Wednesday 31, October 2012

8:00	**Registration**	
	Opening Session	
9:00	**Welcome Addresses**	*Prof. S. Pantelakis EASN Chairman* *Ing. J. Kašpar, General Director of VZLU and President of Assn. of Aviation Manufacturers of the Czech Republic (ALV)*
	Opening of the Conference	*Prof. Th. Panidis, Dr. Z. Patek, Prof. C.C. Wilson Co-Chairmen*
	Session KL.1 - Keynote Lectures *Chair: S. Pantelakis*	
9:30	**The Research Framework Programme Contributing to Europe's Vision for a Sustainable Aviation**, *Dr Diedrich Knoertzer, EC Officer*	
10:00	**Technologies for Environmentally Friendly Aero Engines of the Future**, *Uwe Heßler, Rolls-Royce Deutschland*	
10:30	**Turbulence-Resolving Modelling and its Use in Aeronautic Applications**, *Prof. Shia-Hui Peng, FOI & Chalmers University* **(Publication Approval Pending)**	
11:00	**Coffee Break**	

	Session A.1 *Chair: S.-H. Peng*	Session B.1 *Chair: E. Stumpf*
11:20	**IDIHOM Project** **Industrialization of Higher-Order Methods for Aeronautical Applications - Overview** *N. Kroll* (ID. 28)	**ESPOSA Project** **Efficient Systems and Propulsion for Small Aircraft - A FP7 Project for General Aviation**, *K. Paiger* (ID. 23)
11:40	**Towards Complex Turbulent Flow Computations With Higher-Order Methods**, *T. Leicht, A. Colombo* (ID. 29)	**The Preliminary Analysis of Inlet and Outlet Position in Case of Engine Cooling**, *A. Dziubiński* (ID. 24)
12:00	**High Resolution Discretizations for Reliable and Accurate DNS, LES and Hybrid RANS-LES in an Industrial Context**, *K. Hillewaert* (ID. 30)	**Influence of Non-Uniform Inflow Conditions on Propeller Performance in Tractor Configuration**, *M. Kotsonis, L.Veldhuis, G.Eitelberg* (ID. 25)
12:20	**Numerical Simulation of Subsonic and Transonic Flow Over an Oscillating Wing**, *P.Furmánek, J.Fürst, K. Kozel* (ID.04)	**Simplified Thermo-Fluid Model for Detection of High-Temperature Elements of Engine Cowling in a Small Airplane**, *P. Łapka, M.Seredyński, P. Furmański, A. Dziubiński, J. Banaszek* (ID. 27)
12:40	**HERMES Project** **HERMES Project- Overview Presentation**, *G.Kotsikos* (ID. 44)	**AHEAD Project** **New Engine Architecture for Future Aircraft**, *A. G. Rao* (ID.36)
13:00	**Lunch Break**	

Wednesday 31, October 2012 (afternoon)

	Session A.2 *Chair: Z. Patek*	Session B.2 *Chair: K. Paiger*
14:00	**MARS Project** **An Euro-Chinese Collaborative Research Project**, *G. Bugeda, Sun J., N. Qin, Dong J., J. Pons-Prats* (ID. 37)	**ECATS Project** **Alternative Fuels**, *C.W. Wilson* (ID. 50) **(Publication Approval Pending)**
14:20	**Modifications of Reynolds Stresses by Localized Unsteady Forcing**, N. *Benard, P. Sujar-Garrido, V. Parezanovic, B. Noack, E. Moreau, and J.P. Bonnet* (ID.38)	**The Atmospheric Impacts of Alternative Fuels in Aviation**, *S. Christie, D. Raper* (ID. 20)
14:40	**Hybrid RANS/LES for Active Flow Control Using Oscillating Surfaces and Fluidic Vortex Generator**, *N. Qin* (ID.39)	**Adaptation for Sustainable Fuel**, *R. Kurtenbach, Y.Elshorbany, P. Wiesen* (ID. 19)
15:00	**Formulation of The Optimization Problem for Engine Mount Design – Tractor Propeller Case**, *T. Goetzendorf – Grabowski* (ID. 06)	**Experimental Study on the Influence of Pressure And Temperature on the Burning Velocity and Markstein Number of Conventional and Alternative Jet Fuels**, *V. Vukadinovic, P. Habisreuther, N. Zarzalis* (ID. 22)
15:20	**Aircraft Propeller Simulation in a Rotating Frame of Reference**, *F. Cariglino, N. Ceresola , R. Arina* (ID. 02)	**Assessment of spray characteristics of alternative aviation fuel blends**, An. P. *Vouros, Al. P. Vouros, T. Panidis* (ID. 21)
15:40	**Coffee Break**	
	Session A.3 *Chair: Z. Patek*	Session B.3 *Chair: C.W. Wilson*
		FACTOR Project **Full Aero-Thermal Combustor-Turbine Interaction Research, Overview Presentation**, *C. Battisti* (Id.41)
16:20	**The Preliminary, Parametric Design and Optimisation of the Air-Intake System and the Nacelle as Part of Integration of Turboprop Engine in a Small Aircraft**, *W.Stalewski, J. Żółtak* (ID. 14)	**Factor Project Technical Paper** (ID.42)
16:40	**Optimization of the External Nacelle Shape for a Turboprop Engine**, *S. Kubacki, A. Jaworski, Ł. Łaniewski-Wołłk, J. Rokicki* (ID. 09)	**Modelling of Bypass-Transition in Turbine Blade Cascade** *P. Straka, J. Příhoda* (ID 11)
17:00	**Multiple Objective Optimization of the Power Unit for a Very Light Jet**, *A. Majka* (ID. 01)	**A Numerical Smith Diagram Revision for Modern Low Pressure Turbine Profiles**, *F. Bertini, F. Larocca, E. Ampellio* (ID.03)
17:20	**Numerical Propeller Disk Replacement**, *N. Žižkovský, J. Pelant* (ID. 17)	
17:40	**End of Day One**	

Thursday 1, November 2012

Time	Session / Presentation	
8:00	**Registration**	
	Session KL.2 - Keynote Lectures *Chair: Th. Panidis*	
9:30	**Challenges and Trends in Future Aero Engine Design and Technology**, *Dr. Klaus Rued, MTU Aero Engines Gmbh* **(Publication Approval Pending)**	
10:00	***Technology Developments Required for Electrically Powered Aircraft***, *Prof. Peter Malkin, Cranfield University*	
	Session Pl.1 Plenary	
10:30	**Clean Sky Major Technologies And Demonstrators In Flight Physics And Propulsion**, *Giuseppe Pagnano, Clean Sky JU* (ID. 31)	
10:50	**Coffee Break**	
	Session A.4 *Chair: A. Podsadowskit*	Session B.4 *Chair: M. Guagliano*
11:10	**JTI Clean Sky Project** **SFWA Smart "Laminar Wing": Status and Results of Ground Tests and Manufacturing of Laminar Wings for Flight Test**, *J. Koenig* (ID. 32) **(Publication Approval Pending)**	**AIRCRAFT Fire Project** **Research Problematics To Increase Fire Safety and Survival of the Passengers in the New Generation Aircraft**, *J-M. Most* (ID. 40)
11:30	**Design and Analysis of Noise Shielding after Bodies for Bizjets**, *P. Rostand* (ID. 33)	**Selected Flight Dynamics Models & Computational Procedures Used In Different National and International Projects**, *Z. Goraj* (ID.16)
11:50	**Aerodynamic Design and WT Tests of NLF Wing for Regional A/C in Transonic Cruise and High-Lift Configurations**, *R. Gemma,* (ID. 34)	**A Novel Approach for Trajectory Tracking of UAVs**, *L. De Filippis, G. Guglieri, F. Quagliotti* (ID.05)
12:10	**Multi-Objective Aerodynamic Optimization of Engine Installation Design into Rotorcrafts**, *A. Garavello, E. Benini, R.Ponza* (ID. 35)	
12:30	**Lunch Break**	

Thursday 1, November 2012 (afternoon)

	Session A.5 *Chair:, Z. Goraj*	Session B.5 *Chair: J.M. Most*
13:30	**Simulation of the Helicopter Manoeuvres Close to Boundaries of VRS,** *K.Grzegorczyk* (ID. 08)	**Experimental and Numerical Investigation of a Swirl Stabilized Premixed Methane/Air Flame,** *O. Tunçer, B. Kaynaroğlu* (ID. 10)
13:50	**Bolt-Joint Structural Health Monitoring by Method of Electromechanical Impedance,** *V. Pavelko, I. Ozolinsh, S. Kuznetsov, I. Pavelko* (ID. 13)	
14:10	**EASN Endorsed Projects**	
	EFRA - Environmental Friendly Aircraft, *A.G. Rao* (ID.53)	**MULMON - Multilevel Data Integration in Structural Health Monitoring,** *A. Apicella* (ID. 52)
14:20	**CORSAIR - Cold Spray Radical Solutions for Aeronautic Improved Repairs,** *M. Guagliano* (ID. 45)	**VIVID- Virtual Assessment of Low-Velocity Impact Damage in Composite Airframes,** *K. Tserpes* (ID. 47)
14:30	**Mover2 - Multilevel/Multidisciplinary Optimisation for Design of Aeronautical Structures,** *M. Guagliano* (ID.46)	**ENCOMB+ Validation of Quality Assurance Concepts for Adhesive Bonding of Aircraft Composite Structures by Extended NDT ,** *K. Tserpes* (ID. 54)
14:40	**CAPPADOCIA Project**, *J-L. Bonafe* (ID. 49)	
14:55	**Coffee Break**	
	Session A.6 *Chair: J. Rohacs,*	Session B.6 *Chair: F. Quagliotti*
15:15	**GABRIEL Project**	**EASN Endorsed Projects**
	Using the Magnetic Levitation Technology to Assist the Aircraft Take-Off and Landing, *J. Rohacs* (ID. 43)	**PACIS- Pioneering aircraft-integrated structural sensors,** *H. Pfeiffer*
15:25	**(Publication Approval Pending)**	
15:35	**Discussion on GABRIEL Project**	
16:00	**3nd EASN General Assembly**	
17:30	**End of Day Two**	

Friday 2, November 2012-Excursions to Aeronautic Companies and Research Centres in Prague

2nd EASN Association Workshop on

Flight Physics and Propulsion

Combined with the EASN General Assembly

31st of October- 2nd of November 2012
Prague, Czech Republic

Success stories in the frame of the EASN activities

Prof. Spiros Pantelakis
University of Patras, Greece
Chairman of the EASN Association

Since its establishment, EASN had set a number of priorities:

- ✓ Face research fragmentation in Europe
- ✓ Represent a unique European Academia voice
- ✓ Support and promote innovative research
- ✓ Disseminate knowledge to the engineering base and the scientific community
- ✓ Support the scientific and technical cooperation

- ✓ Face research fragmentation in Europe
- ✓ Represent a unique European Academia voice
- ✓ Support and promote innovative research
- ✓ Disseminate knowledge to the engineering base and the scientific community
- ✓ Support the scientific and technical cooperation

European Aeronautics Science Network

- Mapping of the European Academic institutes active in Aeronautics related research
- Members and contacts established in appx 200 institutes throughout Europe
- More than 10,000 individuals receiving information related to EASN activities

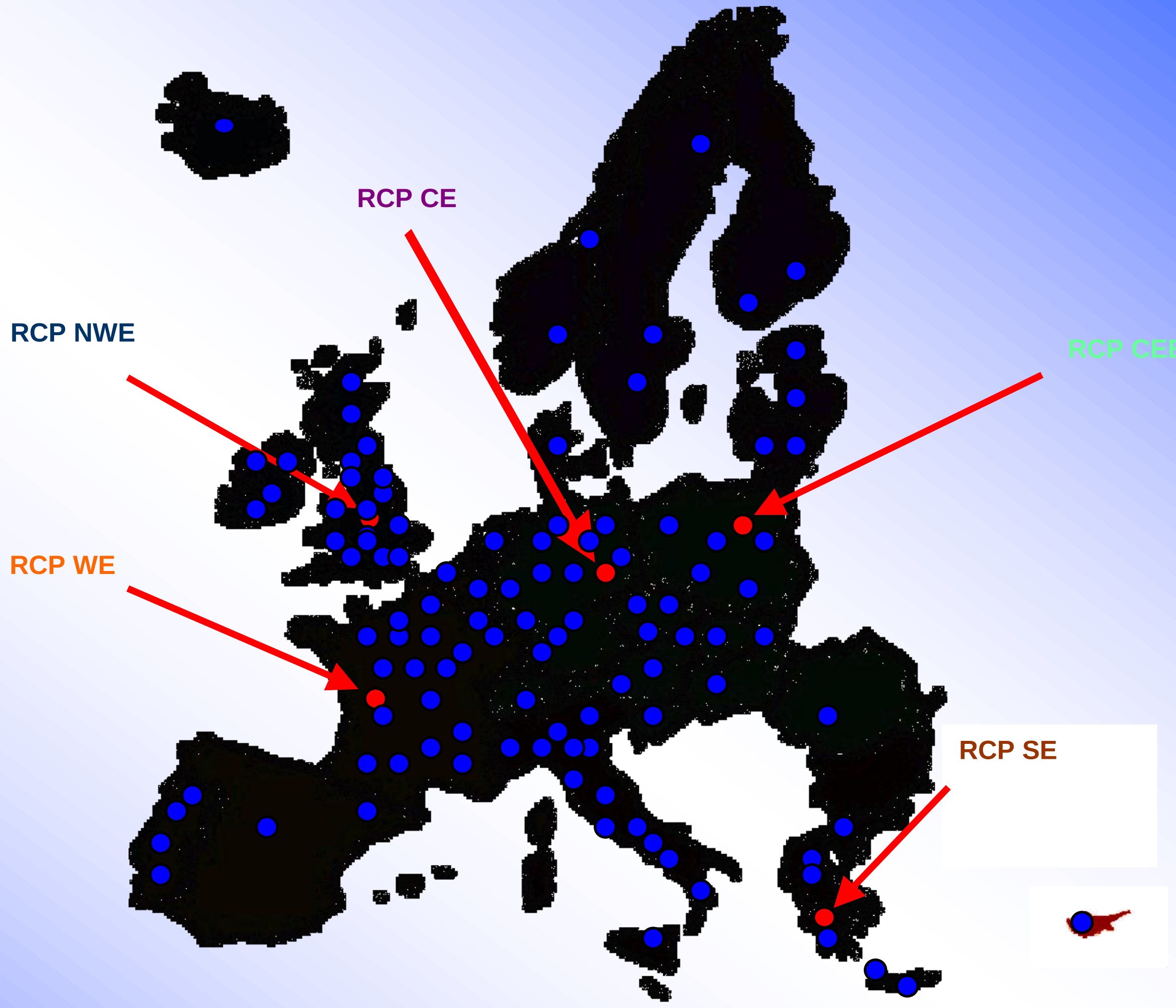

Established EASN Interest Groups

In the frame of EASN a number of *22* Interest Groups could be established so far for different research fields resulting from the needs expressed through the EASN network, corresponding to the classification of aeronautics given by the ACARE Taxonomy. The IGs:

- provide a mechanism for incubating innovation, new technologies and breakthrough concepts
- provide input towards the development of a University Research Strategy for the sector of Aeronautics

- ✓ Face research fragmentation in Europe
- ✓ Represent a unique European Academia voice
- ✓ Support and promote innovative research
- ✓ Disseminate knowledge to the engineering base and the scientific community
- ✓ Support the scientific and technical cooperation

- EASN expresses consolidated Academia views in:
  - ACARE (General Assembly + working groups)
  - The discussions regarding Clean Sky II

Extract from EASN position paper on CS2

…with respect to the role of the Academia in CS

- Although the development of demonstration hardware to high TRL levels is not one of the Academia activities, certain Universities can support such activities through dedicated technology centres.
- Universities could provide validated tools in order to be used by the industry in the design of demonstrators or validate tools that are currently being used
- Specialised researchers and infrastructure provided from European Universities can be better exploited

EASN's role

- Support in broadening academia representation by suggesting Universities and labs
- Participate in the dissemination activities of Clean Sky 2
- The active participation in the CS governing board would provide the academia view on issues relevant to academia and also contribute on implementing the lessons learnt in the frame of Clean Sky.

- EASN expresses consolidated Academia views in:
  - ACARE (General Assembly + working groups)
  - The discussions regarding Clean Sky II
  - The negotiations of the EC with non-EU members on joint calls for proposals (Russia, Japan etc)
  - Support actions and campaigns launched by the EC

European Aeronautics Science Network

- ✓ Face research fragmentation in Europe
- ✓ Represent a unique European Academia voice
- ✓ Support and promote innovative research
- ✓ Disseminate knowledge to the engineering base and the scientific community
- ✓ Support the scientific and technical cooperation

- Endorsement of 19 project proposals in FP6 and 64 in the FP7 calls
- Success rates significantly higher than the global rates indicate high quality proposals and focused research activities

EASN Endorsed projects for the 6th FP7 call

CORSAIR	Cold Spray Radical Solutions for Aeronautic Improved Repairs
ENCOMB+	ENCOMB+ Validation of Quality Assurance Concepts for Adhesive Bonding of Aircraft Composite Structures by Extended NDT
MULMON	Multilevel Data Integration in Structural Health Monitoring
MOVER2	Multilevel/Multidisciplinary Optimisation for Design of Aeronautical Structures
PACIS	Pioneering aircraft-integrated stru-ctural sensors
VIVID	Virtual Assessment of Low-velocity Impact Damage in Composite Airframes
DREAMCOMP	A Universal Approach in Developing Robust and Energy Efficient Monitoring, Optimasation and Control Technologies for Ecolonomic Composites Processing
EFRA	Environmental Friendly Aircraft

- ✓ Face research fragmentation in Europe
- ✓ Represent a unique European Academia voice
- ✓ Support and promote innovative research
- ✓ Disseminate knowledge to the engineering base and the scientific community
- ✓ Support the scientific and technical cooperation

- EASN thematic workshops, disseminating research results and acting as discussion forums towards ideas for future research
  - EASN workshop on Aerostructures (2011)
    - 13/14 projects running at the time of the workshop represented at the workshop
- EASN workshop on Flight Physics and Propulsion
  - 10 projects in the area have confirmed their representation **(9+JTI)**

- EASN thematic workshops, disseminating research results and acting as discussion forums towards ideas for future research
  - EASN workshop on Aerostructures (2011)
    - 13/14 projects running at the time of the workshop represented at the workshop
- EASN workshop on Flight Physics and Propulsion
  - 14 projects in the area have confirmed their representation
- Responsible for the dissemination activities in several currently running FP7 research projects (ENCOMB, INMA, IASS, SARISTU, HAIC….)

- ✓ Face research fragmentation in Europe
- ✓ Represent a unique European Academia voice
- ✓ Support and promote innovative research
- ✓ Disseminate knowledge to the engineering base and the scientific community
- ✓ Support the scientific and technical cooperation

- Participation in support actions aiming to promote research cooperation with technologically advance countries:
  - CooperatEUS: Academia seems to have the largest capacity among all stakeholders to promote upstream collaborative research with the US
  - SUNJET: Establishment of contacts and research collaborations with Japanese Universities and Industry
  - Aero-Ukraine: Integration of Ukrainian institutions in EU research activities
- Direct contacts established with Industrial groups and Associations to enhance the Industry-Academia cooperation
  - ASD
  - Euromart
  - IMG4
- Direct Contacts established with the association of the European research establishments(EREA)

Thank you.

2nd EASN WORKSHOP on Flight Physics and Propulsion
31st of October - 2nd of November
Prague, Czech Republic

Multiple Objective Optimization of the Power Unit For a Very Light Jet

Andrzej Majka
Rzeszow University of Technology

POLITECHNIKA RZESZOWSKA im. IGNACEGO ŁUKASIEWICZA

Aircraft fleet properties

Different conditions of functioning and task performing [source: EROCONTROL]

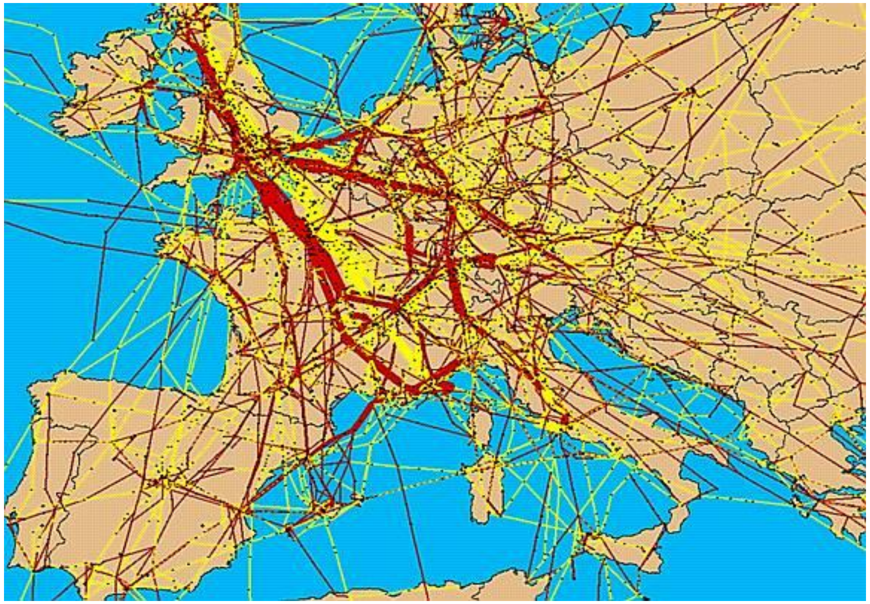

Complex aircraft fleet structure consisting of many different aircrafts

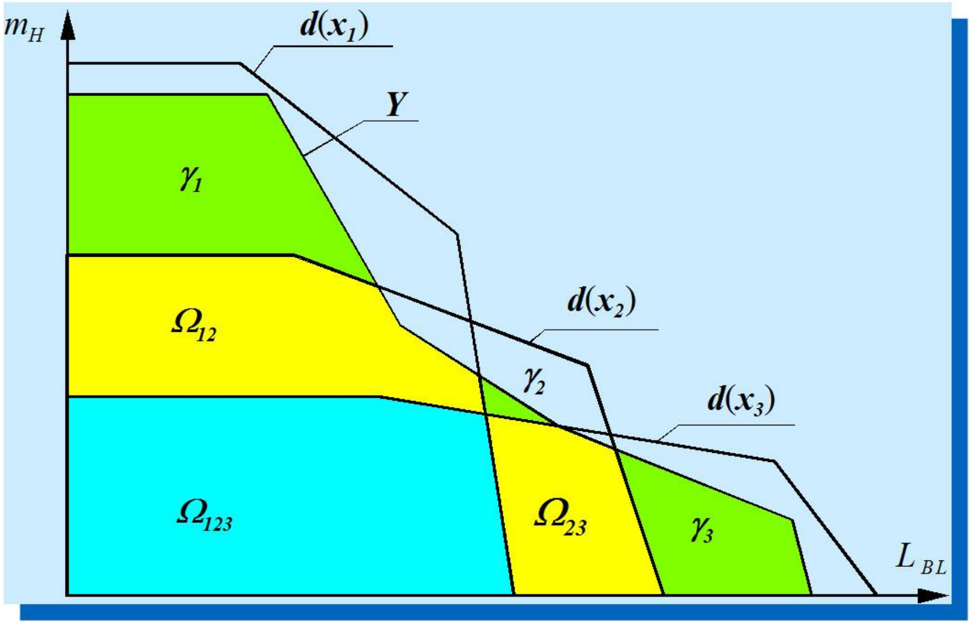

A lot of tasks performed using the aircrafts determine the necessity of using different factors to estimate their effectiveness

Andrzej Majka
Rzeszow University of Technology, Poland

Multitask aviation system

The mathematical model of the aircraft fleet can be a multitask system

X - set of all elements x_i, which can potentially enter the system structure

$A = \{x_i\} \subset X$ where $i = 1,\ldots, m$ – set of system elements

Y - tasks set

$E(y)$ – distribution function (integer type)

D_i - field of specialization of element $x_i \in X$

$$D_i = \{y \in Y \,;\, E(y) = i\} \,;\, i = 1,\ldots, m$$

The fields of specialization must fulfill two criteria:

$$D_i \cap D_k = \varnothing \,; \quad \forall i,k = 1,\ldots,m;\; i \neq k$$

$$\bigcup_{i=1}^{m} D_i = Y$$

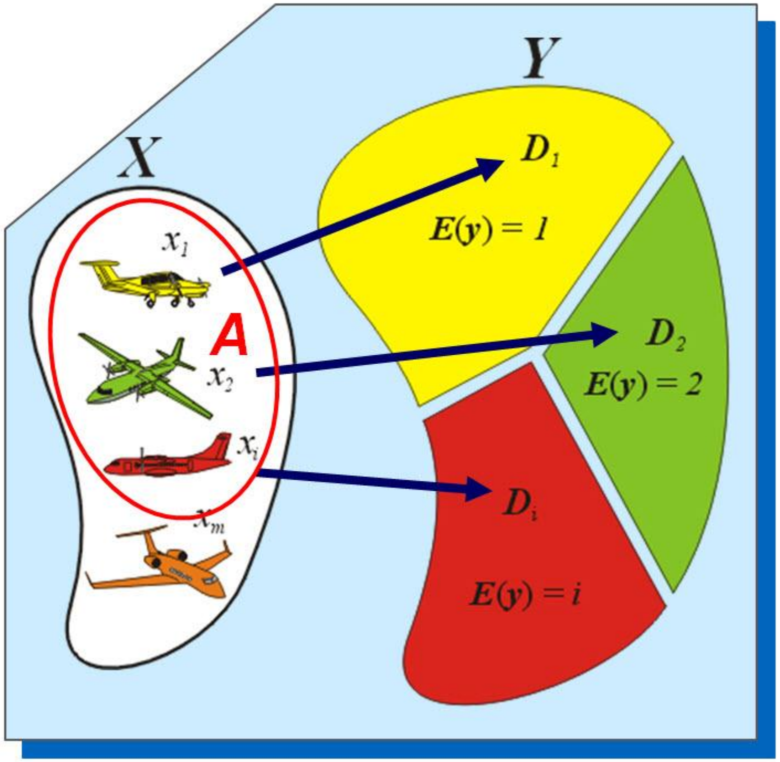

$[A,\ Y,\ E(y)]$ – multitask system

Optimization of multitask aviation system

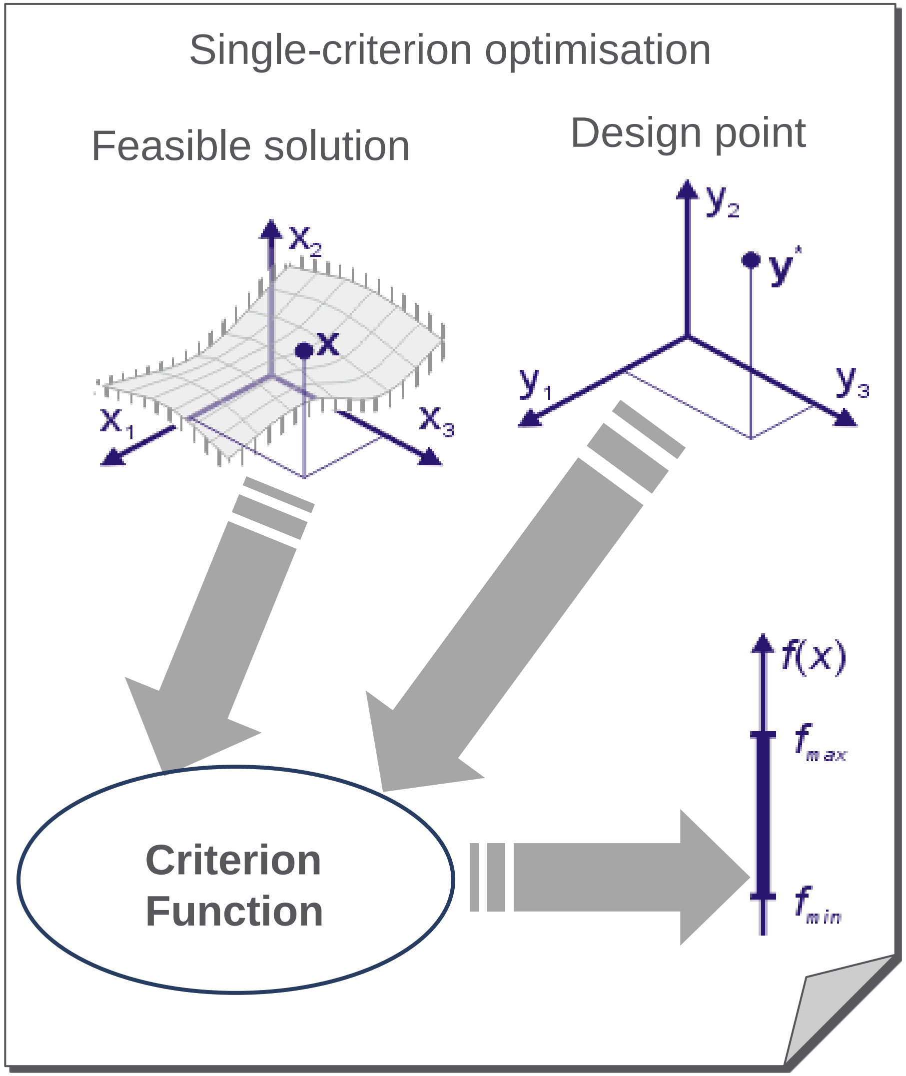

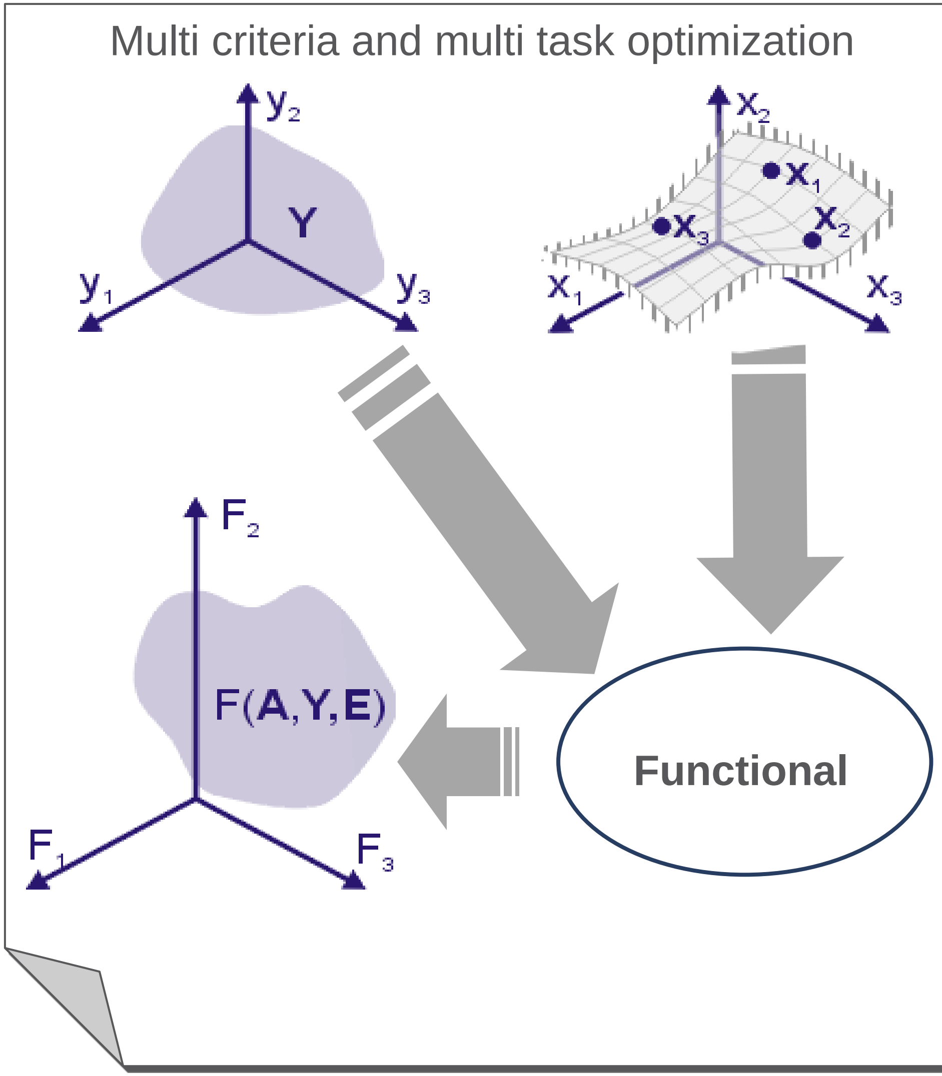

Andrzej Majka
Rzeszow University of Technology, Poland

Optimization of multitask aviation system

Coefficient of the multitask system quality

$$F\left[\boldsymbol{X},\boldsymbol{A},\boldsymbol{E}(x)\right]=\sum_{i=1}^{m}\sum_{y_j\in D_i} f\left[x_i,y_j,\mu\left(\boldsymbol{D}_i\right)\right] \quad \boldsymbol{Y}=\bigcup_{i=1}^{m}\boldsymbol{D}_i$$

Mathematical vector optimization model

$$F\left(x\right)=\underset{x\in X}{opt}\left(F\left(x\right)\right), \quad F=\left\{f_1,\ldots,f_n\right\}$$

The component synthesis method

$$F=\varphi\left[f_1,\ldots,f_n\right]$$

The most widely known method of the synthesis is linear synthesis of the components f_1, ..., f_n to the scalar criterion of the function

$$F\left(x\right)=\sum_{i=1}^{n}w_i f_i\left(x\right) \qquad \sum_{i=1}^{n}w_i=1, \quad w_i\geq 0, \quad i=1,\ldots,n$$

Optimization of multitask aviation system

The weights w_1 and w_2 establishes the essence of the compromise between the elements f_1 and f_2

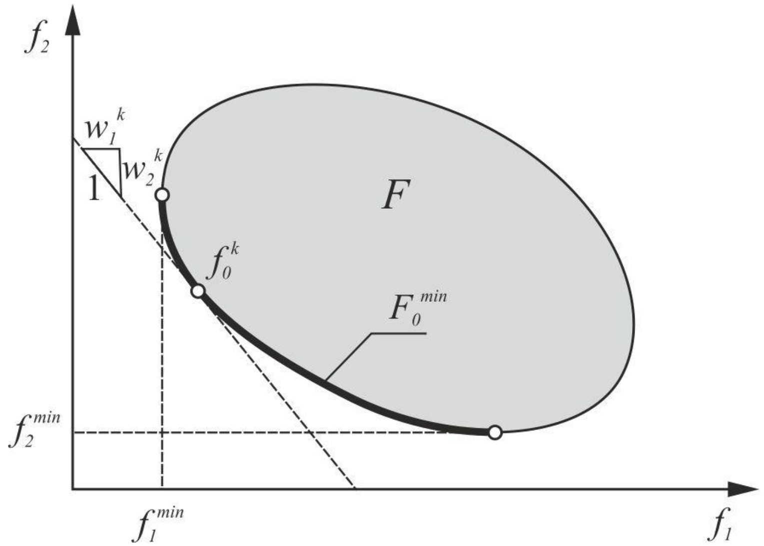

Pareto set - minimization of the factors f_1, f_2

Optimization of multitask aviation system

The question of taking into account the uncertainty in the efficiency estimation and the choice of a relevant solution leads to construction of the weights set and summing of products $w^T \cdot f\,(x, y)$

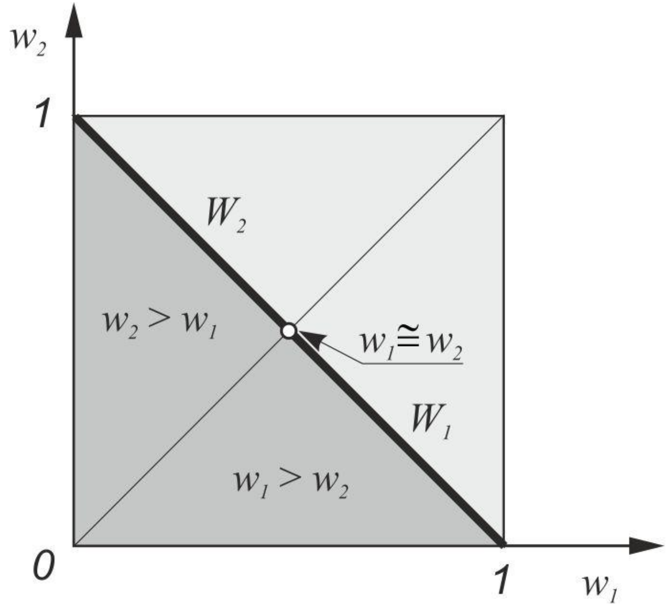

Sets W_1 and W_2 for 2 criteria

Evaluation criteria - aircraft efficiency

Simple technical criteria

The range of velocity

$$\bar{V} = \frac{V_{\max}}{V_{\min}}$$

Weight effectiveness

$$\bar{W}_{useful} = \frac{W_{useful}}{W_{TO}}$$

Transport effectiveness or transport qualitative effectiveness

$$W_T = W_{useful}\frac{L_Z}{T_{BL}} = W_{useful}V_{cru}$$

$$\bar{W}_T = \frac{W_{useful}V_{cru}}{W_{TO}}$$

Economic criteria

DOC (Direct Operating Cost)

$$\frac{USD}{km \times kg}$$

Formulation of the task

The calculations were made for aircraft with geometry similar to Honda HA-420 HondaJet with two jet engines.

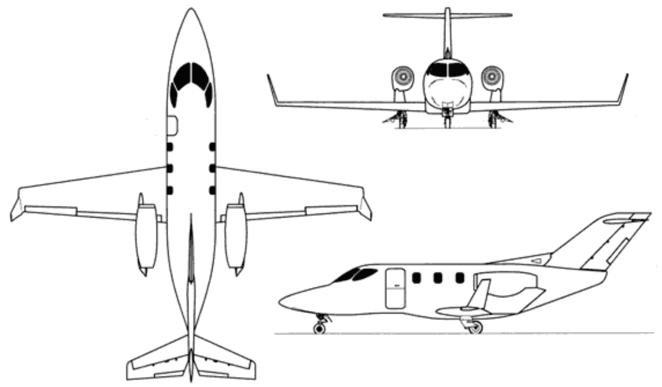

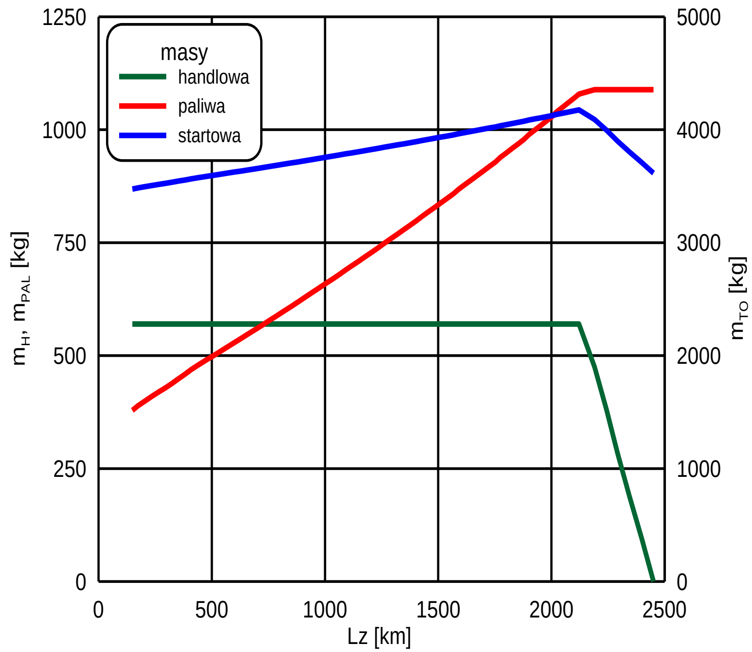

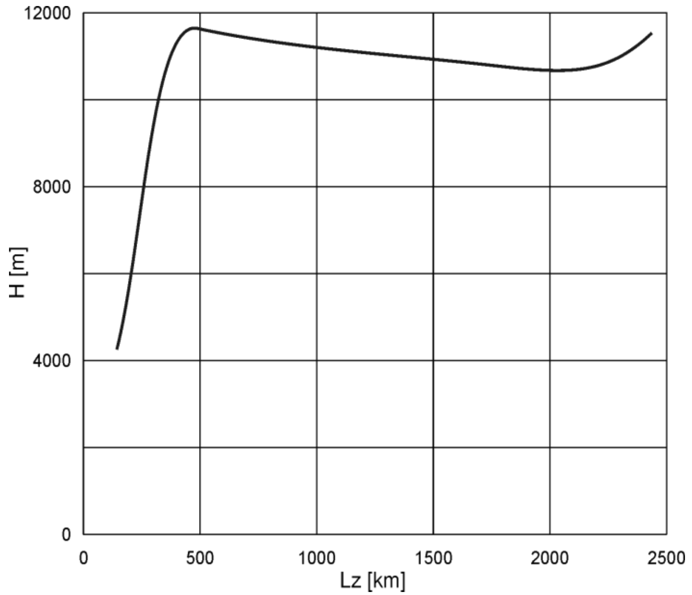

Results

Calculations were made for two criterion of optimization:
specific transport performance and specific fuel consumption

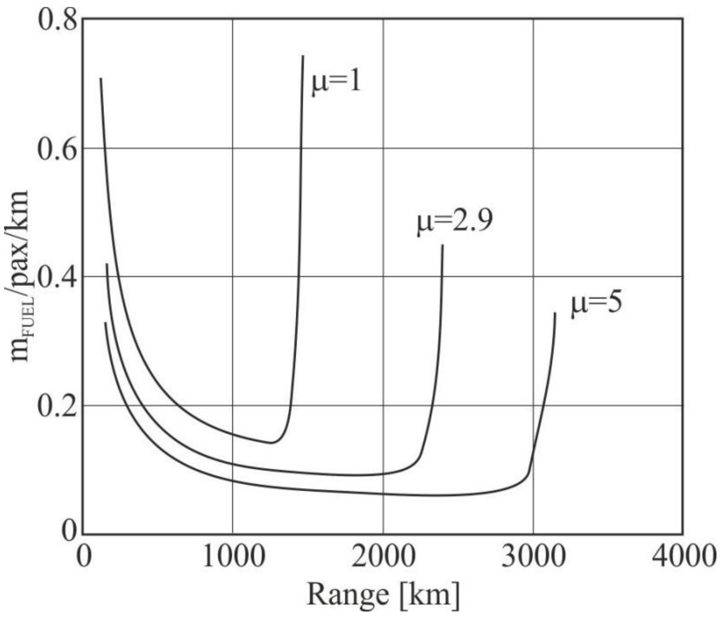

The specific fuel consumption ratio depending of the flying range for the engines with different bypass ratio

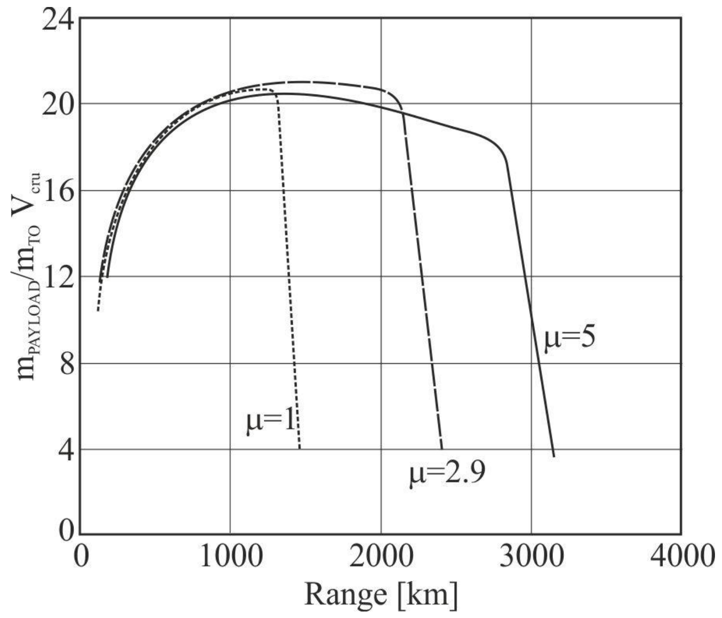

The dependence criterion of the specific transport efficiency on the flying range for the engines with different bypass ratio

Results

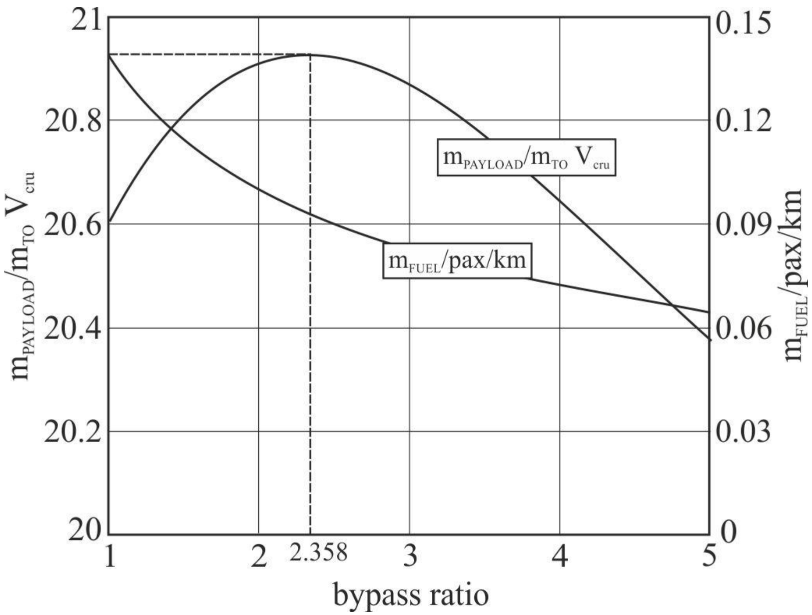

The best values of the analyzed criteria depending on the engine bypass ratio

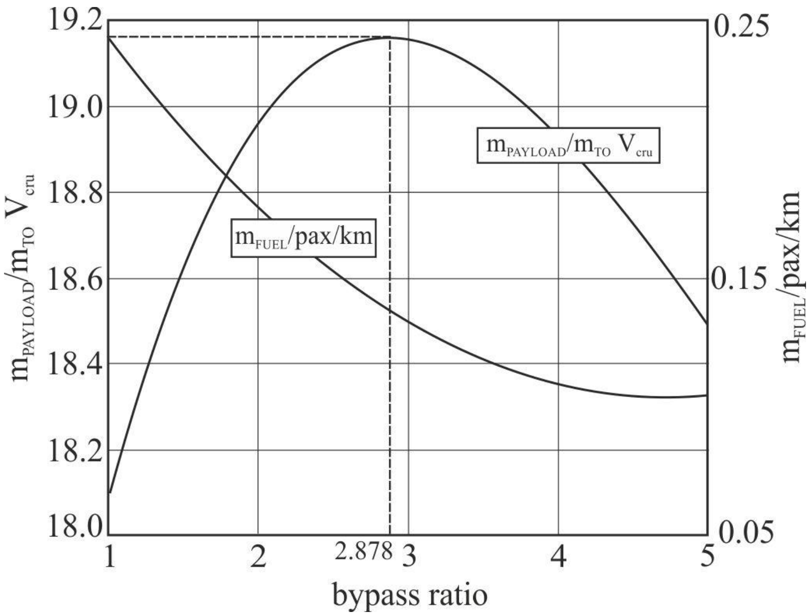

Average values of the analyzed criteria for the complete set of the performed tasks depending on the engine bypass ratio

Results

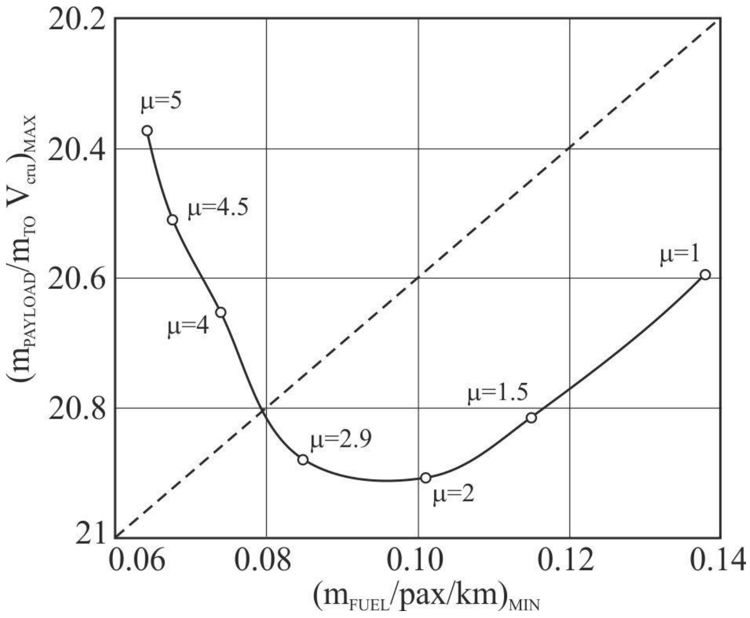

The envelope of the best values of the analyzed criteria (Pareto set) for different engine bypass ratio

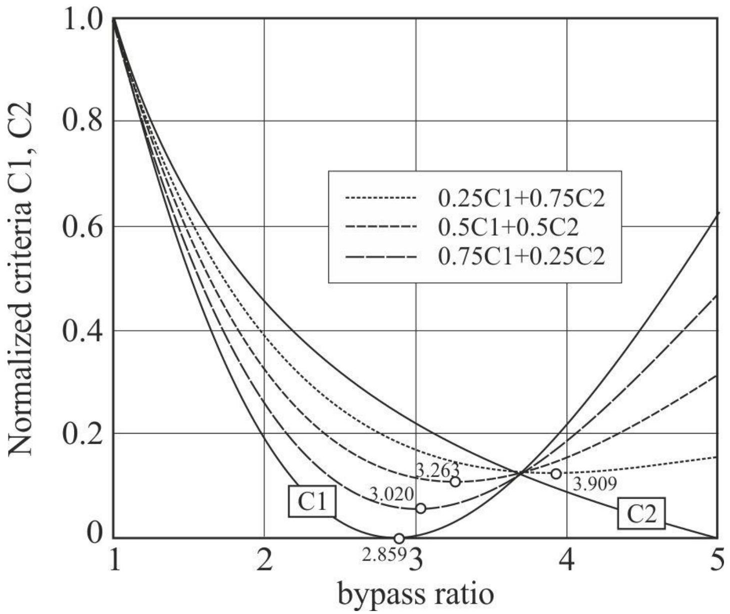

Compromise solutions for the chosen weight factors

Andrzej Majka
Rzeszow University of Technology, Poland

Conclusions

The way to design a competing aircraft is to choose its construction parameters, including the power unit, by using the advanced methods of multiple objective optimization. The main aim of the work was to demonstrate a method of selection chosen parameters of the transport aircraft at the preliminary design stage. The work focuses on the choice of bypass ratio of the jet engine of the Very Light Jet. The method could be helpful at preliminary design stage of a new aircraft to selection another design parameters.

Contact:

Department of Aircrafts and Aircraft Engines

Faculty of Mechanical Engineering and Aeronautics

Rzeszow University of Technology

Address:

ul. Powstancow Warszawy 8

35-959 Rzeszow, POLAND

- phone: +48 17 865 1604

  mobile: +48 602 441 977
- web: www.prz.edu.pl/ksisl
- e-mail: andemajk@prz.edu.pl

Thank You for your attention

EASN Workshop on Flight Physics and Propulsion
31th October – 2nd November 2012

Aircraft Propeller Simulation in a Rotating Frame of Reference

F. Cariglino, R. Arina
Politecnico di Torino, Torino, Italy.
N. Ceresola
Alenia Aermacchi, Torino, Italy.

Outline

- **Introduction:**

  1. Rotating frame of reference for the calculation of the flow field around a propeller

  2. Possible choices for the velocity vector

- **Modelling:**

  1. Formulation of the Navier-Stokes equations in a rotating frame of reference

  2. Computational Fluid-Dynamics (UNS3D) module

- **Applications:**

  1. Propeller flow simulations for three different angular velocities

  2. Comparison between numerical and experimental results in terms of the thrust coefficient

- **Conclusions**

Introduction : Rotating Frame of Reference

- To take into account the *motion of a body,* the formulation of the Navier-Stokes equations in a *rotating frame of reference* represents an alternative to the introduction of a grid velocity in the inertial frame of reference

- This formulation permits to perform the simulations of the unsteady viscous flow around a propeller in a steady-state mode using reduced computational resources

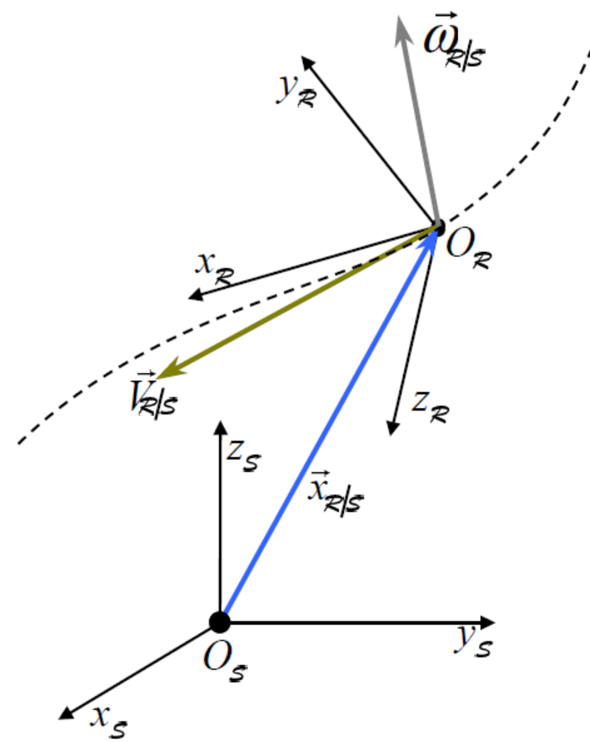

View of inertial coordinates system *S* and general non-inertial coordinate system *R*

Introduction : Rotating Frame of Reference (2)

- Another advantage of the *rotating frame formulation* is the possibility of an easier integration of rotating elements in an aircraft configuration

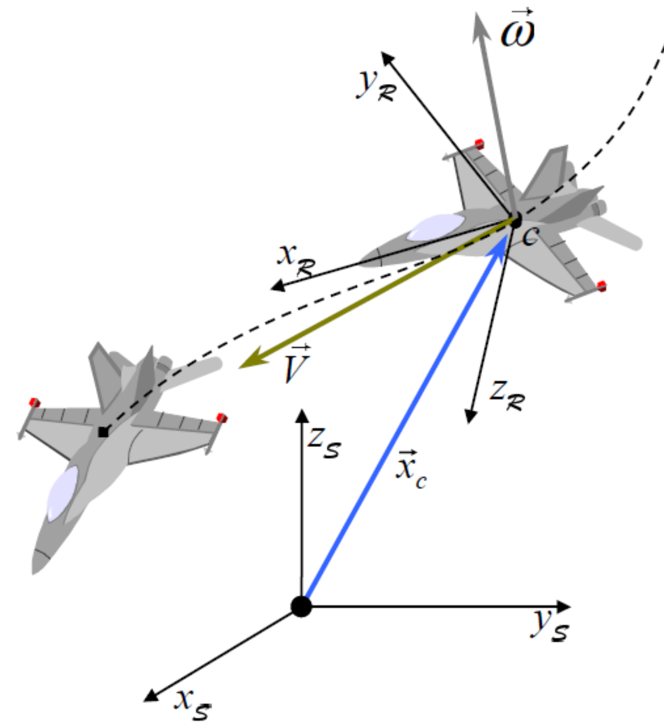

Aircraft flying in an arbitrary motion. View of inertial coordinates system *S* and general non-inertial coordinate system *R*

Introduction: Velocity Vector

The velocity components are expressed with respect to the absolute (inertial) frame

this choice

- *has the advantage to avoid an excess of artificial dissipation in the far field region*.

The contribution of the centrifugal force is implicitly introduced in the rotating frame formulation and consequently a smaller amount of added artificial dissipation is necessary to ensure the numerical convergence.

- *makes easier to interface the propeller computational block inside an aircraft configuration*

Modelling

The formulation of the Navier-Stokes equations in a rotating frame, using absolute velocity components, implies:

– The source term, which take into account the Coriolis force in the momentum equation, is:

$$\vec{Q} = \begin{bmatrix} 0 \\ -\rho(\vec{\omega} \times \vec{v}) \\ 0 \end{bmatrix}$$

– The inviscid flux vectors, considering the rotational speed $\overrightarrow{v_b}$ of the coordinate system, are:

$$F_{Ii} = \begin{bmatrix} \rho v_i \\ \rho v_1 (v_i - v_{b_i}) + p\delta_{1i} \\ \rho v_2 (v_i - v_{b_i}) + p\delta_{2i} \\ \rho v_3 (v_i - v_{b_i}) + p\delta_{3i} \\ (\rho E + p) v_i \end{bmatrix}$$

where $\overrightarrow{v_b} = \vec{\omega} \times \vec{r}$

Modelling

- **The choice of the non inertial reference frame introduces a numerical source error, which can be reduced ensuring conservation of the freestream solution with the inclusion in the Navier-Stokes equations of a new source term:**
  - in our case, with an angular velocity about the x-axis, this source term is equal to

$$\vec{K} = S_{\Omega} \begin{bmatrix} \rho \\ \rho v_1 \\ 0 \\ 0 \\ \rho E \end{bmatrix}$$

where

$$S_{O} = \omega_x \left(-\frac{\partial z}{\partial y} + \frac{\partial y}{\partial z} \right)$$

Application: Rotating Propeller

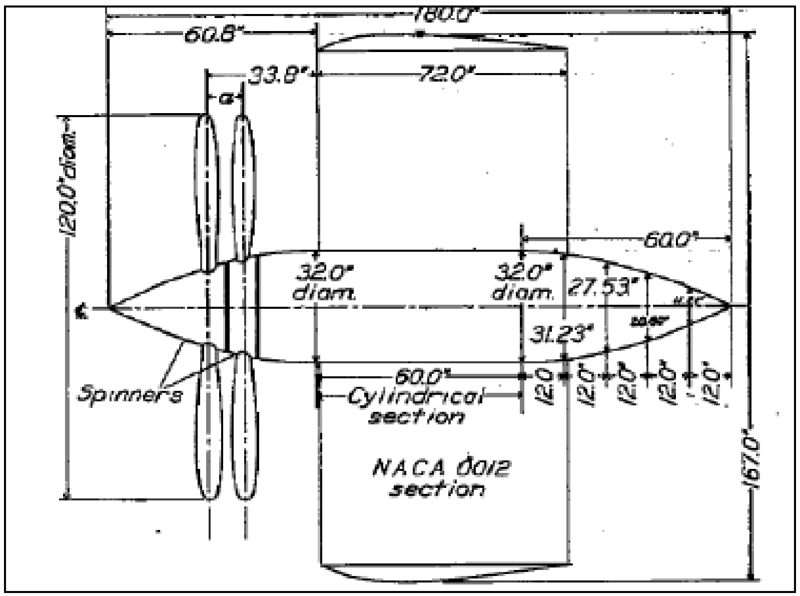

Geometrical and experimental model (Biermann and Haetman)

Geometry of the experimental model used by Biermann and Haetman (NACA-report 747, 1942)
The experimental results are provided for one and two hub propellers

Application: Rotating Propeller

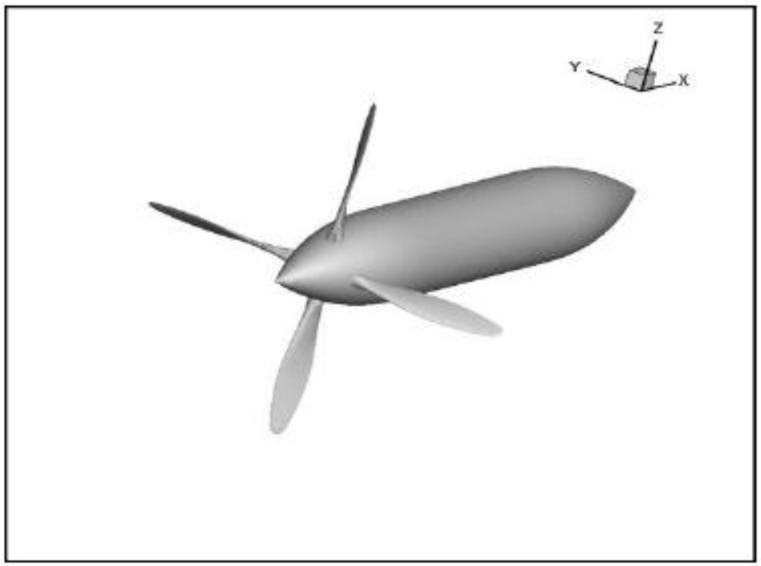

CATIA model of propeller

- The blade angle, from the plane of rotation at the 75% of the blade radius is equal to 45 degrees
- The propeller diameter is equal to 3.08 m
- To obtain the final blade shape, it was decided to design a constant blade profile with a constant pitch of 25 deg and to twist the blade of 20 deg from root to tip

Application: Rotating Propeller

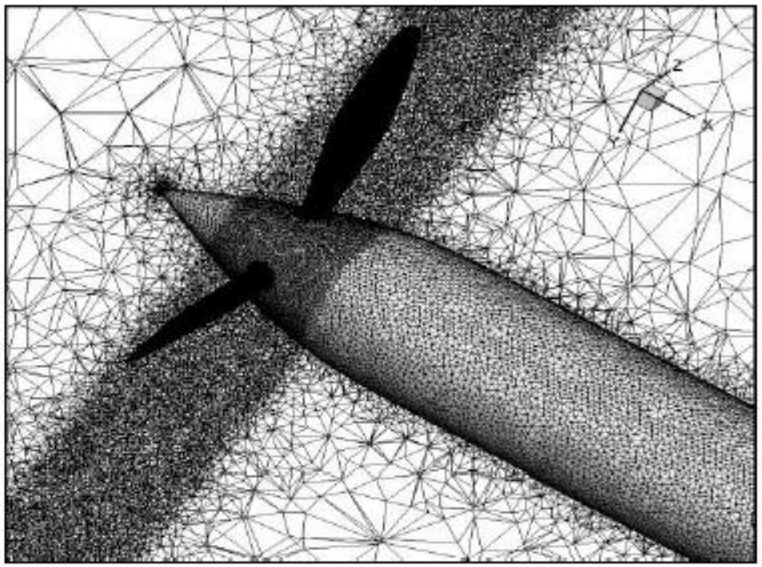

Grid generated with CFD-ICEM

Computational grid

- 5,672,824 nodes
- 16,265,544 elements
- 21 prismatic layers on solid surface to correctly represent the boundary layer
- The grid is refined in the regions around the blades and on the blade surfaces

Operating conditions investigated

Advancement Factor J	Velocity (m/s)	Rotational speed (rps)
1.45	49.1744	11.0
1.8	49.1744	8.9
2.4	49.1744	6.6

Application: Rotating Propeller

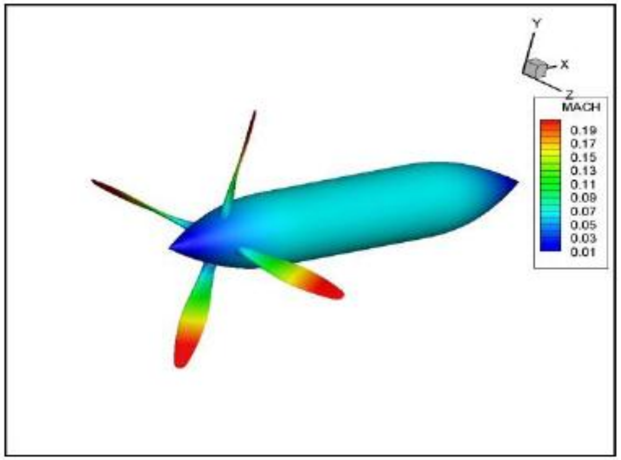

Mach number on the propeller for J=1.8

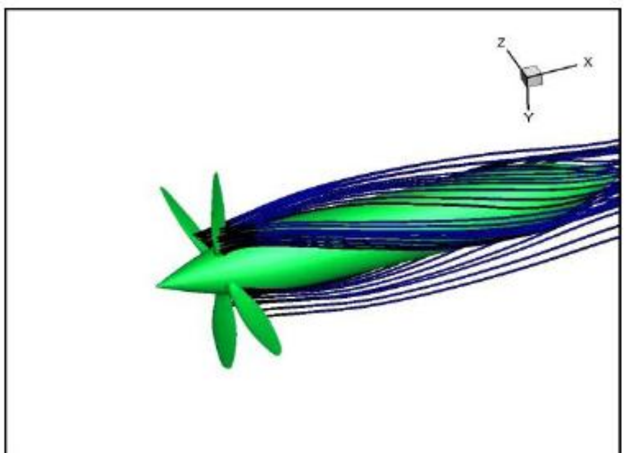

Streamlines around the propeller for J=1.8

<u>Boundary conditions</u>

- On the blade surface no-slip and no-penetration conditions are used by setting the absolute velocity equal to the absolute local blade velocity
- Radial condition to the pressure is imposed

An increasing level of Mach number from the nacelle surface toward the tip, which is the result of the increasing rotational speed with increasing radius

Application: Rotating Propeller

Eddy viscosity contours at blade stall conditions

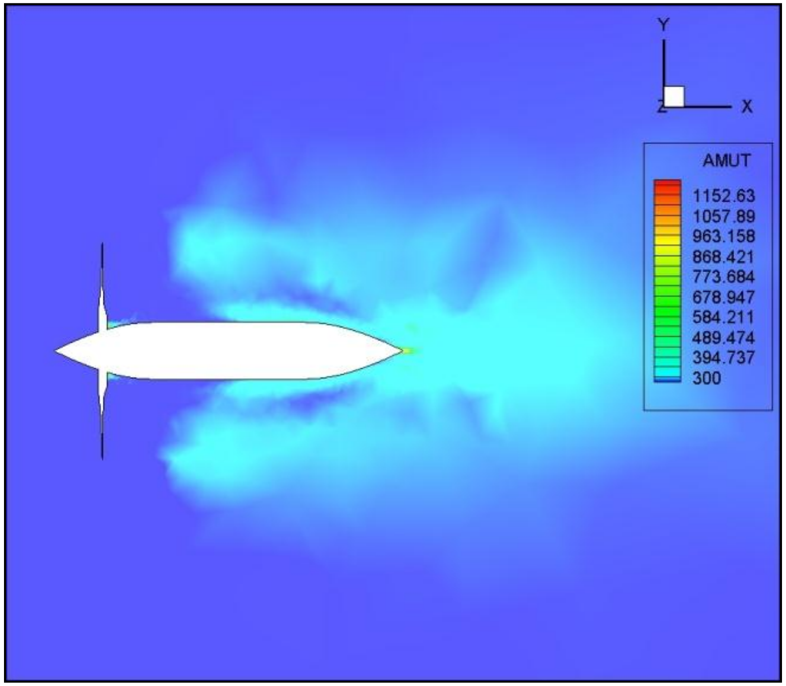

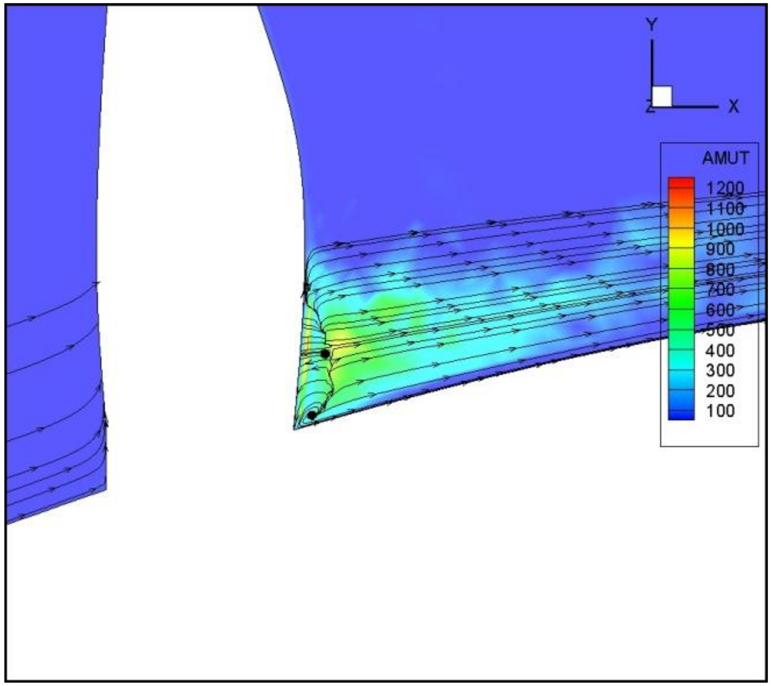

Eddy viscosity on the plane (x,y) for J=1.8

Application: Rotating Propeller

Influence of the rotational speed on the flow past the spinner

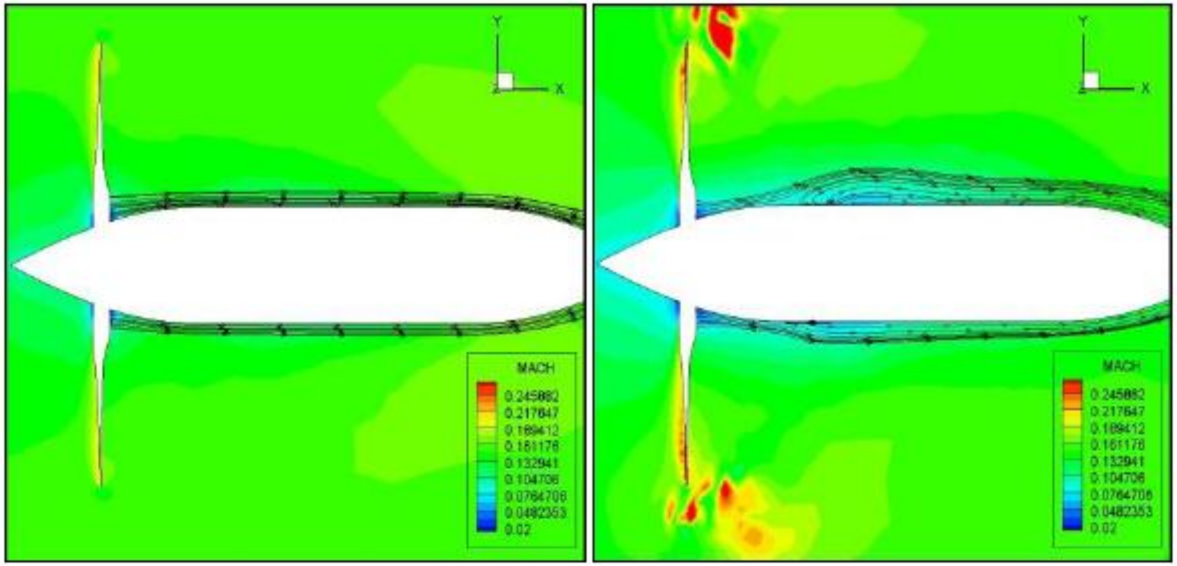

Streamlines around the propeller for J=1.8 and J=1.45

Separation on the spinner due to the increasing of the rotational speed

Application: Rotating Propeller

Pressure coefficient contours at stall conditions

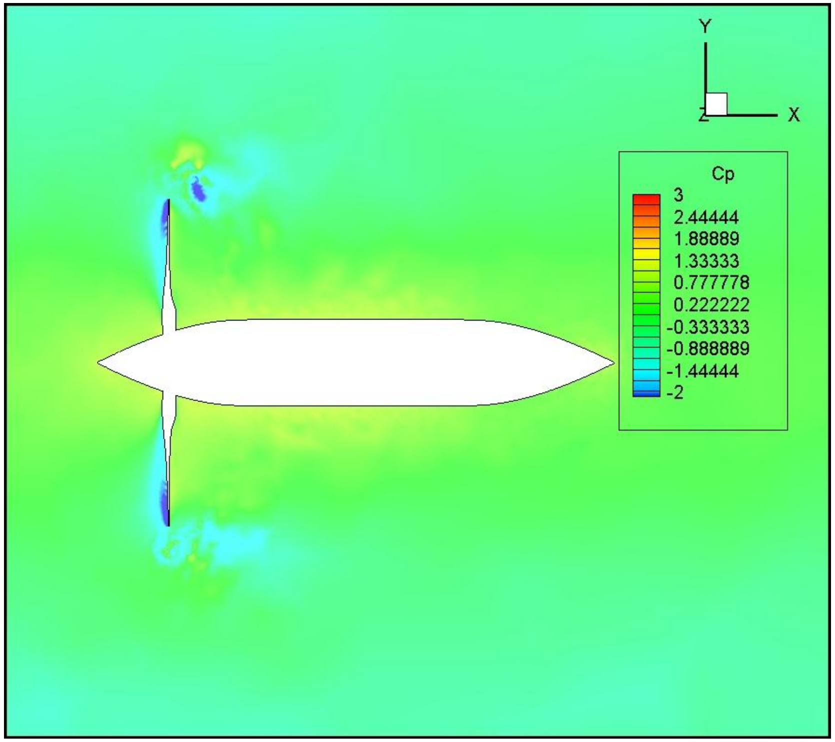

Pressure coefficient in the plane (x,y) for J=1.45

Application: Rotating Propeller

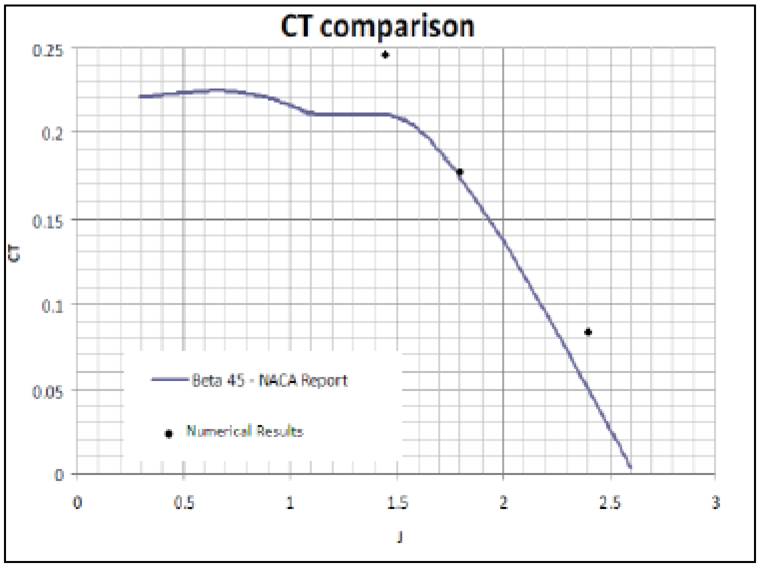

Computed vs experimental thrust coefficient

- *The computed thrust coefficient is in agreement with the experimental values for J=1.8 and in the linear part*
- *The blade stall is qualitatively predicted. However, the thrust coefficient is still over predicted for stall conditions. This maybe due to the fact that in the simulation the spinner is rotating, while in the experiment only the hub is*

Conclusions

- The results are in good agreement with the experimental data within the propeller operating range, while failing to predict propeller stall at the highest rotational speeds
- The present technique allows the simulation of a rotational flow field at a reduced computational cost (the wall clock time for each simulation was of about 4 hours)
- The next step in the application of this method will be the integration of the airframe with the propeller, by the local application of the non inertial frame of reference as a building block in a more complex configuration

2nd EASN Association Workshop on Flight Physics and Propulsion
31st October-2nd November 2012, Prague, Czech Republic

european aeronautics science network

A COMPARISON BETWEEN LOSS CORRELATION MODELS AND SMITH DIAGRAM FOR MODERN LOW PRESSURE TURBINE PROFILES

Francesco Bertini
Avio S.p.A.
Via I Maggio, 99
10040, Rivalta di Torino (TO), Italy
francesco.bertini@aviogroup.com

Francesco Larocca
Enrico Ampellio
Dept. of Aerospace and Mechanical Engineering
Polytechnic of Turin - Corso Duca degli Abruzzi, 24
10129 Torino, Italy
francesco.larocca@polito.it
enrico.ampellio@polito.it

ORIGINAL SMITH DIAGRAM

1. Constant c_{ax} through the stages;
2. DP incidence;
3. R between 0.2 and 0.6;
4. Re between 10^5 and $3 \cdot 10^5$;

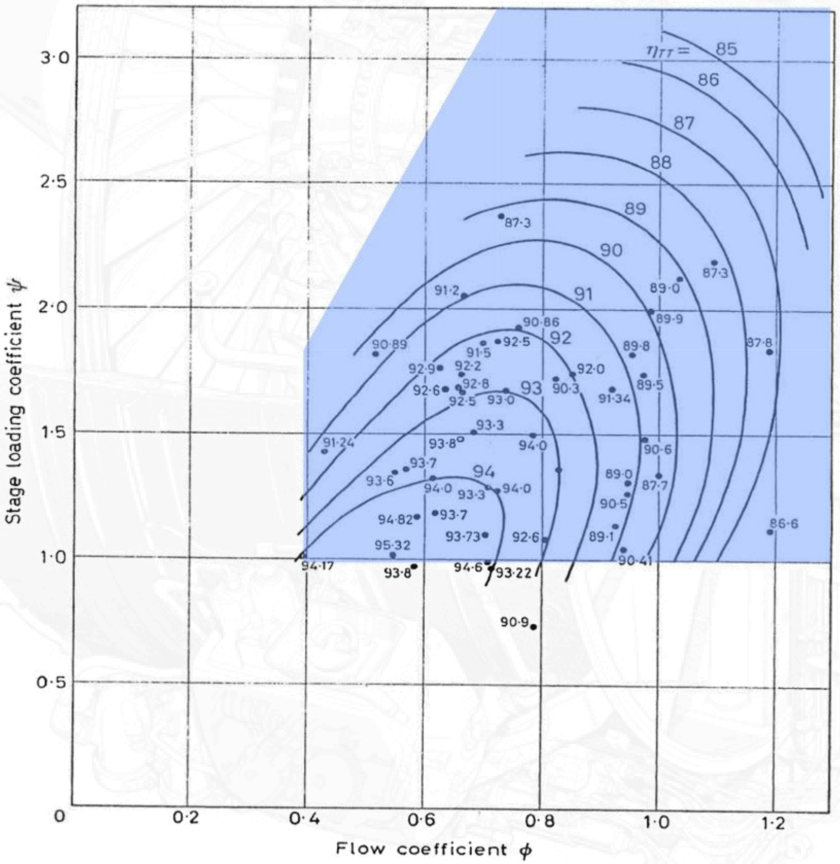

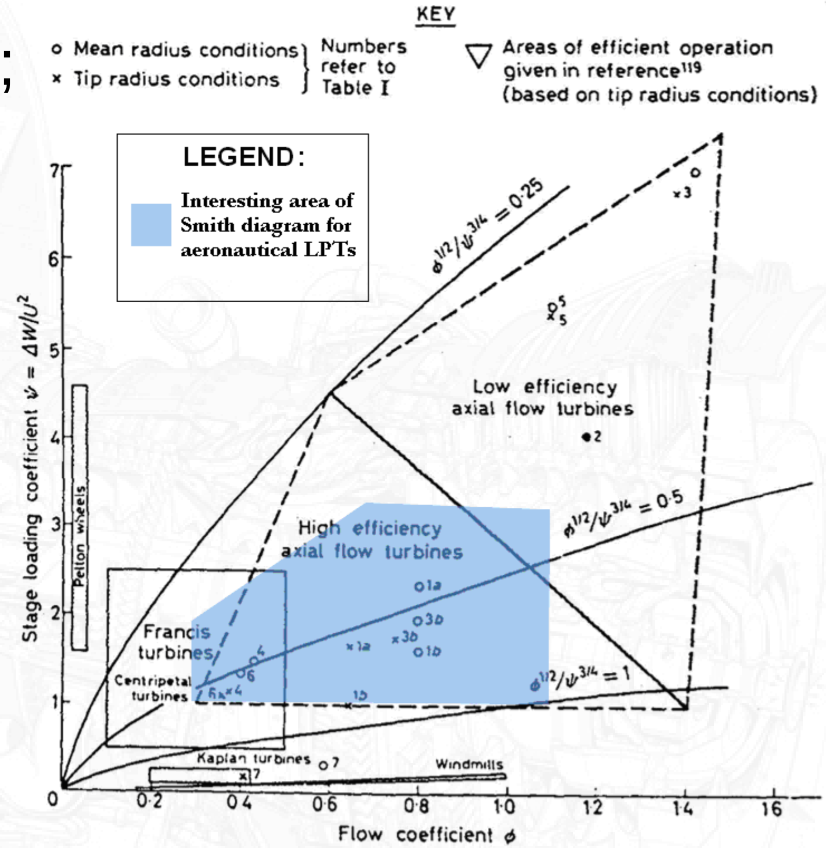

5. AR between 3 and 4;
6. No Mach variation effects;
7. No TE variation effects;
8. RTC losses removal.

PRACTICAL USE OF SMITH DIAGRAM

Main requirements are known from the OEM:

1. Total shaft power supplied;
2. Maximum RPM;
3. Mass flow processed;
4. LPT ecumberance;
5. TtT expansion rate.

Smith diagram permits to manage a great variety of applications.

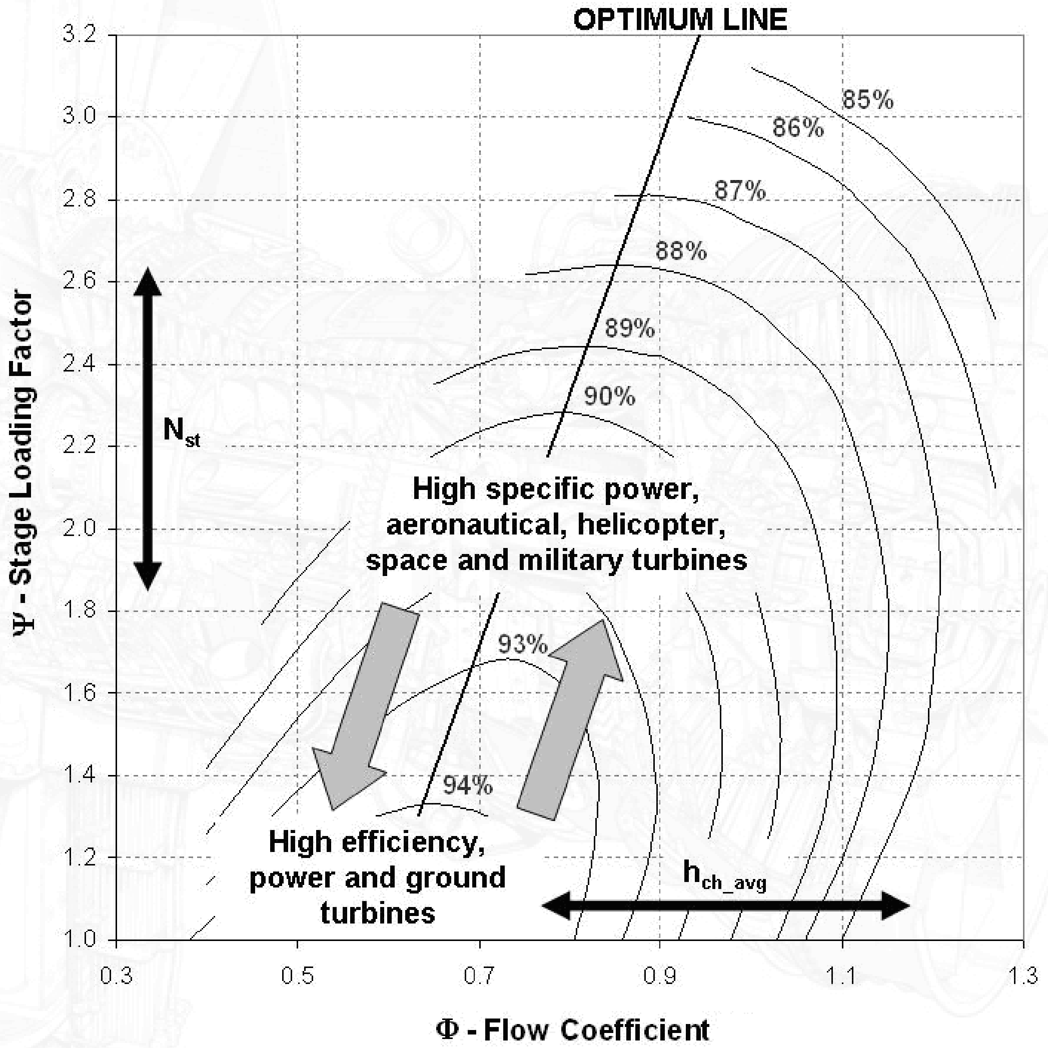

REFERENCE MODULE

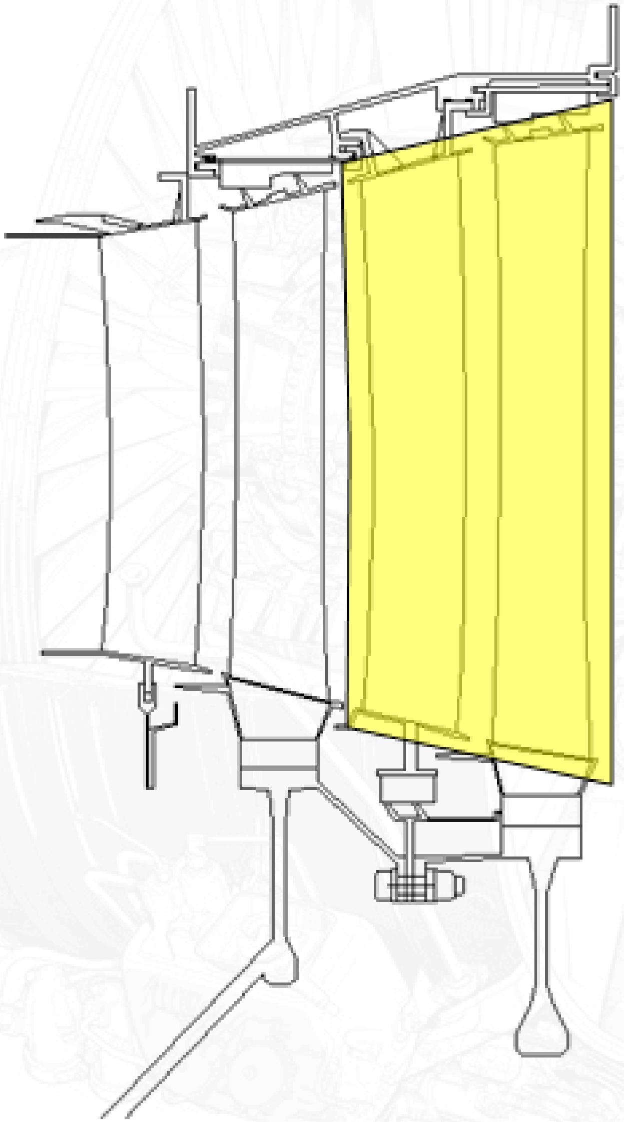

Thermal fluid dynamics		
Inlet Total Pressure	169.0	[kPa]
Inlet Total Temperature	901.5	[K]
Outlet Total Pressure	104.7	[kPa]
Specific Heat Ratio	1.34	[-]
Gas Constant	287.31	[J/kgK]
Geometries		
Inlet Hub Radius	0.660	[m]
Inlet Tip Radius	0.800	[m]
Outlet Hub Radius	0.623	[m]
Outlet Tip Radius	0.837	[m]
Turbine Length	0.186	[m]
Axial chord	0.034	[m]

SAMPLING POINTS ON SMITH DIAGRAM

Meanline analyses

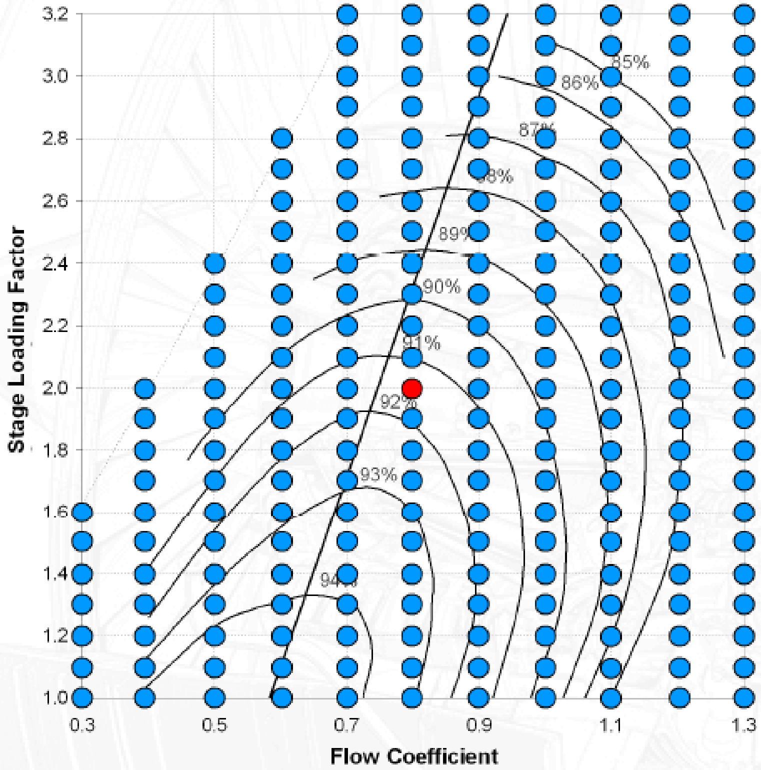

Preliminary CFD 3D

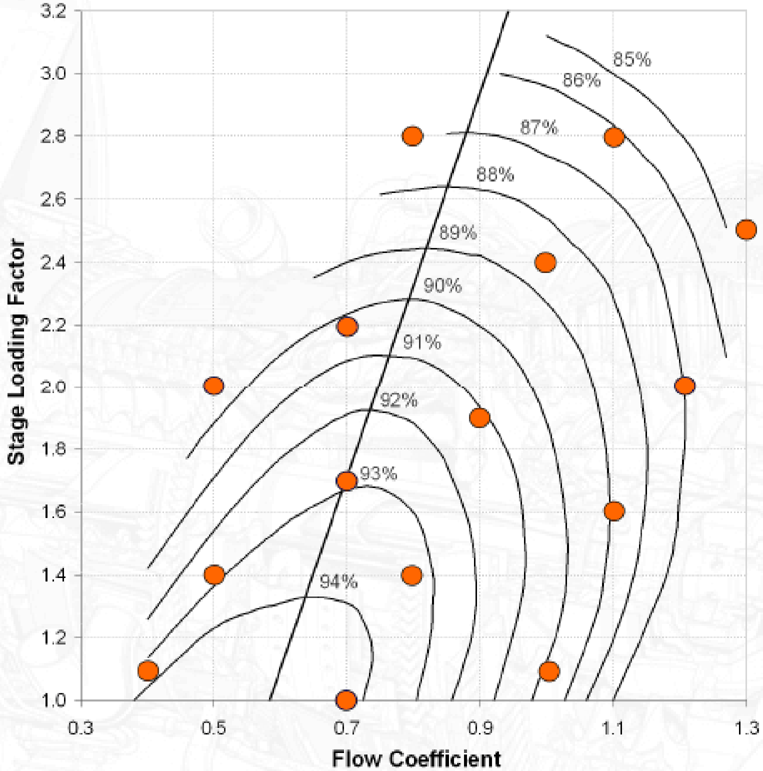

The inlet swirl angle, mass flow and RPM are changed in order to modify R, ϕ and ψ values respectively.

$$
\begin{cases}
\phi = \dfrac{c_{ax}}{U} = \dfrac{MF}{RPM} \cdot \dfrac{1}{\rho \cdot A \cdot r_m} \cdot \dfrac{60}{2\pi} \\[2ex]
\psi = \dfrac{\Delta H}{U^2} = \phi \cdot (tg\alpha_2 - tg\alpha_3) \\[2ex]
R = \dfrac{h_2 - h_3}{H_2 - H_3} = \dfrac{t_2 - t_3}{T_2 - T_3} = 1 - \dfrac{\phi}{2} \cdot (tg\alpha_2 + tg\alpha_3)
\end{cases}
$$

DEFLECTIONS ON SMITH DIAGRAM

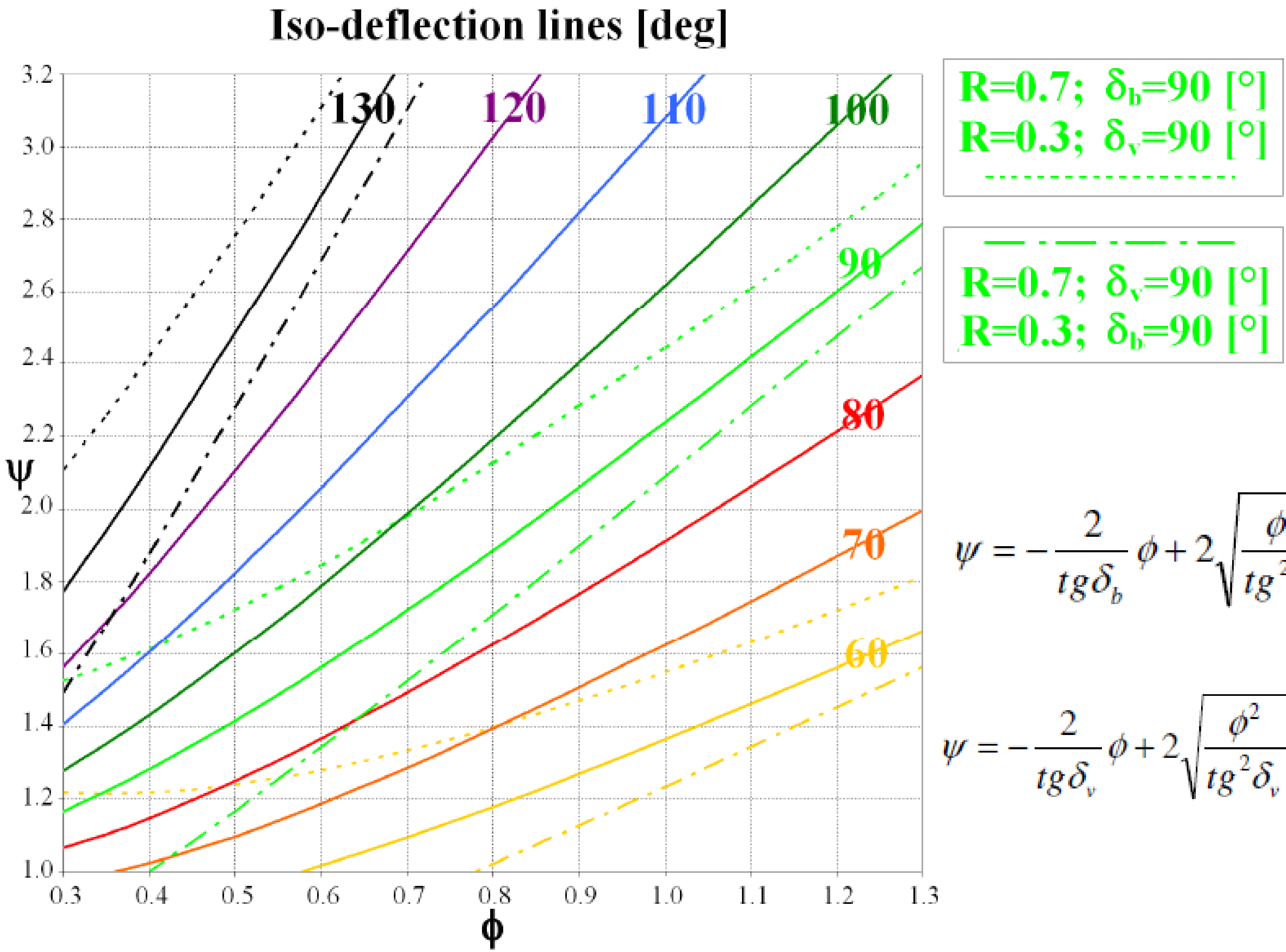

$$\psi = -\frac{2}{tg\delta_b}\phi + 2\sqrt{\frac{\phi^2}{tg^2\delta_b} + R^2 + \phi^2}$$

$$\psi = -\frac{2}{tg\delta_v}\phi + 2\sqrt{\frac{\phi^2}{tg^2\delta_v} + (1-R)^2 + \phi^2}$$

AERODYNAMIC RESULTS: EFFICIENCY

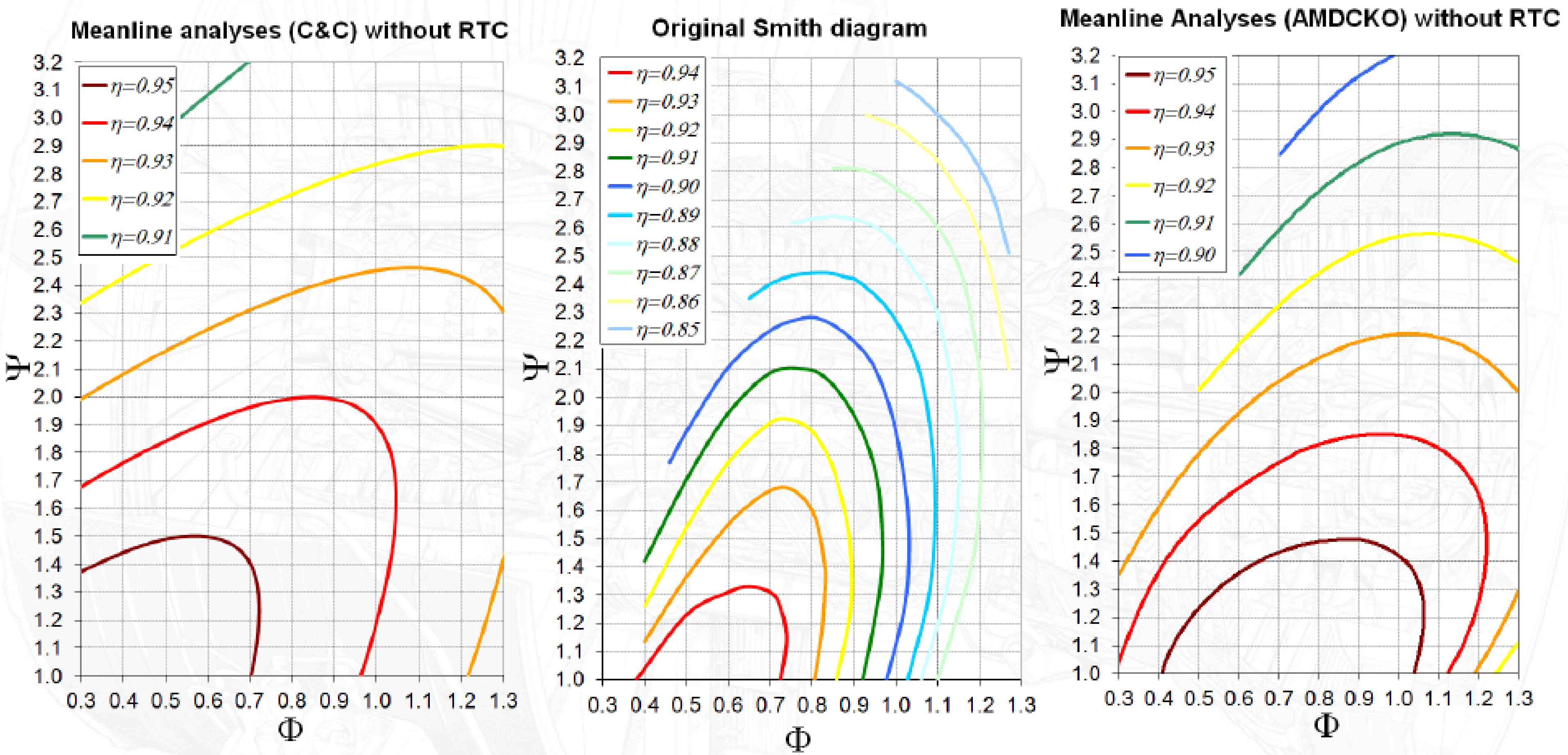

Degree of Reaction=0.4, no Rotor Tip Clearance

AERODYNAMIC RESULTS: RTC EFFECT

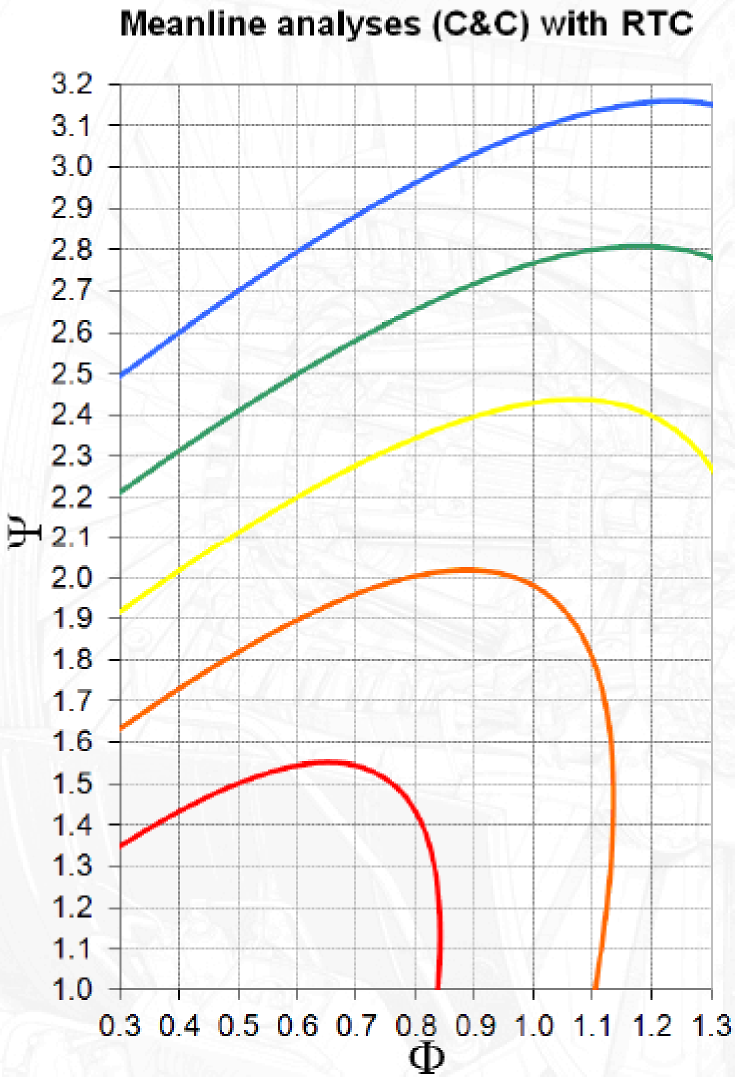

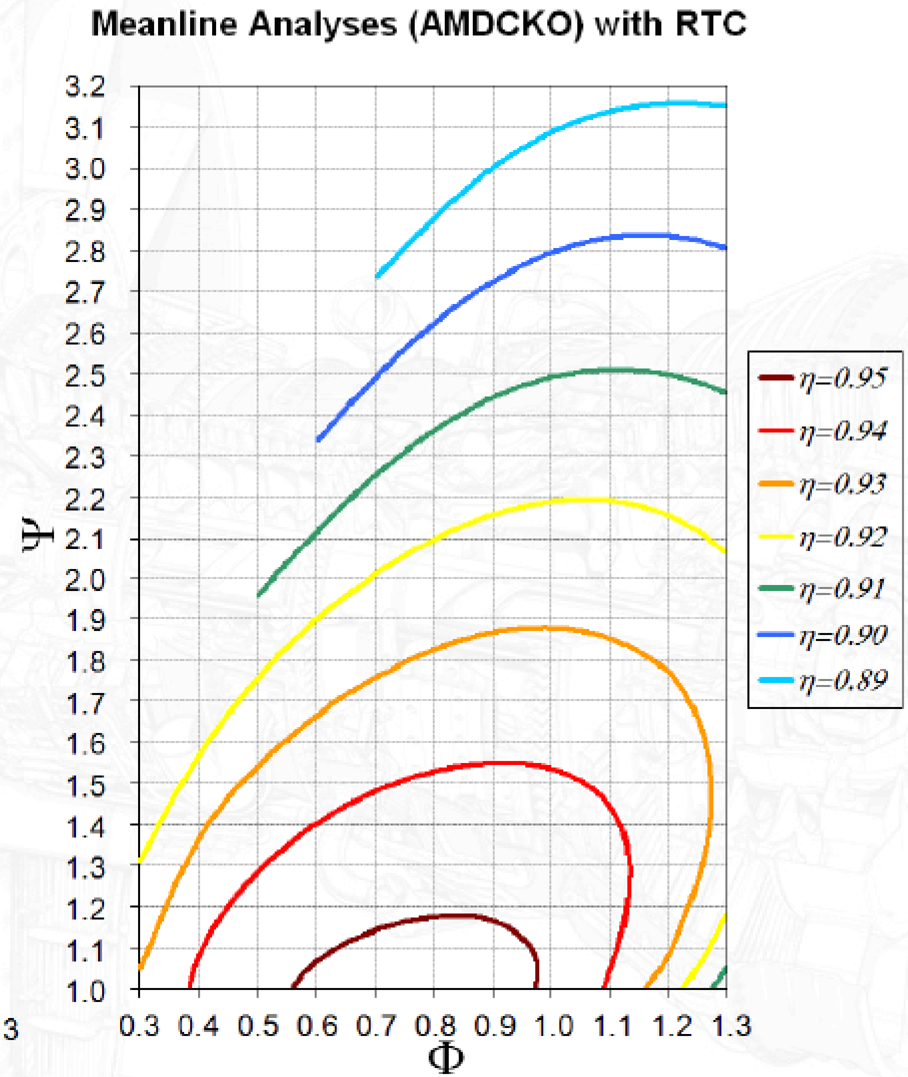

Degree of Reaction=0.4, Rotor Tip Clearance included

AERODYNAMIC RESULTS: R EFFECT FOR C&C

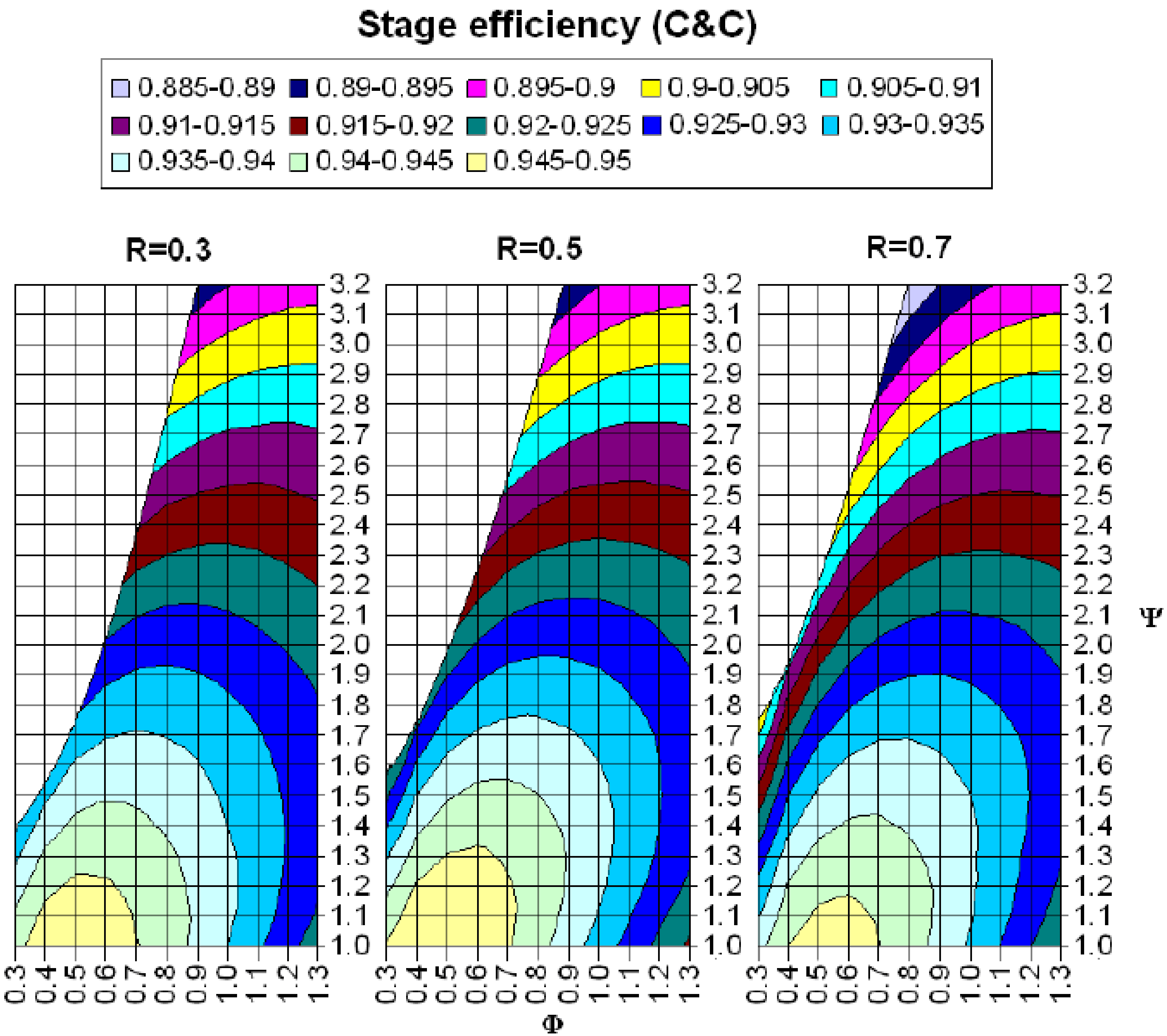

AERODYNAMIC RESULTS: R EFFECT FOR AMDCKO

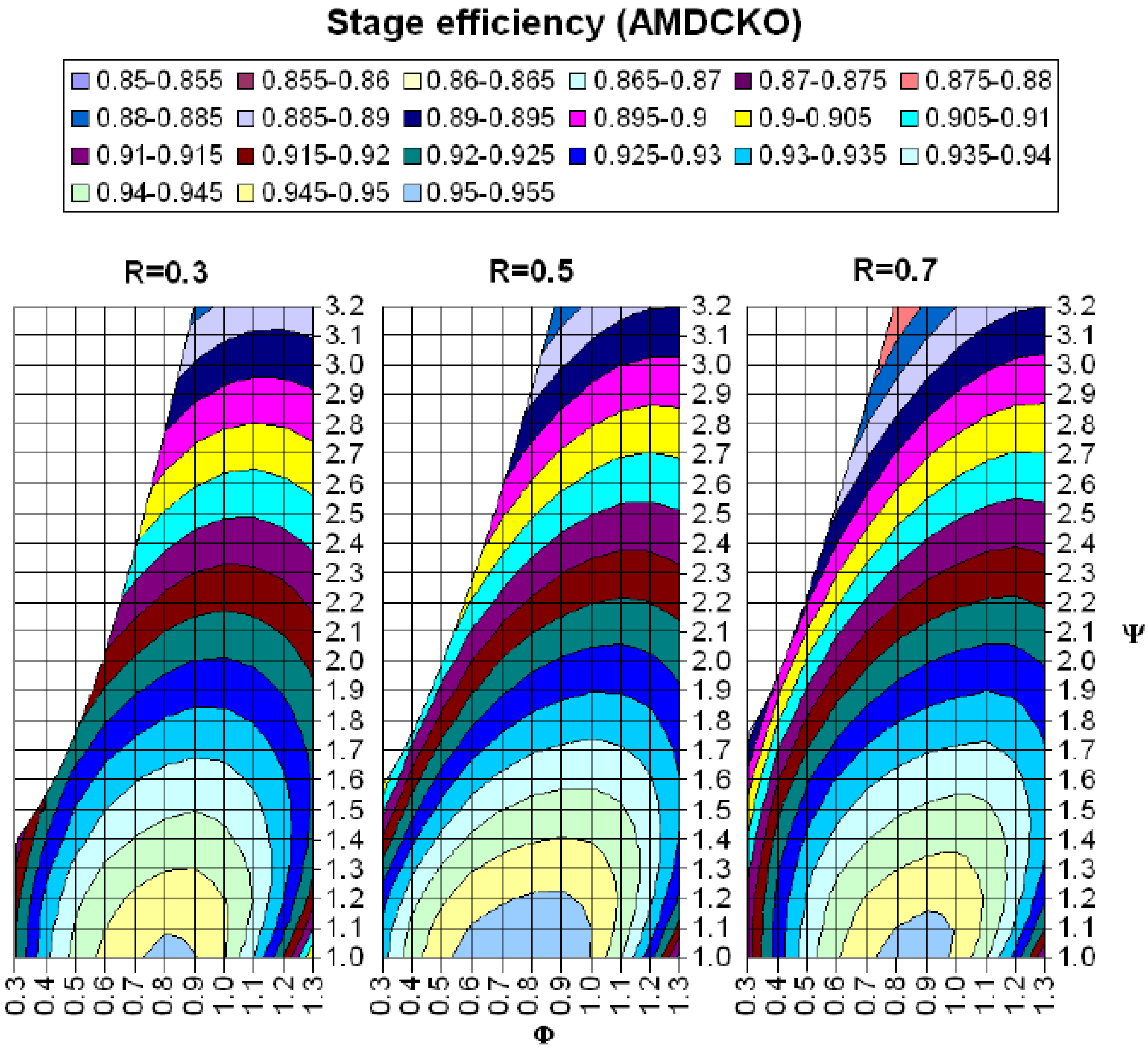

AERODYNAMIC RESULTS: OPTIMUM LINES

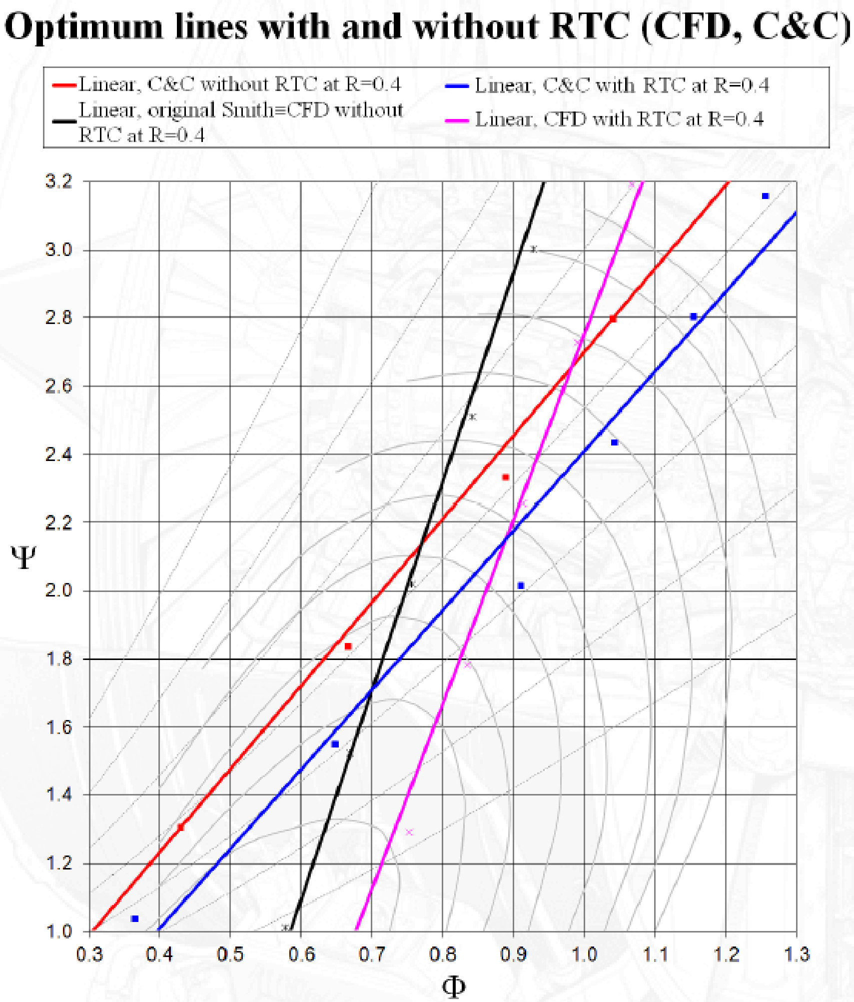

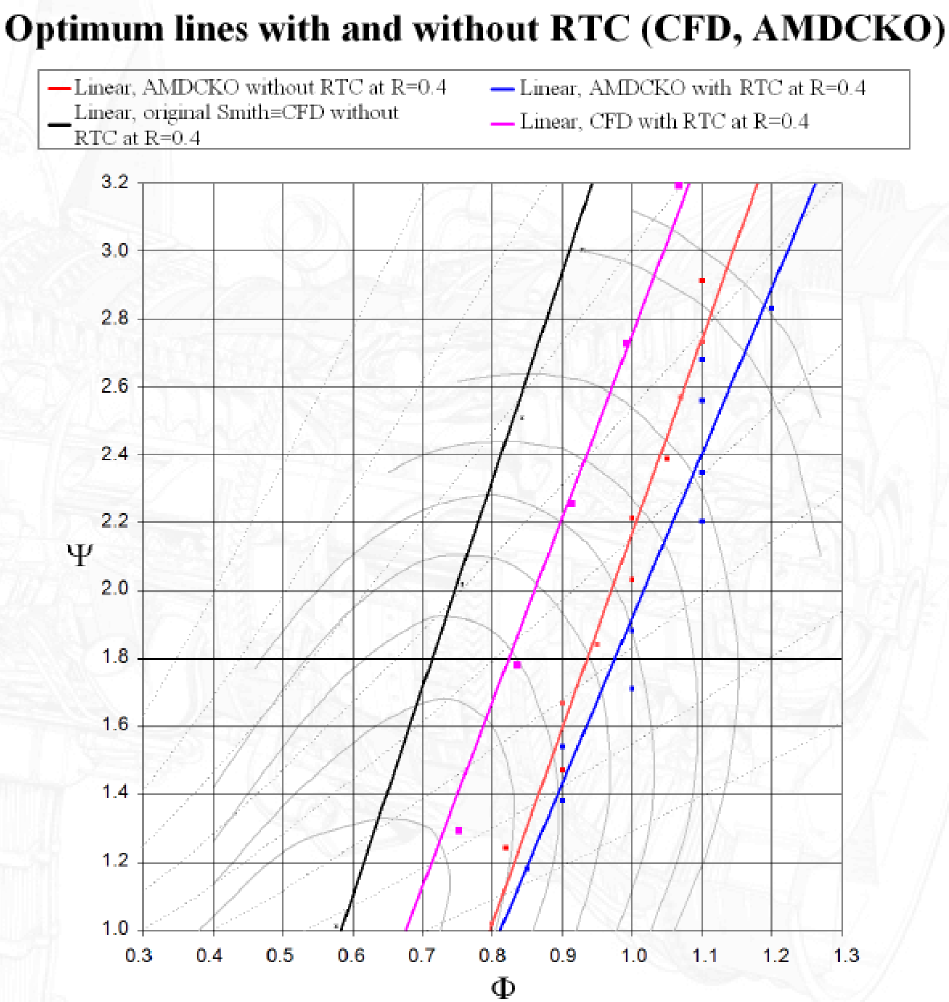

AERODYNAMIC RESULTS: AIRFOIL SHAPE

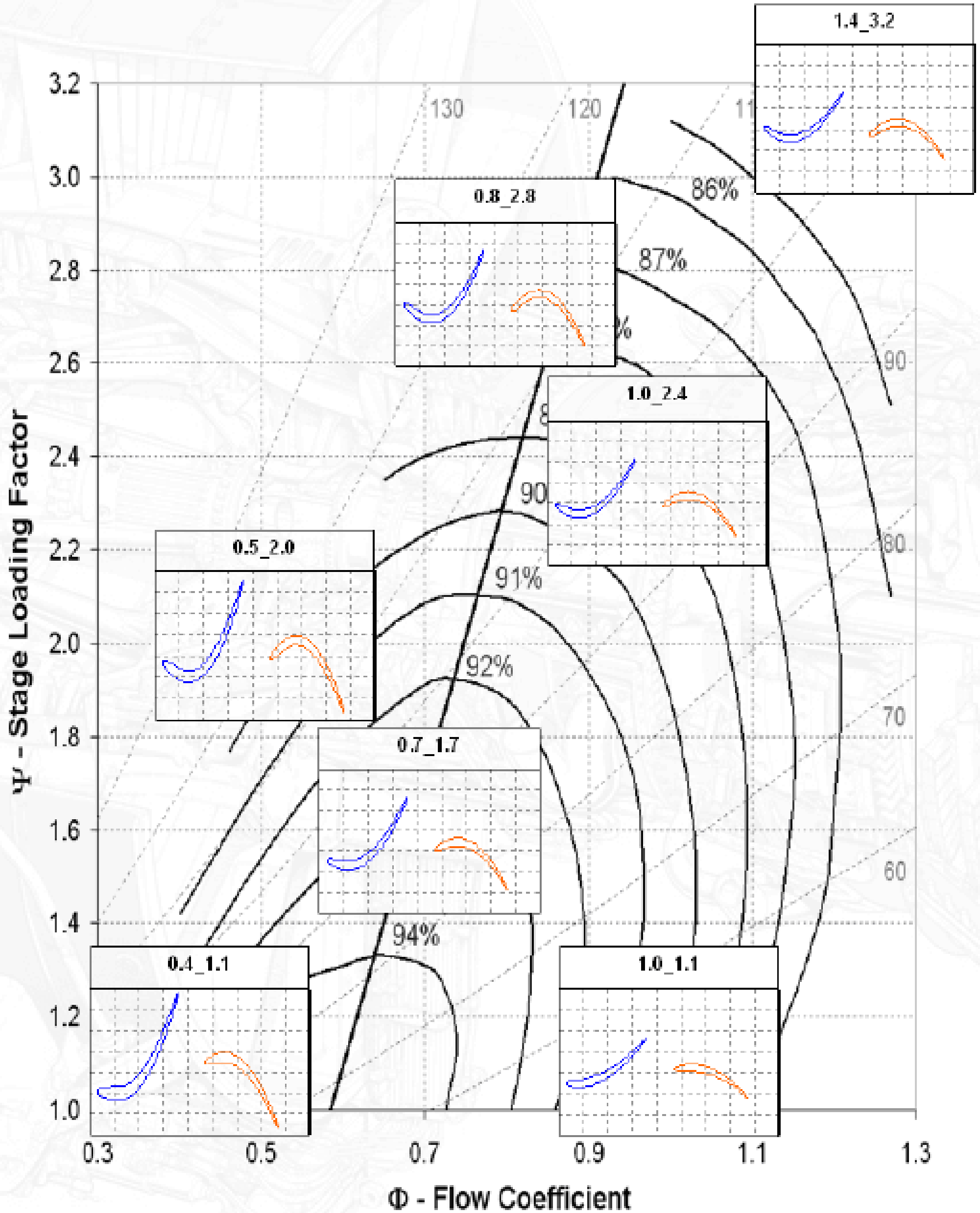

AERODYNAMIC RESULTS : Y=f(δ)

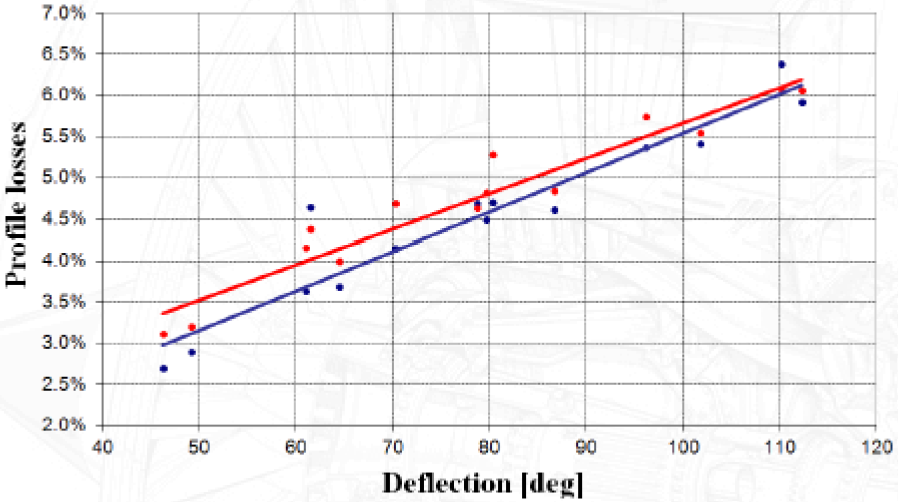

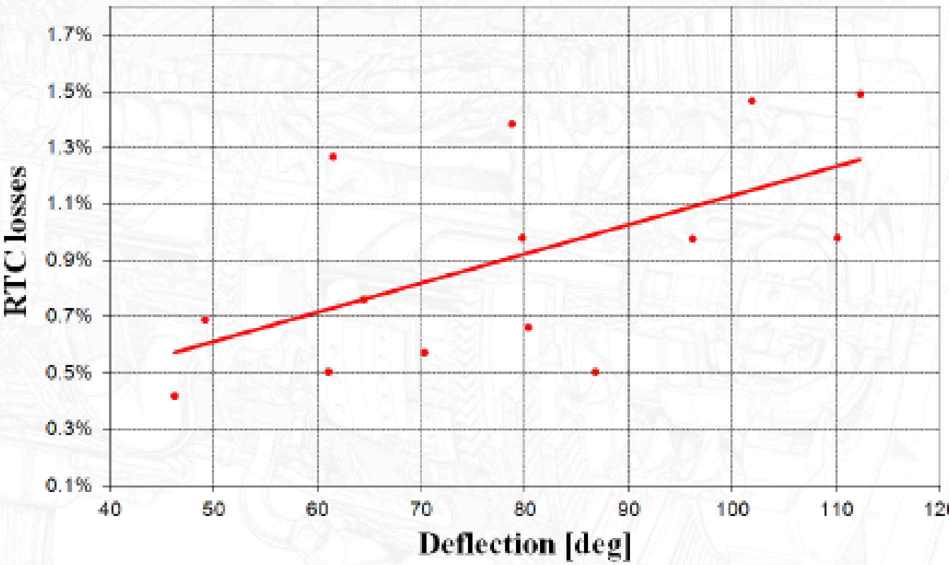

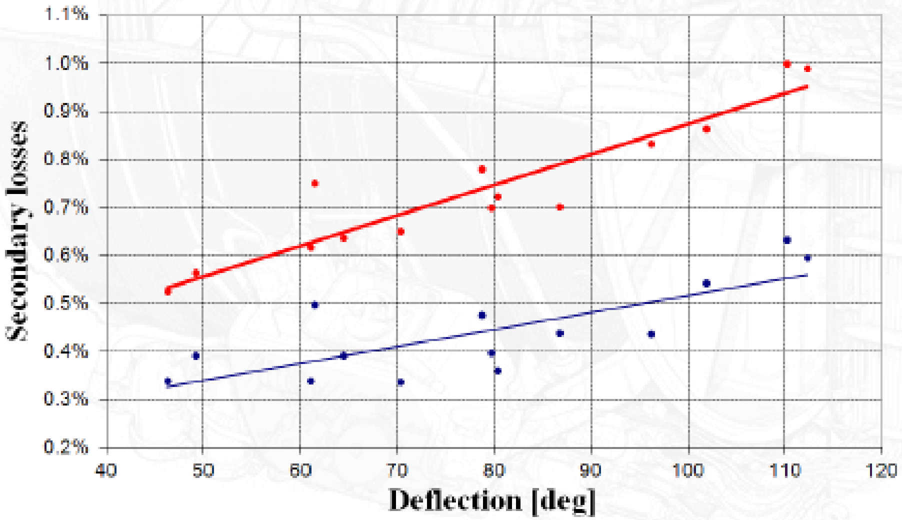

WEAKNESSES OF CORRELATION MODELS

AMDCKO

Y_P on rotor/stator are not symmetric around R=0.5, values are underestimated. The cause is probably the compressible term introduced by Kacker & Okapuu, unbalanced even for R=0.5.
This model overestimates secondary loss values for high δ.

C&C

Profile losses little lower than 3D CFD.
Only this model predicts Y_S that decrease with deflections, this is probably is due to the presence s/b in the evaluation of $(x_s)_b$. The backbone length b seems to underestimates δ effects on the flow when applied to Y_S assessment.

STRUCTURAL RESULTS: N_b ON STATORS

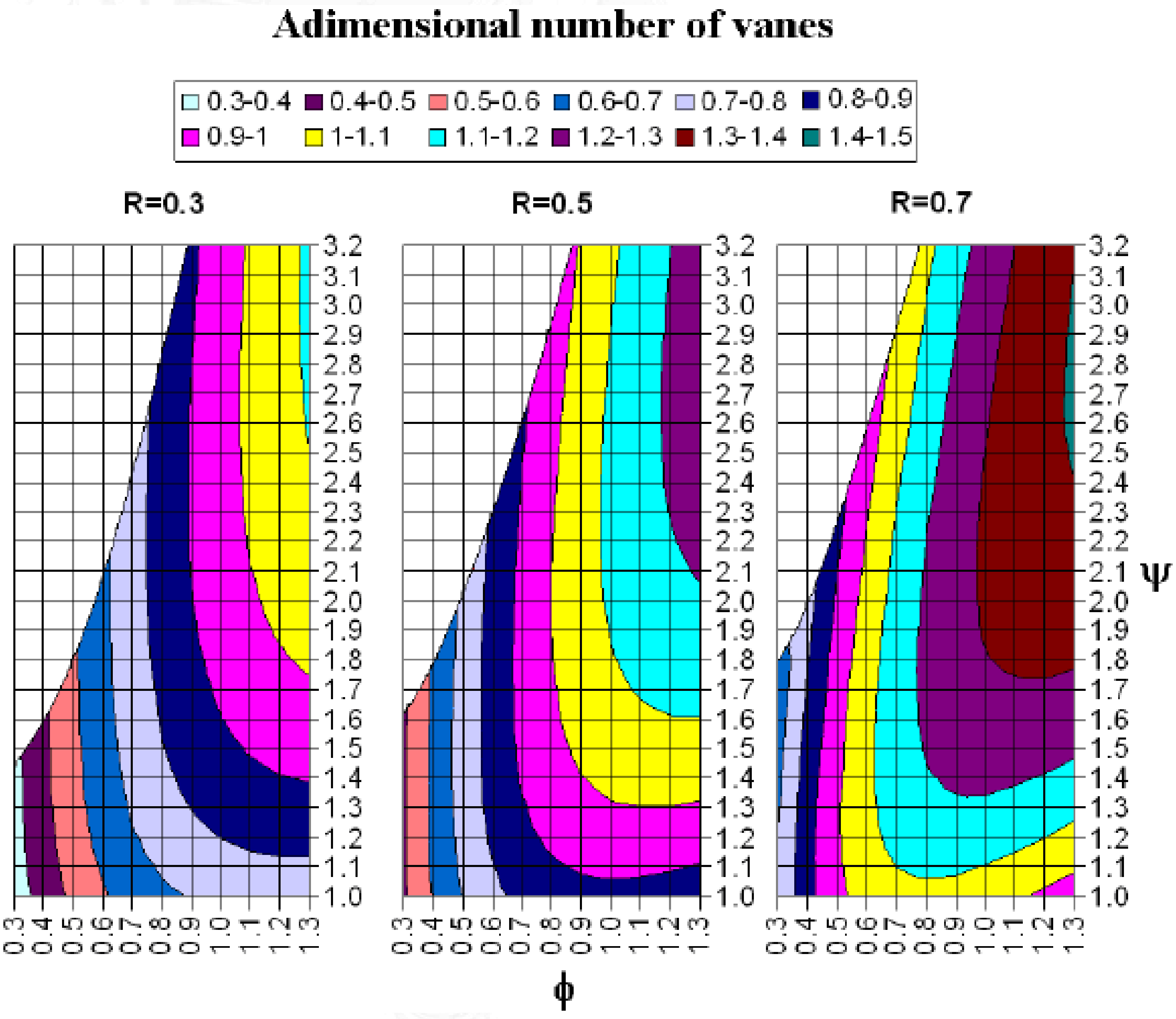

STRUCTURAL RESULTS: STRESS FOR VANES

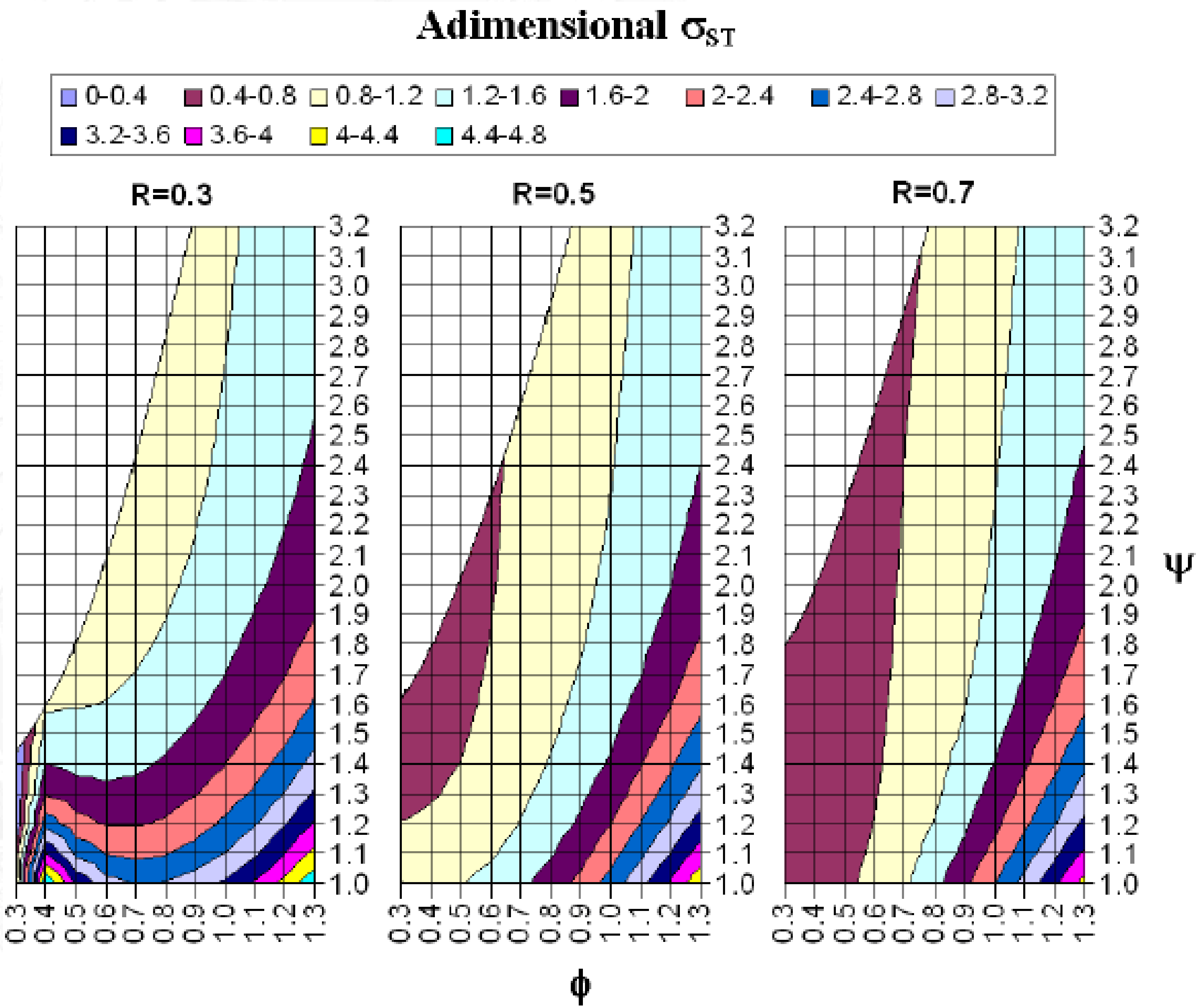

STRUCTURAL RESULTS: STRESS FOR BLADES

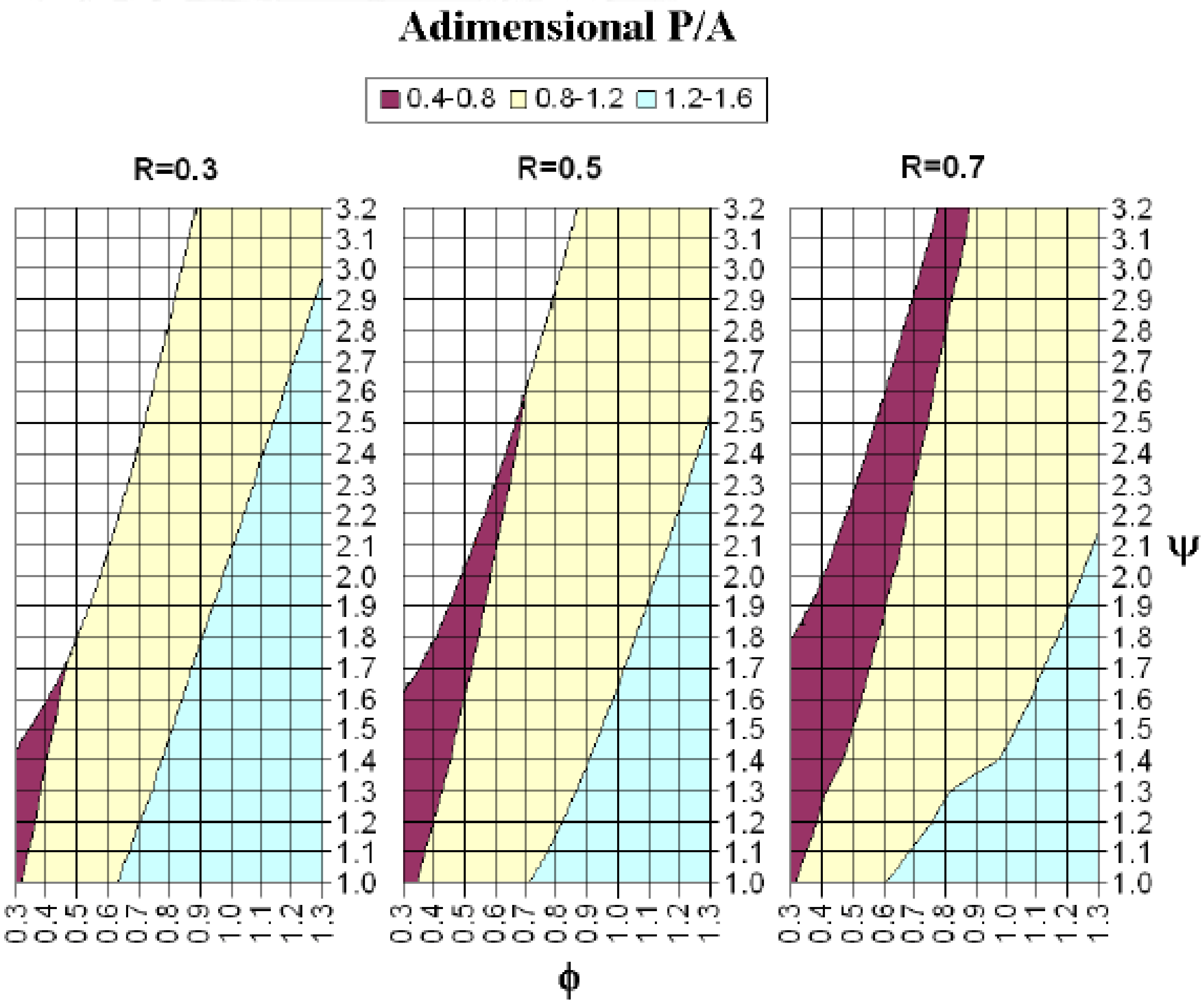

CONLUDING REMARKS

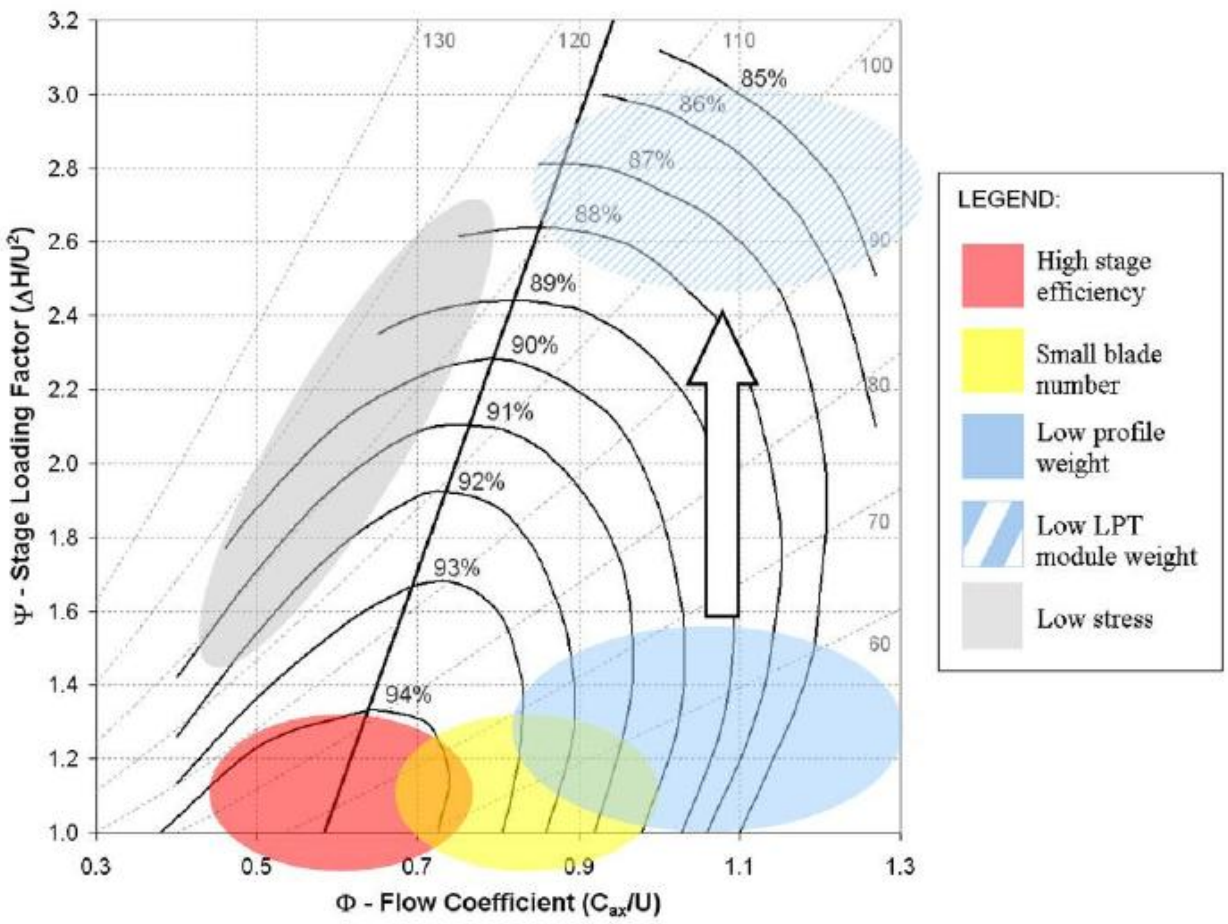

Intermediate R (0.5) are recommended for aerodynamic performances, bigger R for structural ones.

FUTURE ACTIVITY

- Much greater number of 3D CFD simulations;

- Different degrees of reaction, Reynolds numbers, Zweifel numbers and aspect ratios have to be investigated;

- Detailed revision of classical correlation models based on high-fidelity numerical results will become possible;

- The new reliable Smith diagram for modern LPTs will be provided.

THANK YOU FOR THE ATTENTION

Numerical Simulation of Subsonic and Transonic Flow over an Oscillating Wing

PETR FURMÁNEK[1] JIŘÍ FÜRST[2] KAREL KOZEL[2] ALEŠ PRACHAŘ[1]

1) AERONAUTICAL RESEARCH AND TEST ESTABILISHMENT, PRAGUE LETŇANY
2) DEPARTMENT OF TECHNICAL MATHEMATICS, FACULTY OF MECHANICAL ENGINEERING, CTU IN PRAGUE

EASN WORKSHOP ON FLIGHT PHYSICS & PROPULSION

PRAGUE, 31-10-2012

Motivation - research of unsteady effects:

- appear in many physical processes involving fluid dynamics (aerodynamics, turbo-machinery, ABL, bio-mechanical flow, automotive industry...),
- have a great impact on the flow field (e.g. flutter...),
- became a standard part of CFD simulations.

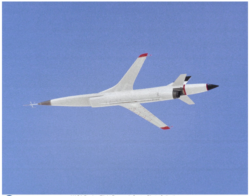

NASA Dryden Flight Research Center Photo Collection
http://www.dfrc.nasa.gov/gallery/photo/index.html
NASA Photo: EC80-14090 Date: 1980 Photo by: NASA photo

DAST in Flight

Dryden Flight Research Center ECN 31306 Photographed 1984
Video frame 07.15.43.9 of DAST just after structural failure of right wing. NASA photo

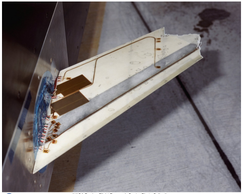

NASA Dryden Flight Research Center Photo Collection
http://www.dfrc.nasa.gov/gallery/photo/index.html
NASA Photo: EC01-0124-1 Date: April 24, 2001 Photo by: Tony Landis
The Aerostructures Test Wing (ATW), which consisted of an 18-inch carbon fiber test wing with surface-mounted piezoelectric strain actuators, following intentional failure on its final flight

Our Aim:

Investigate possibilities of 3D unsteady flow modeling by CFD using two different numerical methods.

Motivation - research of unsteady effects:

- appear in many physical processes involving fluid dynamics (aerodynamics, turbo-machinery, ABL, bio-mechanical flow, automotive industry...),
- have a great impact on the flow field (e.g. flutter...),
- became a standard part of CFD simulations.

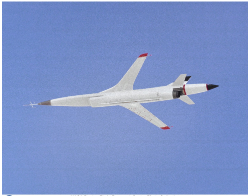

NASA Dryden Flight Research Center Photo Collection
http://www.dfrc.nasa.gov/gallery/photo/index.html
NASA Photo: EC80-14090 Date: 1980 Photo by: NASA photo

DAST in Flight

Dryden Flight Research Center ECN 31306 Photographed 1984
Video frame 07.15.43.9 of DAST just after structural failure of right wing. NASA photo

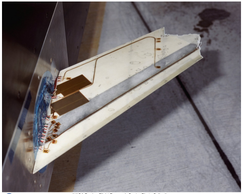

NASA Dryden Flight Research Center Photo Collection
http://www.dfrc.nasa.gov/gallery/photo/index.html
NASA Photo: EC01-0124-1 Date: April 24, 2001 Photo by: Tony Landis
The Aerostructures Test Wing (ATW), which consisted of an 18-inch carbon fiber test wing with surface-mounted piezoelectric strain actuators, following intentional failure on its final flight

Our Aim:

Investigate possibilities of 3D unsteady flow modeling by CFD using two different numerical methods.

Researched Cases

Transonic Flow over The ONERA M6 Wing

Flow Configuration:

- Based on steady flow investigated in AGARD Report AR 138
- Forced oscillatory motion around reference axis going through point $x_{ref} = [0.35c, 0, 0]$ (c - chord length) given by prescription of angle of attack $\alpha_1(t) = \alpha_{init} + A\sin(2\pi ft)$,
- inlet Mach number $M_\infty = 0.8395$, $\alpha_{init} = 3.06^\circ$, $f = 10\mathrm{Hz}$, $A = 1.5^\circ$.
- No experimental data available.

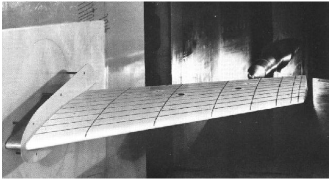

Fig.: ONERA M6 wing.

Subsonic Flow over The AS 28 Wing

Flow Configuration:

- Forced oscillatory motion around reference axis going through point $x_{ref} = [0.25c, 0, 0]$ given by prescription for angle of attack $\alpha_1(t) = \alpha_{init} + A\sin(2\pi ft)$,
- inlet Mach number $M_\infty = 0.51,\ \alpha_{init} = -0.5^\circ,\ f_1 = 15\mathrm{Hz},\ f_2 = 30\mathrm{Hz},\ f_3 = 45\mathrm{Hz},\ A = 3^\circ$.
- Compared with experimental data obtained at VZLÚ a.s.

Fig.: Advanced Light combat Aircraft ALCA L-159.

Numerical Methods

Mathematical Model

- inviscid compressible flow: Euler equations
- turbulent compressible flow: Reynolds-averaged Navier–Stokes equations
- governing systems of equations solved by the **finite volume method**
- unsteady effects: simulated with the use of the Arbitrary Lagrangian–Eulerian method

Modified Causon's Scheme (MCS)

- in-house developed scheme
- derived from simplified TVD form of the classical predictor-corrector MacCormack scheme (Causon)
- not TVD, the results are however qualitatively on the same level; moreover the MCS saves at least 30% of the computational time
- explicit form, cell-centred, parallelised with the OpenMP
- only structured meshes
- used for inviscid simulations

Numerical Methods

Mathematical Model

- inviscid compressible flow: Euler equations
- turbulent compressible flow: Reynolds-averaged Navier–Stokes equations
- governing systems of equations solved by the **finite volume method**
- unsteady effects: simulated with the use of the Arbitrary Lagrangian–Eulerian method

Modified Causon's Scheme (MCS)

- in-house developed scheme
- derived from simplified TVD form of the classical predictor-corrector MacCormack scheme (Causon)
- not TVD, the results are however qualitatively on the same level; moreover the MCS saves at least 30% of the computational time
- explicit form, cell-centred, parallelised with the OpenMP
- only structured meshes
- used for inviscid simulations

Numerical Methods

Edge CFD solver (FOI)

- driven in time by various types of the multistage Runge–Kutta scheme (default: 3-stage RK)
- implicit form, cell-vertex, parallelised with the MPI, unstructured meshes
- spatial discretization: central differences with 4^{th} Jameson's artificial dissipation or upwinding (FDS + limiters)
- convergence improved by geometric multigrid techique and implicit residual smoothing
- dual-time iterations employed in the case of unsteady flow
- used for turbulent simulations

Wallin & Johansson EARSM + Hellsten $k - \omega$ turbulence model

- advanced turbulence model (usually delivers much better results than the eddy-viscosity models)
- solves transport equations directly for Reynolds stresses.

Numerical Methods - Mesh Modification for the ALE method

Prescribed Oscillations around Given Reference Point (MCS, simplified 2D case)

Actual position of the mesh vertices:

$$\vec{x}(t) = \mathbb{Q}\left[\phi(t, ||\vec{x}(0) - \vec{x}_{ref}||)\right](\vec{x}(0) - \vec{x}_{ref}) + \vec{x}_{ref}$$

$$\mathbb{Q}(\phi) = \begin{pmatrix} \cos\phi & -\sin\phi \\ \sin\phi & \cos\phi \end{pmatrix}$$

$$\phi(t, r) = \begin{cases} -\alpha_1(t) & \text{for } r < r_1, \\ -\alpha_1(t) f_D(r) & \text{for } r_1 \le r < r_2, \\ 0 & \text{for } r_2 < r. \end{cases}$$

$$f_D(r) = \left[2\left(\frac{r - r_1}{r_2 - r_1}\right)^3 - 3\left(\frac{r - r_1}{r_2 - r_1}\right)^2 + 1\right]$$

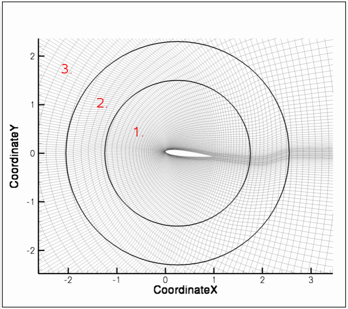

Field of Perturbations (EDGE)

Prescribed motion: field of perturbations of the computational domain is generated in preprocessing procedure. These perturbations are then applied during the computation (no motion of mesh is computed).

Numerical Results - Transonic Flow over the ONERA M6 Wing

Used for testing the in-house code capability of 3D unsteady flow solution.

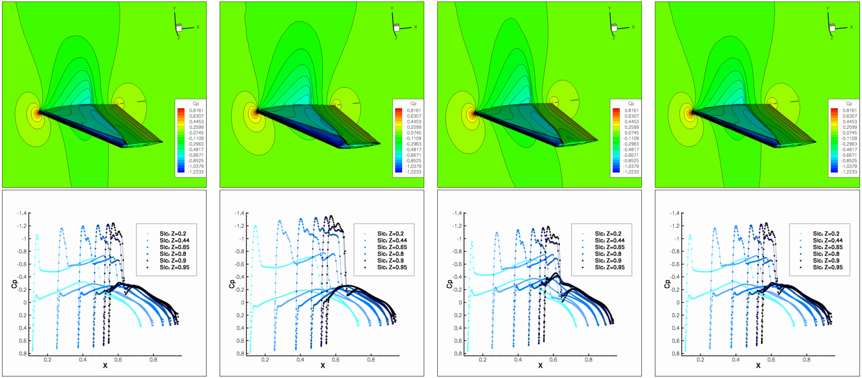

$\omega t = 0\pi$ $\omega t = \frac{1}{2}\pi$ $\omega t = \frac{3}{2}\pi$ $\omega t = 2\pi$

Fig.: c_p isolines (upper figure) and c_p in cuts along the wing (lower figure) during 3^{rd} period of the oscillatory motion.

Numerical Results - Transonic Flow over the ONERA M6 Wing

Numerical Results - Subsonic Flow over the AS28 Wing
MCS Scheme - 15Hz

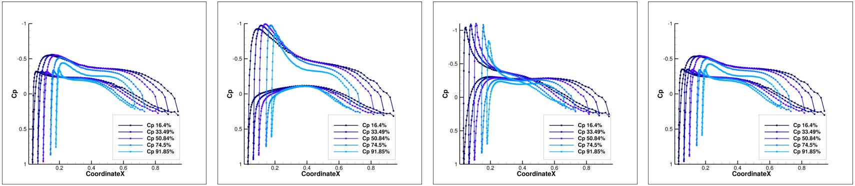

$\omega t = 0\pi$ $\omega t = \frac{1}{2}\pi$ $\omega t = \frac{3}{2}\pi$ $\omega t = 2\pi$

Fig.: c_p isolines (3^{rd} period of the oscillatory motion).

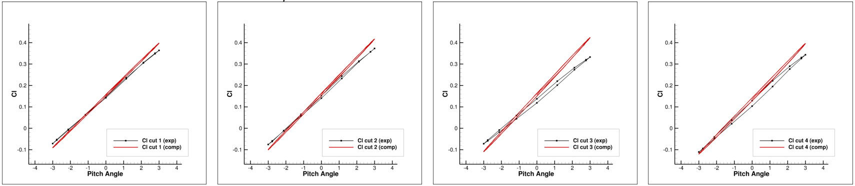

17.05% wingspan 35.38% wingspan 53.72% wingspan 72.05% wingspan

Fig.: c_l behaviour in cuts along the wing (3^{rd} period of the oscillatory motion).

Numerical Results - Subsonic Flow over the AS28 Wing
MCS Scheme - 30Hz

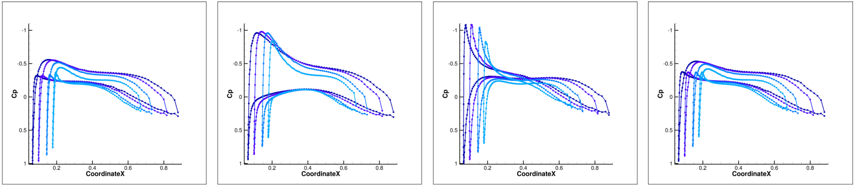

$\omega t = 0\pi$ $\omega t = \frac{1}{2}\pi$ $\omega t = \frac{3}{2}\pi$ $\omega t = 2\pi$

Fig.: c_p isolines (3^{rd} period of the oscillatory motion).

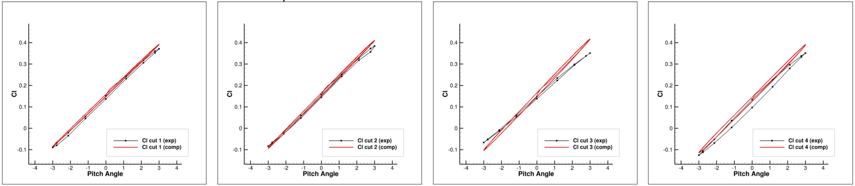

17.05% wingspan 35.38% wingspan 53.72% wingspan 72.05% wingspan

Fig.: c_l behaviour in cuts along the wing (3^{rd} period of the oscillatory motion).

Numerical Results - Subsonic Flow over the AS28 Wing
MCS Scheme - 45Hz

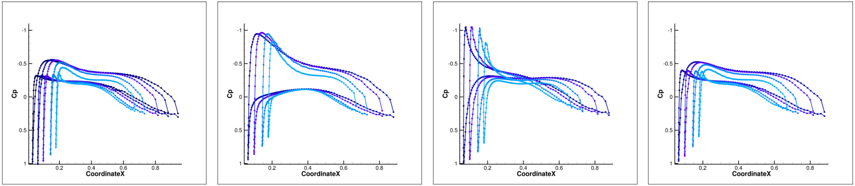

$\omega t = 0\pi$ $\quad$ $\omega t = \frac{1}{2}\pi$ $\quad$ $\omega t = \frac{3}{2}\pi$ $\quad$ $\omega t = 2\pi$

Fig.: c_p isolines (3^{rd} period of the oscillatory motion).

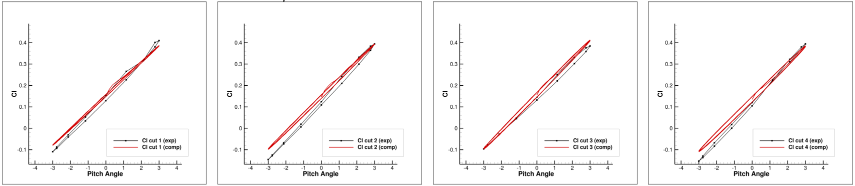

17.05% wingspan $\quad$ 35.38% wingspan $\quad$ 53.72% wingspan $\quad$ 72.05% wingspan

Fig.: c_l behaviour in cuts along the wing (3^{rd} period of the oscillatory motion).

Numerical Results - Subsonic Flow over the AS28 Wing

MCS Scheme $f_1 = 15$ Hz, $f_2 = 30$ Hz, $f_3 = 45$ Hz, c_p isolines.

Numerical Results - Subsonic Flow over the AS28 Wing

EDGE

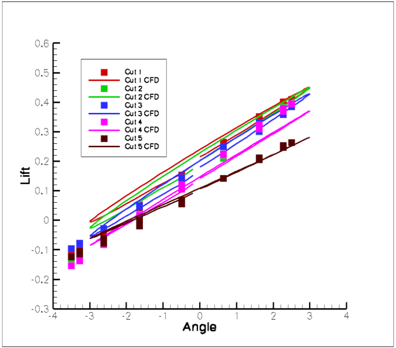

1) $f_3 = 45$ HZ, c_l in cuts (16.14%, 33.49%,50.84%, 74.5% and 91.85%)

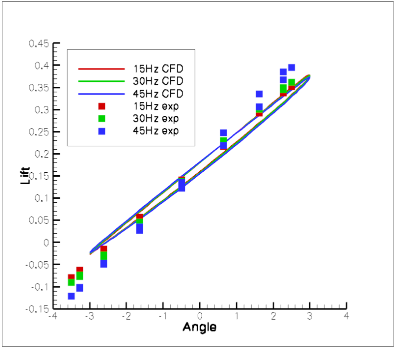

2) c_l for whole wing.

Conclusion

- Both methods can serve as a reliable numerical tool for tested regimes of flow.
- In situations, where approximate results are needed quickly (and no separation or significant turbulent effects are expected), the implemented inviscid code can be used while reasonable level of precision is maintained.

Future Steps Intended

- Implementation of an implicit version of the MCS scheme.
- Implementation of turbulence model into MC scheme (already done in 2D).
- Fluid-structure interaction (already implemented in 2D with 2 degrees of freedom).

THANK YOU FOR YOUR ATTENTION

EASN - European Aeronautics Science Network
31st of October – 2nd of November 2012, Prague, Czech Republic

A Novel Approach for Trajectory Tracking of UAVs

Luca De Filippis, Giorgio Guglieri, Fulvia Quagliotti
Flight Mechanics Research Team of Politecnico di Torino - Italy

System Architecture

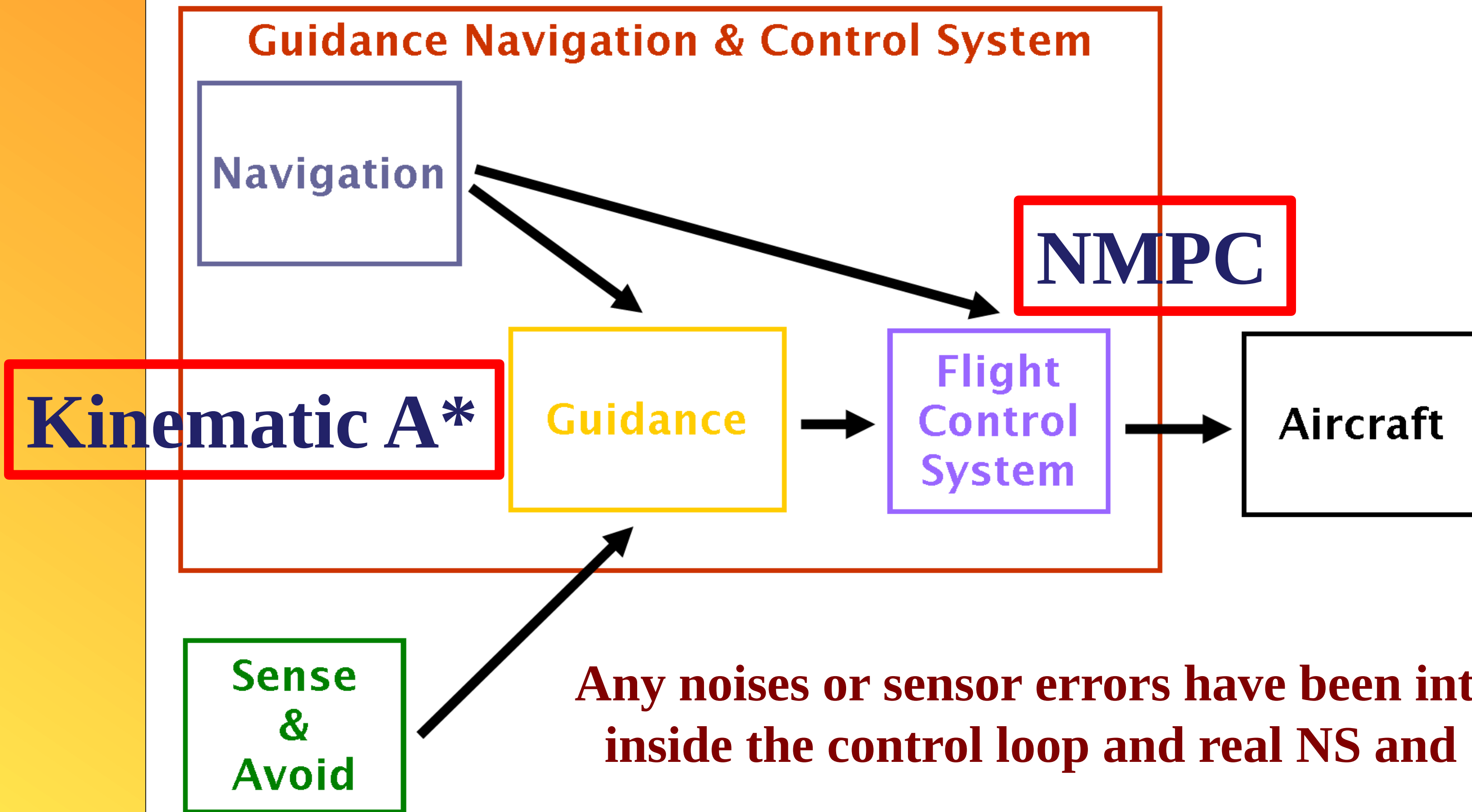

Any noises or sensor errors have been introduced inside the control loop and real NS and S&A-S have not been modeled.

Guidance System

- It exploits the Kinematic A* algorithm to generate the collision avoidance path.
- It receives the obstacle position from the S&A-S and the current aircraft position from the NS.
- It generates a waypoint sequence that avoids the obstacle going back to the reference path provided by the PP.

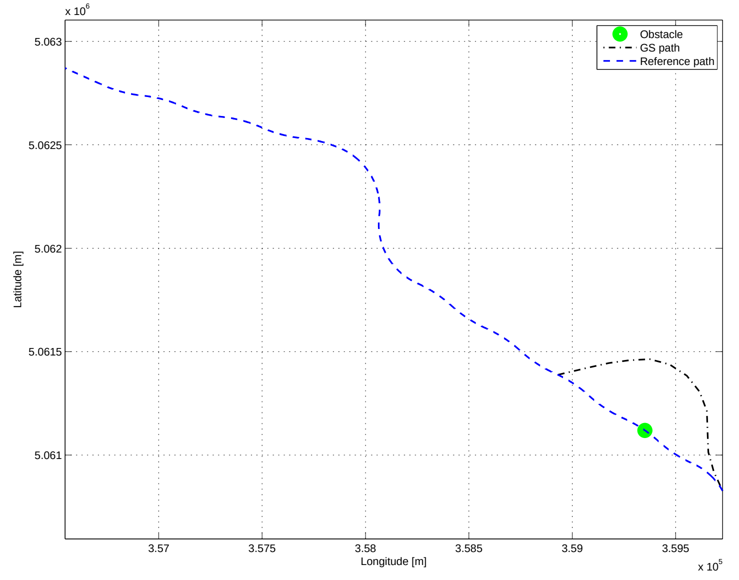

- Dash-dot line: GS.
- Point: static obstacle.
- Dashed line: reference path.

Kinematic A* (KA*)

Primary drawback of classic graph-search algorithms applied to path planning:

Disjunction between optimization logics and kinematic constraints of the aircraft.

Kinematic A* (KA*)

- Exploits the logics of graph search algorithms to find the optimal path.
- Includes a simple kinematic model of the aircraft to evaluate the moving cost between nodes of the graph.
- Lateral and vertical obstacle separations improve flight safety.
- KA* provides the reference to the Flight Control System.

Kinematic Model

$$\begin{cases} \dot{X} = V \cdot \sin(\chi) \cdot \cos(\gamma_{max} \cdot w) & \\ \dot{Y} = V \cdot \cos(\chi) \cdot \cos(\gamma_{max} \cdot w) & |u| \le 1 \\ \dot{Z} = -V \cdot \sin(\gamma_{max} \cdot w) & |w| \le 1 \\ \dot{\chi} = \dfrac{V}{R_{min}} \cdot u & \end{cases}$$

- Wind-frame coincident with Body-frame (small aerodynamic angles).
- Ground frame used to write the equations.

- X,Y, Z = position.
- χ = heading.
- V = aicraft speed.
- R_{min} = minimum turn radius.
- γ_{max}= maximum climb angle

Integrating differential equations over constant time horizon, neighboring nodes become neighboring states and space discretization becomes time discretization.

Path Generation

- The best path is obtained iteratively evaluating the cost function J.
- Each iteration minimizes functional F_{ij} of each state and the global functional J is obtained summing up minimum F_{ij} at each iteration.
- Choosing the smaller value of F_{ij} the algorithm selects a new state that reduces distance from the target and from the current state.

$$J = \sum_{j=S_0}^{j=S_T} \min_i F_{ij} = \sum_{j=S_0}^{j=S_T} \min_i [(\bar{H}_{ij}^T \cdot \boldsymbol{\alpha} \cdot \bar{H}_{ij}) + (\bar{G}_{ij}^T \cdot \boldsymbol{\beta} \cdot \bar{G}_{ij})]$$

S_0 and S_T: starting and target states.
H: cost to go.
G: cost to come.
α and β: diagonal gain matrices.

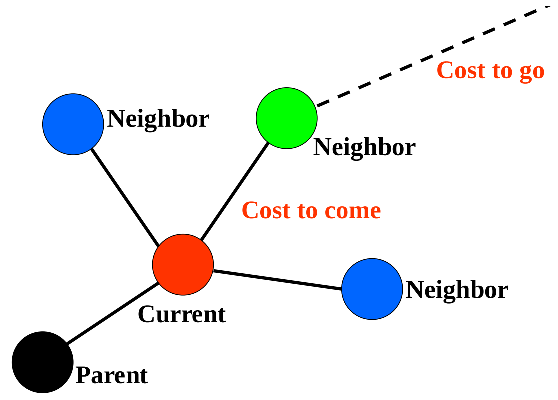

Flight Management System

The Flight Management System provides in real time optimal commands to the Aircraft coping with concurring tasks:

- track the reference trajectory provided with the path planner,
- avoid unpredicted obstacles along the path,

exploiting:

- KA*-state sequence,
- NMPC logics.

GS provides to FCS:
•the aircraft cruise speed *V*,
•the heading angle χ,
•the climb angle γ.

NMPC predicts future aircraft states over the prediction horizon (different from the KA* one) trying to reduce the error between predicted and desired states

Nonlinear Model Predictive Control

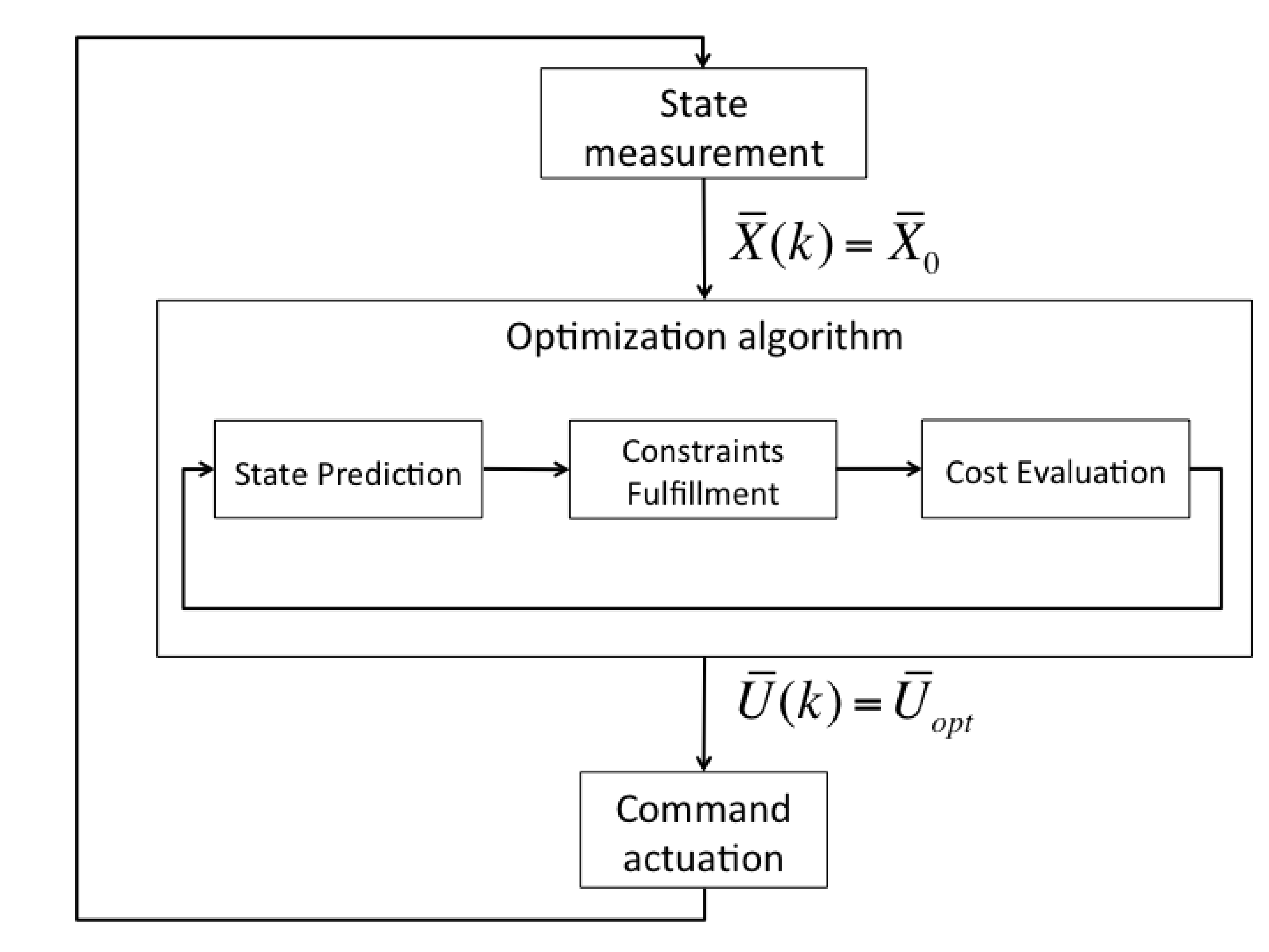

Problem Formulation

$$I = \int_0^{t_f} f(x, u, \pi, t)\, dt$$

Cost function

$$\dot{x} = \phi(x, u, \pi, t) \quad 0 \le t \le t_f$$

Differential constraints

$$S(u, w) \le 0 \quad 0 \le t \le t_f$$

Control inequality constraints

$$[\omega(x, \pi)]_0 = 0$$

Initial conditions

Cost Function

A classic quadratic cost function is implemented

- The first term evaluates the error between the reference and the predicted states.
- The second term evaluates the amount of command needed to minimize the error.

$$\min J(\bar{x}, \bar{u}, \bar{x}_0, \bar{x}_{ref}) = \int_t^{t+T_P} (\bar{x} - \bar{x}_{ref})^T Q (\bar{x} - \bar{x}_{ref}) + \bar{u}^T R \bar{u}$$

where Q and R are diagonal gain matrices and T_p is the prediction horizon.

The control system robustness as not been assessed yet

Genetic Optimizer

- The algorithm computes the optimal solution over a small population (48 individuals) with a reduced number of generations (≈30).
- The chromosomes of each individual are the aircraft commands:

$$chromosome = [\Delta\delta e, \Delta\delta a, \Delta\delta r, \Delta Th]$$

- The population is initialized through a random vector of four numbers:

$$chromosome = \Delta\bar{U}_{min} + (\Delta\bar{U}_{max} - \Delta\bar{U}_{min}) \cdot \bar{R}d$$

Genetic Optimizer

- **Tournament Selection**: half of the total population is randomly selected and two individuals are randomly chosen. The one with lower cost is selected for reproduction and two other solutions are taken. The selection is repeated up to obtain a number of individuals equal to half of the total population.

- **Simulated Binary Crossover (SBX):** it uses a probability distribution around two parents to create two children. The probability distribution is similar to the one of crossover operators used in binary-coded algorithms. The fundamental merit of SBX is its self-adaptive power that guarantees to the offspring to do not narrow near the previous optimal solution.

Genetic Optimizer

- **Polynomial Mutation:** a probability distribution similar to the SBX one is implemented. Then reasons to chose this mutation operator are the same as for the crossover one.

- **Evaluation:** the fitness function to evaluate the individuals is the cost function provided with the NMPC problem.

- **Update**: the update scheme is performed joining old and offspring populations and sorting them with respect to the fitness value. Then a set of individuals equal to the population size is chosen and used for the next algorithm cycle.

Genetic Optimizer

Convergence condition is satisfied when the algorithm converges to the same solution for a prescribed number of times:

$$f_{best} - \frac{\sum_{i=1}^{N-1} f_i}{N} \leq Toll$$

- f_i = the cost of the i_{th} individual
- f_{best} = the cost linked to the best individual
- N = the population size
- Toll is a fixed tolerance

If the algorithm converges to the same local minimum for a given number of times full algorithm convergence is assumed.

Tracking Task

Trim Conditions:

- Speed: (25, 0, 2.6) m/s
- Attitude: (0,0,0) rad
- Angular rate: (0,0,0) rad/s
- Propeller speed: 510 rad/s

Plant: Aerosonde Simulink Model

Initial Commands:

- Throttle: 0.7
- Elevator: 0 rad
- Aileron: 0 rad
- Rudder: 0 rad

Prediction Parameters:

- Integration frequency: 40 hz
- Command frequency: 1 hz
- Integration horizon: 0.3 s
- Command horizon: 0.3 s

Command bounds:

- Throttle: 0 – 1
- Elevator: -0.4 – 0.4 rad
- Aileron: -0.4 – 0.4 rad
- Rudder: -0.4 – 0.4 rad

Tracking Task

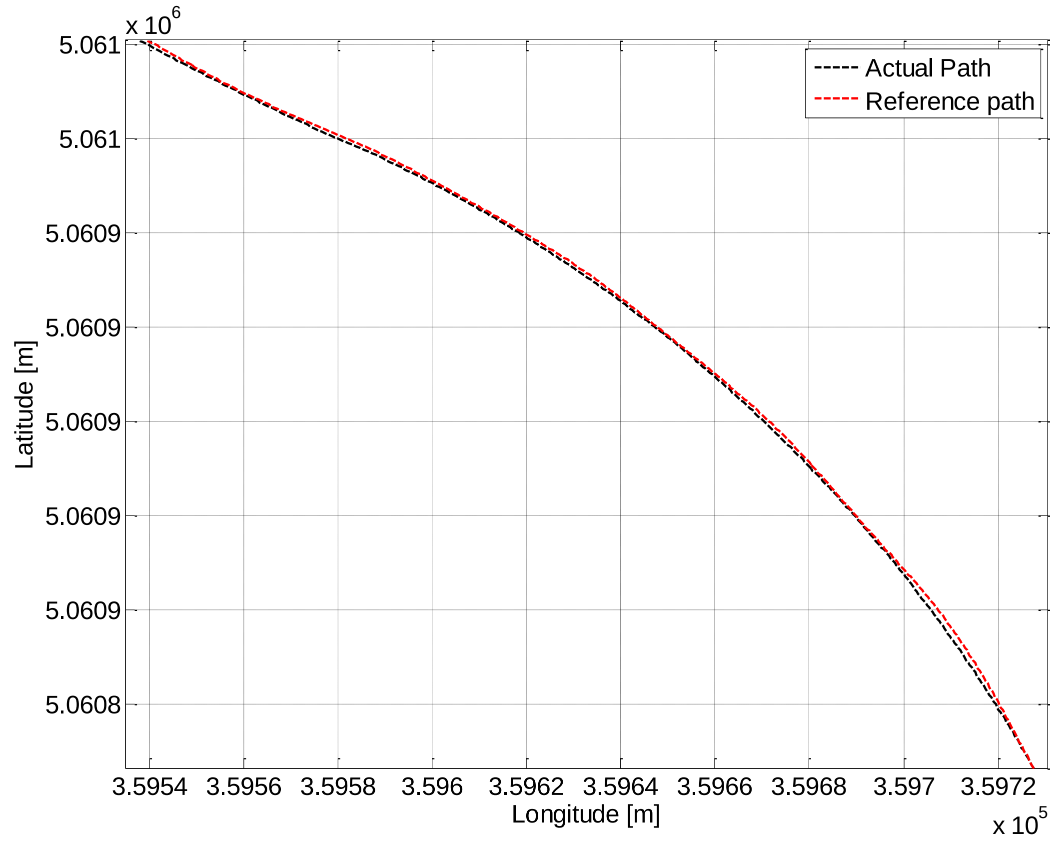

Reference and actual path on the longitude-latitude plane.

Tracking Task

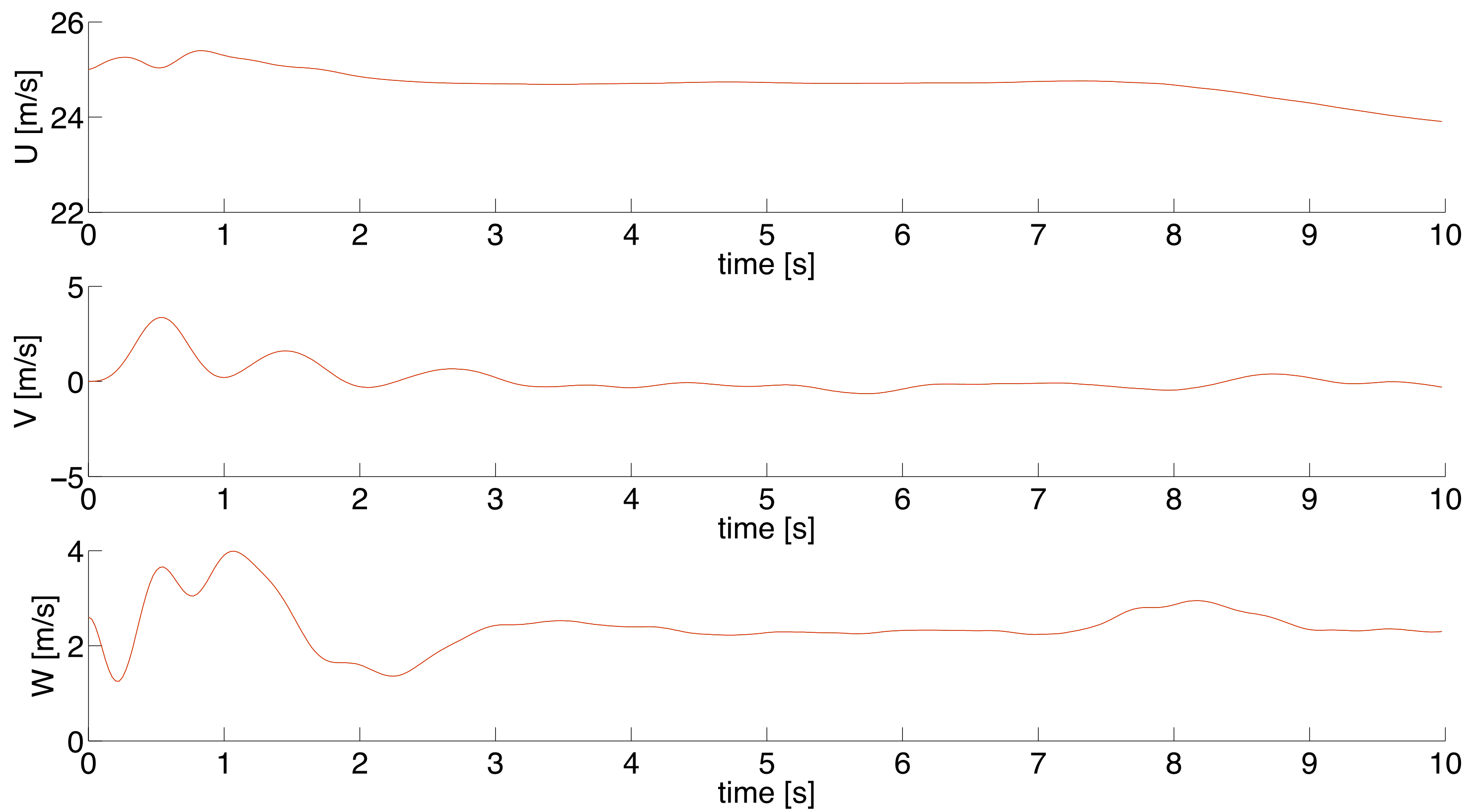

Predicted and actual speed components in body-frame.

Tracking Task

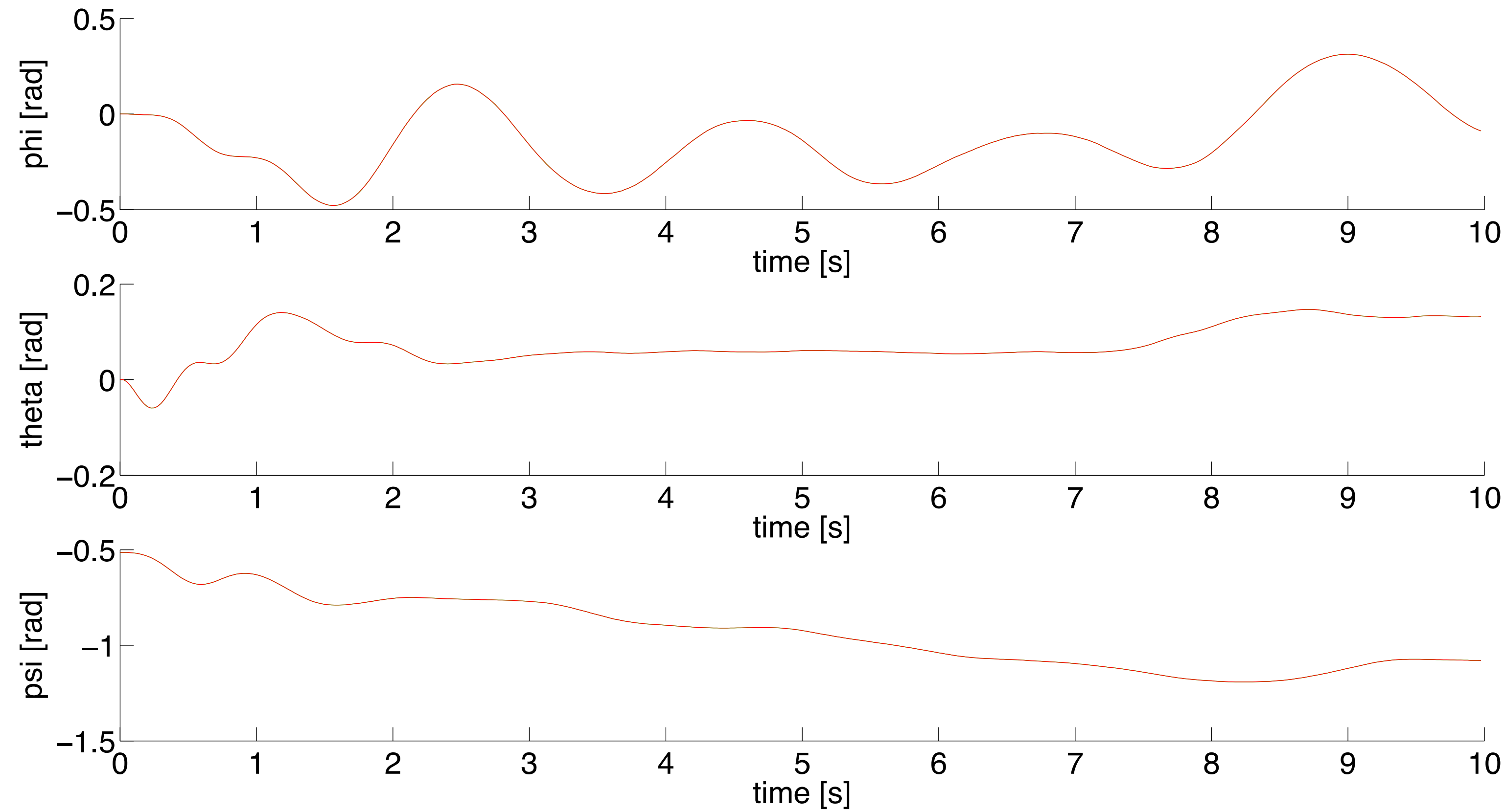

Predicted and actual attitude

Tracking Task

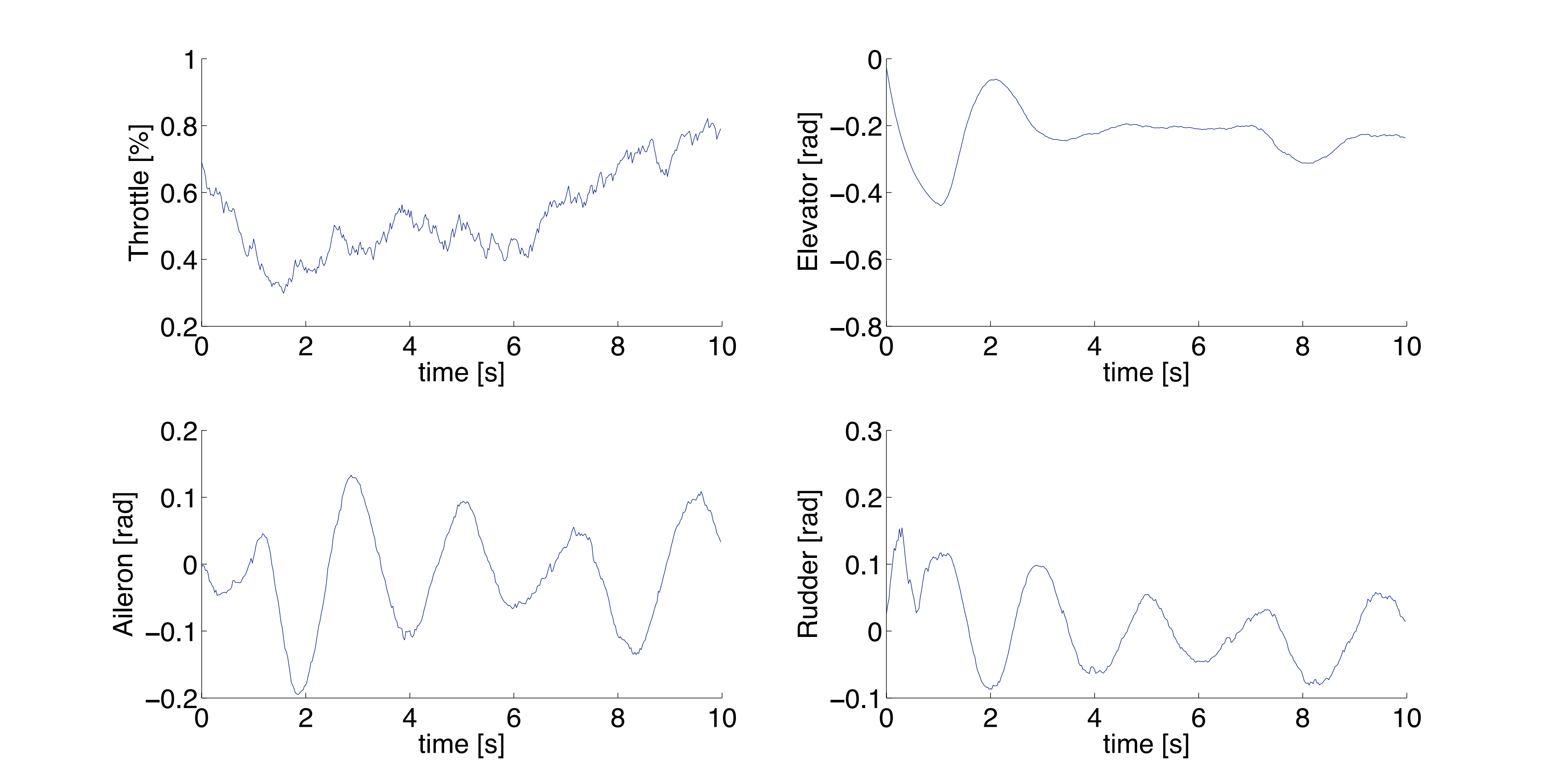

Command sequences

Collision Avoidance Task

Trim Conditions:

- Speed: (25, 0, 2.6) m/s
- Attitude: (0,0,-0.514) rad
- Angular rate: (0,0,0) rad/s
- Propeller speed: 510 rad/s

Plant: Aerosonde Simulink Model

Initial Commands:

- Throttle: 0.7
- Elevator: 0 rad
- Aileron: 0 rad
- Rudder: 0 rad

Prediction Parameters:

•Integration frequency: 40 hz

•Command frequency: 1 hz

•Integration horizon: 0.3 s

•Command horizon: 0.3 s

Command bounds:

•Throttle: 0 – 1

•Elevator: -0.5 – 0.5

•Aileron: -0.5 – 0.5

•Rudder: -0.5 – 0.5

Collision Avoidance Task

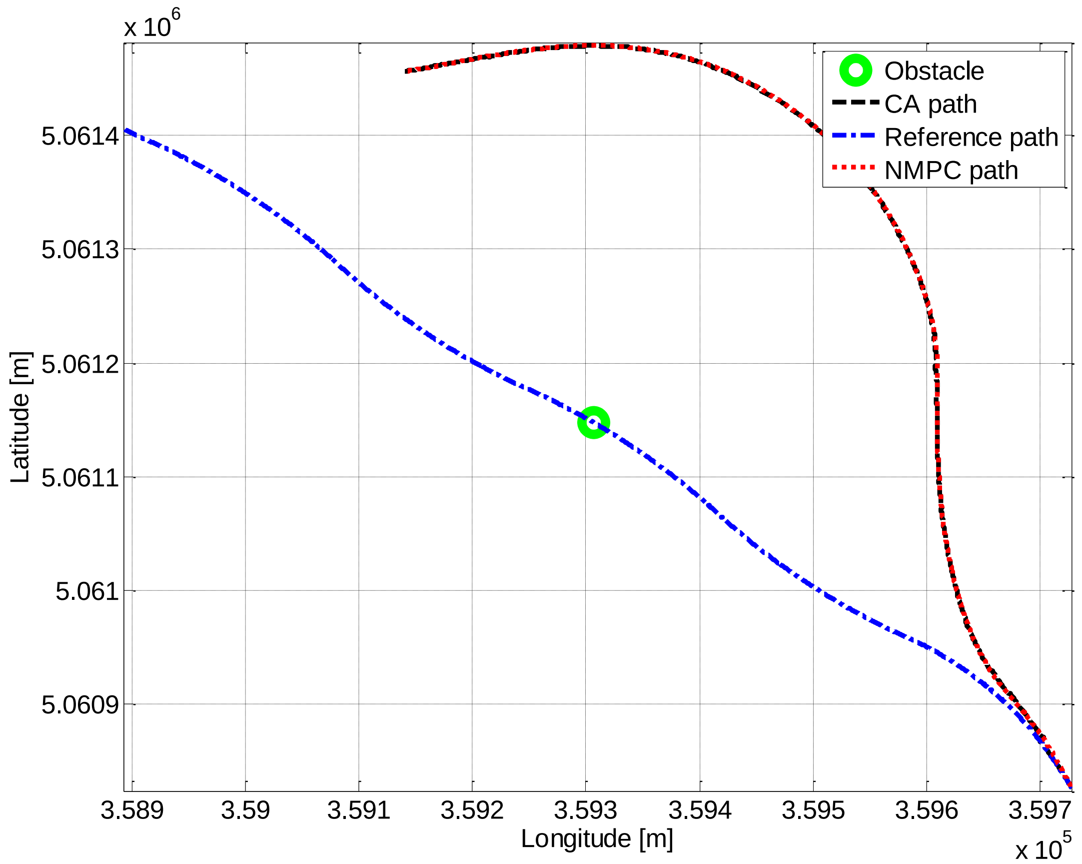

Reference and actual path with static obstacle (green circle)

Collision Avoidance Task

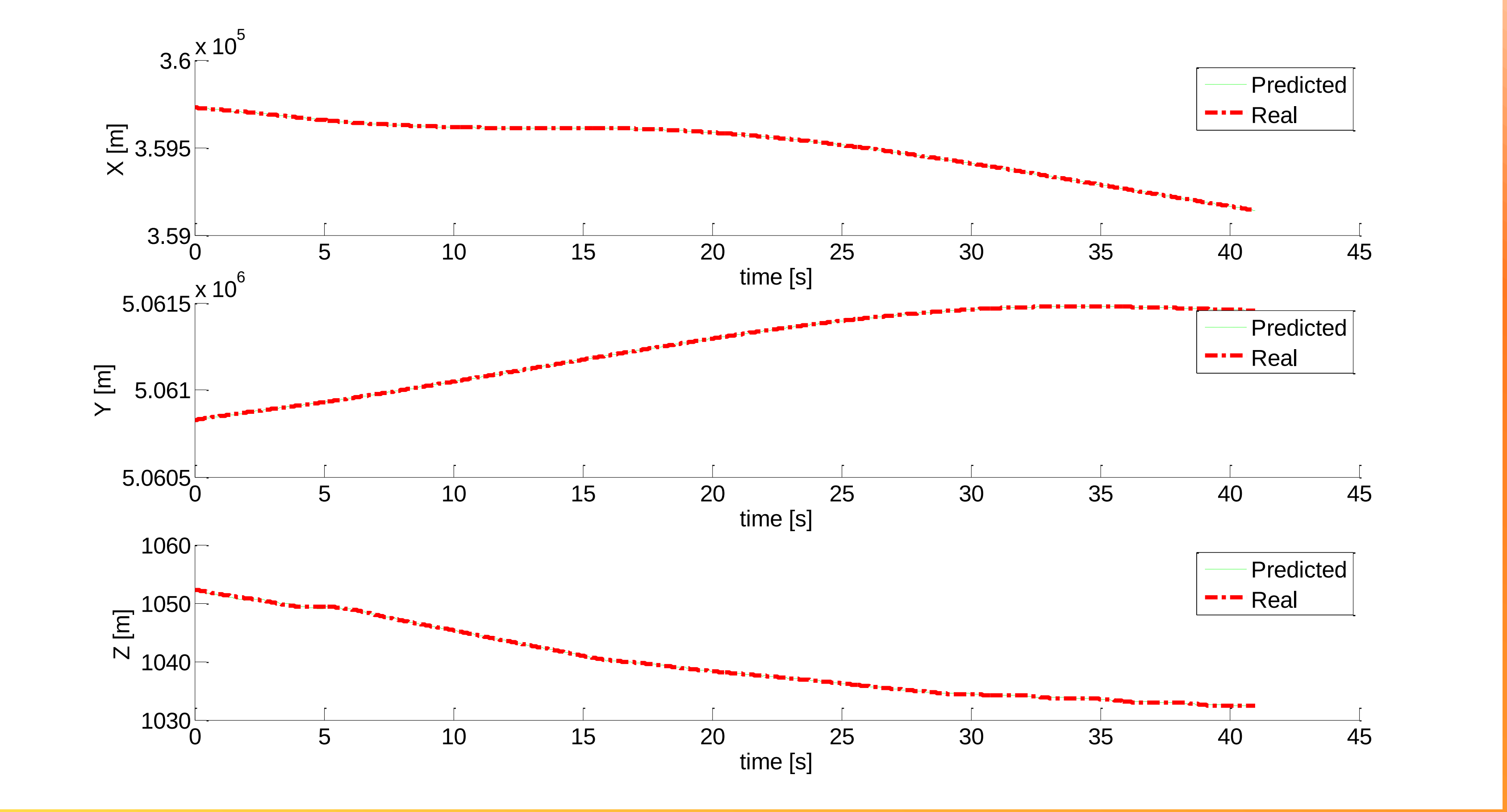

Reference and actual path

Collision Avoidance Task

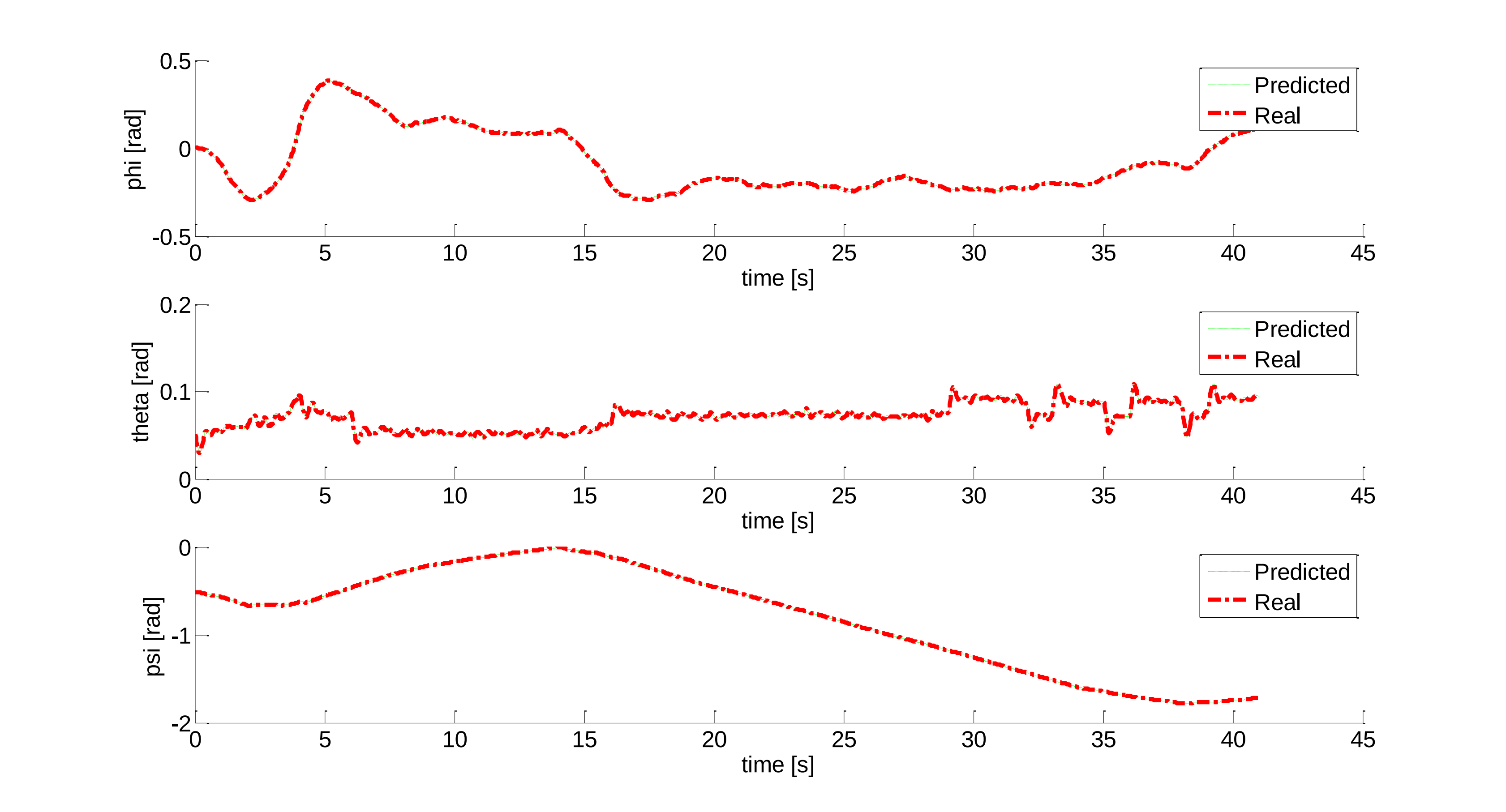

Attitude components in Body Frame

Collision Avoidance Task

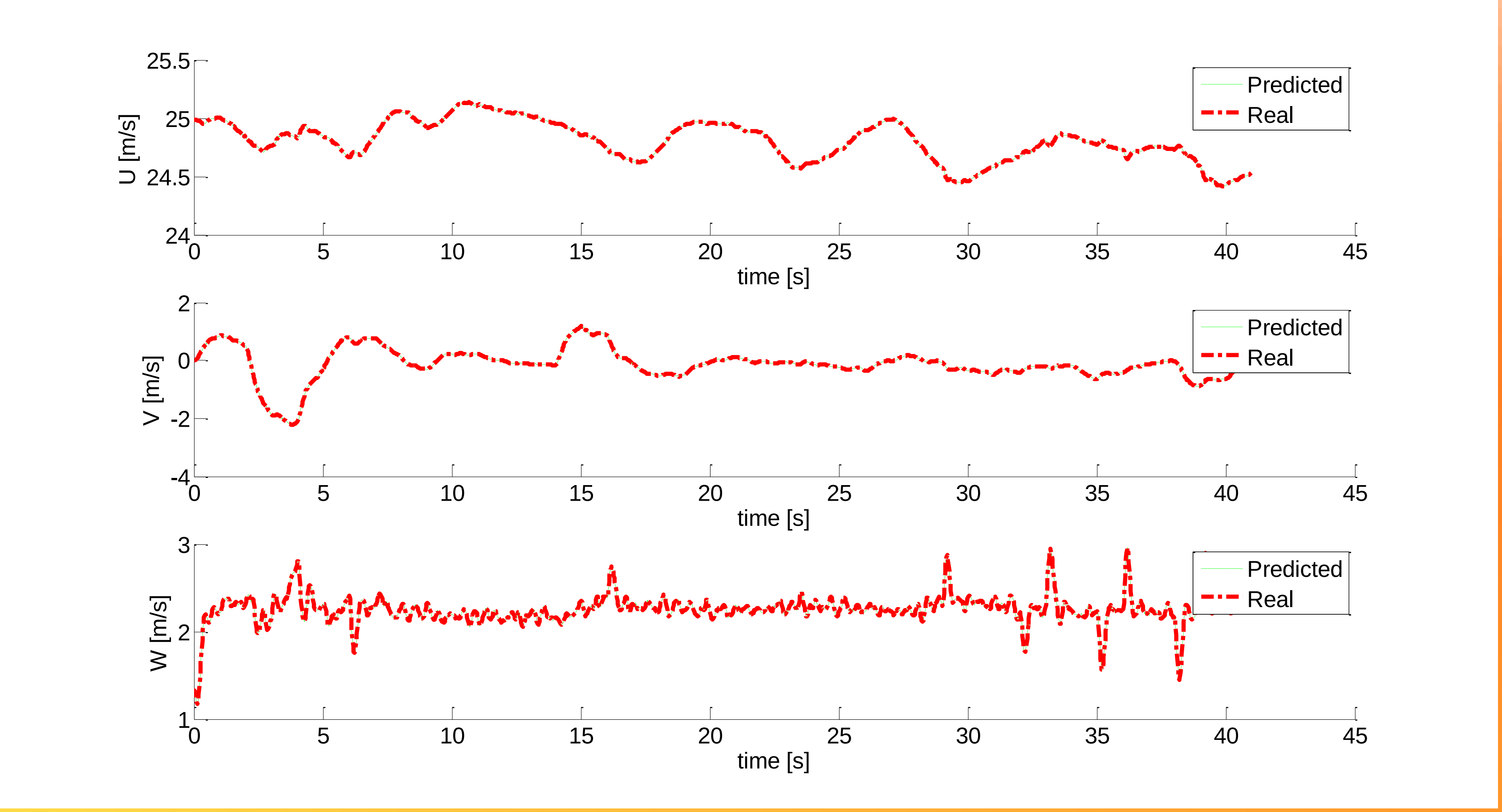

Speed components in Body Frame

Conclusions

- The tracking system proposed in this paper seems to reflect merits of NMPC and to accomplish with all tasks.
- Good tracking performance is evidenced with the results and effective control actions seem to provide smooth and safe paths.

Results:

- A new Guidance System has been implemented, using KA* to generate the avoidance maneuver.
- NMPC works as FCS converting optimum paths and avoidance trajectories in aircraft commands.

2nd EASN Workshop on Flight Physics and Propulsion

Formulation of the Optimization Problem for Engine Mount Design – Tractor Propeller Case

Tomasz Goetzendorf-Grabowski

Praha 31.10-2.11.2012

Introduction

- Engine nacelle is relatively small place, where all demands for the aircraft, power unit and systems, aerodynamics, strength, weight, maintenance, control, etc. are concentrated.
- To meet all requirements, usually iterative process is applied – it is very long and expensive.
- Trial to formulate the optimization problem for engine mount design

Tractor case

I23 - light aircraft

TP-100 small turboprop

Engine mount view

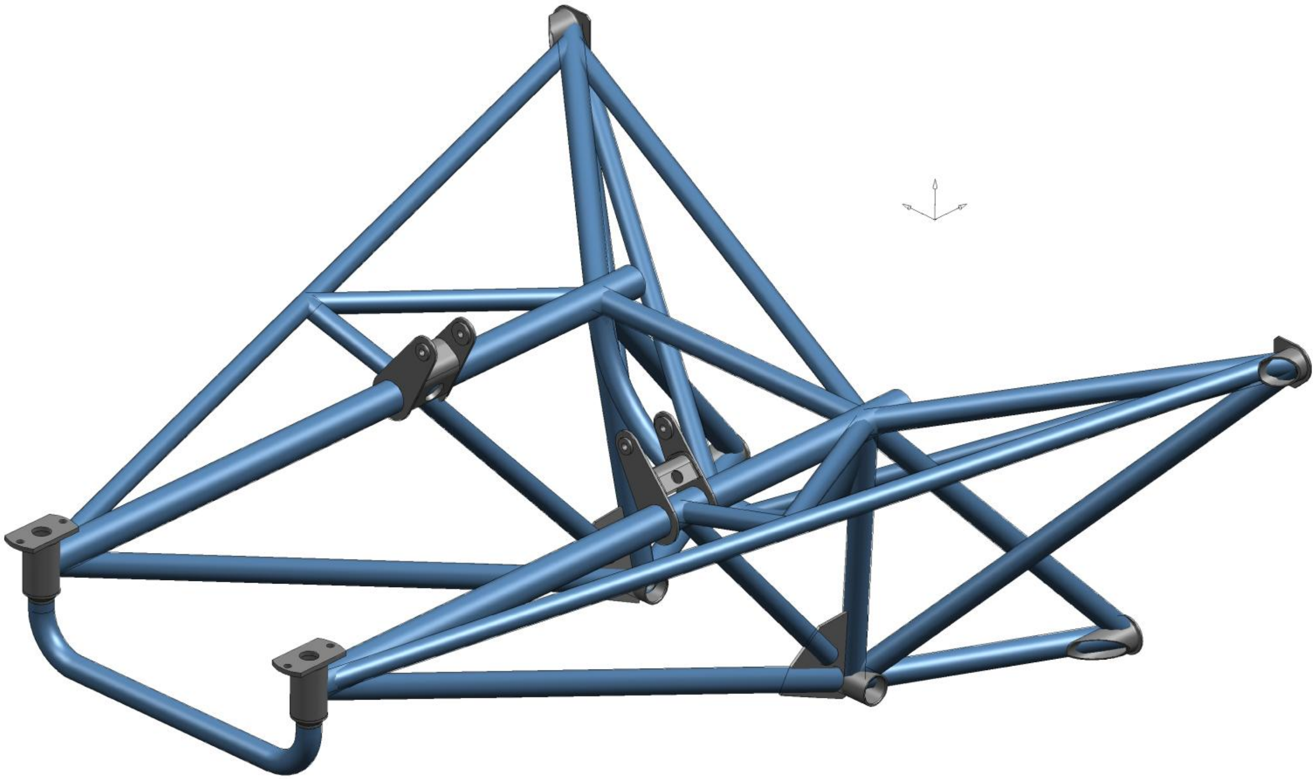

Engine mount – bar truss

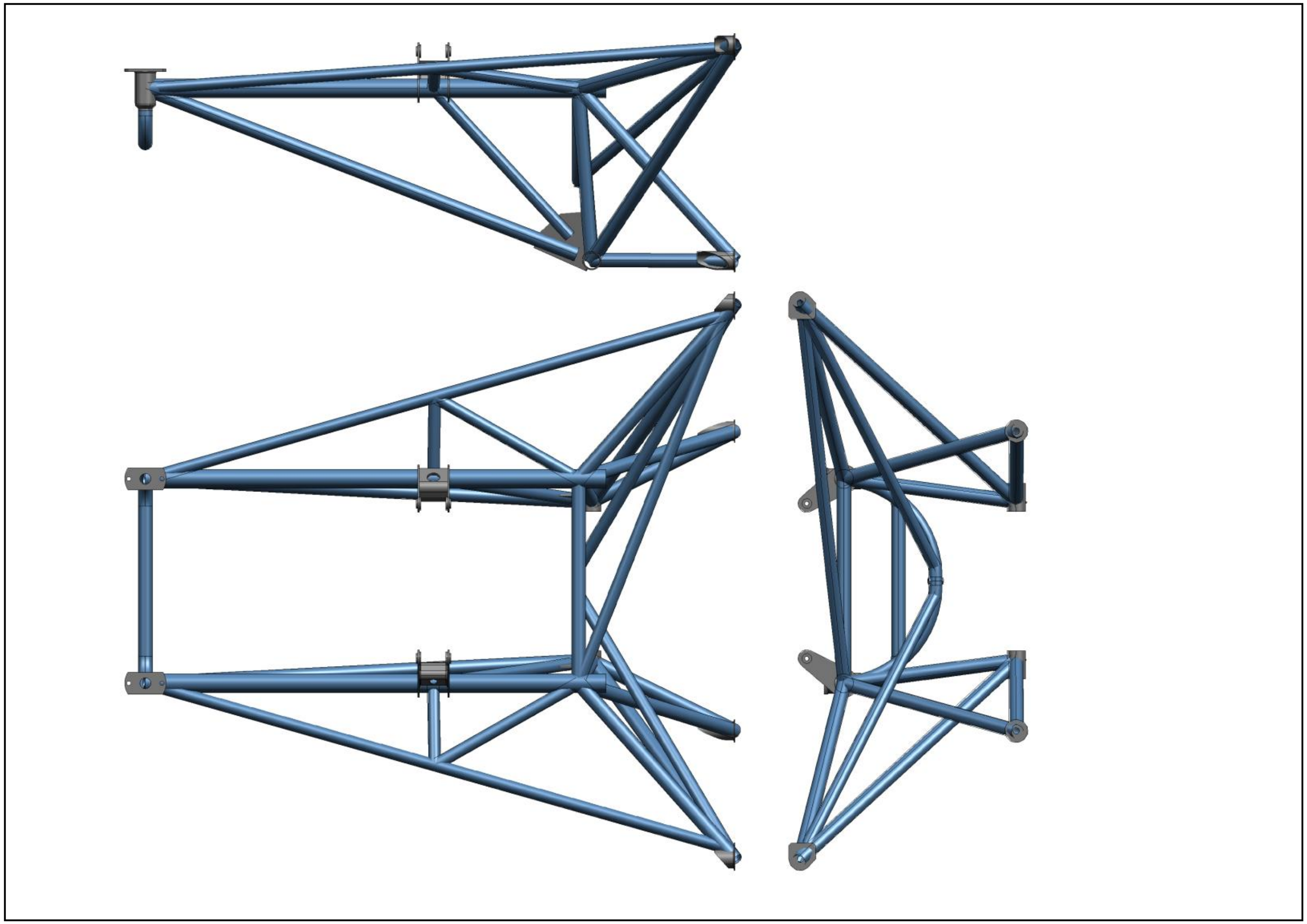

Optimization problem

- the minimization of weight is the main objective
- questions:
  – what parameters should be selected as design variables
  – what are the constraints

Optimization problem

- If the configuration (geometry) of truss is specified, we can formulate optimization problem for usual situation where the design variables are the cross-sectional areas of truss elements and the design objective is the weight of structure:

$$W = \sum_{i=1}^{NE} \rho_i A_i L_i$$

where:

W – weight of engine mount
NE – number of elements
ρ_i – material unit's weight
A_i – cross-sectional area of i-th element
L_i – length of i-th element

Optimization problem

Stress, displacement and eventual frequency criteria are defined by constraints functions:

compressive stress

$$\frac{\sigma_{ij}}{\overline{\sigma}^{-}} - 1 \leq 0 \quad i = 1, NE \quad j = 1, NLC$$

tensile stress

$$\frac{\sigma_{ij}}{\overline{\sigma}^{+}} - 1 \leq 0 \quad i = 1, NE \quad j = 1, NLC$$

Optimization problem – constraints – cont.

Euler buckling

$$\frac{\sigma_{ij}}{\sigma_{bi}} - 1 \le 0 \quad i = 1, NE \quad j = 1, NLC$$

where:

NLC – number of distinct loading conditions
k – number of displacement direction

displacement

$$\frac{\delta_{ijk}}{\overline{\delta}_{ik}} - 1 \le 0 \quad i = 1, NE \quad j = 1, NLC \quad k = 1,2,3$$

frequency (eigenvalues)

$$1 - \frac{\lambda}{\overline{\lambda}} \le 0$$

the lowest eigenvalue λ has to be greater, than a specified minimum $\overline{\lambda}$.

Optimization problem – constraints – cont.

The problem can be transform to reciprocal space:

$$F(X) = W = \sum_{i=1}^{NE} \frac{\rho_i L_i}{X_i}$$

where: $$X_i = 1/A_i$$

This form is useful, because then constraints can be easy linearized and also gradients and second derivatives of objective function can be readily calculated, which allows to build efficient algorithm

Load cases (*NLC*)

- Engine thrust
- Torque
- Gyroscopic moment
- Body forces

Engine thrust

- For jet engines, maximum value of the engine thrust can be given from an engine's characteristic as the a function of airspeed. Usually static thrust is the biggest one. For turboprop and piston engines, maximum value of the engine thrust can be computed from:

$$F_T = \frac{\eta N}{V}$$

where:

η – efficiency of propeller
N – power of engine [W]
V– air speed [m/s]
F_T – thrust of engine-propeller unit [N]

Torque

$$M_{\max} = k\frac{N}{\omega_S}$$

where

ω_S – angular rate of propeller [1/s]

$$k = \frac{M_{\max}}{M_{average}}$$

- The *k* coefficient should be given from engine's characteristic, if the characteristic is unavailable then the coefficient should be given from current regulations of aircraft design (eg CS.361).

Gyroscopic moment

Gyroscopic moment depends on polar moment of inertia J_o of rotating parts of engine, angular velocity of these parts and perpendicular angular velocity of airplane ω_y or ω_z during angular motion around y or z axis. Regulation (CS 23.371) includes the angular velocity values, that should be taken to analysis. The angular velocity ω_y can be calculated based on analysis of circular motion.

Circular motion

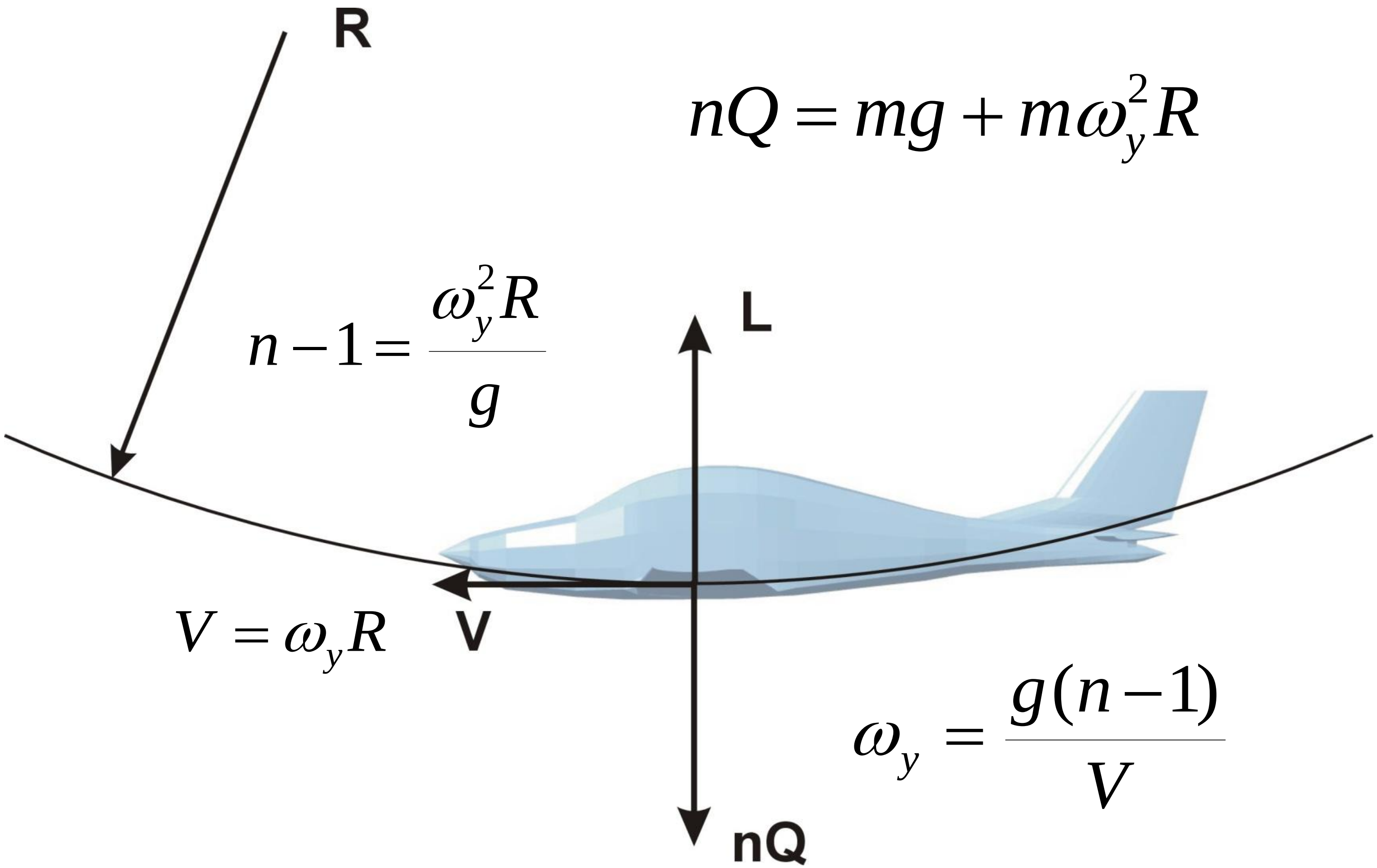

$$nQ = mg + m\omega_y^2 R$$

$$n - 1 = \frac{\omega_y^2 R}{g}$$

$$V = \omega_y R$$

$$\omega_y = \frac{g(n-1)}{V}$$

Gyroscopic moment

$$M_{GYR} = J_O \Omega \omega_y$$

where:

Ω – angular velocity of rotating elements (propeller, turbine, etc.)

J_o – moment of inertia of rotating elements (eg turbine, propeller, etc.)

Should be emphasized, that components of angular velocity and computation cases have to be calculated for the mostly loaded points of the load envelope (V-n diagram), according to regulation requirements.

Body forces

$$F_X = n_X Q_S, \quad F_Y = n_Y Q_S, \quad F_Z = n_Z Q_S$$

Body forces require to calculate the appropriate load factor longwise each axis. The n_z can be taken directly from load envelop. The n_x and n_y are defined in airworthiness regulation or can be calculated by analysis of critical cases.

Engine mount complete loads

Load	Possible critical case
F_X	Take off thrust
F_Y	Body force – turn for Va
F_Z	Body force – point D of load envelop
M_X	Max torque
M_Y	Gyroscopic moment point A
M_Z	Gyroscopic moment point D

Optimization scheme – 1st tier

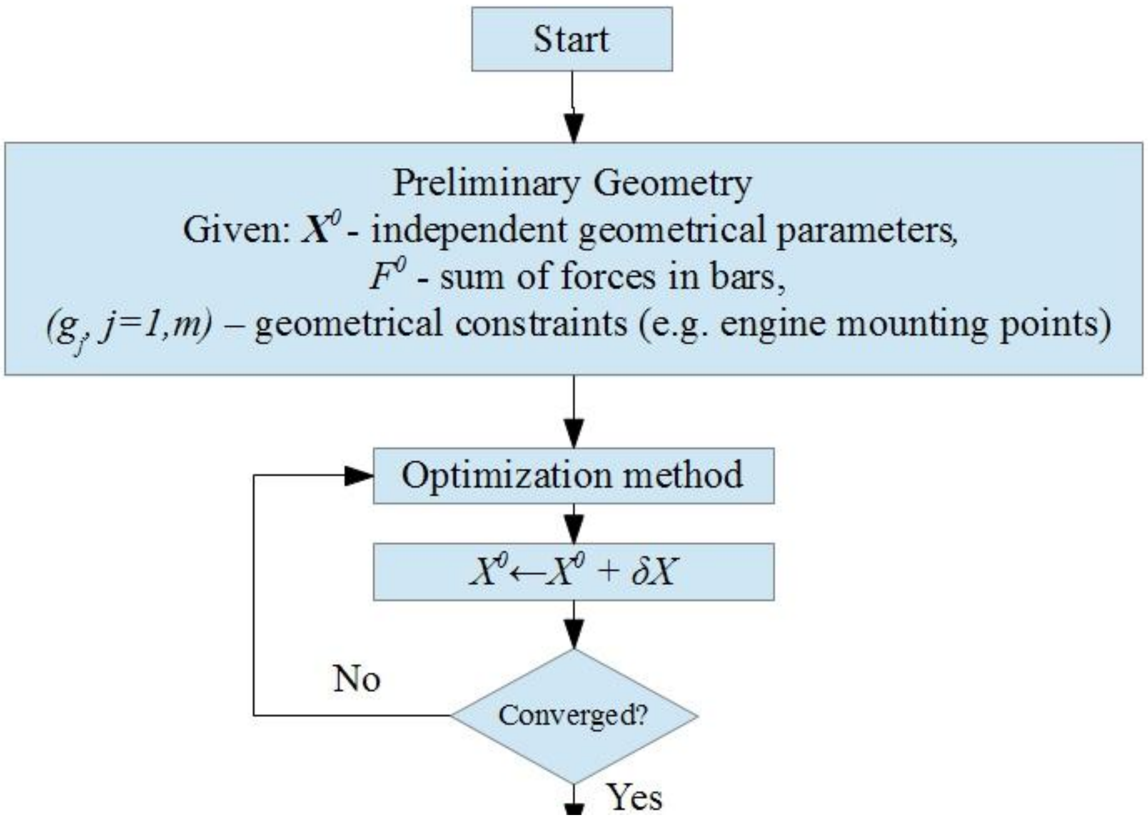

$$G(X) = \sum_{i=1}^{NE} F_i$$

Optimization scheme – 2nd tier

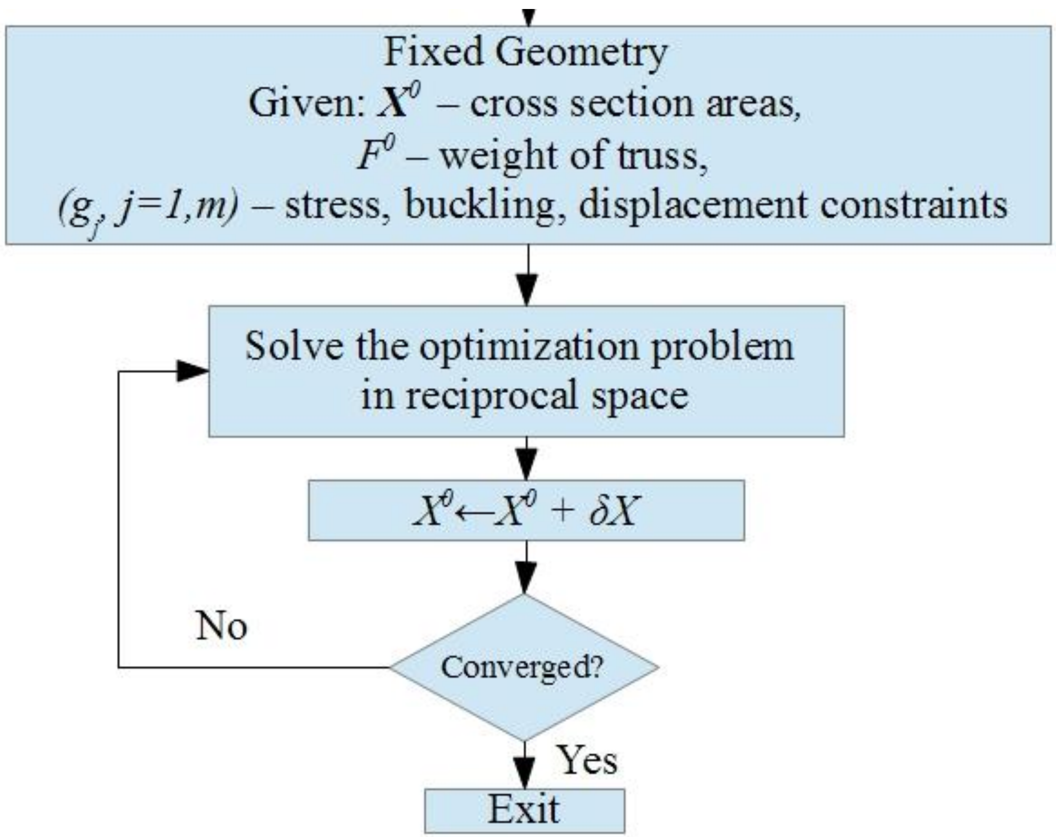

Optimization scheme

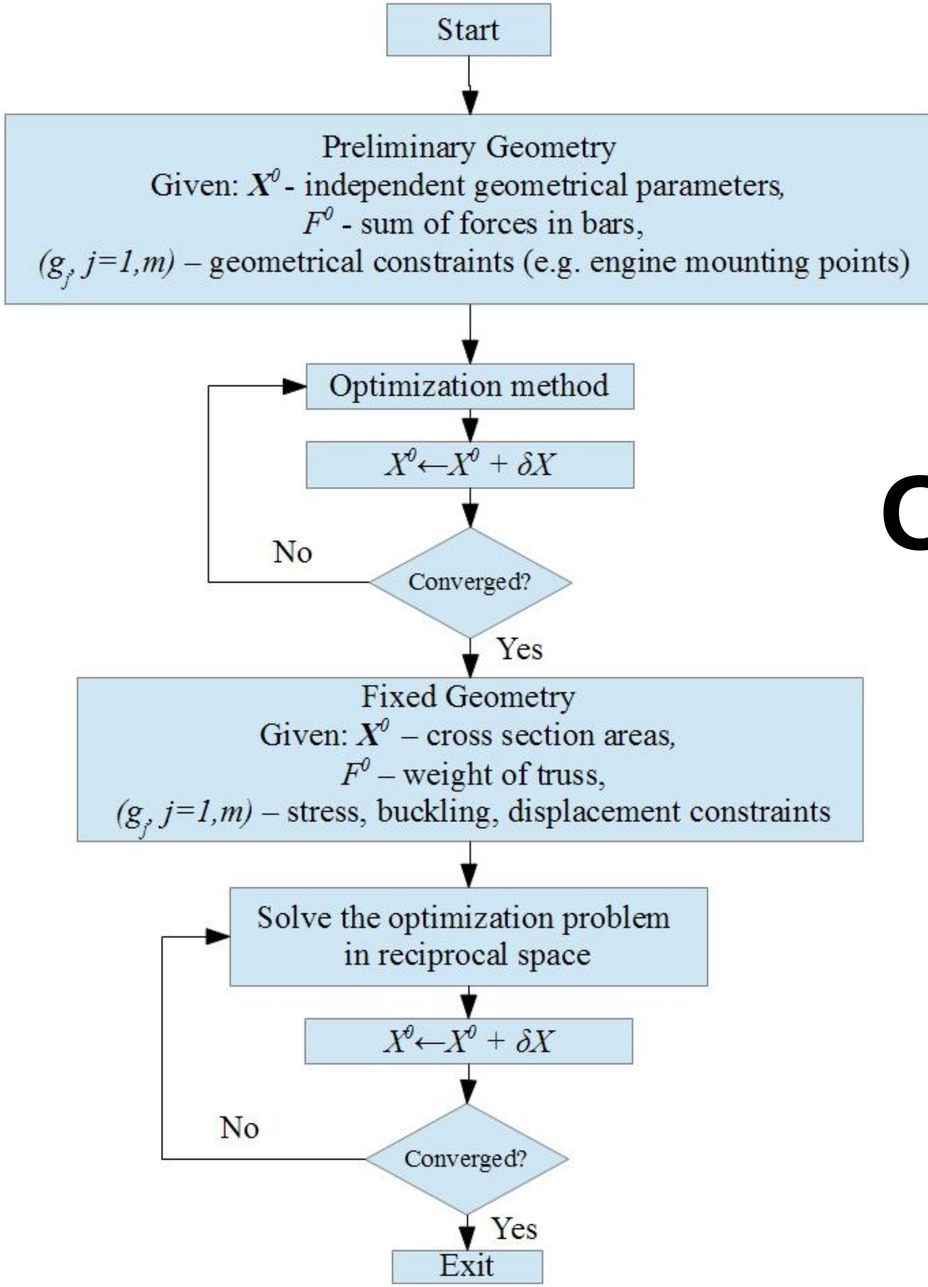

Concluding remarks

- The presentation is merely an attempt to signal optimization problem of engine mounts design.
- The problem of optimizing the truss structure often used in the construction of engine mounts, is relatively well known, it usually assumes a known structure (the number of rods and their length, etc.).
- Two-tier approach allows to design or modify the truss structure in the first step, taking into account constraints in the form of engine mounting points and the engine mounts to the fuselage structure. In the second stage it will be determined the optimal size of truss bar sections.

The End

Thank you for attention

instytutlotnictwa
warszawa, rok założenia 1926

2nd EASN Workshop on Flight Physics and Propulsion

Simulation of the helicopter maneuvers close to boundaries of VRS

mgr inż. Katarzyna Grzegorczyk

research for future

Outline

- background – the rotorcraft speed limitations
  - H-V diagram
  - VRS boundary
- computational cases
  - vertical descent
  - descent with low speed
- results
- conclusions, future development

Helicopter operating limits

- ❑ **Safe** and potentially **dangerous areas of flight** are defined **in flight manual** (performance section) and **air traffic regulations**

- ❑ **Boundaries** are determined **in flight testing** of new helicopter designs **by test pilots**

- ❑ **Boundaries set high risk areas** should be **avoid** or **remain** in them as **short** as possible

- ❑ Flight in this area requires an increased attention because the margin for error is smaller here

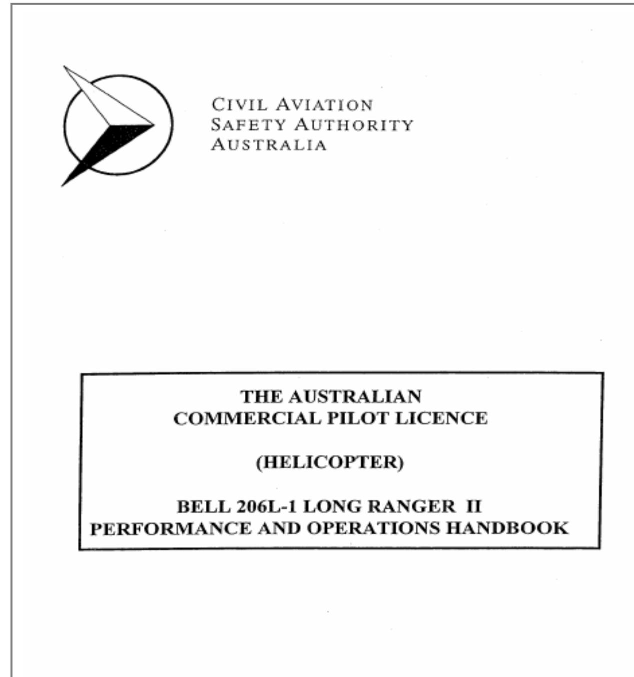
CIVIL AVIATION
SAFETY AUTHORITY
AUSTRALIA

THE AUSTRALIAN
COMMERCIAL PILOT LICENCE

(HELICOPTER)

BELL 206L-1 LONG RANGER II
PERFORMANCE AND OPERATIONS HANDBOOK

THIS HELICOPTER MUST BE OPERATED IN COMPLIANCE WITH THE OPERATING LIMITATIONS SPECIFIED IN THE APPROVED HELICOPTER FLIGHT MANUAL.

Range of usage

***Restrictions for use** the rotorcraft are **determined** to **enhance safety** and **depend on** several groups of factors associated with:*

- *flight conditions*
- *environmental conditions*
- *design of helicopter*

  (range limits for individual components)

Height-Velocity diagram

instytutlotnictwa
warszawa, rok założenia 1926

- A combination of **height-velocity determines** particularly helicopter **flight technique**
- The Height-Velocity Diagram defines conditions from witch a safe landing can be made
- **Dangerous areas** within the H-V curve are especially **important** in the **low-speed and low-altitude flight operations**

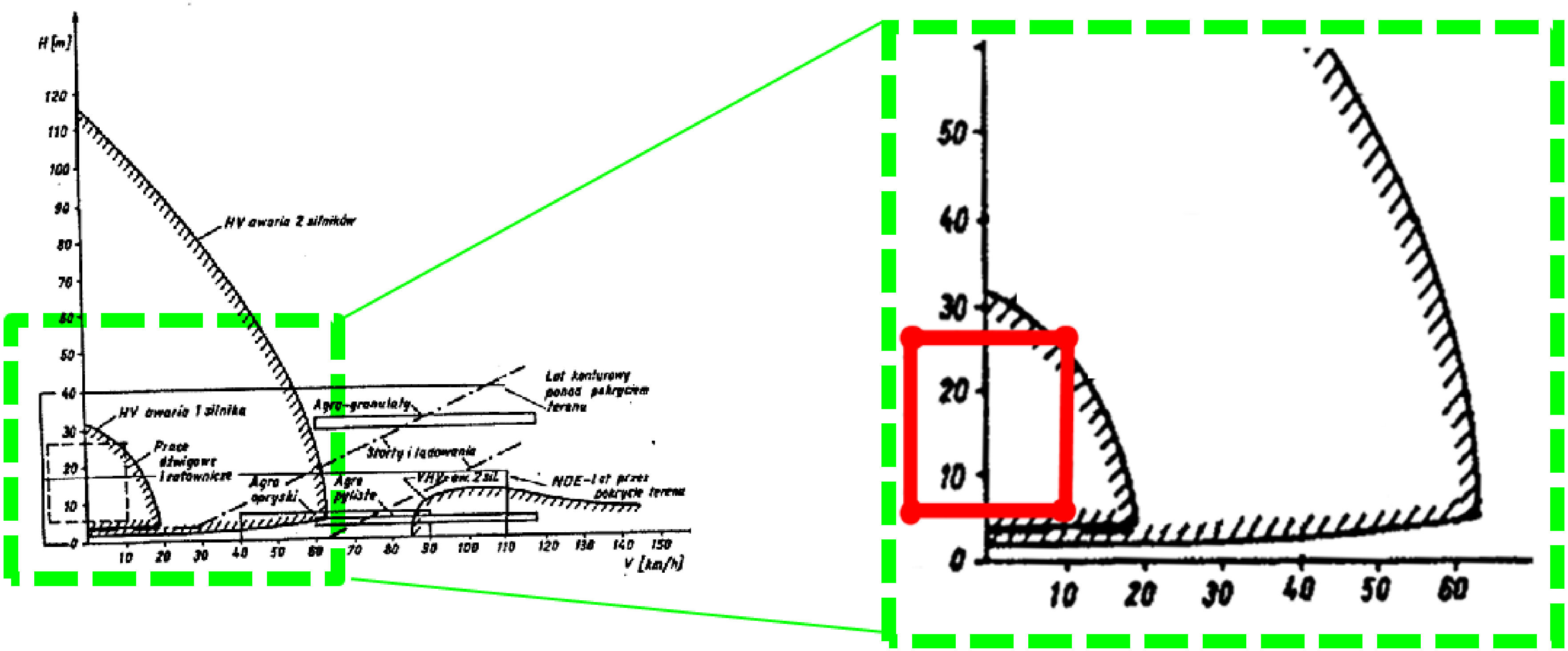

instytutlotnictwa
warszawa, rok założenia 1926

Performance tasks

Velocity descent range – VRS

Another restriction on speed flight which is used in the helicopter operations is the Vortex Ring State boundary

Transport Canada / Transports Canada

TP 9982E
(06/2006)

HELICOPTER FLIGHT TRAINING MANUAL

Second edition

June 2006

TC-1001888

Canada

v

Velocity descent range – VRS

EXERCISE 26 - VORTEX RING

If the helicopter pilot chooses a flight path, airspeed and a rate of descent that coincides with the aircraft's downwash, the helicopter could enter a condition known as the Vortex Ring state. The stall condition formed by the rate of descent flow in opposition to the induced flow

Your instructor will review the causes, conditions and symptoms of vortex ring. During a steep approach, at a high gross weight, high-density altitude and in a downwind or light wind condition; the helicopter may enter its own downwash and the development of vortex ring state. This situation would certainly contribute to the onset of vortex ring, but not necessarily cause it. The phenomenon is most likely to occur when all the conditions listed below are present:

1. in powered flight;
2. high rate of descent, in excess of 500 feet per minute; and
3. low airspeed, less than 20 MPH indicated.

Almost every transition from forward flight to a hover utilizes a powered approach, a rate of descent and a reduced airspeed. To prevent the occurrence of vortex ring, control your rate of descent less than 300 feet per minute.

may only serve to increase the rate of descent. This increase in blade pitch will cause the vortices to intensify in strength and will result in a more rapid descent.

There are some uninformed pilots who use "settling with power" to describe vortex ring, in fact some publications use the terms interchangeably. Confusion results when symptoms are related that do not describe true vortex ring but rather describe "settling with insufficient power". This may occur when a pilot attempts to arrest a rapid, low power descent only to find that he has insufficient power available to bring the helicopter to either a hover or a no-hover landing without exceeding the engine limits. However, this is not a vortex ring situation.

Another situation, 'over-pitching' is often misinterpreted as vortex ring. This is where the pilot rapidly increases collective considerably and the engine cannot produce enough power to overcome the large, swift increase in drag on the rotor system. The result is that the rotor system quickly slows down and loses efficiency causing the helicopter instantly to sink. Again, this is not vortex ring.

The most common situations, where you would be most likely to encounter vortex ring, are usually when you misjudge the wind with a heavy load on a hot day. Downwind approaches to a confined area, or a mountain pad, are two good examples. Always control your rate of descent carefully on these occasions, and make sure an escape route is available. Your instructor will discuss the symptoms and recovery techniques more fully. Demonstration of this exercise is not generally performed, as the stresses on the airframe and rotor system are unknown.

PREVENTION IS BETTER THAN CURE!!!

Velocity descent range – VRS

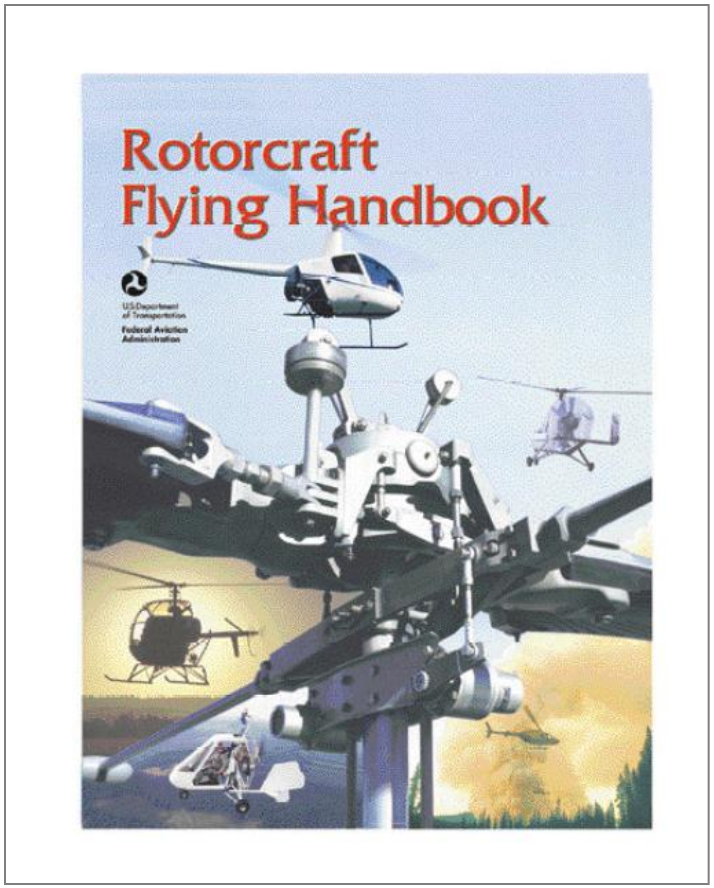

Velocity descent range – VRS

of the helicopter. Therefore, you should always be familiar with the height/velocity diagram for the particular model of helicopter you are flying.

THE EFFECT OF WEIGHT VERSUS DENSITY ALTITUDE

The height/velocity diagram depicts altitude and airspeed situations from which a successful autorotation can be made. The time required, and therefore, altitude necessary to attain a steady state autorotative descent, is dependent on the weight of the helicopter and the density altitude. For this reason, the H/V diagram for some helicopter models is valid only when the helicopter is operated in accordance with the gross weight vs. density altitude chart. Where appropriate, this chart is found in the rotorcraft flight manual for the particular helicopter. [Figure 11-3]

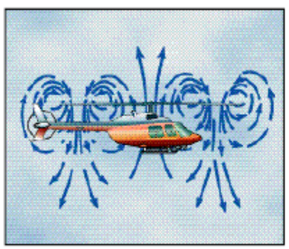

Figure 11-4. Vortex ring state.

Figure 11-3. Assuming a density altitude of 5,500 feet, the height/velocity diagram in figure 11-2 would be valid up to a gross weight of approximately 1,700 pounds. This is found by entering the graph at a density altitude of 5,500 feet (point A), then moving horizontally to the solid line (point B). Moving vertically to the bottom of the graph (point C), you find that with the existing density altitude, the maximum gross weight under which the height/velocity diagram is applicable is 1,700 pounds.

The gross weight vs. density altitude chart is not intended as a restriction to gross weight, but as an advisory to the autorotative capability of the helicopter during takeoff and climb. You must realize, however, that at gross weights above those recom-

mended by the gross weight vs.
chart, the H/V diagram is not rest

VORTEX RING STATE (SET
POWER)

Vortex ring state describes an aer
tion where a helicopter may b
descent with up to maximum pow
little or no cyclic authority. The te
power" comes from the fact that
settling even though full engine p

In a normal out-of-ground-effect
copter is able to remain stationar
large mass of air down through
Some of the air is recirculated ne
blades, curling up from the bottom
tem and rejoining the air enterin
the top. This phenomenon is com
and is known as tip vortices. Tip v
engine power but produce no us
as the tip vortices are small, thei
small loss in rotor efficiency. Ho
helicopter begins to descend ve
into its own downwash, which gre
tip vortices. In this vortex ring st
power developed by the engine is
erating the air in a doughnut pa
rotor.

In addition, the helicopter may d
that exceeds the normal downwa
rate of the inner blade sections.
airflow of the inner blade sections
tive to the disc. This produces a s
ring in addition to the normal tip-v
ondary vortex ring is generated a
the blade where the airflow cha
down. The result is an unstead
over a large area of the disc. Ro
lost even though power is still bei
the engine. [Figure 11-4]
A fully developed vortex ring state
by an unstable condition where the helicopter experiences uncommanded pitch and roll oscillations, has little or no cyclic authority, and achieves a descent rate, which, if allowed to develop, may approach 6,000 feet per minute. It is accompanied by increased levels of vibration.

A vortex ring state may be entered during any maneuver that places the main rotor in a condition of high upflow and low forward airspeed. This condition is sometimes seen during quick-stop type maneuvers or during recoveries from autorotations. The

The following combination of conditions are likely to cause settling in a vortex ring state:

1. A vertical or nearly vertical descent of at least 300 feet per minute. (Actual critical rate depends on the gross weight, r.p.m., density altitude, and other pertinent factors.)

2. The rotor system must be using some of the available engine power (from 20 to 100 percent).

3. The horizontal velocity must be slower than effective translational lift.

tion of at least 1,500 feet AGL.

To enter the maneuver, reduce power below hover power. Hold altitude with aft cyclic until the airspeed approaches 20 knots. Then allow the sink rate to increase to 300 feet per minute or more as the attitude is adjusted to obtain an airspeed of less than 10 knots. When the aircraft begins to shudder, the application of additional up collective increases the vibration and sink rate.

Recovery should be initiated at the first sign of vortex ring state by applying forward cyclic to increase airspeed and simultaneously reducing

Retreating blade stall is a major factor in limiting a helicopter's top forward speed (V_{NE}) and can be felt developing by a low frequency vibration, pitching up of the nose, and a roll in the direction of the retreating blade. High weight, low rotor r.p.m., high density altitude, turbulence and/or steep, abrupt turns are all conducive to retreating blade stall at high forward airspeeds. As altitude is increased, higher blade angles are required to maintain lift at a given airspeed. Thus, retreating blade stall is encountered at a lower forward airspeed at altitude. Most manufacturers publish charts and graphs showing a V_{NE} decrease with altitude.

VRS boundary

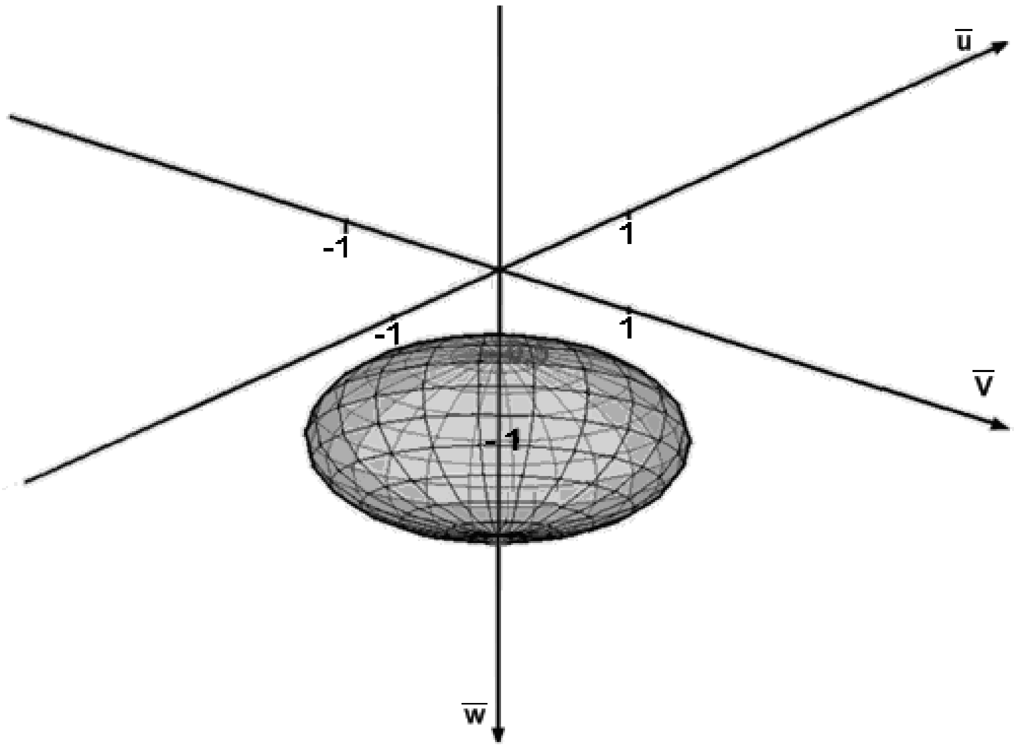

Fig. 3d theoretical area of VRS

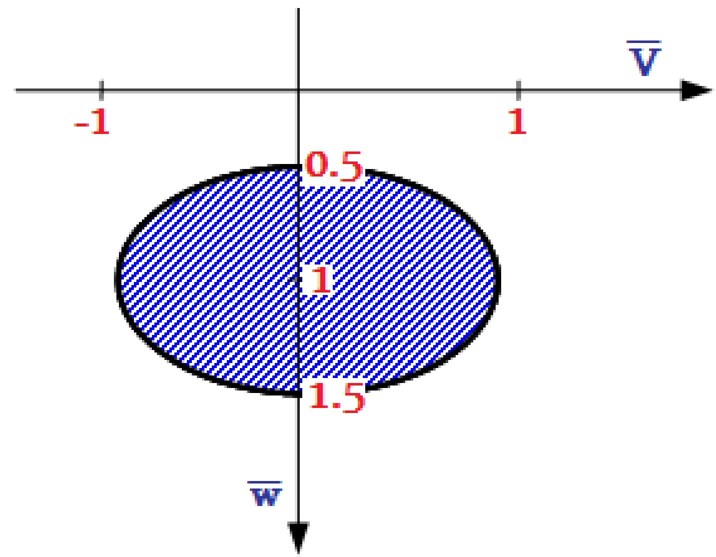

Fig. 2d theoretical area of VRS

$$\overline{V}=\frac{V}{V_{io}} \qquad \overline{u}=\frac{u}{V_{io}} \qquad \overline{w}=\frac{w}{V_{io}} \qquad V_{io}=\sqrt{\frac{T}{2\rho A}}$$

Vortex Ring State phenomenon:

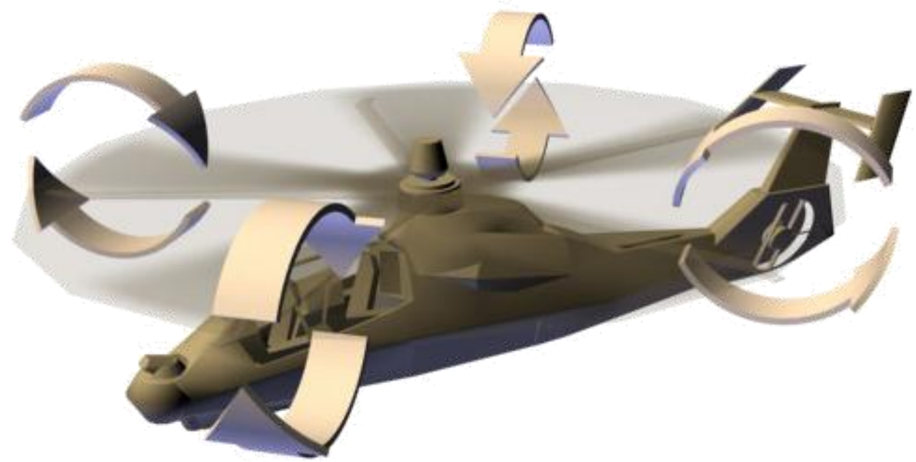

- The **V**ortex **R**ing **S**tate also known as a „**Settling with Power**" is a condition **powered flight** which is characterized by formation of **circulating air stream** moving along a **ring** shaped track **around** the main **rotor** helicopter

- **The reason** for creation and growth of vortex structures is **balancing** rotor **induced flow** and **stream** of air flow **from bottom** to rotor

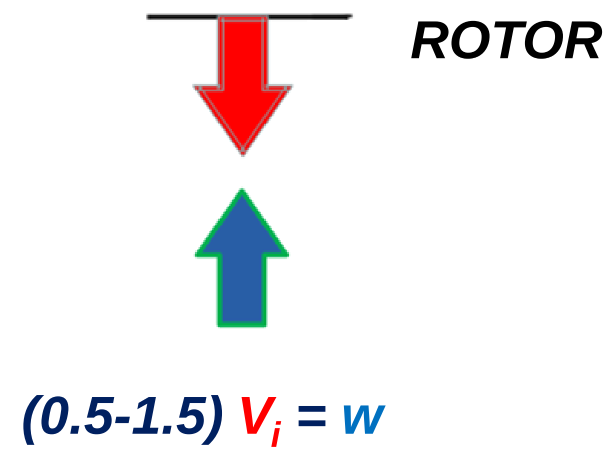

- It is assumed that the **theoretical range of the occurrence of VRS** is $w = (0.5 \div 1.5)\ v_{io}$, where:

  v_{io} - induced velocity for the rotor in hover

Vortex Ring State phenomenon:

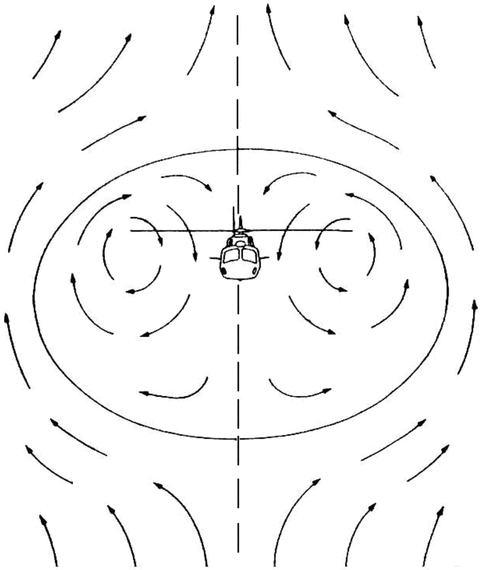

- The **name** of this aerodynamic phenomenon was created by **analogy** to the geometry of the **flow field around a rotor**

- These **specific vortices** disrupt the rotor downwash thus reducing the effectiveness of its operation and **leads** to a **decrease in thrust** and thus **rapidly increasing a rate of descent**

- The **disturbance of the balance**, maneuverability deterioration of a helicopter, **power loss** and **increased levels** of **vibration** are a **consequences of vortex ring**

- In practice, this phenomenon occurs most often during the **vertical descent**

Experimental investigation in Poland

- *SM-1 helicopter*
- *Institute of Aviation*
- *1963 year*

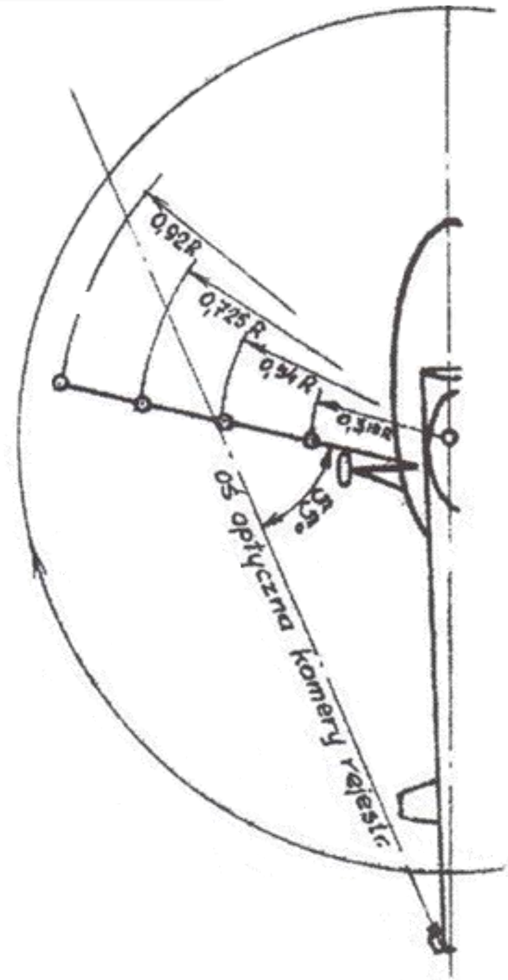

Experimental investigation in Poland

Flow visualization of the flight test the SM-1 helicopter	
w/vio=0,533 	w/vio=0,667 
w/vio= 1,40 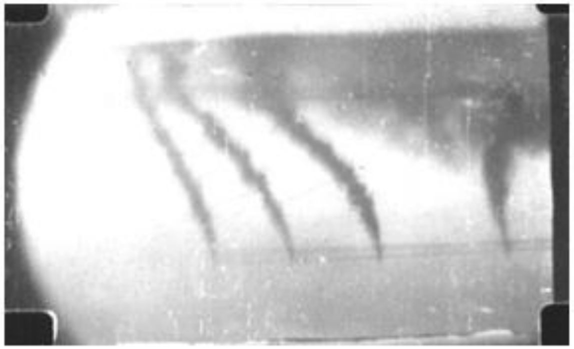	w/vio= 2,09 

Experimental investigation in Poland

- ***PZL W-3 „Sokół" helicopter***
- ***PZL Świdnik SA***
- ***2009 year***

Simulations

Computational model:

- **Geometry: W-3 „Sokół”**

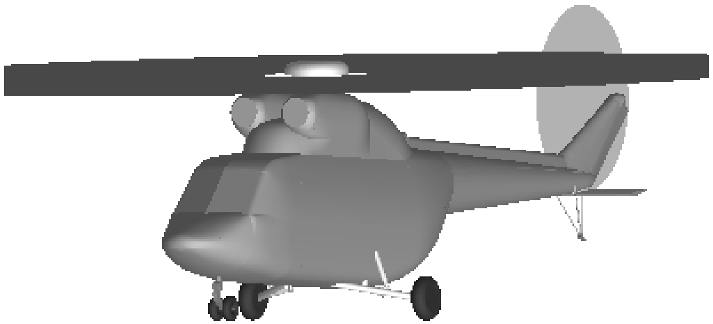

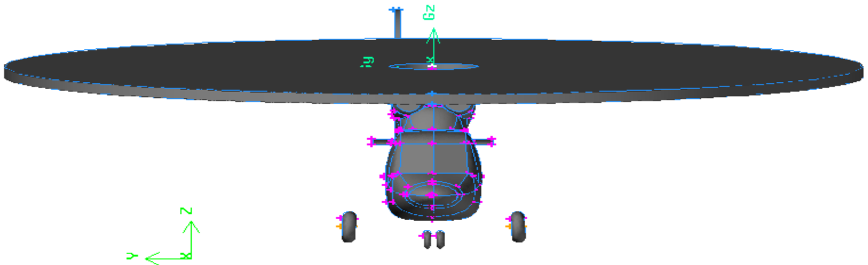

- **Unstructured grid:**

(1133371 cells) ICEM CFD

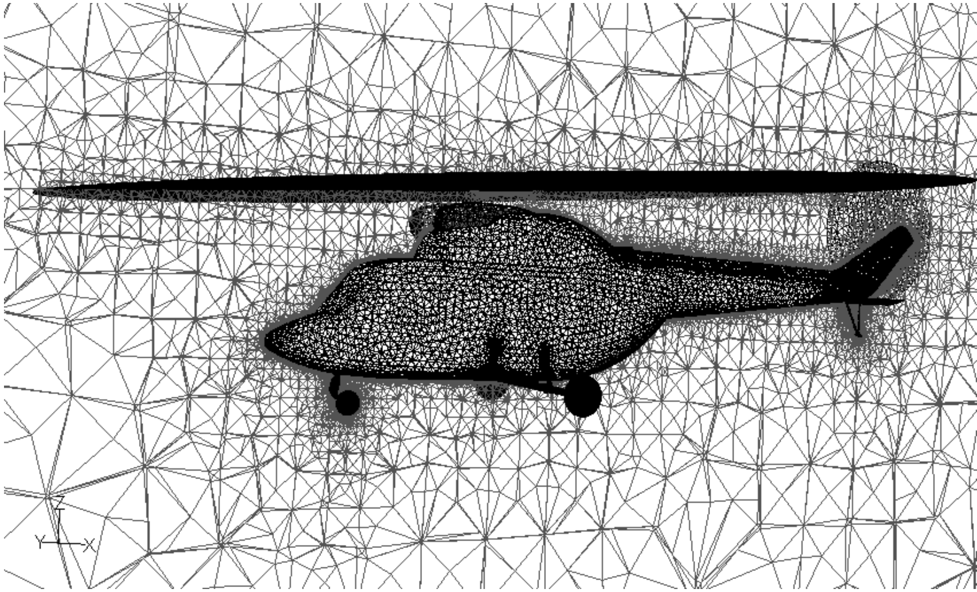

m, vio, R

Modelling assumptions

- **domain:**

  cube 50x50x50

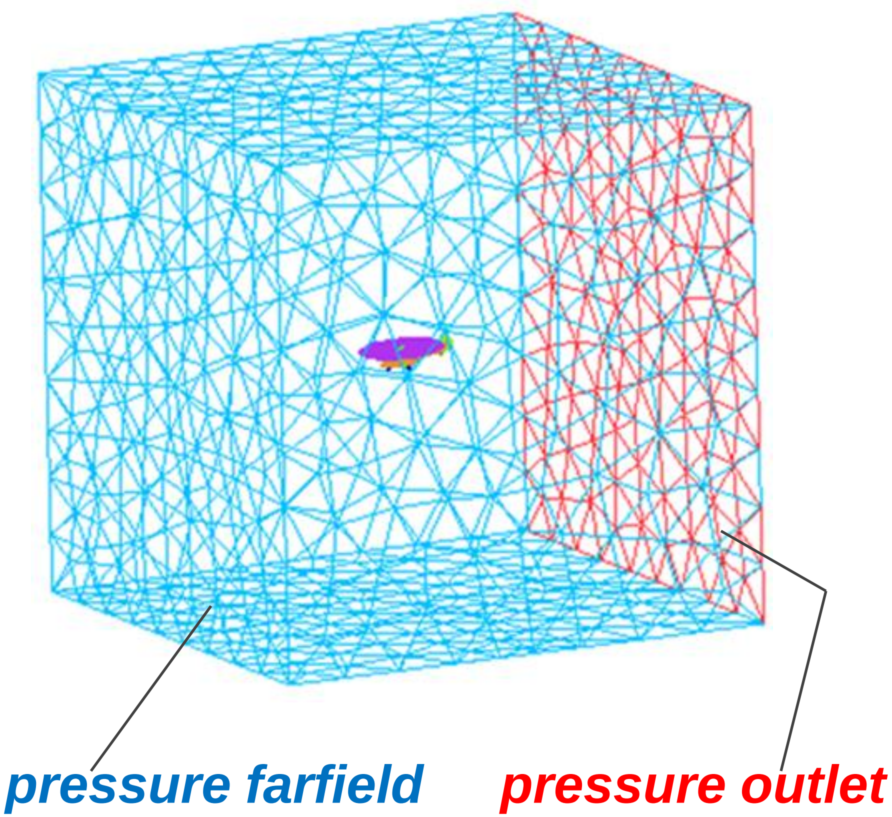

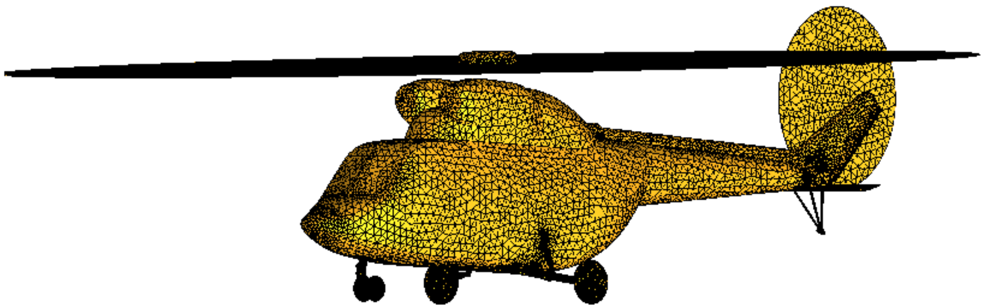

MAIN ROTOR - FAN dp=299 Pa

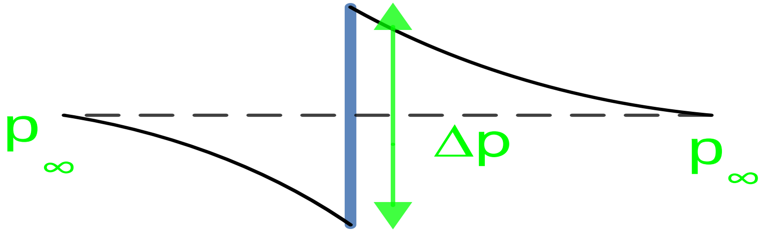

Case I – boundary conditions

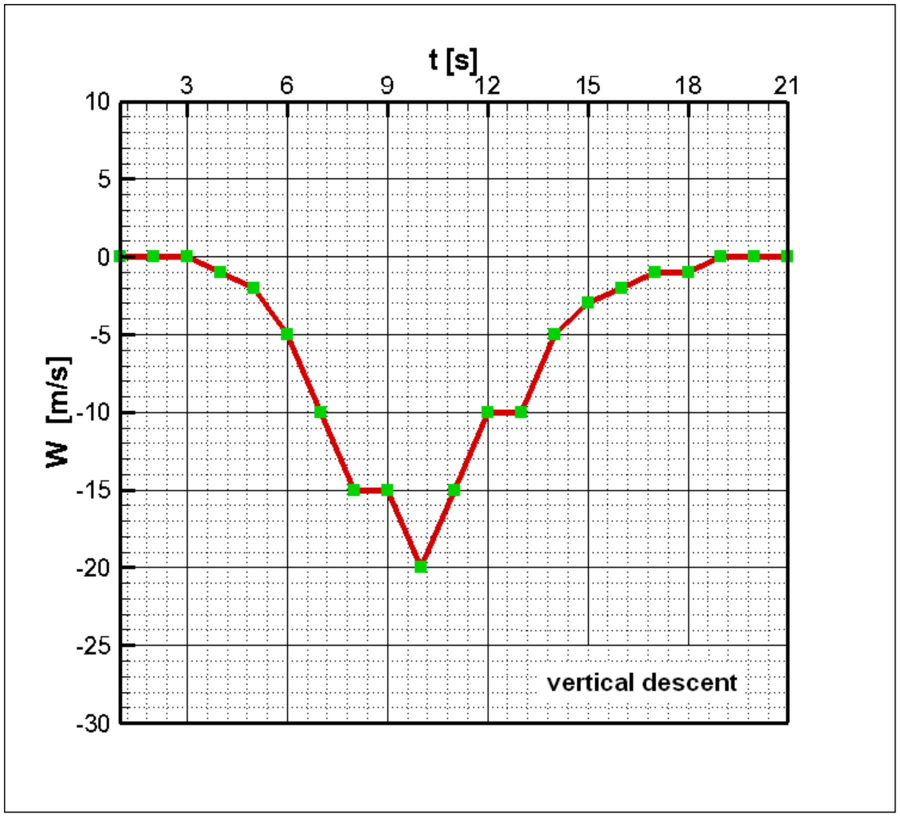

Fig. Velocity descent versus time graph

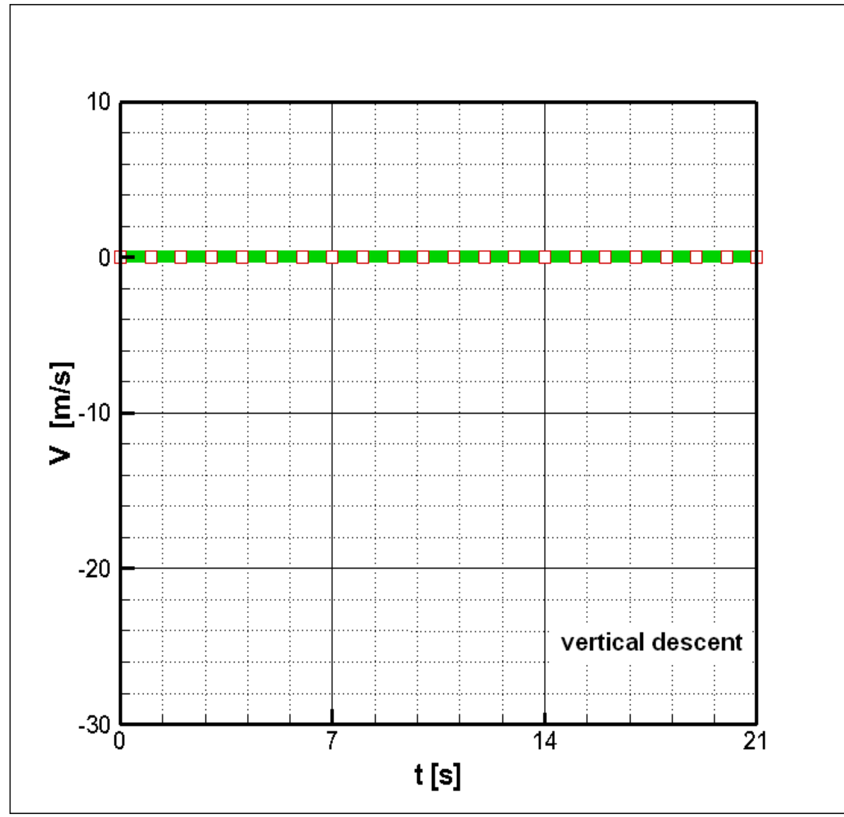

Fig. Airspeed versus time graph

Case I – boundary conditions

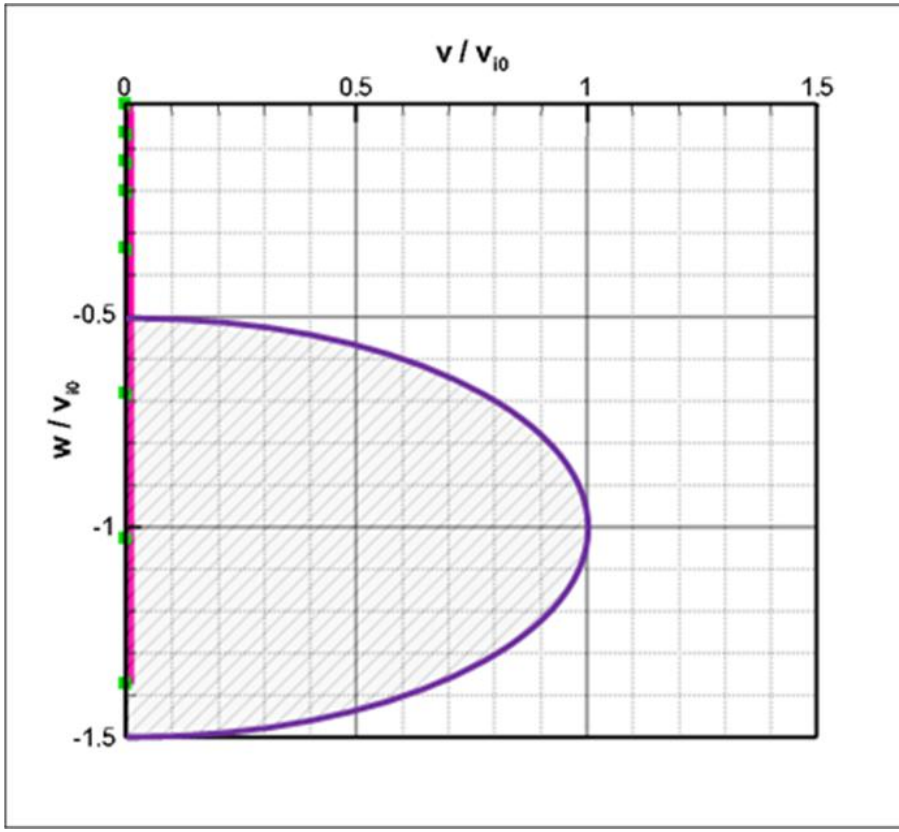

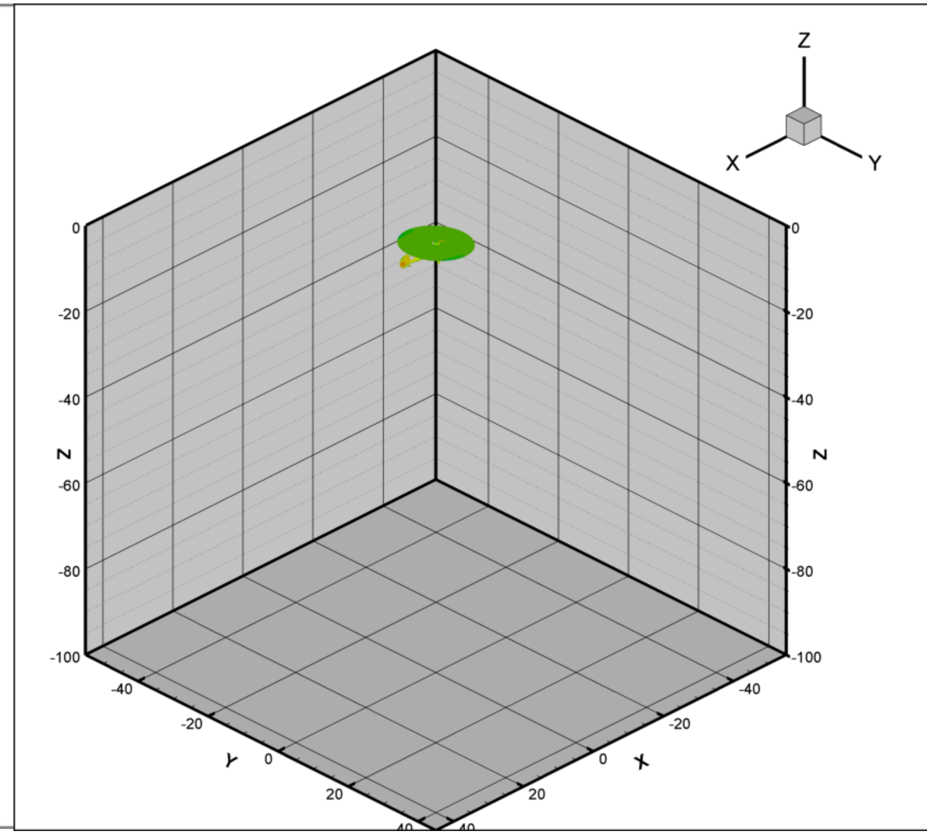

Fig. Velocity descent versus airspeed graph

Case I – start case

- *hover*

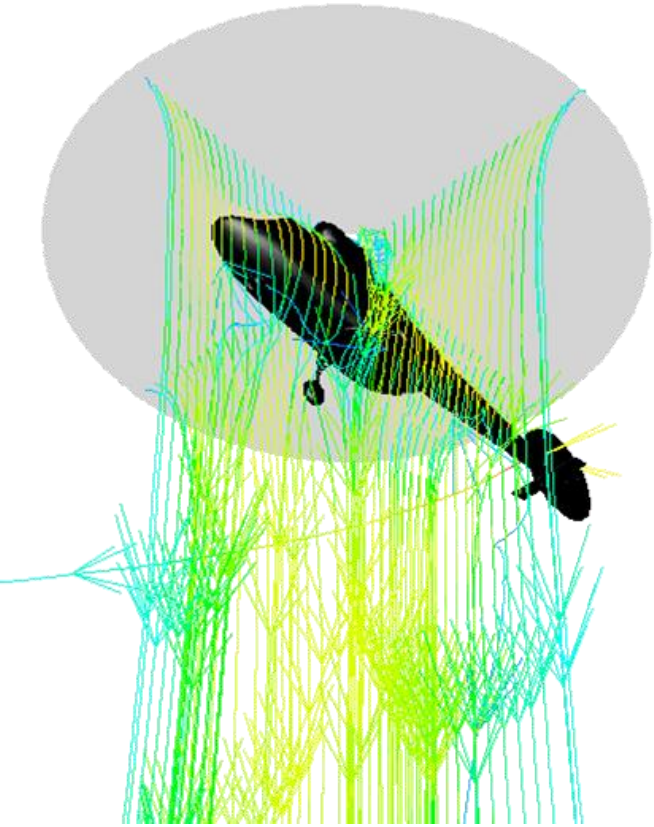

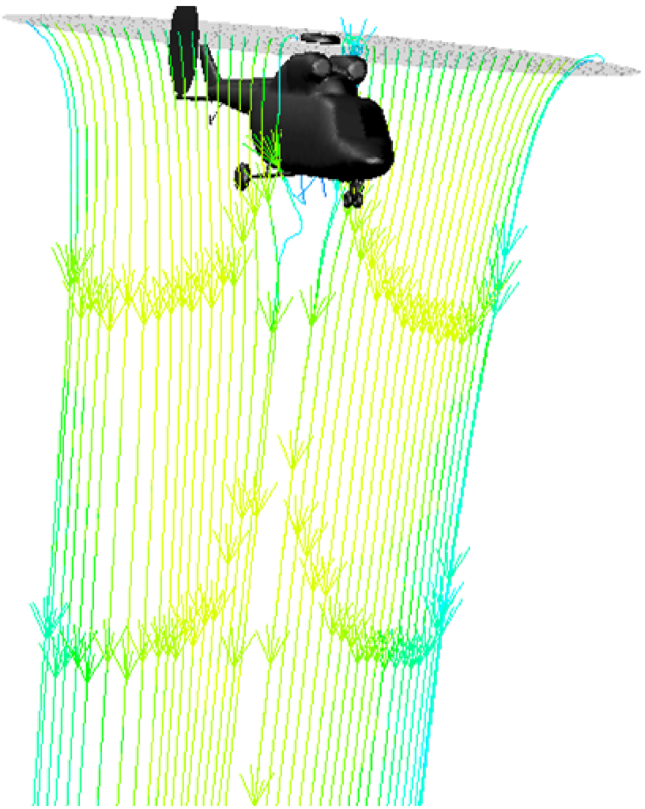

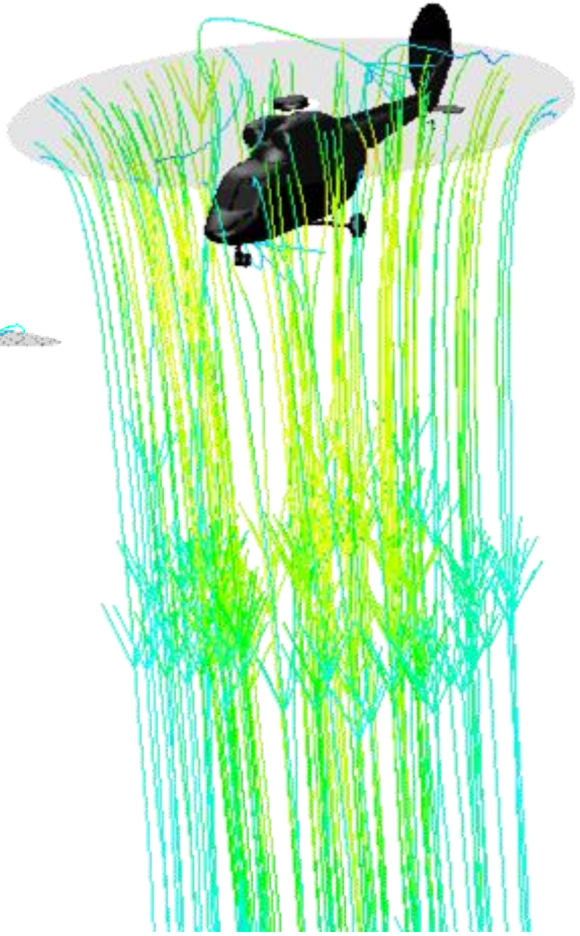

Case I – results (1st part)

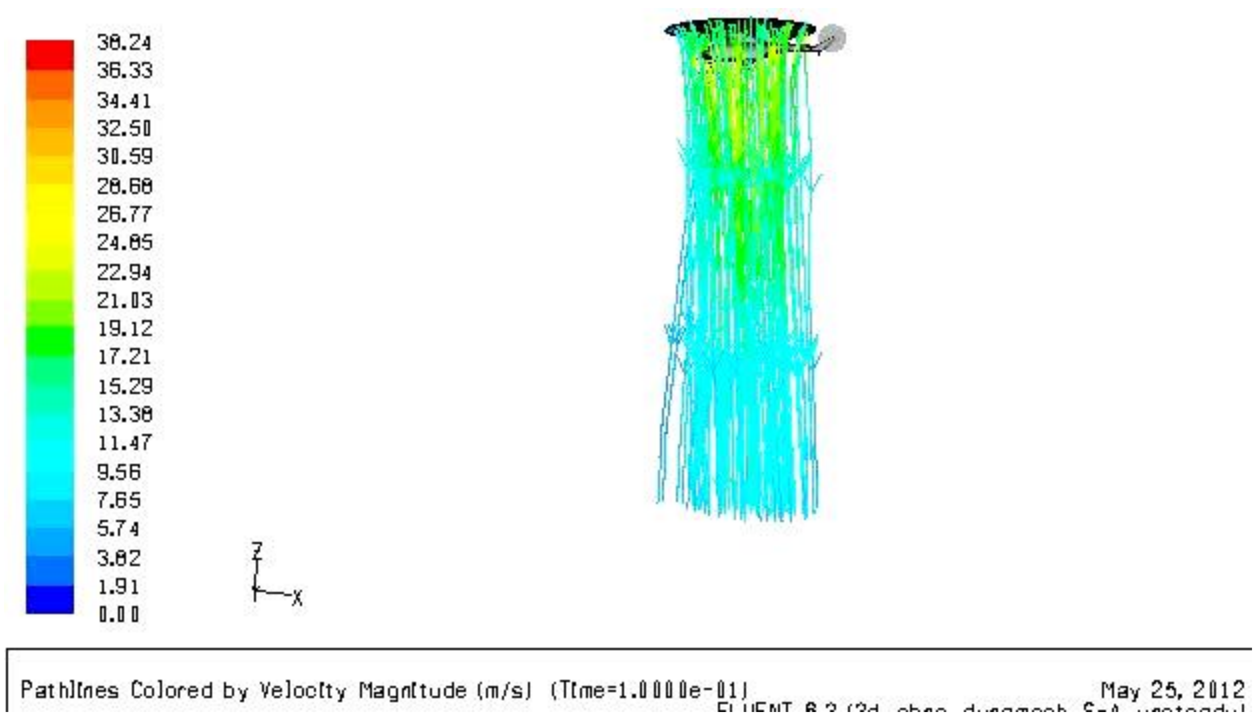

Case I – results (2d part)

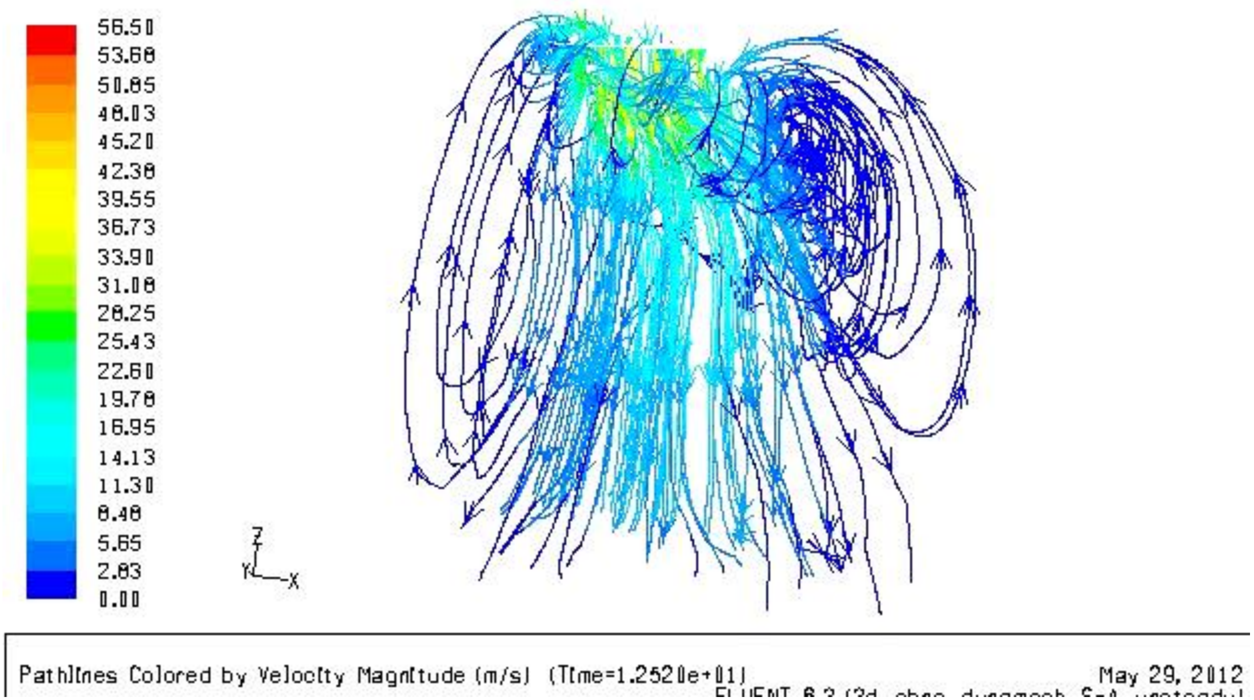

Case II – boundary conditions

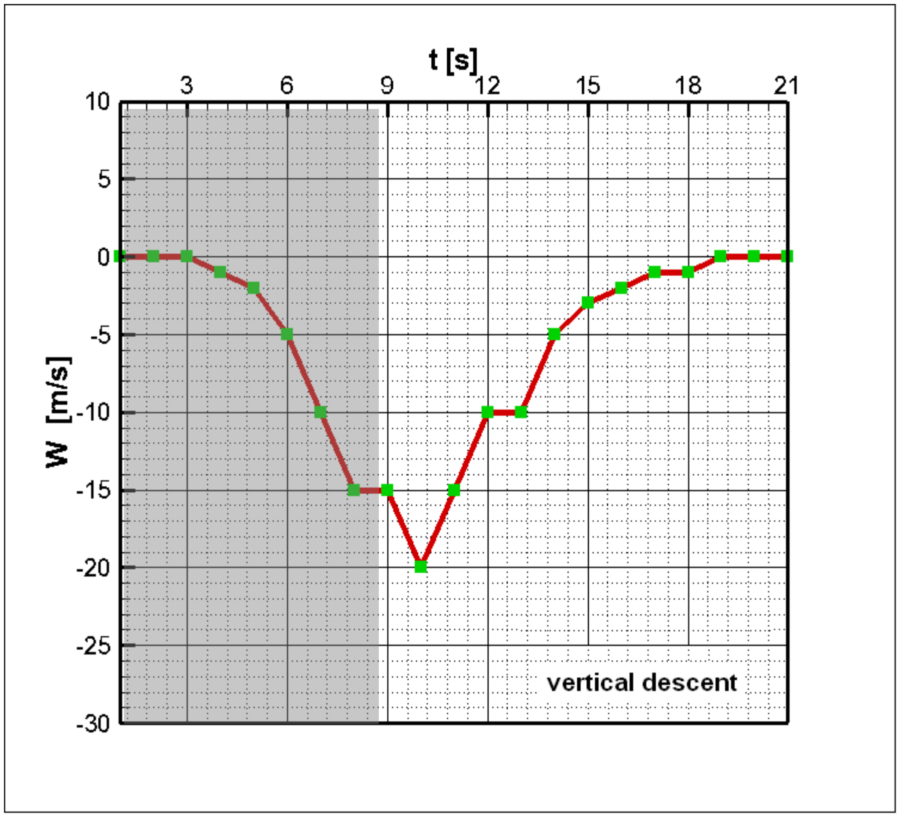

Fig. Velocity descent versus time graph

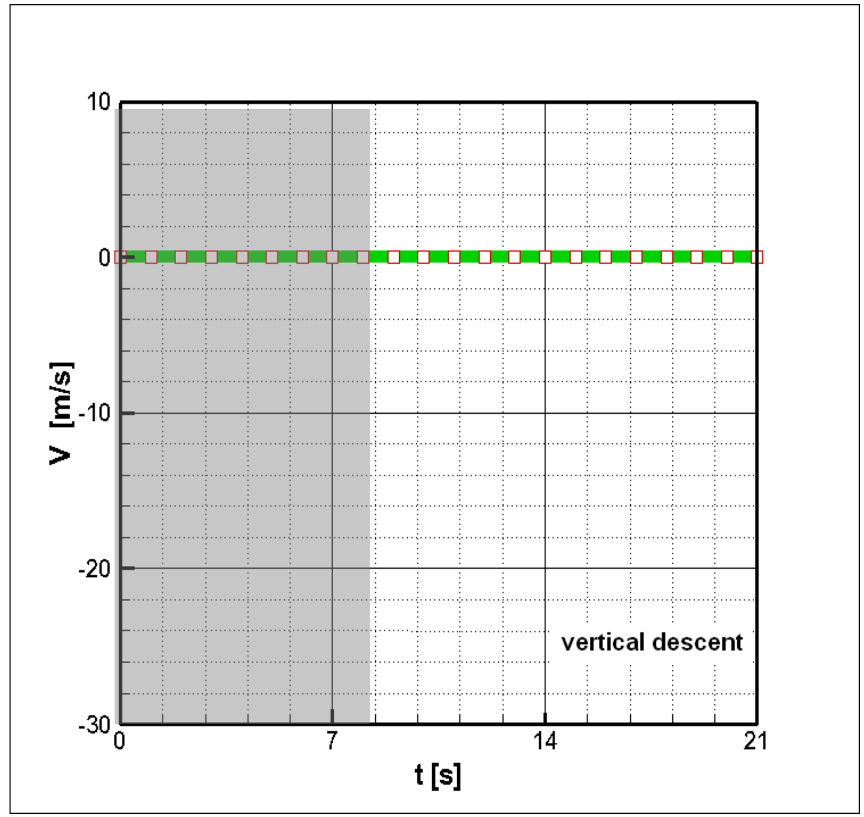

Fig. Airspeed versus time graph

Case II – start case

- *w = -15 m/s*

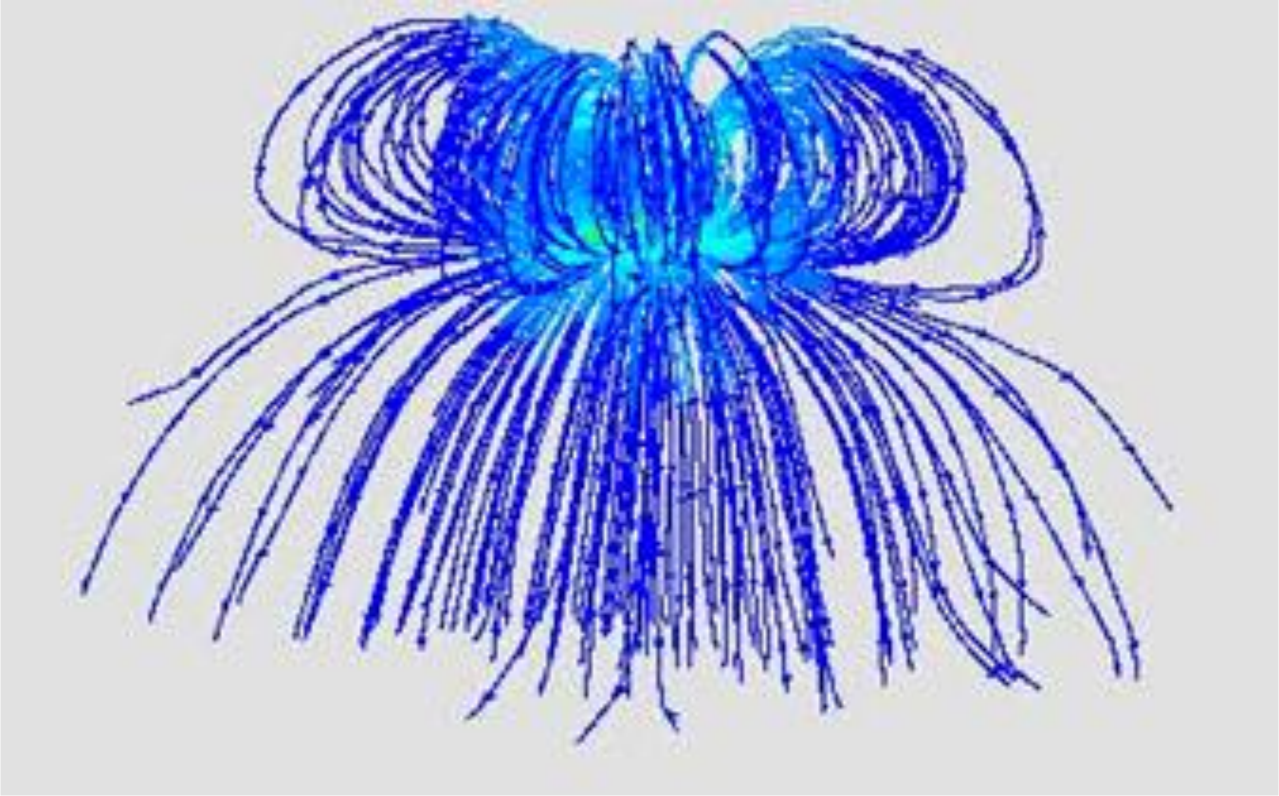

Case II – results

- *w = -15 m/s*

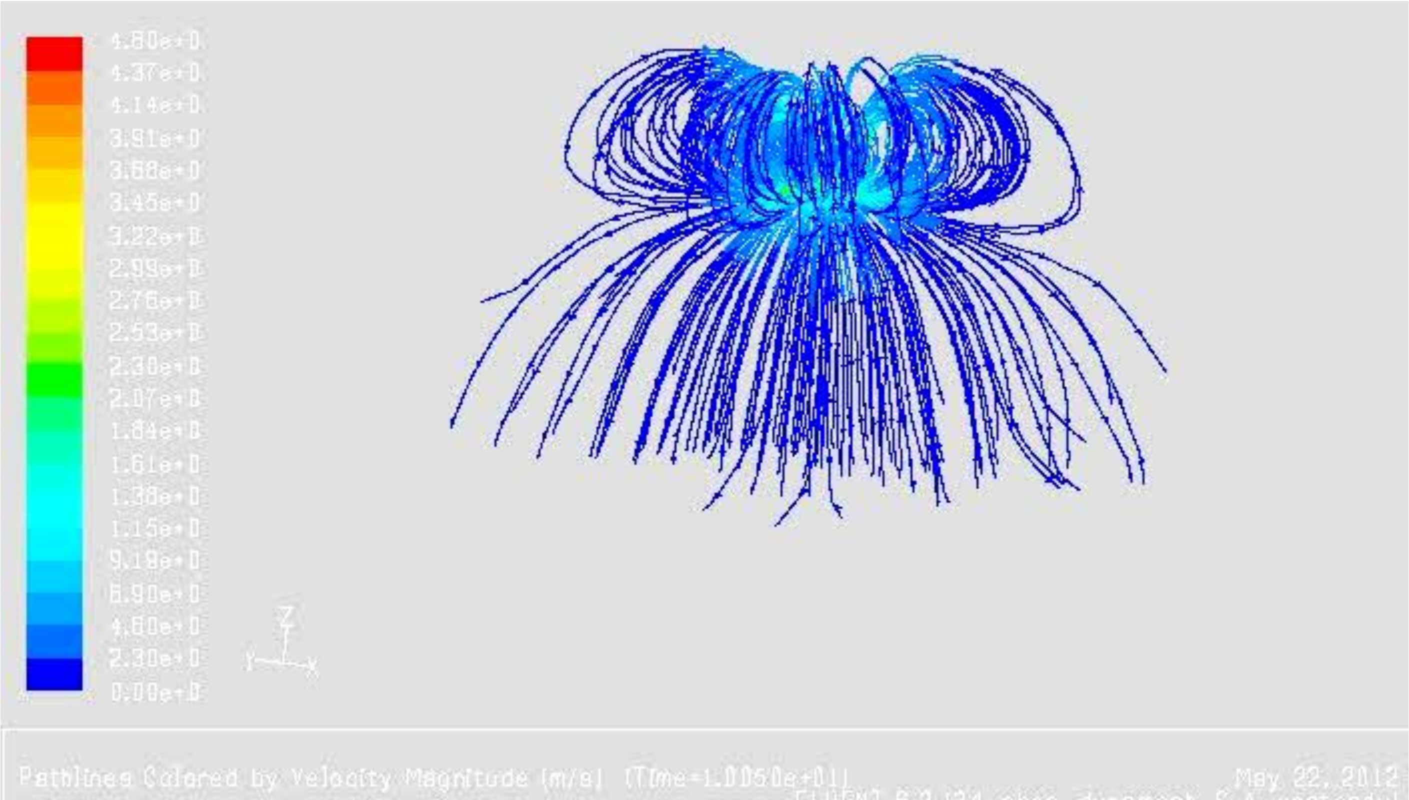

Case III – boundary conditions

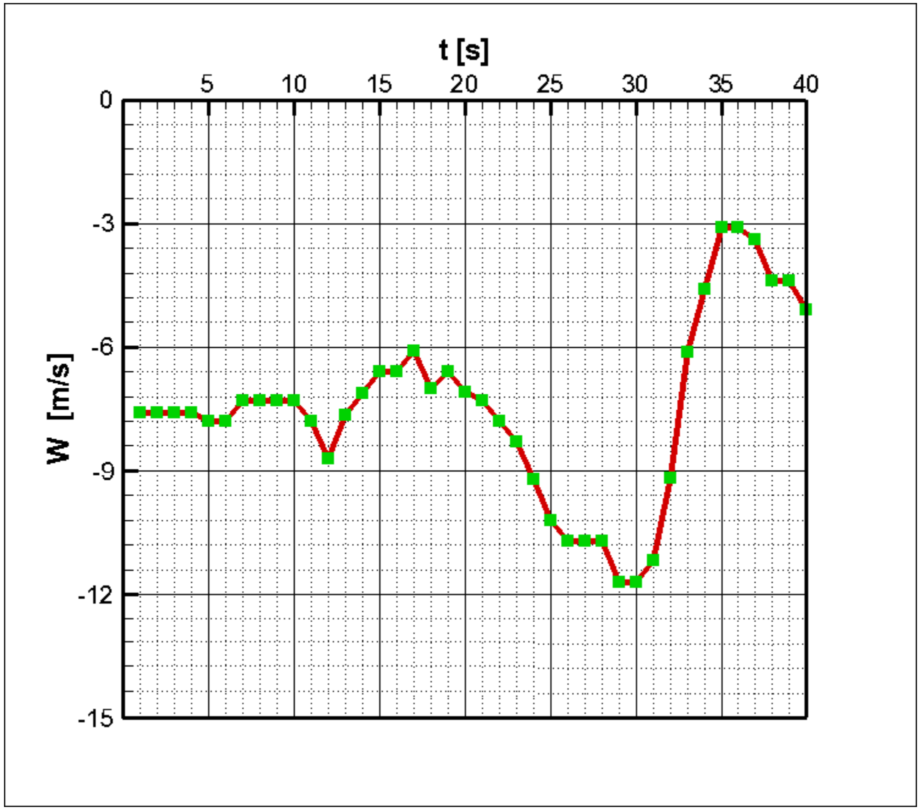

Fig. Velocity descent versus time graph

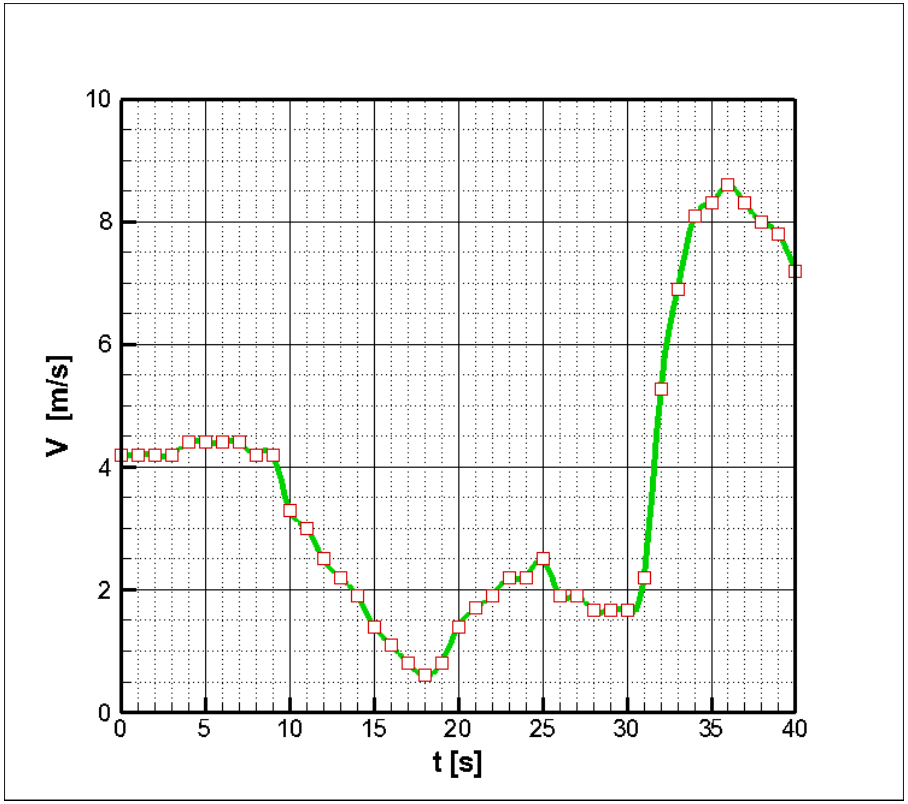

Fig. Airspeed versus time graph

Case III – boundary conditions

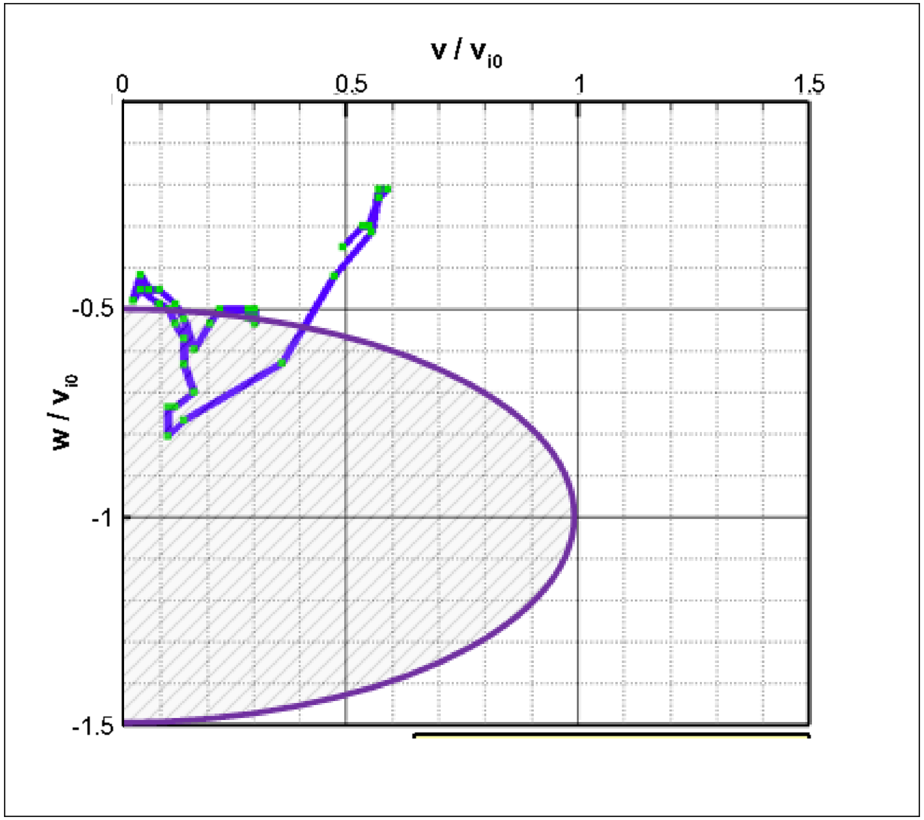

Fig. Velocity descent versus airspeed graph

Case III – boundary conditions

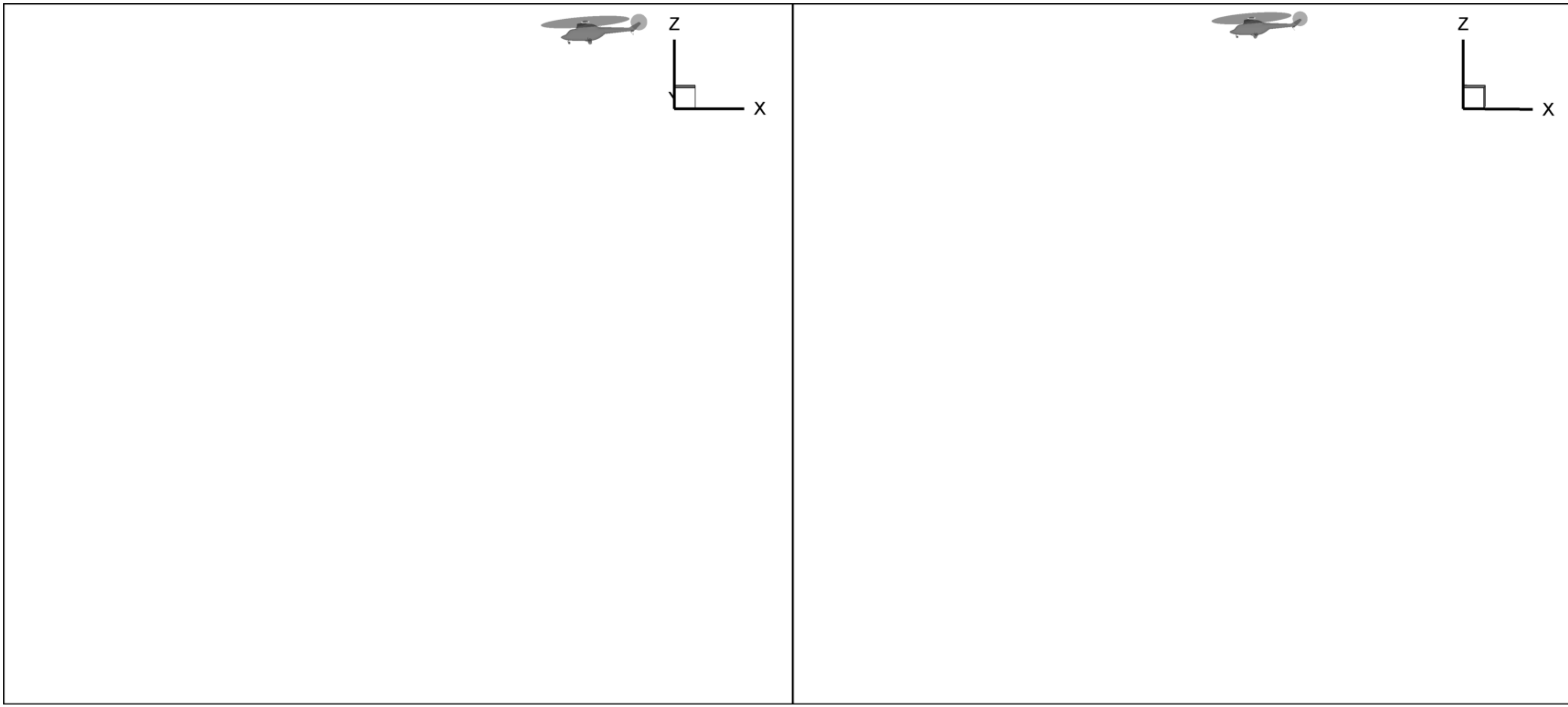

Case III – boundary conditions

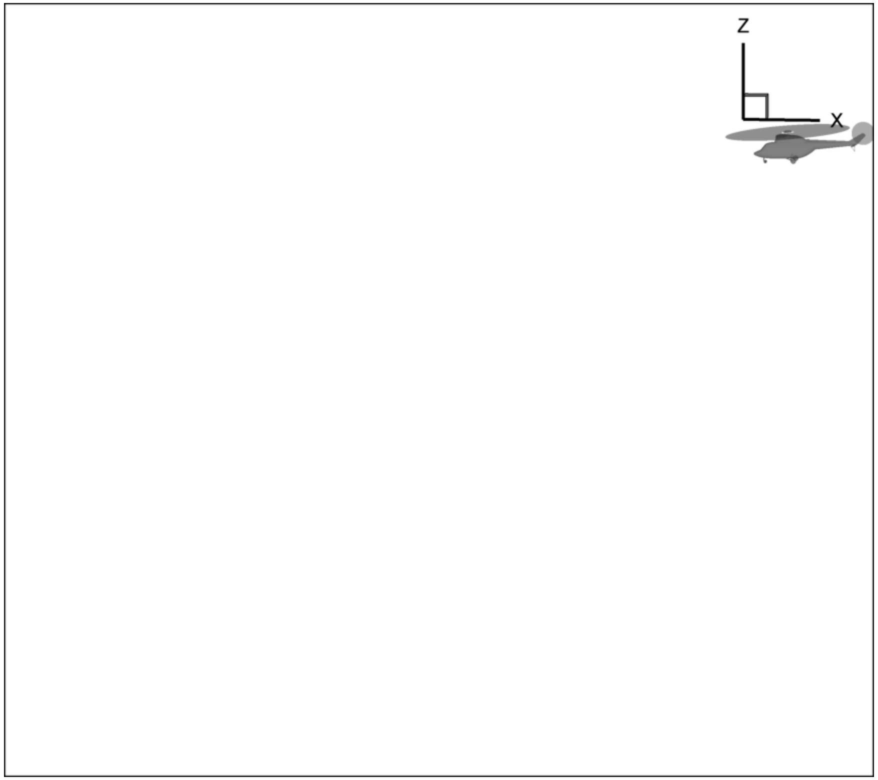

Case III – start case

w = - 7.6 m/s   v = 4.2 m/s

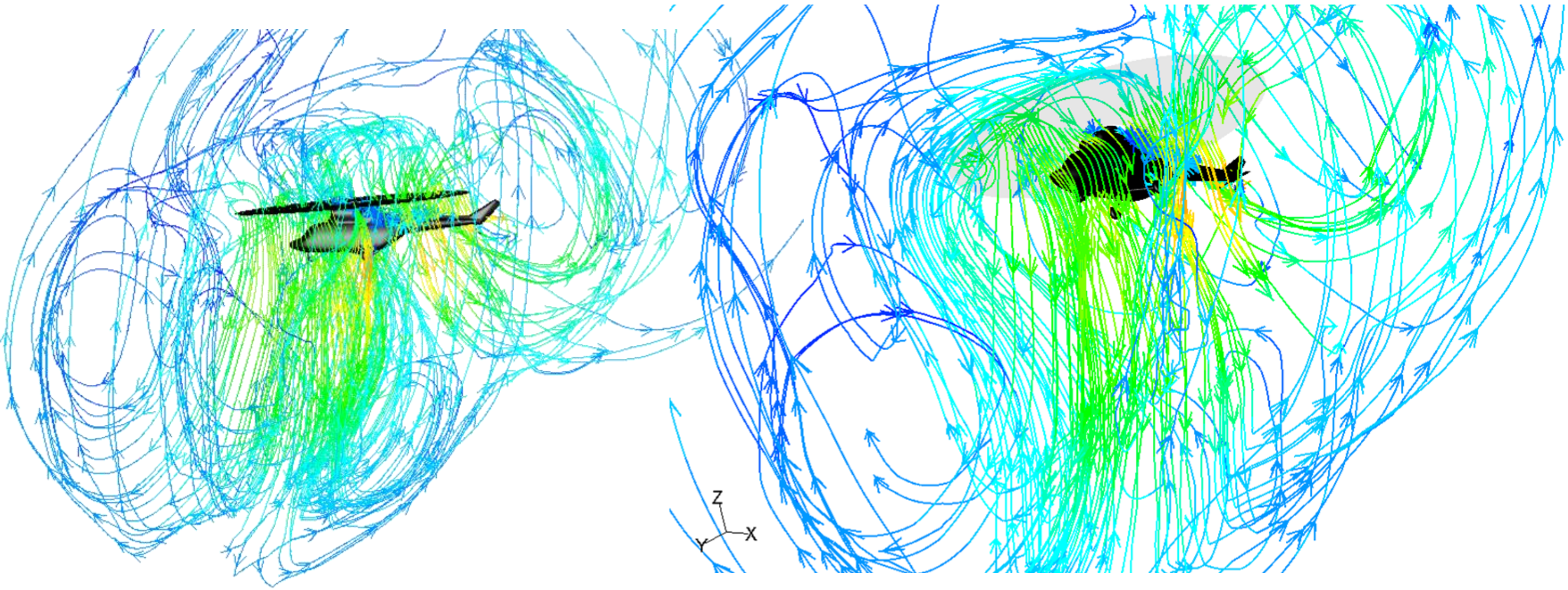

Case III – results

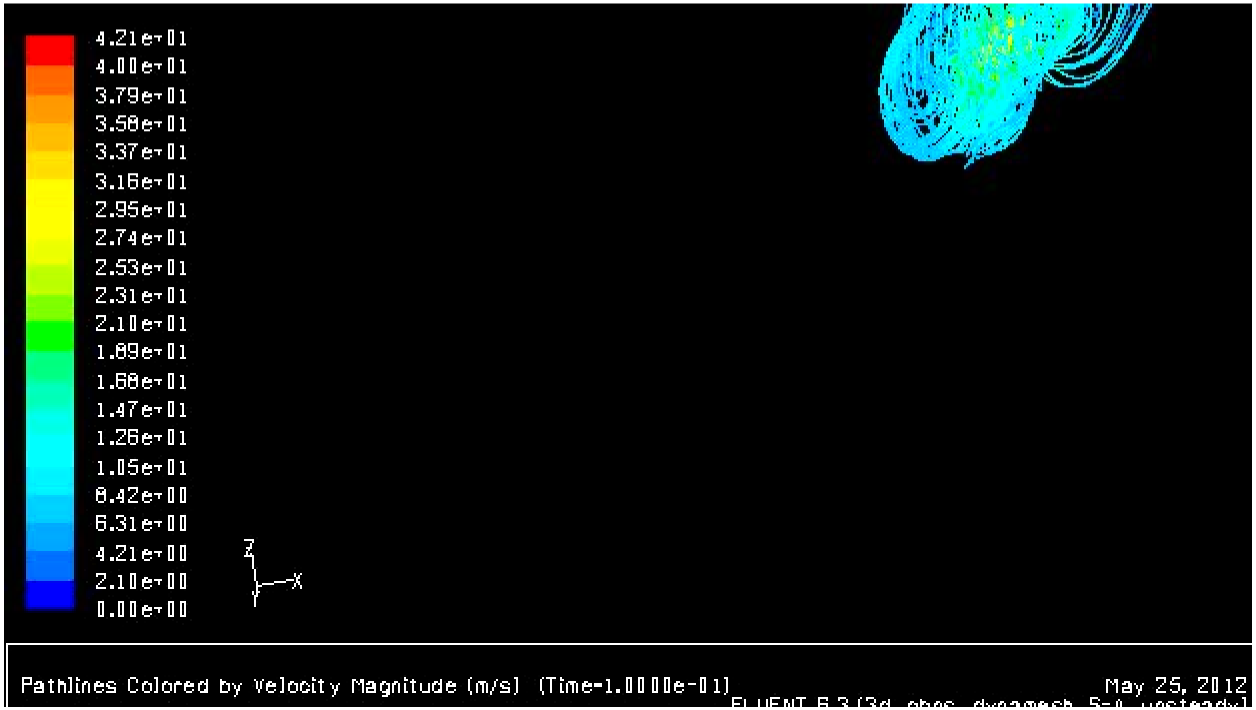

Case III – results

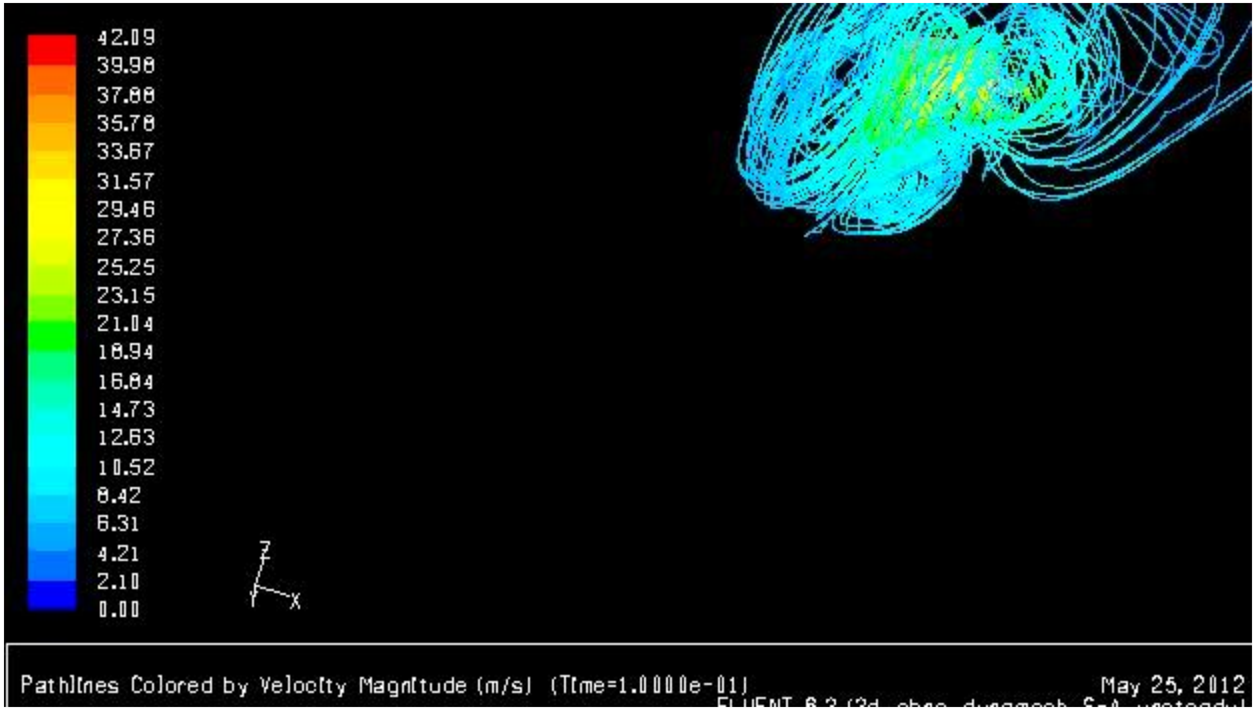

Future work

Experimental investigation

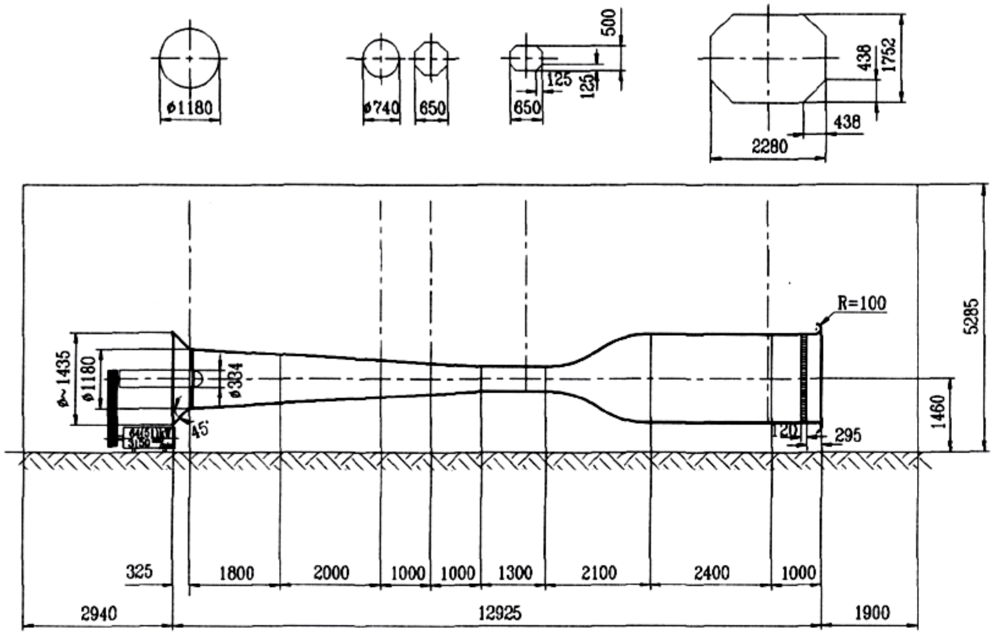

Performance model helicopter:
- ***Main rotor diameter*** ***0,688 [m]***
- ***Blade quantity*** ***2***
- ***Propulsion – electric engine***

Rotor models:

- *FAN model*
- ***V**irtual **B**lade **M**odel (VBM)*
- *Single, multiple reference frame models (SRF - MRF)*
- *Sliding Mesh Model (SMM)*

Virtual Blade Model

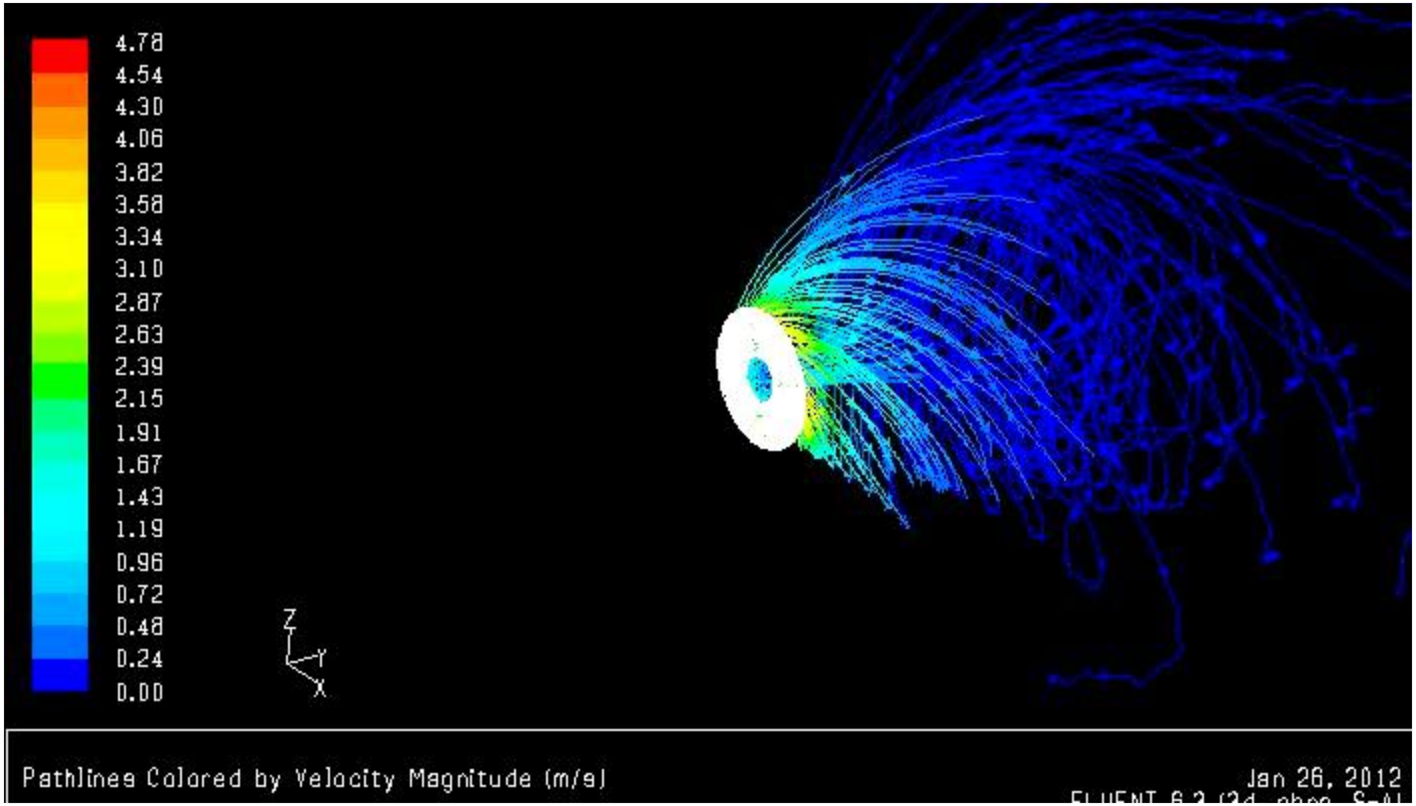

Conclusions

- *A creation and growth the vortex structures depends on rate of descent*
- *In the future computional model will be developed on VBM model*
- *In the future computional model will validate in the experimental invertigation in a wind tunel*

Thank You
for your attention

Katarzyna Grzegorczyk
katarzyna.grzegorczyk@ilot.edu.pl

Optimization of the external nacelle shape for a turboprop engine
(Model Implementation)

Sławomir Kubacki, Łukasz Łaniewski-Wołłk,
Armen Jaworski, Jacek Rokicki

Institute of Aeronautics and Applied Mechanics,
Warsaw University of Technology, Poland

Prague, October 31 – November 2, 2012.

Purpose of work

Testing of the optimization method for two flow problems:

- Laminar flow through the S-bend channel.
Optimization of the channel shape to reduce the pressure drop.

-Turbulent flow over an aircraft (N<1 million).
Optimization of the upper part of the nacelle to reduce the drag force (preliminary results).

Airplane: the optimization problem, parametrization and constraints

- A morphing technique is applied for parametrization of the geometry

- Control points are specified on a selected surface inside the morphing box

- Displacements of the control points along normal to the surface direction is allowed (design parameters)

- The displacements are later distributed among the mesh points by the Radial Basis Method

- The smoothness of the deformation on the borders of the morphing box is ensured

Airplane: the optimization problem, parametrization and constraints

- Definition of the geometric constraints
  - an envelope-geometry consists of simplified engine and exhaust system has been made to impose the geometric constraints,

- Definition of relevant aerodynamic properties
  - design objective - reduced total drag force acting on the airplane surface,
  - unmodified lift force.

Optimization method

Optimization algorithm based on surrogate model can be described in 3 base steps:

0. Select base set of designs using Design of Experiment technique and add them to the data-set.

1. Calculate the objective values for all elements of the data-set.

2. Construct an optimization model.

3. Select new design of a Sampling Criterion, add the design to the data-set and go to 1.

Validation of the optimization tool

First test:

- Laminar flow through S-bend channel,

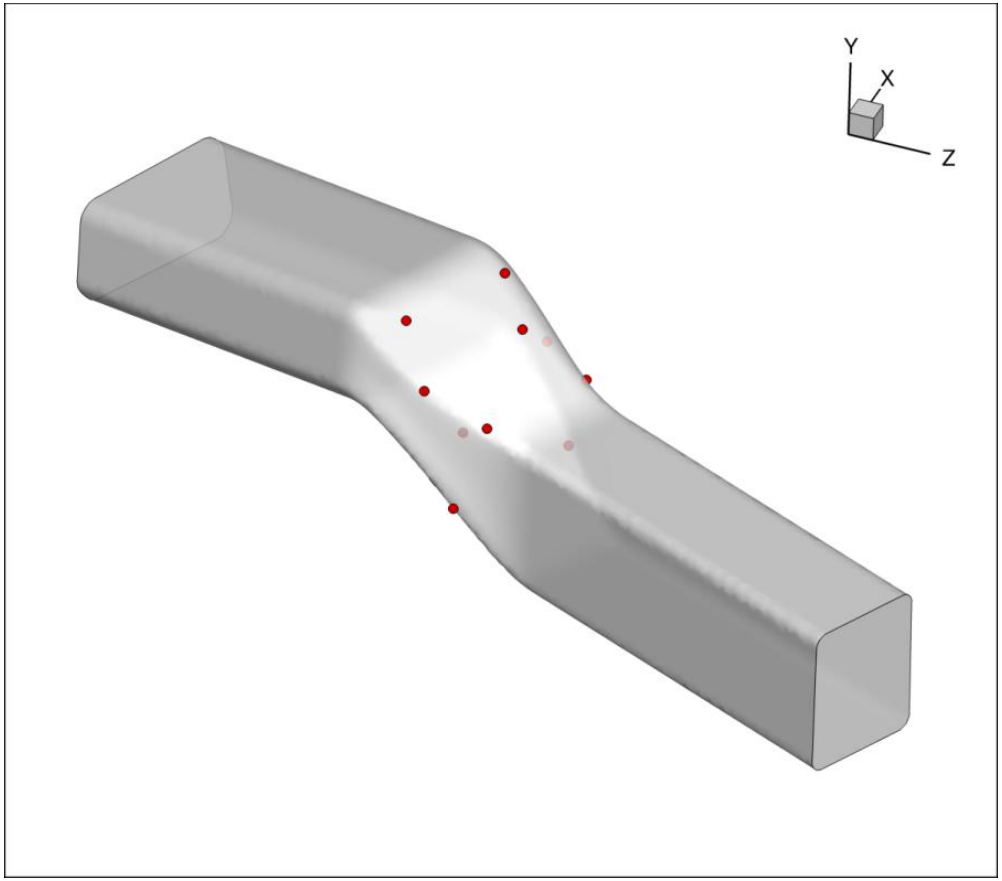

Validation of the optimization tool

First test:

- Good results have been obtained. 17% reduction of the pressure drop

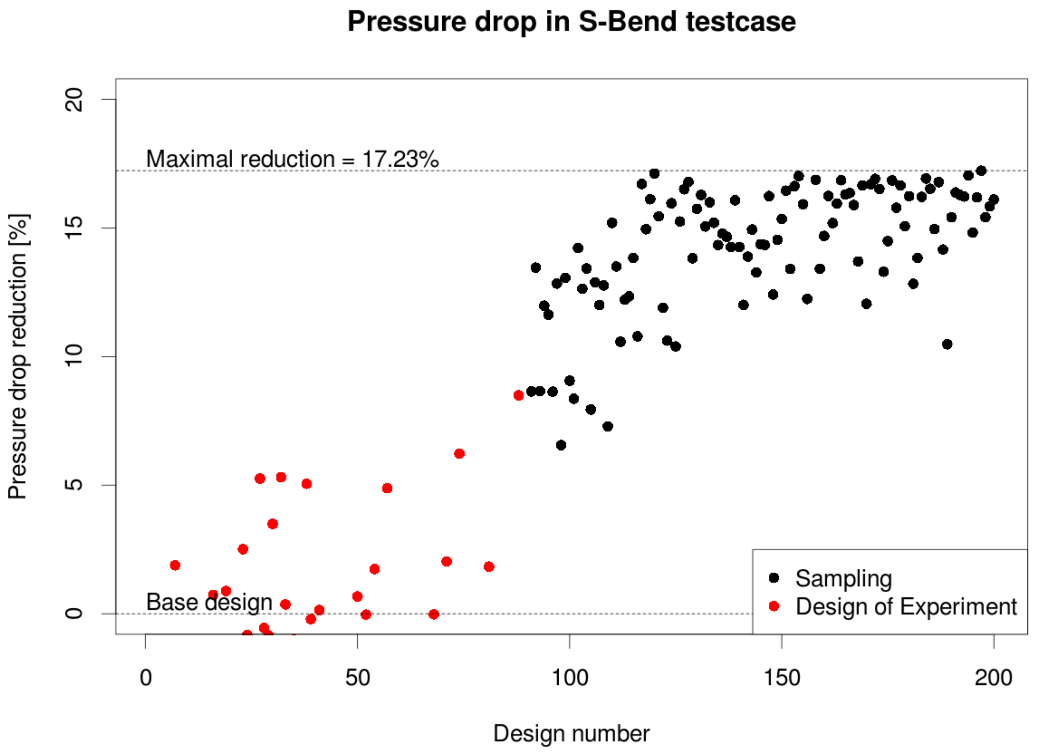

Airplane: RANS

The equations for conservation of mass, momentum and energy

$$\frac{\partial \rho}{\partial t} + \frac{\partial (\rho U_i)}{\partial x_i} = 0$$

$$\frac{\partial (\rho U_i)}{\partial t} + \frac{\partial (\rho U_j U_i)}{\partial x_j} = -\frac{\partial P}{\partial x_i} + \frac{\partial}{\partial x_j}\left(2\mu S_{ij} - \rho\left\langle u_i' u_j'\right\rangle\right)$$

$$\frac{\partial\left(\rho\left(e + \frac{1}{2}U_i U_i\right)\right)}{\partial t} + \frac{\partial\left(\rho U_j\left(h + \frac{1}{2}U_i U_i\right)\right)}{\partial x_j} = \frac{\partial}{\partial x_j}\left(\frac{\mu c_p}{Pr}\frac{\partial T}{\partial x_j} - \rho\left\langle \vartheta' u_j'\right\rangle c_p + U_i\left(2\mu S_{ij} - \rho\left\langle u_i' u_j'\right\rangle\right)\right)$$

Reynolds stress tensor: $-\rho\left\langle u_i' u_j'\right\rangle = \rho\tau_{ij} = 2\mu_t S_{ij} - \frac{2}{3}\rho k \delta_{ij}$

turbulent heat flux: $-\rho\left\langle \vartheta' u_j'\right\rangle = \frac{\mu_t}{Pr_t}\frac{\partial T}{\partial x_j}$

Airplane: Turbulence modelling

The SST k-ω model has been used

- known for its good properties in resolving the attached and separated boundary layers in adverse pressure gradient flows,

- enhanced wall function at walls

$$\frac{\partial(\rho k)}{\partial t}+\frac{\partial(\rho u_j k)}{\partial x_j}=P_k-\beta^* k\omega+\frac{\partial}{\partial x_j}\left[(\mu+\sigma_k\mu_t)\frac{\partial k}{\partial x_j}\right],$$

$$\frac{\partial(\rho\omega)}{\partial t}+\frac{\partial(\rho u_j\omega)}{\partial x_j}=\alpha\rho S^2-\beta\rho\omega^2+2(1-F_1)\frac{\sigma_{\omega 2}}{\omega}\frac{\partial k}{\partial x_j}\frac{\partial\omega}{\partial x_j}+\frac{\partial}{\partial x_j}\left[(\mu+\sigma_\omega\mu_t)\frac{\partial\omega}{\partial x_j}\right].$$

Airplane: computational domain and grid

- Computational domain – sphere with radius R=48.8 m (R equals to 6.5 and 5.5 times the airplane length and span in z- and y-directions, respectively)
- Grid consists of 0.8 million cells
- Boundary layer mesh employed on the major part of the nacelle surface and top part of the fuselage ($y^+ < 150$ on upper part of the nacelle)

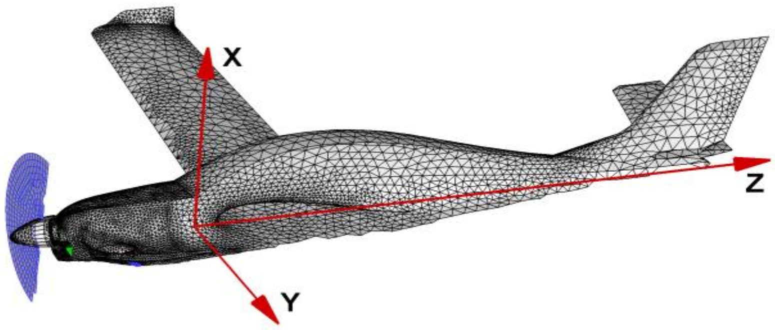

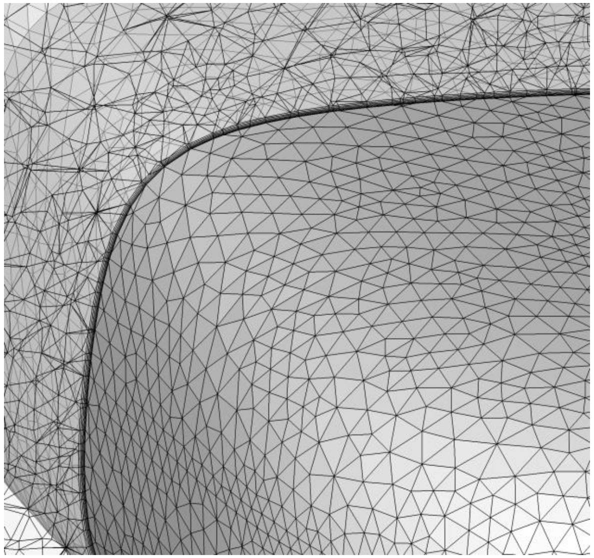

Boundary conditions

Cruise flight at high altitude
(3000 m above the ground, angle of attack: 0 deg)

Name	Boundary type	Mean and turbulent flow conditions	Thermal conditions
Freestream	Pressure far-field	Inlet Mach number: Ma = 0.215 Flow direction: (0, 0, 1) Tu=2%, ν_t/ν=10	Mean temperature: T_∞=269 K
Main air	Mass flow inlet	Mass flow rate: 1.5 kg/sec, Flow direction: outward normal (domain out) Tu=10%, ν_t/ν=100	Mean temperature: T_b = 269K
Auxiliary air	Mass flow inlet	Mass flow rate: 0.6 kg/sec, Flow direction: outward normal (domain out) Tu=10%, ν_t/ν=100	Mean temperature: T_b = 269K
Exhaust gases	Mass flow inlet	Mass flow rate: 0.75 kg/sec, Flow direction: normal to boundary (domain in) Tu=10%, ν_t/ν=100	Mean temperature: T_b = 923K
Airplane surface	Wall (no-slip)	Enhanced wall function	Adiabatic
Particles separator	Wall (no-slip)	Enhanced wall function	Adiabatic

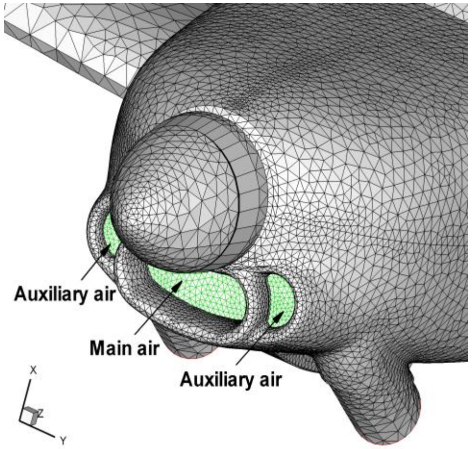

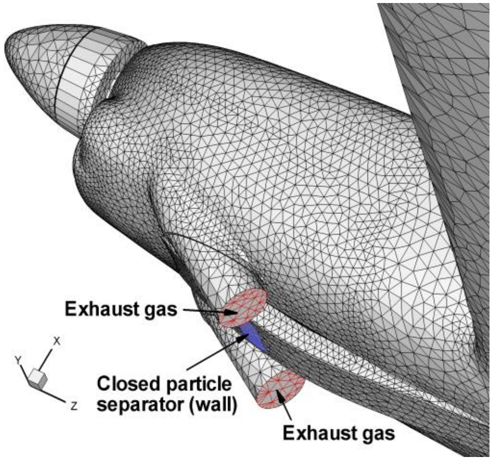

Airplane: Virtual Blade Model

Propeller blades are modelled with actuator disk model
- input data: number of blades, angular velocity, lift and drag coefficients vs. angle of attack etc.
- adjusted blade chords and swift angles to obtain required thrust and engine/propeller power.

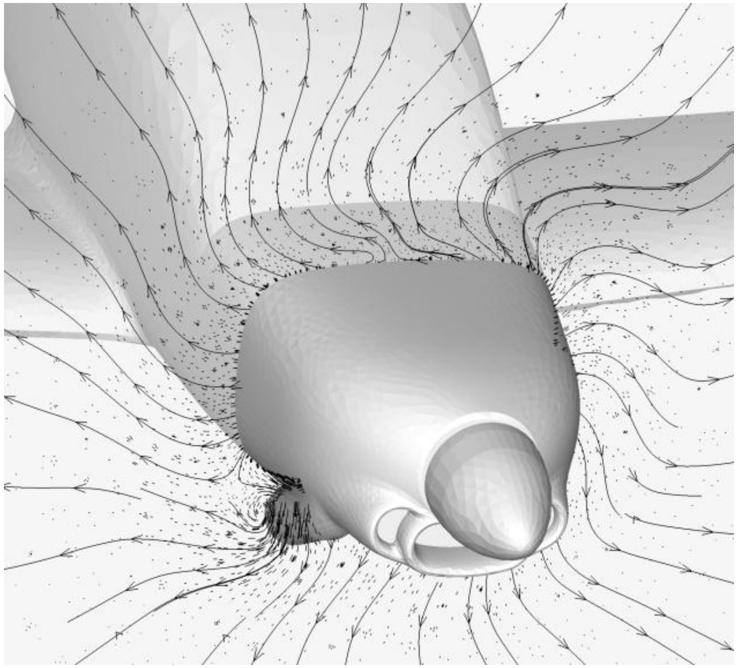

	Target Value	Computed Value	Relative error
Thrust	1100 [N]	1170 [N]	6.4 %
Engine/Propeller power	120 000 [W]	124 900 [W]	4.1 %

Airplane and morphing box

Upper part of the nacelle shape optimization
- control points were selected on the upper part of nacelle inside the morphing box,
- a smoothness of deformations at the borders of the morphing box was ensured.

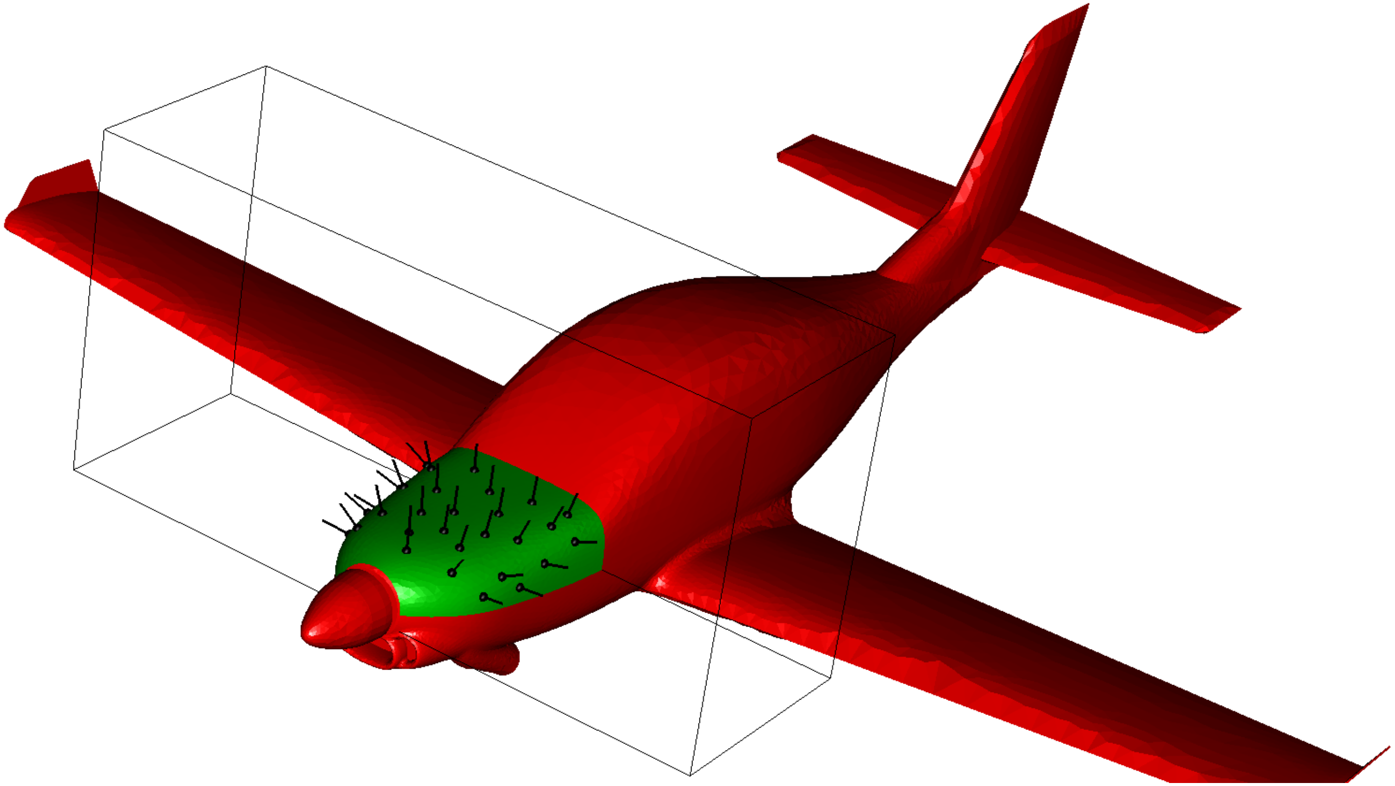

Geometric constraints

Upper part of the nacelle shape optimization

- allowed deformation of the nacelle (green surface) was constrained by surface points located on the envelope-geometry (meshed surface) consists of a simplified engine and exhaust system with an additional safety offset (11 mm),

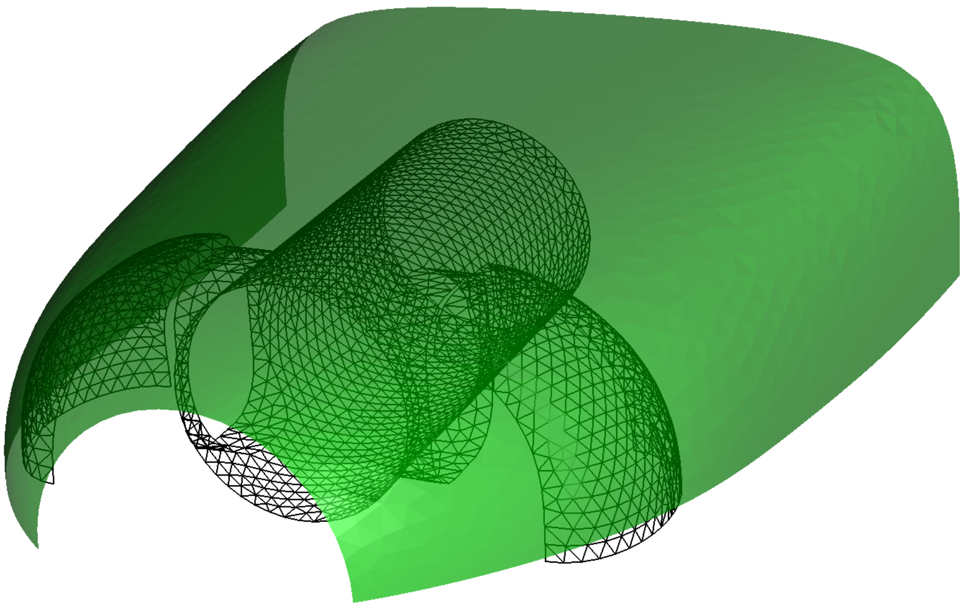

Constraint on the lift force

- A lift force reduction was not allowed,

- The lift force on the modified airplane geometry was compared with the value for the baseline geometry.

Observation (baseline geometry)

- A limited contribution of the total force exerted on the upper part of the nacelle to the total drag force acting on the airplane
- It might be difficult to steer the total drag force by changing only the upper part of the nacelle

	Total force [N]	Force acting tangential to the surface [N]	Pressure force [N]
Airplane surface	1438.2	166.1	1272.0
Nacelle upper	-8.5	14.9	-23.4
Rest of the airplane surface	1446.6	151.2	1295.5

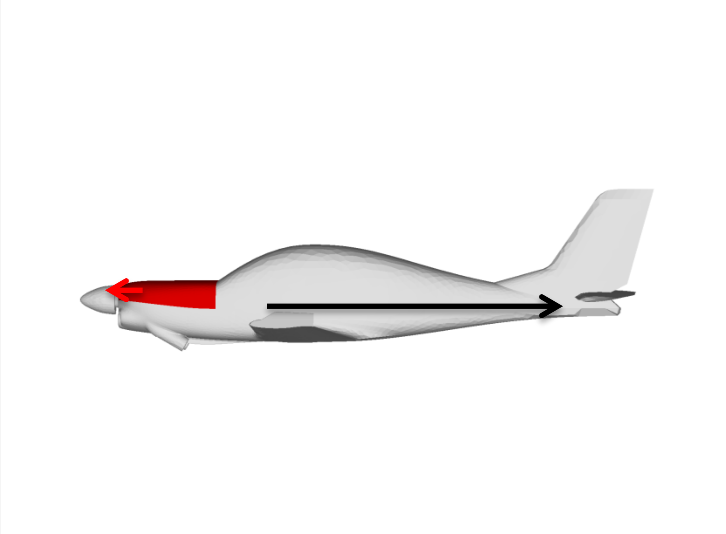

$|F_{\text{nacelle top}}/F_{\text{airplane}}| = 0.6\%$

First results

No significant differences on the contour plots of pressure coefficient

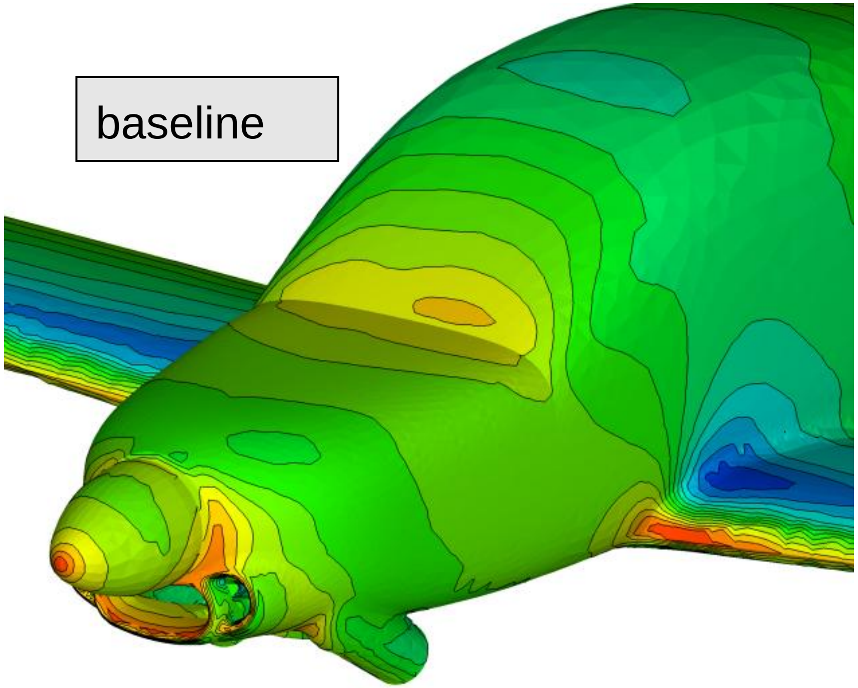

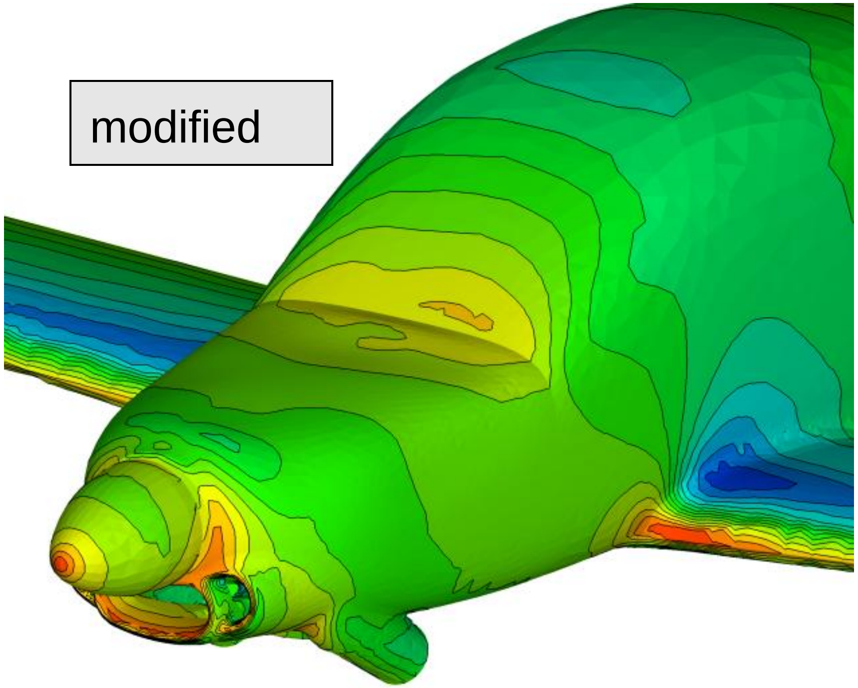

First results

- Small differences on the skin friction distribution (absolute value)
- Low momentum fluid along the geometrical symmetry plane – flow prone to separation

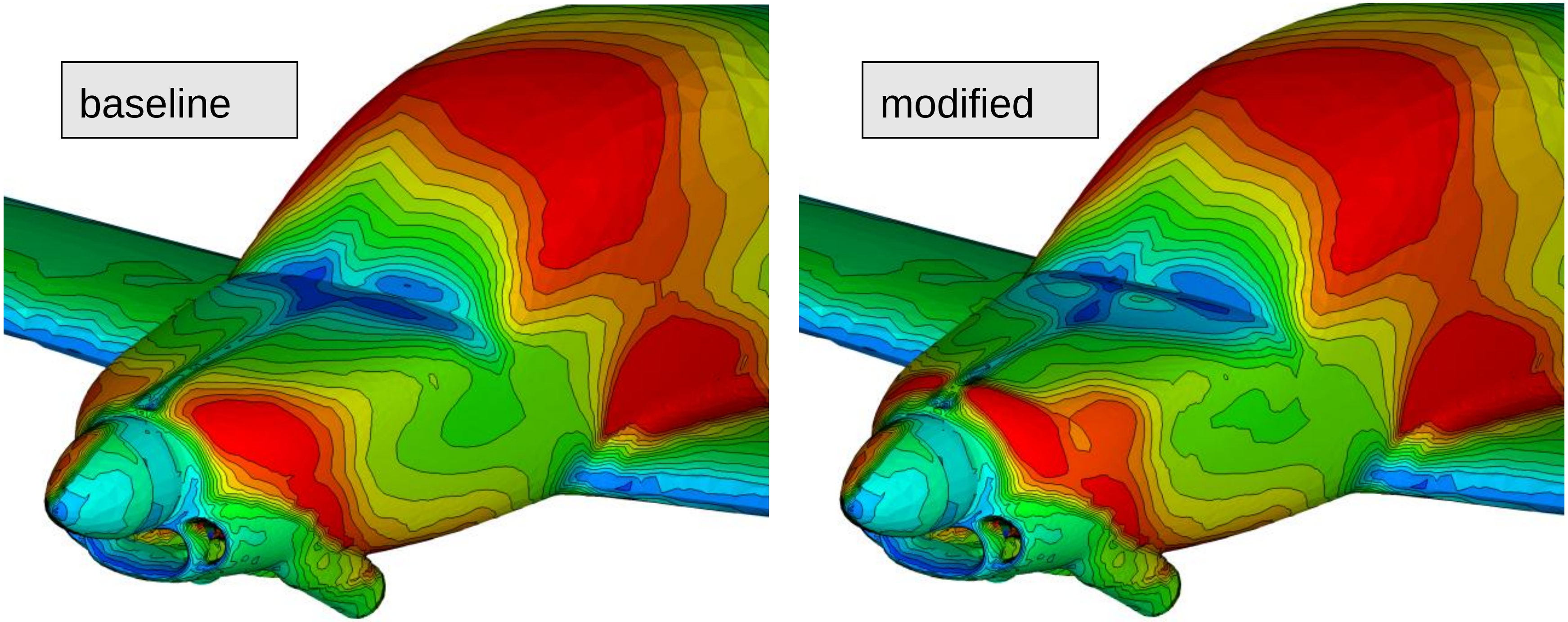

First results

Flow details on the rear part of the nacelle

- Small separation bubble is recovered close to the pilot cabin
- Modified nacelle surface tries to follow more closely the streamlines

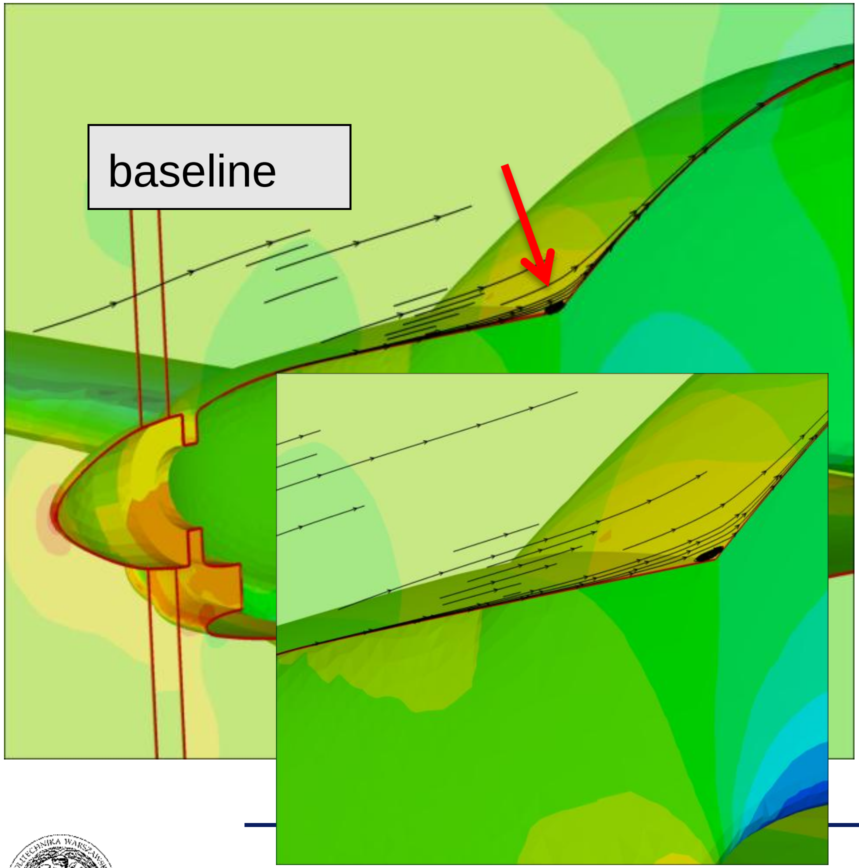

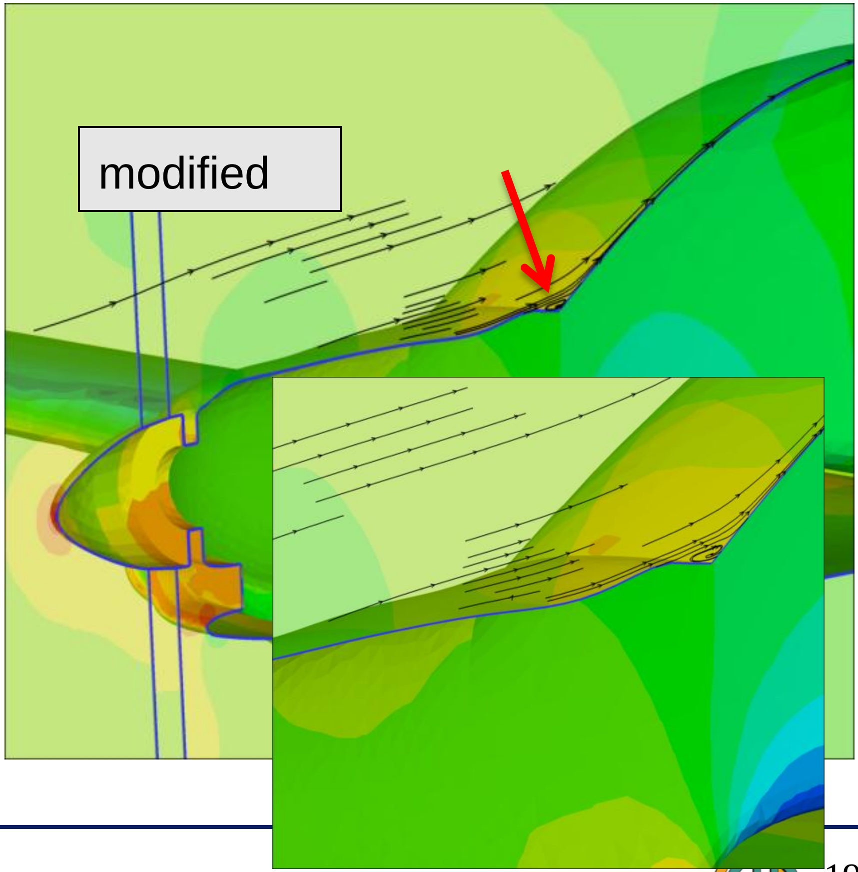

Flow details close to the corner

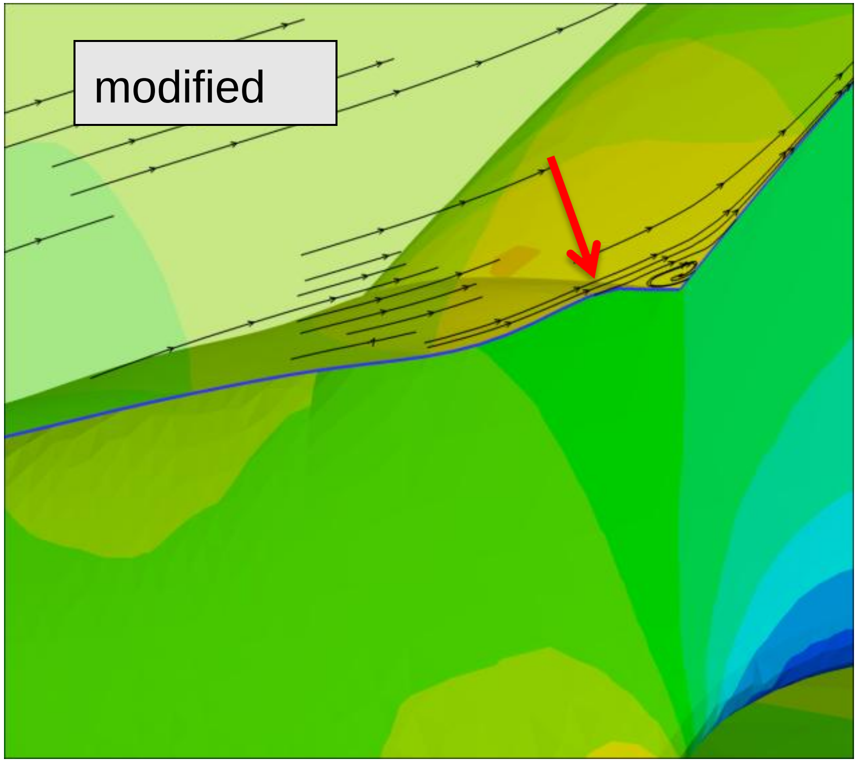

<u>Opposing effects</u>

- Optimisation algorithm tries to smooth out the geometry close to the corner
  (push a high momentum fluid towards the pilot cabin),
  but at the same time
- the nacelle shape cannot be modified there (geometric constraints)

Global result for the airplane

0.6 % reduction in the total drag force acting on the airplane has been obtained

with less than 0.1% increase in the lift force on the modified geometry

We have to take into account a small contribution of the force acting on the upper part of the nacelle to the total drag force acting on the airplane ($|F_{nacelle\ top}/F_{airplane}| = 0.6\%$) !

Summary

- A coupling of the optimization method with the flow solver has been successfully realised

- Very good results have been obtained for optimization of the S-bend channel shape (17% reduction of the pressure drop)

- For the airplane, an improvement in the drag force reduction is relatively small (0.6 %).

Next steps

- An influence of the grid density on the CFD results has to be verified !

- This has to be done together with a simplication of the airplane geometry (limited computer resources). Further analysis will be restricted to the nacelle and a part of the pilot cabin.

The overall quality of the CFD results will improve. This might have a significant effect on final optimization results.

<u>It might be useful to perform this analysis together with a modification of the bottom part of the nacelle using a CAD-based parametrization.</u>

EXPERIMENTAL AND NUMERICAL INVESTIGATION OF A SWIRL STABILIZED PREMIXED METHANE/AIR FLAME

2nd EASN AssociationWorkshop on Flight Physics and Propulsion

Oct 31 – Nov 2, 2012

Onur Tunçer[1], Bertan Kaynaroğlu[2]

[1] Istanbul Technical University, Dept. of Aeronautical Engineering

[2] Istanbul Technical University, Dept. of Aerospace Engineering

Content

Swirl Flows

- Swirl stabilized flames are utilized in a wide range of applications such as gas turbine engines, furnaces, gasifiers, and boilers.
- Sufficient swirling strenght produces large adverse pressure gradient in the streamwise direction , that leads to vortex breakdown and flow reversal.
- The resultant recirculation zone, carries back towards the dump plane of the combustor hot combustion products and free radicals, which act as a stabilizing source for the flame.
- Swirl stabilized combustors have substantial advantages in terms of improved combustion efficiency, better ignition stability, and reduced pollutant emissions.
- These benefits are believed to be the consequence of increased mixing rates due to enhanced turbulence levels.

Swirl Flows – Cont'd

- Gaseous fuel is burnt under lean equivalence ratios. This approach is known as lean premixed combustion.

- It is a well established technology in land based power generation gas turbines for achieving low NOx emissions.

- Although this method is being used for several decades fundamental understanding of flame turbulence interaction is still not satisfactory.

Swirl Flows – Cont'd

- Combustion test rig works on flamelet regime
  - Assuming the reaction layer thickness is smaller than the smallest turbulence scales
- 2 popular models
  - Flame surface density model (Hawkes and Cant, 2001)
  - G-equation model (Williams, 1985; Peters, 2000)
- Another family of model
  - Partial Density Function (PDF) approach (Pope,1985)

Borghi-Peters Diagram for Premixed Flames

- In premixed flames combustion is strongly influenced by interactions between turbulent flow and reaction.

Gas turbine

Otto engine

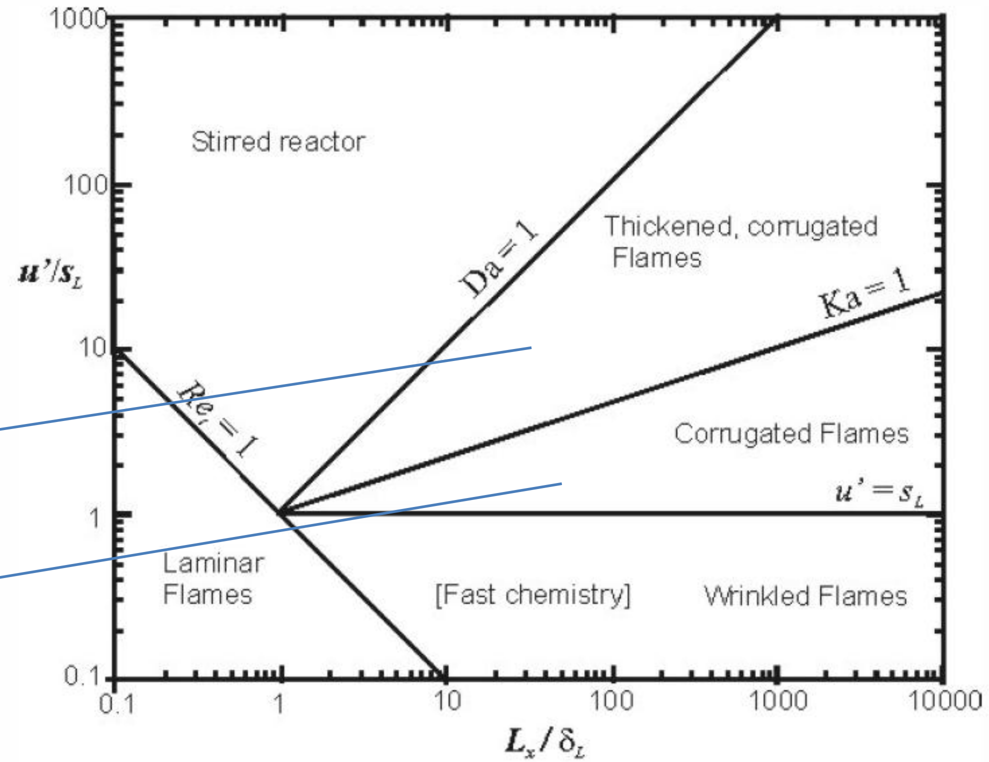

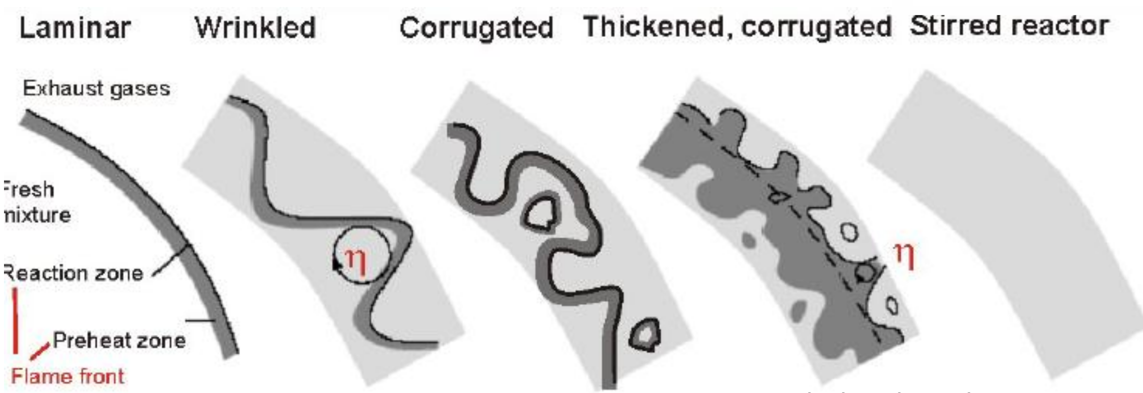

Borghi-Peters Diagram

$$\mathrm{Re}_t = \frac{u' L_x}{\nu} \qquad Da = \frac{\tau_t}{\tau_c} \qquad Ka = \left(\frac{\delta_L}{\eta}\right)^2$$

Particle Image Velocimetry (PIV)

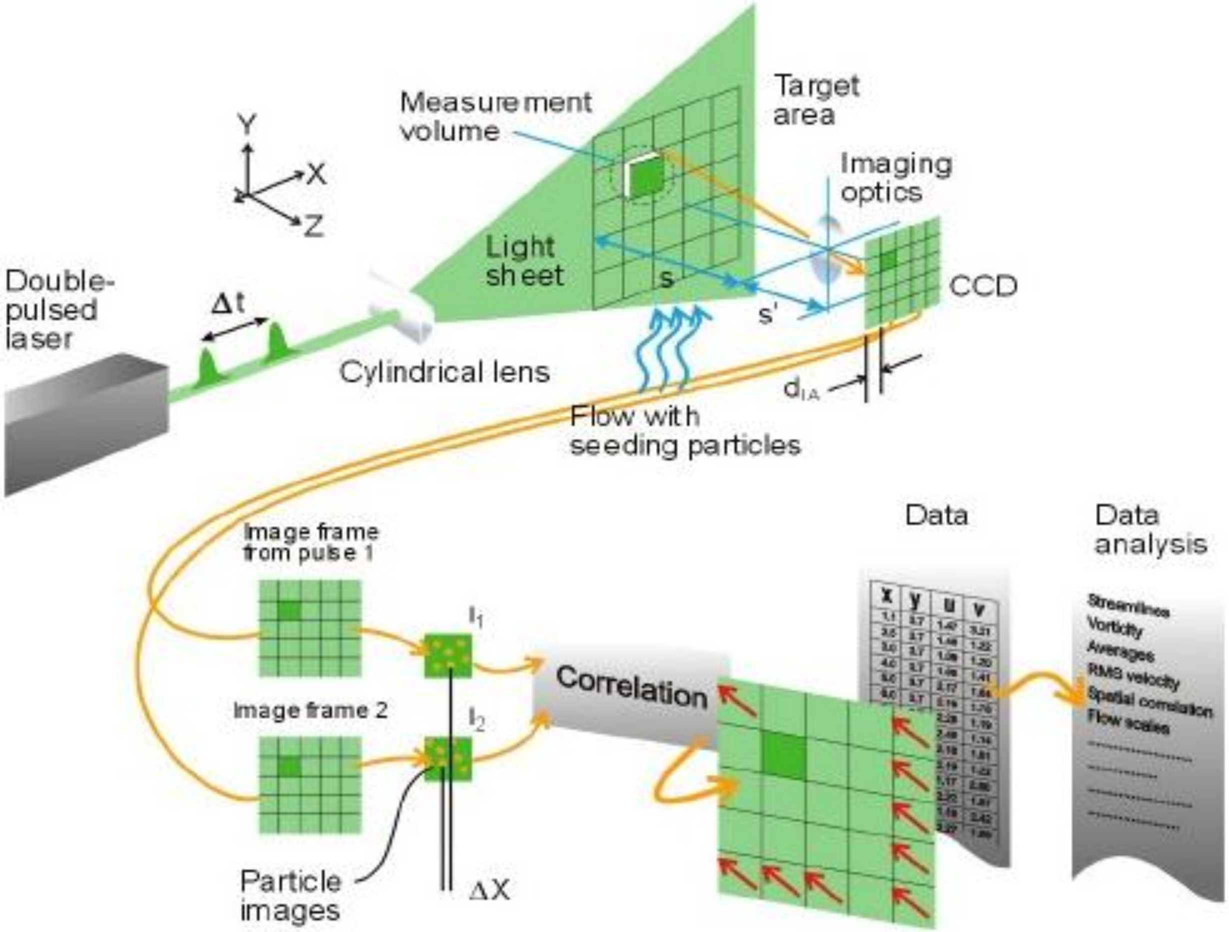

PIV Diagram

Particle Image Velocimetry (PIV) Components

- **Nd-YAG Laser;**
  - ✓ Double cavity
  - ✓ 15 Hz Pulse frequency
  - ✓ 120 mJ at 532 nm
  - ✓ $\pm$ 4% Energy stability
  - ✓ 5 nm Pulse width

- **Camera;**

✓ 2 different types of CCD camera,

  - ✓ Camera 1;
  - ❖ 1600*1200 pixel resolution
  - ❖ 1/14,000 Shutter Speed
  - ✓ Camera 2;
  - ❖ 1344*1024 pixel resolution
  - ❖ 12 bit at 12.2 Hz

- **Seeder**
  - ✓ TiO_2 particles

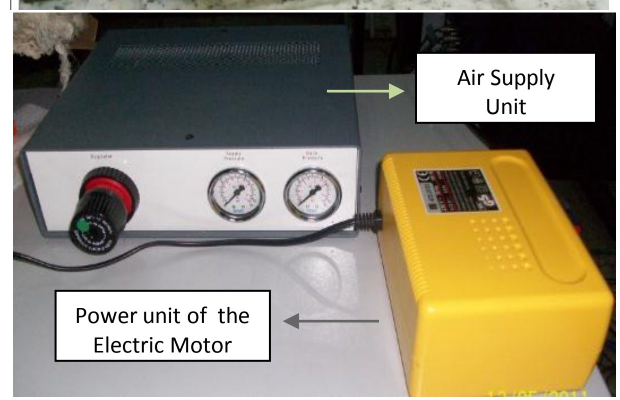

Experimental Setup

- A fully pre-mixed swirl stabilized atmospheric combustor test rig is built under the grant of Aeronautics and Astronautics Engineering Dep. of ITU.
- This laboratory scale combustor can be fired up to 30 kW of thermal power.

Combustion Laboratory

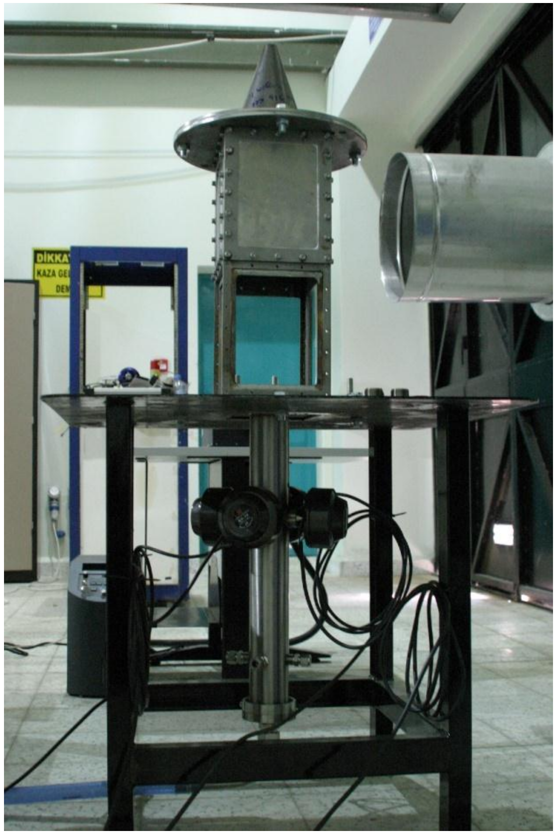

Experimental Test Rig

Experimental Setup – Cont'd

- Swirl vane has 8 blades at an angle of 45 degrees with respect to oncoming flow.
- A conventional type swirler.
- The inner and outer radii of the swirl vane blades are 20 mm and 50 mm respectively.
- Assuming
  - axial and azimuthal velocities are uniform
  - infinitely thin blades

$$S = \frac{2}{3}\left[\frac{1-(R_i/R_o)^3}{1-(R_i/R_o)^2}\right]\tan\varphi \qquad (2)$$

- Swirl number is 0.74.

Top View of Swirl Vane and Center Body Flame Holder

Mathematical Modeling

$$\frac{\partial \bar{\rho}}{\partial t} + \frac{\partial}{\partial x_j}\left(\bar{\rho}\tilde{u_j}\right) = 0.$$

$$\frac{\partial}{\partial t}\left(\bar{\rho}\tilde{u_i}\right) + \frac{\partial}{\partial x_j}\left(\bar{\rho}\tilde{u_i}\tilde{u_j}\right) = -\frac{\partial \bar{P}}{\partial x_j} + \frac{\partial}{\partial x_j}\left(\mu_{eff}\left(\frac{\partial \tilde{u_i}}{\partial x_j} + \frac{\partial \tilde{u_j}}{\partial x_i}\right) - \frac{2}{3}\mu_{eff}\left(\frac{\partial \tilde{u_l}}{\partial x_l}\right)\delta_{ij}\right).$$

$$\mu_{eff} = \mu + \mu_t.$$

$$\bar{P} = \bar{\rho} R(\tilde{Y_m})\tilde{T}.$$

R(Y$_m$) : Gas constant for the mixture

- Menter's *k-ω* SST (shear stress transport) model is used

$$\frac{\partial(\bar{\rho}k)}{\partial t} + \frac{\partial(\bar{\rho}\tilde{u_j}k)}{\partial x_j} = P_k - \beta^* \bar{\rho} k\omega + \frac{\partial}{\partial x_j}\left[\left(\mu + \frac{\mu_t}{\sigma_{k3}}\right)\frac{\partial k}{\partial x_j}\right].$$

$$\frac{\partial(\bar{\rho}\omega)}{\partial \omega} + \frac{\partial(\bar{\rho}\tilde{u_j}\omega)}{\partial x_j} = \alpha_3 \frac{\omega}{k} P_k - \beta_3 \bar{\rho}\omega^2 + \frac{\partial}{\partial x_j}\left[\left(\mu + \frac{\mu_t}{\sigma_{\omega 3}}\right)\frac{\partial \omega}{\partial x_j}\right] + (1 - F_1) 2\bar{\rho}\sigma_{\omega 2}\frac{1}{\omega}\frac{\partial k}{\partial x_j}\frac{\partial \omega}{\partial x_j}.$$

Mathematical Modeling – Cont'd

- Production of turbulent kinetic energy

$$P_k = \mu_t \left(\frac{\partial \tilde{u_i}}{\partial x_j} + \frac{\partial \tilde{u_j}}{\partial x_i} \right) \frac{\partial \tilde{u_i}}{\partial x_j} - \frac{2}{3} \delta_{ij} \left(\bar{\rho} k + \mu_t \frac{\partial \tilde{u_k}}{\partial x_k} \right) \frac{\partial \tilde{u_i}}{\partial x_j}.$$

$$\Phi_3 = F_1 \Phi_1 + (1 - F_1) \Phi_2.$$

Modeling Constants for the k-ω SST Turbulence Model

α_1	α_2	β_1	β_2	β^*	σ_{k1}	σ_{k2}	$\sigma_{\omega 1}$	$\sigma_{\omega 2}$
5/9	0.44	3/40	0.0828	0.09	2	1	2	0.856

$$\nu_t = \frac{a_1 k}{max(a_1 \omega,\ SF_2)}.$$

$$\mu_t = \rho \nu_t.$$

Mathematical Modeling – Cont'd

$$S = \sqrt{\left(\frac{\partial \tilde{u}_i}{\partial x_j} + \frac{\partial \tilde{u}_j}{\partial x_i}\right)\frac{\partial \tilde{u}_i}{\partial x_j}}.$$

$$F_1 = \tanh(arg_1^4).$$

Blending function

$$arg_1 = min\left(max\left(\frac{\sqrt{k}}{\beta^* \omega y},\ \frac{4\rho\sigma_{\omega 2} k}{CD_{k\omega} y^2}\right)\right).$$

$$CD_{k\omega} = max\left(2\rho\sigma_{\omega 2}\frac{1}{\omega}\frac{\partial k}{\partial x_j}\frac{\partial \omega}{\partial x_j},\ 1.0 \times 10^{-10}\right).$$

$$F_2 = \tanh(arg_2^2).$$

$$arg_2 = max\left(2\frac{\sqrt{k}}{\beta^* \omega y},\ \frac{500\nu}{y^2 \omega}\right).$$

Combustion Modeling

- Before ignition fuel and oxidizer mixed in a molecular level
- Turbulence wrinkles and streches the laminar flame sheet that increases its area
- Large turbulent eddies tend to wrinkle and corrugate the flame sheet
- CH_4+ 2(O_2+3.76N_2) → CO_2+2H_2O
- Progress variable (c)
  - Fresh gas = 0
  - Burned gas = unity
  - Can be set by temperature or reactant mass fraction

$$\tilde{c} = \frac{\tilde{T} - T_f}{T_b - T_f}.$$

Combustion Modeling – Cont'd

$\tilde{b} = 1 - \tilde{c}.$ Regression variable

- The transport equation for the regression variable b (Weller and Tabor,2004)

$$\frac{\partial}{\partial t}(\bar{\rho}\tilde{b}) + \frac{\partial}{\partial x_j}(\bar{\rho}\tilde{u_j}\tilde{b}) - \frac{\partial}{\partial x_j}\left(\frac{\mu_t}{Sc_t}\frac{\partial \tilde{b}}{\partial x_j}\right) = -\bar{\rho}S_c.$$

$\Xi = S_t/S_u$ dimensionless wrinkling factor

$$\rho S_c = \rho_u \Xi \sqrt{\left(\frac{\partial b}{\partial x_l}\right)\left(\frac{\partial b}{\partial x_l}\right)}.$$

$$\frac{\partial}{\partial t}(\bar{\rho}\tilde{b}) + \frac{\partial}{\partial x_j}(\bar{\rho}\tilde{u_j}\tilde{b}) - \frac{\partial}{\partial x_j}\left(\frac{\mu_t}{Sc_t}\frac{\partial \tilde{b}}{\partial x_j}\right) = \rho_u \Xi \sqrt{\left(\frac{\partial b}{\partial x_j}\right)\left(\frac{\partial b}{\partial x_j}\right)}.$$

Combustion Modeling – Cont'd

- Equilibrium value for the wrinkling factor Ξ

$$\Xi_{eq} = 1 + 2(1-b)(\Xi_{eq}^{*} - 1).$$

$$\Xi_{eq}^{*} = 1 + 0.62\sqrt{\frac{u'}{S_u}}R_{\eta}.$$

- Laminar flame speed;
  - Gülder's laminar flame speed correlation

$$S_u = W\phi^{n} exp[-\xi(\phi - 1.075)^2]\left(\frac{T}{T_{ref}}\right)^{\alpha}\left(\frac{P}{P_{ref}}\right)^{\beta}.$$

Parameter	Value
W	0.422
n	0.15
Ξ	5.18
α	2.0
β	-0.5

Experimental Results

Visible light emission from the flame, $Re_{Dh} = 19400, Sw = 0.74$, $\phi = 0.7$

Experimental Results – Cont'd

Double exposure of Mie Scattering Images of Cold Flow

(Δt= 30 µs)

a. Frame 1

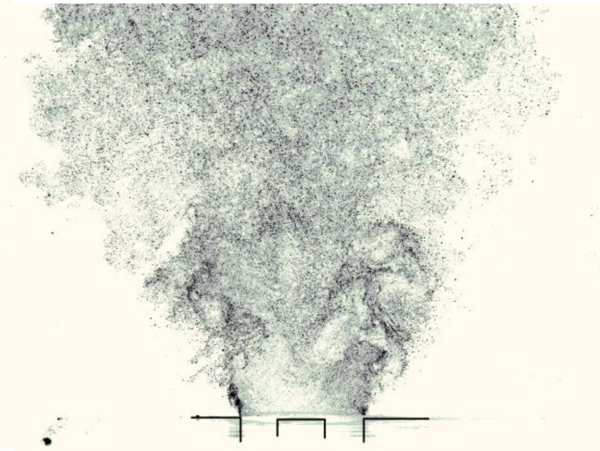

b. Frame 2

Double exposure of Mie Scattering Images of Reacting Flow

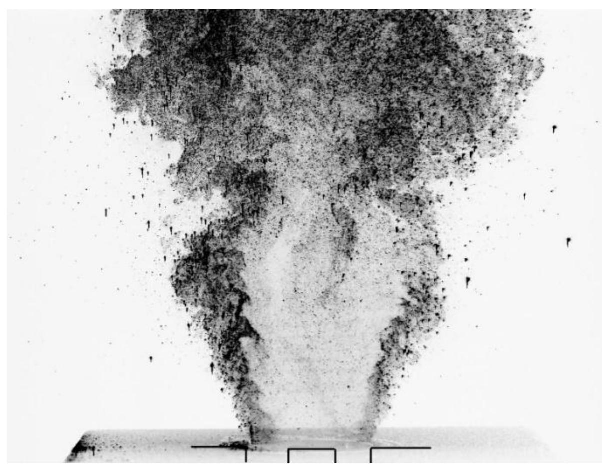

c. Frame 1

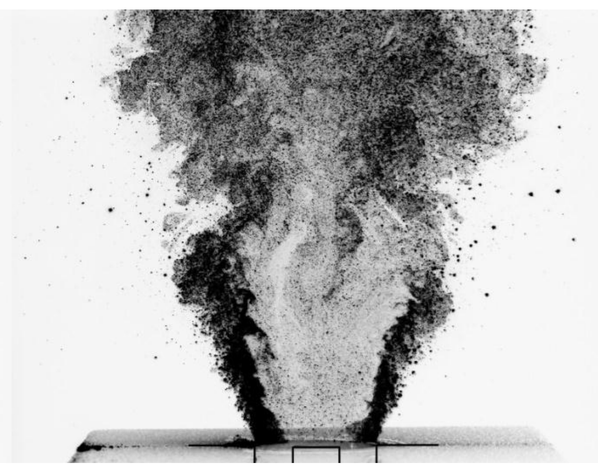

d. Frame 2

Experimental Results – Cont'd

- A few thousand velocity vectors shall be computed from each image pair
- order of N^4 operations are necessary for each N pixel by N pixel interrogation window
- FFT algorithm is used for the cross-correlation operation
- Peak of the correlation function within the interrogation window gives the mean displacement of particles
- Poor signal/noise ratio
- Instead of this procedure average of the correlation function is computed
- At a consequence, erroneous vectors won't be computed insufficient seed density regions.

Experimental Results – Cont'd

Sequence No	Frame A $t=t_0$		Frame B $t=t_0+\Delta t$		Correlation	Peak Search & Vector Determination
1	A_1	*	B_1	=	R_{A1B1}	
					+	
2	A_2	*	B_2	=		
					+	
3	A_3	*	B_N	=		
...	...		...		....	
					+	
N	A_N	*	B_3	=		
	Mean Correlation				$<R_{AB}>$	Mean Velocity Vector

Calculation of mean velocity vector using average correlation (Dantec Dynamics, 2010)

Experimental Results – Cont'd

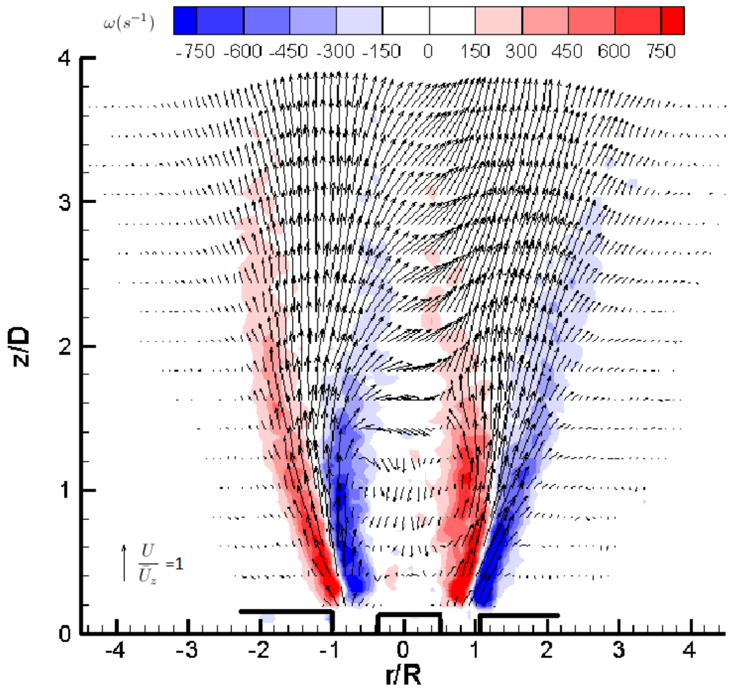

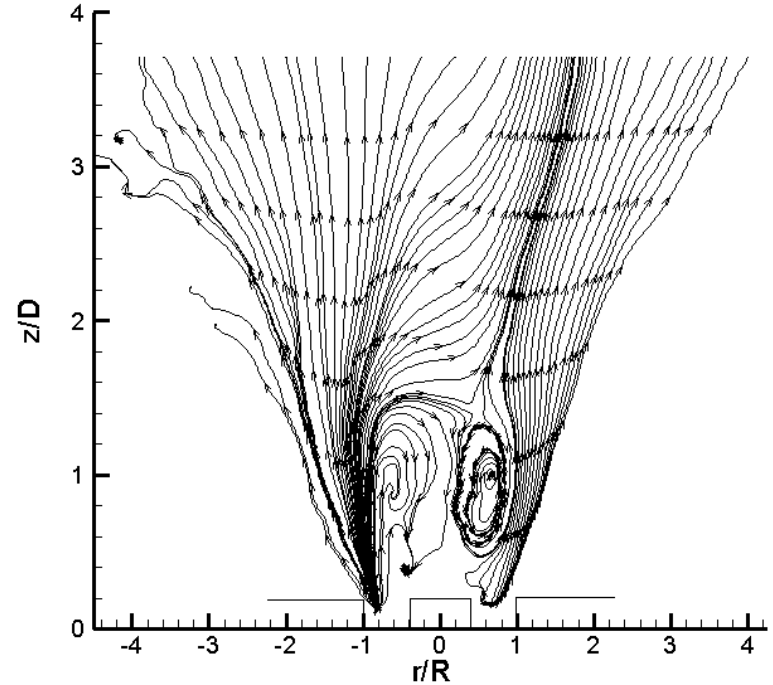

Average Velocity Profiles and Vorticity

Streamlines and Re-circulation Zones

S=0.74 $\mathrm{Re}_{Dh} = 19,400$ $\phi = 0.7$

Numerical Simulation

- Compressible Navier-Stokes, energy and phase equations with turbulence and combustion model solved by using OpenFOAM.
- C++ code library
- Discretized using finite volume method
- A DILU preconditioning scheme used to decrase the possible numerical dificulties.
- Pressure and density
  - geometric agglomerated algebraic multi-grid solver
- Pressure – velocity coupling
  - Hybrid PISO-SIMPLE algorithm.
- Time integration
  - First order implicit Euler scheme.
- Time step
  - Automatically adjusted according to the Courant-Friedrichs-Lewy criteria.

Numerical Simulation – Cont'd

- 1.1 million grid points
- A block structured straight high Reynolds number mesh by BlockMesh dictionary.
- Finer
  - near the wall regions
  - along the centerline
  - in regions close to dump plane

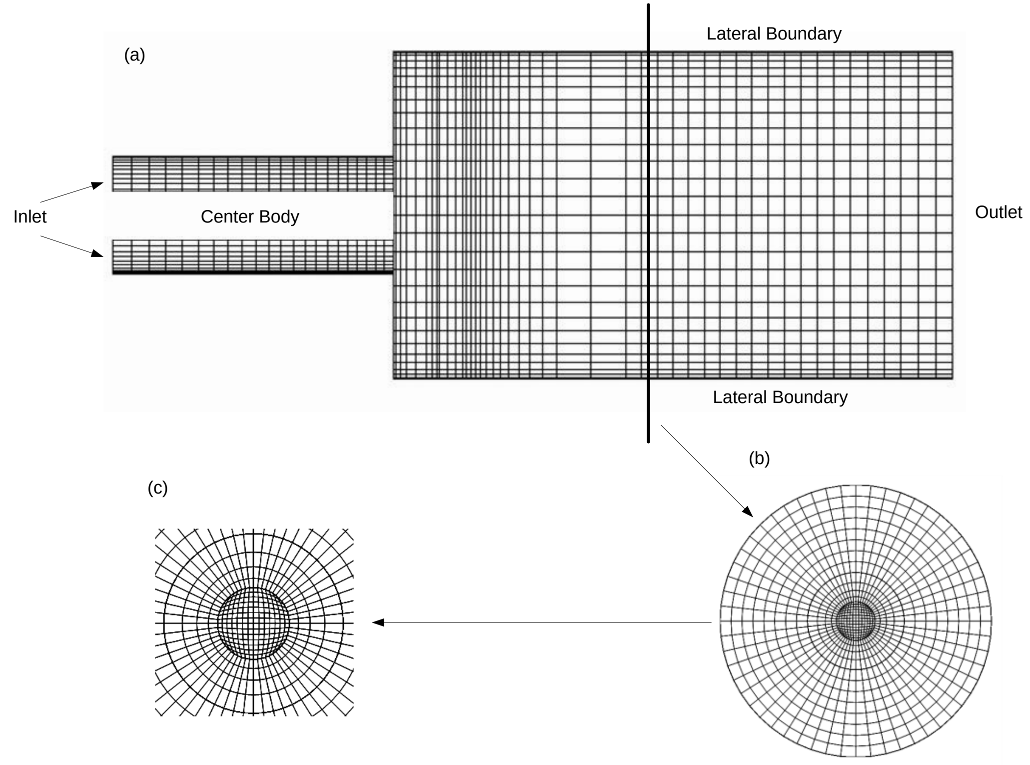

Close-up view of the computational domain (every third grid point in either direction is shown for clarity).

Numerical Simulation – Cont'd

- Inflow boundary condition
  - One-seventh power law profile for axial velocity
- Turbulent boundary condition
  - 10% turbulence intensity
- Outflow boundary condition
  - Convective boundary conditions are prescribed
- Open lateral boundaries
  - zero-gradient boundary conditions
- Assuming
  - constant tangential velocity
  - fuel is completely premixed with air at the inlet
- 128 processor cores works parellel to solve unsteady simulation
- Domain decomposition
  - Hierarchical decomposition scheme

Results of Numerical Simulation

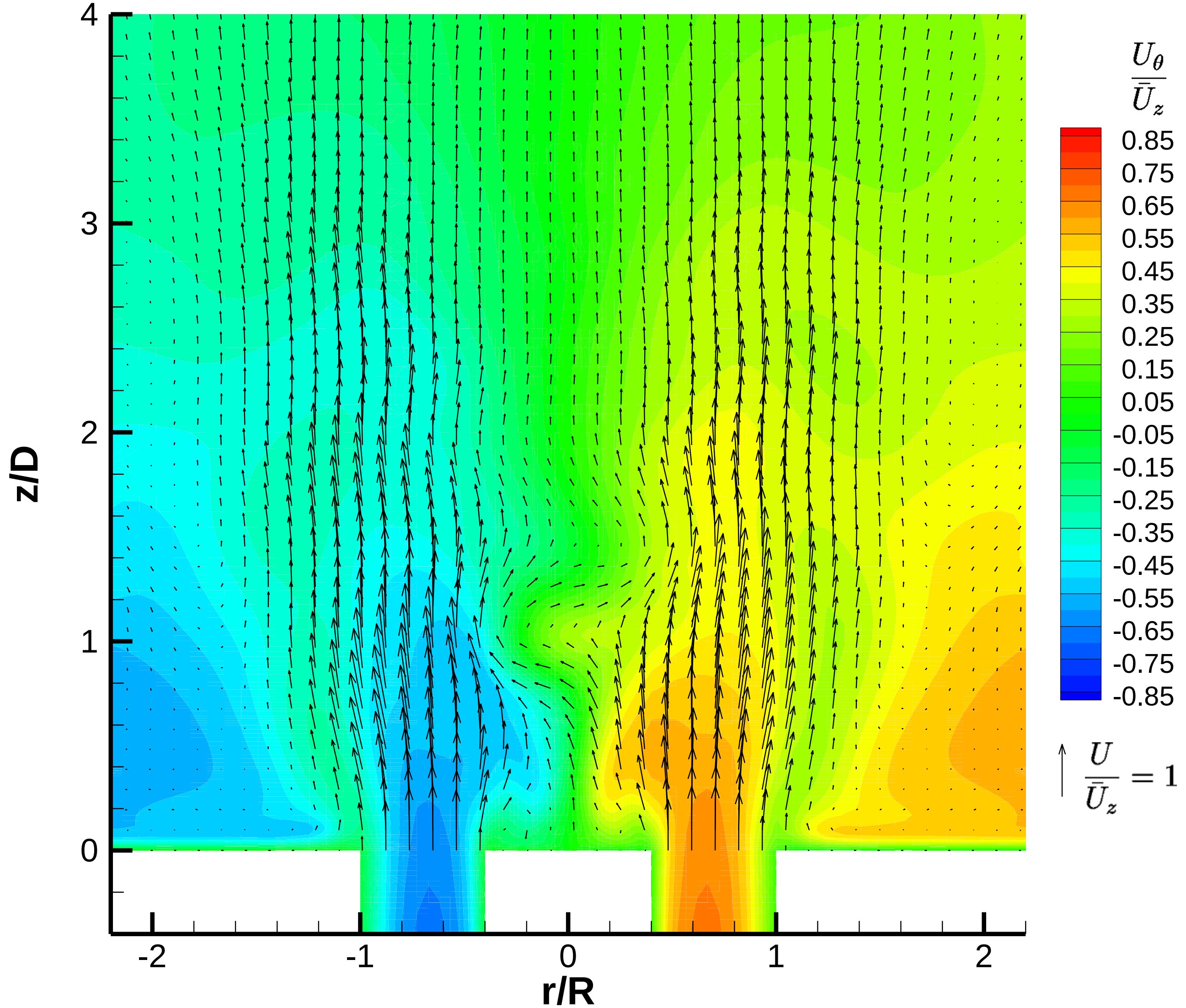

Three dimensional velocity distribution from numerical simulations, $Re_{Dh} = 19400, Sw = 0.74$, $\phi = 0.7$

Results of Numerical Simulation – Cont'd

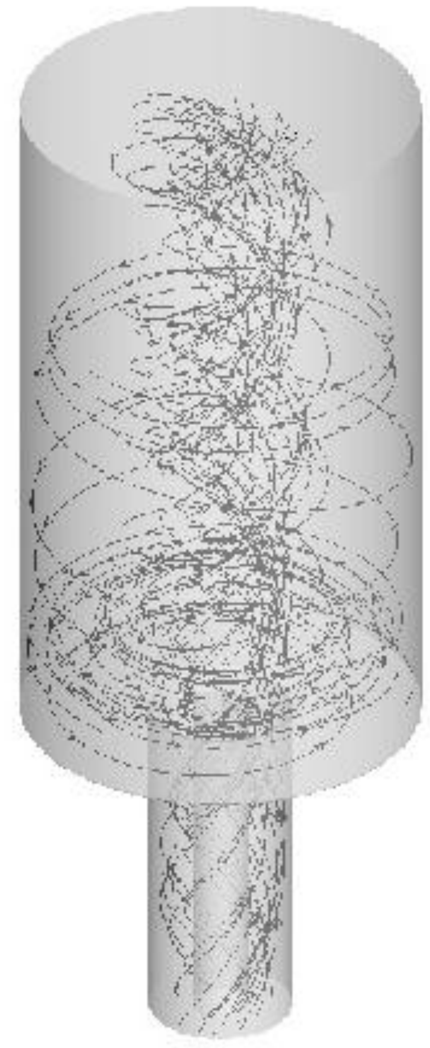

Three dimensional Path lines Inside the Solution Domain, $Re_{Dh} = 19400, Sw = 0.74$, $\phi = 0.7$

Results of Numerical Simulation – Cont'd

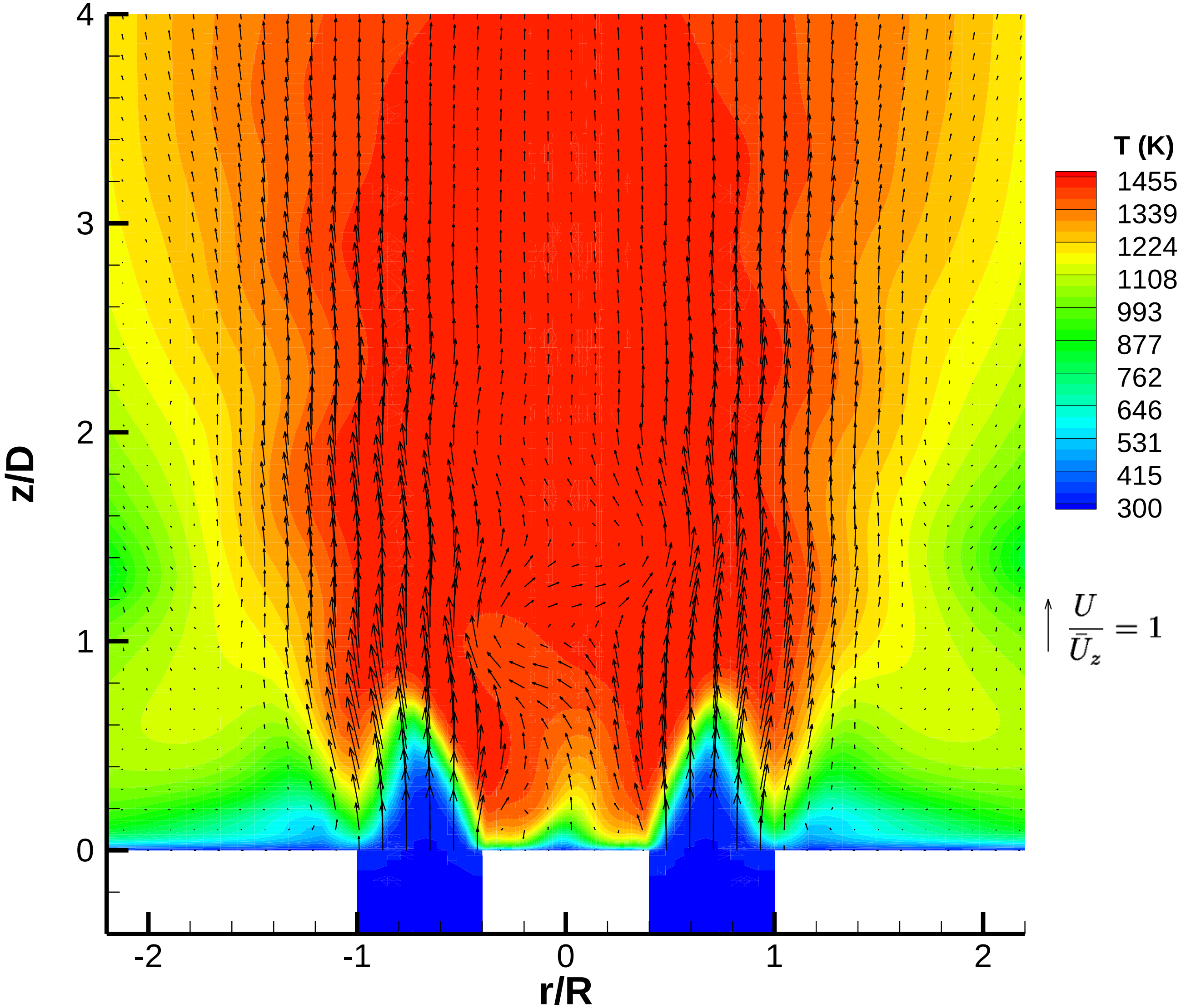

In plane velocity vectors and temperature distribution, $Re_{Dh} = 19400, Sw = 0.74$, $\phi = 0.7$

Conclusion

- Behavior of a swirl stabilized methane/air flame is investigated both experimentally and computationally.
- Both suggest that a central re-circulation zone is instrumental in flame holding. However, numerical results could not predict a re-circulation zone that is as strong as the one that is observed experimentally.
  - This might be attributed to the adequacy of the modeling approach as well as the numerical scheme and grid that were used.
- Both experimental results (Mie scattering images) and numerical ones (temperature distribution) indicate the presence of a wedge shaped flame stabilized both at the tip of the center-body and also at the rim of the delivery tube.

Further works

- Prospective research shall focus on further processing of the Mie scattering images in order to recover the flame front location and the assessment of flame speed from this information, as well as more detailed numerical simulations.
- Experimentally obtained turbulent flame speeds will be compared against numerical results.

Acknowledgement

Authors gratefully acknowledge financial support received from the Turkish Scientific and Technical Research Council (TÜBİTAK) under contract number 109M426 for the experimental part of the study.

Computing resources used in this work were provided by the National Center for High Performance Computing of Turkey (UYBHM) under grant number 1001982012.

Questions ?

MODELLING OF BYPASS-TRANSITION IN TURBINE BLADE CASCADE

Petr Straka

Aeronautical Research & Test Establishment, Prague, Czech Republic

Aerodynamics Deaprtment

Jaromír Příhoda

Academy of Science of the Czech Republic, Prague

Institute of Thermomechanics

2nd EASN WORKSHOP, Prague 2012

Outline

- Physical and Mathematical Model
- Transition Model
  - Algebraic Bypass-Transition Model
  - PTM Model
- Validation
- Application – Flow in Linear Blade Cascade

Physical and Mathematical Model

- Perfect gas
- Compressible flow
- Viscous, transitional
- 2D
- RANS equation + TNT k-ω Kok (2000) + Transition model

Physical and Mathematical Model

$$\frac{\partial \mathbf{W}}{\partial t} + \frac{\partial (\mathbf{F}_i - \mathbf{F}_i^v)}{\partial x_i} = \mathbf{Q}, \quad i = 1,\ 2$$

$$\begin{array}{rcl}
\mathbf{W} & = & [\rho,\ \rho u_j,\ e,\ \rho k,\ \rho\omega]^{\mathrm{T}} \\
\mathbf{F}_i & = & [\rho u_i,\ \rho u_i u_j + \delta_{ij} p,\ u_i(e+p),\ \rho u_i k,\ \rho u_i \omega]^{\mathrm{T}} \\
\mathbf{F}_i^v & = & [0,\ \tau_{ij},\ u_j \tau_{ij} - q_i,\ (\mu + \sigma_k \mu_t)\frac{\partial k}{\partial x_i},\ (\mu + \sigma_\omega \mu_t)\frac{\partial \omega}{\partial x_i}]^{\mathrm{T}} \\
\mathbf{Q} & = & [0,\ 0,\ 0,\ 0,\ P_k - D_k,\ P_\omega - D_\omega - C_D]^{\mathrm{T}}
\end{array}$$

Physical and Mathematical Model

$$
\begin{aligned}
P_k &= \min\left\{P,\ \rho\, k\sqrt{S_{ij}S_{ij}}\right\} \\
P &= \left\{\mu_t\left[\left(\frac{\partial u_i}{\partial x_j}+\frac{\partial u_j}{\partial x_i}\right)-\frac{2}{3}\frac{\partial u_k}{\partial x_k}\,\delta_{ij}\right]-\frac{2}{3}\,\rho\, k\,\delta_{ij}\right\}\ \frac{\partial u_i}{\partial x_k} \\
D_k &= \beta_k\,\rho\, k\,\omega \\
P_\omega &= \alpha\frac{\omega}{k}P_k \\
D_\omega &= \beta_\omega\,\rho\,\omega^2 \\
C_D &= \frac{1}{2}\frac{\rho}{\omega}\max\left(\frac{\partial k}{\partial x_j}\frac{\partial \omega}{\partial x_j},\ 0\right)
\end{aligned}
$$

Physical and Mathematical Model

$$
\begin{aligned}
p &= (\kappa - 1)\left(e - \rho\,\frac{u_j^2}{2}\right) \\
q_i &= -\left(\frac{\mu}{Pr} + \frac{\mu_t}{Pr_t}\right)\,\frac{\kappa\, r}{\kappa - 1}\,\frac{\partial T}{\partial x_i} \\
\tau_{ij} &= (\mu + \mu_t)\left[\left(\frac{\partial u_i}{\partial x_j} + \frac{\partial u_j}{\partial x_i}\right) - \frac{2}{3}\,\frac{\partial u_k}{\partial x_k}\,\delta_{ij}\right] - \frac{2}{3}\,\rho\, k\,\delta_{ij} \\
\mu &= \mu_0\left(\frac{T}{T_0}\right)^{\frac{3}{2}}\,\frac{T_0 + S}{T + S} \\
\mu_t &= \frac{\rho\, k}{\omega}
\end{aligned}
$$

Numerical Method

Mesh:

- structured quadrilateral
- multiblock (block overlapping – “chimera“)

RANS:

- FVM “cell-centered“, implicit
- inviscid fluxes: 1D exact Rieman solver
- 2D lin. reconstruction, limiter: Van Leer
- viscous fluxes: central scheme, “diamond“ dual cells

k-ω TNT Kok

- FVM „cell-centered“, implicit
- convective terms: Steger-Warming
- 2D lin. reconstruction, limiter: Van Leer
- viscous terms: central scheme, “diamond“ dual cells

Algebraic Bypass-Transition Model

$$\gamma = \begin{cases} 0 & ,\dots \text{ lam. domain} \\ 1 & ,\dots \text{ turb. domain} \end{cases}$$

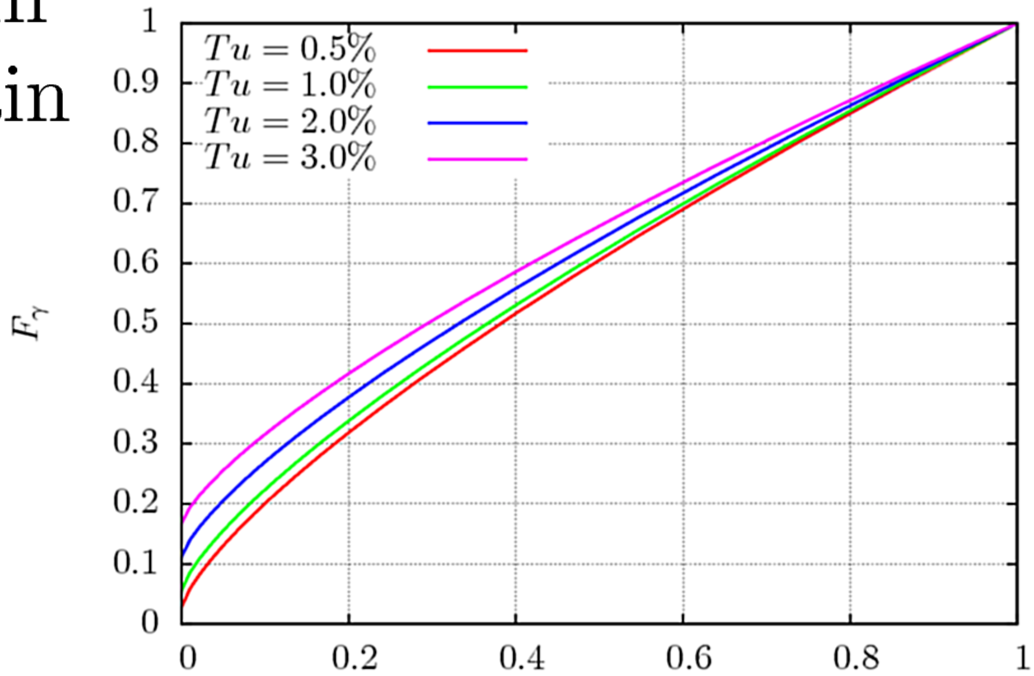

$$\boxed{\mu_{ef} = \mu + \gamma\,\mu_t}$$

$$\boxed{\tilde{P}_k = F_\gamma\, P_k}$$

$$F_\gamma = B + (1 - B)\,\gamma^{3/4}, \quad B = 0,056\,Tu_t$$

Příhoda et al. (1999)

$$\boxed{\tilde{D}_k = \min[\max(\gamma;\ 0.1);\ 1]\,D_k}$$

Algebraic Bypass-Transition Model

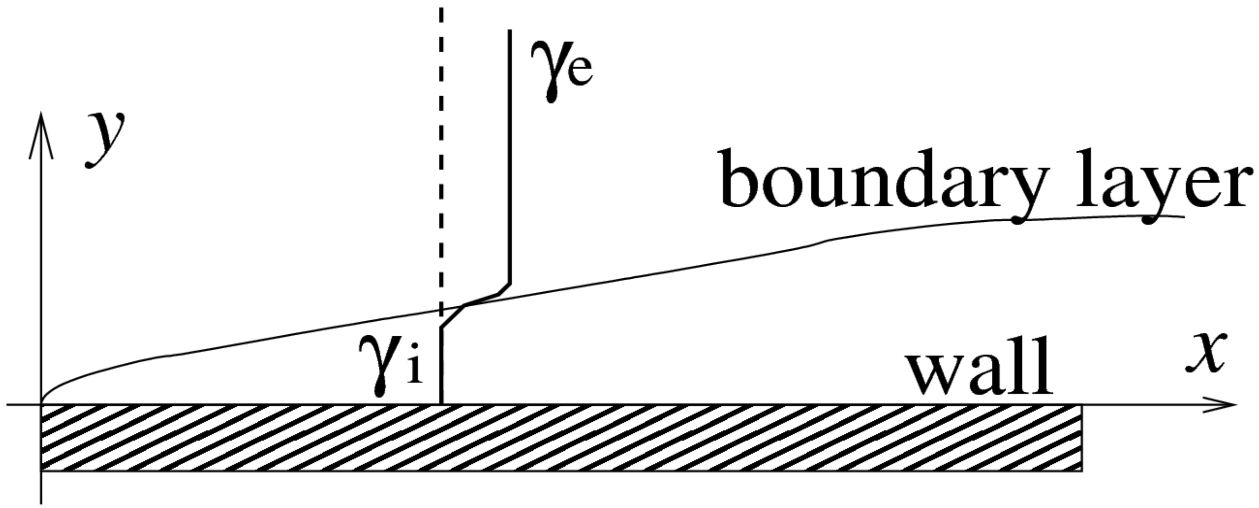

$$\boxed{\gamma = \frac{\gamma_e + \gamma_i}{2} + \frac{\gamma_e - \gamma_i}{2}\,\mathrm{tgh}\left[C_\gamma\left(\frac{y}{\delta_{99.5}} - 1\right)\right]}$$

Straka, Příhoda (2010)

Algebraic Bypass-Transition Model

Narasimha (1985)

$$\boxed{\gamma_i = 1 - \exp\left[-\hat{n}\,\sigma\,(Re_x - Re_{xt})^2\right]}$$

$$Re_{xt} \longrightarrow Re_\theta = Re_{\theta t} \qquad \boxed{Re_\theta = \frac{Re_{v\,\max}}{C}}$$

C = 2.193   Menter at al. (2002)

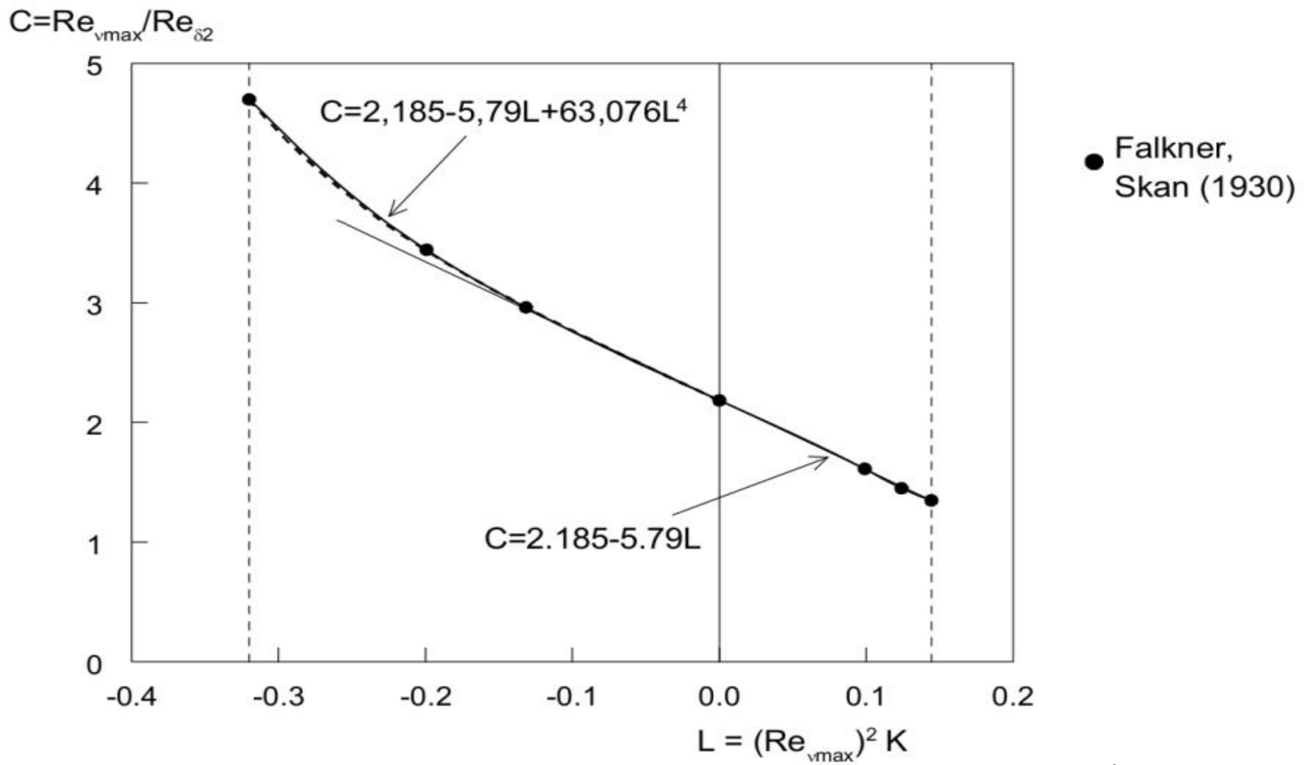

Algebraic Bypass-Transition Model

Narasimha (1985)

$$\boxed{\gamma_i = 1 - \exp\left[-\hat{n}\,\sigma\,(Re_x - Re_{xt})^2\right]}$$

Straka, Příhoda (2010)

$$Re_{\theta t} = Re_{\theta t_0}\,\left[1 + F(Tu_e)\,\frac{1 - \exp(-40\,\lambda_t)}{1 + 0.4\,\exp(-40\,\lambda_t)}\right]$$

$$F(Tu_e) = 0.29\,[1 - 0.54\,\exp(-3.5\,Tu_e)]\,\exp(-Tu_e)$$

$$Re_{\theta t_0} = \begin{cases} 975.8 - 497.2\,Tu_e + \frac{11.4}{Tu_e}\,, & Tu_e \le 1\% \\ 96.7 + \frac{340}{Tu_e} + \frac{53.3}{Tu_e^2}\,, & Tu_e > 1\% \end{cases}$$

$$0.1\% < Tu_e < 8\%$$
$$-0.1 < \lambda < 0.1$$

Algebraic Bypass-Transition Model

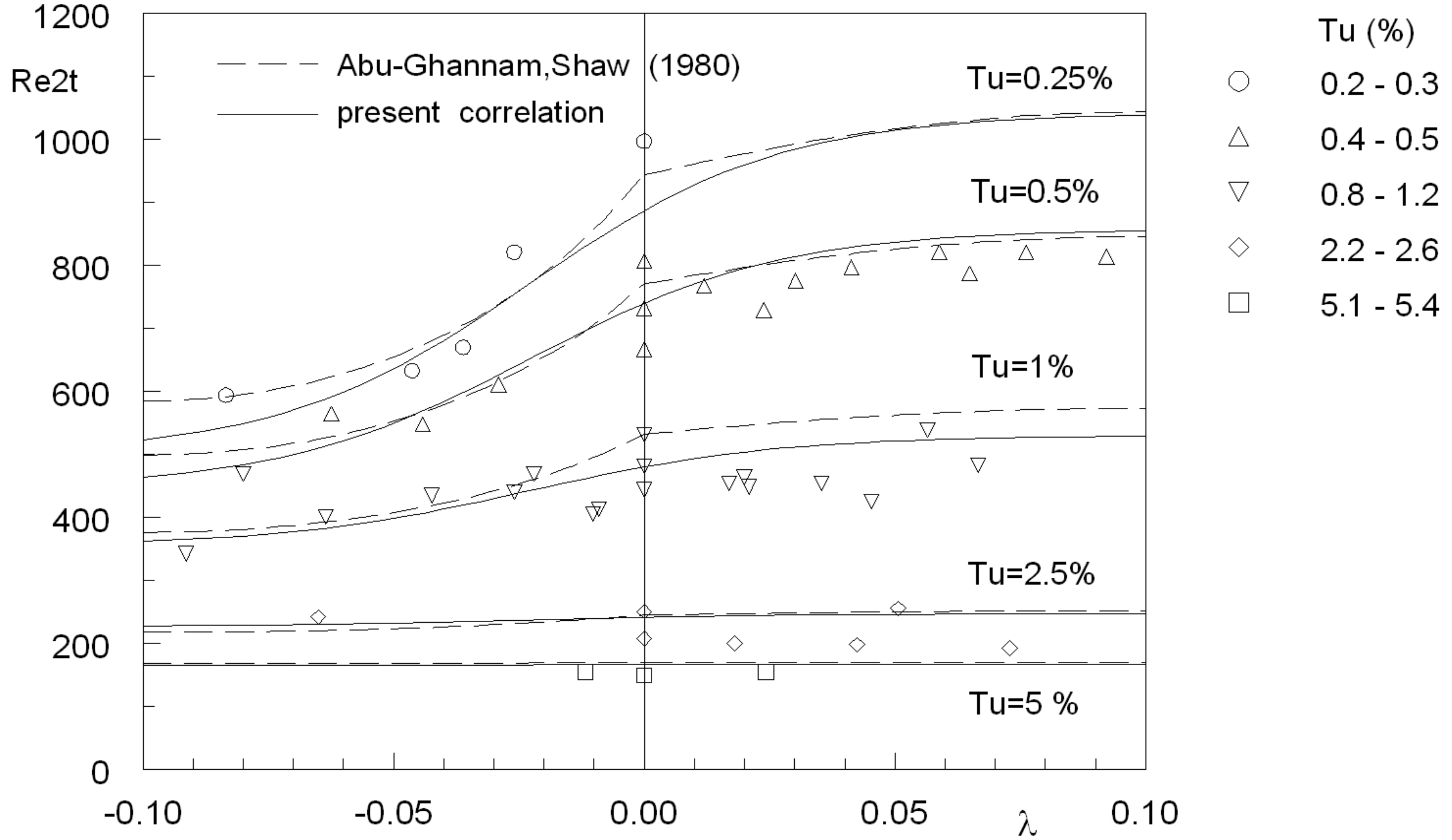

Algebraic Bypass-Transition Model

Narasimha (1985)

$$N = \hat{n}\,\sigma\,Re_\theta^3$$

Gostelov at al. (1992), Solomon at al. (1996)

$$N = f(Tu,\ \lambda)$$

Transition in separation flow:

Mayle (1991)

$$Re_{x\,t} = 300\,Re_{\theta\,s}^{0.7} + Re_{x\,s}$$

Roberts, Yaras (2006)

$$N = \frac{0.55\,H_t - 2.2}{1 - 0.63\,H_t + 0.14\,H_t^2}$$

Validation

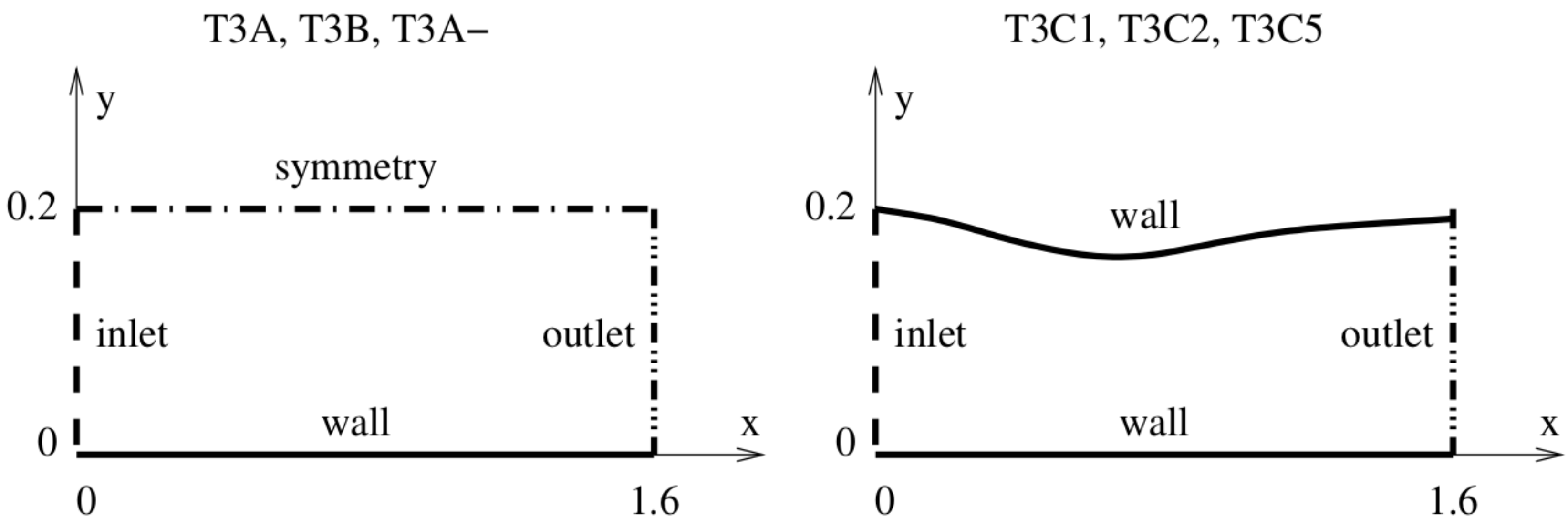

	T3A	T3B	T3A-	T3C1	T3C2	T3C5
$U_0\ (m/s)$	5.4	9.4	19.8	6.3	5.6	9.6
$Tu_0\ (\%)$	3.0	6.0	0.9	6.6	3.0	3.0

Validation

Present correlation

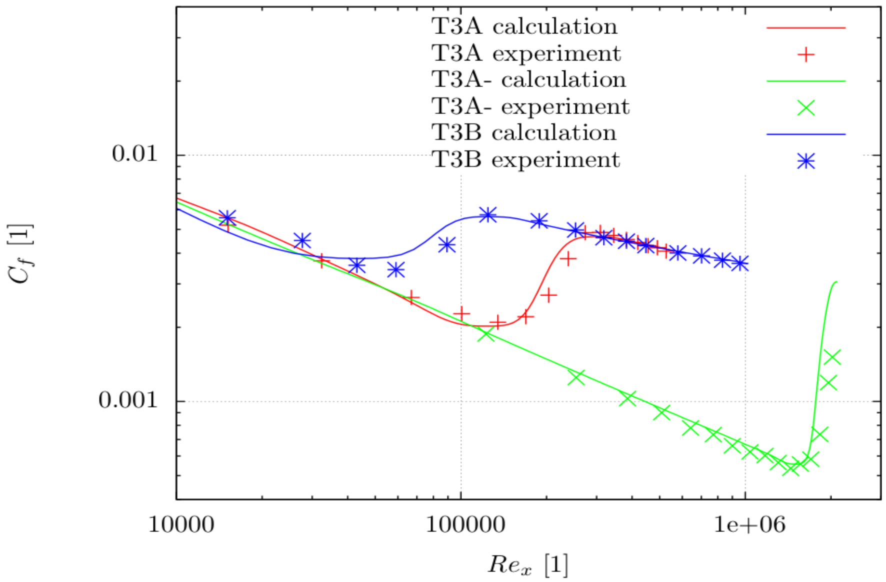

Mayle correlation

$$Re_{\theta\,t} = 402\,Tu^{-0,69}$$

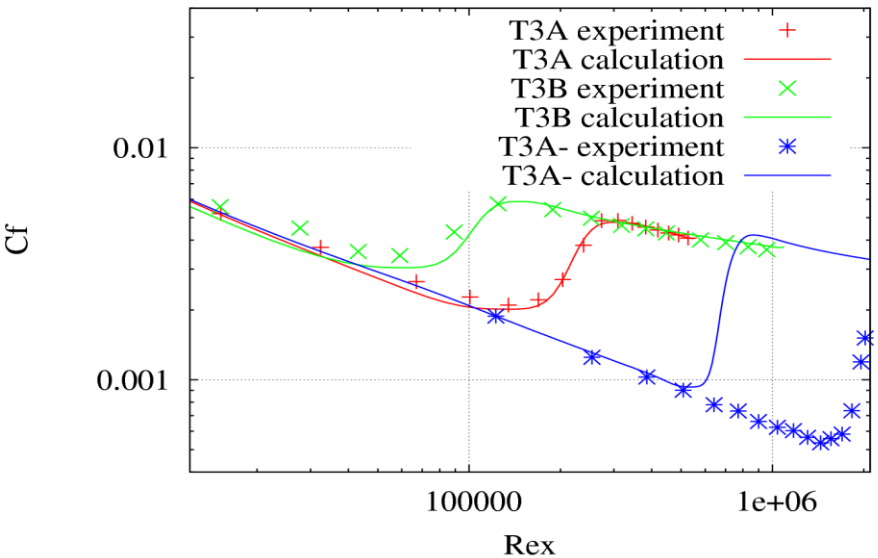

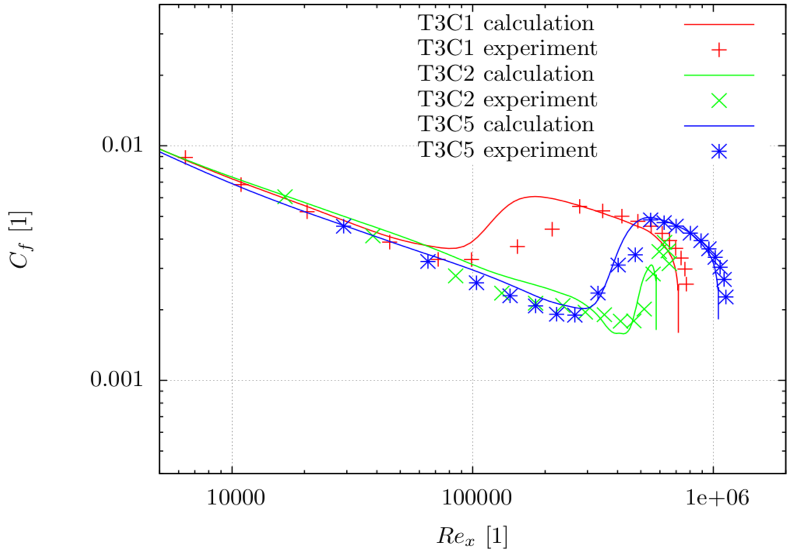

PTM Model

$$\boxed{\tilde{P}_k = PTM \cdot P_k}$$

Langtry Sjolander (2002)

$$PTM = 1 - 0.94\,(PTM1 + PTM2)\,F_3, \quad F_3 = f(R_t)$$

$$PTM1 = f(Re_v)$$

$$PTM2 = f(K,\ Re_v)$$

$$F_3 = e^{\left(-\frac{R_t}{5}\right)^4}$$

Original Langtry Sjolander (2002)

Modified by Nicholas and Denissen (2008)

- Definition of F_3 is not general !!!
- Depends on numerical dissipation – on space discretization scheme

PTM Model

$$F_3 = e^{\left(-\frac{R_t}{5}\right)^4}$$ Original Langtry Sjolander (2002)

$$F_3 = \frac{1}{2} - \frac{1}{2}\tanh\left[C\left(\frac{R_t}{R_t^*} - 1\right)\right]$$ new

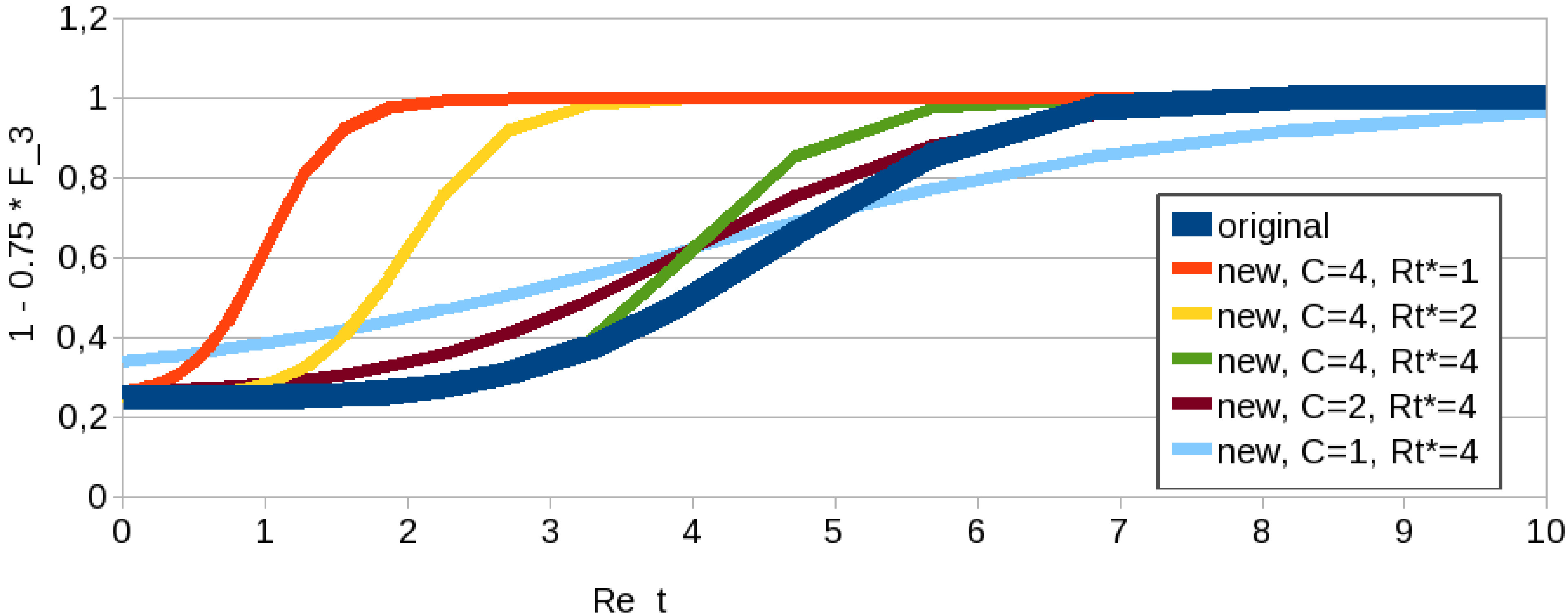

Validation

$$F_3 = \frac{1}{2} - \frac{1}{2}\tanh\left[C\left(\frac{R_t}{R_t^*} - 1\right)\right]$$

Numerical experiment: $2 < C < 5$, $0.3 < Rt^* < 0.8$

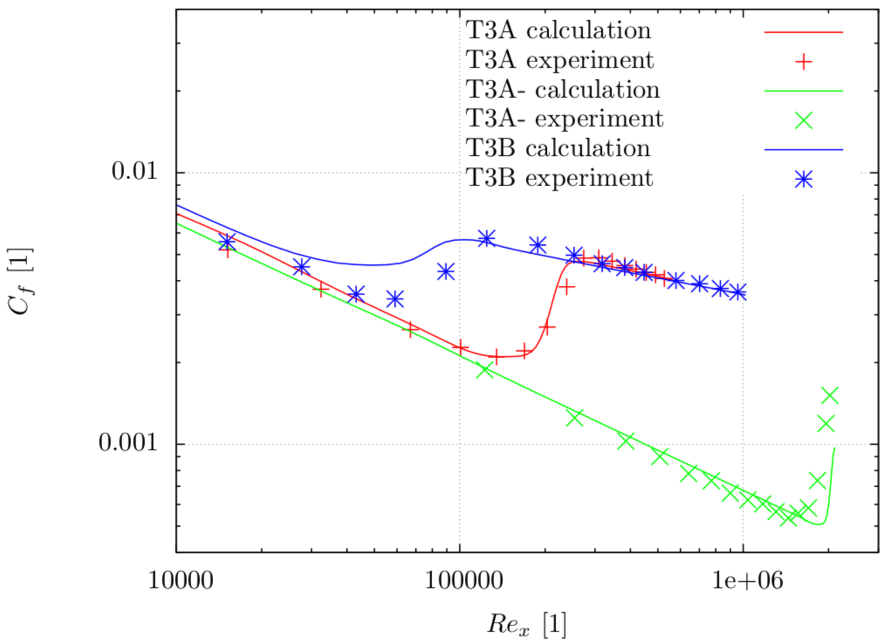

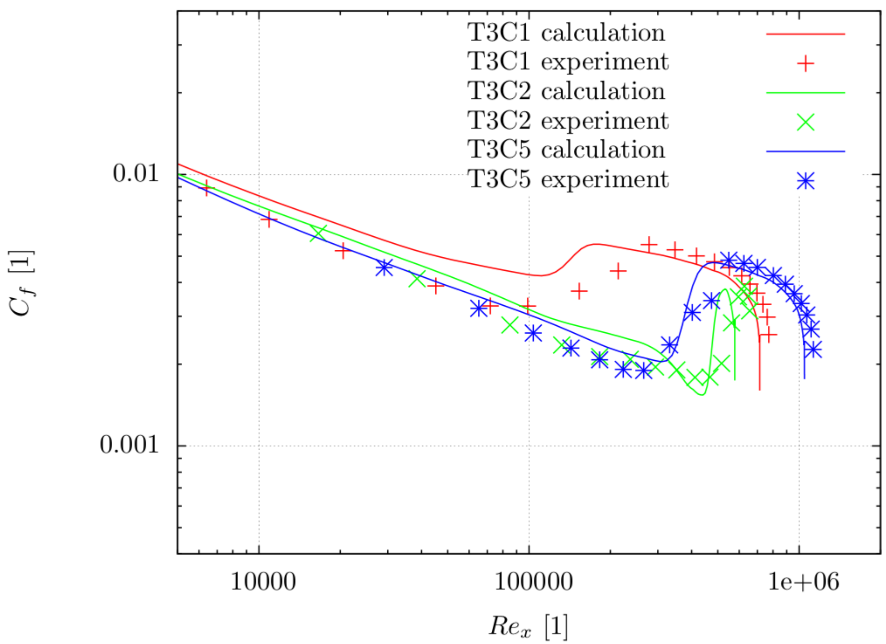

Application

- Unsteady flow in stator-rotor stage

M_{2is}=0.94, Re_{2is}=3x10^5, $alpha_1$=0°, V_{cr}=144 m/s, Tu_1=2%

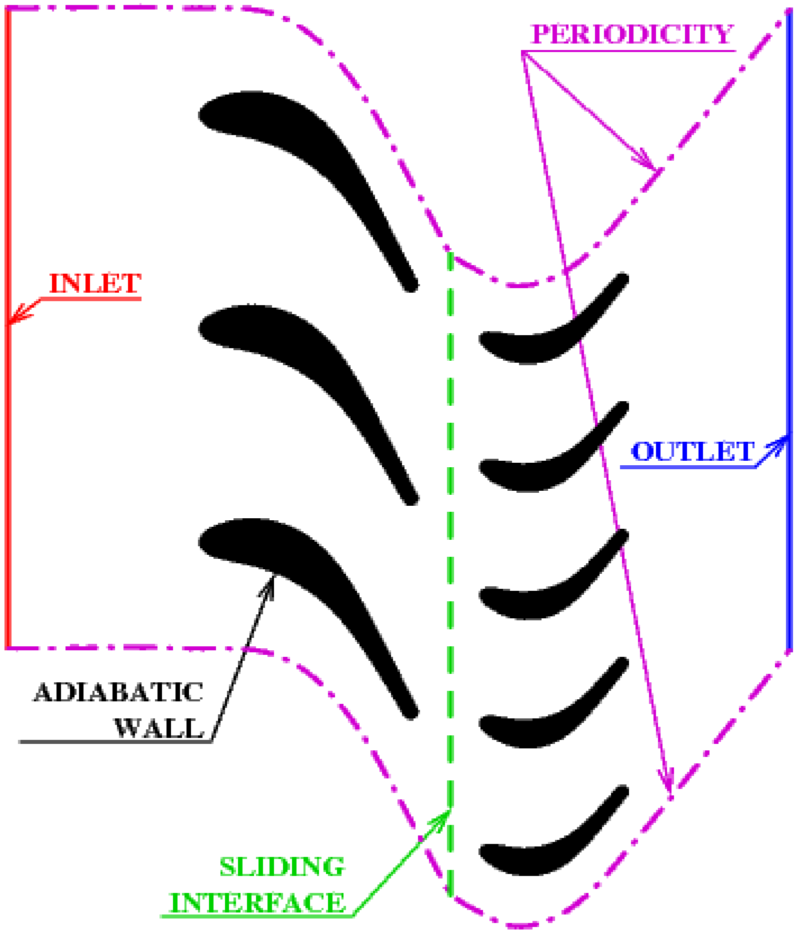

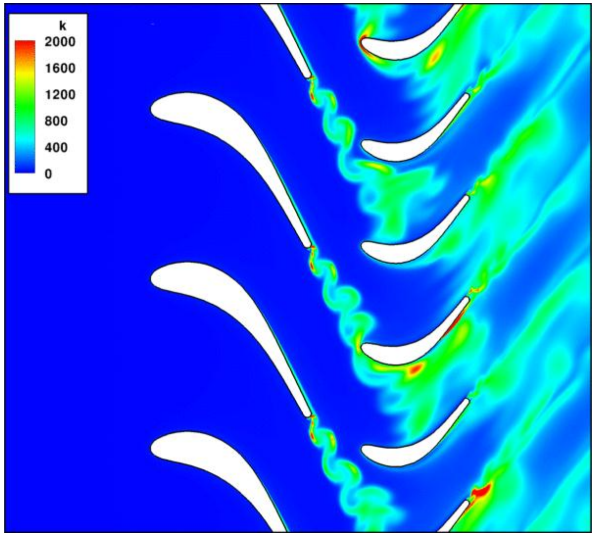

Application`

Algebraic bypass-transition model

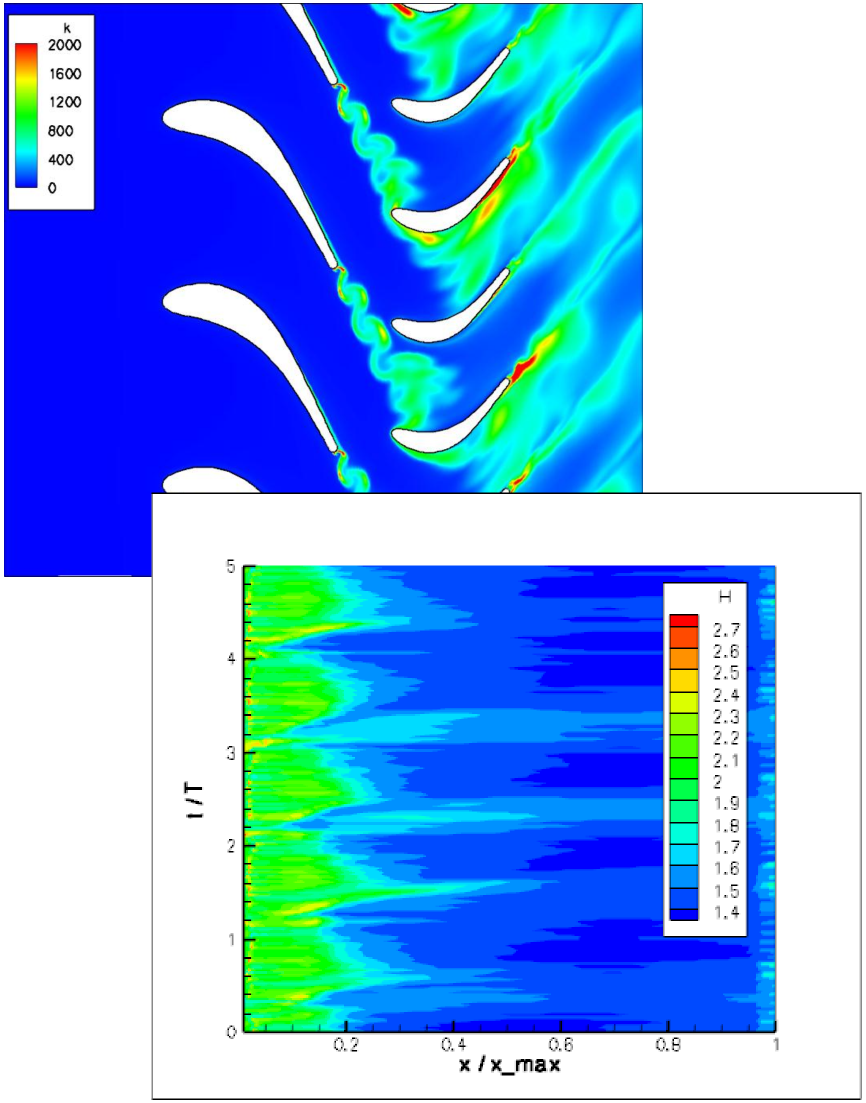

PTM model

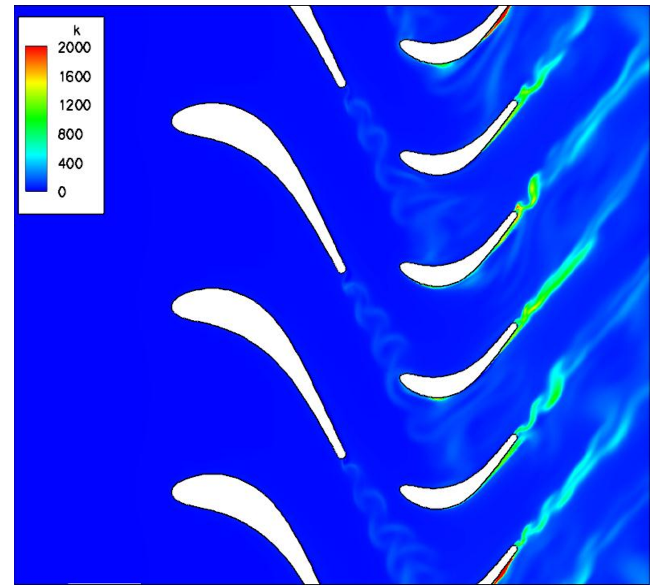

Application

$Re_{2is} = 1.8x10^5$
$M_{2is} = 1.12$
$Tu_1 = 1\%,\ 2\%,\ 5\%$

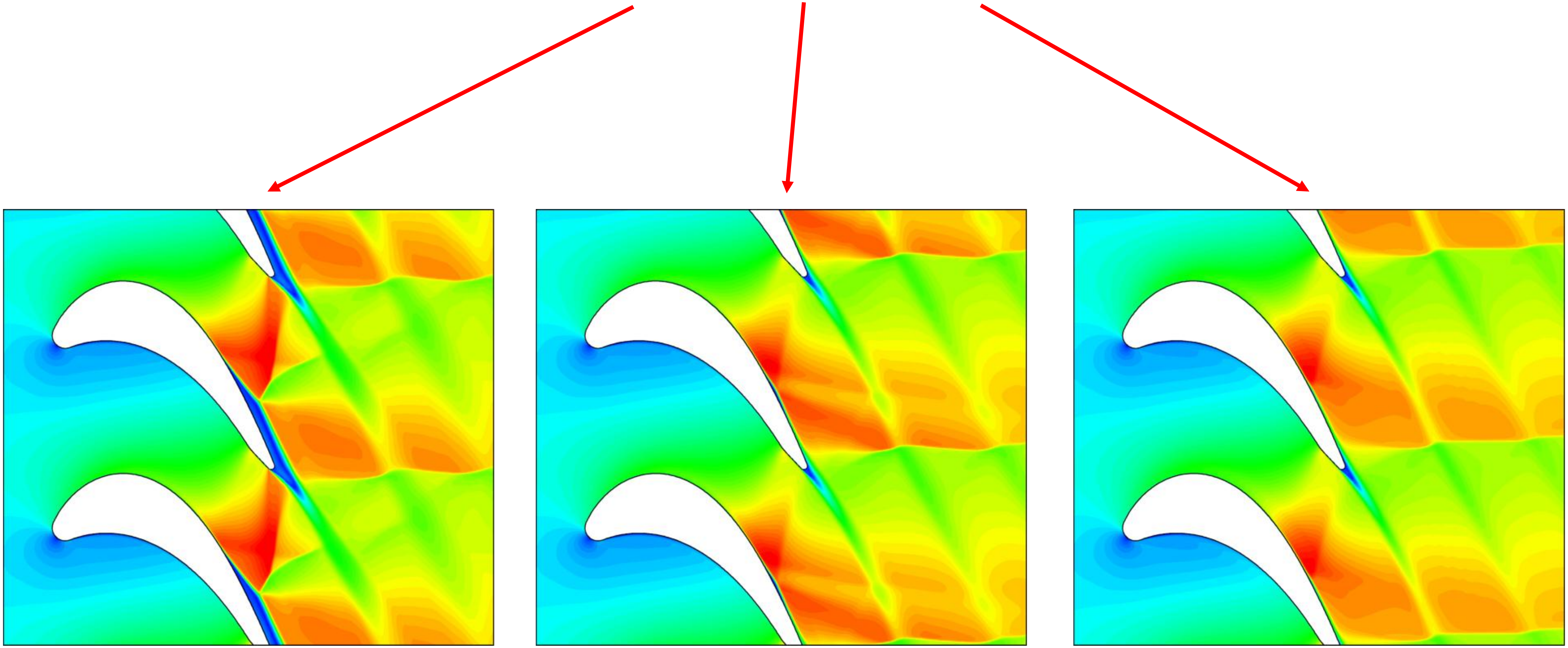

Application

$Re_{2is} = 1.8x10^5$
$M_{2is} = 1.12$
$Tu_1 = 1\%,\ 2\%,\ \ 5\%$

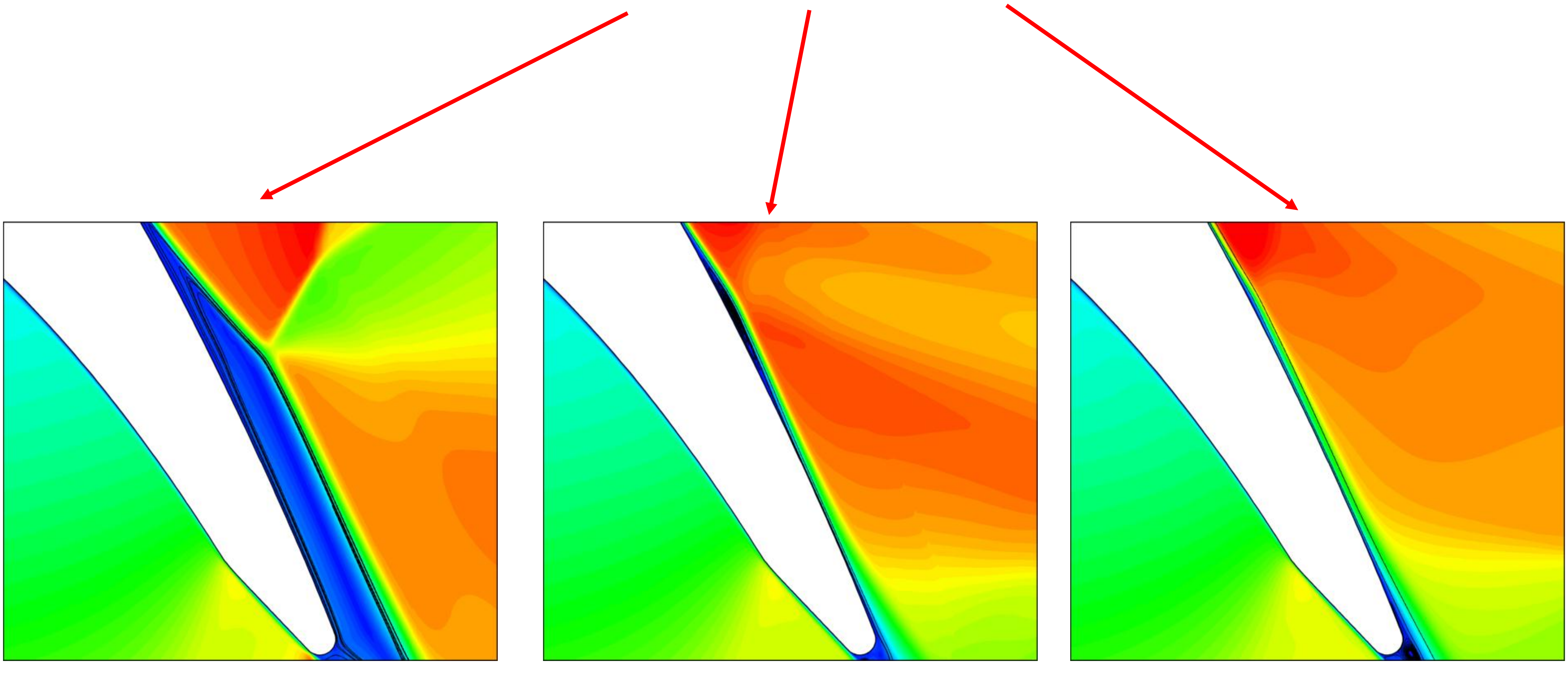

Application

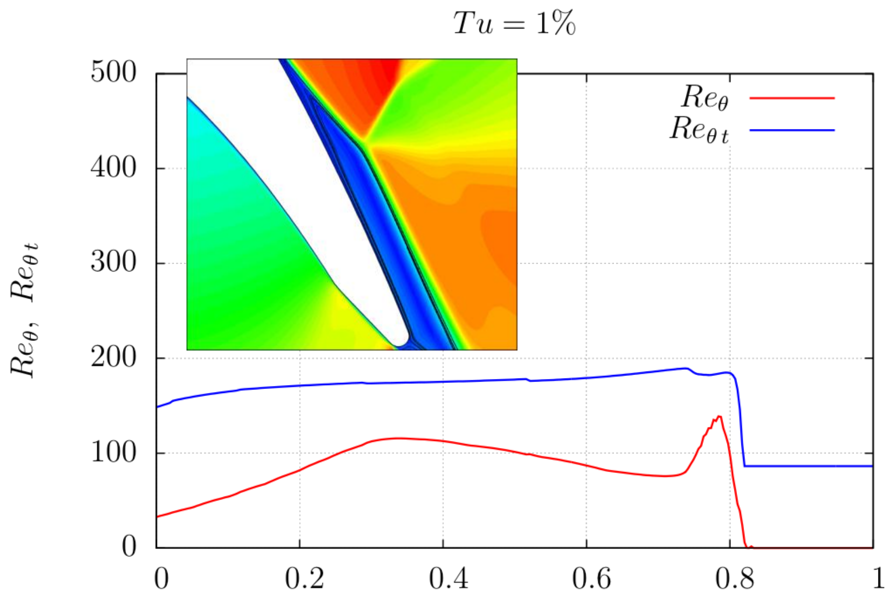

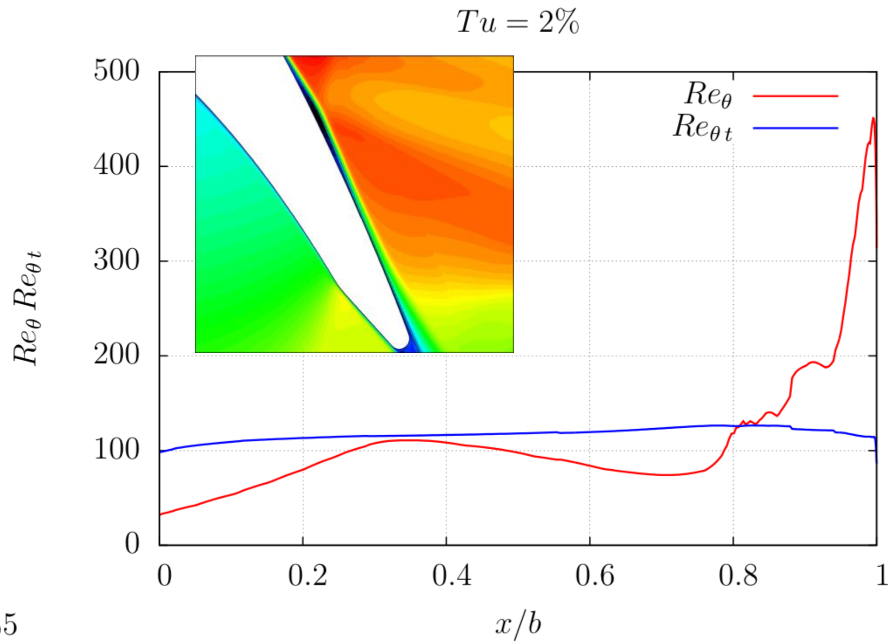

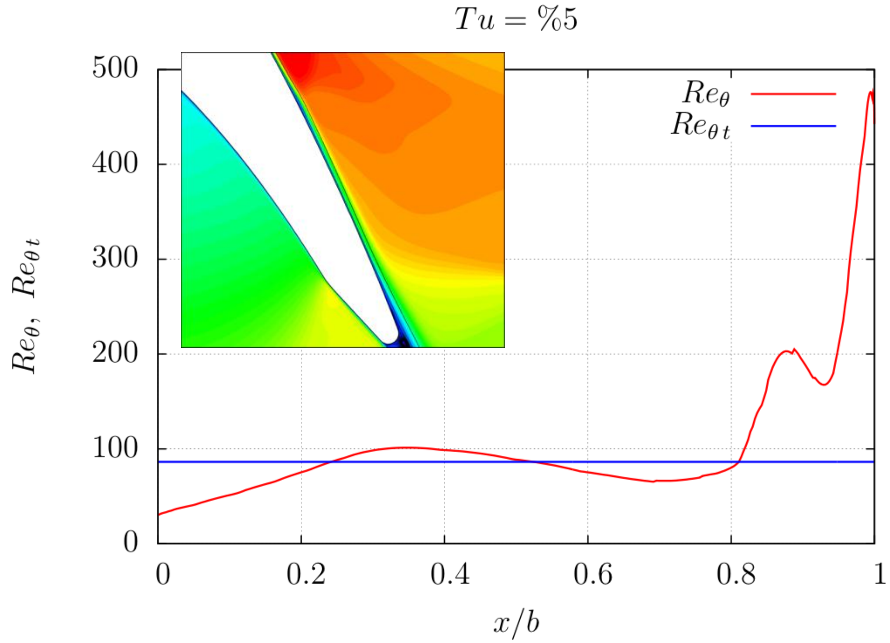

Application

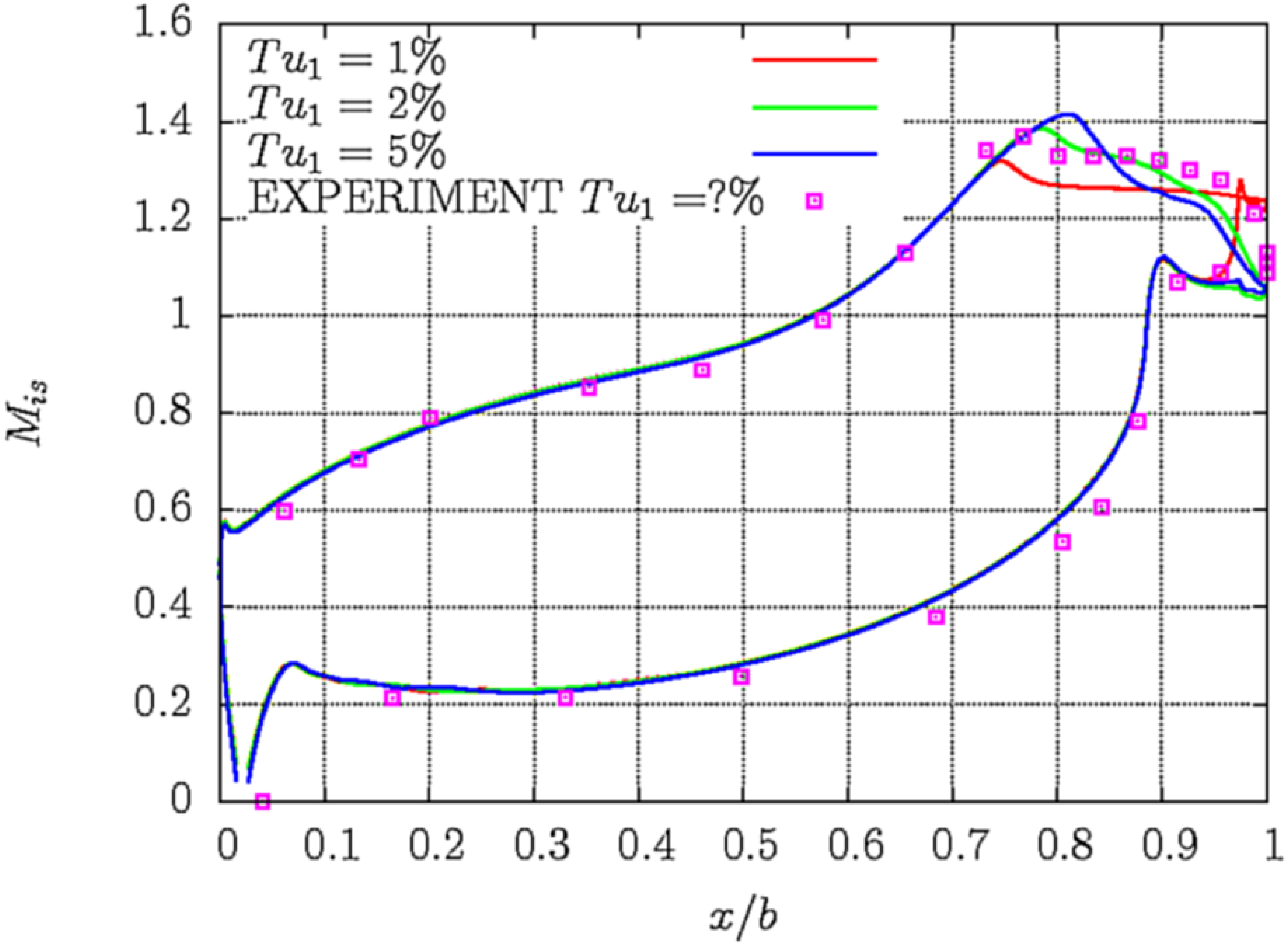

Conclusion

It is necessary to take in account boundary layer transition in turbomachinery application.

Outlook

- Modification of intermittency coefficient distribution across the boundary layer
- To generalize F3 function in PTM model
- Using with EARSM
- Influence of wall-roughness

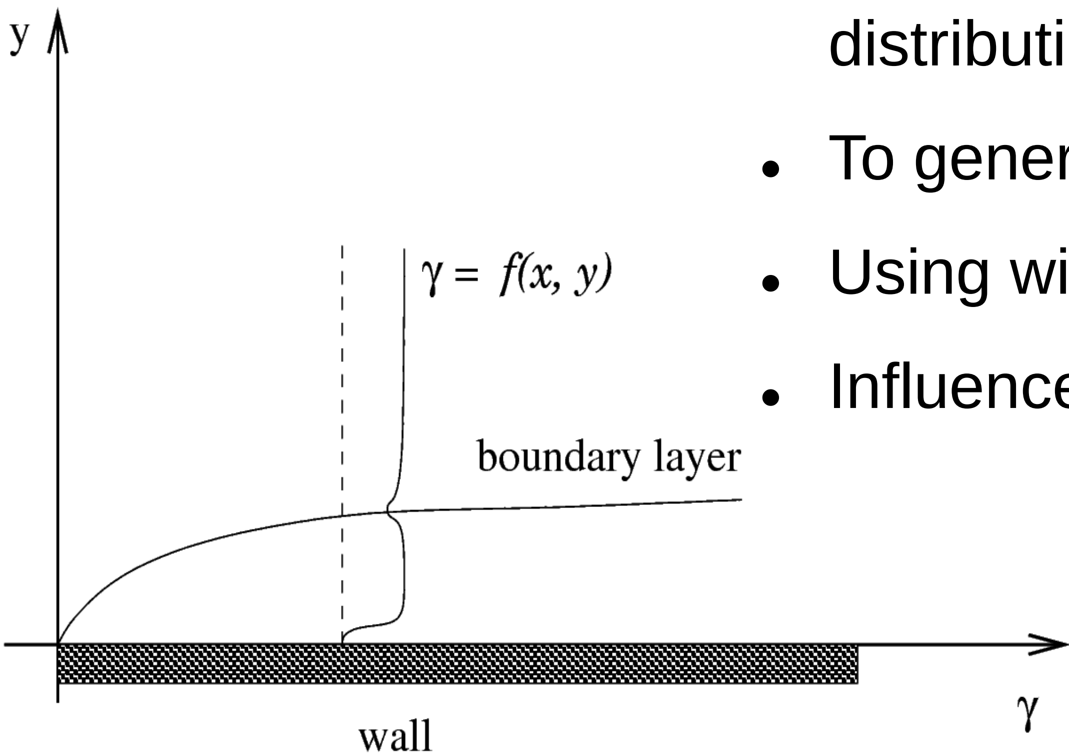

2nd EASN Association Workshop
on **Flight Physics and Propulsion**

31st October – 2nd November 2012
Prague, Czech Republic

BOLT-JOINT STRUCTURAL HEALTH MONITORING BY METHOD OF ELECTROMECHANICAL IMPEDANCE

V. Pavelko*, S. Kuznetsov, I.Ozolinsh, I. Pavelko
Aeronautic Institute, Riga Technical University

BOLT-JOINT STRUCTURAL HEALTH MONITORING BY METHOD OF ELECTROMECHANICAL IMPEDANCE

V. Pavelko[*], S. Kuznetsov, I.Ozolinsh, I. Pavelko
Aeronautic Institute, Riga Technical University

- 1. Introduction
- 2. Experimental study
- 3. Analytical study: 2D model of EMI
- *3.1. The electromechanical impedance of constrained transducer*
- 3.2. Compatibility conditions
- *3.4. Simple case: rectangular shape of transducer*
- *3.3. Interaction force defining using modal decomposition of displacements of a host structure and a transducer*
- 4. Some results of simulation
- 5. Conclusions

BOLT-JOINT STRUCTURAL HEALTH MONITORING BY METHOD OF ELECTROMECHANICAL IMPEDANCE

V. Pavelko, S. Kuznetsov, I.Ozolinsh, I. Pavelko*
Aeronautic Institute, Riga Technical University

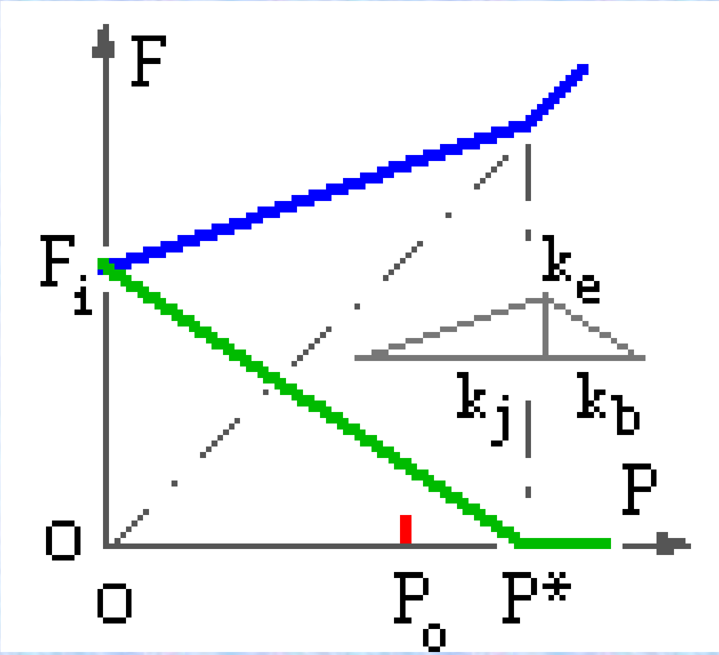

Bolted joints are often applied in the aerospace structures as a general mean of joining of structural units. Usually they are subjected to dynamic load that can cause loosening of joint and accelerating of the fatigue failure

BOLT-JOINT STRUCTURAL HEALTH MONITORING BY METHOD OF ELECTROMECHANICAL IMPEDANCE

V. Pavelko, S. Kuznetsov, I.Ozolinsh, I. Pavelko*
Aeronautic Institute, Riga Technical University

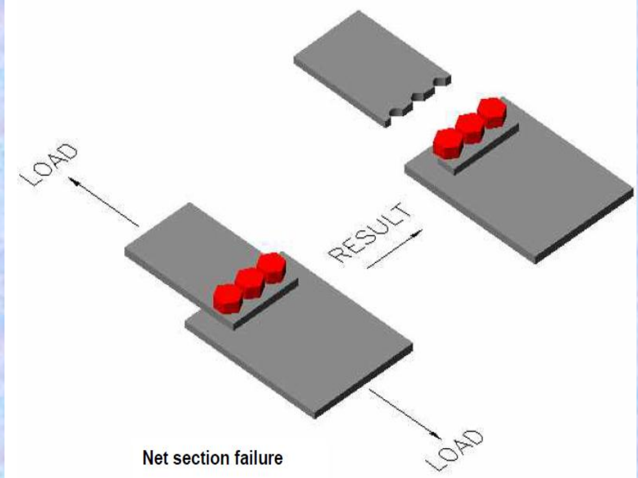

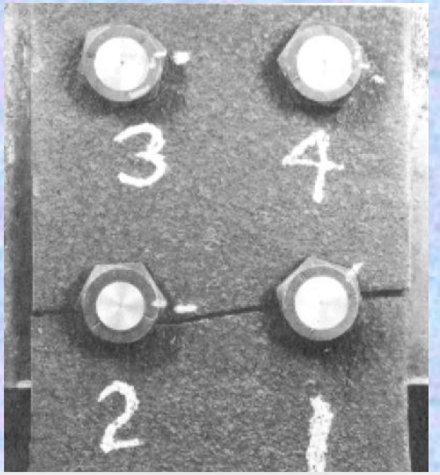

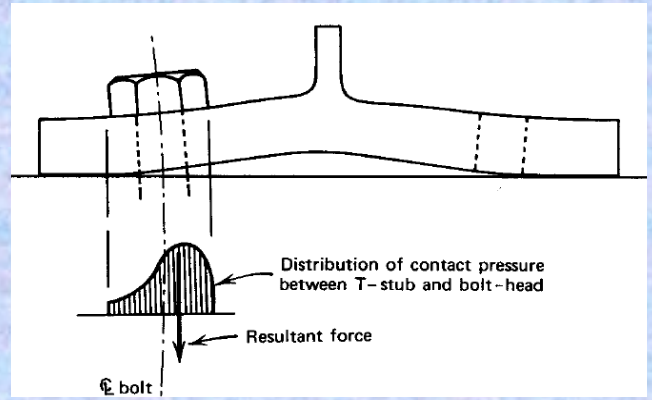

V. Pavelko[*], S. Kuznetsov, I.Ozolinsh, I. Pavelko
Aeronautic Institute, Riga Technical University

E/m impedance for the near field damages detecting

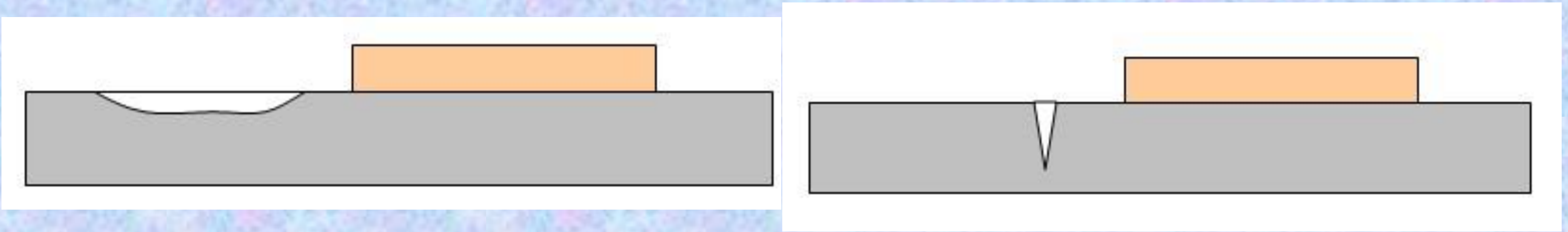

$$Z = \frac{\hat{U}(\omega)}{\hat{I}(\omega)}$$

Mechanical properties cause the changes of electromechanical impedance

- Stiffness
- Attenuation

BOLT-JOINT STRUCTURAL HEALTH MONITORING BY METHOD OF ELECTROMECHANICAL IMPEDANCE

V. Pavelko[*], S. Kuznetsov, I.Ozolinsh, I. Pavelko
Aeronautic Institute, Riga Technical University

Examples of nuts and washers equipped with PZTwafers

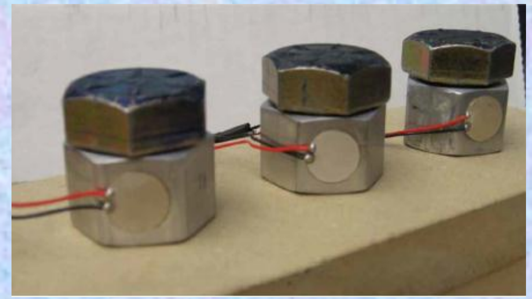

Experimental set-up with PZT enhanced washers

An experimental set-up of PZT stack 1000/25-15/5

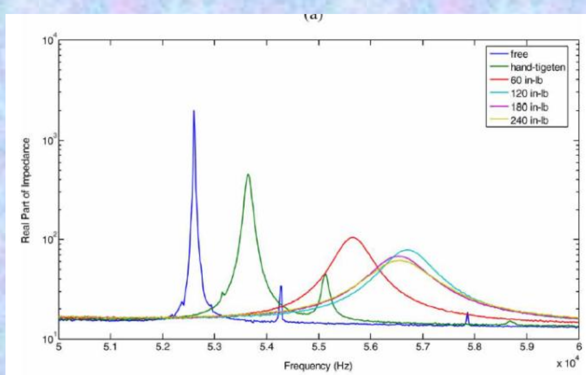

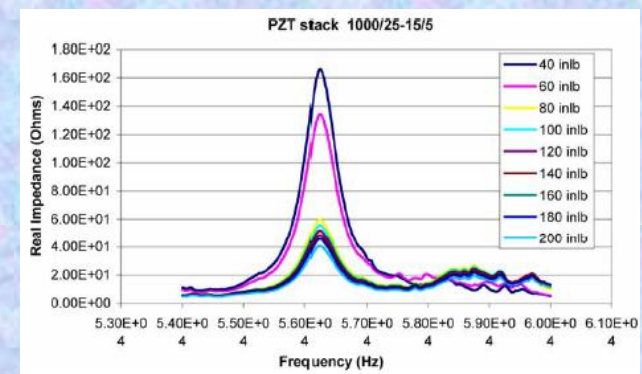

D. L. Mascarenas, G. Park, K.M. Farinholt, M.D. Todd, and C.R. Farrar. (2009) A low-power wireless sensing device for remote inspection of bolted joints. Proc. IMechE Vol. 223 Part G: J. Aerospace Engineering, pp.565-575.

BOLT-JOINT STRUCTURAL HEALTH MONITORING BY METHOD OF ELECTROMECHANICAL IMPEDANCE

V. Pavelko, S. Kuznetsov, I.Ozolinsh, I. Pavelko*
Aeronautic Institute, Riga Technical University

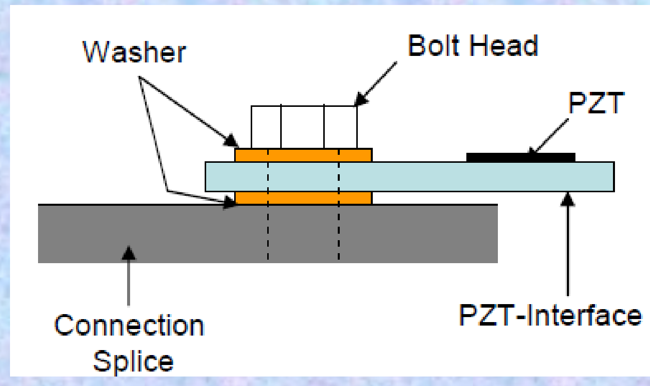

Schematic of PZT-interface and connection splice

Test setup

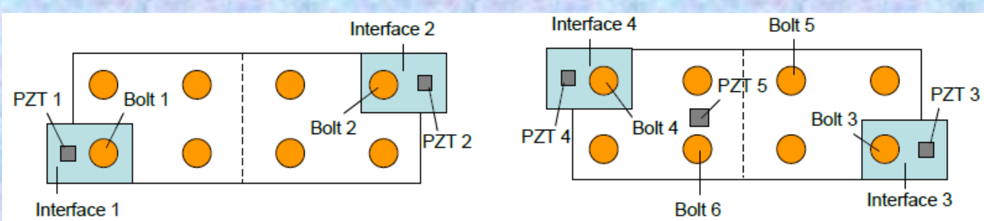

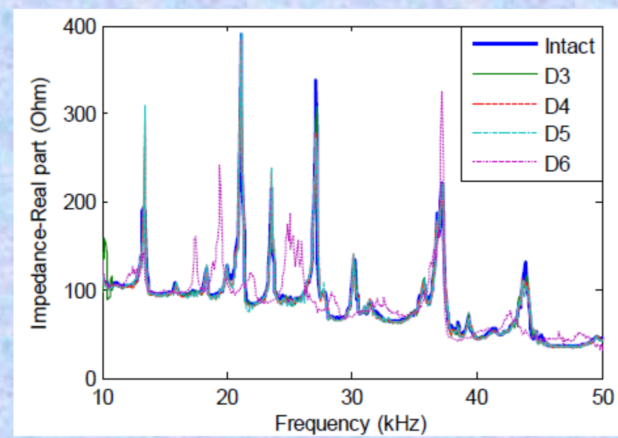

Khac-Duy Nguyen, So-Young Lee, Po-Young Lee and Jeong-Tae Kim. (2011) Wireless SHM for Bolted Connections via Multiple PZT-Interfaces and Imote2-Platformed Impedance Sensor Node. The 6th International Workshop on Advanced Smart Materials and Smart Structures Technology, July 25-26, 2011, Dalian, China.

Electromechanical impedance for SHM of a bolt-joint

Pre-loading of a bolt-joint

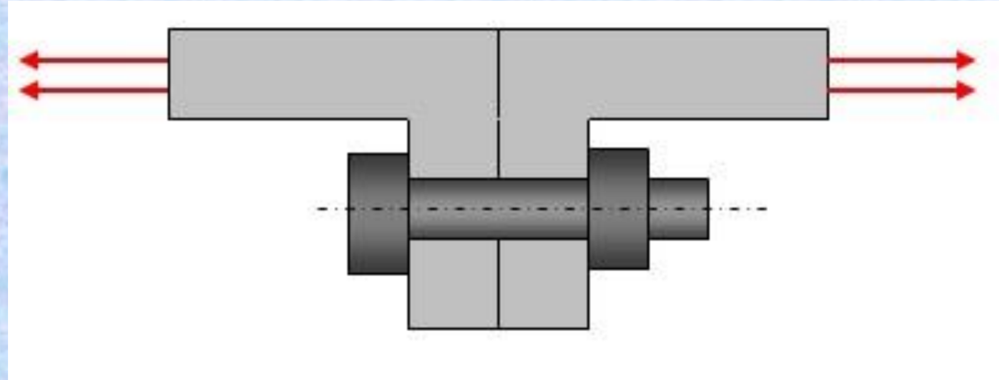

Bolt material: Hihg strength steel
Initil stress: 300MPa
Sensor: Pz27 Plate 6.35 x 6.35 x 1 mm
(Ferroperm Piezoceramics A/S)

V. Pavelko, S. Kuznetsov, I.Ozolinsh, I. Pavelko*
Aeronautic Institute, Riga Technical University

Test results: Pre-loading of a bolt-joint

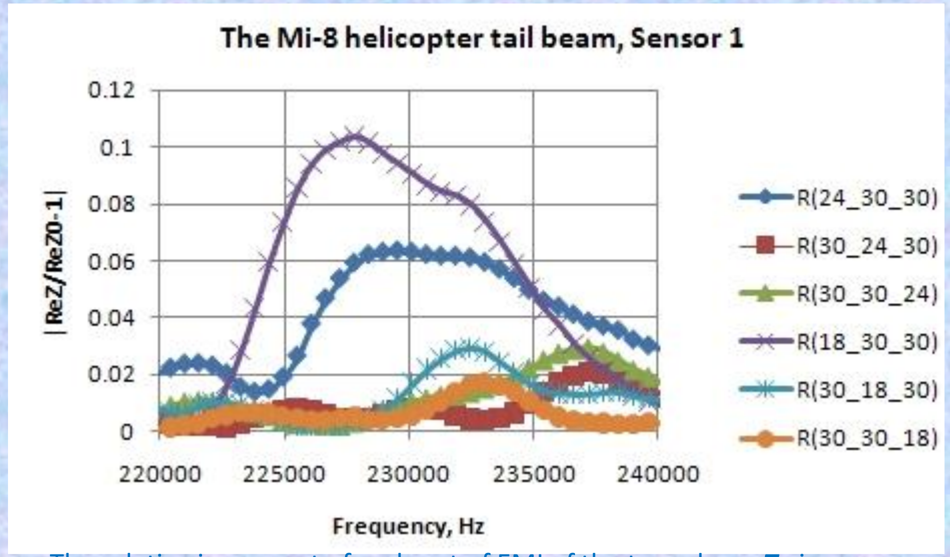

The relative increment of real part of EMI of the transducer T_1 in resonance frequency band as a result of loosing of bolt preload.

$$\Delta\overline{R} = \left| \frac{Re\,Z}{Re\,Z_0} - 1 \right|$$

V. Pavelko, S. Kuznetsov, I.Ozolinsh, I. Pavelko*
Aeronautic Institute, Riga Technical University

Test results: Pre-loading of a bolt-joint

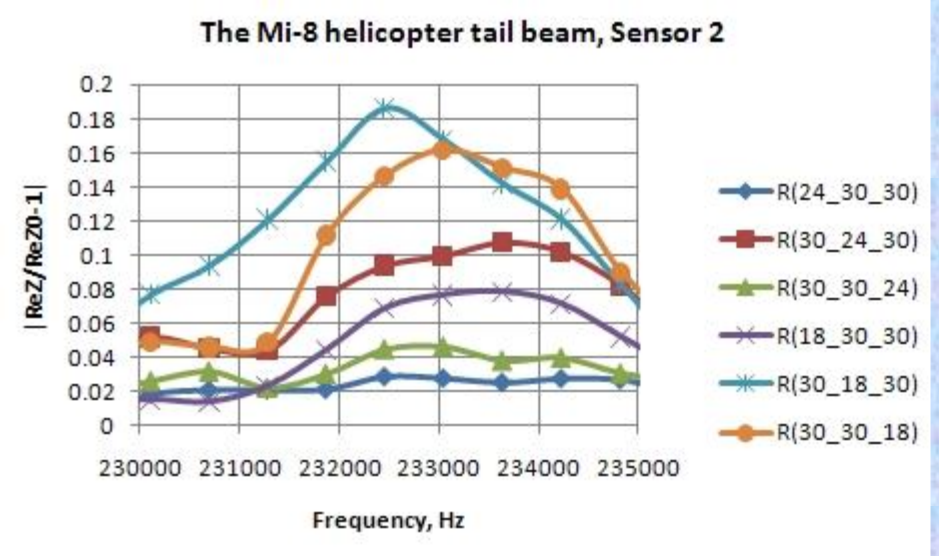

Figure 8. The relative increment of real part of EMI of the transducer T_2 in resonance frequency band as a result of loosing of bolt preload.

BOLT-JOINT STRUCTURAL HEALTH MONITORING BY METHOD OF ELECTROMECHANICAL IMPEDANCE

V. Pavelko[*], S. Kuznetsov, I.Ozolinsh, I. Pavelko
Aeronautic Institute, Riga Technical University

Test results: Pre-loading of a bolt-joint

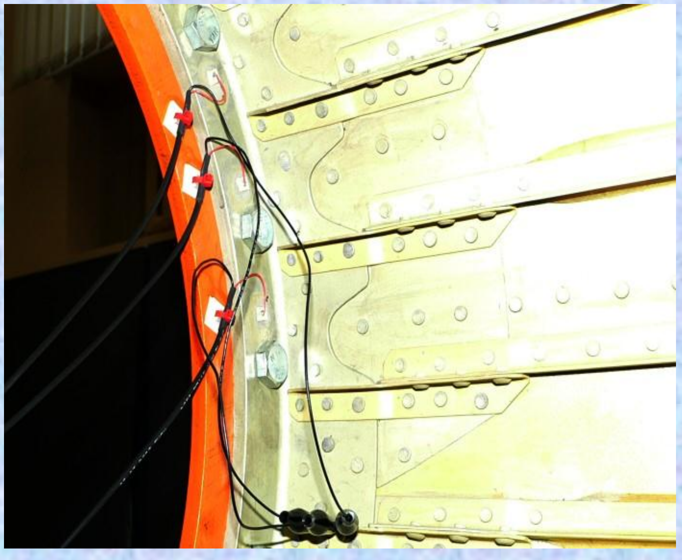

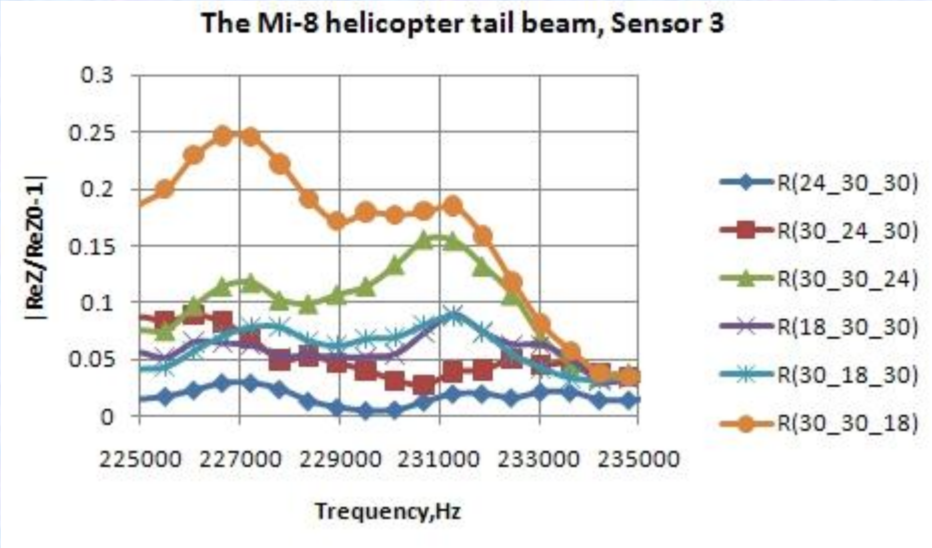

Figure 9. The relative increment of real part of EMI of the transducer $\boldsymbol{T_3}$ in resonance frequency band as a result of loosing of bolt preload.

V. Pavelko, S. Kuznetsov, I.Ozolinsh, I. Pavelko*
Aeronautic Institute, Riga Technical University

Special series of EMI measurements was performed for estimation of statistical stability of this results. The 95% confidence interval for EMI parameter of the transducer $\mathbf{T_1}$

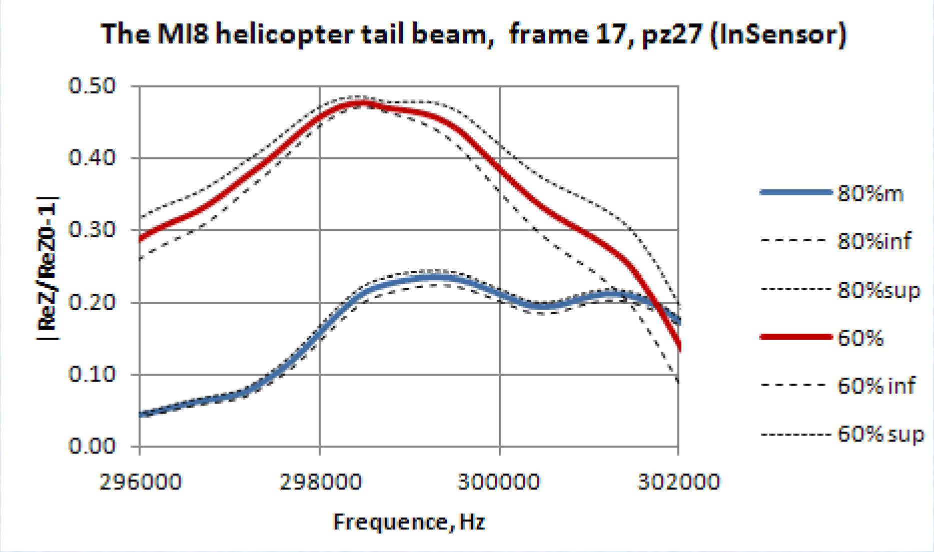

- The 95% confidence interval for EMI parameter of the transducer T_1

V. Pavelko[*], S. Kuznetsov, I.Ozolinsh, I. Pavelko
Aeronautic Institute, Riga Technical University

Computational Simulation

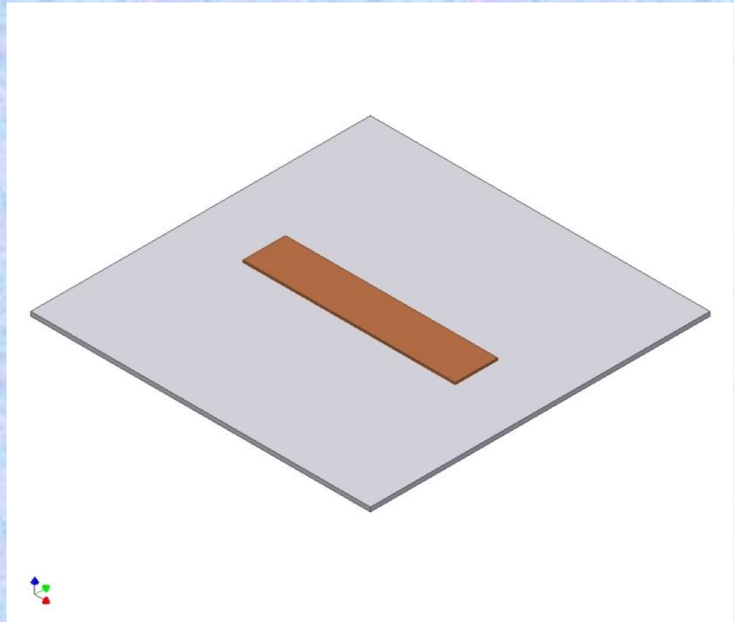

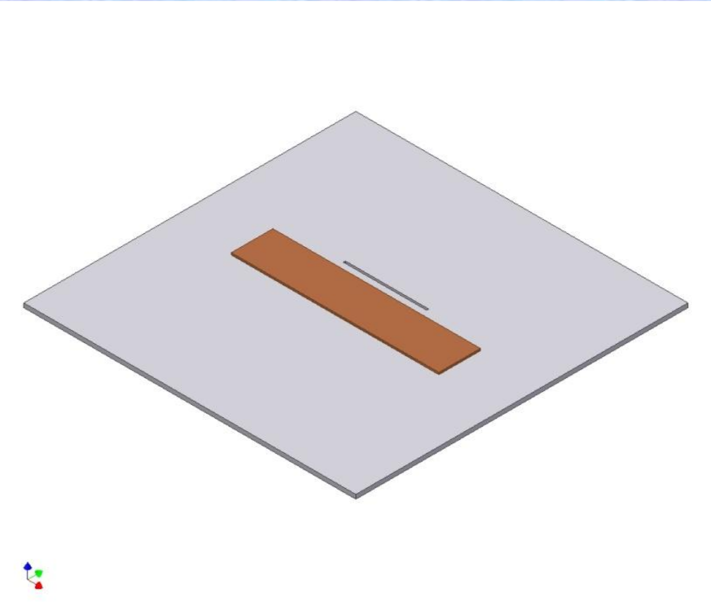

V. Pavelko, S. Kuznetsov, I.Ozolinsh, I. Pavelko*
Aeronautic Institute, Riga Technical University

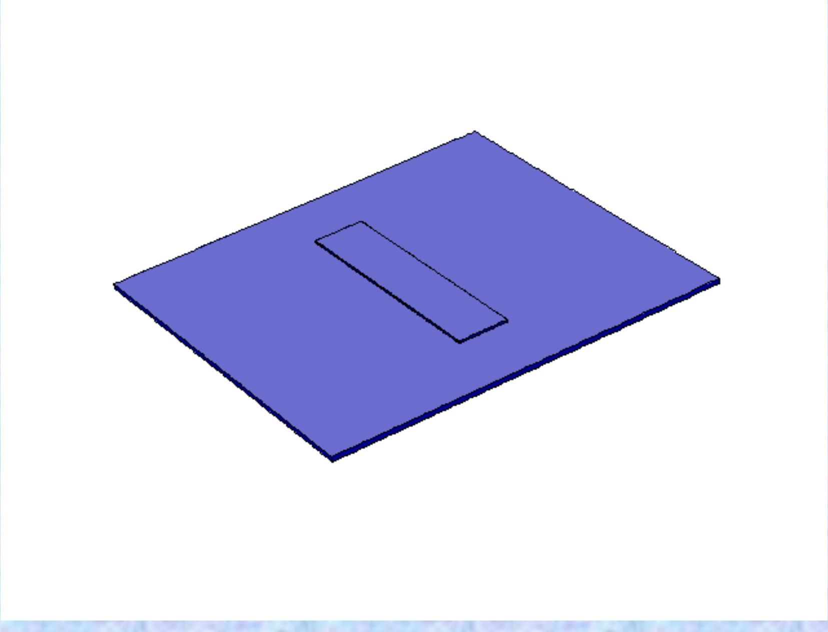

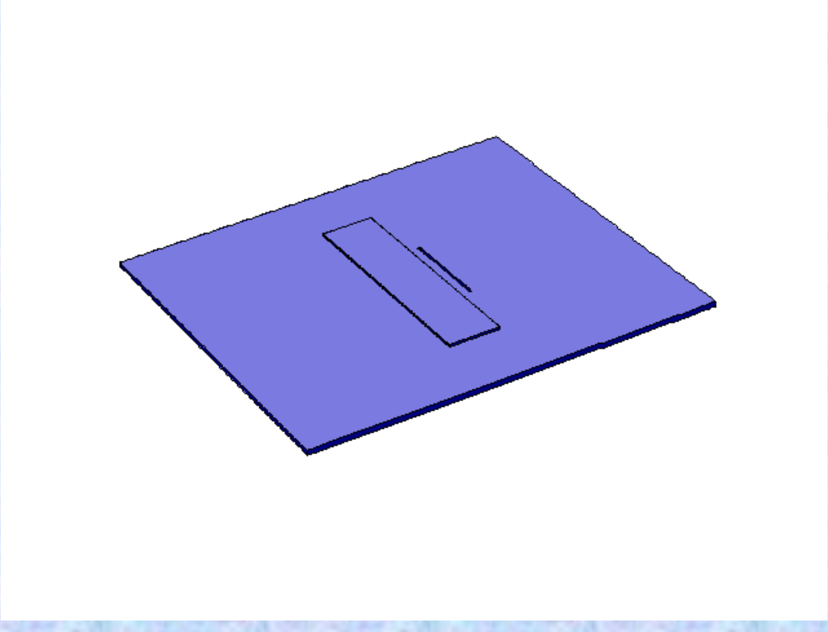

,

BOLT-JOINT STRUCTURAL HEALTH MONITORING BY METHOD OF ELECTROMECHANICAL IMPEDANCE

V. Pavelko, S. Kuznetsov, I.Ozolinsh, I. Pavelko*
Aeronautic Institute, Riga Technical University

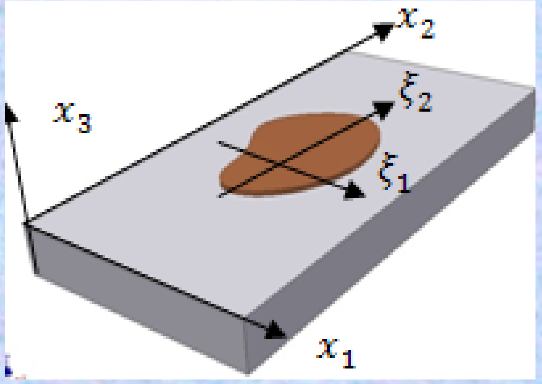

"Host structure-transducer" geometrical model

Analytical study: 2D model of EMI
The electromechanical impedance of constrained transducer

The general constitutive equation

$$D_3 = d_{31}(\sigma_1 + \sigma_2) + \varepsilon_{33}E_3$$

$$D_3 = \varepsilon_{33}E_3\left[1 + \frac{k_{31}^2}{1-\nu}\left(\frac{S_1+S_2}{d_{31}E_3} - 2\right)\right]$$

$$Q = \iint D_3\, d\xi_1 d\xi_2 = \varepsilon_{33}E_3 \iint \left[1 + \frac{k_{31}^2}{1-\nu_{12}}\left(\frac{S_1+S_2}{d_{31}E_3} - 2\right)\right] d\xi_1 d\xi_2$$

$$Q = \varepsilon_{33}E_3 A\left[1 + \frac{k_{31}^2}{1-\nu}\left(\frac{\Delta\bar{A}}{d_{31}E_3 l_1} - 2\right)\right]$$

$$Z = \frac{1}{i\omega C}\left[1 + \frac{k_{31}^2}{1-\nu}\left(\frac{\Delta\bar{A}}{d_{31}E_3} - 2\right)\right]^{-1}$$

BOLT-JOINT STRUCTURAL HEALTH MONITORING BY METHOD OF ELECTROMECHANICAL IMPEDANCE

V. Pavelko, S. Kuznetsov, I.Ozolinsh, I. Pavelko*
Aeronautic Institute, Riga Technical University

Compatibility conditions

equality of vectors of interaction forces (with opposite sign).. $\boldsymbol{p}_s(\zeta) = -\boldsymbol{p}_t(\zeta)$

equality of vectors of displacements…………………………… $\boldsymbol{u}_s(\zeta) = \boldsymbol{u}_t(\zeta) + \varepsilon_{33}E_3\zeta$

Interaction force defining using modal decomposition of displacements of a host structure and a transducer

Second compatibility condition can be transformed to following form

$$\sum_{k=1}^{\infty}\frac{U_{tk}(x)\Phi_{tk}}{M_{tk}\left(\omega_{tk}^2-\omega^2\right)}+d_{13}E_3x=\sum_{k=1}^{\infty}\frac{U_{sk}(x)\Phi_{sk}}{M_{sk}\left(\omega_{sk}^2-\omega^2\right)}$$

or in a form more convenient for numerical analysis

$$\iint K(x,\zeta)\boldsymbol{p}(\zeta)\,dA = d_{13}E_3x \qquad K(x,\zeta)=\sum_{k=1}^{\infty}\frac{U_{sk}(x)U_{tk}(\zeta)}{M_{sk}\left(\omega_{sk}^2-\omega^2\right)}+\sum_{k=1}^{\infty}\frac{U_{tk}(x)U_{tk}(\zeta)}{M_{tk}\left(\omega_{tk}^2-\omega^2\right)}$$

BOLT-JOINT STRUCTURAL HEALTH MONITORING BY METHOD OF ELECTROMECHANICAL IMPEDANCE

V. Pavelko, S. Kuznetsov, I.Ozolinsh, I. Pavelko*
Aeronautic Institute, Riga Technical University

Simple case: rectangular shape of transducer

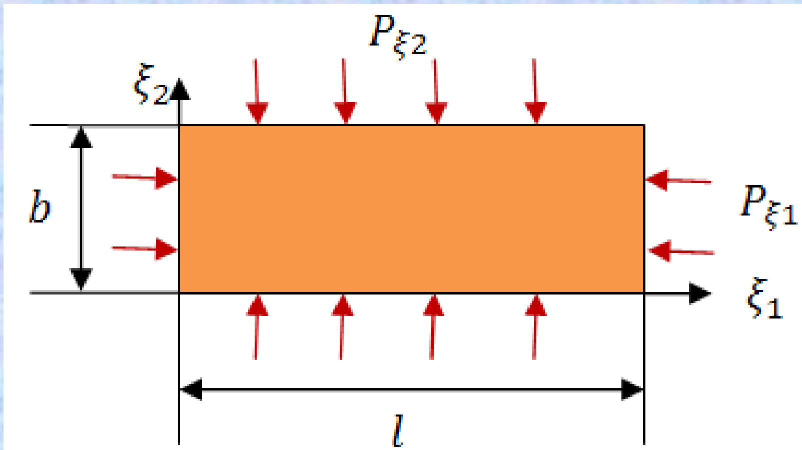

Shape of transducer and pin-end force model

$$F_{\xi 1} = \int_0^b P_{\xi 1} d\xi_2 , \qquad F_{\xi 2} = \int_0^b P_{\xi 2} d\xi_1$$

$$\begin{cases} C_{11}F_{\xi 1} + C_{12}F_{\xi 2} = d_{13}E_3 l \\ C_{21}F_{\xi 1} + C_{22}F_{\xi 2} = d_{13}E_3 b \end{cases}$$

$$C_{11} = \sum_{k=1}^{\infty} \frac{\Delta U_{t1k}^2}{M_{tk}(\omega_{tk}^2 - \omega^2)} + \sum_{k=1}^{\infty} \frac{\Delta U_{s1k}^2}{M_{sk}(\omega_{sk}^2 - \omega^2)}$$

$$C_{12} = C_{21} = \sum_{k=1}^{\infty} \frac{\Delta U_{t1k}\Delta U_{t2k}}{M_{tk}(\omega_{tk}^2 - \omega^2)} + \sum_{k=1}^{\infty} \frac{\Delta U_{s1k}\Delta U_{s2k}}{M_{sk}(\omega_{sk}^2 - \omega^2)}$$

$$C_{22} = \sum_{k=1}^{\infty} \frac{\Delta U_{t2k}^2}{M_{tk}(\omega_{tk}^2 - \omega^2)} + \sum_{k=1}^{\infty} \frac{\Delta U_{s2k}^2}{M_{sk}(\omega_{sk}^2 - \omega^2)}$$

$$\boldsymbol{\Delta U} = \Delta U_1 \boldsymbol{i} + \Delta U_2 \boldsymbol{j} = \sum_{k=1}^{\infty} \frac{\boldsymbol{\Delta U_k}\left(F_{\xi 1}\Delta U_{1k} + F_{\xi 2}\Delta U_{2k}\right)}{M_k\left(\omega_k^2 - \omega^2\right)}$$

$$\Delta \bar{A} = \frac{1}{A}(\Delta U_1 b + \Delta U_2 l)$$

BOLT-JOINT STRUCTURAL HEALTH MONITORING BY METHOD OF ELECTROMECHANICAL IMPEDANCE

V. Pavelko[*], S. Kuznetsov, I.Ozolinsh, I. Pavelko
Aeronautic Institute, Riga Technical University

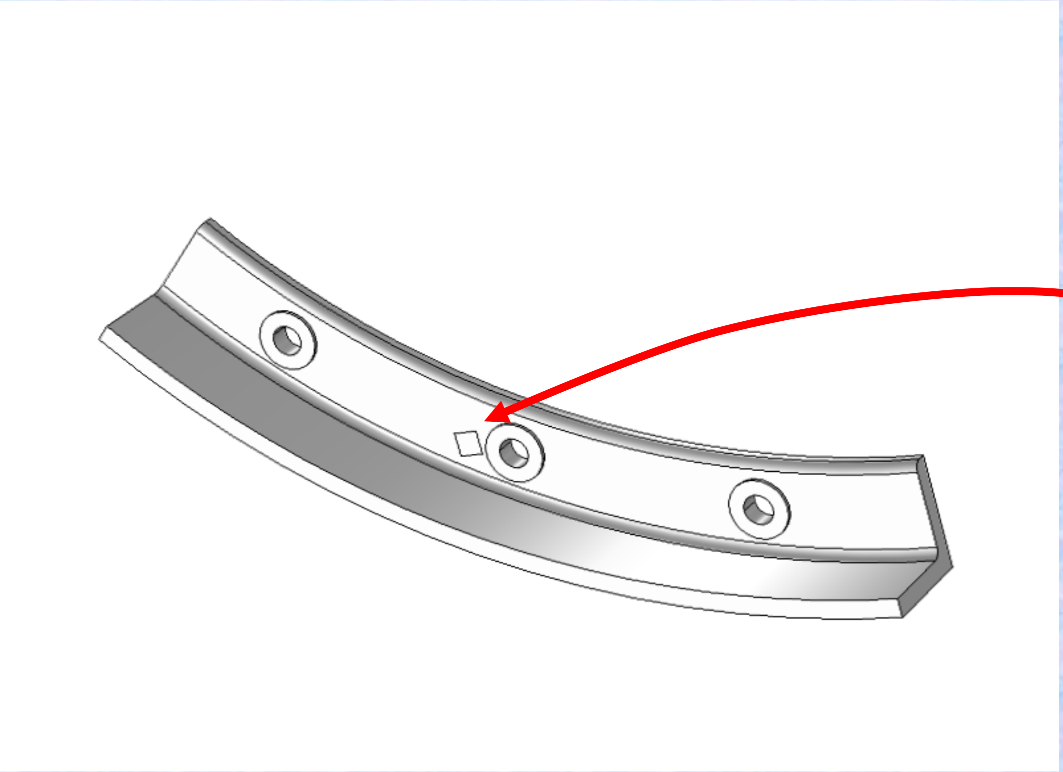

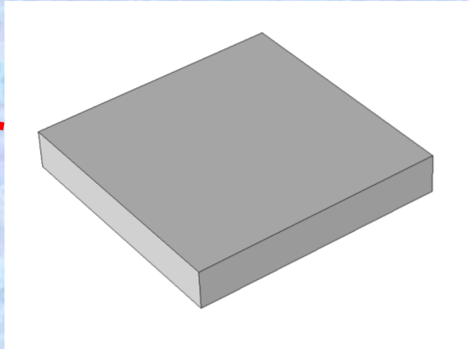

BOLT-JOINT STRUCTURAL HEALTH MONITORING BY METHOD OF ELECTROMECHANICAL IMPEDANCE

V. Pavelko, S. Kuznetsov, I.Ozolinsh, I. Pavelko*
Aeronautic Institute, Riga Technical University

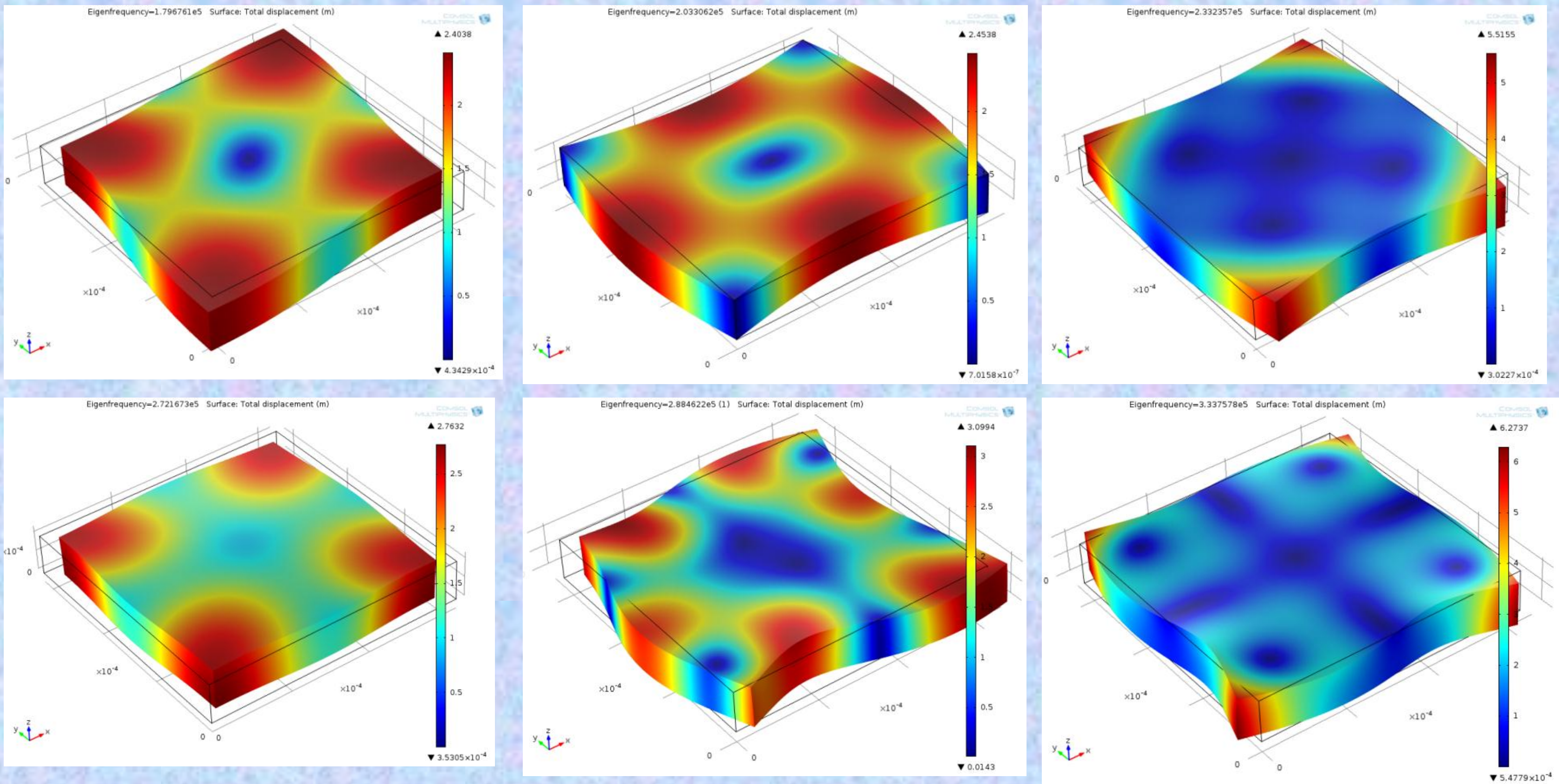

BOLT-JOINT STRUCTURAL HEALTH MONITORING BY METHOD OF ELECTROMECHANICAL IMPEDANCE

V. Pavelko[*], S. Kuznetsov, I.Ozolinsh, I. Pavelko
Aeronautic Institute, Riga Technical University

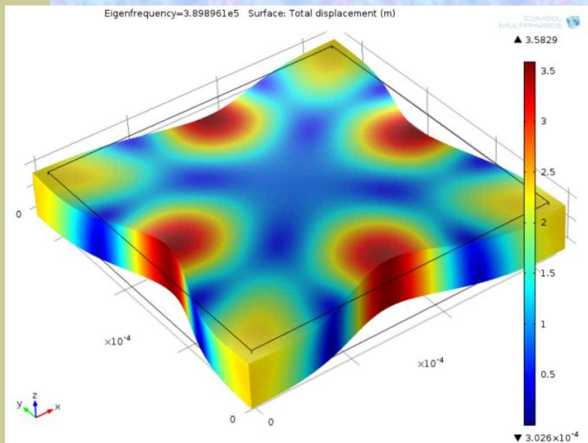

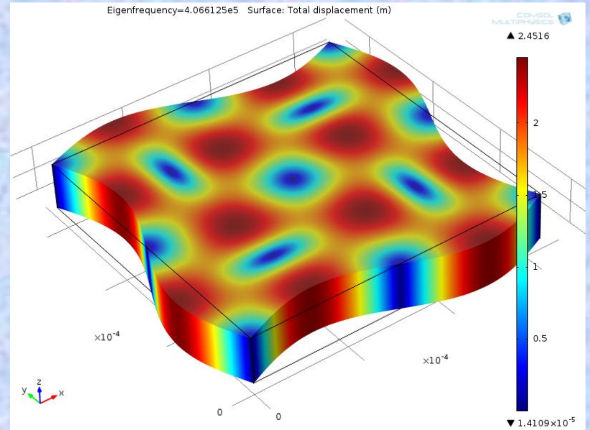

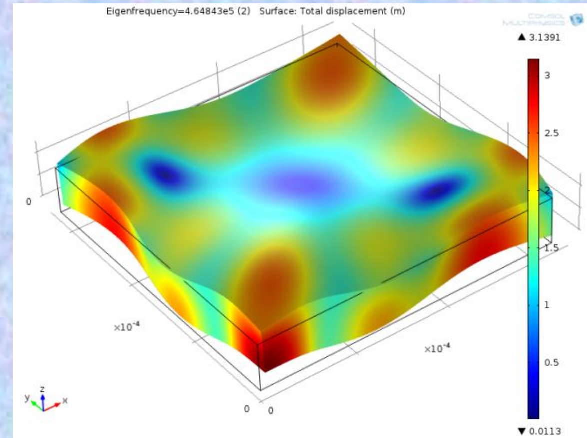

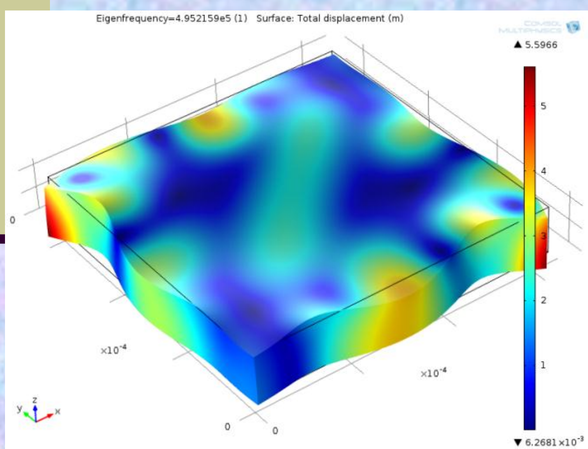

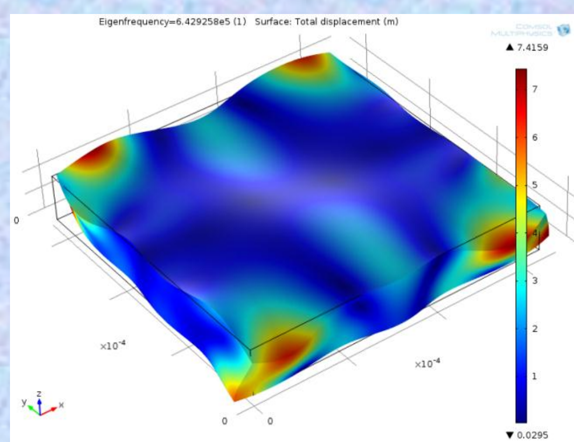

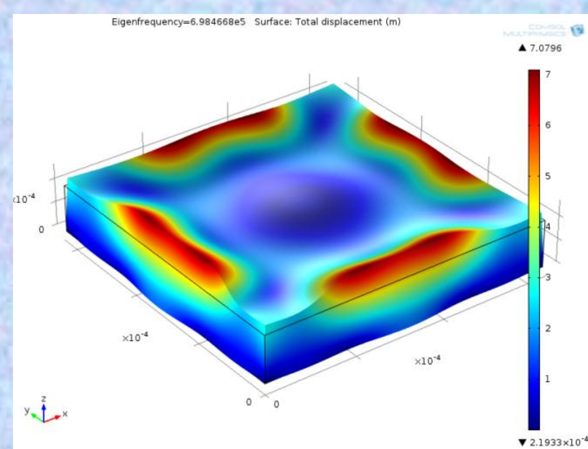

BOLT-JOINT STRUCTURAL HEALTH MONITORING BY METHOD OF ELECTROMECHANICAL IMPEDANCE

V. Pavelko, S. Kuznetsov, I.Ozolinsh, I. Pavelko*
Aeronautic Institute, Riga Technical University

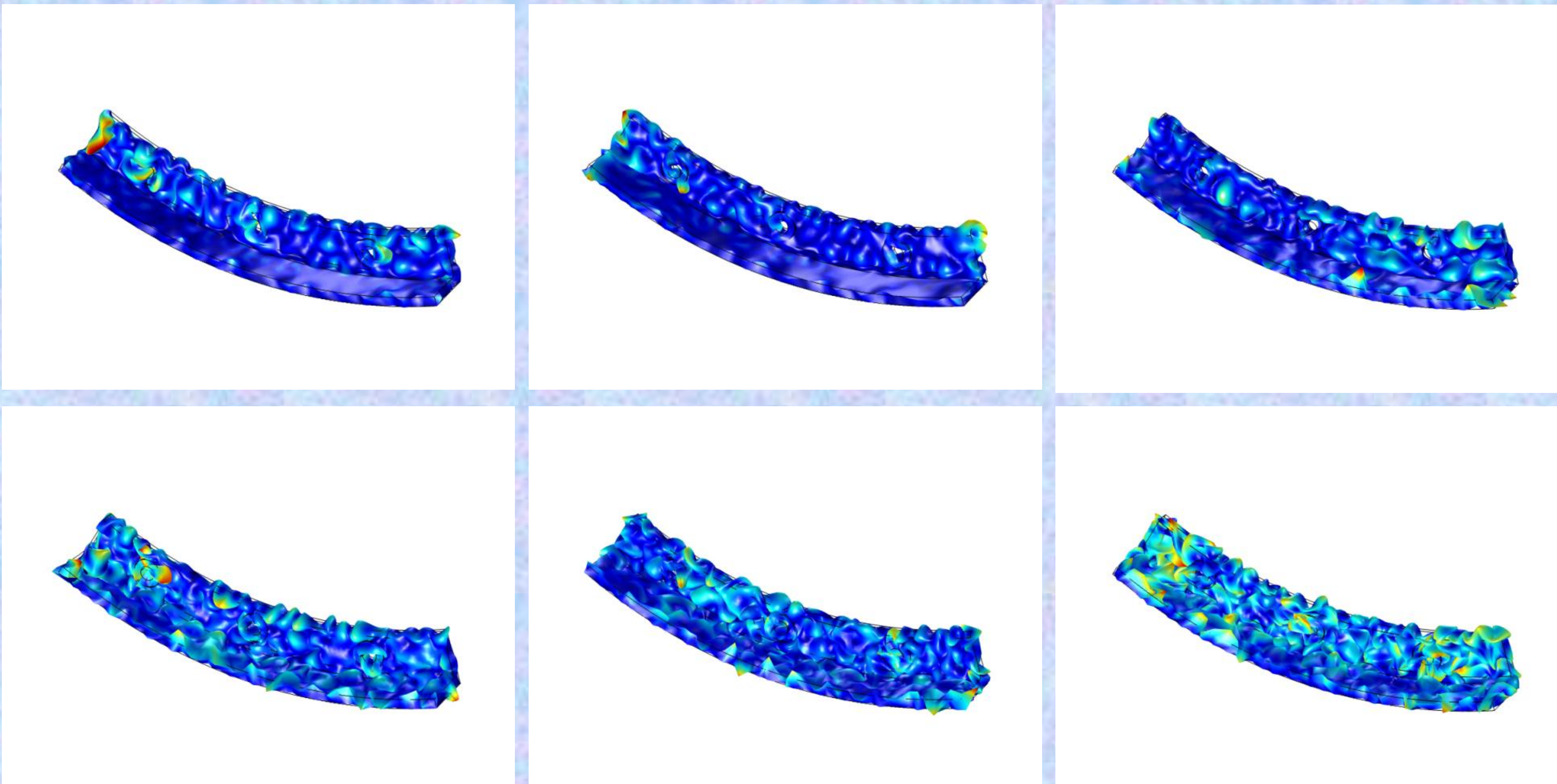

BOLT-JOINT STRUCTURAL HEALTH MONITORING BY METHOD OF ELECTROMECHANICAL IMPEDANCE

V. Pavelko, S. Kuznetsov, I.Ozolinsh, I. Pavelko*
Aeronautic Institute, Riga Technical University

Some results of simulation

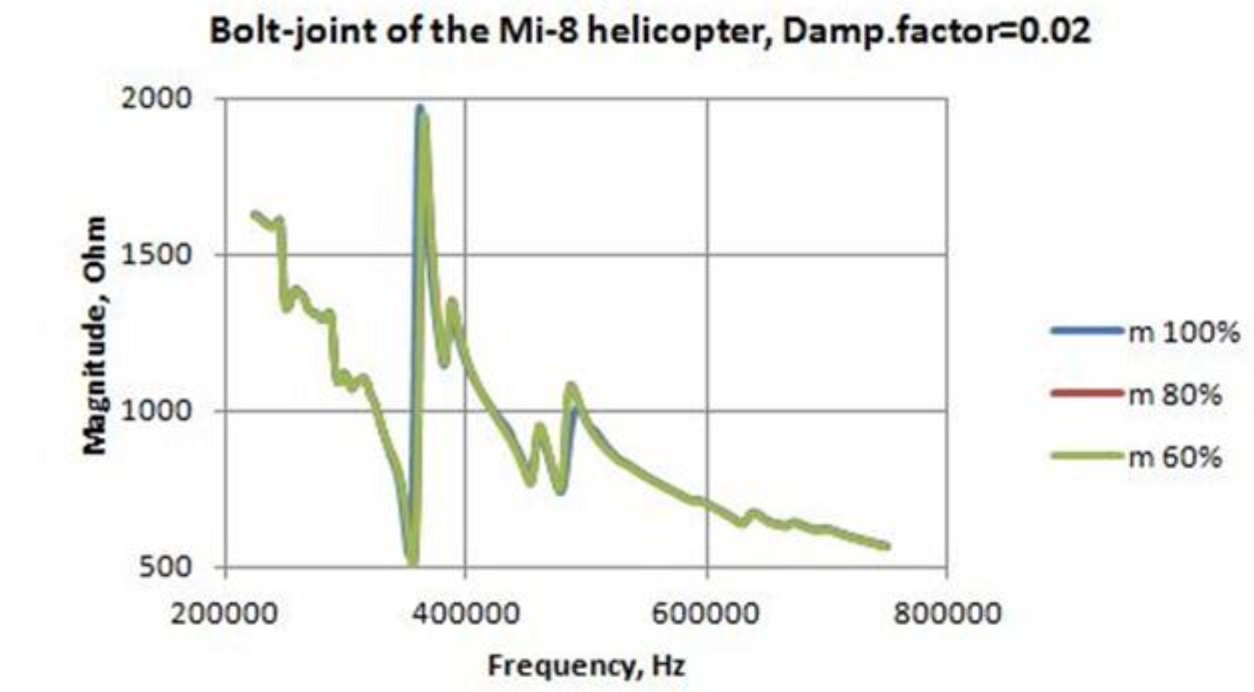

BOLT-JOINT STRUCTURAL HEALTH MONITORING BY METHOD OF ELECTROMECHANICAL IMPEDANCE

V. Pavelko, S. Kuznetsov, I.Ozolinsh, I. Pavelko*
Aeronautic Institute, Riga Technical University

Some results of simulation

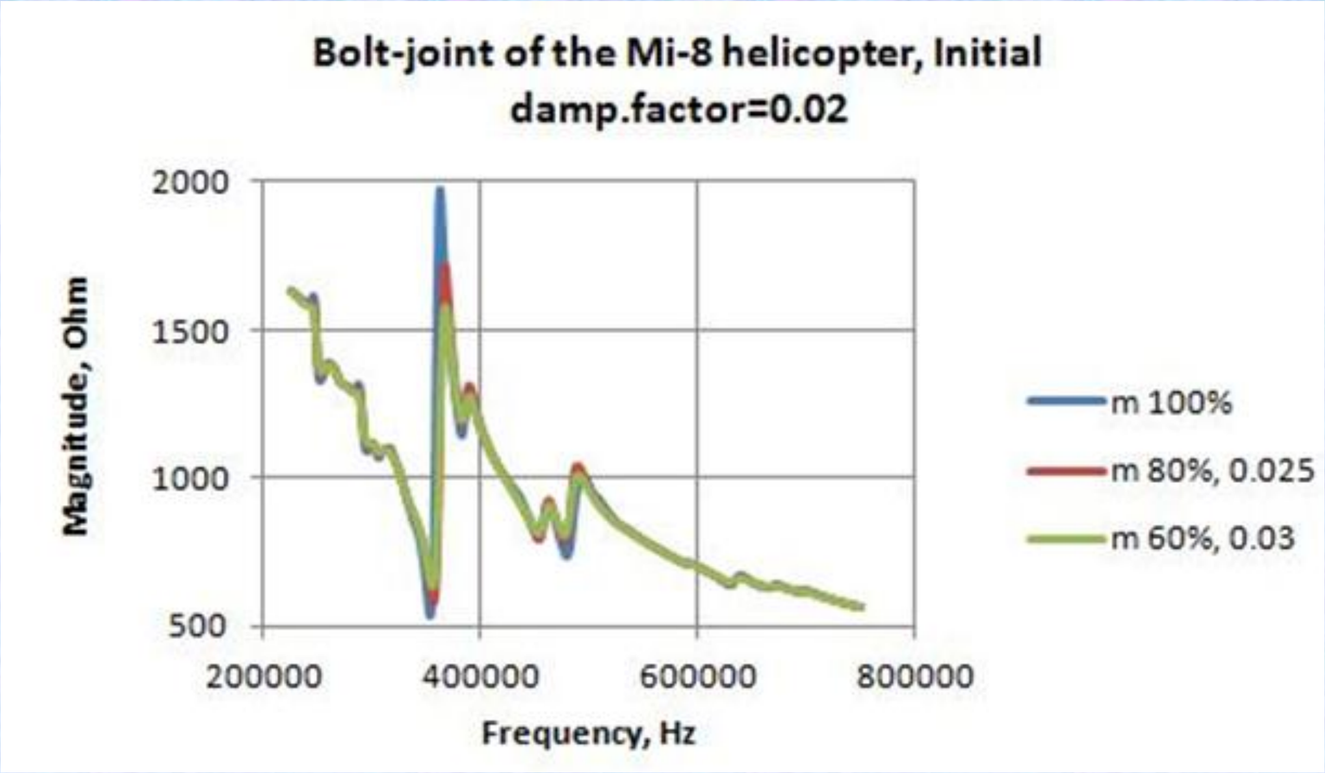

BOLT-JOINT STRUCTURAL HEALTH MONITORING BY METHOD OF ELECTROMECHANICAL IMPEDANCE

V. Pavelko, S. Kuznetsov, I.Ozolinsh, I. Pavelko*
Aeronautic Institute, Riga Technical University

Conclusions

•The effect of structural damage is associated with the changes of dynamic properties of a structure and can be effectively defined by identification of EMI of system ‘transducer - host-structure’.
•Test result shows that there is stable response of EMI to loosening of bolt-joint. This can be used for SHM of bolt-joints of aerospace structure. It can suppose that effect of loosening of bolt-joint to EMI is caused by friction changing.
•The developed 2D model of constrained PZT can be used for analysis of the elastic and geometrical parameters effect to properties of constrained piezoceramics transducer, and for structural health monitoring of element with different possible damages including bolt-joint loosening.
•Results of simulation with developed model confirm the assumption of dominant influence of friction in a bolt-joint to EMI.
•There is needed additional investigation and development of adequate model of friction in bolt-joint.

BOLT-JOINT STRUCTURAL HEALTH MONITORING BY METHOD OF ELECTROMECHANICAL IMPEDANCE

V. Pavelko[*], S. Kuznetsov, I.Ozolinsh, I. Pavelko
Aeronautic Institute, Riga Technical University

Acknowledgement

- The research leading to these results has received funding from the European Community's Seventh Framework Program [FP7/2007-2013] under grant agreement n°212912. The authors are grateful to European Commission for financial support and all partners for scientific and technological collaboration.

Thanks you for your attention!

2nd EASN WORKSHOP
on Flight Physics and Propulsion

The Preliminary, Parametric Design and Optimisation of the Air-intake System and the Nacelle as a Part of Integration of Turboprop Engine in a Small Aircraft

institute of aviation
warsaw, since 1926

Wienczyslaw Stalewski
Jerzy Zoltak

Prague Czech Republic 31st October - 2nd November 2012

Outline

1. **Background and Goals of the Research**
2. **Definition of the Problem**
3. **Methodology**
4. **Description of the Design Process**
5. **Conclusions**

Research Background

- EU Project **ESPOSA**
  Efficient Systems and Propulsion for Small Aircraft
- "The goal of the ESPOSA project is to develop new key components for small gas turbine engines up to 1000 kW and to develop new lean manufacture technologies.
  The project will also deal with engine related systems that will contribute to the overall propulsion unit efficiency, safety and pilot workload reduction." (#)
- The ESPOSA Subproject:
  "**Advanced Design Methods for Engine Integration**"

(#) ESPOSA official website: http://www.esposa-project.eu

Research Goals

- To develop a preliminary concept of the **Integration** of:
  - **TP100 Gas Turbine Engine**
    (one of ESPOSA baseline engines,
    manufactured by the PBS Velká Bíteš)
  - **I-23 Aircraft**
    (one of ESPOSA flying demonstrators: small aircraft, single-engine, propeller driven in a tractor configuration)
- The research should be focused on fluid-dynamics aspects of the integration, and should concern the following components of the aircraft:
  - **Engine Nacelle**
  - **Air Delivery** and **Cooling Systems**
  - **Exhaust System**

Problem Definition - Requirements

- The inlet duct shape and dimensions must ensure sufficient and steady air delivery without excessive pressure loses and distortion
- Due to engine protection it is recommended to design the foreign particles separator, activated in low-altitude flight
- The shape of the nacelle must comply with the rest of the fuselage and must not collide with its internal content, including the turboprop engine with its necessary equipment
- The design of the nacelle must ensure to introduce the auxiliary air ducts, delivering the air for the cooling and air-conditioning purposes
- The designed nacelle and air-delivery ducts must comply with simultaneously designed ducts of the exhaust system

Problem Definition - Constraints

- **Integration Constraints**

  fixed Shapes and Positions of:
  - turboprop engine
  - engine mounting truss
  - front landing gear
  - propeller and spinner
  - battery

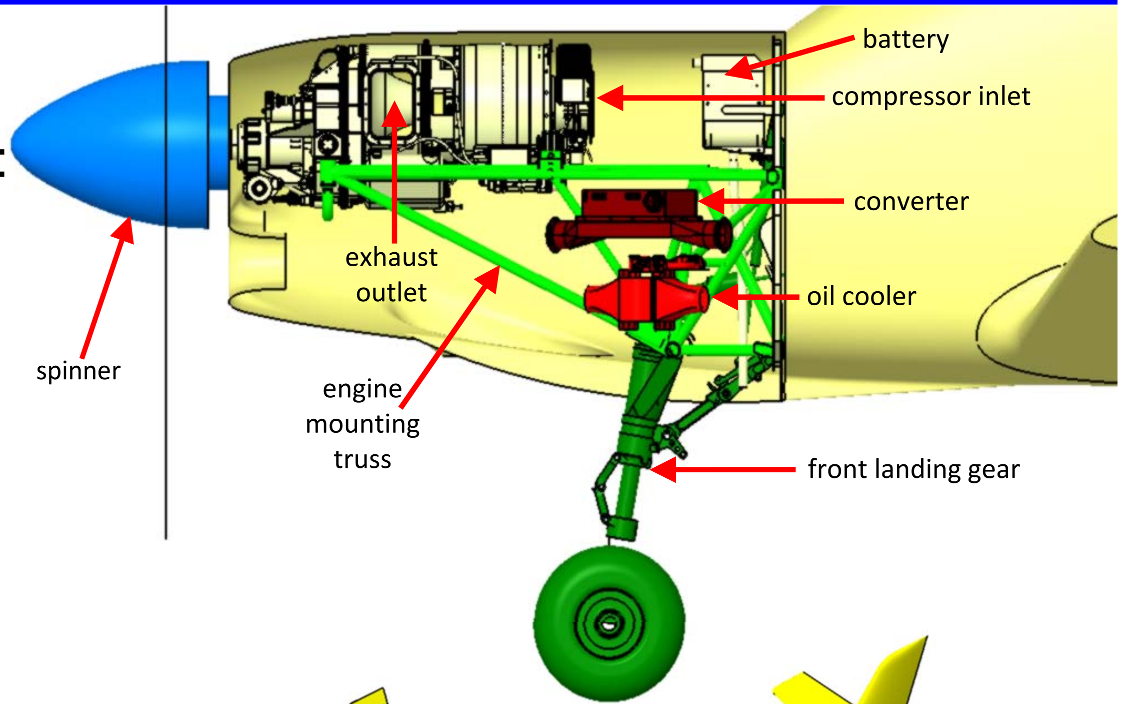

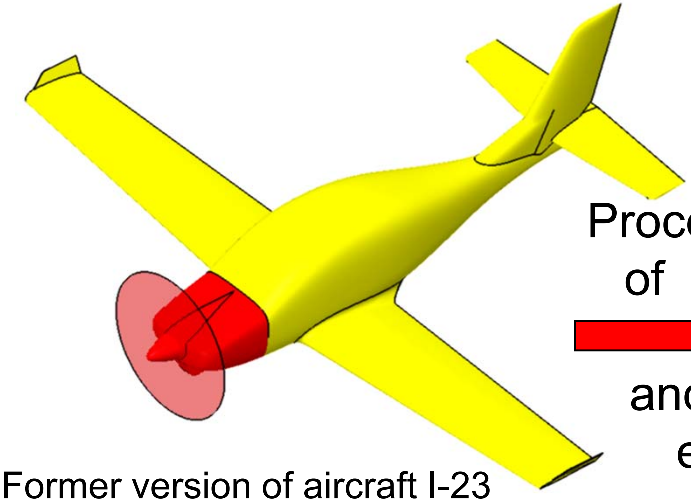

Former version of aircraft I-23
with piston propulsion

Process of integration of the aircraft **I-23**

and the turboprop engine **TP100**

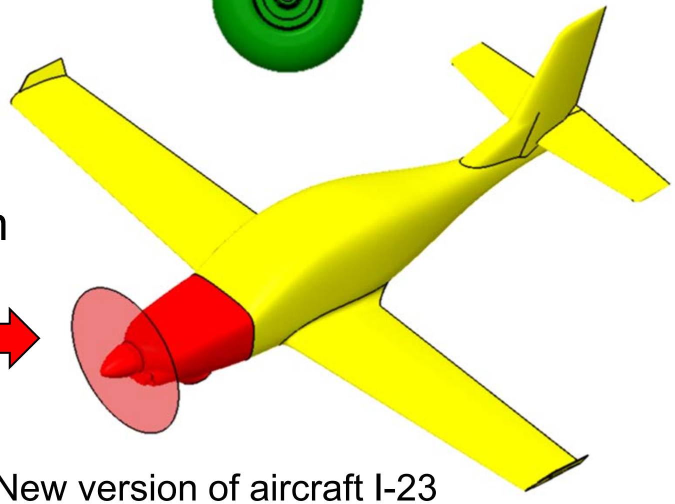

New version of aircraft I-23
with turboprop propulsion

Methodology

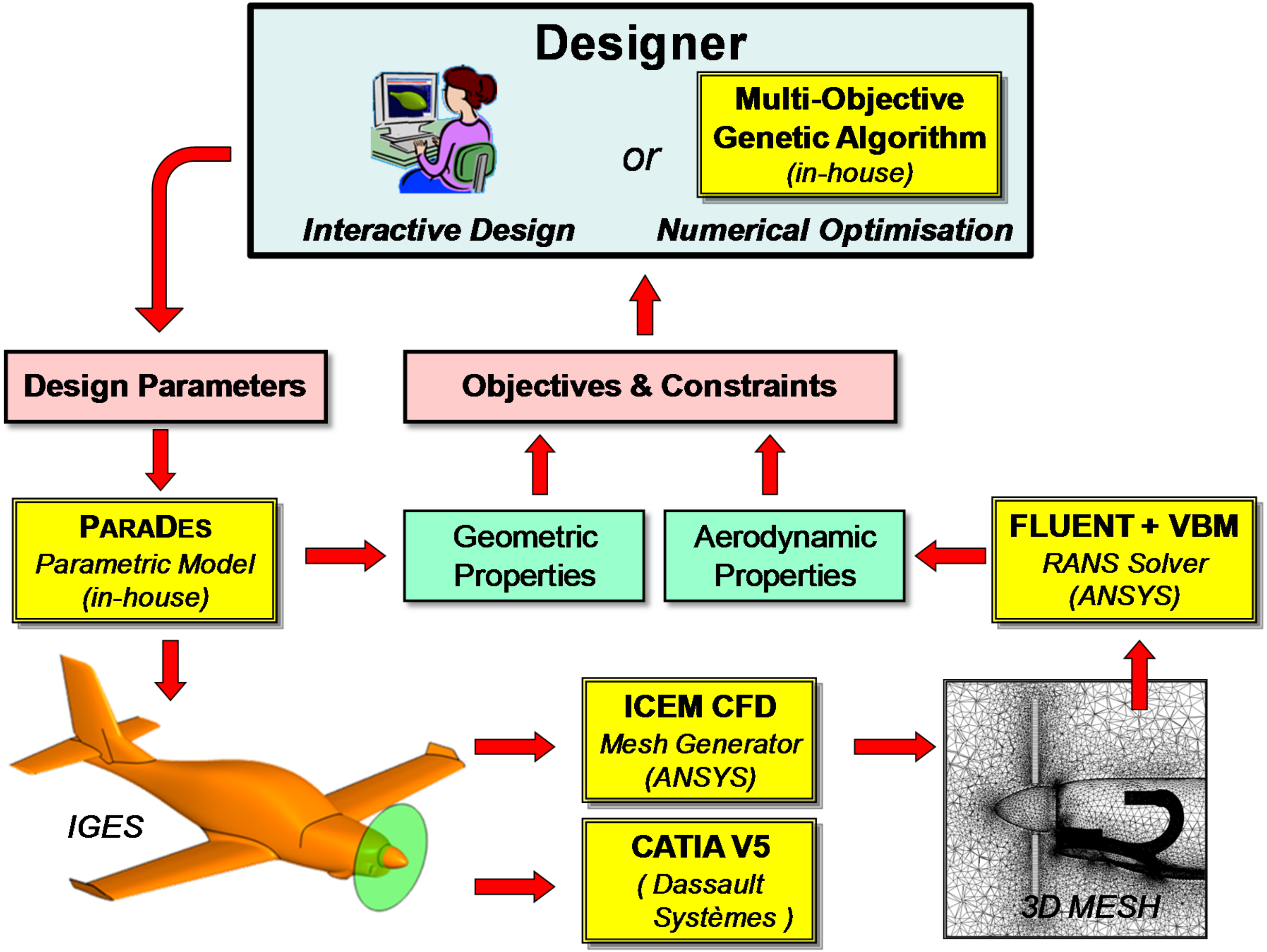

Methodology – Parametric Modelling

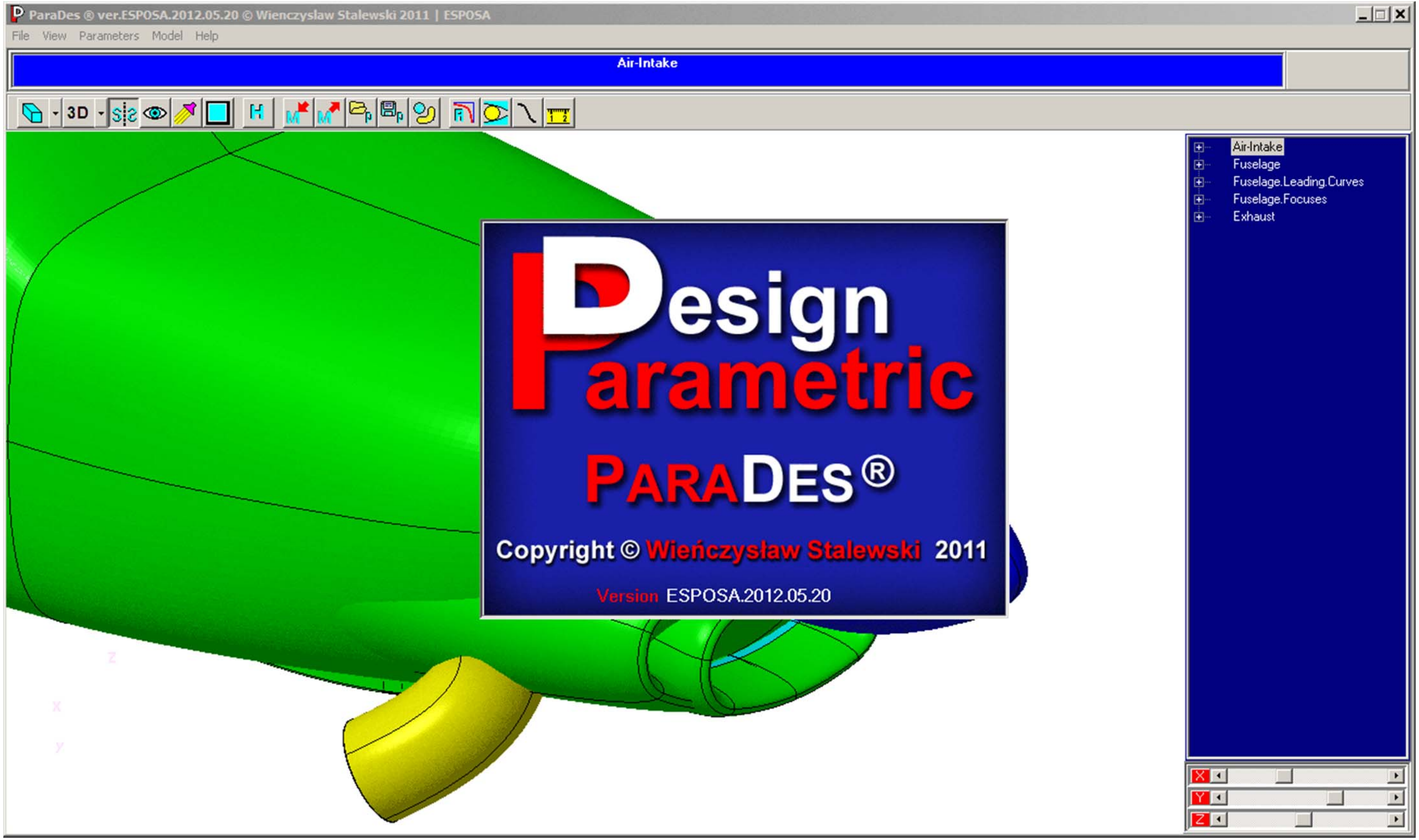

PARADES - parametric modelling software

Methodology – Parametric Modelling

Standard **P**   **Morphing** **W**

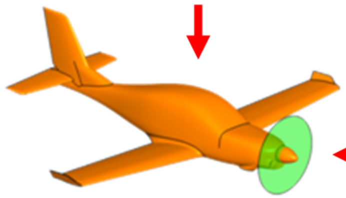

P = B • W (convex combination)

P	- Set of Design Parameters
B = [$B_1,\ldots,B_N$]	- Base Sets of Design Parameters
W = [$w_1,\ldots,w_N$]	- Morphing Weights $w_1+\ldots+w_N=1$, $w_i \geq 0$

- **Morphing**

Advantages

- Significantly reduced number of Design Parameters
- Inheritance of feasibility, smoothness, etc.

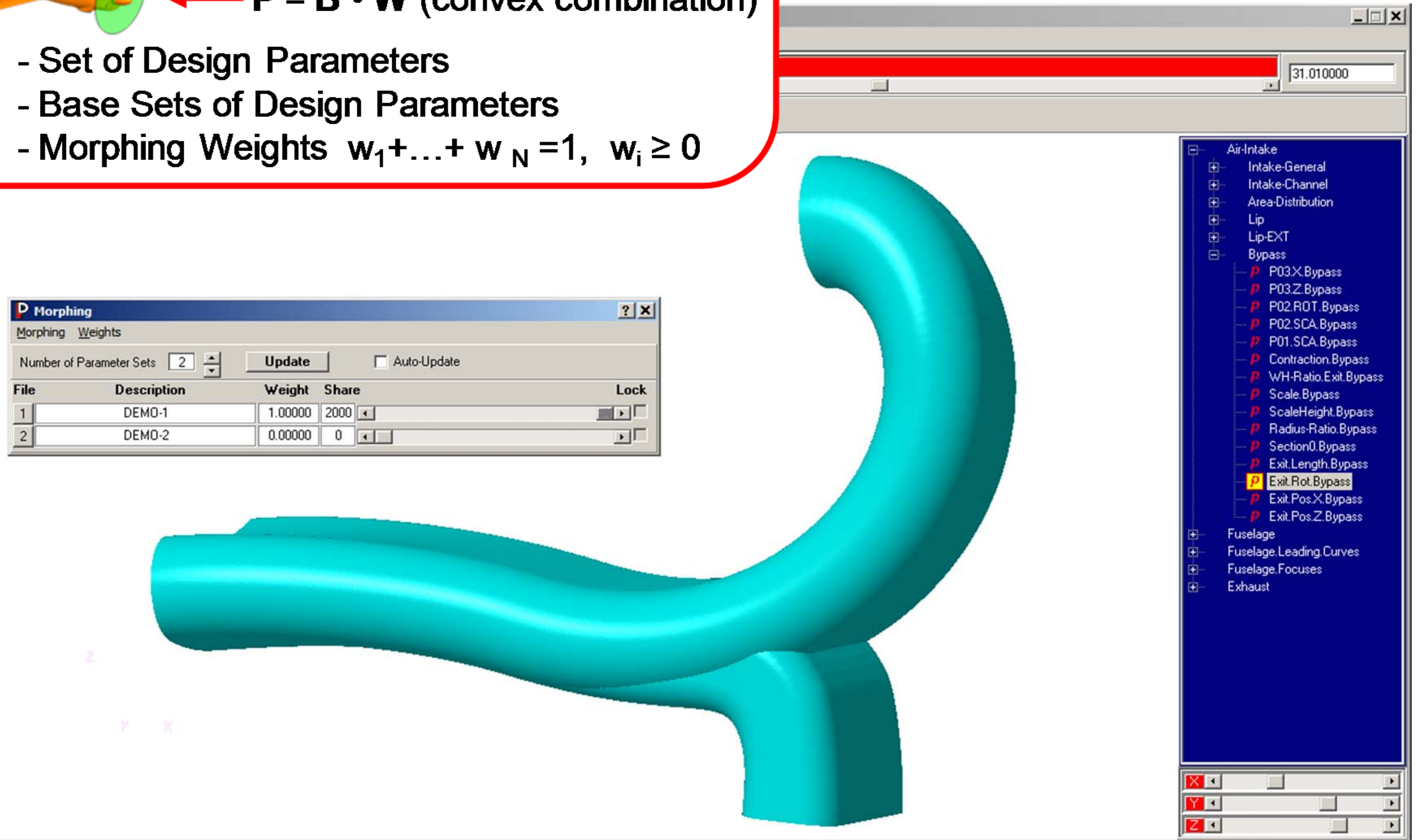

Methodology – CFD Analyses

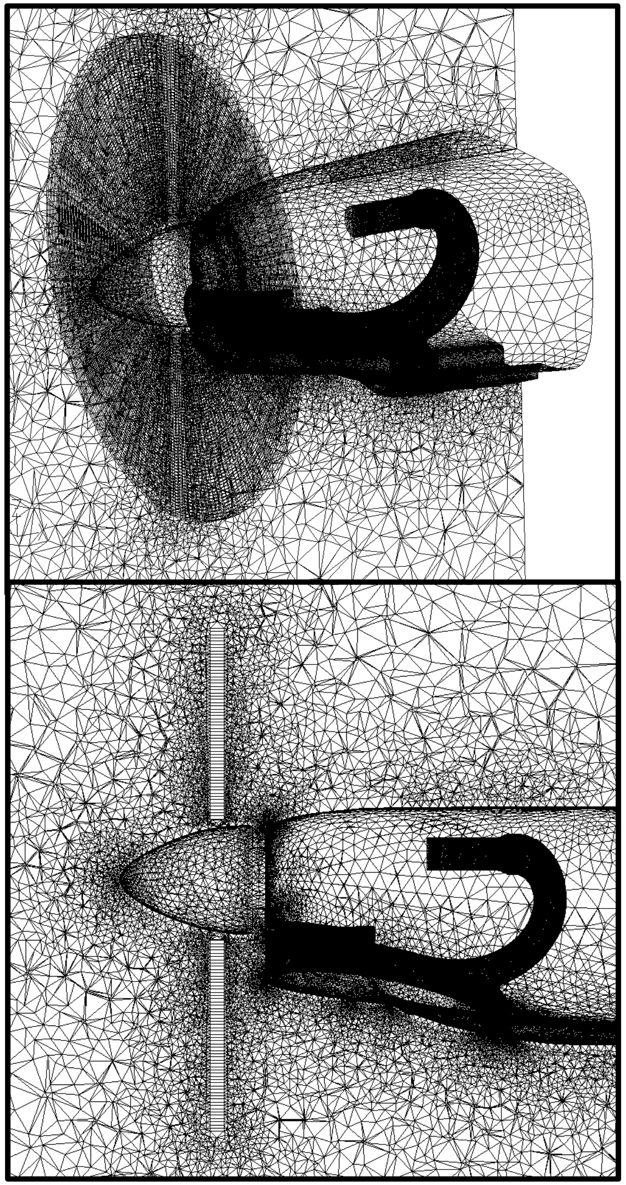

CFD computations

- RANS solver: **FLUENT** (ANSYS)
- mesh generator: **ICEM CFD** (ANSYS)
- computational model:
  - flow model: steady, compressible, viscous
  - turbulence model: k-ω, SST
  - mesh quality: fine (y+ ≈1)
- effect of rotating propeller**: Virtual Blade Model**

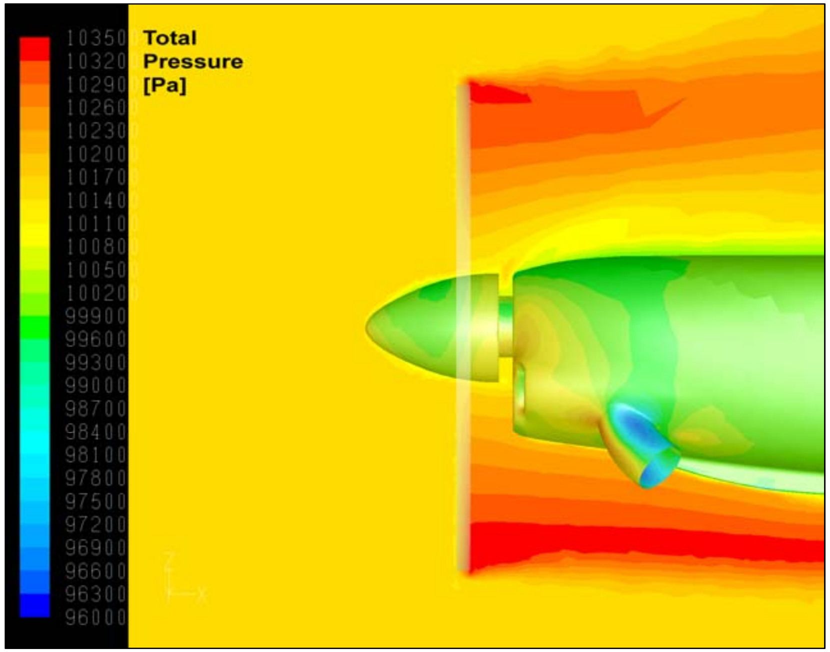

Methodology – CFD Analyses

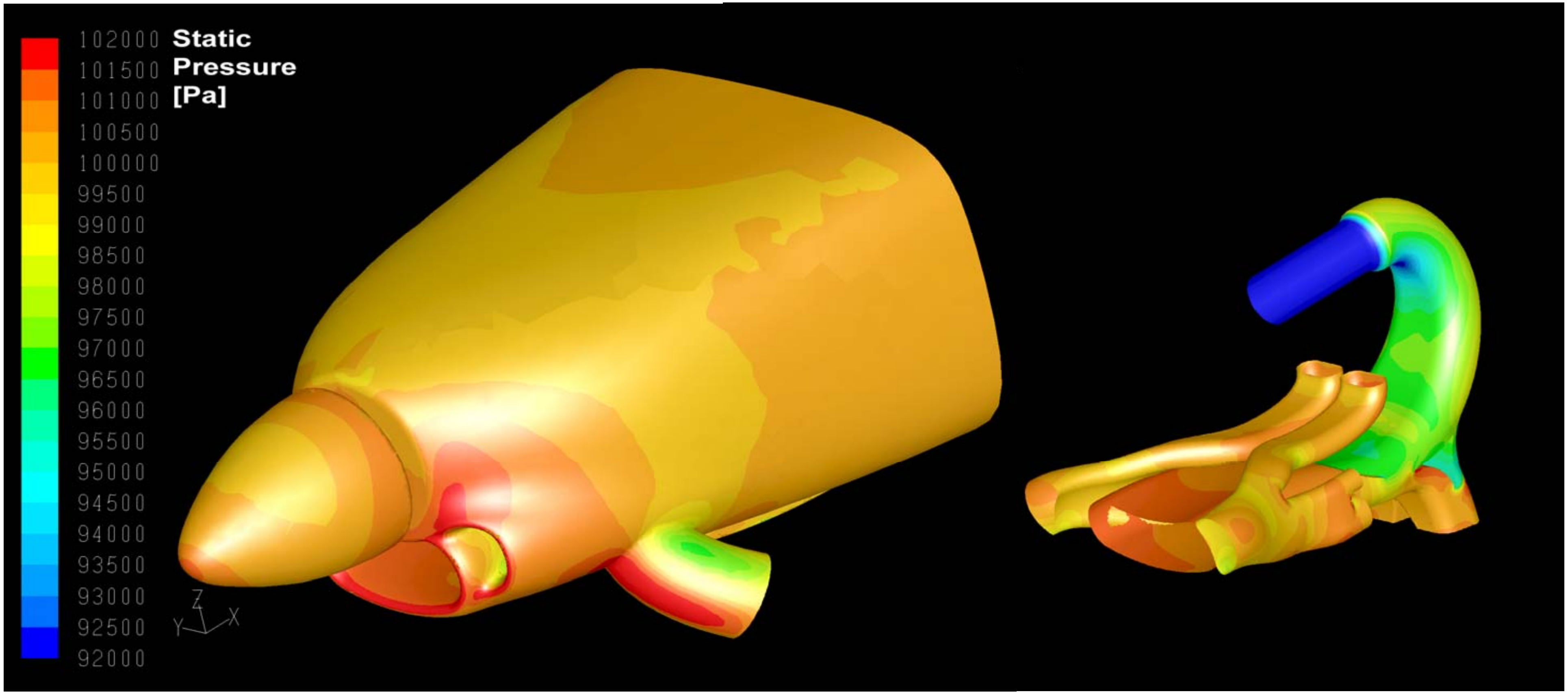

Contours of Static Pressure on the walls of the Air-Delivery-System ducts and on the Nacelle.
Results of RANS simulation of flow around the nacelle and inside the internal ducts
with active modelling of flow effects caused by the rotating propeller.

The Concept of the Integration

- **Concept of the Air-Intake duct delivering the air to the engine compressor**

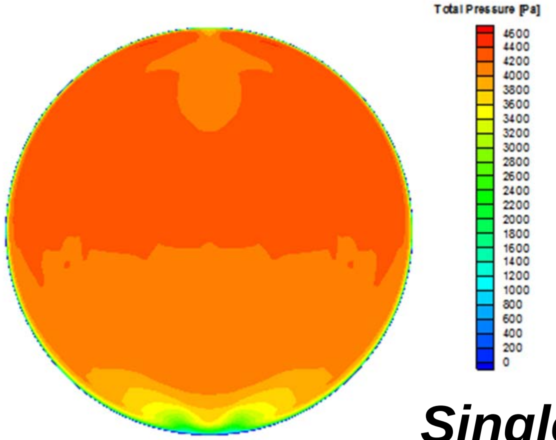

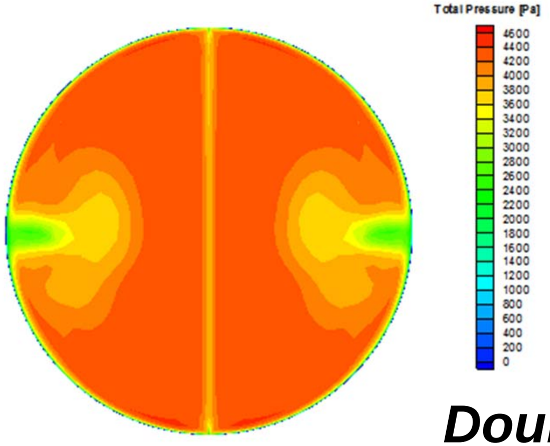

Single-Bottom

Double-Side

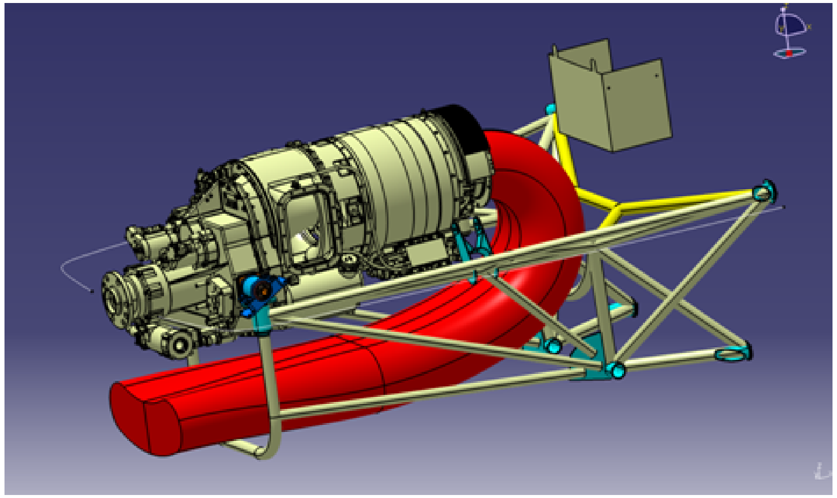

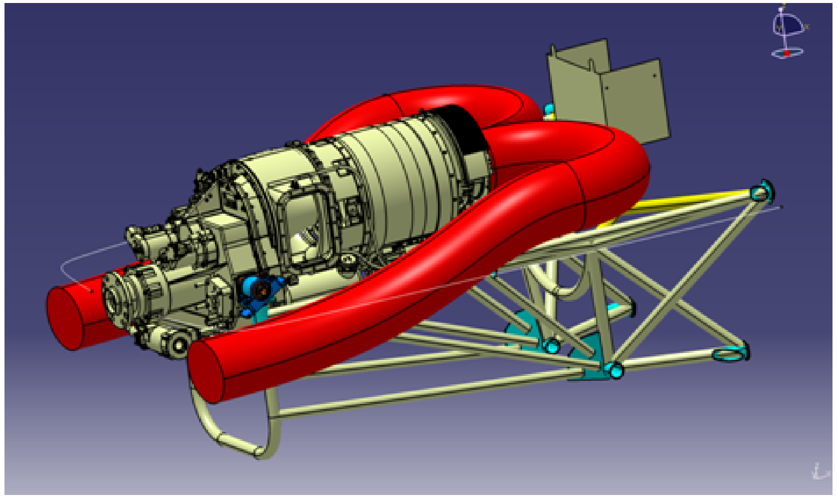

The Concept of the Integration

- **Parametric model of the Air Intake and Bypass**

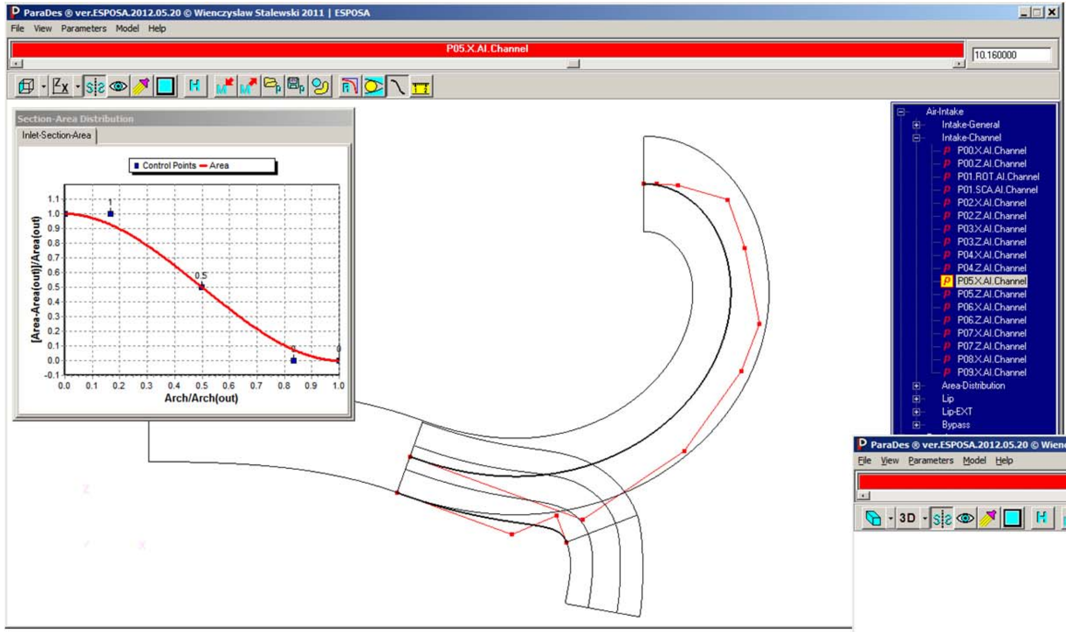

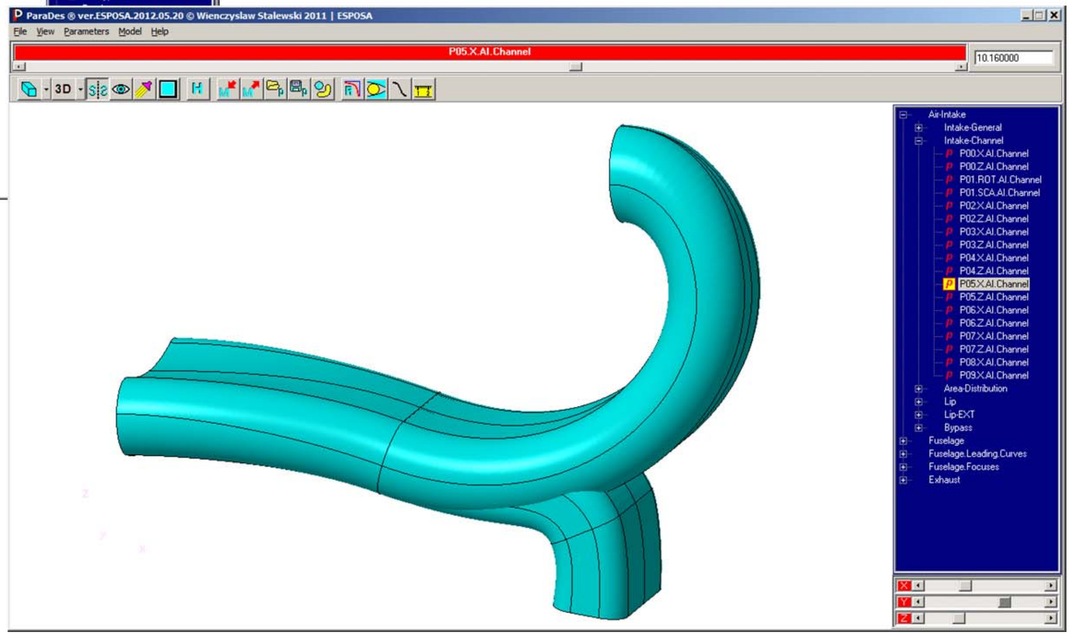

Air-Intake Geometry

defined by curves describing:

- *Shape of the Central Line*
- *Cross-Section-Area Distribution*

The Concept of the Integration

- **Parametric model of the Nacelle and the Exhaust System**

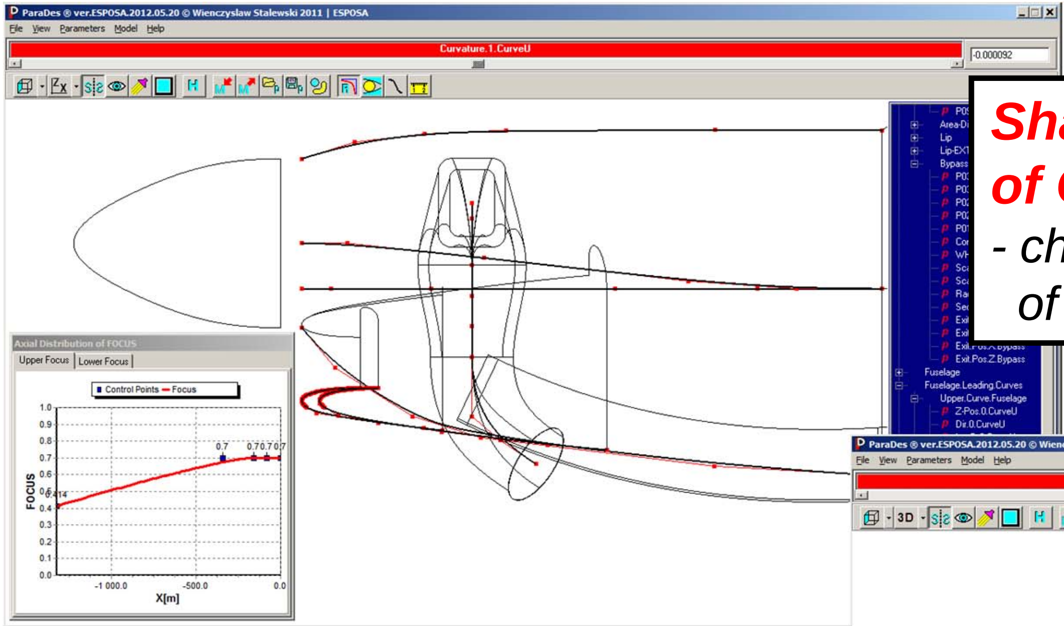

Shapes of Guiding and Section Curves
- changed by smooth changes of their Control Points

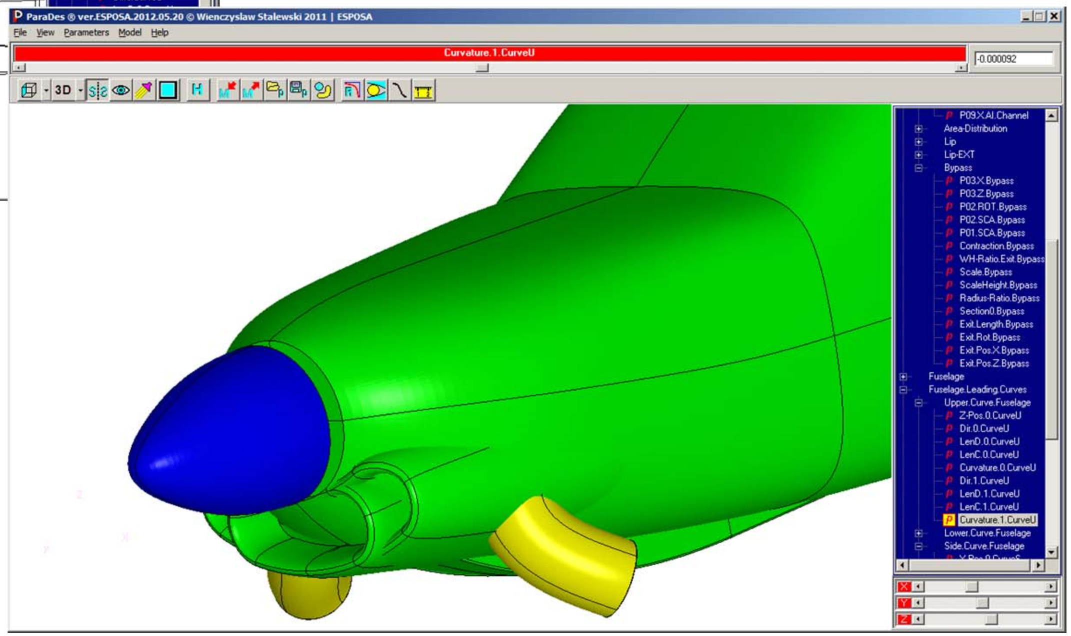

Surface of the Nacelle
- NURBS Multi-Section Surface, defined by family of Section Curves swept along Guiding Curves

The Concept of the Integration

- **Air-Intake with Bypass**
  - fulfilment of all geometrical constraints
  - sufficient air mass flow rate at the engine compressor inlet

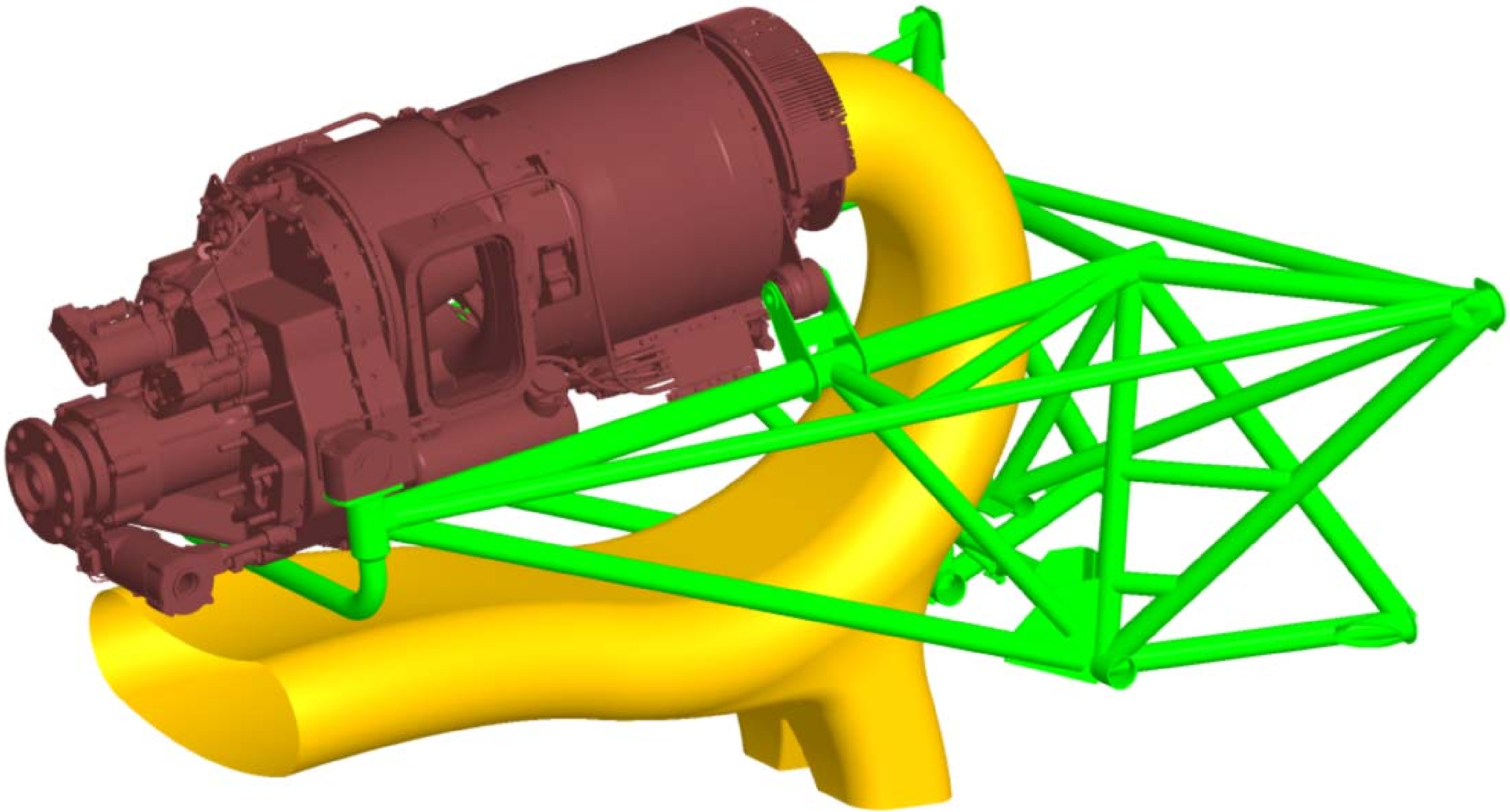

The Concept of the Integration

- **Foreign-Particle Separator**

Injection of 1mm Quartz Particles

Number of Particles escaped through the COMPRESSOR	Number of Particles escaped through the BYPASS
94	6981
Separation Efficiency	98.7%

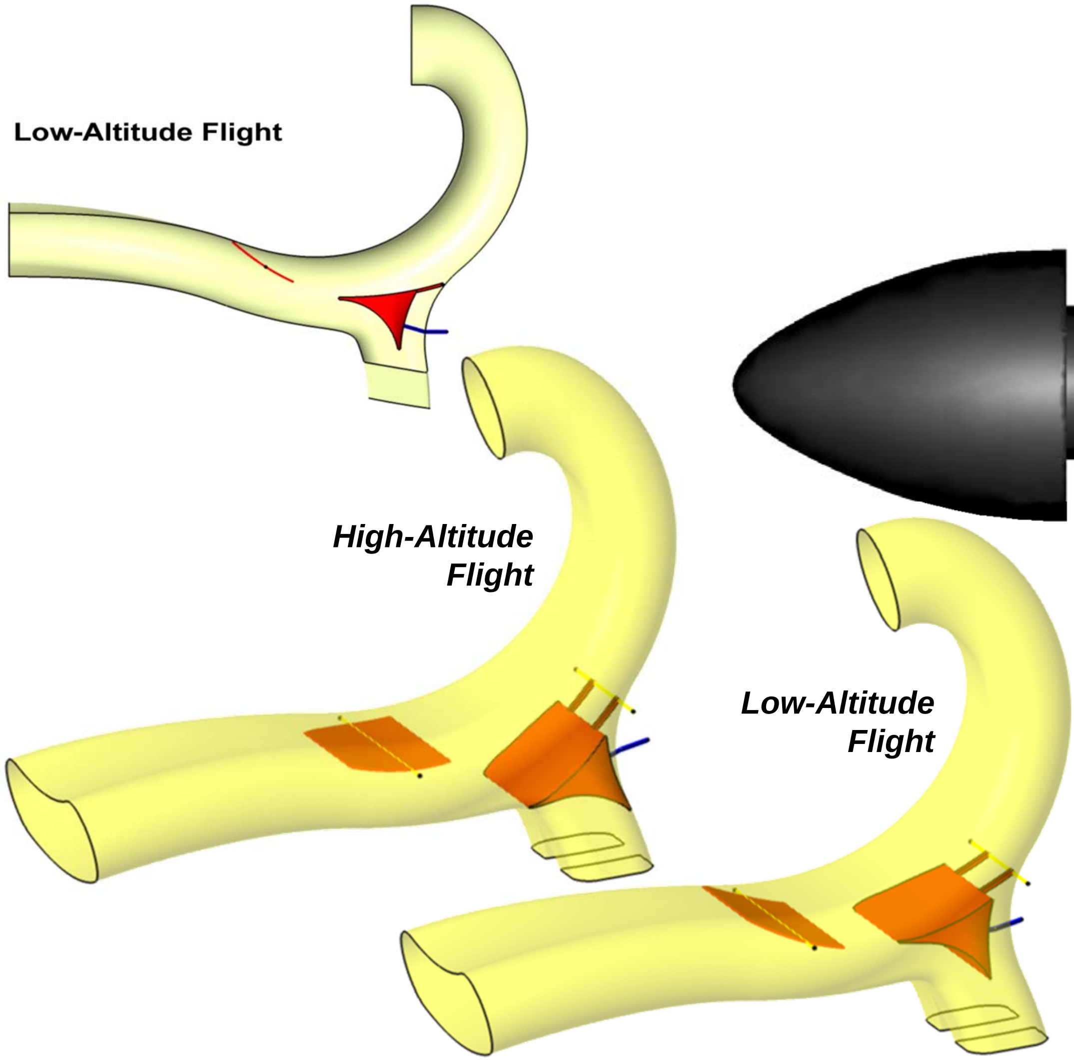

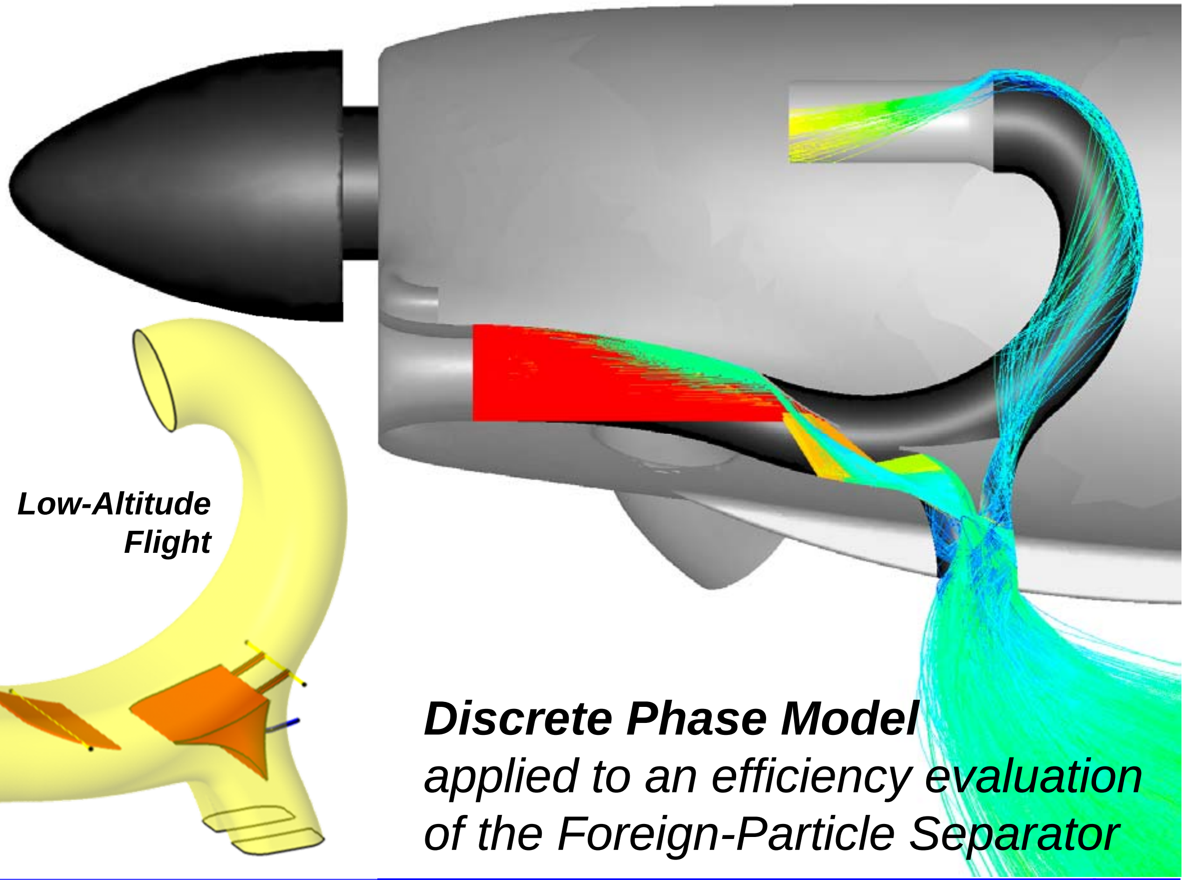

Discrete Phase Model
applied to an efficiency evaluation of the Foreign-Particle Separator

The Concept of the Integration

- **Complete air delivery system, cooling system, cooled devices and cockpit-air-conditioning system**

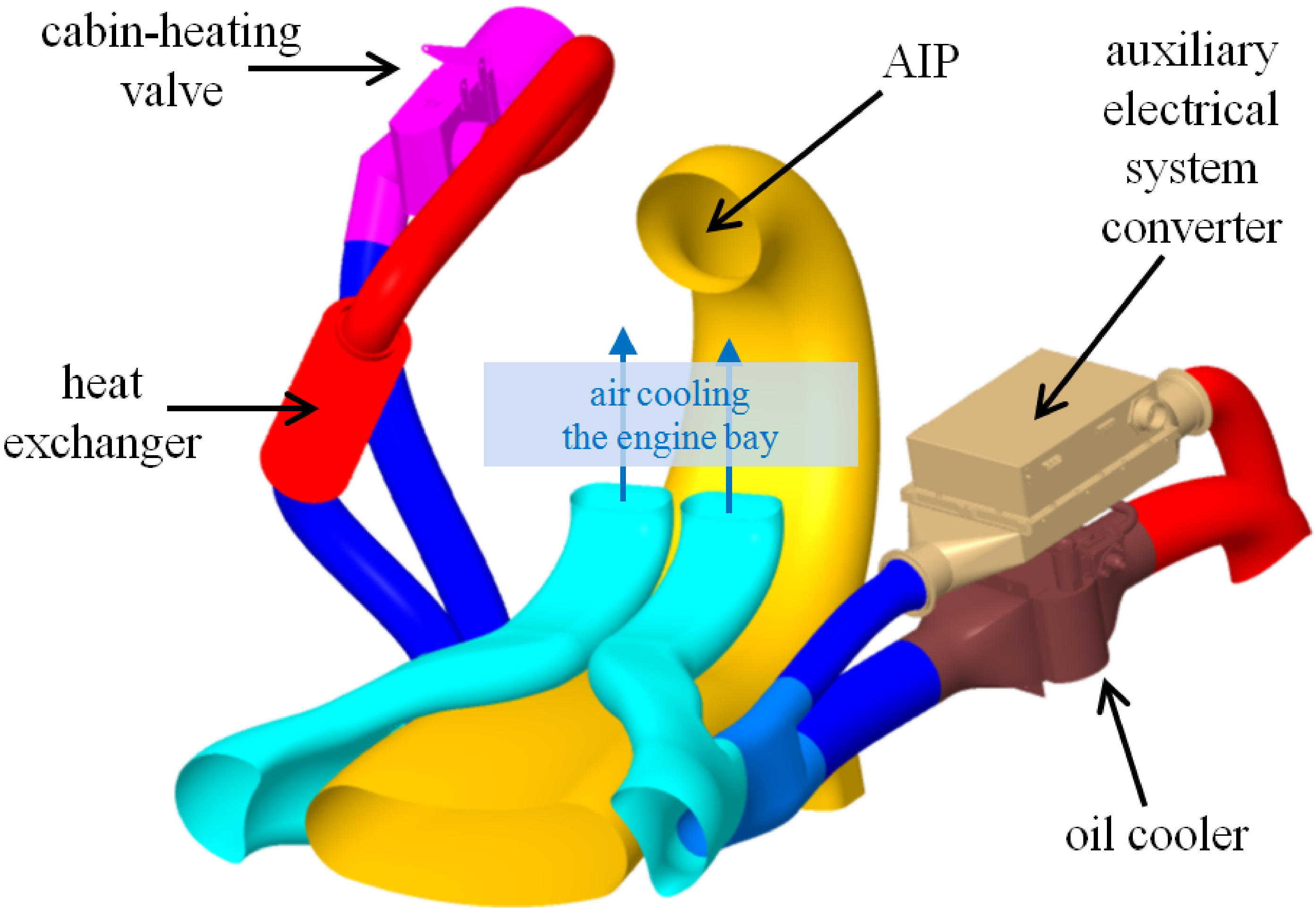

The Concept of the Integration

- **The Exhaust System**

Apart from removing exhaust, the system is designed to remove hot air from the engine bay, utilising the ejector-pump effect. The exhaust stream generates an under-pressure, sucking the hot air through the ejector slot. To protect the most heated parts of the nacelle shell, the additional protective covers have been introduced.

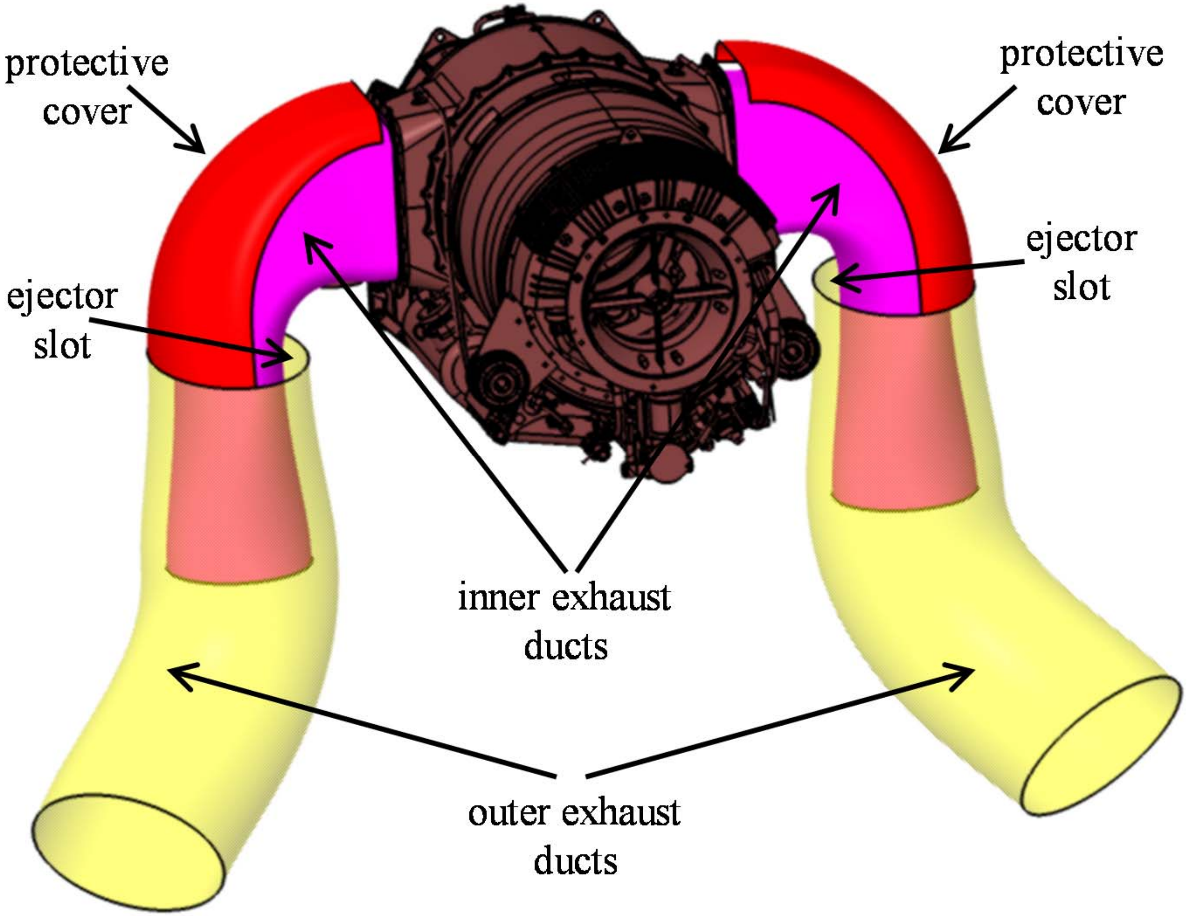

The Concept of the Integration

- **The Nacelle**

designed taking into account:

- avoiding overheating and potential conflicts with internal content
- achieving satisfactory aerodynamic properties in external flow

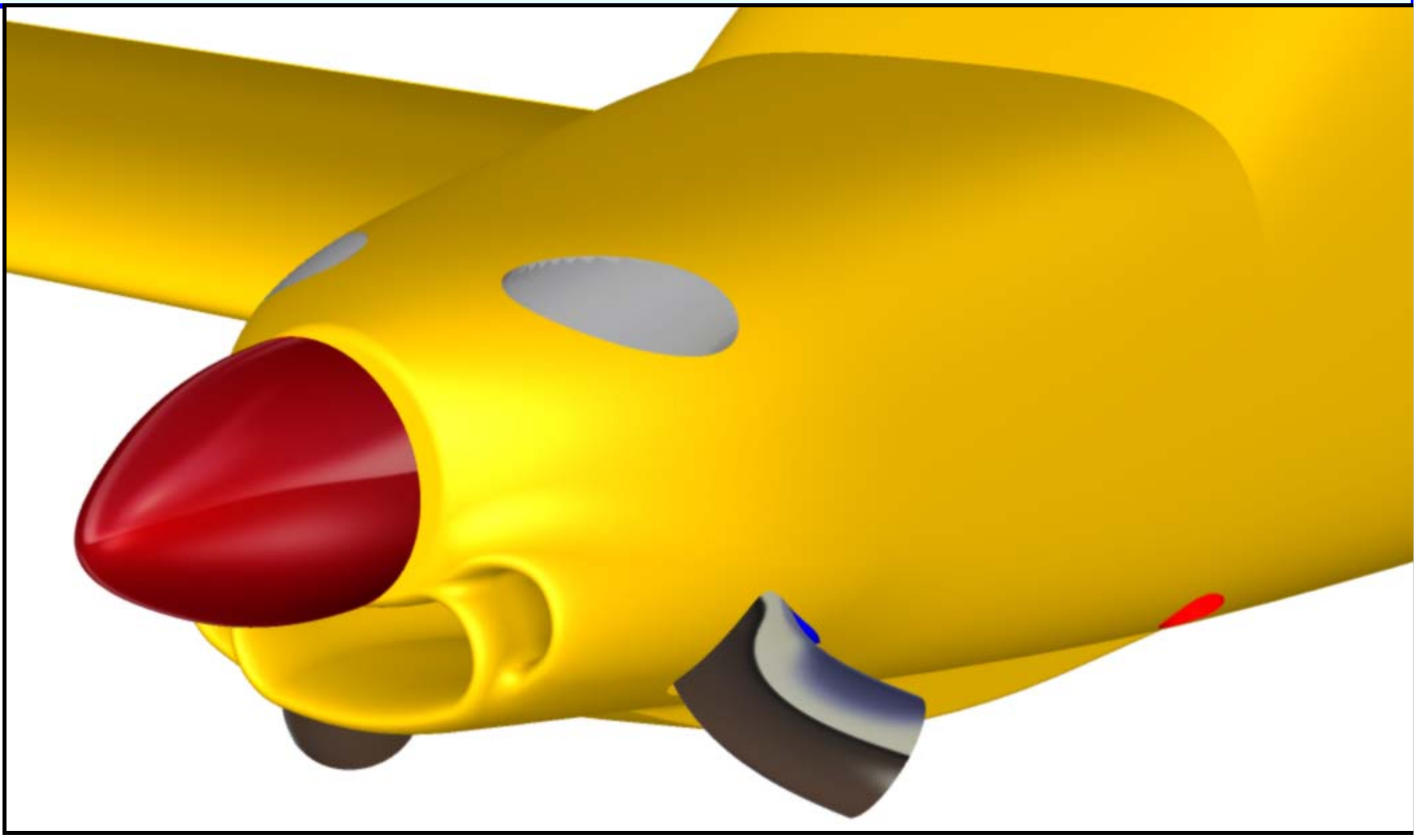

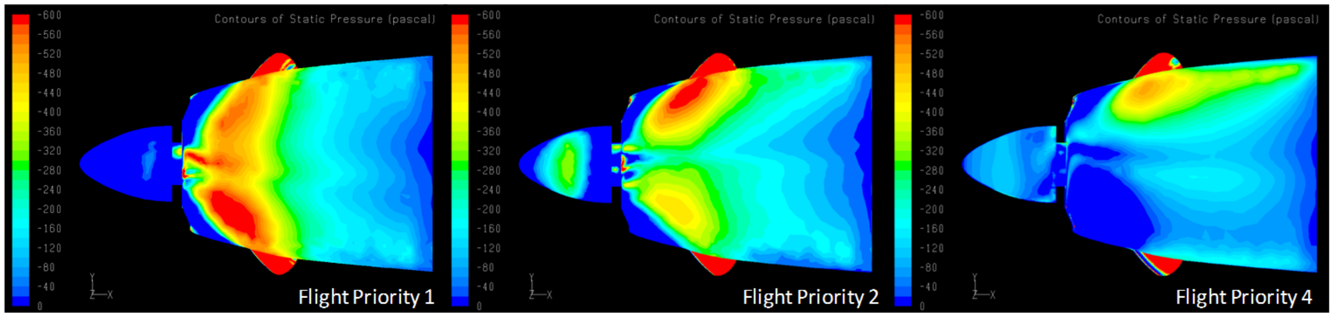

CFD analyses aiming at an optimal localisation of ventilation grilles on the nacelle shell

Conclusions

- The main goal of the research was to develop the preliminary concept of integration of the turboprop engine TP100 and the aircraft I-23. The research were focused on fluid-dynamics aspects of the integration.
- The integration designing was conducted using the Interactive Parametric Design methodology, utilising several commercial and in-house codes.
- As a result of the research, the concepts of the following components of the integration have been developed:
  - engine nacelle
  - air intake together with the foreign particles separator
  - auxiliary intakes delivering the air for cooling and air-conditioning purposes
  - ventilation system of the engine bay
  - exhaust system
- Within next stages of the ESPOSA project, the improvements and optimisation of above components will be conducted, so as to develop a fully useful and implementable technical project of the integration.

Thank You
for Your Attention

2nd EASN WORKSHOP on Flight Physics and Propulsion

Selected Flight Dynamics models & computational procedures used in different national and international projects

Zdobyslaw Goraj: goraj@meil.pw.edu.pl

Warsaw University of Technology

Prague, 31st of October – 2nd of November 2012

Experience - Selected projects (1/2)

KUSY

GROT-2

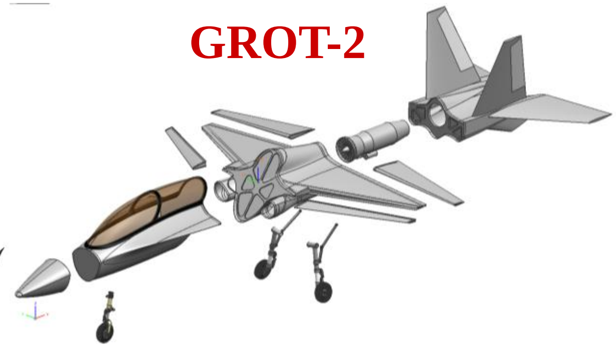

HELENA

SAMONIT-1

SAMONIT-2

SAMONIT-3

PW-114

PW-103

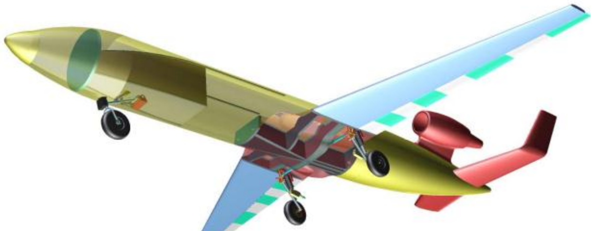

NACRE IEP

Experience - Selected projects (2/2)

HAAMRT

Family Jet

B2-2

B2-1

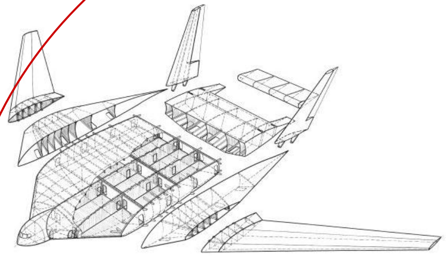

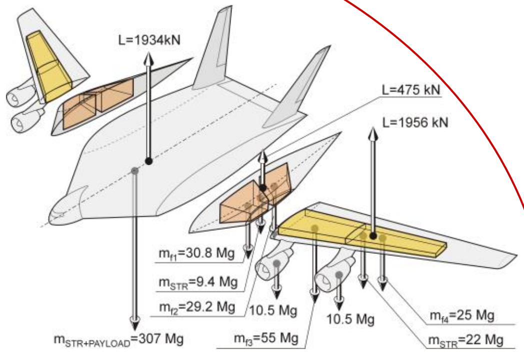

NACRE

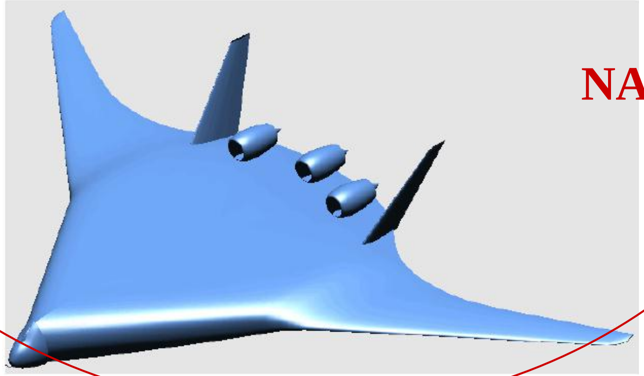

Mathematical background

$$\dot{\mathbf{x}} = \mathbf{A}\mathbf{x} + \mathbf{B}\boldsymbol{\eta}$$

$$\mathbf{x} = \mathbf{x}_0 e^{\lambda t}$$

$$\left[\lambda_r \mathbf{I} - \mathbf{A}\right]\mathbf{x}_r = \mathbf{0}$$

$$C_{z_u} = \frac{\partial C_z}{\partial\left(\dfrac{u}{u_0}\right)} = -2C_L - 2C_{Lu}$$

Numerical simulation

20,009	-0,45438	0,60513	-0,45438	-0,60513	-2,95E-03	0,52442	-2,95E-03	-0,52442	-0,51601	0,00E+00	-7,09E-03	4,90E-02	-7,09E-03	-4,90E-02	5,72E-03	0,00E+00
21,007	-0,45277	-0,53309	-0,45277	0,53309	-3,53E-03	0,52178	-3,53E-03	-0,52178	-0,51559	0,00E+00	-6,82E-03	-4,74E-02	-6,82E-03	4,74E-02	5,38E-03	0,00E+00
22,005	-0,45137	-0,45007	-0,45137	0,45007	-4,11E-03	0,51919	-4,11E-03	-0,51919	-0,51518	0,00E+00	-6,53E-03	4,50E-02	-6,53E-03	-4,50E-02	5,04E-03	0,00E+00
23,003	-0,45015	-0,34821	-0,45015	0,34821	-4,69E-03	0,51663	-4,69E-03	-0,51663	-0,51476	0,00E+00	-6,24E-03	-4,11E-02	-6,23E-03	4,11E-02	4,68E-03	0,00E+00
24,002	-0,51434	-4,12E-08	-5,29E-03	0,51411	-5,29E-03	-0,51411	-0,44887	0,20012	-0,44887	-0,20012	-6,18E-03	-3,35E-02	-6,18E-03	3,35E-02	4,32E-03	0,00E+00
25	-0,65111	0,00E+00	-0,51392	0,00E+00	-5,88E-03	0,51161	-5,88E-03	-0,51161	-0,24101	0,00E+00	-1,57E-02	0,00E+00	3,96E-03	0,00E+00	-9,86E-08	0,00E+00
25,998	-0,7973	3,89E-06	-0,51349	0,00E+00	-6,48E-03	0,50915	-6,48E-03	-0,50915	-7,59E-02	-4,86E-02	-7,59E-02	4,86E-02	4,32E-02	-3,59E-06	3,58E-03	0,00E+00
26,997	-0,89832	5,93E-09	-0,51307	0,00E+00	-7,08E-03	0,50672	-7,08E-03	-0,50672	-4,48E-02	7,38E-02	-4,48E-02	-7,38E-02	8,37E-02	0,00E+00	3,20E-03	0,00E+00
27,995	-0,98076	-5,54E-09	-0,51263	0,00E+00	-7,69E-03	0,50432	-7,69E-03	-0,50432	0,13521	0,00E+00	-2,88E-02	7,43E-02	-2,86E-02	-7,43E-02	2,81E-03	0,00E+00
28,993	-1,0524	4,57E-09	-0,5122	0,00E+00	-8,31E-03	-0,50195	-8,31E-03	0,50195	0,19274	0,00E+00	-2,12E-02	7,13E-02	-2,11E-02	-7,13E-02	2,41E-03	0,00E+00
29,991	-1,117	1,11E-10	-0,51176	0,00E+00	-8,93E-03	-0,4996	-8,93E-03	0,4996	0,25044	0,00E+00	-1,74E-02	-6,87E-02	-1,74E-02	6,87E-02	2,00E-03	0,00E+00
30,99	-1,1764	-1,28E-08	-0,51132	0,00E+00	-9,56E-03	-0,49728	-9,56E-03	0,49728	0,30597	0,00E+00	-1,54E-02	6,68E-02	-1,54E-02	-6,68E-02	1,58E-03	0,00E+00
31,988	-1,2319	-4,25E-10	-0,51087	0,00E+00	-1,02E-02	0,49498	-1,02E-02	-0,49498	0,35887	0,00E+00	-1,41E-02	6,54E-02	-1,41E-02	-6,54E-02	1,15E-03	0,00E+00
32,986	-1,2844	2,11E-09	-0,51042	7,00E-09	-1,08E-02	-0,49271	-1,08E-02	0,49271	0,40925	0,00E+00	-1,33E-02	-6,43E-02	-1,33E-02	6,43E-02	7,11E-04	0,00E+00
33,985	-1,3346	1,02E-08	-0,50996	-2,07E-08	-1,15E-02	-0,49046	-1,15E-02	0,49046	0,45739	4,69E-09	-1,27E-02	-6,35E-02	-1,27E-02	6,35E-02	2,61E-04	0,00E+00
34,983	-1,3828	-5,04E-09	-0,50949	0,00E+00	0,50356	0,00E+00	-1,22E-02	-0,48823	-1,22E-02	0,48823	-1,23E-02	6,29E-02	-1,23E-02	-6,29E-02	-2,00E-04	0,00E+00
35,981	-1,4295	-1,14E-09	0,54803	1,14E-09	-0,50902	2,59E-08	-1,28E-02	-0,48601	-1,28E-02	0,48601	-1,19E-02	-6,23E-02	-1,19E-02	6,23E-02	-6,72E-04	0,00E+00
36,979	-1,4749	-1,73E-09	0,59101	9,18E-09	-0,50855	0,00E+00	-1,35E-02	0,48382	-1,35E-02	-0,48382	-1,17E-02	-6,19E-02	-1,17E-02	6,19E-02	-1,16E-03	0,00E+00
37,978	-1,5193	-5,93E-09	0,63271	0,00E+00	-0,50806	0,00E+00	-1,42E-02	0,48164	-1,42E-02	-0,48164	-1,14E-02	-6,15E-02	-1,14E-02	6,15E-02	-1,65E-03	0,00E+00
38,976	-1,5629	7,09E-10	0,6733	0,00E+00	-0,50757	0,00E+00	-1,49E-02	-0,47948	-1,49E-02	0,47948	-1,13E-02	-6,12E-02	-1,13E-02	6,12E-02	-2,17E-03	0,00E+00

xc	SP_R1	SP_I	SP_R2	X1	H_R	X2	H_I	X3	R	X4	PH_R	PH_I	SPIRAL
20,00900	-0,45438	0,60513	-0,45438	0,60513	-0,00295	0,52442	0,00524	0,00000	-0,51601	0,00000	-0,00709	0,04905	0,00572
21,00700	-0,45277	0,53309	-0,45277	0,53309	-0,00353	0,52178	0,00522	0,00000	-0,51559	0,00000	-0,00682	0,04743	0,00538
22,00500	-0,45137	0,45007	-0,45137	0,45007	-0,00411	0,51919	0,00519	0,00000	-0,51518	0,00000	-0,00653	0,04503	0,00504
23,00300	-0,45015	0,34821	-0,45015	0,34821	-0,00469	0,51663	0,00517	0,00000	-0,51476	0,00000	-0,00624	0,04113	0,00468
24,00200	-0,44887	0,20012	-0,44887	0,20012	-0,00529	0,51411	0,00514	0,00000	-0,51434	0,00000	-0,00618	0,03348	0,00432
25,00000	-0,65111	0,00000	-0,24101	0,00000	-0,00588	0,51161	0,00512	0,00000	-0,51392	0,00000	-0,01568	0,00000	0,00000
25,99800	-0,79730	0,00000	-0,07588	0,00000	-0,00648	0,50915	0,00509	0,00000	-0,51349	0,00000	-0,07588	0,04862	0,00358
26,99700	-0,89832	0,00000	-0,04482	0,00000	-0,00708	0,50672	0,00507	0,00000	-0,51307	0,00000	-0,04482	0,07376	0,00320
27,99500	-0,98076	0,00000	0,13521	0,00000	-0,00769	0,50432	0,00504	0,00000	-0,51263	0,00000	-0,02876	0,07434	0,00281
28,99300	-1,05240	0,00000	0,19274	0,00000	-0,00831	0,50195	0,00502	0,00000	-0,51220	0,00000	-0,02115	0,07134	0,00241
29,99100	-1,11700	0,00000	0,25044	0,00000	-0,00893	0,49960	0,00500	0,00000	-0,51176	0,00000	-0,01744	0,06873	0,00200
30,99000	-1,17640	0,00000	0,30597	0,00000	-0,00956	0,49728	0,00497	0,00000	-0,51132	0,00000	-0,01540	0,06680	0,00158
31,98800	-1,23190	0,00000	0,35887	0,00000	-0,01020	0,49498	0,00495	0,00000	-0,51087	0,00000	-0,01414	0,06538	0,00115
32,98600	-1,28440	0,00000	0,40925	0,00000	-0,01084	0,49271	0,00493	0,00000	-0,51042	0,00000	-0,01330	0,06432	0,00071
33,98500	-1,33460	0,00000	0,45739	0,00000	-0,01150	0,49046	0,00490	0,00000	-0,50996	0,00000	-0,01271	0,06350	0,00026
34,98300	-1,38280	0,00000	0,50356	0,00000	-0,01216	0,48823	0,00488	0,00000	-0,50949	0,00000	-0,01227	0,06286	-0,00020
35,98100	-1,42950	0,00000	0,54803	0,00000	-0,01283	0,48601	0,00486	0,00000	-0,50902	0,00000	-0,01193	0,06232	-0,00067
36,97900	-1,47490	0,00000	0,59101	0,00000	-0,01351	0,48382	0,00484	0,00000	-0,50855	0,00000	-0,01166	0,06188	-0,00116
37,97800	-1,51930	0,00000	0,63271	0,00000	-0,01420	0,48164	0,00482	0,00000	-0,50806	0,00000	-0,01144	0,06152	-0,00165
38,97600	-1,56290	0,00000	0,67330	0,00000	-0,01490	0,47948	0,00479	0,00000	-0,50757	0,00000	-0,01126	0,06121	-0,00217

CFD + Panel Methods (to compute stability derivatives)

NACRE IEP-15

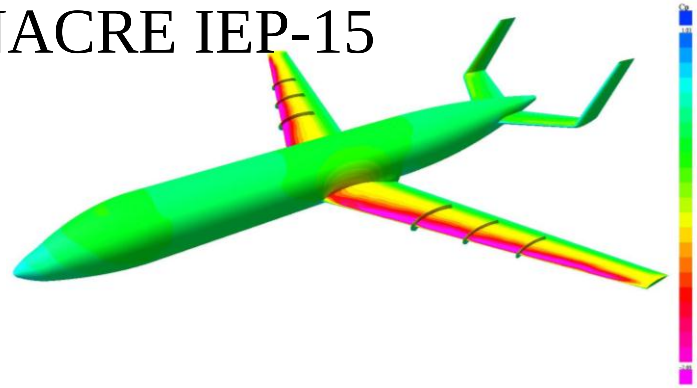

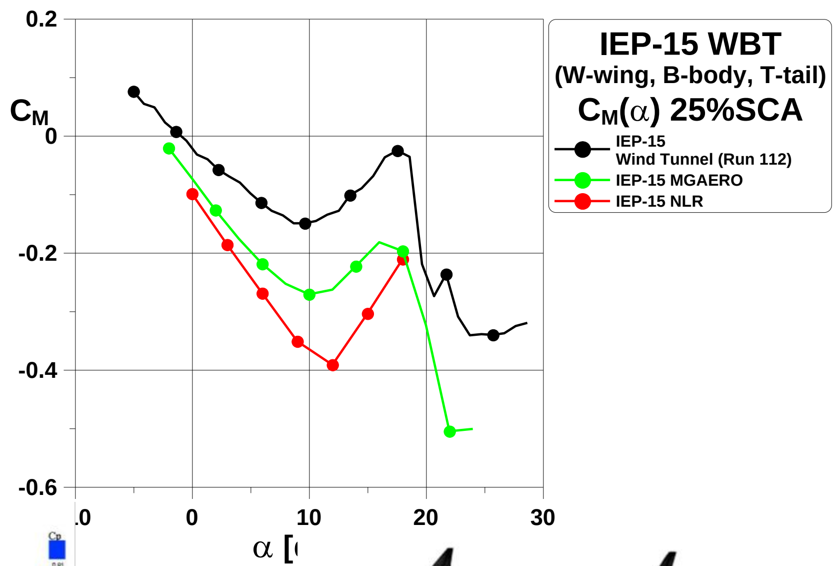

FAMILY JET-2

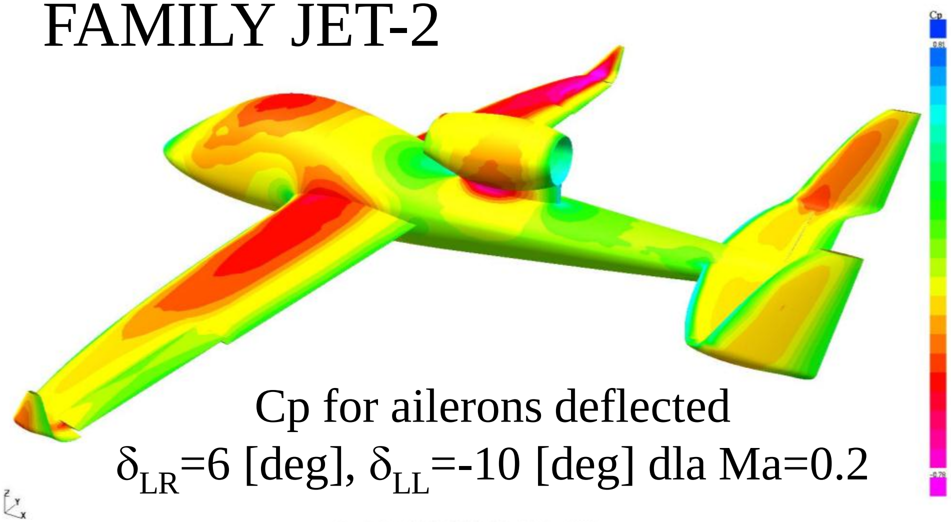

Cp for ailerons deflected
δ_{LR}=6 [deg], δ_{LL}=-10 [deg] dla Ma=0.2

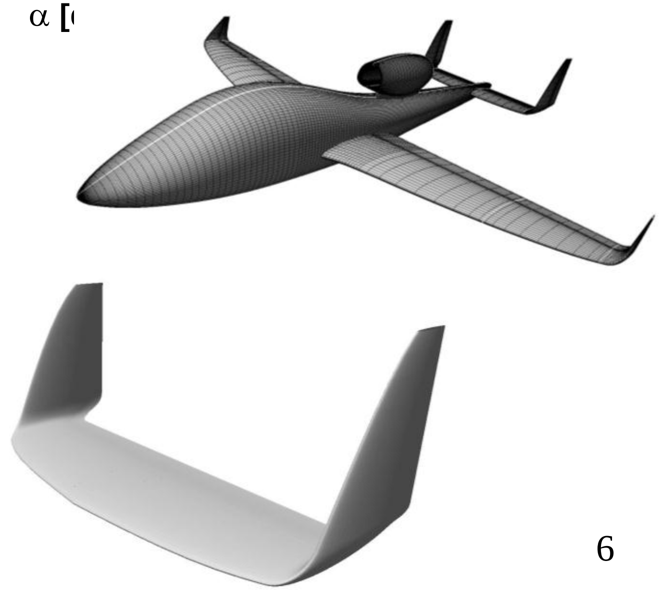

$$\left.\frac{dC_l}{d\delta_L}\right|_{Ma=0.2} = -0.230\ [1/rad]\ (0.004\ [1/\deg])$$

Envelope of CG position

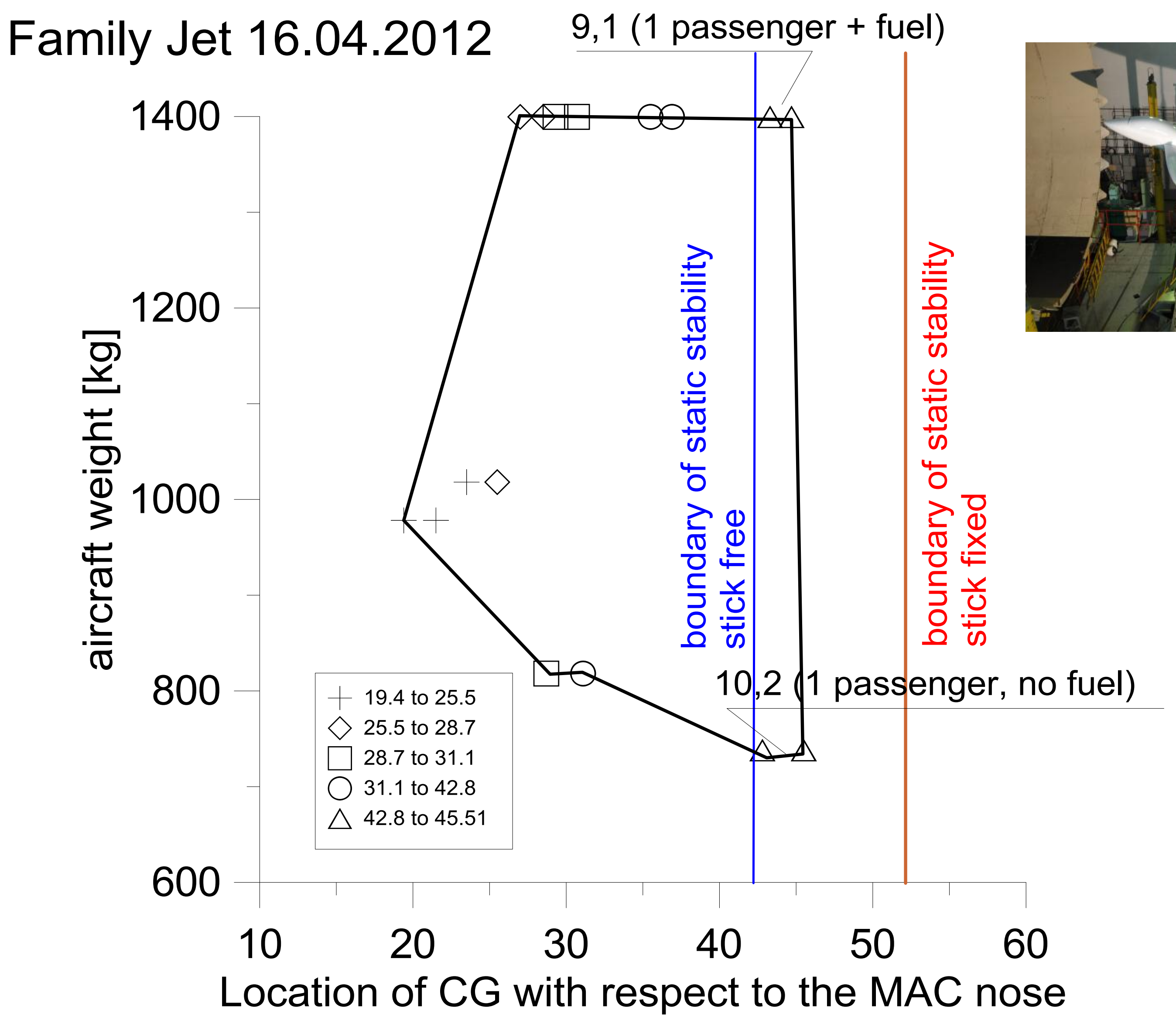

NACRE BWB, Ma=0.85, C_L=0.28

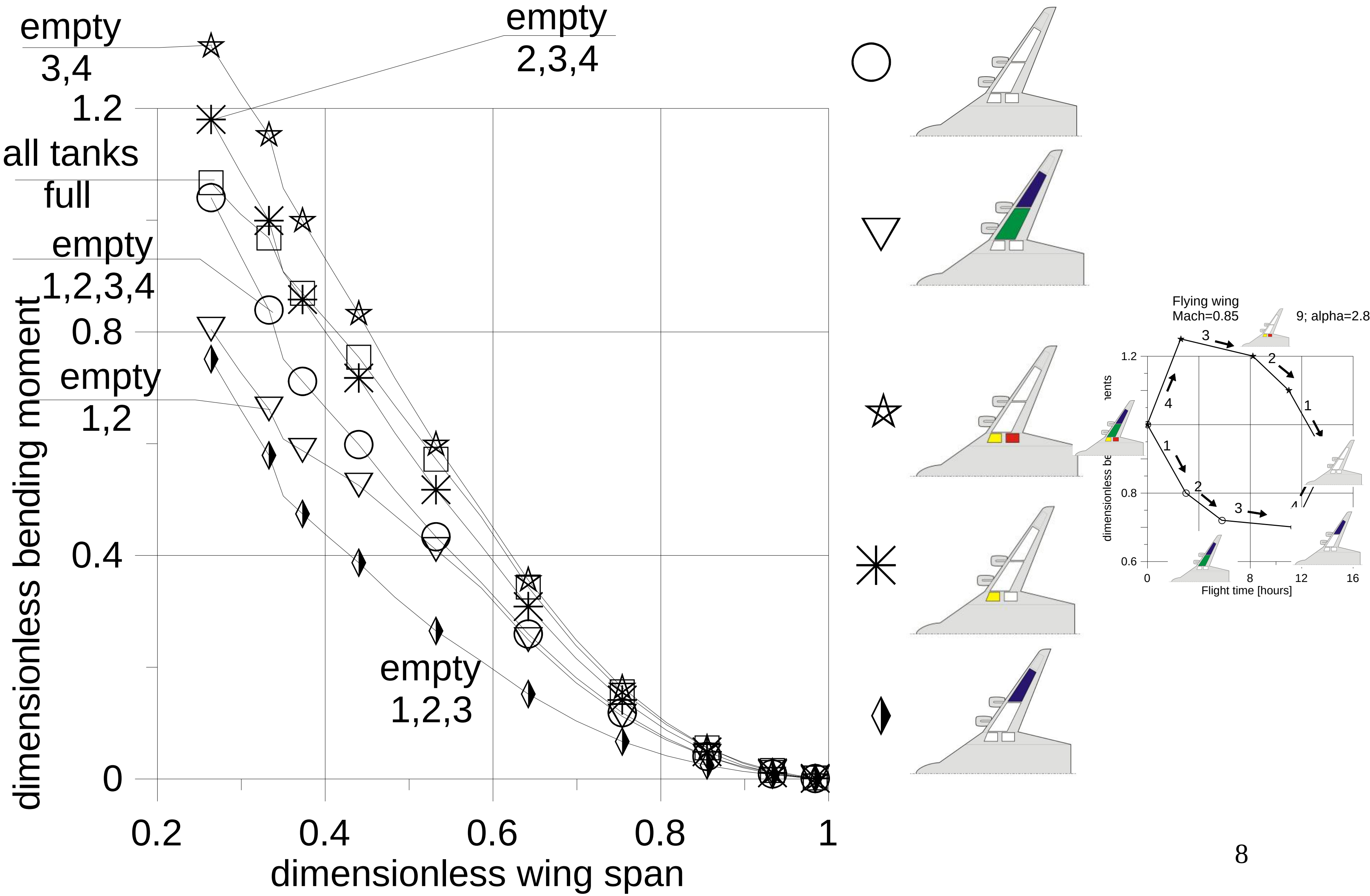

Flight parameters in trim – deflected flap no 4 only

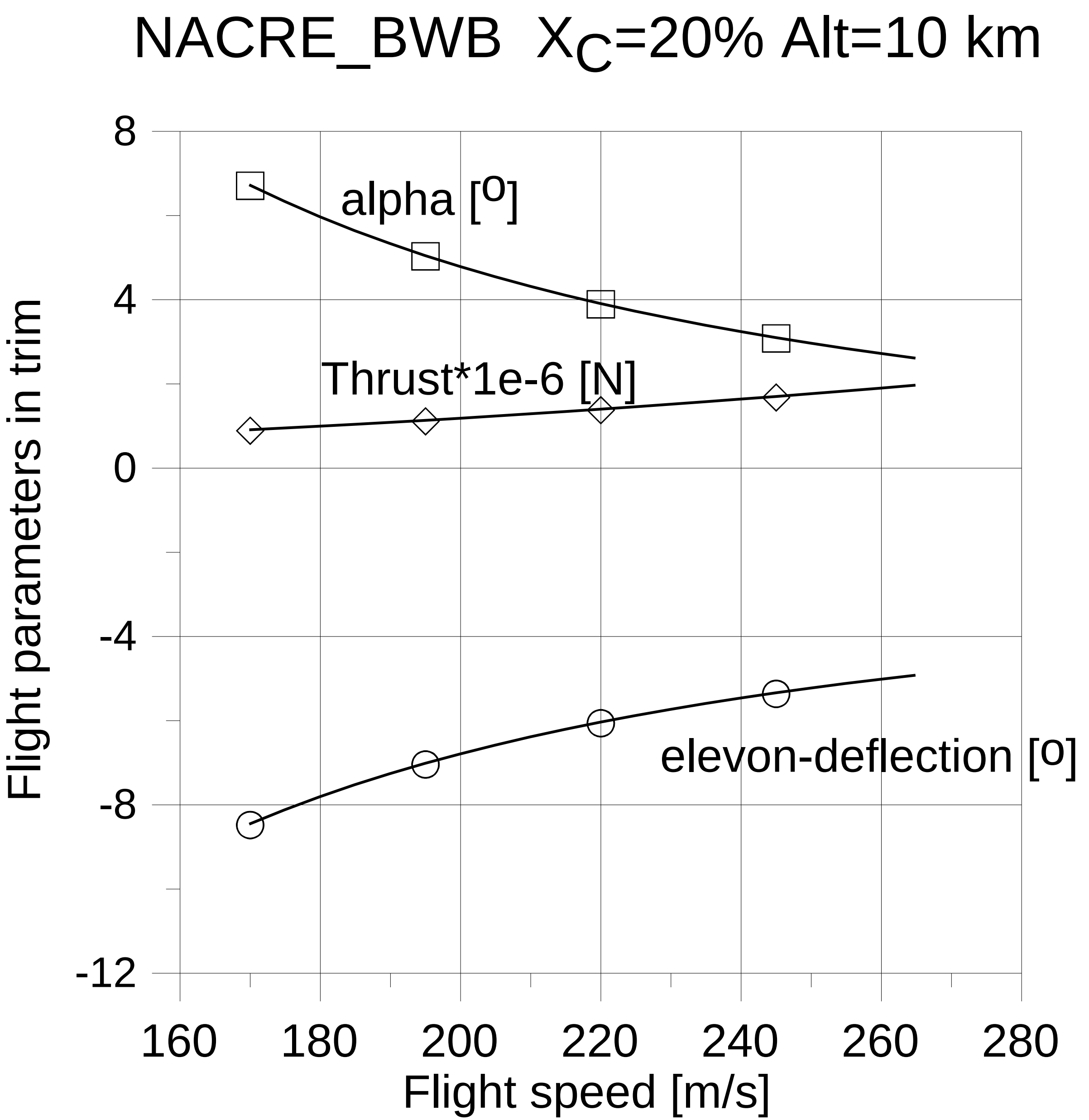

Damping and frequency coefficients versus flight speed, MTOW=700 tons

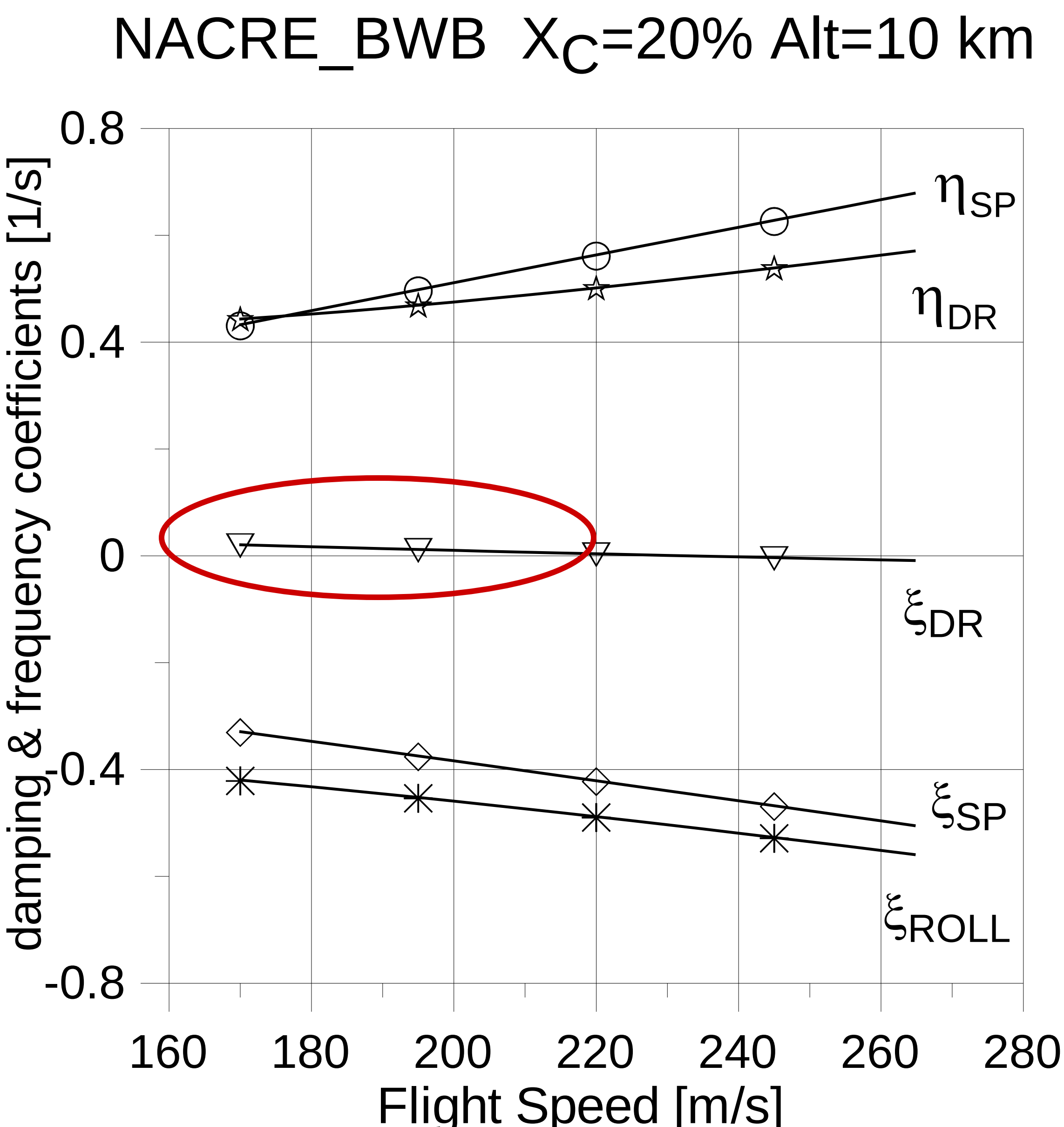

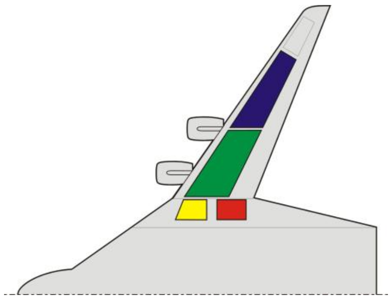

Damping and frequency coefficients versus CG location computed for Short Period mode (SP)

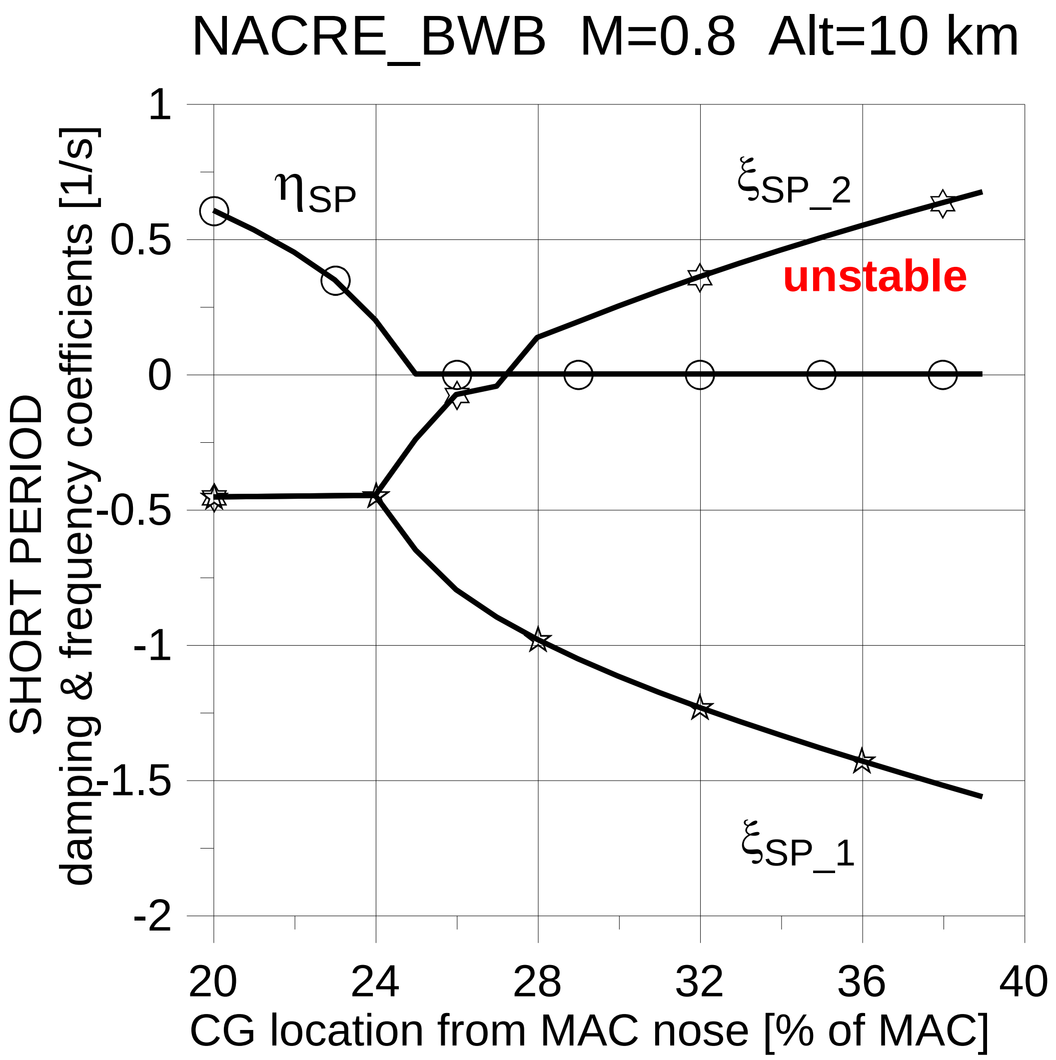

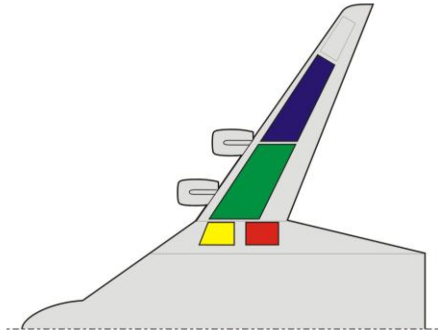

Damping and frequency coefficients versus CG location computed for Phugoid (PH) and Spiral modes (SP)

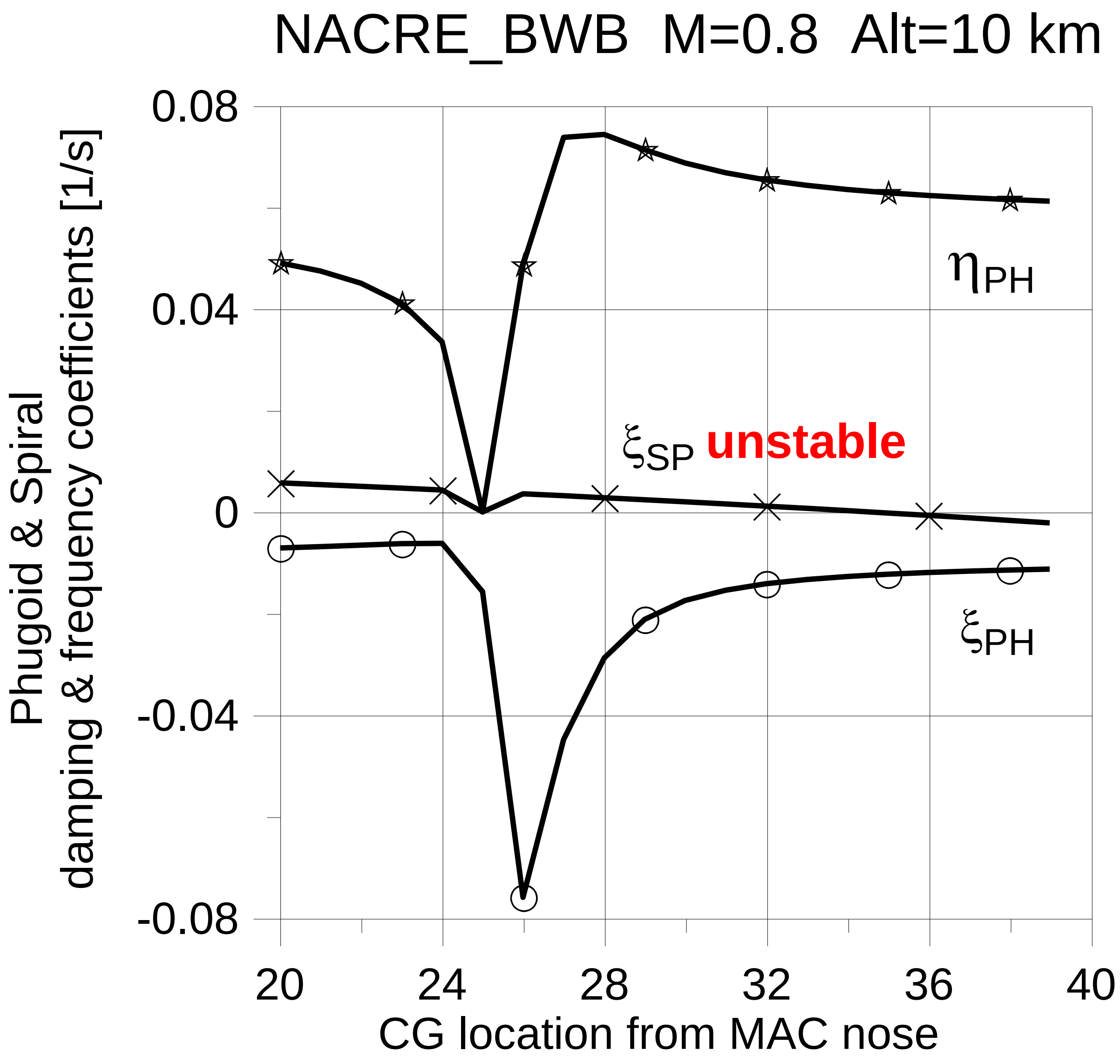

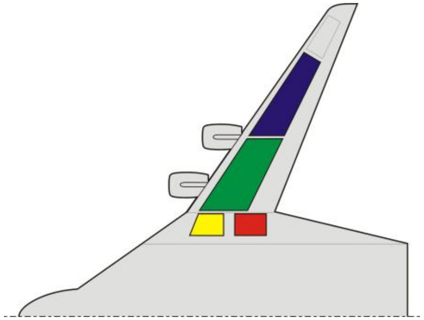

Damping and frequency coefficients versus CG location computed for Short Period mode (SP), aircraft weight equal to 420 tons

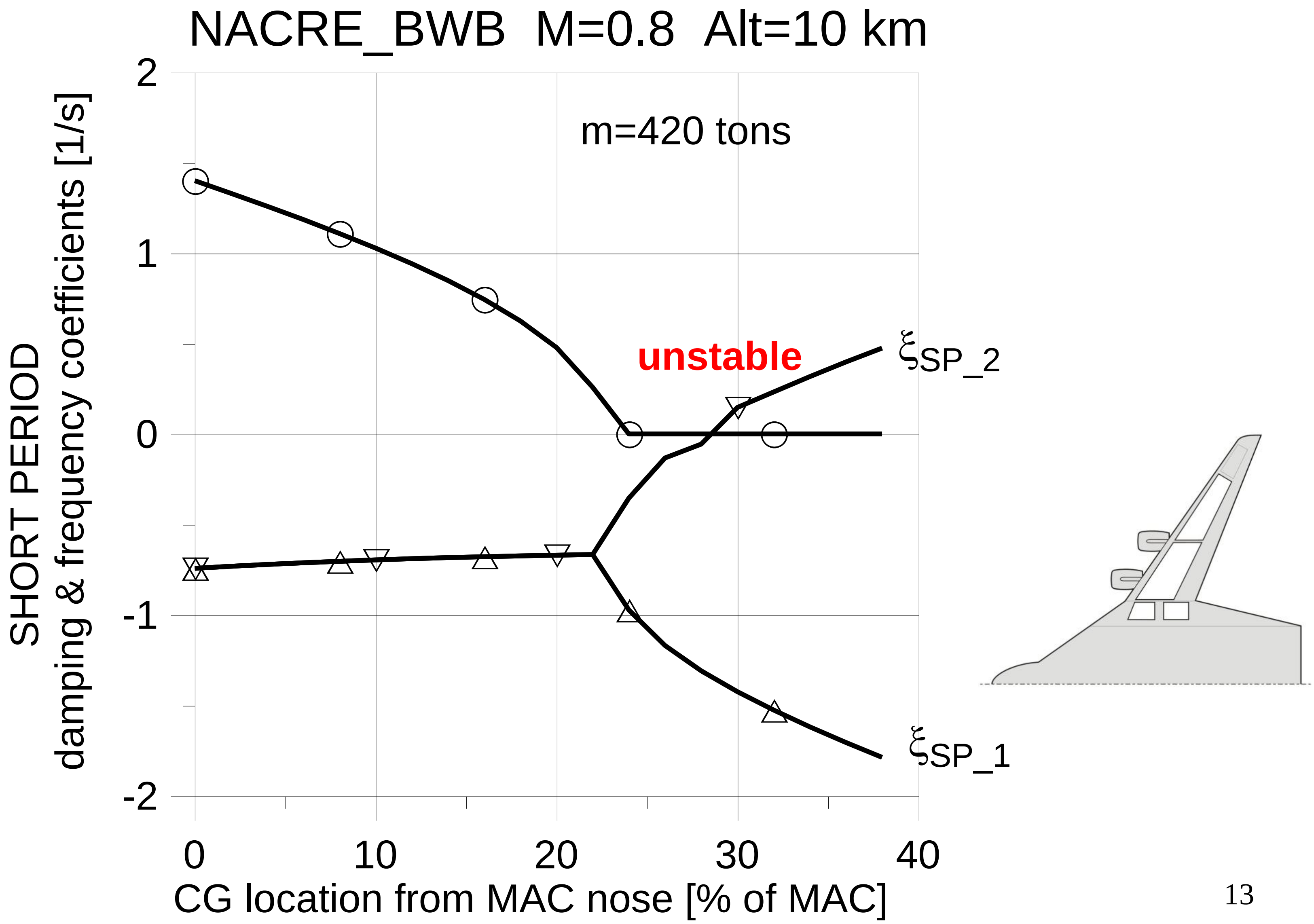

Damping and frequency coefficients versus CG location computed for Phugoid (PH) and Spiral modes (SP). Weight equal to 420 tons

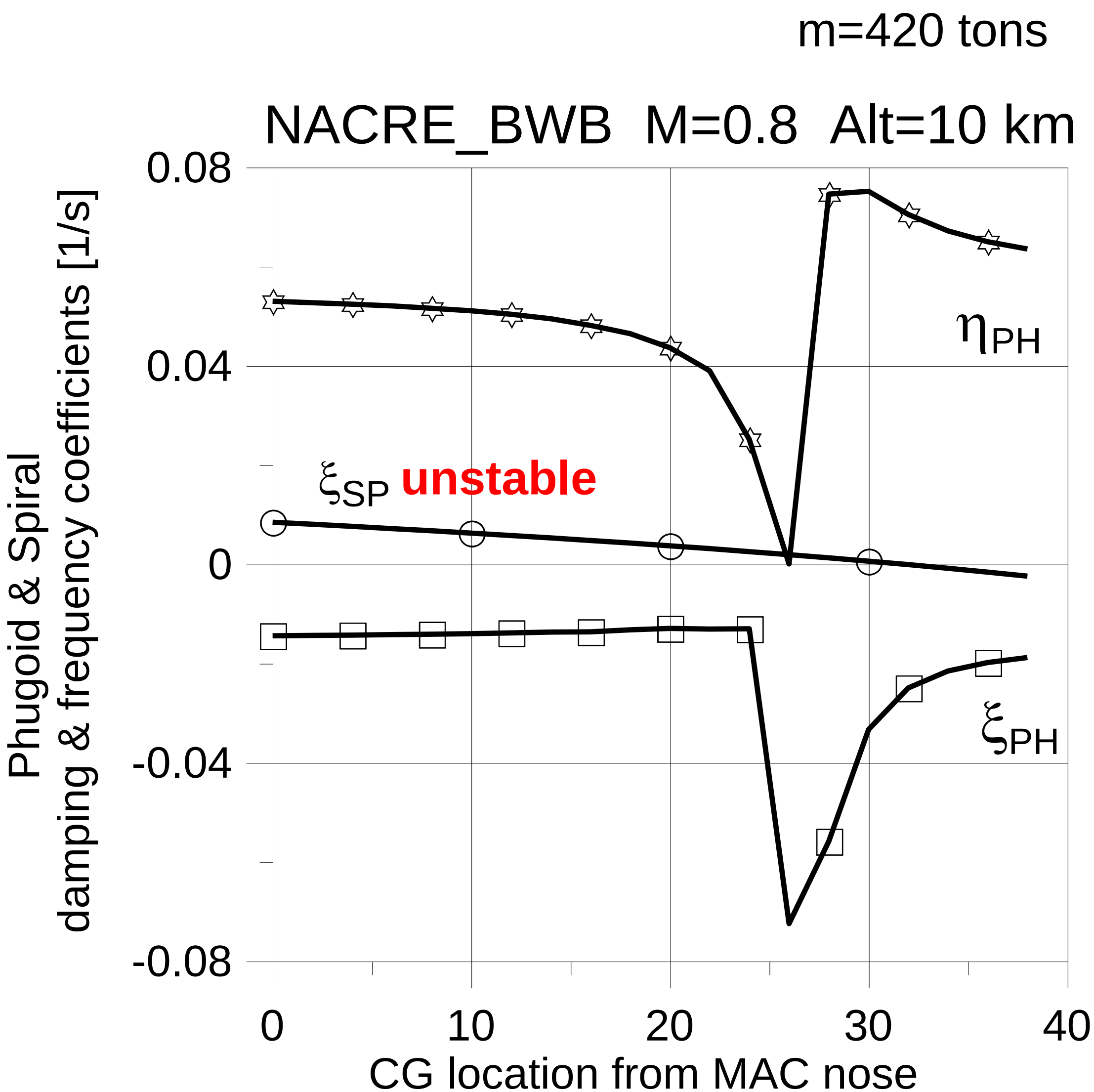

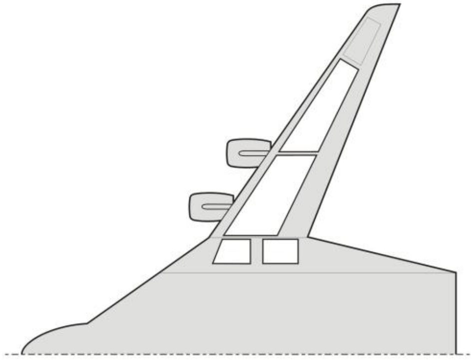

Damping and frequency coefficients versus CG location computed for Short Period mode (SP), aircraft weight equal to 700 and 420 tons

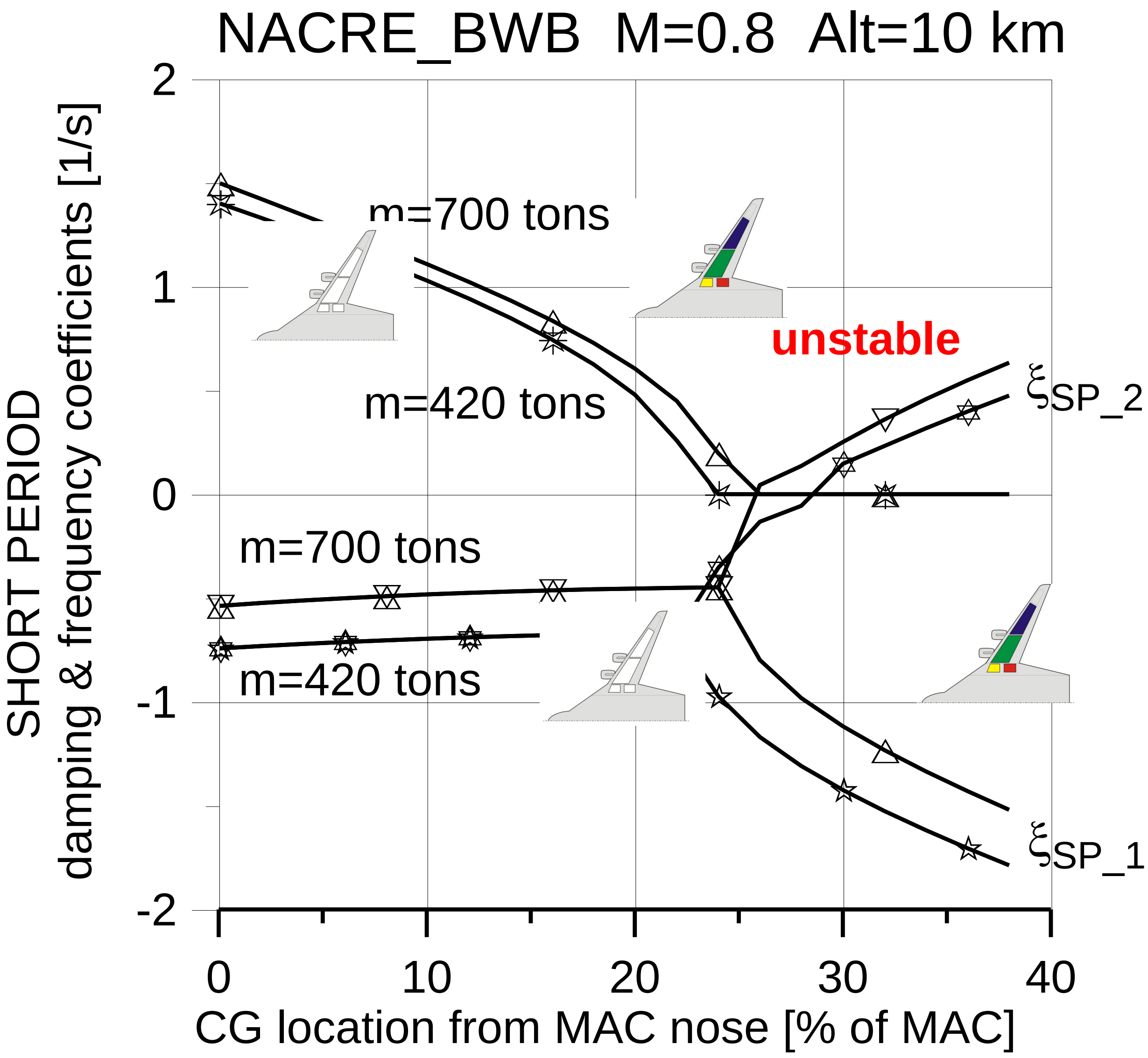

Less fuel more stable!

Damping coefficients versus CG location computed for Short Period mode (SP), aircraft weight equal to 420, 470 and 700 tons. The lighter aircraft the better damped SP mode. Time to half ($T_{1/2}$) decreases on 0.35 s when weight increases from 420 tons till 700 tons

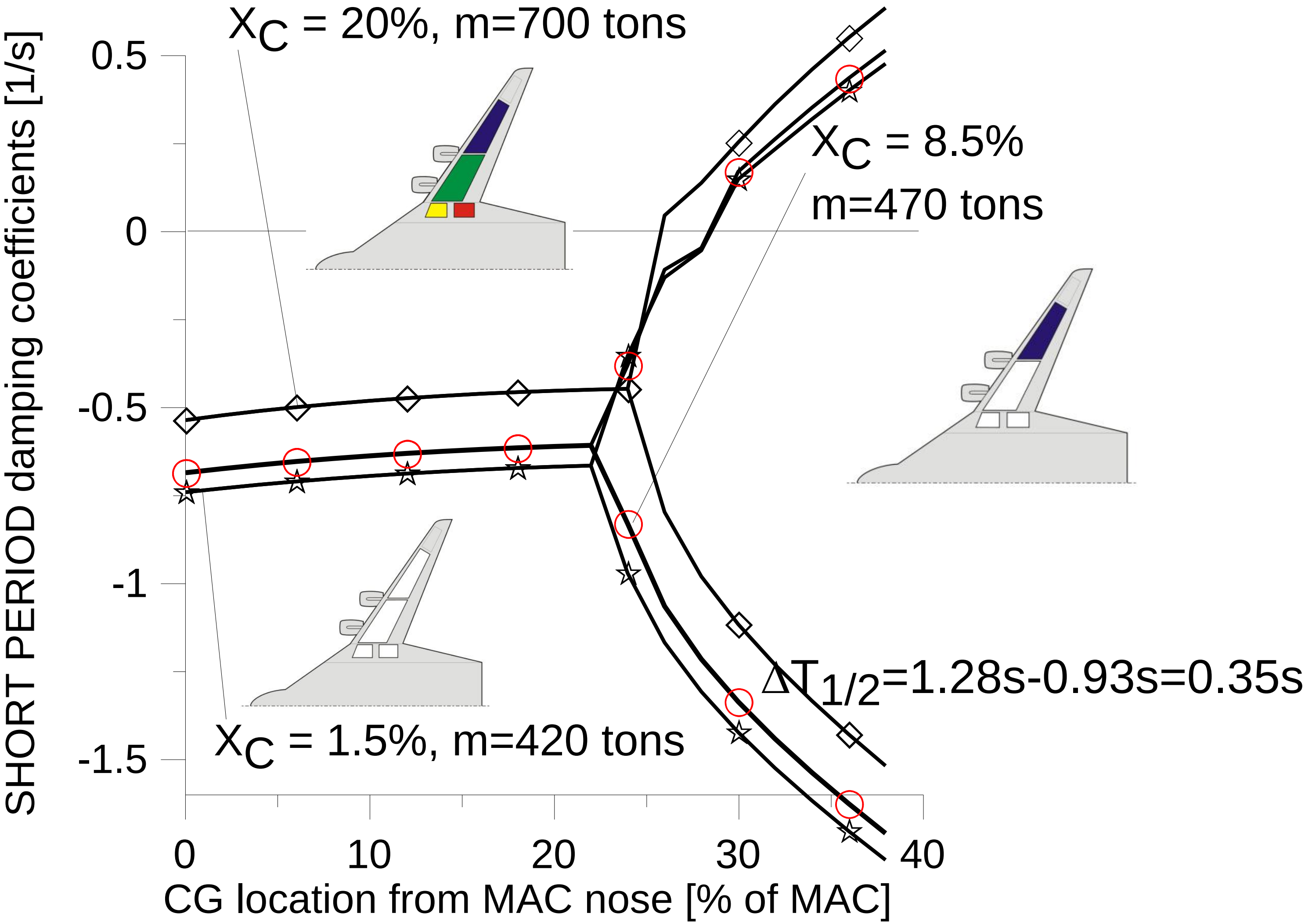

Damping & frequency coefficients of Short Period mode versus CG location, m_A=700 tons. Two cases are shown here: (1) all wing flaps are deflected on zero deg ($\delta_{F2}=\delta_{F3}=\delta_{F4}=0^o$) and aircraft is trimmed due to flap F1 deflected up (red colour) and; (2) aircraft is trimmed due to flap F4 deflected up on -10 deg (black colour) ($\delta_{F1}=\delta_{F2}=\delta_{F3}=0^o$).

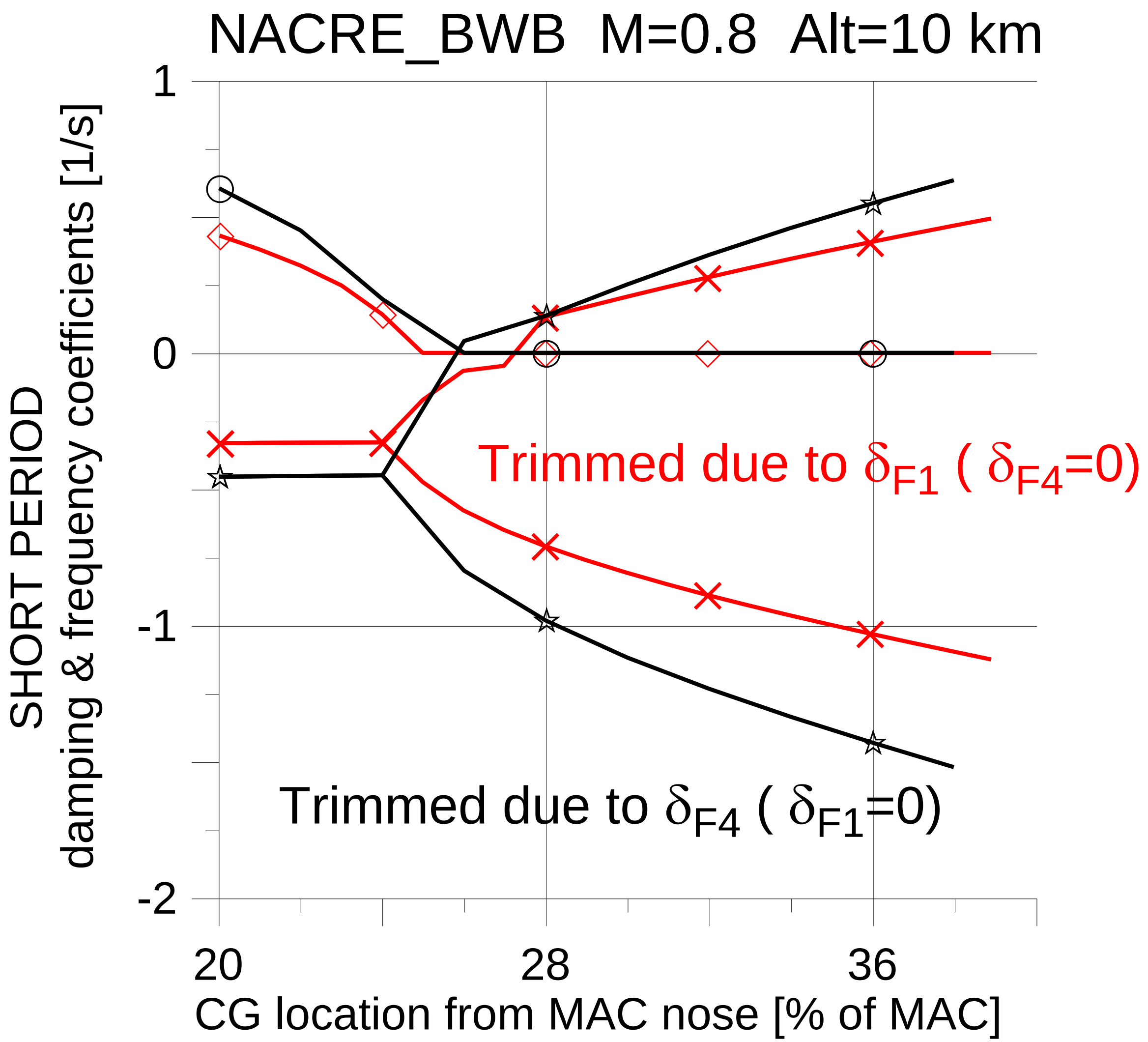

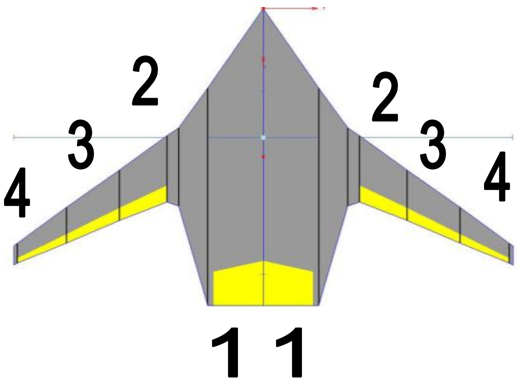

CG position depending on fuel mass distribution

Case number	1	2	3
Fuel tank graph (white colour means no fuel)	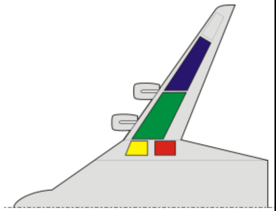	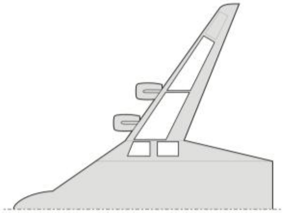	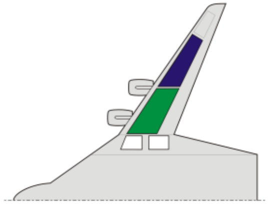
Fuel weight [tons]	280	0	160
Airplane weight [tons]	700	420	580
$x_{CG,A}^{Fuel\ only}\ [m]$	8.24	0	10.07
$x_{CG,A}^{Full\ Aircraft}\ [m]$	-1.82	-8.53	-3.4
$x_{CG,NA}^{Full Aircraft}$ [% of MAC]	20.0	1.5	15.6

Rear trim fuel tank

Case number	13	14
Fuel tank graph (white colour means no fuel)	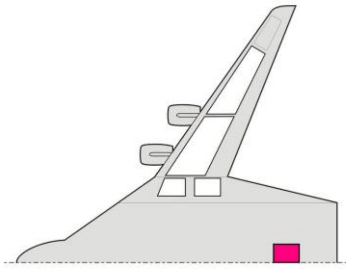	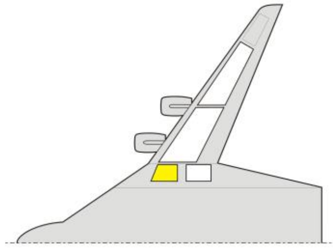
Fuel weight [tons]	60	60
Airplane weight [tons]	480	480
$x_{CG,A}^{Fuel\ only}$ [m]	24.68	2.1
$x_{CG,A}^{Full\ Aircraft}$ [m]	-4.38	-7.20
$x_{CG,NA}^{Full\ Aircraft}$ [% of MAC]	12.9	5.2

$$\Delta\delta = \Delta x_{CG}\frac{1}{\frac{\partial C_{m,A}^{F}}{\partial\delta}} = \frac{-0.077}{-0.00482} = 16^{o}$$

$$\Delta C_D = A\left(C_{L,1}^2 - C_{L,2}^2\right) + B\left(C_{L,1} - C_{L,2}\right) =$$
$$A * \Delta C_L * 2C_L + B * \Delta C_L = 0.025 * 0.138 * 0.56$$
$$+ 0.001 * 0.138 = 0.003312$$

$$\Delta C_D[\%] = \frac{0.003312}{C_{D,ref}} * 100\% = \frac{0.003312}{0.0724} * 100\% = 4.57\%$$

BSSA Long range Business Jet B2

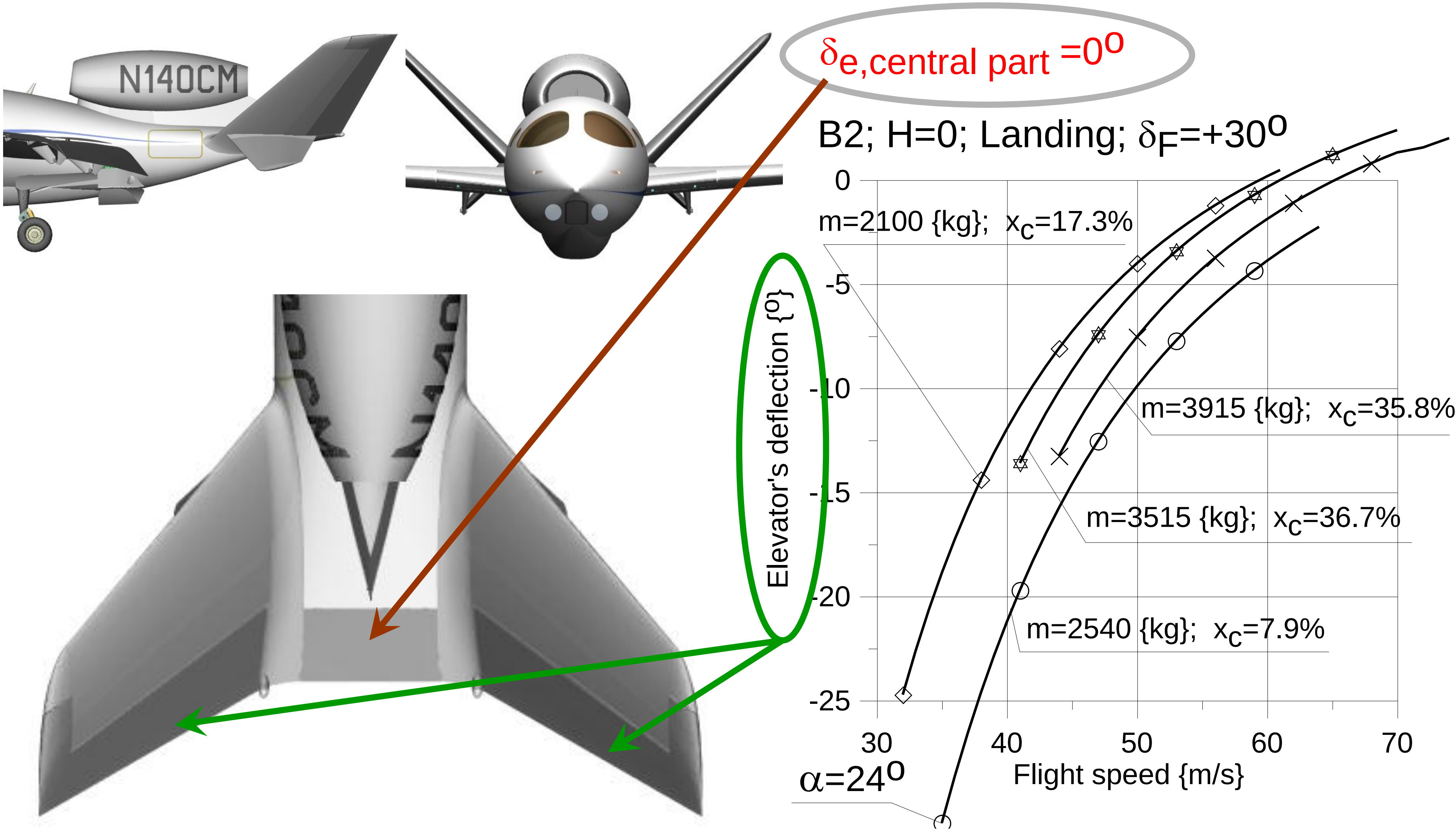

Courtesy of BSSA

Mach = 0.75
Range = 5600 km
Engine: PW 530
Seating: pilot + 10
Rescue: 3 parachutes

Damping ratio & natural frequency

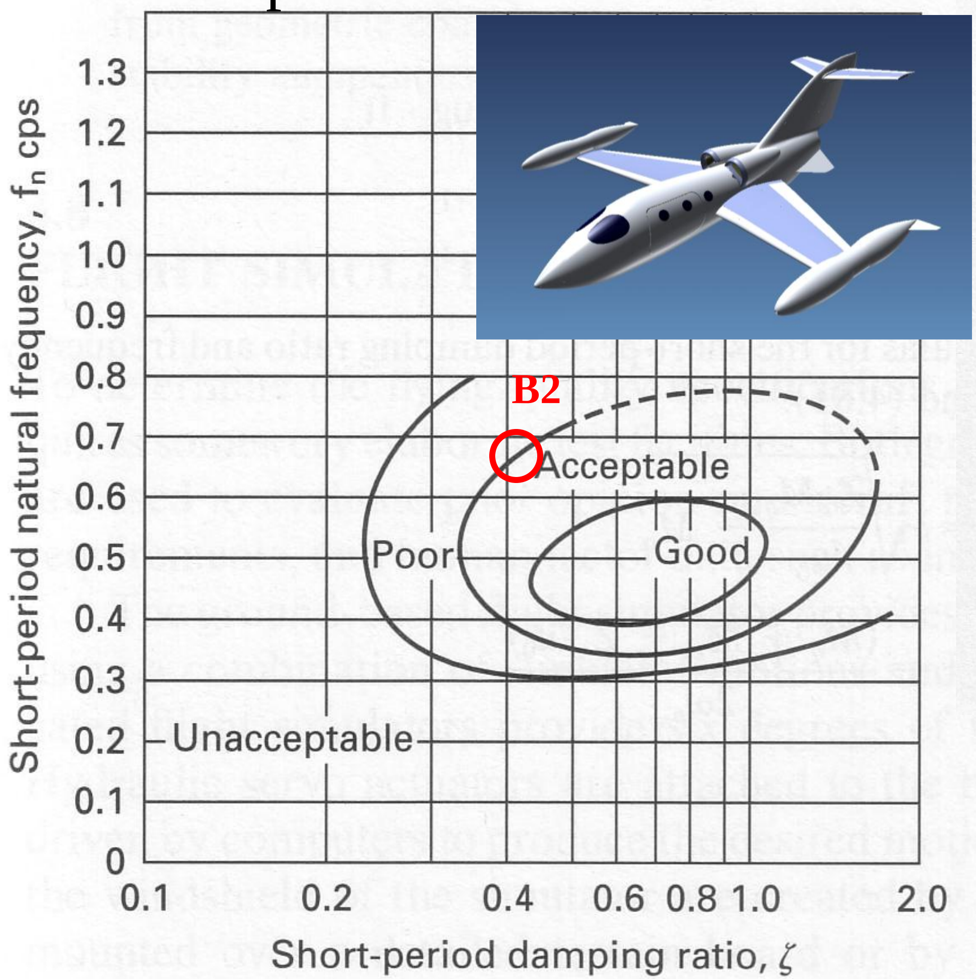

TABLE 4.10
Longitudinal flying qualities

Phugoid mode

Level 1	$\zeta > 0.04$
Level 2	$\zeta > 0$
Level 3	$T_2 > 55$ s

Short-period mode

	Categories A and C		Category B	
	ζ_{sp}	ζ_{sp}	ζ_{sp}	ζ_{sp}
Level	min	max	min	max
1	0.35	1.30	0.3	2.0
2	0.25	2.00	0.2	2.0
3	0.15	—	0.15	—

$$\omega_n = \sqrt{\xi^2 + \eta^2} \quad ; \quad \zeta = \frac{-\xi}{\sqrt{\xi^2 + \eta^2}}$$

Wind tunnel tests, IoA, May 2009

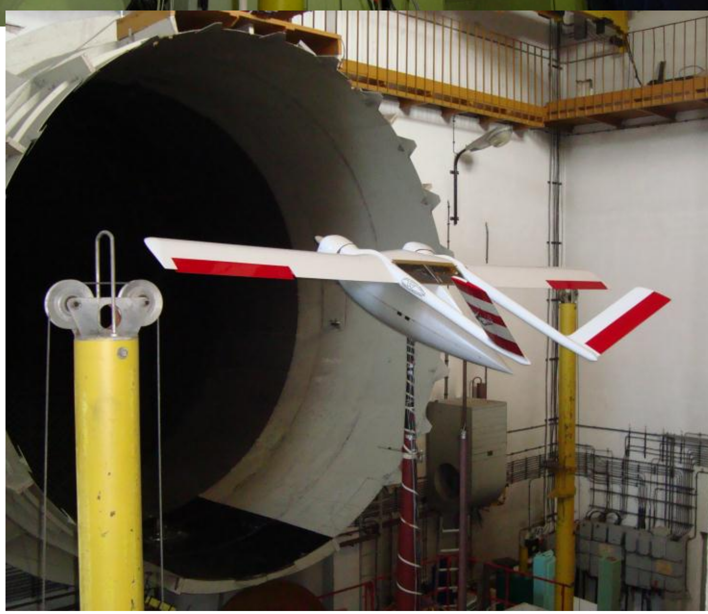

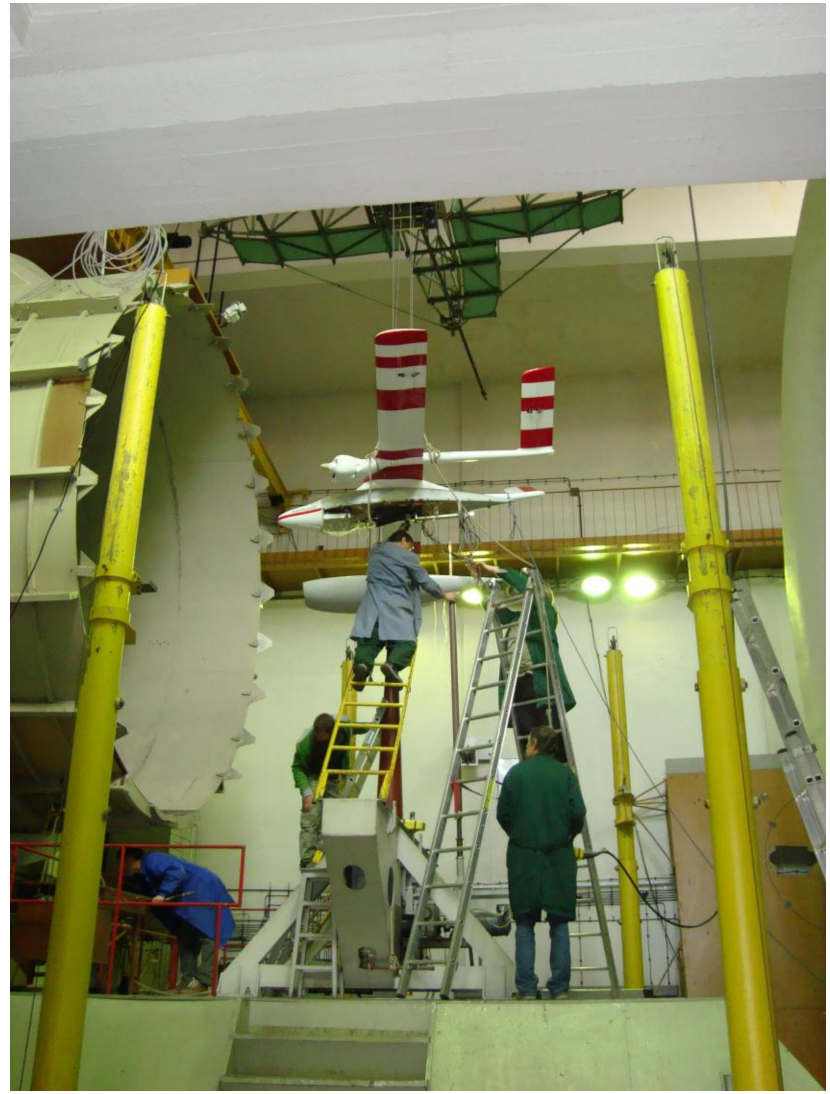

Wind tunnel tests, IoA, May 2009

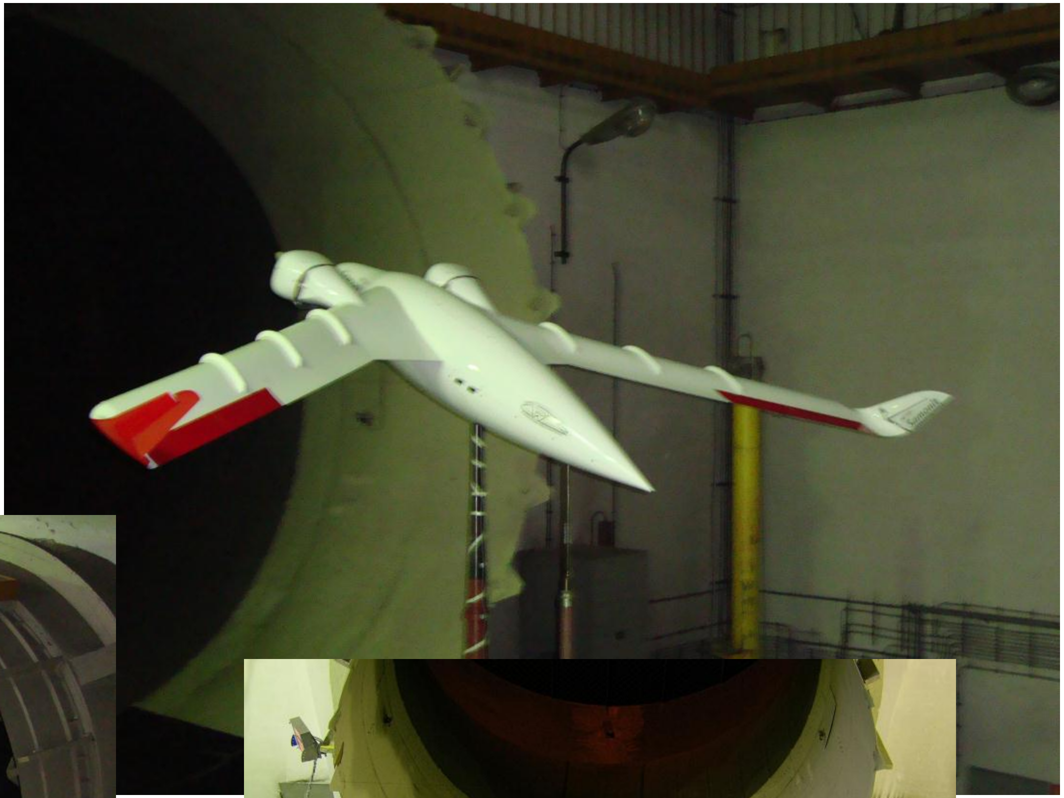

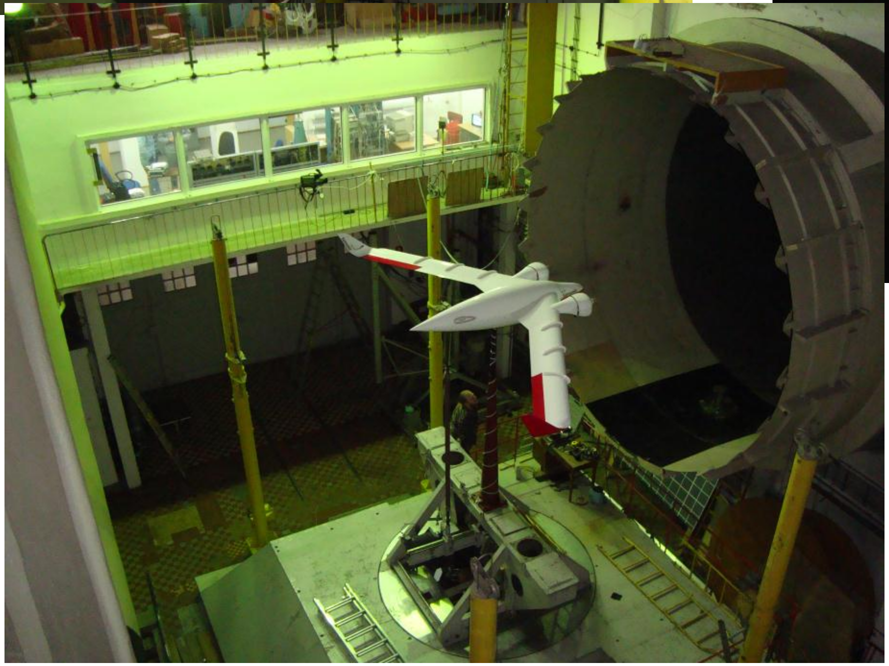

Unmanned Aerial Vehicle - SAMONIT

SAMONIT - Version_2: Flying wing
Results of computation versus
CG location, V=40 m/s

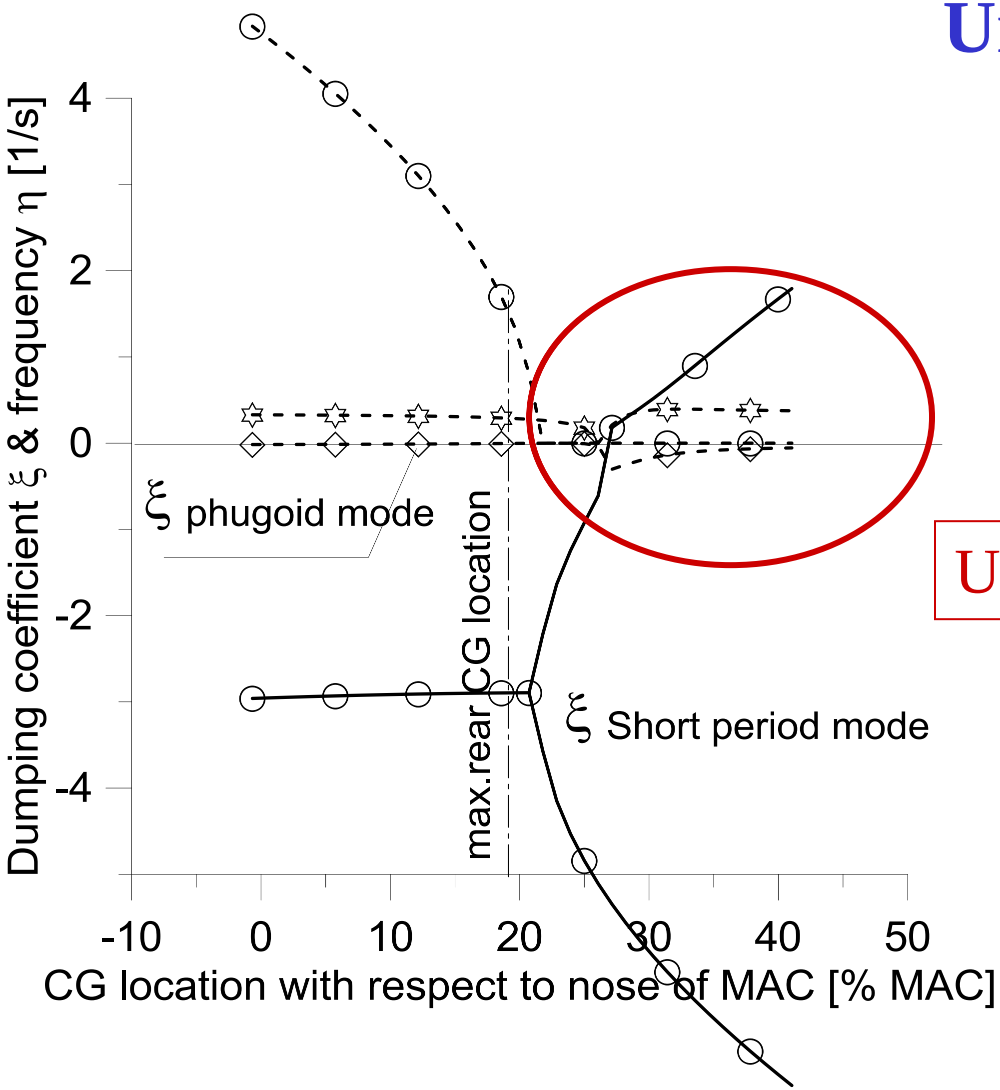

Unstable range of CG location

SAMONIT - tailless tractor configuration

$m=48$ kg, $x_C=8^o$ of MAC, $x_N=29\%$ MAC

static stability margin = 21% of MAC,

sideslip $\beta=-15^o\div+10^o$; only right engine in operation; $2S_{VS}=0.048\ m^2$; $2S_{VU}=0.132\ m^2$

Lateral control

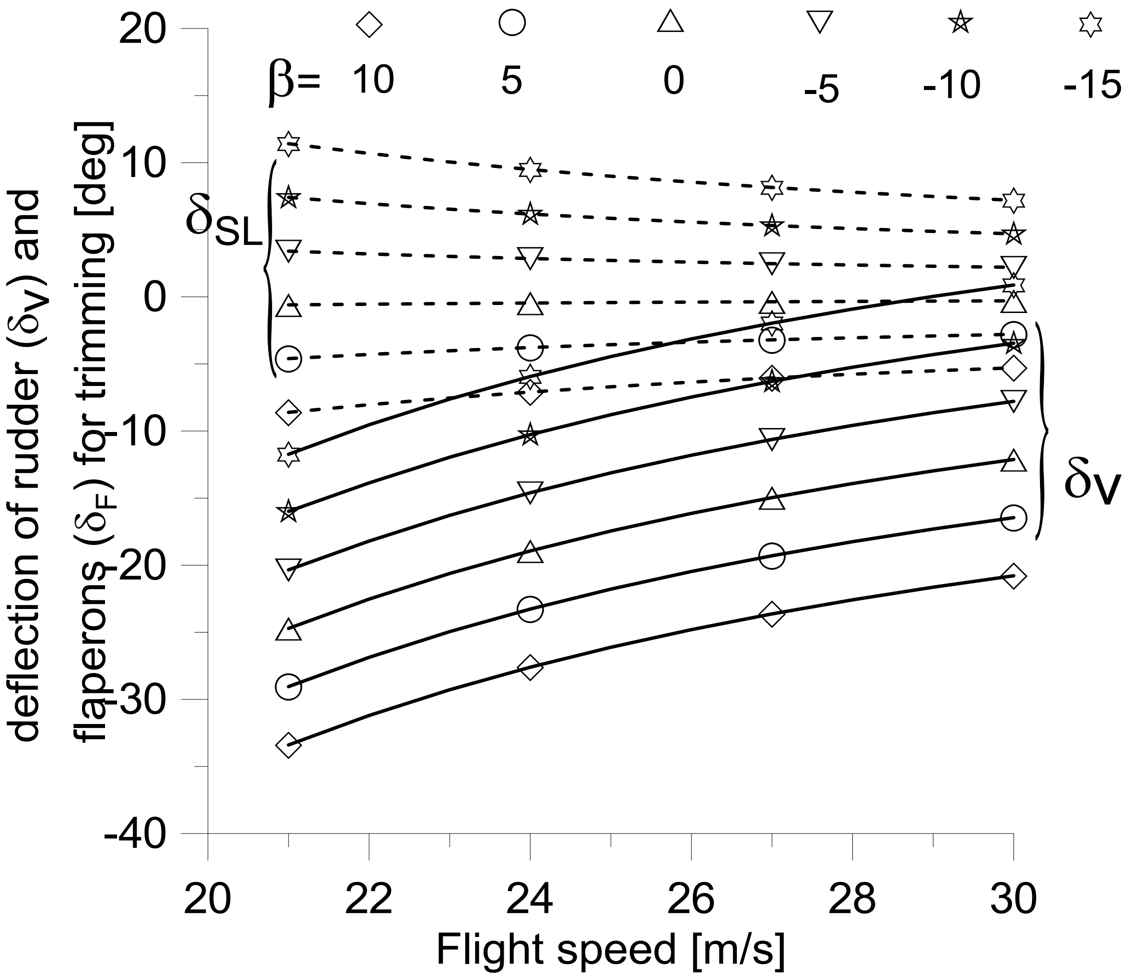

Spiral instability

SAMONIT - tailless tractor configuration

m=48 kg, x_C=8% MAC, x_N=29% MAC

static stability margin = 21% MAC

Unstable Spiral, dihedral angle = 2^o

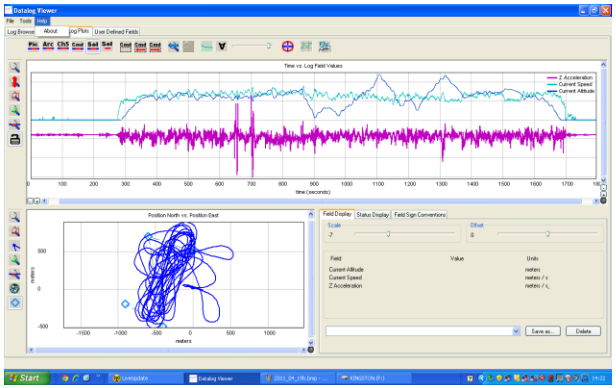

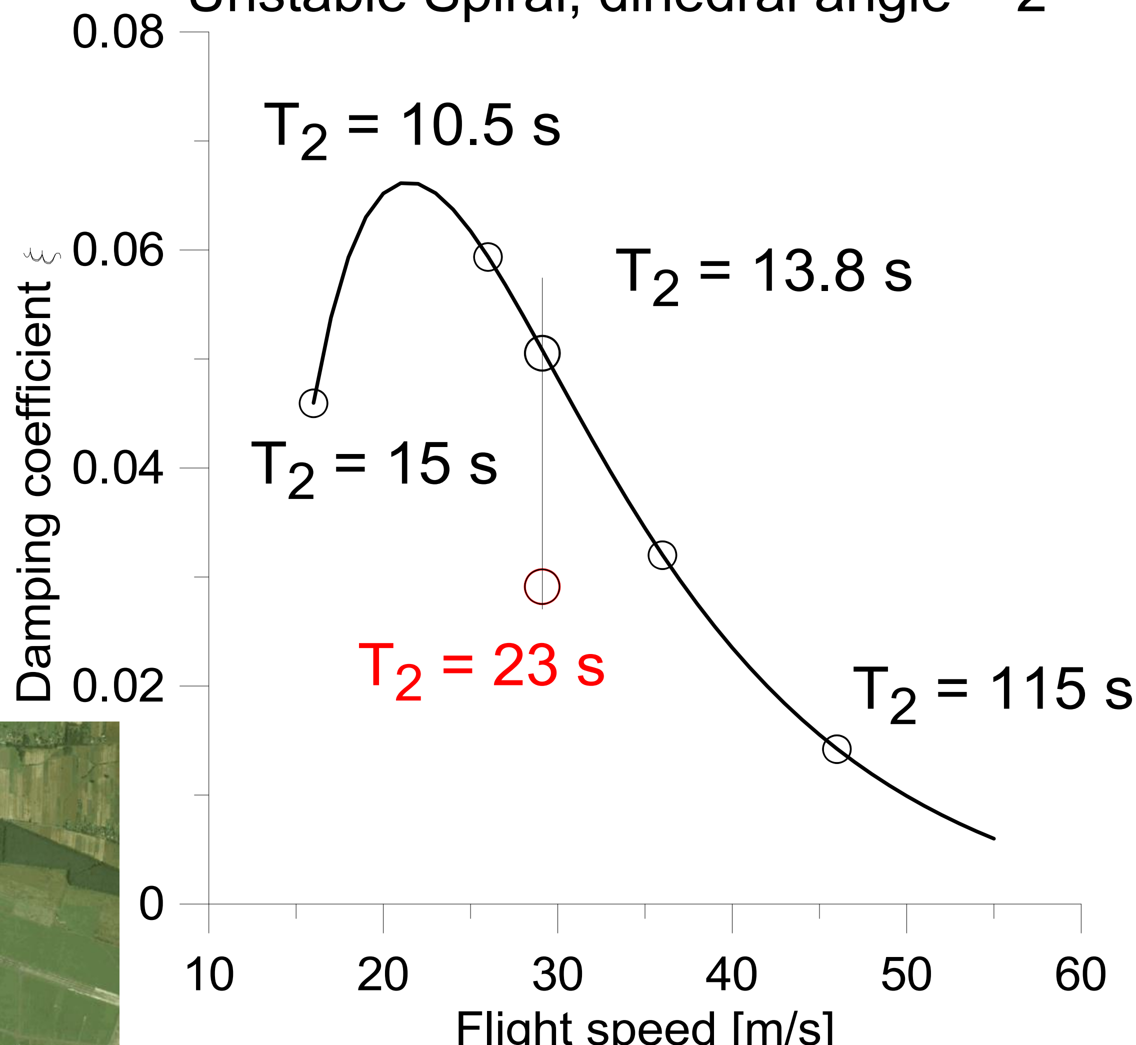

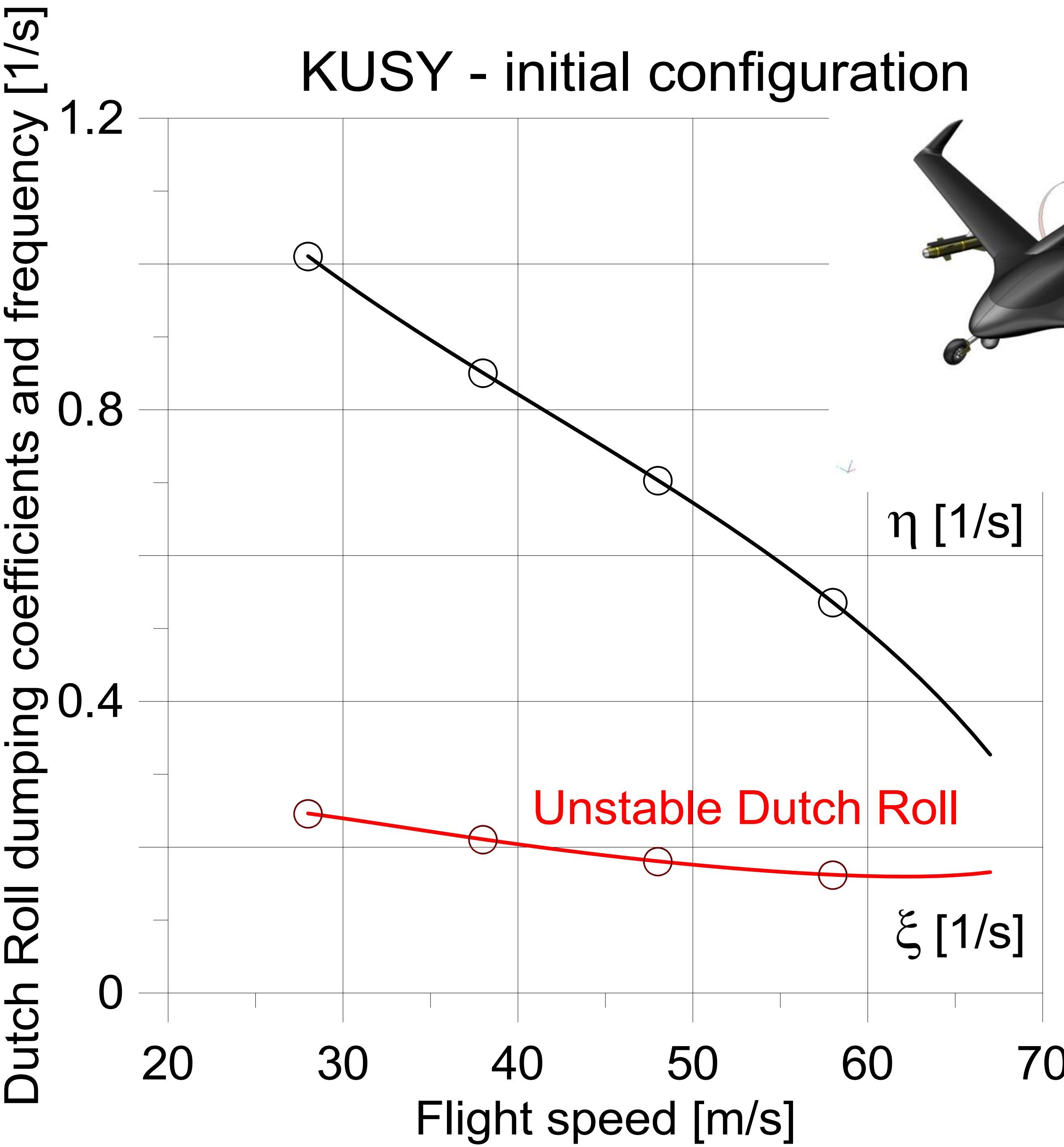

KUSY – a UAV in progress

Family Jet, m=1400 kg, Xc=26.4% MAC
Geometry: July-October 2010
Aerodynamcs: M=0.65, Tunel Φ5 + Prandtl coefficient
Control surface characteristics modified Feb 2012

H=7 km, Tailplane setting angle = -3°
Short Period, sticks free/fixed

Stick free versus stick fixed dynamic stability

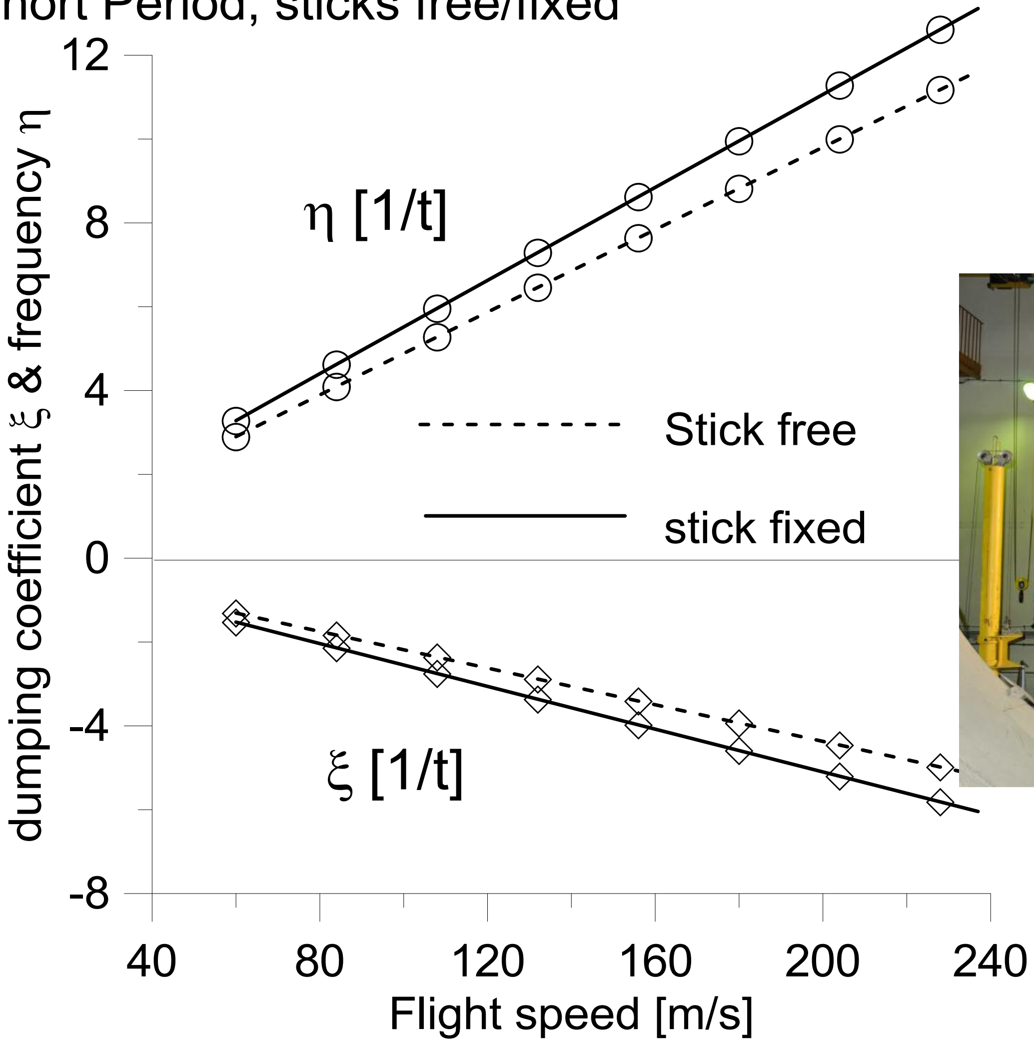

Neutral points, manoeuvrability points

Family Jet, m=1400 kg, Xc=26.4% MAC
Geometry, July/Oct 2010
Aerodynamics: M=0.2, Tunnel Φ5
Modified aerodynamic characteristics of tailplane Feb 2012
H=0 km, tailplane setting angle = -3^{o}

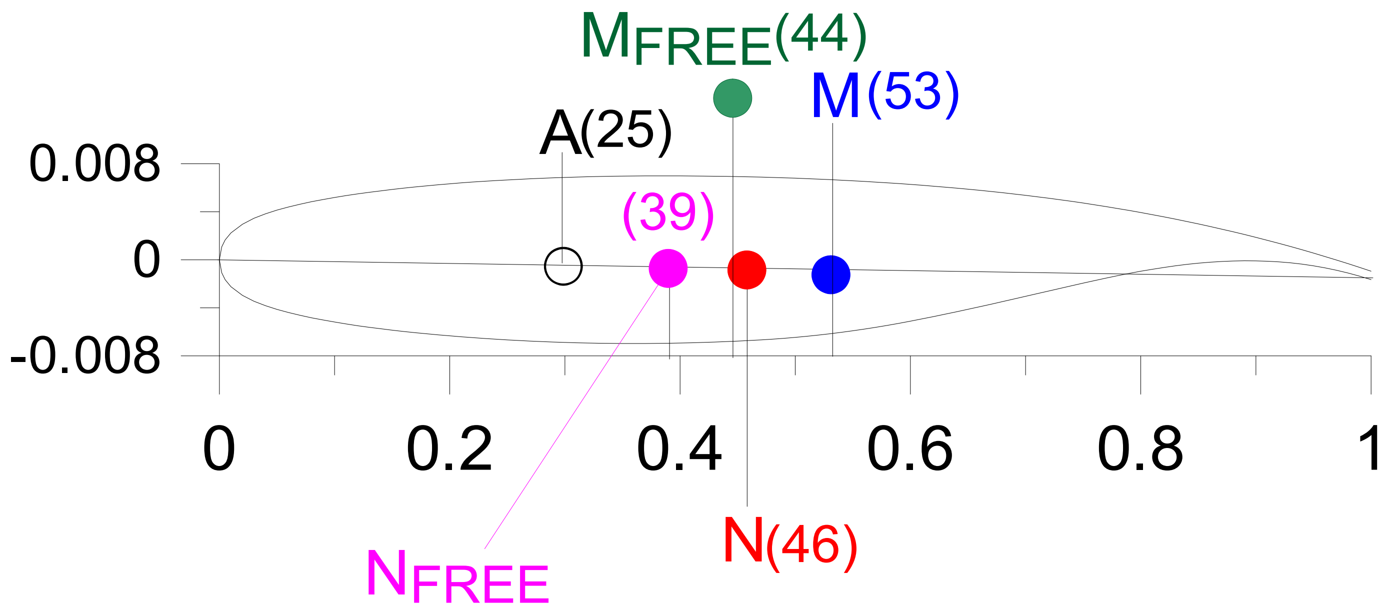

Conclusions

- STB software has been developed at Warsaw University of Technology and intensively tested and improved since 1982. This effort could be measured by more than 40 man-years;
- more than 20 industrial and research projects were supported using STB, and also many student's projects;
- in any case this software must be combined either with CFD or Wind Tunnel testing; it is especially sensitive to lateral stability derivatives.

Simulation of a Propeller Disk Represented by Distribution of Velocities

N. Žižkovský J. Pelant M. Kyncl

Aerospace Research and Test Establishment

EASN workshop, Prague, 2012

Outline

1. Motivation
   - Application
   - Standard Implementation
   - Formulation
2. Test case
   - Case description
3. Solution
   - Home code solution
   - Commercial code implementation

Outline

1. Motivation
   - Application
   - Standard Implementation
   - Formulation
2. Test case
   - Case description
3. Solution
   - Home code solution
   - Commercial code implementation

Isolated solution

An independent design / optimization for each part of propulsor, like:

- Propeller blade
- Duct / channel
- Engine nacelle

Outline

1. Motivation
   - Application
   - Standard Implementation
   - Formulation
2. Test case
   - Case description
3. Solution
   - Home code solution
   - Commercial code implementation

Present CFD code implementation

Blade/fan/propuslor solver is implemented in both of our main CFD codes:

- FOI's Edge - generally for external aerodynamics
  - Propeller solver uses blade length distribution of aerodynamics coefficient
- CD-Adapco's Star-CCM+ - for external and internal aerodynamics
  - Fan solve uses pressure drop characteristic $\Delta p = f(\dot{m})$

Outline

1. Motivation
   - Application
   - Standard Implementation
   - Formulation
2. Test case
   - Case description
3. Solution
   - Home code solution
   - Commercial code implementation

Input values

From isolated solver of propeller blade we'll receive blade span distribution of velocities in cylindrical coordinates.

- Axial velocity $v_A = f(R)$
- Tangential velocity $v_T = f(R)$
- Radial velocity $v_R = f(R)$ - neglected

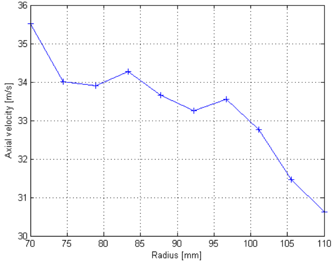

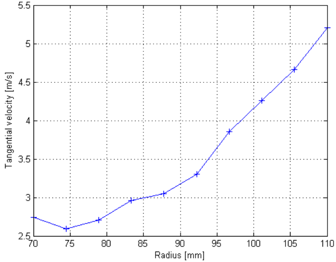

Expressions

Basic expressions for compressible flow:

$$p = p_0 \cdot \left(1 - \frac{1-\kappa}{1+\kappa} \cdot \lambda^2\right)^{\kappa/\kappa-1} \tag{1}$$

$$\rho = \rho_0 \cdot \left(1 - \frac{1-\kappa}{1+\kappa} \cdot \lambda^2\right)^{1/\kappa-1} \tag{2}$$

$$c^2 = c_0^2 \cdot \left(1 - \frac{1-\kappa}{1+\kappa} \cdot \lambda^2\right) \tag{3}$$

$$T = T_0 \cdot \left(1 - \frac{1-\kappa}{1+\kappa} \cdot \lambda^2\right) \tag{4}$$

$$\lambda^2 = \frac{v^2}{c_*^2} = \frac{v_A^2 + v_T^2 + v_R^2}{c_*^2} \tag{5}$$

Expressions

Derived expressions - Total state values:

$$c_*^2 = \frac{2 \cdot \kappa \cdot p}{(\kappa + 1) \cdot \rho} + \frac{\kappa + 1}{\kappa + 1} \cdot v^2 \tag{6}$$

$$p_0 = p \cdot \frac{1}{\left(1 - \frac{1-\kappa}{1+\kappa} \cdot \lambda^2\right)^{\kappa/\kappa-1}} \tag{7}$$

$$\rho_0 = \rho \cdot \frac{1}{\left(1 - \frac{1-\kappa}{1+\kappa} \cdot \lambda^2\right)^{1/\kappa-1}} \tag{8}$$

$$T_0 = T \cdot \frac{1}{\left(1 - \frac{1-\kappa}{1+\kappa} \cdot \lambda^2\right)} \tag{9}$$

Outline

Ducted propeller with internal flow

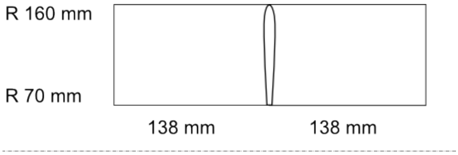

- compressible, viscid, turbulent flow
- Inlet total state values: $T_0 = 273.15^\circ K$, $p_0 = 101325 Pa$, $R = 287.04$, $\kappa = 1.4$
- Pressure outlet: $p_s = 101325 Pa$, $T = 273.15^\circ K$
- $k_0 = 0.05576$, $\omega_0 = 0.321 \cdot 10^6$

Ducted propeller with external flow

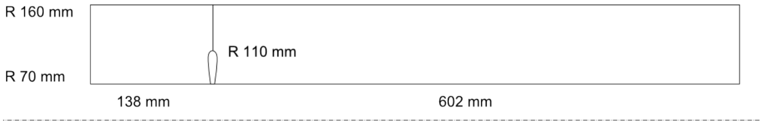

- compressible, viscid, turbulent flow
- Inlet total state values: $T_0 = 273.15^\circ K$, $p_0 = 101325 Pa$, $R = 287.04$, $\kappa = 1.4$
- Pressure outlet: $p_s = 101325 Pa$, $T = 273.15^\circ K$
- $k_0 = 0.05576$, $\omega_0 = 0.321 \cdot 10^6$

Outline

1. Motivation
   - Application
   - Standard Implementation
   - Formulation
2. Test case
   - Case description
3. Solution
   - Home code solution
   - Commercial code implementation

Simulation setup overview

Own code written in Fortran and it's focused to rotational disk solution

- 2D structured mesh
- 3D axisymmetrical solver with tangential component
- Turbulence model k-ω
- Explicit unsteady time
- Compressible flow
- Two cases of propeller disk
  - in the entire diameter of the pipe
  - occupies only about 34% of section of the pipe

Boundary conditions definition

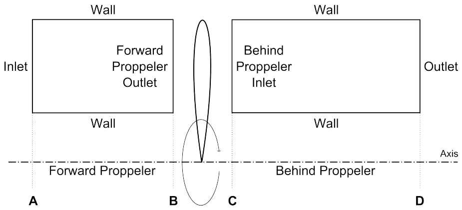

- **A** Stagnation Inlet - Total state
- **B**
  - Mass Flow Outlet
  - Internal Interface - for smaller propellers than tube diameter
- **C**
  - Stagnation Inlet - Total state
  - Internal Interface - for smaller propellers than tube diameter
- **D** Pressure Outlet

Full cross section propeller

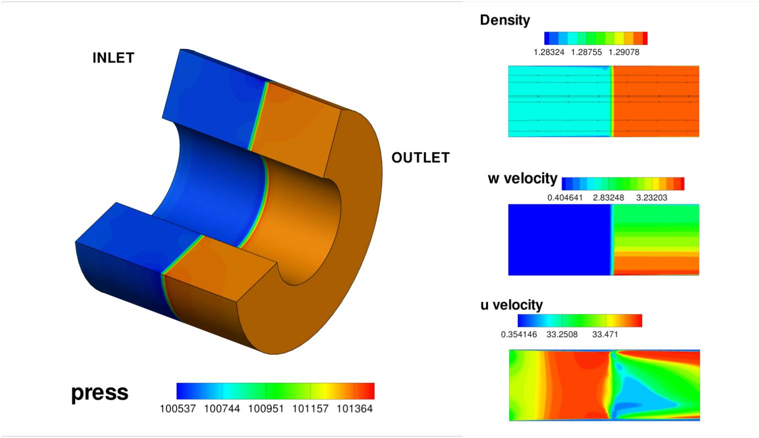

Partial cross section propeller

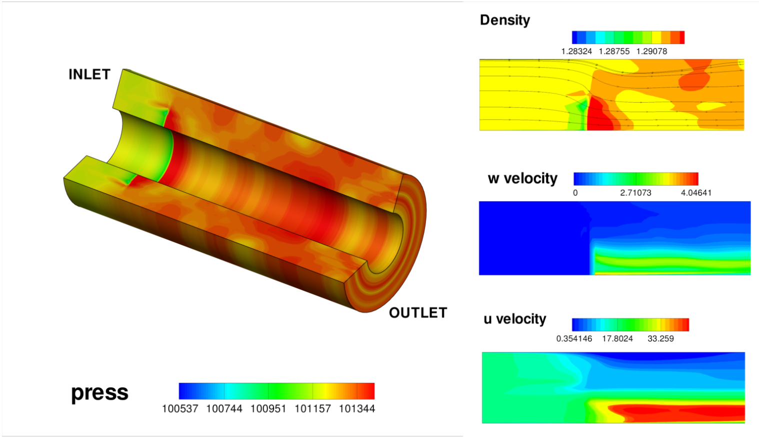

Outline

Simulation setup overview

- Full scale 3D model - unstructured mesh
- Turbulence model k-ω SST
- Implicit unsteady simulation
- Compressible flow
- Two cases of propeller disk
  - in the entire diameter of the pipe
  - occupies only about 34% of section of the pipe

Boundary conditions definition

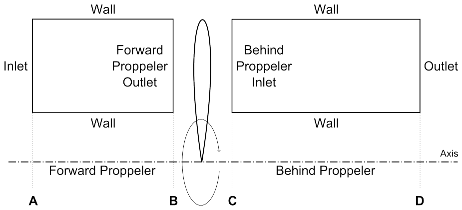

A Stagnation Inlet

B
- Mass Flux
- Internal Interface - for smaller propellers than tube diameter

C
- Stagnation Inlet
- Internal Interface - for smaller propellers than tube diameter

D Pressure Outlet - with radial equilibrium

Simulation setup

C boundary defined by Field Functions

- p_0 correspond to eq. (7)
- T_0 correspond to eq. (9)
- Data of Mass Flux and Temperature are stored in R-table
  - values are averaged around perimeter
  - data from R-table are extracted each time step - by macro

B boundary values of Mass Flux are defined by R-table

Simulation's problem

- Stability of calculated total state values (p_T and T_T) at **C** boundary condition
  - Using Average values from R-table as well for **C** boundary
- Convergence problem
  - Minimize time step
  - Increase mesh quality/using of mapped mesh

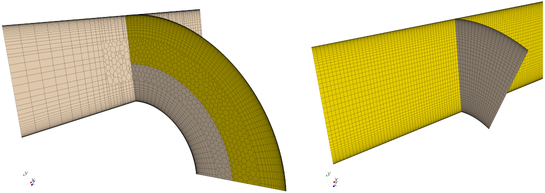

Results for ducted propeller with internal flow

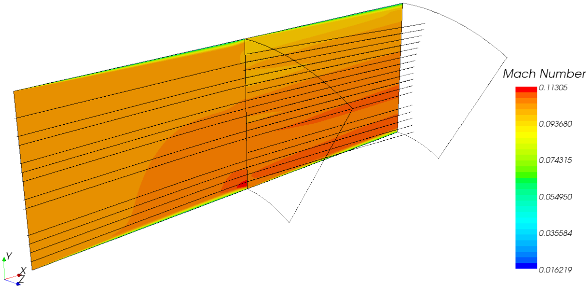

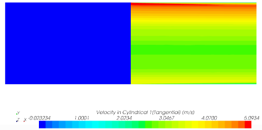

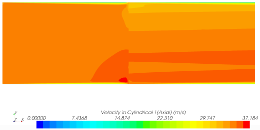

Results for ducted propeller with external flow

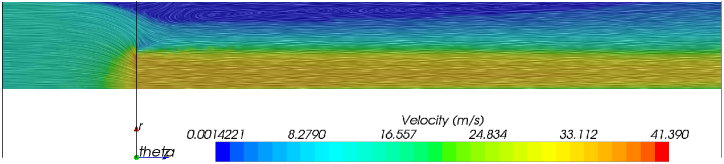

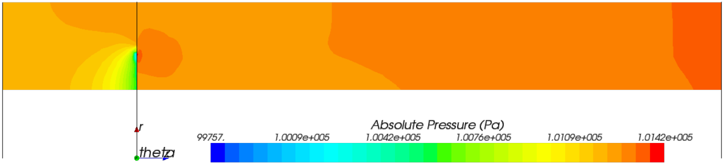

Summary

- Home code - stable solution for axisymmetrical simulations
- Solution in Star-CCM+ can be applied in complex simulations
- Difference between solvers is caused by
    - different mesh
    - different velocity profile input (spline in Star-CCM+)

- Outlook
    - Comparison to experimental data
    - Full shape optimization

Acknowledgement

This result originated with the support of Ministry of Industry and Trade of Czech Republic for the long-term strategic development of the research organisation.

References I

- Liepmann, H. W. and A. Roshko.
  Elements of Gasdynamics. Galcit Aeronautical series.
  New York: Willey, 1957, p. 53. ISBN 0471534609.

- Pelant, J.
  Boundary value Conditions For Three-Dimensional Flow Round an Axis Symetrical Ring With Proppeler Disk.
  Prague: VZLÚ, Z-65: 8–17, 1995.

- Pelant, J.
  Boundary value Conditions For Three-Dimensional Flow Round an Axis Symetrical Ring With Proppeler Disk.
  Prague: VZLÚ, Z-72: 8–17, 2000.

Adaptation for Sustainable Fuel

Ralf Kurtenbach[1], Yasin Elshorbany[2] and Peter Wiesen[1]

1: University of Wuppertal, Wuppertal, Germany
2: Max Planck Institute for Chemistry, Mainz, Germany

2nd EASN Association Workshop on Flight Physics and Propulsion, 31st – 2nd November 2012, Prague, Czech Republic

Objective:
Exhaust measurements and reactivity study

- Analysis of the chemical composition of the exhaust emissions from different alternative fuels; GTL, aromatic blend (B+Ar), naphthalene blend (B+N) and aromatics+naphthalens blend (B+Ar+N) in comparison to the conventional Jet A-1

Objective: Exhaust measurements and reactivity study

- Determine the environmental impact of the alternative fuels as well as of the conventional Jet-A1 fuel. For this, the reactivity of the exhaust emitted non-methane volatile organic compound (NMVOC) profiles was determined.
- The modelling analysis is largely depending on the components and species included in the emission data base.

- The hydroxyl radical (OH) is the primary photochemical oxidant of trace gases (e.g. NMVOCs) in the atmosphere.
- The photochemical oxidation of NMVOCs in the present of nitrogen oxide (NO_x) results in the formation of harmful photooxidants, like ozone (O_3) and peroxyacetylnitrate (PAN).
- Since the OH-radical is the determinant species for the oxidation capacity in the atmosphere, the identification of the OH-reactivity of the NMVOC profiles R_{OH} is important.

- R_{OH} is defined as the sum of the respective oxidation rates of the molecules Y_i (NMVOCs) by the OH-radical:

$$R_{OH} = \sum k_{Y_i} * [Y_i]$$

where k_{Yi} is the bimolecular rate constants for the reaction of Y_i with OH-radicals. $[Y_i]$ is the concentration of Y_i (NMVOCs)

- The O_3 isopleths illustrate the importance of NMVOC and NO_x as well as there ratio in formulating O_3 control strategies. The TNMVOC/NO_x ratio indicate which compound has to be reduced, NMVOCs or NO_x to reduce efficiently the ozone level.

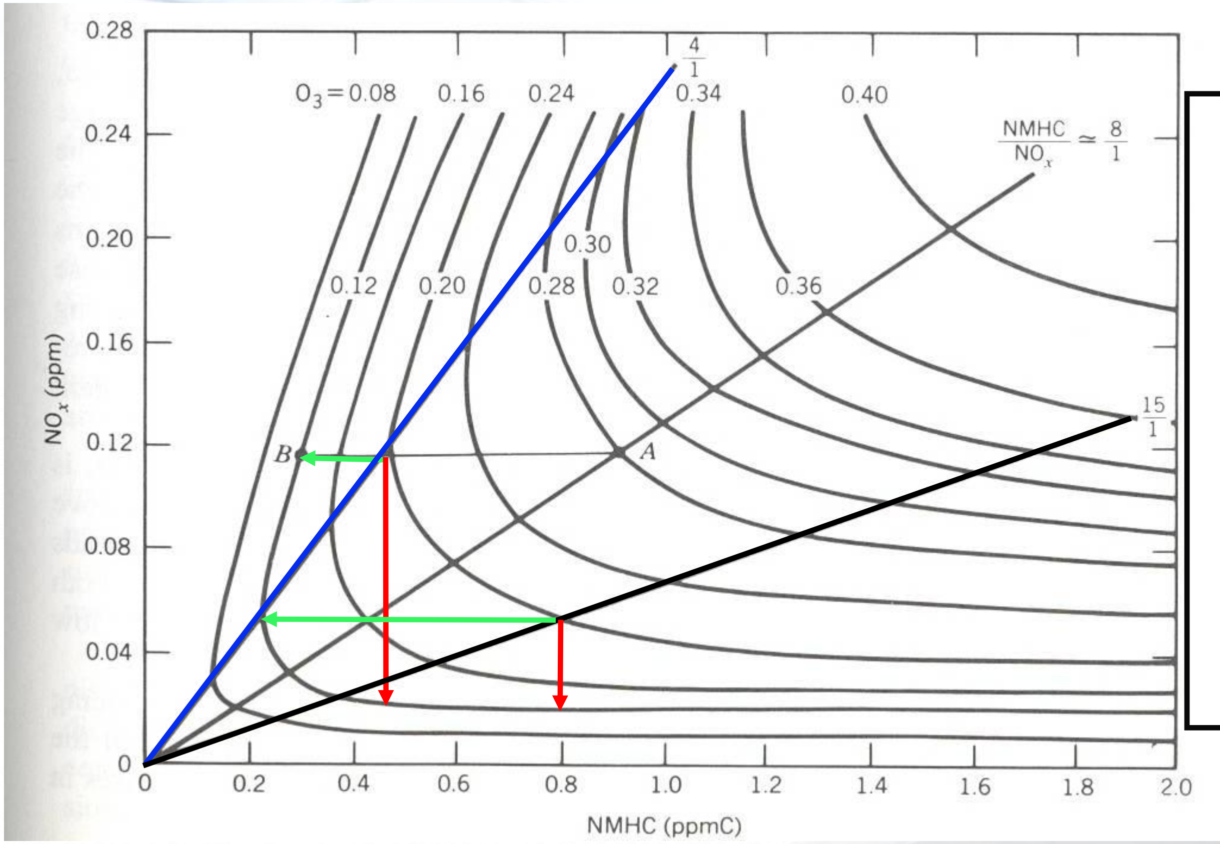

Ozone isopleths used in EKMA approach, Dodge 1977

Ozone reduction:
e.g. 0.20 ppm to 0.12 ppm

low TNMVOC/NO_x ratio e.g. 4
NMVOC reduce by ≈ 33%
NO_x reduce by ≈ 83%
➢NMVOC sensitivity

high TNMVOC/NO_x ratio e.g. 15
NMVOC reduce by ≈ 74%
NO_x reduce by ≈ 60%
➢NO_x sensitivity

Generic composition of GTL blends under study

Fuel	Blend	Compound content
1	B	Paraffins (99%)
2	B-Ar	Paraffins (80%) + Aromatics (20%)
3	B-N	Paraffins (60%) + Naphthenes (40%)
4	B-N-Ar	Paraffins (50%) + Naphthenes (30%) + Aromatics (20%)

Measurement compounds and techniques

- Nitrogen monoxide (NO) and nitrogen dioxide (NO_2): chemiluminescence based analyzer with molybdenum converter (AC 31M, ansyco)
- Carbon dioxide (CO_2): IR absorption based monitor (Carbondio, Pewatron and LI-7000, Licor)
- Carbon monoxide (CO): resonance fluorescence technique (AL5002, Aero-Laser)
- Non-methane volatile organic compounds (NMVOC): preconcentrator (Entec 7100) and GC-FID technique (HP 6890)

Measurement techniques

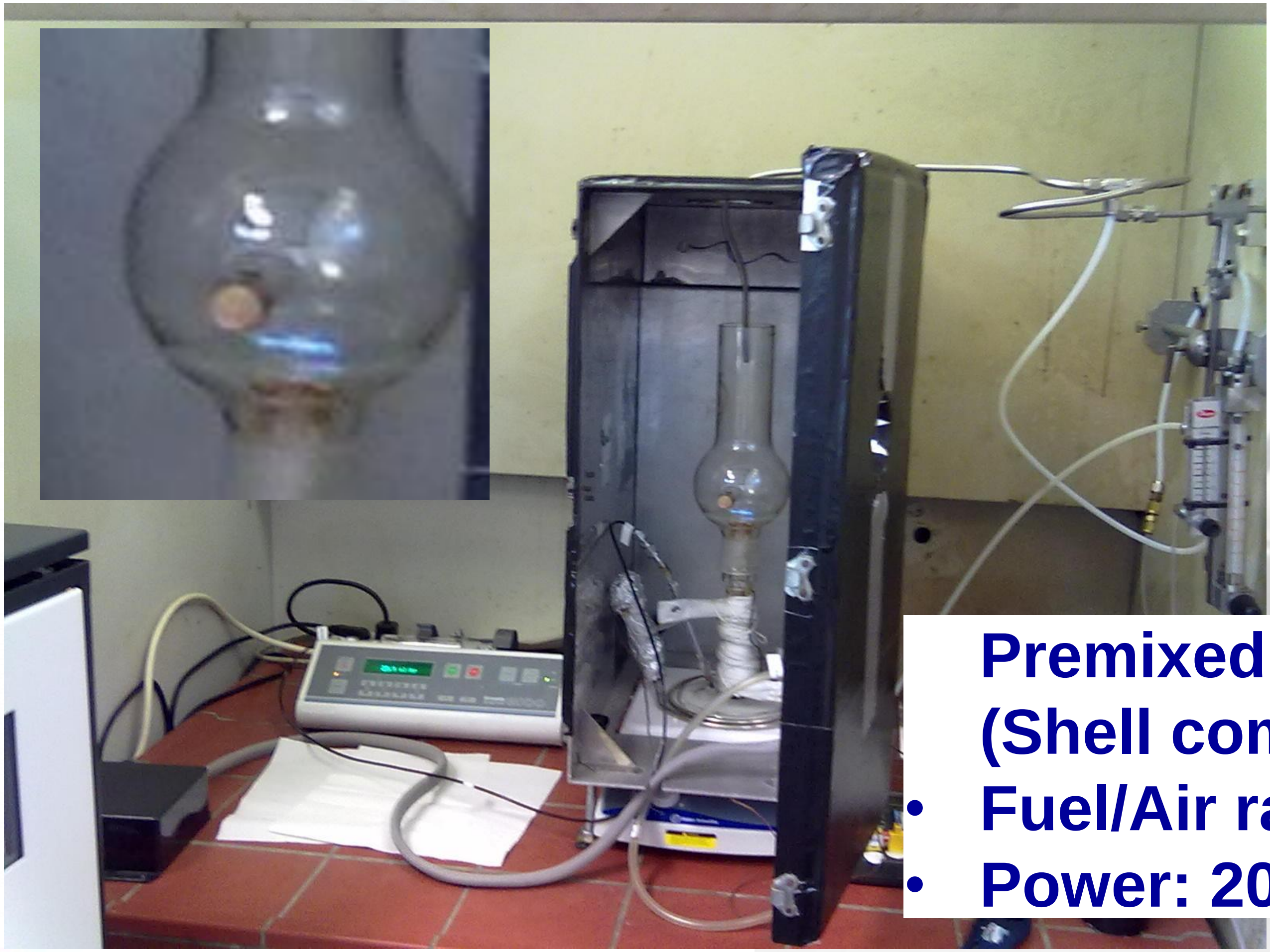

Premixed burner (Shell company)

- Fuel/Air ratio: 1-1.15
- Power: 200 Watt

Measurement techniques

Average measured mixing ratios

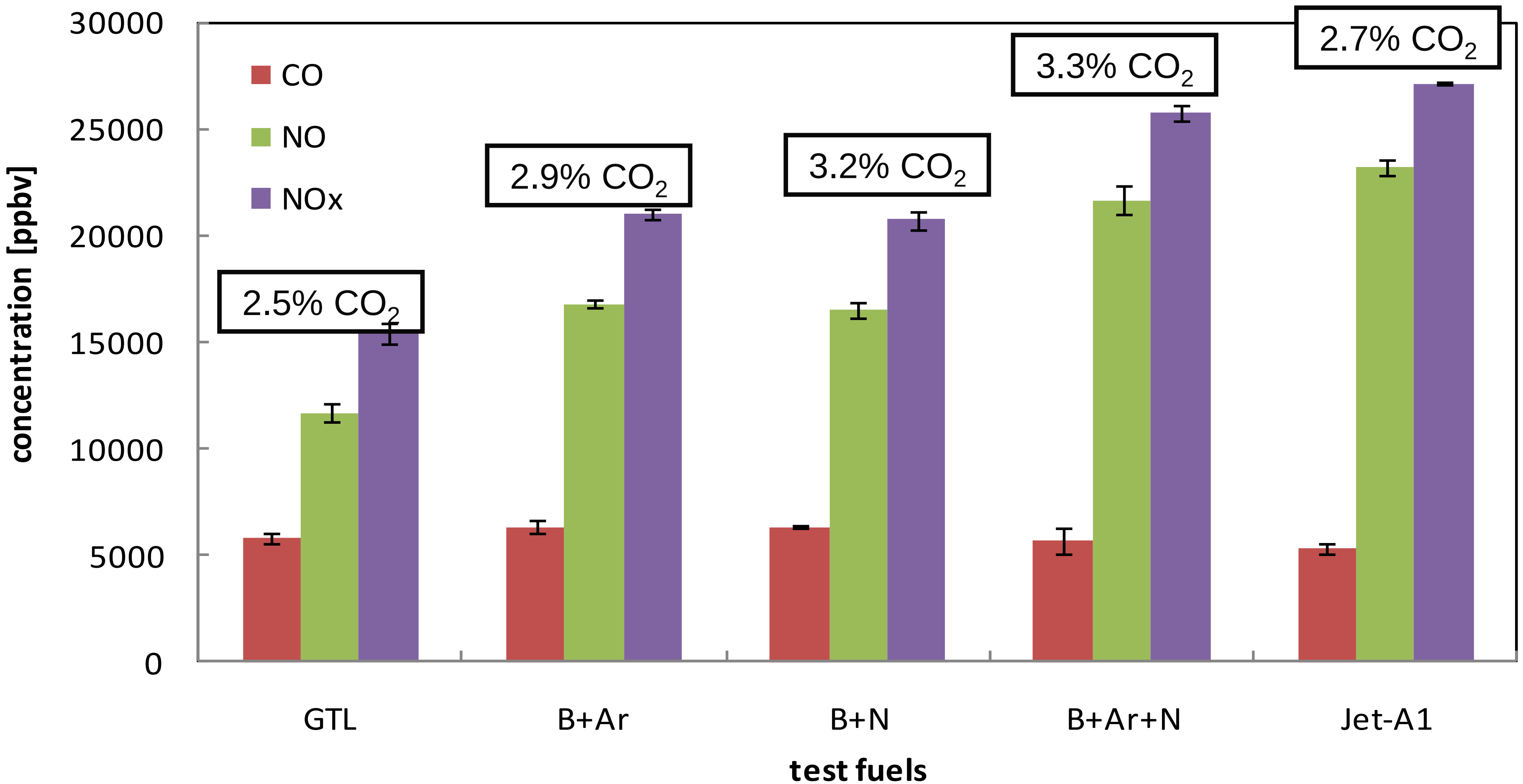

- More than 60 NMVOCs were measured
- Different NMVOC profiles were obtained for the different test fuels

For example:

- Jet A-1 lowest mixing ratios for ethene, ethyne, i-butene, 1-butene and 1,3-butadiene, but highest levels for n-butane, 2-methylbutane and 2-methylpentane and m-&p-xylenes
- GTL has the highest decane mixing ratio but the lowest levels of 1,2,4-trimethylbenzene, which is expected in terms of its paraffinic structure

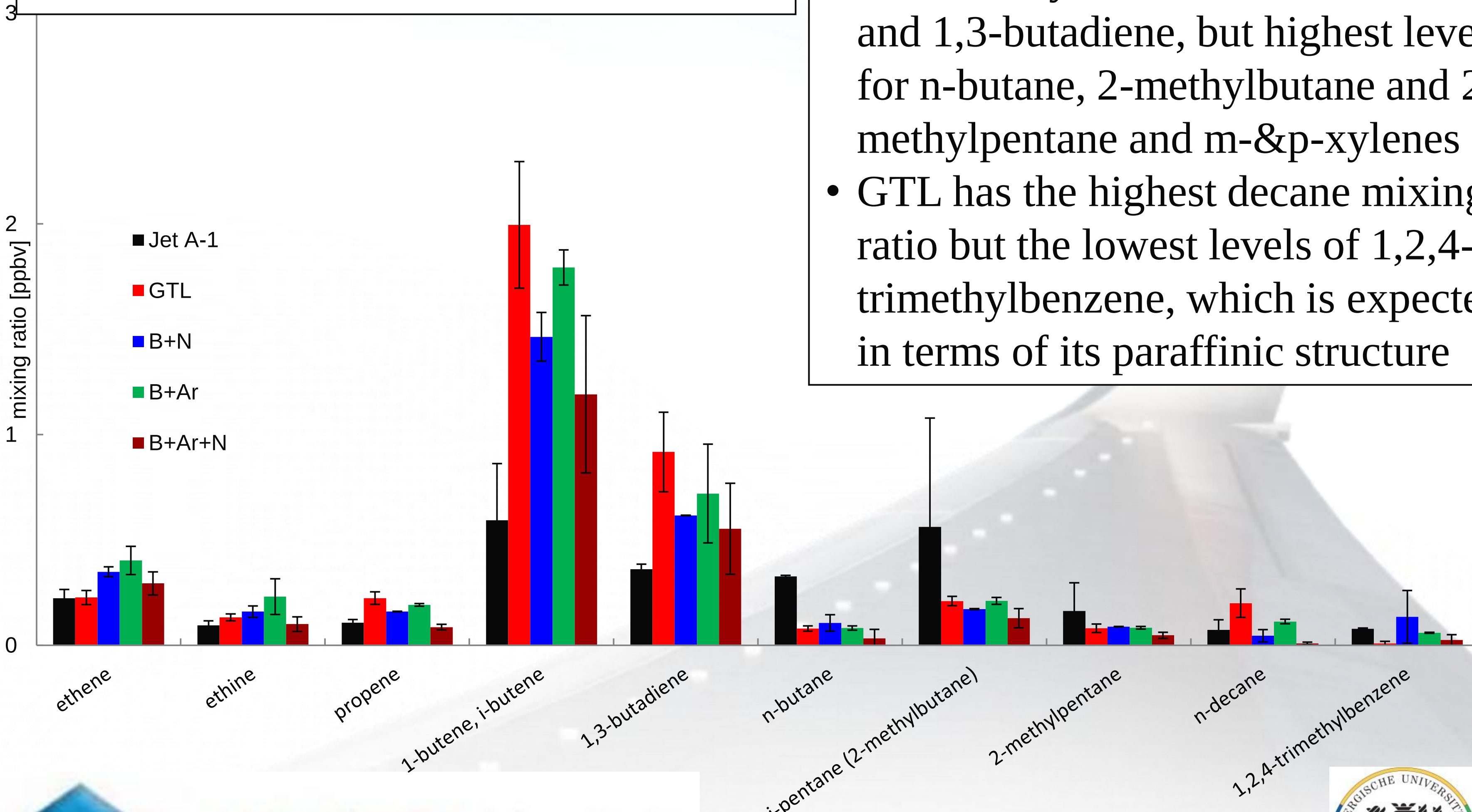

Emission indices [g/kg]

Fuel	NO_x	NO_2	CO	TNMVOC
GTL	2.02 ± 0.05	0.49 ± 0.02	0.46 ± 0.01	0.0051 ± 0.0003
B+Ar	2.43 ± 0.03	0.49 ± 0.01	0.45 ± 0.02	0.0037 ± 0.0002
B+N	2.15 ± 0.01	0.44 ± 0.01	0.40 ± 0.01	0.0041 ± 0.0001
B+Ar+N	2.57 ± 0.04	0.41 ± 0.04	0.34 ± 0.05	0.0017 ± 0.0001
Jet-A1	3.30 ± 0.21	0.47 ± 0.08	0.39 ± 0.04	0.0041 ± 0.0001

- GTL had the lowest NO_x levels, but the highest CO and TNMVOC level
- Jet-A1 and B+Ar+N had the highest NO_x levels, but the lowest CO levels
- B+Ar+N had the lowest TNMVOC level

Comparison with ICAO data base

- NO_x levels in the range of 2-3 g/kg, comparable with idle condition
- CO levels in the range of 0.4-0.5 g/kg, TNMOC levels in the range of 0.002-0.005 g/kg, comparable with take off conditions

ICAO data base

conditions	NO_x	CO	TNMVOC
idle	4.0 ± 1.1	31.8 ± 22.3	7.9 ± 16.6
approach	9.2 ± 2.9	5.3 ± 7.4	0.7 ± 1.7
cruise	21.4 ± 8.5	0.9 ± 1.3	0.2 ± 0.2
take-off	27.3 ± 11.9	0.7 ± 0.7	0.1 ± 0.3

R_{OH} [s^{-1}] of the NMVOC profile for different fuels

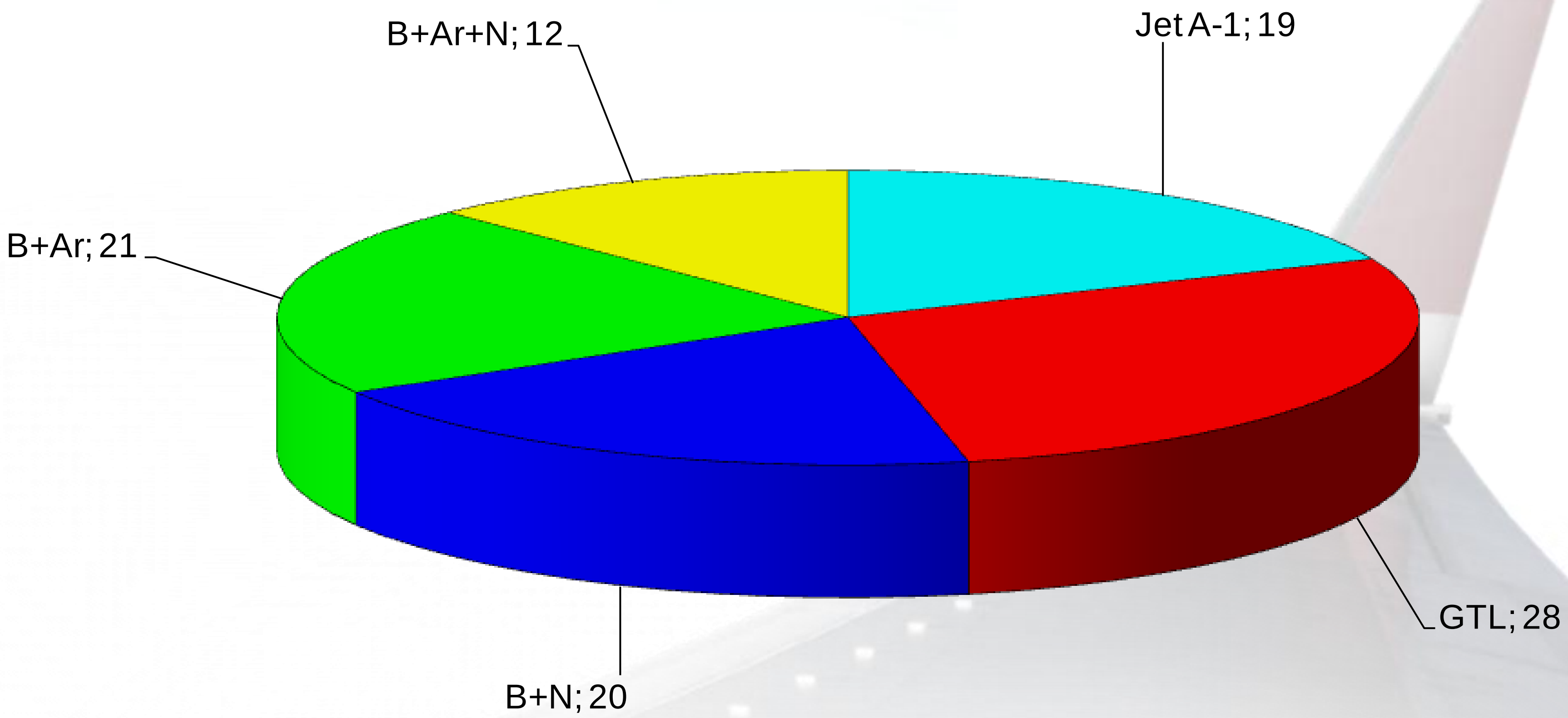

R_{OH} [s^{-1}] of the saturated NMVOCs (alkane) for different fuels

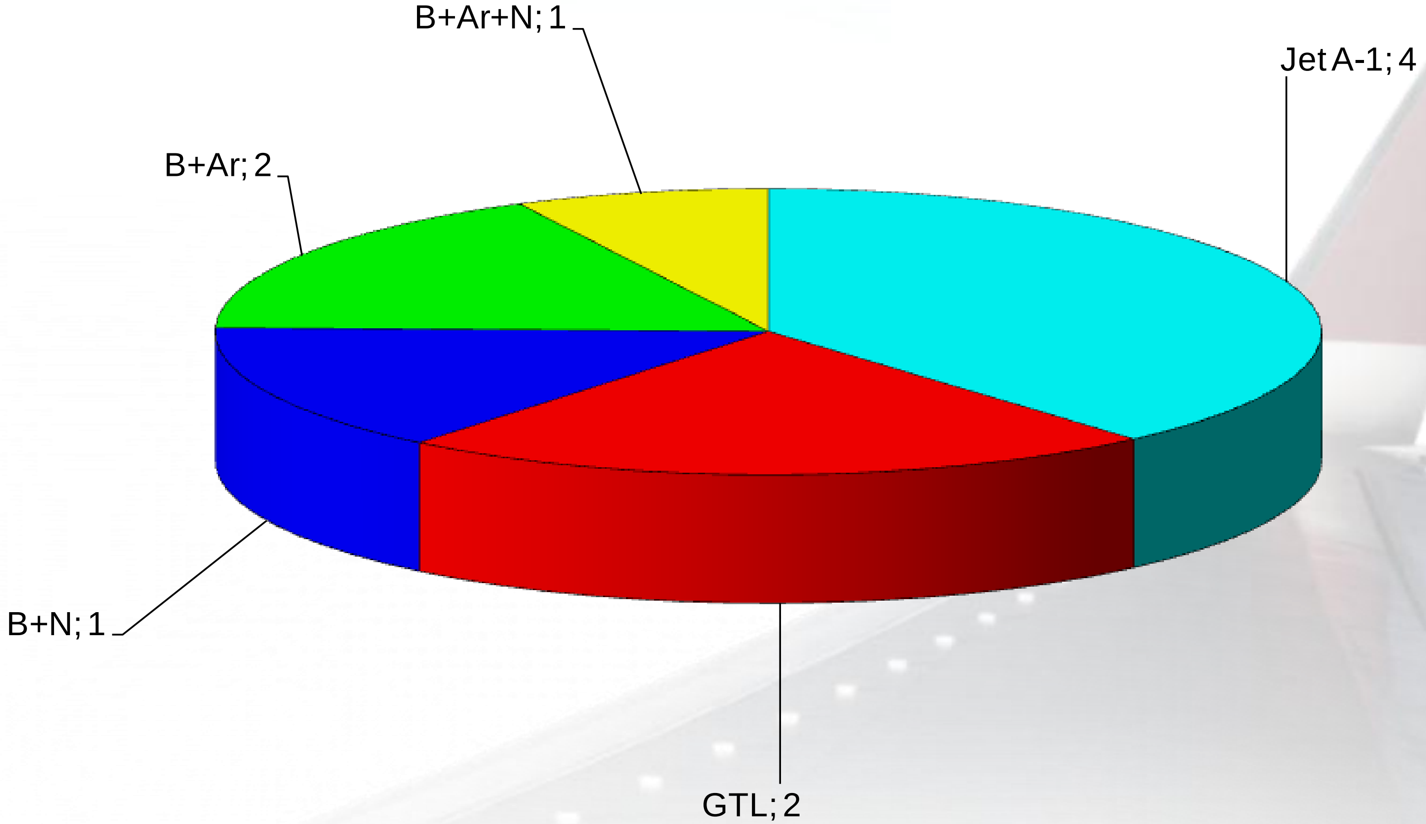

R_{OH} [s^{-1}] of the unsaturated NMVOCs (alkene/alkyne) for different fuels

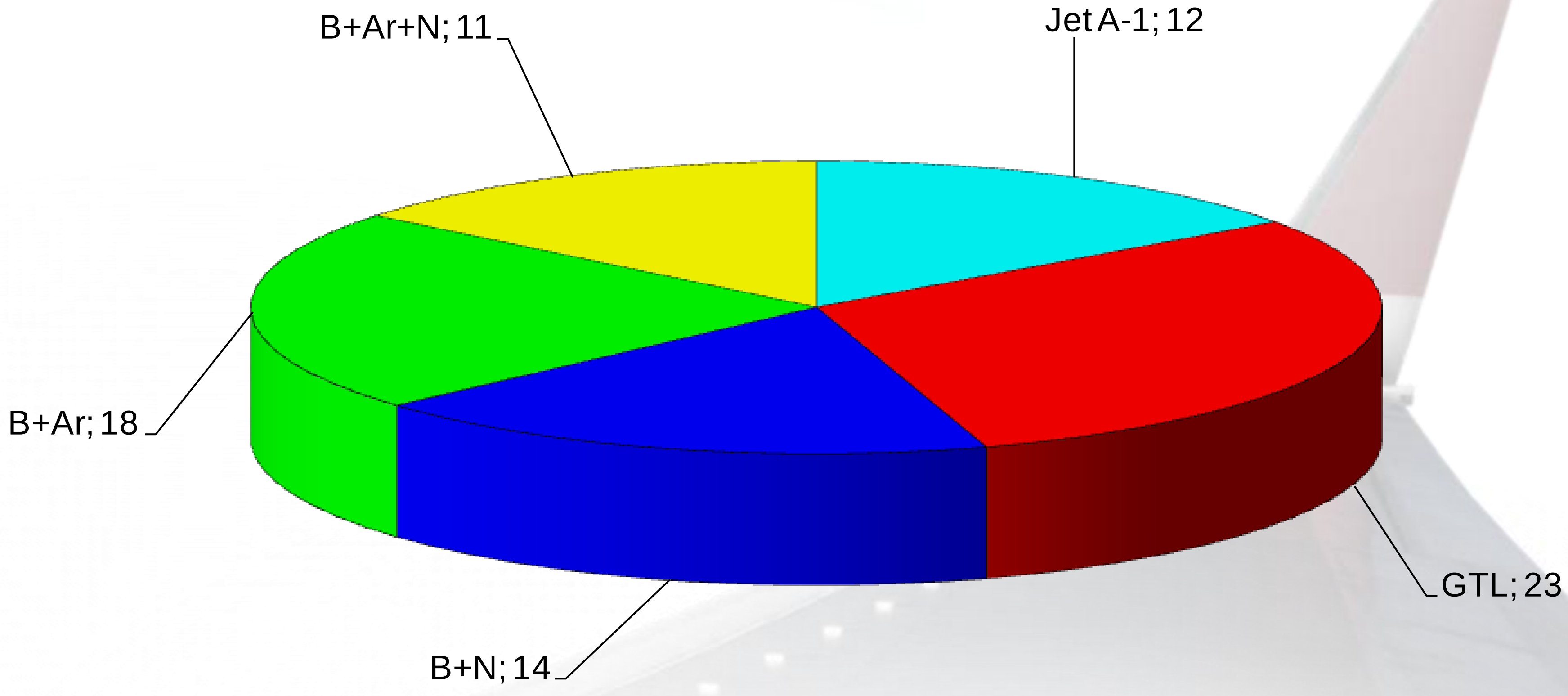

R_{OH} [s^{-1}] of the aromatic NMVOCs for different fuels

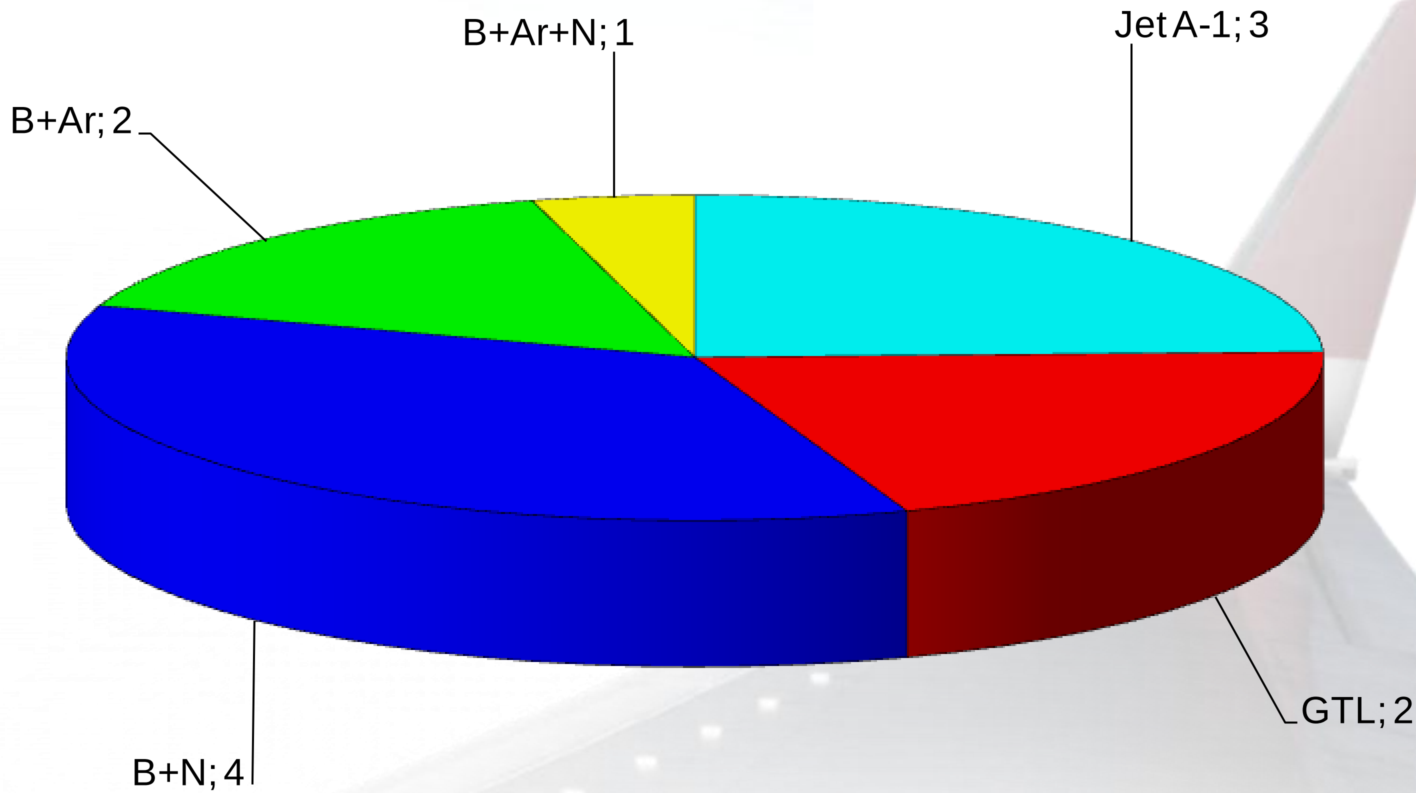

Percentage distribution of the R_{OH} (19 s^{-1}) for Jet A-1 fuel

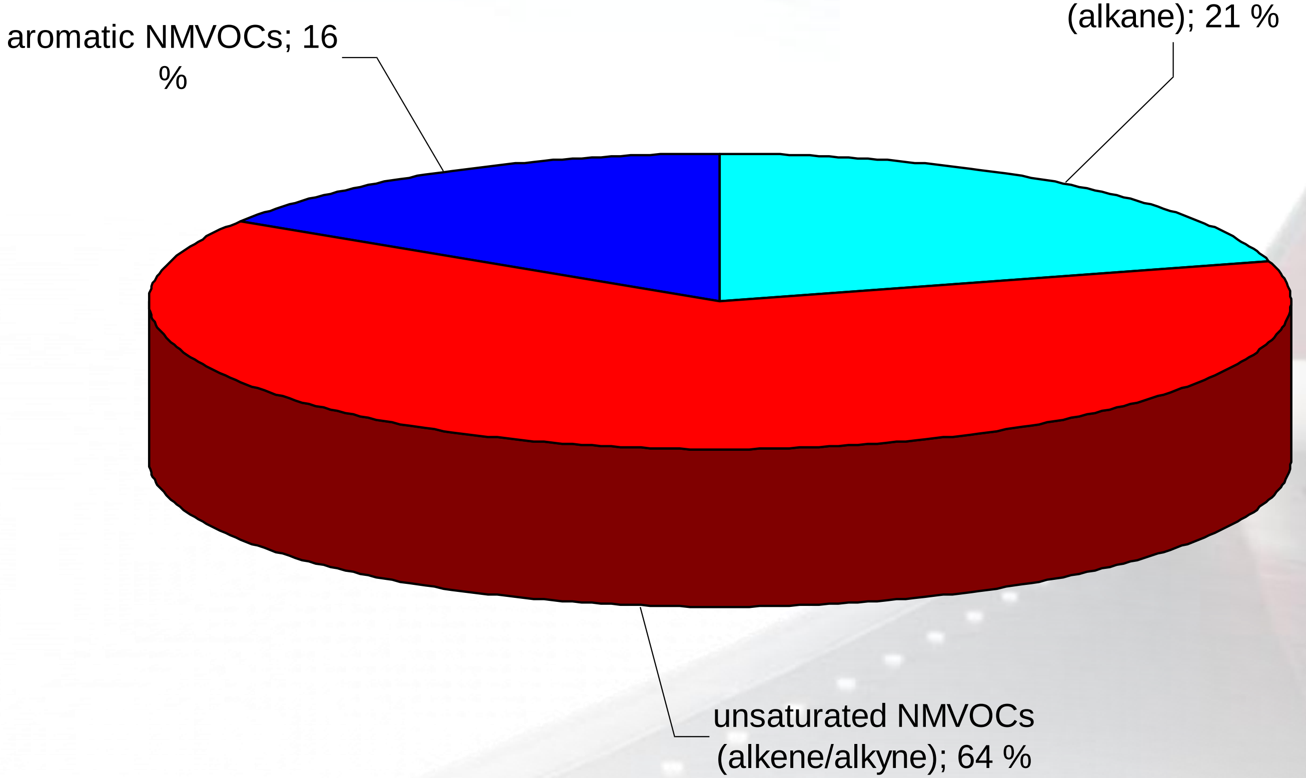

Percentage distribution of the R_{OH} (20 s^{-1}) for B+N fuel

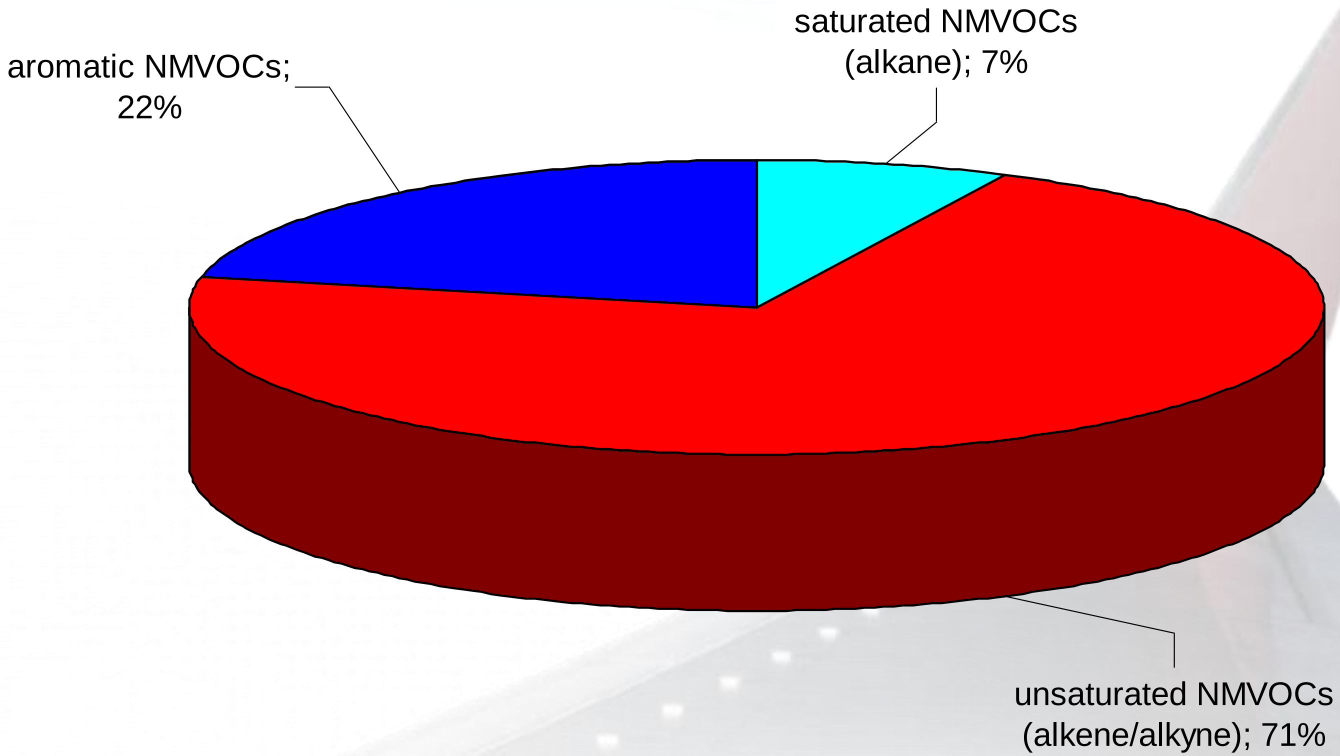

Percentage distribution of the R_{OH} (21 s^{-1}) for B+Ar fuel

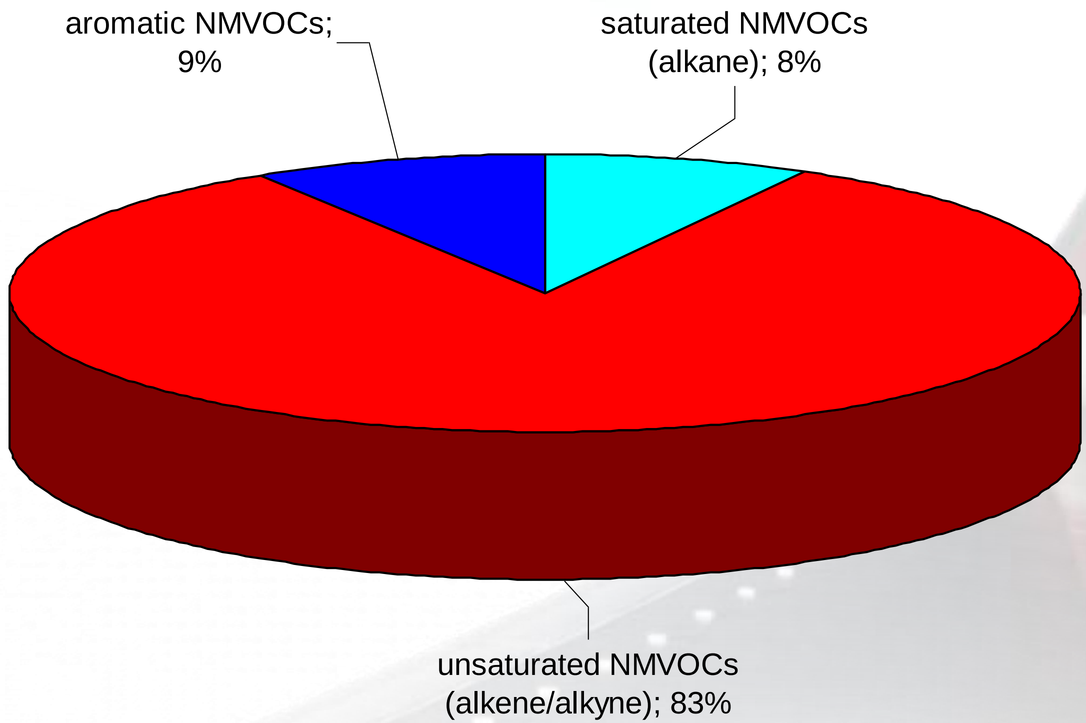

Percentage distribution of the R_{OH} ($12\ s^{-1}$) for B+Ar+N fuel

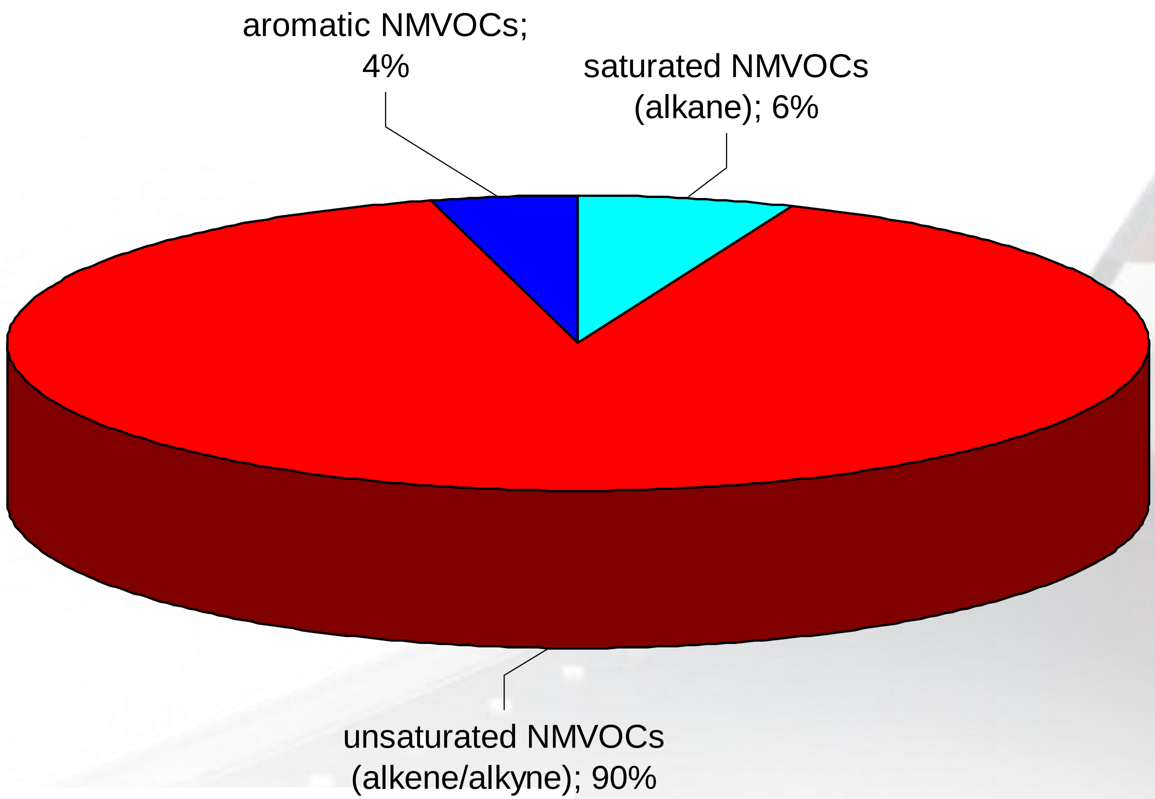

Percentage distribution of the R_{OH} (28 s^{-1}) for GTL fuel

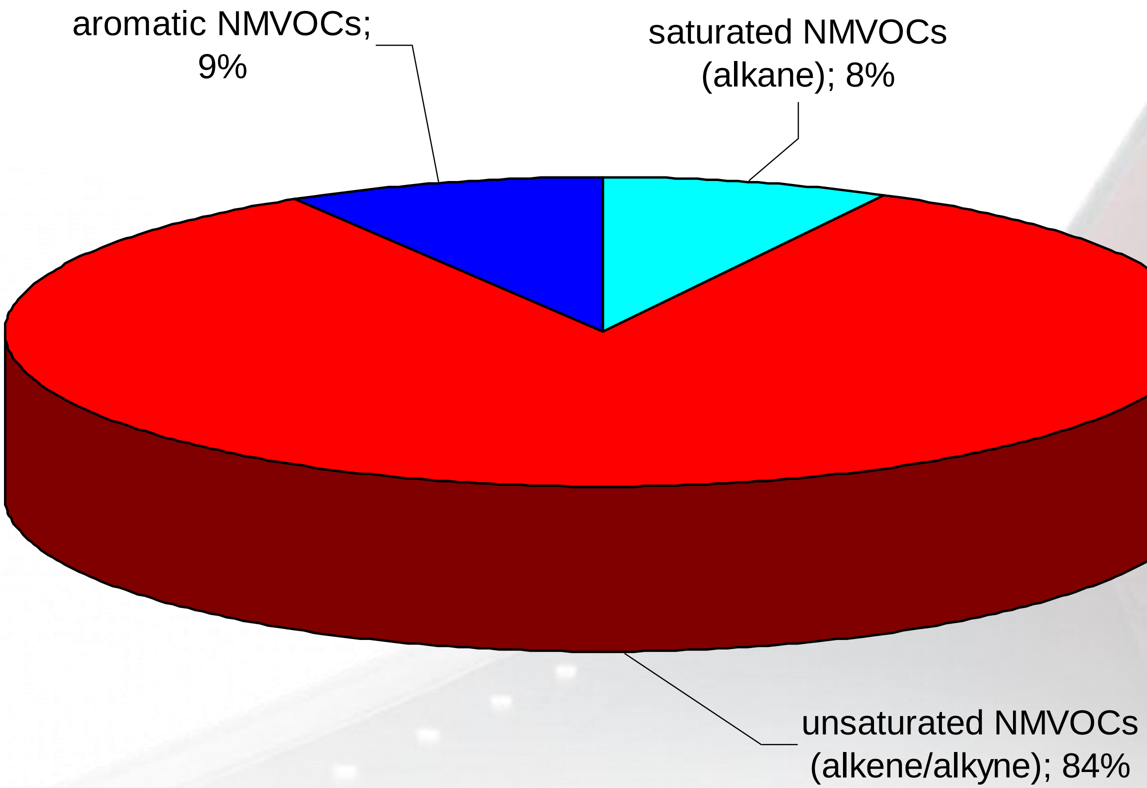

TNMVOC/NO_x (ppbC/ppbV) ratio for different fuels

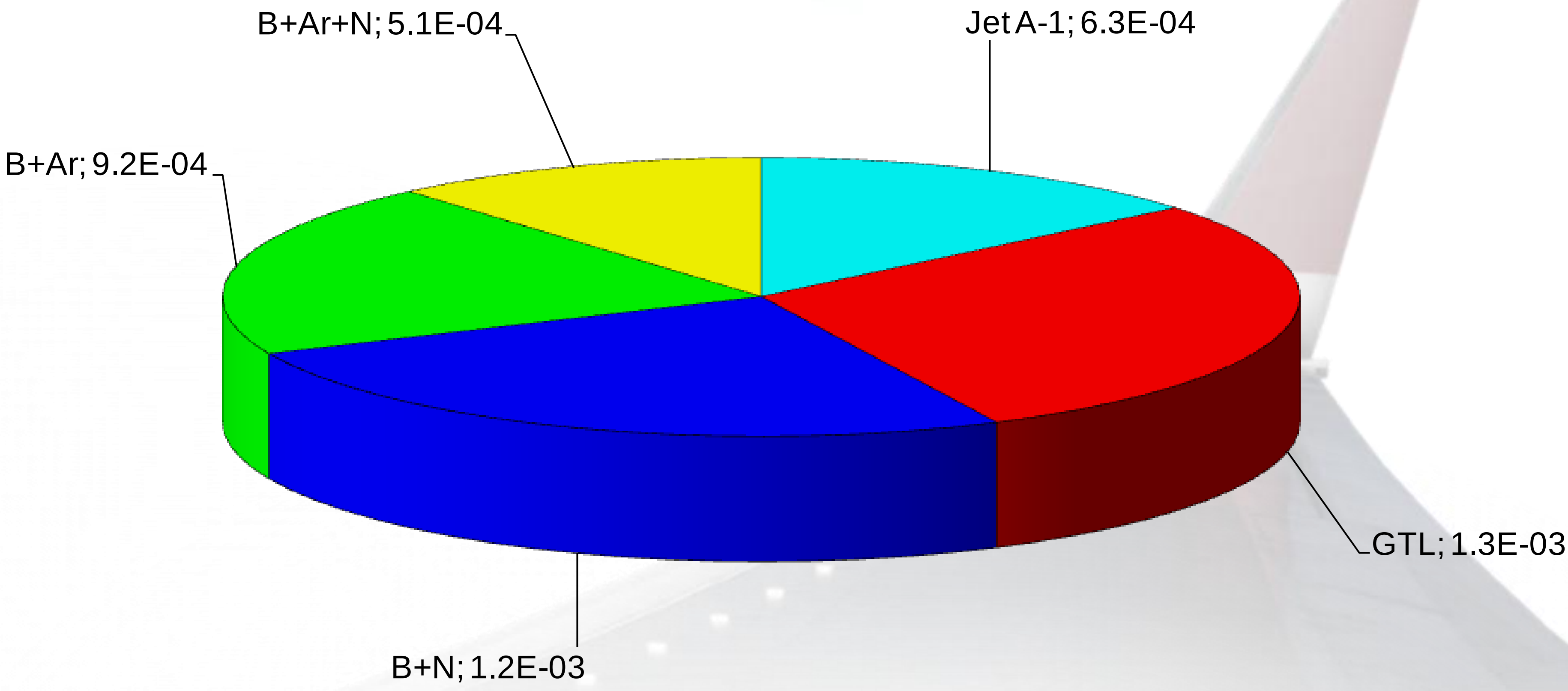

Conclusion

- Observed relative high NO_x but very low NMVOC emissions from the different test fuels
- Most apparent difference between the exhaust emissions from test fuels are the emitted NO_x levels which are lowest in GTL and highest in Jet A-1 and B+Ar+N.
- NMVOC split are different

Conclusion

- In comparison to the Jet A-1 fuel the GTL, B+Ar and B+N fuels have a higher OH-reactivity R_{OH} and TNMVOC/NO_x ratio, among which GTL fuel have the highest R_{OH} and TNMVOC/NO_x ratio.

- In contrast, the B+Ar+N fuel has a lower and the lowest OH-reactivity R_{OH} and TNMVOC/NO_x ratio of all fuels, respectively.

Conclusion

- Unsaturated NMVOCs (alkene/alkyne) have the highest contribution (64-90%) to the R_{OH} for all fuels. Contribution of saturated and aromatic NMVOCs to the R_{OH} variegated from 6-21% and 4-22%, respectively.

- Very low TNMVOC/NO_x ratios are found for all fuels, indicating a NMVOC sensitivity of the exhaust gas. Accordingly a reduction of ozone levels is achieved by reducing the NMVOC emissions.

Thanks for your attention

The atmospheric impact of alternative fuels in aviation

Simon Christie and Dave Raper
Manchester Metropolitan University, UK

ECATS International Association

Combustion products from a gas turbine

- Combustion of fuel in a gas turbine engine is a highly efficient process:

CO_2	72.0%
H_2O	27.6%
NO_x	0.336%
CO	0.047%
UHC	0.016%
SOx	0.020%
Soot	0.004%

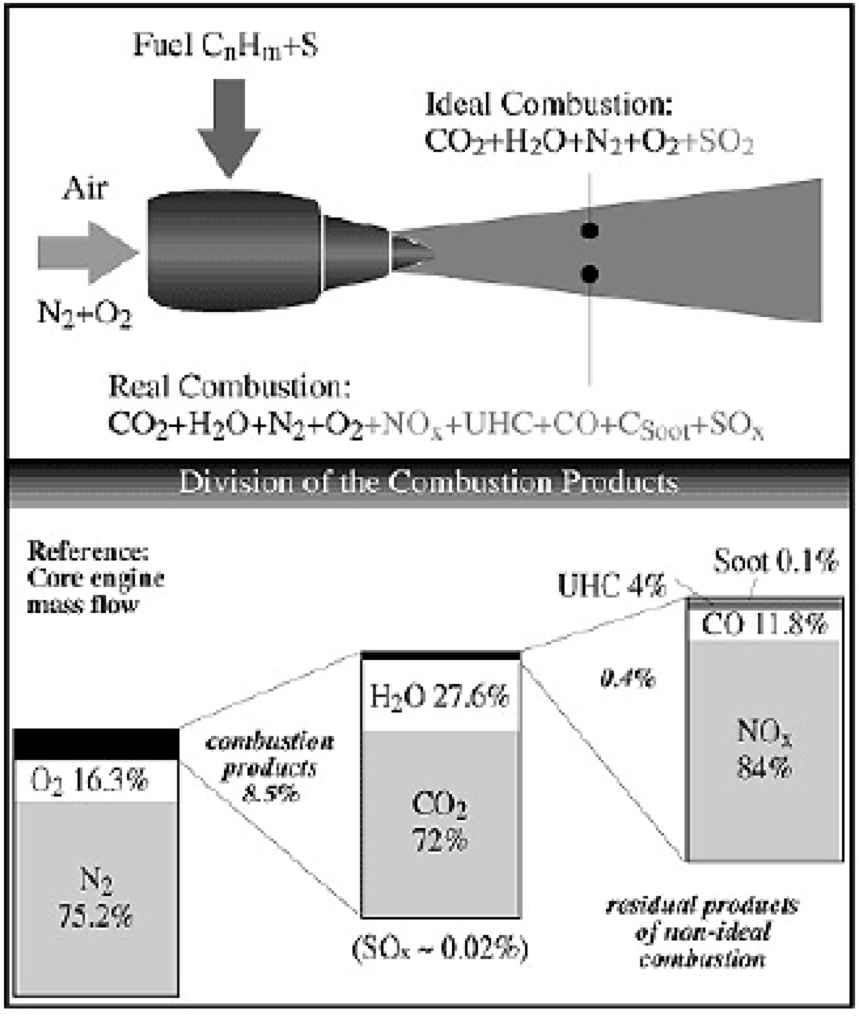

Aircraft emissions

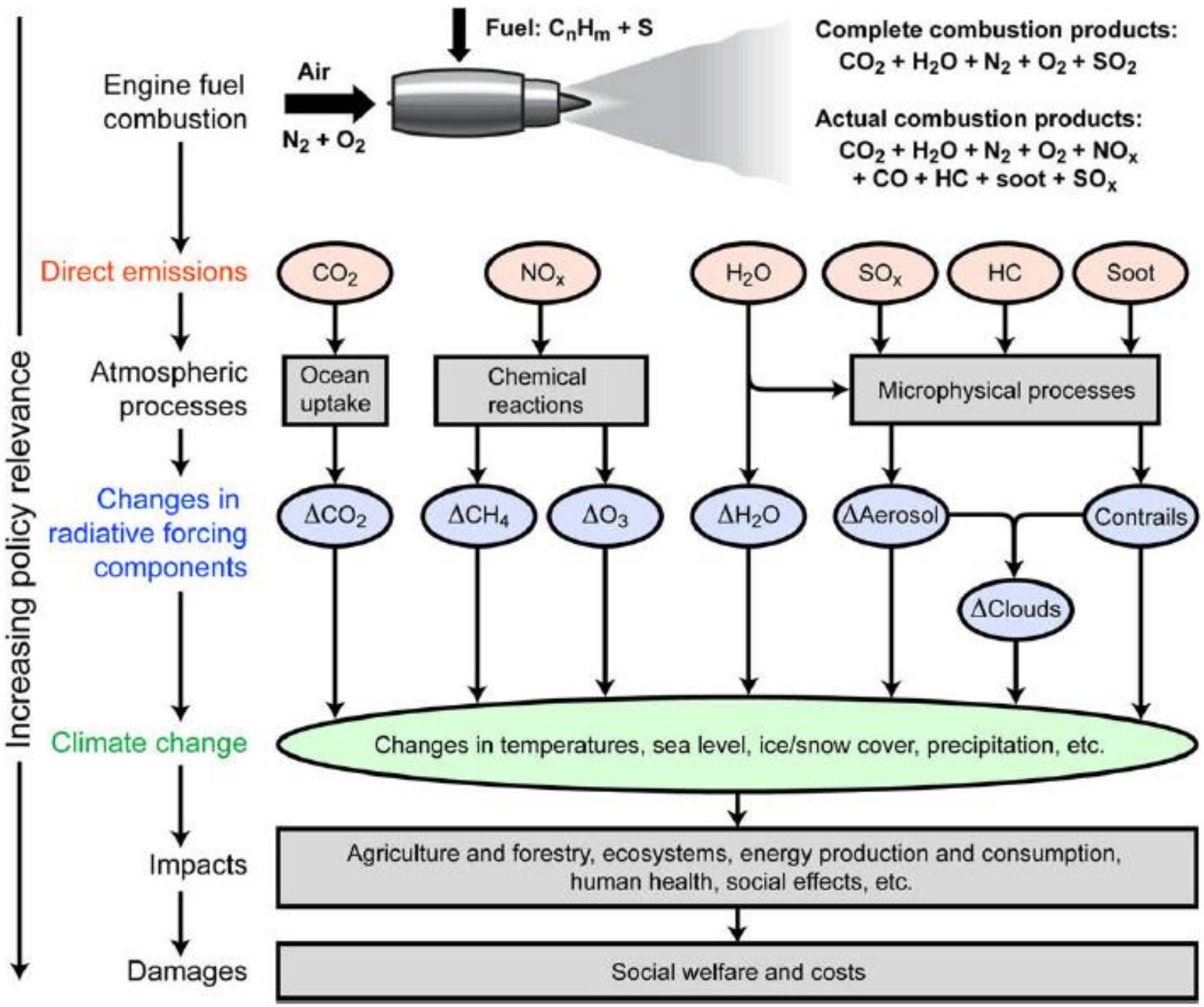

ECATS International Association

Aviation radiative forcing components

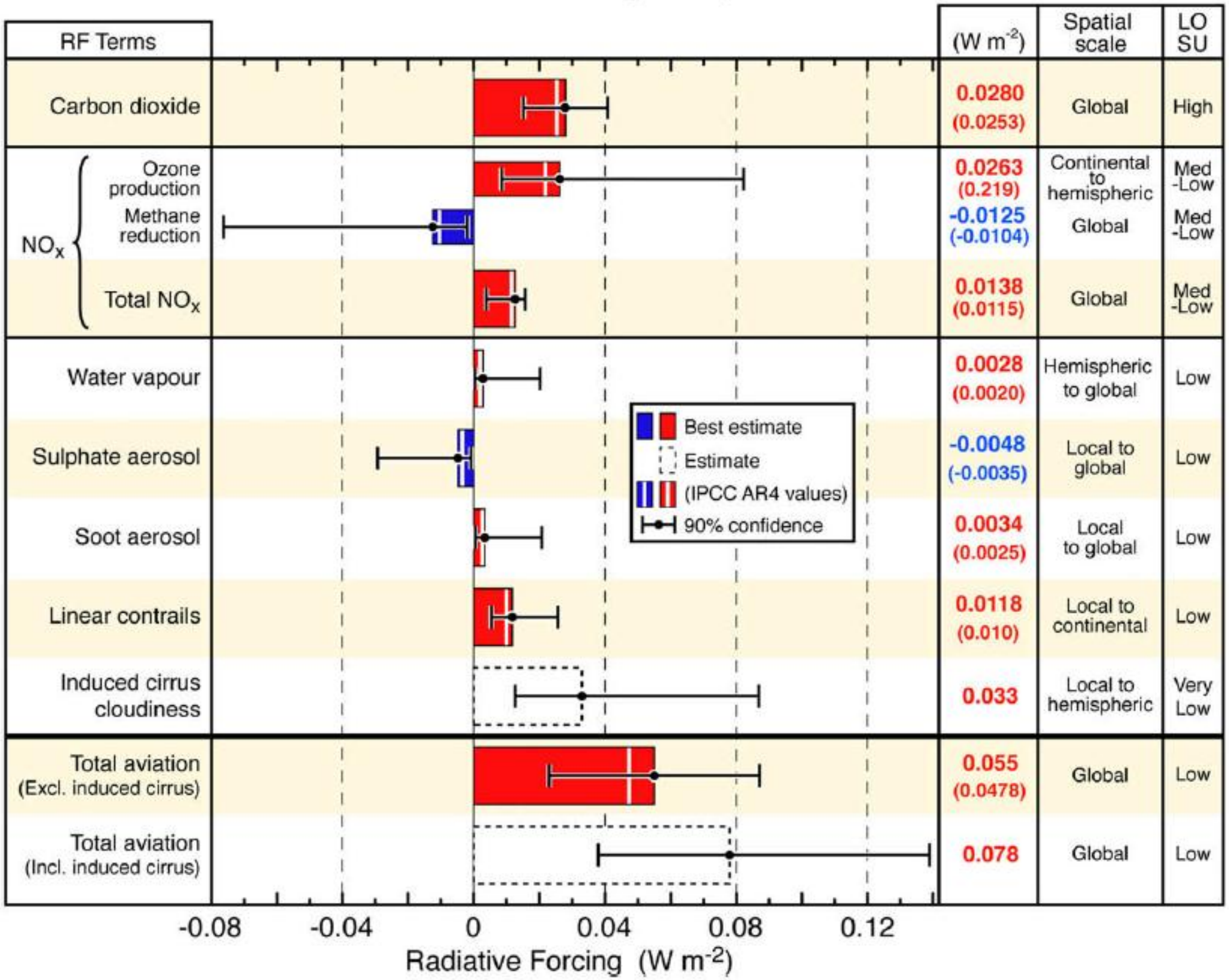

ECATS International Association

The atmospheric impact of alternative fuels

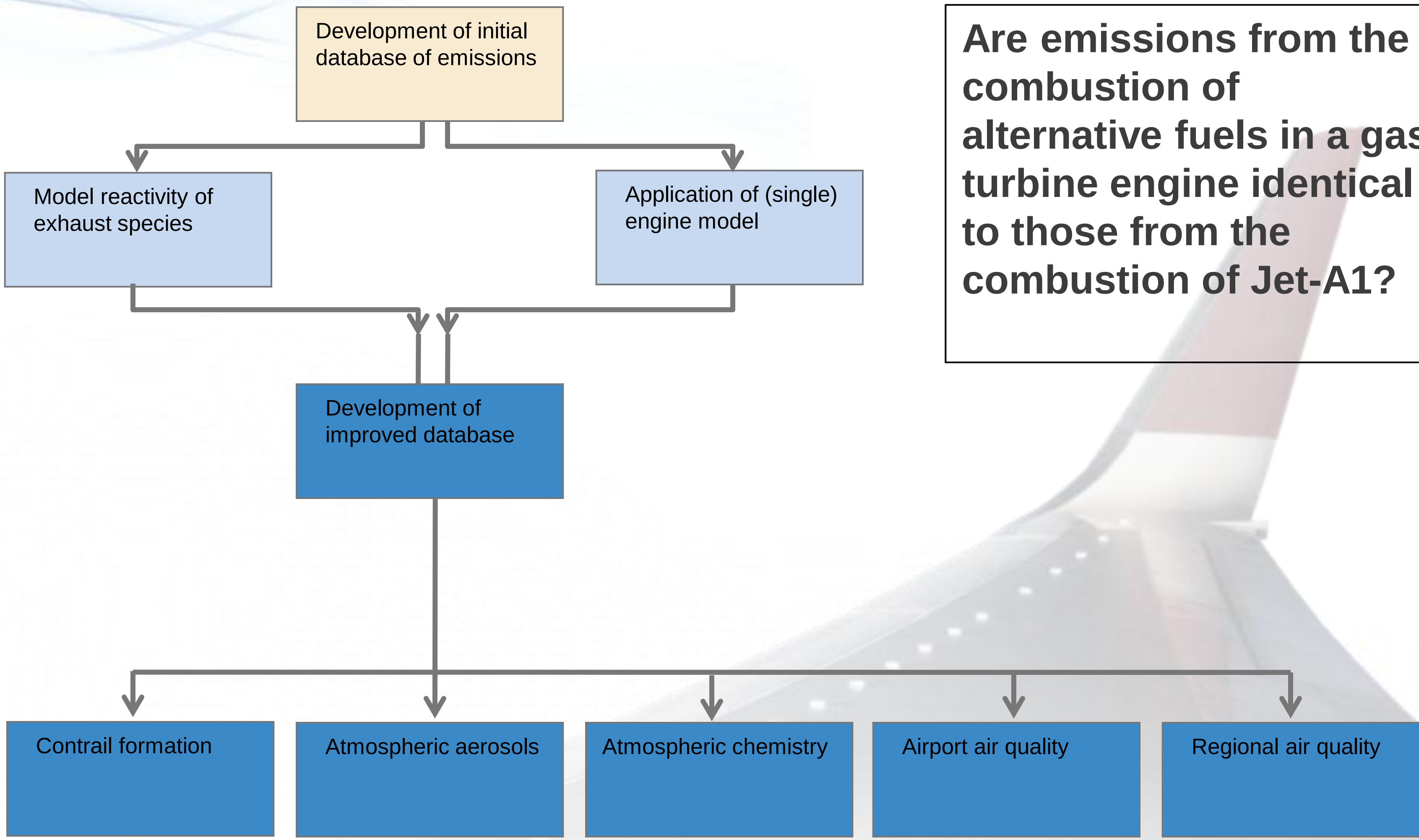

Are emissions from the combustion of alternative fuels in a gas turbine engine identical to those from the combustion of Jet-A1?

ECATS International Association

Database of combustion products from alternative fuels relative to Jet-A1

1. CO_2
2. H_2O
3. NO_x
4. CO
5. UHC
6. PM

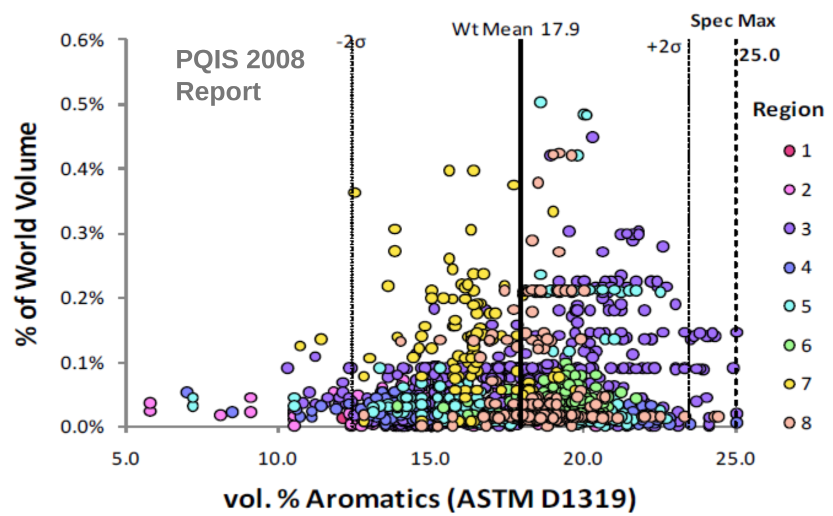

Caveats:

- Properties of Jet-A1 fuel are variable
- Properties of hardware are variable
- The inter-comparison of characterised emission data from multiple sources requires great care to deal with the uncertainties
- Characterised emission data from alternative fuels is sparse

PM from combustion of alternative fuel

- All alternative fuel tests have shown PM emissions to be reduced in both number based and mass based EI (due to lower aromatic and sulphur content)
- Reduced sulphur in fuel will also reduce secondary PM formation
- Most studies do not differentiate between volatile and non-volatile PM

Fuel	Operating Condition					
	Idle			Full Power		
	SN	EIn (#/kg fuel)	EIm (mg/kg fuel)	SN	EIn (#/kg fuel)	EIm (mg/kg fuel)
Jet A1	10.3 ± 0.6	(1.2 ± 0.4) $x10^{16}$	50.7 ± 14.1	27.3 ± 0.6	(1.9 ± 0.6) $x10^{16}$	188.3 ± 59.5
FSJF	2.6 ± 1.5	(0.7 ± 0.2) $x10^{16}$	12.9 ± 3.5	10.3 ± 1.2	(1.9 ± 0.7) $x10^{16}$	84.9 ± 24.3
gTL	0.7 ± 0.6	(0.02 ± 0.007) $x10^{16}$	7.5 ± 2.7	0.7 ± 0.6	(0.3 ± 0.1) $x10^{16}$	18.1 ± 5.1
50:50 gTL: Jet A1	2.0 ± 1.0	(0.5 ± 0.2) $x10^{16}$	10.5 ± 2.8	6.3 ± 0.6	(1.5 ± 0.5) $x10^{16}$	66.1 ± 18.9

PM and smoke

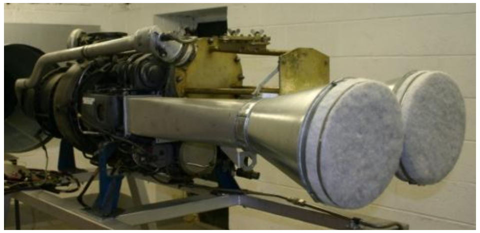

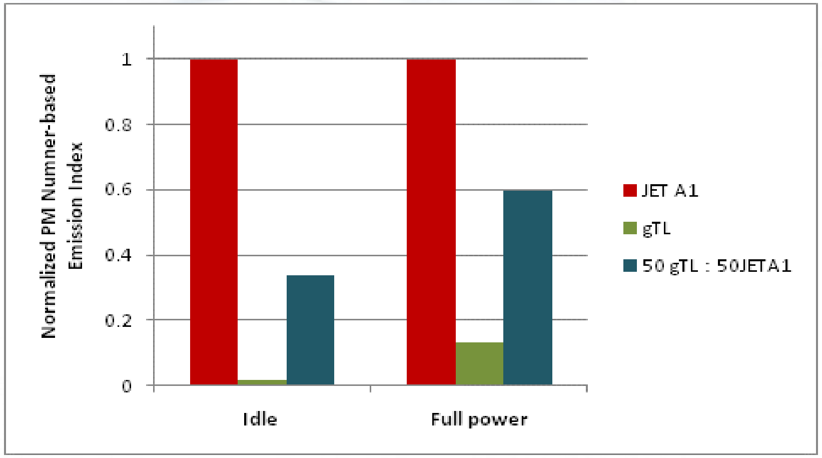

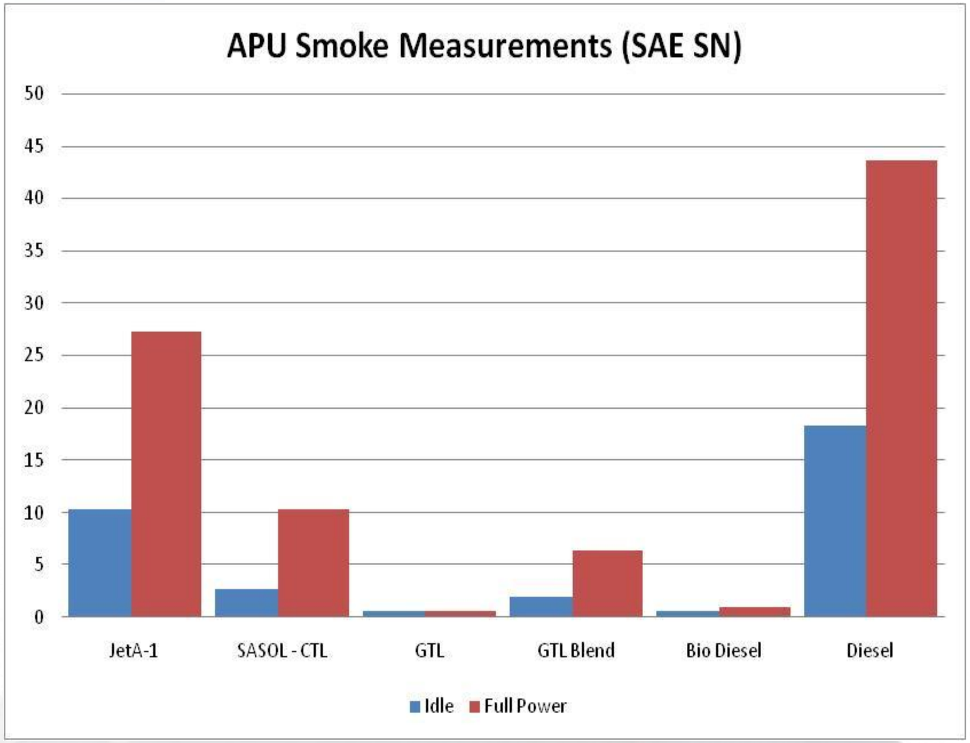

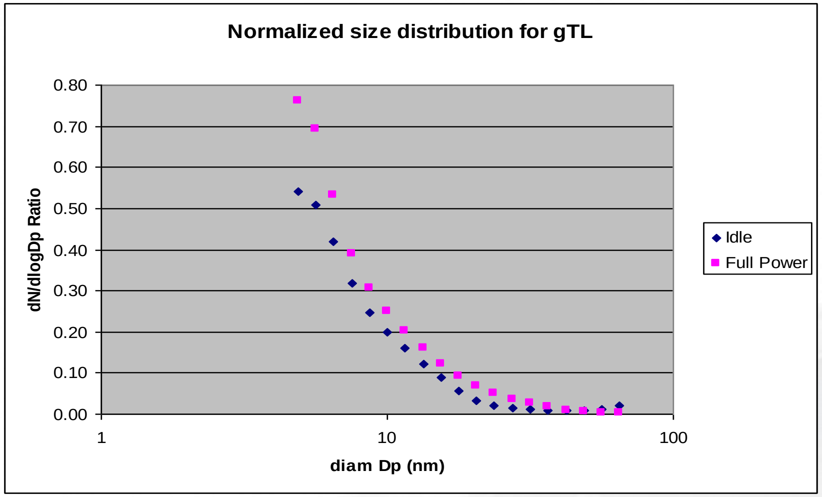

ECATS International Association

Speciation of VOC exhaust emitted species

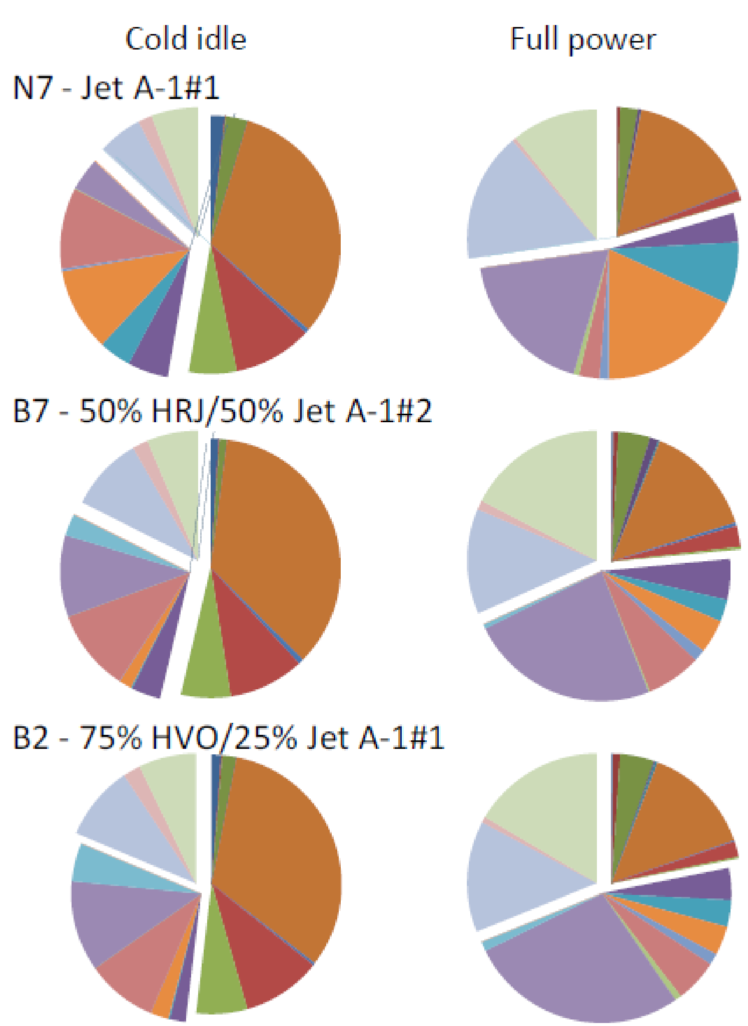

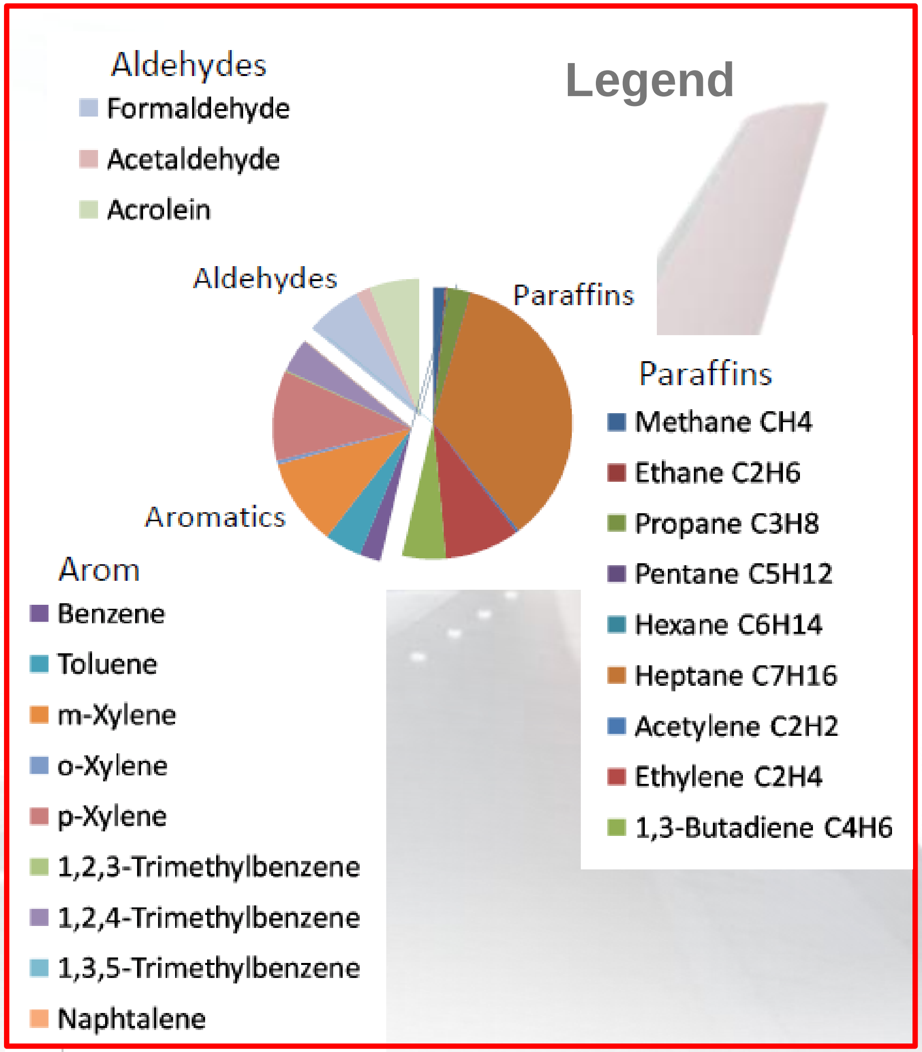

ECATS International Association

Emissions from combustion of alternative fuels in a gas turbine

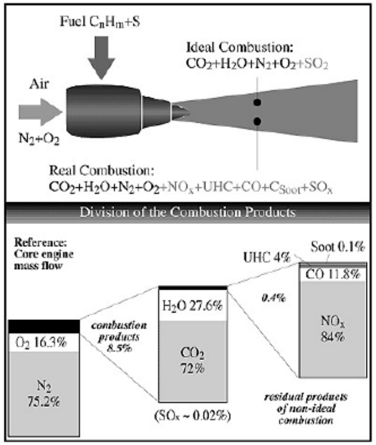

Species	**Jet A1**	**50:50 blend JetA1/SPK**
CO_2	72.00%	small reduction (1.5% reduction)
H_2O	27.60%	small increase (3.5% increase)
SO_x	0.02%	reduced by 50%
NO_x	0.336%	technology dependent (similar perhaps small reduction)
CO	0.047%	technology dependent (2 - 8% reduc. aromatic sensitive)
UHC	0.016%	technology dependent (2 - 8% reduc. aromatic sensitive)
PM	0.004%	reduced by > 40% (up to 90% at idle, aromatic sensitive)
Parameter		
Prop. Effic.		same
H:C ratio	1.90	2.02 (6% increase)
Energy	43MJ/Kg	44MJ/Kg (2% increase)
Fuel flow		~1% reduction (higher energy density)
PM EI(#/Kg)	$10^{14}/10^{15}$	$10^{12}/10^{13}$ (reduction up to x100)

ECATS International Association

Local and regional air quality

Atmospheric species:

LAQ at airports can constrain development (NOx and PM)

- Small reduction in NOx, CO, UHC
- Reduced primary PM (soot and SOx)
- Reduced precursors for secondary PM (NOx and SOx)

Improved air quality and health benefits (reduced emission inventories)

Atmospheric chemistry:

Meteorological, emissions, chemistry transport modelling

- EIs of CO, NOx, HC, aircraft movements and fuel flow rate
- HC speciation from Genetic Algorithm – Chemical Reactor Model
- VOC/NOx ratio lower for alternative fuels (VOC sensitive)

Improved air quality at larger scale

ECATS International Association

Contrail formation

Contrail formation is thermodynamically controlled

(Schmidt-Appleman criteria has no reference to PM)

However expect a change in contrail occurrence due to a change in the energy specific emission indices of water vapour (EI_{H2O} / Q)

- for kerosene = 0.029
- for alternative fuels ≥ 0.029 (0.030 – 0.032)

JetA1 → Alt fuels: H/C: 1.9→2.0 (~4% increase in EI_{H2O})

Q: 43→ 44 MJ/kg (~2% increase in Q)

Assuming equal overall propulsion efficiency, then contrails from alternative fuels may be produced at higher ambient temperatures and hence lower altitudes

The Schmidt-Appleman criterion for contrail formation: dependence on energy specific emission index of water vapour

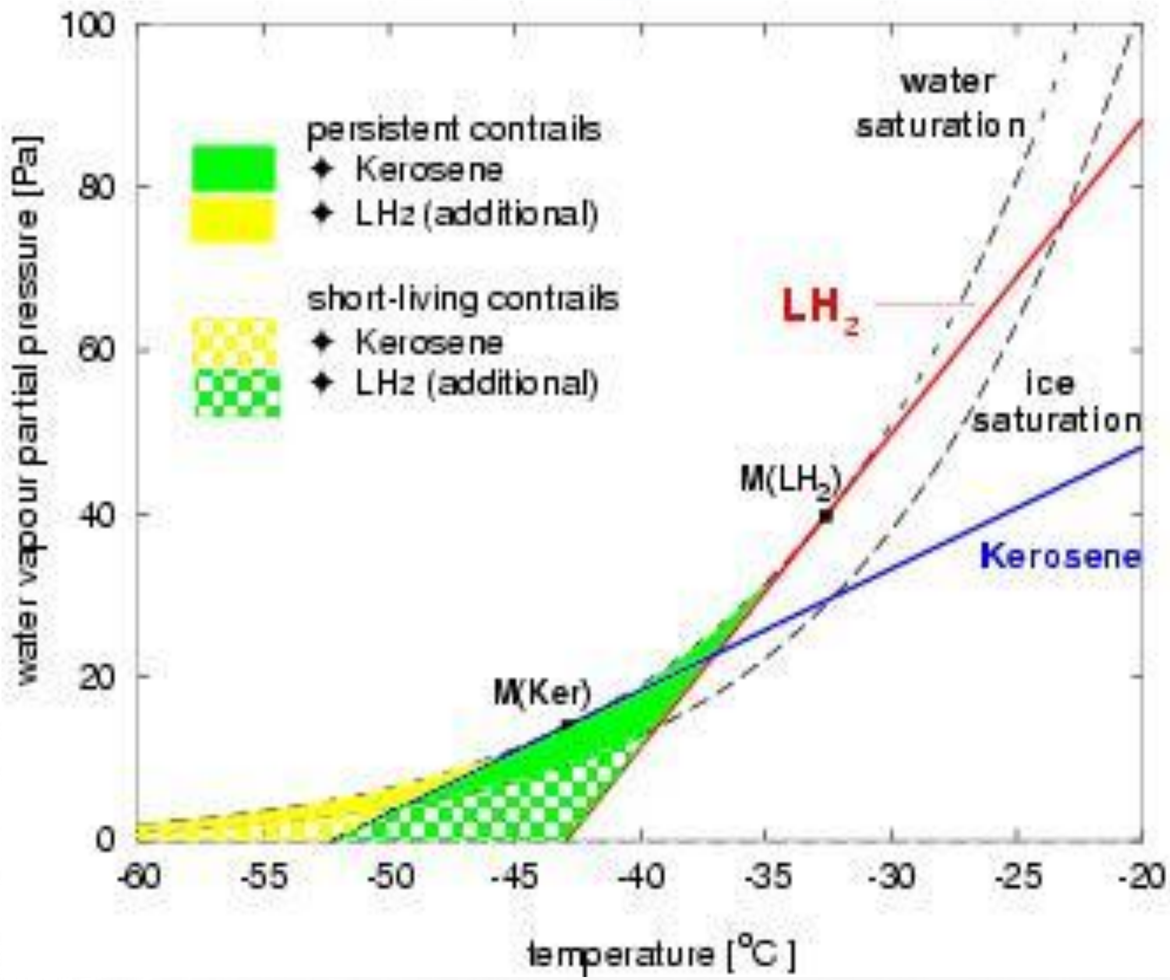

Case 1. Kerosene
Case 2. LH_2 (included to demonstrate dependence)

- EI_{H2O}/Q is 2.55 times larger for LH_2 than for Kerosene
- LH_2 contrails formed at higher Temperatures, i.e. at lower altitudes

ECATS International Association

Contrail characteristics

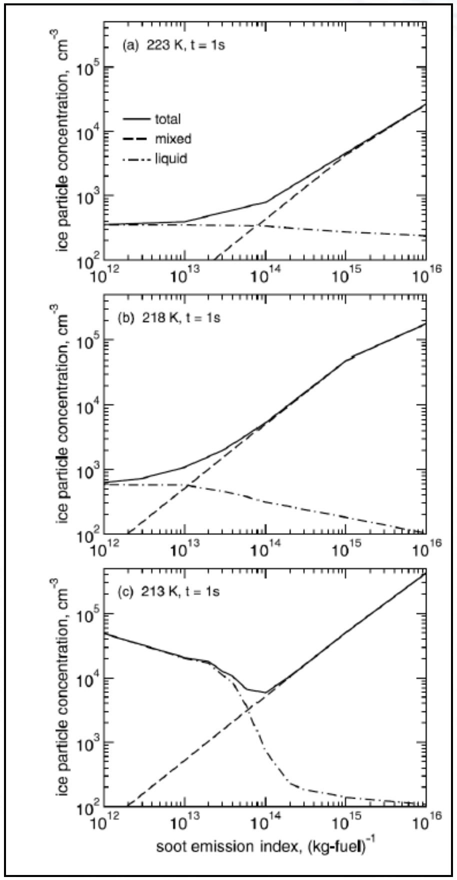

Karcher & Yu (2009)

- Reduced emissions of non-volatile particulate matter
  - EI_{soot} (kerosene) 10^{14} to 10^{15} particles/kg fuel
  - EI_{soot} (Alt. fuel) 10^{12} to 10^{13} particles/kg fuel
  - $EI_{volatile}$ (kerosene) >> $EI_{volatile}$ (Alt. Fuel)
- Initial contrail ice crystal formation dependent upon soot number based emission index (for certain range) and ambient temperature
- At temperatures below S-A threshold every soot particle produces an ice crystal
- EI_{soot} reductions below 10^{13} have little effect
- At temps 10K below S-A threshold can get rise in number of ice crystals as nucleates on volatile PM

Contrail properties

- Alternative fuels may result in more contrails and these may occur at lower altitudes (higher temperatures)
- These contrails may contain a reduced number of larger ice crystals making them optically thinner (a soot reduction by factor 5 will half initial optical thickness)
- Contrails containing a reduced number of larger ice crystals will have a reduced lifetime as the crystals will fall out more rapidly

It is conceivable (but not yet proven) that aerosol emitted from jet engines can also lead to cirrus formation at a later time, even though no contrail was formed initially.

ECATS International Association

Conclusions

- Alternative fuels offer local and regional air quality benefits
- Mapping the relation between fuel parameters and the speciated HC emissions is required to better model impacts (chemistry & aerosols)
- Many new fuels and fuel process pathways are under development: physical, chemical, biological (although FT and HEFA dominate)
- Mapping the relation between fuel parameters and emissions is allowing the design of fuels with improved environmental credentials
- Potential for tailor made fuels
- Validation of contrail formation and characteristics needs to be pursued
- Developing a wide-ranging and integrated assessment of how combustion products impact atmospheric chemistry


Thank you!

Assessment of spray characteristics of alternative aviation fuel blends

Andreas P. Vouros,
Alexandros P. Vouros and
Thrassos Panidis

Lab of Applied Thermodynamics
University of Patras

ECATS International Association

Outline

- Objectives
- Alternative Fuels Family - What is an xTL alternative fuel?
- Focus of UP-LAT Experiment
- Phase Doppler Anemometry (PDA)
- Description of tested fuels
- Experimental Results
- Conclusions
- References
- Acknowledgments

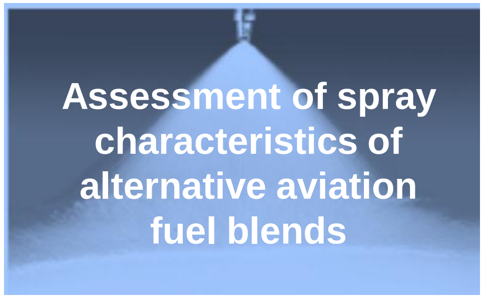

Objectives

- The experimental assessment of alternative fuel blends spray characteristics in relation to the standard used JET A-1
- The contribution of experimental data on jet fuel atomization at high injection pressures (5 – 11 bar)
- The identification of the (drop-in) fuel physical properties influencing the atomization process
- The monitoring of the droplets characteristics (velocity field and droplet size) using Phase Doppler Anemometry

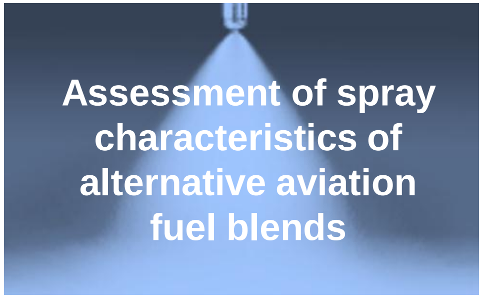

Alternative fuel requirements

- Since aircrafts carry their fuel, new fuels have to have high energy density
- Since they are flying at high altitudes fuel must remain liquid at -50 °C.
- Since they travel long distances fuels must be compatible throughout the world.
- Since aircrafts remain many years in service new fuels should be compatible with current fleet.
- Ideal option a fuel similar to current JET-A1 fuel (drop-in) with lower CO2 budget.

Alternative Fuels Family
What is an xTL alternative fuel?

“x" equals "anything"

The anything-to-liquid (xTL) process can turn virtually any carbon-containing material (x) into a clean, odourless and colourless liquid. Whether it’s natural gas, biomass or coal that goes in, we can get an identical liquid out.

The xTL- family

- Gas to liquids (GTL),
- Biomass to liquids (BTL) and
- Coal to liquids (CTL)

created through the same 3-step process (Fisher – Tropsch)
and producing identical results whatever the source material.

Fisher – Tropsch (FT) synthesis provides

- Fuel product virtually free from the sulfur-, oxygen- and (occasionally) nitrogen-containing compounds found in conventional jet fuel.
- FT fuel emits fewer particulates than conventional jet fuel. It is a sulfur-free fuel leading to complete elimination of SOx emissions.
- There are no sulfur dioxide (SO_2) or sulfuric acid (H_2SO_4) aerosol emissions, which also form contrails.
- The synthetic FT fuels are very similar in performance to conventional jet fuel but show a reduction in pollutants such as SOx, NOx, particulate matter, and hydrocarbon emissions.
- The disadvantages of the low aromatics content (such as low fuel density or elastomer shrinkage) disappear if the FT synthetic fuel is blended with conventional jet fuel, although the advantage of lower emissions is reduced.

Jet A-1 Fuel Composition

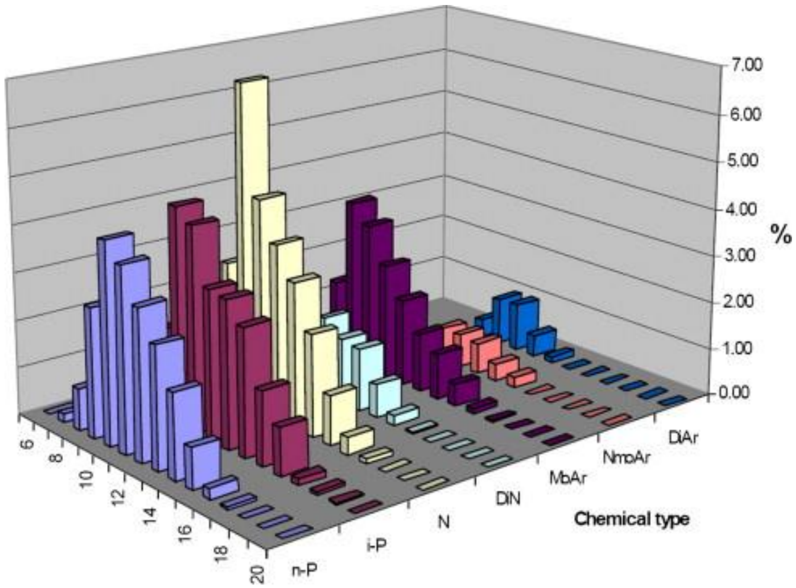

Preparation description :

- Complex mixture of hydrocarbons consisting of paraffins, cycloparaffins, aromatic and olefinic hydrocarbons with carbon numbers predominantly in the C7 to C16 range.
- May also contain several additives at <0.1% v/v each

Chemical Identity:

- Kerosene (petroleum) hydrodesulphurised, kerosene

Material Safety Data Sheet (MSDS), Effective 19.01.2009, Regulation 1907/2006/EC

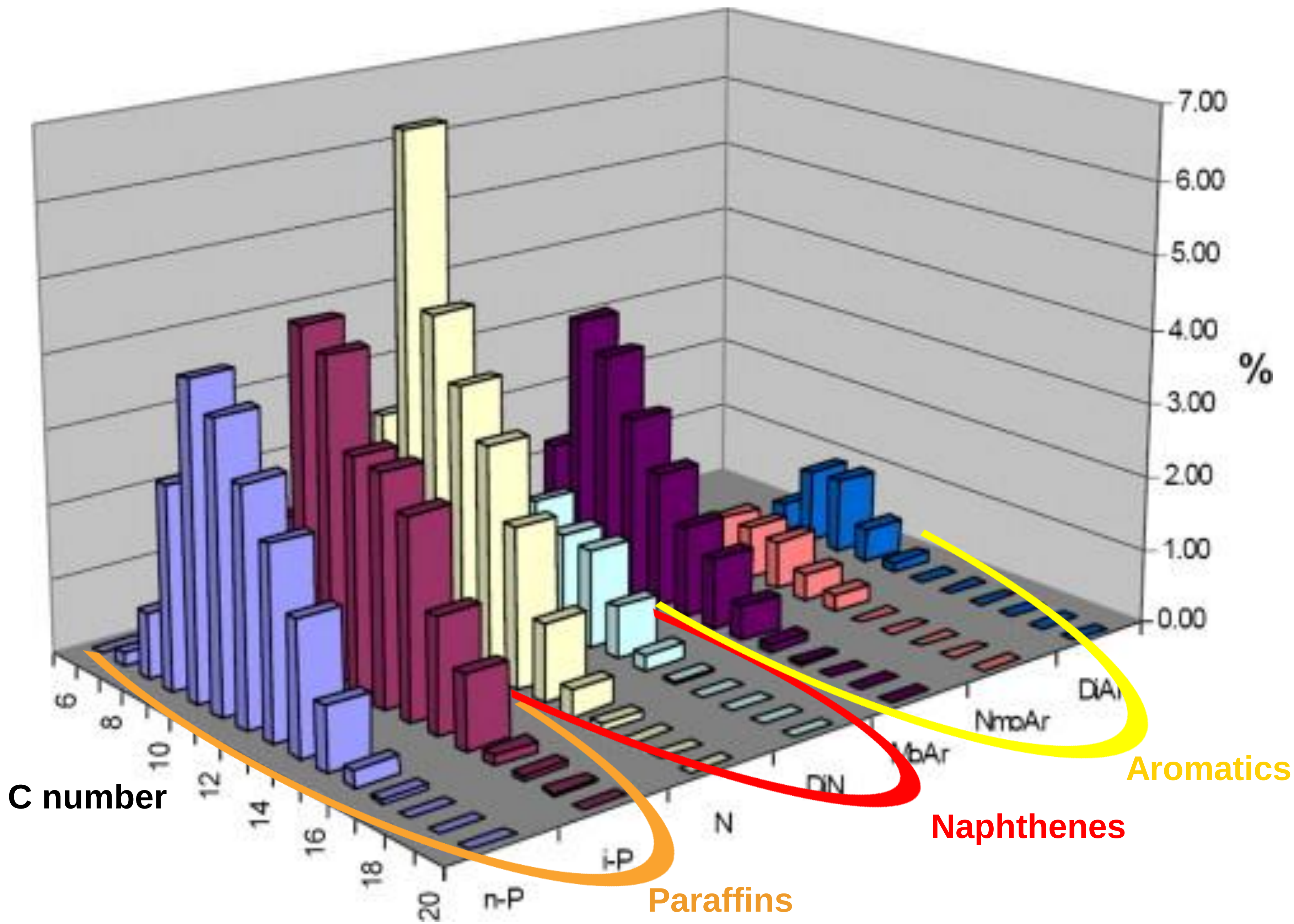
7.00
6.00
5.00
4.00
3.00
2.00
1.00
0.00
%
6
8
10
12
14
16
18
20
C number
n-P
i-P
N
DiN
MbAr
NmoAr
DiAr
Paraffins
Naphthenes
Aromatics

Generic composition of Shell GTL blends

Assessment of spray characteristics of alternative aviation fuel blends

Blend	Compound content	Molecular Formulae
P (GTL)	*Paraffins (99%)*	$C_{10.14}H_{22.25}$
P-Ar	*Paraffins (80%) + Aromatics (20%)*	$C_{10.08}H_{20.35}$
P-N	*Paraffins (60%) + Naphthenes (40%)*	$C_{12.18}H_{25.28}$
P-N-Ar	*Paraffins (50%) + Naphthenes (30%) + Aromatics (20%)*	$C_{11.48}H_{22.18}$

Properties of Candidate Alternative Fuels

Liquid Fuel Properties → **Fuel Spray Process**

Liquid Fuel properties affecting atomization
- density
- viscosity
- surface tension
- blending ratio

Fuel Spray Process
- atomization
- evaporation
- mixing

Fuel Spray Process

↓

fuel / air
mixture formation
combustion process

↓

Engine Performance
/ Emissions

Physical Properties of the test blends

Blend Code	Fuel Density (15 ^{o}C) ρ (g/ml)	Kinematic Viscosity ν (cSt)	$v/v_{Jet\ A\text{-}1}$ at same temperature	Surface Tension (22 ^{o}C) σ (10^{-3} kg/s^2)
JET A-1	*0.8210*	*0.99 at 24.95 ^{o}C*	*100.0%*	*29.84 ± 0.06*
P (GTL)	*0.7376*	*1.01 at 25.02 ^{o}C*	*102.2%*	*26.28 ± 0.05*
P – Ar	*0.7687*	*0.98 at 25.04 ^{o}C*	*99.2%*	*27.43 ± 0.04*
P – N	*0.7879*	*1.13 at 20.61 ^{o}C*	*107.2%*	*28.87 ± 0.05*
P – N – Ar	*0.8054*	*1.15 at 22.75 ^{o}C*	*112.5%*	*29.43 ± 0.02*

Characteristic non-dimensional numbers

- Reynolds number $$Re = \frac{\rho_l u D}{\mu_l}$$
- Weber number $$We = \frac{\rho_l u^2 D}{\sigma}$$
- Onhesorge number $$Oh = \frac{\sqrt{We}}{Re} = \frac{\mu_l}{\sqrt{\sigma \rho_L D}}$$

Spray formation regimes in relation to Re and Oh

Assessment of spray characteristics of alternative aviation fuel blends

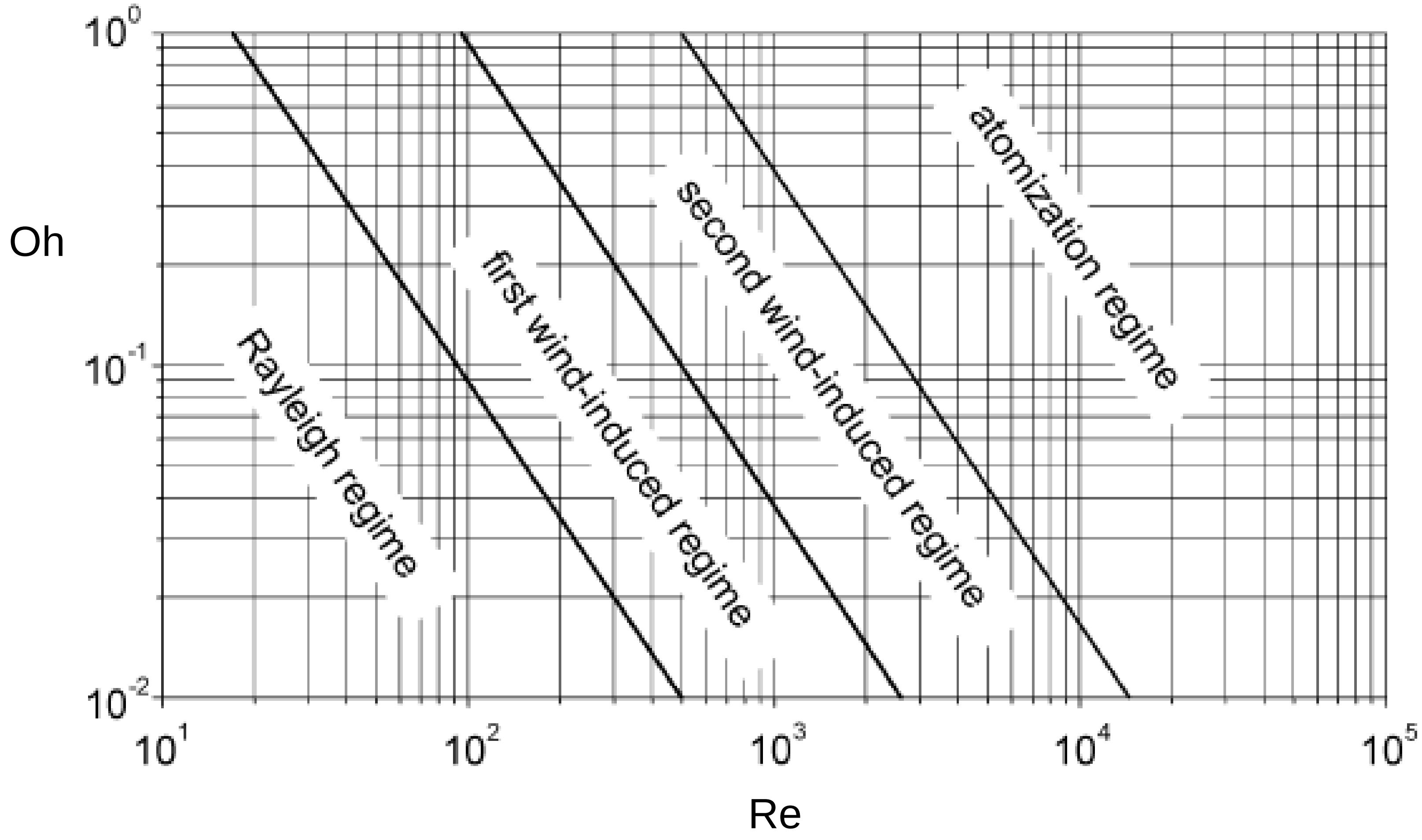

Experimental approach

- Parametric study to investigate alternative fuels atomization characteristics
- Generic configuration independent of specific application
- Generic, isothermal tests at room conditions, designed to facilitate optical diagnostics for the comparison of sprays produced by the different blends.
- Not expected to provide information on the operational characteristics in actual applications.

Liquid Fuel Spray Parameters

- nozzle type
- nozzle discharge coefficient
- spray shape
- cone angle
- initial velocity profile
- injection pressure
- jet axial momentum
- droplet size distribution
- number density
- gas/liquid velocity profiles
- recirculation zones
- evaporation time

Assessment of spray characteristics of alternative aviation fuel blends

Spray Performance

Characteristics	Increase in Operating Pressure	Increase in Specific Gravity	Increase in Viscosity	Increase in Fluid Temperature	Increase in Surface Tension
Pattern Quality	*Improves*	*Negligible*	*Deteriorates*	*Improves*	*Negligible*
Drop Size	*Decreases*	*Negligible*	*Increases*	*Decreases*	*Increases*
Spray Angle	*Increases then decreases*	*Negligible*	*Decreases*	*Increases*	*Decreases*
Capacity	*Increases*	*Decreases*	*Full/hollow cone increases Flat – decreases*	*Depends on fluid and nozzle*	*No effect*
Impact	*Increases*	*Negligible*	*Decreases*	*Increases*	*Negligible*
Velocity	*Increases*	*Decreases*	*Decreases*	*Increases*	*Negligible*
Wear	*Increases*	*Negligible*	*Decreases*	*Depends on fluid and nozzle*	*No effect*

Adapted from Spraying Systems Co Catalog

Parameters' selection for spray experiment

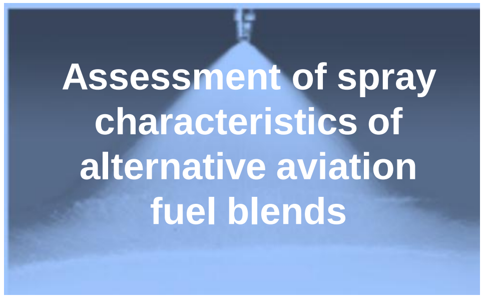

- Nozzle type (full cone)
- Capacity (small)
- Spray angle (<30°)
- Injection pressure (1.5 - 11 bar)

Selected nozzle Type - **full-cone 1/4 D1-35** *Spraying Systems Co*

Nozzle type	Orifice Diam. (mm)	Capacity (liters per minute) at stated pressure in bar										Spray Angle (°) at stated pressure in bar		
		0.7	1.5	2	3	4	6	7	10	15	20	1.5	3	6
1/4 D1-35	.79	*.30*	*.39*	*.48*	*.58*	*.65*	*.78*	*.90*	*.97*	*1.2*	*1.3*	*19*	*23*	*26*

Experimental set up & PDA instrumentation

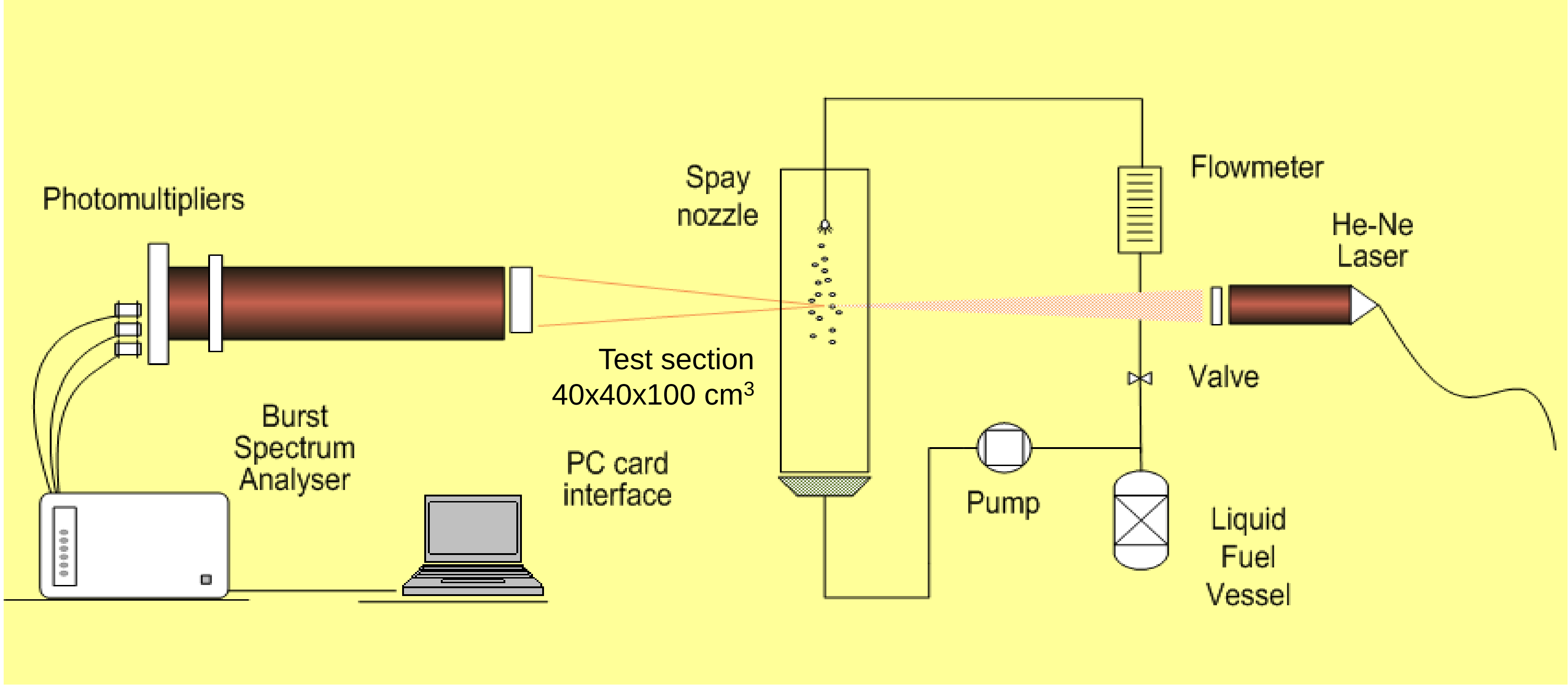

Principle of PDA

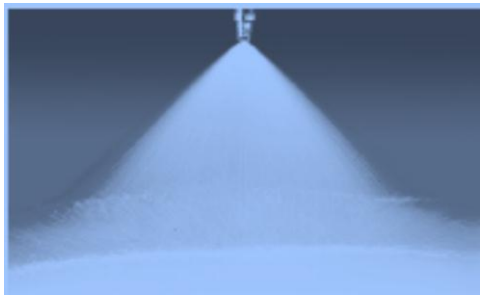

- A particle scatters light from two incident laser beams
- Both scattered waves interfere in space and create a beat signal with a frequency which is proportional to the velocity of the particle
- Two detectors receive this signal with different phases
- The phase shift between these two signals is proportional to the diameter of the particle

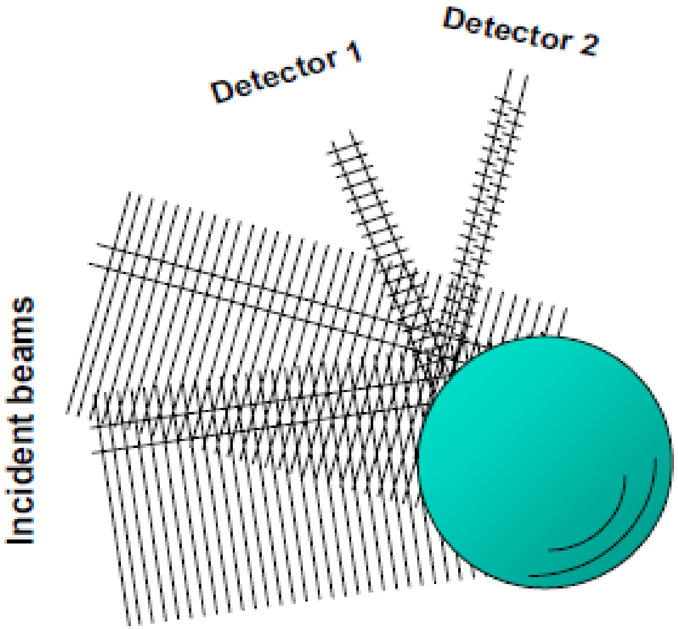

Scattering Modes of Ray Transmission

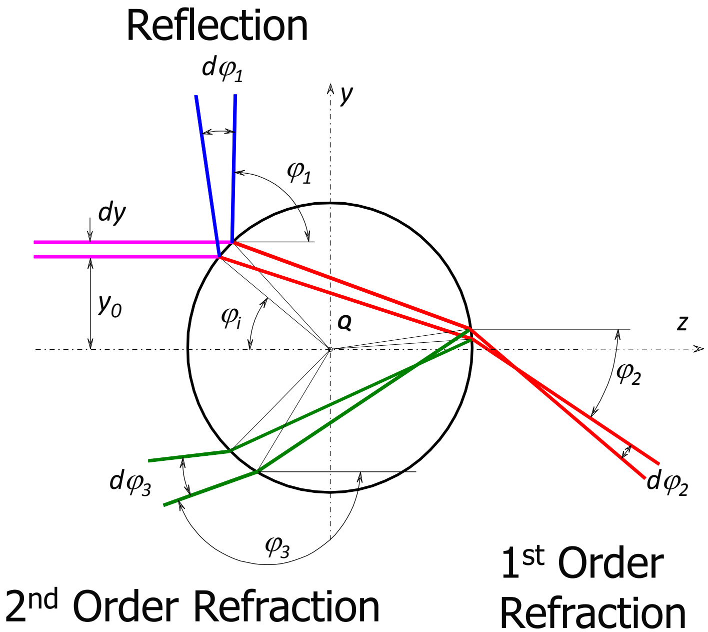

Scattering Light Polar Chart

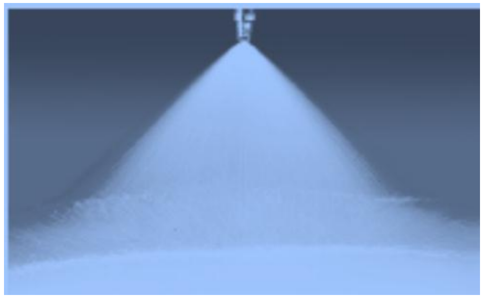

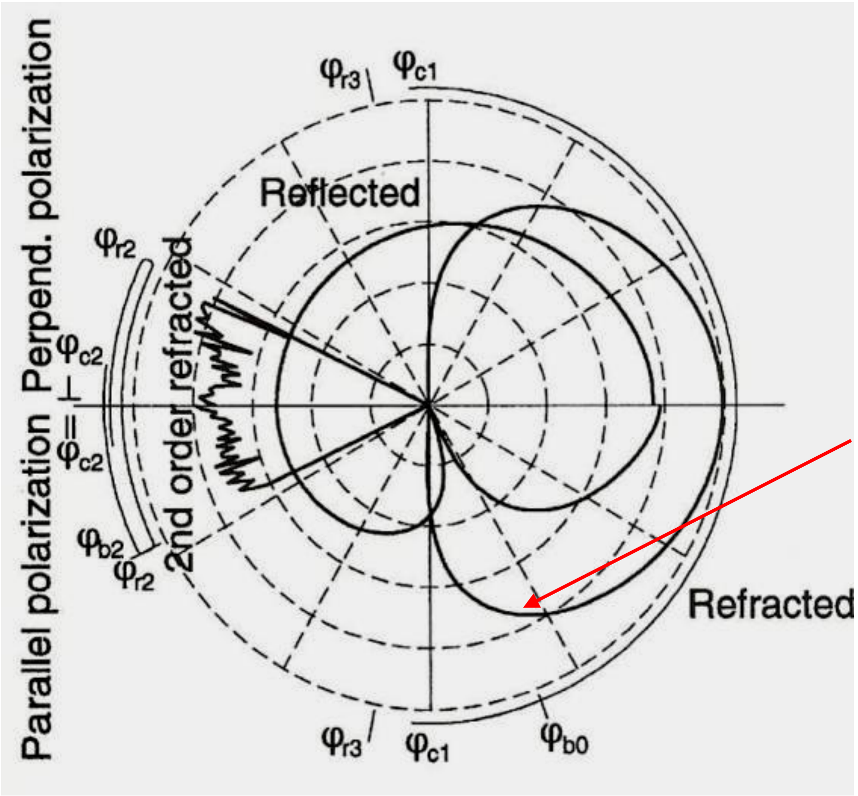

UP/LAT experiments

Characteristic scattering modes
for droplet of $n \approx 1.46$

Phase size relation in PDA

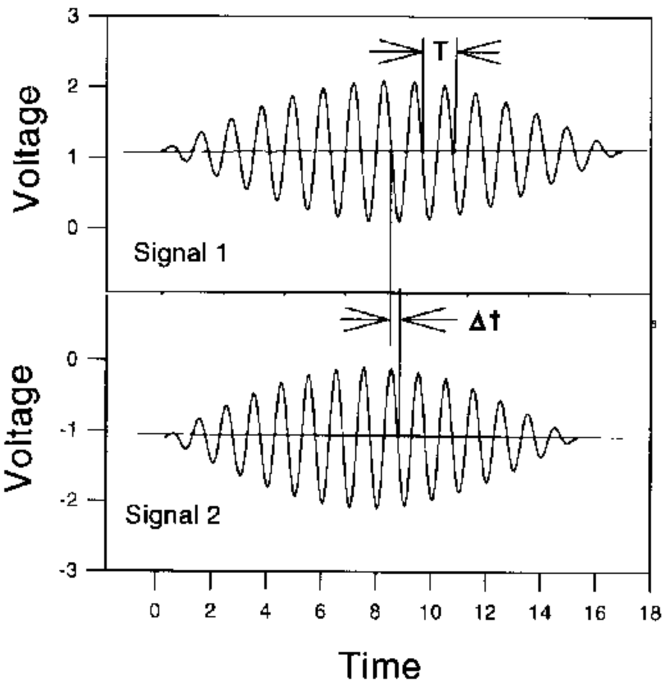

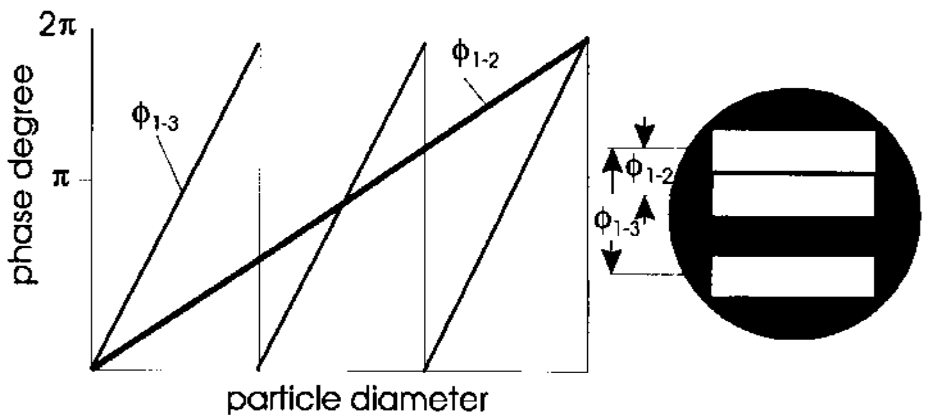

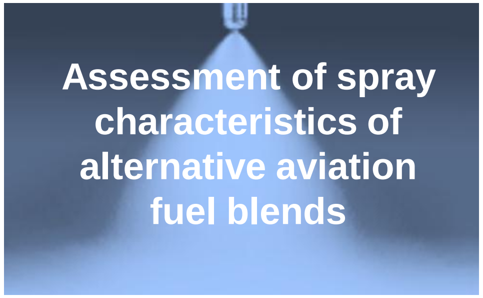

Phase Doppler Anemometry

Non intrusive - Optical Technique

Provides **Local, Instantaneous** or **Time Averaged Measurements** of

- Fluid or Particle **Velocities**
- Particle **Size** Distribution
- **Correlation** of Size and Velocity
- Particle **Concentration** and **Mass Flux**
- **Refractive Index** of Particle

Suitable for **Dispersed** Two Phase Flows with **Spherical** Particles

Examples:

- Gas Droplet Flows (e.g. Sprays)
- Bubbly Flows (only for Spherical Bubbles usually less than 1 mm)
- Gas-Solid Flows (e.g. Spherical Beads)

PDA set up

Laser source	*HeNe*
Wavelength	*632.8 nm*
Laser source power	*20 mW*
Transmitting Optics	
Focal length	*250 mm*
Frequency shift	*40 MHz*
Receiving Optics	*PDA 57X10*
Focal length	*310 mm*
Receiving Angle	*67^o to forward*

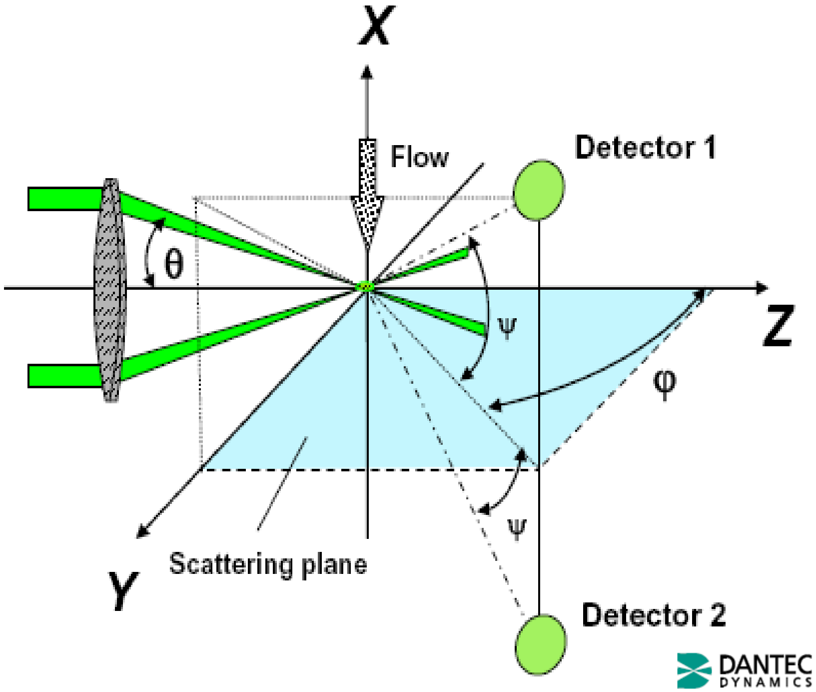

Fuel Atomization and Spray Testing Protocol

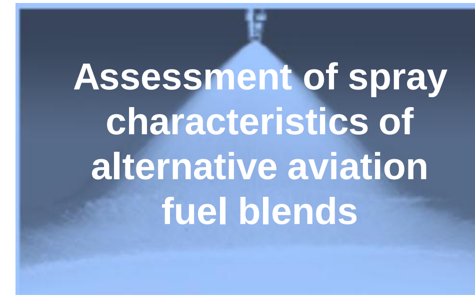

Experimental test cases for each fuel

Test Case	Working pressure (bar)		Experimental measurements
1	Low	1.5	a. *Jet – spray Axial evolution (velocity distribution),* b. *Radial profiles (velocity and droplet size at z/d = 73.4, 124.1)*
2		3.0	
3	High	5.0	a. *Radial profiles (velocity and droplet size at z/d = 73.4, 124.1, 174.7, 225.3)*
4		7.0	
5		9.0	
6		11.0	

Low Pressure Results
Axial mean velocity

Assessment of spray characteristics of alternative aviation fuel blends

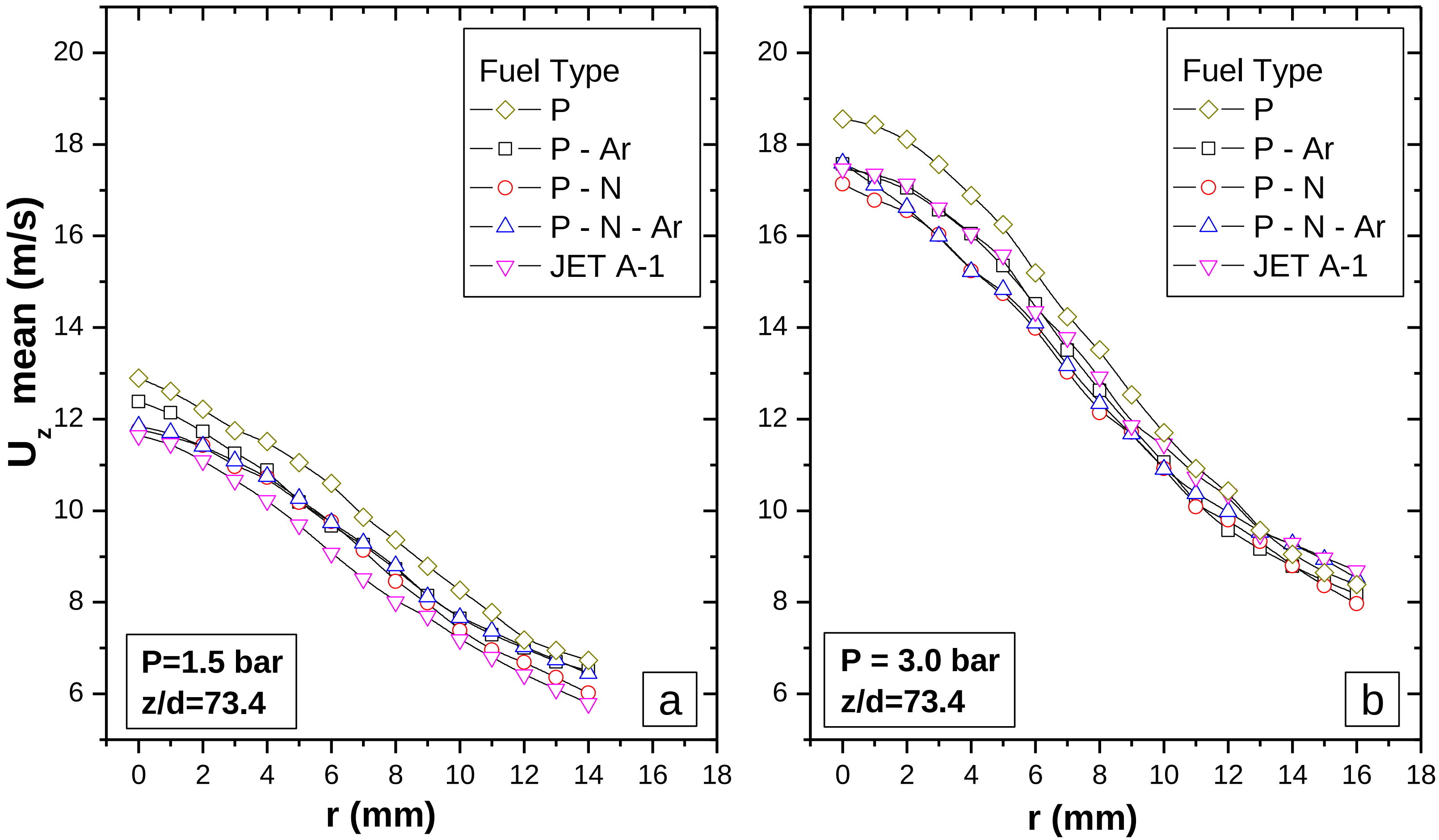

Low Pressure Results
Sauter mean diameter

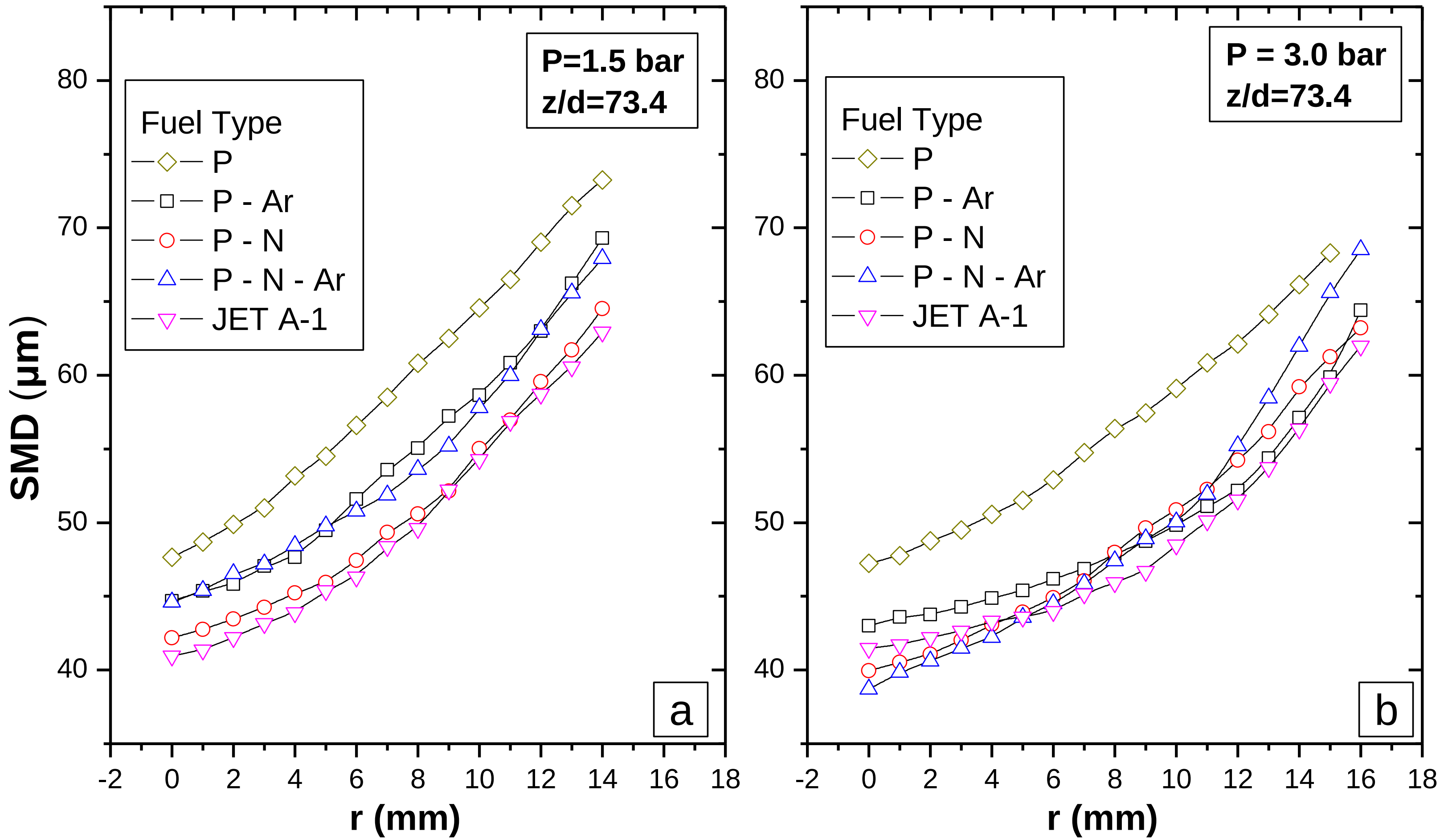

Low Pressure Results
Diameter PDF

Assessment of spray characteristics of alternative aviation fuel blends

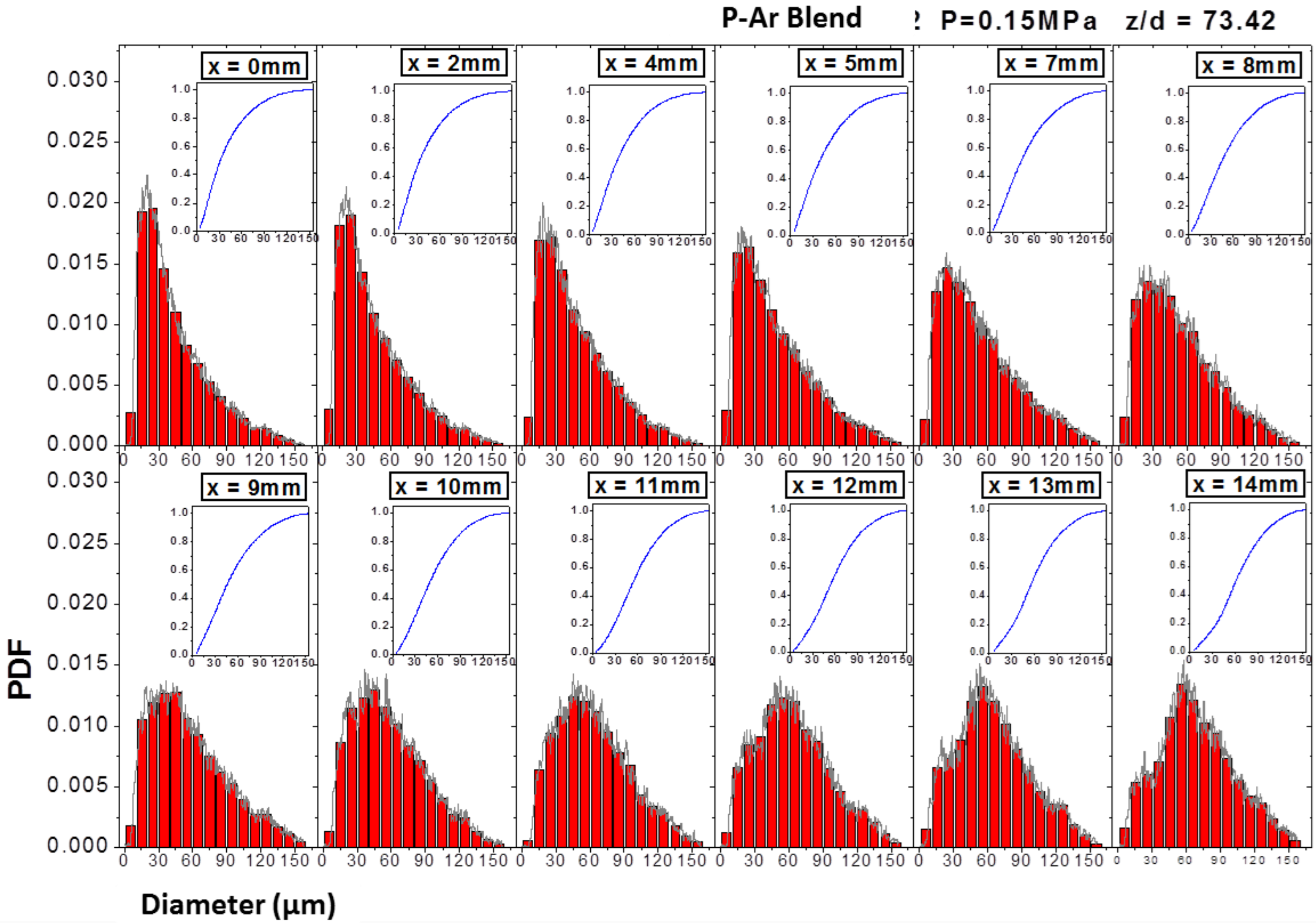

Low Pressure Results
Diameter PDF

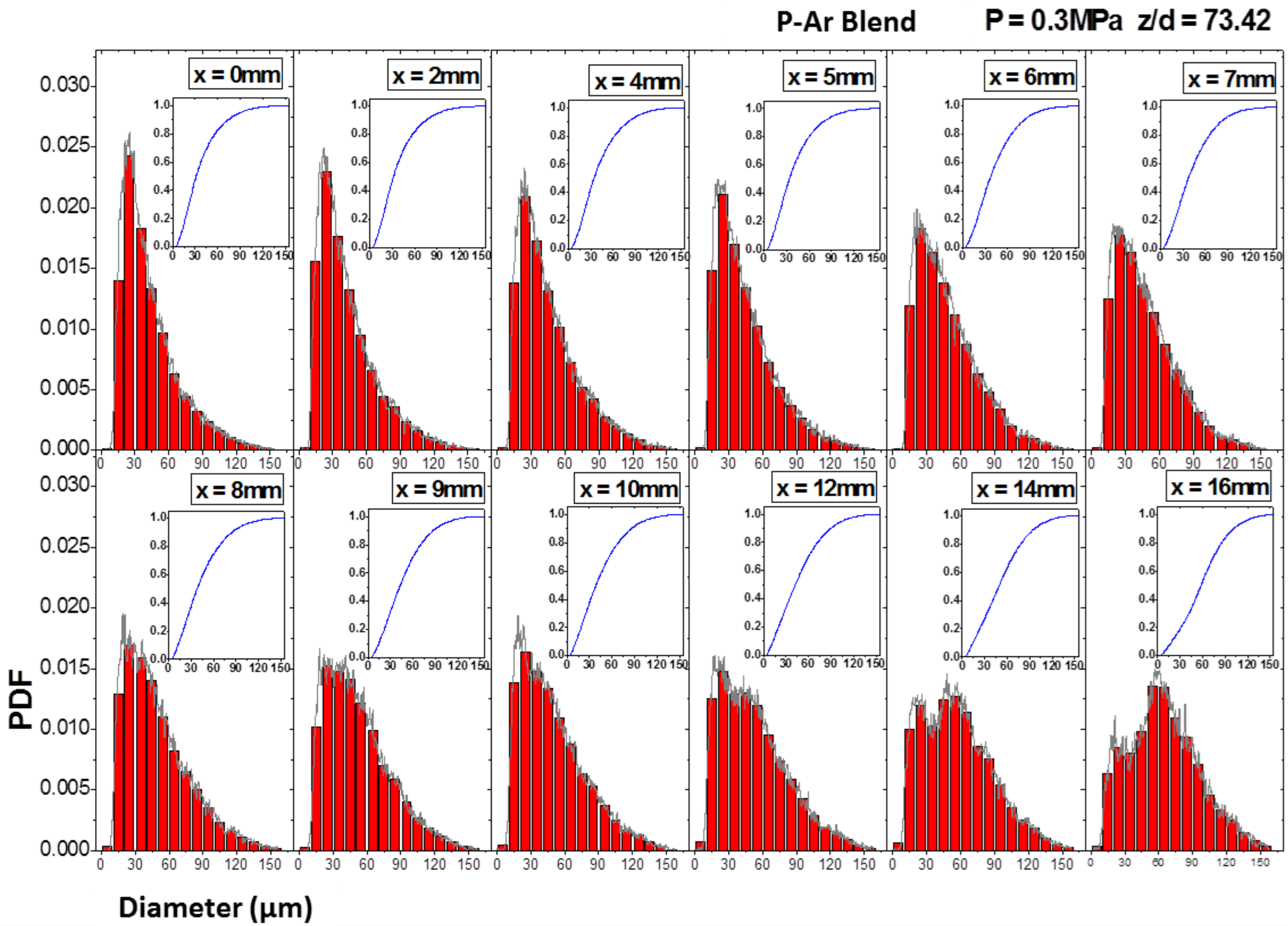

Low Pressure Results

Diameter PDF

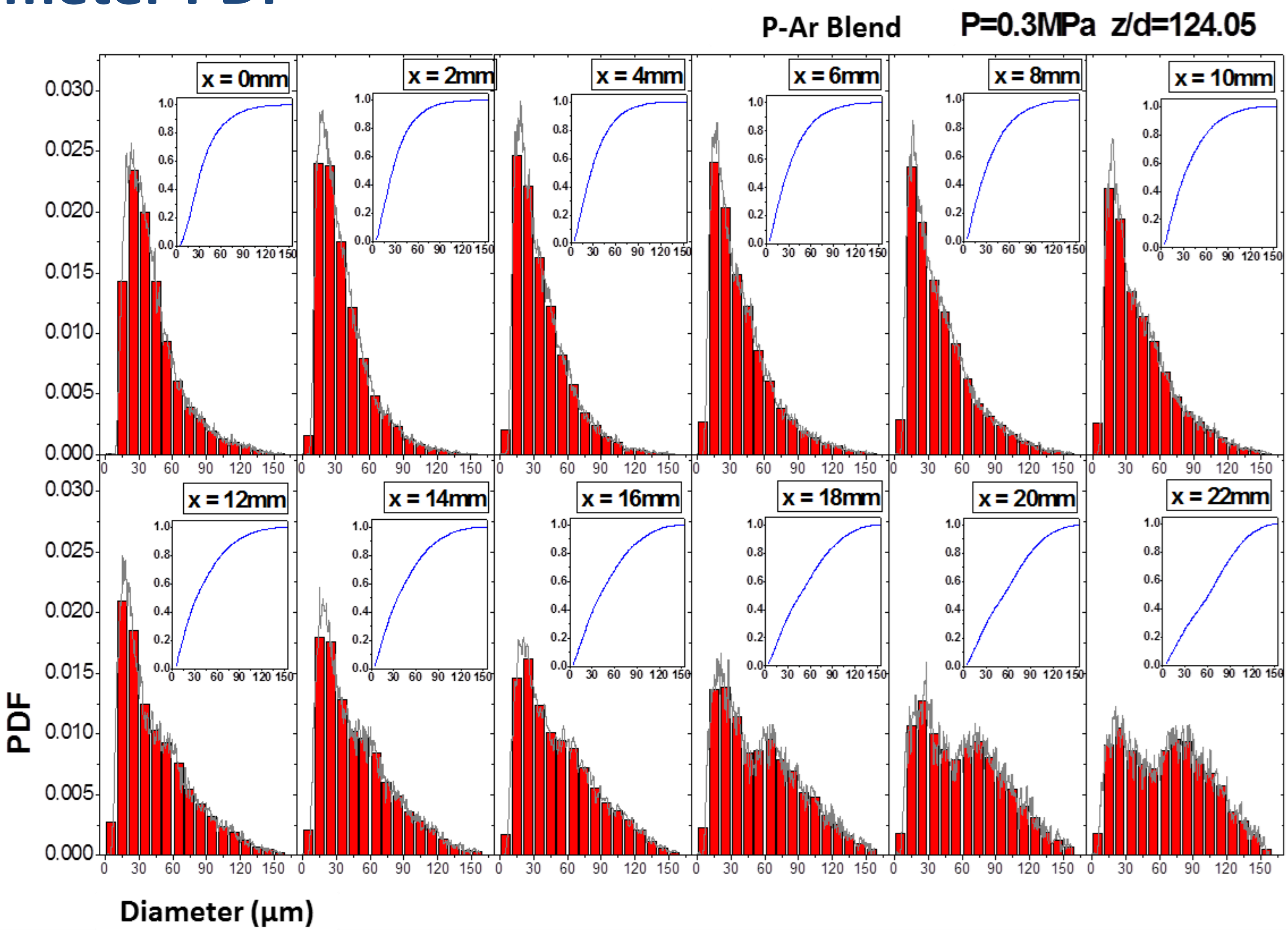

High Pressure Results
Axial mean velocity

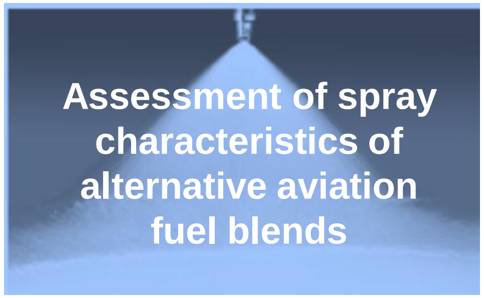

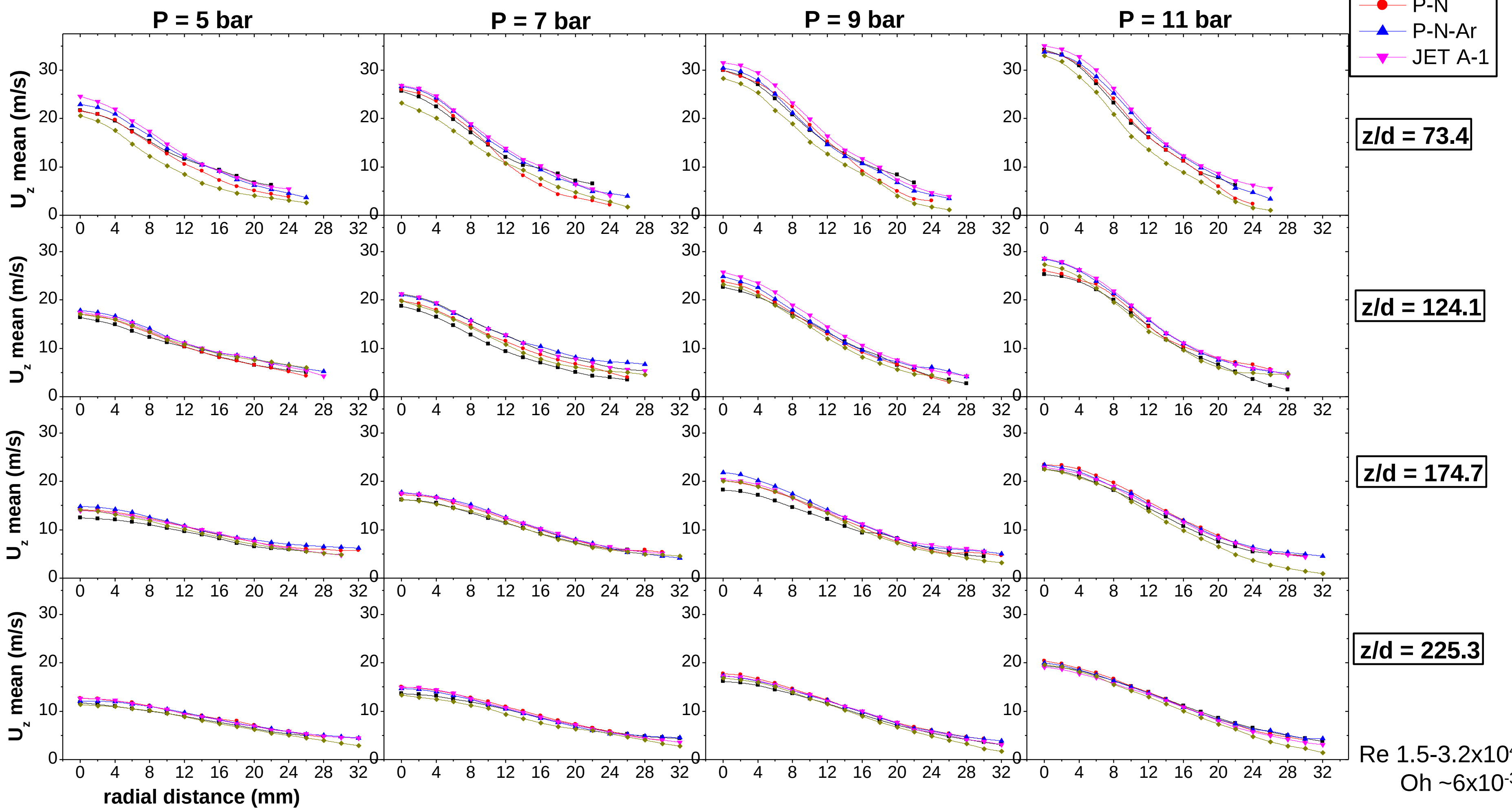

High Pressure Results

Axial velocity rms

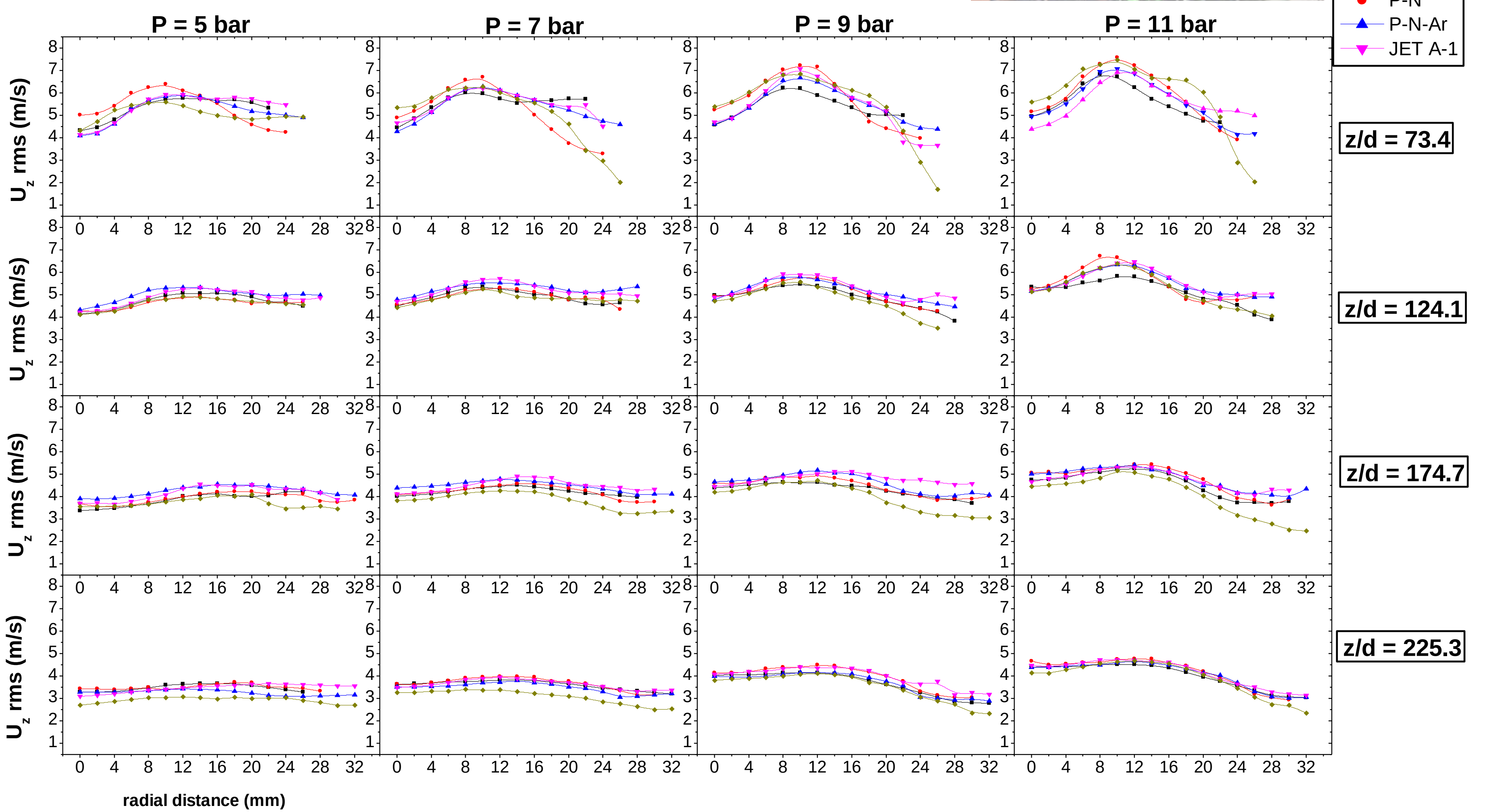

High Pressure Results
Sauter mean diameter

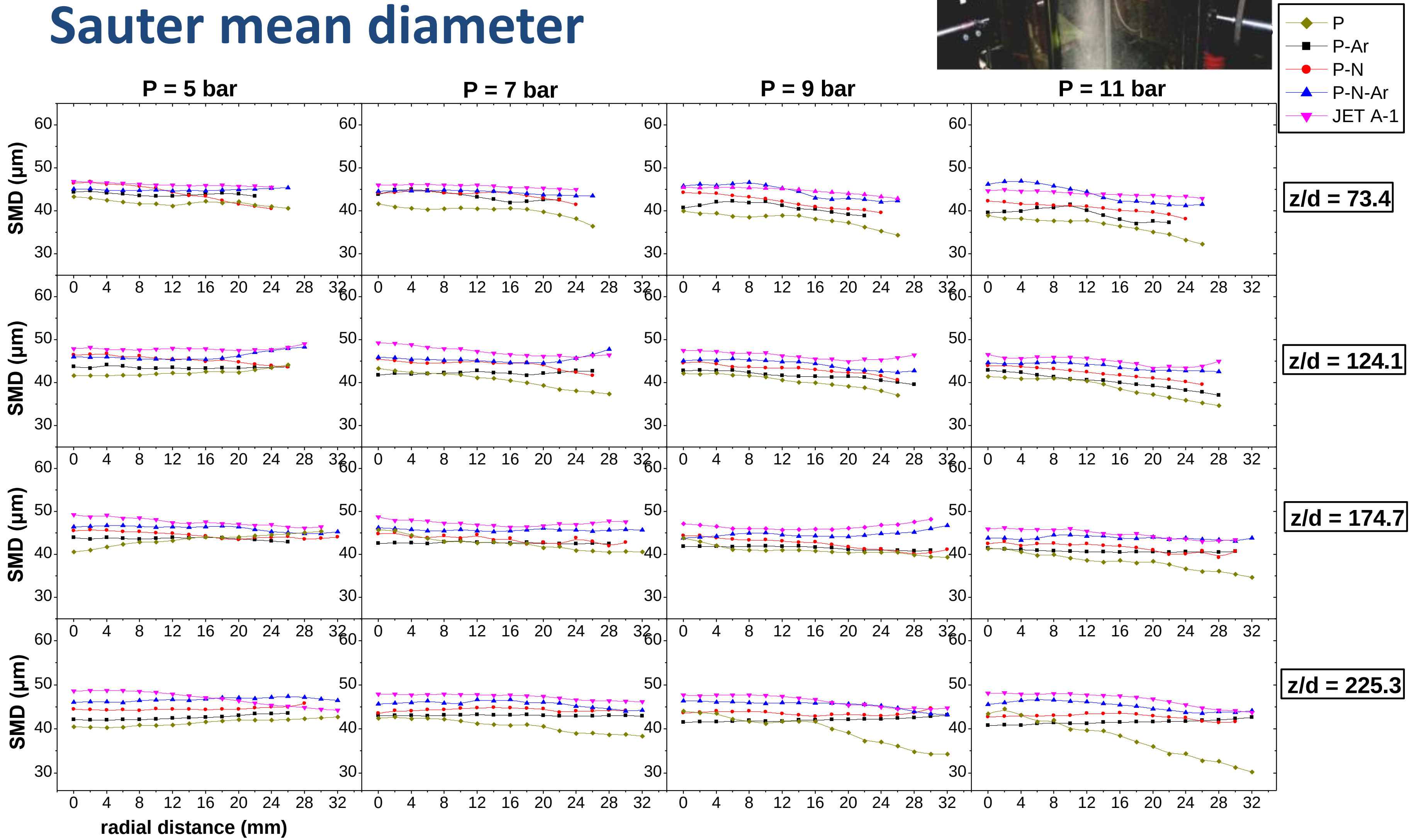

Conclusions

- The results indicate that all tested blends have similar physical properties and produce similar sprays with the reference Jet A-1 fuel, under the testing conditions used in the present study.
- As drop in fuels, they may be expected to behave similar to the reference fuel, as far as spraying characteristics are concerned.
- For this purpose, the P – N – Ar blend (Paraffins, 50% - Naphthenes, 30% - Aromatics, 20%) seems to provide the best candidate. It has a density and a surface tension very close to those of the reference fuel and produces a similar spray pattern with matching droplet velocity and Sauter mean diameter distributions.

THANK YOU

Acknowledgment
The work was funded through the ECATS (Environmentally Compatible Air Transport System) The authors are grateful to Shell Global Solutions (UK) for providing the tested blends.

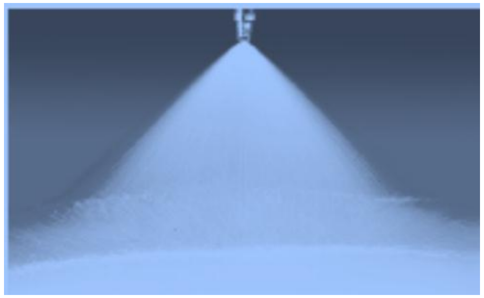

References

Dantec Dynamics, Laser Doppler Anemometry Introduction to principles and applications

Dantec Dynamics, Principles of Phase Doppler Anemometry

Sommerfeld, M., Application of Optical Non-Intrusive Measurement Techniques for Studies of Gas- Solid Flows, LSTM, Erlangen, 1994.

Tropea C., Yarin A. L., Foss J.F. (2007) Handbook of Experimental Fluid Mechanics, Springer.

L.Q. Maurice, H. Lander, T. Edwards, W.E. Harrison, Fuel 80 (5) (2001) 747-756

Blakey, S., Rye L., Wilson C.W., (2011) Aviation gas turbine alternative fuels: A review, Proc. Comb. Institute 33:2863-2885

Chevron Corporation: Alternative jet fuels, A supplement to Chevron aviation fuels review, 2006

Lefebvre H. A. Atomization and Sprays CRC Press, 1988

IP-365-Density and Relative Density of Liquids by Digital Density Meter, The Institute of Petroleum, 2003

Spraying Systems Co, “Industrial Spray Products” Catalog 60M, 2009

PDA User’s Guide, Dantec Dynamics, 1990

Tropea, C.,Yarin A.L., Foss J.F. Handbook of Experimental Fluid Mechanics, Springer, 2007

G. Pitcher, G. Wigley, and M. Saffman, "Sensitivity of drop size measurements by phase doppler anemometry to refractive index changes in combusting fuel sprays", in Applications of Laser Techniques to Fluid Mechanics: 5th International Symposium, Lisbon, Portugal 9-12 July 1990

Fuel Atomization and Spray Testing Protocol

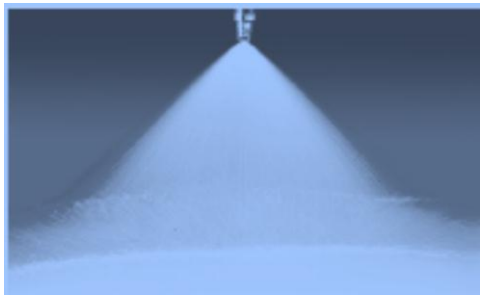

The experimental facility during measurements

EXPERIMENTAL STUDY ON THE INFLUENCE OF PRESSURE AND TEMPERATURE ON LAMINAR BURNING VELOCITY AND MARKSTEIN NUMBER OF CONVENTIONAL AND ALTERNATIVE JET FUELS

V. Vukadinovic, P. Habisreuther, N. Zarzalis

ENGLER-BUNTE-INSTITUTE; DIVISION OF COMBUSTION TECHNOLOGY

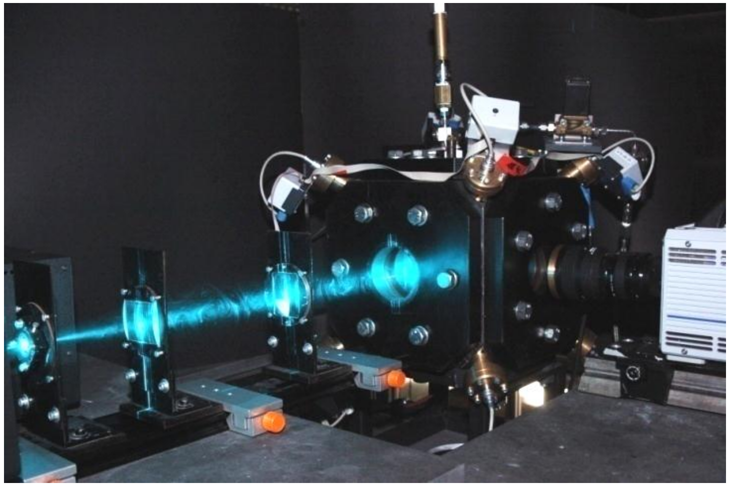

Contents

Motivation

Motivation

- Design of gas turbine combustor relies strongly on turbulent burning velocity. This velocity depends of laminar burning velocity and Ma.

- Attempt to replace conventional with alternative fuels requires their comparison in order to find the most appropriate substitute

- The experimental data of Kerosene Jet A-1 and alternative fuels are needed. Nevertheless, they are scarce, especially at higher pressure condition.

Important Fuel Characteristics

Laminar Burning Velocity and Markstein Number

Engler-Bunte-Institute
Division of Combustion Technology

Laminar Burning Velocity S_L

- The most important parameter of a combustion process
- Velocity of the unburned mixture entering into the flame front (consumption velocity)
- It depends on the thermal diffusivity and the reaction kinetic

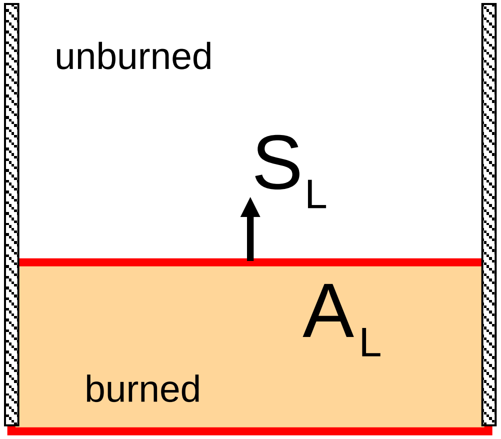

$$S_L \propto \sqrt{\frac{a}{\tau}}$$

a ← thermal diffusivity

τ ← heat release time

Markstein Number

Problem in prediction of a burning velocity

S_L (planar flame) ≠ S_L (counterflow flame) ≠ S_L (spherically expanding flame)

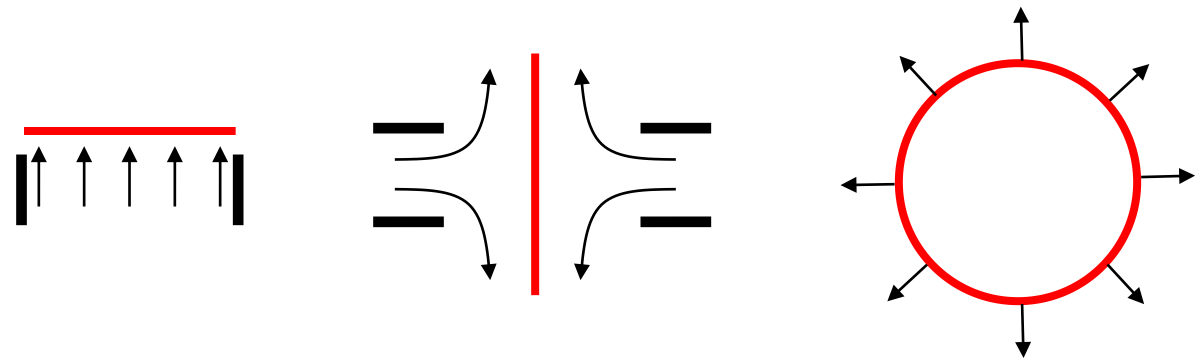

Reason

The flame is strained

The flame is curved and strained

-> The laminar flames are exposed to stretch effects.

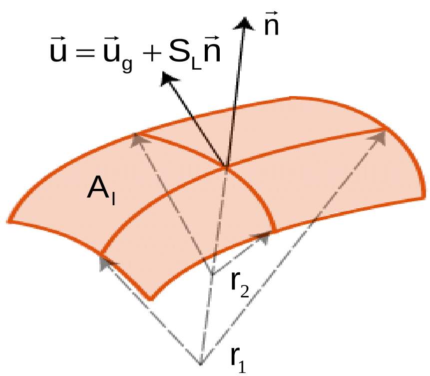

stretch rate => $K = \frac{1}{A} \cdot \frac{dA}{dt}$

Markstein Number

- Stretch effect has a linear influence on the laminar burning velocity
- This influence can be quantified by Markstein number - Ma

$$\frac{S_u}{S_L} = 1 - Ma \cdot Ka$$

<u>Example for Ma=0.6:</u>

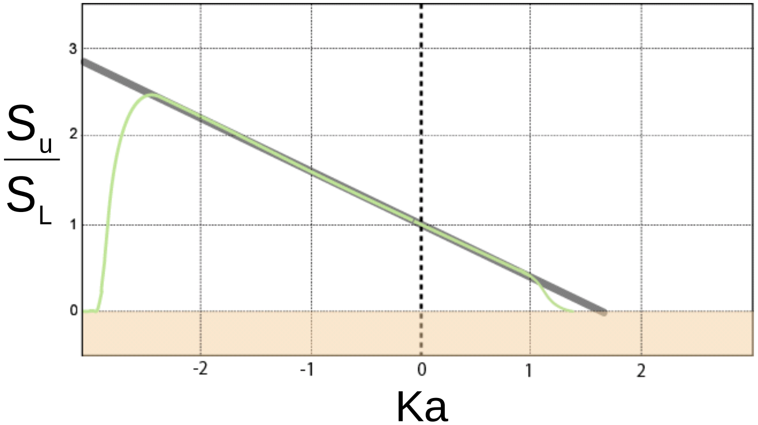

S_u	Stretched laminar burning velocity
S_L	Unstretched laminar burning velocity
$Ka = K \cdot \tau$	Karlovitz number
Ma	Markstein number

Engler-Bunte-Institute
Division of Combustion Technology

Markstein Number

Influence of Markstein number
on turbulent flame speed

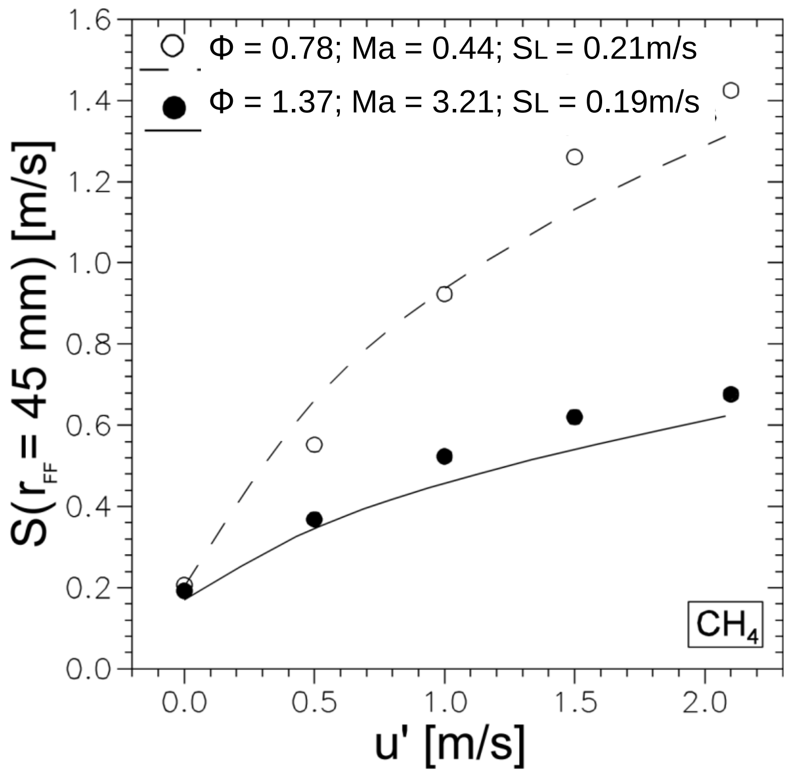

Engler-Bunte-Institute
Division of Combustion Technology

Markstein Number

- For one component and small hydrocarbon molecules (CH_4, C_2H_6) the laminar burning velocity and Markstein number can be calculated

- For multi component fuels, which consist of large hydrocarbon molecules, **the computation of burning velocity and Ma is difficult and must experimentally be determined**.

- An experimental determination of S_L and Ma as a function of equivalence ratio and thermodynamic state (pressure and temperature) is necessary.

- Entire information: Laminar burning velocity of unstretched flame and Markstein number.

Strategy for Measurements of Liquid Fuel Characteristics

Strategy for Measurements of Liquid Fuel Characteristics

- Main difficulty in the present experiments is pre-evaporation of the fuel and achieving the homogeneous gaseous fuel/air mixture prior to ignition

- Mounting the heating system into the walls of the vessel that provides an uniform temperature distribution in the vessel

- Measurement process is practically done through the following steps:
  - Heating the vessel up to requested temperature (max 250 °C)
  - Filling the vessel with appropriate mixture by partial pressure method (providing a fuel in gaseous state through the liquid fuel injection and its instantaneous evaporation due to the elevated temperature)
  - Attaining the uniform mixture by means of fans
  - Ignition and acquisition of the data
  - Post-processing and data analyses

Applied Measurement Technique

Applied Measurement Technique

- Optical laser method based on the Mie-scattering of the laser light by smoke particles

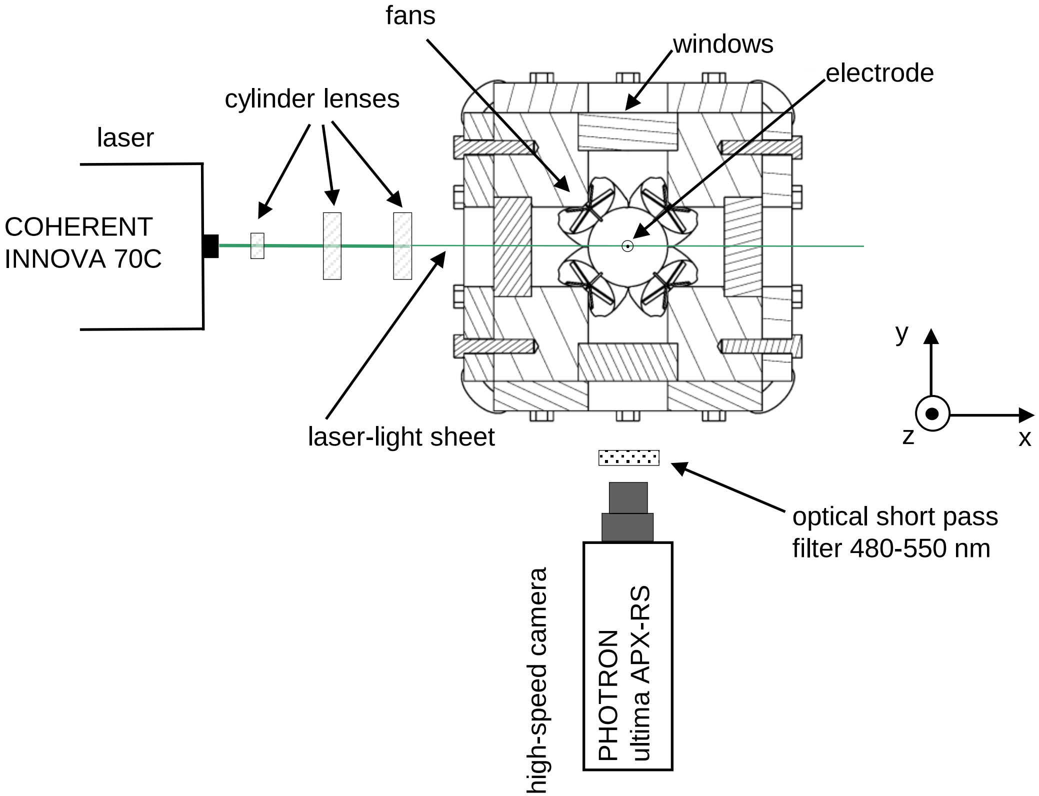

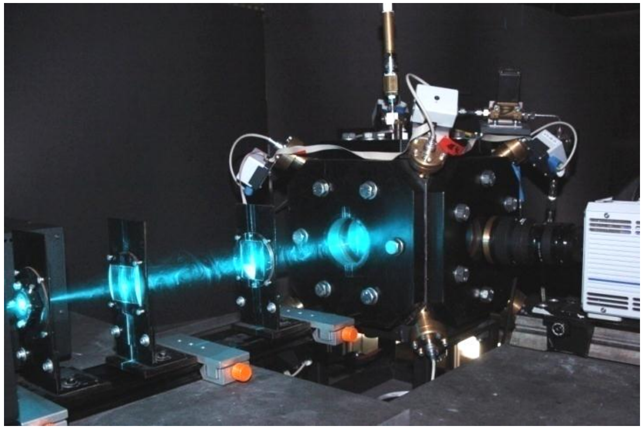

Experimental facility in the process of measurement

Applied Measurement Technique

- Recorded 2D flame front propagation

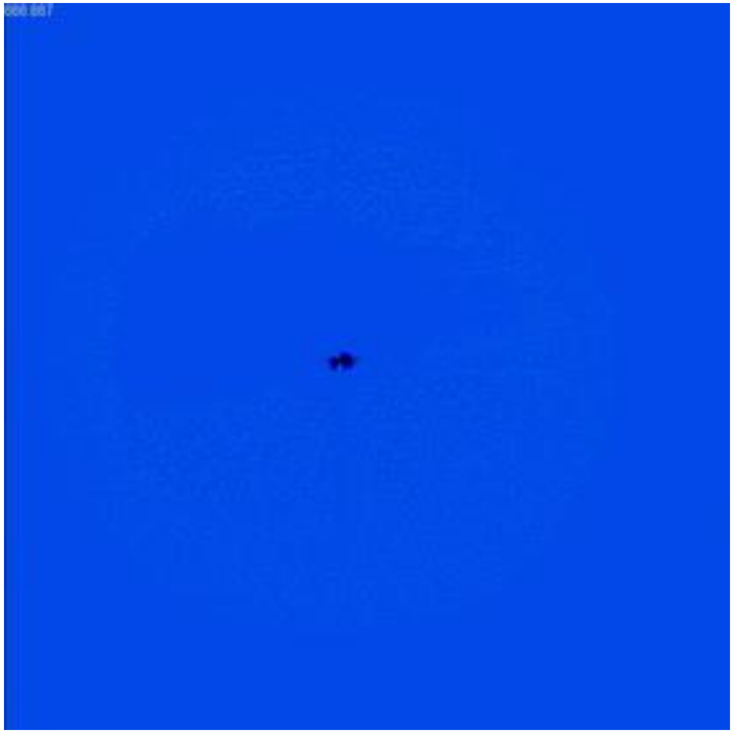

Applied Measurement Technique

- Procedure to determine the unstretched laminar burning velocity and the Markstein number

Processed image

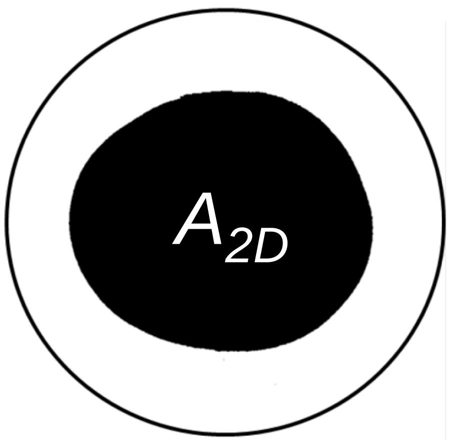

$$R = \sqrt{\frac{A_{2D}}{\pi}}$$

$$Flame\,front\;speed = \frac{\Delta R}{\Delta t}$$

Considering the mass conservation:

$$Burning\,velocity\;S = Flame\,front\;speed \cdot \frac{\rho_b}{\rho_u}$$

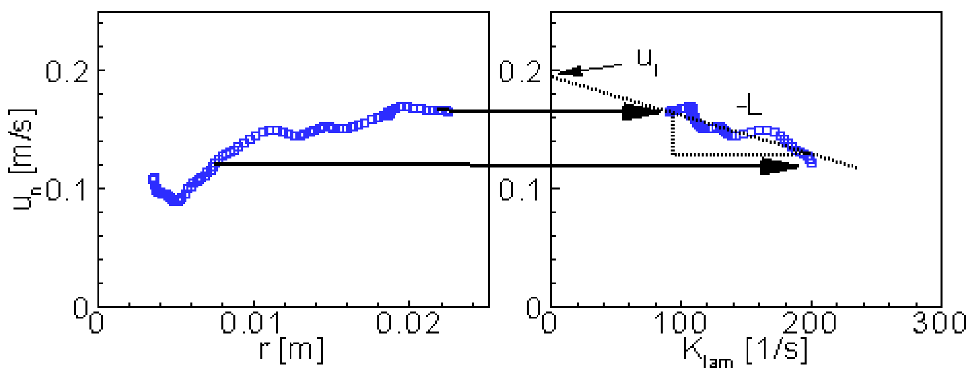

Experimental Results and Discussion

Investigated Fuels and Conditions

- **Investigated fuels**:

  Kerosene Jet A-1, average formulation ($C_{11.16}H_{20.82}$)

  GTL(Gas-To-Liquid), average formulation ($C_{10.14}H_{22.25}$)

- **Influence of all three important initial parameters on burning velocity:**

  Initial temperatures 100°C, 150°C and 200°C

  Initial pressures 1, 2 and 4 bar

  Wide range of equivalence ratio

Laminar Burning Velocity

Karlsruhe Institute of Technology

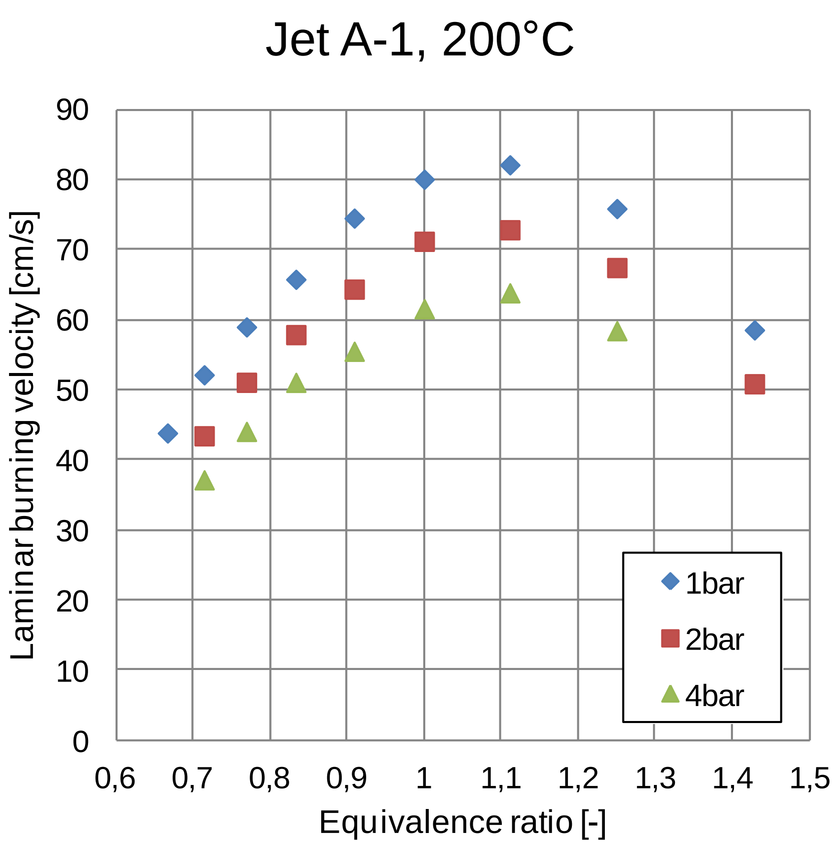

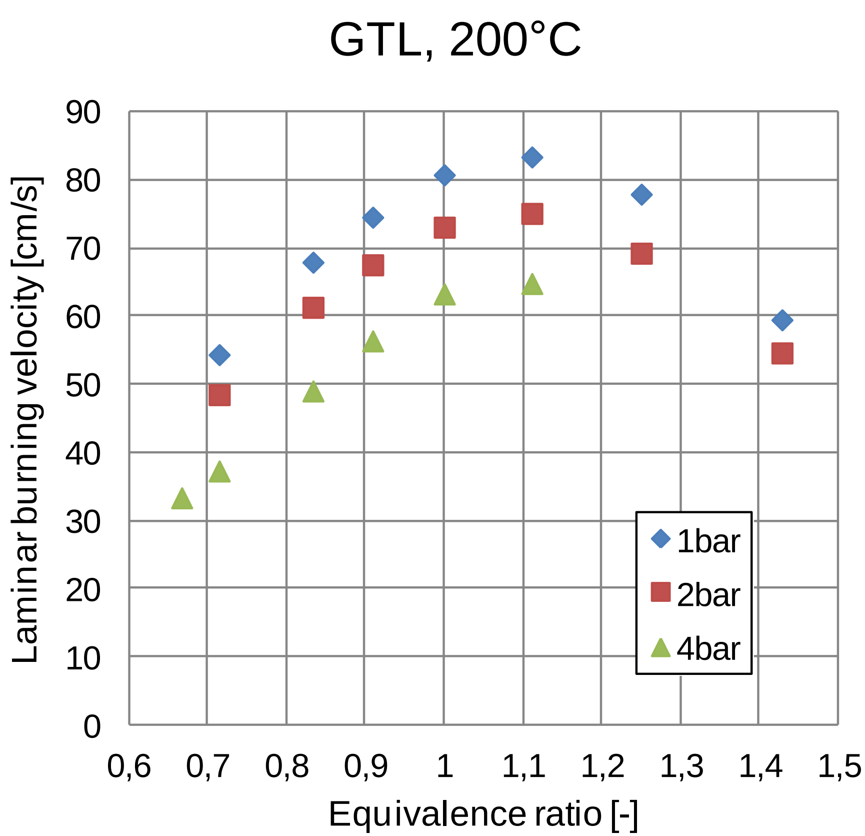

Laminar Burning Velocity

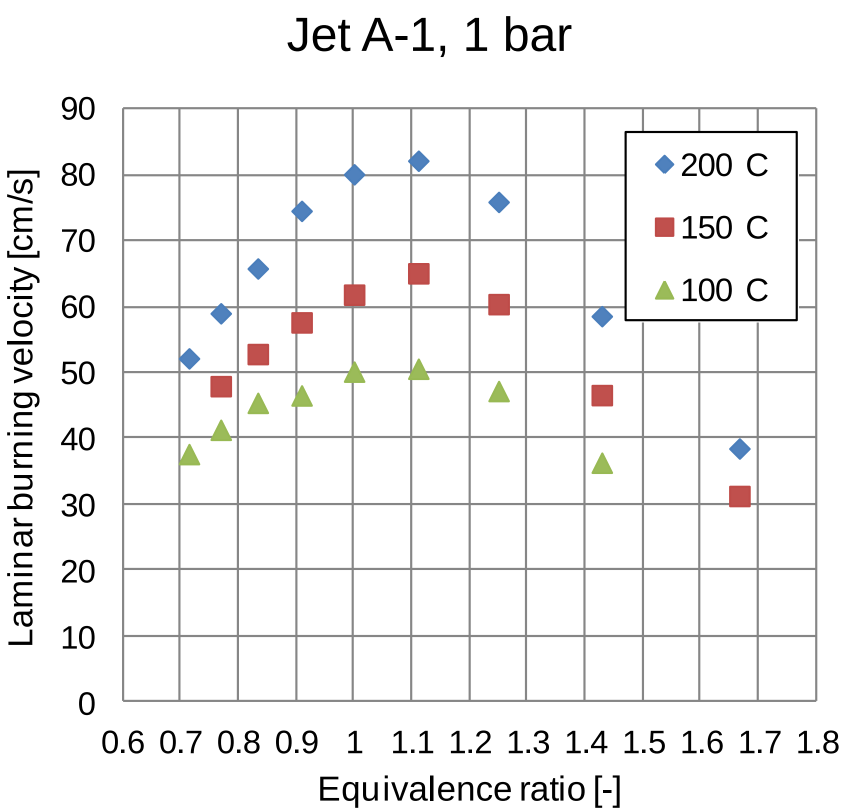

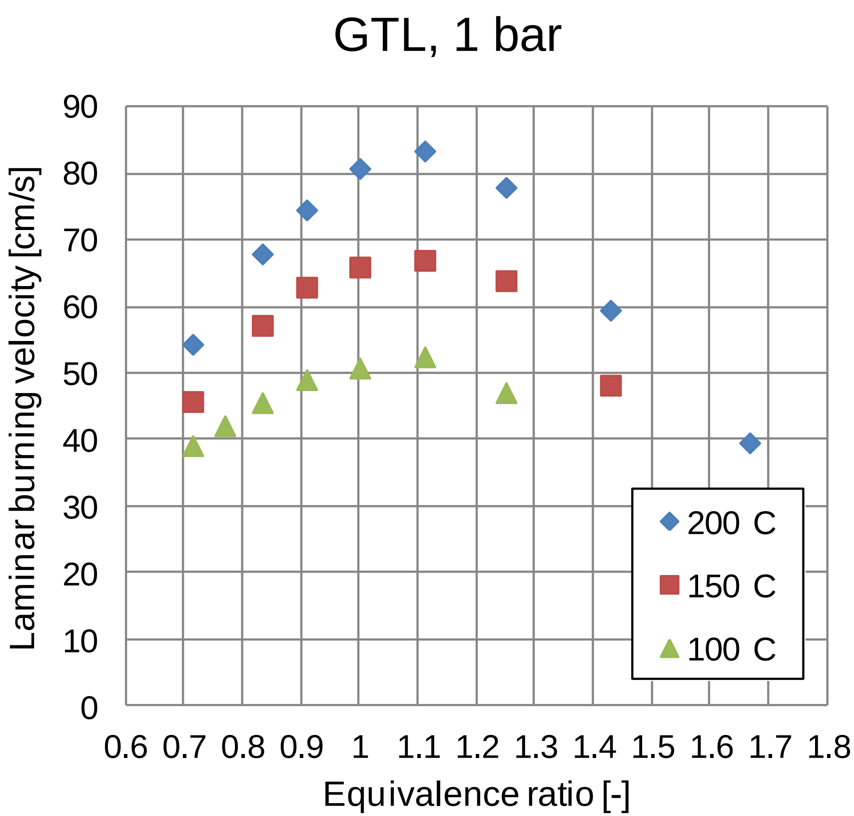

Markstein Number

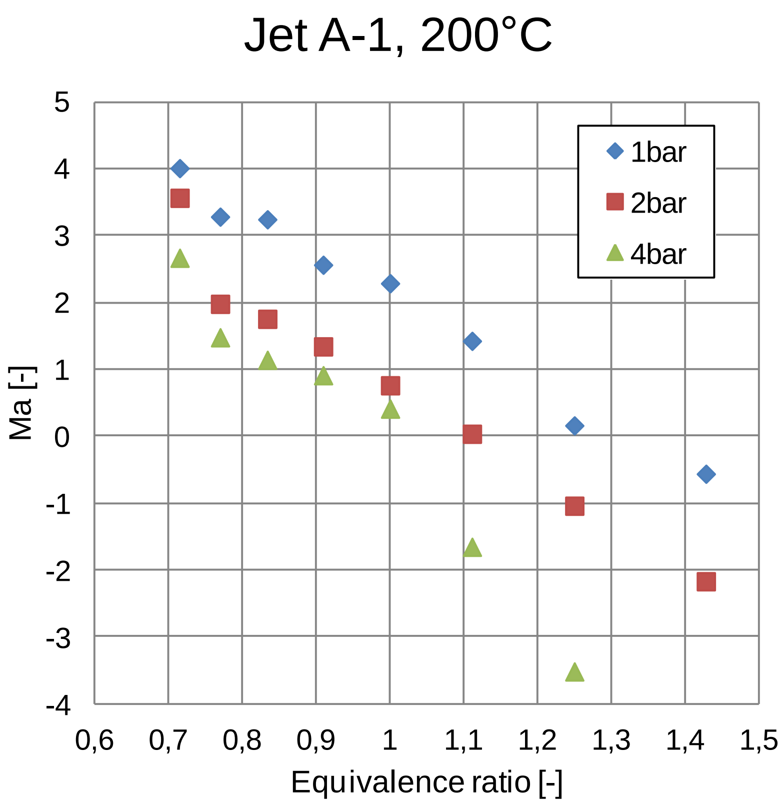

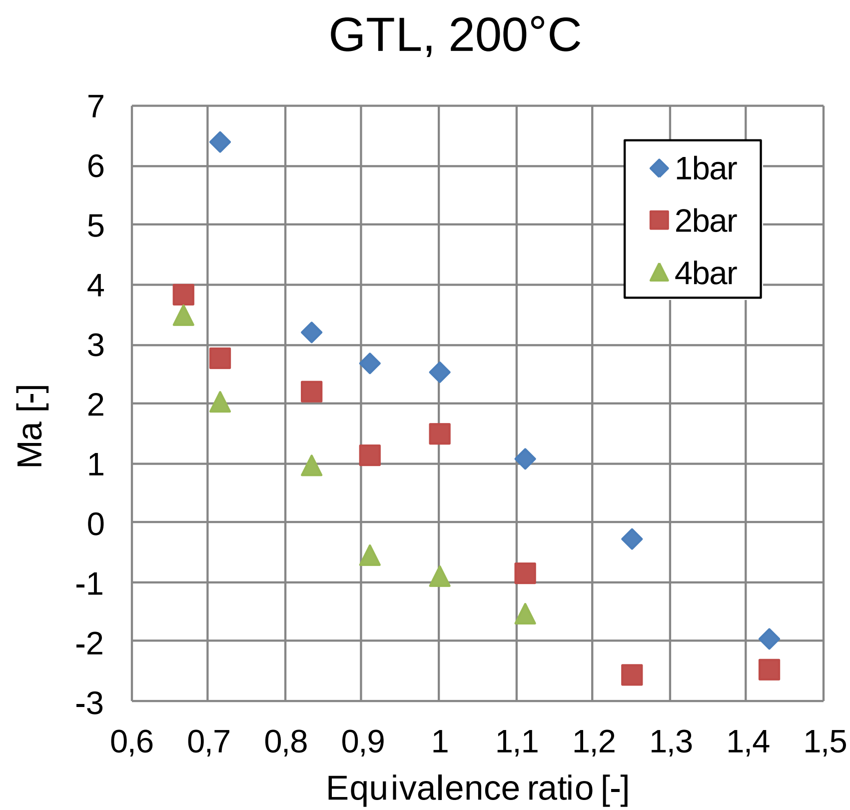

Summary

Summary

- Important fuel characteristics: the laminar burning velocity and Markstein number as one complete information for predicting the flame front propagation
- Experimental method and strategy for measurement of liquid fuels combustion characteristics
- Applied measurement technique and validation
- Comparison of combustion characteristics of kerosene Jet A-1 and GTL
  The characteristics are very similar!
- Further investigation should be performed on GTL blend that contains minimum 8% aromatics
- Additionally, other important properties of GTL blends such as: high energy density, good atomization, rapid evaporation, low explosion risk, etc. also need to be examined.

Thank you for your attention!

ACKNOWLEDGMENTS
We kindly acknowledge financial support by the European Commission through the **ECATS network of excellence** (Contract No. ANE-CT-2005-012284) and DFG SFB 606 (Deutsche Forschungsgemeinschaft Sonderforschungsbereich 606) and making the fuels available for the investigation by **Royal Dutch Shell**.

ESPOSA EFFICIENT SYSTEMS AND PROPULSION FOR SMALL AIRCRAFT

SEVENTH FRAMEWORK PROGRAMME

The research leading to these results has received funding from the European Union Seventh Framework Programme [FP7/2007-2013] under grant agreement n° [284859]

EUROPEAN COMMISION

EFFICIENT SYSTEMS AND PROPULSION FOR SMALL AIRCRAFT

EASN workshop on Flight Physics and Propulsion

Prague, Czech Republic, 31st of October - 2nd of November 2012

Presentation of ESPOSA project

Title : ESPOSA = Efficient Systems and Propulsion for Small Aircraft

level 2 project of 4th call of FP7, (ACP1-GA-2011-284859-ESPOSA)

Duration: 48M**, start: Oct 2011 – end: Sept 2015**

Website: www.esposa-project.eu

Coordinator : **PBS Velka Bites, a.s. (+ VZLU)**

Consortium:

- **39 partners (incl. 10 SMEs)**
- **18 industrials, 11 research centres, 10 universities**
- 15 countries :
  CZ(7), PL(5), DE(5), ES(1), IT(4), HU(1), RO(2), FIN(1), UK(1), BE(3), NL(2), SVK(1), UKRAINE(2), RU(1), TR (3)

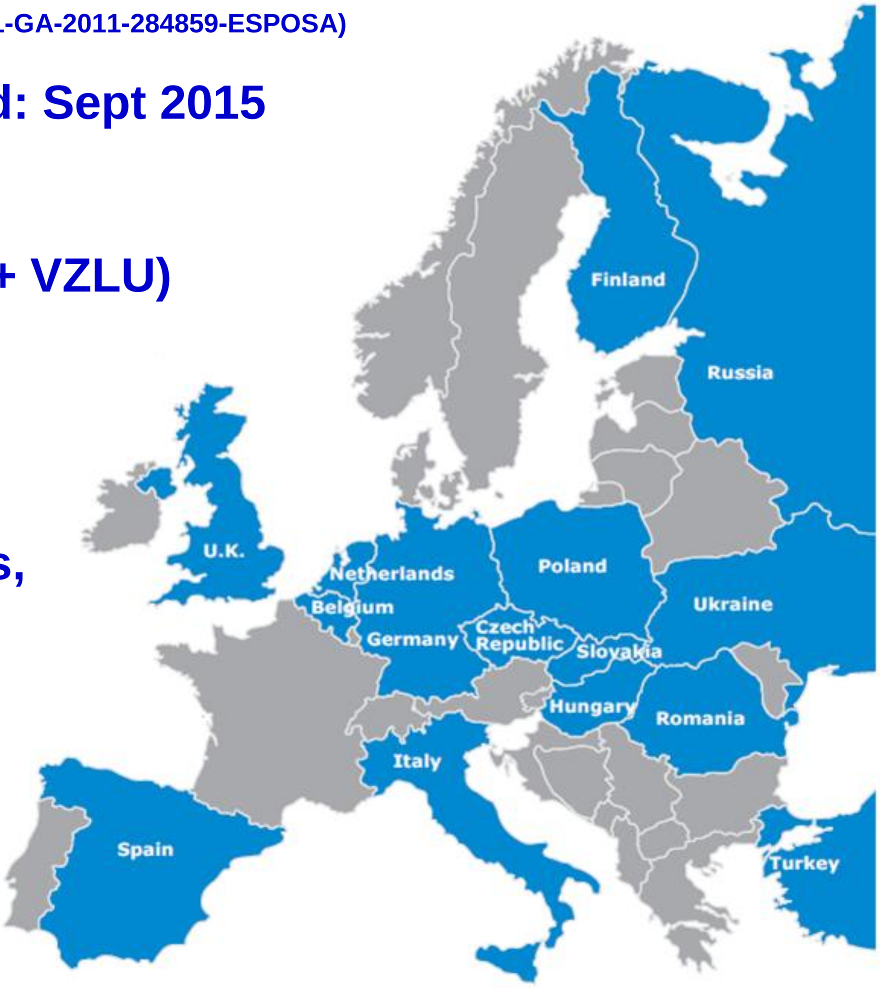

ESPOSA – Project future impact

ENGINES

- turbo propeller and turbo shaft gas turbine engines
- two power categories (160÷250 kW and 300÷550 kW)

FLYING VEHICLES

- small turboprop aircraft, light helicopters
- transport utility aircraft, small commuter aircraft
- unmanned aircraft systems for civil use

160-250 kW
(~ 2-5 seats)

Turboprop
Turboshaft

Baseline Engine 1
(160-180 kW)

300-550 kW
(~ 5-9 seats)

Turboprop
Turboshaft

Baseline Engine 2
(400-470 kW)

ESPOSA – Project technical areas

- **New engine components and its technical solutions** (for efficient engine operation)
- **Optimized new production technologies for lean manufacture** of critical engine components (to improve engine affordability)
- **New affordable solutions for electronic engine control and engine health monitoring** (to contribute to the overall propulsion unit efficiency, safety and pilot workload reduction)
- **Complex design methodologies for turboprop/turboshaft engines installation** (to improve readiness for new turbine engines installation into various aircrafts)

ESPOSA – Engine parts

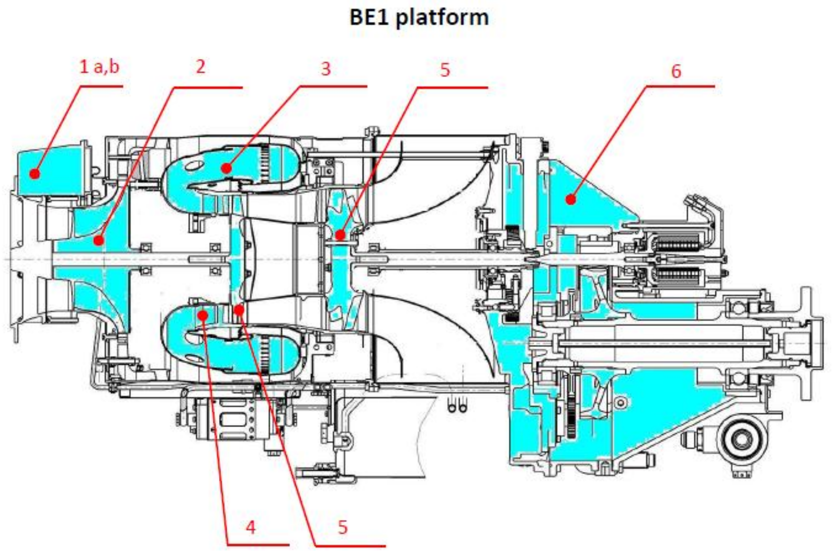

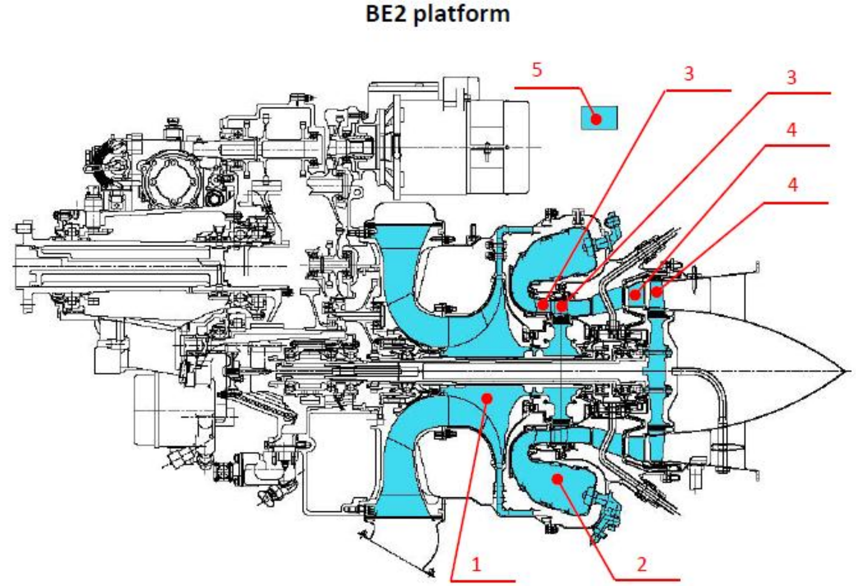

1 - Dual channel EECU - Engine Electronic Control Unit (a) + engine data recorder (b) for engine maintenance (

2 - Compressor - only from the point of view of lower production cost. The compressor design should remain unchanged unless the design change is required by lowering of production costs.

3 - Combustion chamber - from the point of view of lower production cost, higher efficiency and lifetime.

4 - Guide vanes of gas generator turbine - from the point of view of definition and validation of cooled guide vanes concept.

5 - Turbine wheel bliscs (castings) - from the point of view of improved casting technologies resulting in better mechanical properties.

6 – Gearbox - overall concept - from the point of view of defining the key characteristics of a performance to cost efficient gearbox (aimed at BE1 power range). Improving weight, reliability and component cost based on gearbox dynamic analyses.

- 5a - Fadec + 5b- Automatic Control System (fuel control unit, propeller speed governor, electronic module of ACS) + 5c - EMM (engine monitoring module)
- 1-4 - all component of flow path (compressor inlet - 1, compressor - 2, combustion chamber - 3, guide vanes and blades of power turbine (LPT) - 4 and gas generator turbine (HPT) - 3).

ESPOSA – Work flow

ESPOSA EFFICIENT SYSTEMS AND PROPULSION FOR SMALL AIRCRAFT

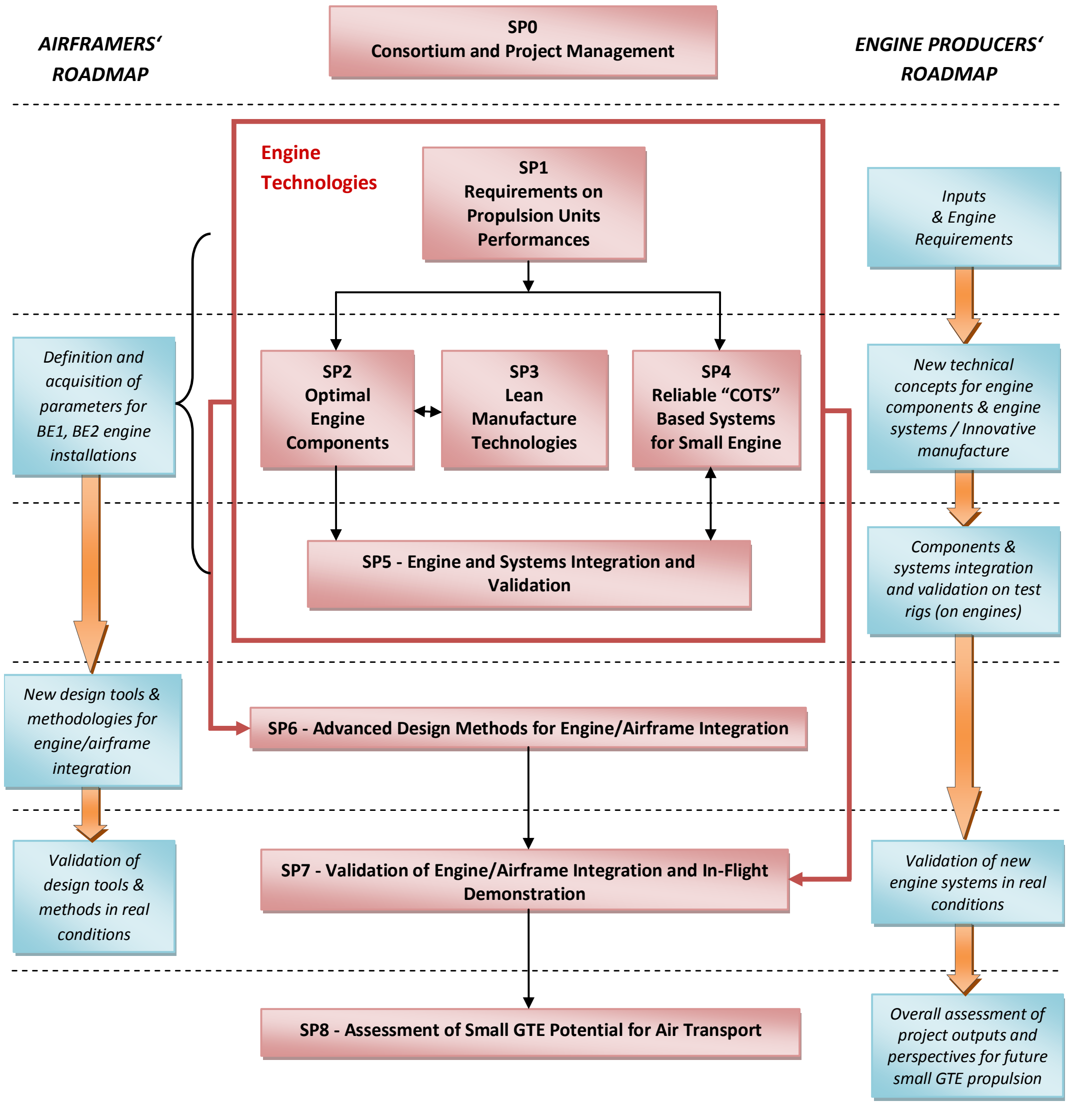

- **SP1 start technical activities with definition of high level requirements (airframers - req. on propulsion unit, engine producers - req. on engine components / systems)**
- **SP2 and SP3 work comprises performance improvements of key engine components, their improved manufacture in terms of costs and quality.**
- **SP4 is dedicated to novel modern electronic engine control based on COTS, pioneering the engine health monitoring for small engines and providing advanced more electric solutions for fuel control systems.**
- **SP5 summarizes particular achievement of SP2,3,4 in functional complex and provides the space for their validation on engine test benches**
- **SP6 addresses problematic design areas connected with turboprop/shaft engine installation into airframe structure, including the use of composite materials. The work will be conducted taking into account specifics of different aircraft configurations.**
- **SP7 validates not only installation technologies developed in SP6 but also selected engine in operational conditions**

ESPOSA – Work Packages

ESPOSA EFFICIENT SYSTEMS AND PROPULSION FOR SMALL AIRCRAFT

SP1 - Requirements on Propulsion Units Performances
WP 1.1 - Requirements on GTE propulsion used in General Aviation
WP 1.2 - Performance and economic specifications for baseline engines
WP 1.3 - Enhanced mathematical modelling of gas turbine engines

SP 2 - Optimal Engine Components
WP 2.1 - Optimal small compressor
WP 2.2 - Advanced cooled small turbine
WP 2.3 - Efficient combustion concept
WP 2.4 - Optimal gear box design
WP 2.5 - Advanced dynamic modelling of high speed turbomachinery

SP 3 - Lean Manufacture Technologies
WP 3.1 - Low-cost machining for compressors
WP 3.2 - Precise and low-cost casting technologies for turbine wheels
WP 3.3 - Development of progressive coating solutions for engine parts
WP 3.4 - Low-cost gearbox manufacturing

SP 4 - Reliable "COTS" Based Systems for Small Engine
WP 4.1 - Advanced automatic control system for small engines
WP 4.2 - Smart health monitoring system
WP 4.3 - Affordable more electric solution for fuel and propeller control s

SP 5 - Engine and Systems Integration and Validation
WP 5.1 - Validation of BE1 on test rig
WP 5.2 - Validation of BE2 on test rig
WP 5.3 - Validation of BE2 in altitude test chamber

SP 6 - Advanced Design Methods for Engine/Airframe Integration
WP 6.1 - Complex design methodology for engine mechanical integration
WP 6.2 - Reliable design methodology for aerodynamic engine/airframe integration
WP 6.3 - Tools for engine and nacelle aeroelastic integration – "Whirl Flutter"
WP 6.4 - Reliable simulation tools for engine thermal integration
WP 6.5 - New design and manufacturing approaches for "hot" composite nacelles

SP 7 - Validation of Engine /Airframe Integration and In-Flight Demonstration
WP 7.1 - Validation of integration design methodologies
WP 7.2 - Qualification activities for flight testing
WP 7.3 - Overall demonstration in In-flight conditions

SP 8 - Assessment of Small GTE Potential for Air Transport
WP 8.1 - Overall assessment of SP results toward ESPOSA objectives

ESPOSA – Tests / Demonstrators

- **Project activities will include extensive validation on the test rigs (validation on component level)**

- **The most promising technologies (value/cost benefit) will be selected and integrated into higher functional complexes and further evaluated on the engine test beds (validation on engine level)**

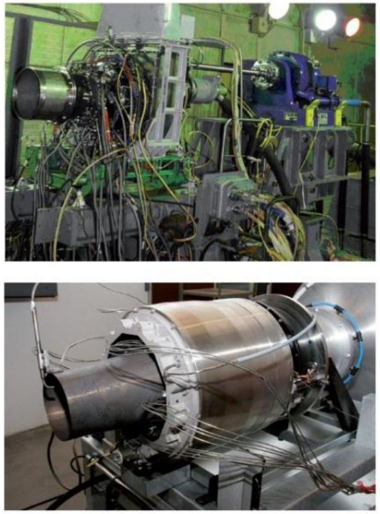

Test benches

RTD

INTEGRATION AND VALIDATION

DEMONSTRATION

- **The functionality of certain project outcomes will also be demonstrated and validated in flight conditions to reach higher TRL level (validation on aircraft level)**

ILOT: I23 - tractor single engine a/c

M-M: Orka - pusher twin-engine a/c

Winner Helico: single engine light helicopter

ESPOSA EFFICIENT SYSTEMS AND PROPULSION FOR SMALL AIRCRAFT

ESPOSA – Objectives

Targeted objective of ESPOSA	BE1 engine platform *160-200 kW*	BE2 engine platform *400-470 kW*
Engine affordability (price reduction target)	establishing new category (by 60%)	by 15-20%
Reduction of fuel consumption (fuel costs)	maintain standard	by 10-15%
Reduction of maintenance (MRO) costs	standard, or improved	by 40%
Weight (Mass reduction)	45-58% (significant mass reduction)	6% (PT6A-21)
Engine systems improvement and pilot workload reduction	electronic EEC control low-cost engine health-monitoring system	low-cost FADEC low-cost engine health-monitoring system.
Time to market reduction for propulsion related technologies speeding up the new aircraft development process	reliable and efficient design tools and methodologies for engine integration, development of “plug- in” solutions for engine systems	reliable and efficient design tools and methodologies for engine integration, development of “plug- in” solutions for engine systems
Pioneering the emissions standards for small turbine engines	Provision of basic data about small GTE emissions	Provision of basic data about small GTE emission and emission reduction of BE2

ESPOSA – Objectives / Engines

The target for "BE2" engine
(measured in DOC) :

- Reduction of depreciation costs - by 1,5 ÷ 3%
- Reduction of fuel consumption (fuel costs) – by 2,5÷5%
- Reduction of maintenance and MRO related costs – by 6%

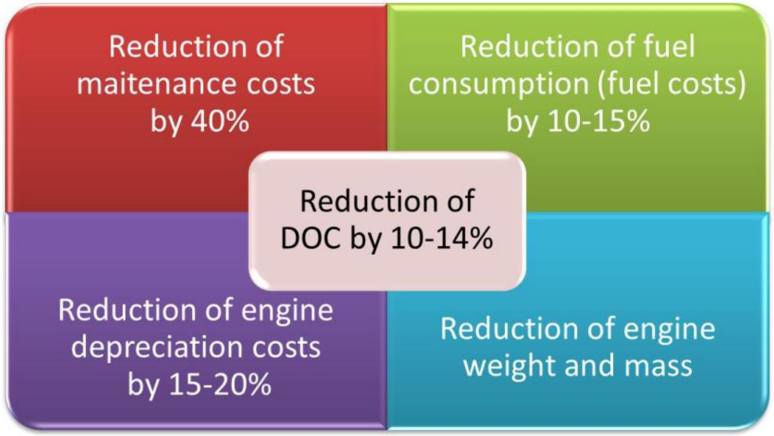

The target for "BE1" engine :

- about 60% price reduction compare to the gas turbine engine currently available
- lower maintenance costs (TBO prolongation) compare to piston engines.
- EECU system
- create new engine segment

Figure 9 - Visualization of expected mass reduction of BE1

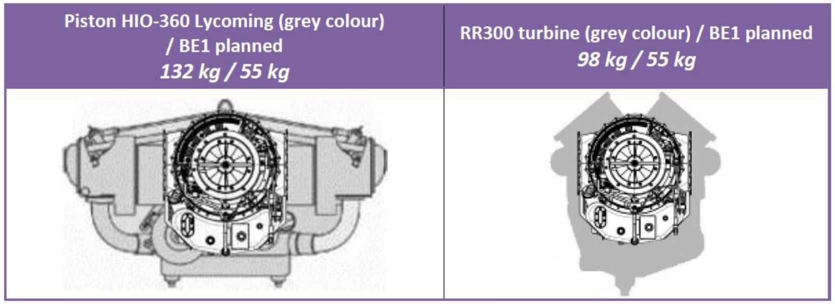

ESPOSA – Contacts

Motto: "The project ESPOSA should encourage both aircraft and engine producers in using new solutions for their aircrafts and gas turbine engines by demonstrating their feasibility and by proving their advantages."

Thank you for your attention !

COORDINATION

První brněnská strojírna Velká Bíteš, a.s.
Vlkovská 279, 595 12 Velká Bíteš
Czech Republic, www.pbsvb.cz

Zdeněk Palát & Pavel Wolf, project coordinators
e-mail: palat.zdenek@pbsvb.cz, wolf.p@pbsvb.cz

ADMINISTRATION

Výzkumný a zkušební letecký ústav, a.s.
Beranových 130, 199 05 Prague
Czech Republic, www.vzlu.cz

Karel Paiger, project administrator
e-mail: paiger@vzlu.cz

INFO

More information about ESPOSA project:
www.esposa-project.eu

The Preliminary Analysis of Inlet and Outlet Position in Case of Engine Cooling

Adam Dziubiński
Aerodynamics and Flight Mechanics Division
Al. Krakowska 110/114,
Warsaw, 02-256,Poland
adziubinski@ilot.edu.pl
http://www.ilot.edu.pl

research for future

EASN workshop on Flight Physics and Propulsion
31st of October - 2nd of November 2012. Prague, Czech Republic

easn

Presentation Schedule:

1. Mesh and zones description
2. Boundary conditions and test program
3. Results of inlet analysis
   a. Surface temperature distribution
   b. Flow field temperature distribution
   c. Convection heat flux comparison
   d. Radiation heat flux comparison
4. Results of outlet analysis
   a. Surface temperature distribution
   b. Flow field temperature distribution
   c. Convection heat flux comparison
   d. Radiation heat flux comparison
5. Conclusions

Adam Dziubiński

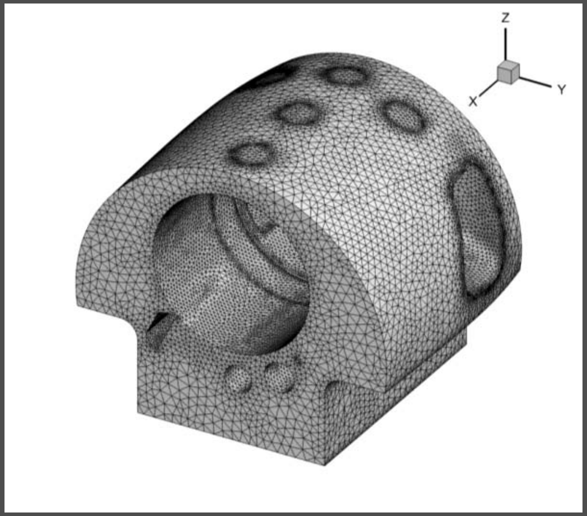

Mesh properities:

- All tetrahedral
- 0.5 mln of cells

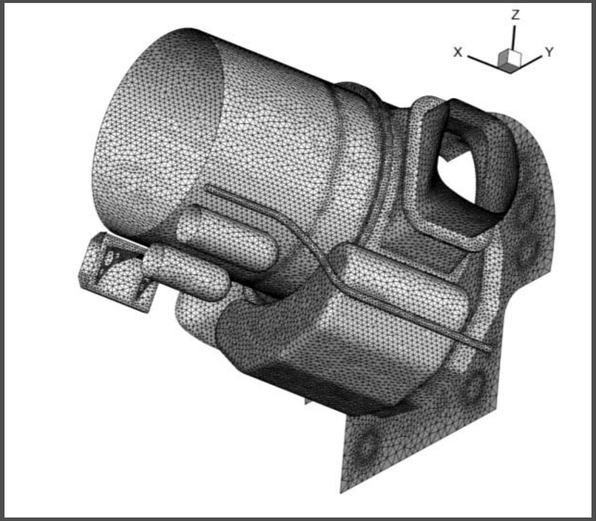

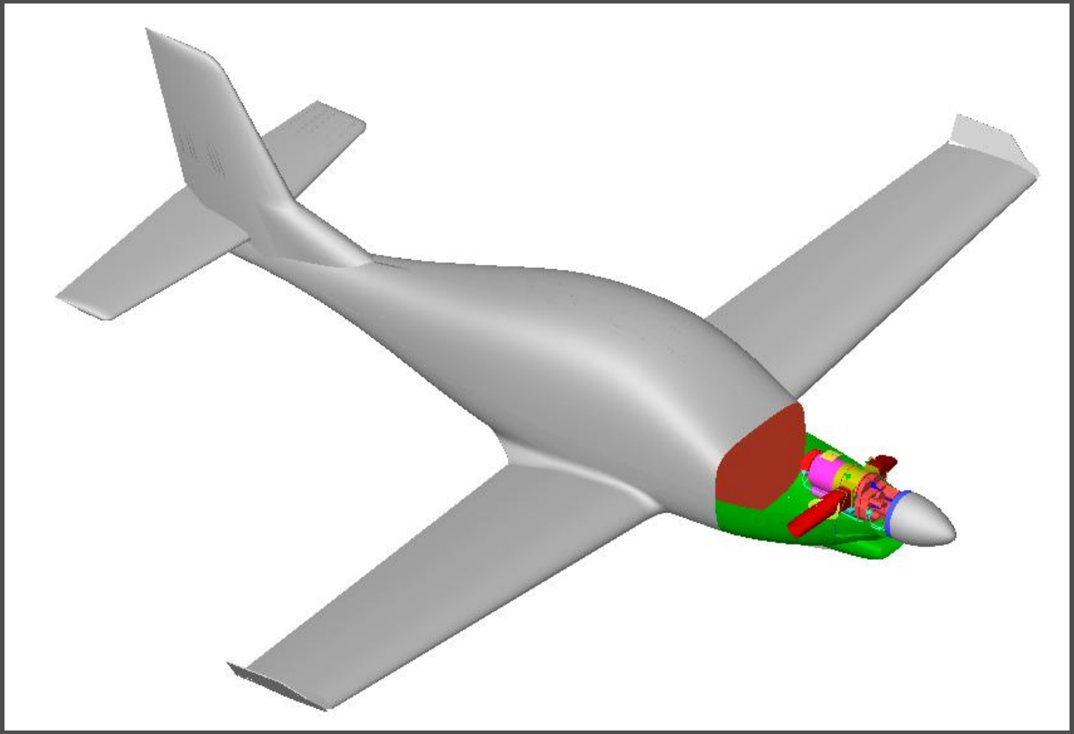

Mesh boundary division into zones

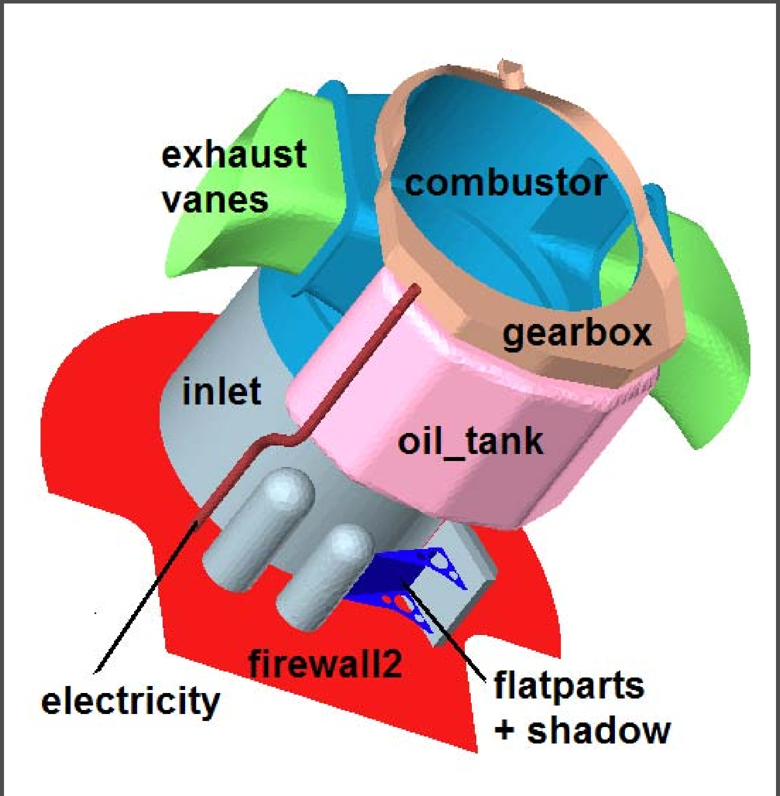

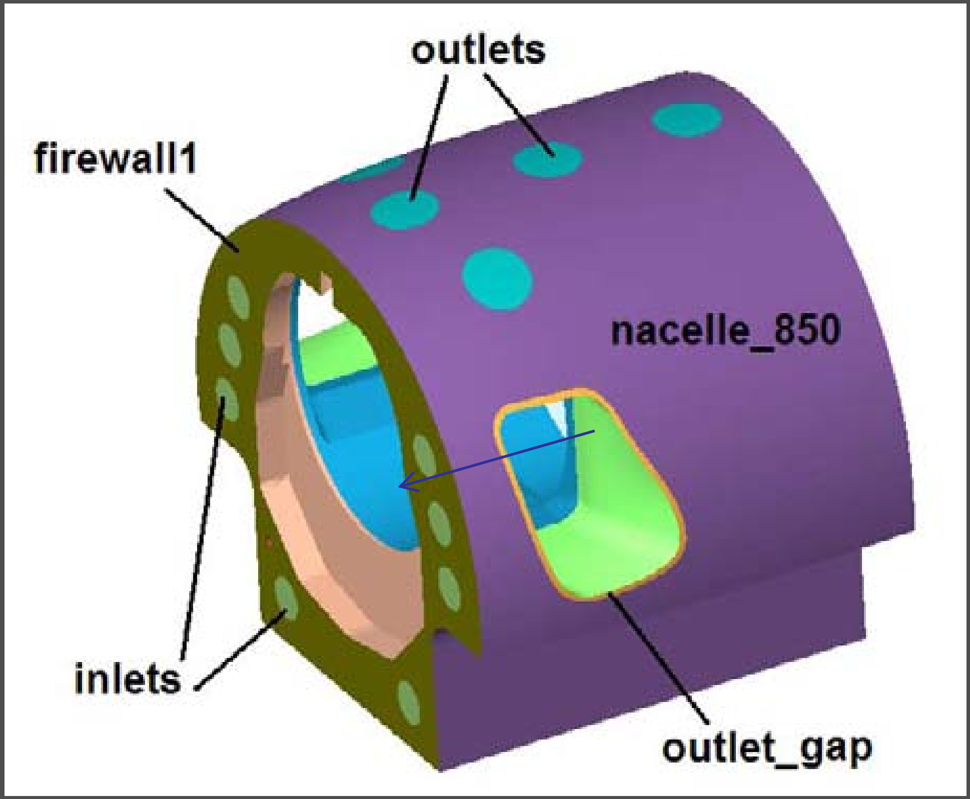

NACELLE WALL (aluminium alloy) max. allowable temp. 180 C (453 K)

COOLING OUTLETS (alternative), 15 C (288.15 K)

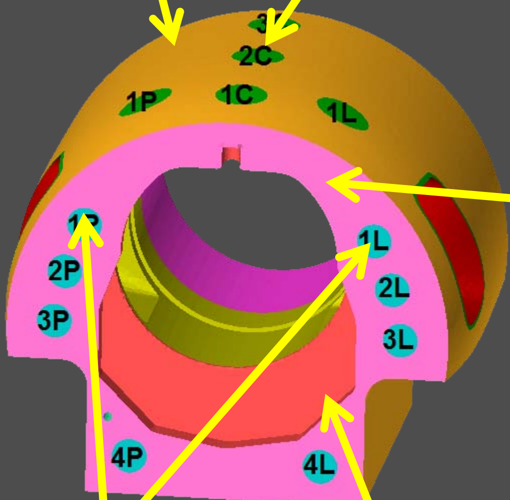

FIREWALL FRONT / AFT dQ/dt = O

COOLING INLETS (alternative), 15 C (288.15 K)*

MAIN GEARBOX, 100 C (373 K)

EXHAUST VANES, Steel 1.5 mm, hot gases temperature inside: 650 C (923K)

COMBUSTOR CHAMBER 220 C (493 K)

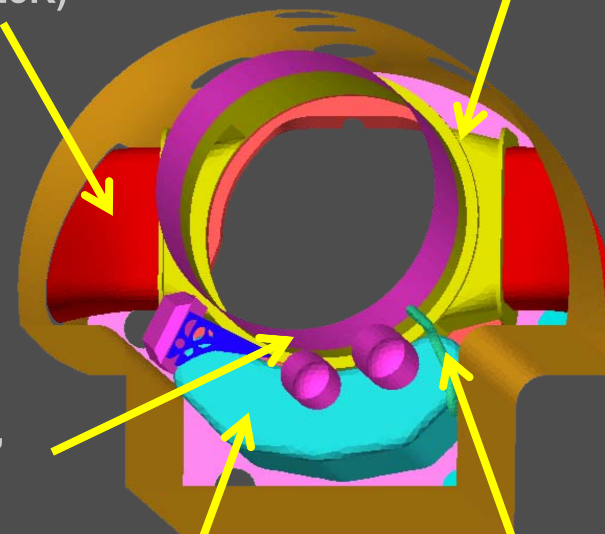

COMPRESSOR, 235 C (508 K)

OIL TANK 100 C (373 K)

ELECTRICAL INSTALLATION, 60 C (333 K)

*Dynamic pressure on inlets corresponding to 150 km/h stagnation pressure

INLETS AND OUTLETS DEFINITION

A mesh has been equipped with **all inlets and outlets**, on which user **can set**, if this is a **wall or opening**.

Naming sequence has been assumed **as self explaining**:

1 – forward, top,

4 – backward, bottom

L-Left

C- Center

P- Right (pol. „Prawy”, for curiosity)

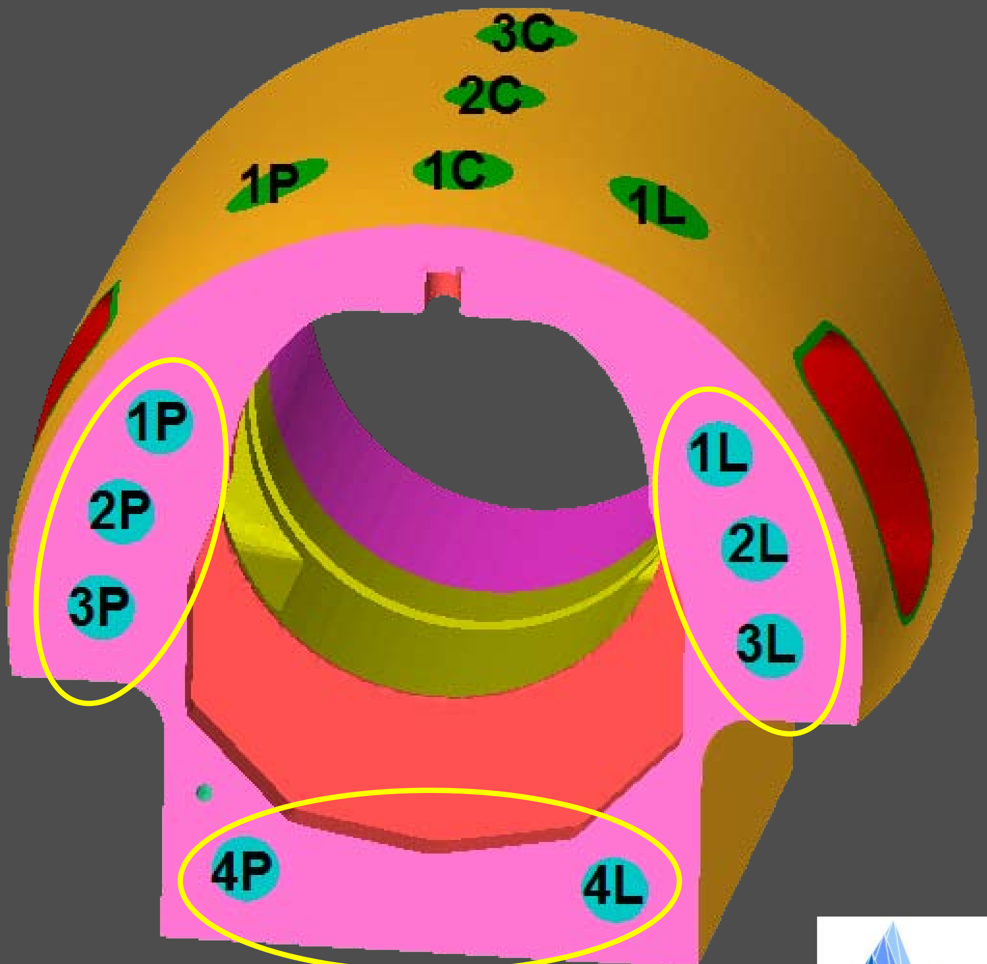

INLET POSITION CASES

Case **naming system** has been assumed as **straight – forward**

case name:

2L2P 3C

means:

Open inlets: **2L i 2P**

Open outlet **3C**

Only exception:

+G means, that only **the gap around exhaust vane** is open

1L1P 3C

2L2P 3C

3L3P 3C

4L4P 3C

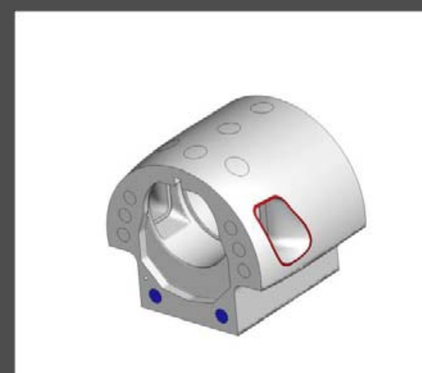

4L4P +G

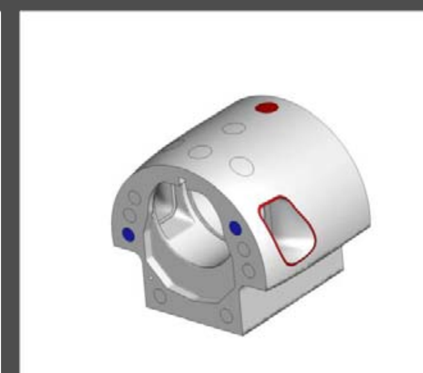

1L3P 3C

Surface Temperature Comparison

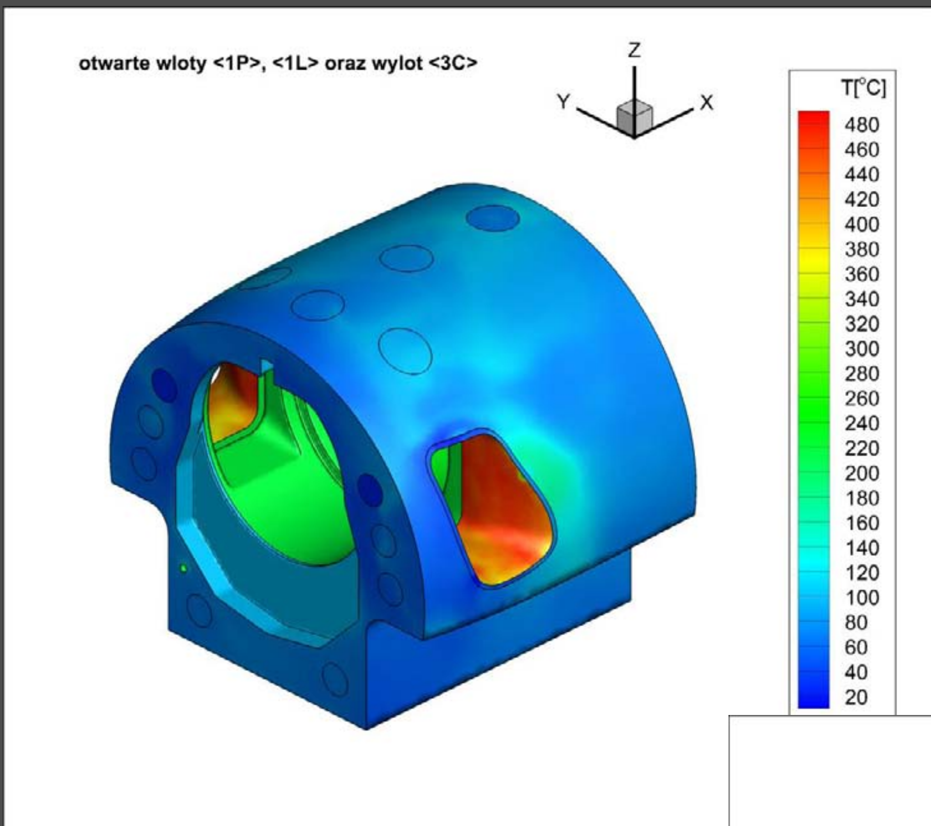

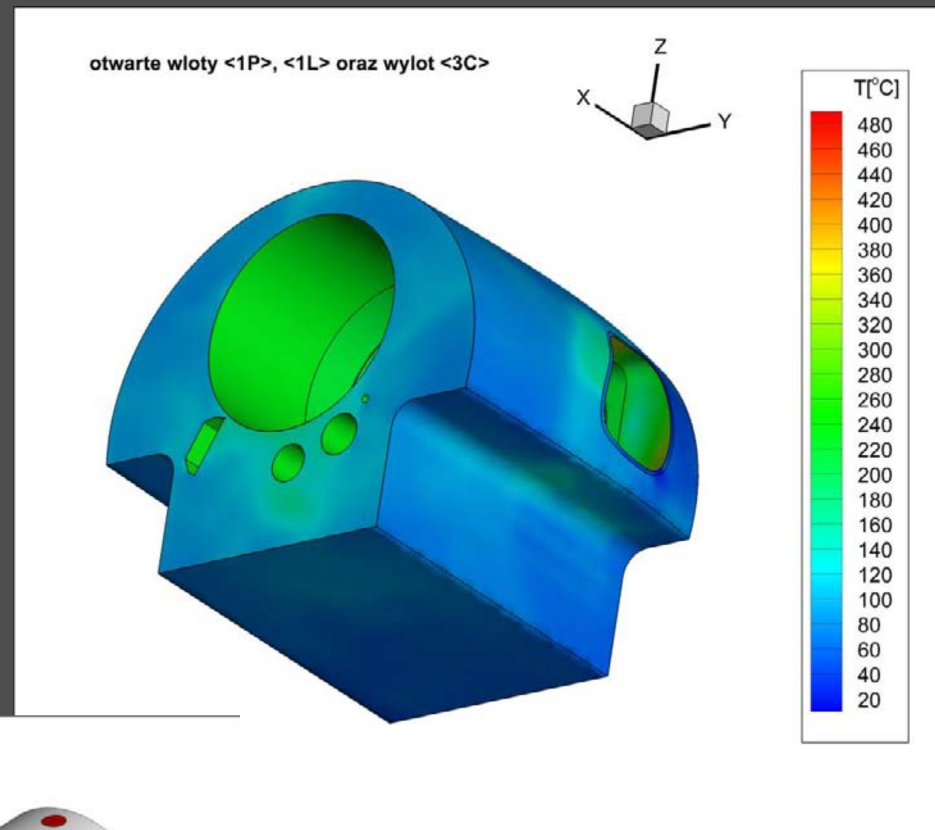

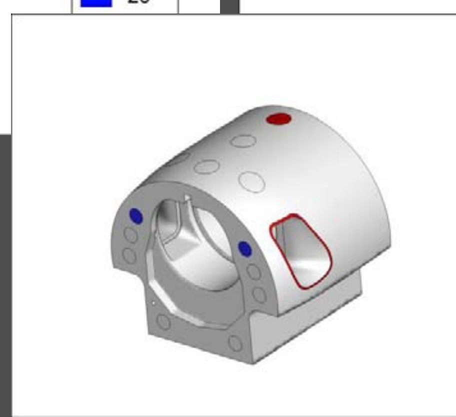

1L1P 3C

Inlet position influence

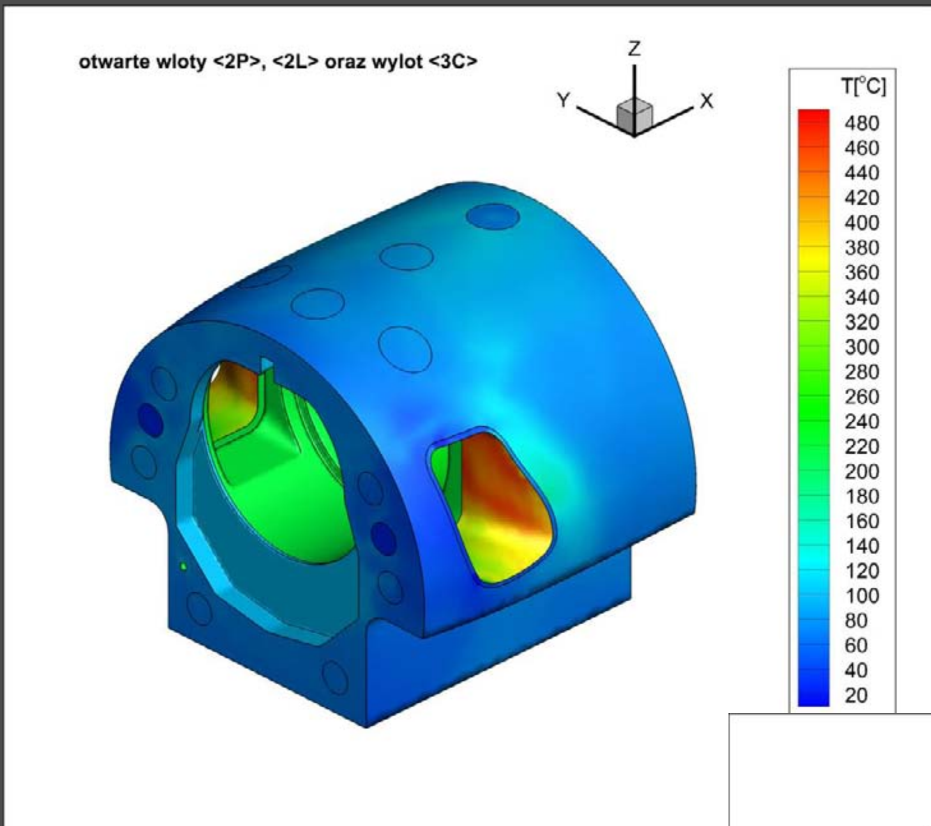

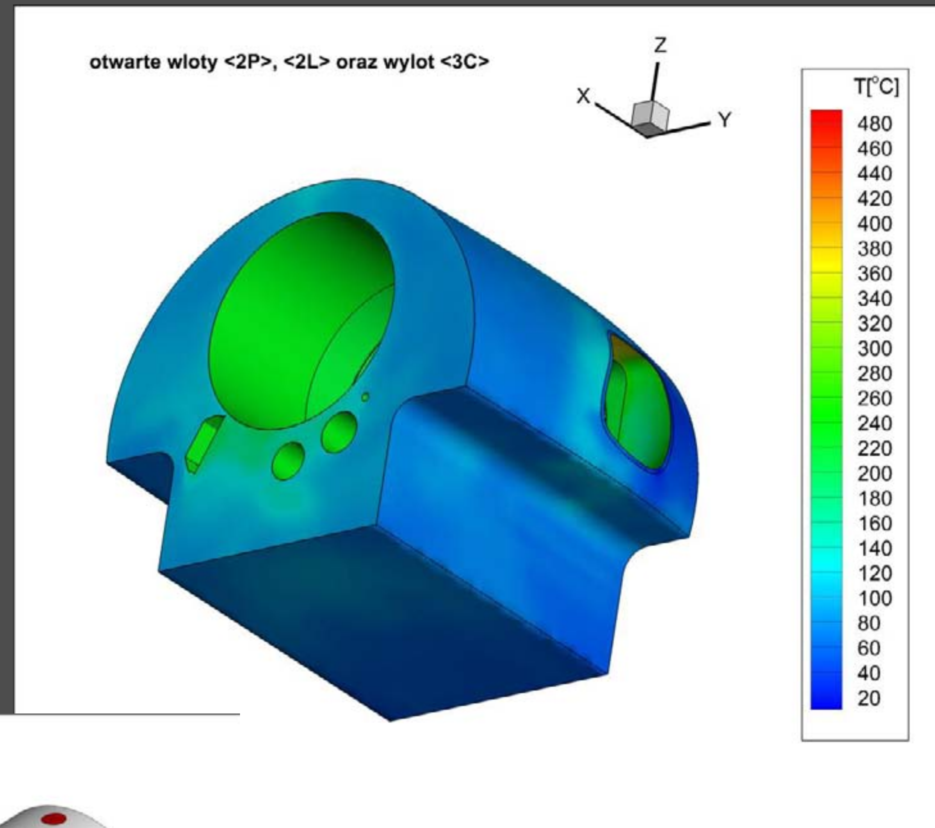

2L2P 3C

Inlet position influence

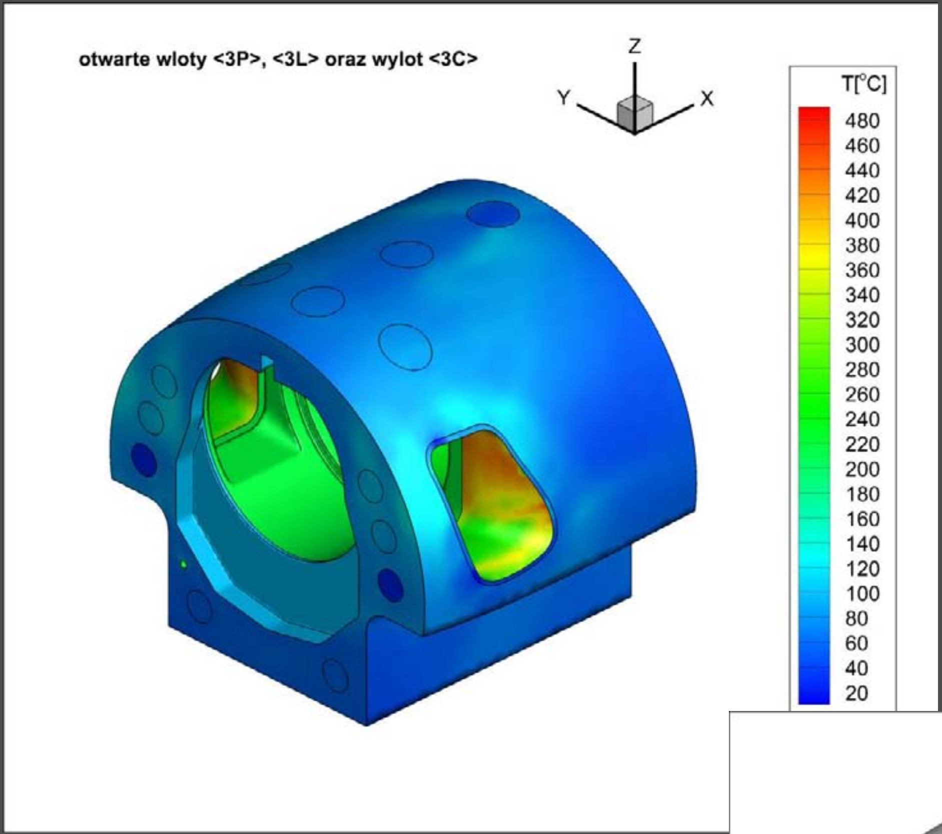

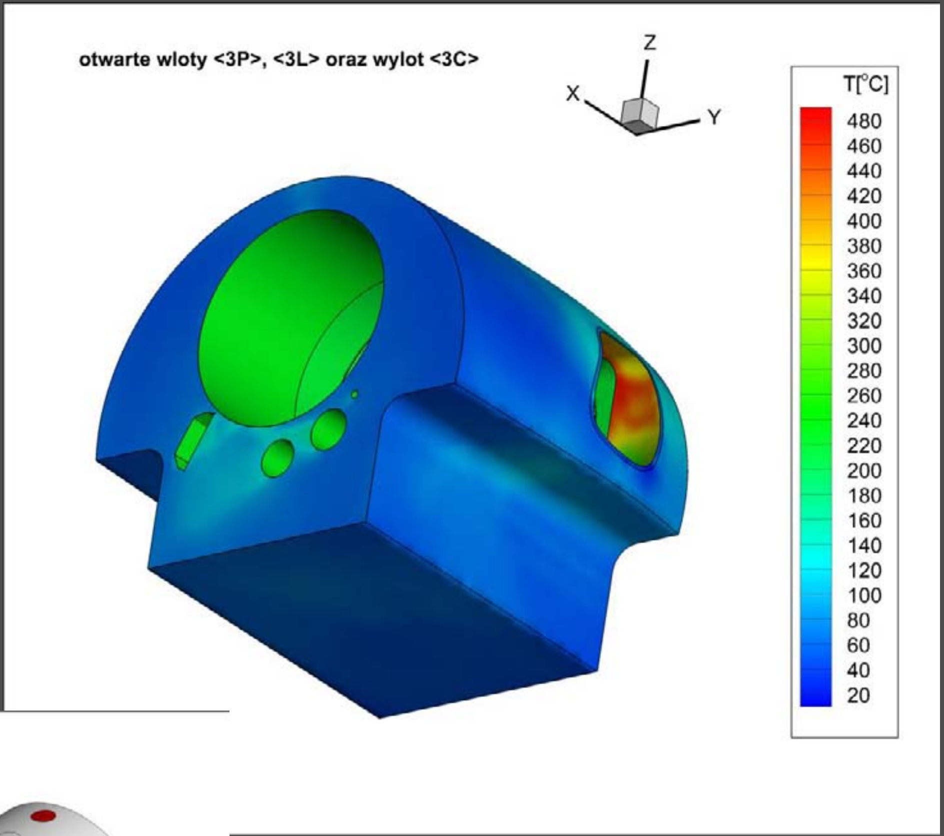

3L3P 3C

Inlet position influence

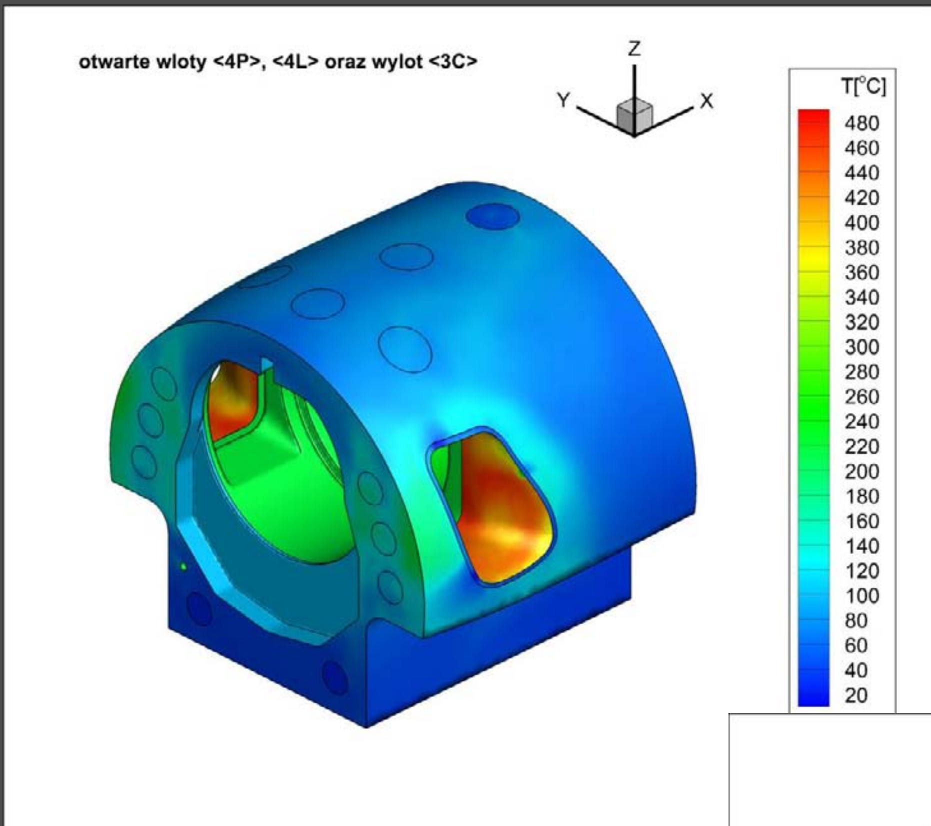

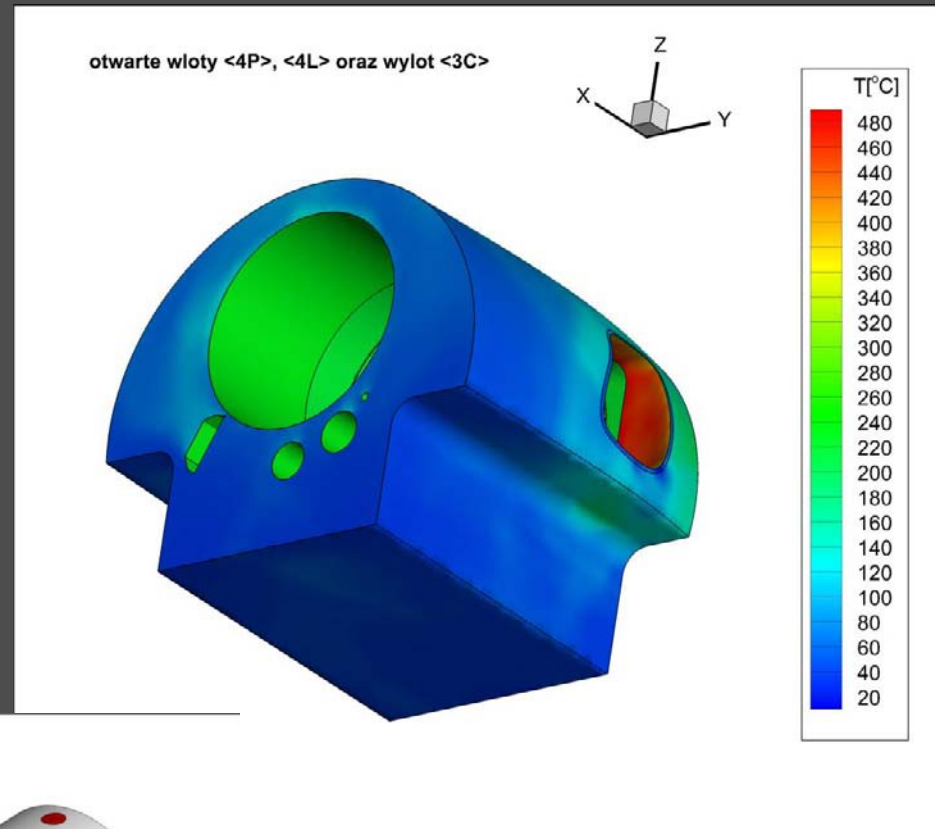

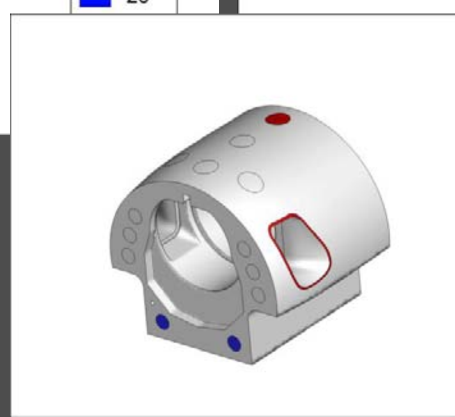

4L4P 3C

Inlet position influence

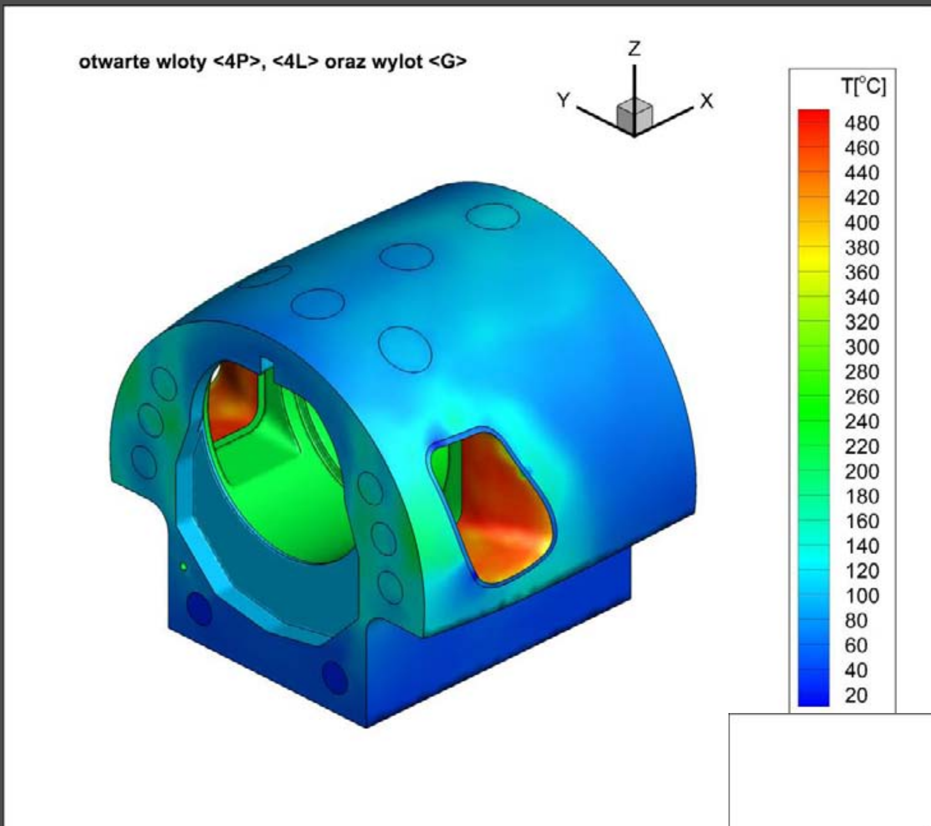

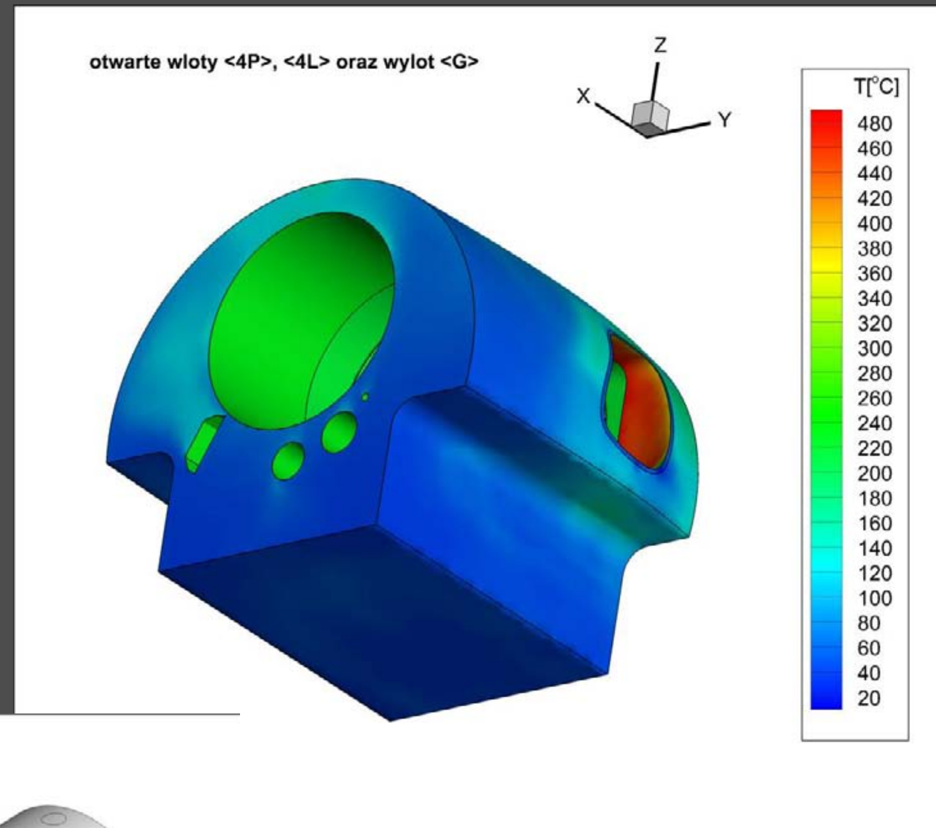

4L4P +G

Inlet position influence

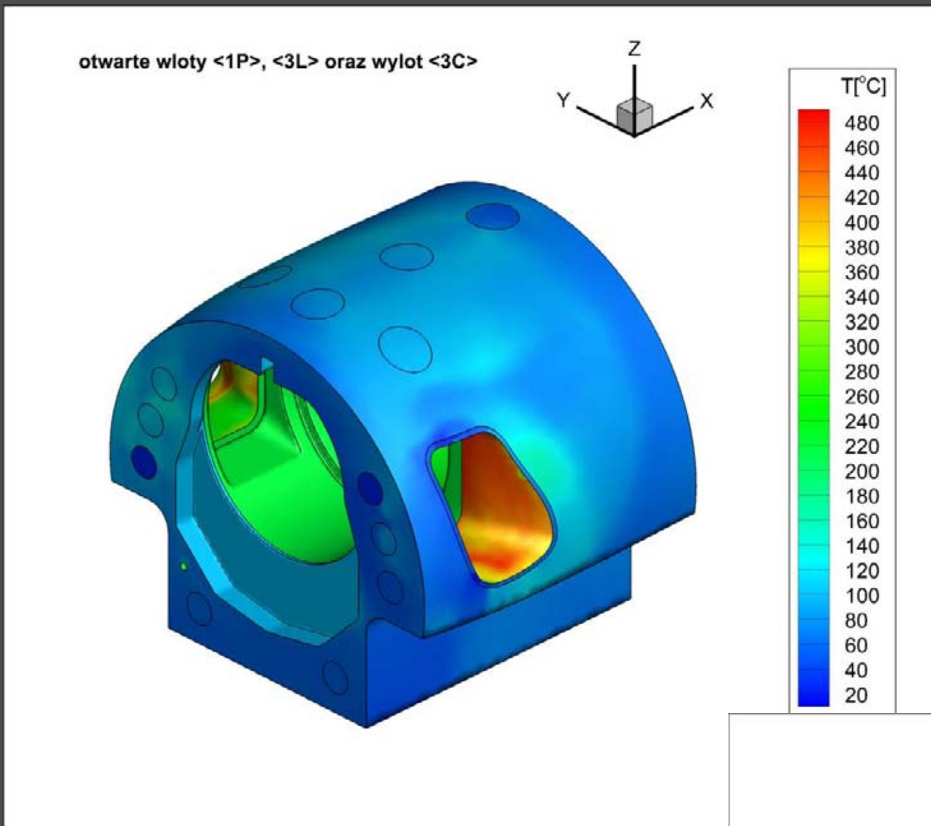

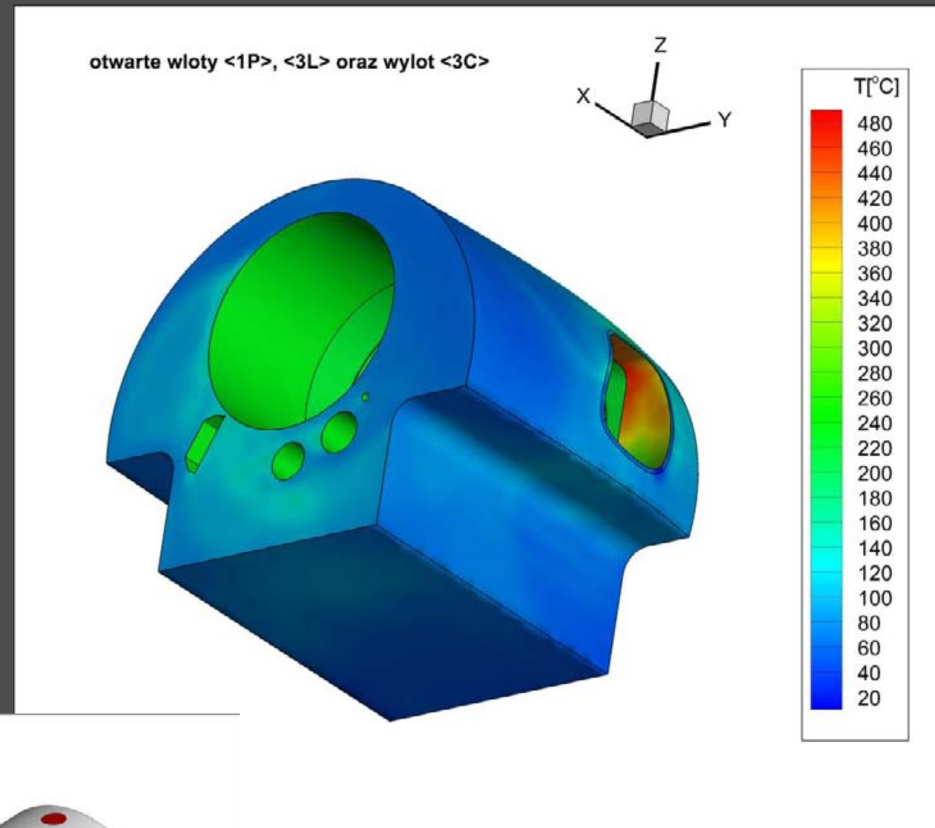

1L3P 3C

Inlet position influence

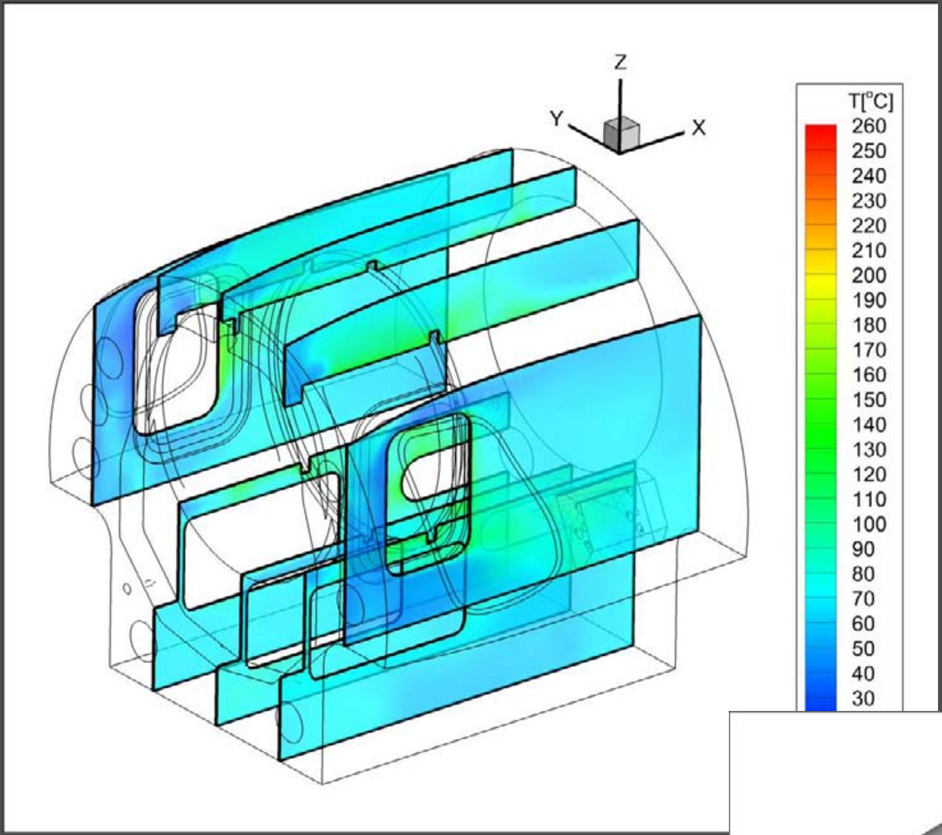

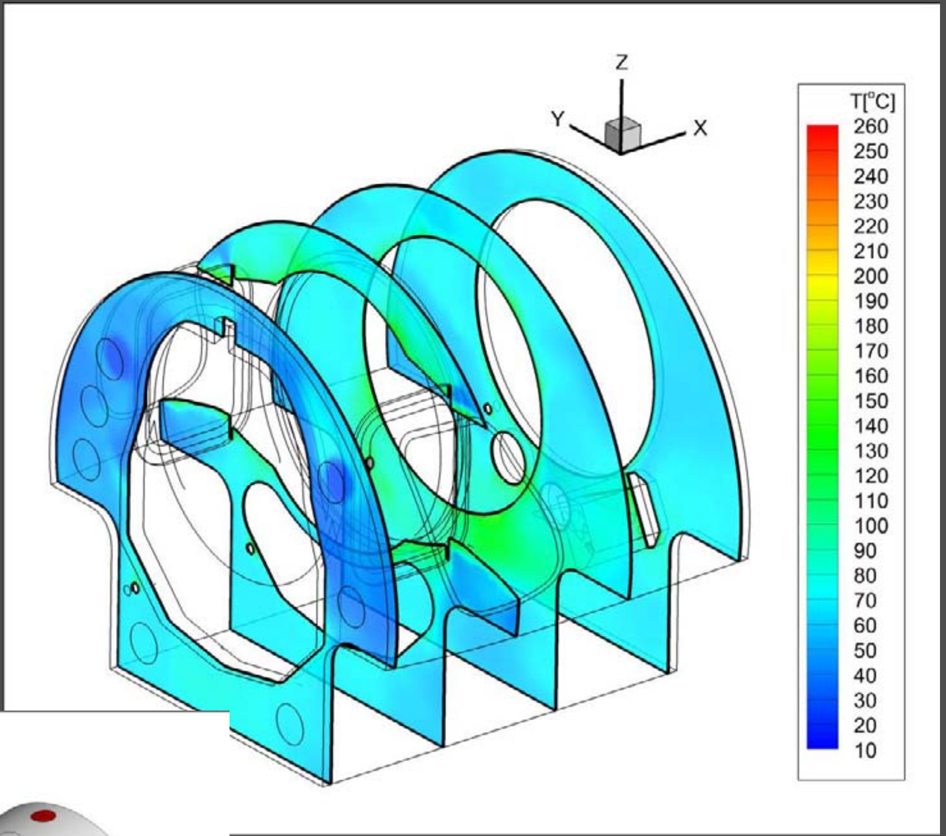

Inlet position influence

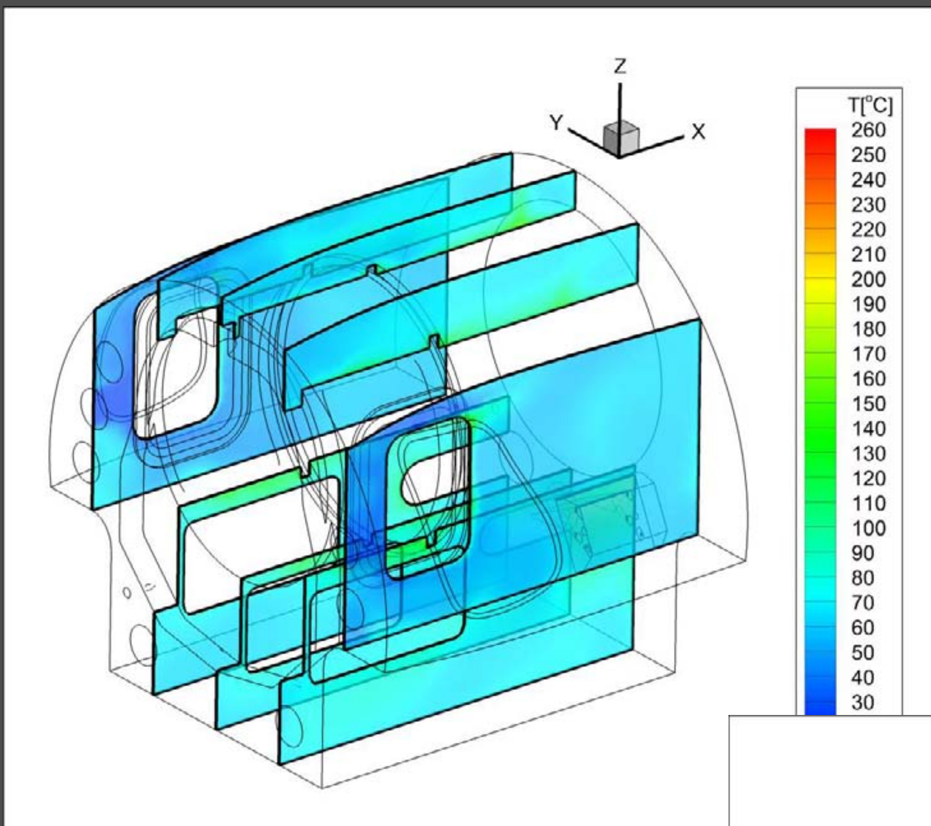

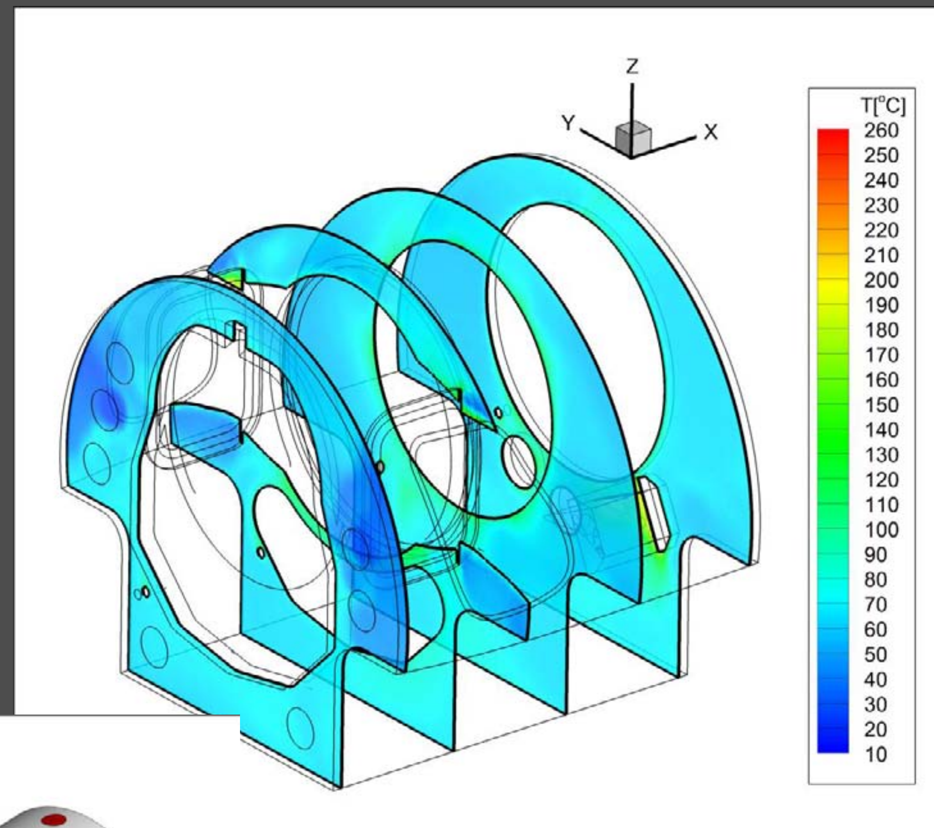

Inlet position influence

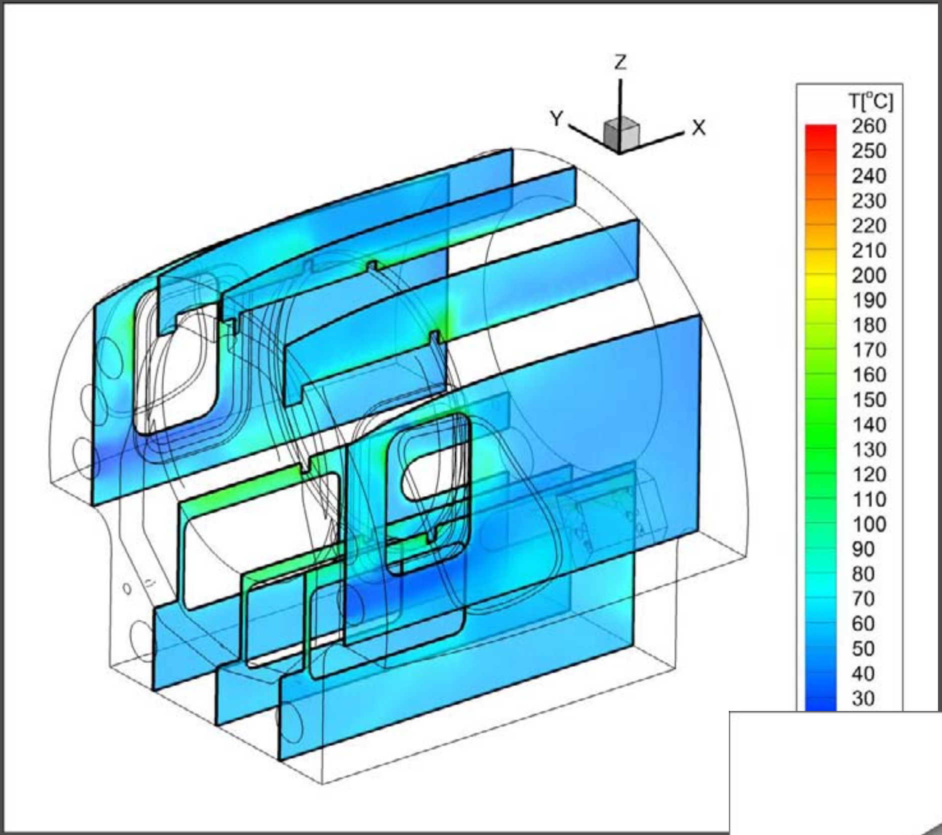

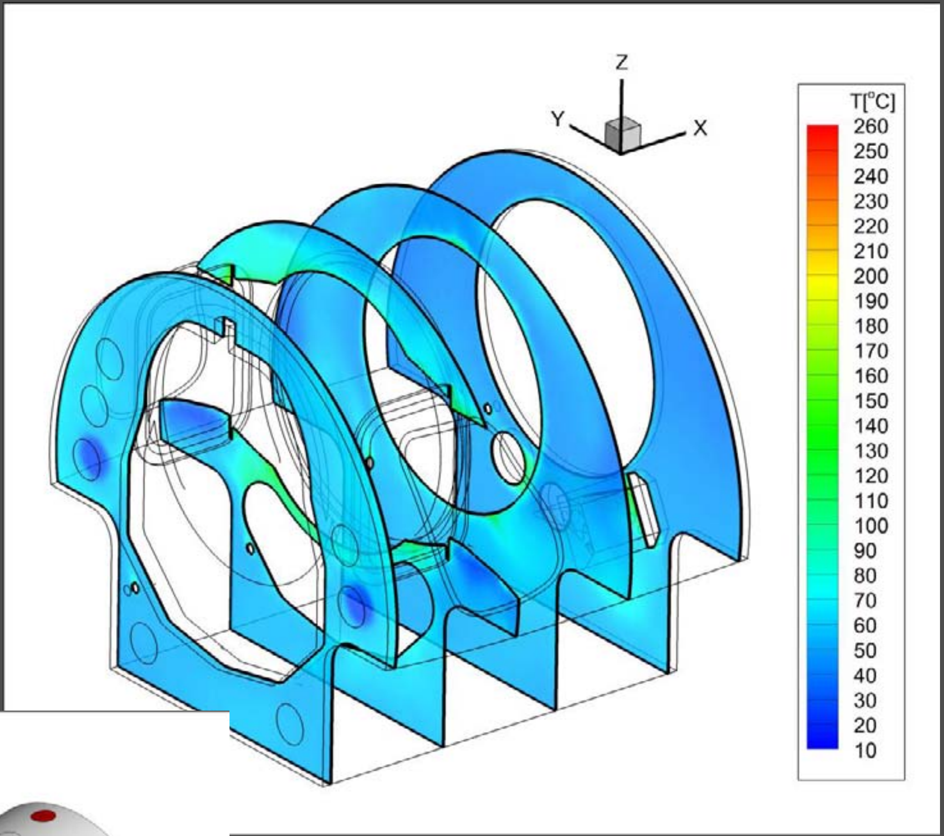

Adam Dziubiński

Inlet position influence

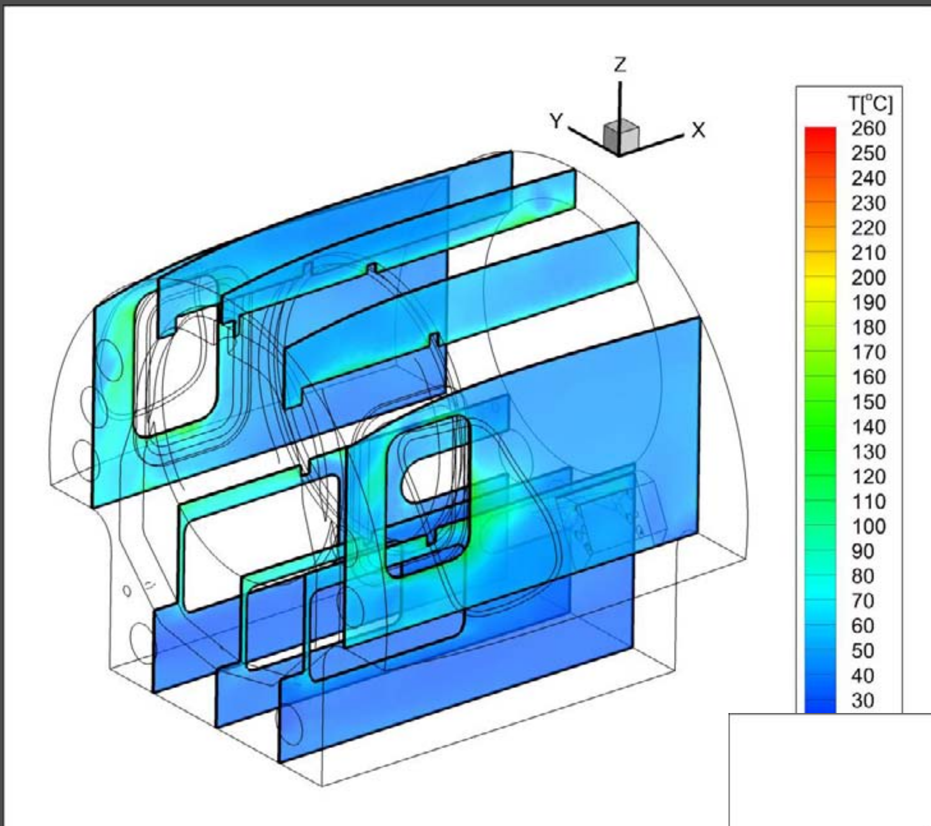

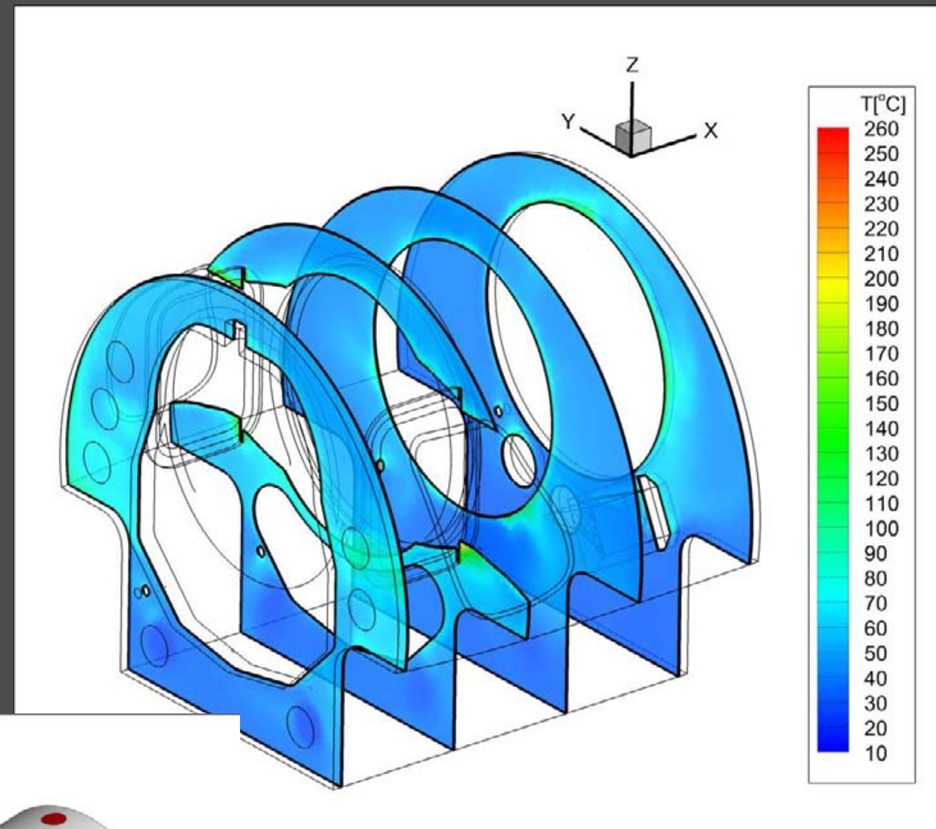

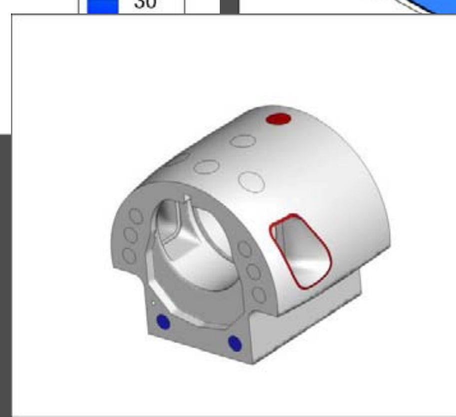

institute of aviation
warsaw, since 1926

Inlet position influence

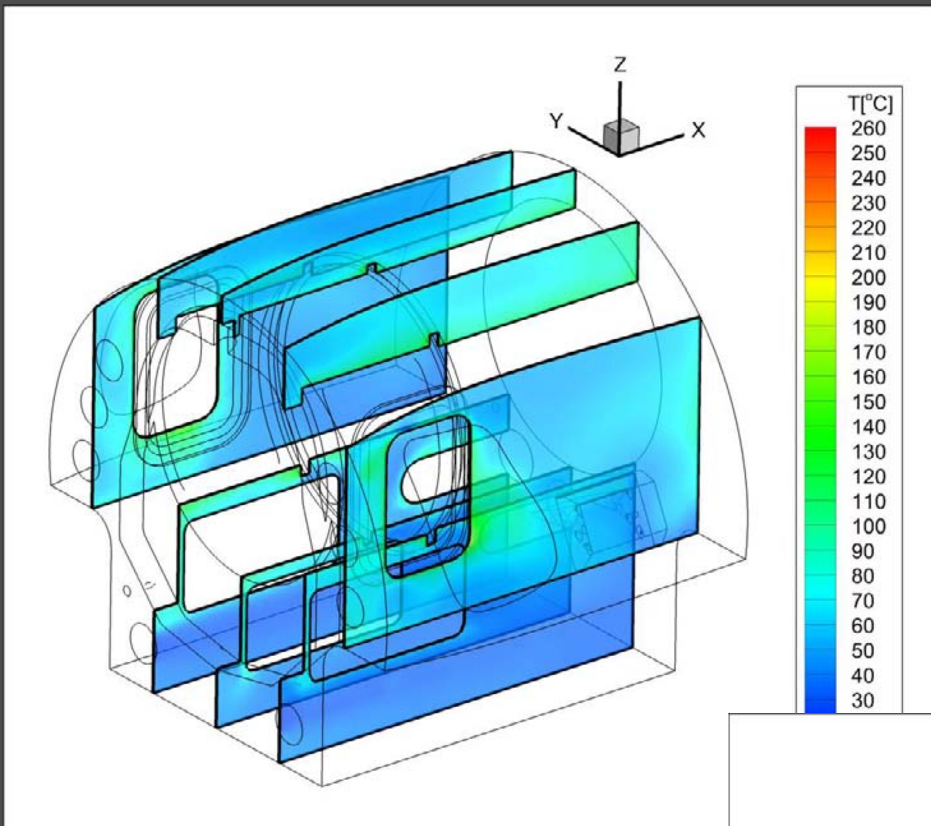

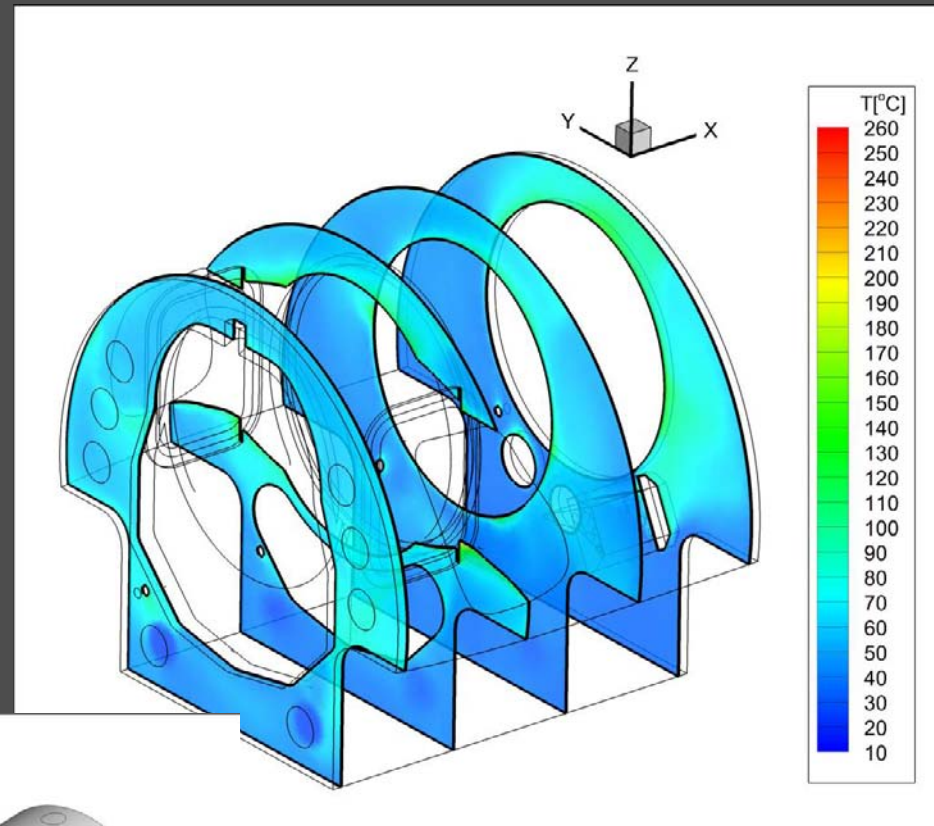

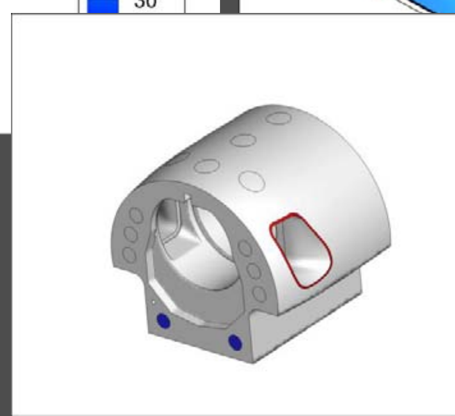

4L4P +G

Inlet position influence

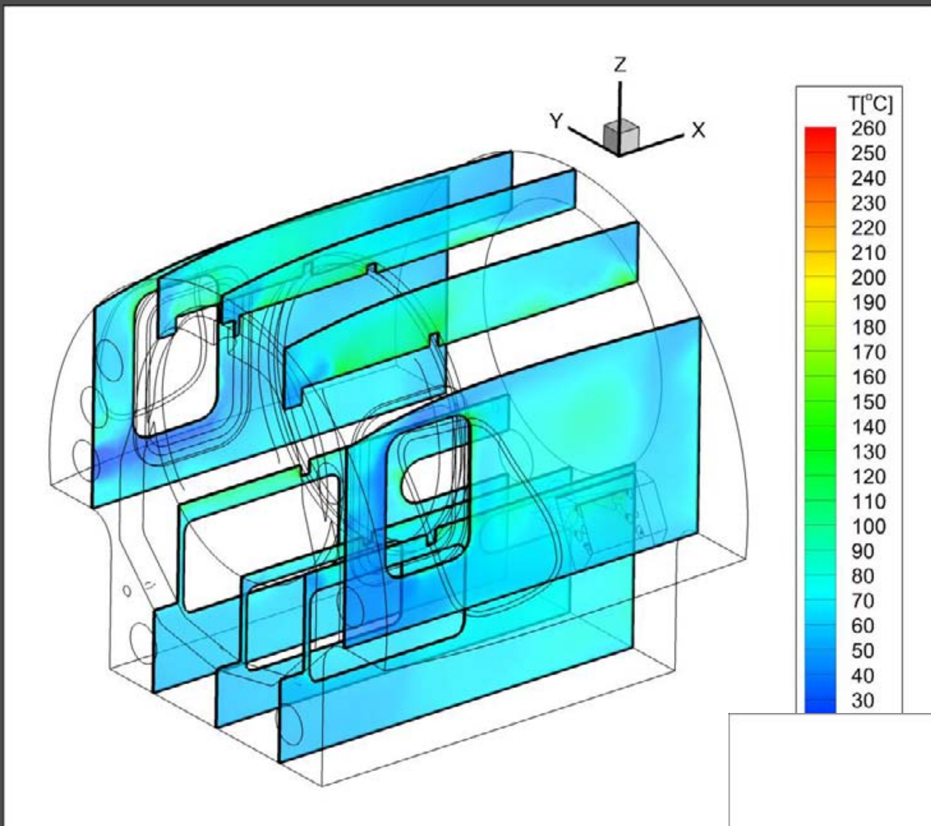

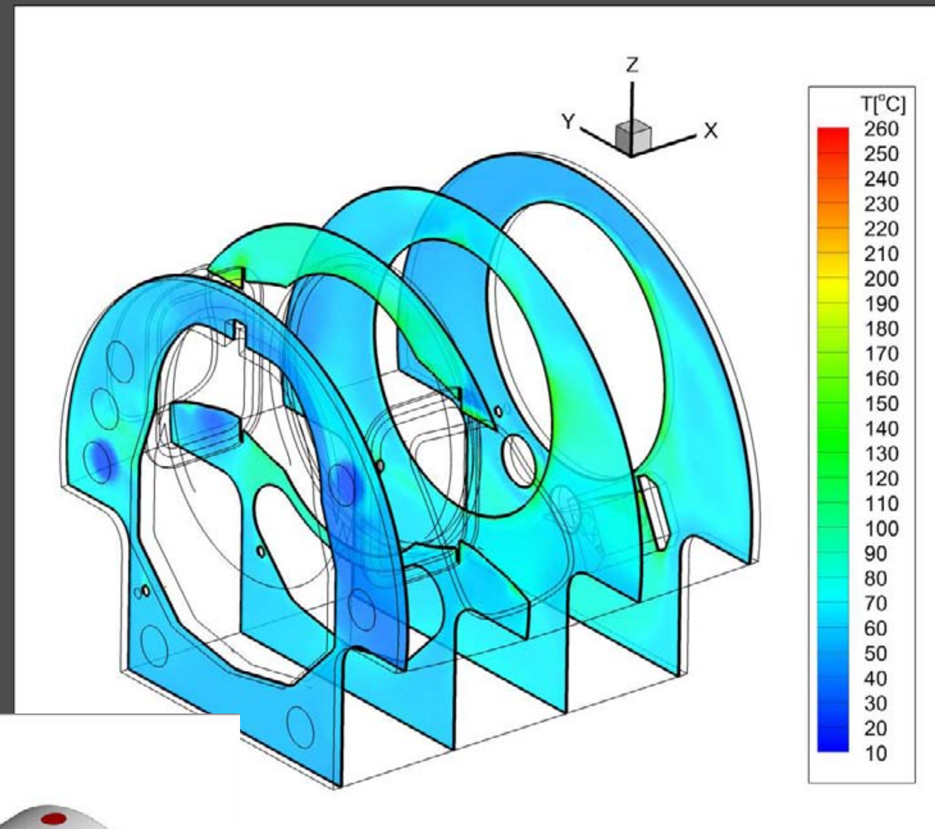

institute of aviation
warsaw, since 1926

Inlet position influence

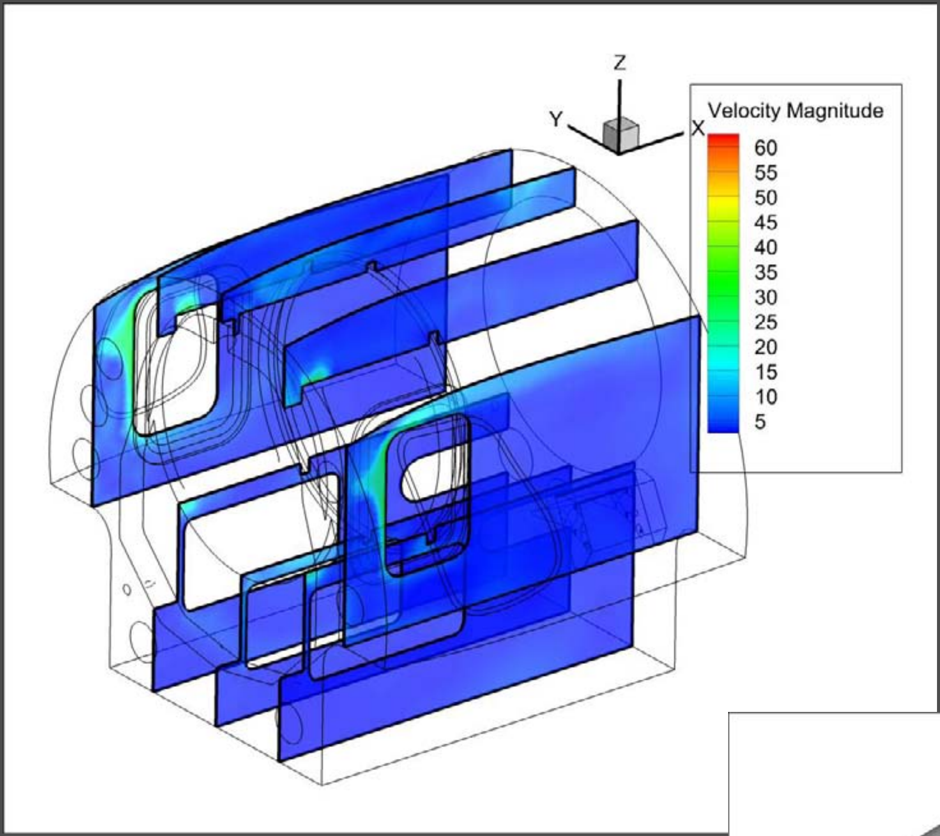

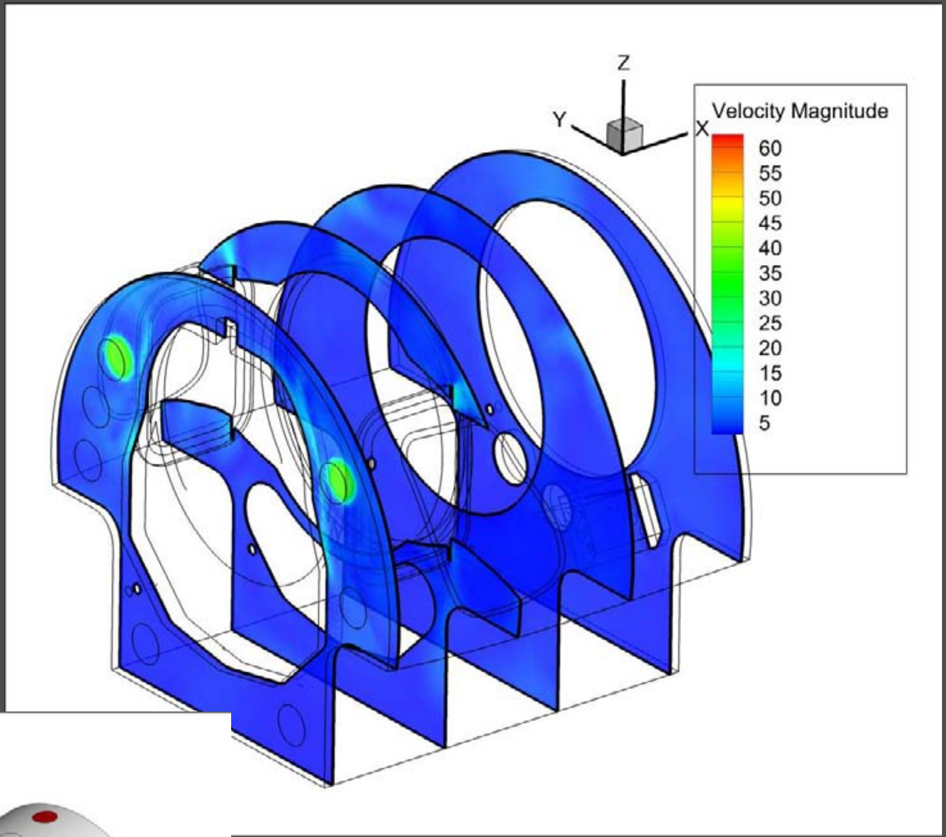

research for future

1L1P 3C

easn

Inlet position influence

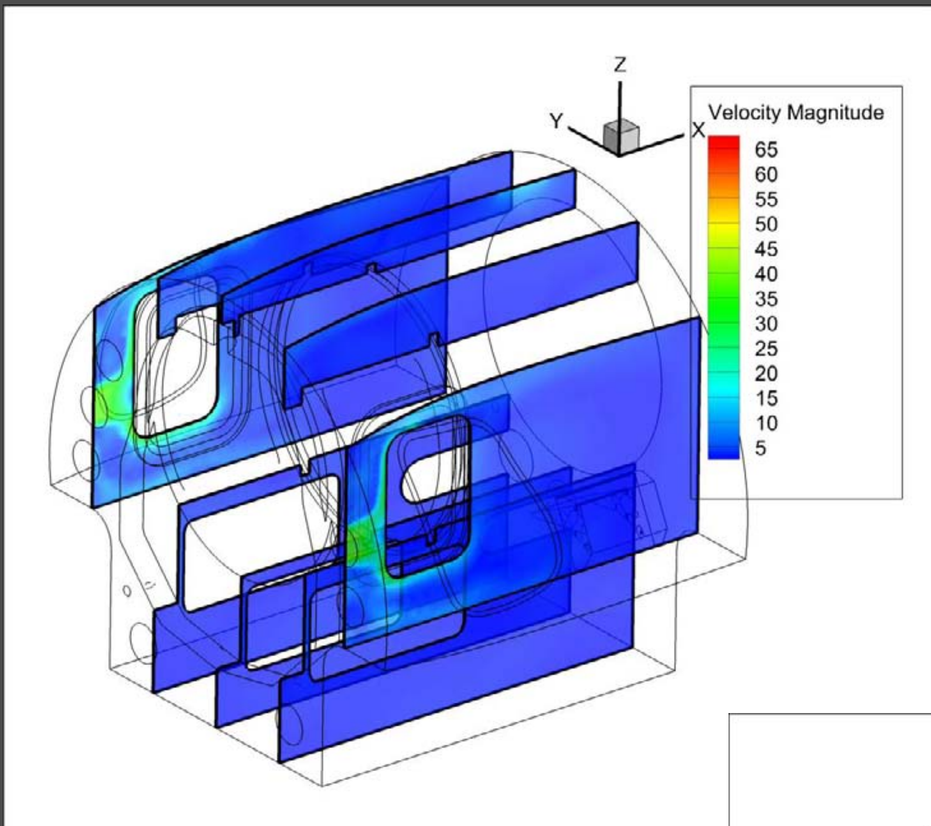

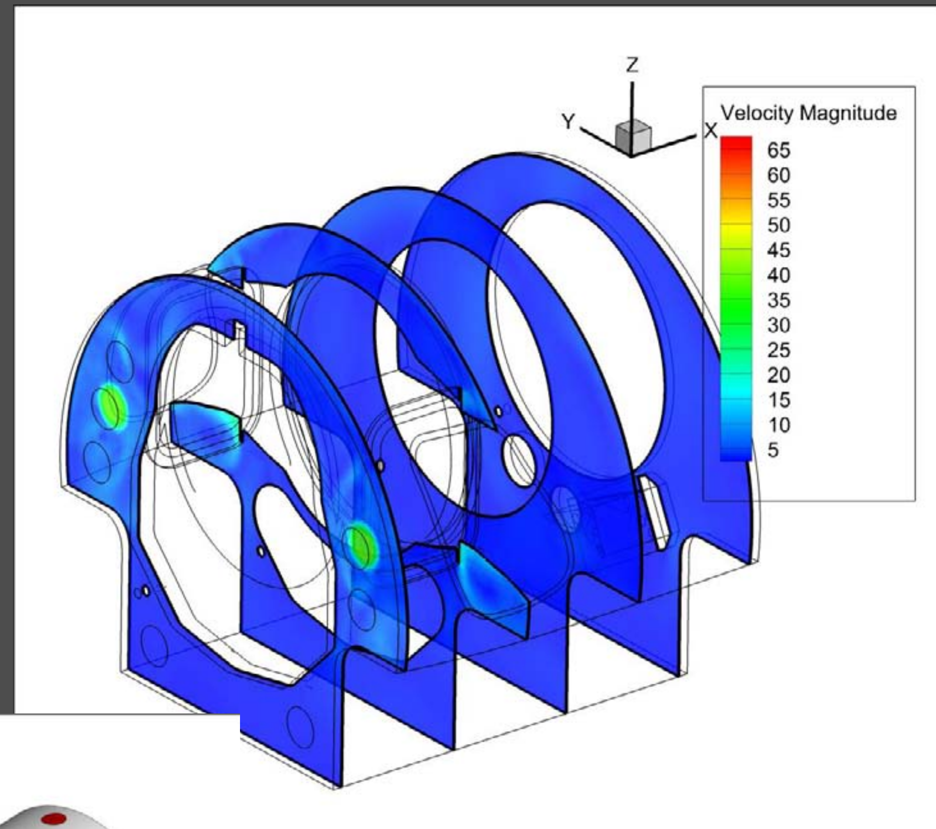

Inlet position influence

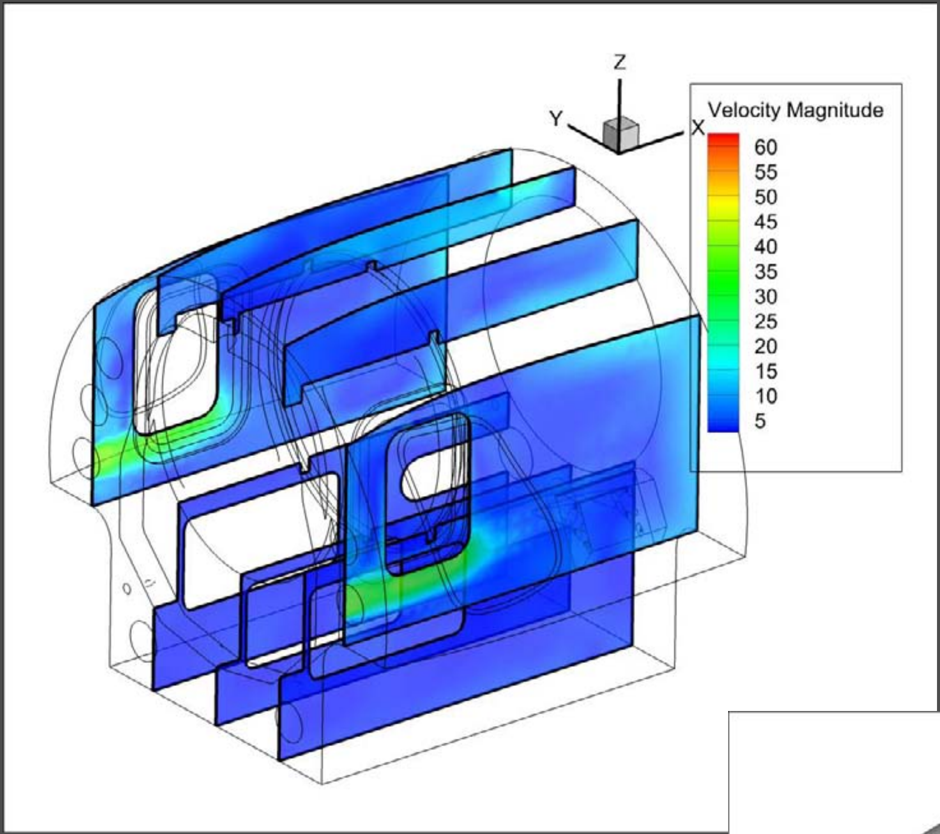

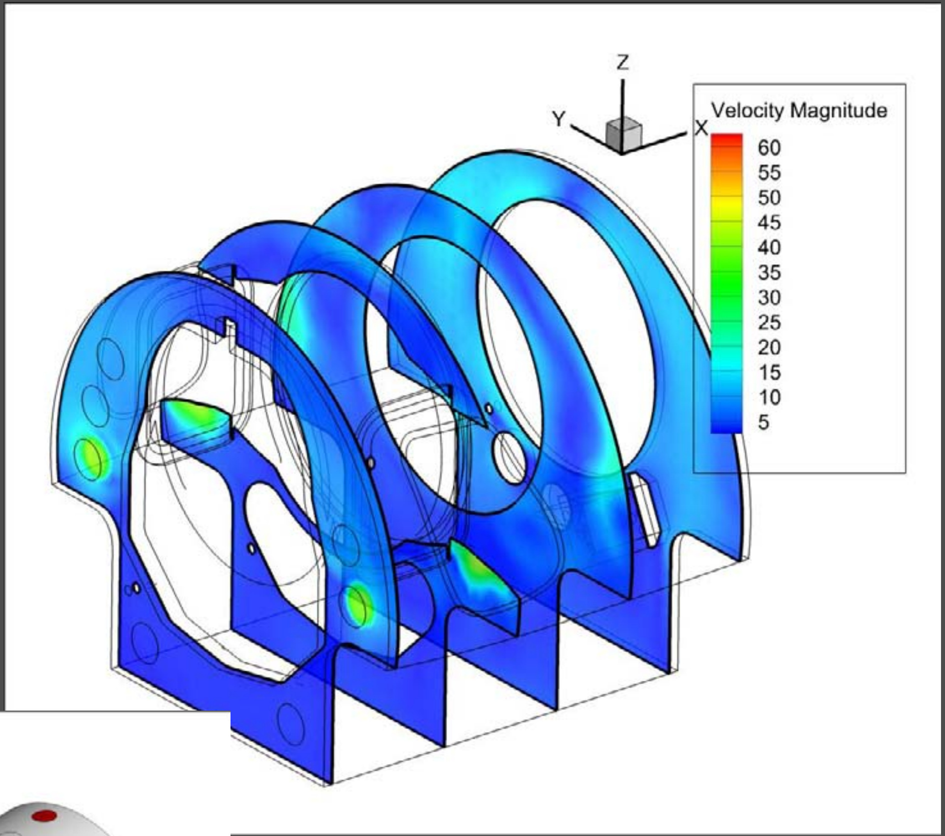

Inlet position influence

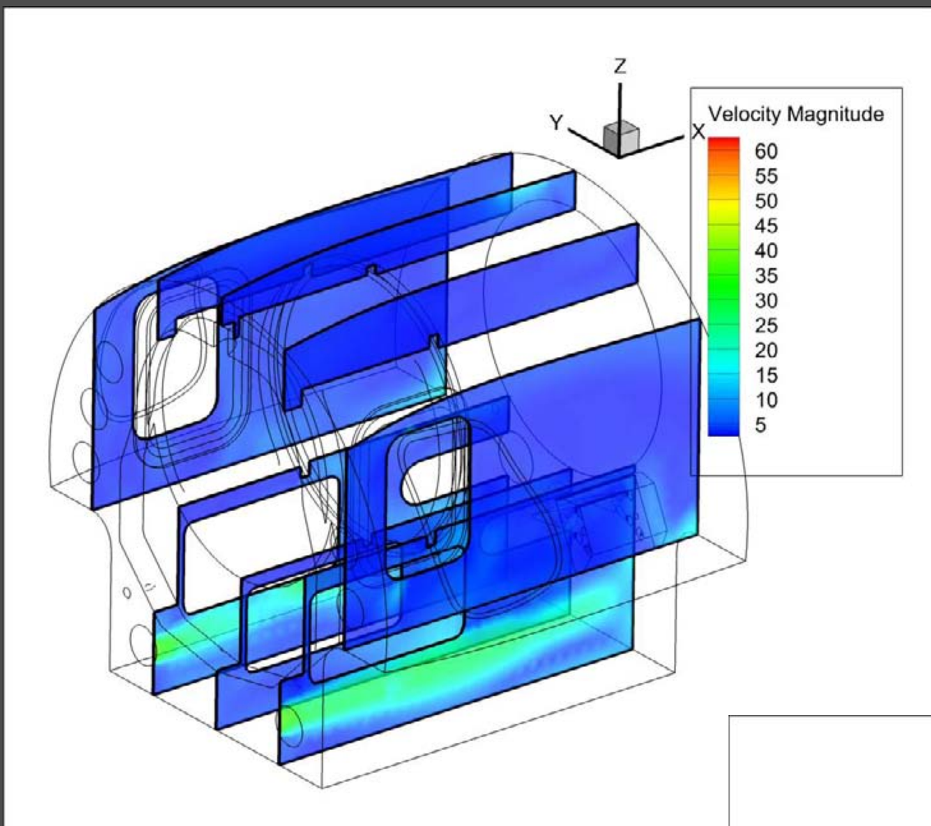

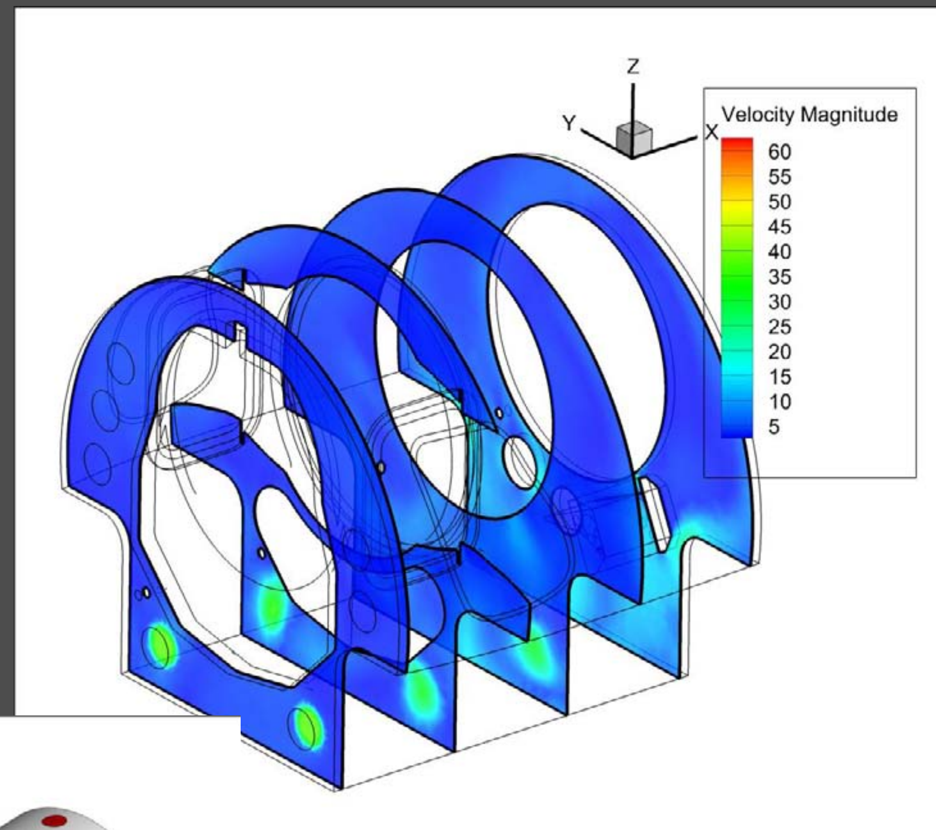

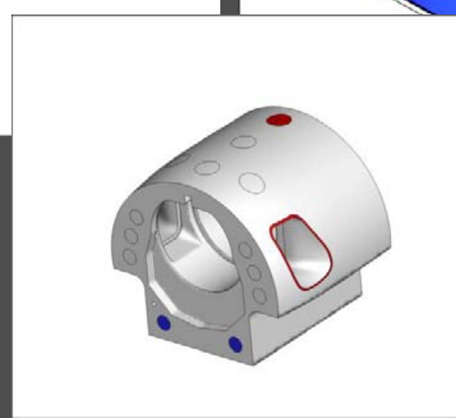

Inlet position influence

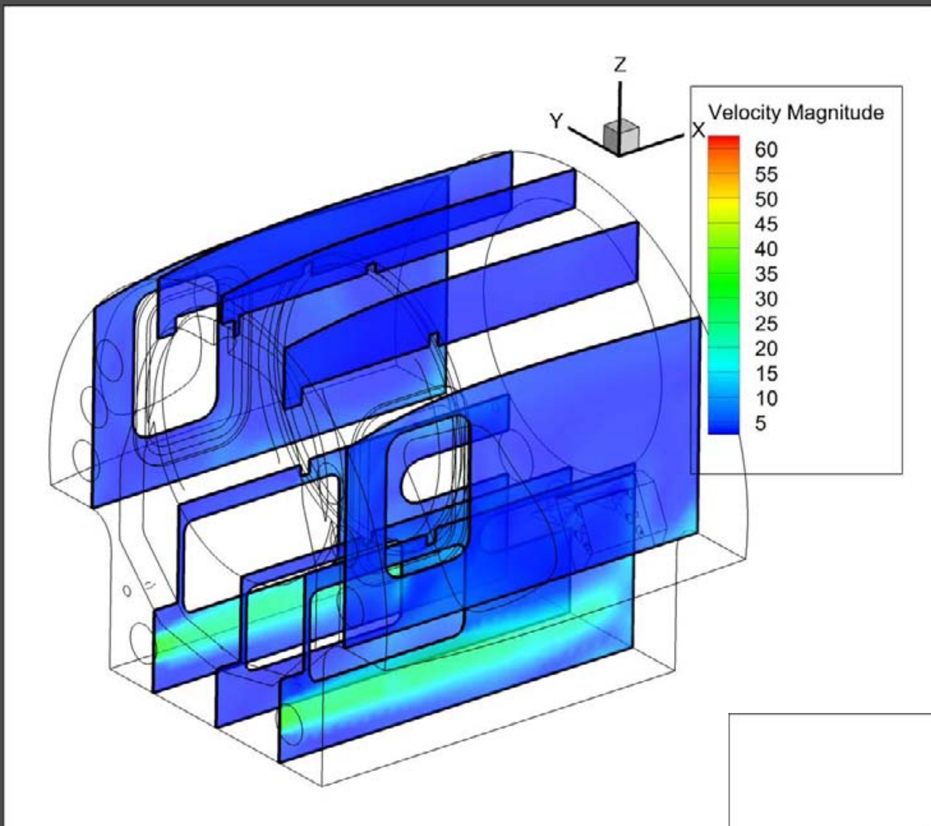

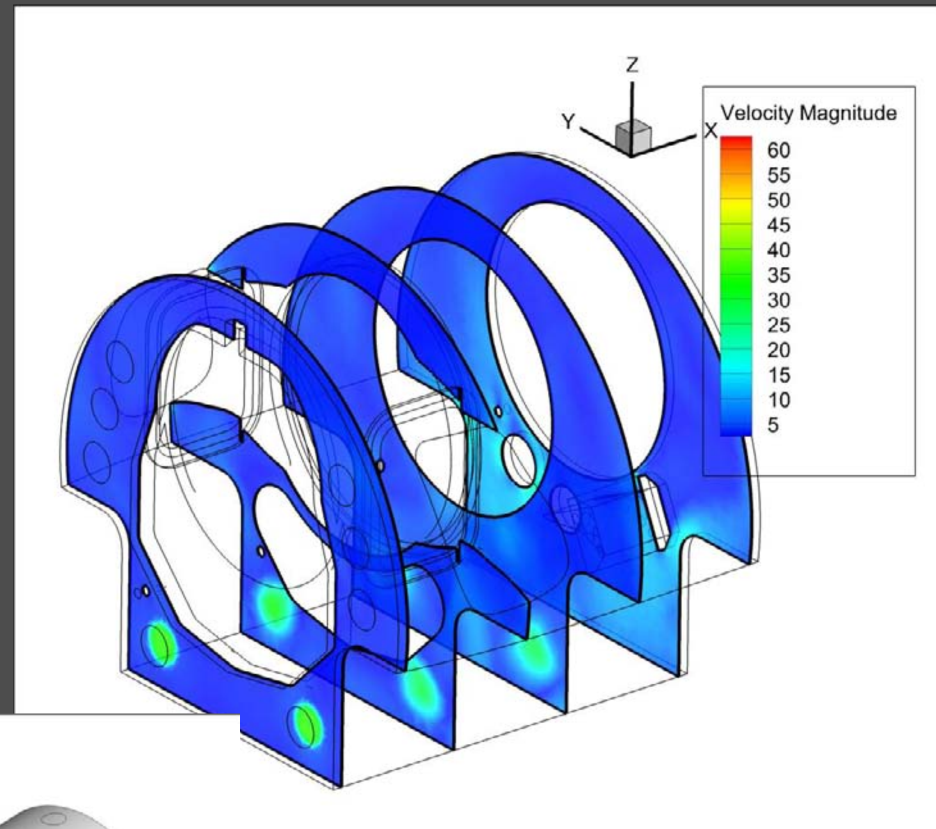

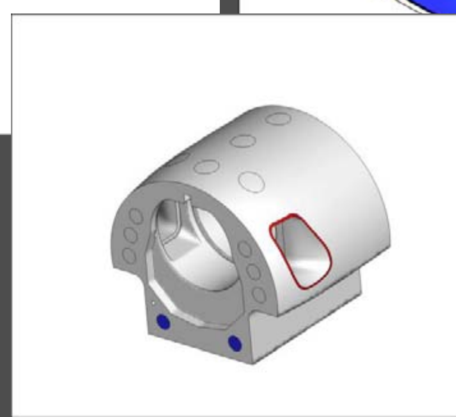

instituteofaviation
warsaw, since 1926

Inlet position influence

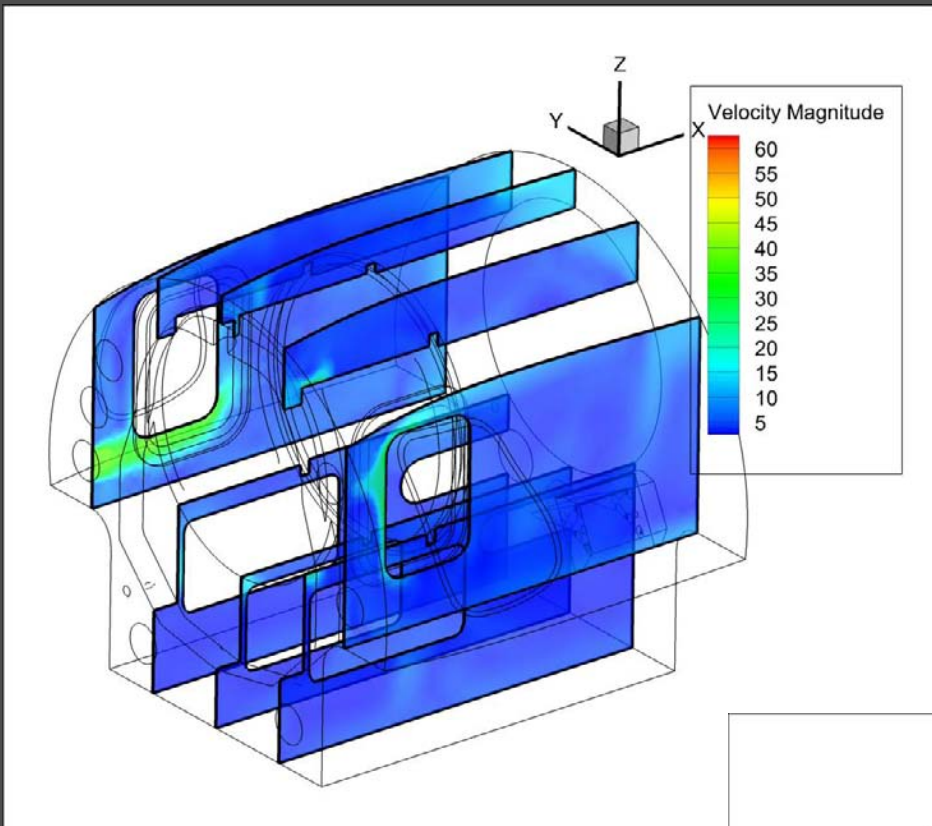

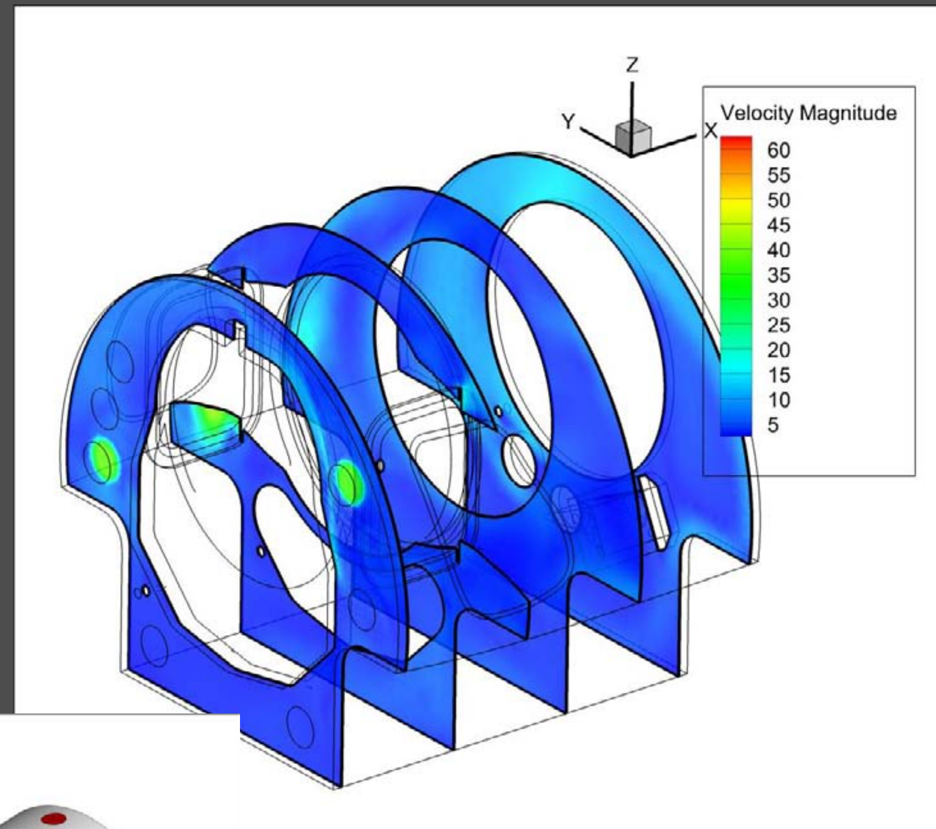

research for future

1L3P 3C

easn

Convection Heat Flux Sources and Receivers

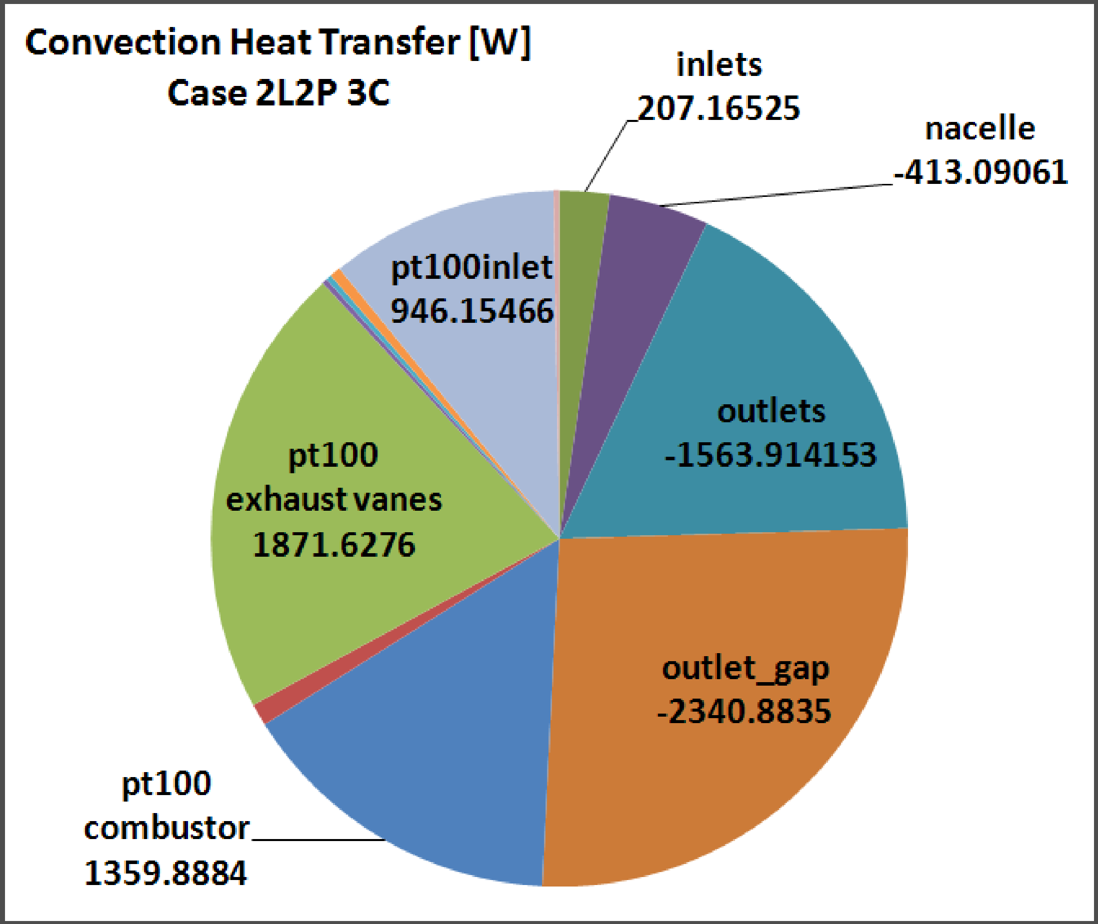

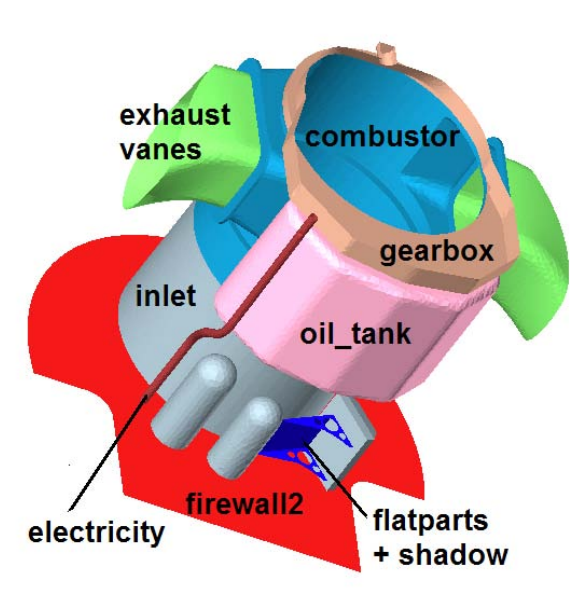

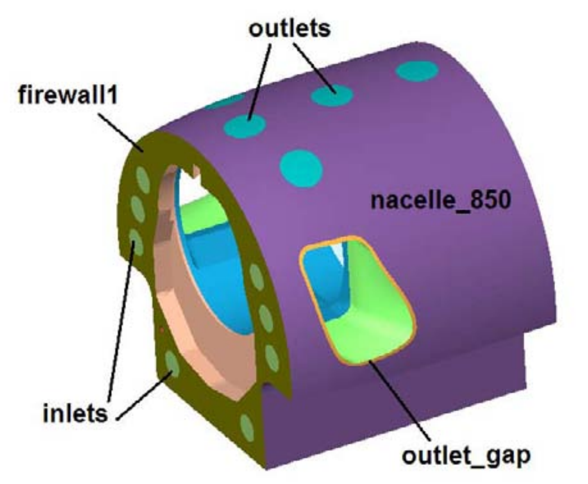

Boundaries that have biggest part in heat flow, these proportions are similar in all cases.

Convection Heat Transfer Rate

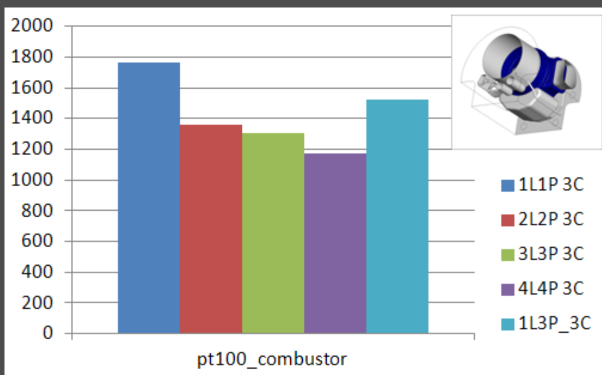

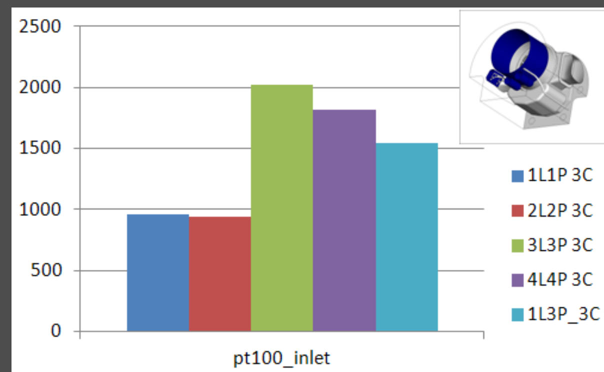

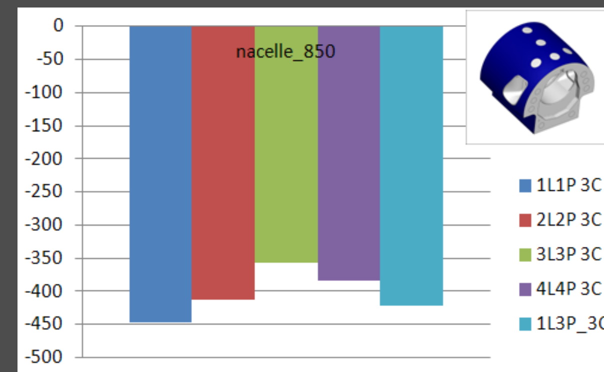

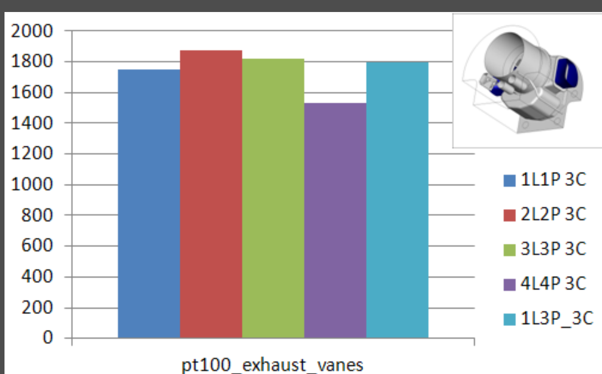

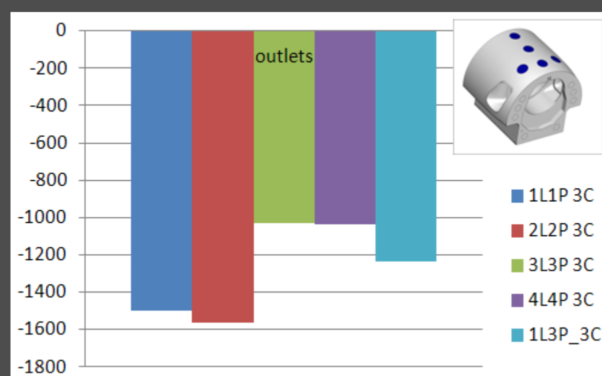

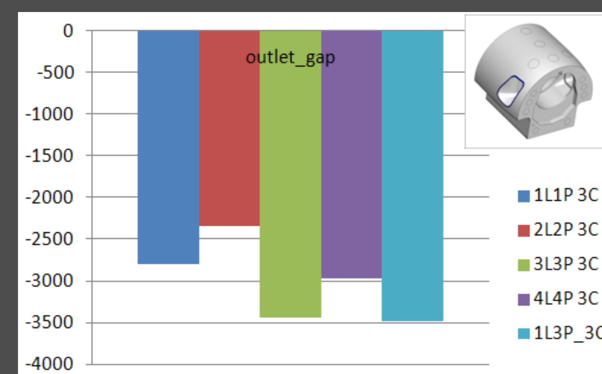

Inlet Analysis Radiation Heat Flux Sources and Receivers

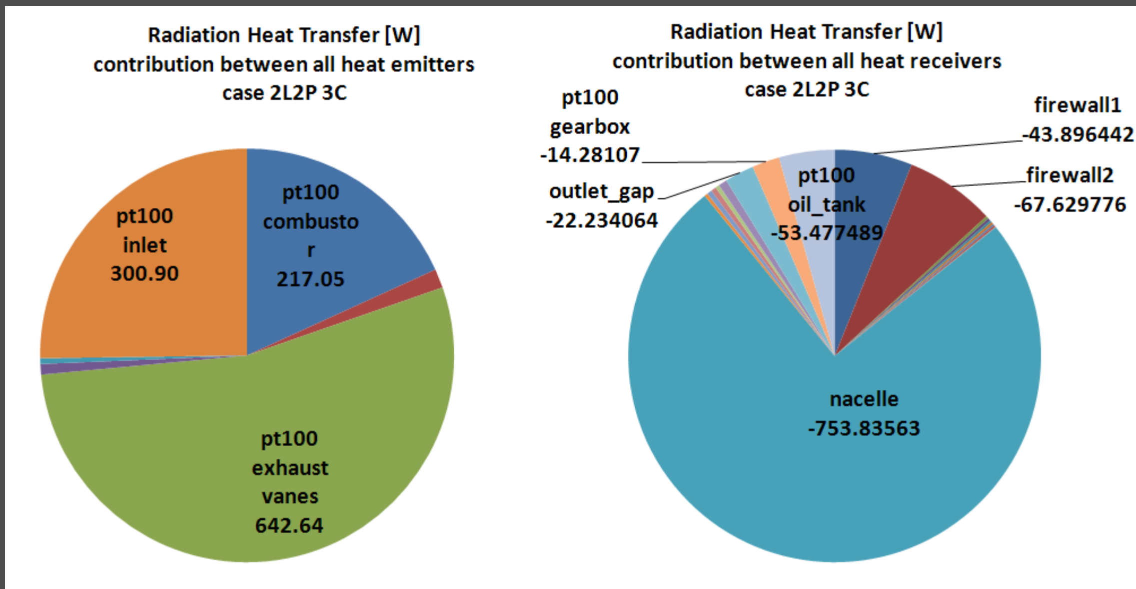

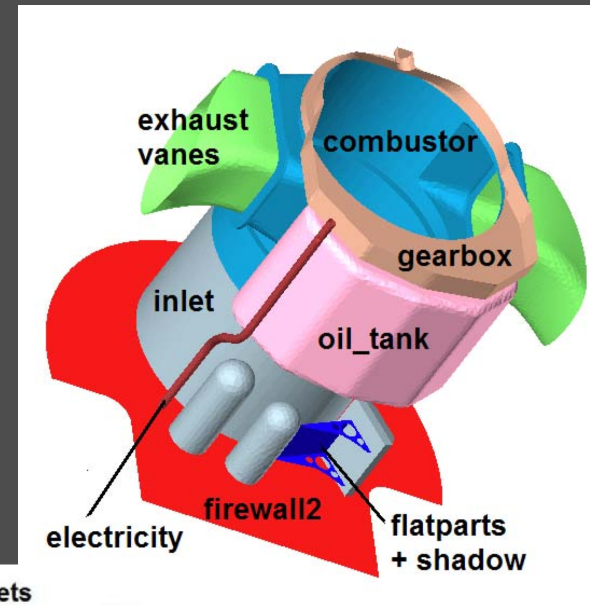

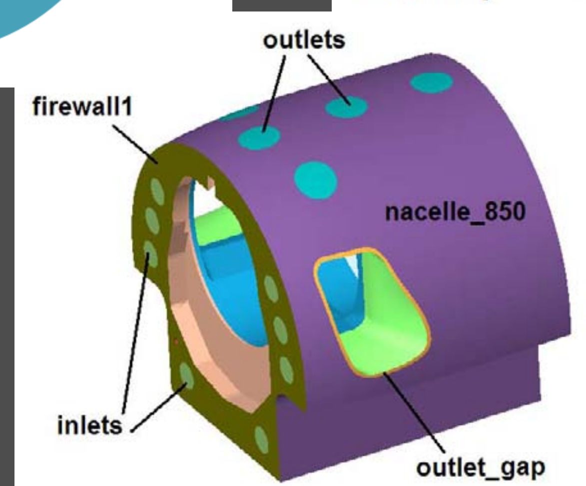

Boundaries that have biggest part in radiation heat flow, these proportions are similar in all cases.

Inlet Analysis Radiation Heat Transfer Rate

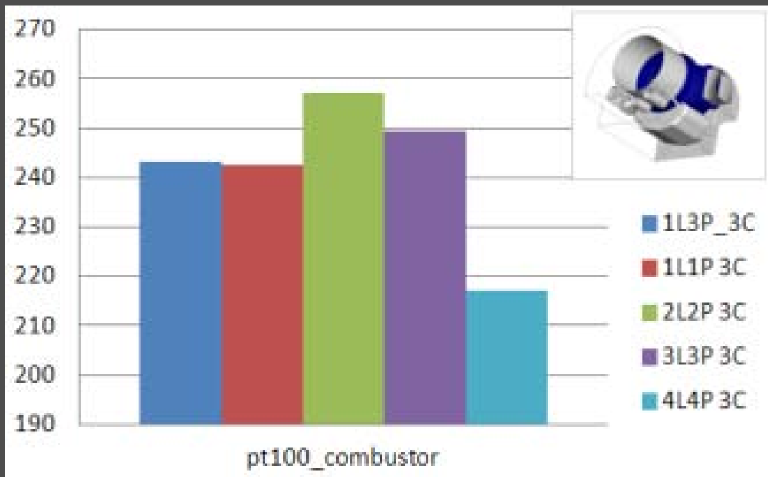

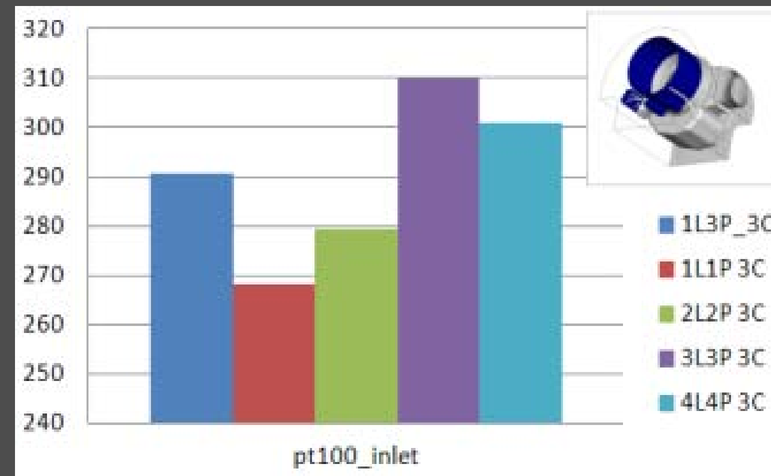

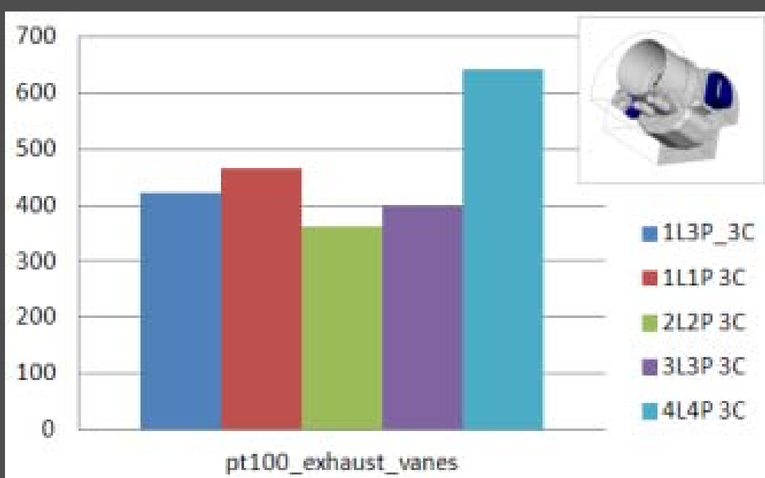

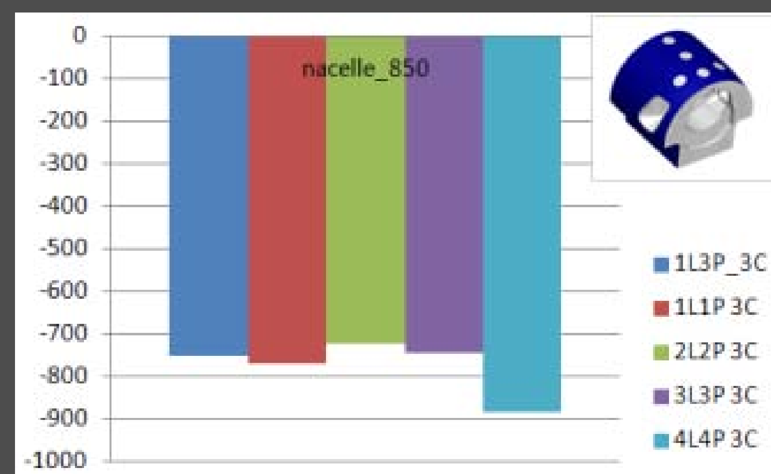

Conclusions from inlet analysis

•Minimum temperature of air inside the nacelle was obtained for the 4L4P configuration the air is only blown through the nacelle bay, heat transport through convection is not sufficient

• 1L1P and 2L2P air temperature is well balanced

• Case 1L3P shows, that asymmetry of inlets does not bring about much advantage

•Composite material on surface of the nacelle should be secured from heat at the back side of exhaust vanes, because none of the inlet positions allows for good cooling of this part of cover

• 4L4P is producing lowest wall temperature at the expense of high temperatures around exhaust vanes.

• Combustor is well cooled in the cases with inlets 1L or 1P opened. On the other hand the inlet is better cooled with inlets 3L,3P, 4L and 4P.

• For case 2L2P most of the heat flows out by the upper outlet, as for cases with 3L or 3P inlets open, most of the heat goes through the gap around exhaust vanes. Those inlets also providing best cooling for the nacelle

• Radiation analysis provides similar results as for convection heat transfer

OUTLET POSITION INFLUENCE

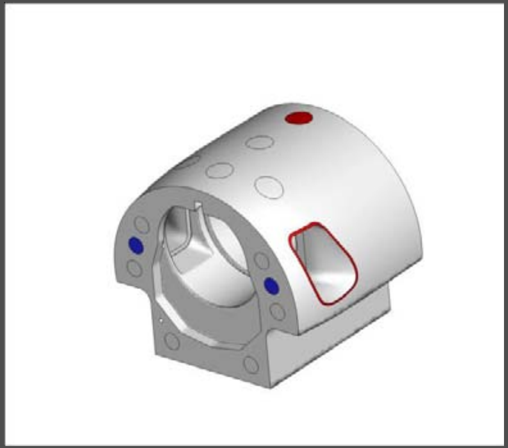

2L2P 3C

2L2P 2C

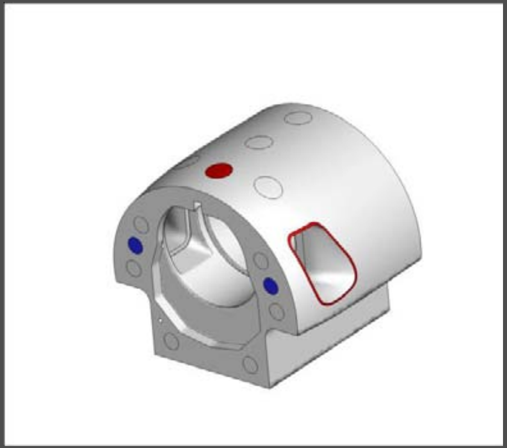

2L2P 1C

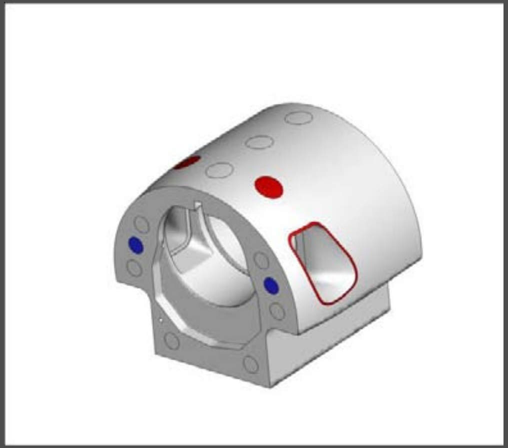

2L2P 1L1P

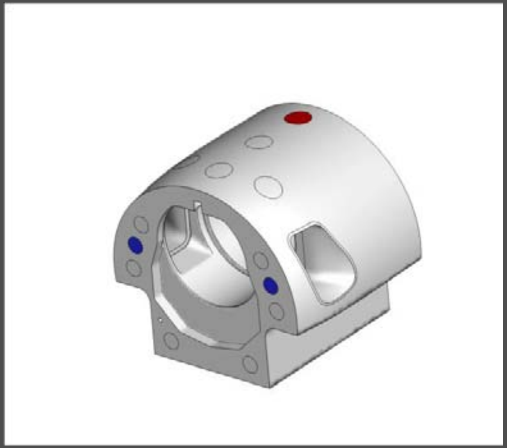

2L2P 3C -G

Outlet position influence

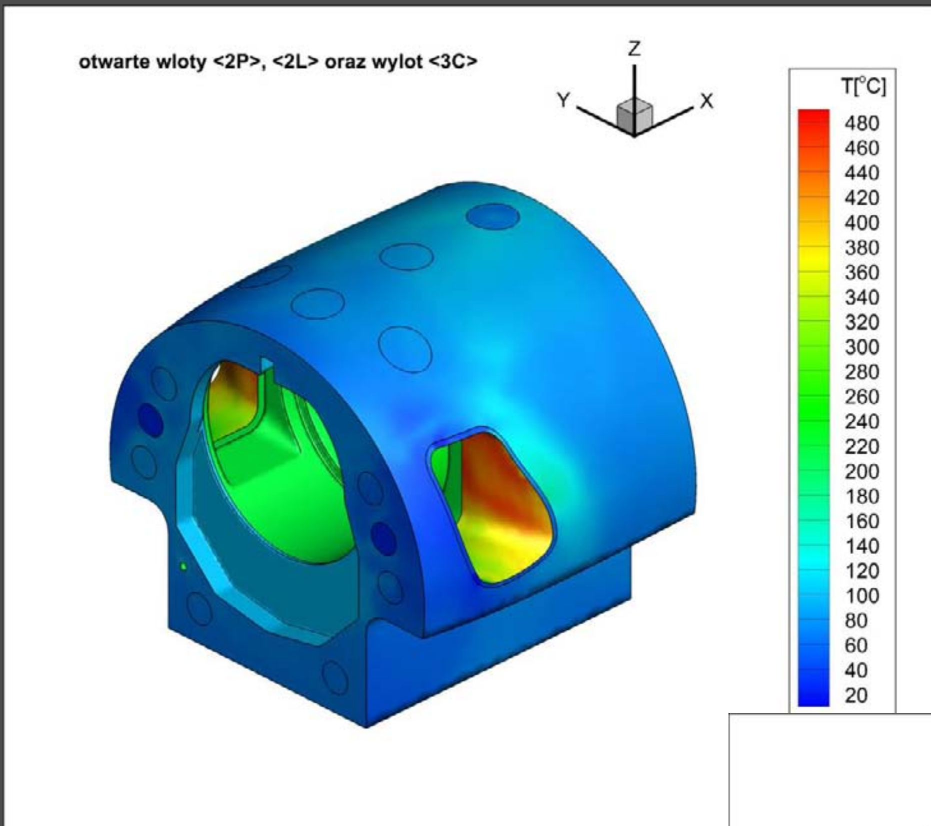

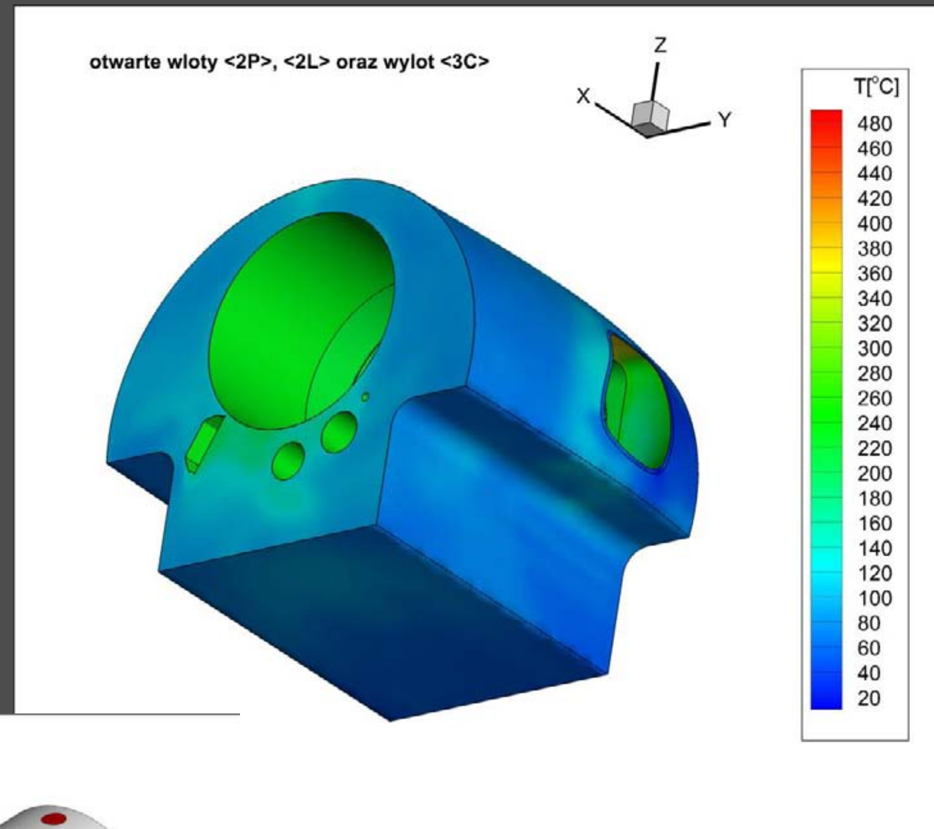

2L2P 3C

Outlet position influence

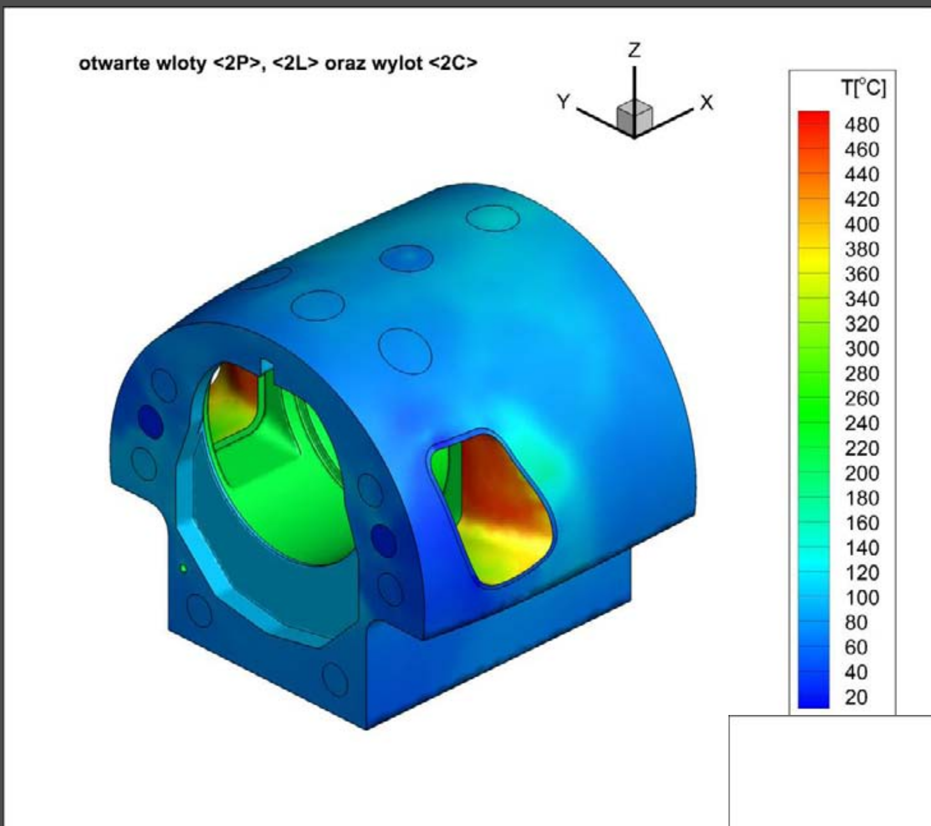

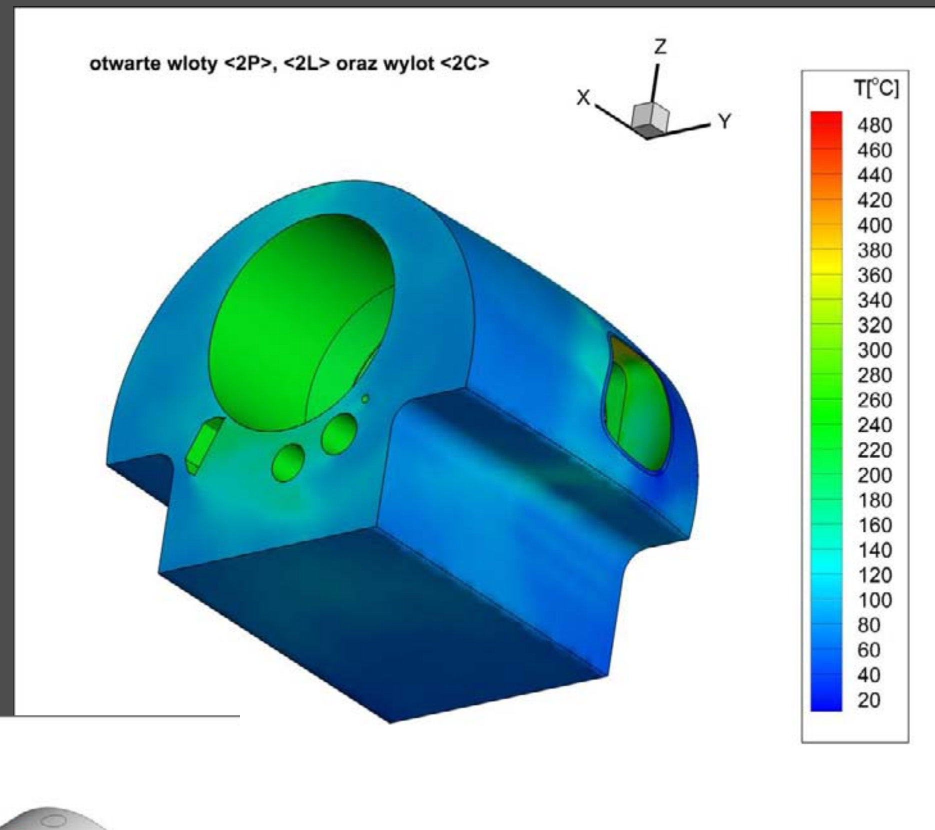

2L2P 2C

Outlet position influence

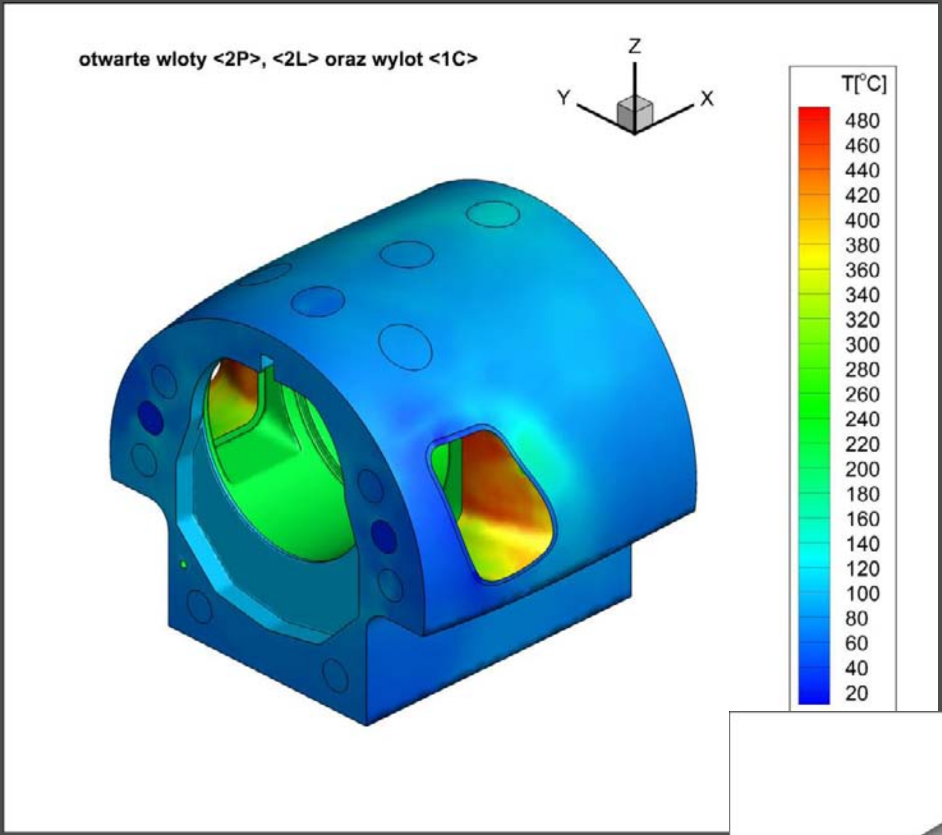

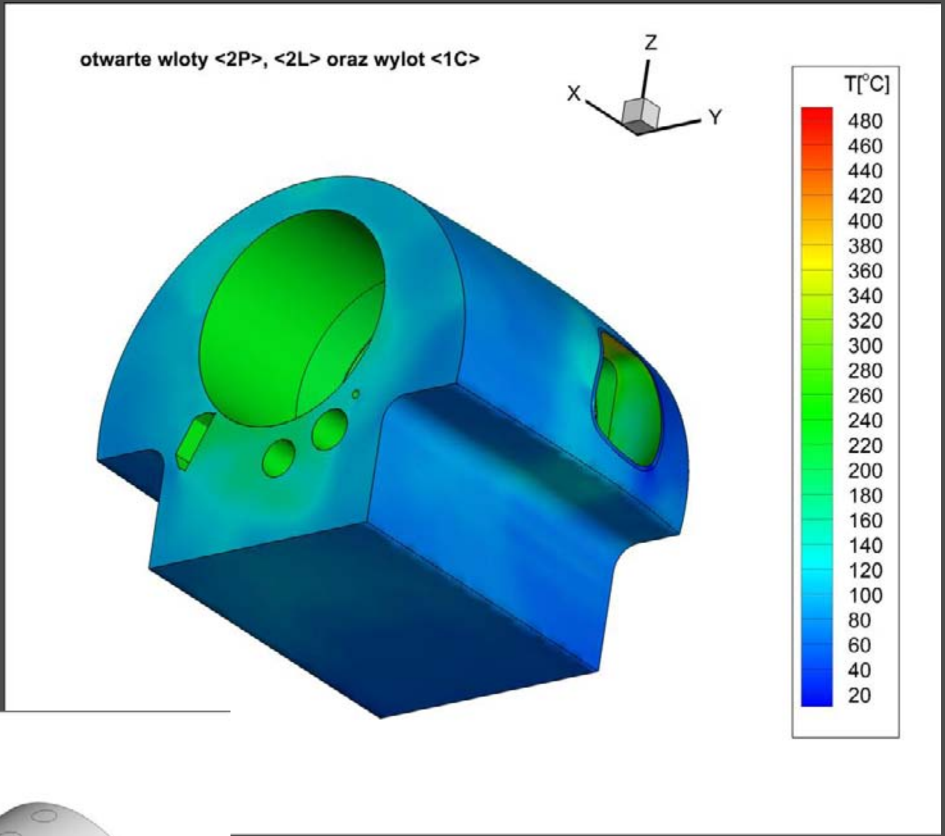

2L2P 1C

Outlet position influence

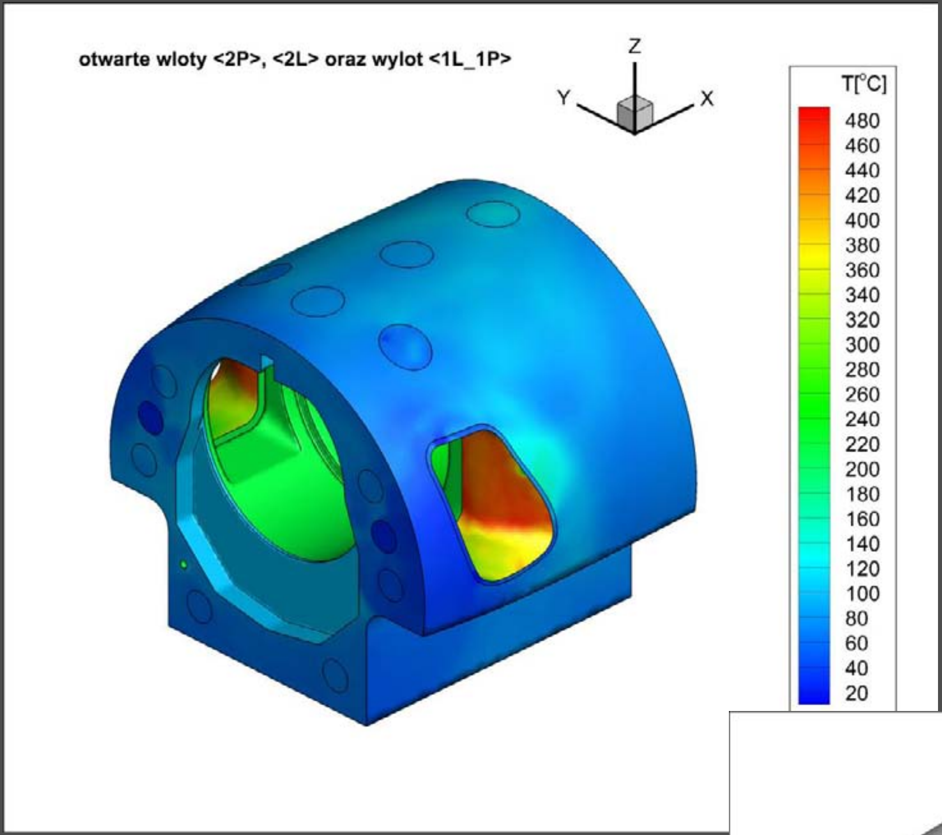

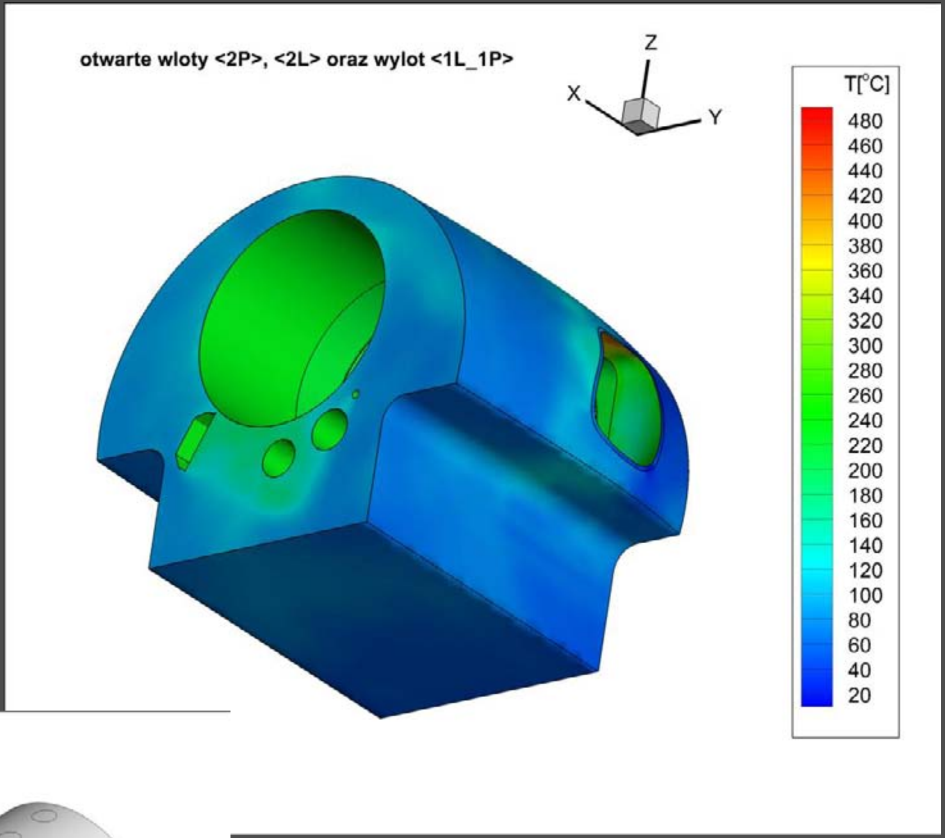

2L2P **1L1P**

Outlet position influence

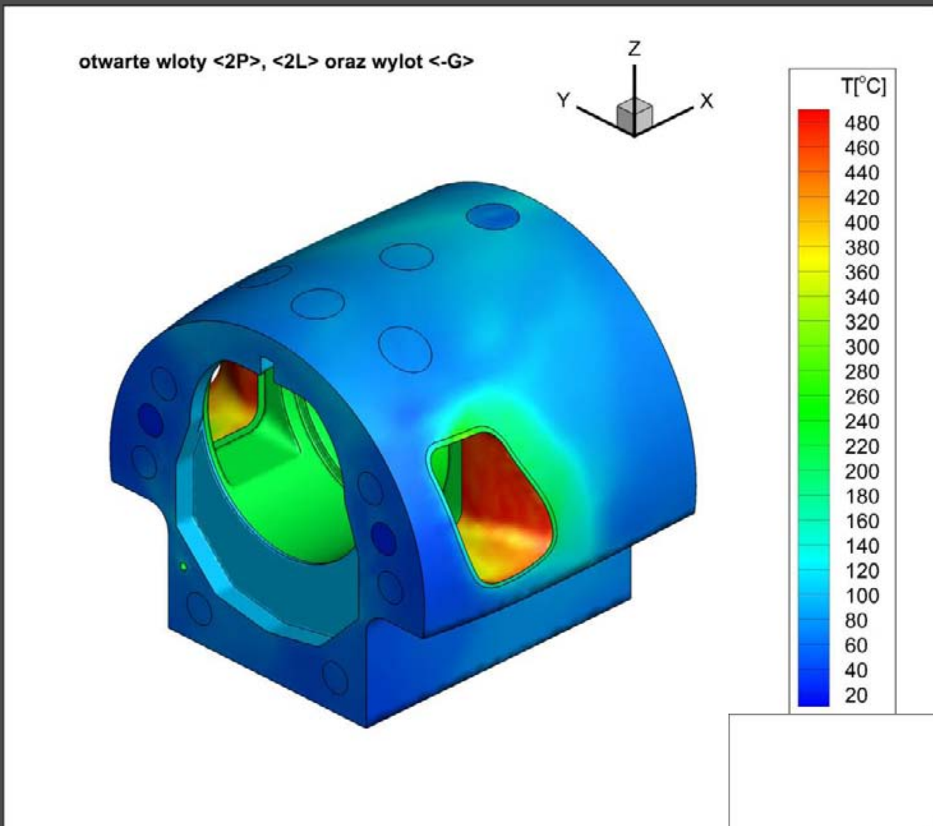

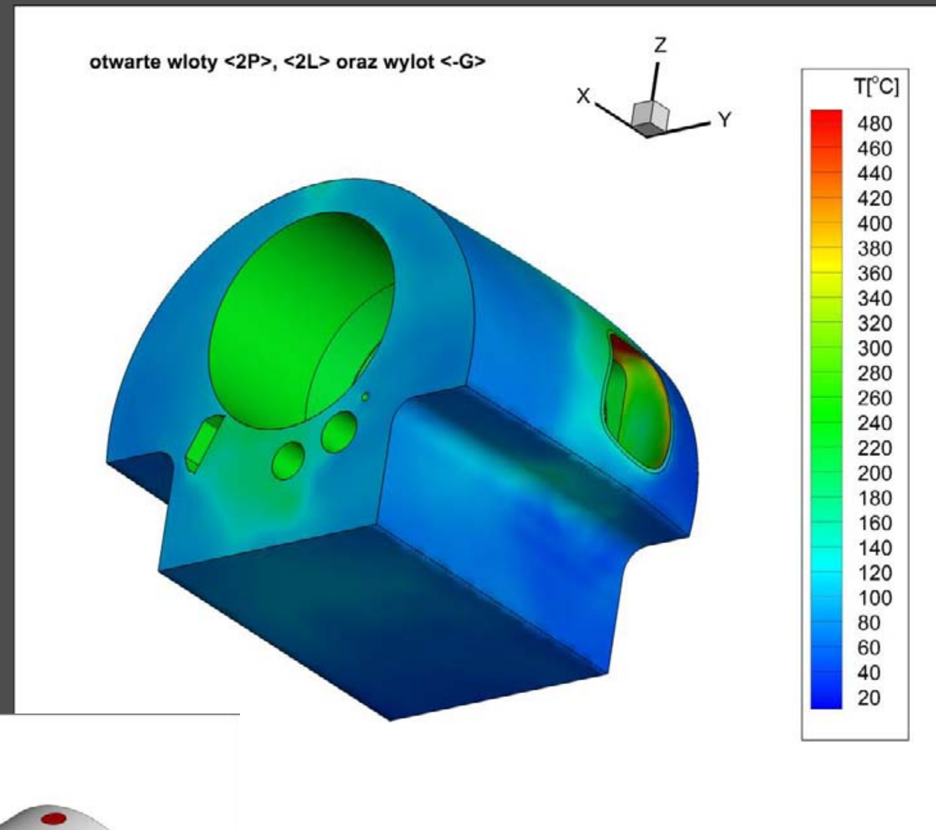

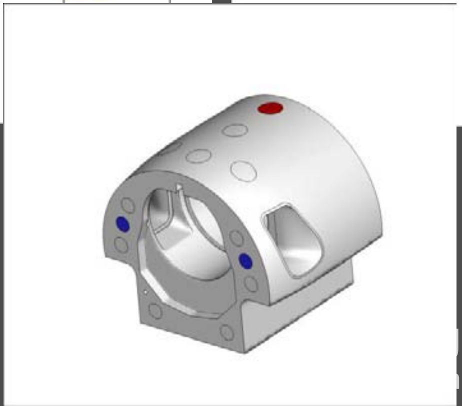

2L2P 3C -G

Outlet position influence

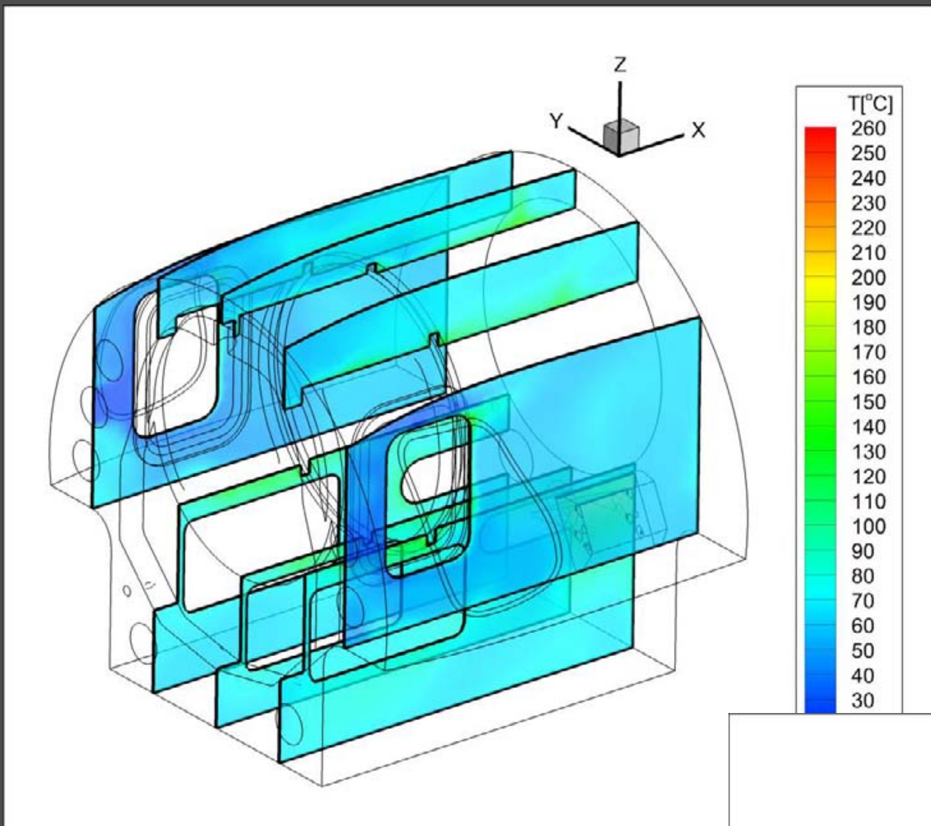

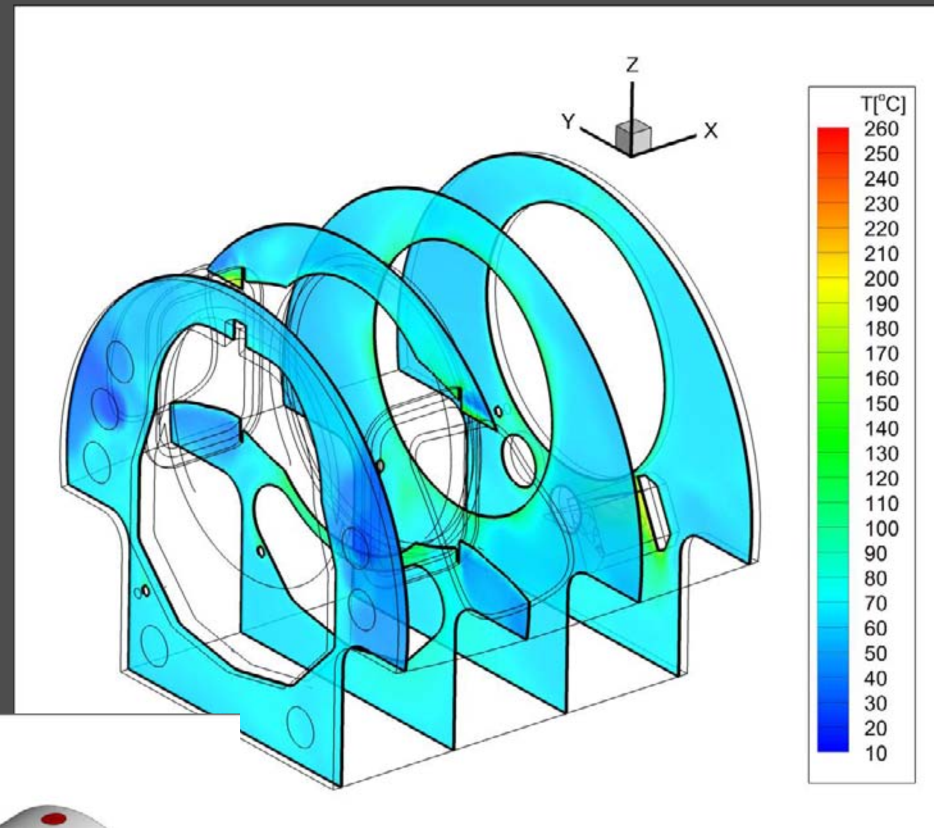

Outlet position influence

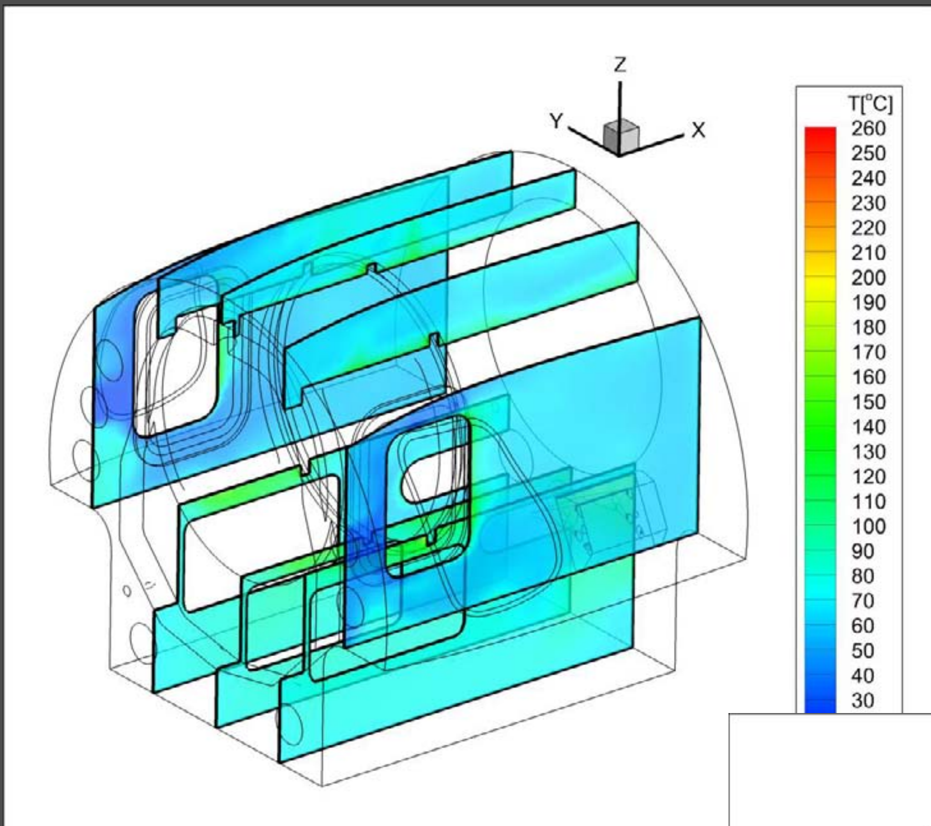

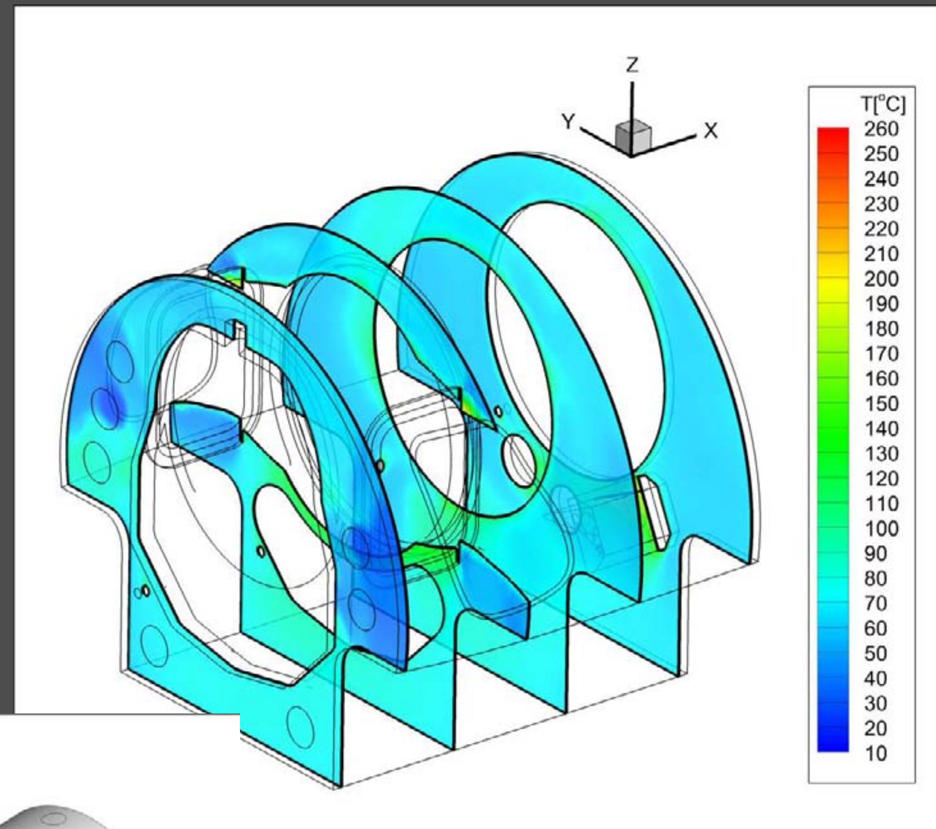

Outlet position influence

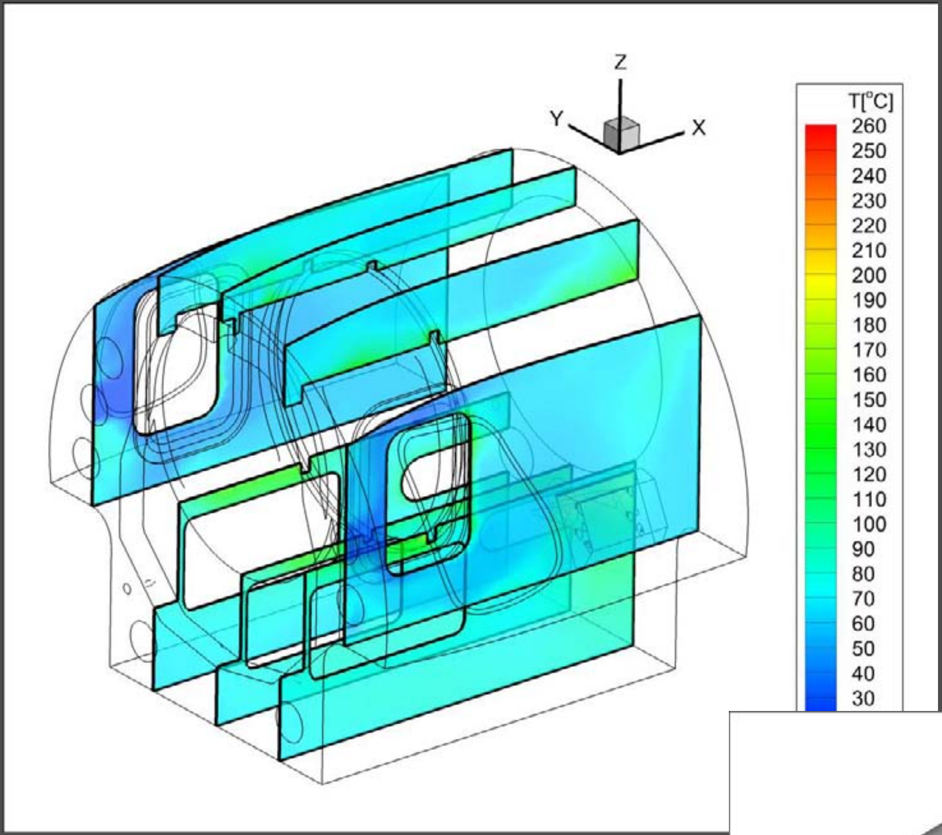

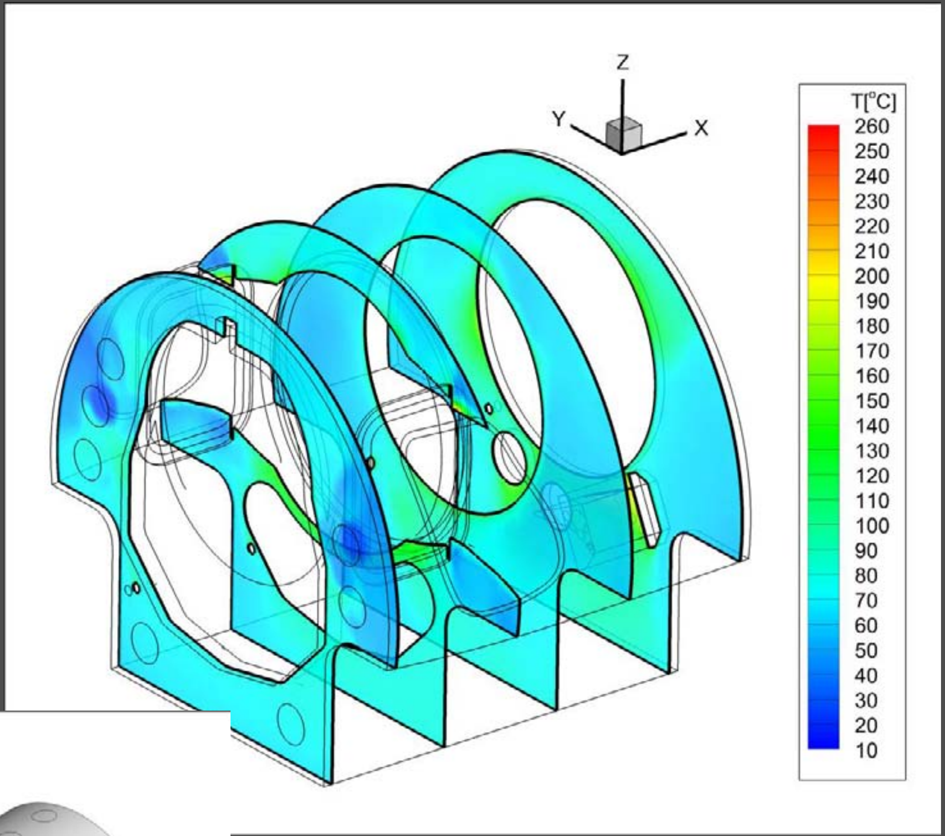

Outlet position influence

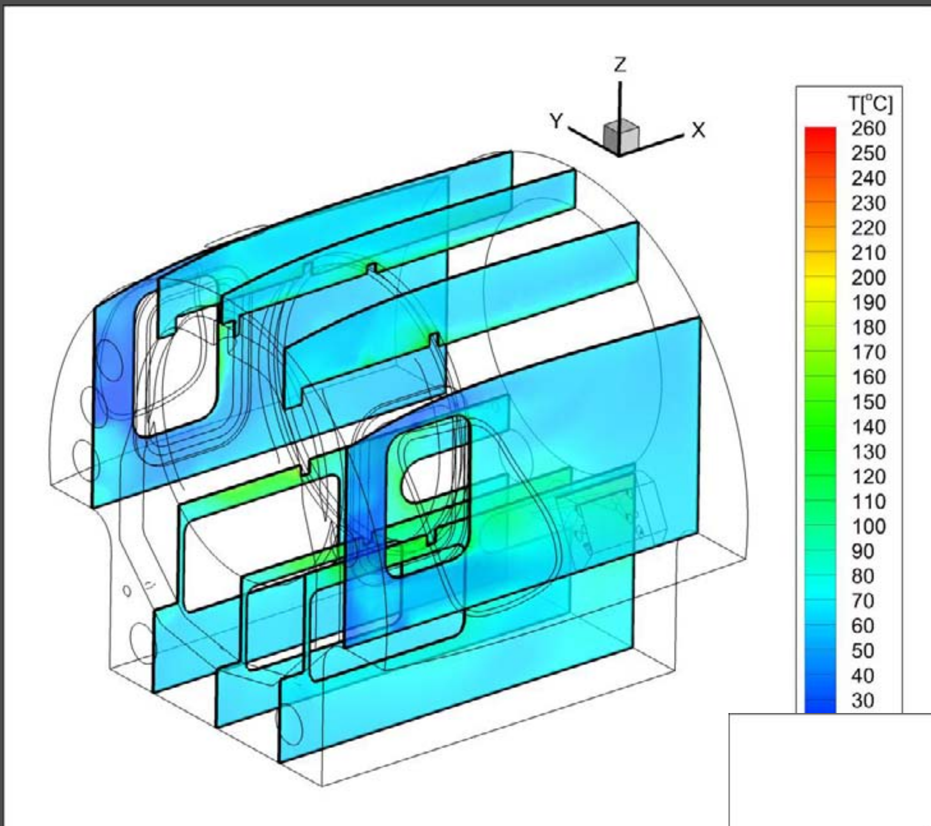

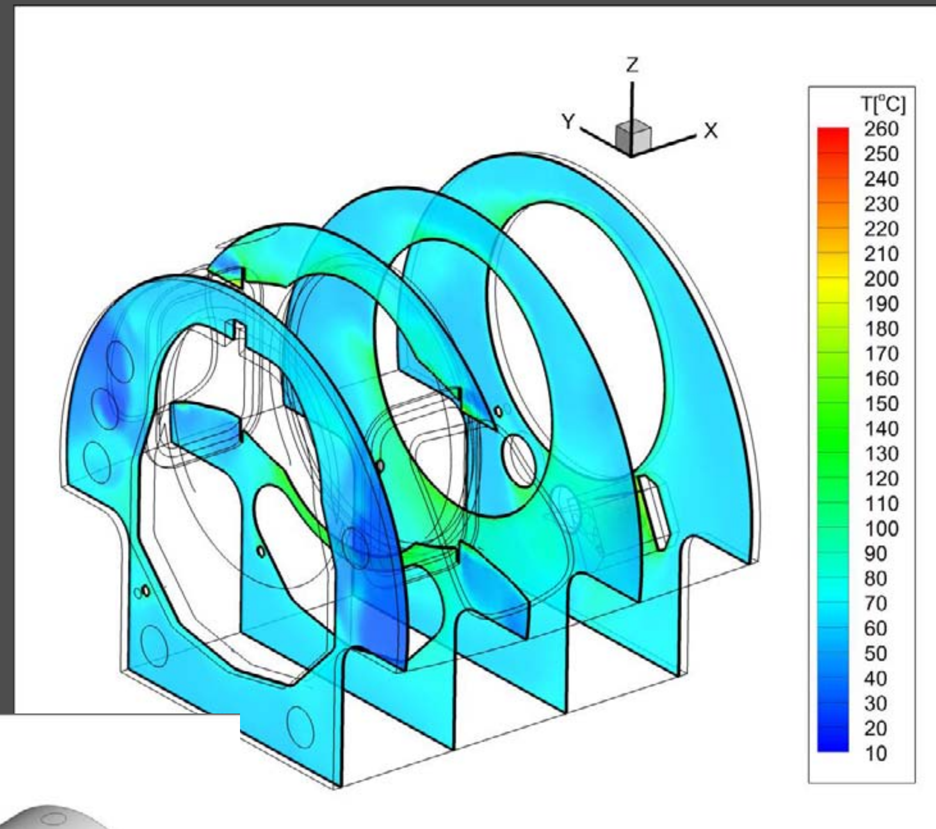

2L2P **1L1P**

Outlet position influence

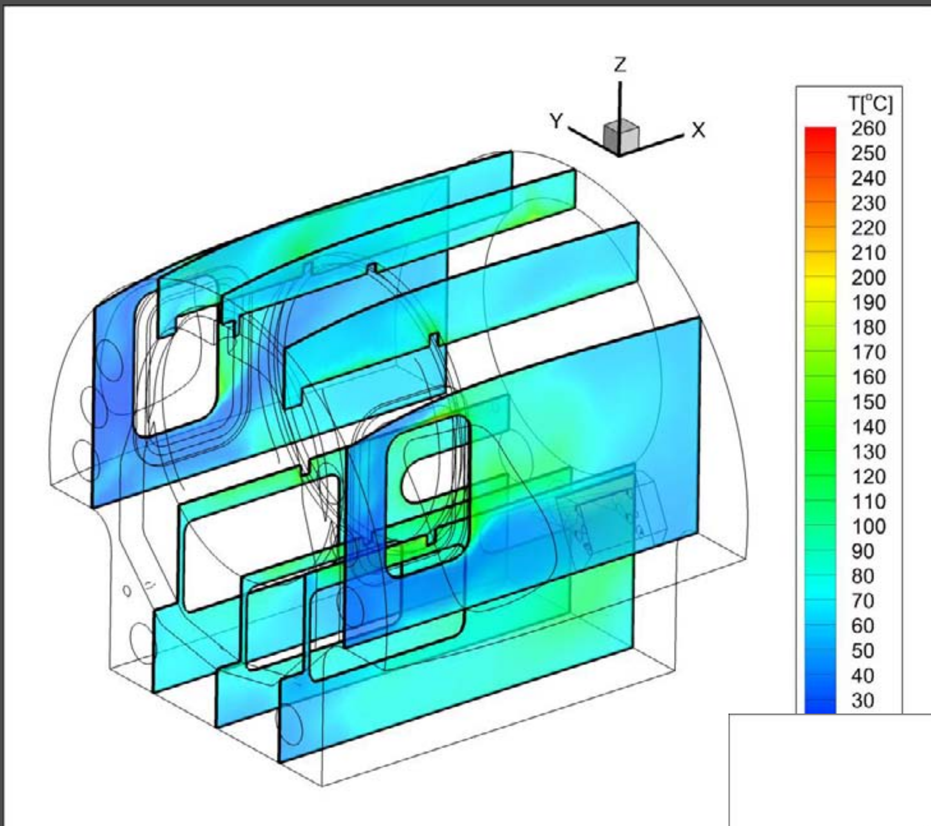

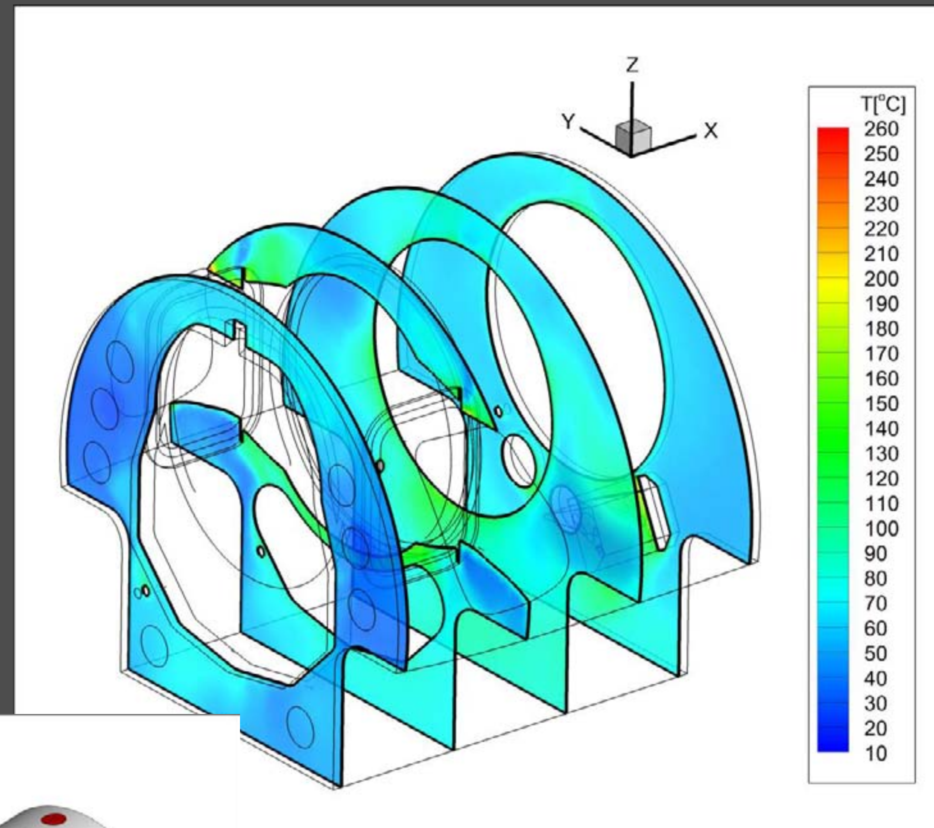

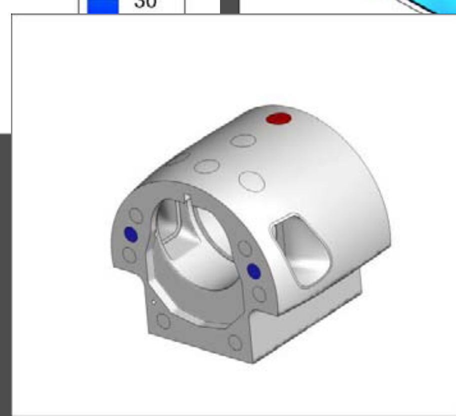

Outlet position influence

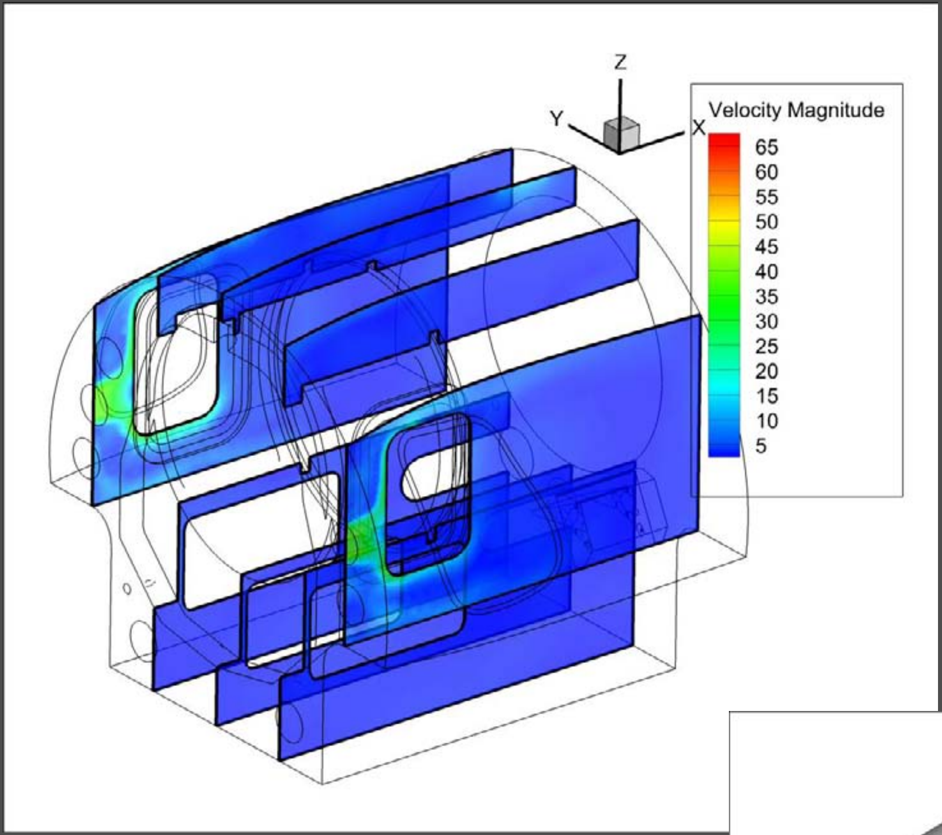

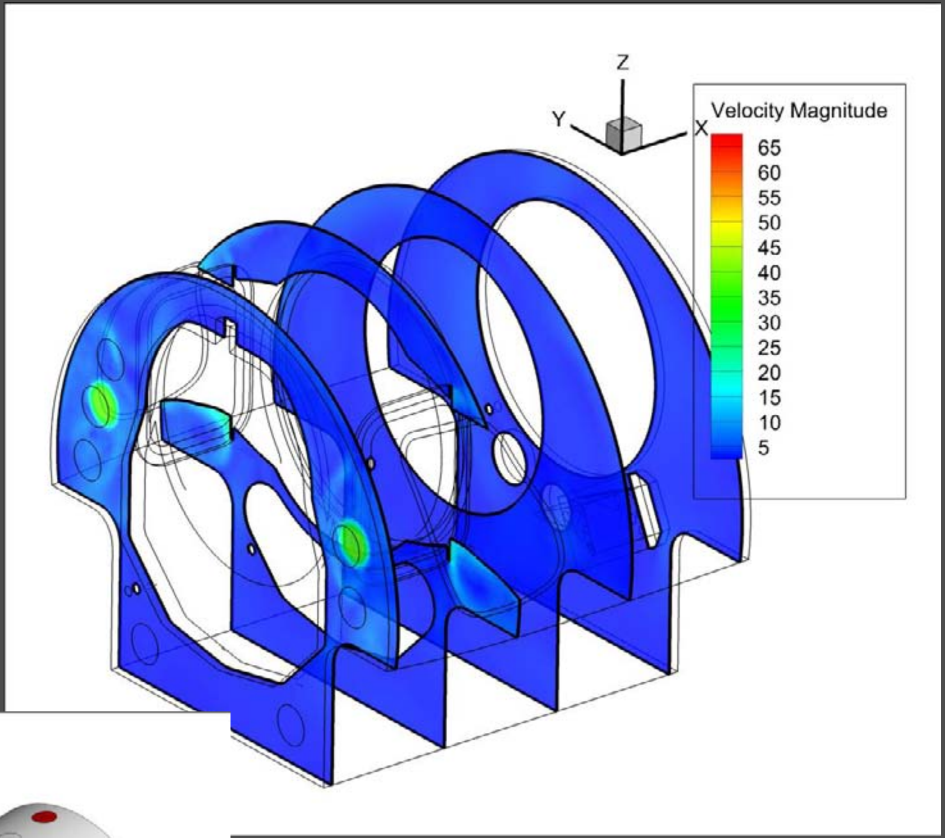

Outlet position influence

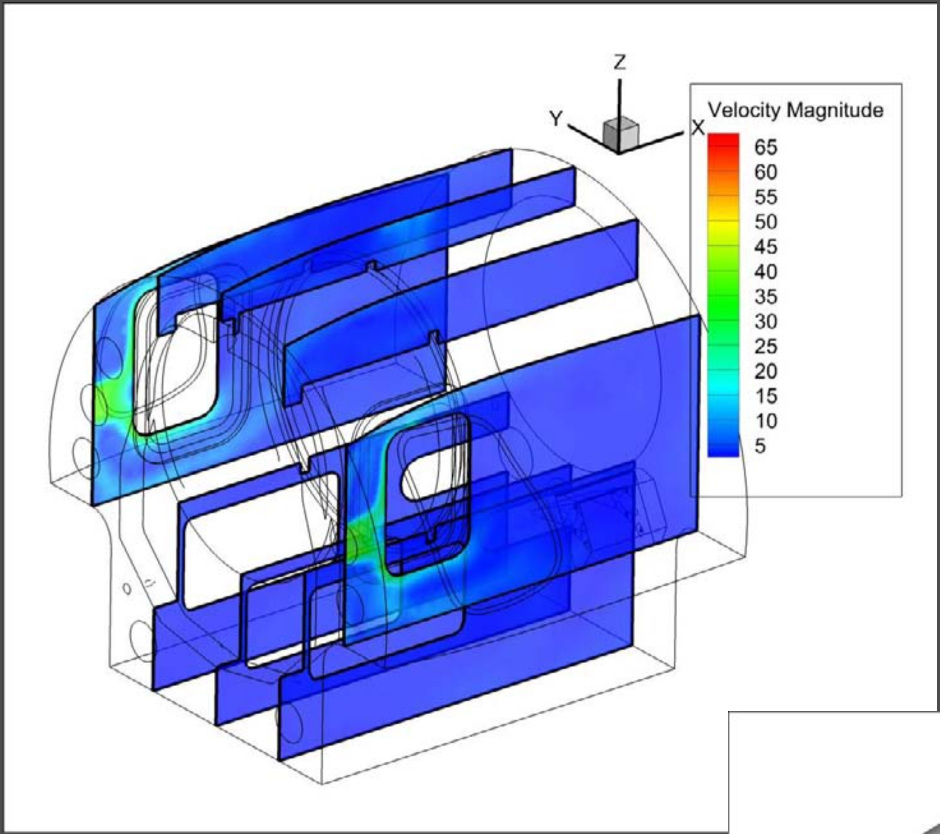

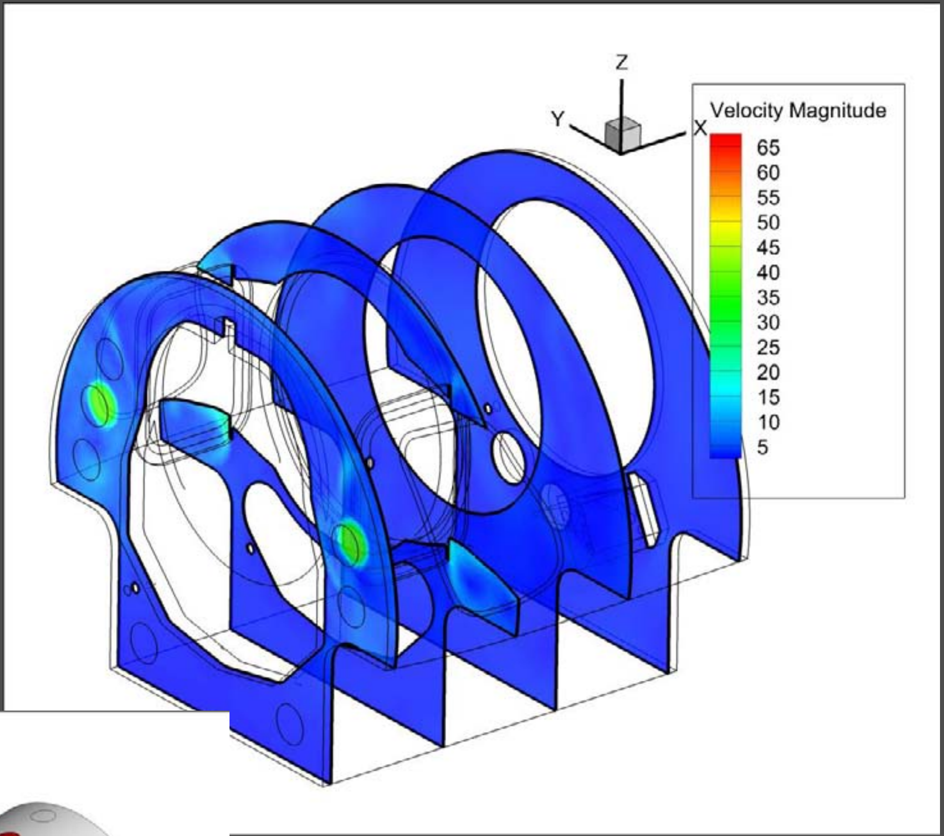

Outlet position influence

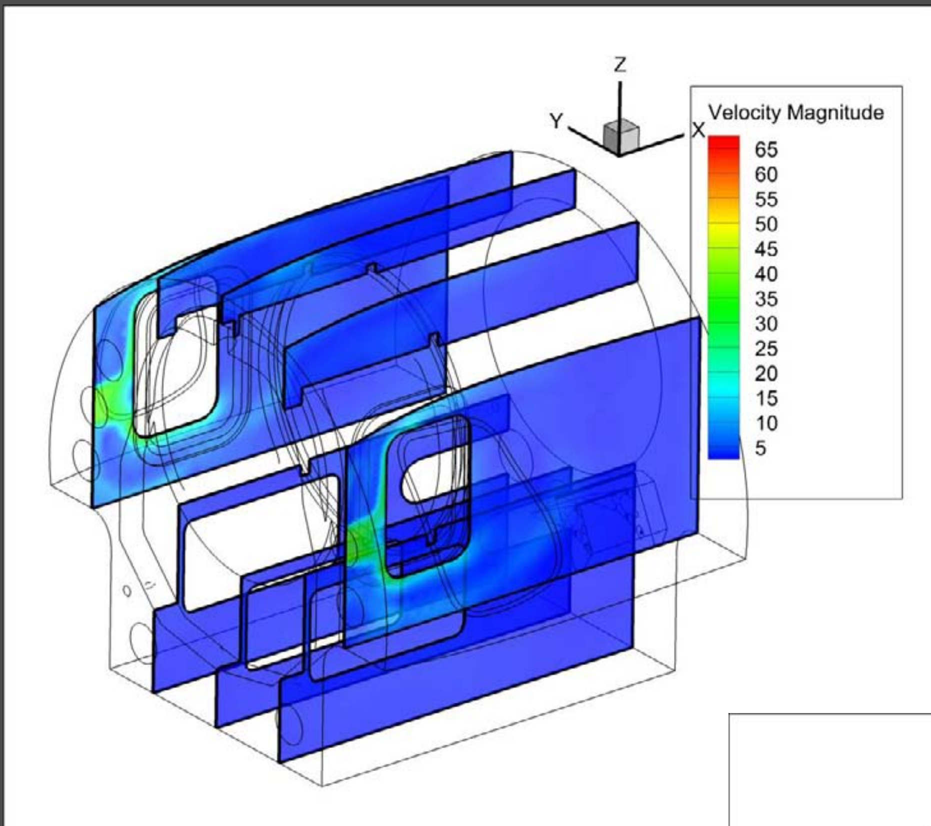

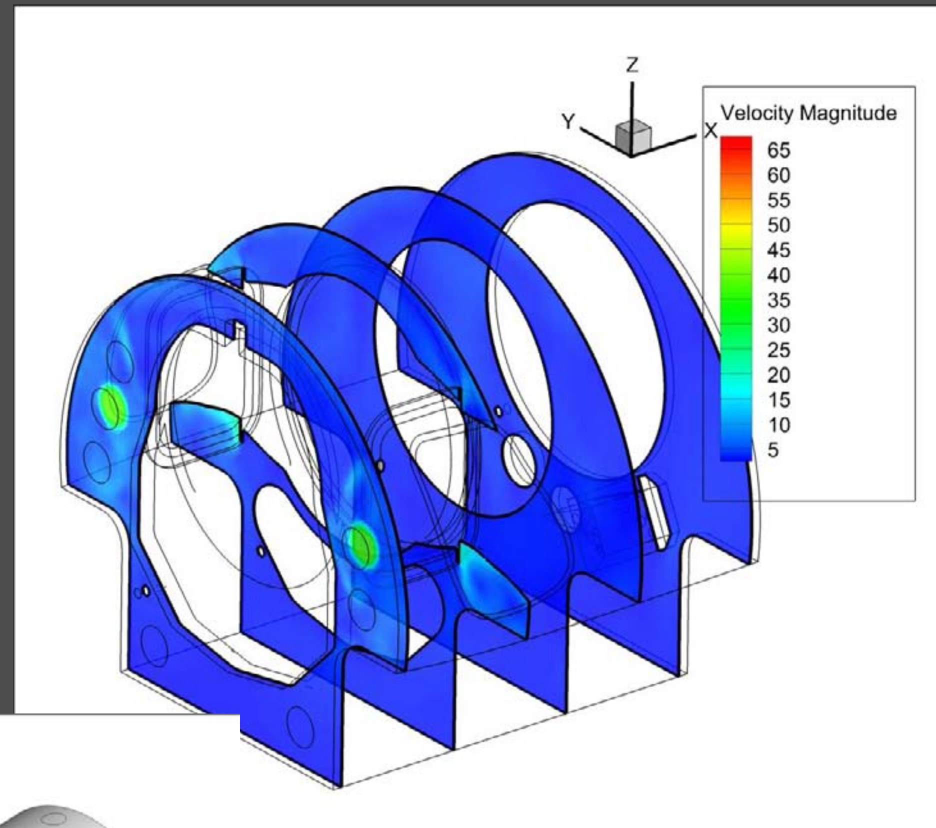

Outlet position influence

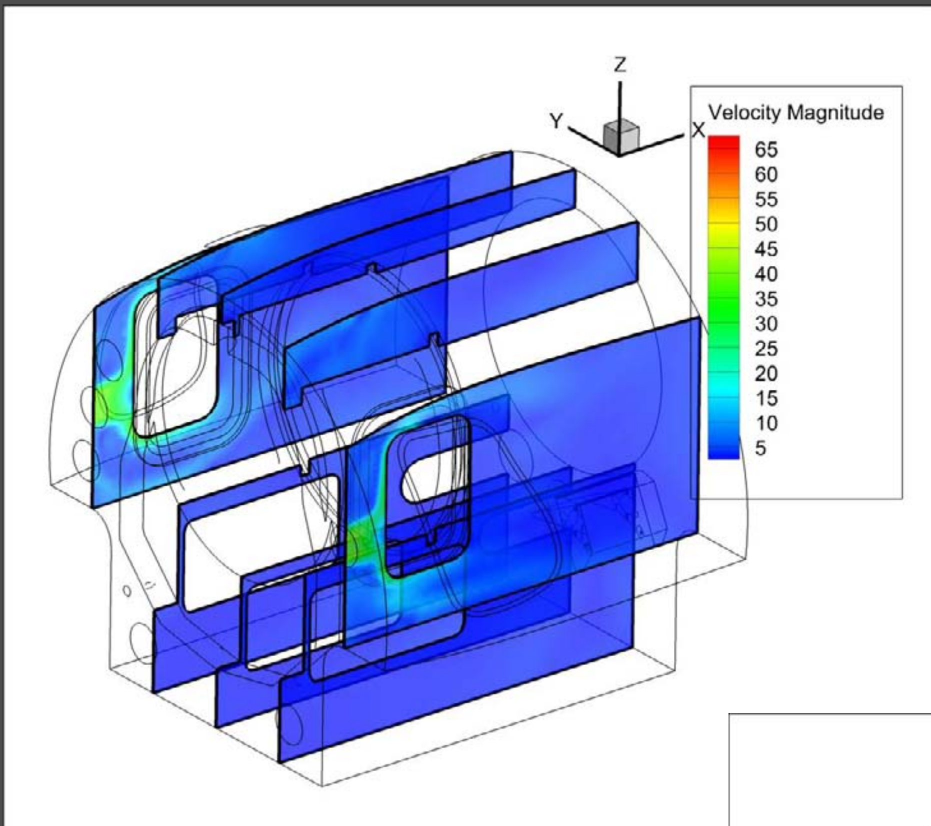

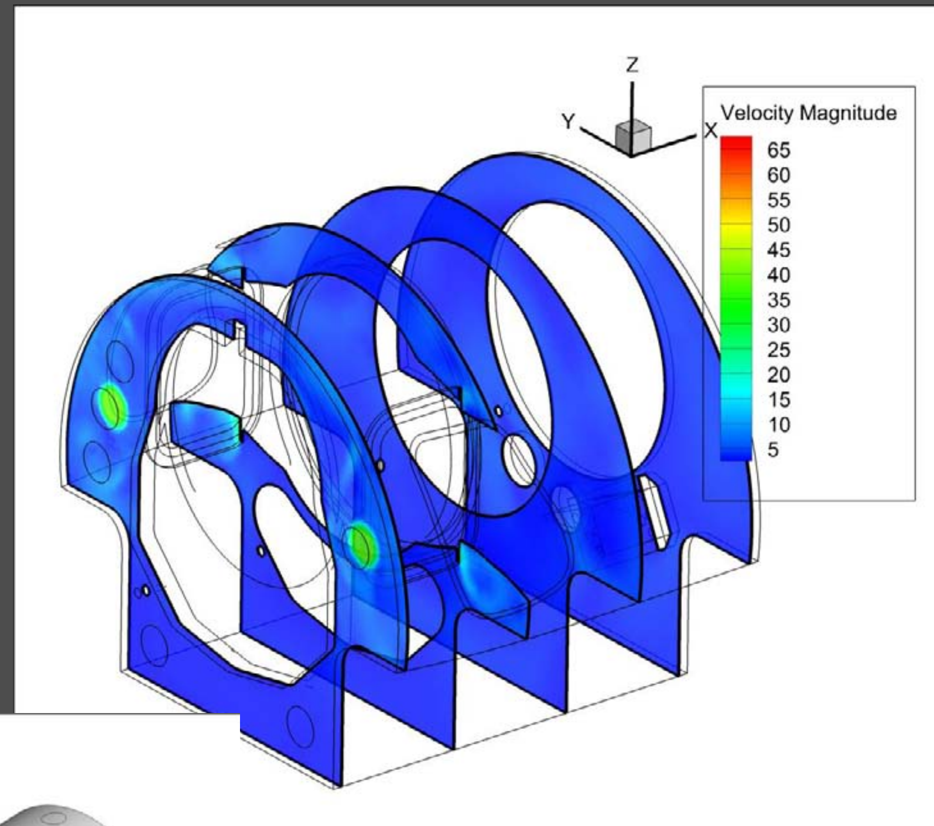

2L2P **1L1P**

Outlet position influence

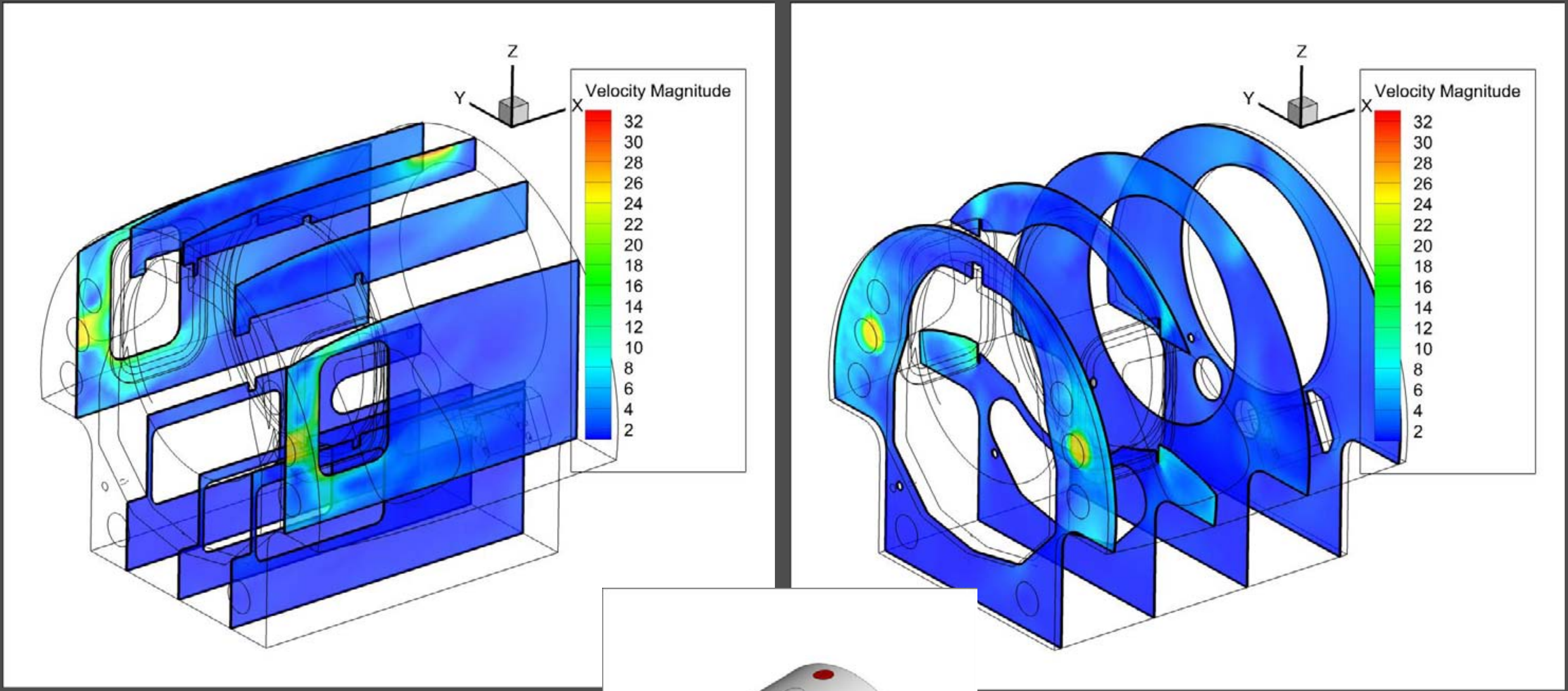

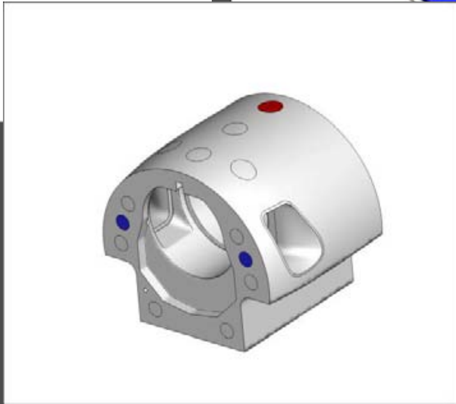

Outlet analysis - Convection Heat Transfer Rate

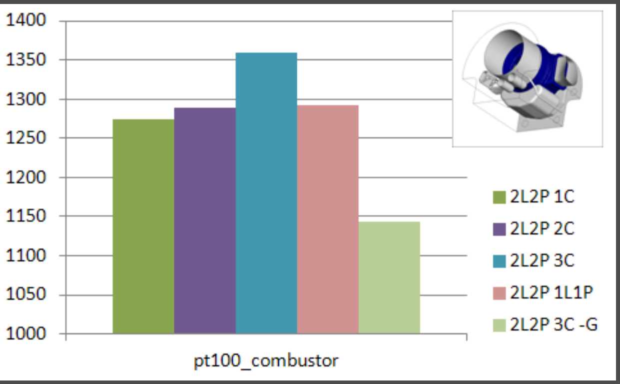

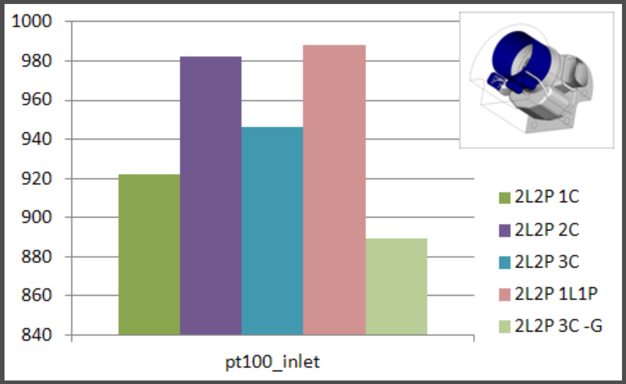

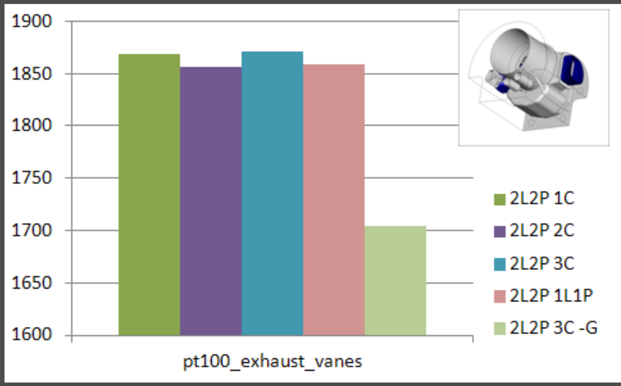

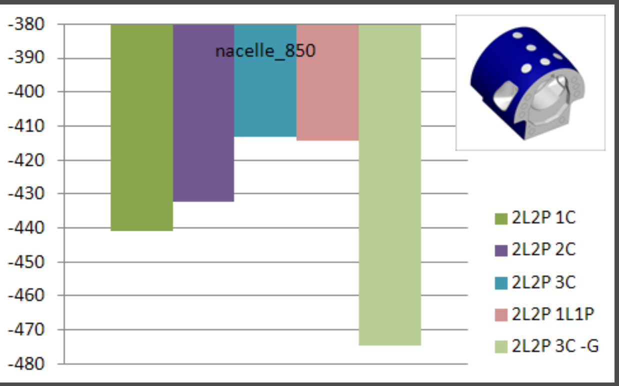

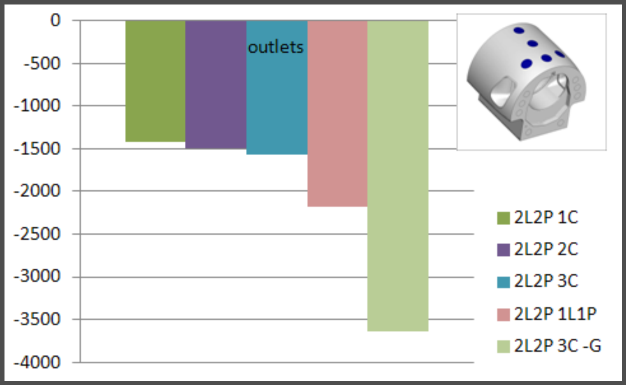

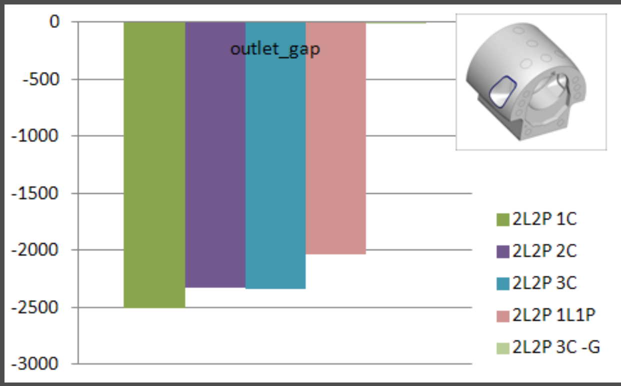

Outlet position influence

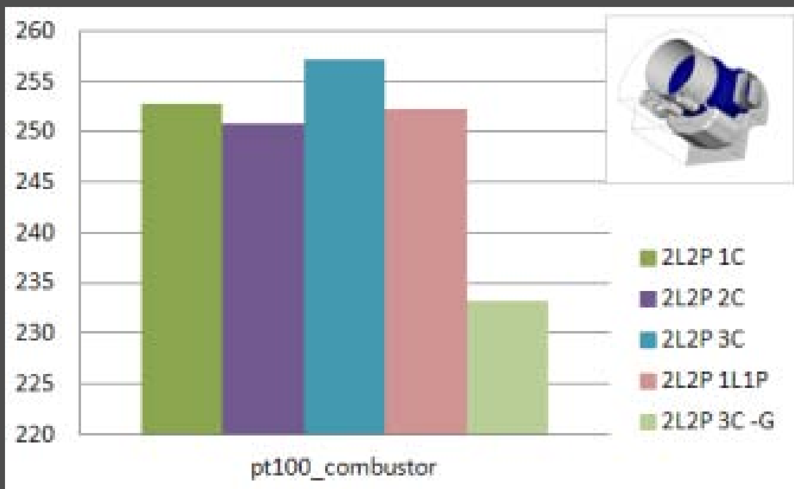

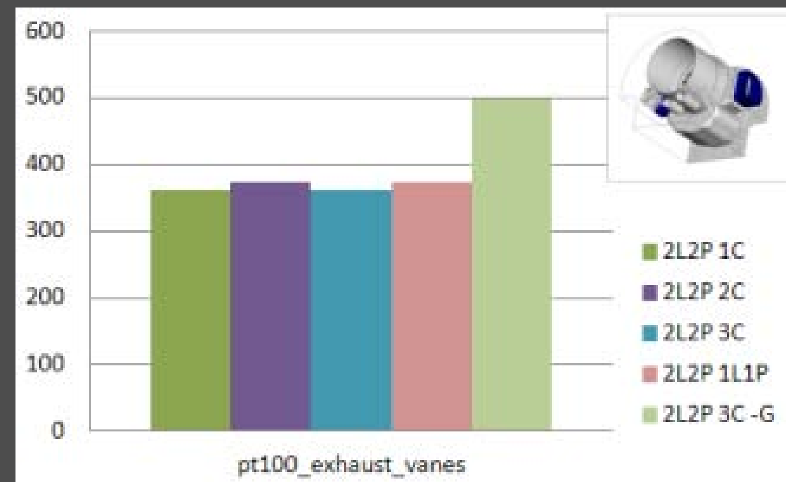

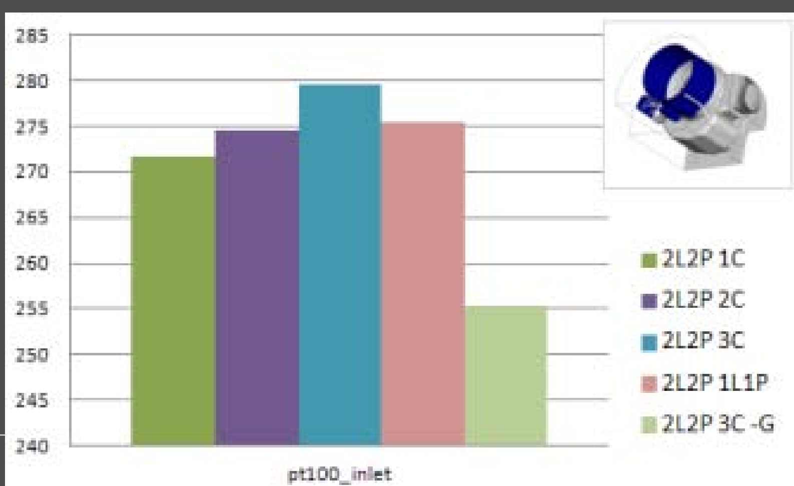

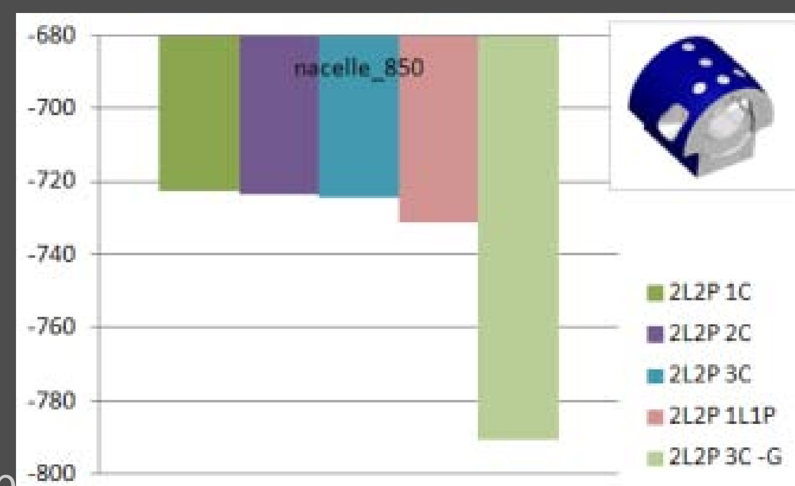

Conclusions from outlet analysis

• The position of outlet does not have significant influence on temperature distribution inside nacelle.

• The case with closed gap had more significant influence on this distribution as well, as in wall temperature comparison

• The combustor cooling gets better with more aft position of outlet

• The more backward position for the outlet, the more heat transfers through outlets and less through the gap, but case (1L1P) defies this tendency, and appears an even better solution.

•**Best cases** for nacelle cooling are **3C and 1L1P.**

• Significant but **negative change** in radiation transfer brings **closing the gap** around the exhaust vane

Conclusions

A rough analysis of engine cooling system allows to obtain proper positions for inlet and outlet, even allowing to some kind of sensitivity analysis.

The best solutions have been down selected (cases “2L2P 3C” and “2L2P 1L1P”), and a database for position influence for inlet and outlet has been obtained

These data have been used in design of flying test bed for TP-100 engine integration with PZL I-23 “Manager” aircraft.

Thank you.

Influence of Non-Uniform Inflow Conditions on Propeller Performance in Tractor Configuration

Phase 0: Commissioning test of the propeller setup

ESPOSA

E. van Berkel (Msc student)

Delft University of Technology

Contents

- Introduction
- Phase 0: Commissioning test
- ESPOSA test preparations
- Preliminary conclusions
- Outlook

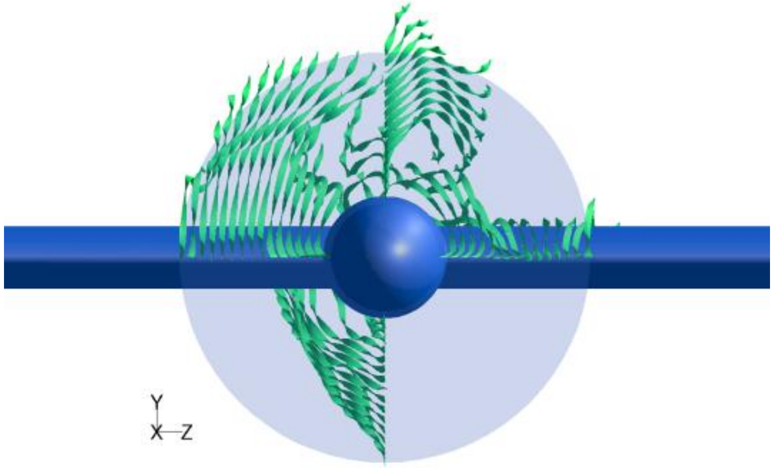

ESPOSA – WP 6.2

ESPOSA EFFICIENT SYSTEMS AND PROPULSION FOR SMALL AIRCRAFT

- Experimental Campaign on Non-uniform Inflow Conditions on Propeller Performance

SEVENTH FRAMEWORK PROGRAMME
www.esposa-project.eu
FUNDED BY THE EUROPEAN COMMISSION
IN THE SEVENTH FRAMEWORK PROGRAMME
GRANT AGREEMENT NO. ACP1-GA-2011-284859-ESPOSA

ESPOSA – DOW/TU Delft

- **Description of Work**:
  - "A small scale Wind Tunnel campaign will be performed aimed at analyzing the effect of non-uniform inflow on propeller performances."
  - "TUD will perform parametric studies of simplified wing-propeller configuration and will perform data collection and analysis"
- **Output**
  - Propeller performances as function of wing-propeller relative position.
- **Deliverables**

Deliverable Number [61]	Deliverable Title	Lead beneficiary number	Estimated indicative person-months	Nature [62]	Dissemination level [63]	Delivery date [64]
D62.1	Propeller-wing parametric study and aerodynamics data-set	31	18.10	R	CO	12
D62.2	BE1 tractor nacelle and inlet design requirements	22	18.10	R	CO	6
D62.3	BE2 tractor nacelle and inlet design requirements	18	18.10	R	CO	6
D62.4	BE1 pusher nacelle and inlet design requirements	15	18.10	R	CO	6
D62.5	BE1 tractor: nacelle design process and optimized geometry	33	18.20	R	CO	30

DNW wind tunnel tests

Commissioning tests

- Goals:
  - Checking of propulsion system (air motor) and Rotating Shaft Balance (RSB) equipment
  - Training of TUD staff
- Determination of basic system characteristics
- Check of predicted trends

- Windtunnel:
  - DNW-LST low speed windtunnel
  - DNW high pressure feeding system

Theory

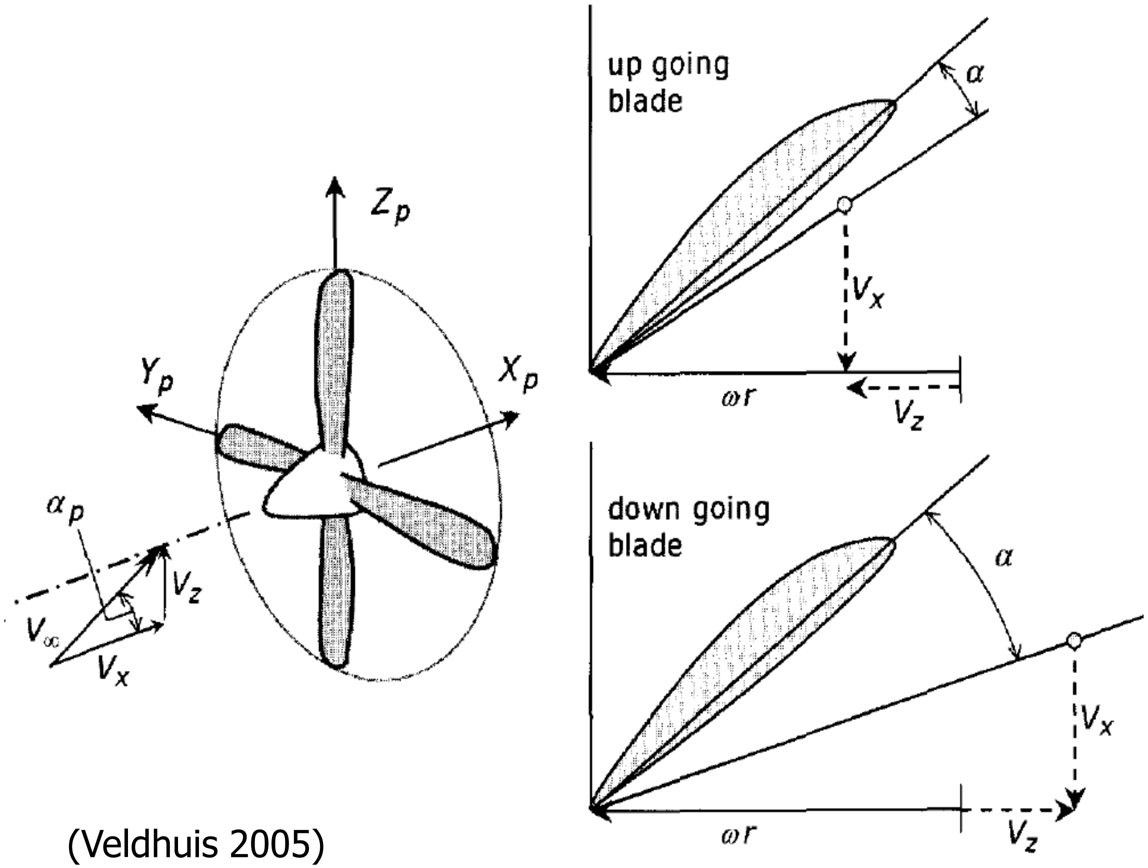

(Veldhuis 2005)

- Propeller at non-zero angle of attack leads to inflow non-uniformity.
- A.o.a. increase of down going blade is larger than a.o.a. decrease of up going blade => Thrust increase at same J.
- Wing induced flow effect is different from pure propeller a.o.a.
- Adapted BEM model for trend analysis

DNW wind tunnel tests

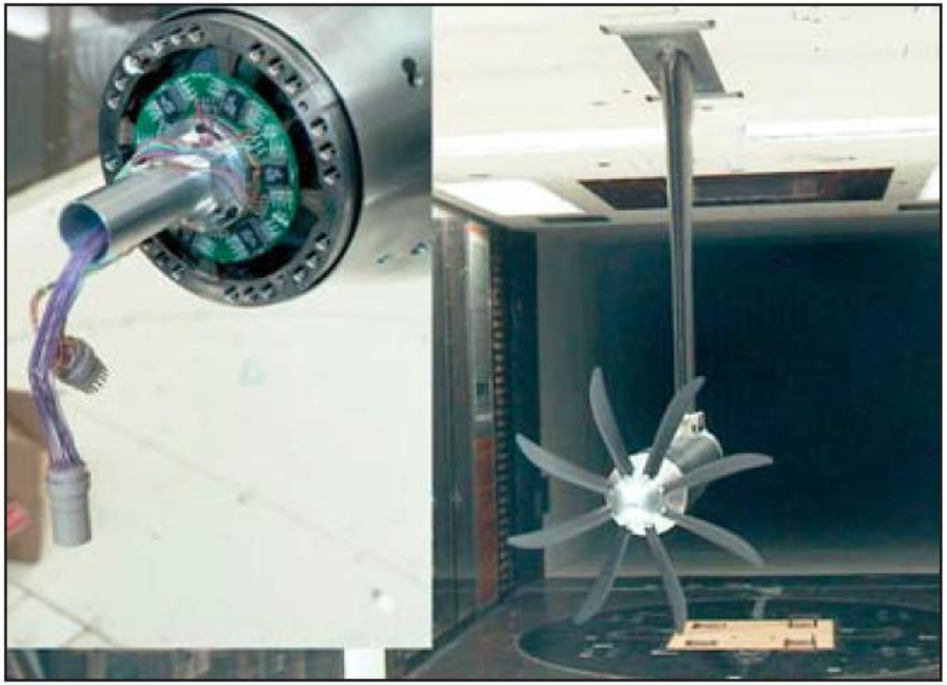

Typical propeller test in DNW-LST facility.
Insert: Rotating shaft balance

German-Dutch Wind Tunnels

ESPOSA – setup

Propeller

- Fokker F29 experimental propeller
- Configurations of 4 and 8 blades possible

ESPOSA - setup

Pneumatic drive

- Driven by a TDI 1999 air motor
- Max rpm 16000
- Max. thrust: 400 N
- Max. torque: 40 Nm

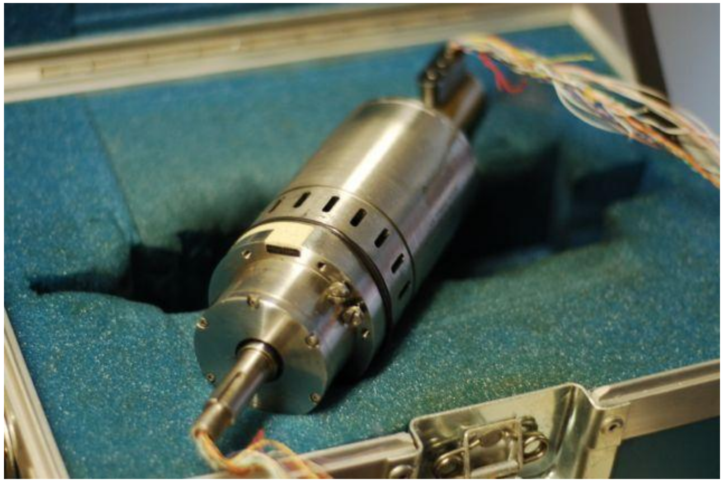

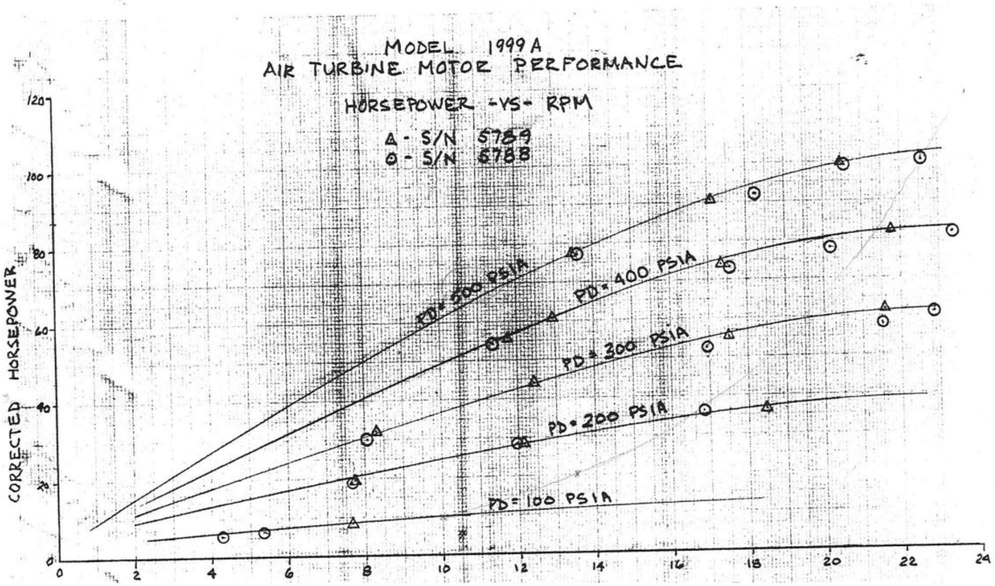

ESPOSA - setup

Rotating Shaft Balance (RSB)

- 6 component RSB
- Developed by NLR
- Direct reading of DC components (thrust, torque)
- Possibility for in-plane loads measurement

ESPOSA - setup

Test rig

- Constant diameter nacelle
- Internal temperature and performance monitoring systems
- Combined with a simplified wing geometry

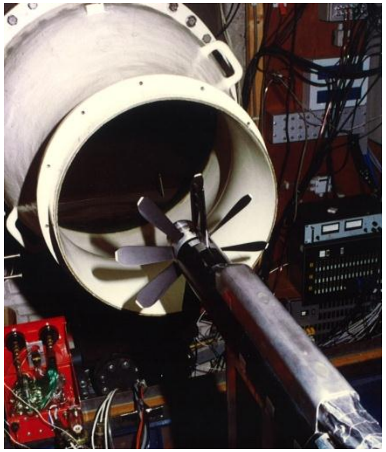

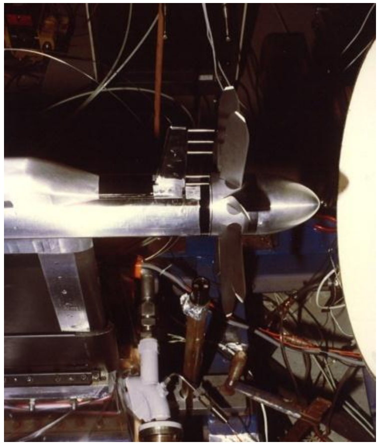

Calibration setup at DNW

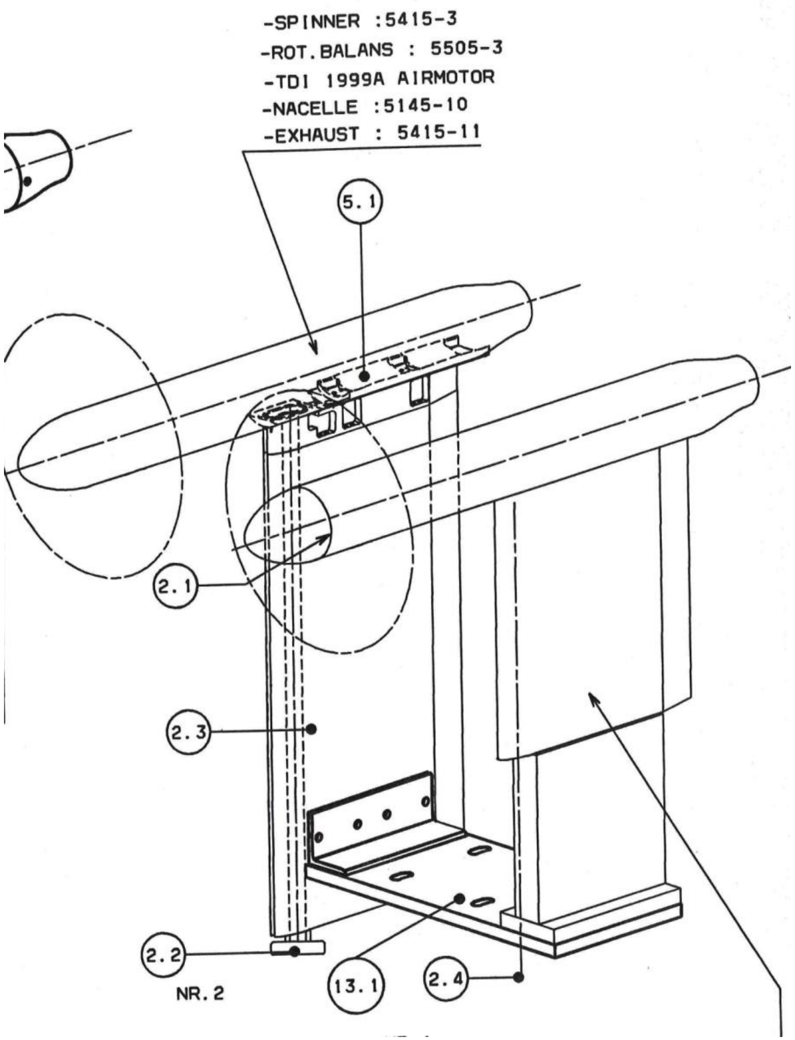

Test setup DNW

Commissioning tests

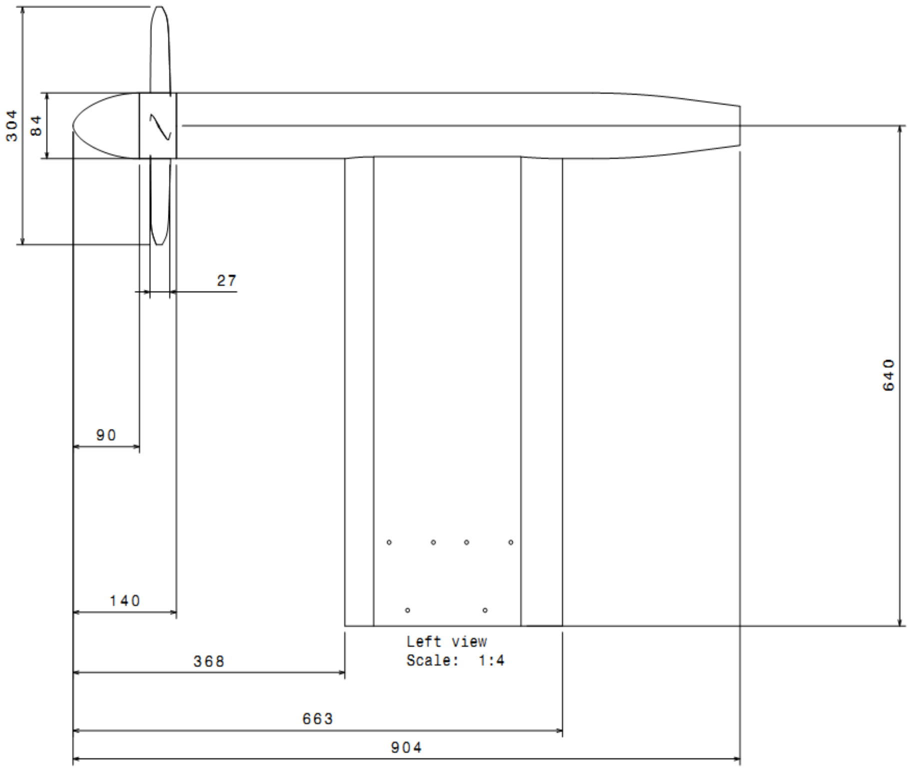

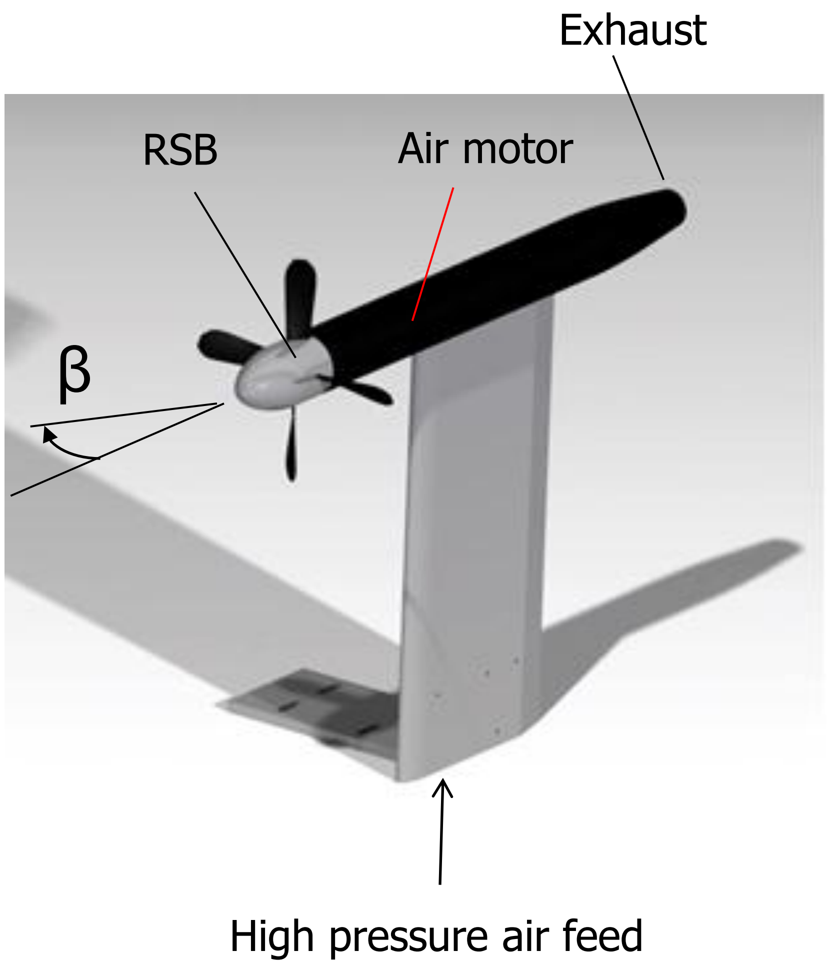

Test results (1/6)

RPM sweep

Thrust and torque coefficient

$$C_T = \frac{T}{n^2 D^4 \rho}$$

$$C_Q = \frac{T}{n^2 D^5 \rho}$$

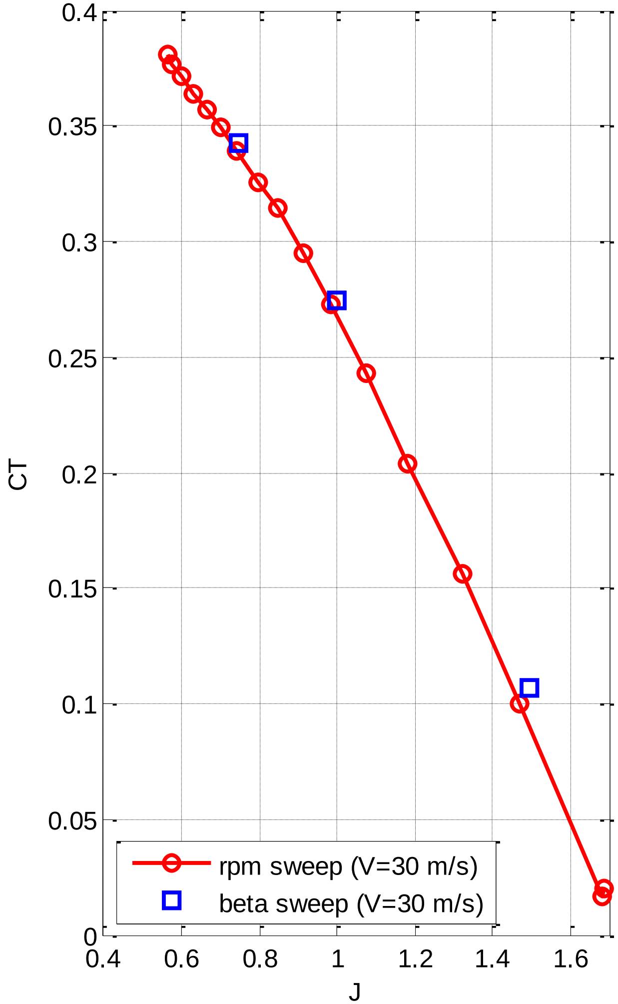

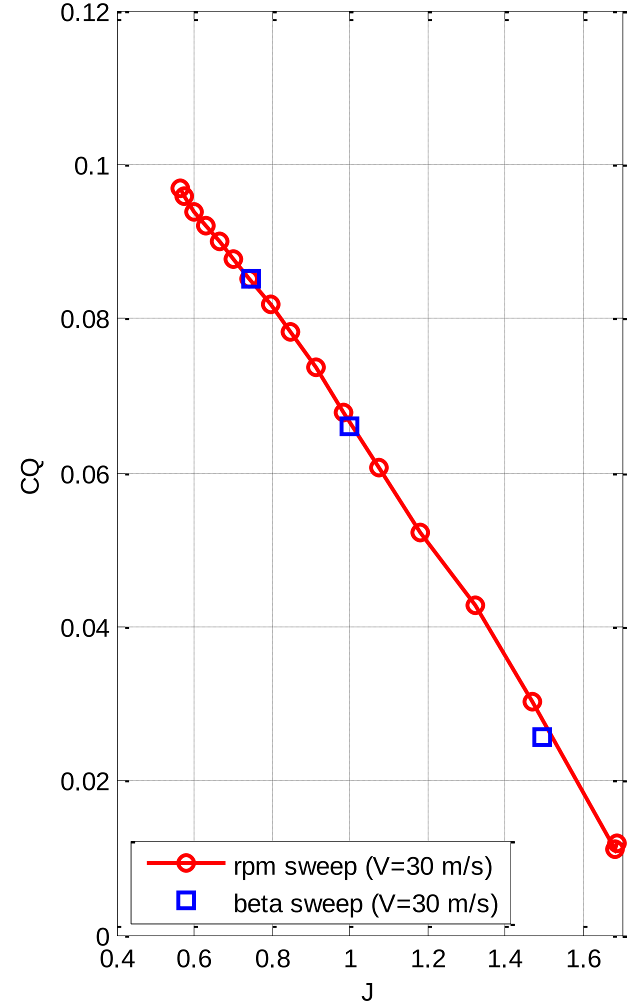

Test results (2/6)

RPM sweep

Propeller efficiency

$$\eta = \frac{J}{2\pi}\frac{C_T}{C_Q}$$

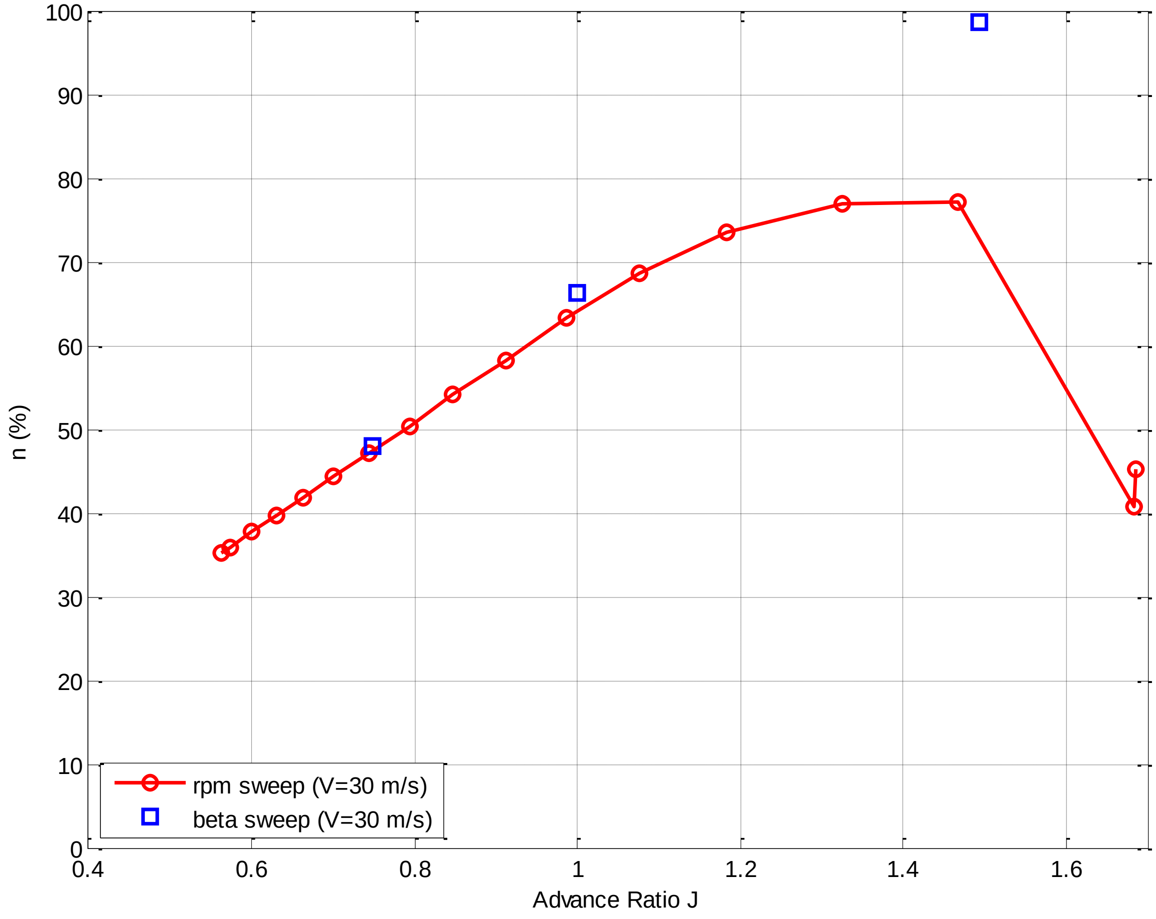

Test results (3/6)

Beta sweep

Comparison with BEM analysis

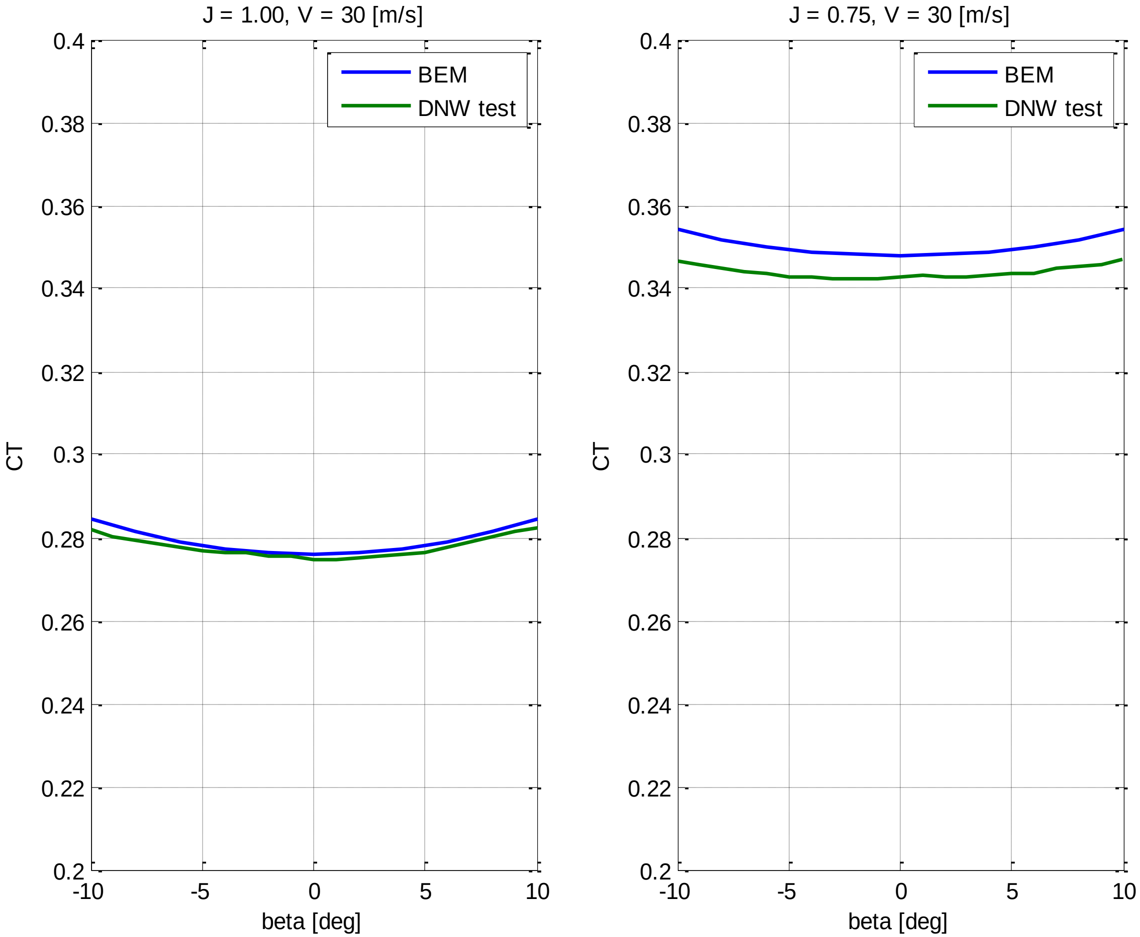

Test results (4/6)

Beta sweep

Efficiency based on thrust in axis direction increases for non-zero angle of attack

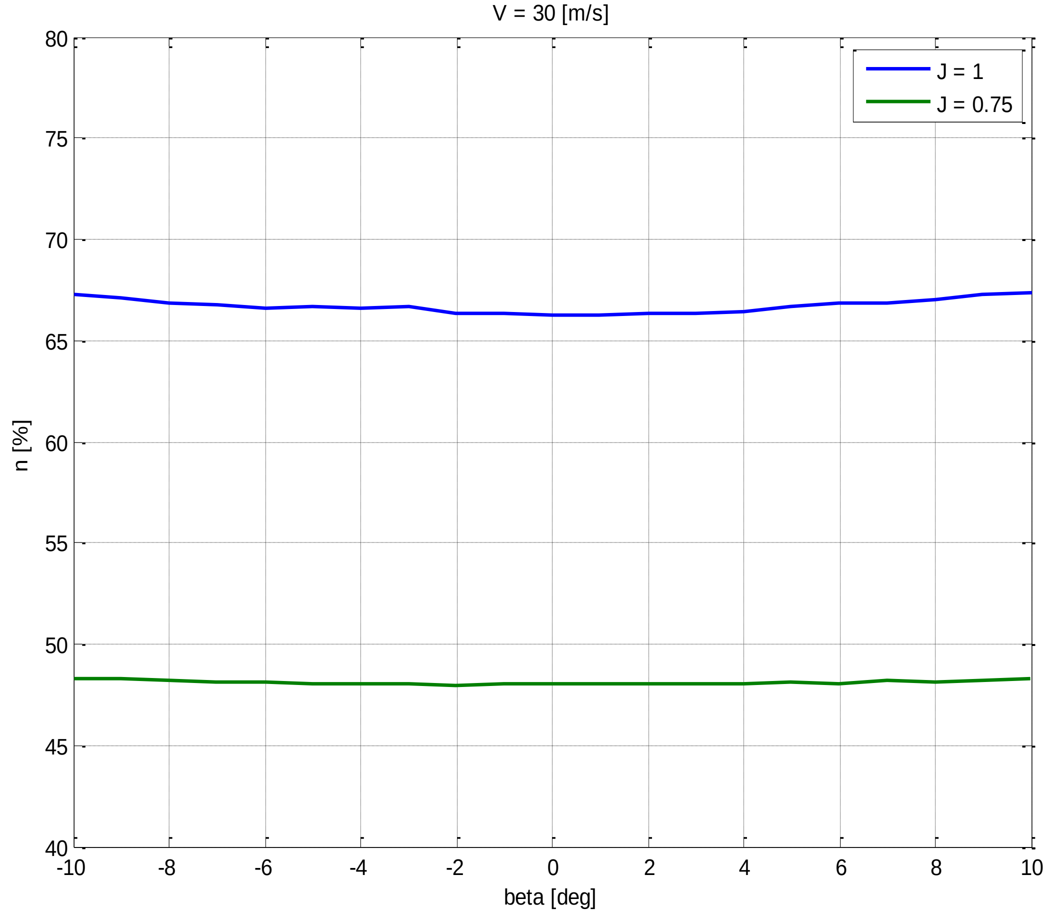

Test results (5/6)

Velocity distributions from 5-hole probe data. Traverses at x/D=0.18 behind the propeller

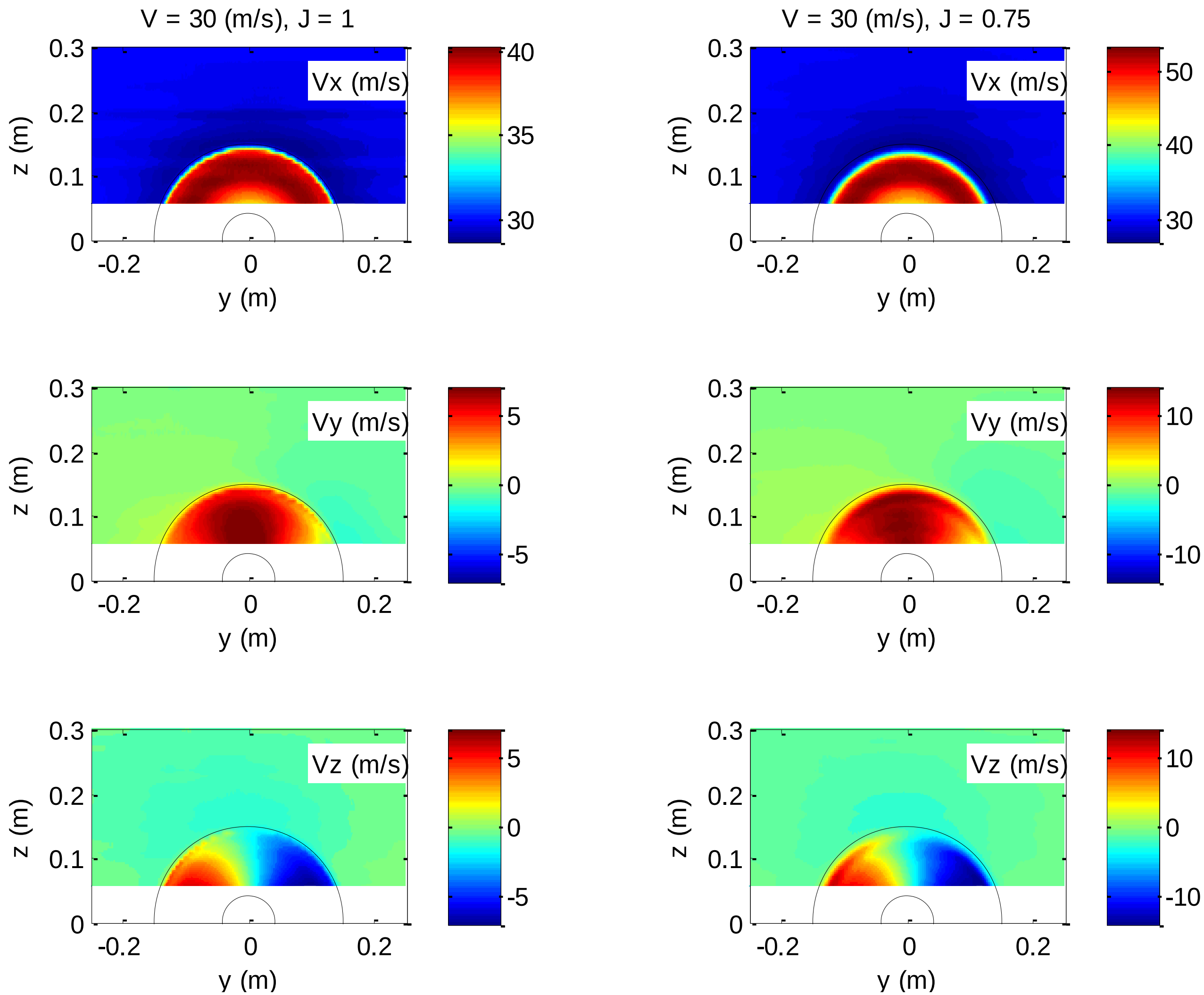

Test results (6/6)

Beta

Radial swirl angle distribution at x/D=0.18 behind the propeller.

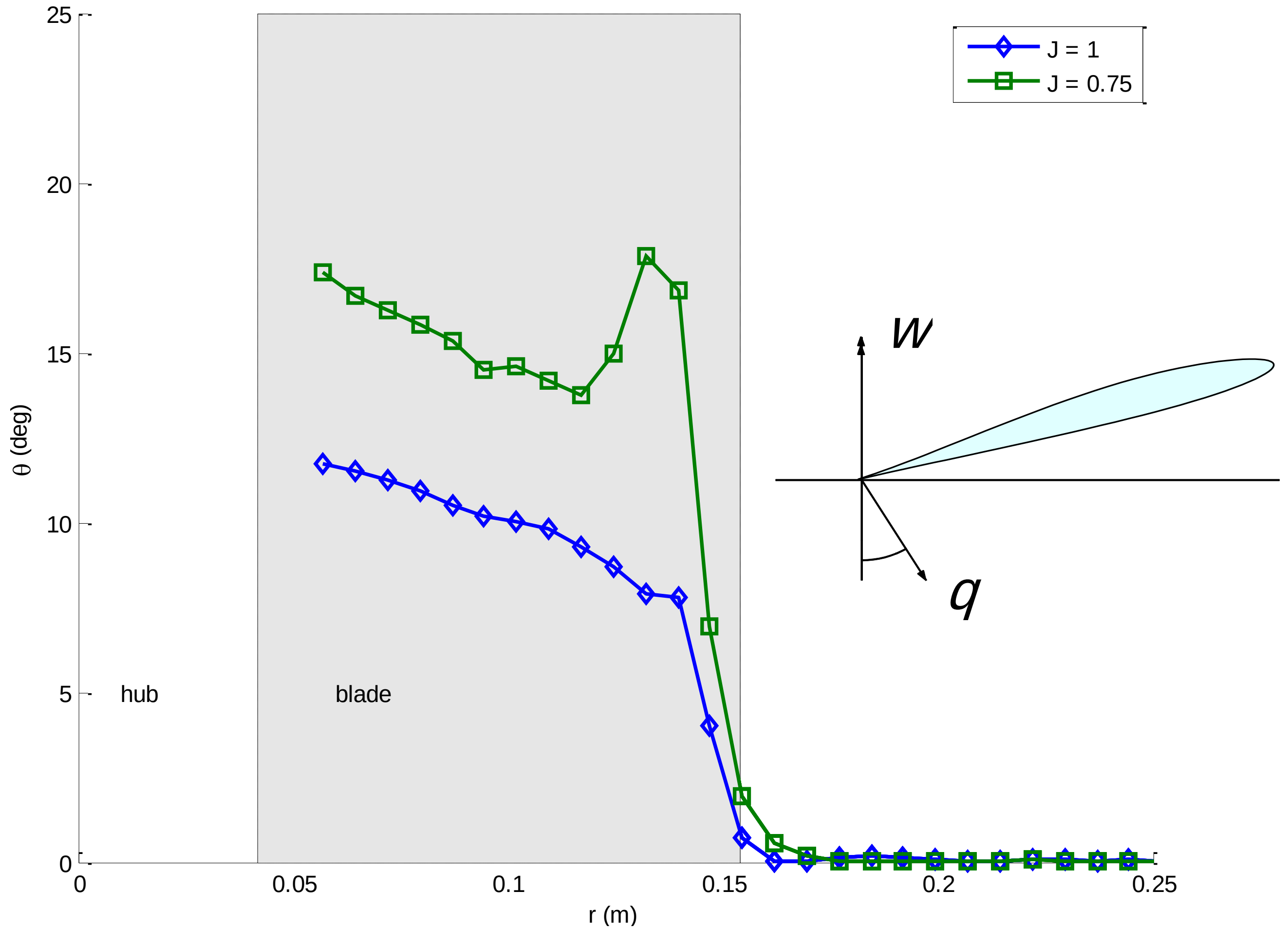

Upcoming tests TUD

Non-uniform inflow field

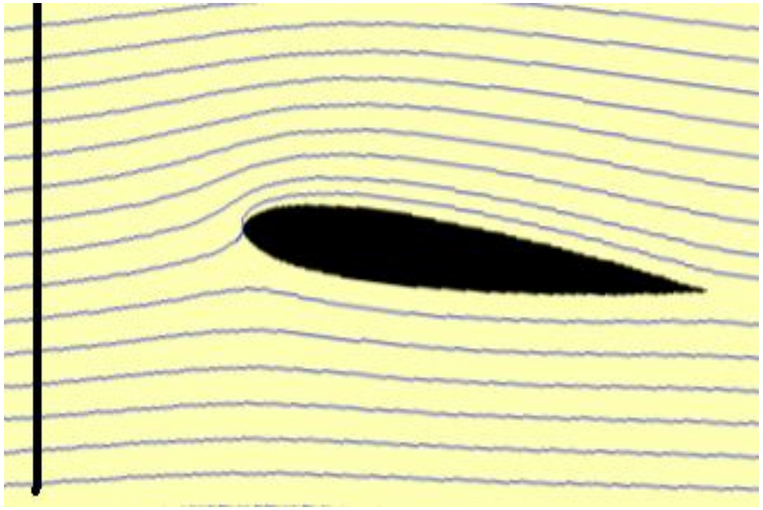

Propeller in wing upwash field

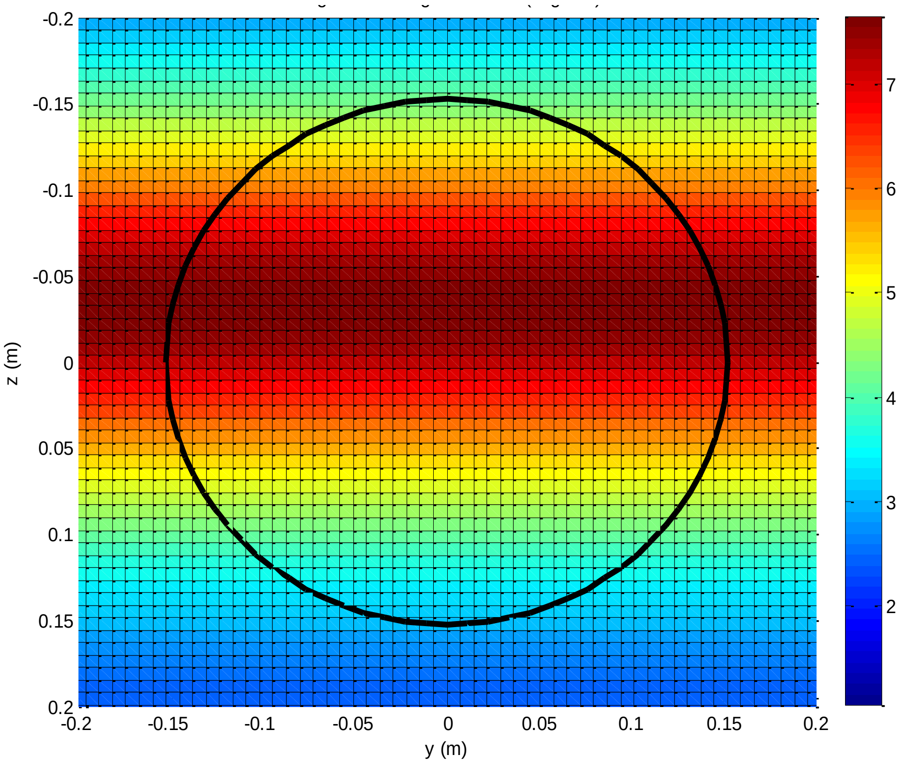

Wing induced angle of attack in propeller plane

Upcoming tests TUD

Test setup

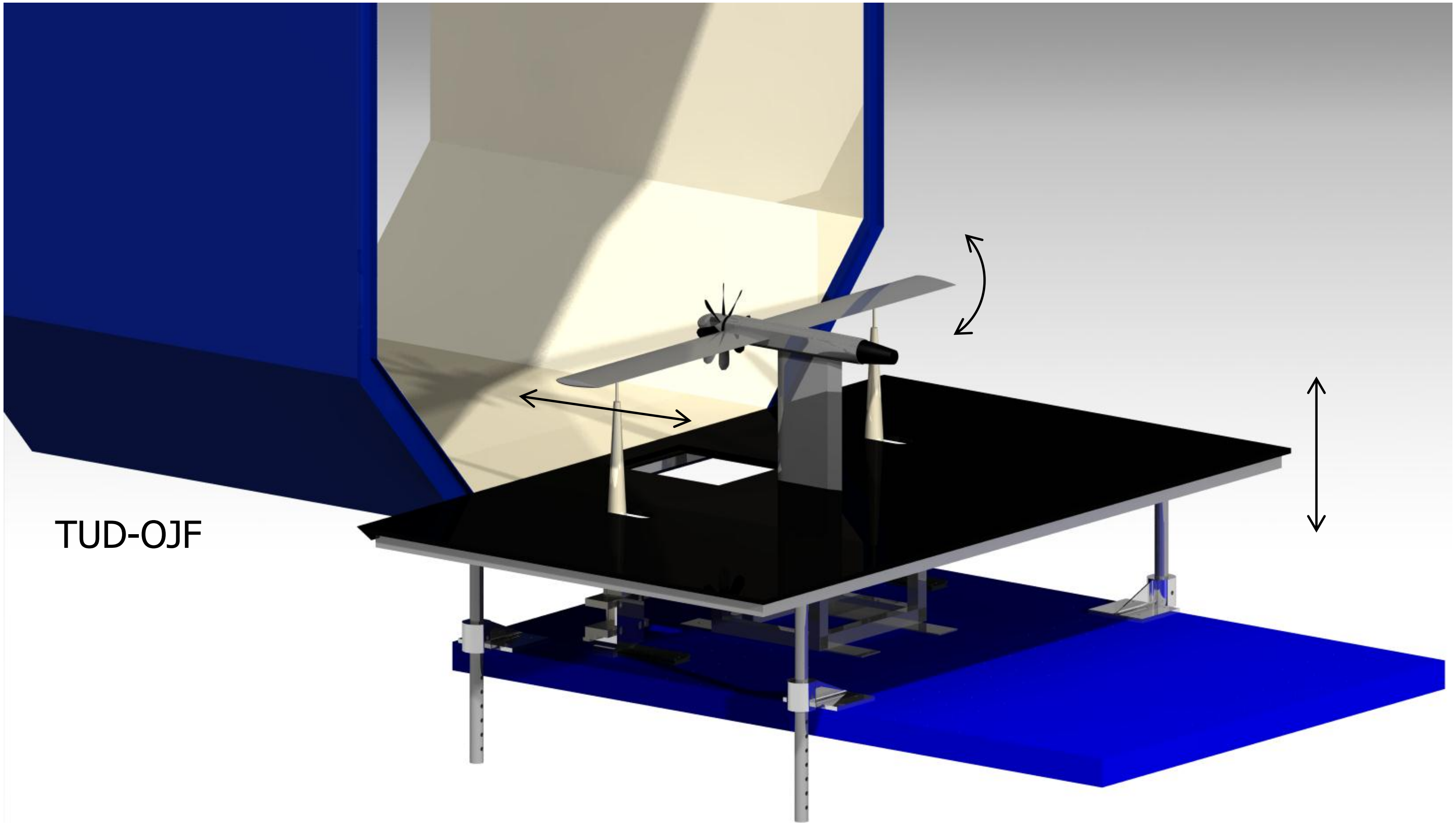

Upcoming tests TUD

Test setup

Propeller with Rotating Shaft Balance (RSB) inside.

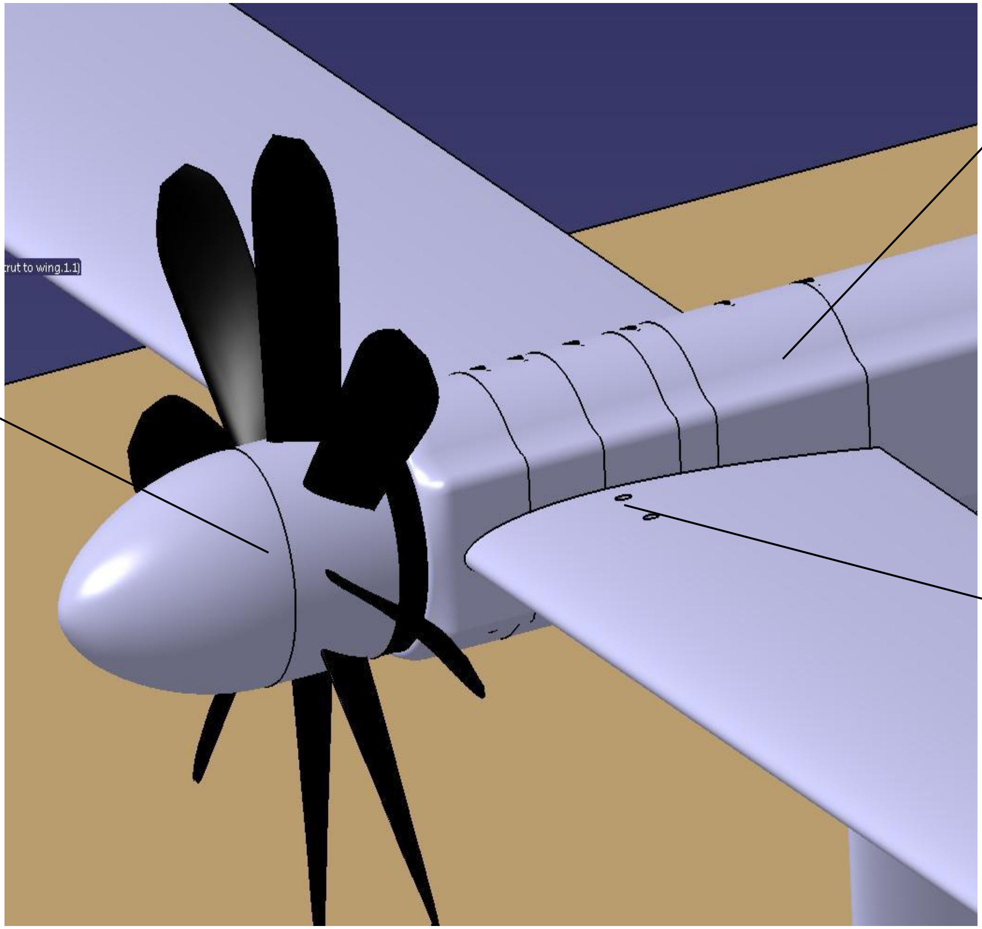

Interchangeable rings for adjustment of propeller-wing distance

Pivot point for changing wing angle of attack

Conclusions

- Preliminary investigations on the influence of a non-uniform inflow field on the propellers performance have been performed successfully during a commissioning test.
- Non-zero propeller angle of attack increases the thrust, torque and efficiency of the propeller for fixed J, as expected.
- This effect increases with advance ratio. For a free stream velocity of 30 m/s and an advance ratio of 0.75 the efficiency increase with angle of attack is less than 0.3% and 1.1% for an advance ratio of 1.
- An adapted BEM model that takes non-zero propeller angle of attack into account predicted propeller performance with reasonable accuracy.
- Tip vortex becomes dominant for low advance ratios. This is not explicitly incorporated in the BEM.
- Preparations for the ESPOSA test campaign are well under way. Phase 1 tests will commence on 12 Nov. 2012.

Outlook

Running research projects

- Propeller induced ground vortex

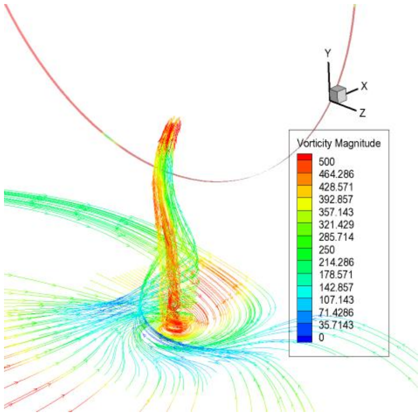

- Pylon TE blowing

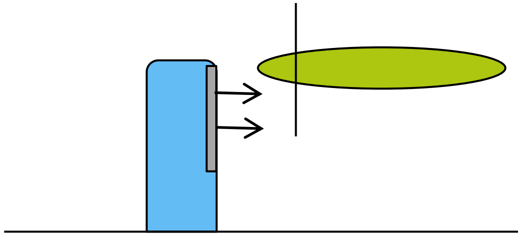

- Swirl Recovery Vanes

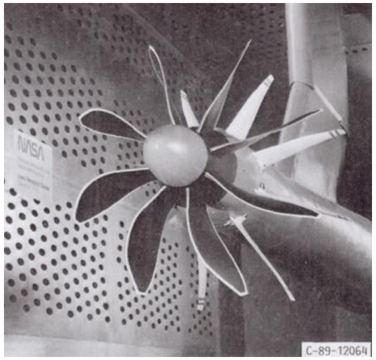

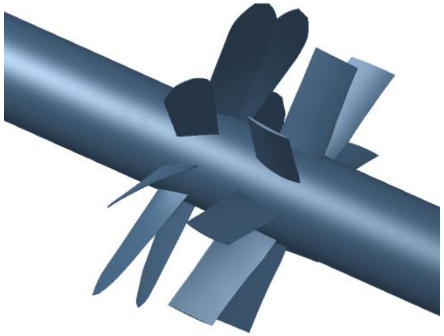

Piotr ŁAPKA[1]

Mirosław SEREDYŃSKI[1]

Piotr FURMAŃSKI[1]

Adam DZIUBIŃSKI[2]

Jerzy BANASZEK[1]

[1] Institute of Heat Engineering, Warsaw University of Technology , Poland

[2] Institute of Aviation, Warsaw, Poland

Simplified thermo-fluid model for detection of high-temperature elements of engine cowling in a small airplane

ITC

Outline

1. Introduction
2. Geometrical model
3. Numerical simulation
4. Results
5. Conclusions and future development

1. Introduction

Introduction

One of challenges faced during the development of a new aircraft is to ensure that temperatures of the engine nacelle are within the allowable limits during operation under normal and extreme conditions.

- The cowling is usually made of plastic composites e.g.: fiberglass or carbon fibers:
  - ❑ good mechanical properties,
  - ❑ cannot be exposed to high temperature.

- Many elements inside the engine bay reach very high temperatures and by heat conduction, convection and thermal radiation heat up the interior of the nacelle:
  - ❑ Special ventilation and cooling systems as well as heat shields should be developed to reduce temperature in the cowling and other elements,
  - ❑ Materials used for e.g.: exhaust systems, thermal heat barriers and engine cowling should be selected according to expected most adverse thermal conditions.

Thermal analysis is necessary in order to verify that an adequate cooling is ensured in all flight conditions.

Purpose of the work

- The main objective of the work was to develop simplified numerical model of fluid flow and heat transfer inside the engine bay prototype of the airplane I-23 in the tractor configuration equipped with turboprop engine TP100 in the fuselage.

- Analysis of an impact of different inlets and outlets configurations and different inlet conditions on flow field and temperature distribution in the cowling were carried out to find high-temperature spots on the internal side of the nacelle.

- The obtained results will help in future studies on a new design of ventilation and cooling systems and will contribute to select materials for parts of the engine bay.

2. Geometrical model

Geometrical model

Geometrical model of the cowling and the TP100 engine bay

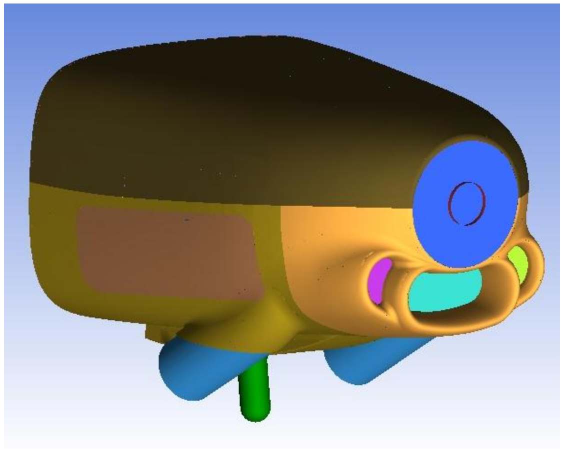

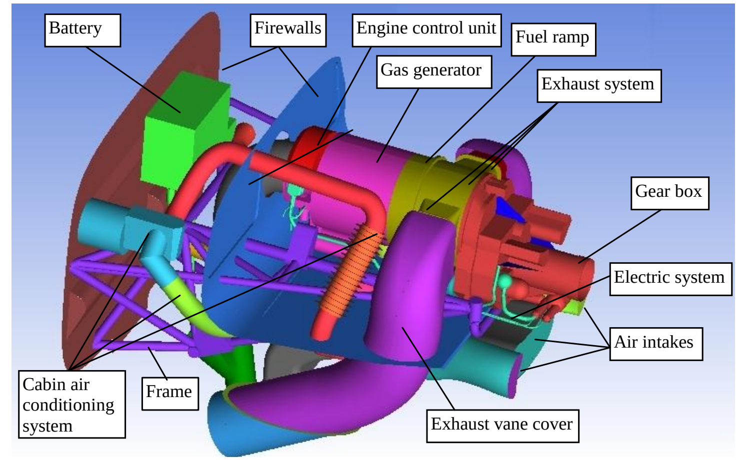

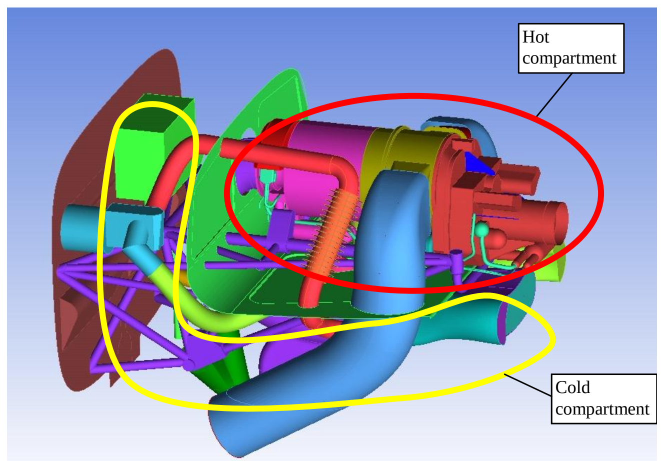

ITC

Geometrical model

Locations of air inlets and outlets

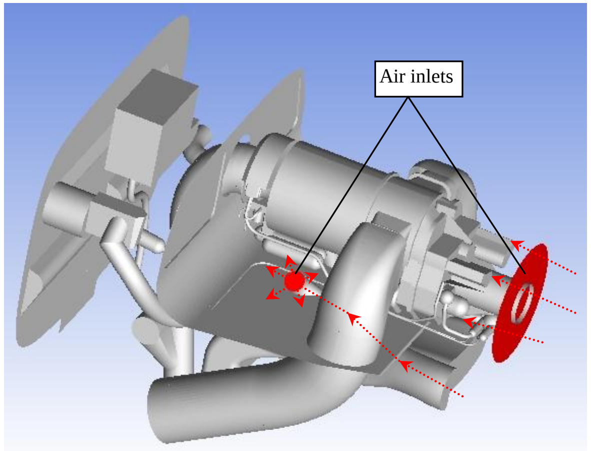

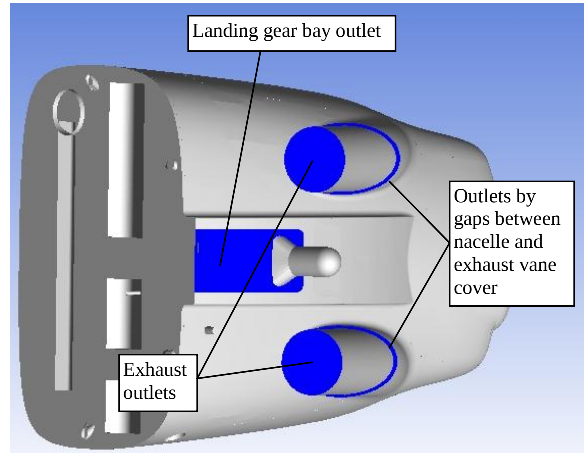

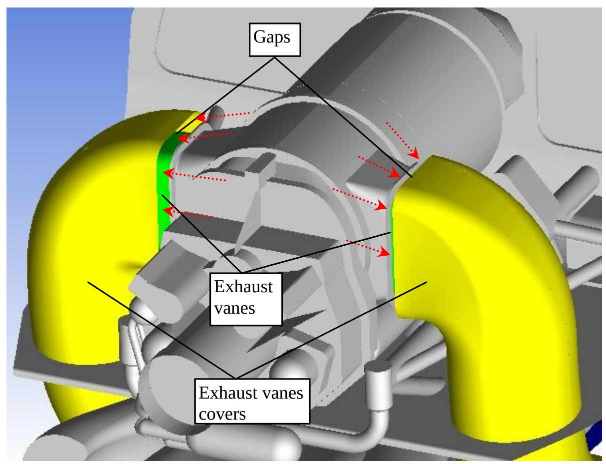

3. Numerical simulation

Numerical simulation

Mesh

- Over 11 millions of tetrahedral control volumes with almost 23 millions of faces,
- Refined close to the boundaries, near small elements, hot surfaces and in the gap between exhaust vanes and exhaust vane covers.

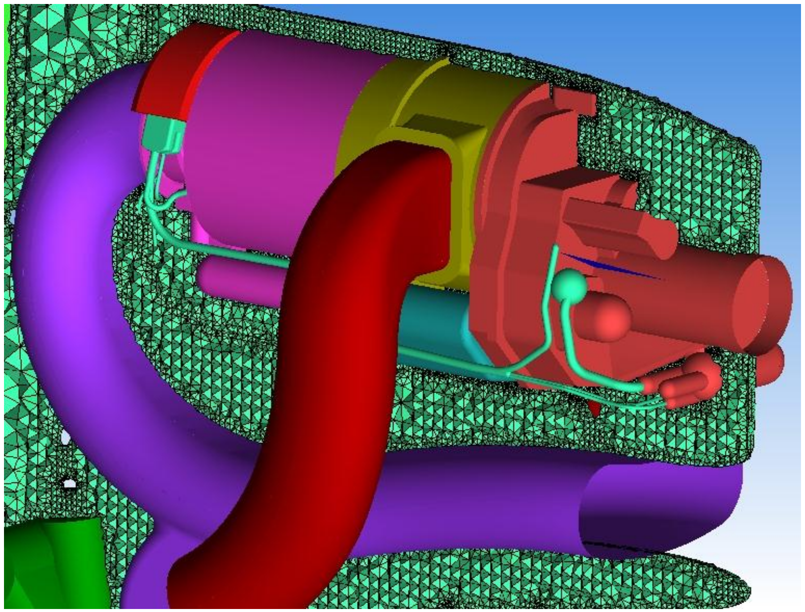

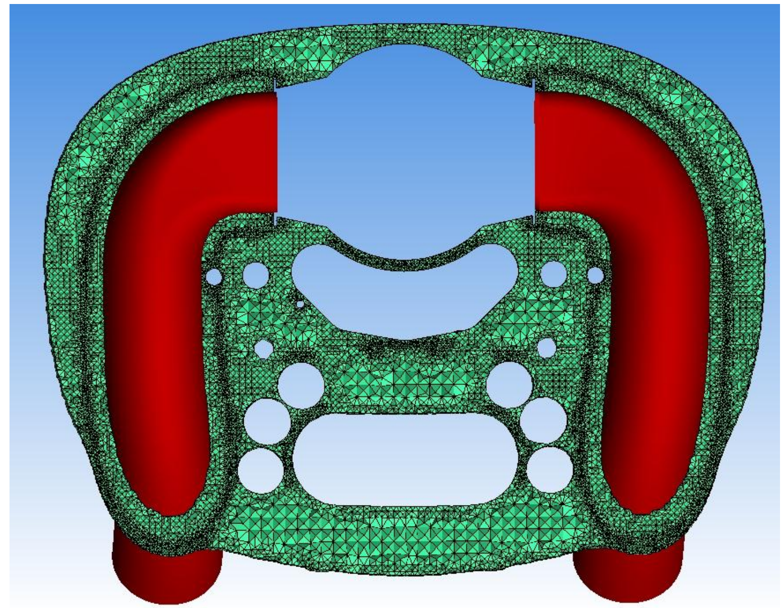

Numerical simulation

Solution

ANSYS FLUENT 14.0

Assumptions

- Steady state simulation,
- Thermal radiation was neglected due to time limitation,
- *Realizable k-ε model* for turbulence with *Scalable Wall Function* approximation,
- Momentum and pressure variables were coupled with the SIMPLEC procedure,
- *Second order upwind* scheme was applied to all balance equations,
- To include air buoyancy effects the perfect gas model was utilized,
- 1D shell heat conduction model was applied to some internal and external surfaces.

Numerical simulation

Boundary conditions

Simulations were performed for the airplane waiting for takeoff (case A) and additionally for three velocities of its operation (cases B, C and D).

Case	Velocity of ambient air [km/h]	Common inlet gauge pressure [Pa]	$\overline{\mathrm{Nu}}_L$	$\bar{h}_L$ [W/m^{2}K]
A	30	0	1265.86	24.7
B	100	472.61	3285.79	83.6
C	200	1890.15	6114.63	155.6
D	300	4253.47	8661.09	220.3

Numerical simulation

Boundary conditions

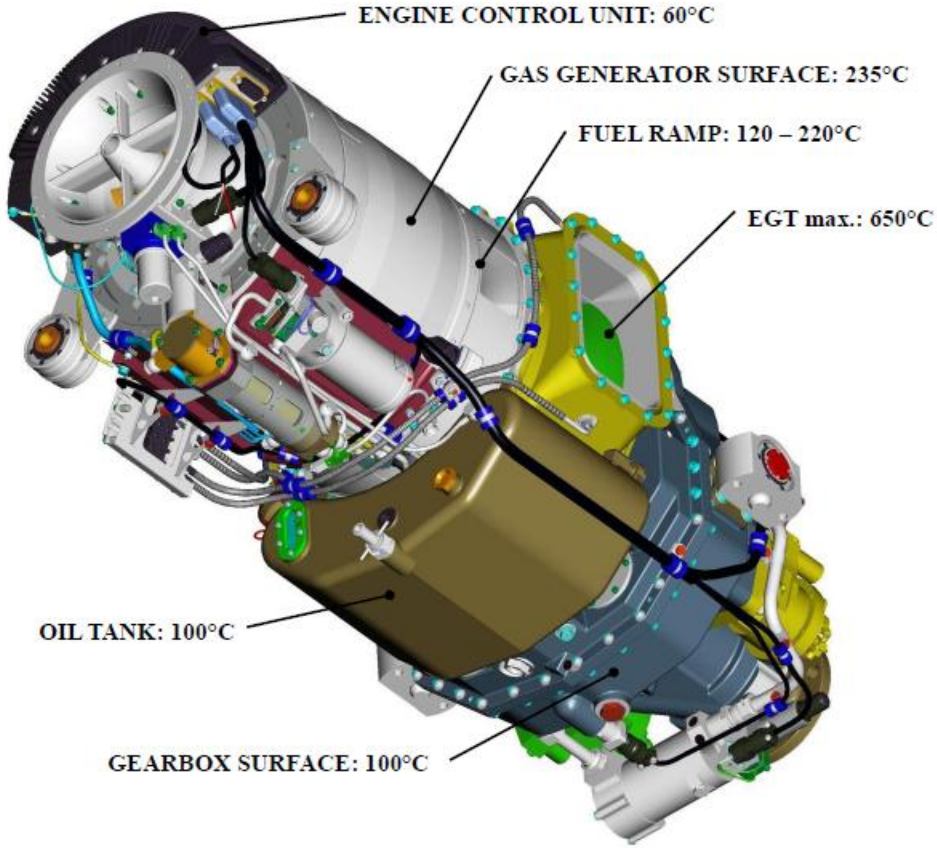

Data taken from „*Recommendations for engine - airframe installation within ESPOSA project*"

Numerical simulation

Inlets and outlets configurations

Four different inlets and outlets configurations were analyzed. For all cases fixed locations of inlets below the engine as well as fixed locations of the outlets in the gaps (between nacelle and exhaust vanes covers) and in the exhaust system (air flow induced by ejector effect) were assumed. The additional inlet around the spinner mount and the optional outlet in the landing gear bay were assumed.

	Inlets in nacelle	Inlet round the spinner	Outlets in the gap and in exhaust system	Outlet in the landing gear bay
Case I	x	x	x	-
Case II	x	-	x	-
Case III	x	x	x	x
Case IV	x	-	x	x

4. Results

Results

Temperatures and mass flow rates

	Air velocity [km/h]	Maximum temperature [K]: Nacelle	Maximum temperature [K]: Exhaust vane covers	Mass flow rate [kg/s]: Inlets in nacelle	Mass flow rate [kg/s]: Inlet round the spinner	Mass flow rate [kg/s]: Outlets in the gap	Mass flow rate [kg/s]: Outlets in the exhaust system	Mass flow rate [kg/s]: Outlet in the landing gear bay	Heat transfer rate [kW]
Case I	A: 30	322.05	664.13	0.028	0.402	0.055	- 0.485	-	- 21.78
	B: 100	322.76	629.22	0.051	1.024	- 0.493	- 0.582	-	- 27.16
	C: 200	322.68	558.79	0.085	1.757	- 1.004	- 0.838	-	-38.60
	D: 300	322.84	504.41	0.122	2.577	- 1.518	- 1.181	-	-52.28
Case II	A: 30	322.09	673.00	0.096	-	0.366	- 0.462	-	- 22.88
	B: 100	322.30	660.01	0.200	-	0.276	- 0.476	-	- 23.96
	C: 200	322.16	666.73	0.375	-	0.101	- 0.476	-	- 25.84
	D: 300	321.93	666.07	0.559	-	- 0.084	- 0.475	-	- 27.66
Case III	A: 30	322.22	624.31	0.028	0.403	0.052	- 0.485	0.001	- 21.65
	B: 100	323.91	623.17	0.076	1.708	- 0.317	- 0.575	- 0.891	- 28.67
	C: 200	324.02	572.73	0.137	3.158	- 0.660	- 0.807	- 3.157	- 40.49
	D: 300	323.70	527.76	0.203	4.670	- 1.005	- 1.123	- 2.744	- 54.90
Case IV	A: 30	322.54	667.41	0.061	-	0.144	- 0.479	0.274	- 23.04
	B: 100	322.66	657.57	0.191	-	0.105	- 0.486	0.190	- 23.75
	C: 200	322.01	667.03	0.373	-	0.049	- 0.478	0.056	- 25.75
	D: 300	322.11	668.44	0.558	-	0.002	- 0.476	-0.084	- 27.22

Results

Contours of temperature

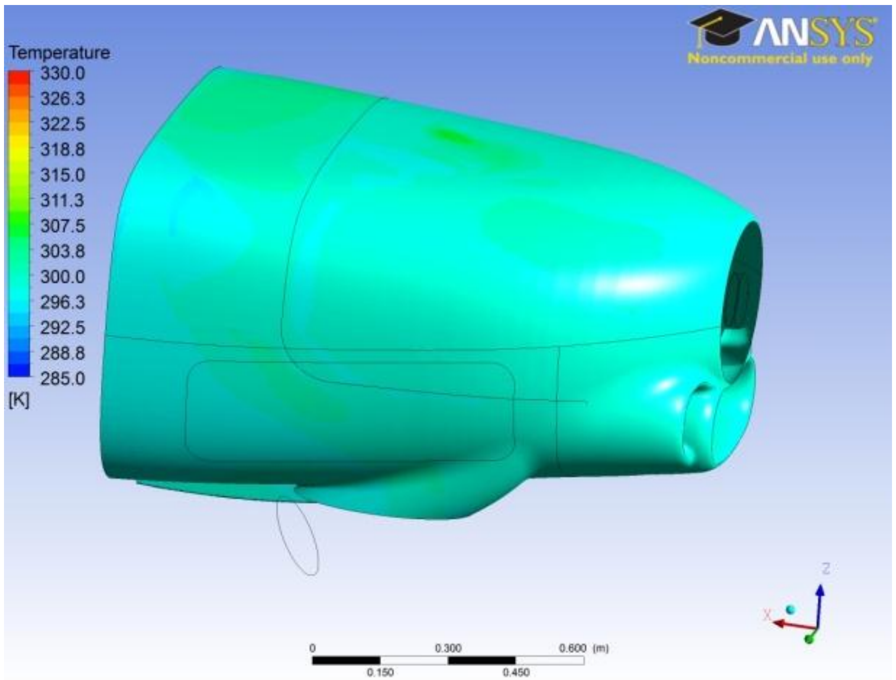

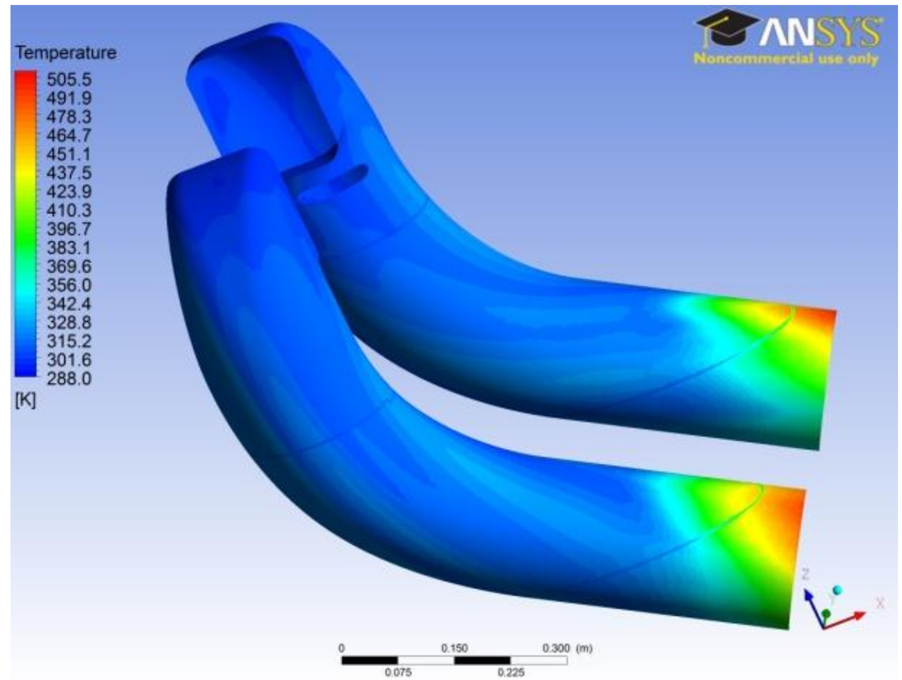

Results

Stream lines originated from inlet round spinner mount and inlets in nacelle for case I-D

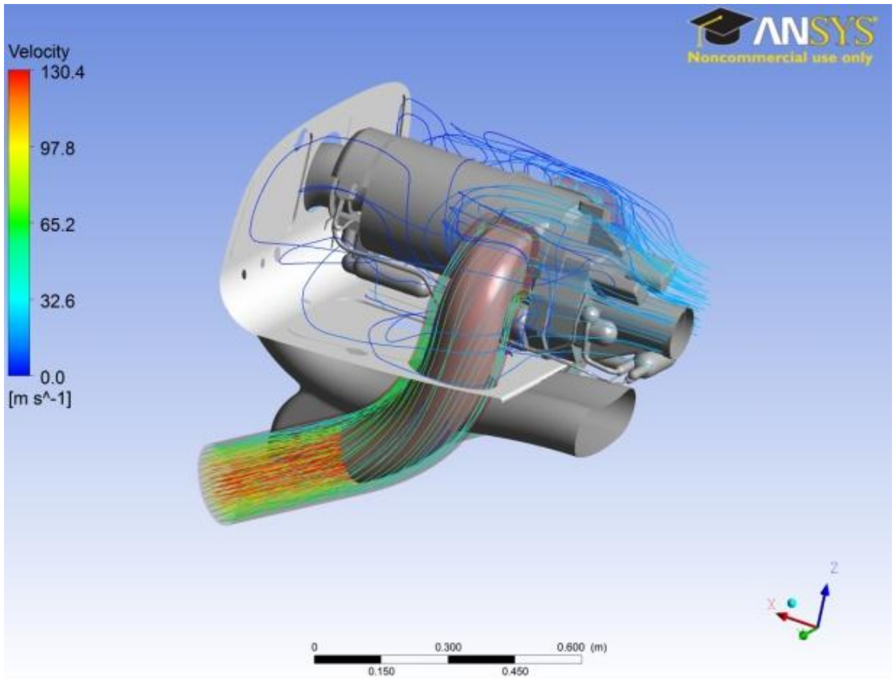

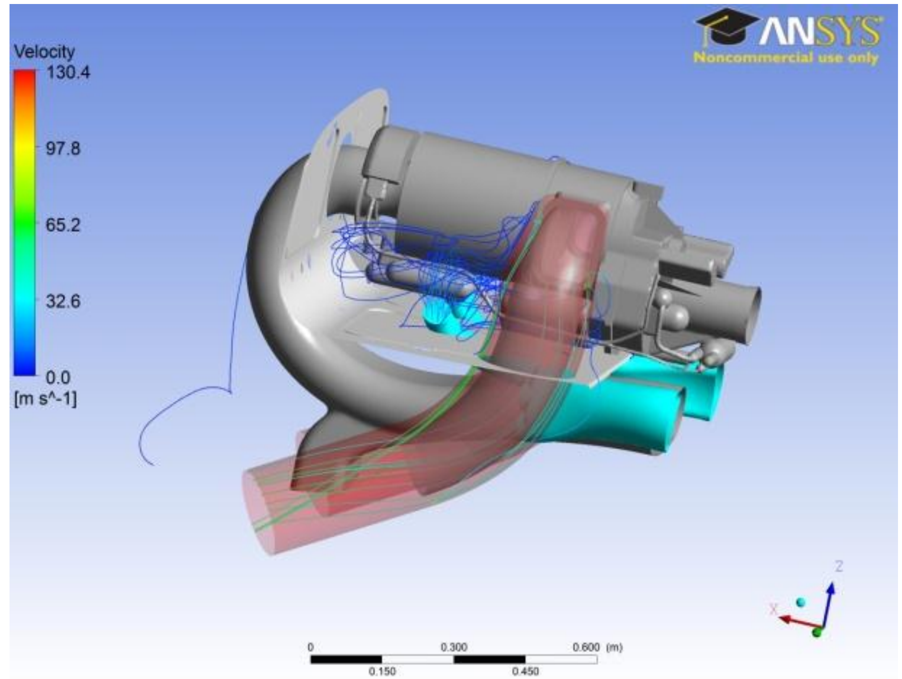

5. Conclusions and future development

Conclusions

- Simplified numerical model was developed as well as fluid flow and heat transfer simulations in the engine bay were performed for different conditions at the air inlets and for different inlets and outlets configurations,

- The results show that the inlet round the spinner mount is beneficial and ensures effective cooling of the exhaust system,

- Additional inlet in the cold part of the nacelle is suggested instead of the outlet located in the landing gear bay,

- The maximum temperature at the nacelle surface was observed just above the engine and near exhaust vanes covers. The highest temperature of the exhaust covers was found in the region close to their outlets.

Future development of the model

Future work

- Modeling of thermal radiation emitted or reflected on surfaces and emitted by hot exhaust gases:
    - ❑ P-1 or FVM for radiative heat transfer.

- Thermal analysis concentrated on selected regions or parts of cowling:
    - ❑ Fine mesh,
    - ❑ Optimization.

Thank You

IDIHOM

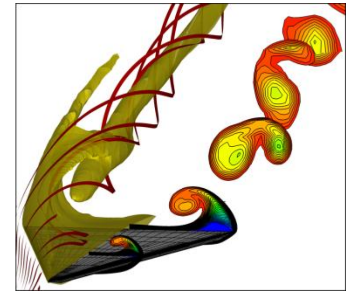

IDIHOM -

European project on Industrialization of High-Order Methods for Aeronautical Applications

Collaborative Research Project, 7th European Framework Programme

SEVENTH FRAMEWORK PROGRAMME

Norbert Kroll

German Aerospace Center

DLR

2nd EASN Workshop on Flight Physics and Propulsion, Prague, 31st October – 2nd November 2012

Flightpath 2050

Europe's Vision for Aviation

- Maintaining Global Leadership & Serving Society's Needs

Goals *(relative to typical aircraft in 2000)*

- CO_2 emissions reduced by 75%
- NOx emissions reduced by 90%
- 65% reduction in perceived aircraft noise

Consequence

- Heavy demands on future product performance
- Step changes in aircraft technology required
- New design principles mandatory

Numerical Simulation - Key Enabler for Future Aircraft Design

Future aircraft

- Design may be driven by unconventional layouts
- Flight characteristics may be dominated by non-linear effects

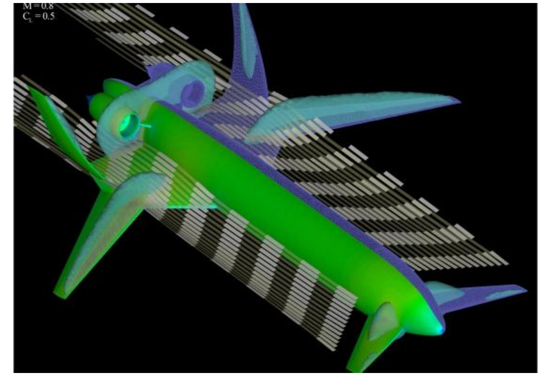

High-fidelity simulation methods indispensable for design & assessment of step changing aircraft

- Reliable insight to new aircraft technologies
- Comprehensive sensitivity analysis with risk & uncertainty management
- Best overall aircraft performance through integrated aerodynamics / structures / systems design
- Consistent and harmonized aerodynamic and aeroelastic data across flight envelope

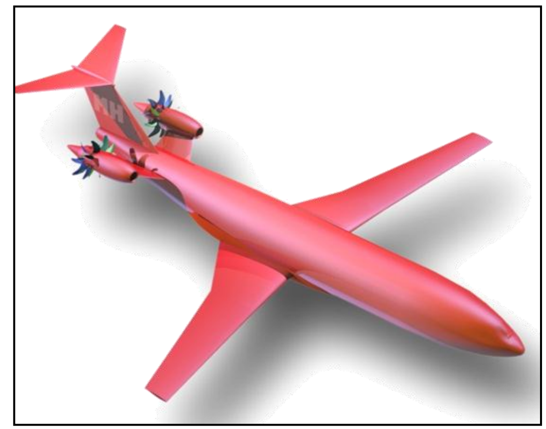

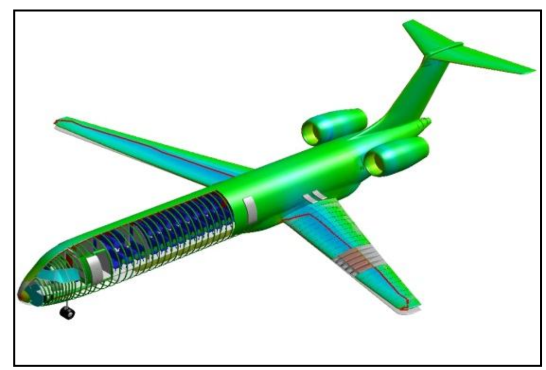

Numerical Simulation

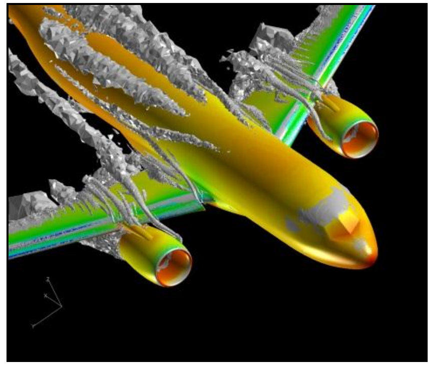

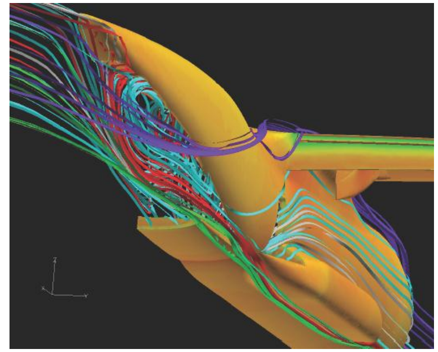

Status

- Computational Fluid Dynamics (CFD) has significantly evolved over the last 25 years
- Mature tool for configurations at their design point in flight envelope
- Complementary to wind tunnel testing and flight tests
- **Total potential not yet exploited:**
  - **Full flight envelope**
  - **Integration of all relevant disciplines**
  - **Multi-disciplinary optimization**

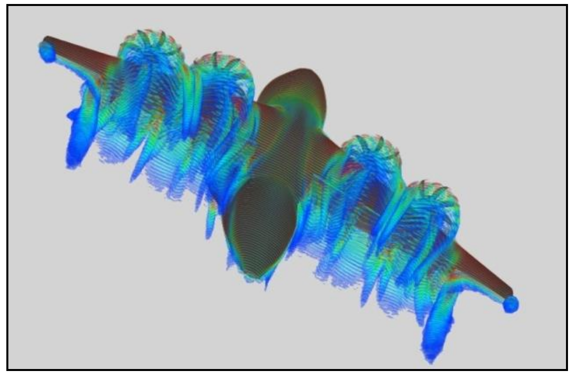

Limitations

- Physical modeling
- Computational complexity

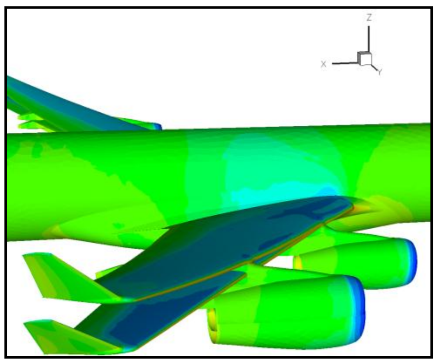

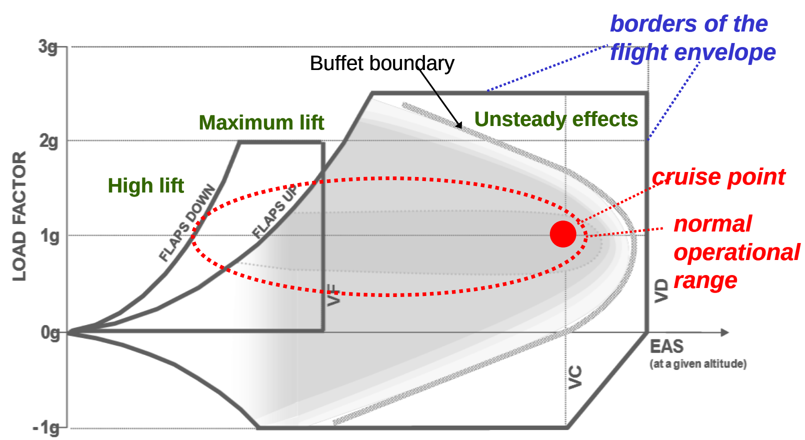

CFD Tools in Aeronautical Industry

Status

- Based on 2nd order methods
- Effective order often between 1st and 2nd order due to irregular meshes

- Very fine meshes for complex applications required

→ **Large scale applications very expensive**

Mesh independent solutions often not feasible

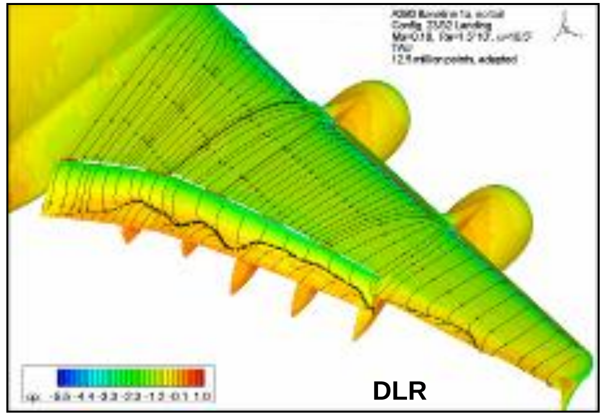

complete aircraft, high-lift
objective: aerodynamic forces
grid: > 30 million grid points

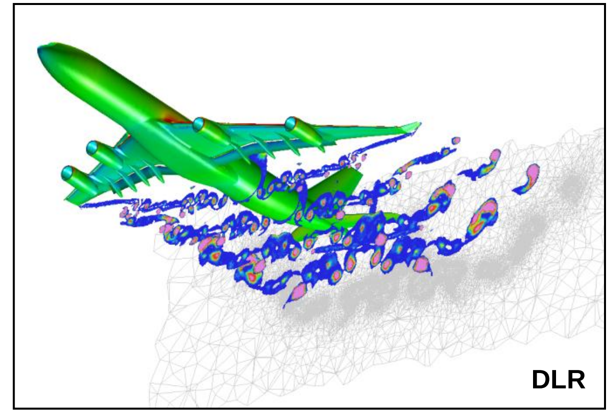

complete aircraft, high-lift
objective: wake vortex
grid: > 40 million grid points

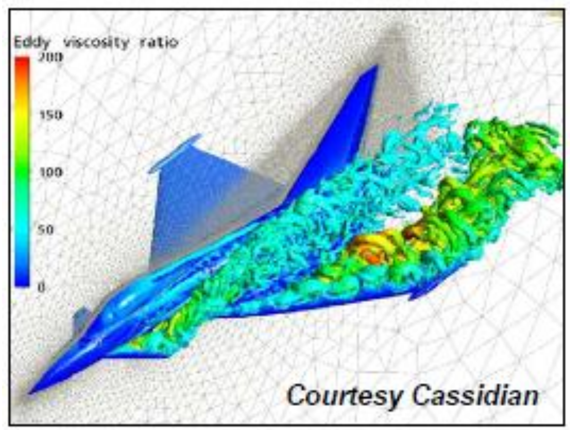

complete fighter, full conf.
objective: vortical flow, high α
grid: > 30 million grid points

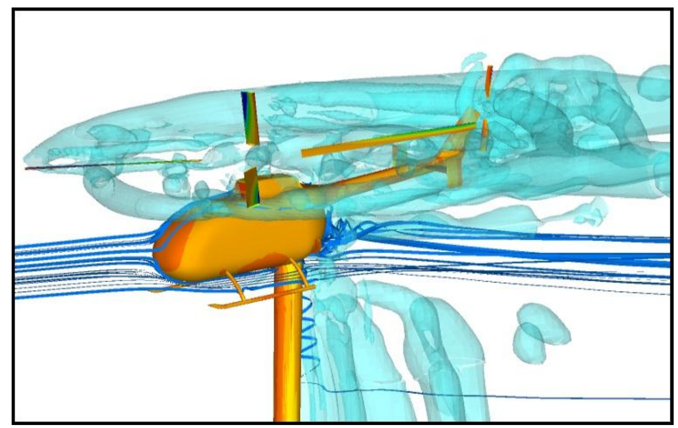

complete helicopter
objective: wake interaction
grid: > 50 million grid points

Need for Innovative Numerical Algorithms / Strategies

Adaptive Higher-Order Methods best suited to

- Meet high accuracy requirements
- Capture widest range of scales
  at acceptable cost
- Enable grid independent solutions

Function to be approximated

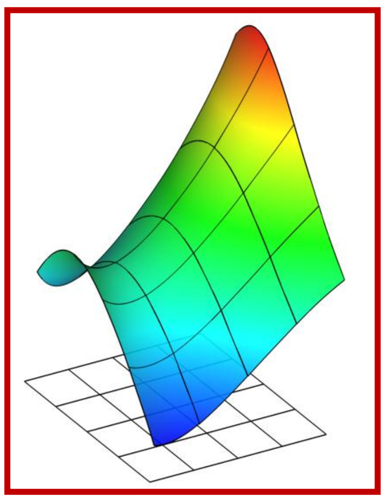

Levels of Approximation

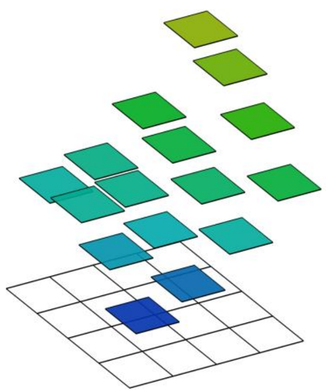

piecewise constant functions

1st order method

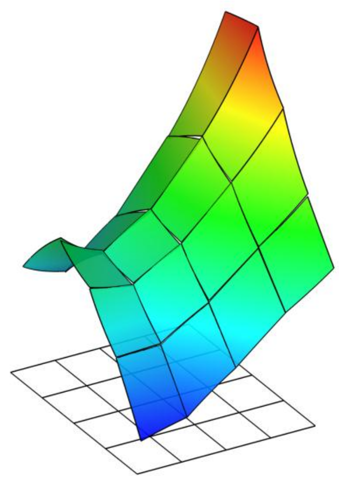

piecewise linear functions

2nd order method

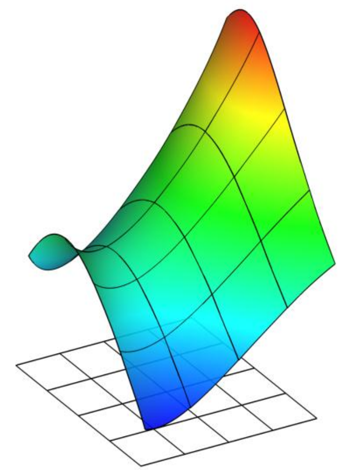

piecewise quadratic functions

3rd order method

Need for Innovative Numerical Algorithms / Strategies

Adaptive Higher-Order Methods best suited to

- Meet high accuracy requirements
- Capture widest range of scales at acceptable cost
- Enable grid independent solutions

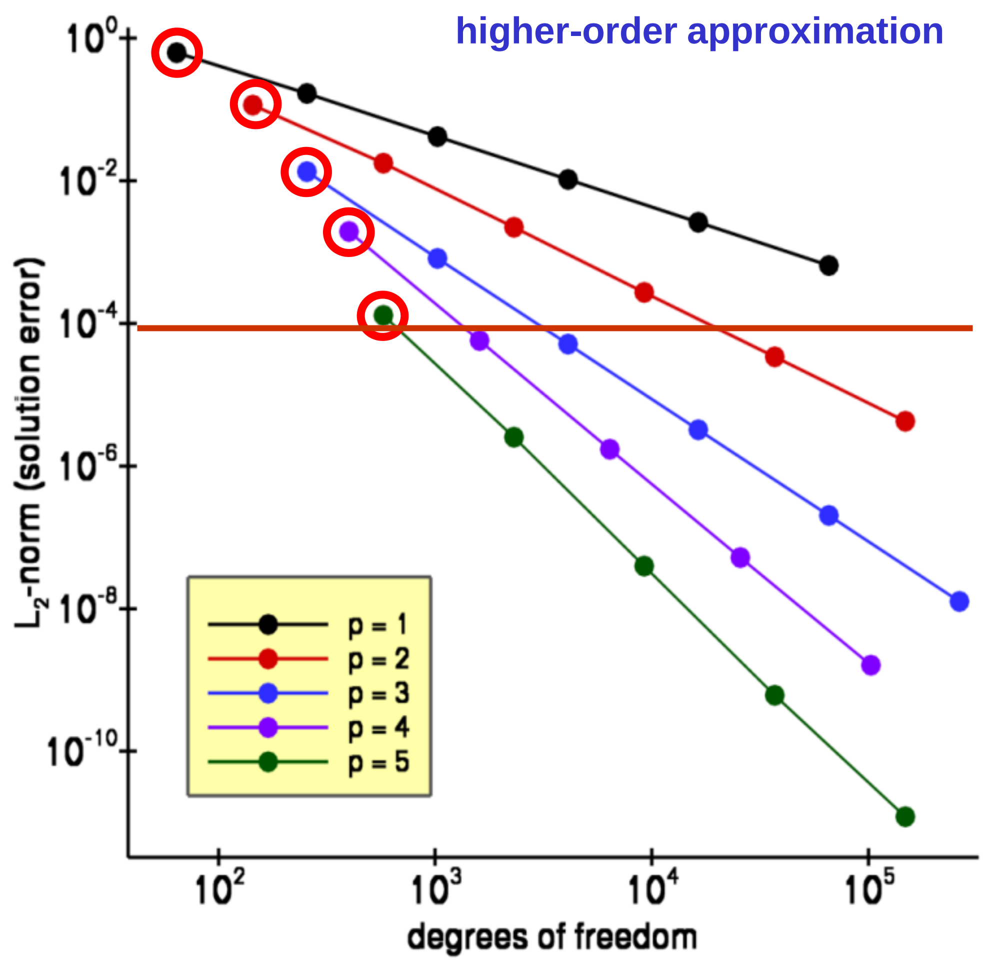

Need for Innovative Numerical Algorithms / Strategies

Adaptive Higher-Order Methods best suited to

- Meet high accuracy requirements
- Capture widest range of scales
  at acceptable cost
- Enable grid independent solutions

adaptive resolution

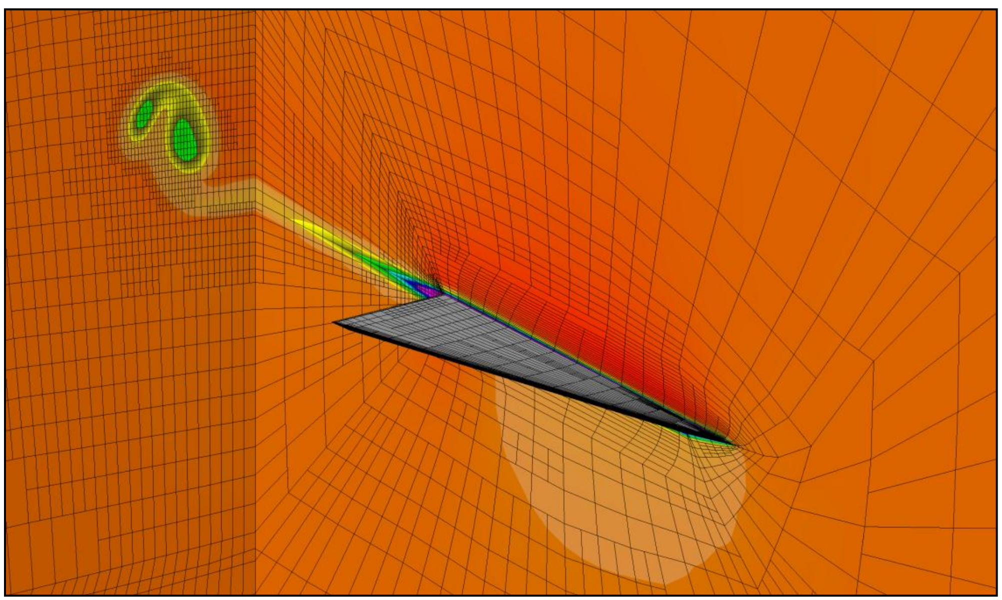

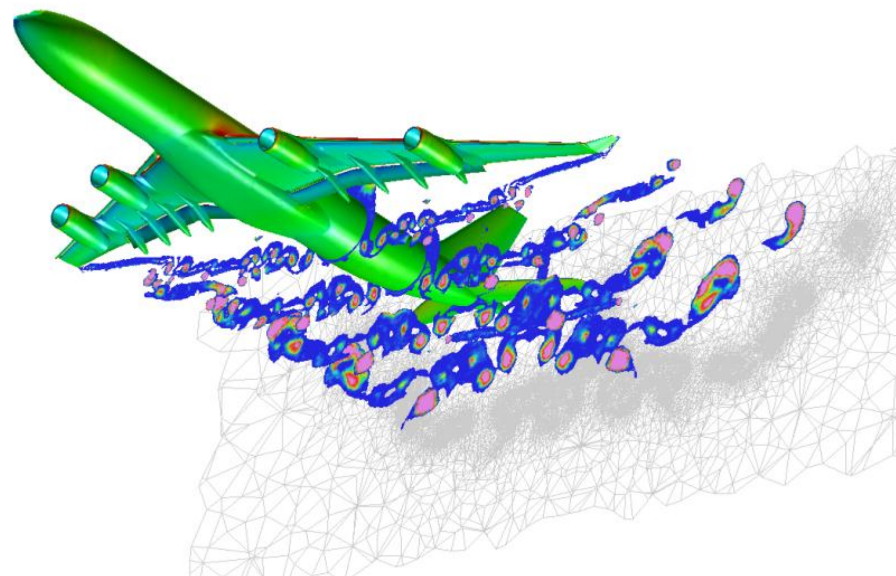

Need for Innovative Numerical Algorithms / Strategies

Adaptive Higher-Order Methods best suited to

- Meet high accuracy requirements
- Capture widest range of scales at acceptable cost
- Enable grid independent solutions

Limitations / restrictions

- Resolution of discontinuities
- Complex bodies with curved boundaries
- Efficient solution strategies for large scale applications
- Reliable refinement techniques and error estimates
- Prediction of turbulent flows

Major research activity worldwide

- **2 EU projects: ADIGMA & IDIHOM**

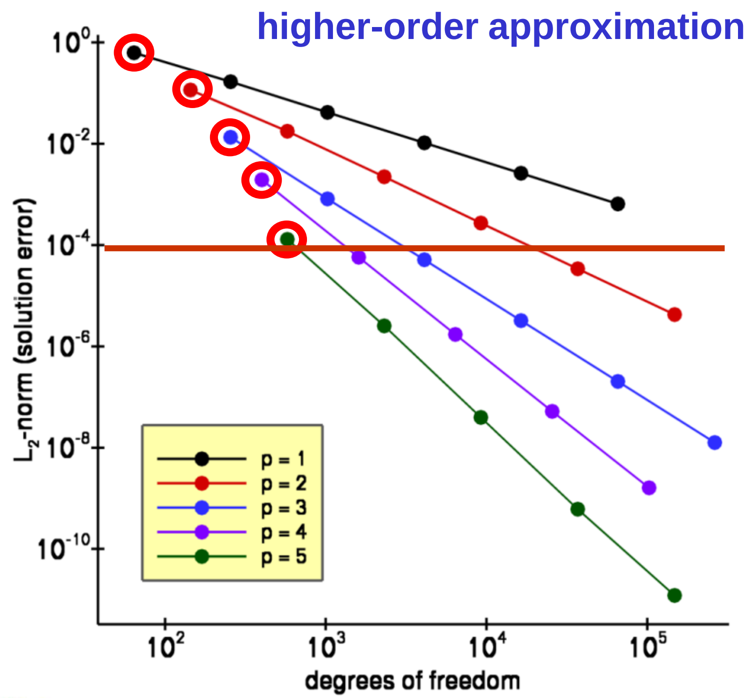

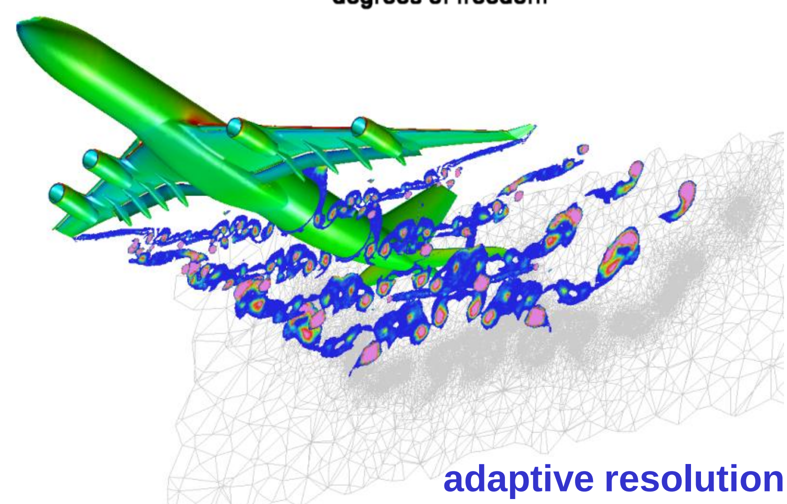

EU Research Project (2006-2009)

ADIGMA — **Adaptive Higher-Order Variational Methods for Aerodynamic Applications in Industry**

Objective

- To add a major step towards the development of next generation CFD methods for aeronautical applications
  - Development of innovative higher-order methods
  - Development of advanced and reliable error estimation & adaptation techniques
  - **Critical assessment of novel techniques based on industrial conditions**

Approach

- Restriction to variational methods (FE)
- Industrial assessment

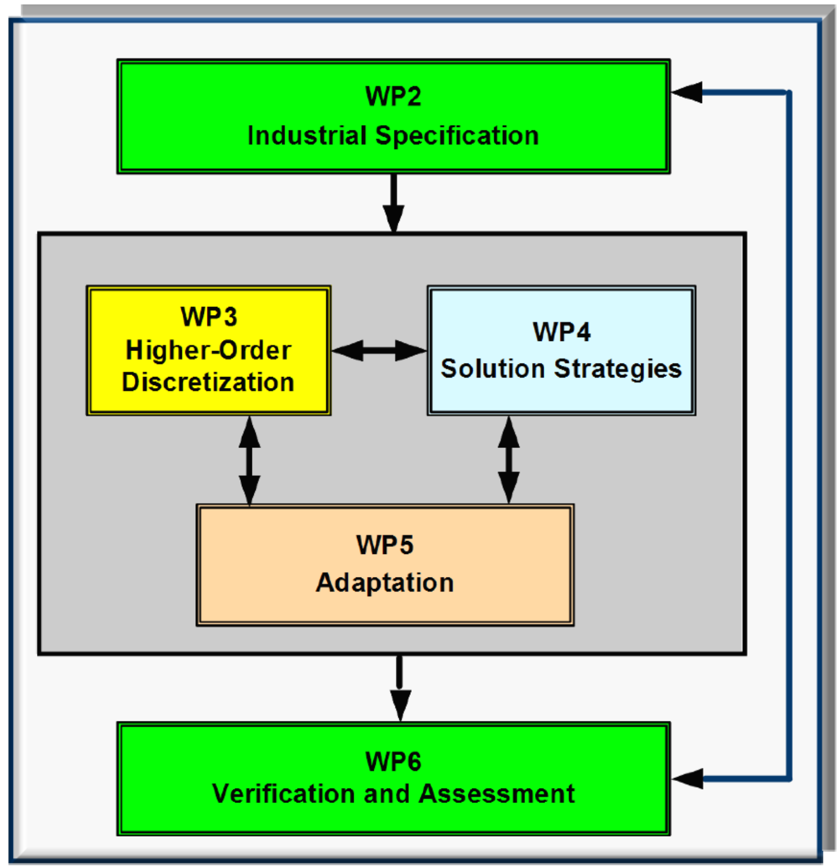

Consortium: 22 partners

Assessment

2006-2009

MTC2: NACA0012, inviscid flow, M=0.8, α=1.25^0

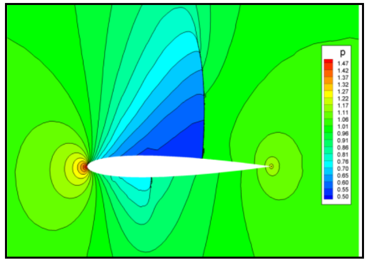

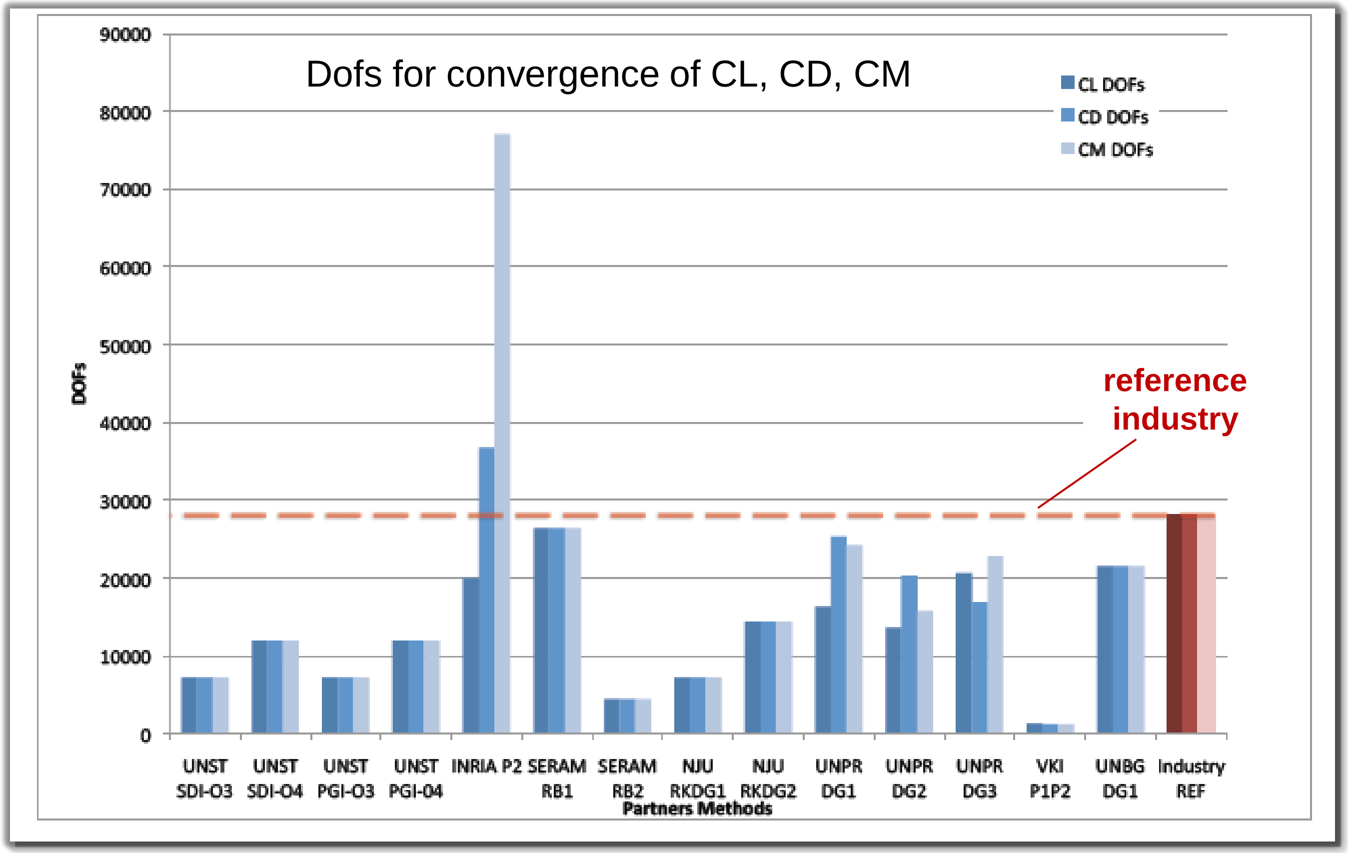

Observations

- Most of higher-order codes show improvements compared to industrial reference codes
    - Reduction of DoFs by factor 3, mainly by increasing the order from 2 to 3

2006-2009

Assessment

MTC2: NACA0012, inviscid flow, M=0.8, $\alpha=1.25^0$

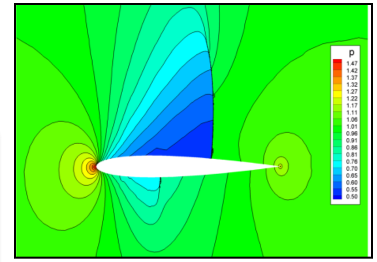

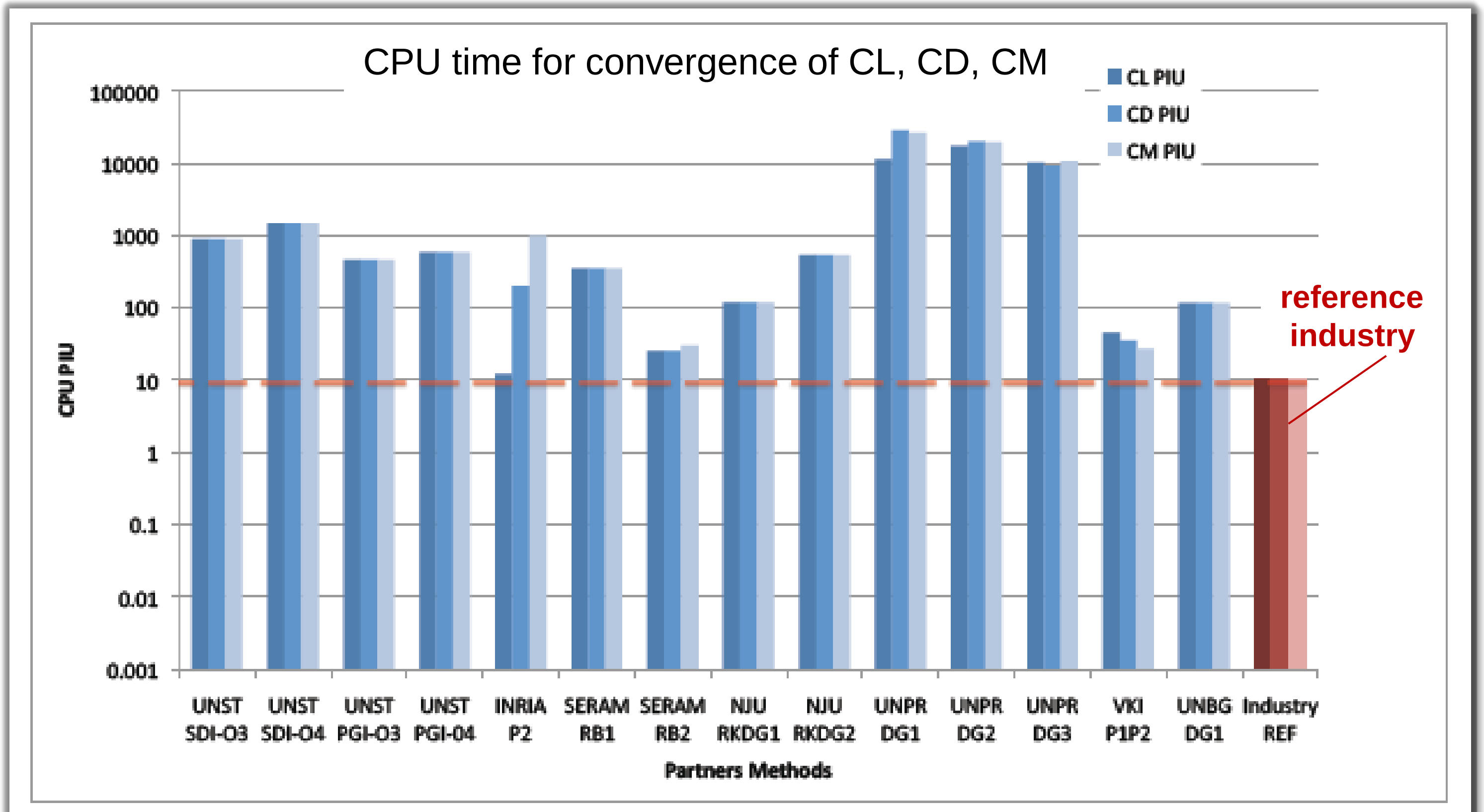

Observations

- Most of higher-order codes show improvements compared to industrial reference codes
  - Reduction of DoFs by factor 3, mainly by increasing the order from 2 to 3
- **Higher-order codes are not yet competitive in terms of computational cost**

Complex Test Case

- F6 wing-body, M=0.75, C_L=0.5, Re=5x10^6
- DLR DG code PADGE, k-ω turbulence model
- Higher-order, error estimation, goal-adjoint adaptation
- Comparison with industrial baseline code TAU

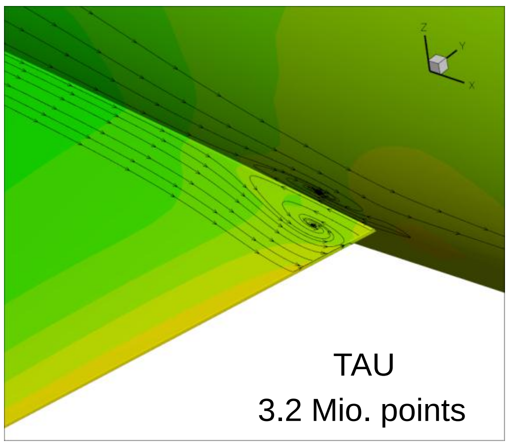

TAU
3.2 Mio. points

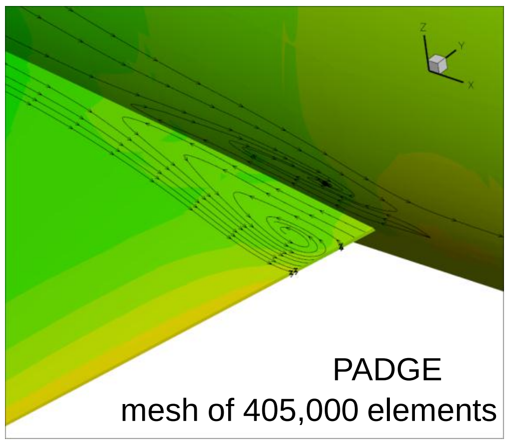

PADGE
mesh of 405,000 elements

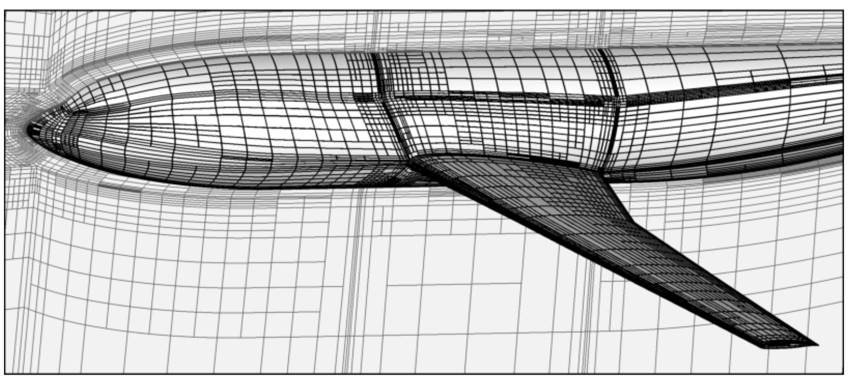

Adjoint-based refined mesh

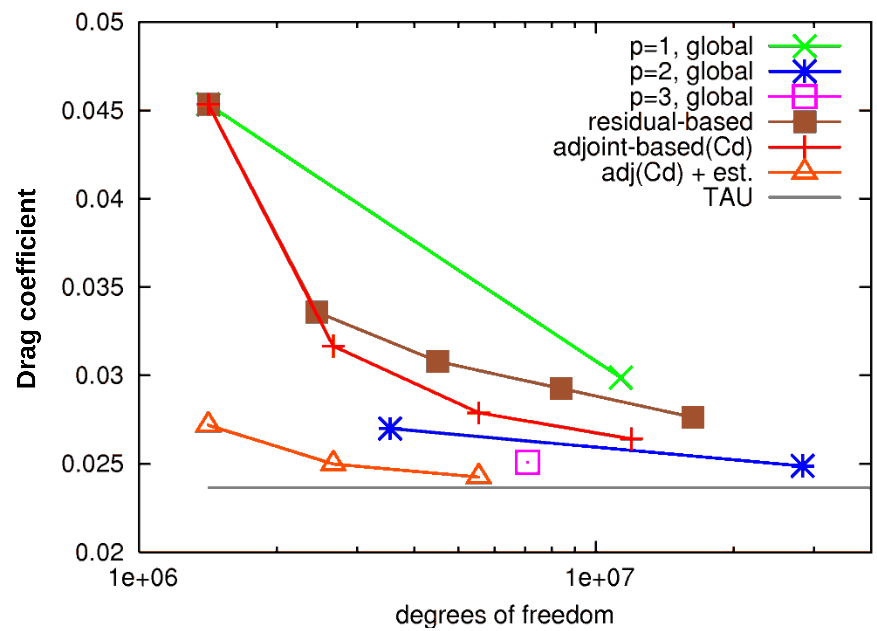

Convergence of drag coefficient
(global & local mesh refinement)

R. Hartmann, J. Held, T. Leicht

ADIGMA 2006-2009

Main Conclusions

Adaptive higher-order methods

- Potential demonstrated for aerospace applications
  - Reduction of degrees of freedom
  - Reliable adaption techniques & error estimates
- Limitations identified for industrial use
  - Solver efficiency for turbulent flows at high Reynolds number
  - Higher-order meshing

Necessary steps for industrialization

- Meshing capabilities for generation of coarse higher-order meshes
- Memory efficient solver strategies for large scale applications
- Demonstration of adaptive higher-order methods to complex applications

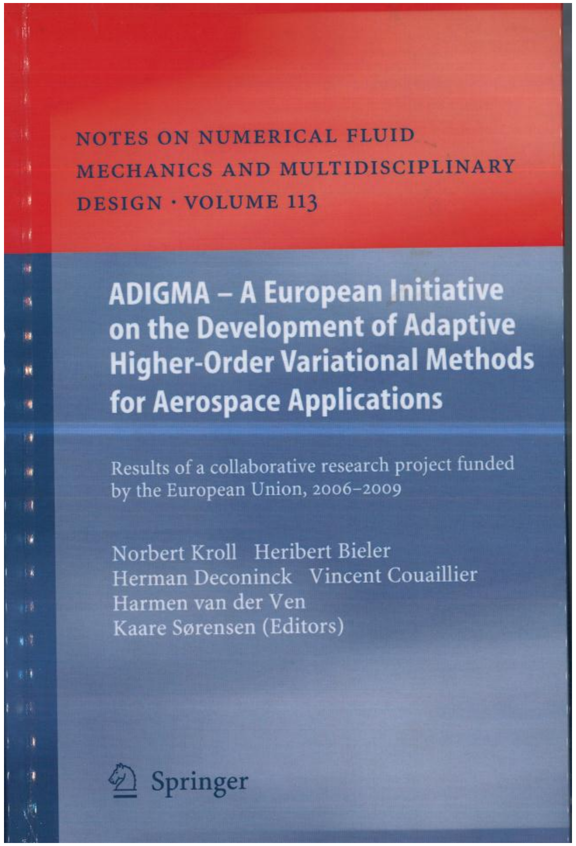

EU Research Project (10/2010-9/2013)

IDIHOM **Industrialization of Higher-Order Methods - A Top-Down Approach**

Objectives

- To overcome limitations identified in ADIGMA (grid generation, solver complexity)
- To extend higher-order methods to advanced turbulence models
- To demonstrate the industrial applicability of higher-order methods to
  - Application challenges/business cases (external & internal flows)
  - Multi-disciplinary applications
- To advance the Technology Readiness Level to TLR 5

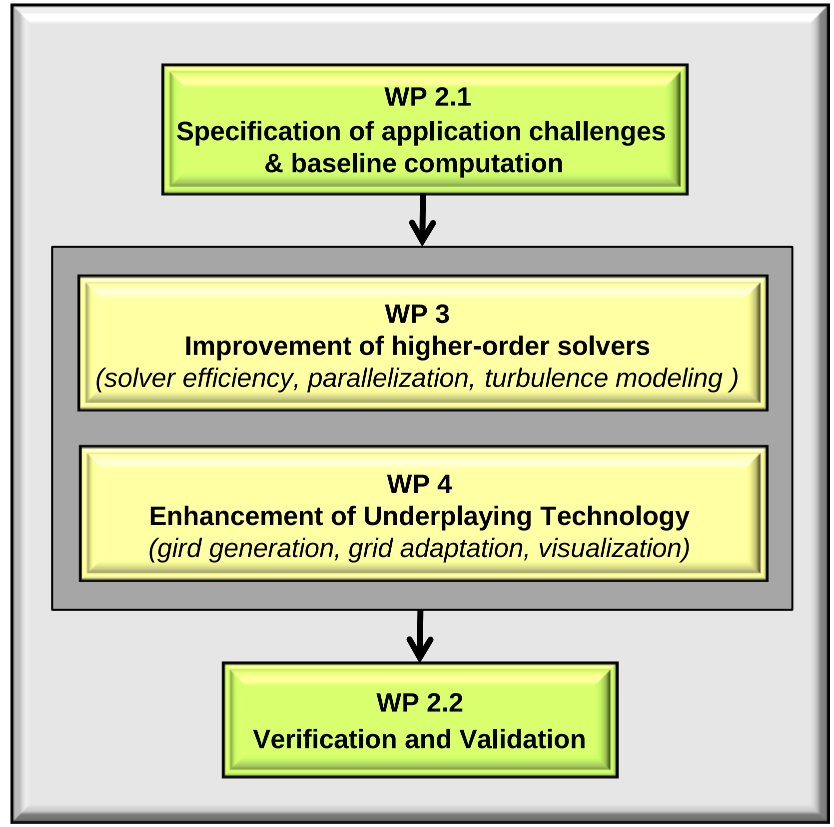

Consortium

- 21 partners from 8 countries
- Well balanced between upstream research, applied research and industry
- Partners with well proven expertise in CFD (higher-order adaptive schemes)

Industry
- **Dassault Aviation, (F)**
- **EADS-Cassidian, (DE)**

SME
- **CENAERO, (B)**
- **NUMECA, (B)**

Research Organization
- **ARA, (UK)**
- **DLR, (D)**
- **FOI (S)**
- **INRIA, (F)**
- **NLR, (NL)**
- **ONERA, (F)**
- **TSAGI, (RUS)**
- **VKI, (B)**

Universities
- **ARTS, (F)**
- **Bergamo, (I)**
- **Brescia, (I)**
- **ICL, (UK)**
- **Linköping, (S)**
- **Louvain, (B)**
- **Poznan, (PL)**
- **Stuttgart, (D)**
- **Warsaw, (PL)**

Project Co-ordinator: DLR

Associated Partners: Airbus, SAAB, MTU, SNECMA, RR, Bombardier, …

Application Challenges (1/3)

External Aerodynamics

Clean Sky | **EADS-Cassidian** | **Airbus** | **DASSAULT**

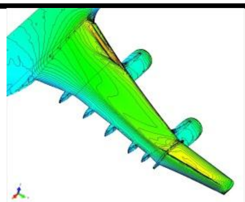	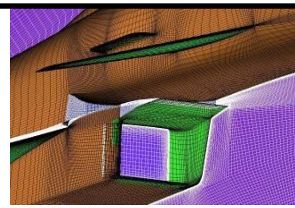	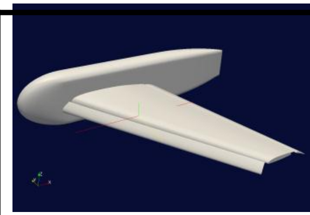	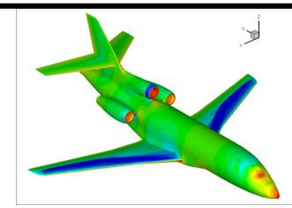	
A.1 - CleanSky configuration:	**A.2 - FA5 A/C** DES: M=0.1, α=15°, Re_m=1x10^6 RANS: M=0.85, α=24°, Re_m =1x10^8	**A.3 - High-lift prediction workshop, case 1** M=0.2, Re_{mac}=4.3×10^6, α=13° (linear regime) and α=28° (max. lift)	**A.4 - Falcon business jet** M=0.80, a=2.0°, z=40,000 ft	
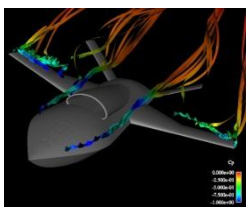		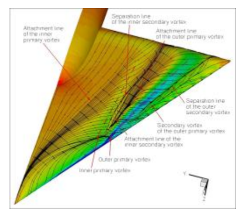	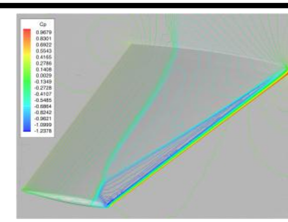	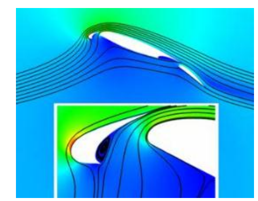
A.5 - UAV(Ma=0.17, α=18°, Re=1.7×10^6	**A.6 - Train head** 70 m/s, Re = 1.4×10^6 based on ref. length=3m, yaw=**30°/40°/50°/60°**	**U.1 - VFE-2 delta wing** M=0.869, α=24.7°, Re_{mac}=59.5x10^6	**U.2 - ONERA M6 wing** M=0.84, α=3.06°, Re=11.72x10^6	**U.3 - L1T2 high-lift config.** M=0.197, Re=3.52×106 α=20.18°

SAAB | **Bombardier**

IDIHOM

Application Challenges (2/3)

Internal Aerodynamics

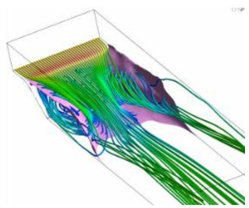		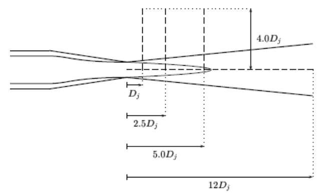	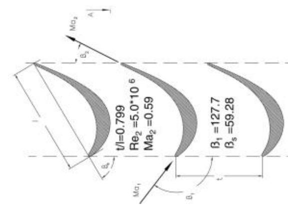	
A.11 - Water tunnel experiment (DESider) M=incom., Re/m=7x106 *Figure: Menter/Egorov, ANYSY*	**A.7 - NASA Rotor 37** 36 multiple-circular-arc blade Tip speed=1500 ft/sec, Pressure ratio =2.106	**A.8 – JEAN nozzle** M=0.75, $Re=5\times10^4$, $T_{jet}/T_{\infty}=1$	**A.9 - MTU Cascade** Ma-in=0.28, Ma-out=0.59 Inflow angle=127.7° Outflow angle=26.8° Outflow Re=500,000	**A.10 – Transonic fan** M=1.38 at tip, $Re=5x10^6$ at tip

Rolls Royce	SNECMA	MTU	TechSpace Aero

Application Challenges (3/3)

Eurocopter

Aero-elastics

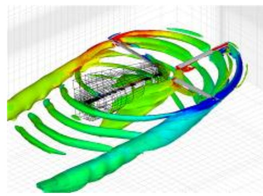	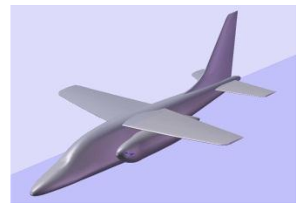	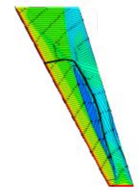
A.12 - HART-II helicopter rotor M_{Tip}=0.64, μ=0.15, Re_{Tip}=1.8x10^6	**A.13 - IRYDA I22 M-93 A/C** M=0.14, α=0°, Re=1.5x10^6 Structure: Normal modes	**U.4 - LANN wing - CT9** M=0.82, α=2.6°, Re=7.17x10^6 *Figure: DLR*

Aero-acoustics

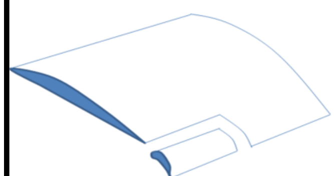	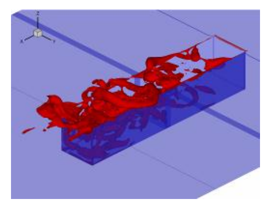	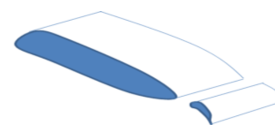
A.14 – VALIANT case, wing-flap-tip interaction ("3D" case) Simulation of airframe noise M=0.16, α=20°, α_{Flap}=20°, Re=3.6x10^6	**A.15 - M219 cavity** M=0.85, Re=13.47x10^6 *Figure: Strelets, NTS, a DDES computation*	**U.5 – VALIANT case, wing-flap-tip interaction ("2D" case)** Simulation of airframe noise M=0.16, α=0°, α_{Flap}=20°, Re=3.6x10^6

Range of Application

- High-order DG computation
- kω-based EARSM turbulence model
  (Explicit Algebraic Reynolds Stress Model)
- Structured curvilinear grid
- Applications
  - VFE-2 delta wing (U.1)
    M=0.4, AoA=13,3^0, Re=3x10^6
  - FA5 fighter configuration (A.2)
    M=0.85, AoA=24^0, Re=1x10^8

FA5 fighter configuration (Cassidian)

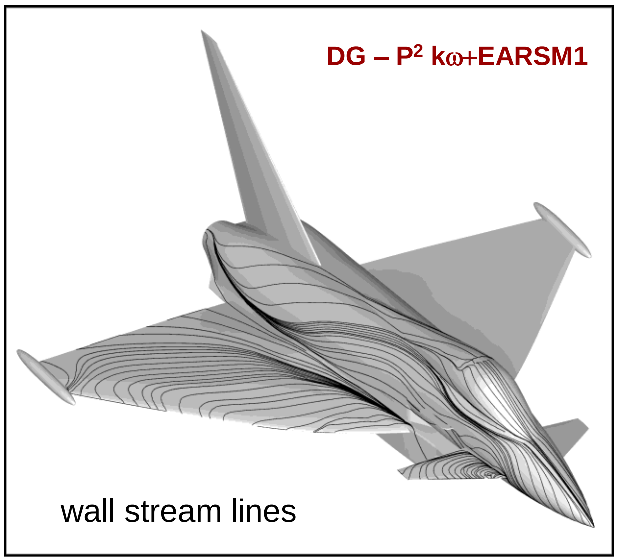

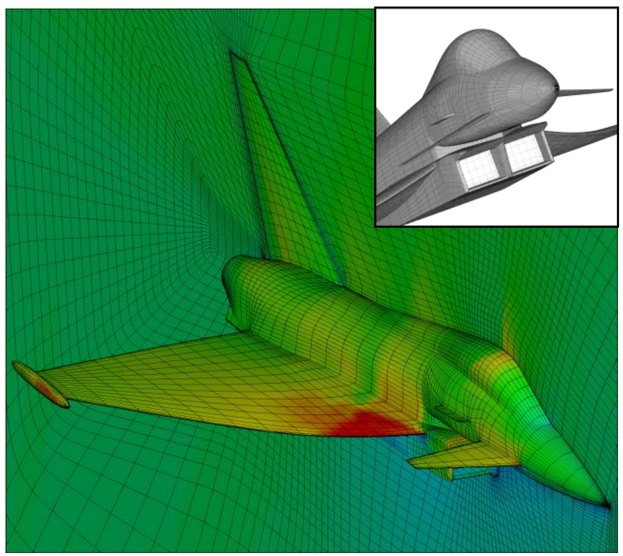

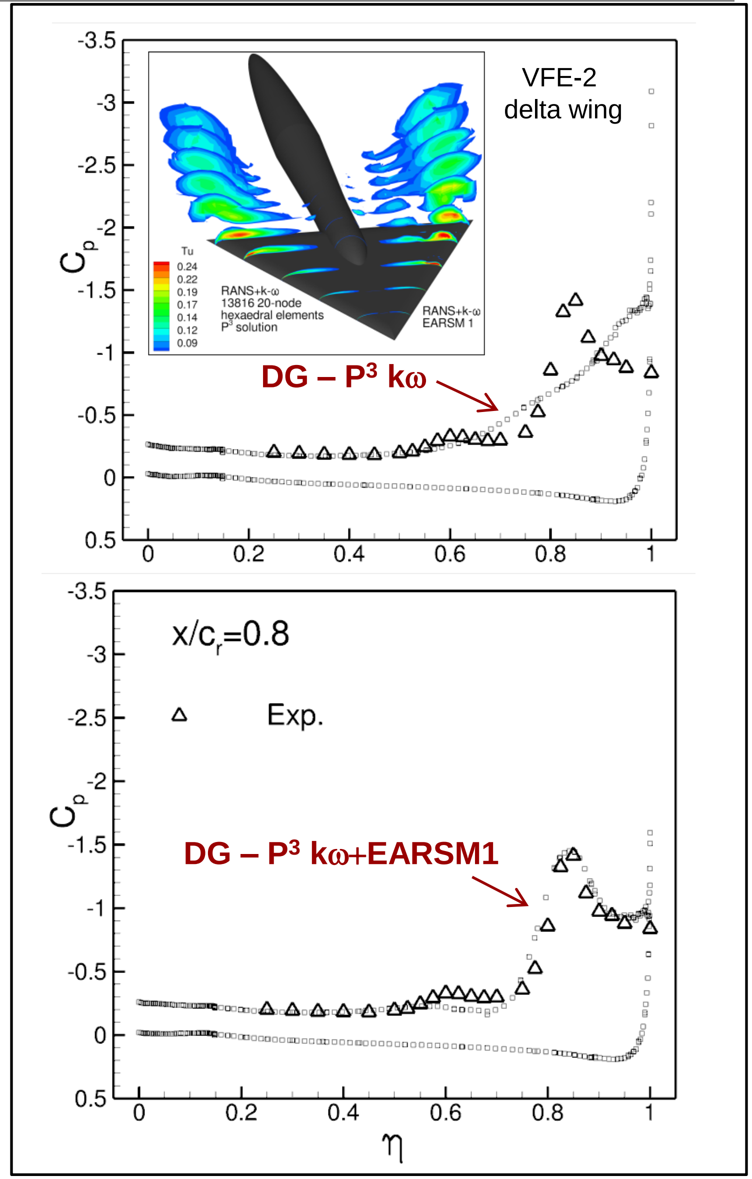

F. Bassi, et. al. , ECCOMAS 2012

Grid Generation

Challenges for higher-order methods

- Coarse meshes required
  (3rd-order: 10 Dof/Element)
- Order of method/accuracy of solution limited by geometry approximation

  Issue: Turbulent high-Reynolds number flow around complex configuration

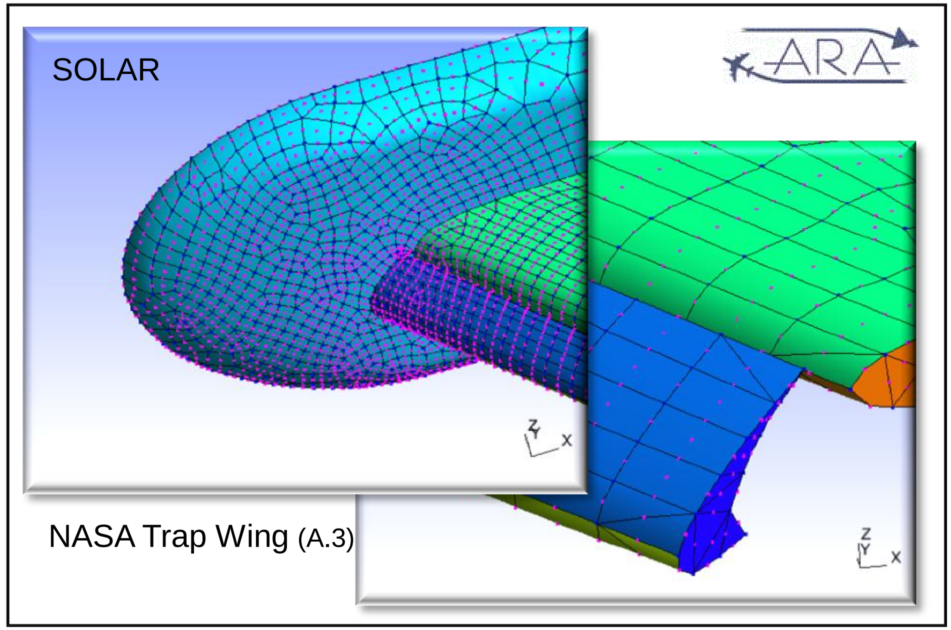

Activities

- Extension of ARA SOLAR mesh generator
- Extension of GMES
  - Robust estimates for validity assessment of curvilinear meshes
  - Techniques to curve linear meshes
  - Optimization framework for improving high-order meshes

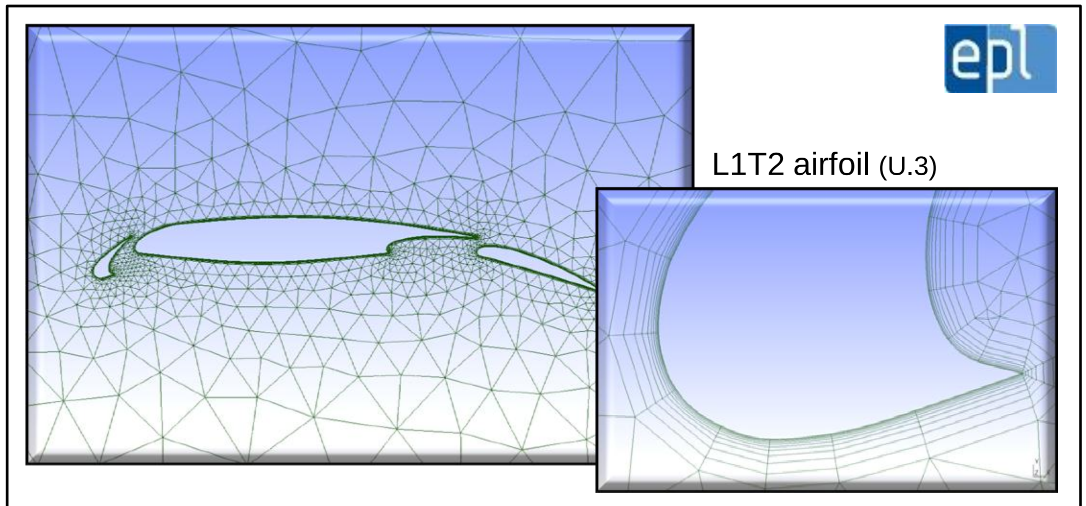

B. Gorissen, J. Remacle, ECCOMAS 2012

Solver Improvement

Challenges for higher-order methods

- Memory and CPU efficient solution strategies for large scale applications

  Issue: Turbulent high Reynolds number flows (highly stretches meshes)

Approaches

- p - multigrid with suitable smoothers
- h – multigrid on agglomerated grids *(as preconditioner and solver)*
- Combination of p- and h- multigrid

U. Brescia

p - Multigrid

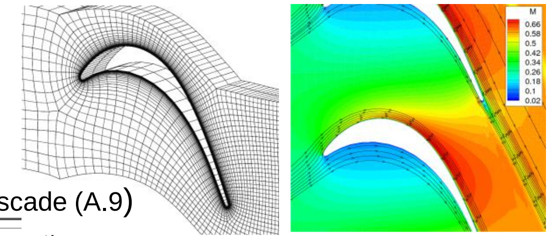

MTU Cascade (A.9)

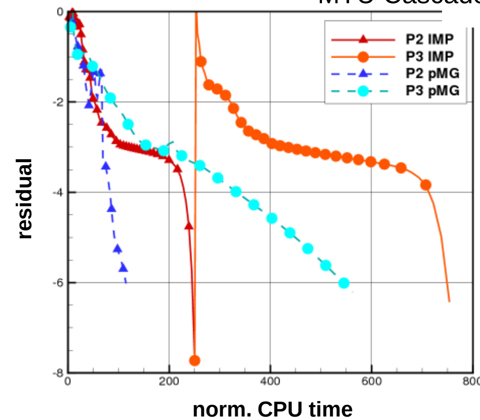

		P^2	P^3
p-MG	time [IU]	114	563
	Mem [Gb]	1	2.5
BE *implicit*	time [IU]	250	753
	Mem [Gb]	4.1	8.6

A. Ghidoni, ECCOMAS 2012.

DLR

h - Multigrid

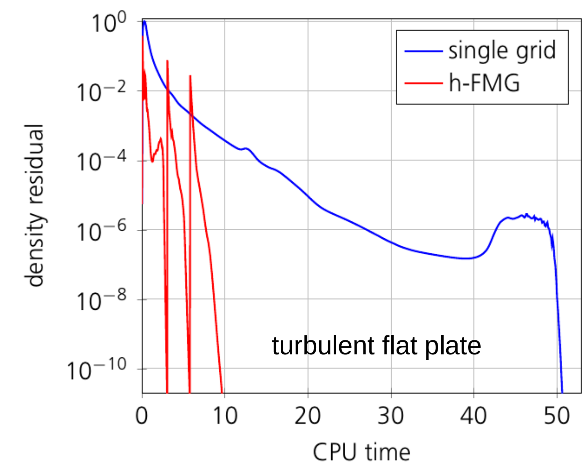

T. Leicht, ECCOMAS 2012,

Grid Adaptation

- Subsonic turbulent flow around VFE-2 delta wing
  M=0.4, AoA=13.3^0, Re=3x10^6
- Adaptive higher-order DG method,
  kω turbulence model (DLR PADGE Code)
- **Adjoint-based adaptation improves overall time-to-solution**

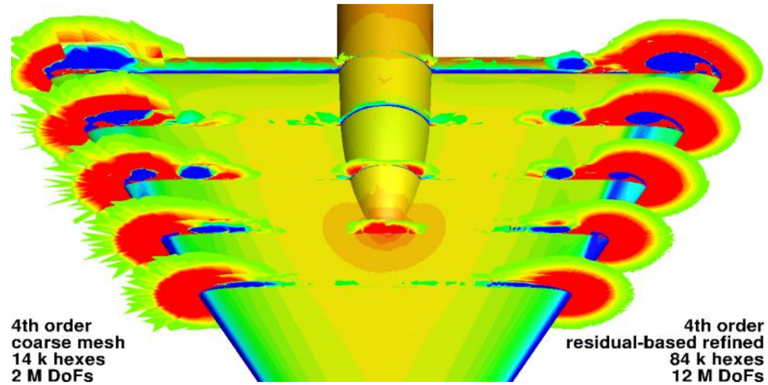

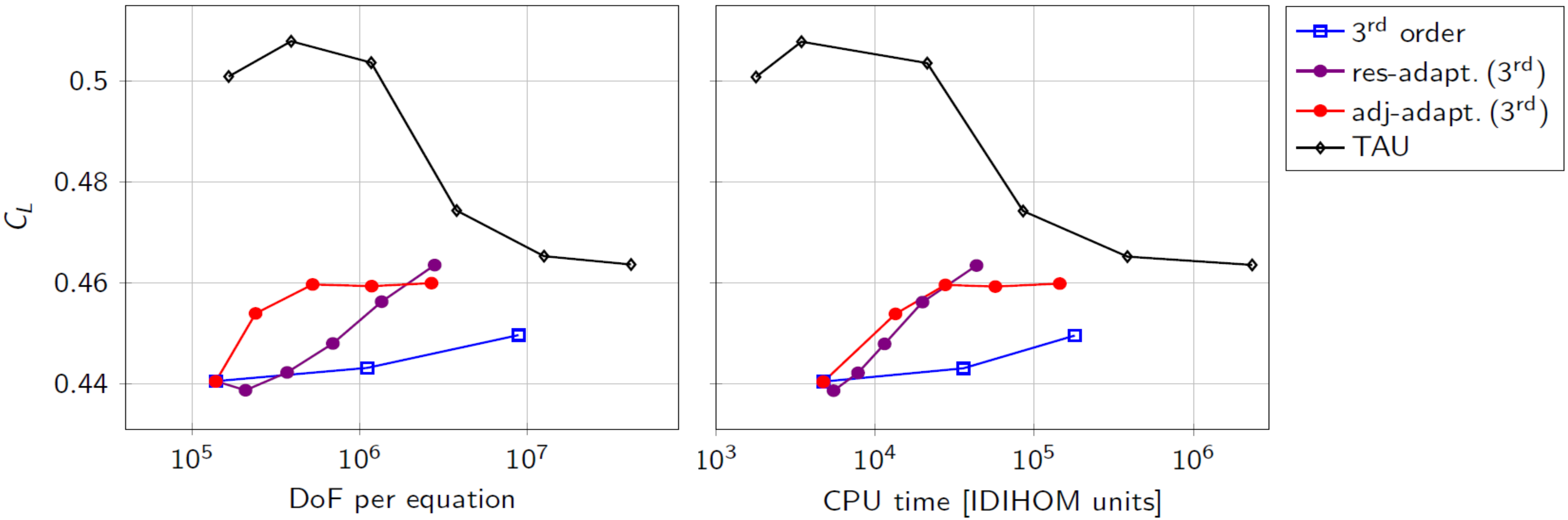

R. Hartmann, ECCOMAS 2012

Physical Modeling

Activities

- Evaluation of high-order methods (DG) for LES, hybrid RANS/LES on unstructured meshes
  - dissipation / dispersion properties
- Demonstration of potential through large scale applications (bump, cavity, Jean nozzle, HART rotor, ..)

Preparatory DNS results (4^{th}-order DG) for T106A turbine at Re=50.000

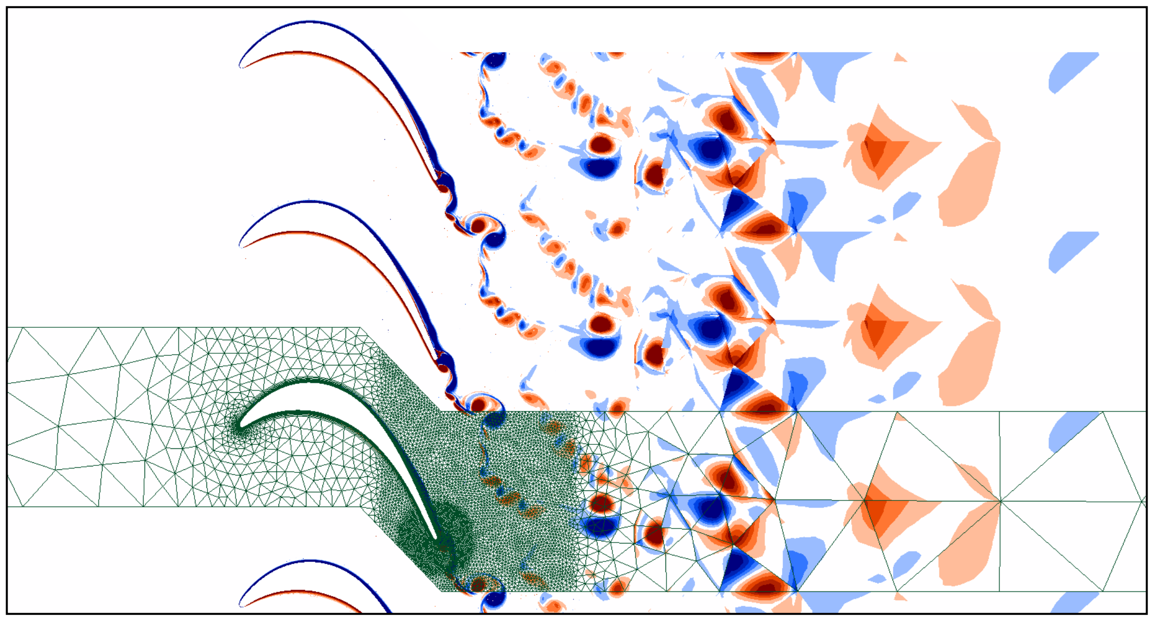

Expected Result / Outcome

- Industrialisation of higher-order methods
  - Improved predictive accuracy or reduced computational time for business cases or application challenges
  - Improved multi-disciplinary simulations
  - Identification of application areas best suited for higher-order methods

→

  - Advantages for faster and/or more accurate designs
  - Strengthen the competitiveness of European industry
- Closer co-operation between industry and research organizations and academia

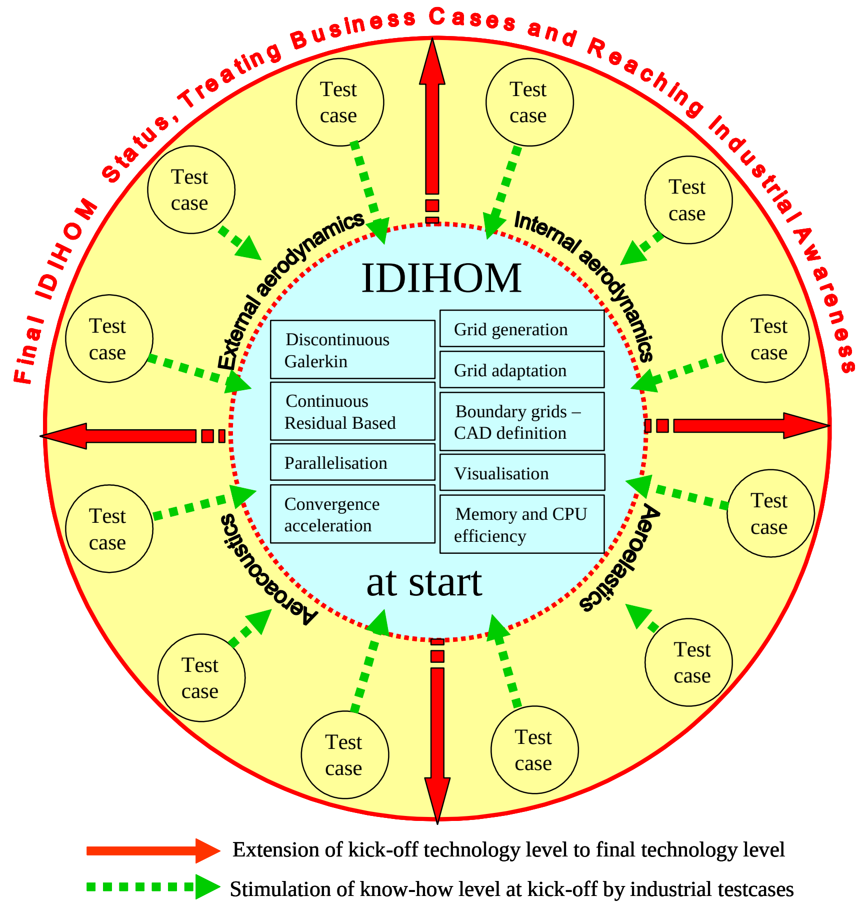

Intermediate Conclusion

Adaptive Higher-order methods

- Potential for challenging applications demonstrated
- For RANS simulations superiority to classical industrial codes not yet proven
  - Some issues still to be solved (grid generation, post processing, solver complexity, …)
- Clear advantages for scale resolving turbulence (Hybrid RANS/LES, LES, DNS)
  - Further dedicated research required

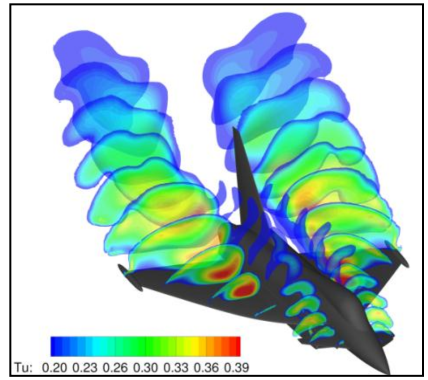

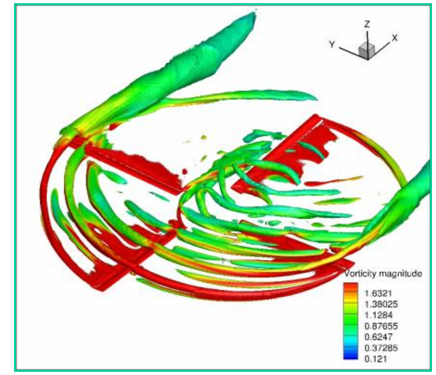

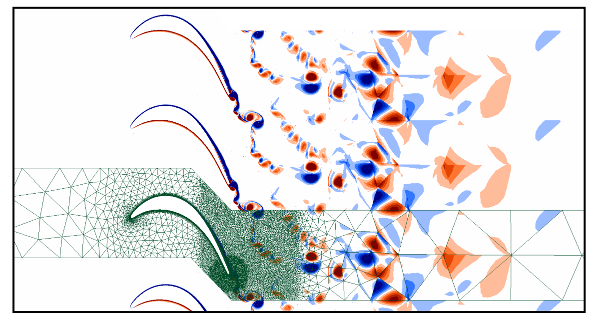

IDIHOM based on EU projects

IDIHOM: Industrialization of Higher Order Methods

ATAAC: Advanced Turbulence Simulation for Aerodynamic Application Challenges

Intensive world wide research: **http://www.nianet.org/CFDConference/index.aspx**

IDIHOM

Towards complex turbulent flow computations with higher-order methods

prepared by

Alessandro Colombo and Tobias Leicht

with contributions from all IDIHOM partners

2nd EASN Workshop on Flight Physics and Propulsion, Prague, 31st October – 2nd November 2012

Outline

- overview

- fixed wing aerospace applications
- turbomachinery applications
- helicopter applications

- summary

Overview

status in ADIGMA / prior to IDIHOM

- ADIGMA concentrated on inviscid and laminar viscous flows
- first results for turbulent flow (RANS) for some partners

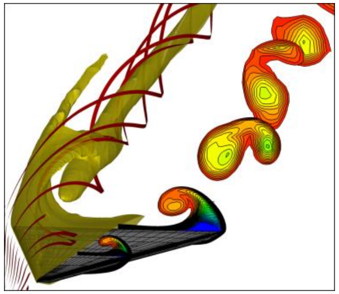

focus of IDIHOM

- turbulent flows (all partners)
  - RANS
  - scale-resolving schemes: LES/DES, DNS
- increased complexity
  - geometric
  - physical aspects: complex flowfields

Fixed wing aerospace applications

- cruise conditions (ADIGMA status)
  - ONERA M6 wing
  - Dassault Falcon
- high lift
  - L1T2 airfoil
  - NASA trap wing
- vortical flows
  - VFE-2 delta wing
  - FA 5 fighter aircraft

ONERA M6 wing

- widely used CFD evaluation case
- was a complex case in ADIGMA
  is now an underlying case treated by more partners

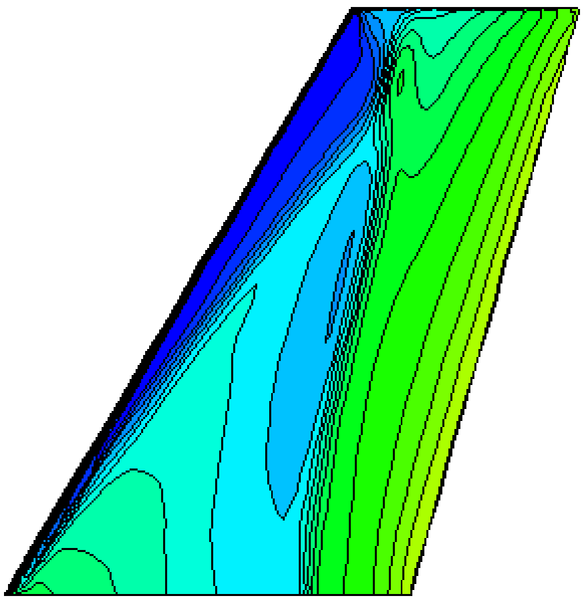

ONERA M6: flowfield and convergence

- P2 computation on 215,632 quadratic hexes
- order sequencing solution (P0 → P1 → P2)

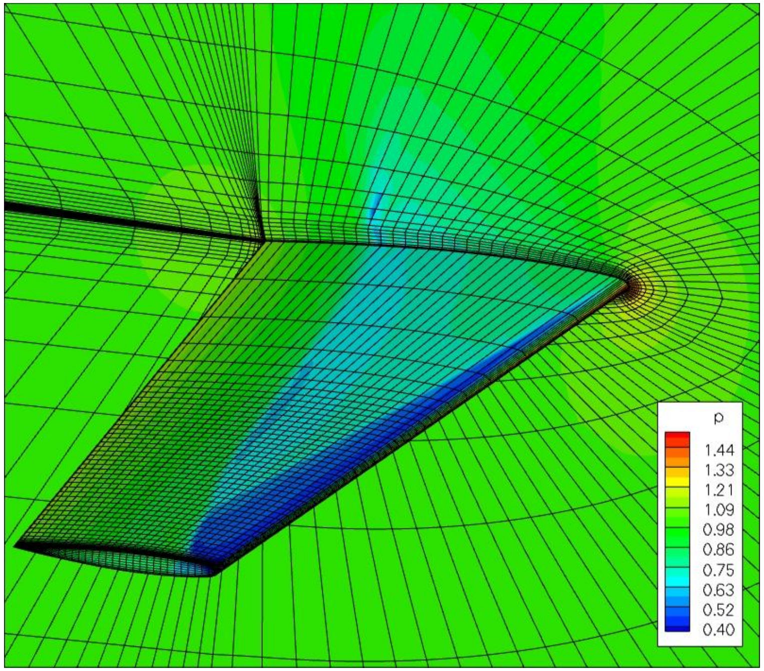

pressure contours

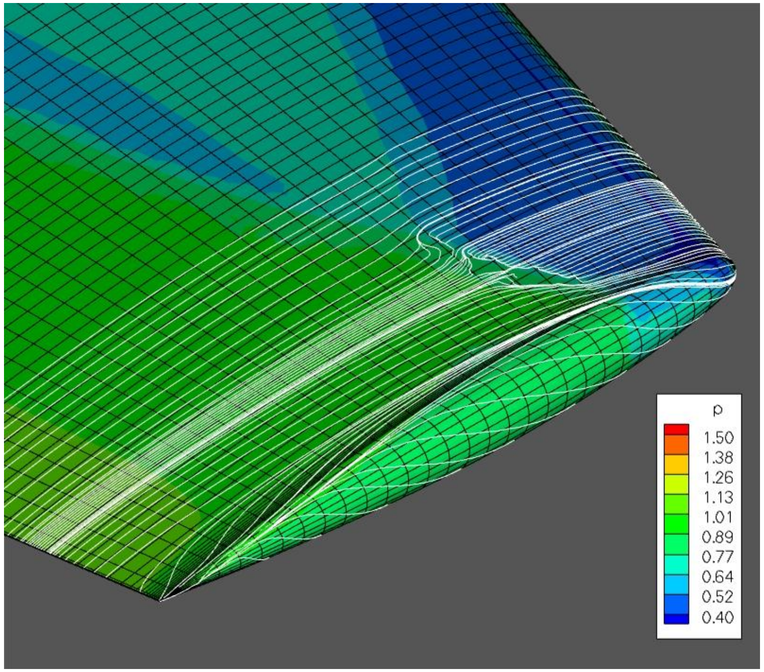

separation bubble (suction side)

ONERA M6 wing: C_p comparison

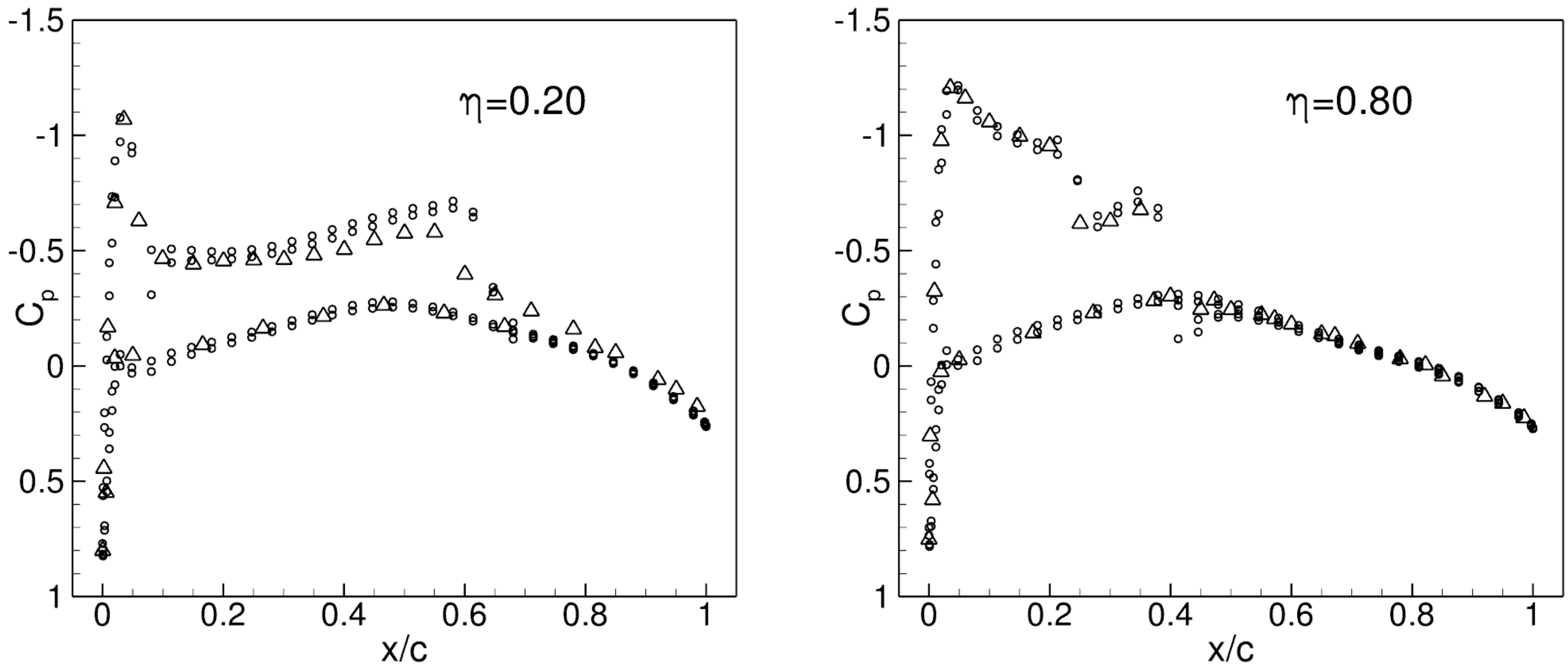

○ DG-$\mathbb{P}^2$, Δ Exp.

Dassault Falcon

- complete air craft in cruise condition
- generic version to be treated by several partners
- solution computed with 2^{nd} and 3^{rd} order FE methods

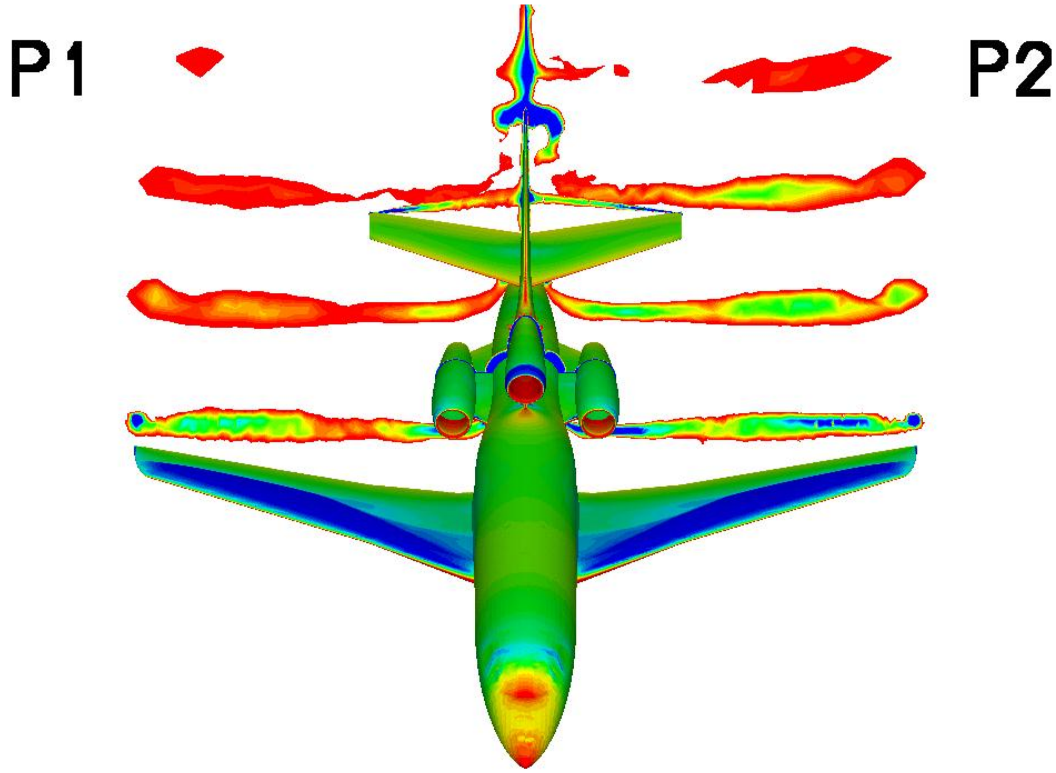

Falcon: spurious drag analysis

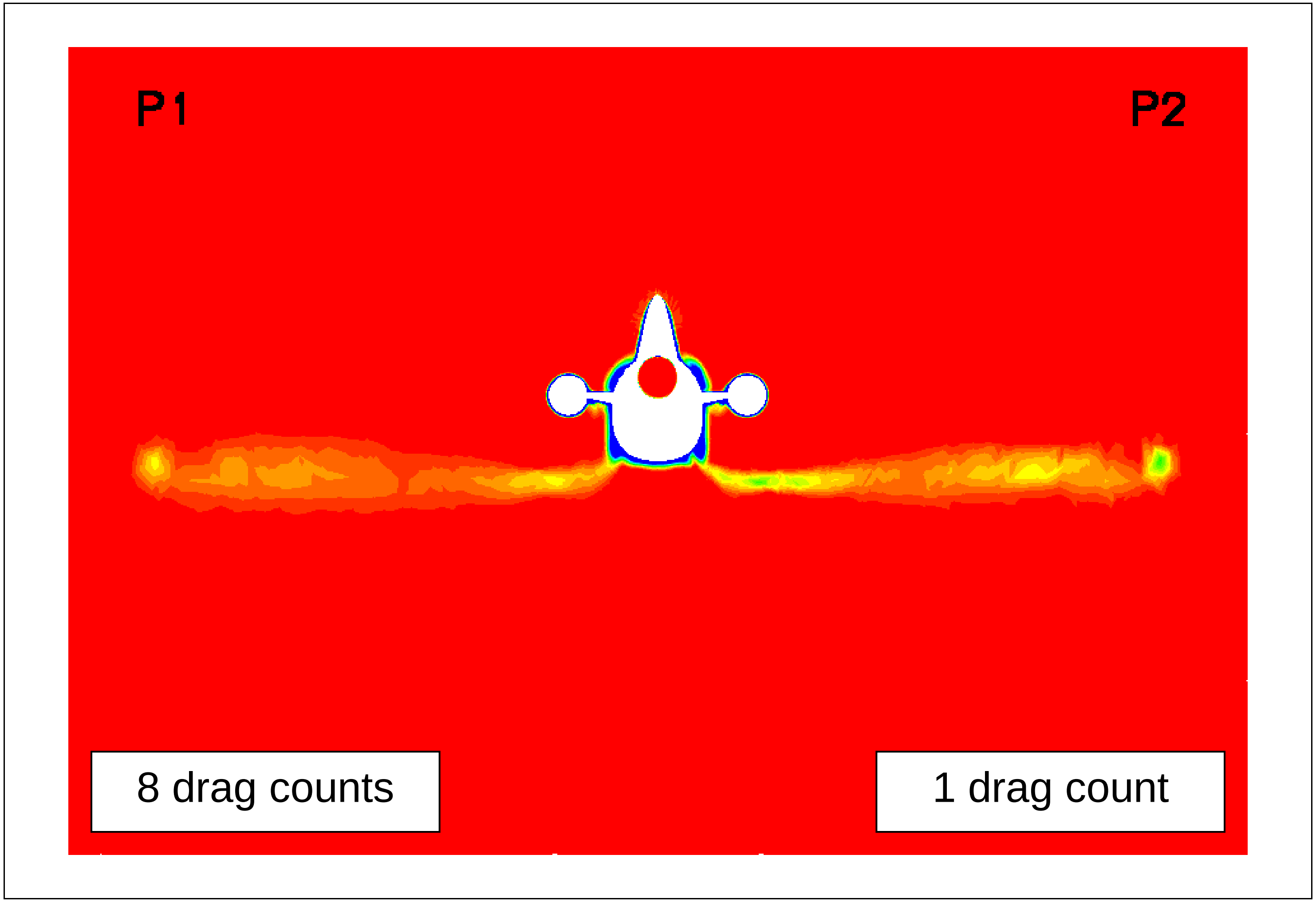

L1T2: high lift airfoil

- 2D high lift case
- high-end application in ADIGMA
  now treated by many partners as „underlying case“
- detailed analysis possible

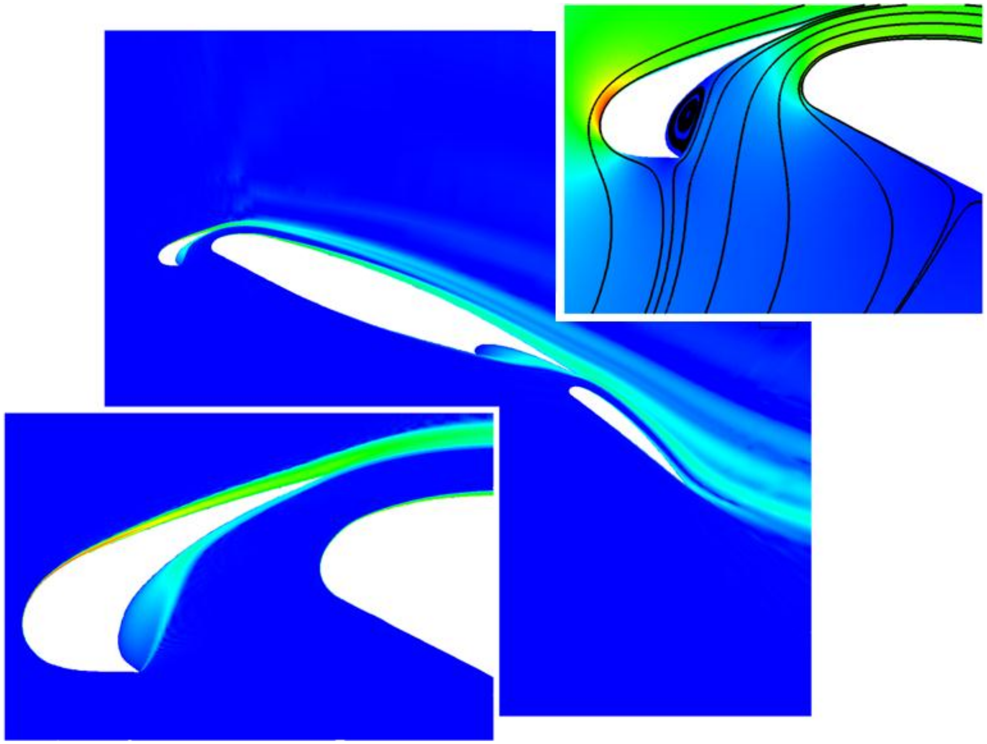

- M = 0.197
  α = 20.18°
  Re = 3.52 ×10^6

L1T2: comparison with experiments

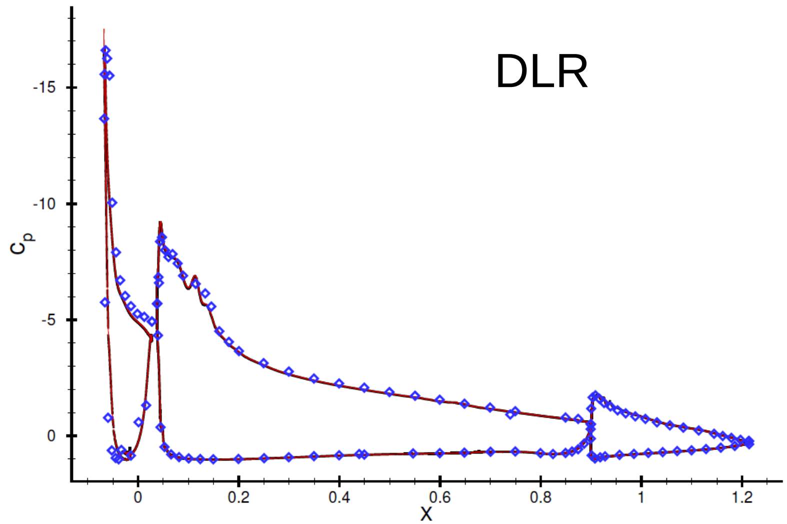

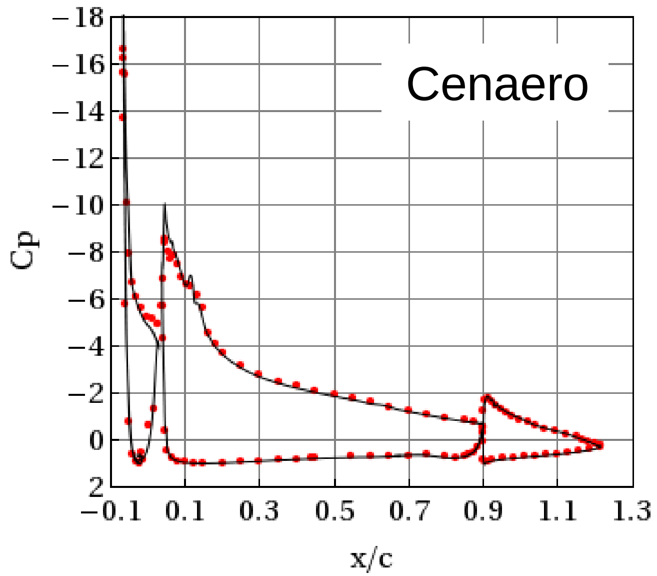

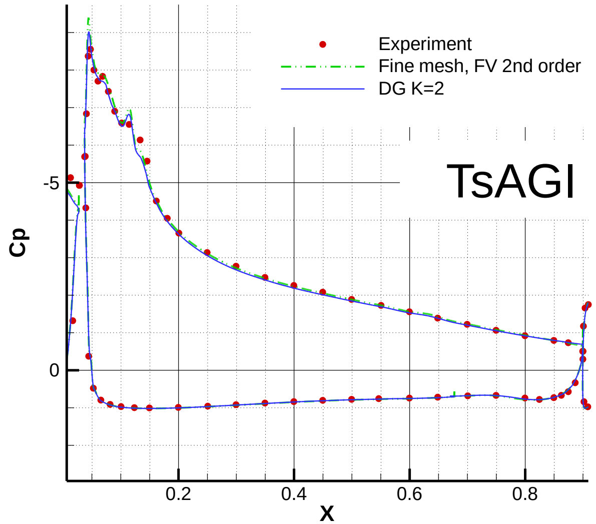

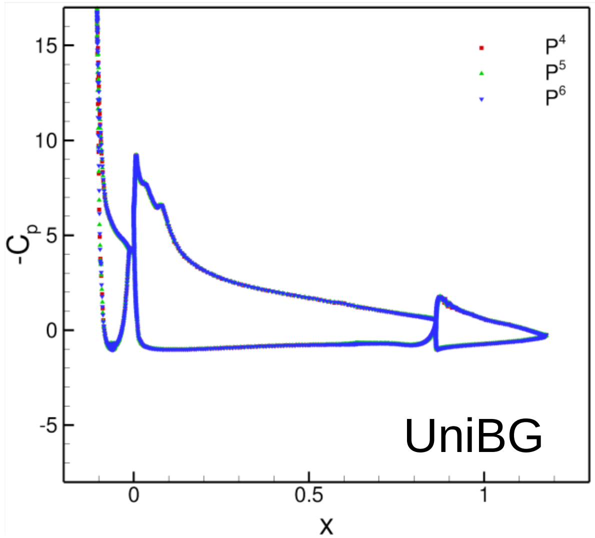

L1T2: FV / DG comparison: meshes

unstructured hexahedral meshes with hanging node refinement

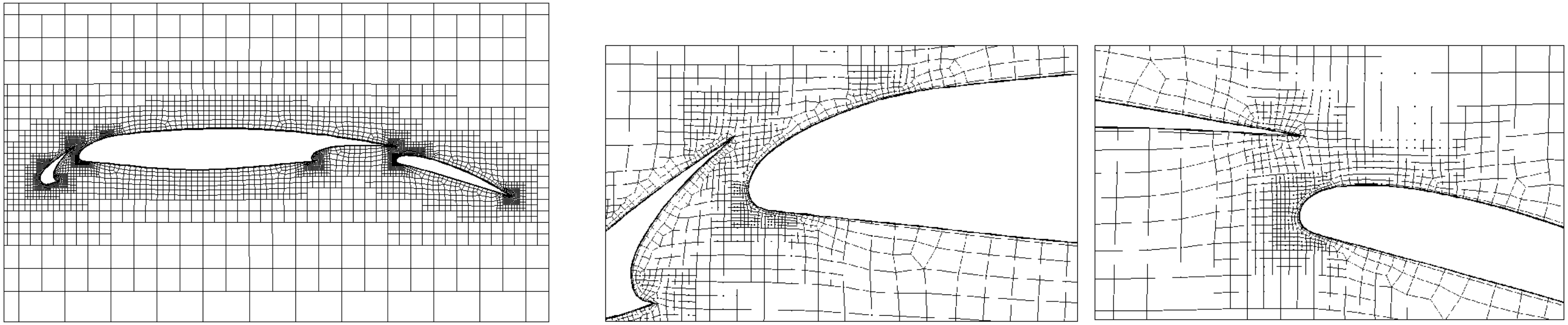

coarse: 6,111 elements

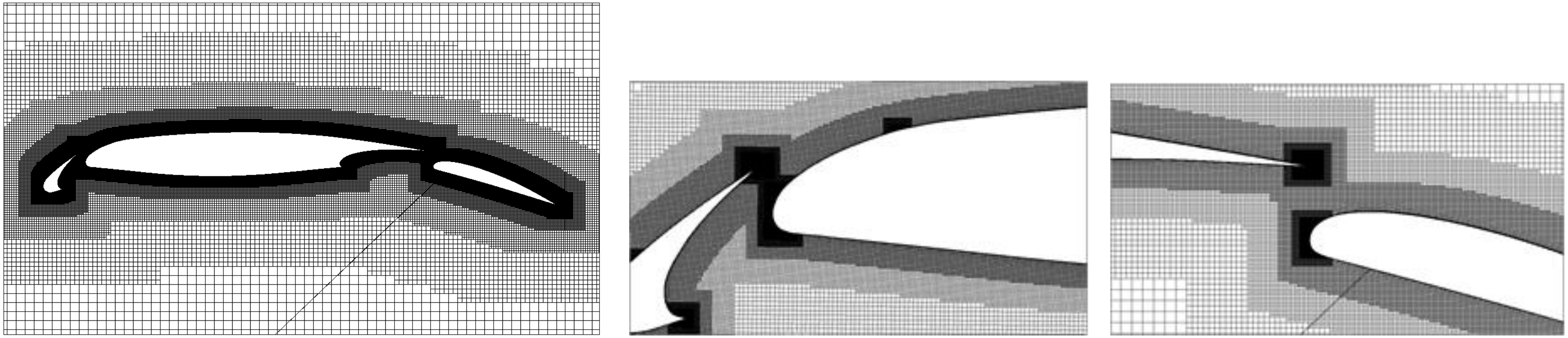

fine: 319,966 elements

L1T2: FV / DG comparison: flowfield

FV, coarse	FV, fine	3^{rd} order DG, coarse

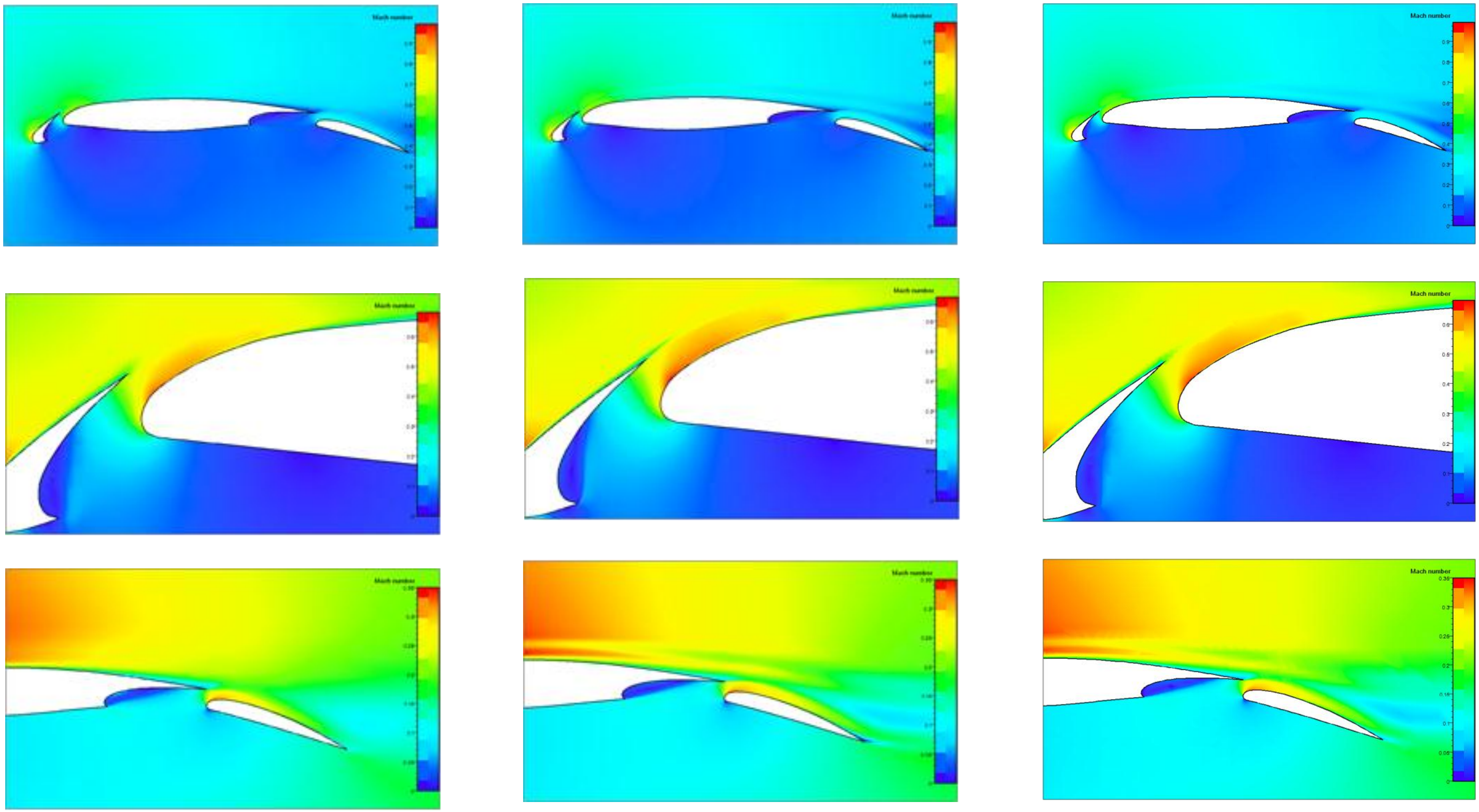

IDIHOM

L1T2: unstructured curvilinear meshes

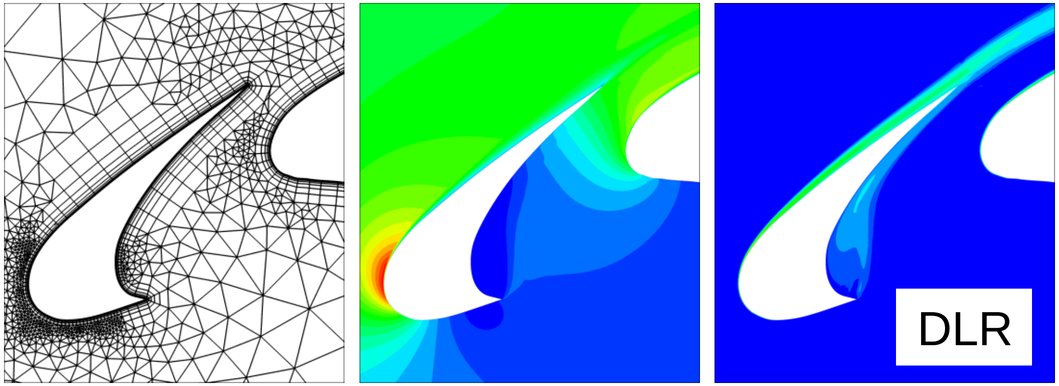

mesh *Mach* *Tu*

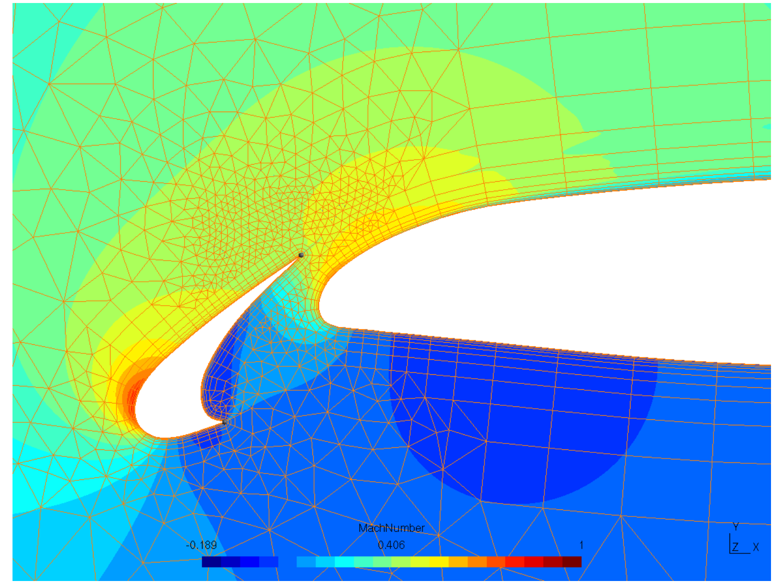

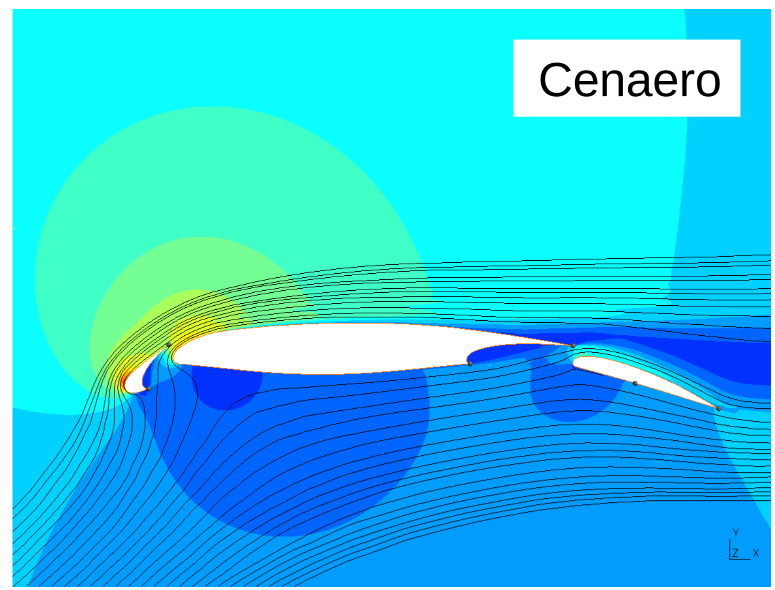

unstructured meshes (UCL)

- hybrid / mixed-element
- boundary layer structure
- curvilinear elements
- attractive alternative to legacy structured mesh sequences

L1T2: mesh convergence analysis

close to ideal mesh convergence

lift and drag coefficients *errors in lift and drag coefficients*

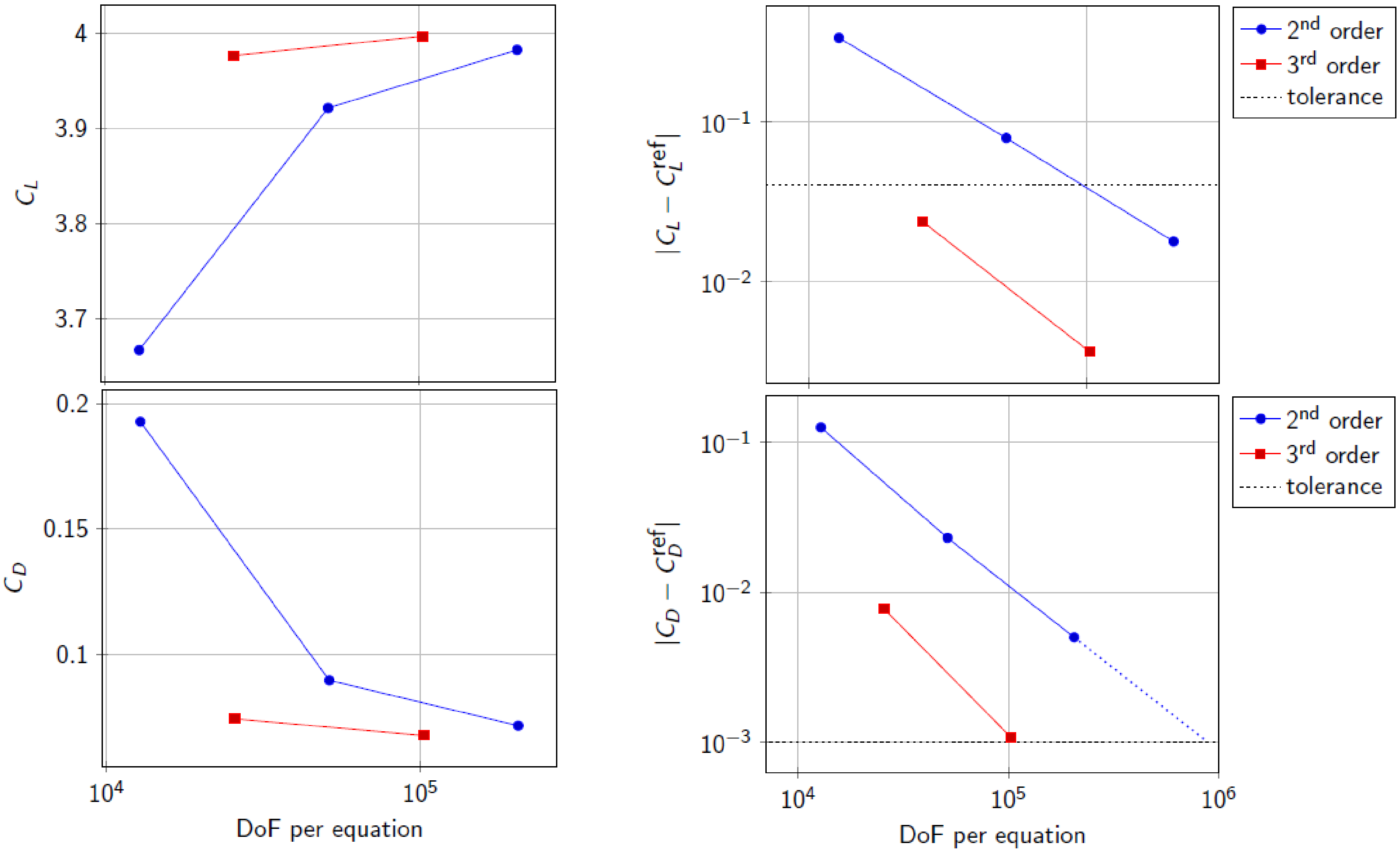

L1T2: convergence issues / geometry effects

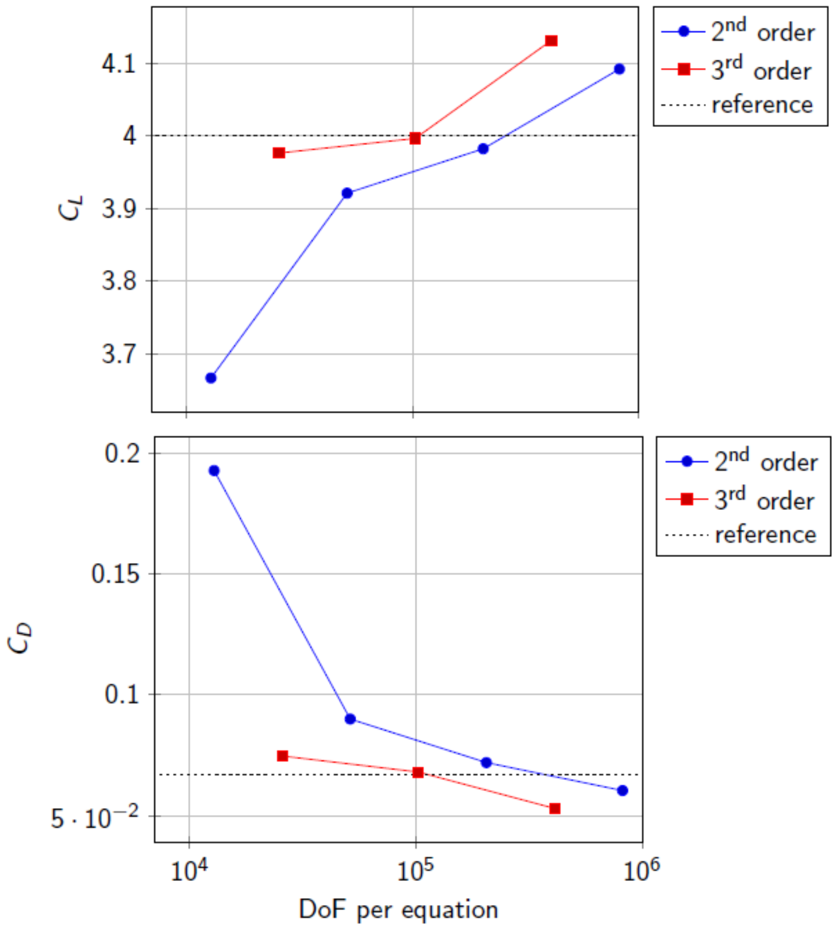

- high resolution „destroys“ mesh convergence
- due to geometric disturbance (original data)
- „exact geometry“ is an issue for HO methods

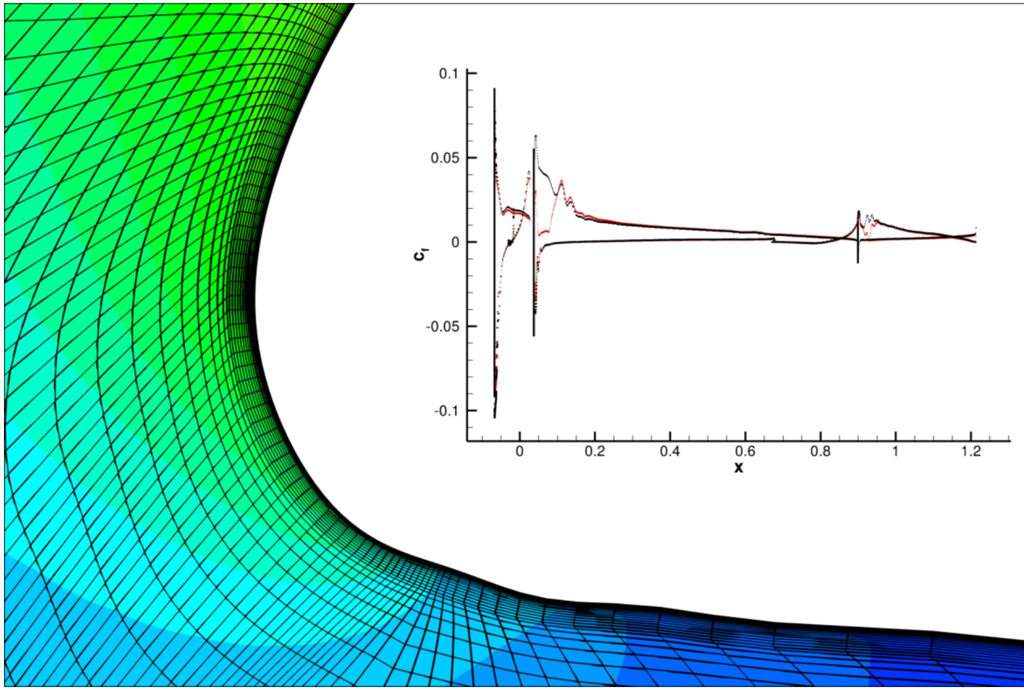

NASA trap wing

- 3D wing-body high lift configuration
- well documented case, available meshes
- focus of 1st AIAA High Lift Prediction Workshop

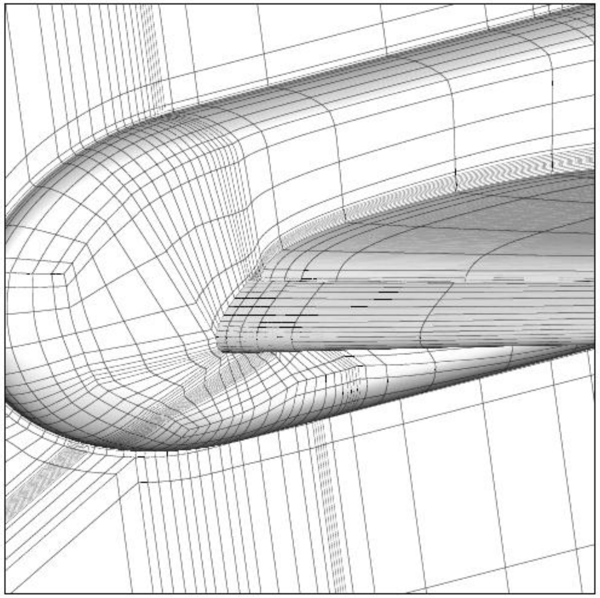

coarse curvilinear block-structured mesh

NASA trap wing: results

pressure coefficient (body) and Mach number (symmetry plane) contours

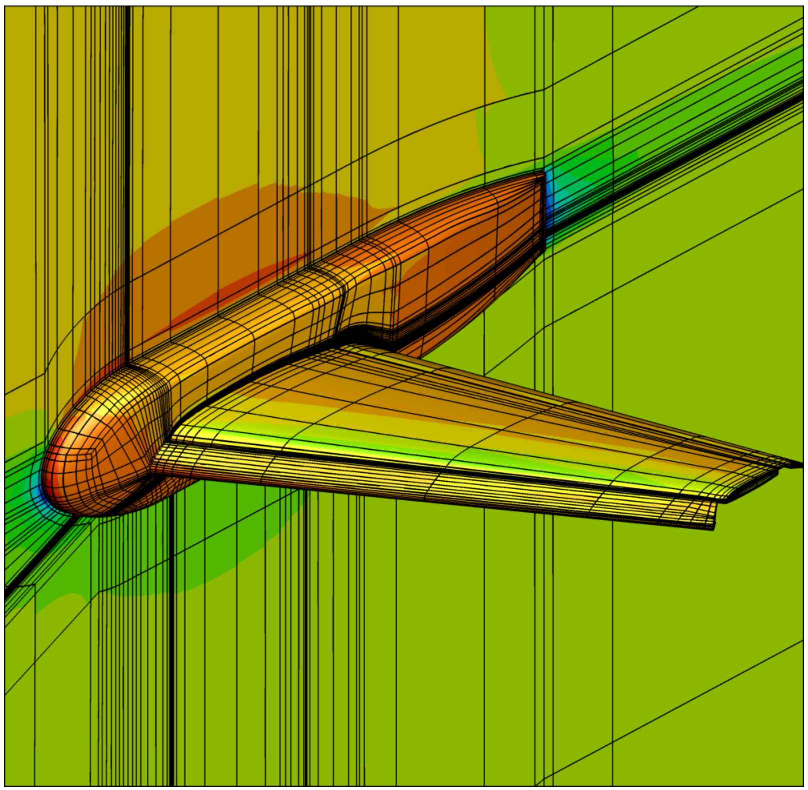

second order DG

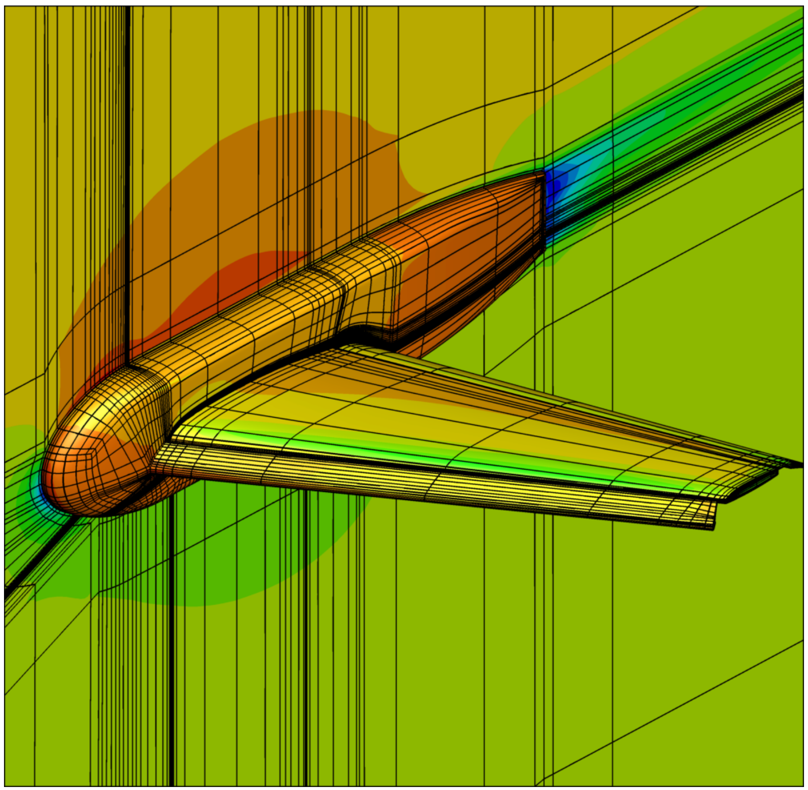

third order DG

NASA trap wing: separation behind body

pressure coefficient (body) and Mach number (symmetry plane) contours

streamlines on the symmetry plane

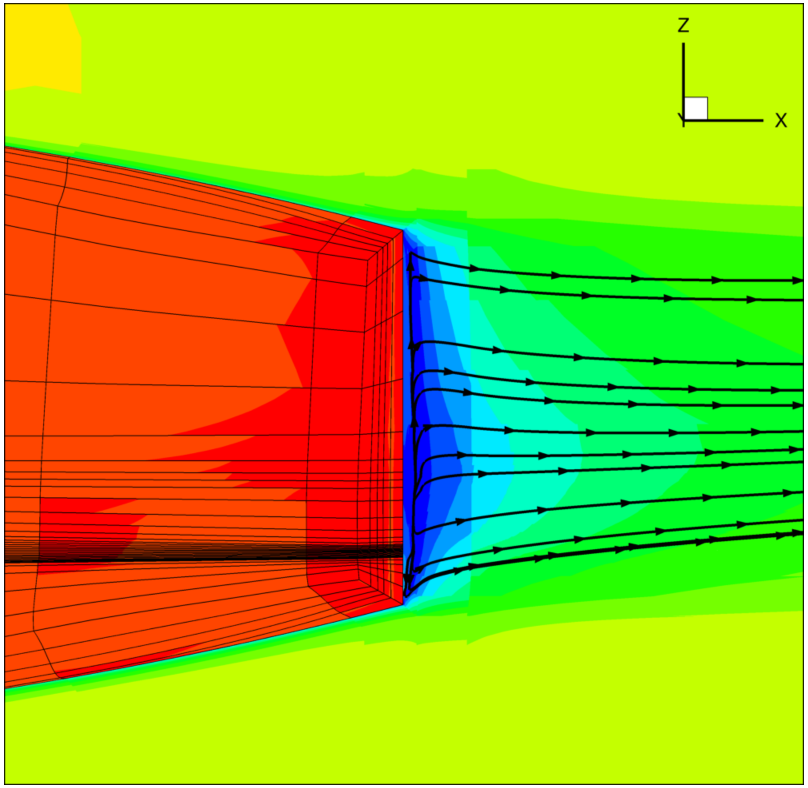

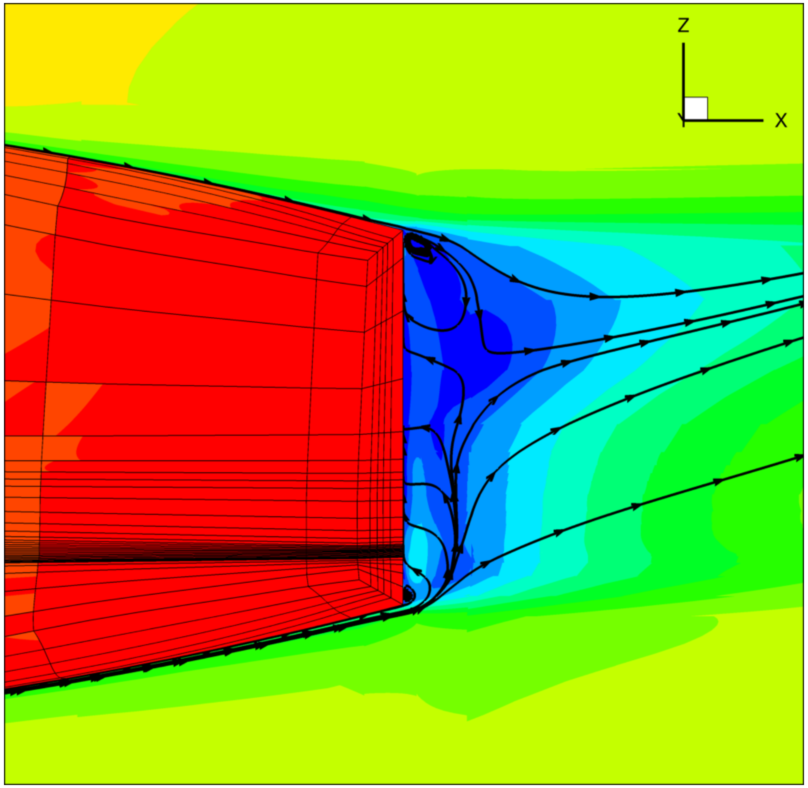

second order DG third order DG

VFE-2 delta wing

- widely used in the second vortex flow experiment (experiments and CFD)
- vortex-dominated flowfield
- purely subsonic case
- transonic case with shock-vortex interaction (requires shock-capturing)

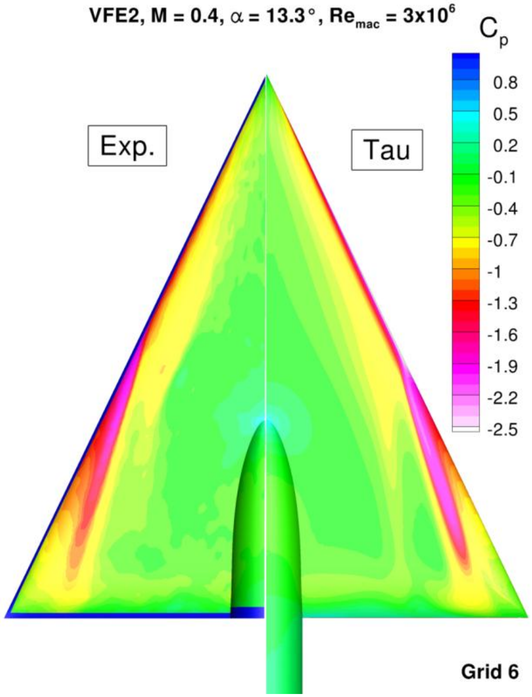

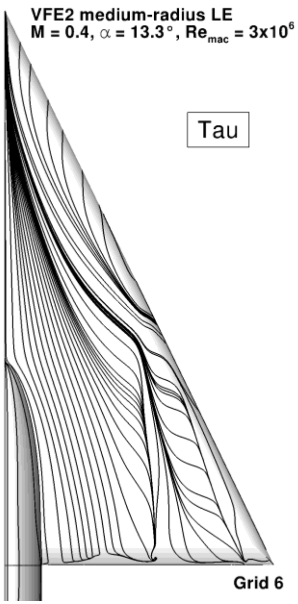

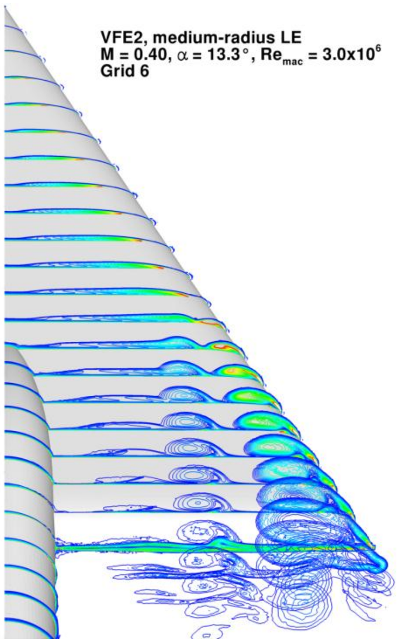

VFE-2 delta wing: meshes

computed on

- a sequence of block-structured meshes 13 k,110 k and 880 k hexes (DG)
- locally solution-adapted meshes
- a sequence of unstructured meshes (FV)

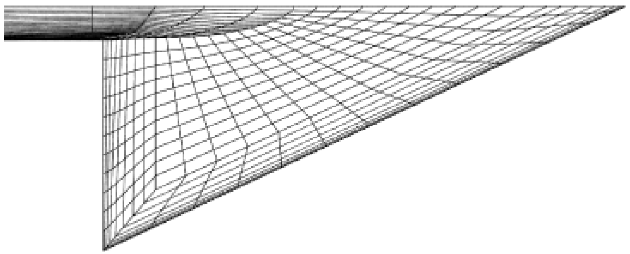

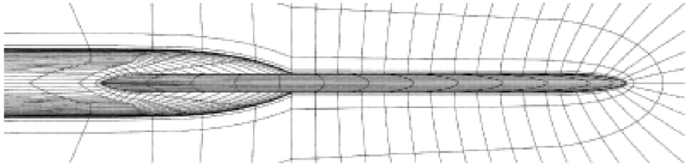

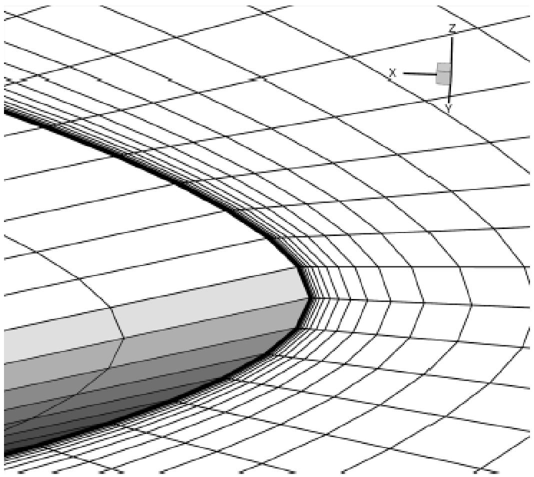

straight-sided

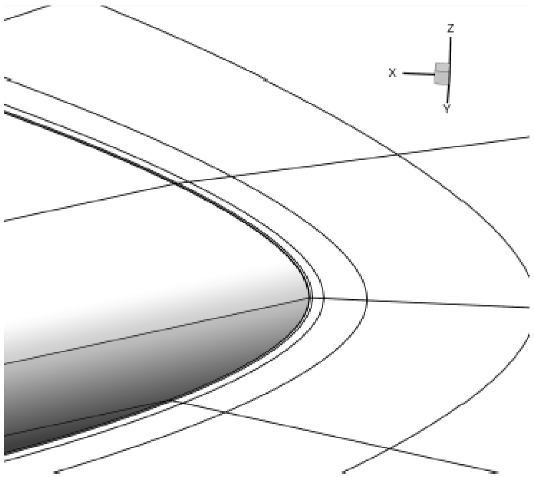

curvilinear
quartic polynomials

VFE-2 delta wing: adaptation

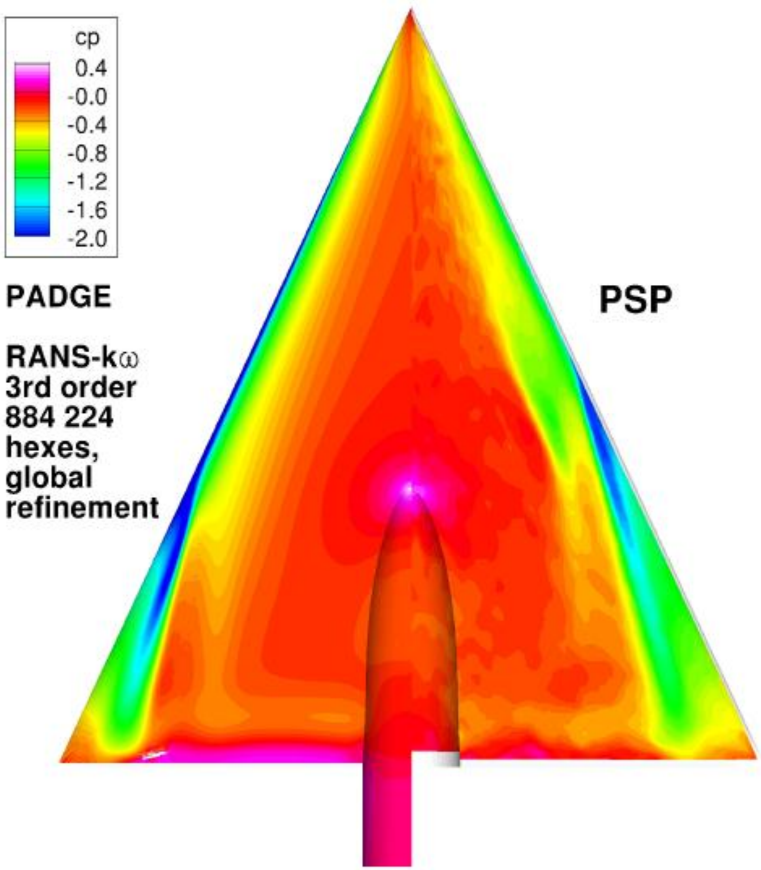

structured mesh

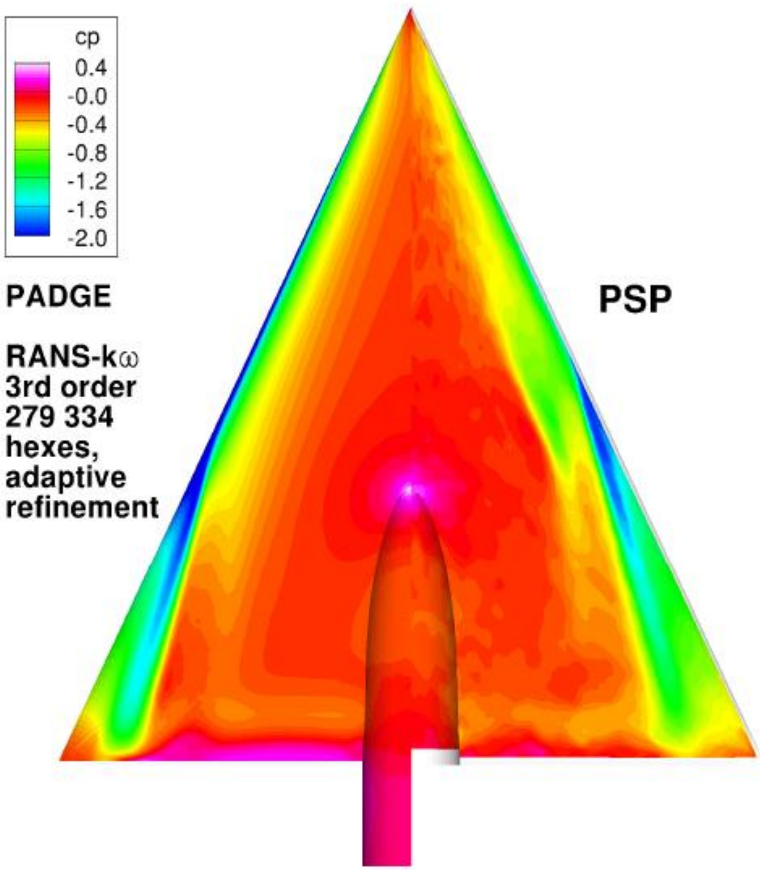

adapted mesh

3[rd] order solution vs. experiment (c_p)

VFE-2 delta wing: adaptation

- adapation improves the overall time to solution, in particular if based on an adjoint problem
- timings include adaptation and computations on coarser meshes

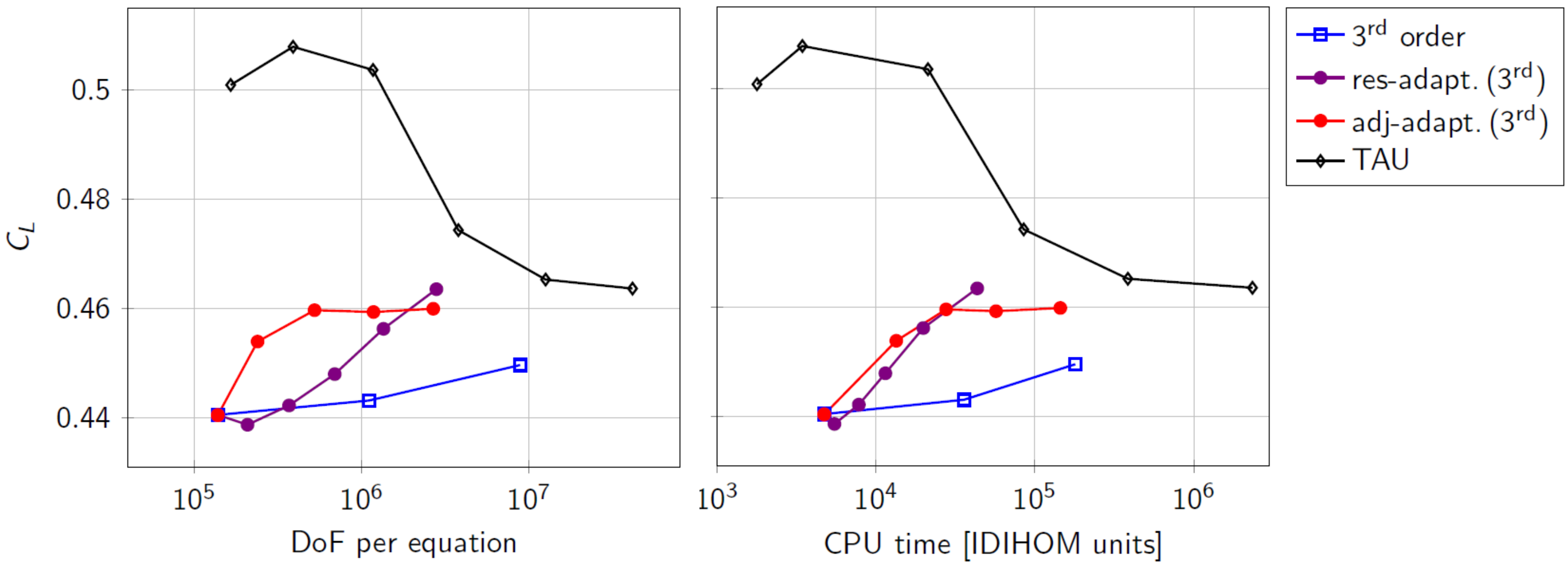

VFE-2 delta wing: EARSM

EARSM: Explicit Algebraic Reynolds Stress Model (Wallin & Johansson)

EARSM 1: including linear terms of the anisotropy tensor
EARSM 2: including linear & quadratic terms of the anisotropy tensor
EARSM 3: including linear & quadratic & cubic terms of the anisotropy tensor

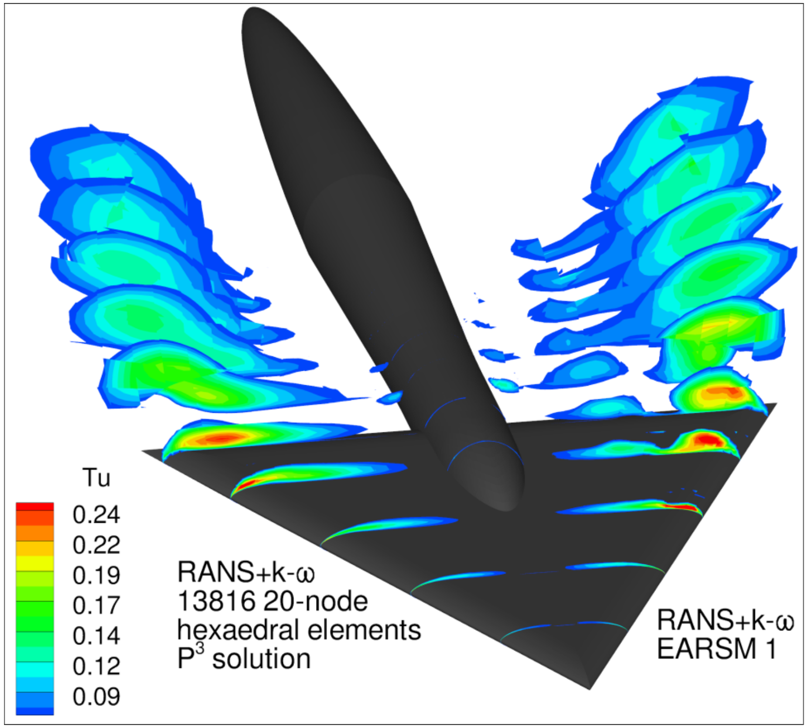

kω vs. EARSM 1

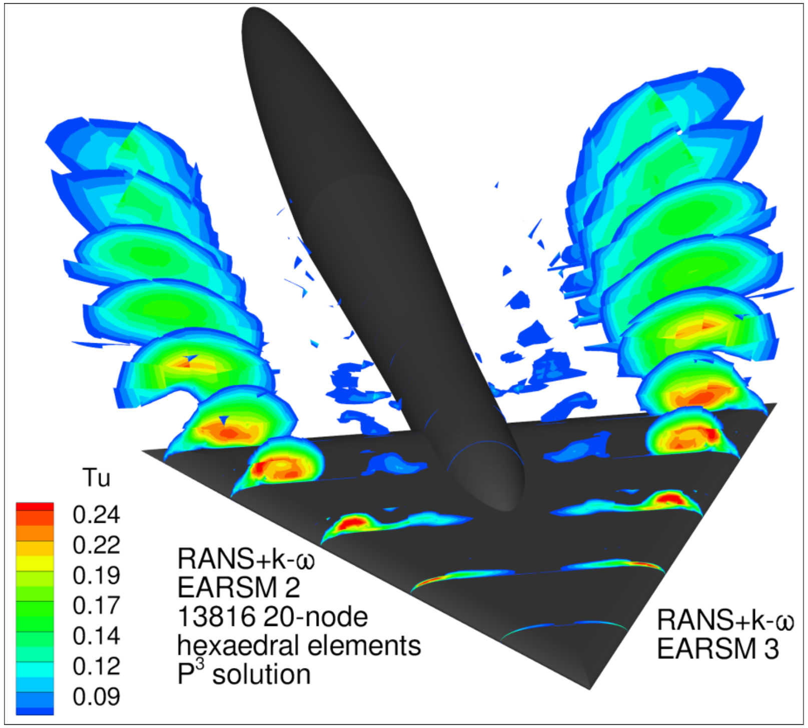

EARSM2 vs. EARSM 3

VFE-2 delta wing: EARSM

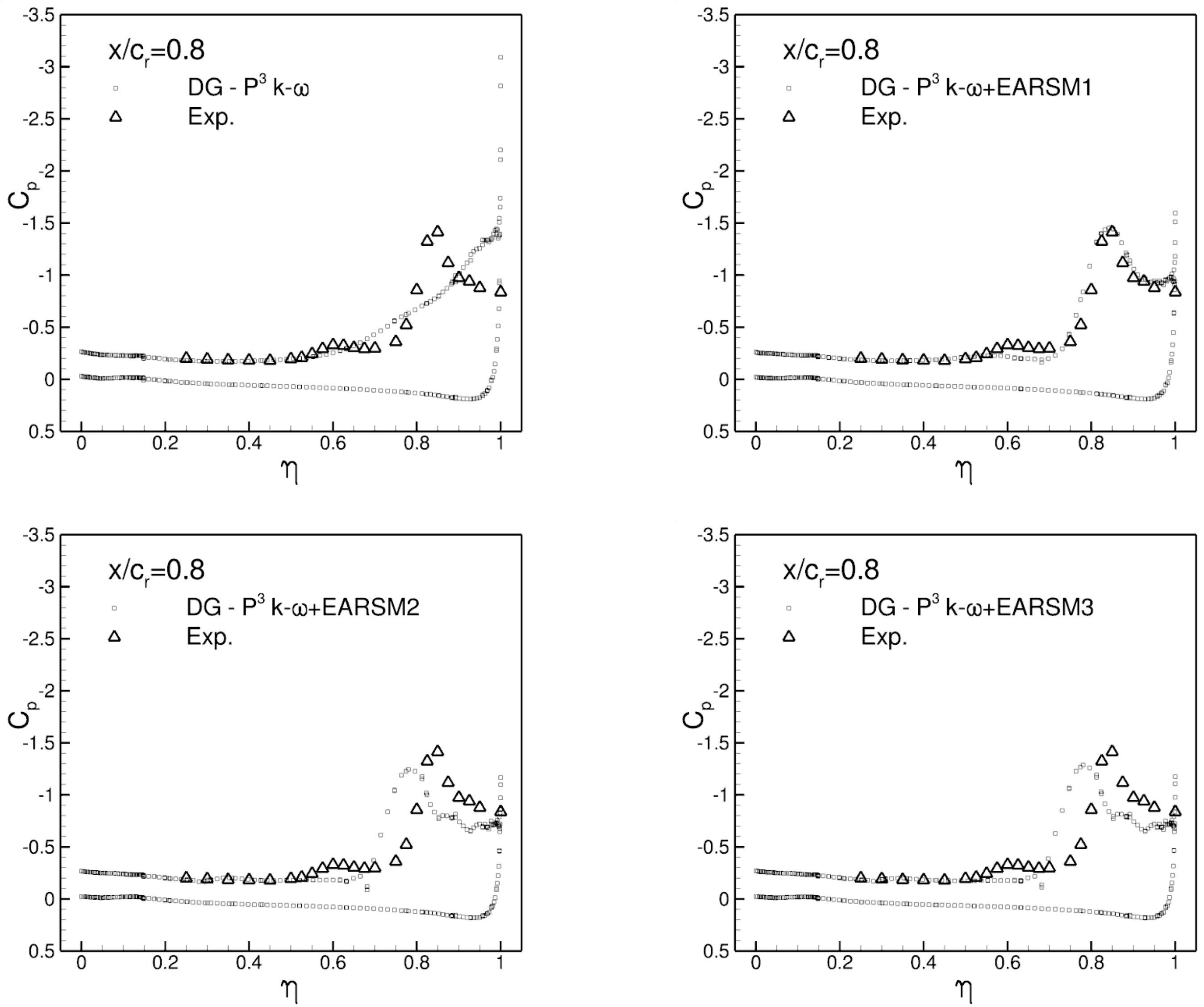

VFE-2 delta wing: transonic flow

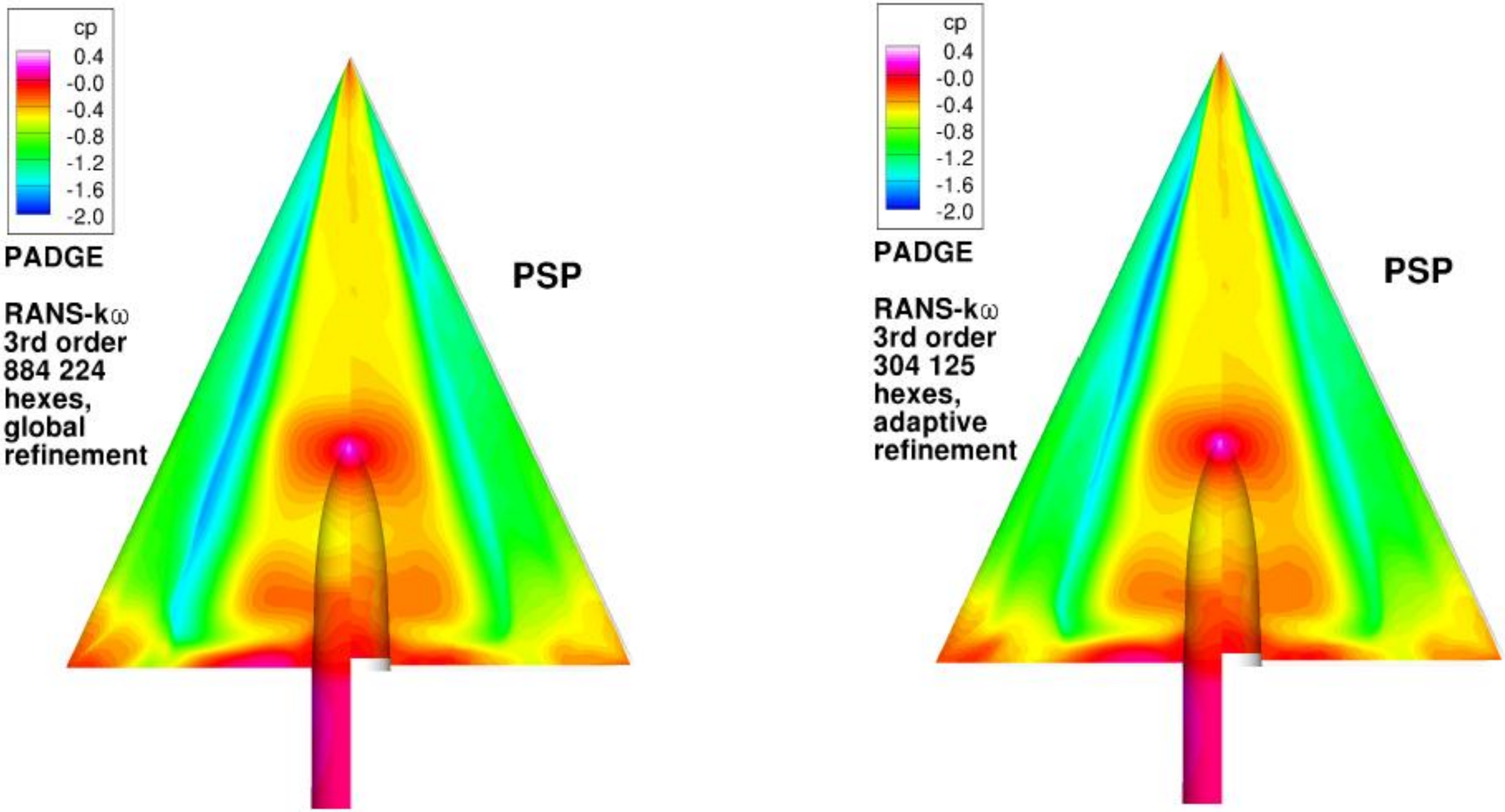

structured mesh | adapted mesh

3[rd] order solution vs. experiment (c_p)

VFE-2 delta wing: transonic flow

Mach and pressure contours, λ_2 criterion

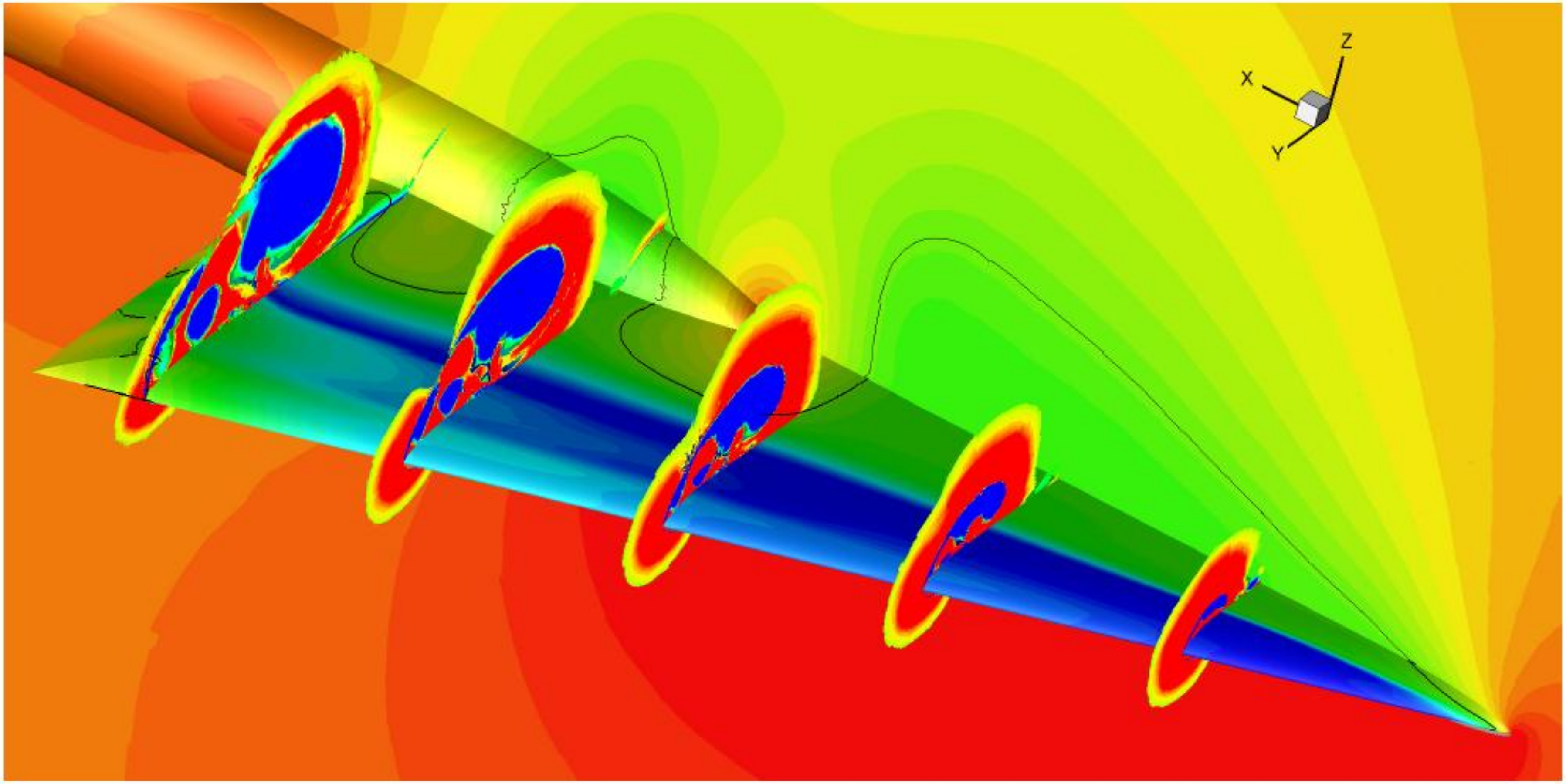

good resolution of three vortices already on coarse meshes (300 k elements) with a 3rd order DG solution

FA 5 fighter configuration

- transonic high angle of attack case by CASSIDIAN
- structured curvilinear mesh
- 3rd order DG EARSM results

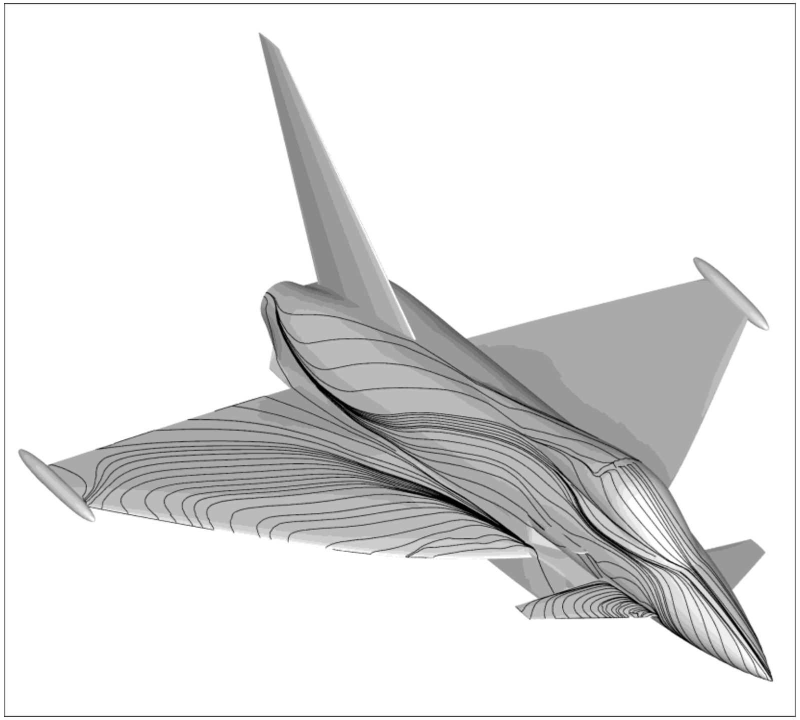

wall stream lines

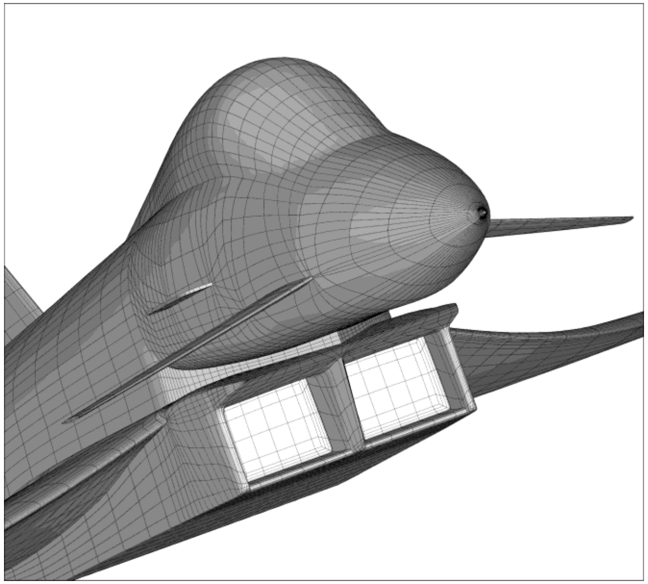

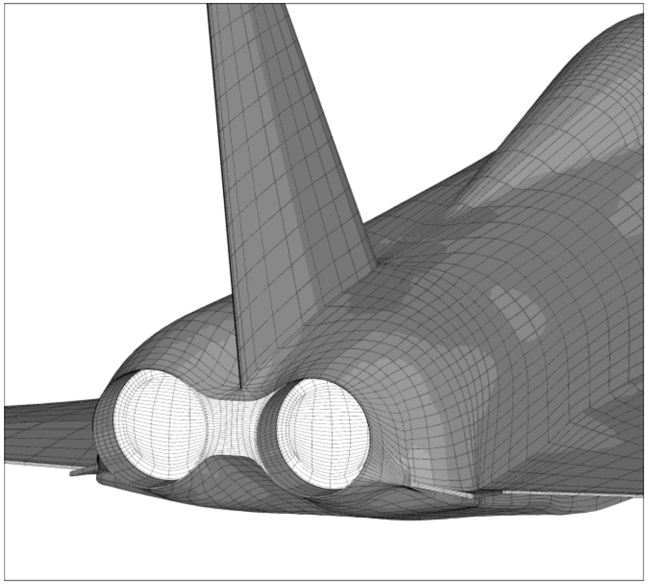

FA 5: C_p distribution

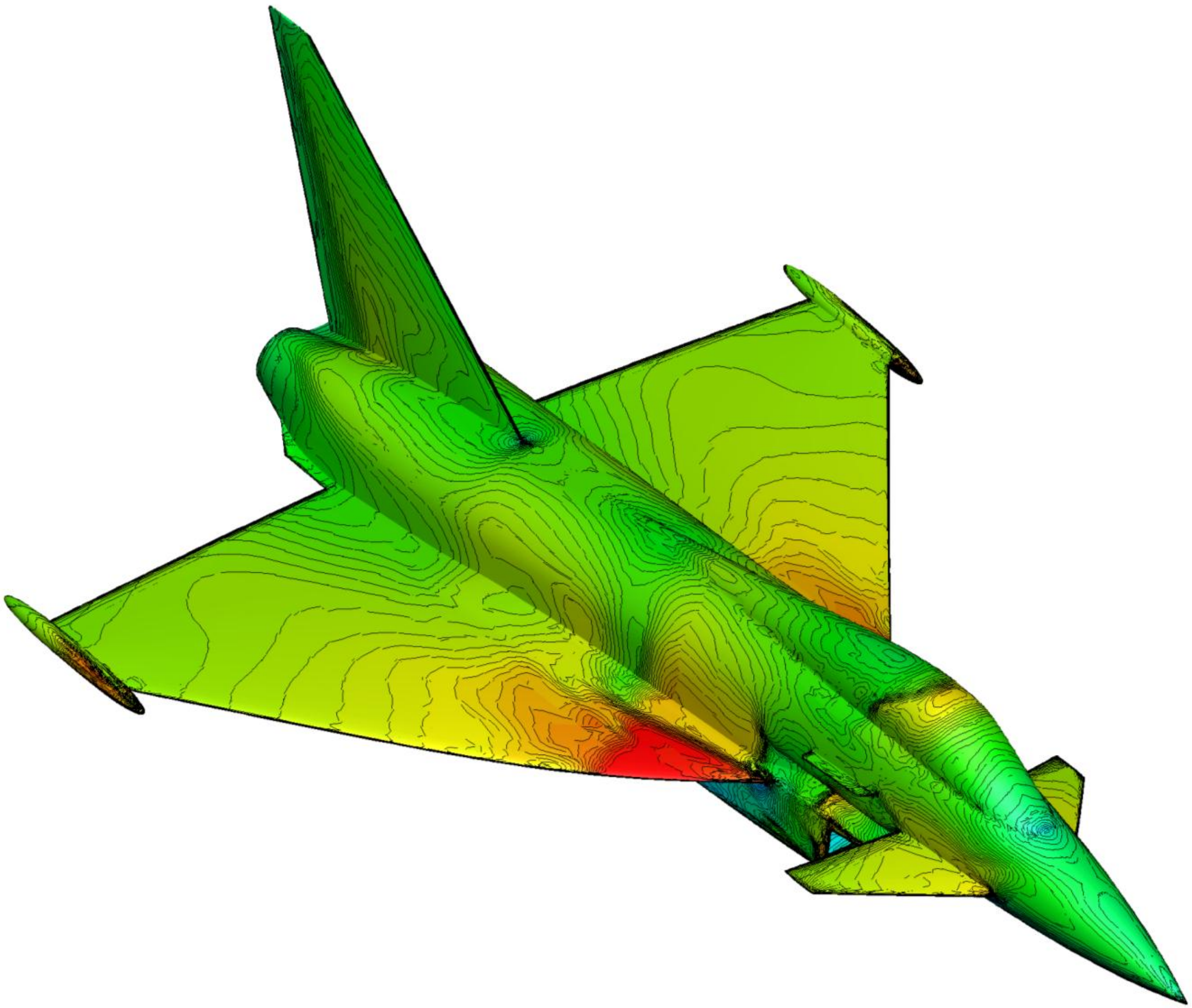

FA 5: turbulence intensity

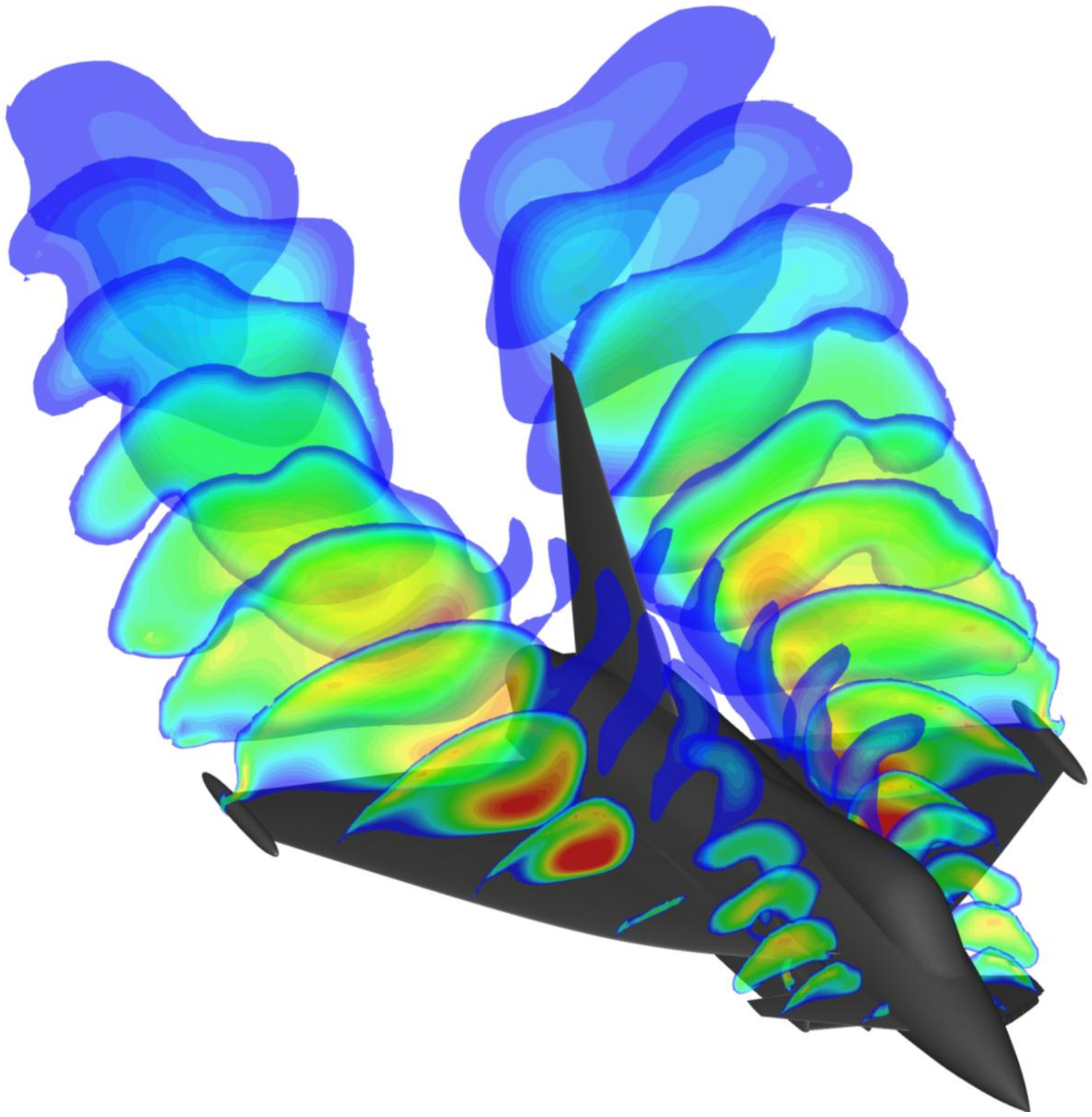

Turbomachinery applications

- T106A LP-Turbine
- NASA Rotor 37

LP turbine: mesh

two meshes have been used:
coarse (43,000 hexahedra) and medium (77,600 hexahedra)

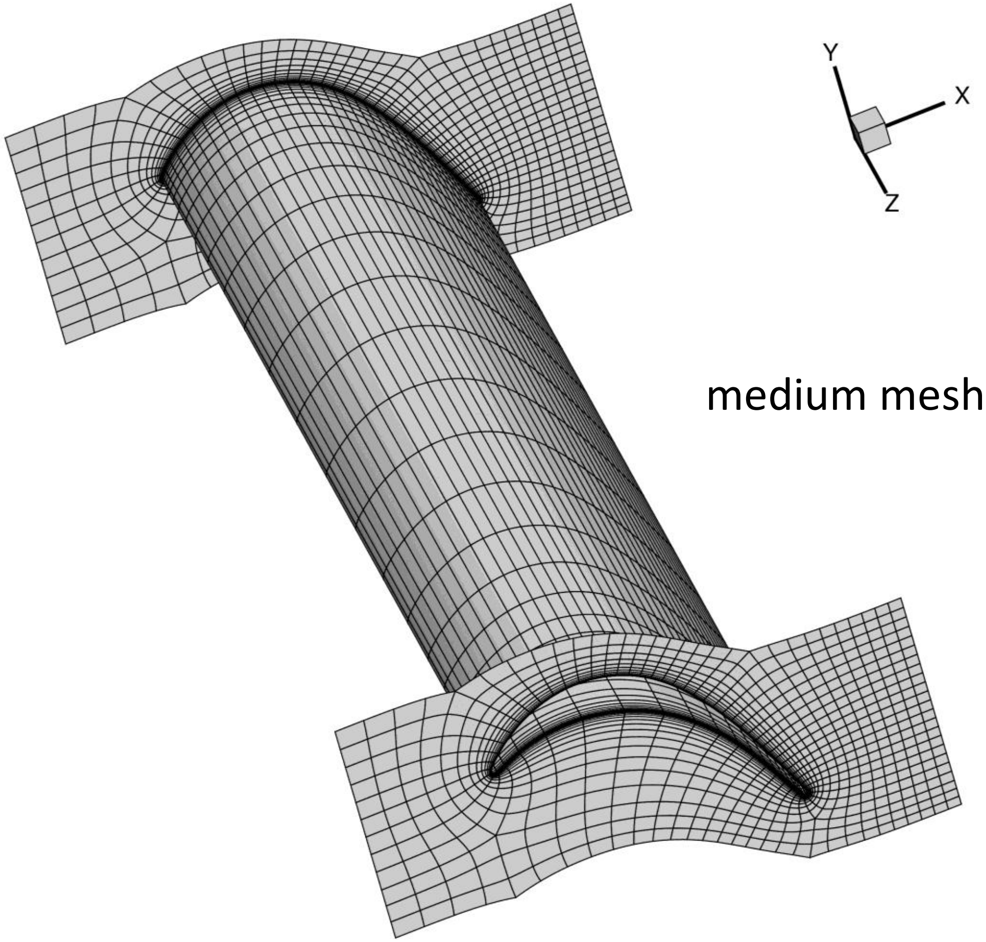

medium mesh

LP turbine: Mach contours (midspan)

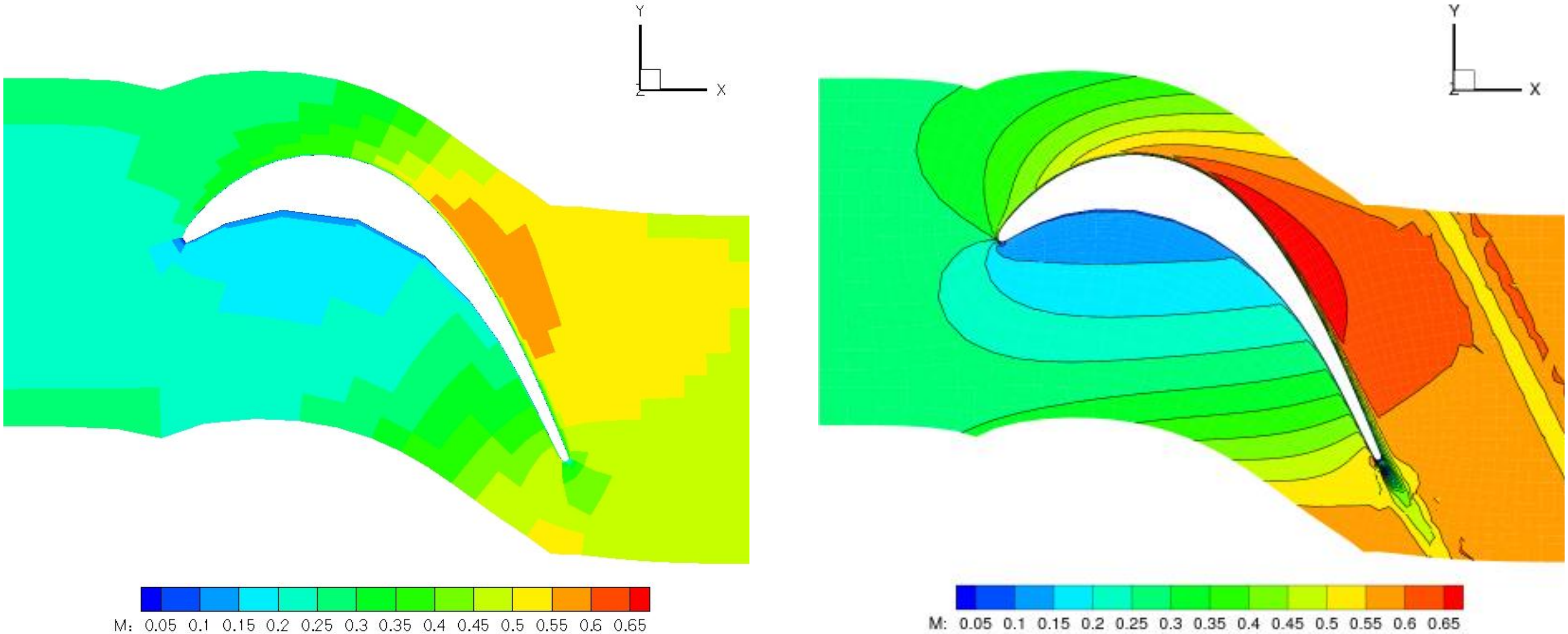

Mach number contours on the coarse grid for different polynomial order: P^0 (left) and P^3 (right)

LP turbine: C_p distribution

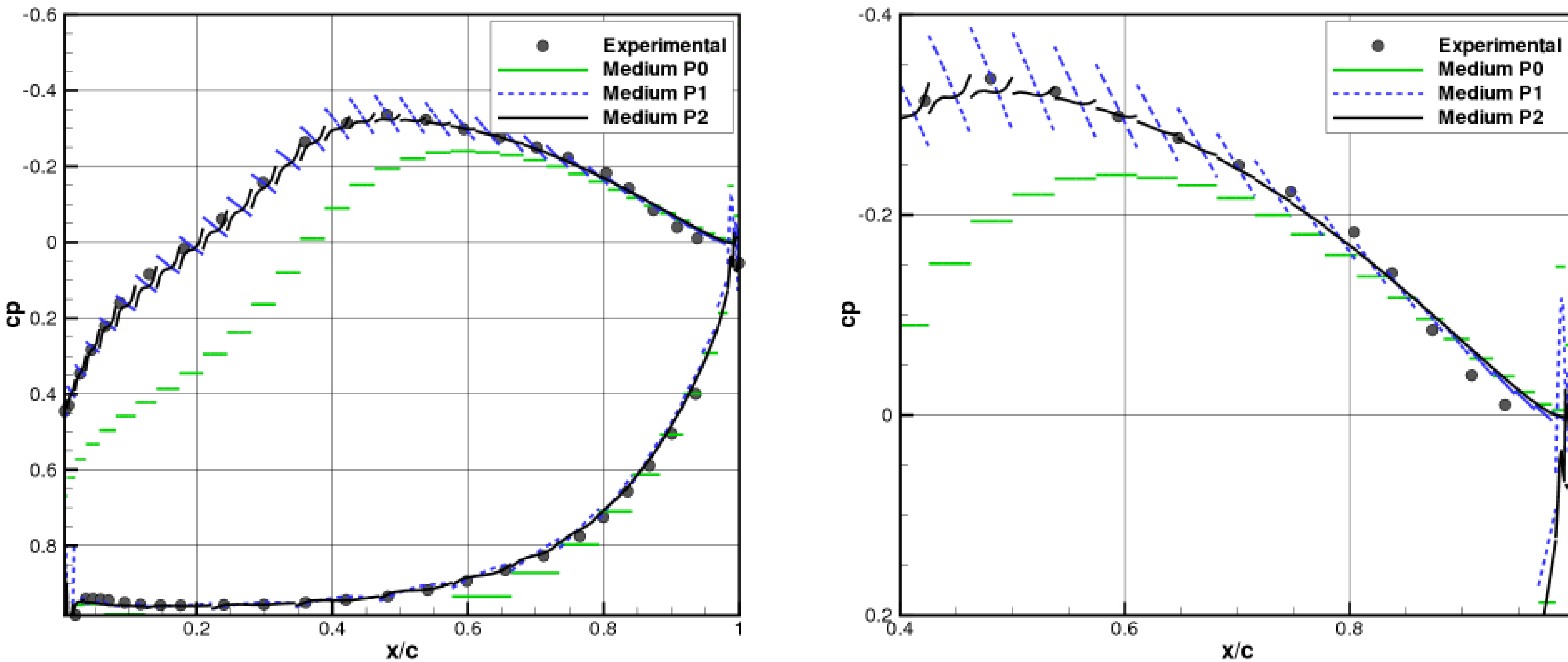

pressure coefficient distribution
computed on the medium grid for different polynomial orders

LP turbine: horseshoe vortices

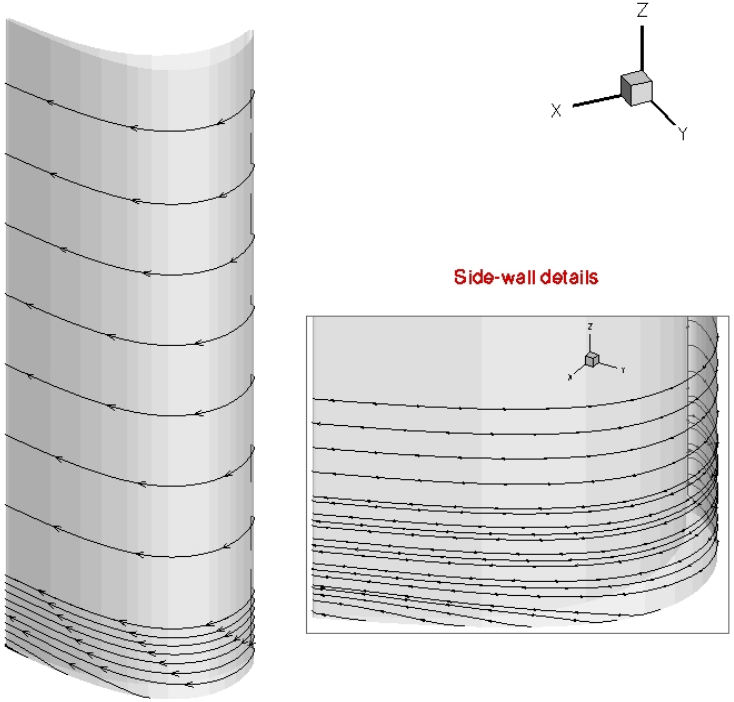

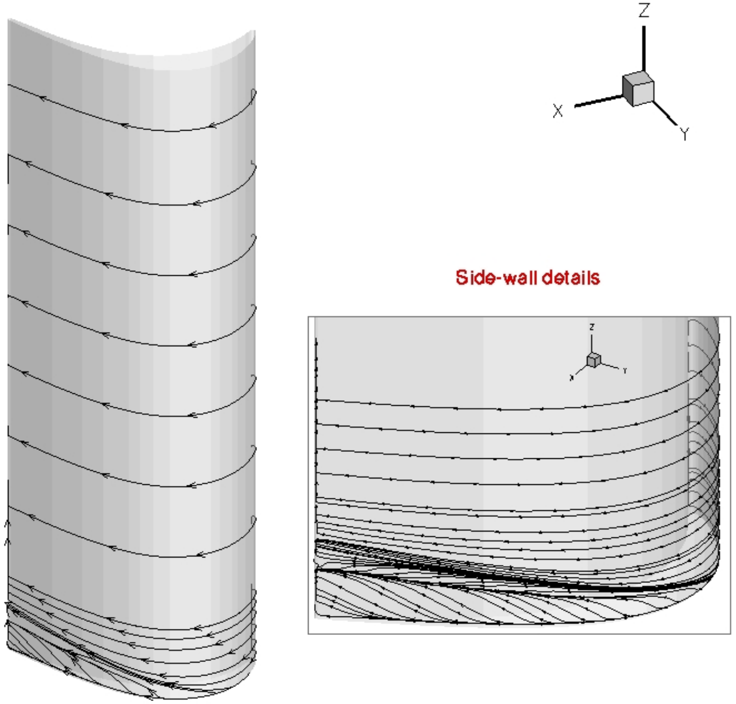

horseshoe vortices on the coarse grid for P^0 (left) and P^3 (right) solution

LP turbine: DNS

- 2D study to identify turbulent structures (preparation for 3D)
- reduced transitional reynolds number (50,000)
- 4^{th} order DG, mesh adapted on vorticity discontinuities

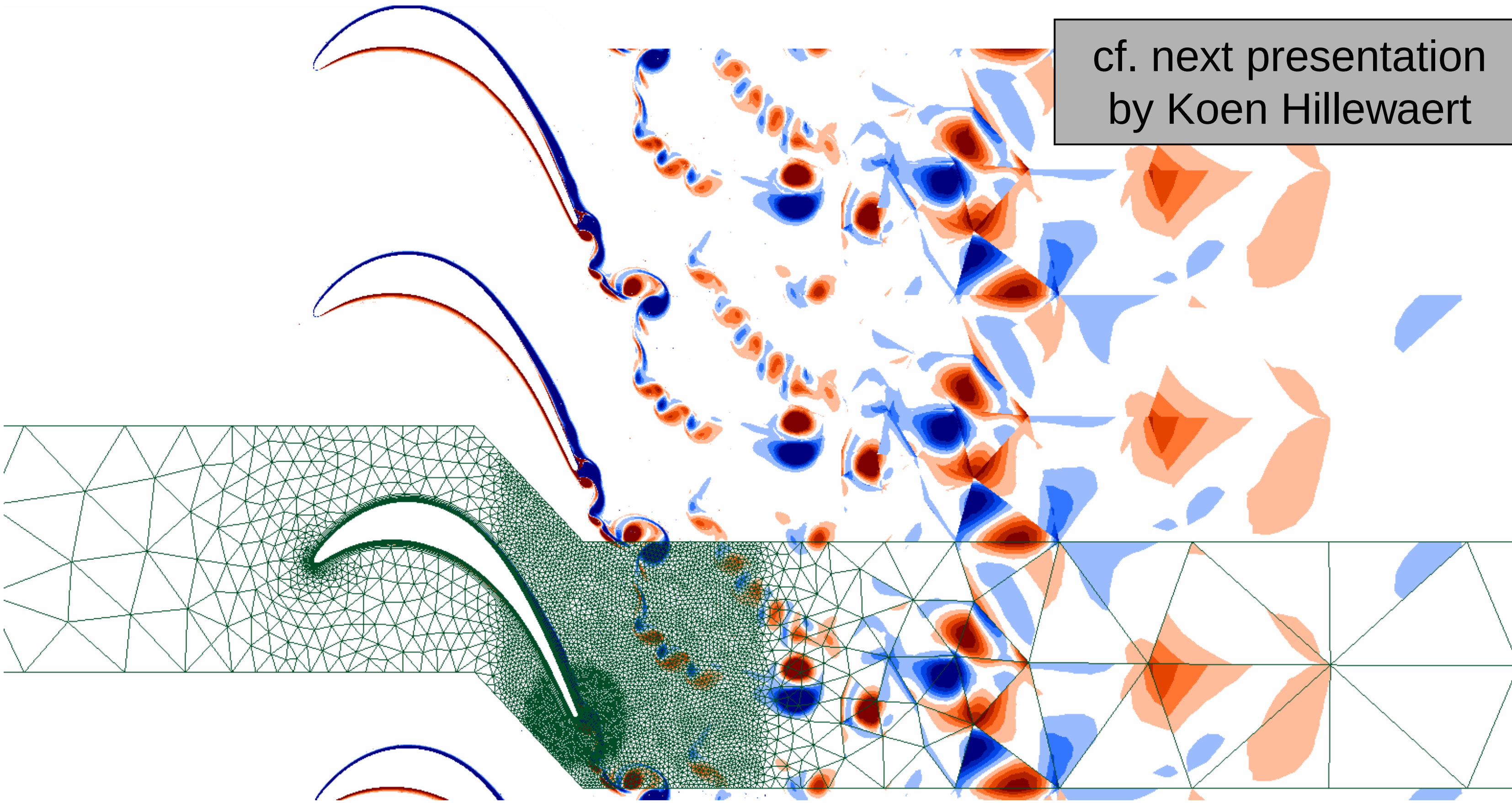

IDIHOM

NASA Rotor 37

highly loaded transonic compressor

- widely tested in the 1990’s
- design pressure ratio of 2.106
- choke mass flow 20.93 kg/s
- computed at 98% choke conditions

Rotor 37: convergence

- fine grid computations with SA: 6 blocks, about 1.5M cells
- target mass flow condition at outlet

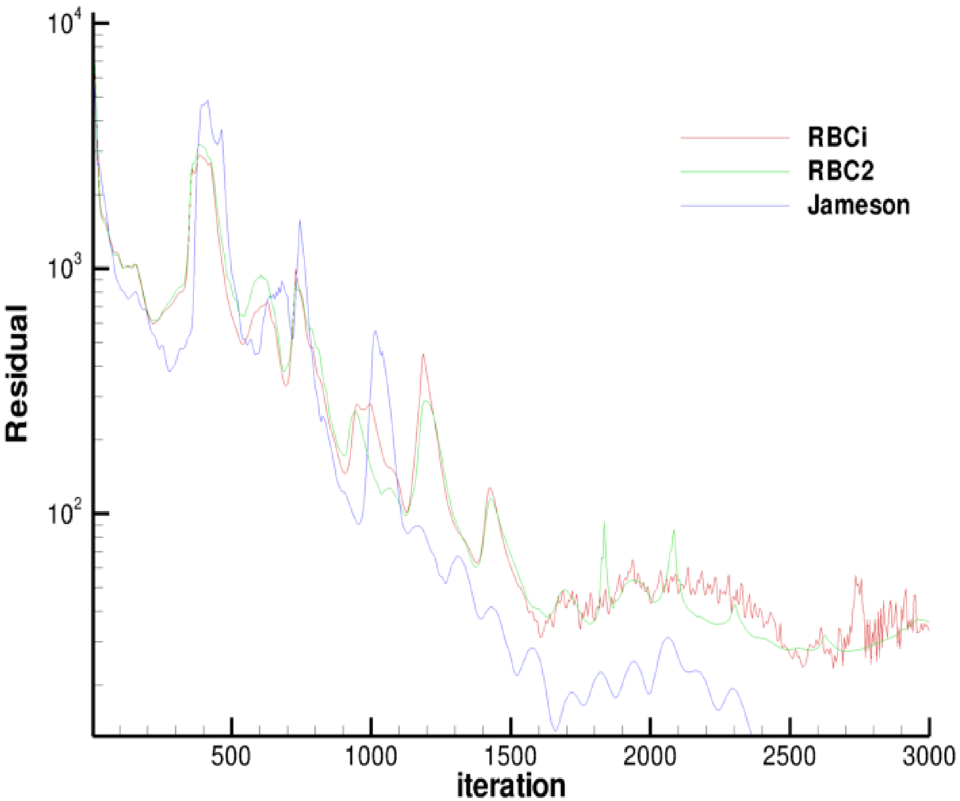

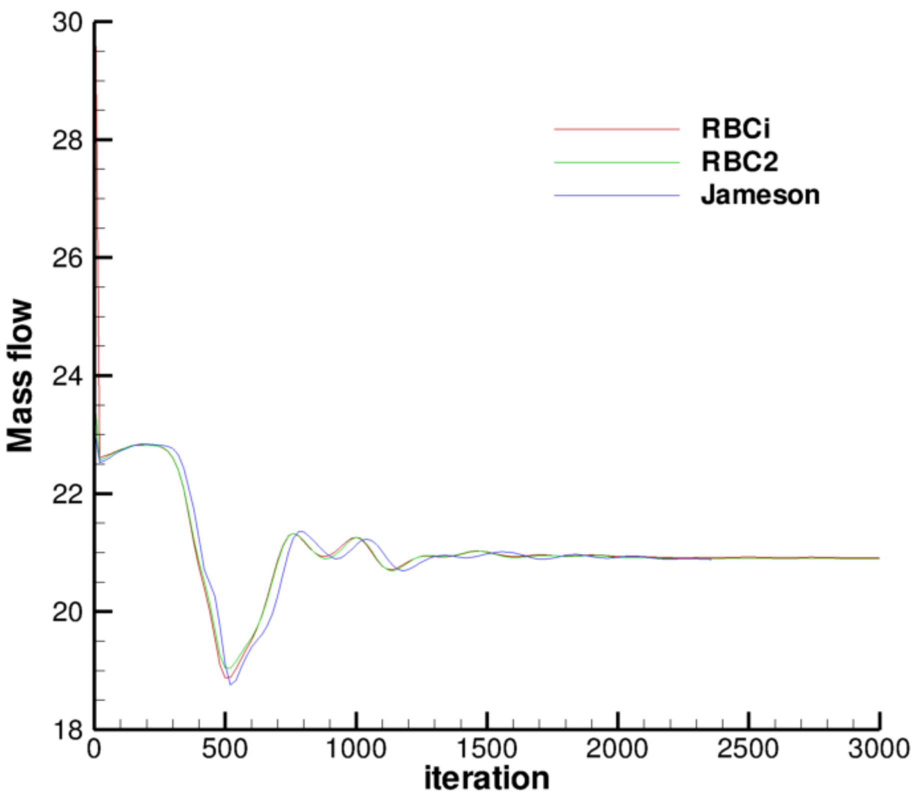

Rotor 37: 3D view of flowfield

iso-Mach contours, pressure isolines, stream ribbons (RBCi scheme)

bow shock

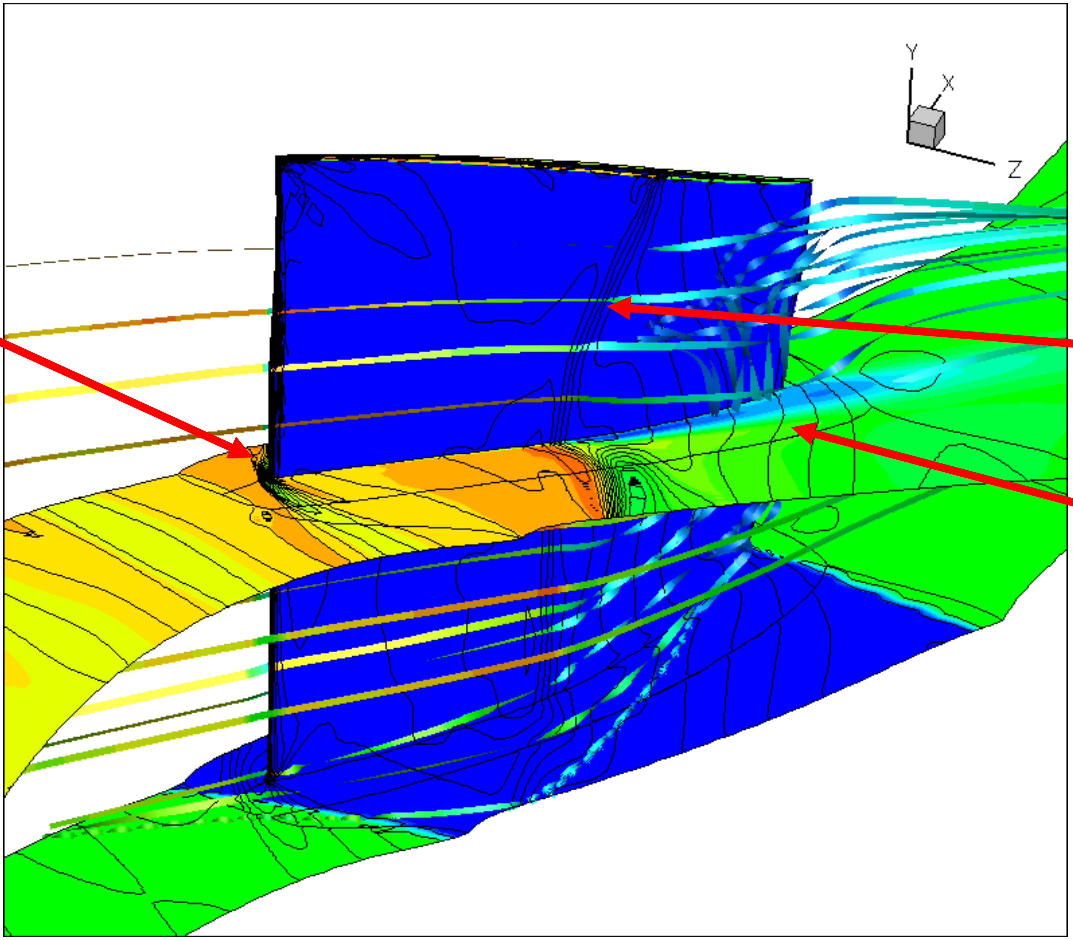

passage shock

separated flow

Rotor 37: iso-Mach (midplane)

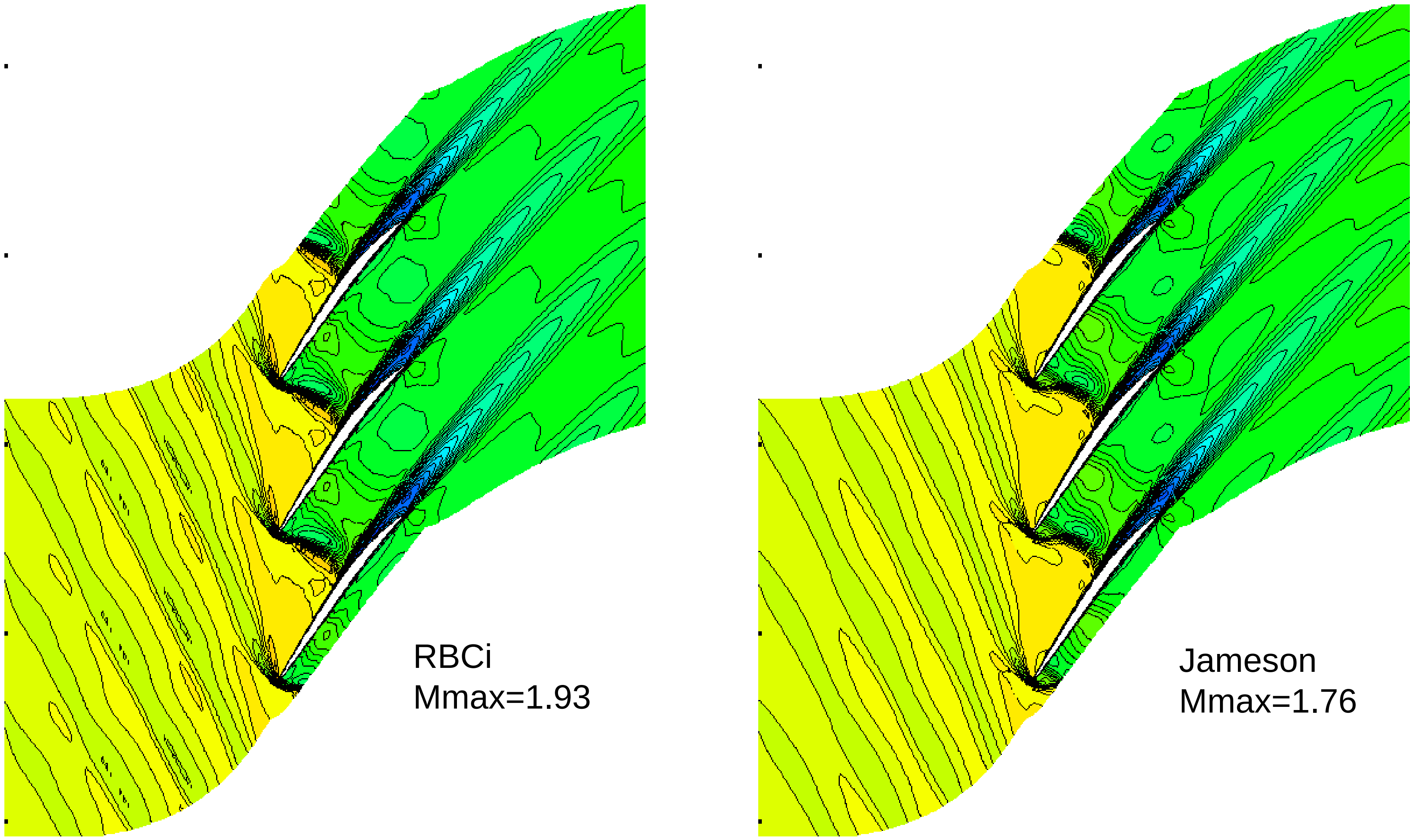

Rotor 37: complete characteristic

coarse grid results (approx. 200,000 cells)

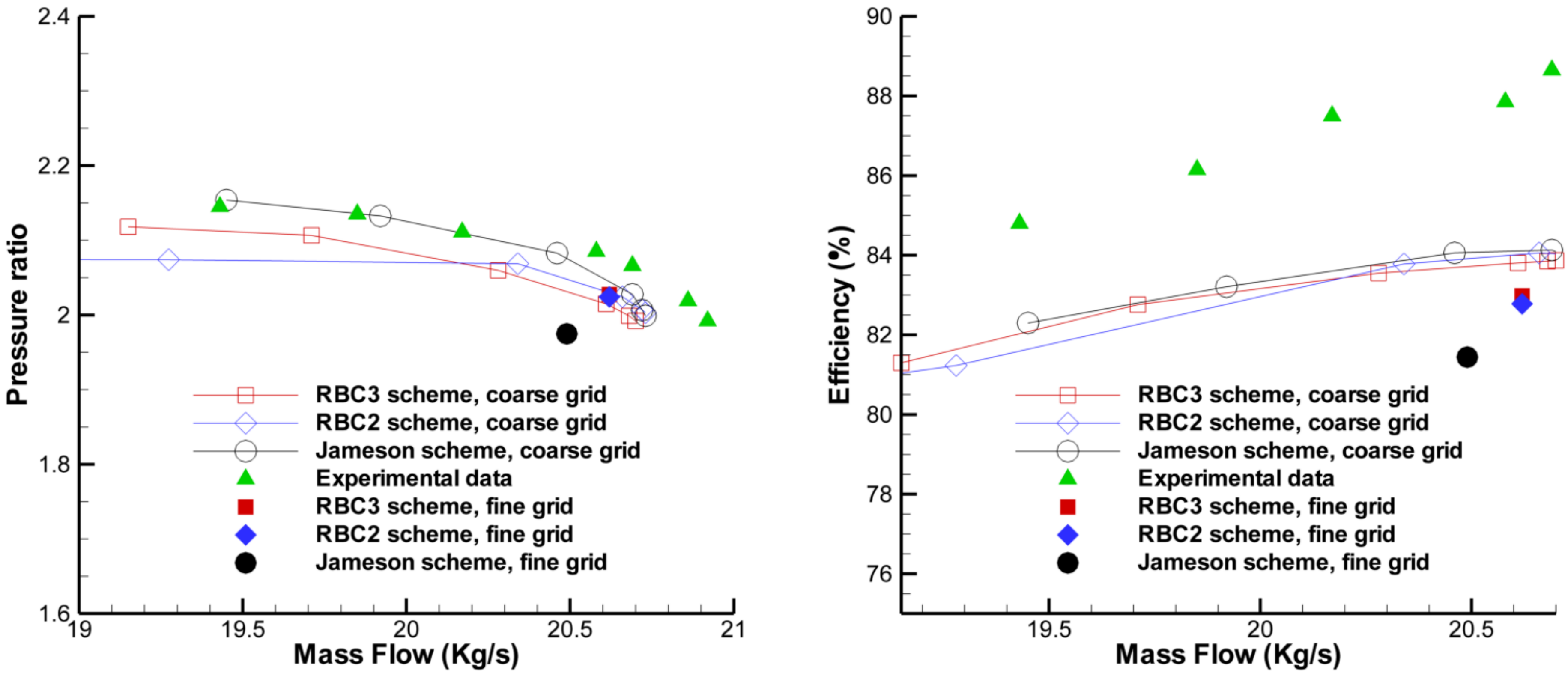

- all schemes underestimate the pressure ratio and adiabatic efficiency
- coarse grid values for the RBC schemes at 98% choke close to fine grid results
- Jameson's scheme coarse grid results fortuitously close to experimental

IDIHOM

Rotor 37: DG flowfield

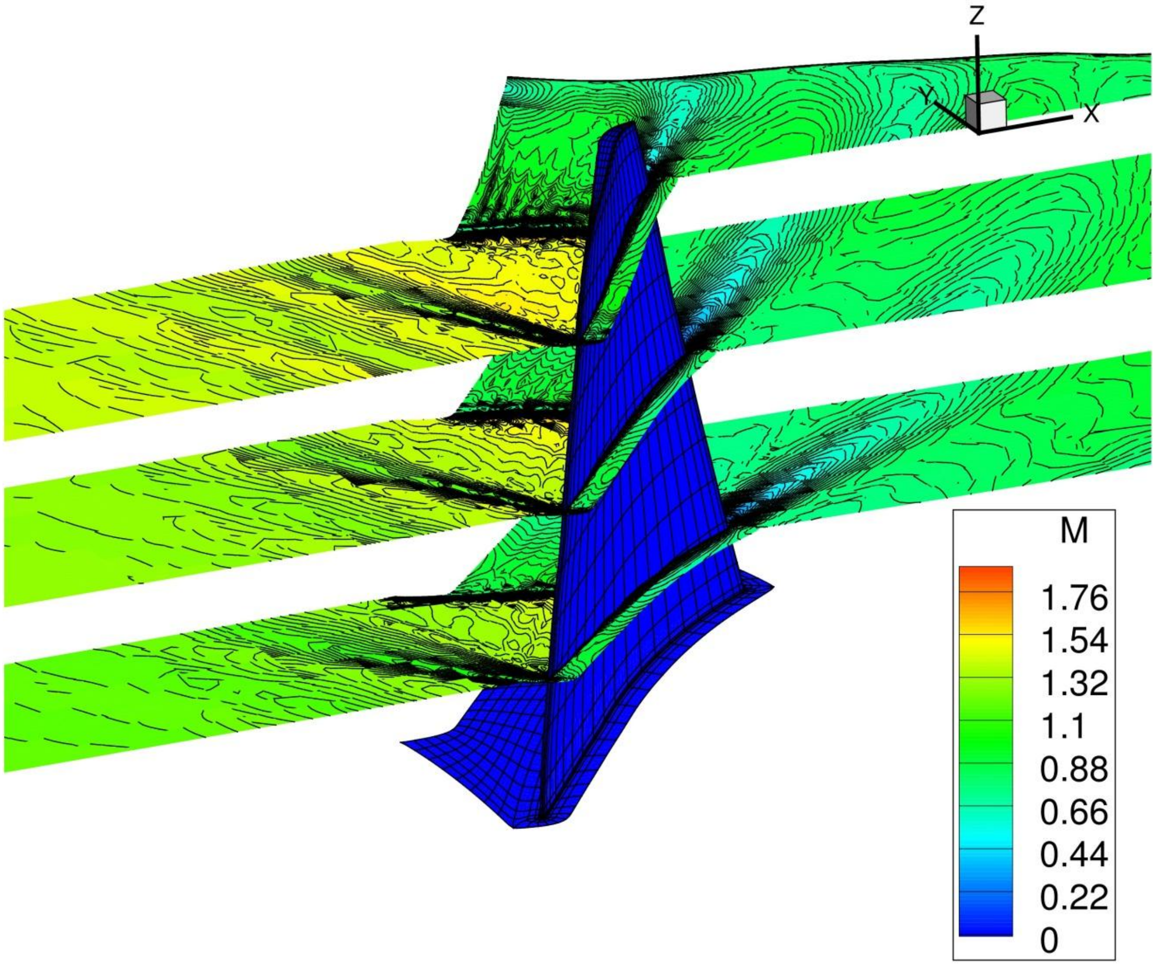

Mach number contours

3rd order DG computation

Helicopter applications

HART-II experiment: helicopter rotor in blade-vortex interaction conditions

- challenge is to convect tip vortex over 1.5 to 2 revolutions without dissipating it

baseline and HO simulations performed

- baseline: 4^{th} order FV on unrefined mesh (13 M cells)
- HO: 4^{th} order FV on refined mesh (26 M cells)
- all simulations performed with a time step equivalent with 0.5° azimuth
- rigid blades, no trim

refined mesh

- obtained using the algorithm developed within IDIHOM
- aims at obtaining a uniform mesh in the rotor disk area

HART-II rotor: mesh

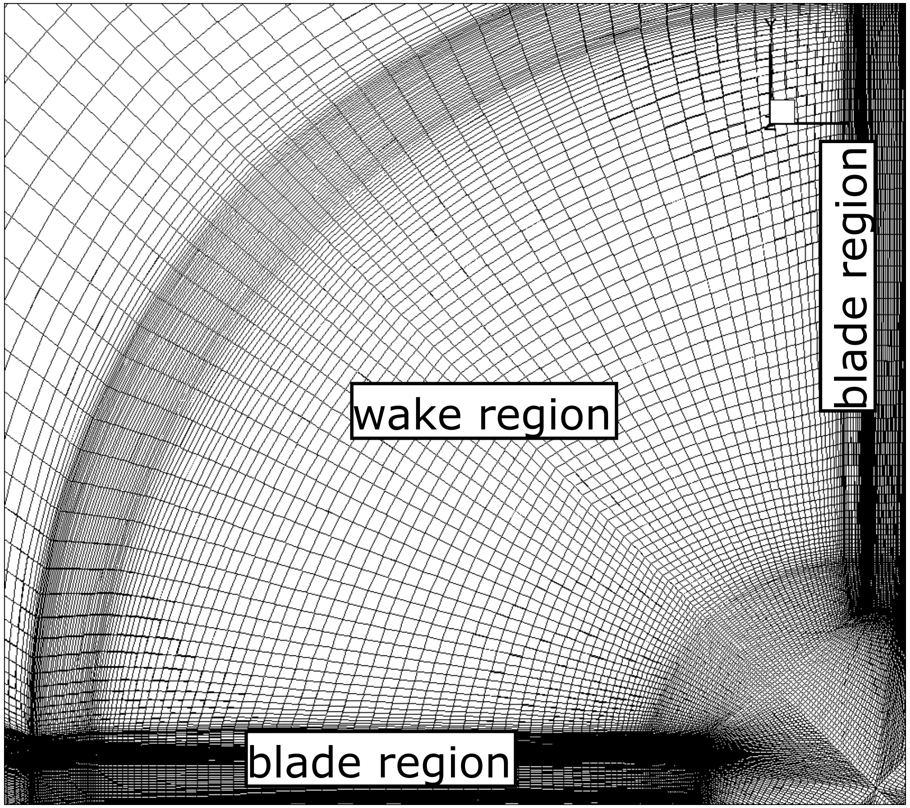

unrefined mesh

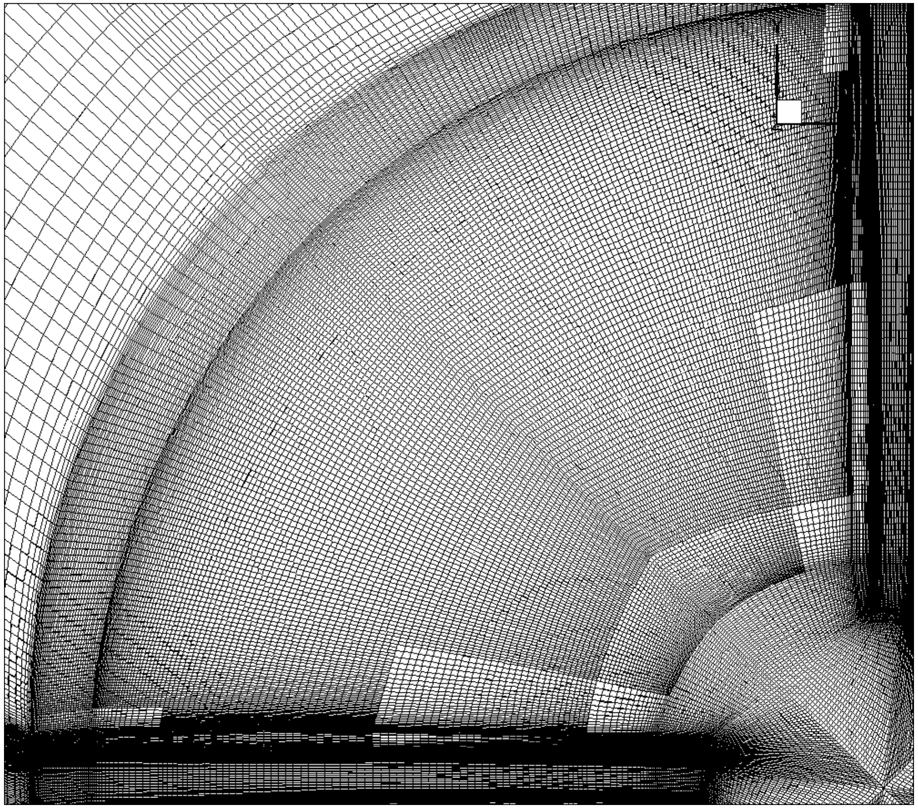

refined mesh

in the rotor disk a uniform mesh width of 1% blade span is obtained

HART-II rotor: results

iso-contour of Q coloured with vorticity magnitude

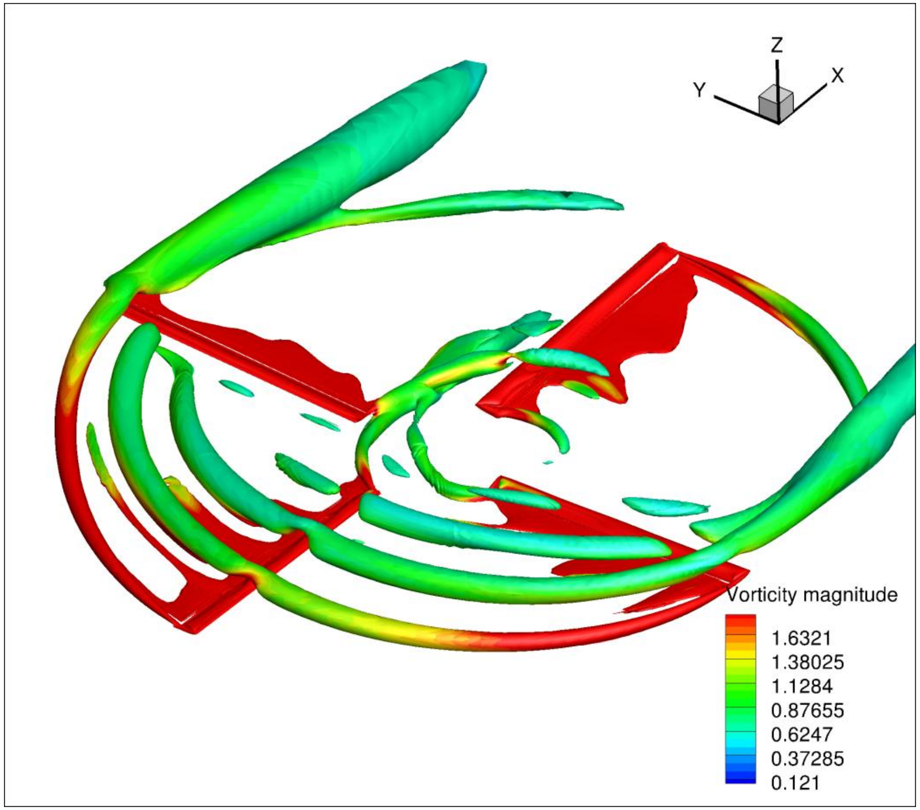

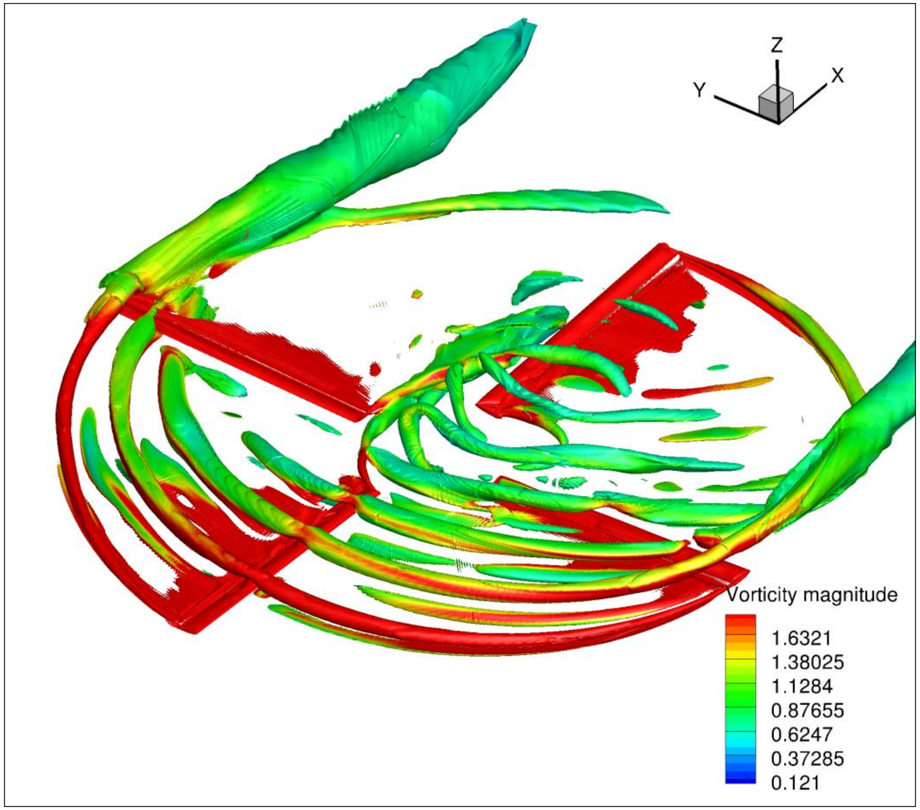

unrefined mesh

refined mesh

the local refinement results in improved vortex capturing

HART-II rotor: results

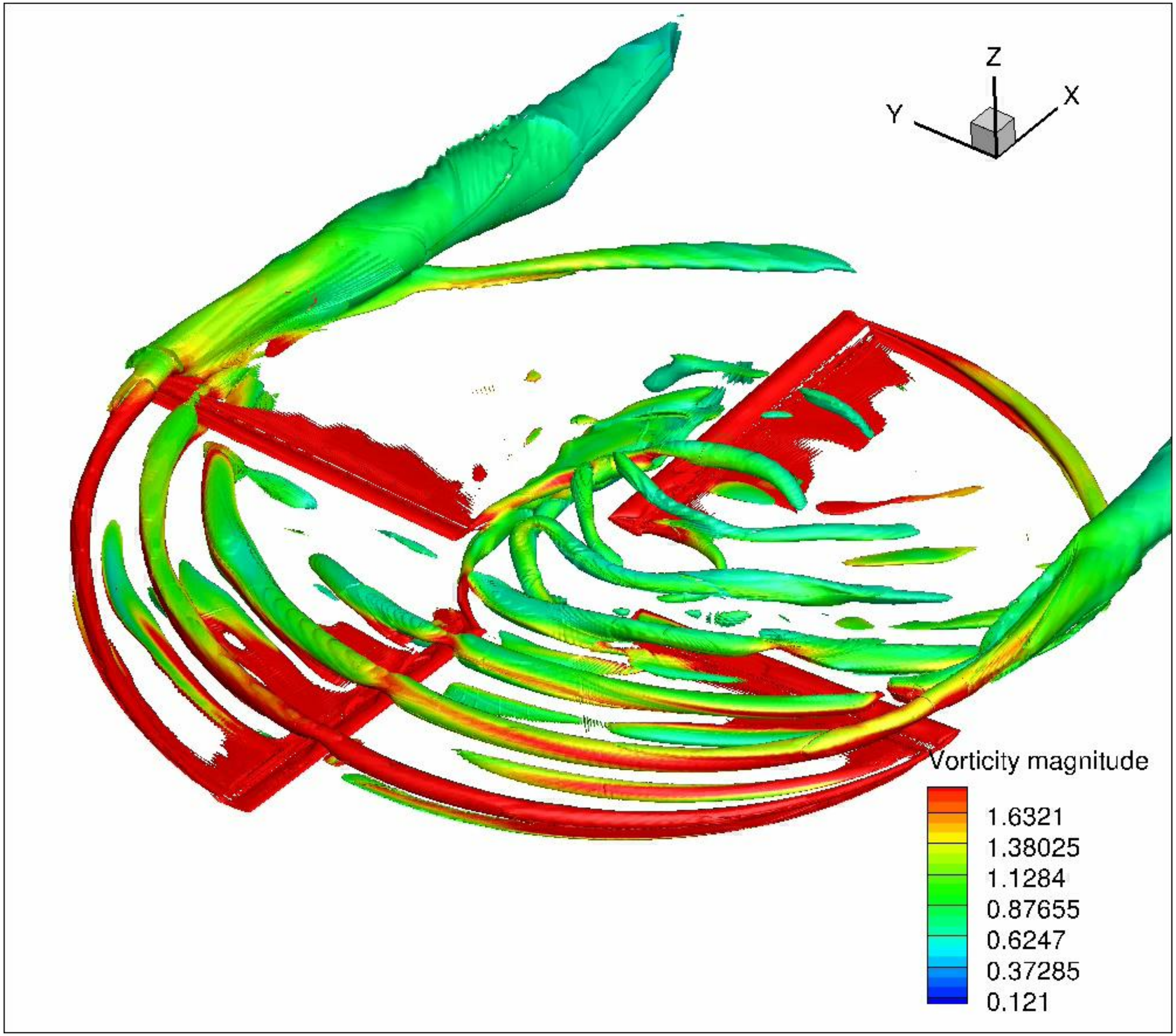

HART-II rotor: vorticity magnitude

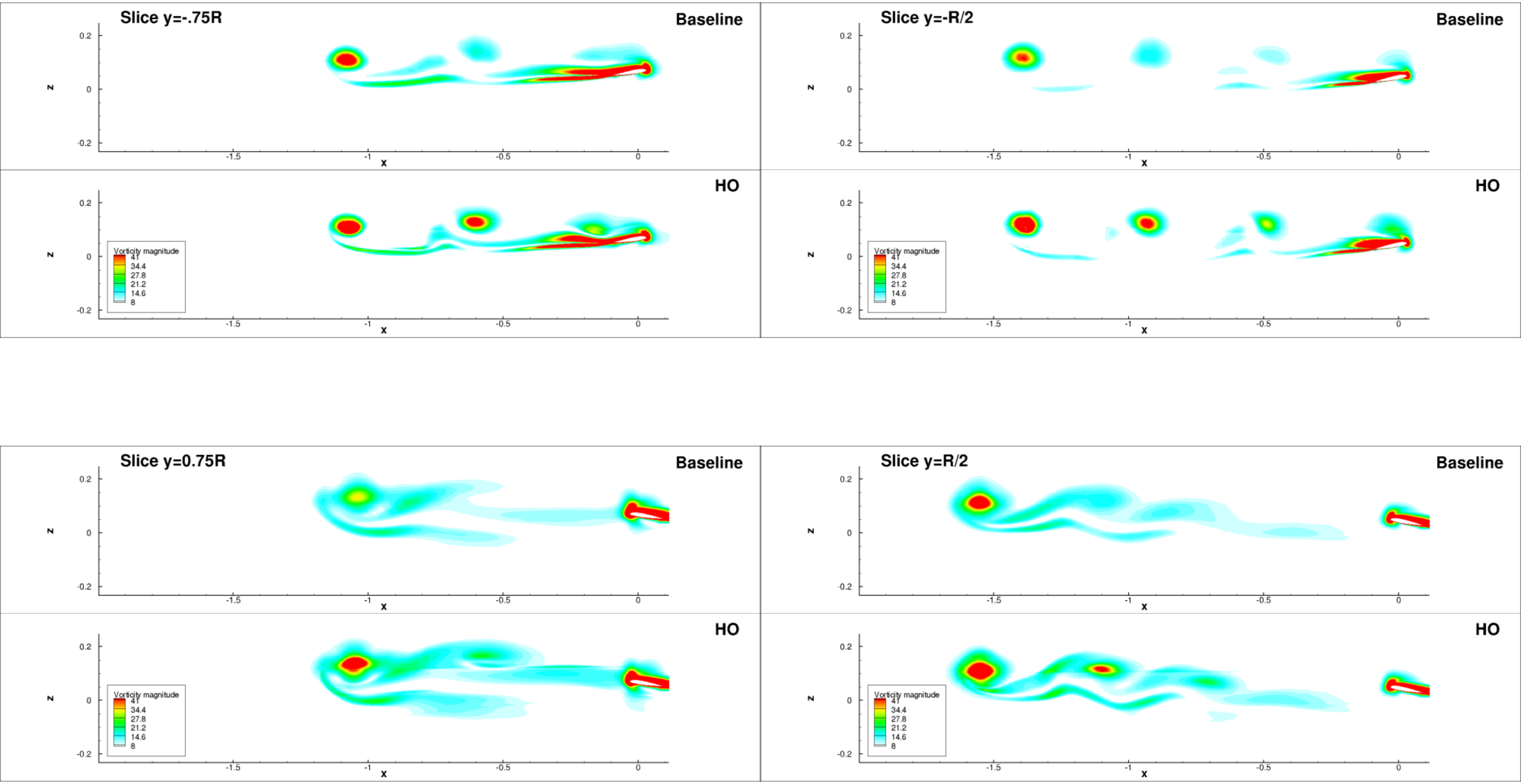

Summary

- The complete range of aerospace CFD, including fixed and rotary wing cases as well as turbomachinery applications, has been tackled.
- High order methods have been shown to produce accurate results.
- For most cases, further progress concerning more detailed analyses of individual flows is forseen during the second half of the project.

- Geometric complexities can be handled, concerning both high order meshes and flow solvers.
- Structured (initial) meshes are (still) predominantly used in those cases.

other areas to be treated in the second half of the project

- aero-elasticity
- aero-acoustics
- ground vehicle aerodynamics (train)

Cenaero

High resolution discretisations for reliable and accurate DNS, LES and hybrid RANS-LES in an industrial context

EASN workshop on flight physics and propulsion
Prague, October 31st 2012

IDIHOM

Koen Hillewaert
Argo team leader, Cenaero
Contact: koen.hillewaert@cenaero.be

Doc. ref.: ARGO-NS-025-00

PROD-F-015-01

Turbulent flow regimes

$$Re = \frac{uc}{\nu}$$

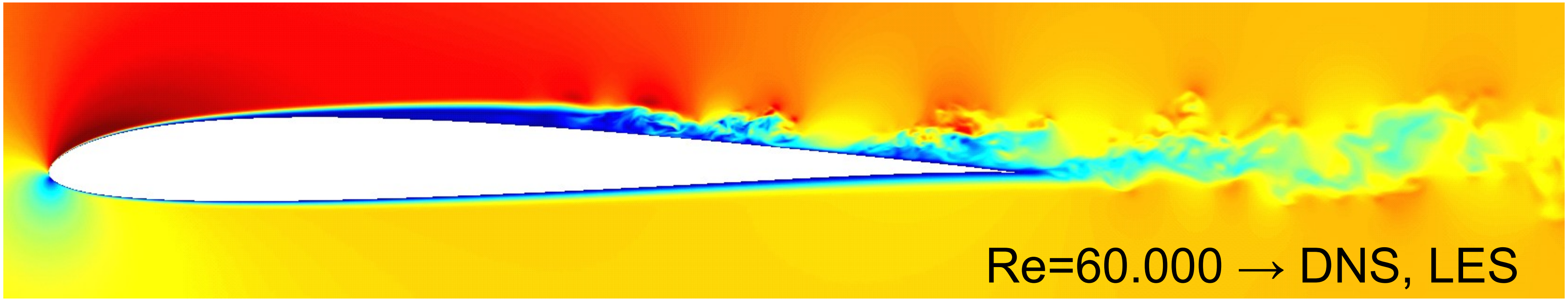

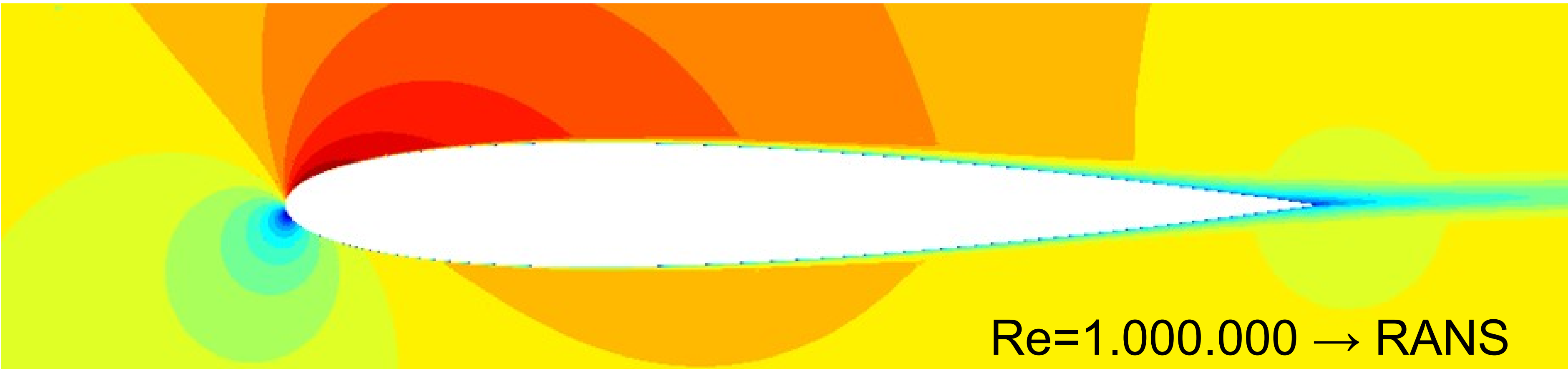

PROD-F-015-01

Cenaero IDIHOM

Paul Tucker – Progress in Aerospace Sciences 47 (2011)
Resolved turbulence (DNS/LES) in turbomachinery CFD ?

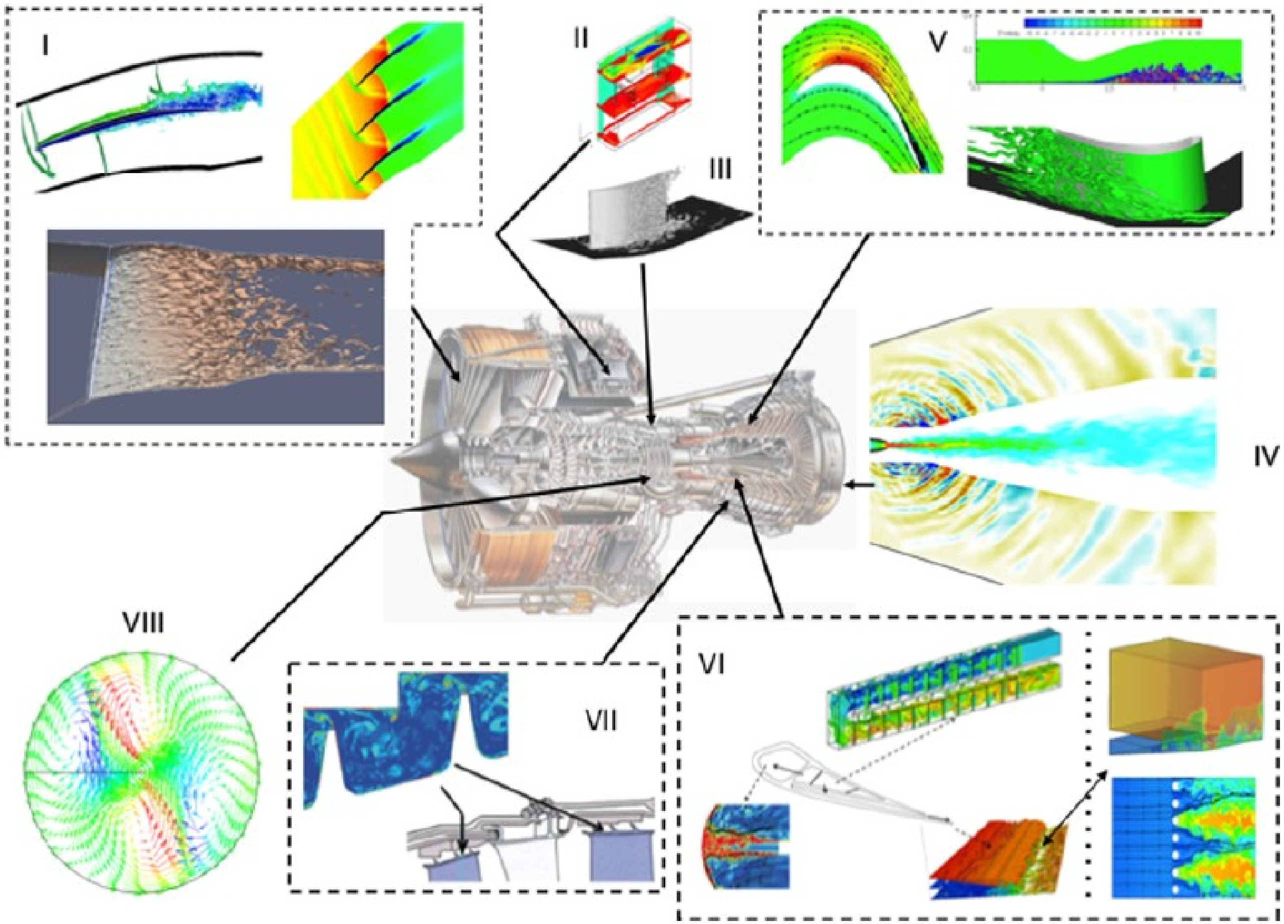

- Only averaged models (RANS) used for design
- Often more resolution (DNS/LES/hybrid RANS-LES) needed

PROD-F-015-01

Cenaero IDIHOM

Scale-resolving computations: not only a question of models, but also discretisation

- Dedicated codes (PSP, FD, …) → fundamental studies, LES model development
  - High accuracy
  - High efficiency
  - Low flexibility
- Industrial grade codes
  - High flexibility
  - High stability
  - Efficiency ?
  - Low accuracy
- New computational cores :
  - High accuracy
  - Flexible mesh
    - Unstructured FEM: DGM/RDS/SDM
    - curved multiblock: CRB, SBS/SAT
  - High parallellisability / CPU efficiency

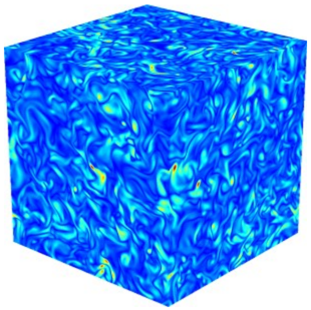

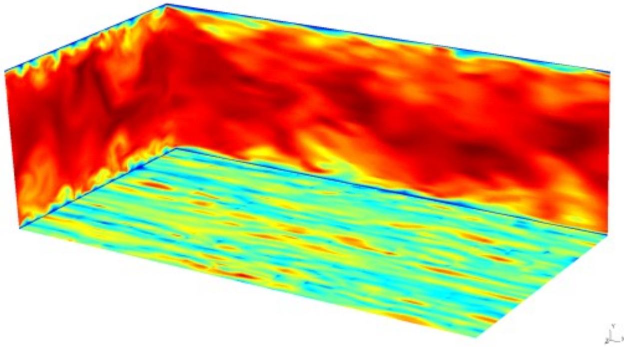

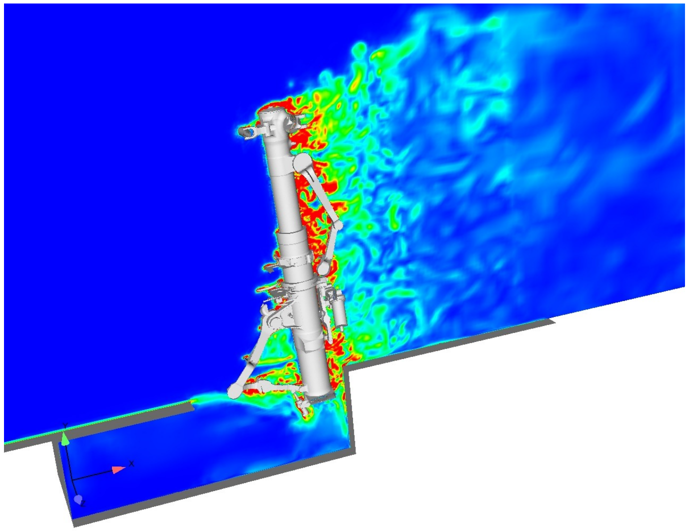

PROD-F-015-01

Cenaero IDIHOM

Paul Tucker – Progress in Aerospace Sciences 47 (2011)

State of the art DNS and LES for turbomachinery flows

"Although LES is, obviously, much less model dependent than RANS, grids currently used for more practical simulations are clearly insufficiently fine for the LES model and numerical schemes not to be playing an excessively strong role."

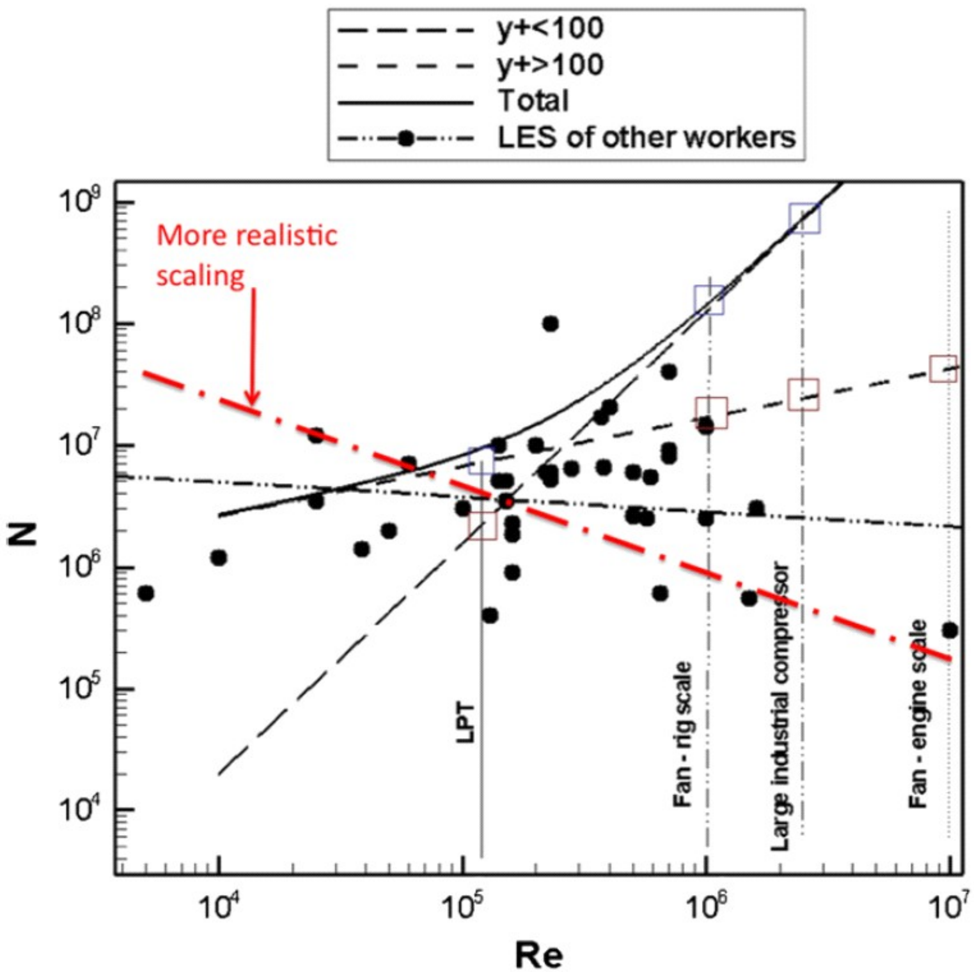

PROD-F-015-01

Cenaero IDIHOM

What are high-order methods ?

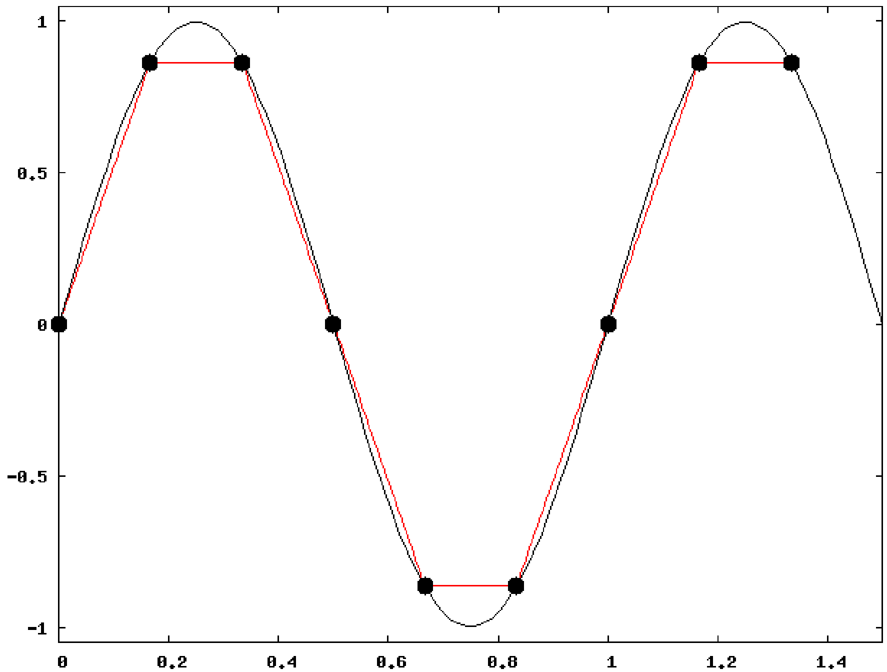

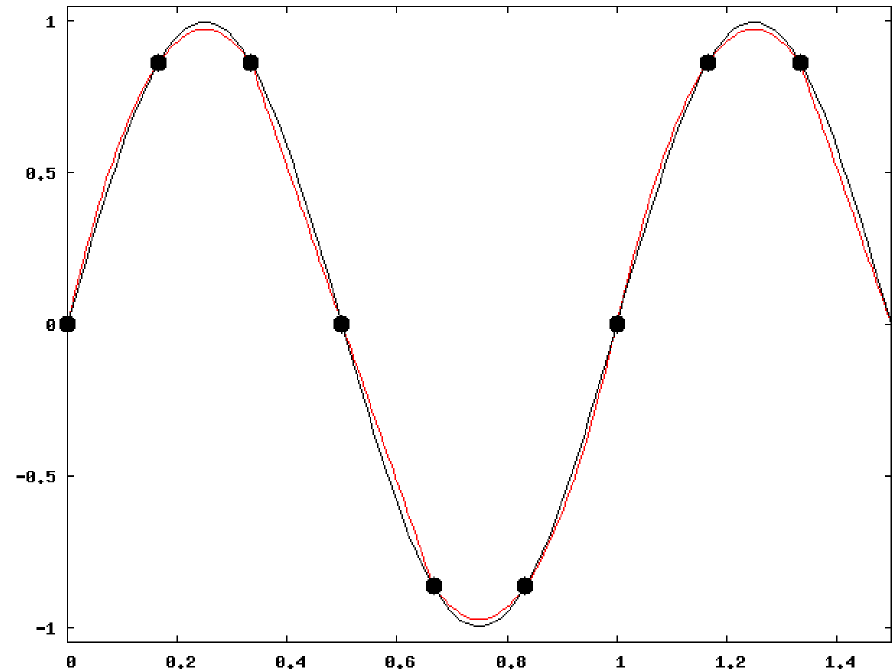

- **Classical : highly structured**
  - **pseudospectral, finite differences**
- **Novel**
  - **Unstructured FEM like: *DGM/SEM/RDS*/SDM**
  - **Unstructured FVM : ENO, WENO, ...**
  - **Flexibilisation of structured mesh: *CRB***

PROD-F-015-01

Cenaero IDIHOM

IDIHOM (FP7) – Industrialisation of High Order Methods
Implementation, calibration, validation on realistic conditions

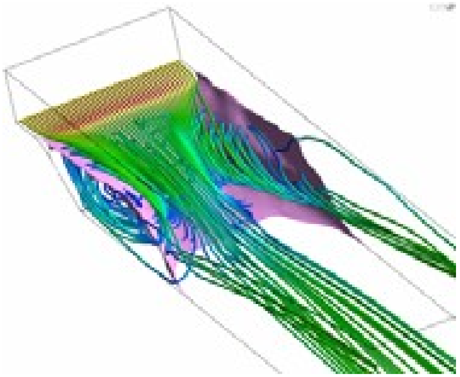

Desider bump, Re=7M, hybrid RANS-LES

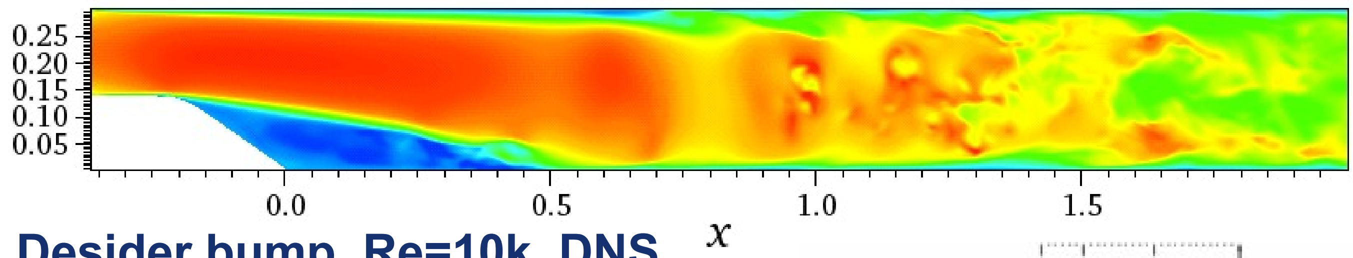

Desider bump, Re=10k, DNS

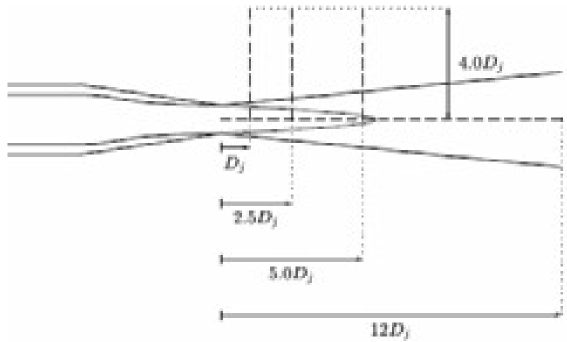

Jean Nozzle, Re=50k, LES

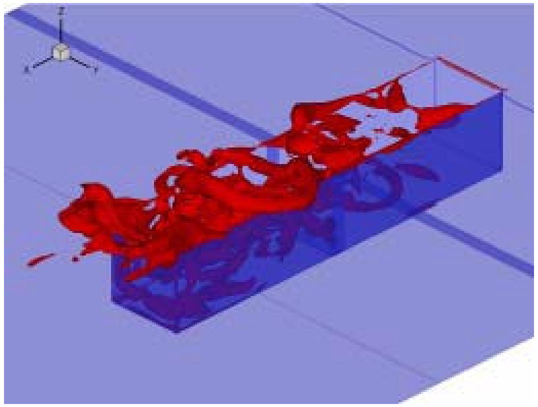

M219 cavity, Re=13M
Hybrid RANS-LES

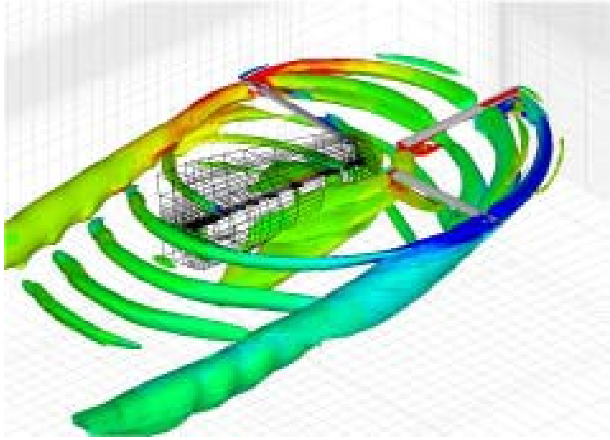

Hart II Rotor, Re=1.8M, hybrid RANS-LES

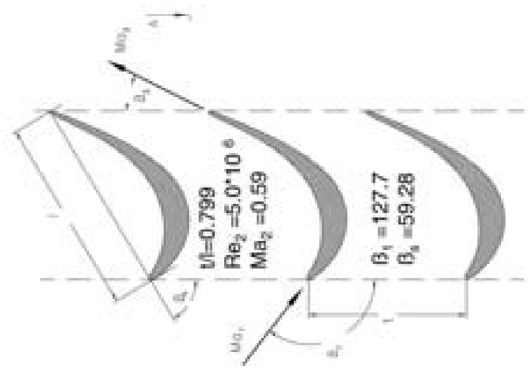

T106A, Re=50-120k, DNS &LES

PROD-F-015-01

Cenaero IDIHOM

Validation on canonical testcases

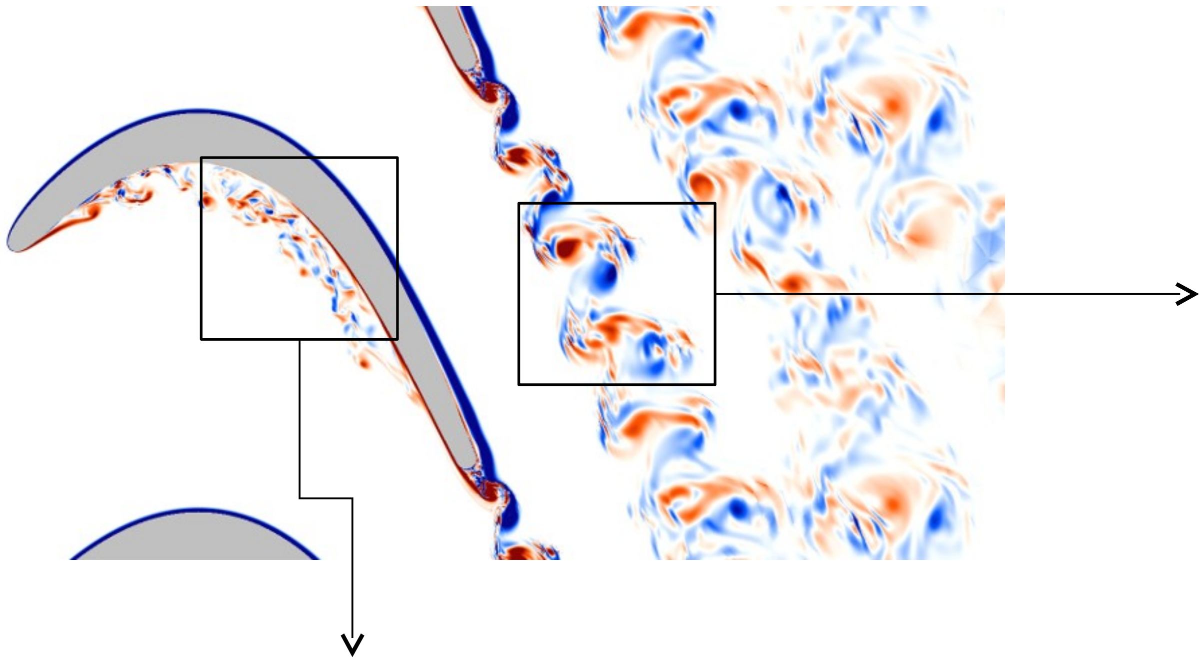

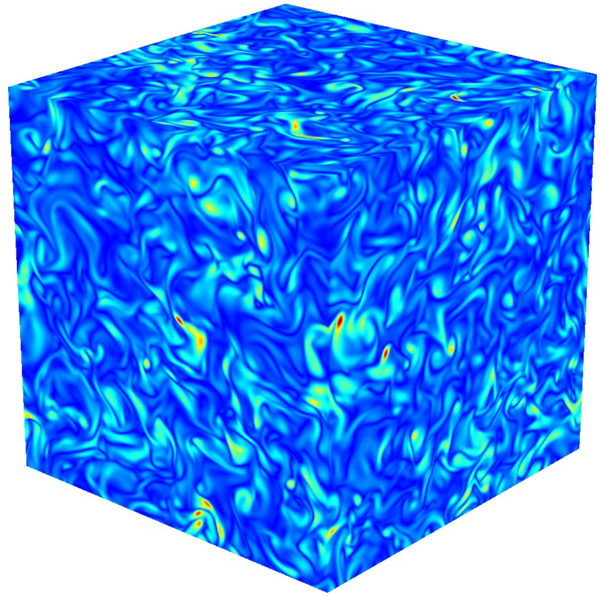

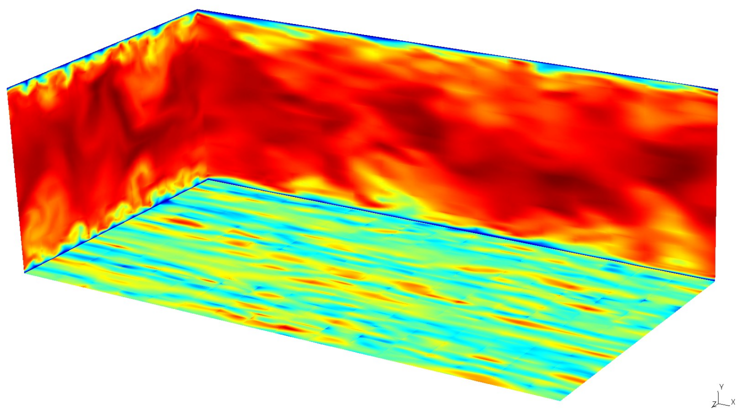

Validation/calibration for :

- **free field turbulence**
- **near-wall turbulence**

PROD-F-015-01

Cenaero

IDIHOM

Basic validation: DNS of Transition and Decay of the Taylor-Green vortex (Re=1600)

Testcase C3.5 1st Intl. Workshop on high order methods for CFD

- Reference: spectral DNS 512^3
- Criterion: dissipation rate

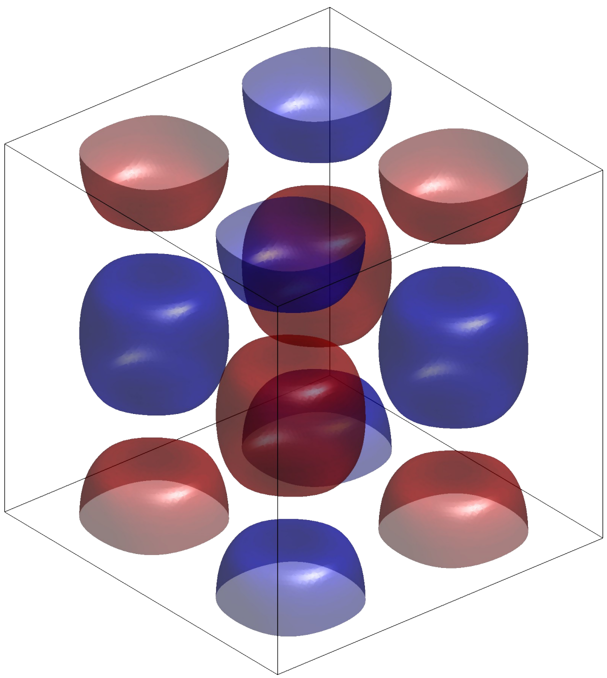

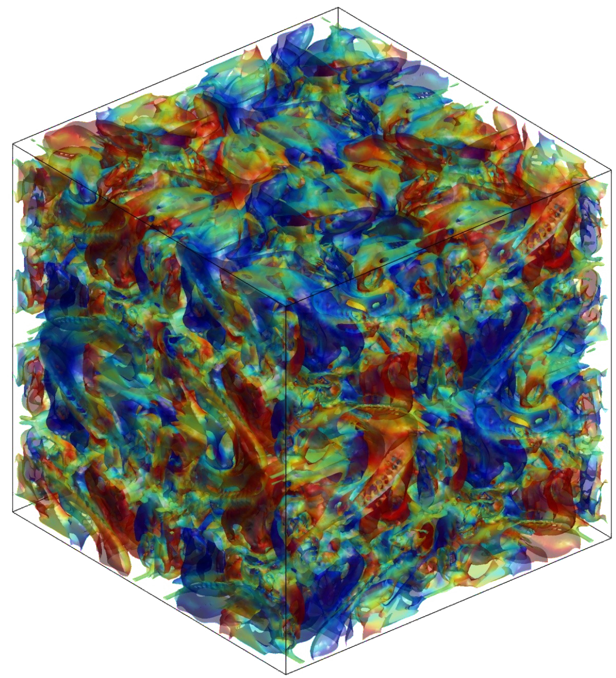

- DGSEM/DGM/FDM/FVM/CPR
- IDIHOM partners: IAG, Onera, Cenaero

PROD-F-015-01

Measured vs theoretical dissipation rate
256x256x256

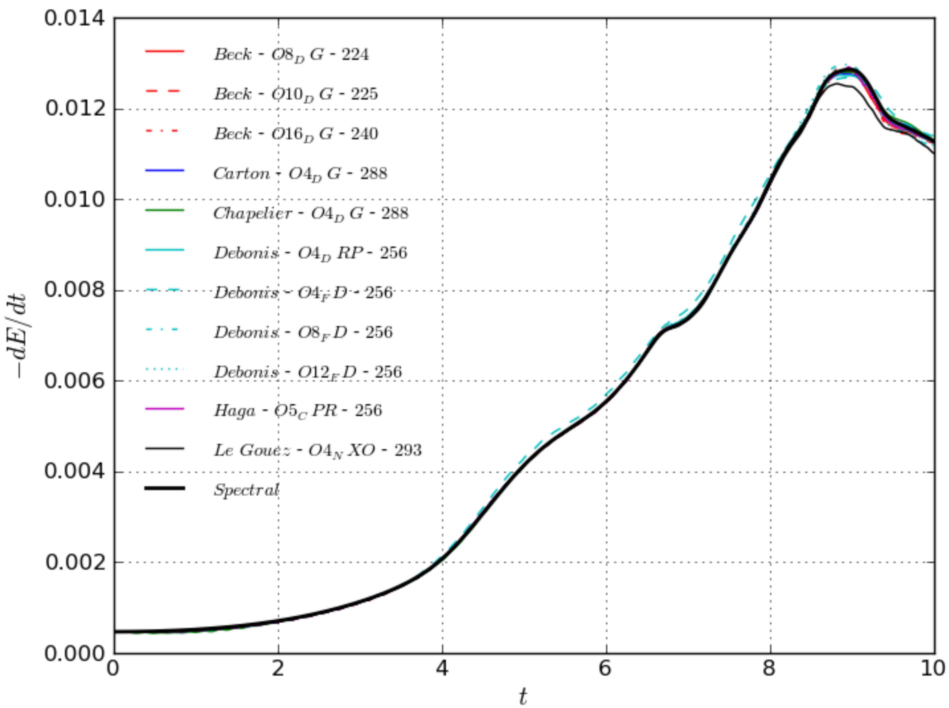

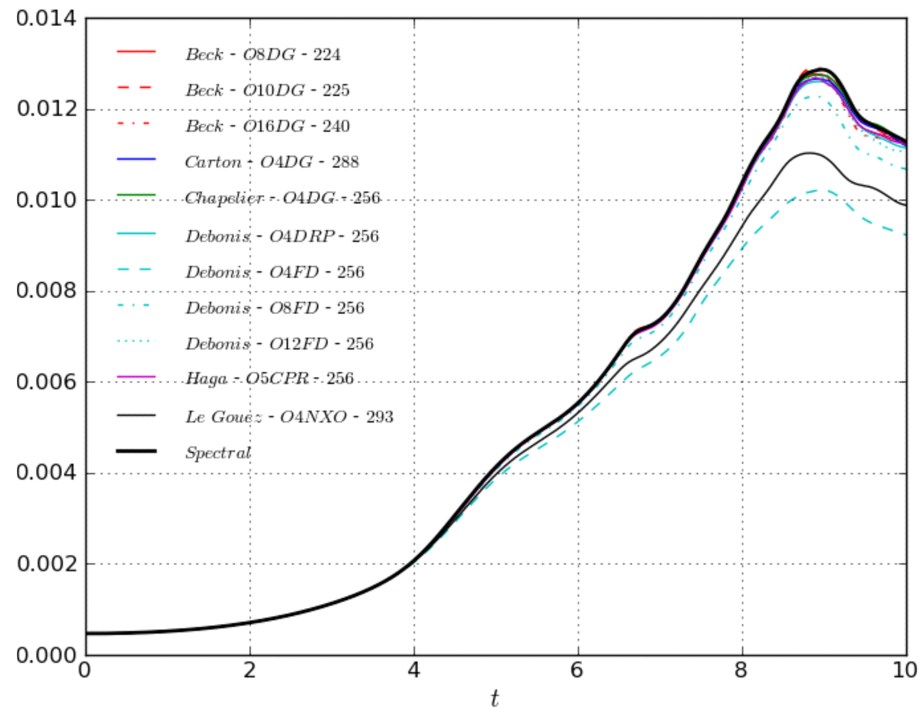

PROD-F-015-01

Taylor-Green vortex: spatial convergence

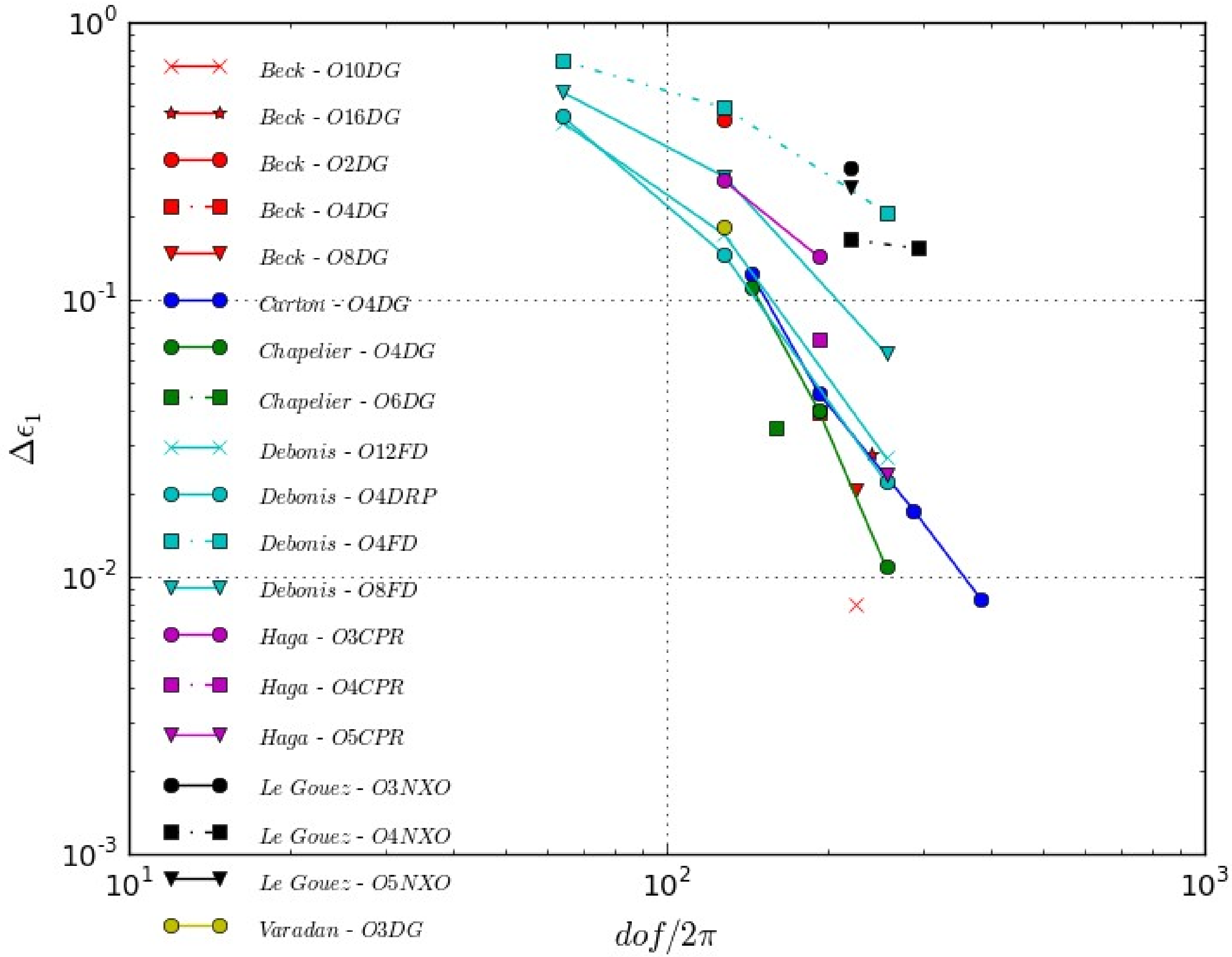

PROD-F-015-01

Cenaero IDIHOM

Importance of dispersion
FD4 vs DGM4 on 256^3

PROD-F-015-01

Cenaero IDIHOM

Typical dissipation and dispersion for high order methods

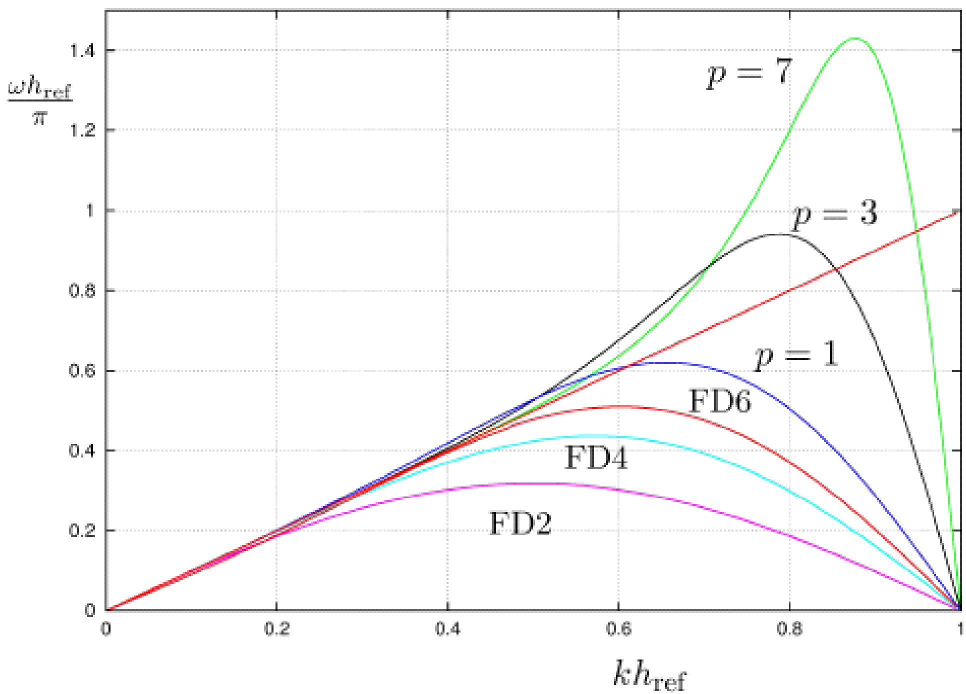

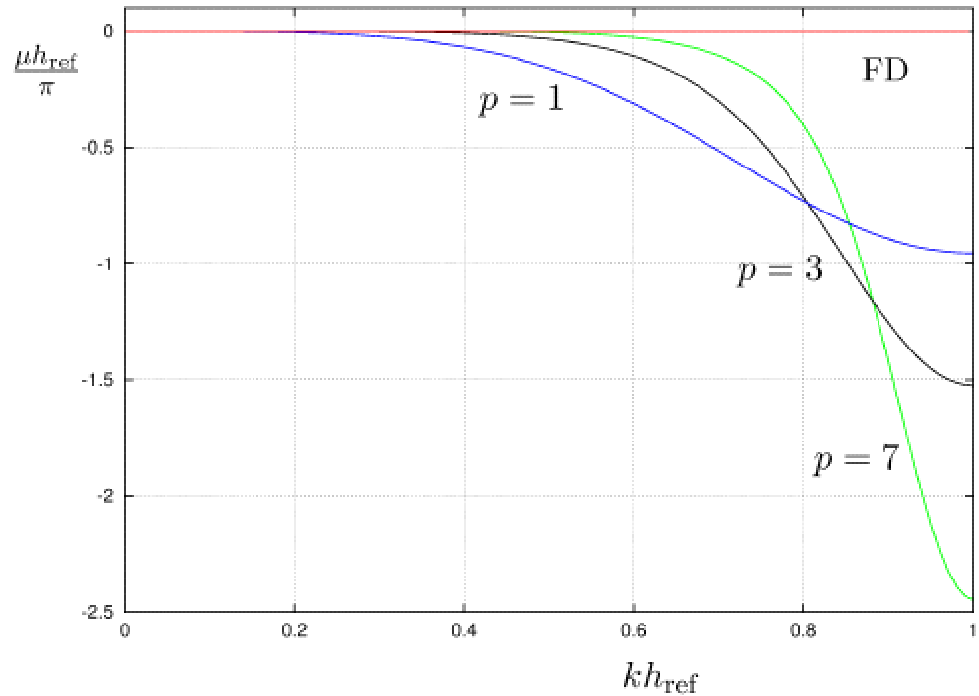

PROD-F-015-01

Cenaero IDIHOM

Taylor-Green vortex: effort convergence

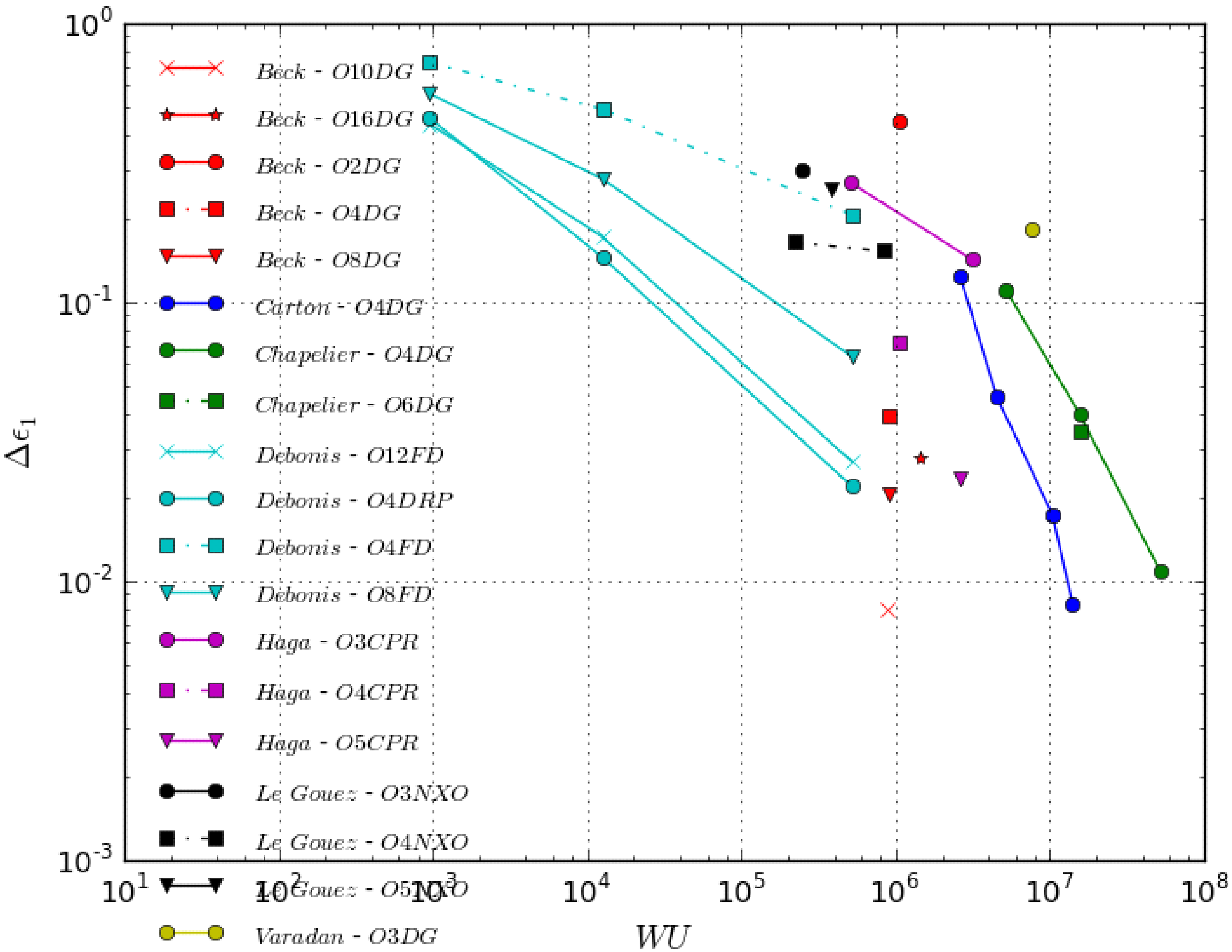

PROD-F-015-01

Cenaero IDIHOM

IAG/DGSEM: mesh vs order convergence
Taylor-Green Re=800

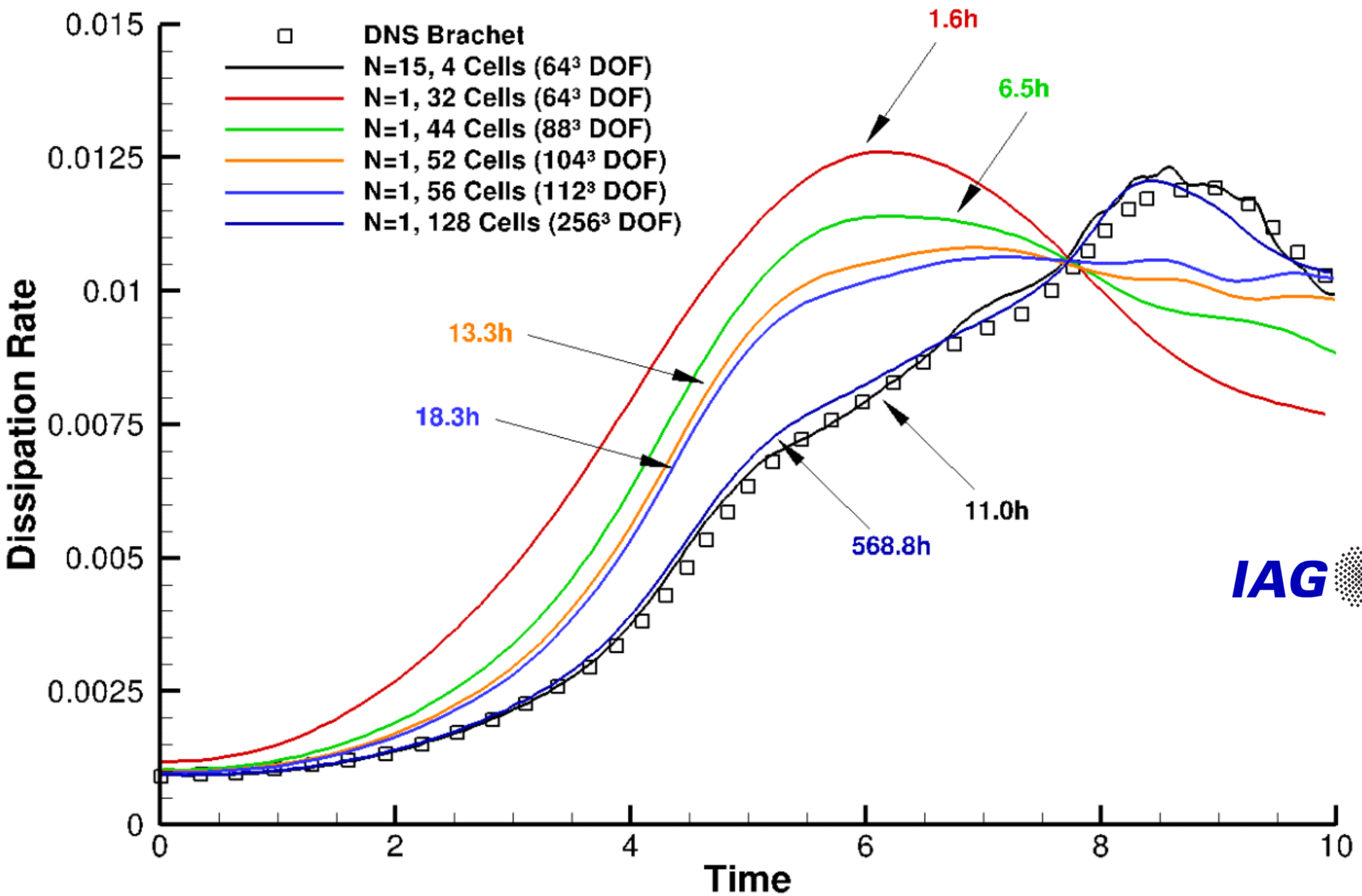

IAG Universität Stuttgart Germany

PROD-F-015-01

Cenaero IDIHOM

Developing subgrid scale models for complex flows

Requirements

- not dedicated
- local
- no tuning

Candidates

- Smagorinski
- WALE
- SVV
- ...
- ILES

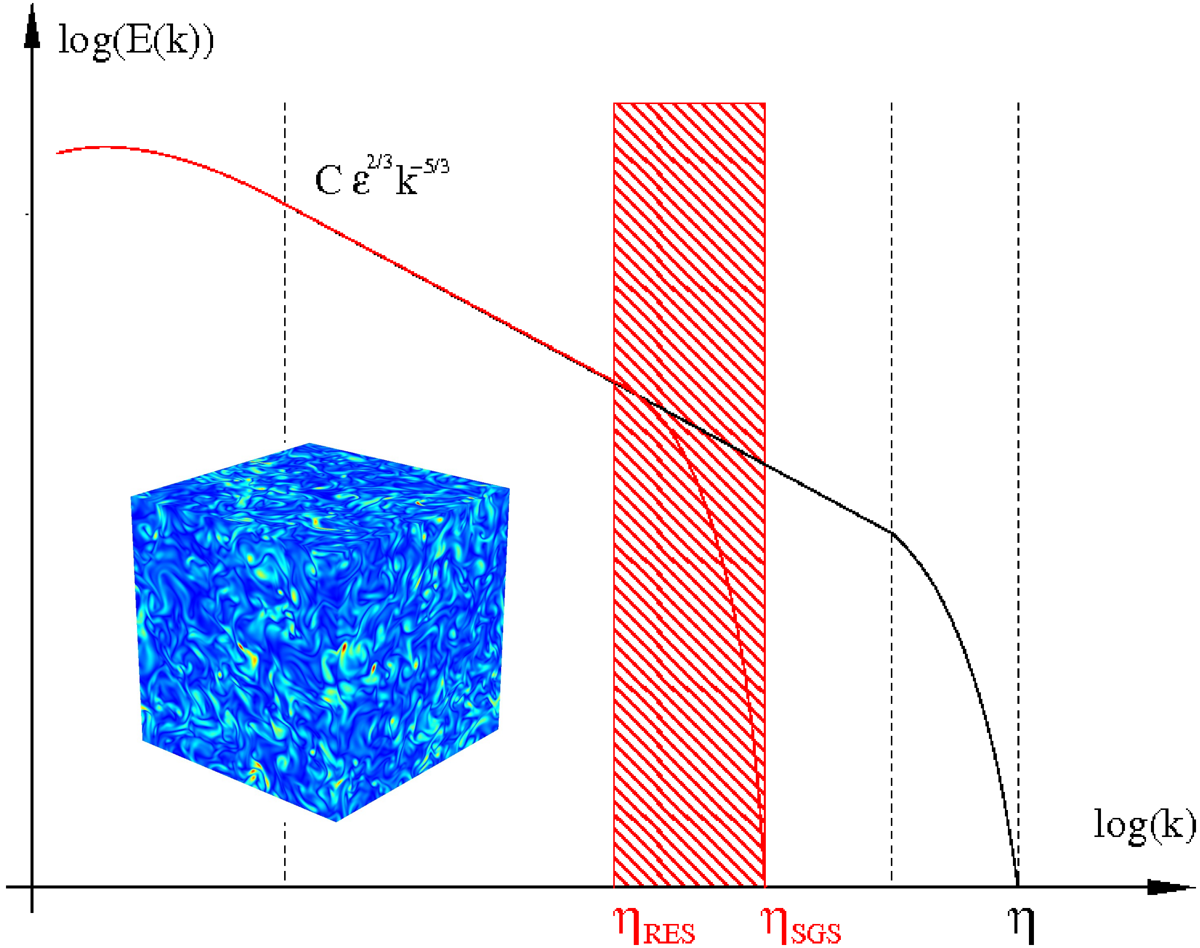

Validation on HIT, channel flow, ...

IAG/DGSEM: underresolved computations

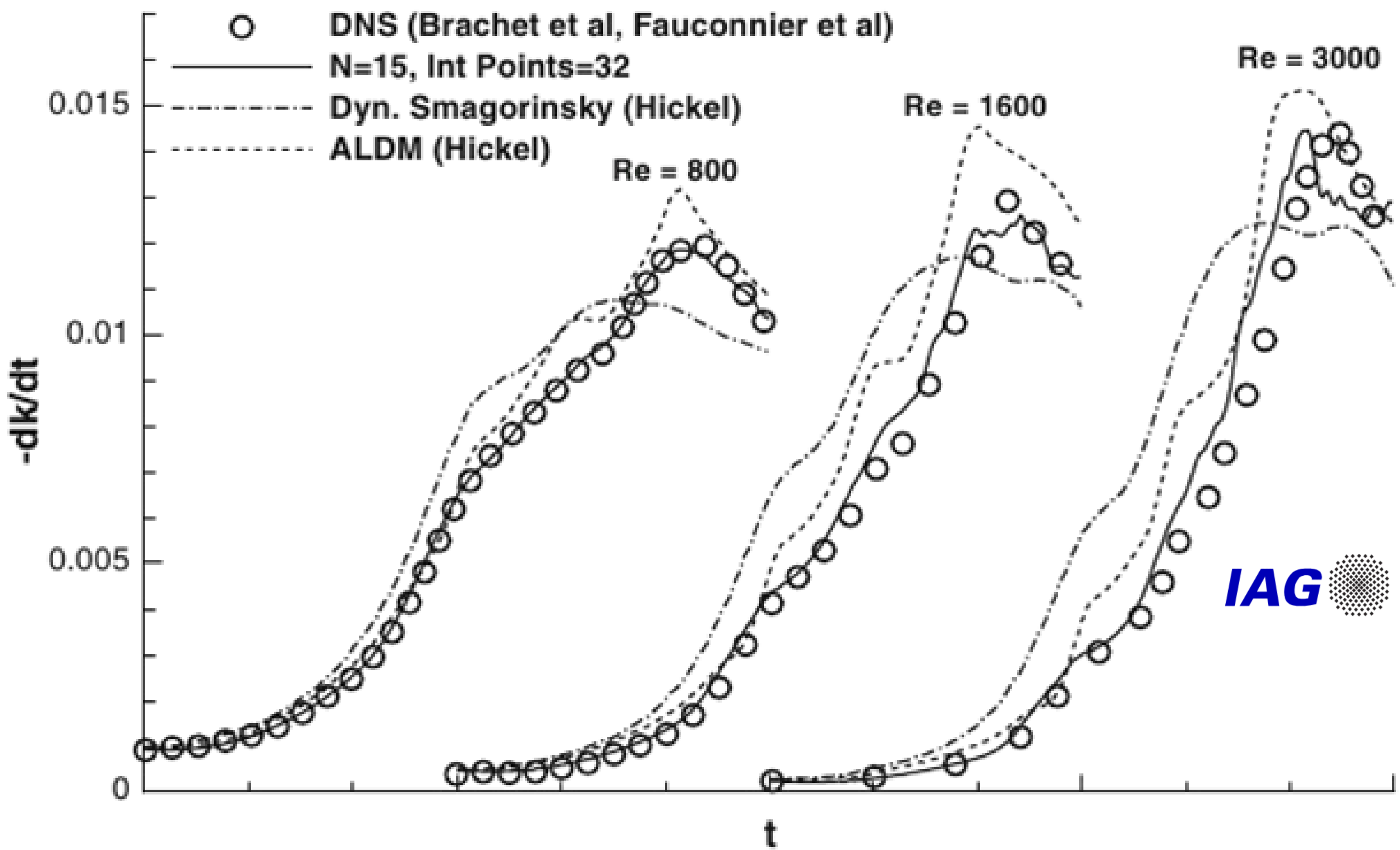

IAG Universität Stuttgart Germany

PROD-F-015-01

Cenaero IDIHOM

Practical example: transitional flow on airfoil

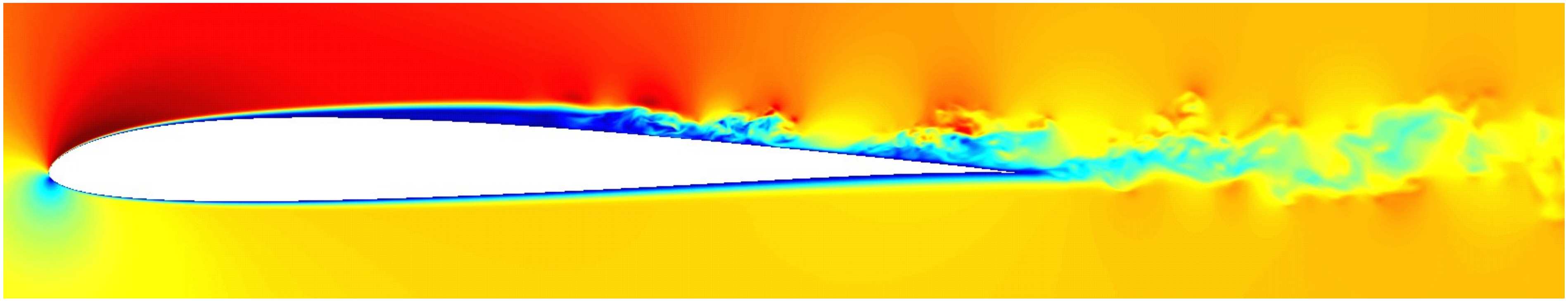

- SD7003 Re=60.000, AoA=4°
- Testcase C3.3 Intl. Workshop on HOM for CFD
- DNS vs ILES with DGM

PROD-F-015-01

DNS vs ILES on SD7003 airfoil – Re=60k mesh resolution

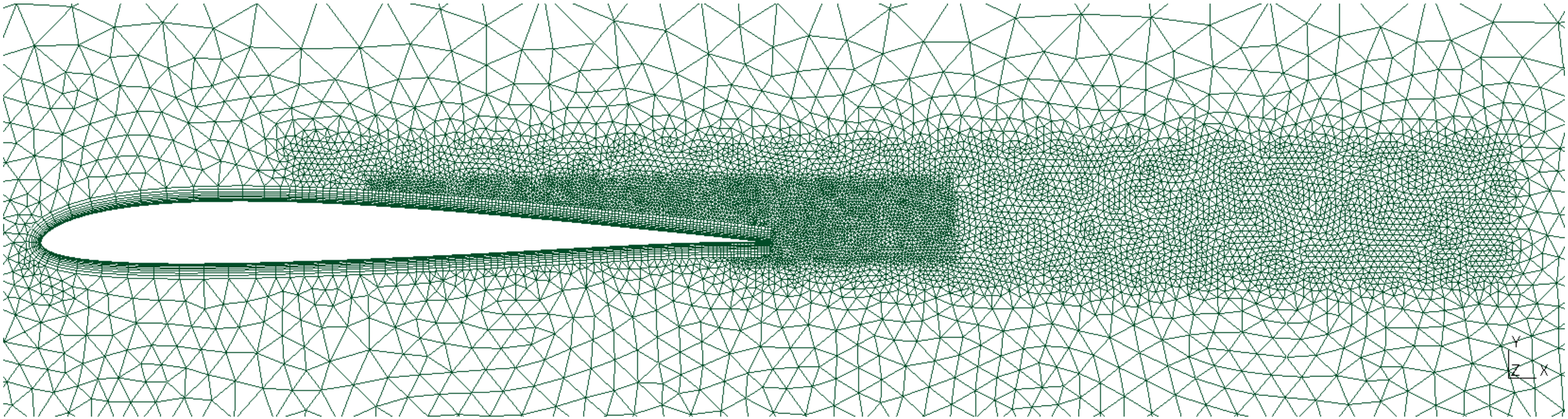

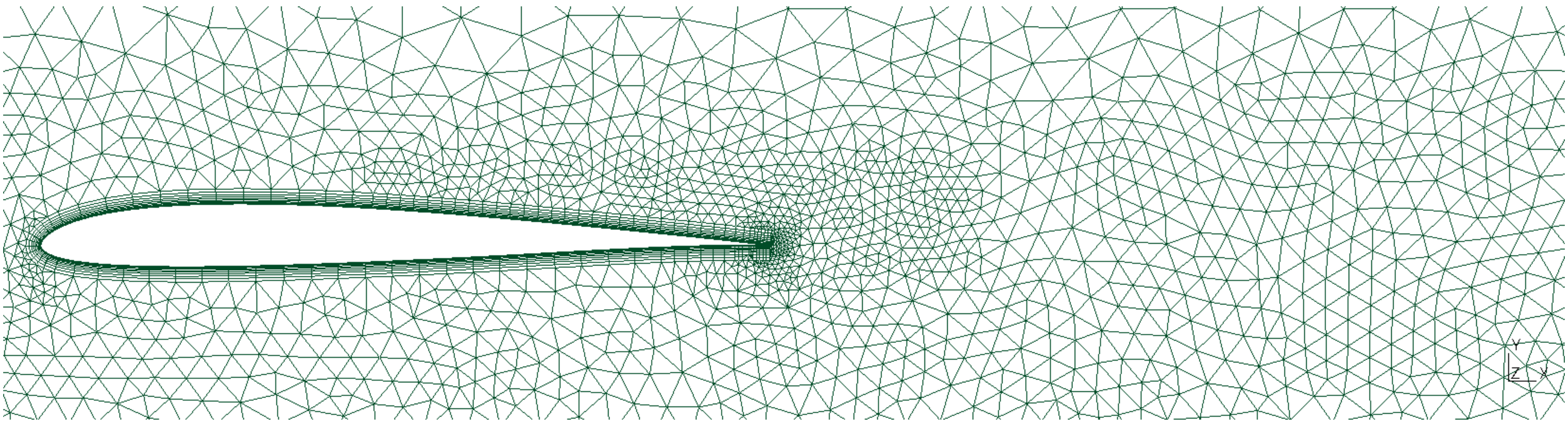

PROD-F-015-01

Cenaero IDIHOM

DNS vs ILES on SD7003 – Re=60k
Vortical structures in cut

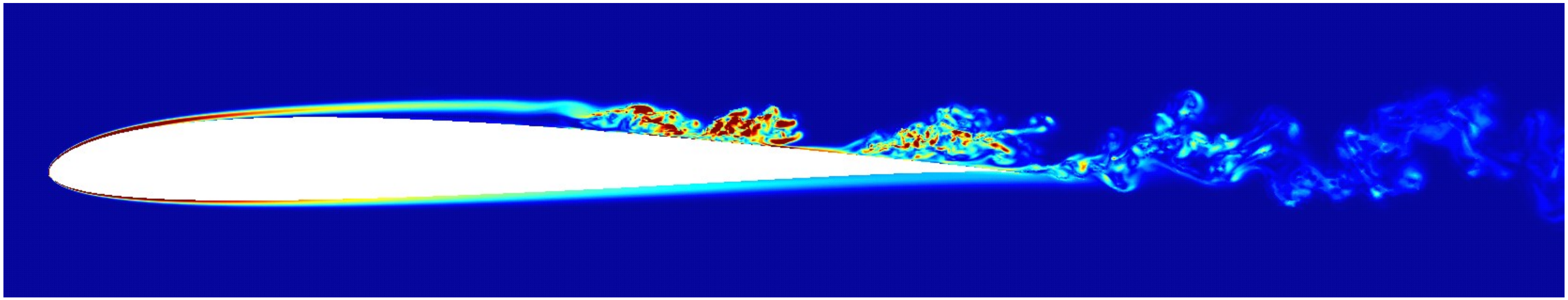

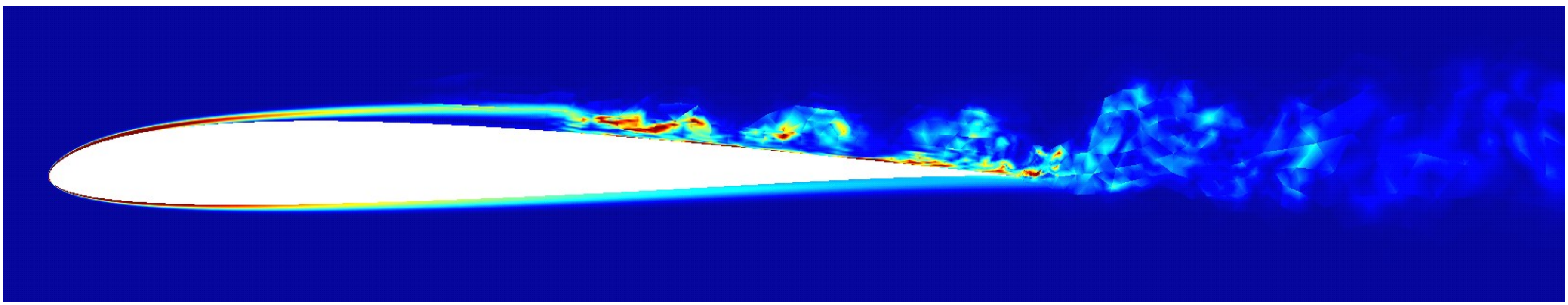

PROD-F-015-01

Cenaero IDIHOM

DNS vs ILES on SD7003 – Re=60k
Skin friction

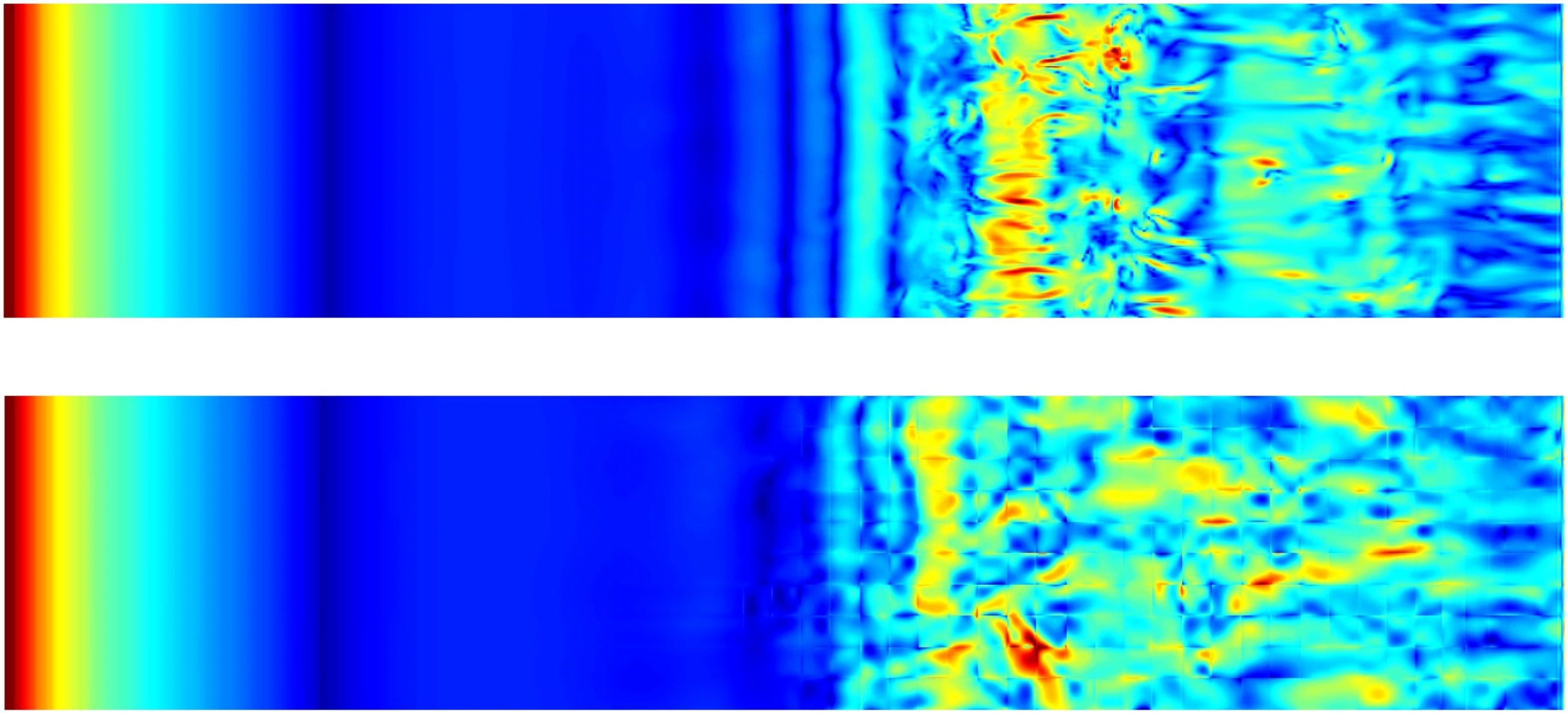

PROD-F-015-01

DNS vs ILES
SD7003 airfoil

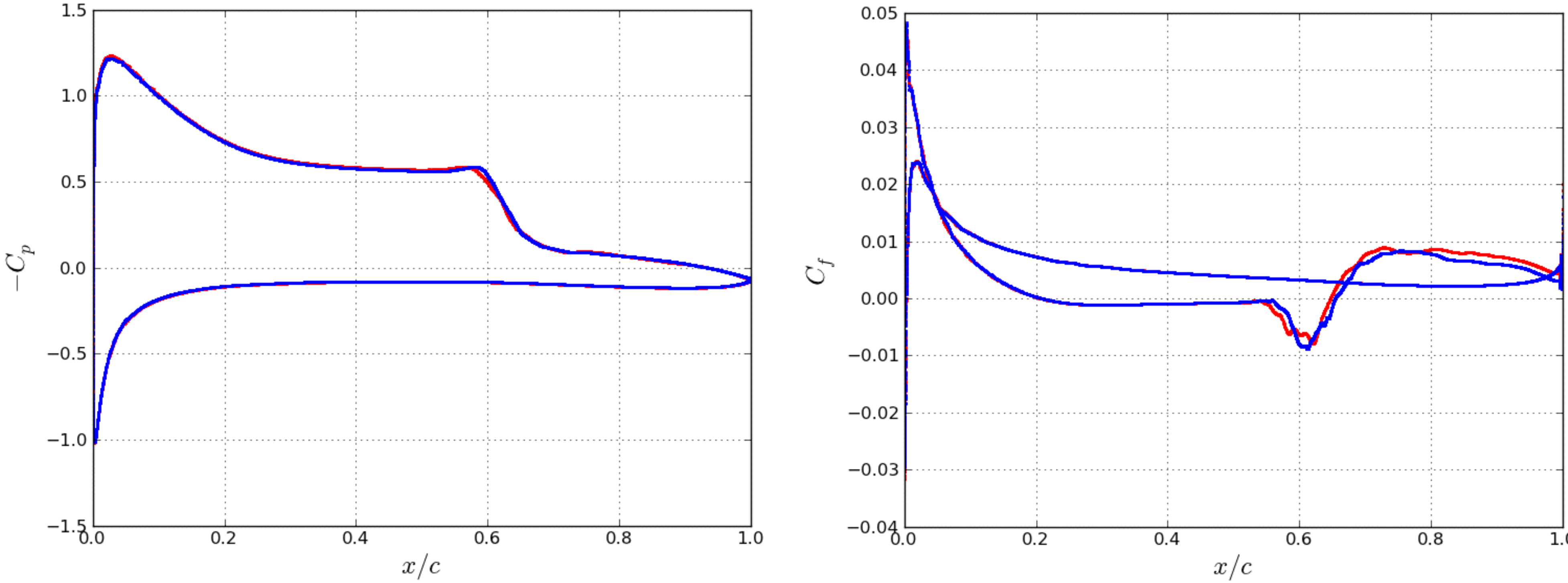

PROD-F-015-01

Same L&D for 10 times less CPU, *no explicit model*

Cenaero IDIHOM

NoFUDGE: DNS LP Turbine (M_2=0.6, Re_2=85,000)

PRACE industrial pilot "noFUDGE" - ASME GT2012-68900

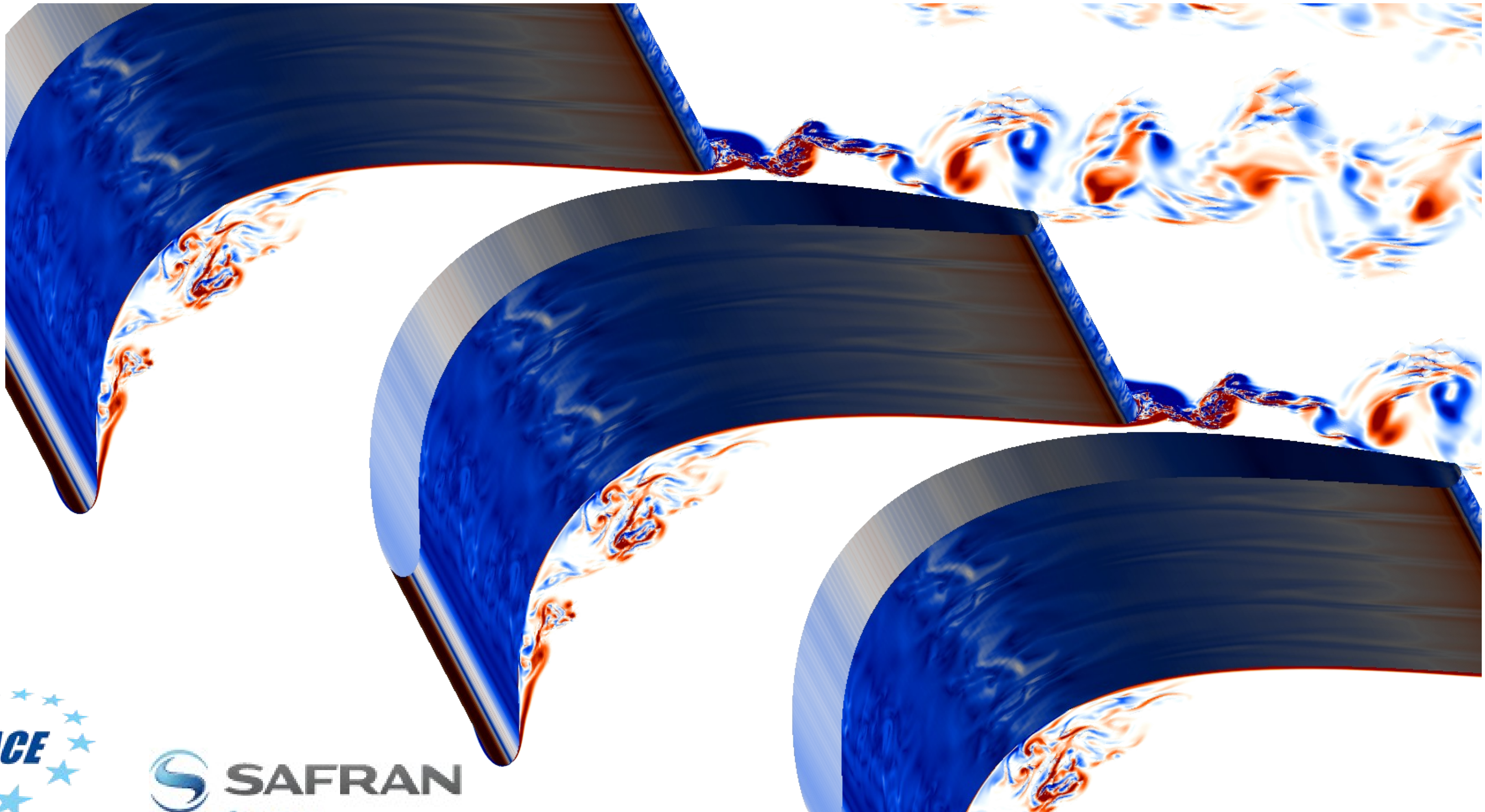

PROD-F-015-01

PRACE

SAFRAN Snecma

Cenaero

IDIHOM

Total Pressure in the Wake

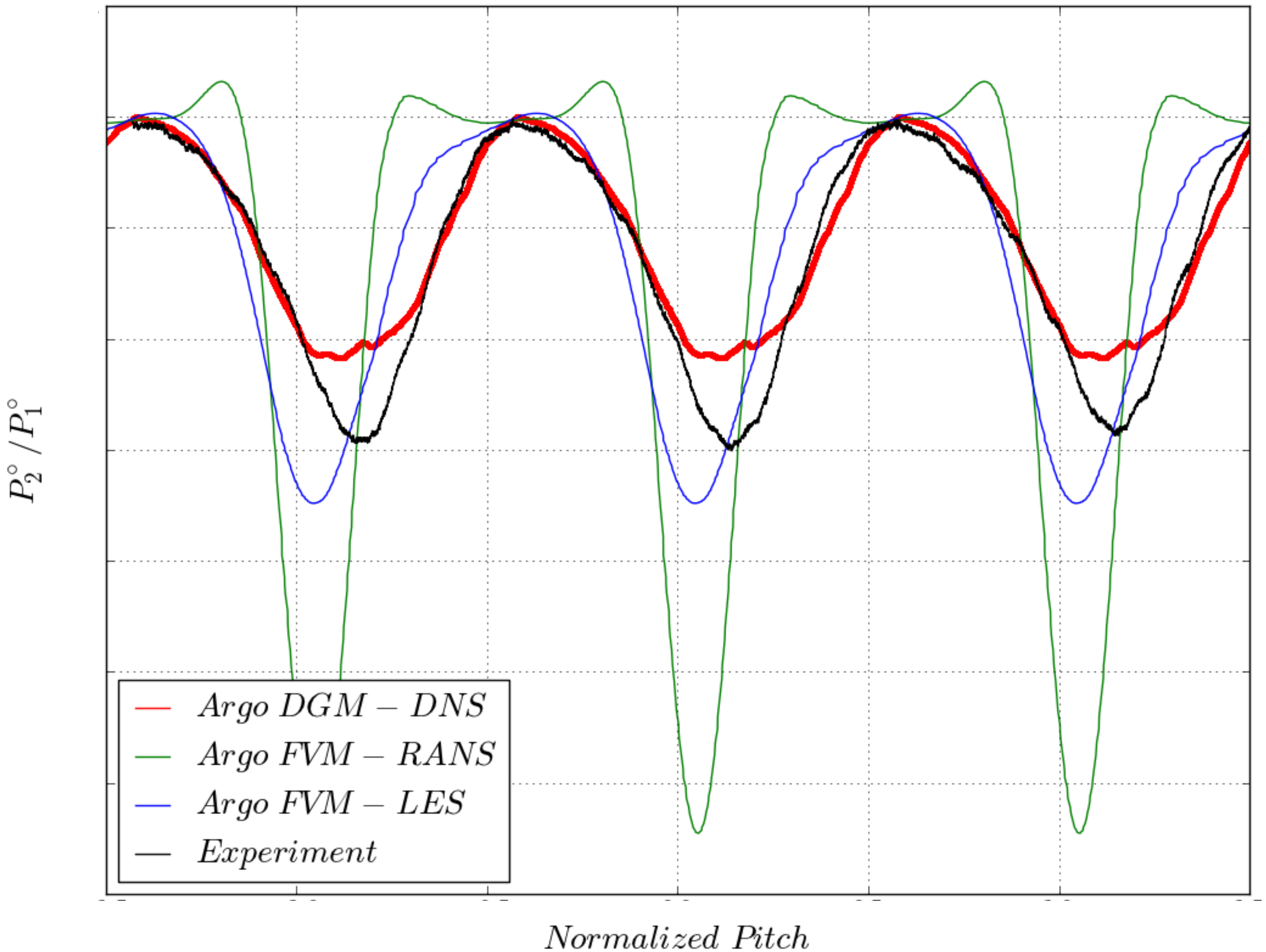

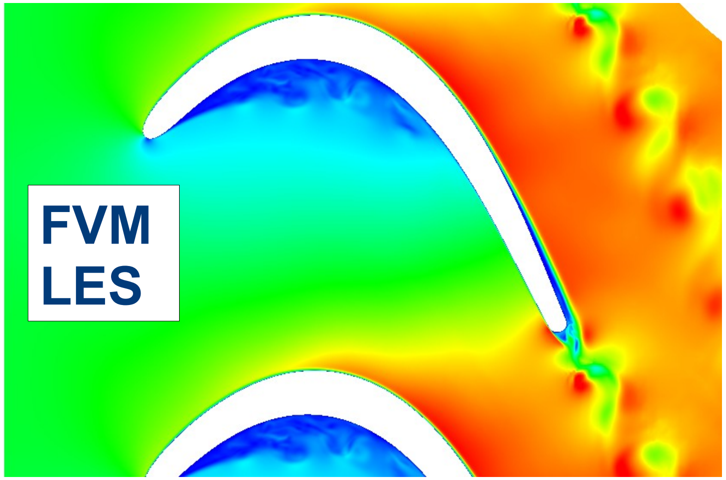

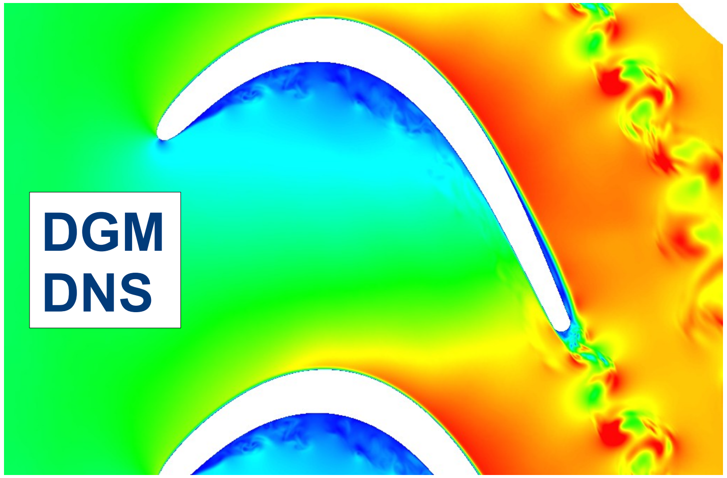

Cenaero IDIHOM

FVM (KE-scheme) Mesh vs DGM (Cubic Polynomial) Mesh

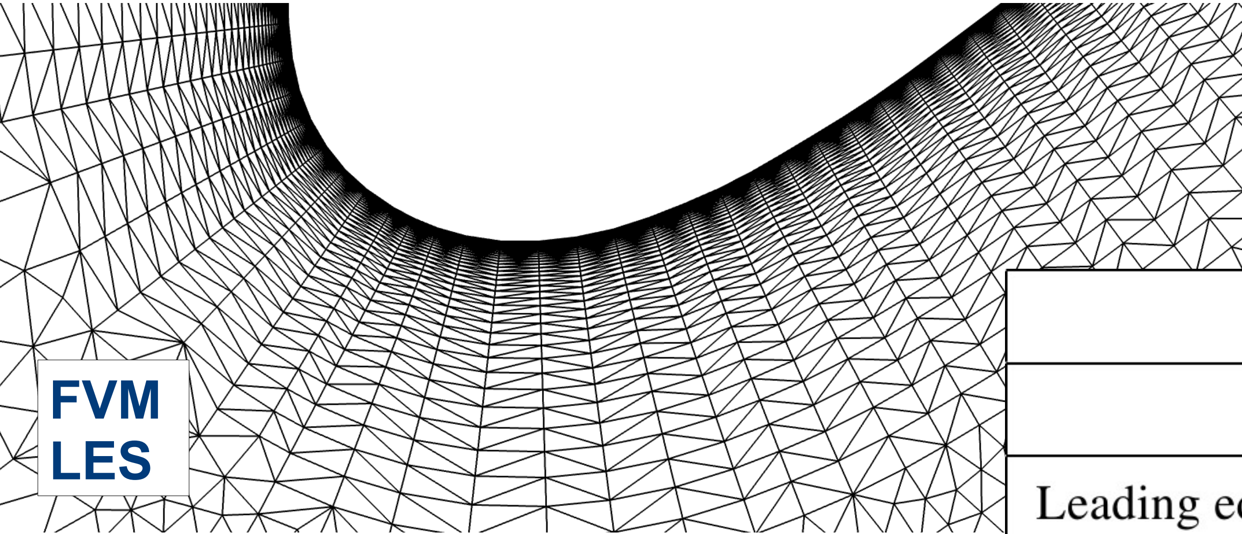

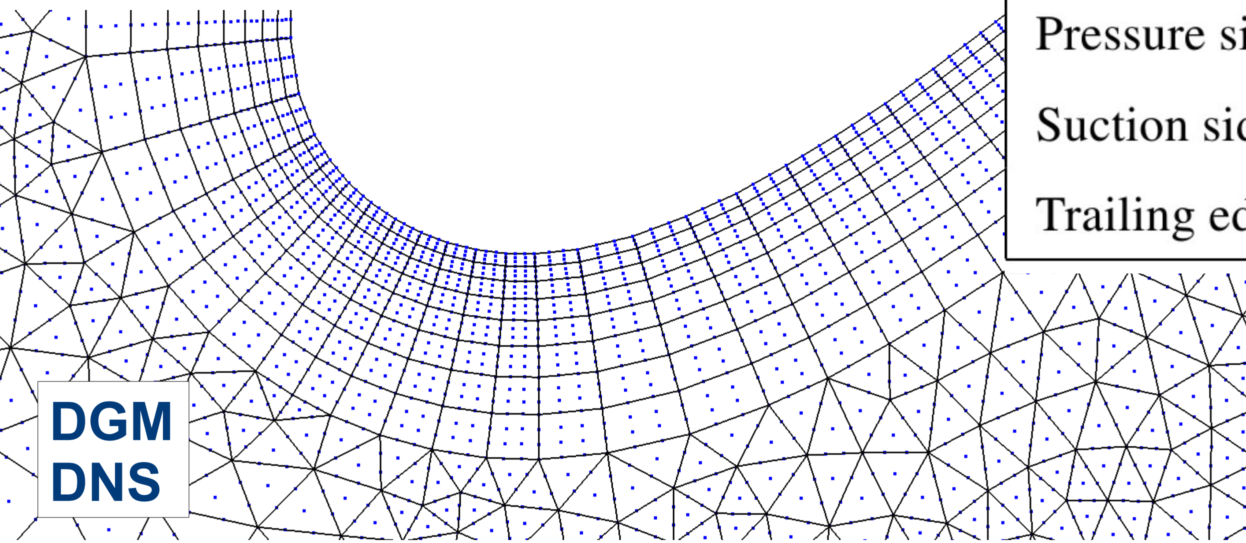

	FVM		DGM		
	$x^+ = z^+$	y^+	x^+	z^+	y^+
Leading edge	35	0.5	15	30	3
Pressure side	5	0.1	3	3	0.3
Suction side	50	0.3	15	15	1.5
Trailing edge	10	0.3	2	10	1

8.5M dof/variable FVM LES
15M dof/variable DGM DNS

(Rough) Cost Estimate (FVM on Intel; DGM on BlueGene/P)

	FVM LES	DGM DNS
Order of accuracy	2	4
# dof / variable (M dof)	8.5	15
CPU time for one t_c (kCPUh)	11	112
Memory per core (MB)	700	500
Number of cores	256	4096
CPU time / # dof	0.0013	0.0075
Memory / # dof	0.02	0.036

- **Intel ~ 4 times faster than BlueGene/P**
- **DGM 40% more expensive in equivalent CPU / dof**
- **But, DGM more accurate, more stable and less dissipative**

PROD-F-015-01

Cenaero IDIHOM

HOM enabling technology?

- Resolution obtained on complex(er) geometry
  - Fully unstructured methods ~ FEM (DGM/RDS)
  - Flexibilisation of structured HOM (FDM, CRB)
- Dissipation not as problematic as for low order FVM
  - Dissipation HOM only for high-frequency content ~ ILES
  - Dispersion becomes dominant error
- DGM already used for industrial DNS
  - Jet flows (IAG): gas injector acoustics
  - Transitional flows (Cenaero): LP turbines, low Re/laminar wing
- Subgrid scale modeling in development
  - Current research : both ILES and explicit SGS
  - VMS filters easy to implement in discontinuous methods
- Resolution and adaptation
  - discontinuous interpolation : resolution check for DNS
  - Order convergence much faster than resolution
  - FEM : flexibility (non-conforming, order adaptation)
- Efficient exploitation of HPC infrastructure

PROD-F-015-01

Cenaero IDIHOM

Concluding remarks

- Industrial need for resolved turbulence in complement to and verification of RANS
  - Transitional flows
  - Bluff body flows and maneuvering
  - Vortex blade interaction
  - Instabilities, partial regimes in turbomachines
  - Acoustics
  - …
- Increased availability of HPC (PRACE)
- HOM and turbulence modeling $\rightarrow$ FP8 ?
- High-order workshop in Cologne, 24-25 april
  - 2D periodic hill from ERCOFTAC QNET CFD
  - DNS transitional LP turbine blade ?

Clean Sky major technologies and demonstrators in flight physics and propulsion

Giuseppe Pagnano,

Clean Sky Coordinating Project Officer

2nd EASN Workshop on Flight Physics & Propulsion

Prague, 01 November 2012

www.cleansky.eu

outline

- Introduction: ACARE, FP7, JTI
- Clean Sky: structure, ITDs, budget, JU
- Achievements; Technology Evaluator
- Calls for proposals: academia participation
- Way forward in H2020
- Concluding remarks

JTI in FP7

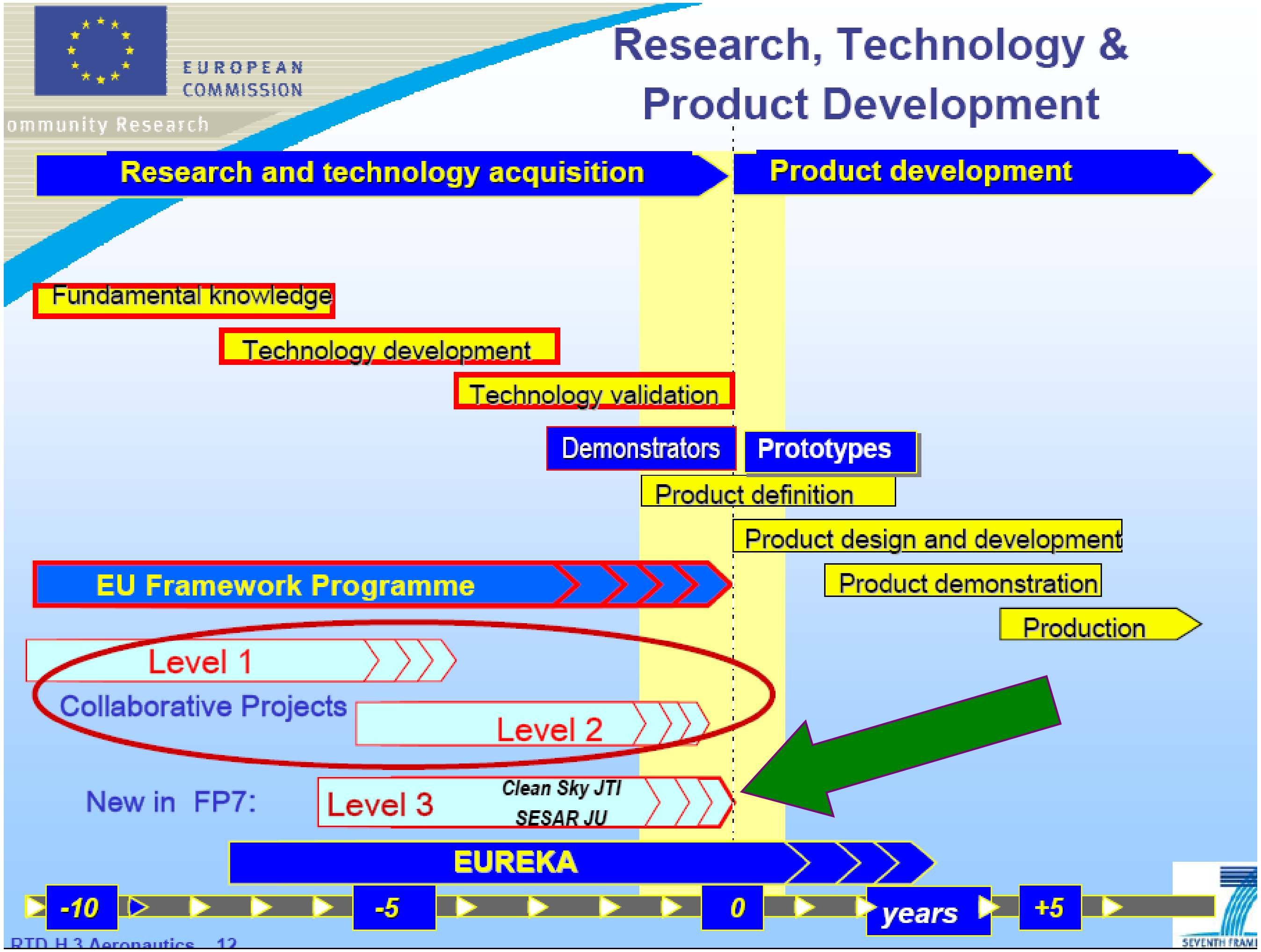

Level 3: closer to the market research, based on demonstrators of high technology readiness levels

ACARE Goals

Vision 2020 (January 2001)
- **To meet Society's needs**
- **To achieve global leadership for Europe**

ACARE
October 2002 : The Strategic Research Agenda (SRA) → 5 Challenges

Quality and Affordability	Environment	Safety	Air Transport System Efficiency	Security

October 2004 : The SRA 2 → High level Target Concepts

Very Low Cost ATS	Ultra Green ATS	Highly Customer oriented ATS	Highly time-efficient ATS	Ultra Secure ATS	22nd Century

80% cut in NOx emissions
Halving perceived aircraft noise
50% cut in CO_2 emissions per pass-Km by drastic fuel consumption reduction
A green design, manufacturing, maintenance and disposal product life cycle

In Flightpath 2050:
NOx 90%;
Noise 65%;
CO_2 75%

ACARE: Advisory Council for Aviation Research (and Innovation) in Europe

Reaching the ACARE Goals

	ACARE goals	Technology Domains
50%CO2 80% NOx	Reduced Fuel Consumption (CO_2 & NOx reduction)	➢ Engines ➢ Loads & Flow Control ➢ New Aircraft Configurations ➢ Low Weight Configurations ➢ Aircraft Energy Management ➢ Mission Management
50% noise	External noise reduction	➢ Engines ➢ Trajectory Management ➢ New Aircraft Configurations ➢ Low noise Configurations ➢ Rotorcraft Noise Reduction ➢ Rotorcraft optimised configuration
Green design..	« Ecolonomic » life cycle	➢ Aircraft Life Cycle

Clean Sky Integrated Technology Demonstrators (ITD)

Smart Fixed Wing Aircraft	
	Airbus (F, D, UK, E)
	SAAB (SE)
Green Regional Aircraft	
	Alenia Aeronautica (I)
	EADS CASA (E)
Green Rotorcraft	
	AgustaWestland (I, UK)
	Eurocopter (F, D)
Sustainable and Green Engines	
	Rolls-Royce (UK, D)
	Safran (F)
Systems for Green Operation	
	Thales (F)
	Liebherr (D)
Ecodesign	
	Dassault Aviation (F)
	Fraunhofer Gesellschaft (D)

Technology Evaluator
Thales
DLR

SESAR JOINT UNDERTAKING

Split of the EC Contribution

Maximum Overall EC Contribution:
800 M€

Members
(max. 600 M€ i.e. 75%)

ITD Leaders
(max 400 M€ i.e. 50%)

match EC contribution 50% (in-kind)

Associates
(max 200 M€ i.e. 25%)

match EC contribution 50% (in-kind)

Partners
(min 200 M€ i.e.25%)

Call for Proposals

The Clean Sky Joint Technology initiative

It is a **Public-Private Partnership** between Commission and Industry implementing the Level 3 project approach of FP7

Starting date: 02/2008

Multi-year research project on Greening of Aeronautics: 2008-2015

Total budget 1.6 billion €

- **800 million € from Commission in-cash**
- 800 million € from industry in-kind

Since Nov 2009 an independent legal entity (the Clean Sky Joint Undertaking), with own staff of 24, placing the contracts / grant agreements and coordinating the programme

Concept Aircraft – assessing the environmental benefits

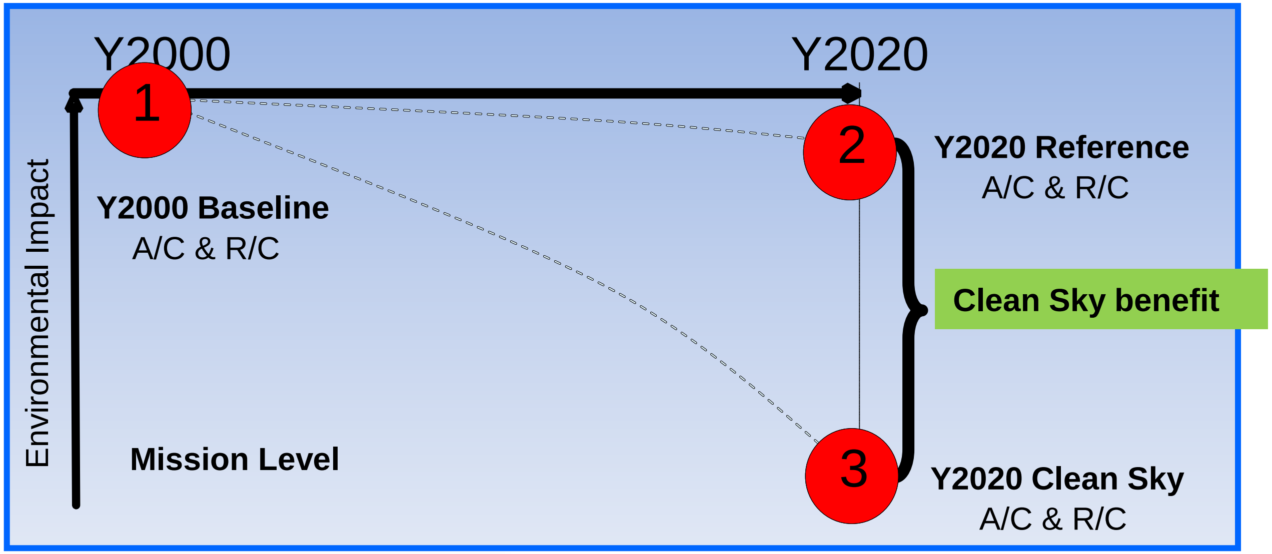

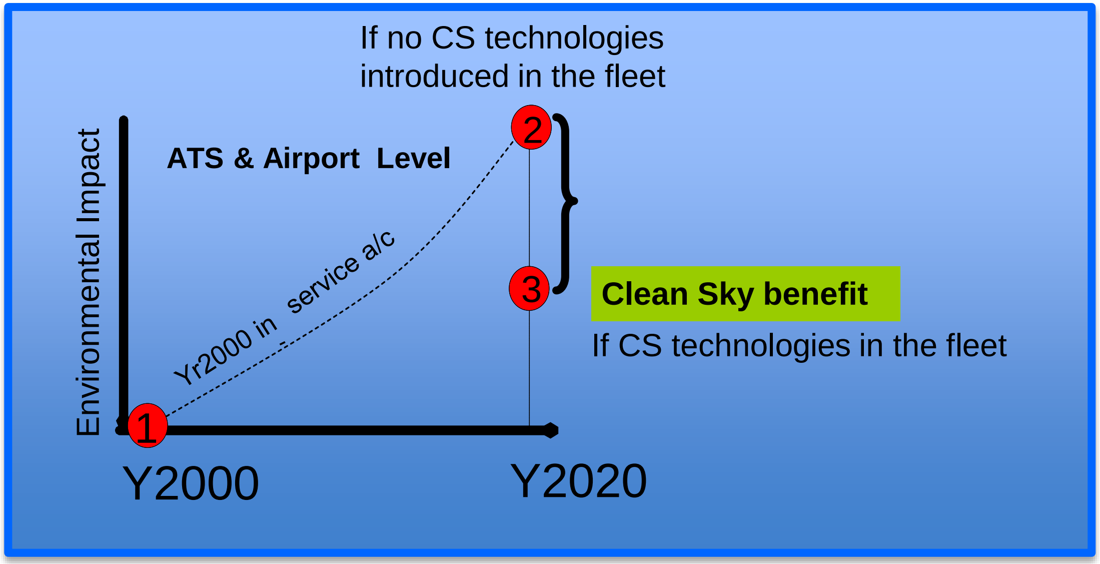

Integrating the technologies and enabling the assessment

- at aircraft (mission) level
- at airport level
- at air transport system level

TE: Results of the 1st evaluation

First Clean Sky Technology Evaluation

Game-changing potential advances in environmental performance (re-)confirmed compared to equivalent Y2000 aircraft

1. SMR aircraft with open rotor engines and laminar-flow wing technology could deliver **up to 30% better fuel efficiency** and related CO_2 emissions reductions.
2. Next-generation **Regional aircraft** for 90–130 passengers show similar potential - against today's best in-service aircraft.
3. Important **reductions in noise** in business aviation and rotorcraft operations.
4. Clean Sky has successfully implemented a unique Technology Evaluation process involving robust and independent analysis of performance gains and extensive simulation of aircraft in airport and air transport system level scenarios.

SFWA: major demonstrators

Input interfacing with:

SAGE ITD – **CROR engine**

SGO – **Systems for Green Operation**

Innovative Powerplant Integration

- **Technology Integration**
- **Large Scale Flight Demonstration**
  - Impact of airframe flow field on Propeller design (acoustic, aerodynamic, vibration)
  - Impact of **open rotor** configuration on airframe (Certification capabilities, structure, vibrations...)
  - Innovative empennage design

Smart Wing Technologies

- **Technology Development**
- **Technology Integration**
- **Large Scale Flight Demonstration**
  - **Natural Laminar Flow (NLF)**
  - Hybrid Laminar Flow (HLF)
  - Active and passive load control
  - Novel enabling materials
  - Innovative manufacturing scheme

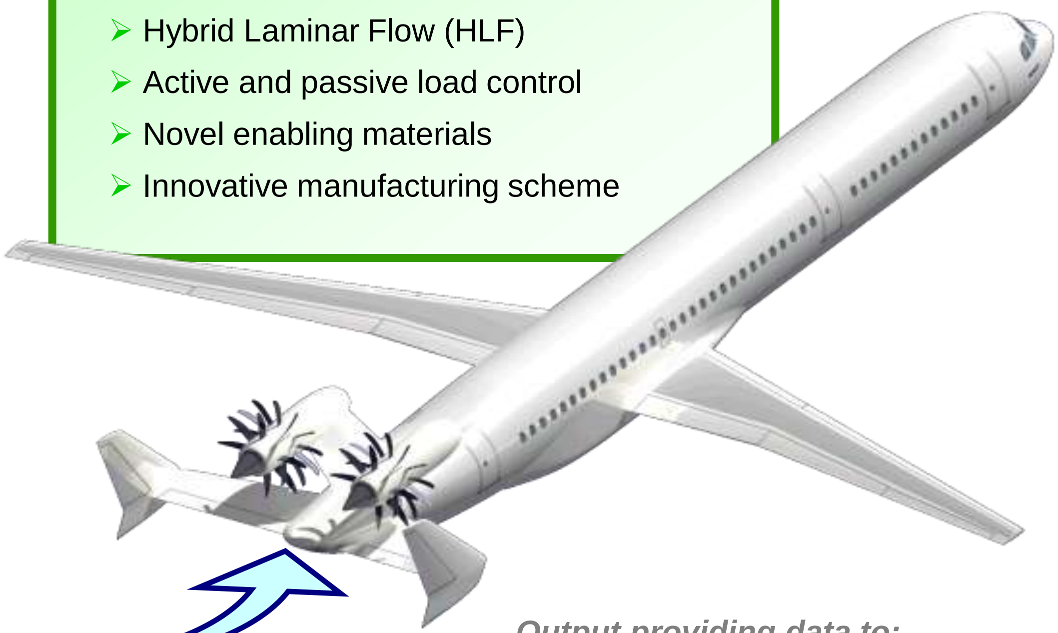

Output providing data to:

TE– **SFWA technologies for a Green ATS**

GRC: examples of achievements

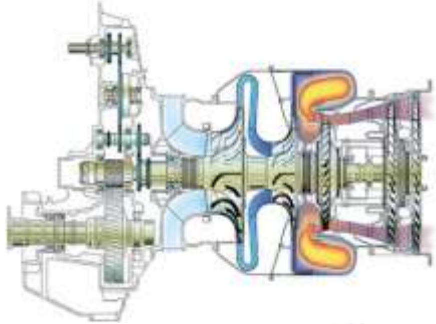

Advanced Turboshaft Demonstrator

Q1/2013

- High efficiency compressor, combustion chamber, high- and low-pressure turbines
- Full scale & life cycle validation

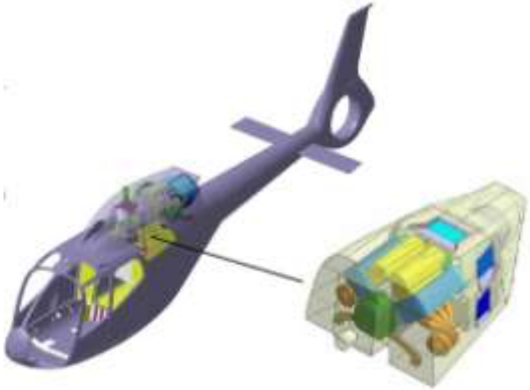

Diesel Demo

Q2/2014

- Diesel core engine
- Power pack integration

- Innovative Rotor blades:
  - Active twist blade
  - Gurney flap rotor
  - 3D blade profile optimised for dual speed rotor

Q2/2016

Calls for Proposals

Peculiarities of Clean Sky CFPs

1. TOPICS instead of research themes, defined by Topic Managers of ITDs
2. Threshold in terms of Topic VALUE instead of funding
3. A single APPLICANT may apply, no need for a consortium
4. One winner per topic

Clean Sky Calls statistics

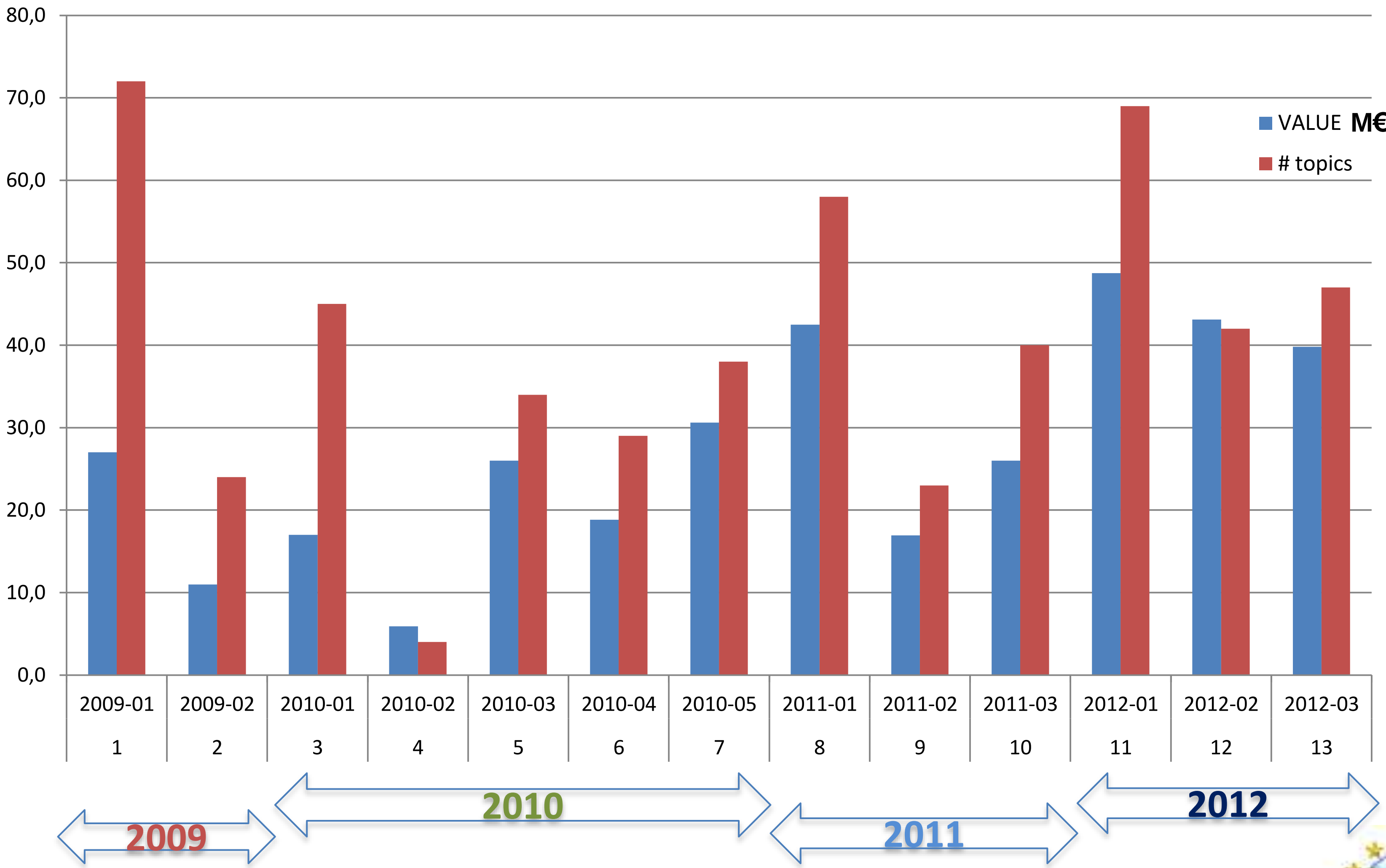

University Participation for Calls 1-12

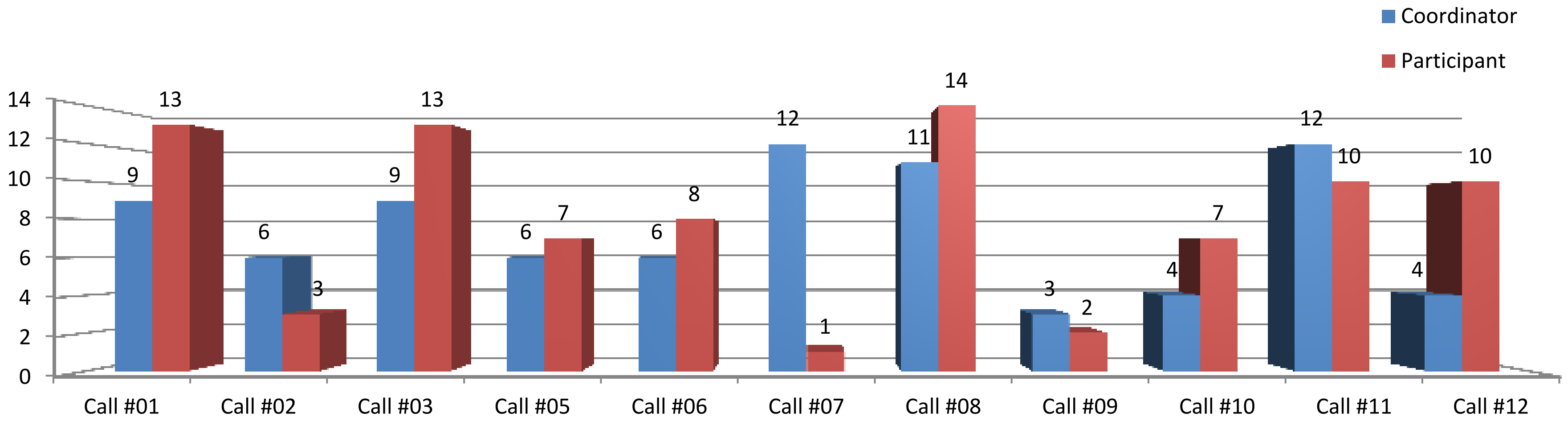

- More than 400 topics published
- > 30% success rate for applicants
- Average topic value 500 K€
- > 400 partners involved (i.e. ~500 participants incl. Members)
- > 50% of newcomers, not involved in previous European programmes

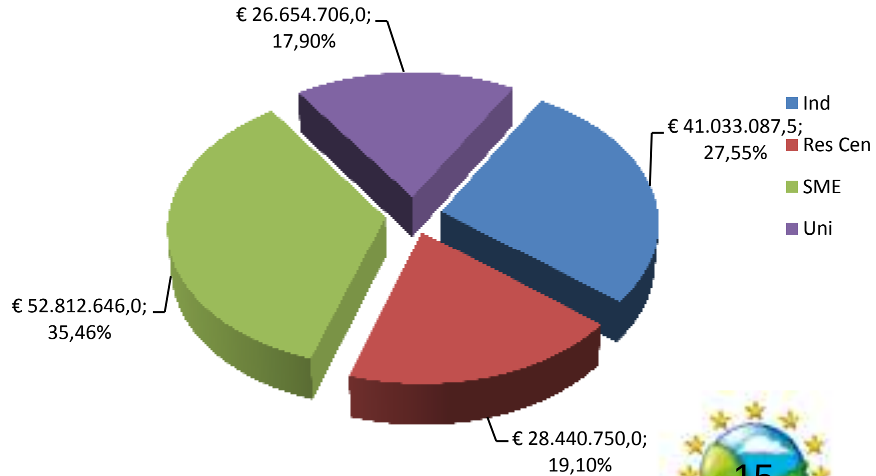

Way forward

Clean Sky is confirming the validity of the L3 approach.

As for the other JTIs, a possible continuation in H2020 is considered.

The current members have produced a proposal (Clean Sky 2) submitted by the EC to assessment by an external panel of experts, and to public consultation. A dedicated event took place at ILA.

The concept of IADP (Integrated Aircraft Demonstration Platform) complements the ITD approach.

The Process for finalizing the proposal for formal approval and submission as part of the H2020 framework for aviation is ongoing.

Concluding remarks

Clean Sky is aimed at reaching TRL up to 6 for the most effective technologies to improve the environmental impact of aviation.

It is using the complex demonstrator approach complemented by advanced tools .

The Technology Evaluator performs a continuous assessment of the actual achievement of environmental benefits for the chosen technologies and conceptual aircraft.

Clean Sky is engaging the most important players of the aeronautical sector in Europe, as well as several academic partners and SMEs.

It is the basis for continuing the approach in H2020 for further improvements.

CLEANSKY

EASN workshop on flight physics and propulsion

"Smart Fixed Wing Aircraft Integrated Technology Demonstrator" (SFWA-ITD):

SFWA smart "laminar wing": Status and results of ground tests and manufacturing of laminar wing sections for validation testing onboard the Airbus A340-300 test aircraft

Prague, 1st & 2nd November 2012

J. Koenig (Airbus)

SFWA-ITD *Smart Wing* R&T program status

Presentation Content

- Introduction
- SFWA-ITD key objectives; The SFWA-ITD *Smart Wing*
- Potentials and Challenges for the *Smart Wing*
- Strategy and programme to mature the *Smart Wing* in CleanSky
- *Smart Wing* Ground tests, status and intermediate results
- Preparation of the *BLADE* flight test demonstration
- Conclusion

SFWA-ITD *Smart Wing* R&T program status

Presentation Content

- **Introduction**
- SFWA-ITD key objectives; The SFWA-ITD *Smart Wing*
- Potentials and Challenges for the *Smart Wing*
- Strategy and programme to mature the *Smart Wing* in CleanSky
- *Smart Wing* Ground tests, status and intermediate results
- Preparation of the *BLADE* flight test demonstration
- Conclusion

CleanSky Nature of Programme

CLEANSKY
Joint Technology Initiative
for Aeronautics & Air Transport
www.cleansky.eu

Joint Technology Initiative (JTI) „Clean Sky“

- New instrument in European Commission Frame Programme FP7
- Single Frame Demonstrator R&T program for „Greening of the Air Traffic System“
- Representing the European large civil aero-industry
- 1.6 B€ programme budget out of ~4.6 B€ Aero R&T in FP7
- 7 years runtime
- Annual update of workplan, annual „Grant Agreement“
- Run via a dedicated „Joint Undertaking“ (JU)

SFWA-ITD organisation and setup

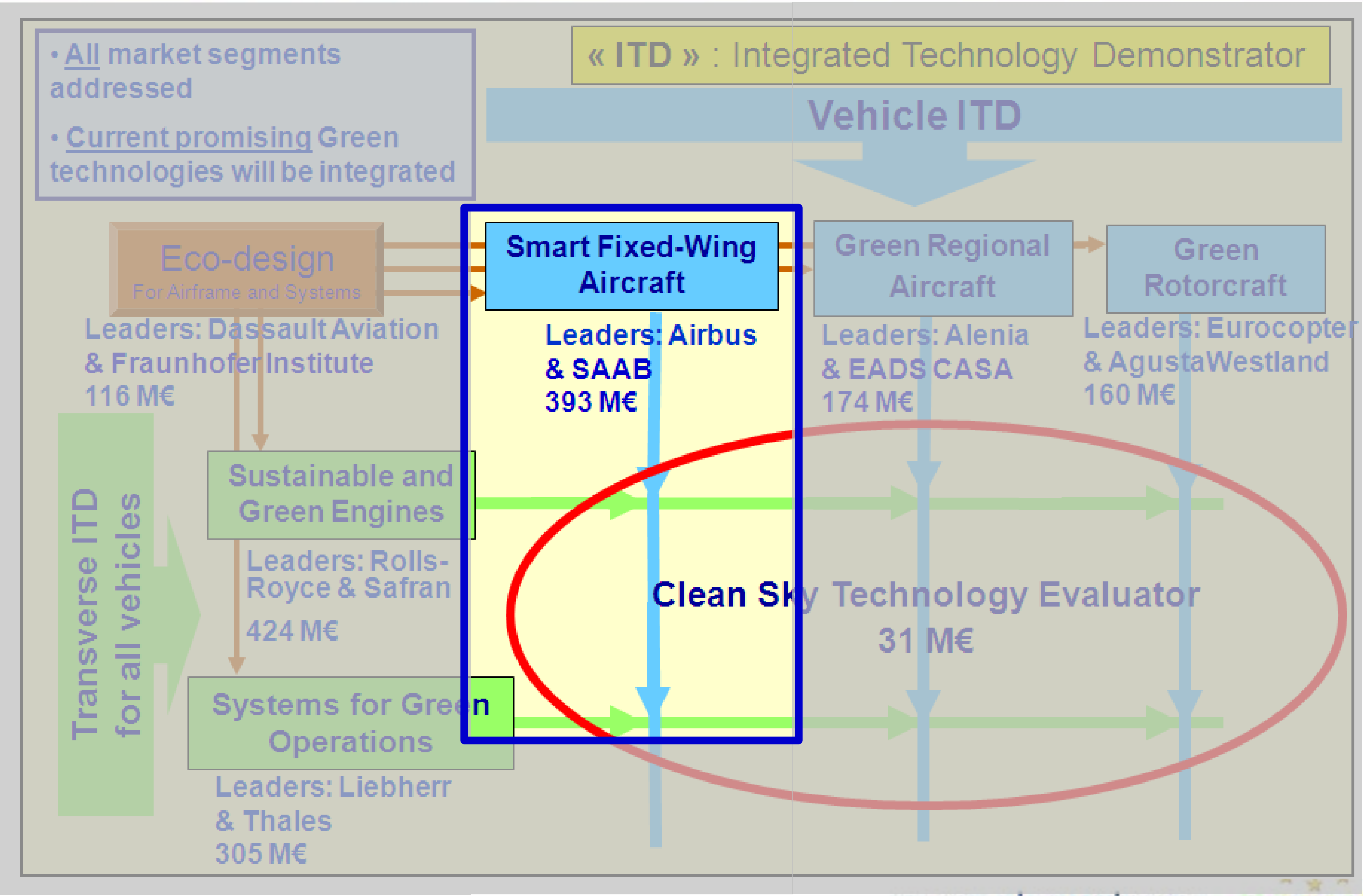

SFWA-ITD *Smart Wing* R&T program status

Presentation Content

- Introduction
- **SFWA-ITD key objectives; The SFWA-ITD *Smart Wing***
- Potentials and Challenges for the *Smart Wing*
- Strategy and programme to mature the *Smart Wing* in CleanSky
- *Smart Wing* Ground tests, status and intermediate results
- Preparation of the *BLADE* flight test demonstration
- Conclusion

Smart Fixed Wing Aircraft - ITD Key objectives

Input connecting to:

SAGE ITD – **CROR engine**

SGO – **Systems for Green Operation**

Smart Wing Technologies

- **Technology Development**
- **Technology Integration**
- **Large Scale Flight Demonstration**
  - Natural Laminar Flow (NLF)
  - Hybrid Laminar Flow (HLF)
  - Active and passive load control
  - Novel enabling materials
  - Innovative manufacturing scheme

Innovative Powerplant Integration

- **Technology Integration**
- **Large Scale Flight Demonstration**
  - Impact of airframe flow field on Propeller design (acoustic, aerodynamic, vibration)
  - Impact of open rotor configuration on airframe (Certification capabilities, structure, vibrations...)
  - Innovative empennage design

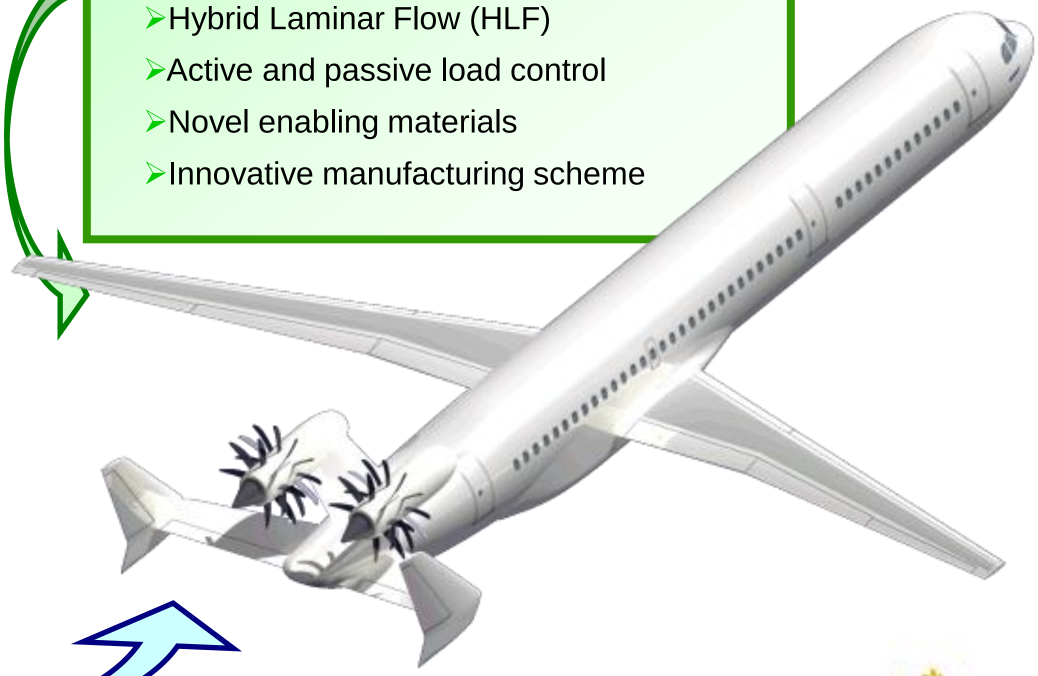

Output providing data to:

TE– **SFWA technologies for a Green ATS**

www.cleansky.eu CLEANSKY

Smart Fixed Wing Aircraft - ITD Key objectives

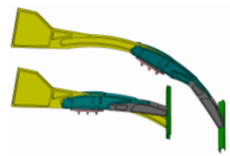

WP3 – Lead AI-F
Flight Demonstration

WP31 – AI-SAS Low Drag Demonstrator	WP32 – Dassault Low Speed Demonstrator	WP33 – AI-F Innovative Engine Demonstrator	WP34 – AI-D Long –Duration flight Trials	WP35 - Dassault After-body Demo Option
Airbus Aernnova Dassault Incas Saab Onera DLR NLR	Dassault NLR Incas	Airbus DLR Rolls-Royce Snecma Microflown	Airbus Qinetiq	Dassault Incas Onera Ruag

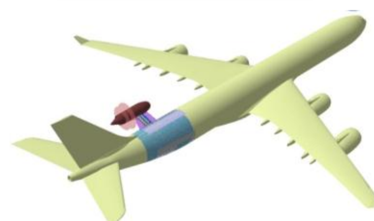

CfP partners
Asco / FTI Group
BIAS / GKN
ITA / Sertec /
Aritex/ASCAAM

Presentation Content

- Introduction
- SFWA-ITD key objectives; The SFWA-ITD *Smart Wing*
- **Potentials and Challenges for the *Smart Wing***
- Strategy and programme to mature the *Smart Wing* in CleanSky
- *Smart Wing* Ground tests, status and intermediate results
- Preparation of the *BLADE* flight test demonstration
- Conclusion

Aerodynamic drag reduction through laminar flow

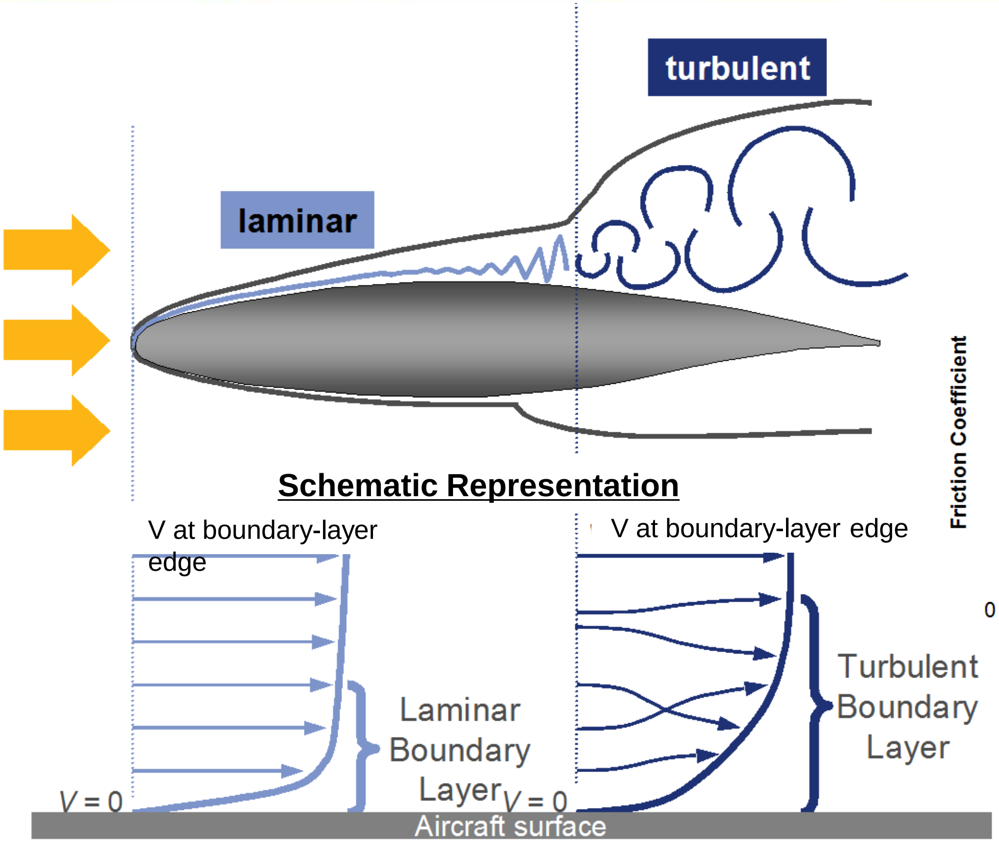

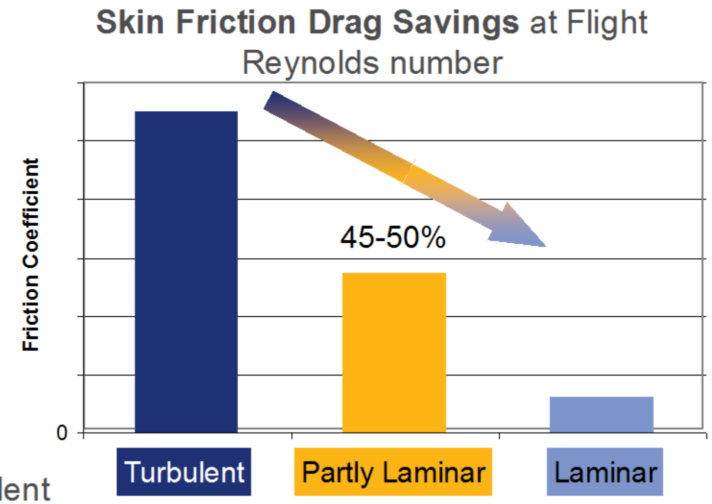

Achieving a laminar flow on the upper cover of the wing has the potential to provide 25% drag reduction at wing level, and 6-7% drag reduction at aircraft level

SFWA- High Speed Demonstrator Passive (HSDP) – The „BLADE“ Demonstrator

Smart Passive Laminar Flow Wing

- Design of an all new natural laminar wing
- Proof of natural laminar wing concept in wind tunnel tests
- Use of novel materials and structural concepts
- Exploitation of structural and system integration together with tight tolerance / high quality manufacturing methods in a large scale ground test demonstrator
- Large scale flight test demonstration of the laminar wing in operational conditions

Port wing

Laminar wing structure concept
Option 2

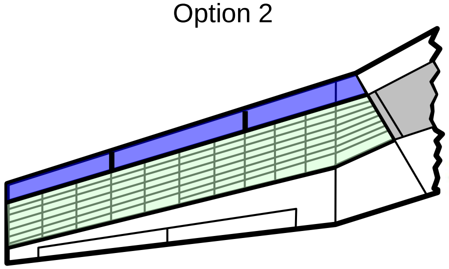

Starboard wing

Laminar wing structure concept
Option 1

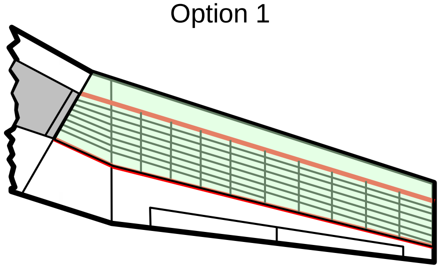

Laminar flow flight demonstrations 1985 - 2008

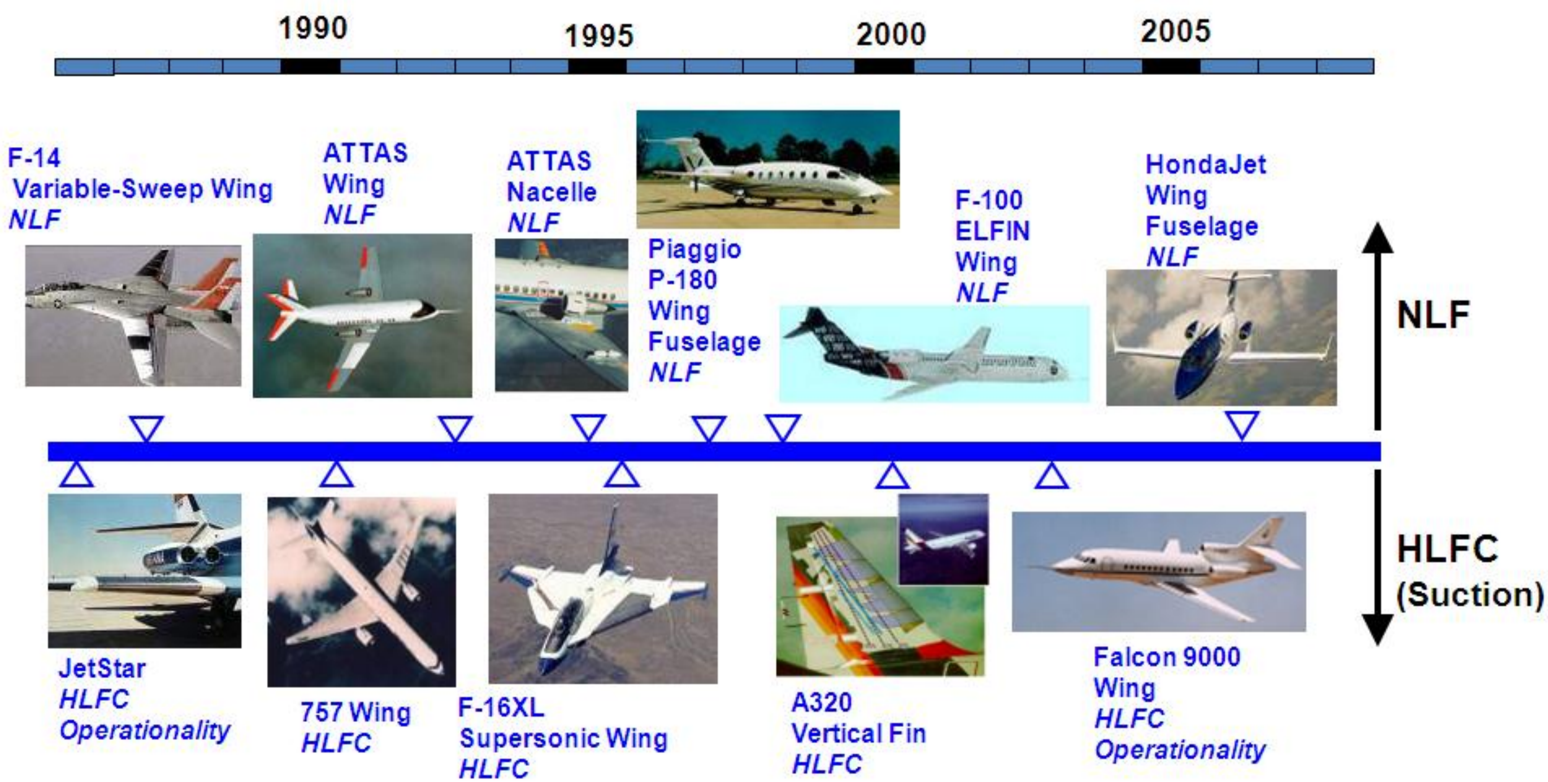

Aerodynamic design feasible and high performance possible <u>but</u>

Key for introduction of laminar technology is

- **<u>High surface quality</u>**
- **Avoidance of insect contamination**
- **Simplified suction system**

SFWA-ITD *Smart Wing* R&T program status

Presentation Content

- Introduction
- SFWA-ITD key objectives; The SFWA-ITD *Smart Wing*
- Potentials and Challenges for the *Smart Wing*
- **Strategy and programme to mature the *Smart Wing* in CleanSky**
- *Smart Wing* Ground tests, status and intermediate results
- Preparation of the *BLADE* flight test demonstration
- Conclusion

SFWA-ITD “NLF Wing Technology Stream”

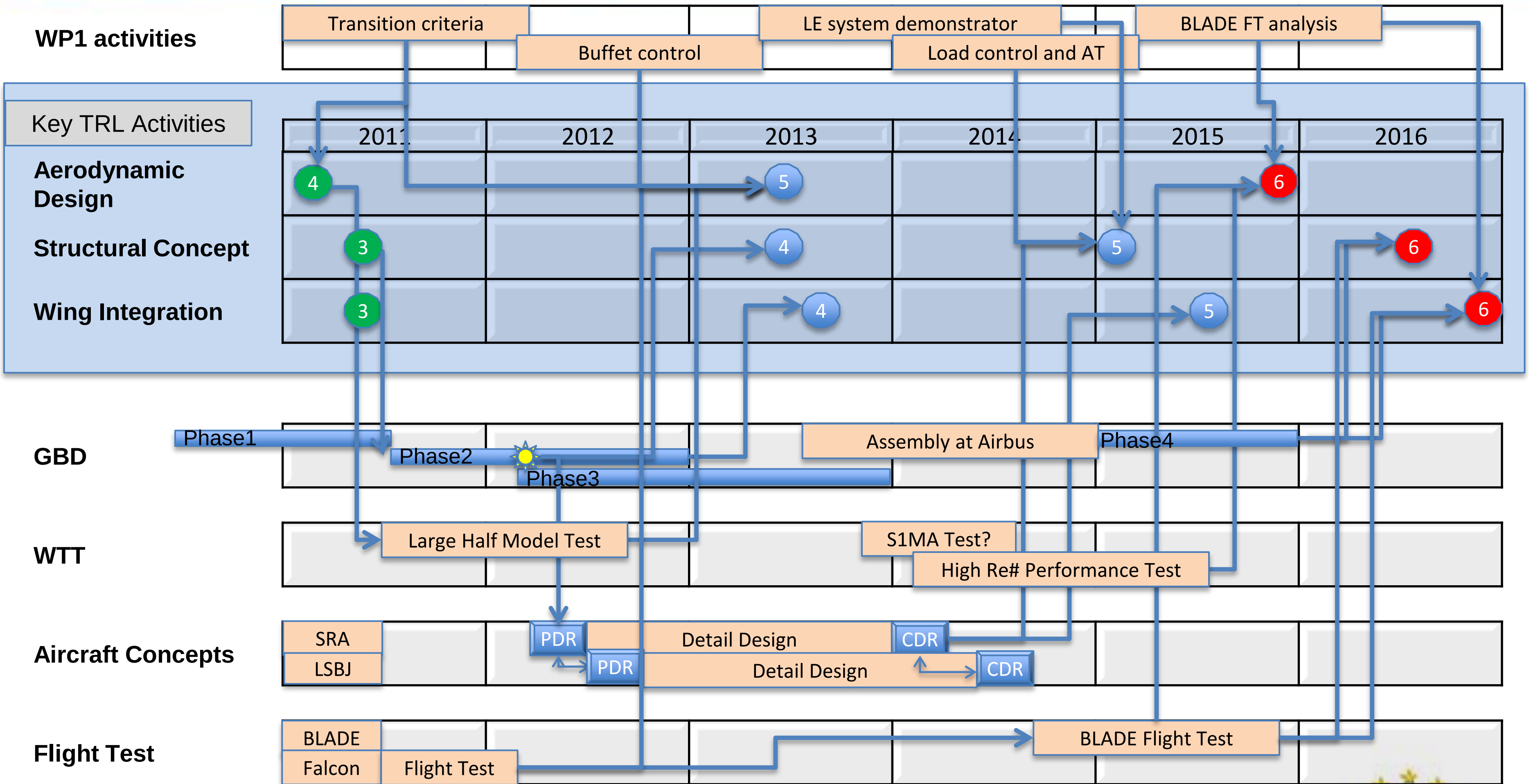

Only major inputs / outputs are shown

Laminar Wing Structure Options & Valiadtion

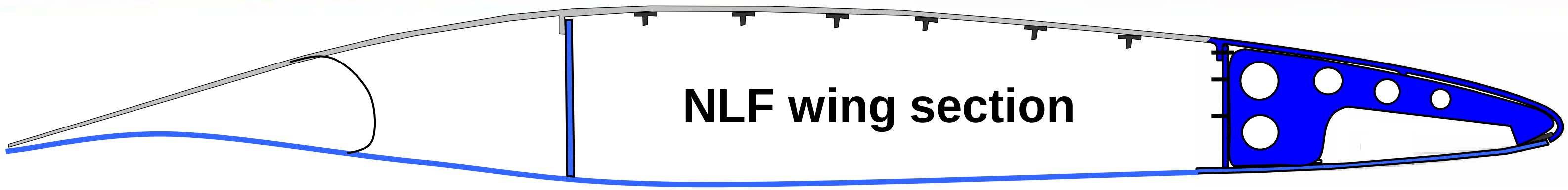

Examples of two upper cover options

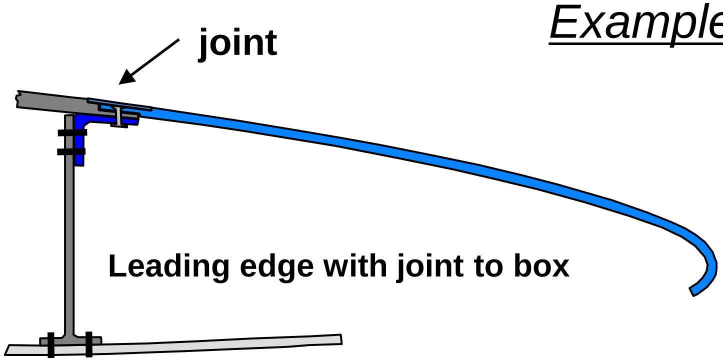

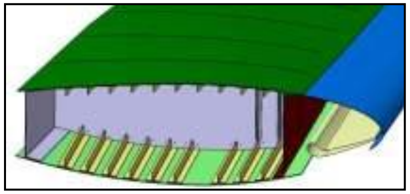

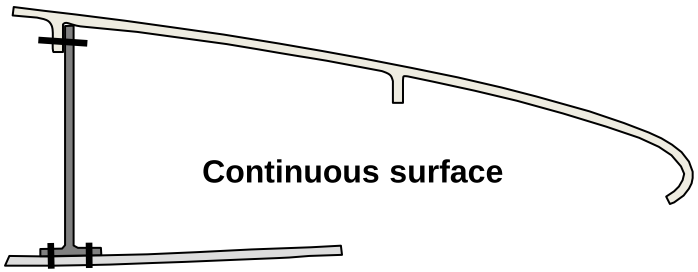

Other options under investigation

downselection

process

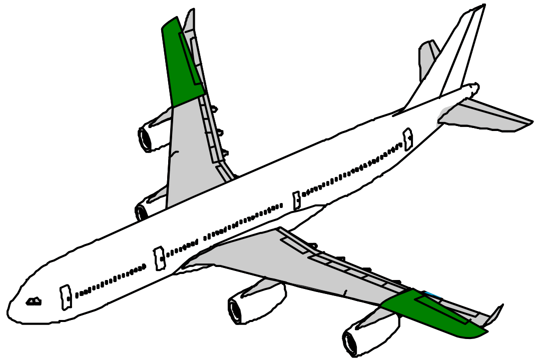

Validation on A340 FTD

Validation by specific ground tests

Operational Challenges

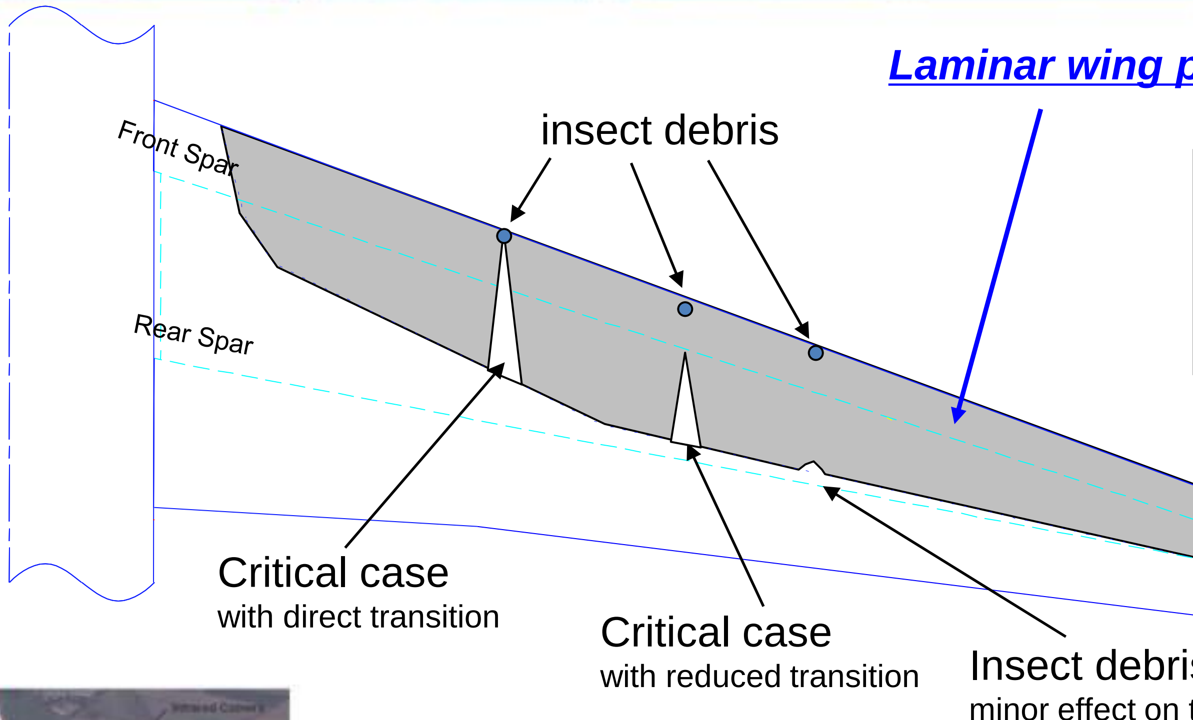

insect impact on surface

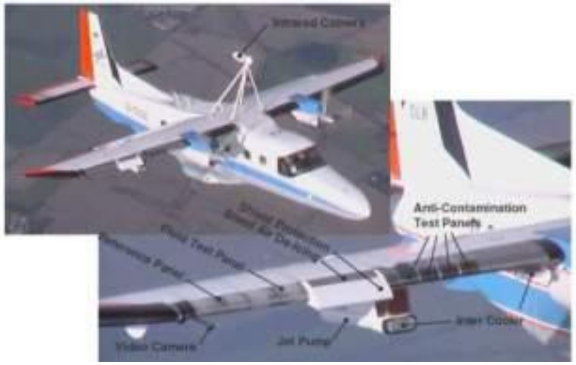

Krueger shielding

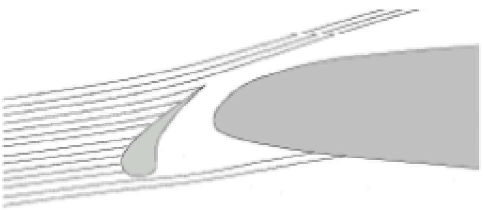

Shielding effect

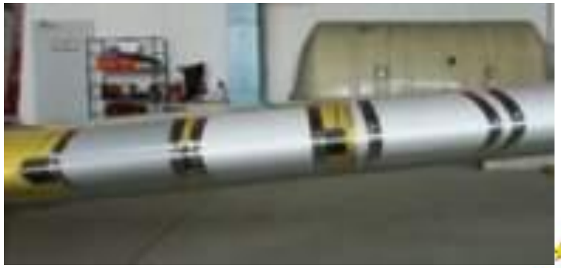

Anti-contamination coating

Aeronautics priority R&T in CleanSky

Major Objective:

Demonstrate the feasibility of a structure concept enabling laminar flow

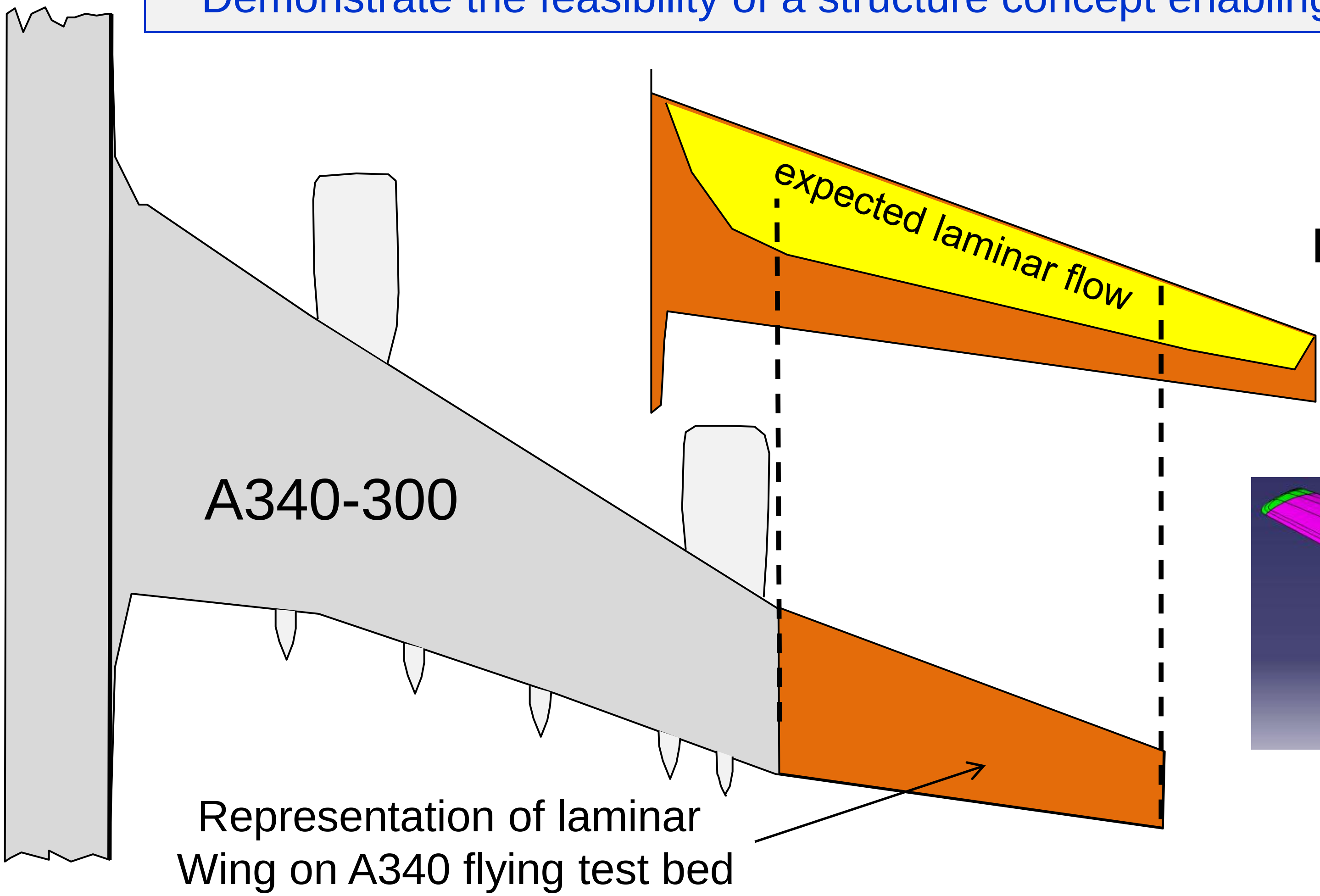

Laminar wing

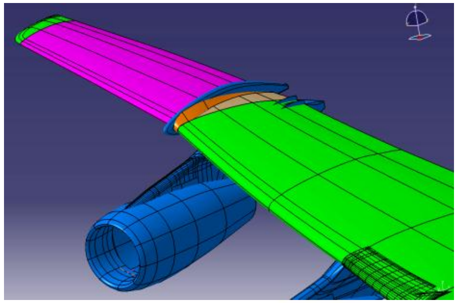

SFWA-ITD *Smart Wing* R&T program status

Presentation Content

- Introduction
- SFWA-ITD key objectives; The SFWA-ITD *Smart Wing*
- Potentials and Challenges for the *Smart Wing*
- Strategy and programme to mature the *Smart Wing* in CleanSky
- ***Smart Wing* Ground tests, status and intermediate results**
- Preparation of the *BLADE* flight test demonstration
- Conclusion

SFWA-ITD *Smart Wing* Ground Based Demonstration

- **Key Objectives**
  - To demonstrate the functionality and fit to requirements of a fully integrated full scale representation of the SRA leading edge zone.

- **Engagement**
  - A team activity, led by Airbus with input from SAAB and supported the CFP process (GKN for Phases 1, 2 and 3)

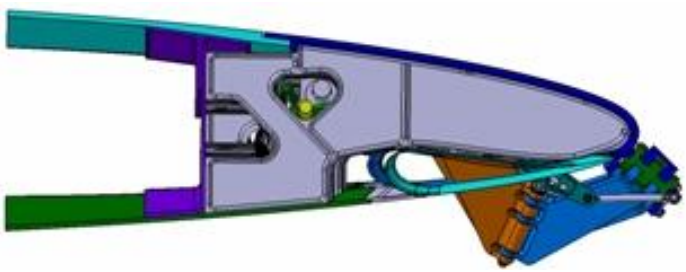

- **Deliverables**
  - 5 connected phases of activity
  - Phase 1: Leading Edge joint
  - Phase 2: Definition of LE architecture
  - Phase 3: Manufacturing
  - Phase 3a: Assembly
  - Phase 4: Test and Analysis

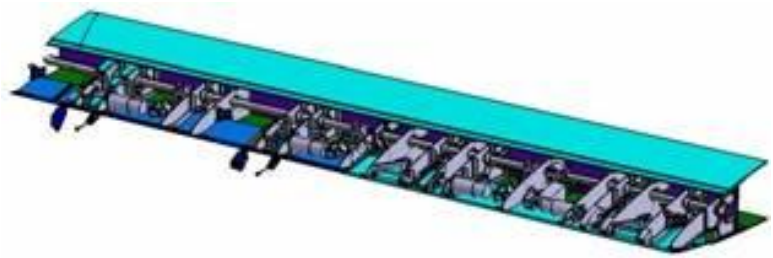

SFWA-ITD *Smart Wing* Ground Based Demonstration

ID	Task Name
1	**CFP Phase 1 LE Joint Design**
2	Joint definition and testing
3	WIPS feasibility
4	**CFP Phase 2 Design of Integrated LE**
5	Icing tunnel tests and WIPS definition
6	Detailed structure definition
7	6 month extension to cover feature demos in Phase 3
8	**CFP Phase 3 Component Manufacturing**
9	Continuation of feature demonstrators
10	Manufacturing of structural components
11	**Assembly of GBD (Airbus)**
12	Tooling
13	Assembly
14	**CFP Phase 4 GBD Testing and Analysis**
15	Test and analysis
16	Report construction
17	***Major milestones***
18	Completion of Phase 1 GBD CFP activity
19	Downselection of GBD configuration following SRA PDR
20	Completion of Phase 2
21	Phase 3 launch
22	Phase 3 completion
23	Supply of Krueger surface and kinematics from LUFO
24	Airbus assembly launched
25	Airbus assembly completed
26	Phase 4 launched
27	Phase 4 completed and report delivered

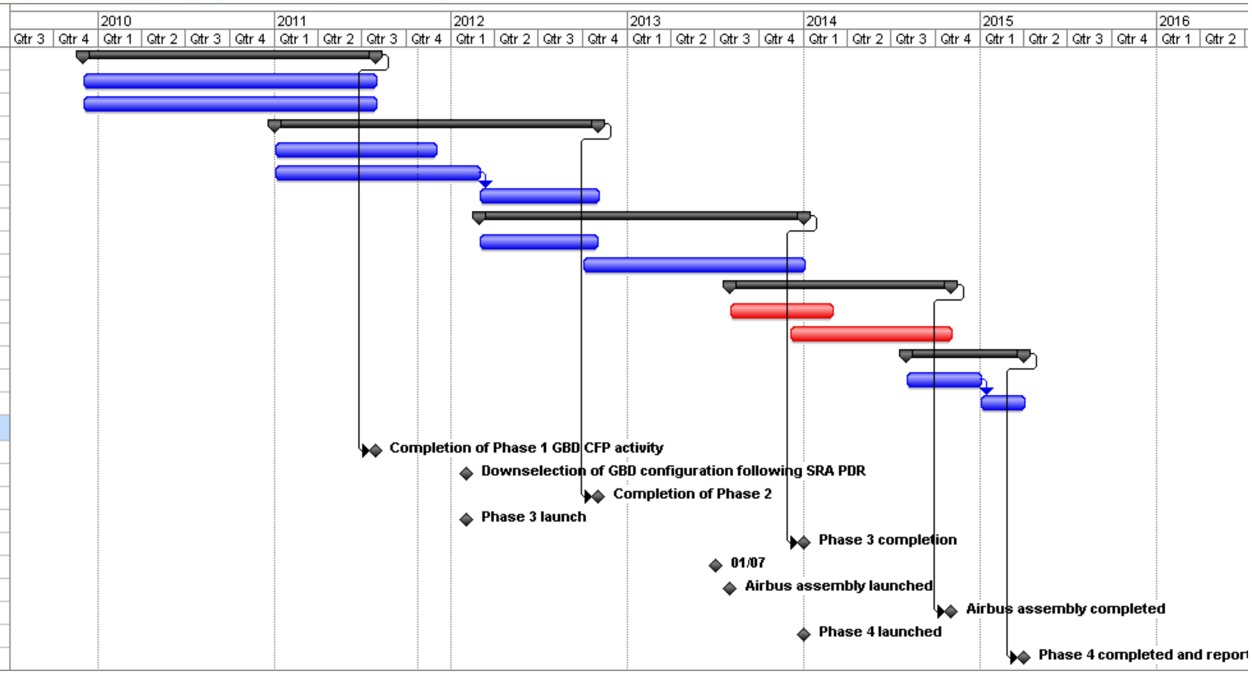

- Phase 1 CFP (GKN) completed and LE joint concept selected
- Phase 2 CFP (GKN) well under way and feeding down selection review
- Phase 3 CFP (GKN) Negotiations completed – contract in place
- Down selection review held 1st March 2012 with GKN, Airbus and SAAB
- Key issues have been identified for further investigations prior to commitment to DFM

All aspects of leading edge design, assembly and operation considered in down selection review process

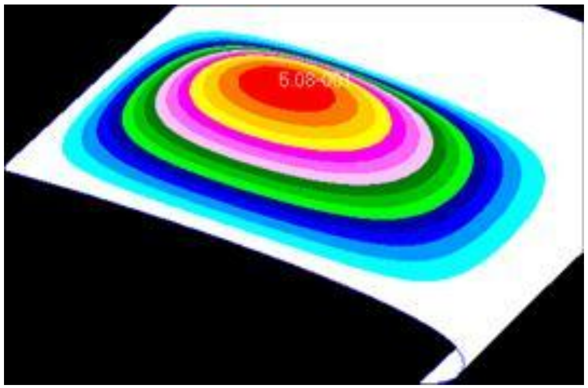

Skin panel sized by flight loads to meet the waviness criteria

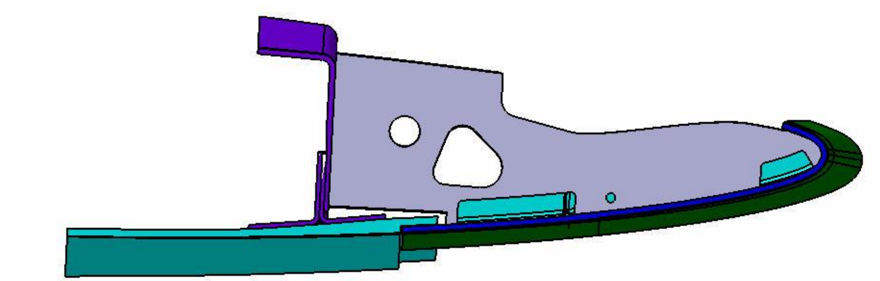

Outside/ In assembly option

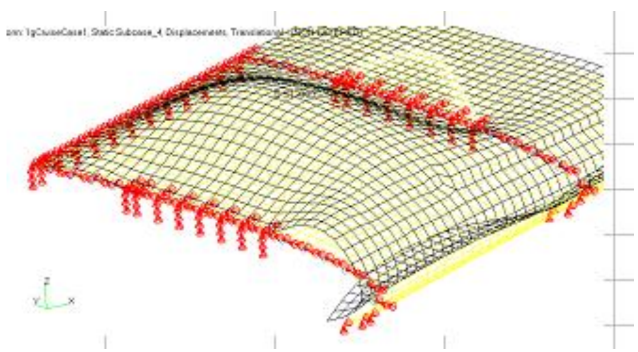

FE analysis that now accounts for rib attachment geometry

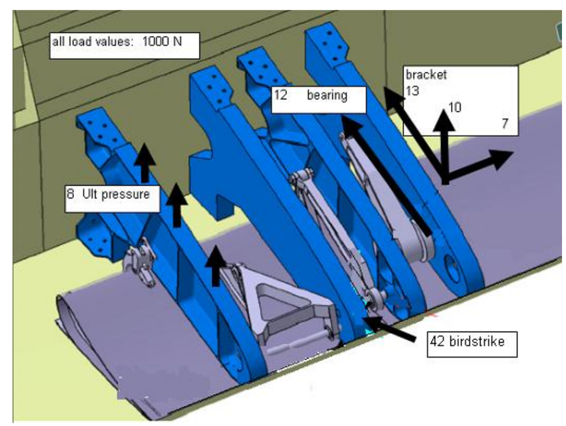

Rib layout taken from Krueger system and sized for flight loads and bird strike

SFWA-ITD *Smart Wing* Ground Based Demonstration

- To understand fully the potential **impact of surface imperfections upon NLF wings**, a series of wind tunnel tests are being performed.
- A series of 2d step tests have been performed in KRG to **assess surface tolerance limits for forward and backward facing steps** at different x/C
- The latest in KRG was conducted in July 2012 to **assess the effect of waviness and steps** and in particular, to model the effect of interaction between LE waves and wingbox waves.
- The **results of these tests are being used to update surface tolerance requirement documents** to enable design for manufacture to minimise the risk of transition due to waviness and steps.

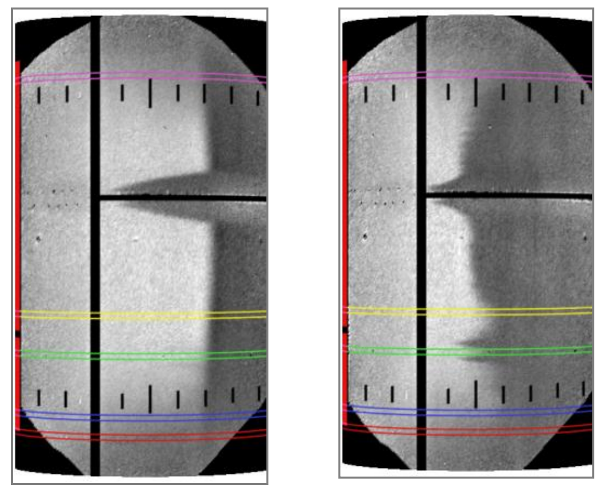

Shift of laminar - turbulent transition line as function of waviness at Ma0,75

SFWA-ITD Demo on manufacturing and assembly

Current manufacturing of the Smart Wing integrated upper panel (SAAB)

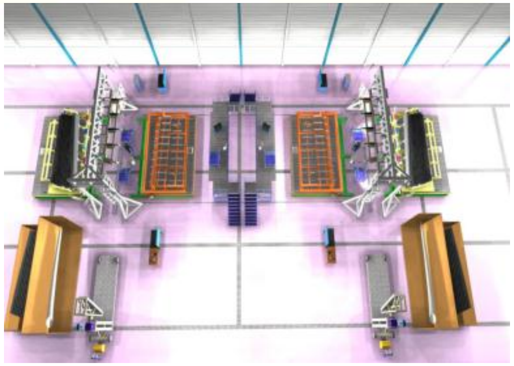

Smart Wing industrial assembly scenarios (Aernnova)

Smart Wing semi-assembly ground transportation (Aernnova)

The manufacturing and assembly of a future *Smart Wing* is of key relevance for the industrial application

- **Cost of tooling**
- **Cost of material and manufacturing**
- **Production ramp up and flexibility of production rate**
- **Quality of products**

SFWA-ITD *BLADE* flight test demo preparation status

- Down-selection review for the GBD selecting the concepts to be combined for the "SFWA laminar wing" held in May 2012.
- Phase 3 of the GBD is launched and first manufacturing of components will commence.
- Major wind tunnel tests at high Reynolds number were successfully conducted to confirm the required tolerances of surface, waviness, steps and gaps.
- A TRL3 review of Transition Health Monitoring and Fuel Planning was successfully held in September 2012

- *Tests ongoing to select and deploy a robust anti contamination and erosion protection for the wing surface*
- *Major effort ongoing to implement WIPS for the NLF wing concept, in particular installation and assembly*
- *Highly motivated team*
- *Work closely on track versus plan*

31.Oct - 02.Nov 2012
EASN workshop on Flight Physics & Propulsion

SFWA-ITD *Smart Wing* R&T program status

Presentation Content

- Introduction
- SFWA-ITD key objectives; The SFWA-ITD *Smart Wing*
- Potentials and Challenges for the *Smart Wing*
- Strategy and programme to mature the *Smart Wing* in CleanSky
- *Smart Wing* Ground tests, status and intermediate results
- **Preparation of the *BLADE* flight test demonstration**
- Conclusion

SFWA-ITD *BLADE* flight test demo preparation status

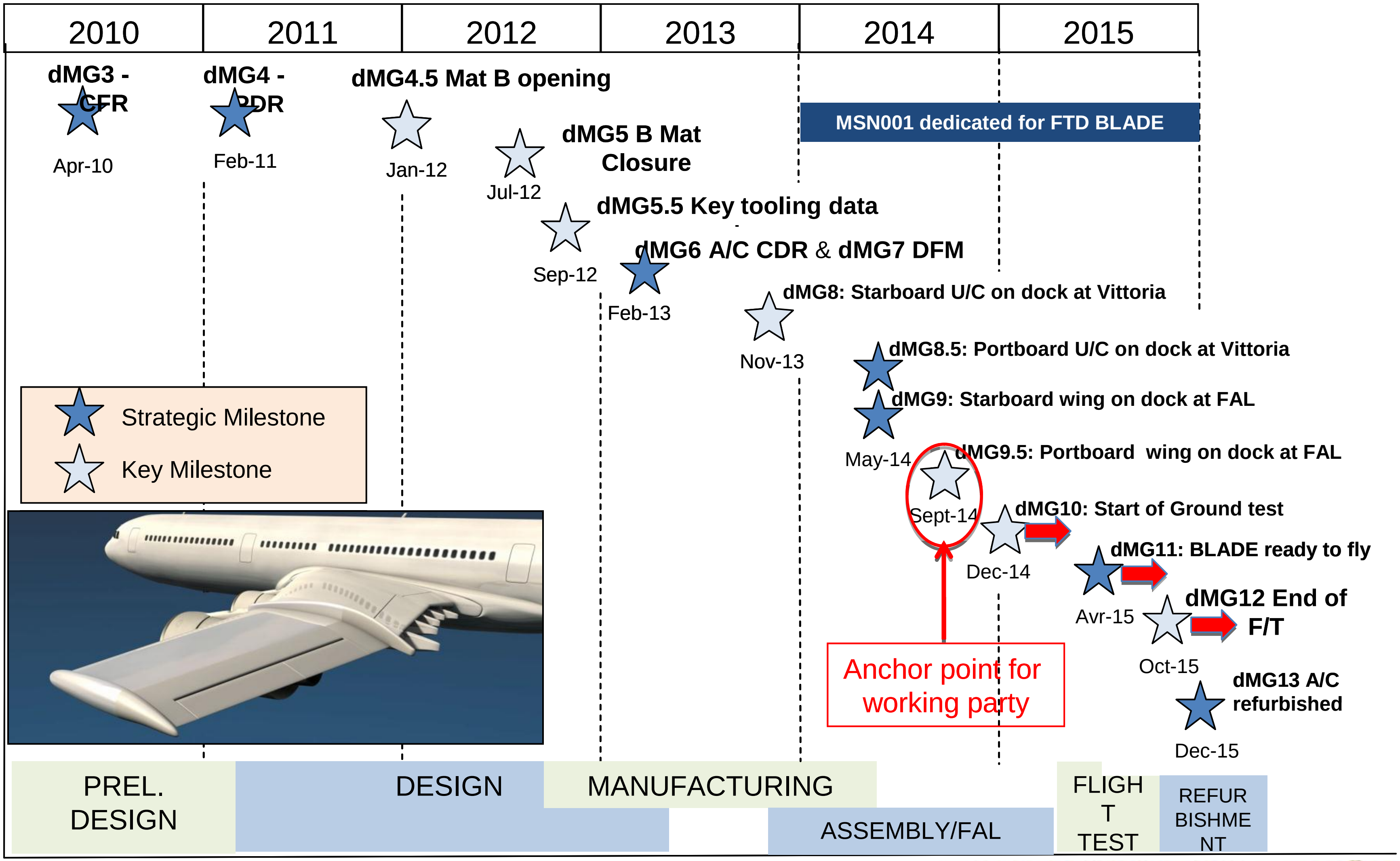

The Integrated Smart Wing Upper Cover Concept (SAAB concept)

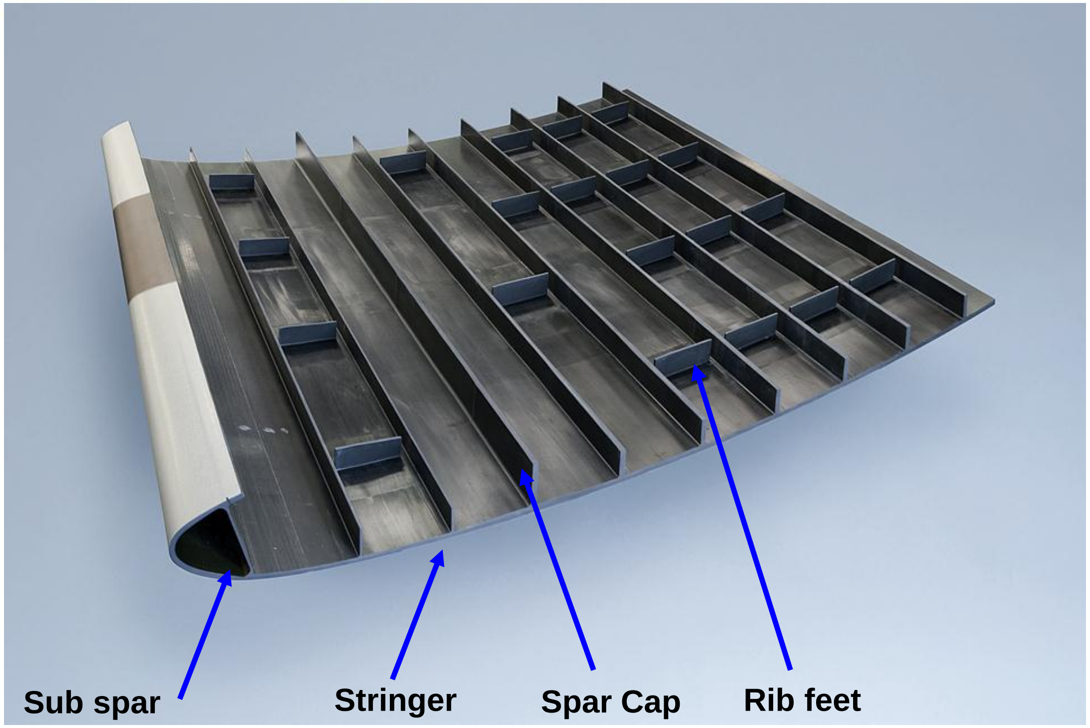

Complexity

– The panel combines several advanced design principles into an fully integrated solution, co-cured in one step.

– Fulfilling very challenging requirements regarding surface quality

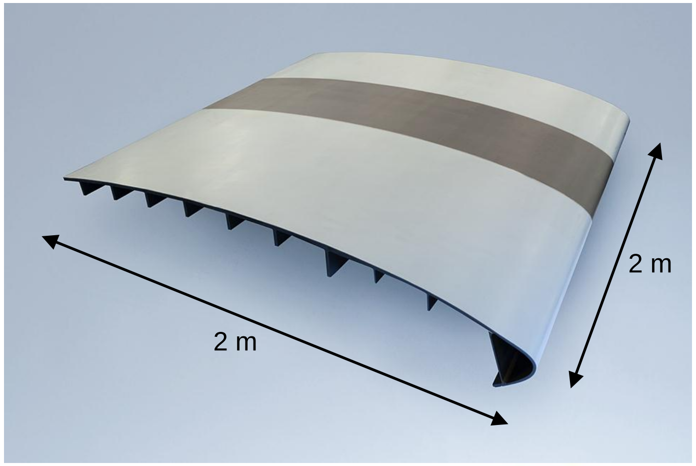

Test/Trial Panel

– A test/trial panel has been manufactured and is used for several purposes, i.e. evaluation design concepts, tooling, surface measurement etc.
– Manufacturing of starboard wing test panels completed to validate tooling concept and spring back analysis

SFWA-ITD *BLADE* flight test demo preparation status

BLADE Wing DMU populated

- All MSN 001 datum wing and smart wing structures
- Datum systems and system modfications for flight controls, fuel, electrical and hydraulic lining, ports, connectors, etc
- Ports, vents, access doors

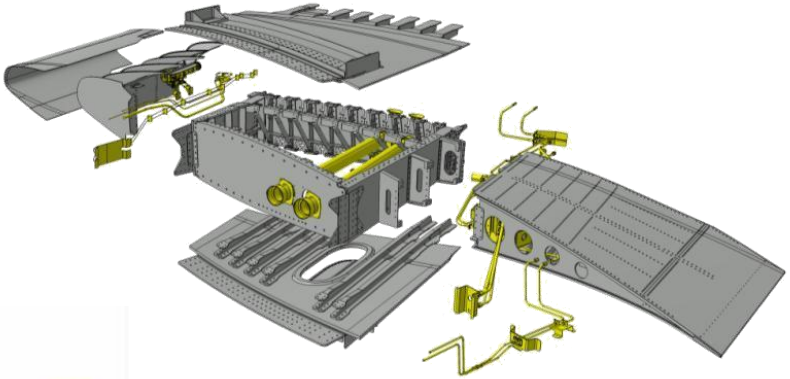

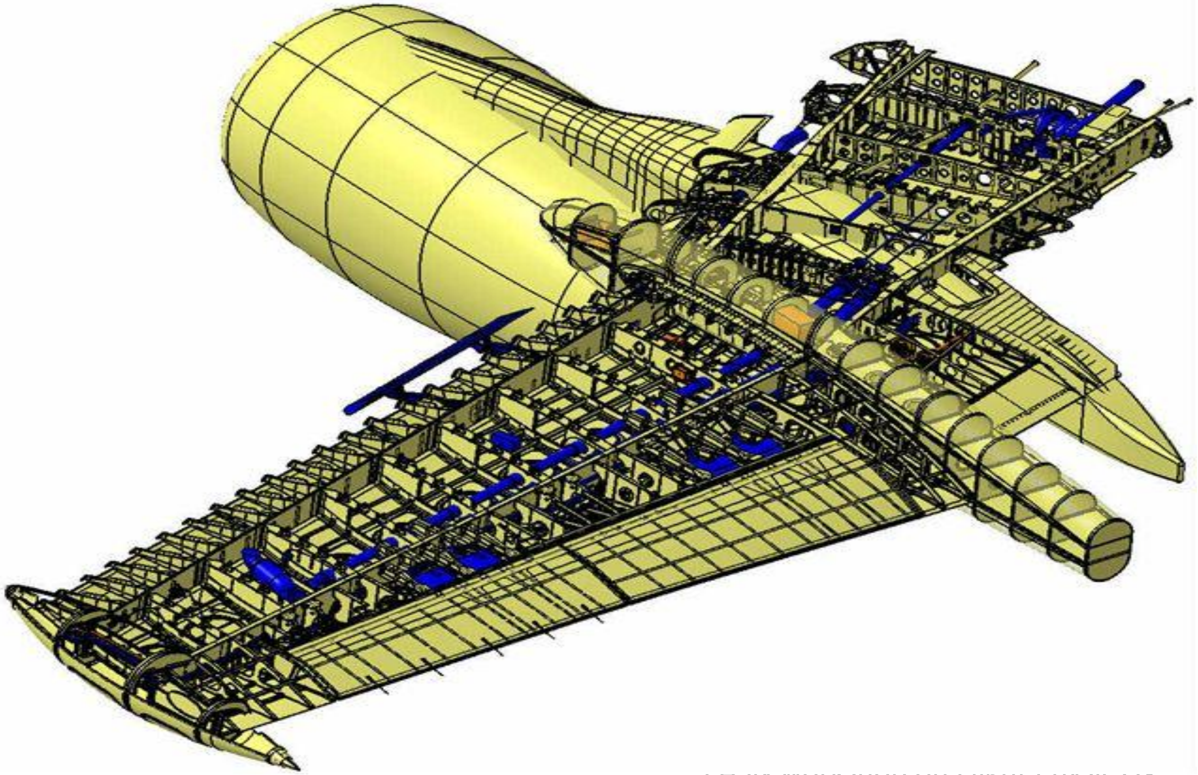

Transition zone

- Detailed design and drawings available
- Design of toolings close to completion
- Bill of parts available
- Start of production planned for Q1/2013

www.cleansky.eu CLEANSKY

31.Oct - 02.Nov 2012
EASN workshop on Flight Physics & Propulsion

SFWA-ITD *BLADE* flight test demo preparation status

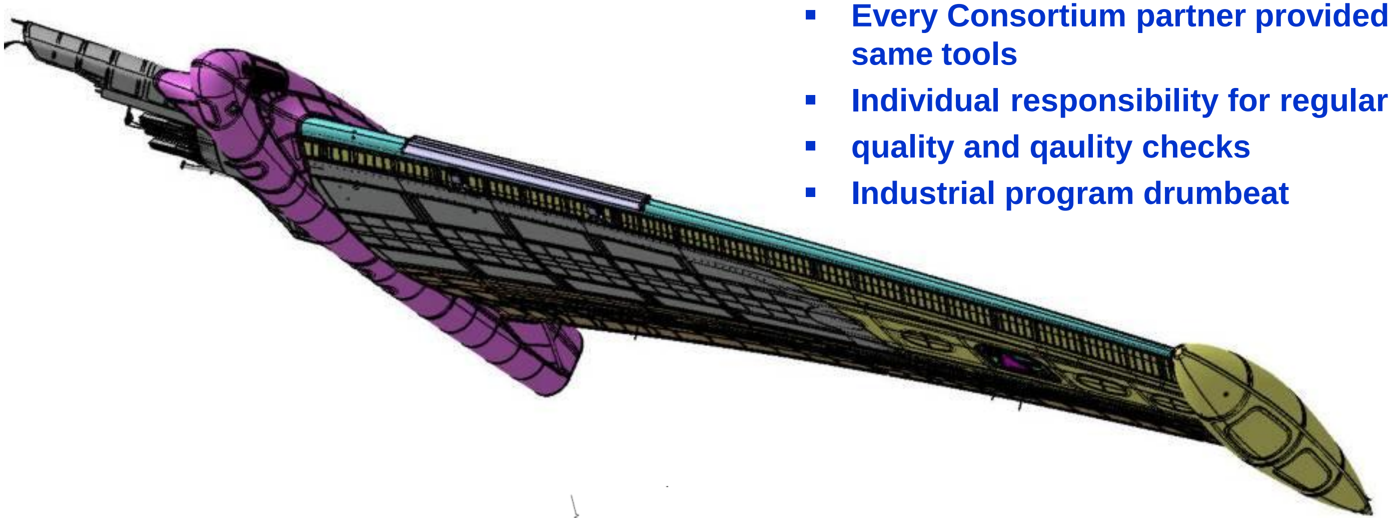

Complete wing design managed through DMU

- Every Consortium partner provided full set of data prepared with same tools
- Individual responsibility for regular updating
- quality and qaulity checks
- Industrial program drumbeat

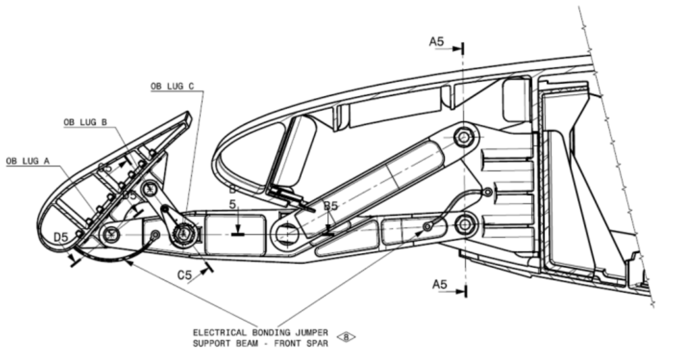

Krueger Flap

- Mechanism design improved
- Assembly test conducted

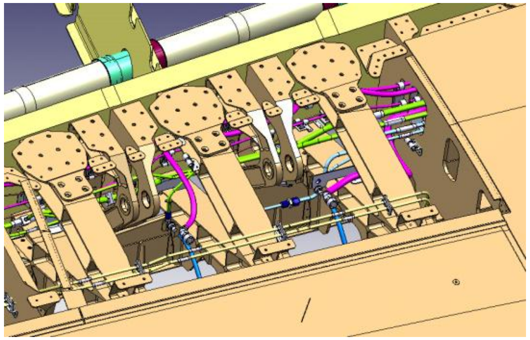

Wing system installation

- Flight control geometry compliance checked
- Aileron and actuator installation maturity validated

www.cleansky.eu CLEANSKY

31.Oct - 02.Nov 2012
EASN workshop on Flight Physics & Propulsion

SFWA-ITD *BLADE* flight test demo preparation status

L/E Demo 1

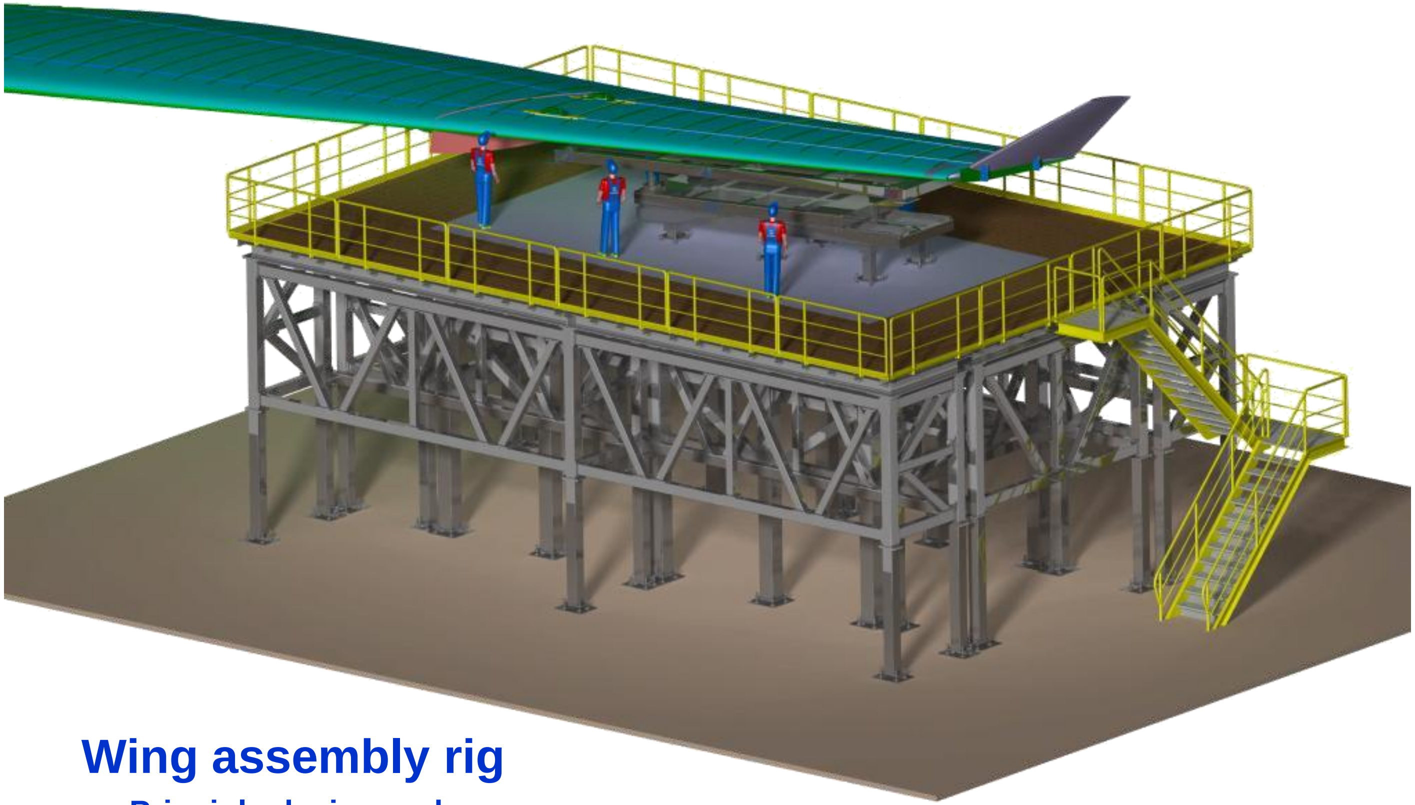

FTI installations

- **Installation of diverse types of flight test instrumentation ongoing**

Wing assembly rig

- **Principle design and drawings available**
- **Compliance with assembly tools and rigs checked**
- **Capability to conduct ground wing load tests**

SFWA-ITD *BLADE* flight test demo preparation status

Qualification of IR camera – based boundary layer measurements

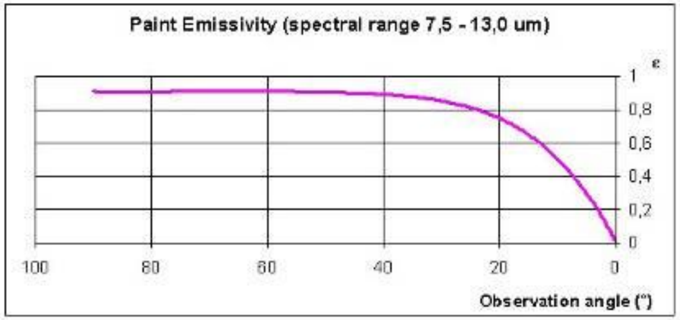

- Isolated infrared camera and sample holder with heating
- Cooling down to – 50 ° C
- Measurement of digital level (radiation signal)
- Varying the viewing angle from 90° (perpendicular) down to 5°

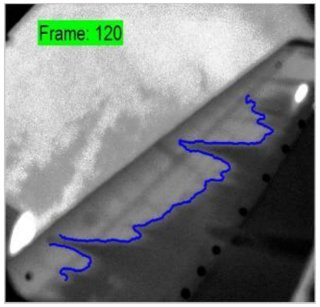

Status :

- *From IR data analysis, the minimum sun illumination required is estimated to about 600 W/m2*
- *Transposed to BLADE, this defines the possible time window for flight trials*

Toulouse

Condition/ Duration	3 hours	2 hours	1 hours
Left & Right	13/03 - 29/09	09/03 – 04/10	05/03 – 06/10
Left OR Right	20/02 – 19/10	13/02 – 31/10	09/02 – 01/11

Seville

Condition/ Duration	3 hours	2 hours	1 hours
Left & Right	26/02 – 14/10	22/02 – 20/10	17/02 – 24/10
Left OR Right	02/02 – 08/11	19/01 – 24/11	16/01 – 26/11

SFWA-ITD *BLADE* flight test demo preparation status

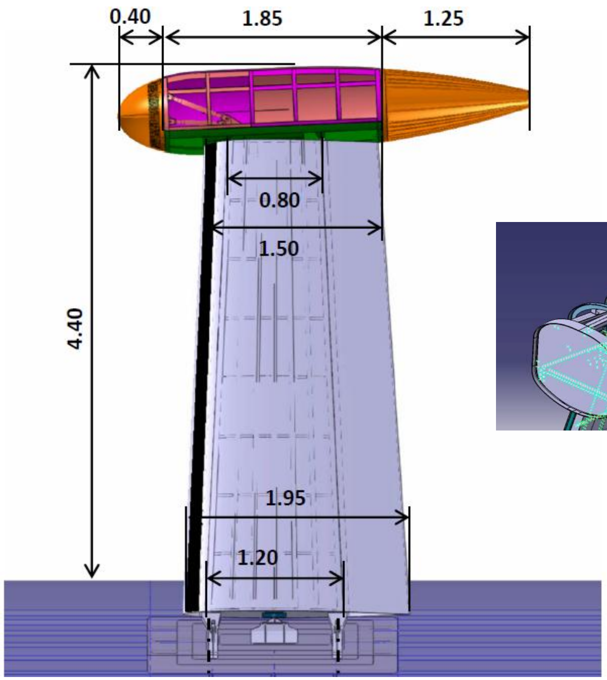

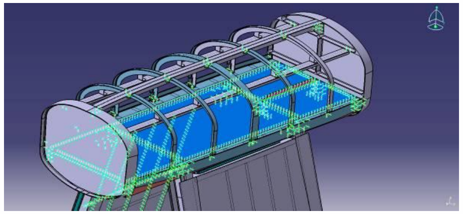

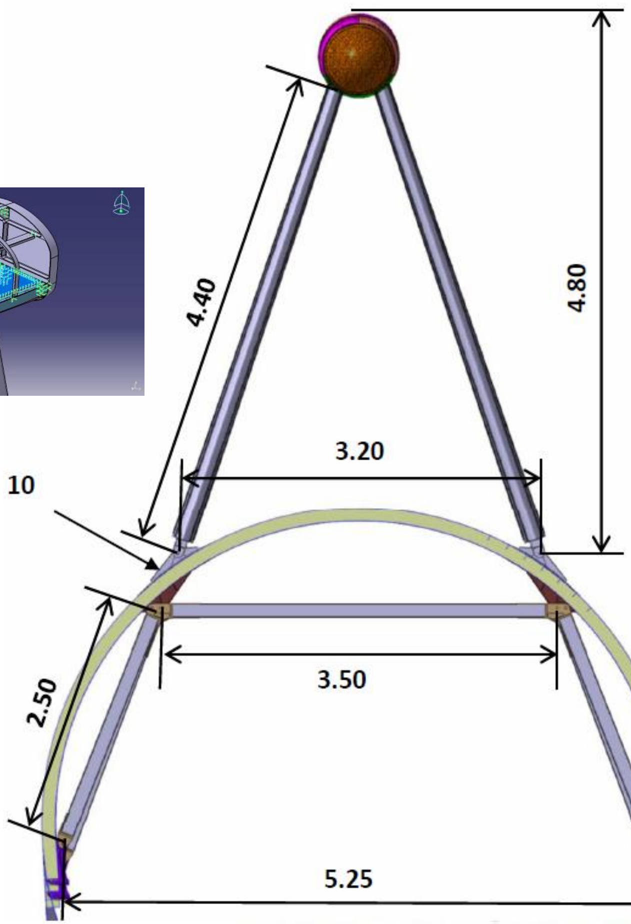

Camera pod design

- **Structural design of pod and carrier structure available**
- **Principle assembly of cameras, and supplementary equipment and systems frozen**

SFWA-ITD *BLADE* flight test demo preparation status

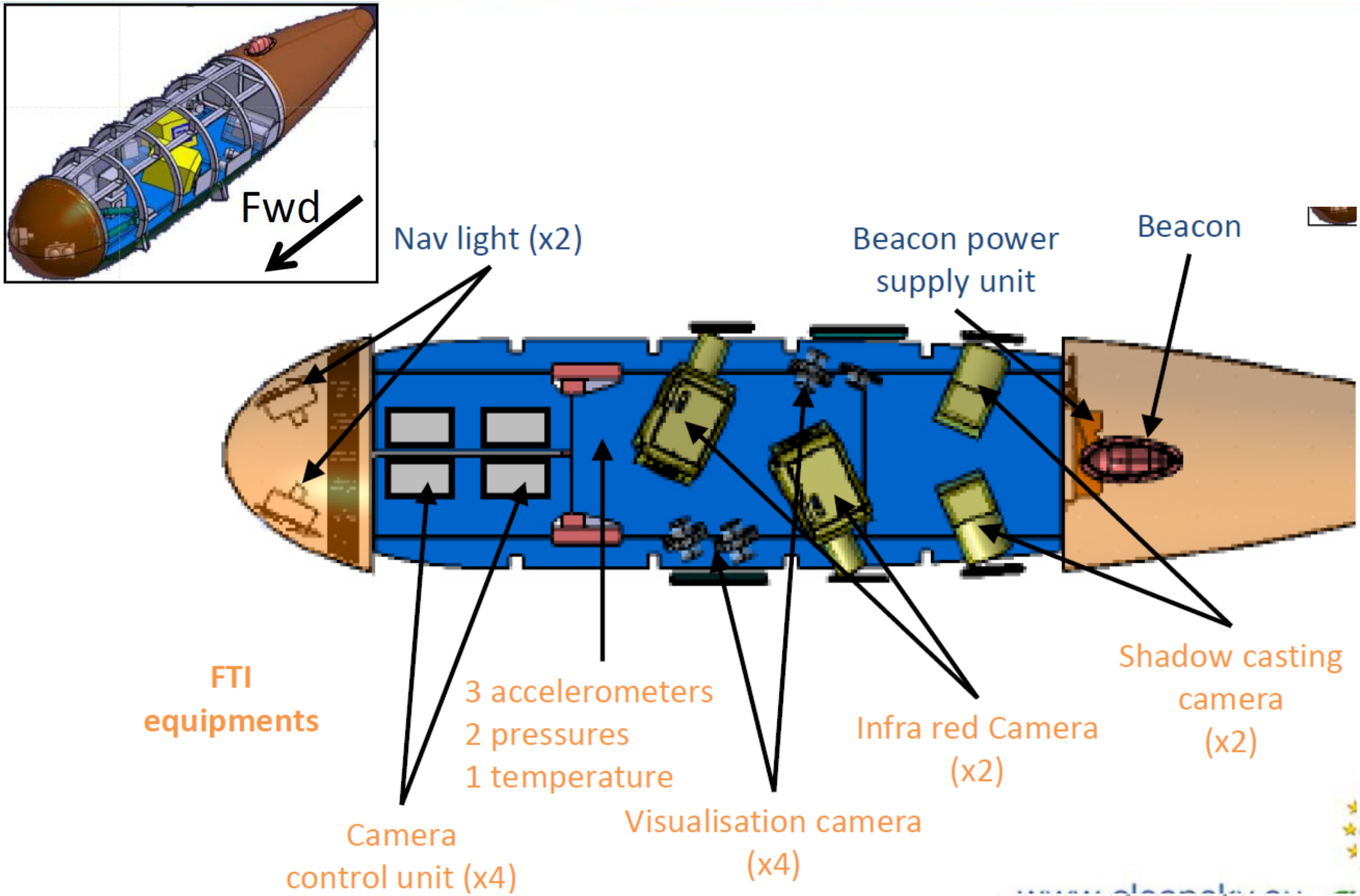

SFWA-ITD *BLADE* flight test demo preparation status

- Preliminary design review for flight test on A340-300 MSN passed in Q1/ 2011
- Detailed design of most major components completed
- Laminar wing test articles detailed design almost complete
- Start of manufacturing & assembly planned in Q1/ 2013
- „Permit to Fly“ process started with authorities
- Assembly of parts at aircraft May 2013
- Flight test planned to start in April 2015

- *Challenge to work on high TRL R&T under „industrial conditions“*
- *Combining targets of the demonstration with rules and procedures to be respected for flight clearance and flight testing is posing a severe constraint*
- *Highly motivated team*
- *Work on track, but still significant challenges ahead!*

31.Oct - 02.Nov 2012
EASN workshop on Flight Physics & Propulsion

SFWA-ITD *Smart Wing* R&T program status

Presentation Content

- Introduction
- SFWA-ITD key objectives; The SFWA-ITD *Smart Wing*
- Potentials and Challenges for the *Smart Wing*
- Strategy and programme to mature the *Smart Wing* in CleanSky
- *Smart Wing* Ground tests and accomplishments
- Preparation of the *BLADE* flight test demonstration
- **Conclusion**

Conclusion

- A flight test programme of complexity and size of BLADE is as challenging as an industrial aircraft programme, with constraints of an R&T project
- “High TRL” RnT is demanding to generate and share foreground knowledge and foreground IP
- SFWA requires a integrated, seamless single programme planning for R&T on numerical simulation, ground based demonstration, wind tunnel testing and flight test demonstration
- A programe of size and duration of SFWA requires a strong and reliable commitment of the key stakeholders respectively consortium members

Conclusion

A program like CleanSky is the way to go for large scale "high TRL" Research and Technology in Aeronautics

SFWA-ITD *Smart Wing* R&T program status

Design and Analysis of Noise shielding after bodies for Bizjets

2nd EASN Association Workshop

Sébastien Barré, Stéphane Lemaire, Floriane Rey
DASSAULT AVIATION

Motivations for reduction of future Falcon aircraft noise levels :

- **More and more stringent noise constraints around airports:**
  - enforcement of acoustic certification constraints expected within coming years
  - specific local constraints depending on airports: night curfews, more stringent noise levels, fines if maximum levels not respected
- **Our customers seek flexibility in term of day slots and operate at community airports where the noise constraints are the strongest**

  → need to design aircraft capable to operate at airports applying very severe noise constraints

    - **challenge** for engineers to cope with these **requirements**
    - **noise impact** must be considered from **early stages of aircraft design**
    - need **to predict accurately** the noise signature of future aircraft
- The **european aircraft industry** is committed to **reduce noise** levels by **10 EPNdB per operation** (take off, landing) between 2000 and 2020 (technological objectives corresponding to TRL 6). It will be **difficult to reach** this objective **without considering new aircraft architectures** shielding engine noise.

Noise Reduction Objectives & Technology Paths (Future Projects)

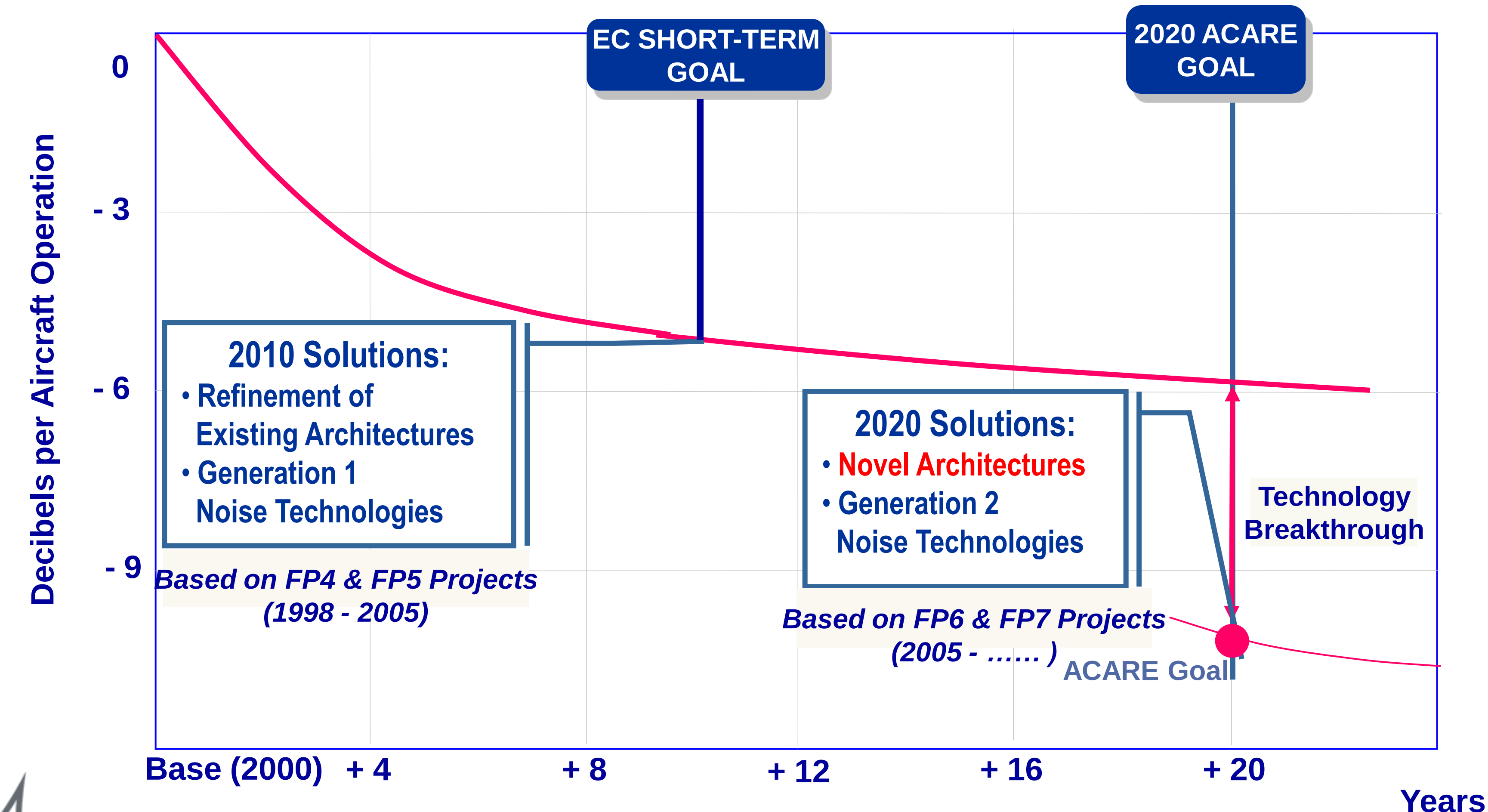

Investigation of innovative business jet aft-bodies in CleanSky EU project

- **Innovative business jet aircraft architectures** with an **engine noise shielding aft-body** have been investigated in the **SFWA (Smart Fixed Wing Aircraft)** platform of **CleanSky EU project (**2008-2016, 7FP, grant agreement n° CSJU-GAM-SFWA-2008-001)
- **Different partners** are participating to these studies **: ARA, INCAS, ONERA, RUAG** and **SNECMA ;**
- Design of these **innovative architectures** must be performed by **accounting** not only **for noise constraints** but also for **other main topics** like **aerodynamics, structures** and **flight performances ;**
- **Evaluation of noise levels** are performed by **Dassault Aviation** using prediction tools which will be **validated and calibrated** using **dedicated wind tunnel** and **static tests ;**

Overall strategy for evaluation of noise levels

Prediction of engine noise installation effects & A/C noise levels

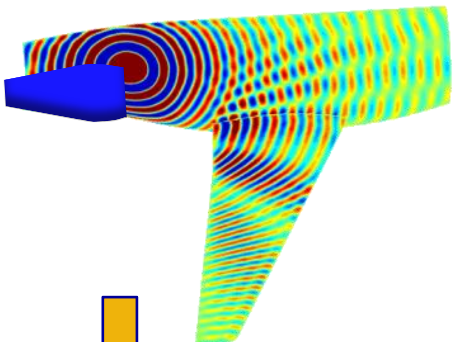

Tests specification

Calibration & validation of noise prediction tools

Experimental campaigns

Assessment of the noise shielding potential of aft-bodies and downselection of the most promising concepts for futher studies

Falcon aircrafts noise sources

- **Falcon business jets:** typical noise contributions to overall noise

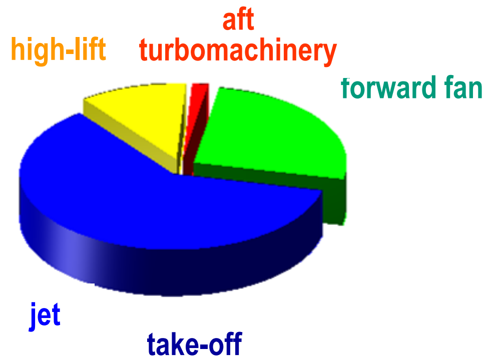

→ all engine and airframe components have to be accurately estimated to predict overall noise

- **Engine noise (jet, forward fan, aft fan, core, turbine):**
  - noise from **isolated static engine** provided by **engine manufacturers**
  - noise from engines **installed on aircraft: corrections must be applied** to isolated static data

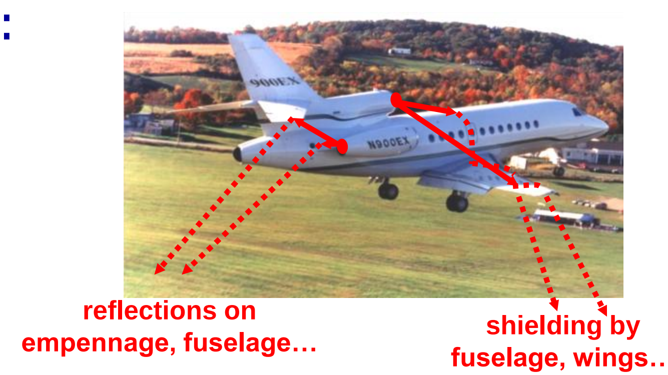

- **Airframe noise (high-lift, landing gears):**
  - **noise** sources depend on **local geometric and aerodynamic environment**
  - noise modeling must account for **interactions between components** (gear/wing, gear/bay, slat/flap…)

DASSAULT AVIATION
DGT/DTIAE

Prediction of A/C noise levels using ANIS code

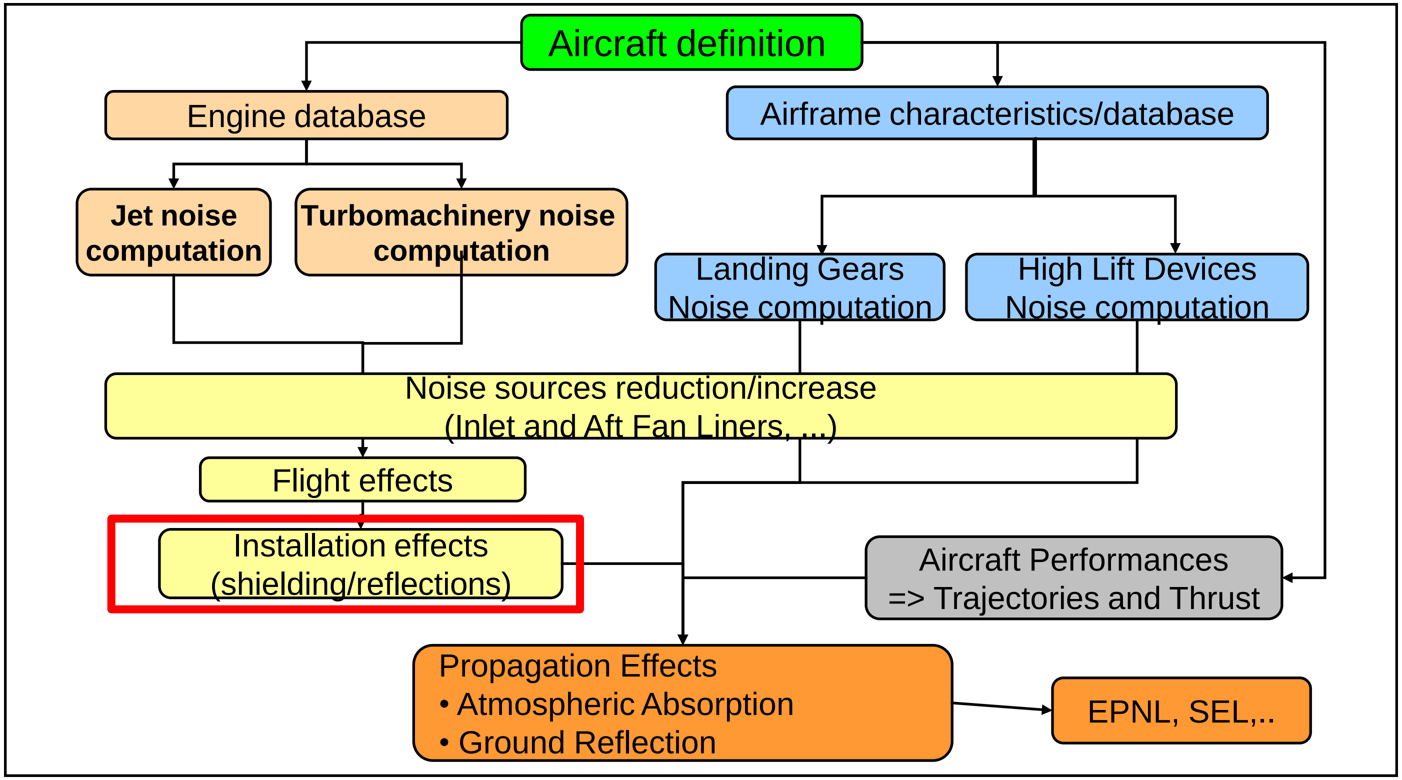

- **ANIS computes Falcon aircraft noise :**
  - **on trajectory** and in **adequate metrics (**EPNdB, dBA) using **A/C description** and **performance data ;**
  - with **engine noise** sources fully **modeled or provided by engine manufacturers (static tests data) ;**
  - **accounting for engine installation effects :** shielding or reflections of acoustic waves on the aircraft body

Prediction of engine noise installation effects

- **Turbo-machinery noise (rearward fan, combustion & turbine noise sources):**
  - Simplified **noise sources** are located **at nozzle exit** using equivalent **rings of monopoles**;
  - **Boundary Element Methods** (BEM) are used to **propagate noise** from sources taking into account the **aircraft geometry** ;

- **Jet noise:**
  - **Internal jet noise sources** are located at nozzle exit (internal mixing through the lobe mixer of primary and secondary flows) using equivalent **rings of monopoles**;
  - **External jet noise sources** are **spread within the full 3D jet volume** downstream the nozzle (external mixing between internal mixed jet and ambient flow);
  - **Tam & Auriault theory** is used to predict **external noise sources** from a **3D RANS computation** of the jet mean flow;
  - **Boundary Element Methods** (BEM) are used to **propagate noise** from sources taking into account the **aircraft geometry.**

Experimental campaigns : DNW wind tunnel tests

- **Objective : validation** of the **noise reduction potential** of various **aft-bodies, including mean flow effects** but with **simplified engine** noise sources **:**
  - **1/5th scale mock-up ;**
  - **engine noise sources** produced by **TPS** (Turbofan Propulsion Simulator) ;
  - **acoustic modes** radiated by the TPS **characterized** using **rings of kulites ;**
  - **airframe noise sources localization** using a specific antenna ;
  - large **parametric configuration** matrix with **different TPS operating conditions, A/C configurations, isolated TPS & A/C without TPS.**

- **Partners :**
  - **ARA & INCAS:** mockup design and manufacturing;
  - **DNW:** measurements and facility operation, TPS;
  - **ONERA**: contribution to test specifications and acoustic calculations.

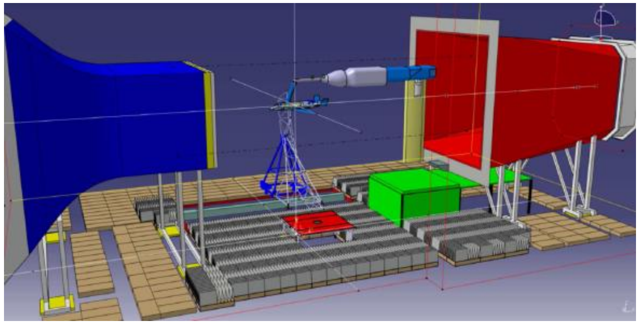

- **Test scheduled in late 2013**

Experimental campaigns : Istres static tests

- **Objective : validation** of the **noise reduction potential** of the **U-tail** concept**, without mean flow effects** but with **realistic Falcon engine** noise sources**:**
  - **U-tail** on a dedicated support located **behind the aircraft central engine;**
  - large **parametric configuration** matrix with **different engine operating conditions, A/C configurations** (different axial and lateral support positions)**;**
  - **Far-field noise** measurements using **ground inverted microphones** and **acoustic velocities measurements;**
  - Only **jet** and **aft turbo-machinery noise** will be **recorded** at far-field microphones by **isolating** the noise radiated by the **inlet using a shielding plate.**

- **Partners :**
  - **INCAS:** U-tail support design and manufacturing;
  - **MicroFlown:** innovative measurement technique for acoustic velocities characterization.

- **Test scheduled in 2015**

Assessment of the noise shielding potential of aft-bodies

- **Trade-off on a U-tail configuration:** U-tail axial position

aftbody axial position	U-tail leading edge at the nozzle exit	U-tail leading edge $+1.5D_{nozzle}$ downstream the nozzle exit
impact on cumulative certification noise levels	REF	+5 EPNdB

Best axial position: at the nozzle exit

- **Trade-off:** aft-body configuration

	Fixed U-tail (no trim capability) 	**Adjustable U-tail (with trim)** 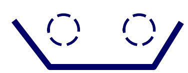	**Inverted T-tail** 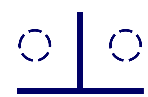	**Cross-tail** (usual Falcon tail) 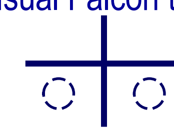
cumulative certification noise levels	-6 EPNdB	-5 EPNdB	-2 EPNdB	REF

DASSAULT AVIATION
DGT/DTIAE

Conclusion and perspectives

- **Novel A/C configurations** are **mandatory to reach 2020 ACARE objectives** of -20 EPNdB noise reduction**;**
- **Dassault Aviation** is investigating **innovative aft-bodies to shield rearward** propagating **engine noise** in **Cleansky SFWA** platform**;**
- **An overall strategy** mixing **prediction tools** and **experimental tests campaign** is proposed to downselect the **most promising noise shielding configurations;**
- **U-tail** concepts combined **with 2020 engine technologies** could allow to **reach the ACARE 2020 noise objectives;**
- An expected **TRL of 5 is targeted** at the **end of Cleansky** (2016) for the selected **noise shielding after-bodies;**
- **Further work** is **planned in CleanSky 2** to **increase maturity** of the concepts

Acknowledgments to the EU commission for funding works performed in CleanSky (grant agreement n° CSJU-GAM-SFWA-2008-001) and to all partners involved in studies relative to innovative aft-bodies

2nd EASN Association Workshop on Flight Physics and Propulsion

Multi-Objective Aerodynamic Optimisation of Engine Installation Design into Rotorcrafts

Andrea Garavello
Hit09 s.r.l

Rita Ponza
Hit09 s.r.l

Ernesto Benini
University of Padova

Outline

- **Background**
  - The UNIPD-hit09 Aerodynamic Optimisation Method;
  - The TILTOp & the *HEAVYcOPTer* programs;
- **Optimisation of the ERICA Tilt-Rotor air Intake System**
  - ERICA Engine Installation Description;
  - Intake geometry parameterization;
  - Intake Objective function formulation;
  - Optimisation results.
- **AW101 Engine Installation Optimisation**
  - AW101 Engine Installation Description;
  - Geometry Parameterisation;
  - Formulation of the Optimisation Problem;
  - Optimisation Results;
- **Concluding Remarks**
- **Acknowledgements**

Background

The TILTOp & HEAVYcOPTer Programs
Aerodynamic Optimisation at UNIPD-hit09

Background

The TILTOp & HEAVYcOPTer Programs

TILTOp

Contribution to the study of the air intake and exhaust integration into a tiltrotor nacelle

HEAVYcOPTer

Contribution to optimisation of heavy helicopter engine installation design

Clean Sky **Call for Proposal**

Issued by AgustaWestland S.P.A. For improving the European ERICA tilt rotor engine installation efficiency

Clean Sky **Call for Proposal**

Issued by AgustaWestland Ltd. For improving AW101 engine installation efficiency

Objectives

Reduction of heavy class helicopters and tilt rotors engine/airframe integration loss

- **Engine Air Intakes system aerodynamic shape optimisation;**
- **Engine Exhaust system aerodynamic shape optimisation.**

Method

UNIPD/hit09 GDEA based optimisation method

Background

Aerodynamic Optimisation at UNIPD-hit09

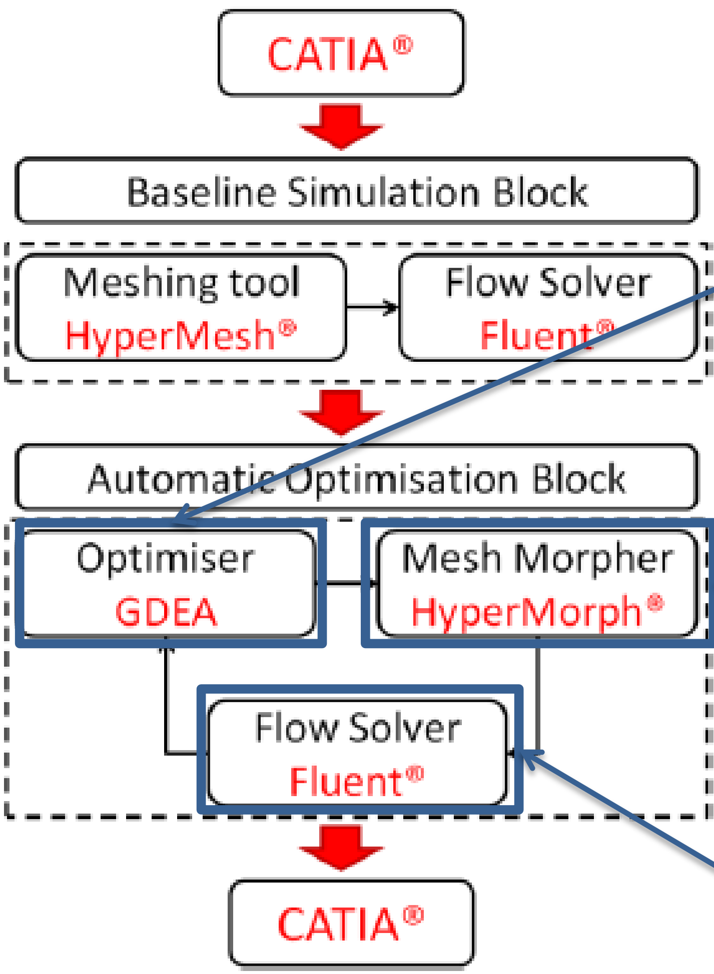

General purpose aerodynamic optimisation loop
Developed in the framework of the *Clean Sky GRC2*

GDEA
UNIPD Multi-objective genetic algorithm

ALTAIR HyperMorph®
Application of parametric changes to FE models

ANSYS FLUENT®
Flow solver for objective function evaluation

Optimisation of the ERICA Tilt-Rotor air Intake System

ERICA Installation Description

Geometry Parameterisation

Optimisation Problem Formulation

Optimisation Results

Optimisation of the ERICA air Intake System

ERICA Installation Description

Architectural Constraints for Shape Modification

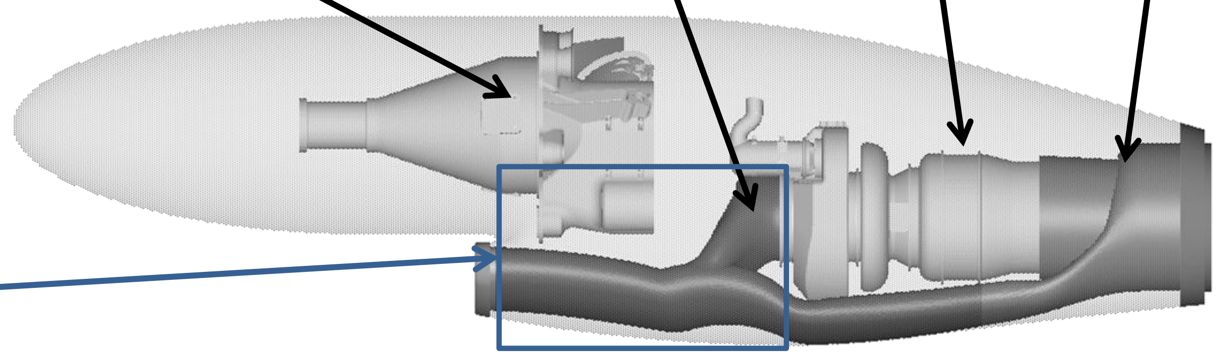

Intake duct geometrical definition given by the linear combination of 8 basic shapes

$$v(\alpha_i) = \sum_{i=1}^{8} \alpha_i Sh_i$$

Global displacement vector

Shapes scaling factors chosen by GDEA

User defined Basic shapes

Optimisation of the ERICA air Intake System

Geometry Parameterisation

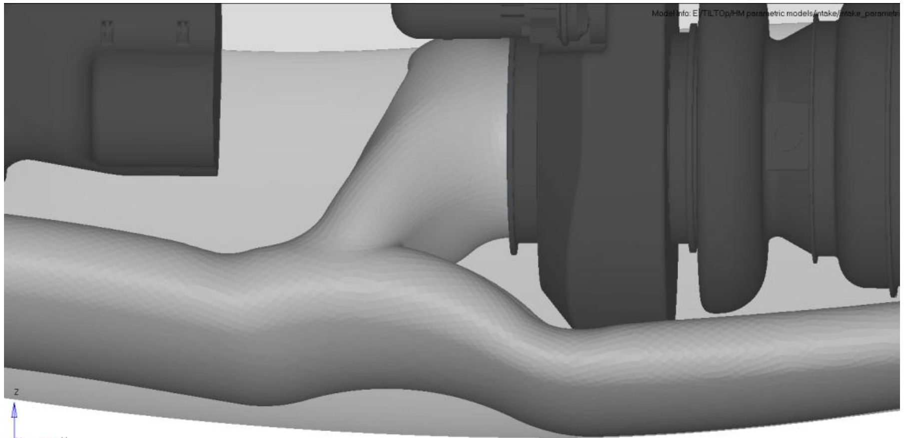

Shape-1: Second bend inner surface shape

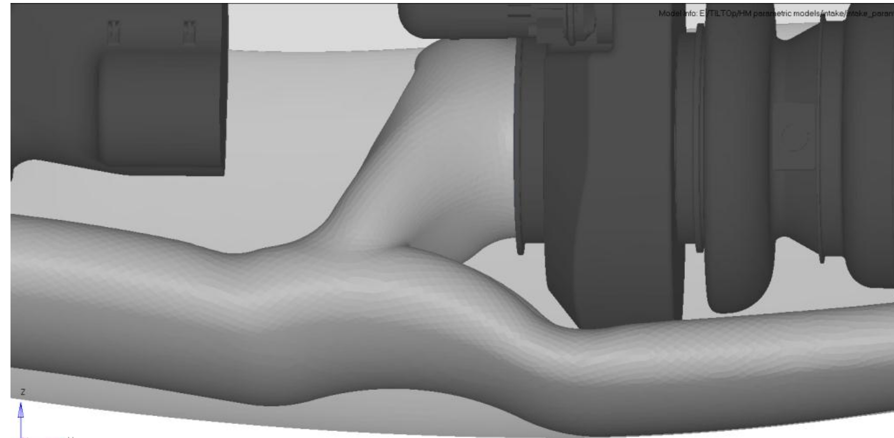

Shape-2: By-pass duct shape

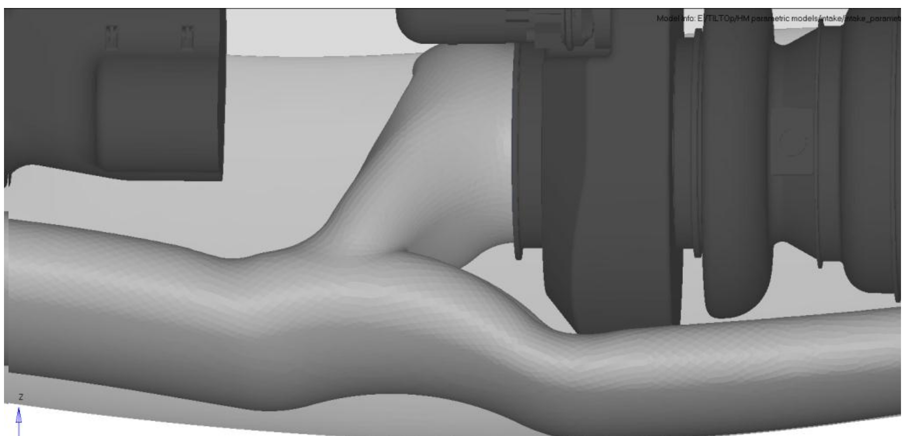

Shape-3: Entry duct shape

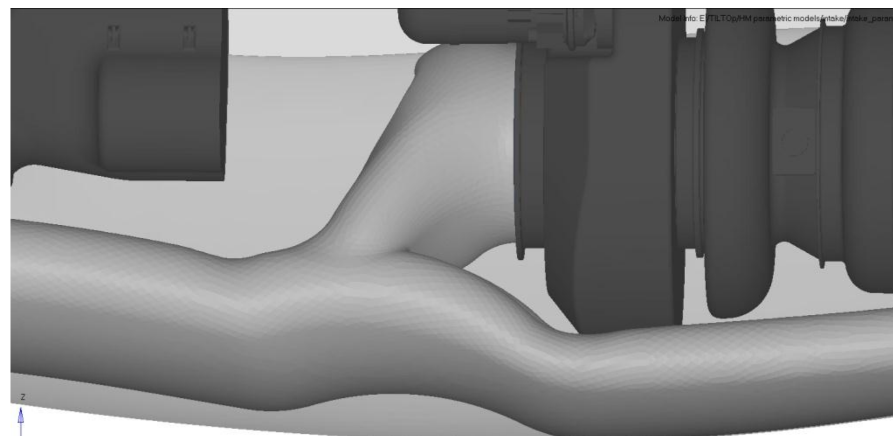

Shape-4: S-connection “x” position

Optimisation of the ERICA air Intake System

Geometry Parameterisation

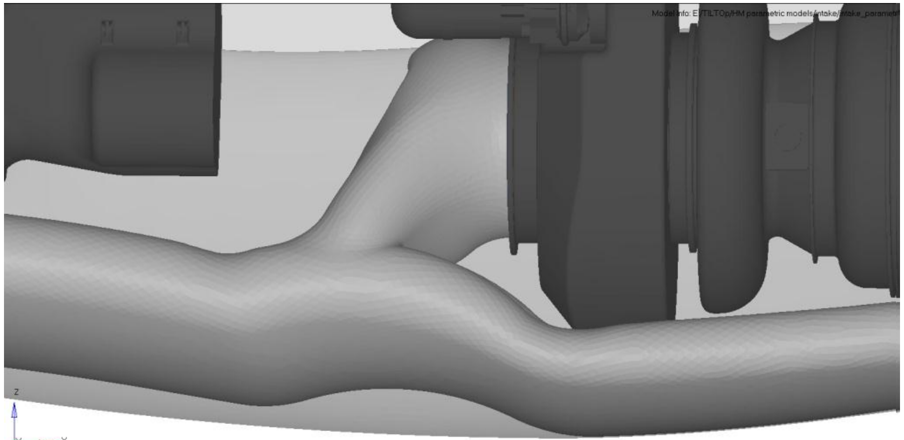

Shape-5: First bend inner surface shape

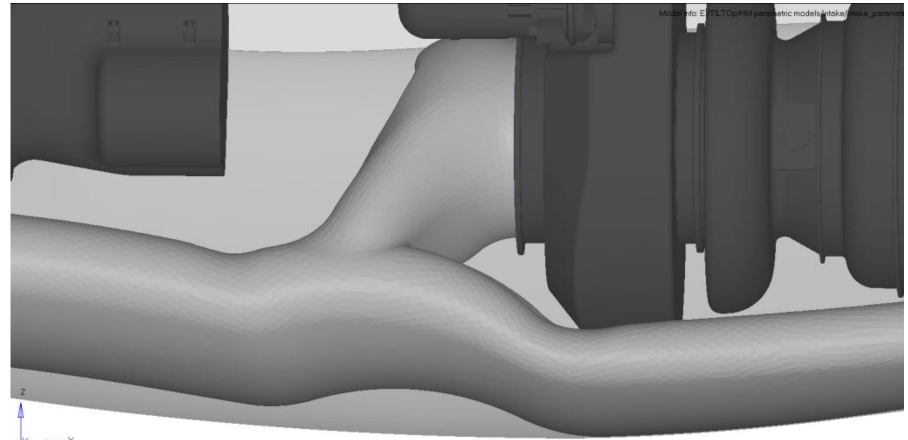

Shape-6: First bend outer surface shape

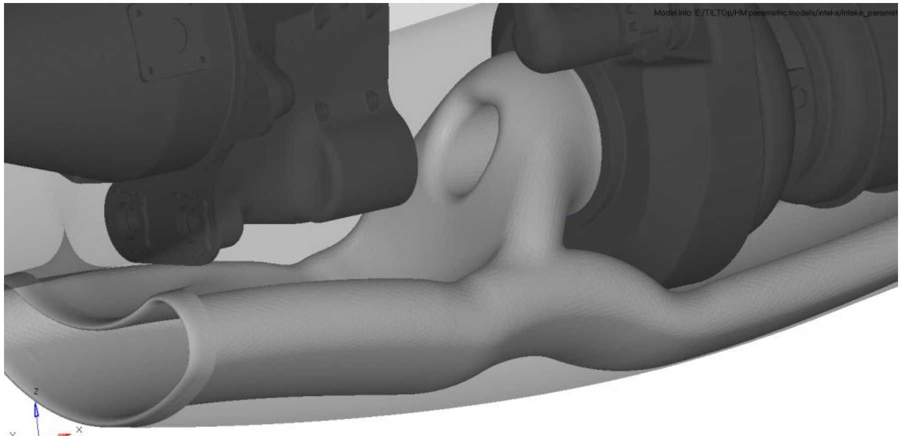

Shape-7: Second bend outer surface shape

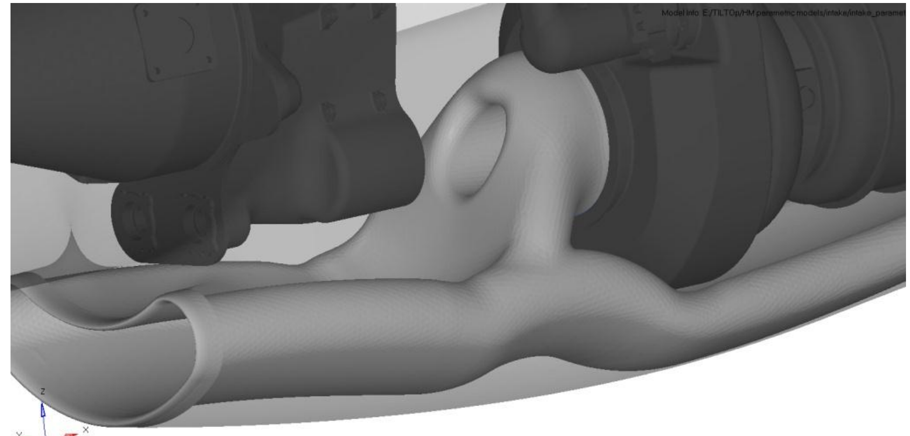

Shape-8: Second bend outer surface shape

Intake Aerodynamic optimisation using UNIPD/hit09 automatic design method at cruise condition

Reduction of inlet total pressure loss → *Increasing Power Output/Decreasing Fuel consumption*

Reduction of Flow Distortion at the engine AIP → *Increasing compressor surge margin and stability*

$$Maximize[\eta_p(\alpha_i); -DC60(\alpha_i)]$$

$$\eta_P = \frac{P_f}{P_\infty}$$

f: AIP section

∞: free stream condition

$$DC(\theta) = \frac{P_f - P_\theta}{q_f}$$

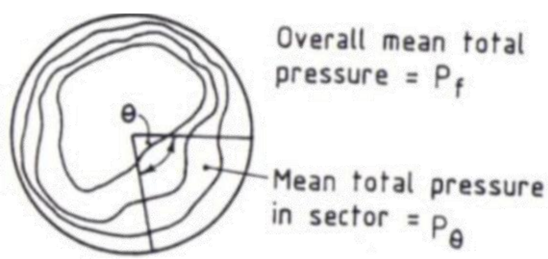

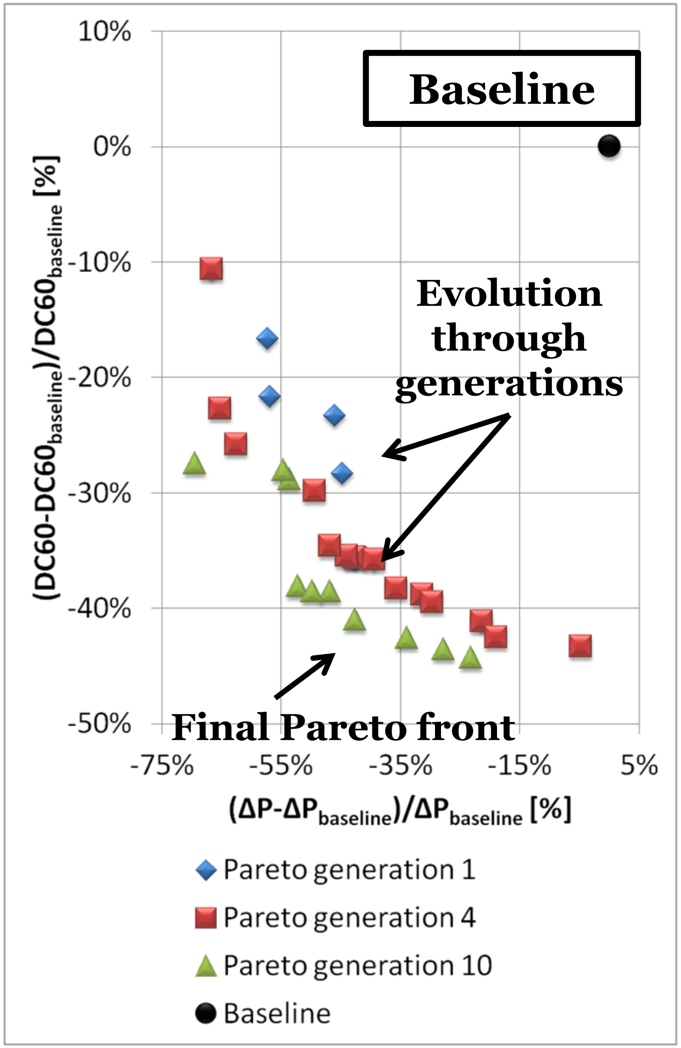

Baseline
Evolution through generations
Final Pareto front
10%
0%
-10%
-20%
-30%
-40%
-50%
-75%
-55%
-35%
-15%
5%
(DC60-DC60baseline)/DC60baseline [%]
(ΔP-ΔPbaseline)/ΔPbaseline [%]
Pareto generation 1
Pareto generation 4
Pareto generation 10
Baseline

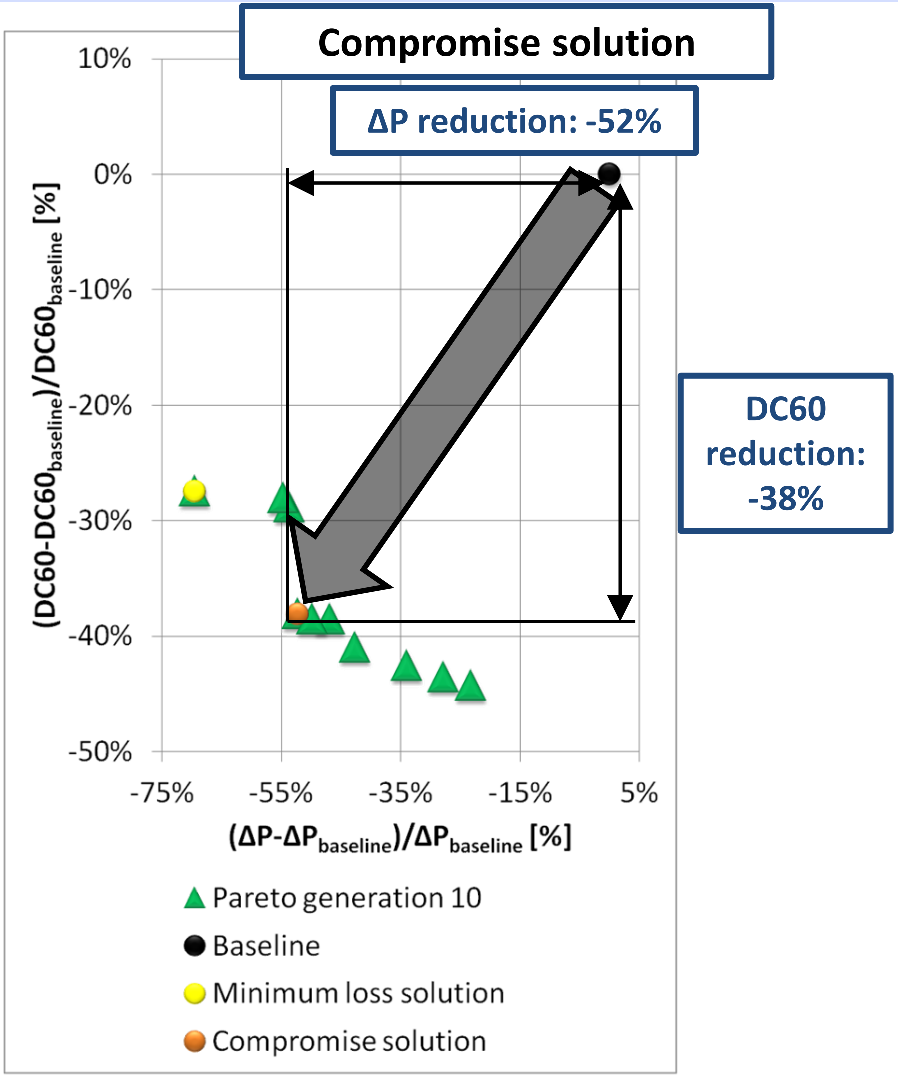

Compromise solution
ΔP reduction: -52%
DC60 reduction: -38%
10%
0%
-10%
-20%
-30%
-40%
-50%
-75%
-55%
-35%
-15%
5%
(DC60-DC60baseline)/DC60baseline [%]
(ΔP-ΔPbaseline)/ΔPbaseline [%]
Pareto generation 10
Baseline
Minimum loss solution
Compromise solution

Optimisation of the ERICA air Intake System

Optimisation Results

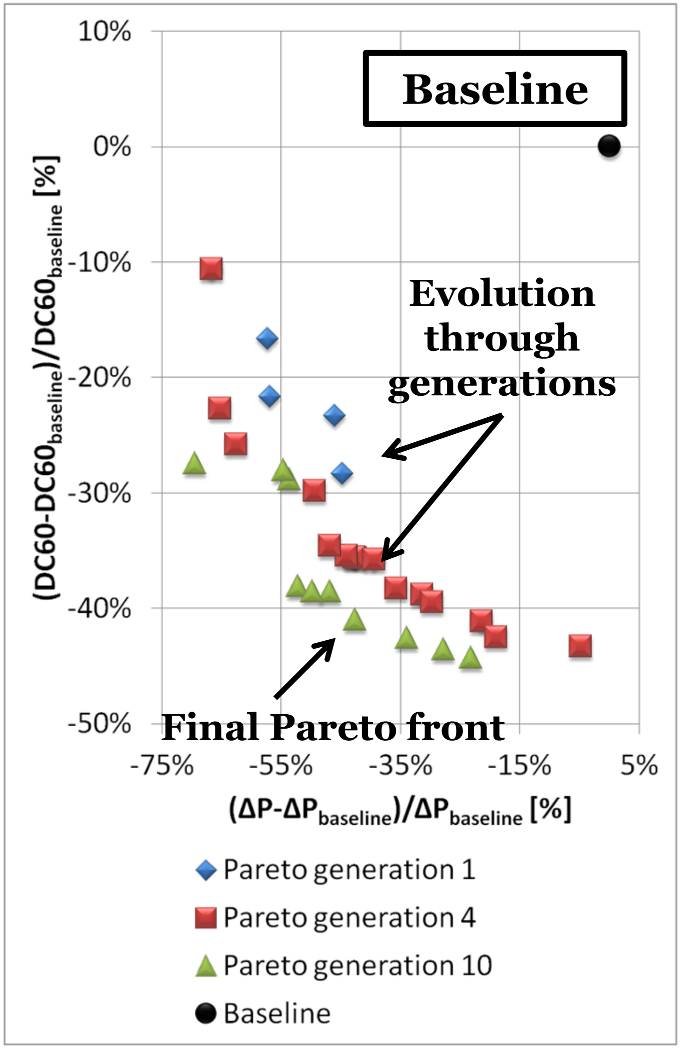

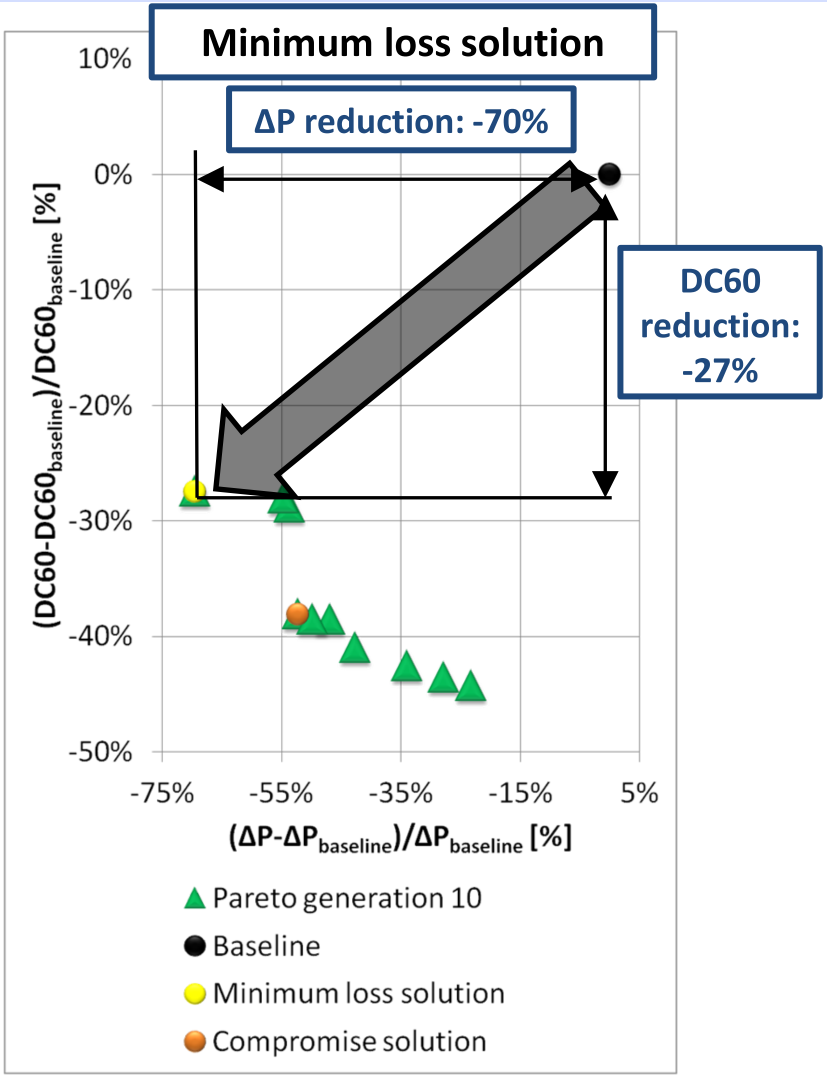

Optimisation of the ERICA air Intake System

Optimisation Results

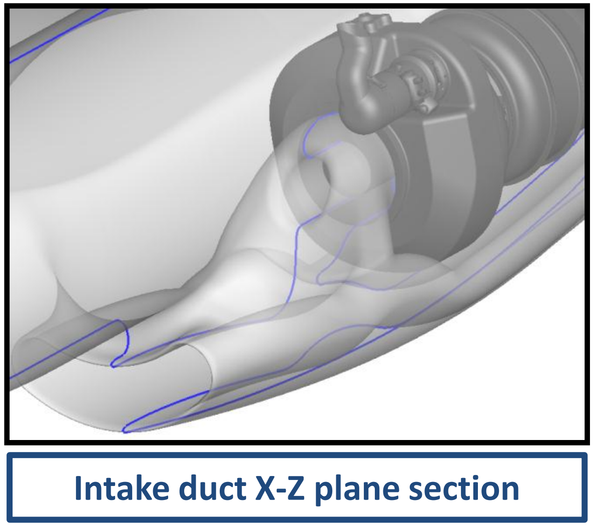

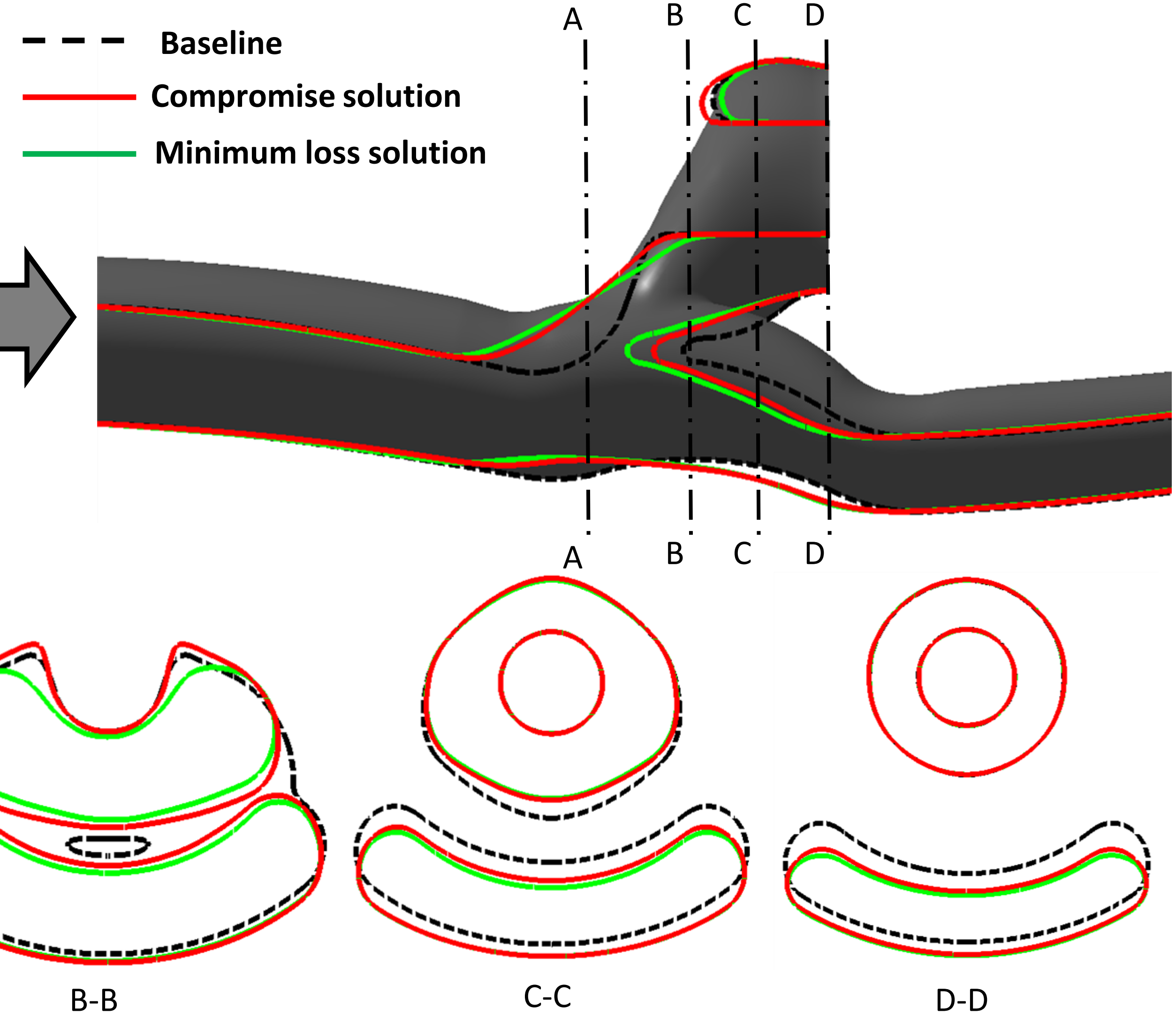

Intake duct streamlines coloured by normalized total pressure

Baseline	Compromise solution	Minimum loss solution

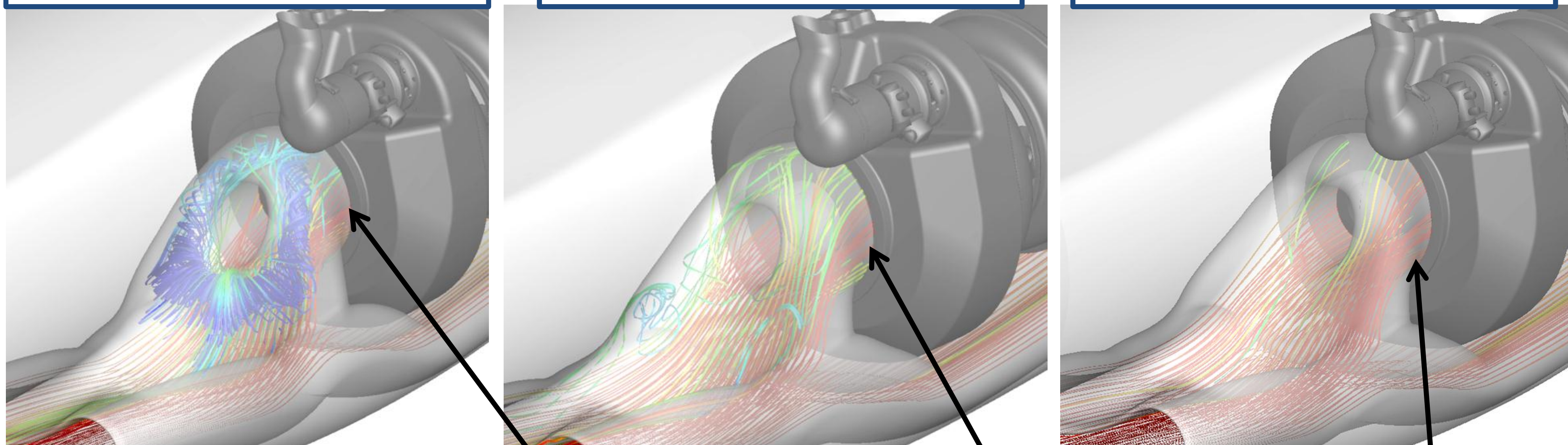

AIP Normalized Total Pressure Contours

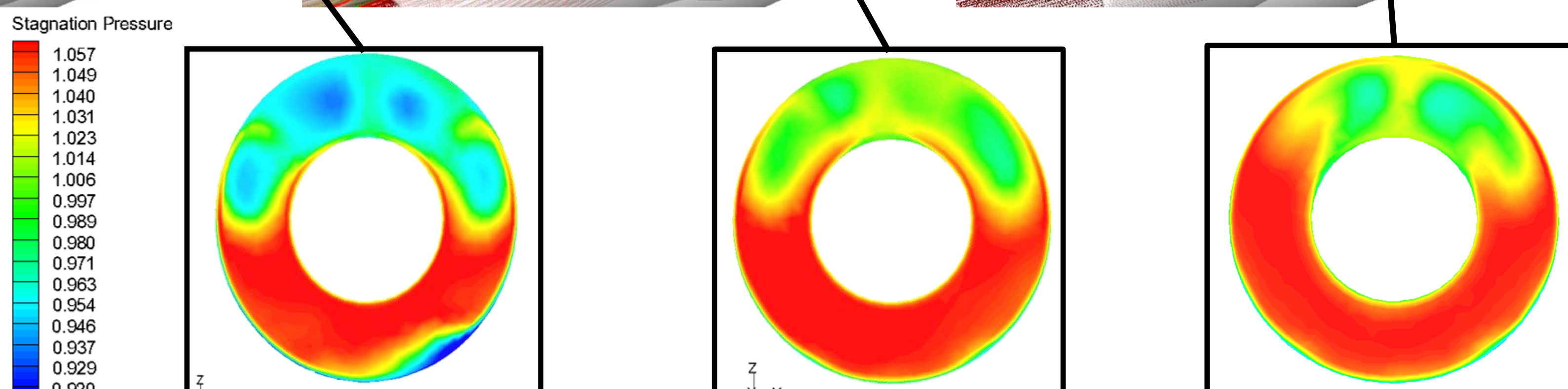

AW101 Engine Installation Optimisation

Installation Description
Geometry Parameterisation
Optimisation Problem Formulation
Optimisation Results

AW101 Engine Installation Optimisation

Installation Description

3 engines configuration

- engine#1 and engine#3 are arranged symmetrically on the two sides of the fuselage;
- engine#2 is positioned on top of the fuselage roof.
- Intakes and exhausts are numbered accordingly.

Intake#1, intake#2 and exhaust#2 are submitted to optimisation within the HEAVYcOPTer framework

Here, results relative to intake#1 optimisation are presented

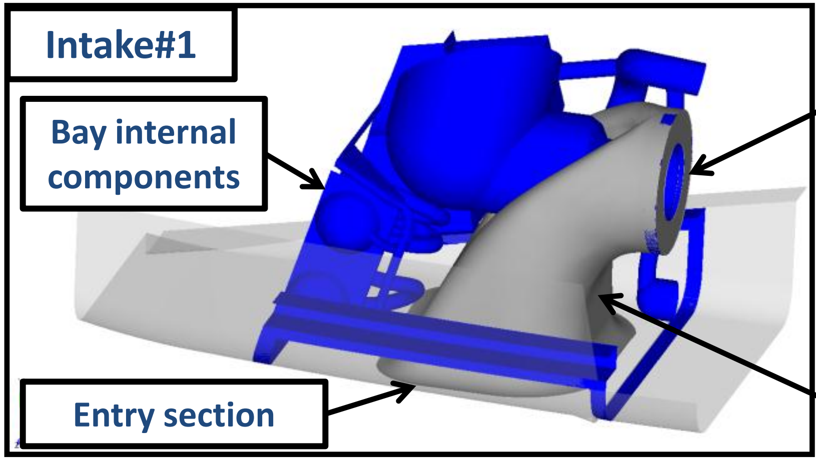

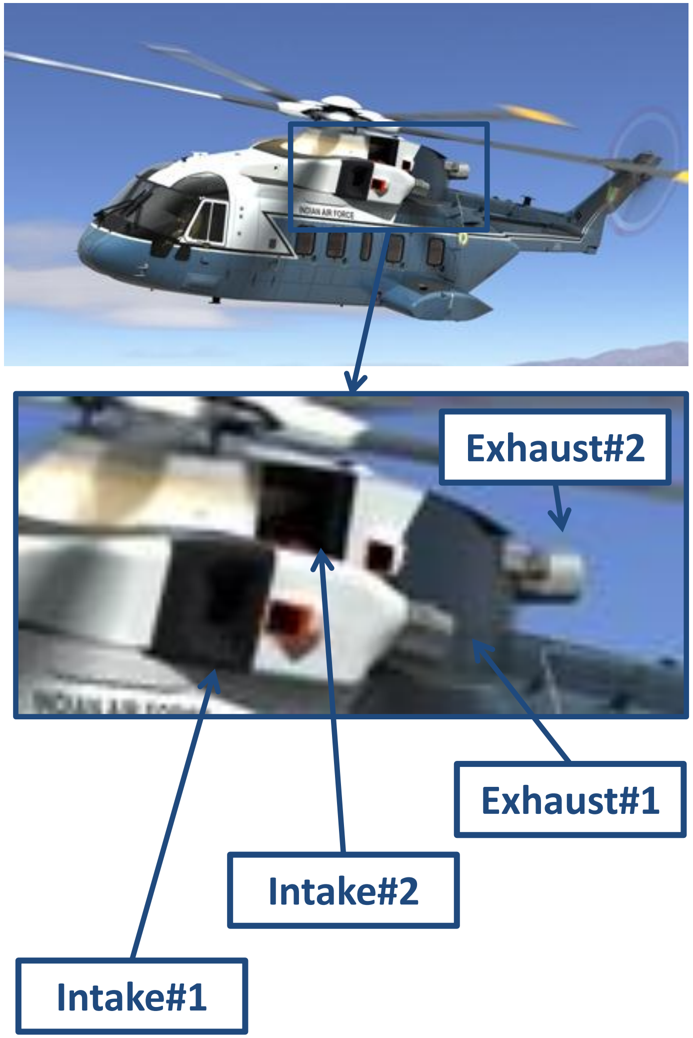

AW101 Engine Installation Optimisation

Geometry Parameterisation

Intake duct geometrical definition given by the linear combination of 14 basic shapes

$$v(\alpha_i) = \sum_{i=1}^{14} \alpha_i Sh_i$$

Global displacement vector

Shapes scaling factors chosen by GDEA

User defined Basic shapes

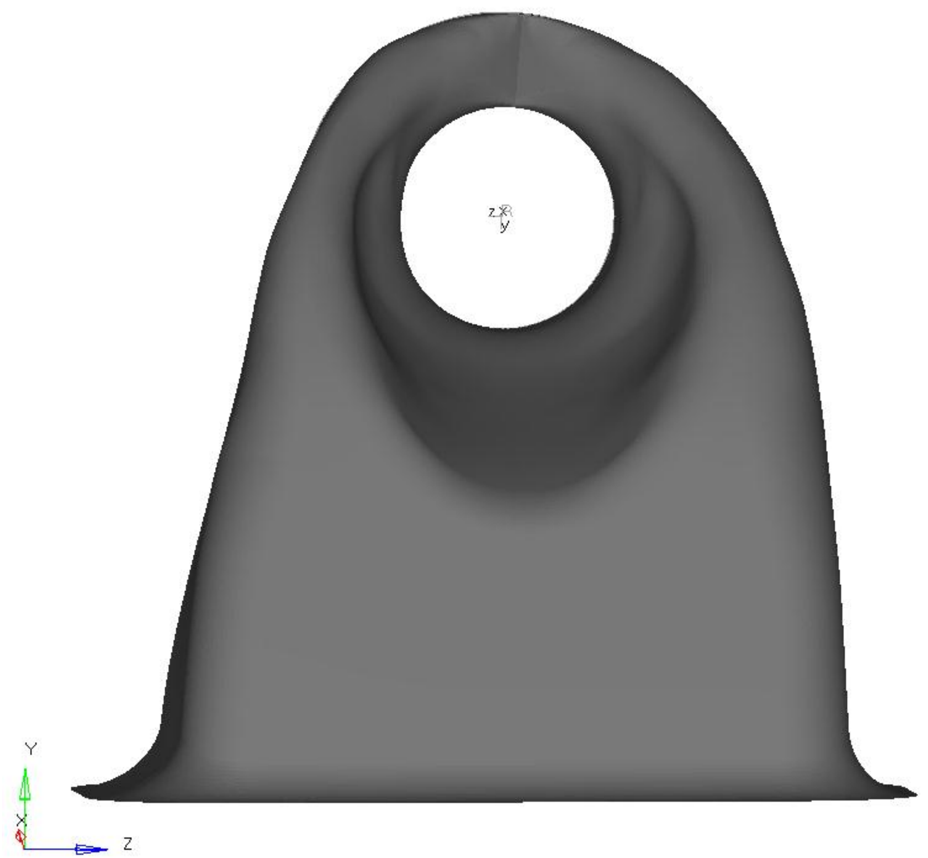

Baseline → **Sh1** → **Sh2**

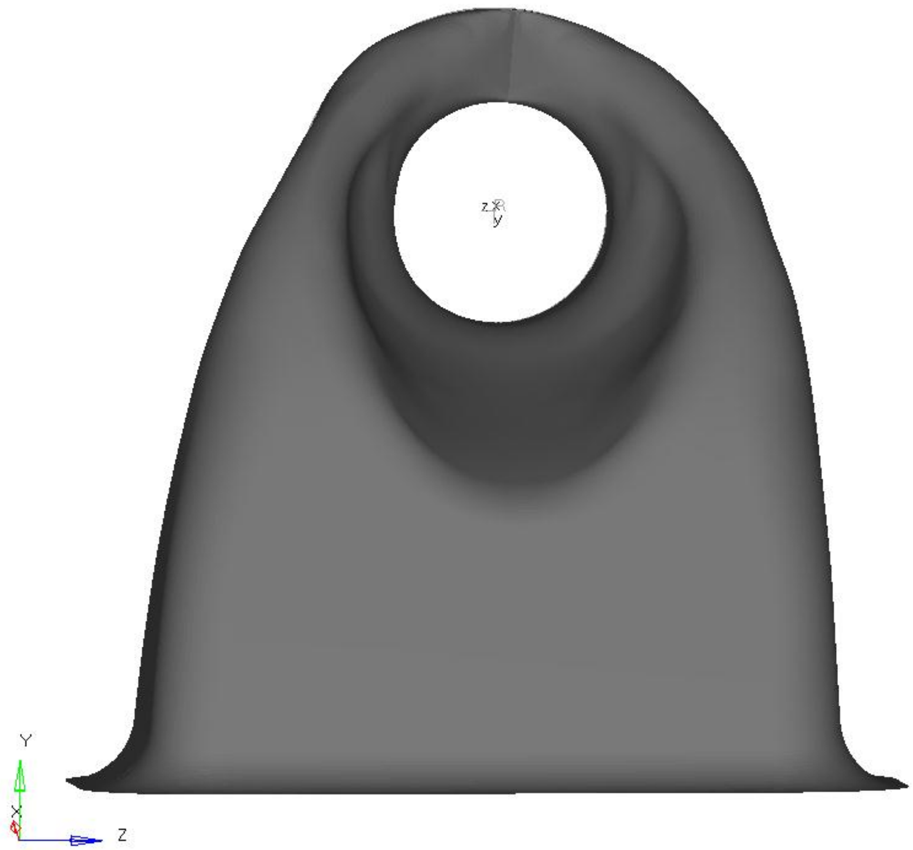

Baseline → **Sh6** → **Sh7**

Baseline → **Sh3** → **Sh4**

Geometry Parameterisation

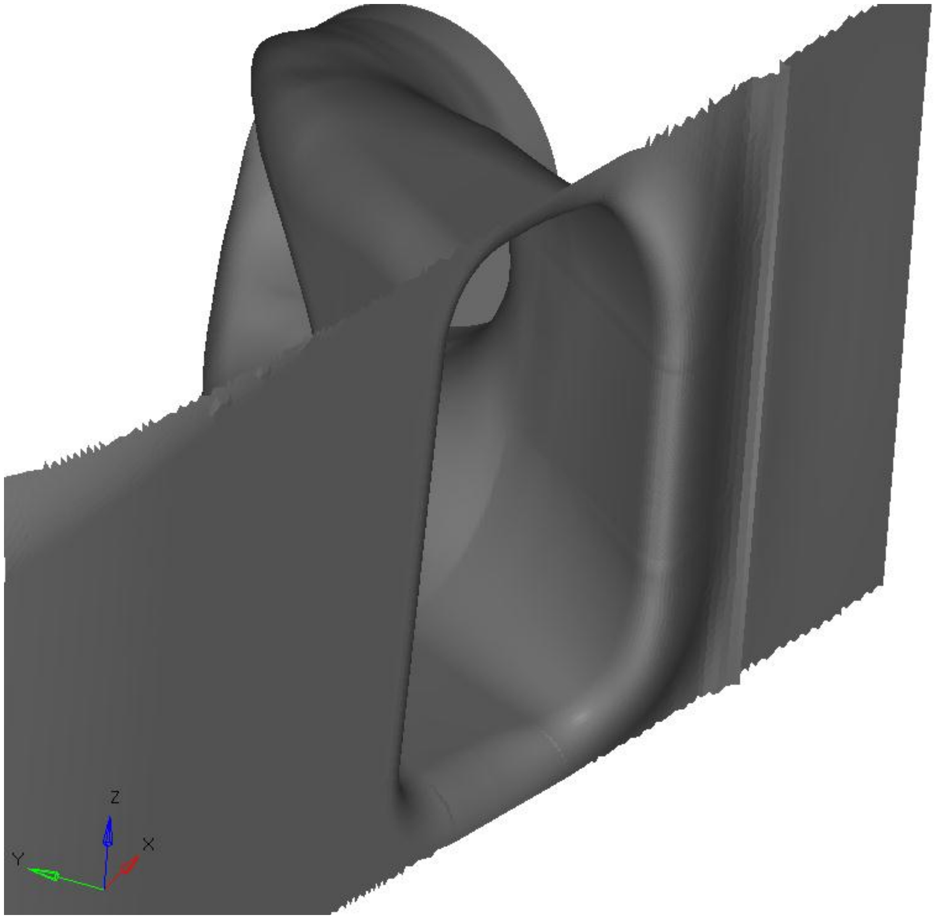
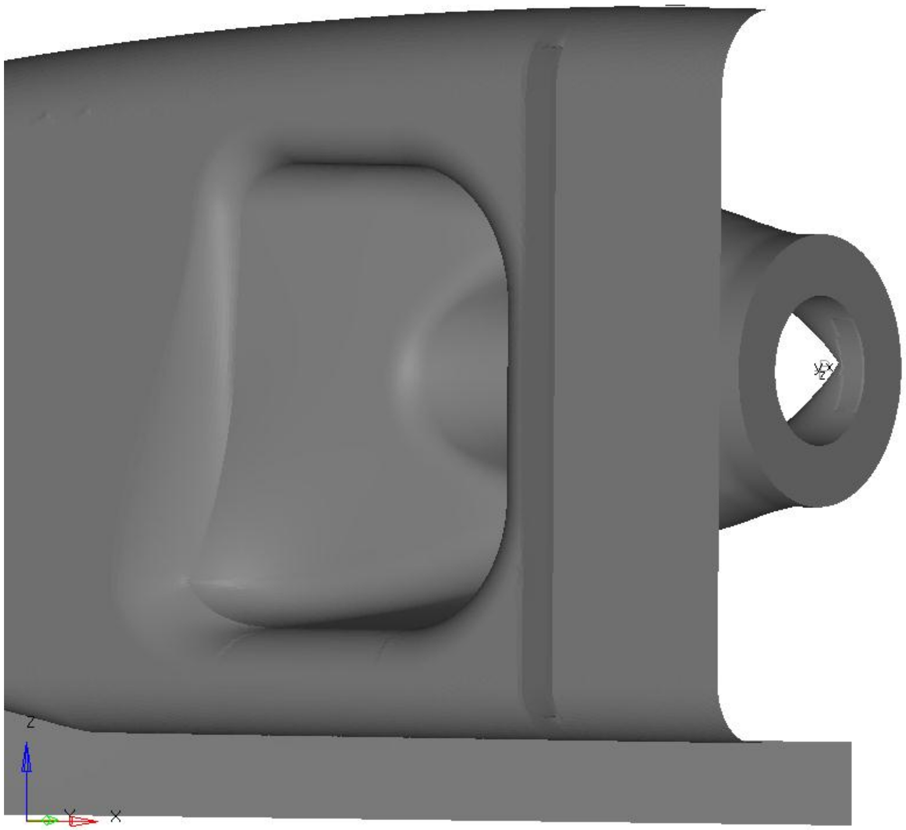

Baseline → **Sh5** → **Sh11**

Baseline → **Sh8** → **Sh9**

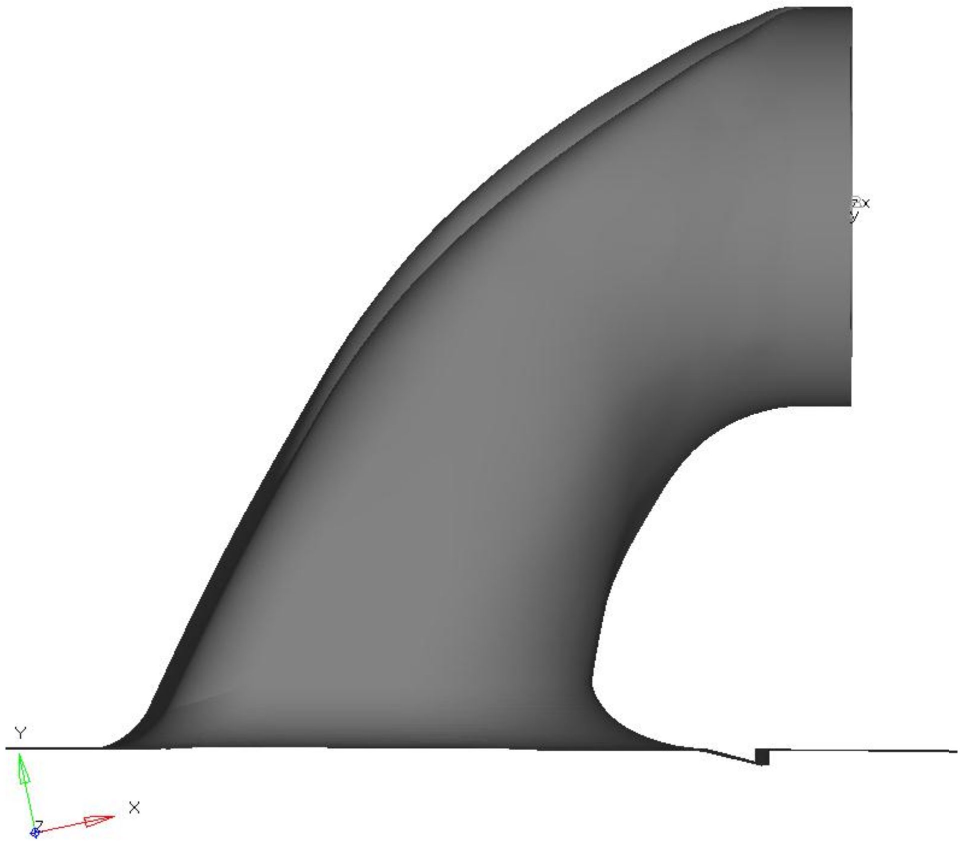

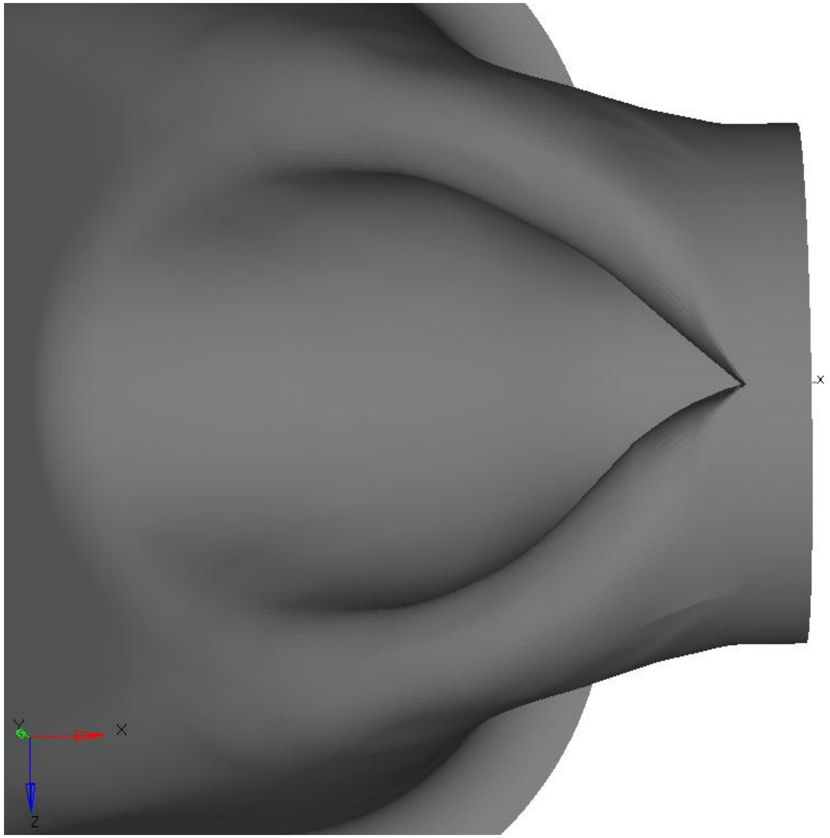

Baseline → Sh10 → Sh14

Baseline → Sh12 → Sh13

Multi-point/Multi-objective approach;

- Two flight conditions are optimised at the same time;
- This is possible thanks to the multi-objective capabilities of GDEA.

Design parameters vector

$$x = [\alpha_1 \ldots\ldots \alpha_{14}]$$

$$\text{minimize } \{G(x) = [F(x) + PF(x)]\}$$

Multi-Point objective function

Total pressure loss are minimised at hover and forward flight simultaneously.

$$F(x) = \begin{bmatrix} \Delta P_T \mid @\,hover \\ \Delta P_T \mid @\,cruise \end{bmatrix}$$

Penalty function

DC60 distortion index must be equal or lower than the baseline for a new design to be considered;
Distortions are taken into account by means of penalty functions.

$$PF(x) = \begin{bmatrix} 0 & \text{if } \mathrm{DC60} \le \mathrm{DC60}_{\mathrm{baseline}} \\ \beta \left| \dfrac{DC60 - DC60_{baseline}}{DC60_{baseline}} \right|^{\gamma} & \text{if } \mathrm{DC60} > \mathrm{DC60}_{\mathrm{baseline}} \end{bmatrix}$$

AW101 Engine Installation Optimisation

Optimisation Results

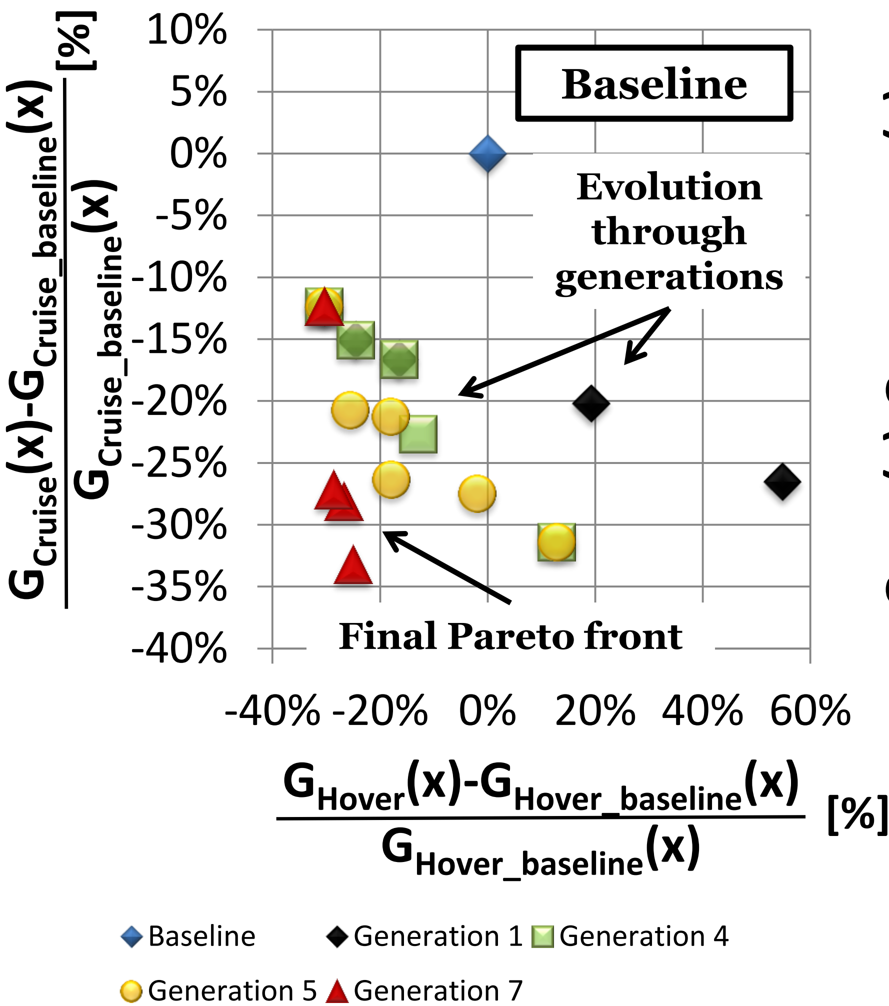

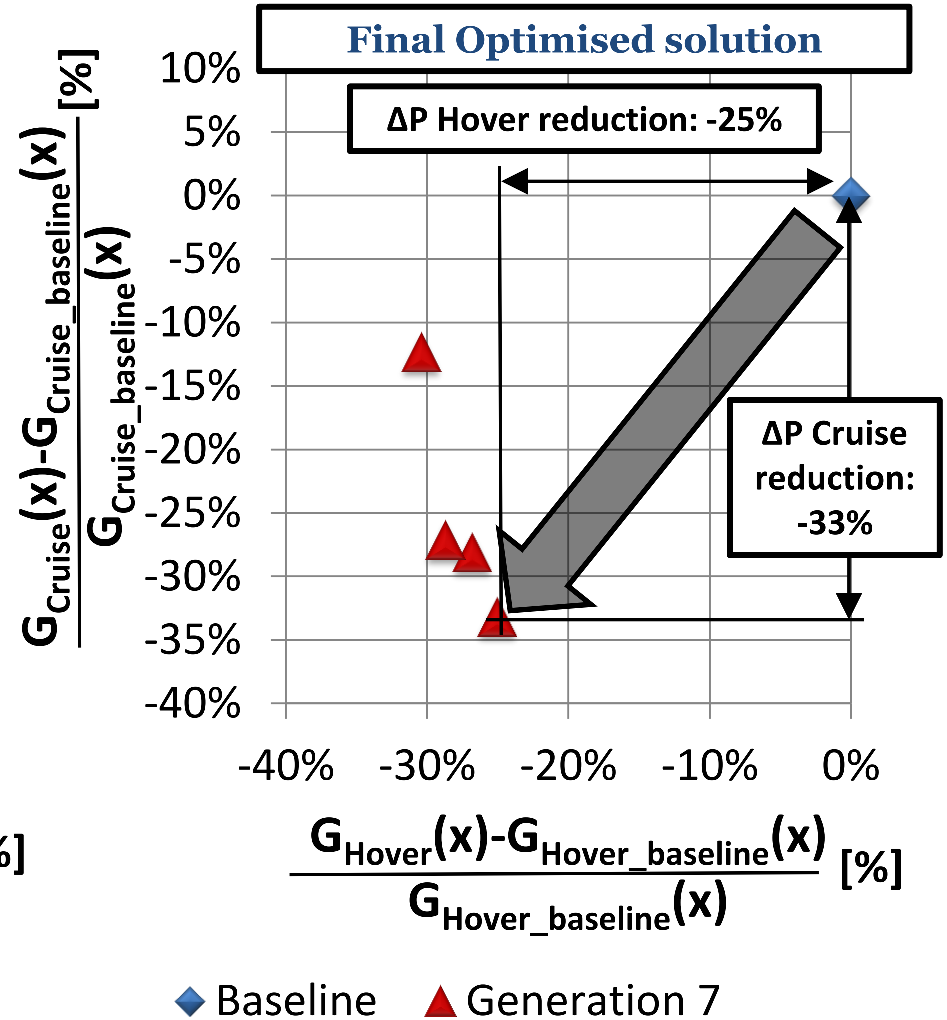

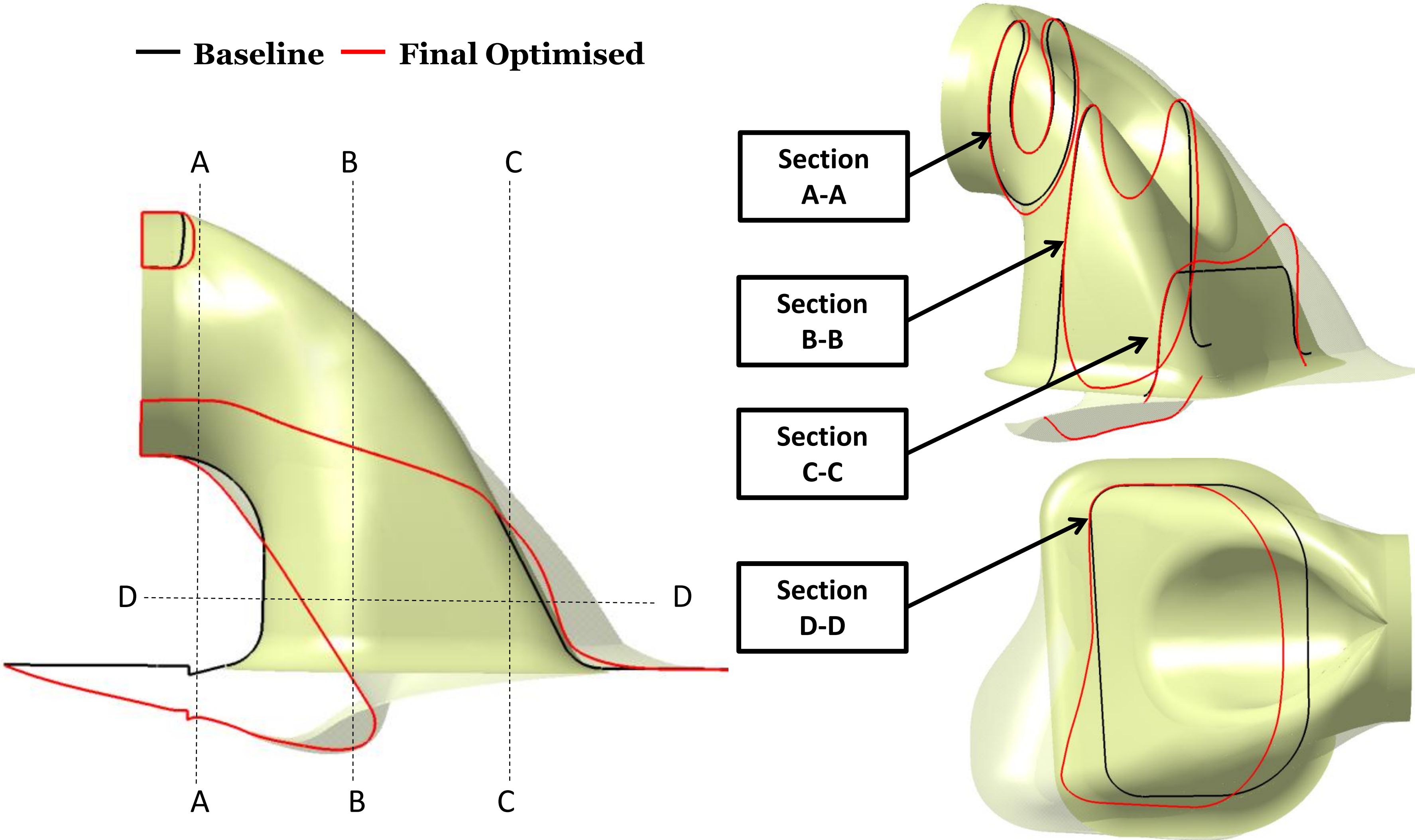

Baseline
Final Optimised
A
B
C
D
D
A
B
C
Section A-A
Section B-B
Section C-C
Section D-D

AW101 Engine Installation Optimisation

Optimisation Results

AIP Total pressure distribution comparison	Total pressure distribution along the duct

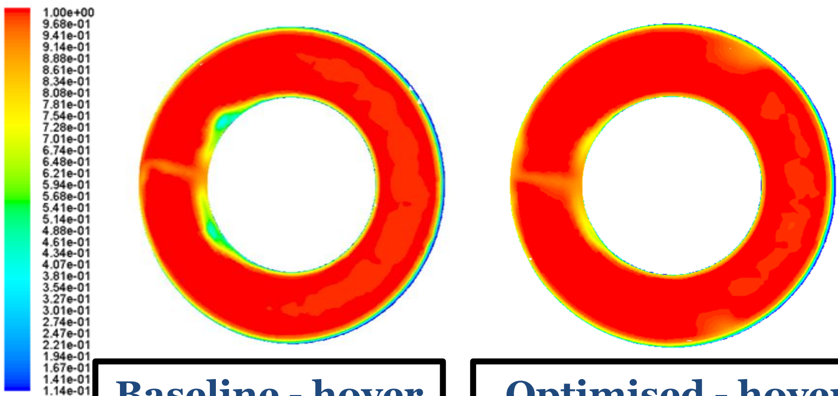

Baseline - hover | Optimised - hover

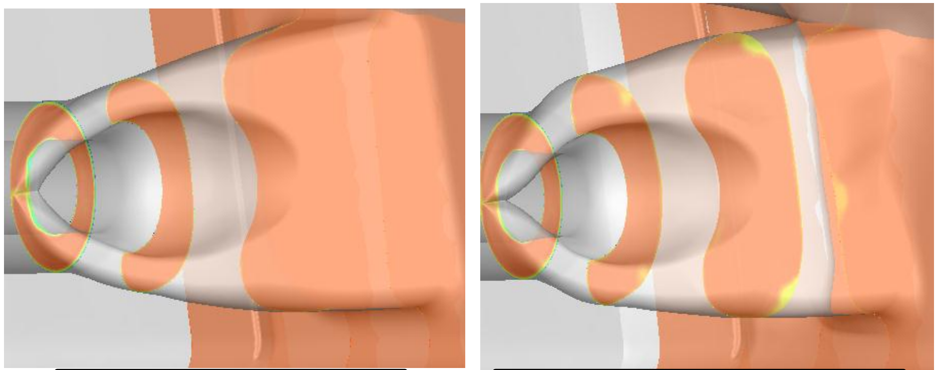

Baseline - hover | Optimised - hover

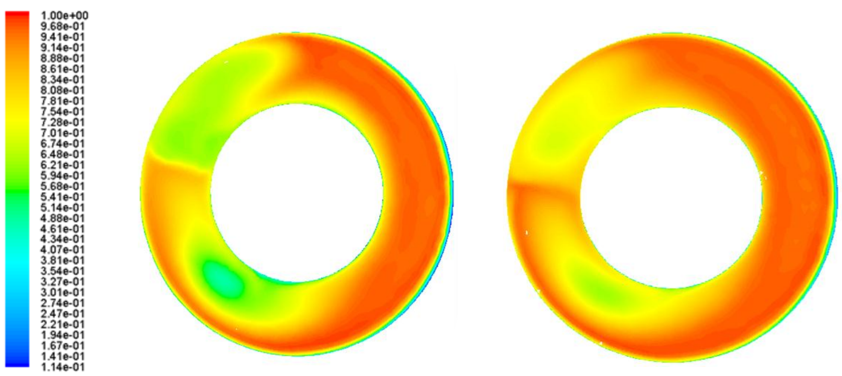

Baseline - cruise | Optimised - cruise

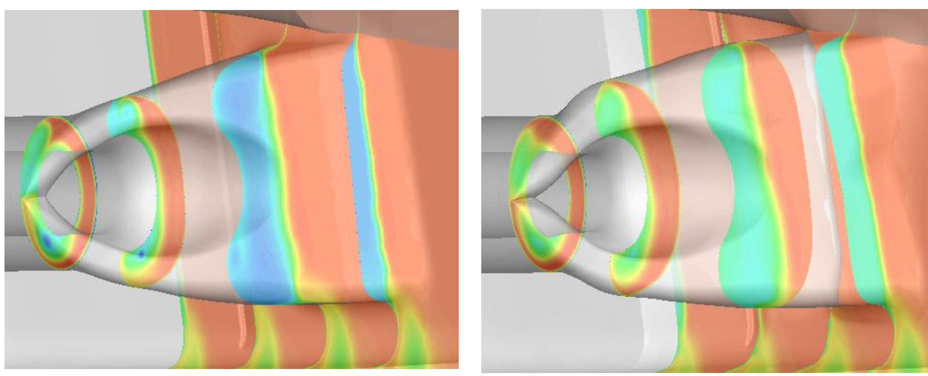

Baseline - cruise | Optimised - cruise

Concluding Remarks

Concluding Remarks

- The GDEA based optimisation method demonstrated its capabilities in dealing with general shape components and complex constraints configurations;
- Optimisations of ERICA and AW101 components showed the possibility to improve performance of existing designs by means of automatic methods;
- The adopted multi-objective approach allowed to easily deal with conflicting design objectives;
- Significant improvement margins have been highlighted for the engine installation performance, for both aircrafts, in particular considering the forward flight case;
- The parametric and multi-objective approach chosen proved its effectiveness in providing robust and optimal design alternatives to the current aircrafts intake configurations.

Acknowledgements

Acknowledgements

- **Clean Sky Joint Undertaking**

These research activities are partially funded by the Clean Sky Joint Undertaking (CSJU) under projects GAM-GRC, related to activities performed within the ITD Green Rotorcraft. The authors would like to thank the CSJU for the financial support and *Dr. Sebastian Dubois* from the CSJU for the management monitoring of the HEAVYcOPTer program;

- **AgustaWestland aerodynamic department**

All the research work described throughout this presentation was carried out in tight cooperation with the AgustaWestland aerodynamic department. The authors would like to thank engineers *Antonio Saporiti*, *Alessandro Scandroglio*, *Alessandro Stabellini*, *Andrew Ramage*, *Nigel Scrase* and *Karl Baverstock* from AgustaWestland for their precious advice and support.

Advanced Hybrid Engine for Aircraft Development

2nd EASN Workshop on Flight Physics and Propulsion

Dr. Arvind Gangoli Rao, TU Delft

Improvement in aircraft fuel burn

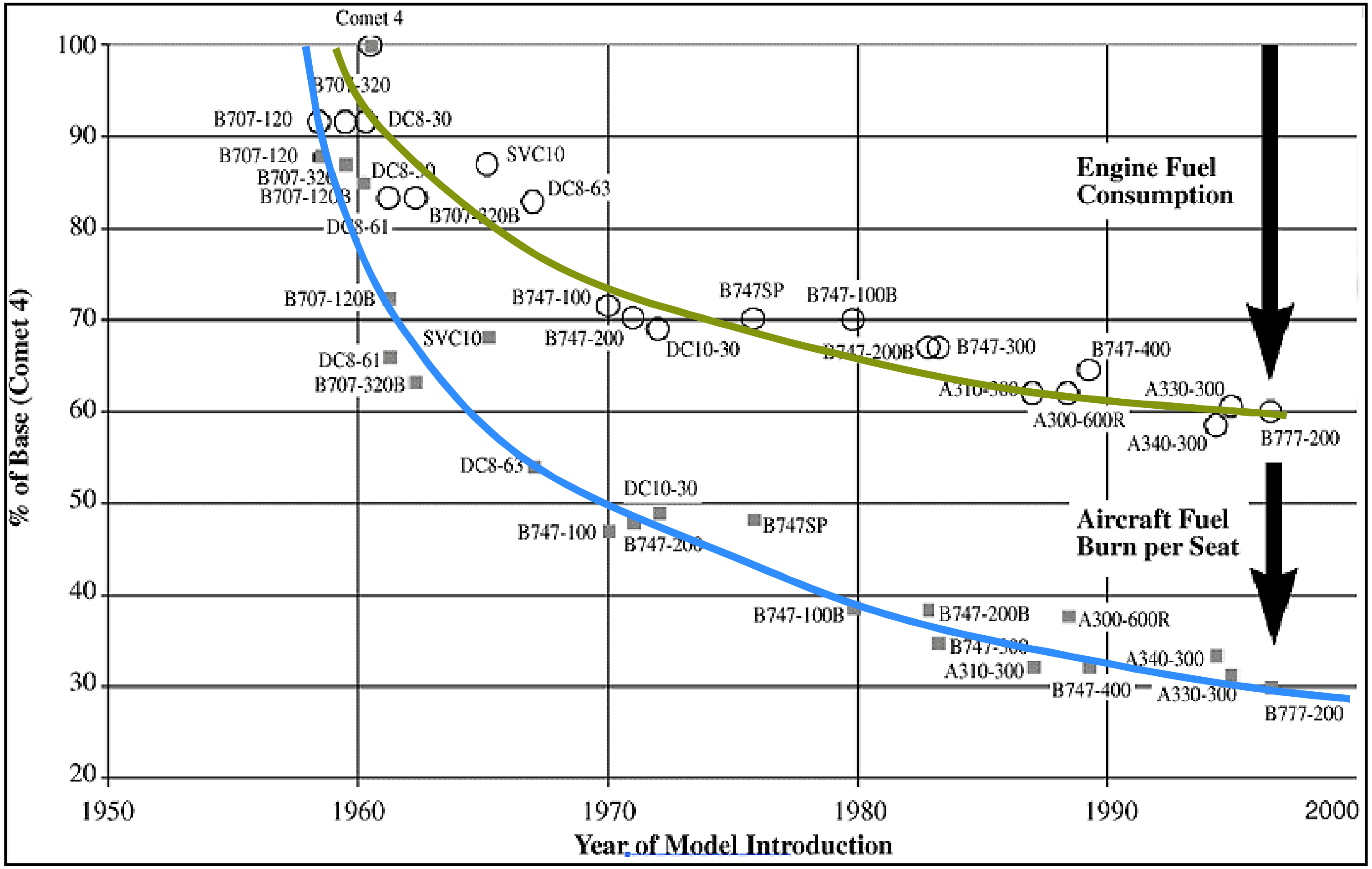

http://www.grida.no/publications/other/ipcc_sr/?src=/climate/ipcc/aviation/avf9-3.htm

Aircraft Seating Efficiency

Then ☺

Now ☹

Growth of civil aviation

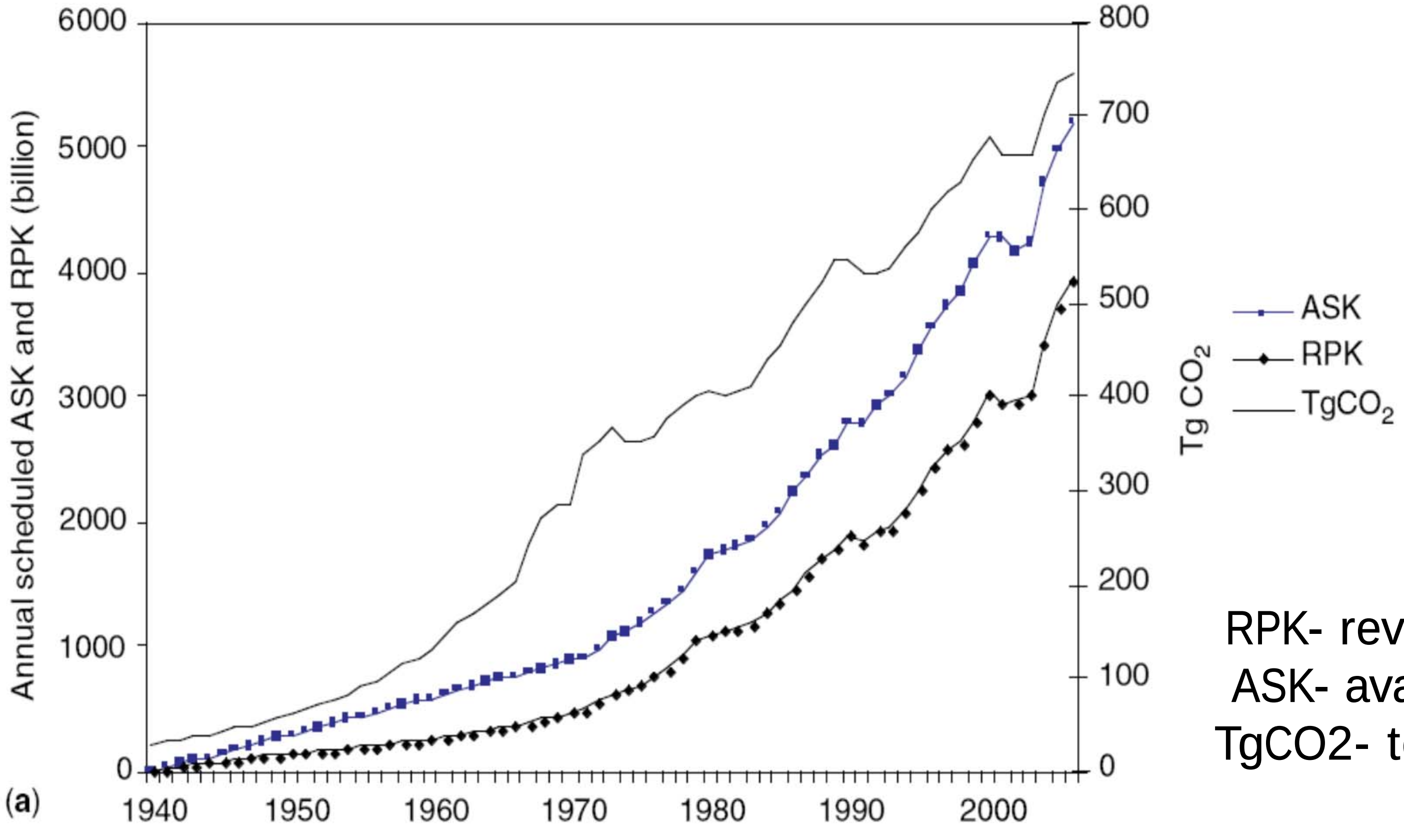

RPK- revenue pass. Km
ASK- available seat km
TgCO2- terra gm of CO2

B. Owen & David Lee "Aircraft Emissions", Encyclopedia of aerospace engg. John Wiley &Sons

Global CO_2 emissions from commercial airlines

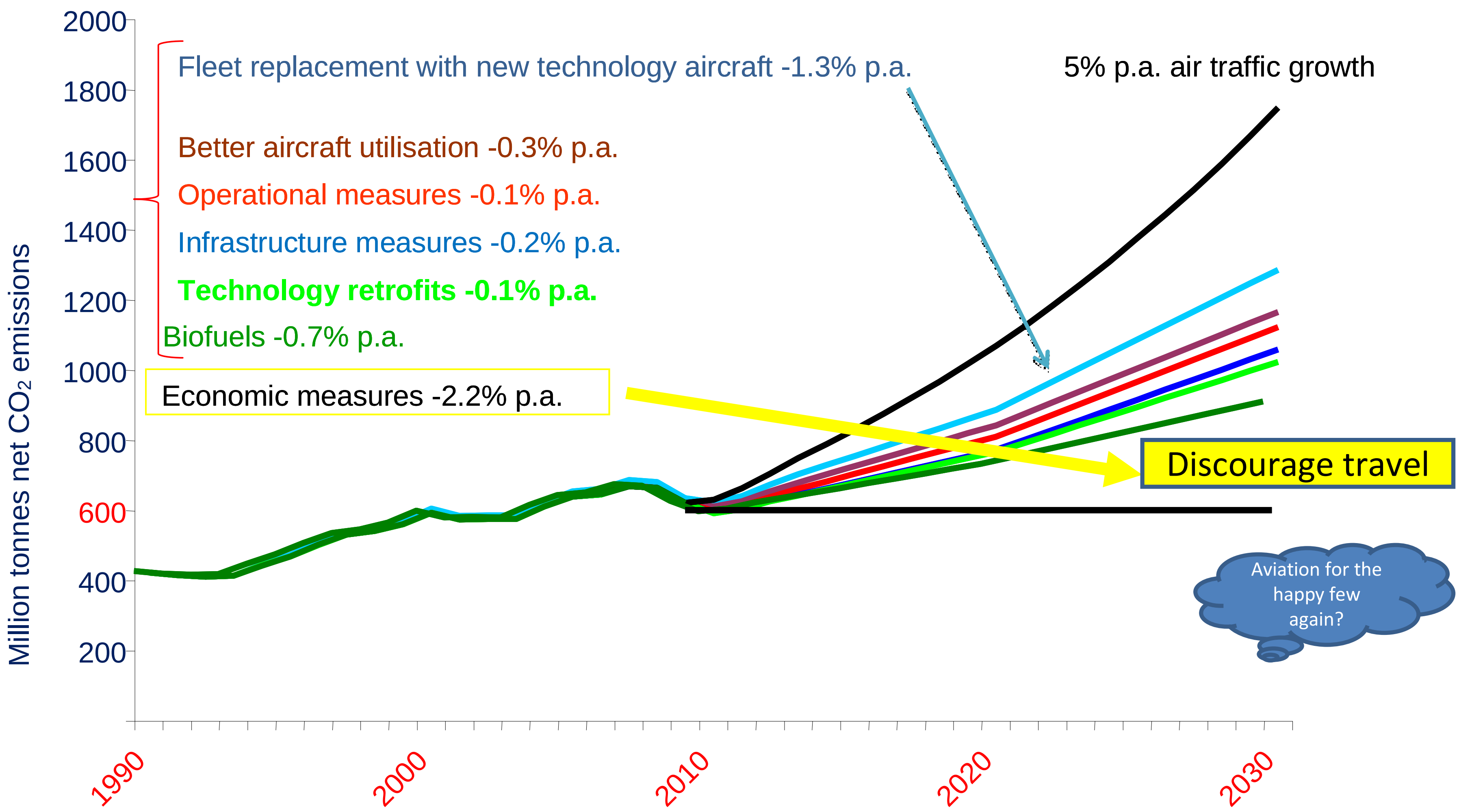

© 2009 IATA

Main Challenges of Civil Aviation

EFFICIENCY

EMISSION

Energy Source

NOISE

ACARE Goals for EU

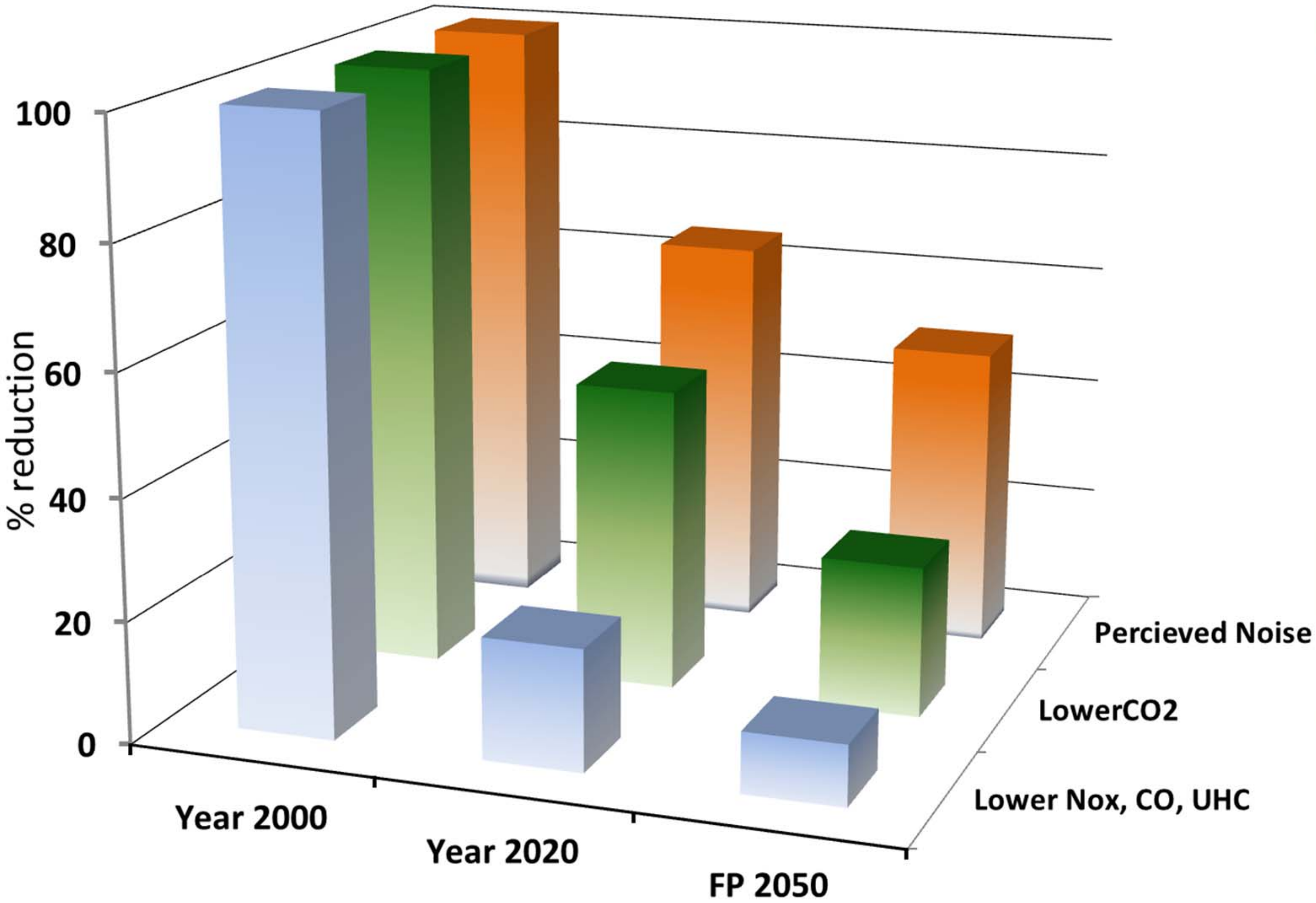

Fuel consumption

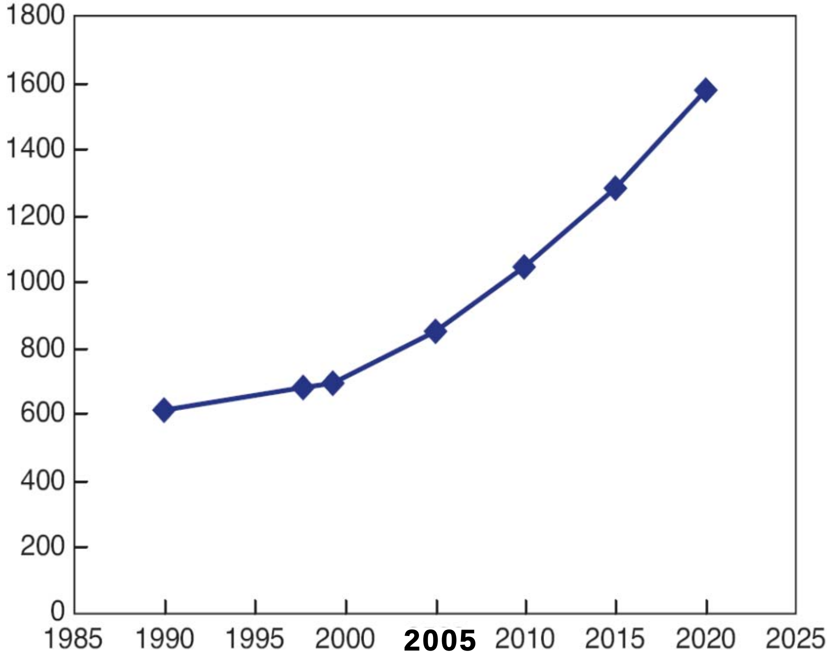

Source: US Department of Energy

World jet fuel consumption between now and 2020 (Million liters per day)

Hubbert's Peak Theory

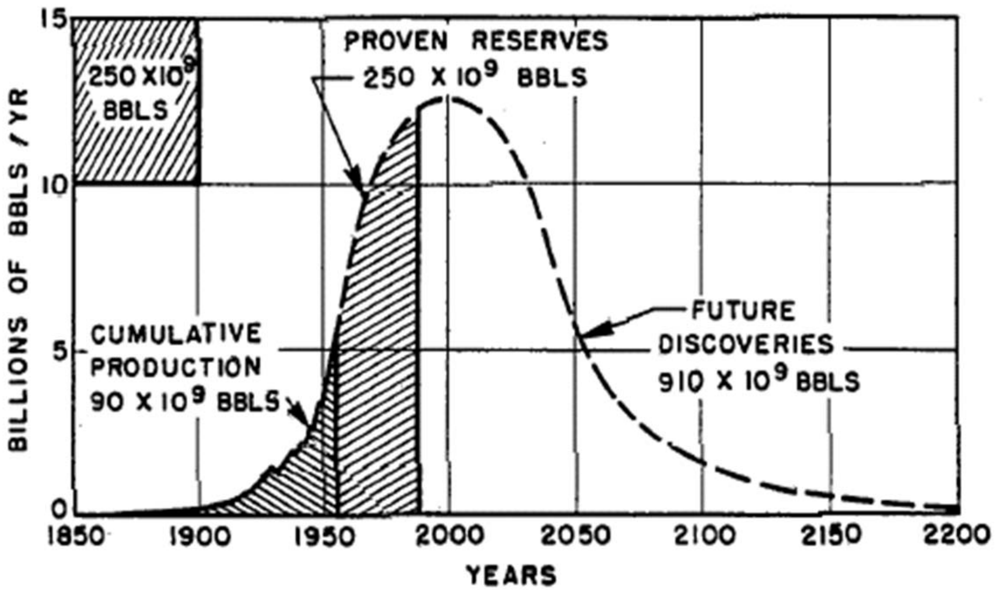

- Oil production in decline in 33 out of 48
- 2 out of 3 largest oil fields have peaked

Possible energy sources for long range aircraft

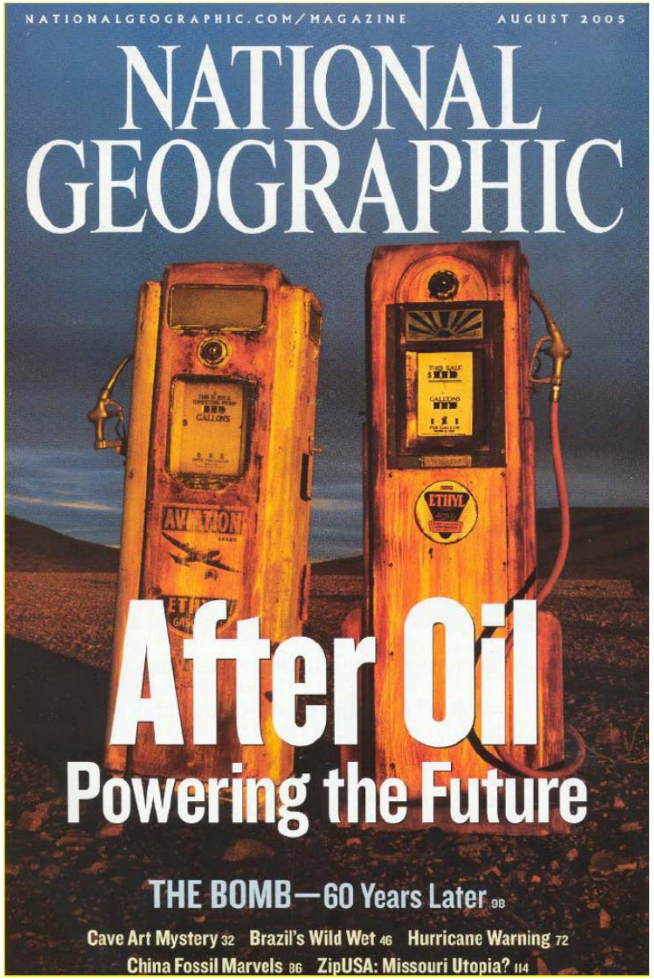

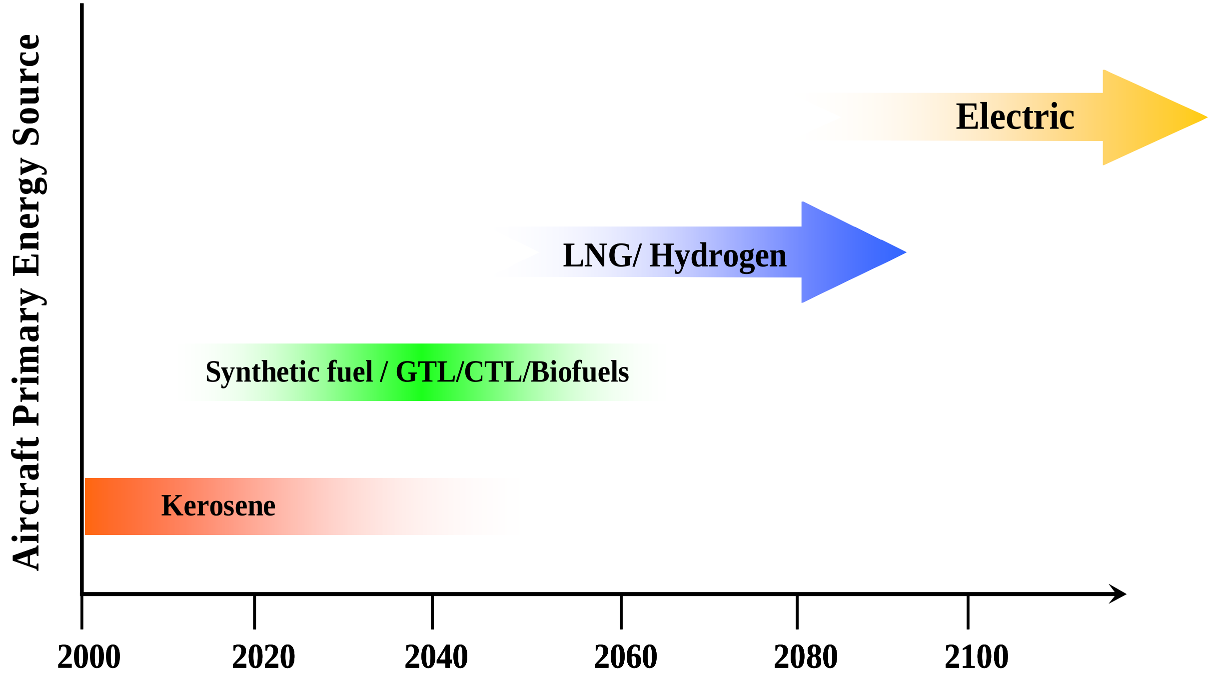

Fuels for Aviation

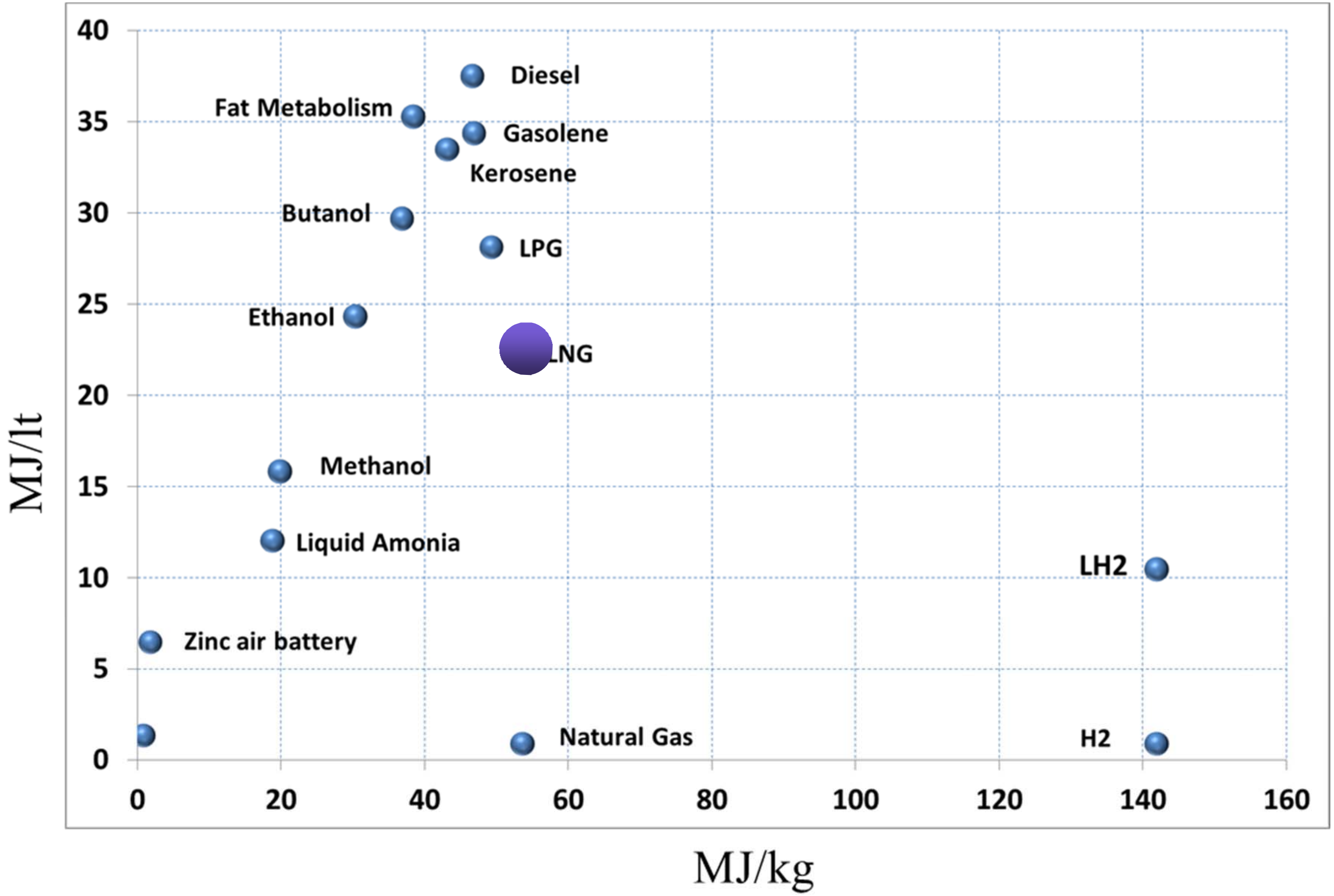

LNG Fuel

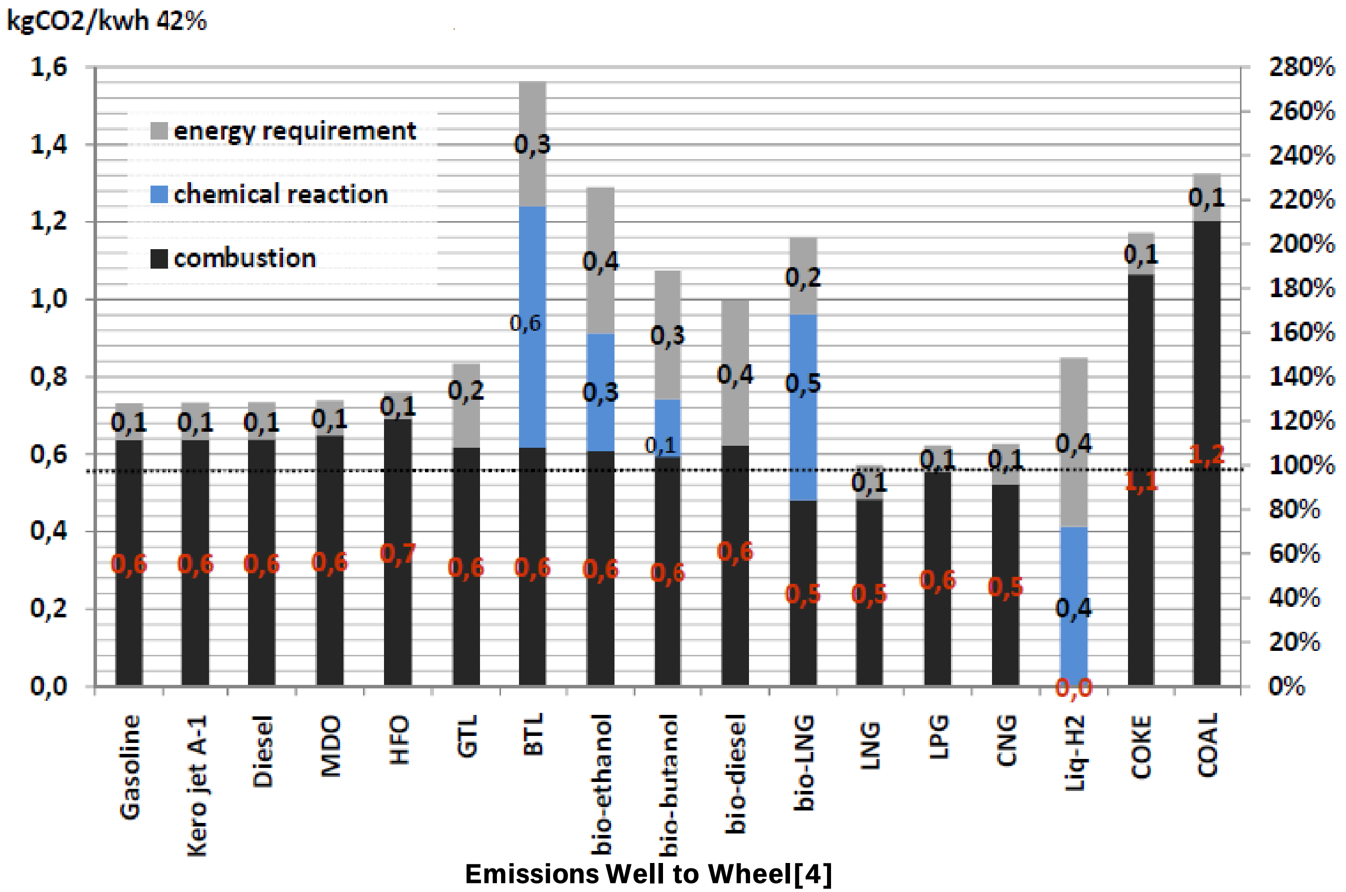

- Decrease of CO_2 by 25%
- Decrease of NOx by 80%
- Particulate emissions eliminated

Storage of hydrogen rich fuels in conventional aircraft

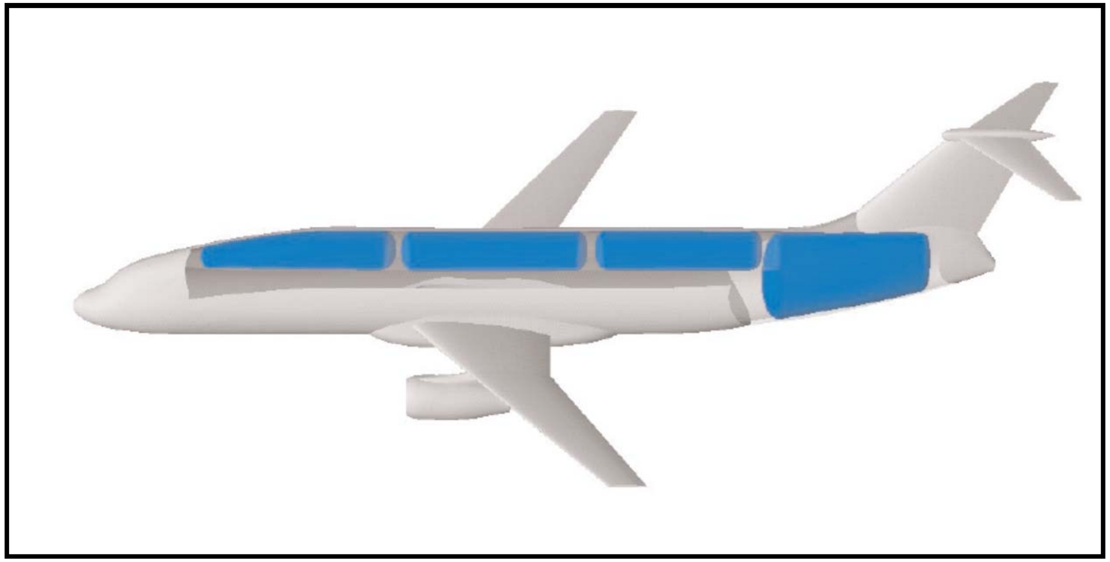

Cryoplane Project

- Cyrogenic fuels should be stored in cylindrical tanks
- Fuel storage was the biggest challenge

Storage of hydrogen rich fuels in BWB

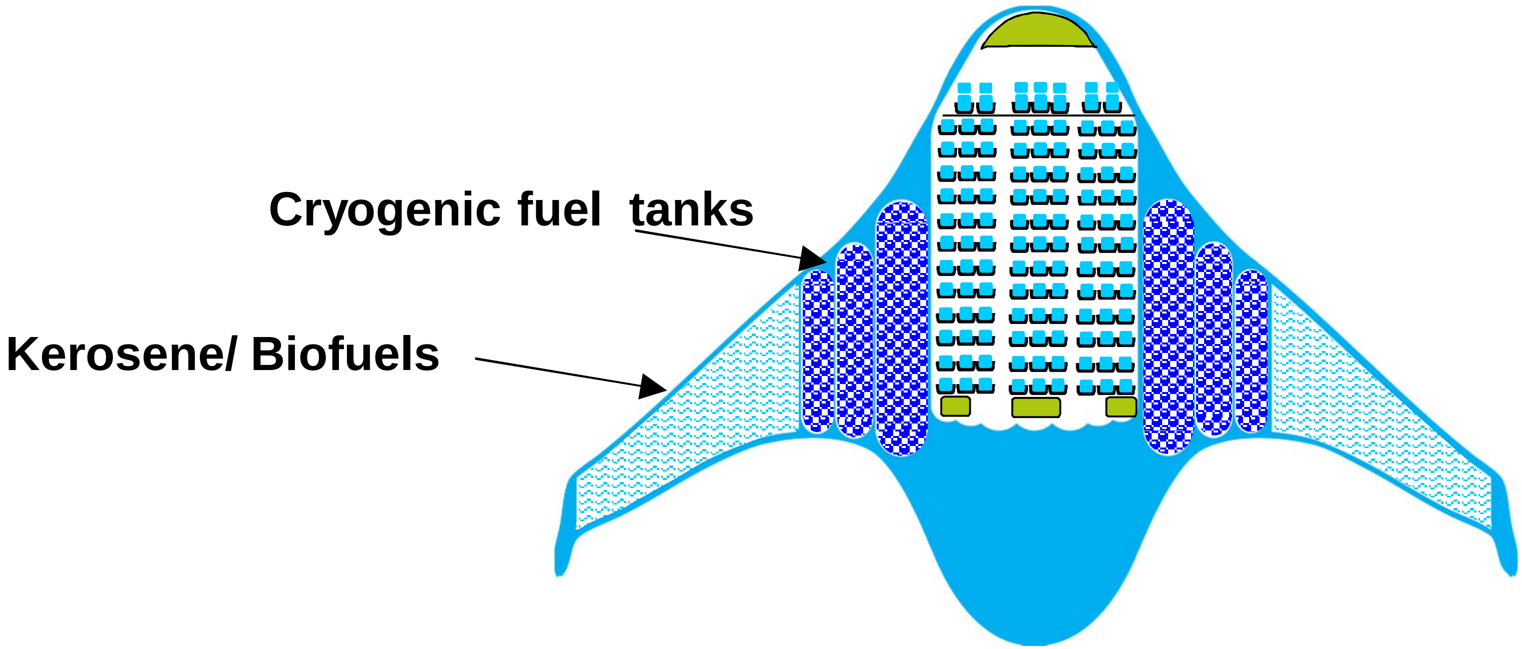

- BWB has inherently has extra volume which can be used to accommodate the cylindrical fuel tanks
- This novel idea of multi fuel BWB is unique which optimizes the usage of space in a BWB

Engine requirements from a future aircraft

- **High fuel Efficiency**
- **Low Emissions**
- **Low noise**
- **Reduced Aerodynamic Drag**
- **Low Installation Penalty**
- **Boundary Layer Ingestion**

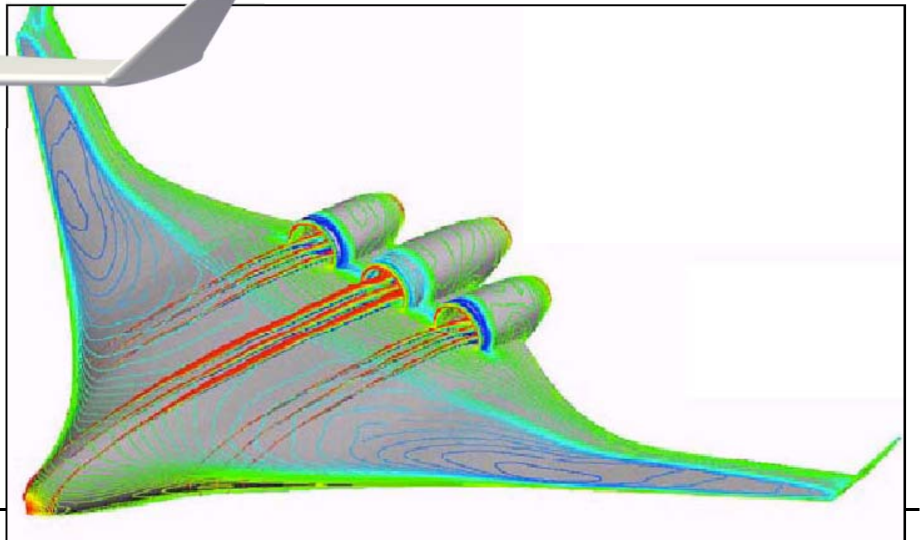

Can we design an engine taking into account all the above mentioned considerations

Next generation hybrid engine

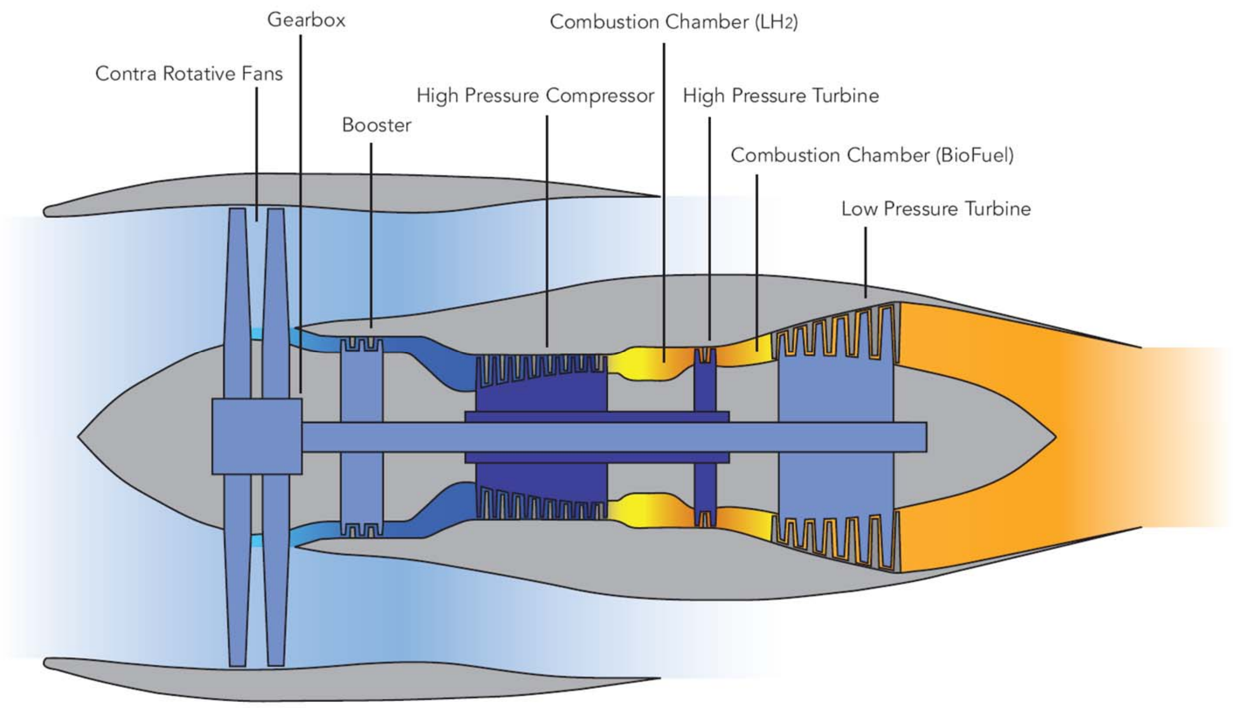

- ✓ **LNG/ LH2 Main Combustor**
- ✓ **Kerosene/ Biofuel Secondary Flameless Combustor**
- ✓ **Bleed cooling by LH2**
- ✓ **Counter rotating shrouded fans**
- ✓ **Higher Specific Thrust**
- ✓ **Low Installation Penalty**

The hybrid combustion system

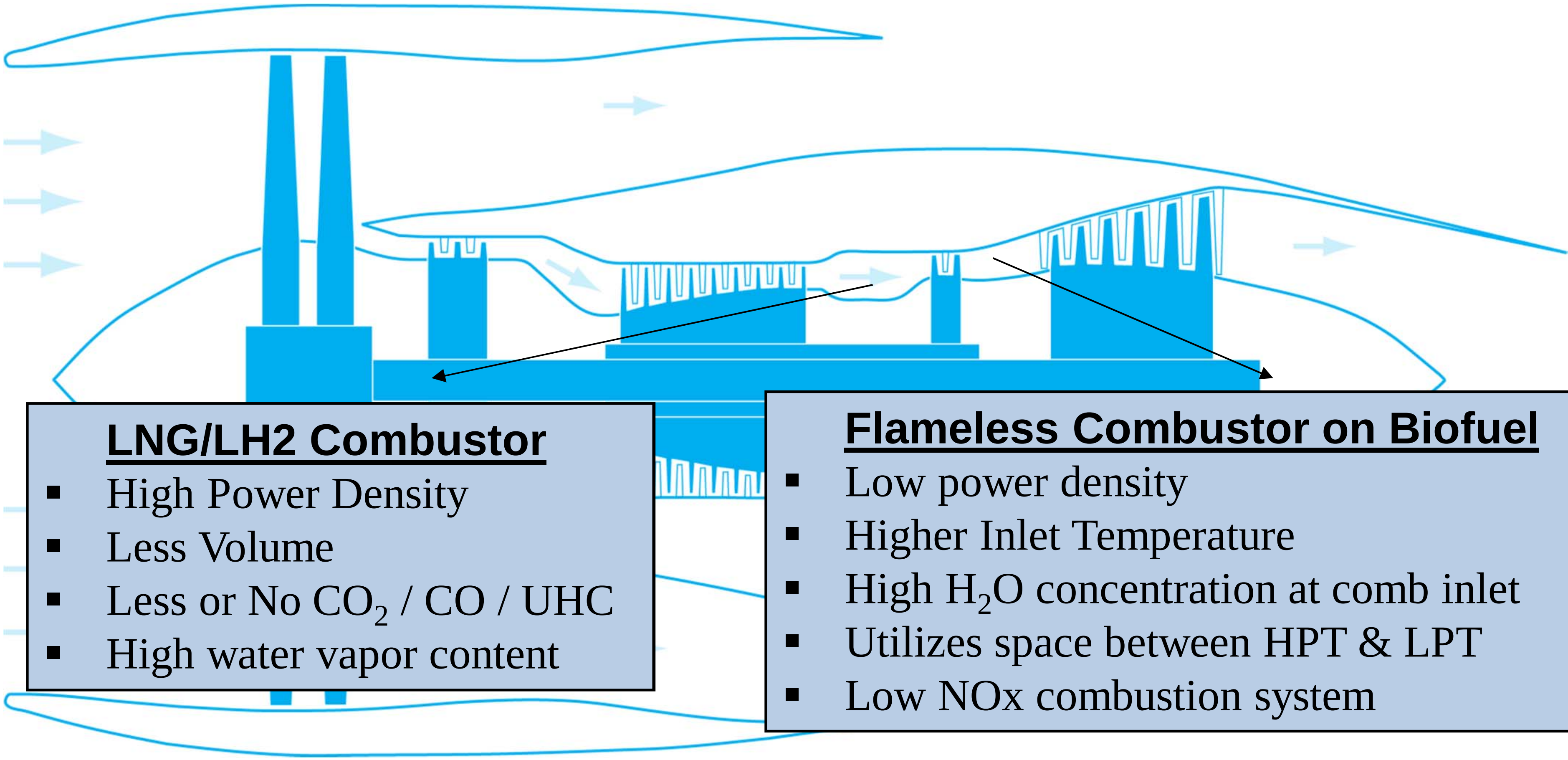

LNG/LH2 Combustor

- High Power Density
- Less Volume
- Less or No CO_2 / CO / UHC
- High water vapor content

Flameless Combustor on Biofuel

- Low power density
- Higher Inlet Temperature
- High H_2O concentration at comb inlet
- Utilizes space between HPT & LPT
- Low NOx combustion system

Overview of the workpackage structure

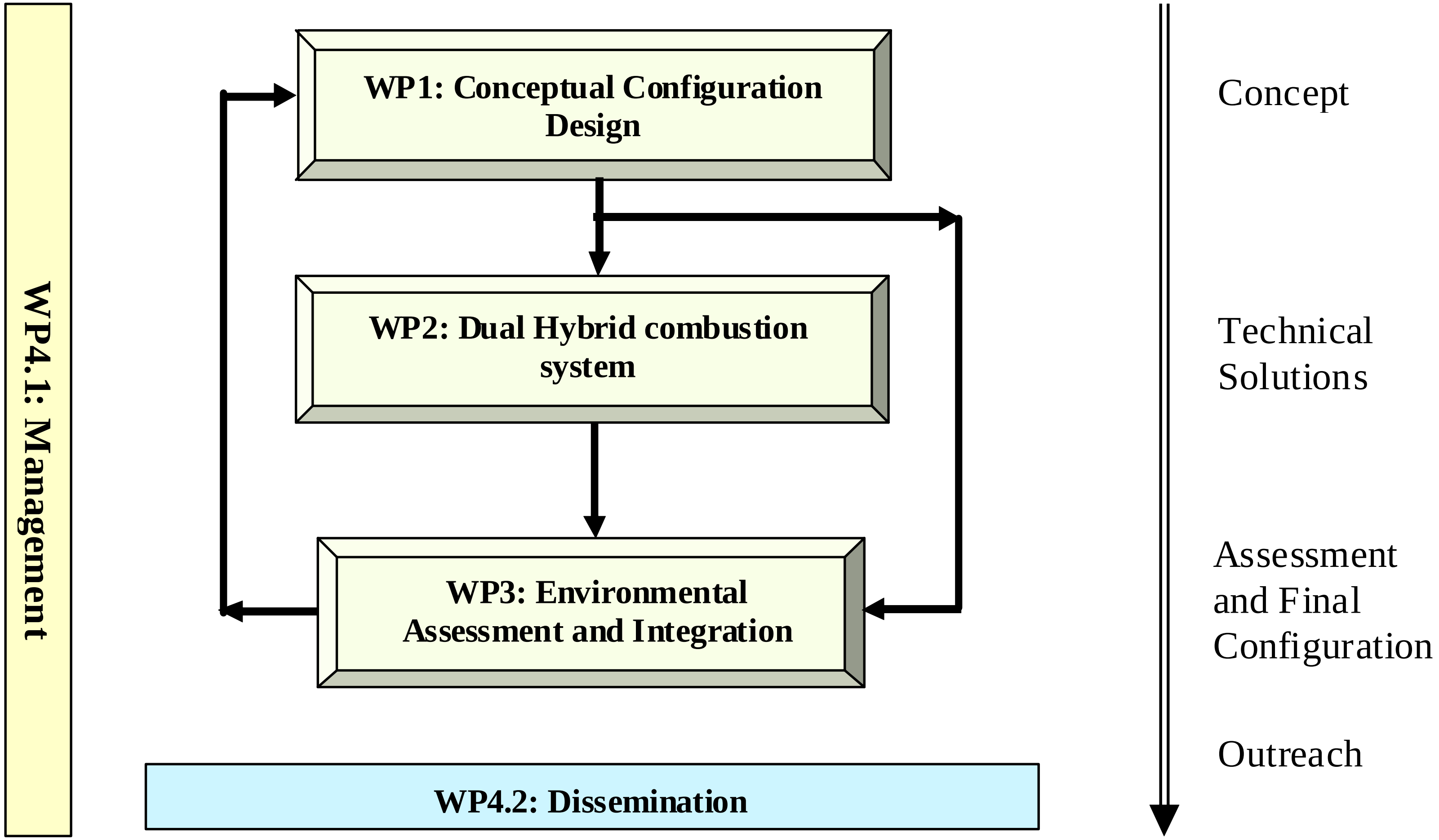

Work Package

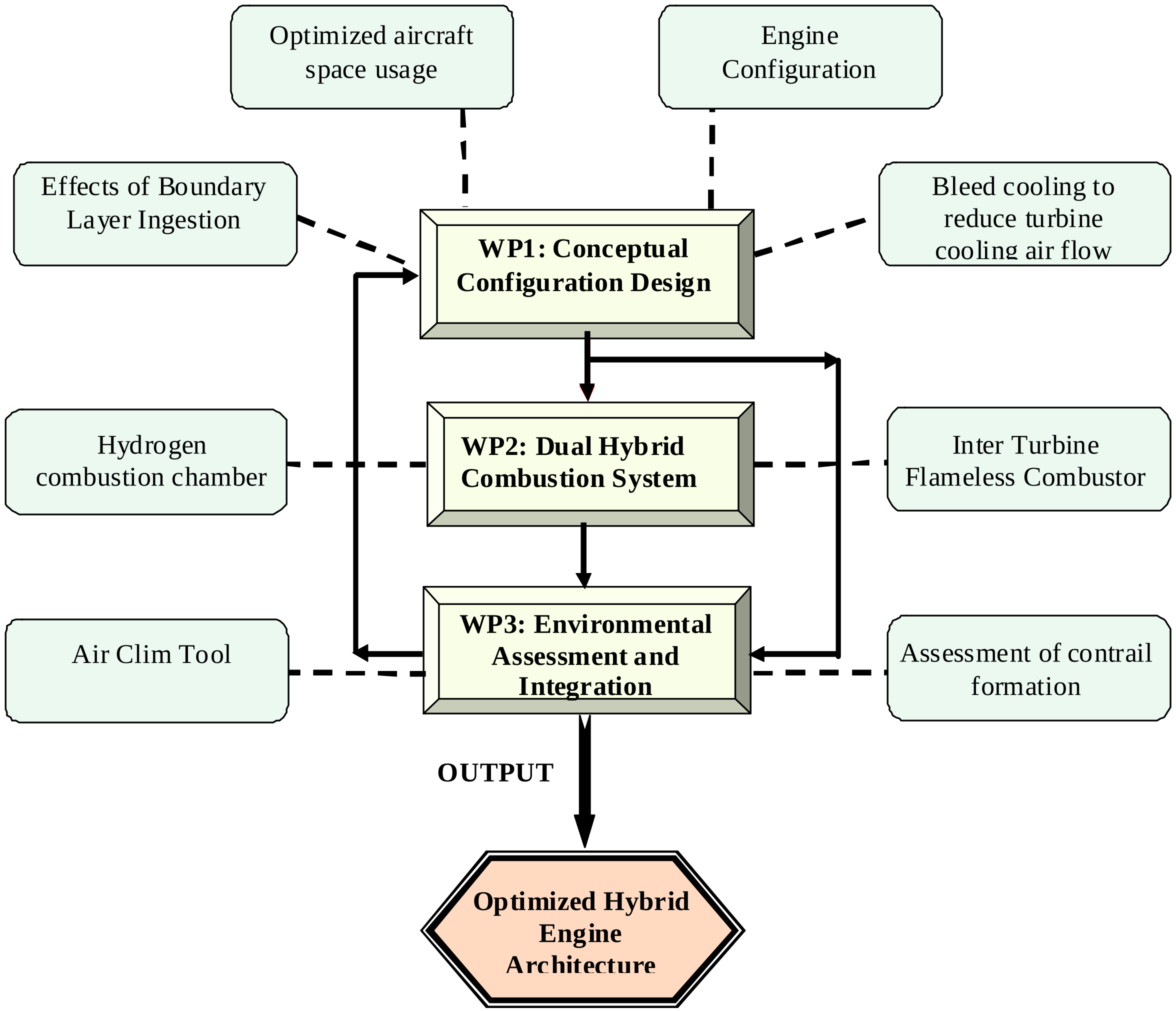

Various hybrid engine architectures:

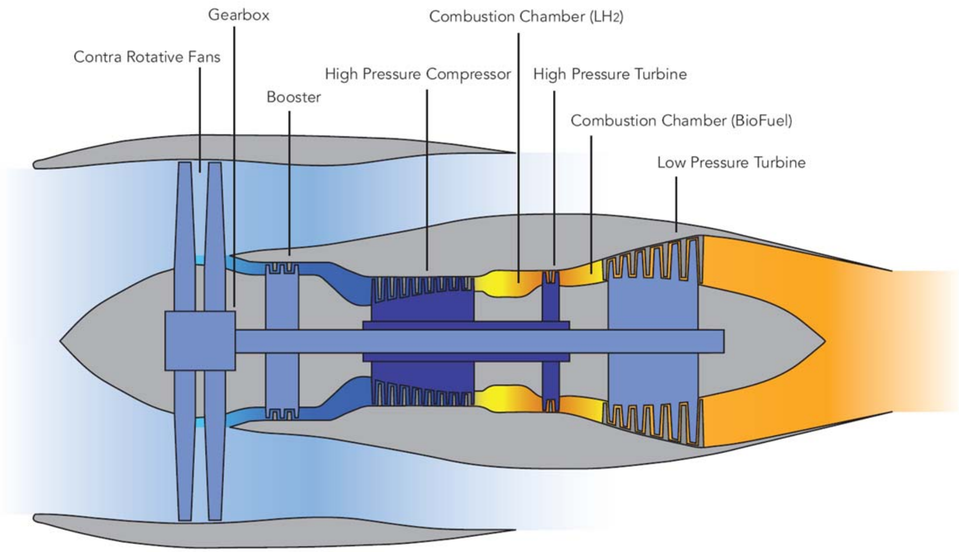

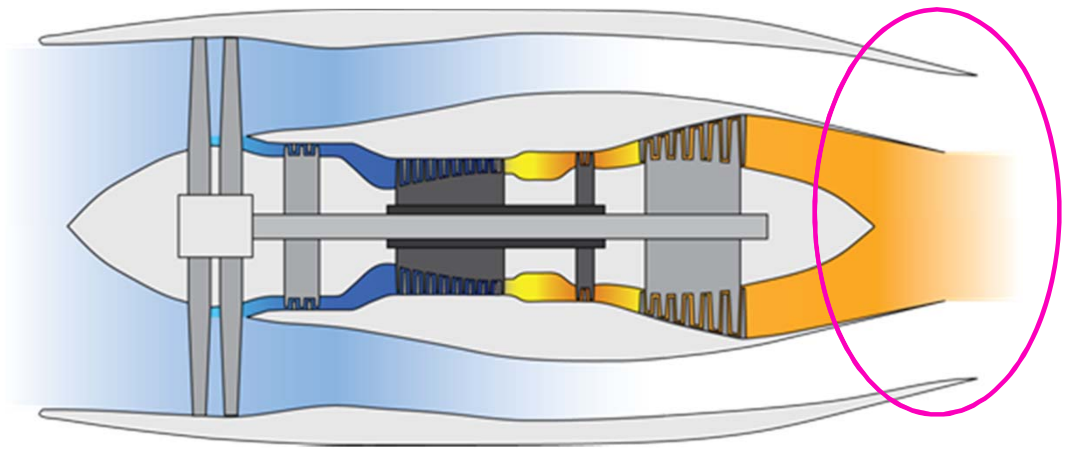

The Hybrid Engine Architecture

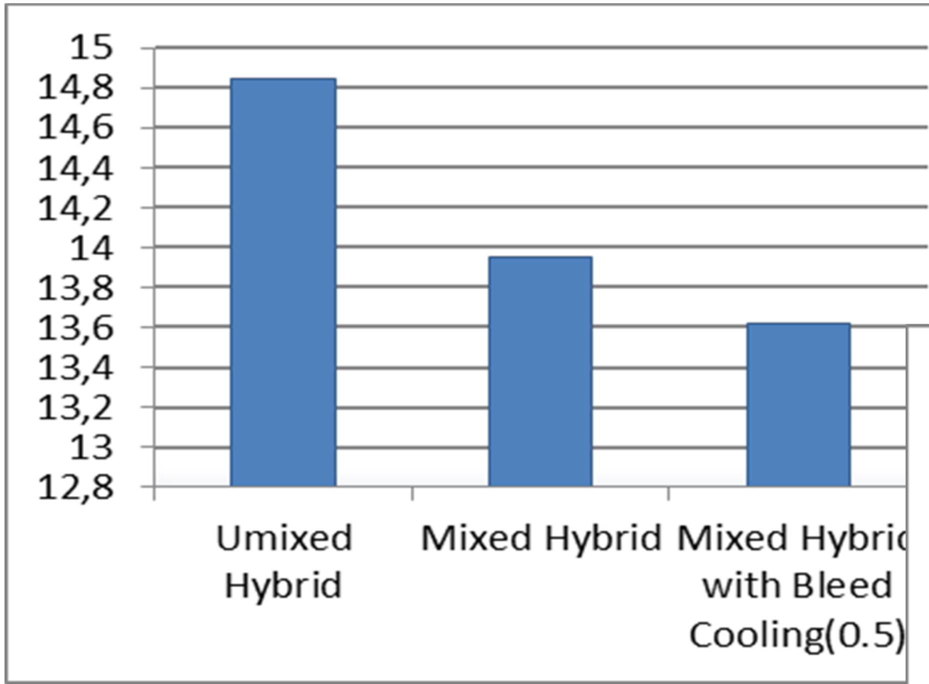

Variation of Sp. Fuel consumption for different engine architecture

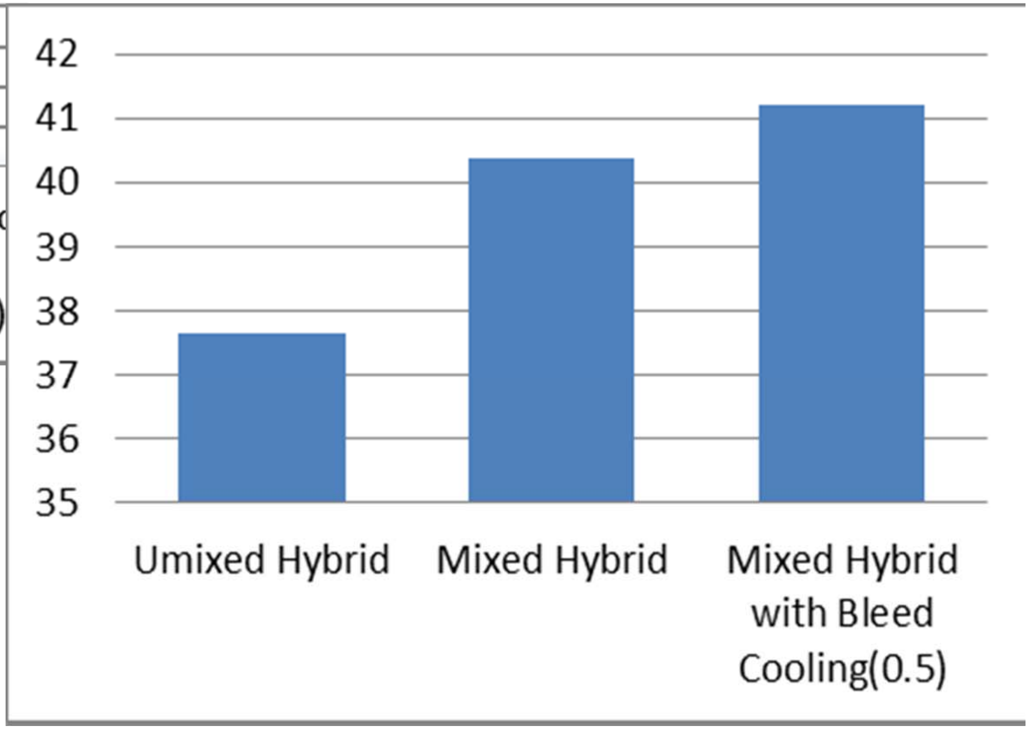

Variation of specific Thrust with various engine architecture

Comparison of hybrid engine with GE90-94B

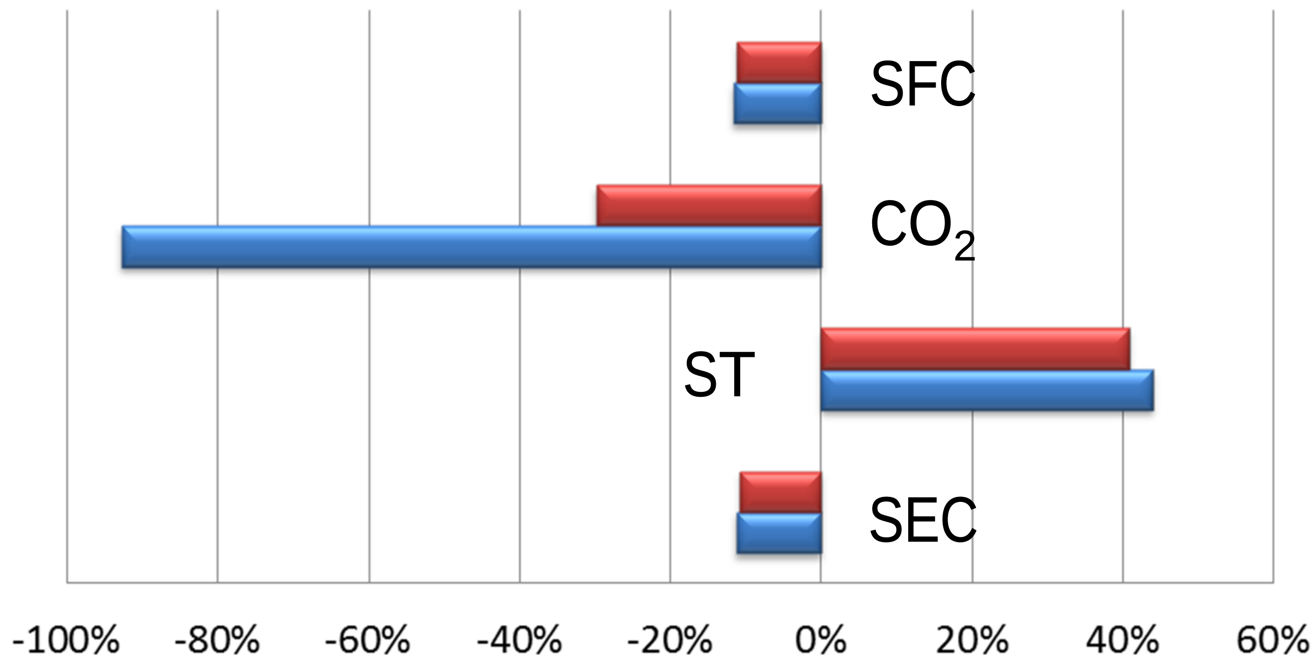

	SFC [g/kN.s]	ST [N.s/kg]	CO2 [kg/s]	SEC [MJ/kN.s]
LNG	-11%	41%	-30%	-11%
LH2	-11%	44%	-93%	-12%

The Multi-fuel Blended Wing Body

Preliminary design

Results – Planform and arrangement

The most important components:

- Main body
- Passenger compartment
- Cargo hold
- Pressure vessels (LNG)
- Fuel tanks (kerosene)
- Landing gear
- Engines

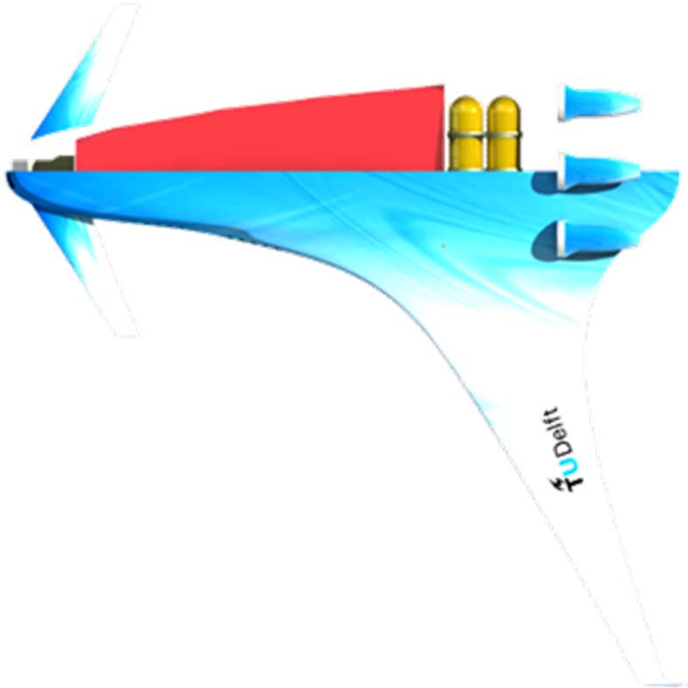

Preliminary design

Results – Passenger compartment

- 302 seats
- 8 lavatories and 7 galleys
- 6 Type-A emergency exits

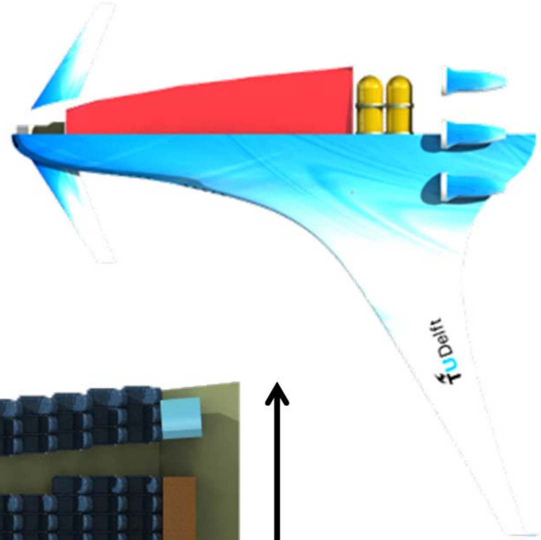

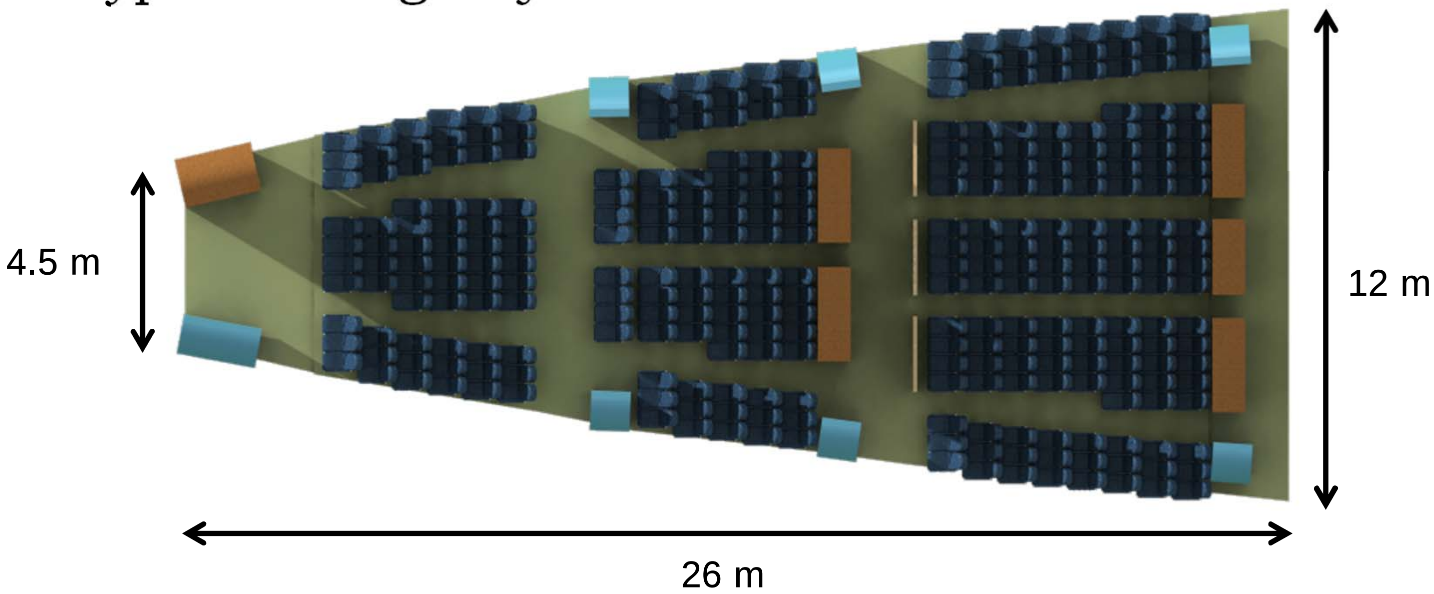

Multi Fuel BWB Design

Comparison with B777-200ER (1)

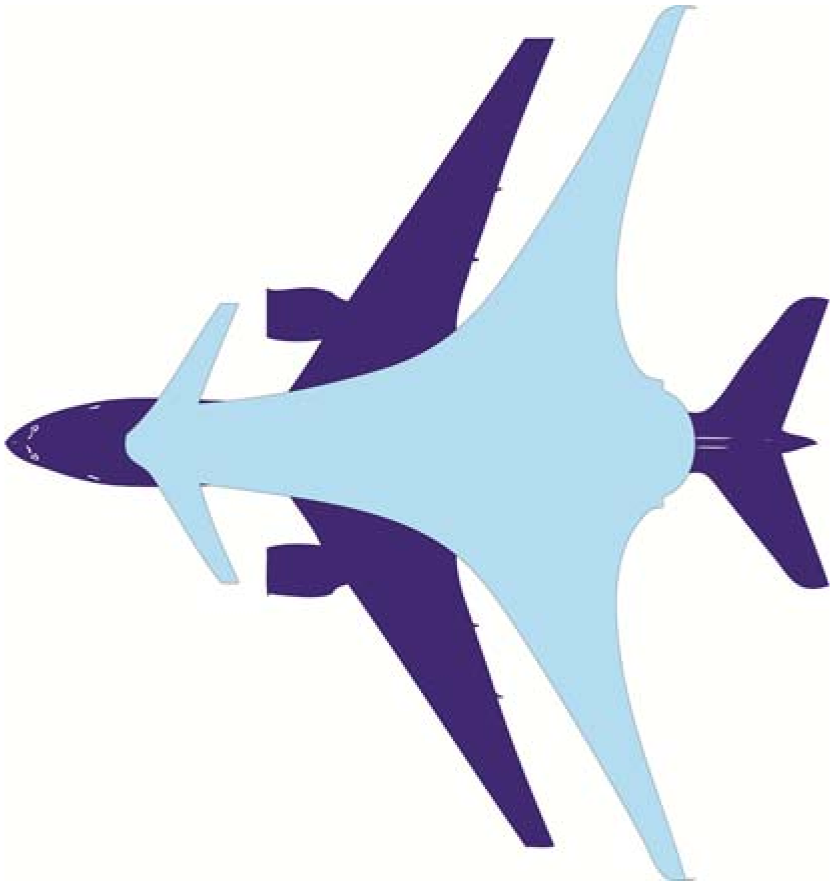

CO_2 Emission

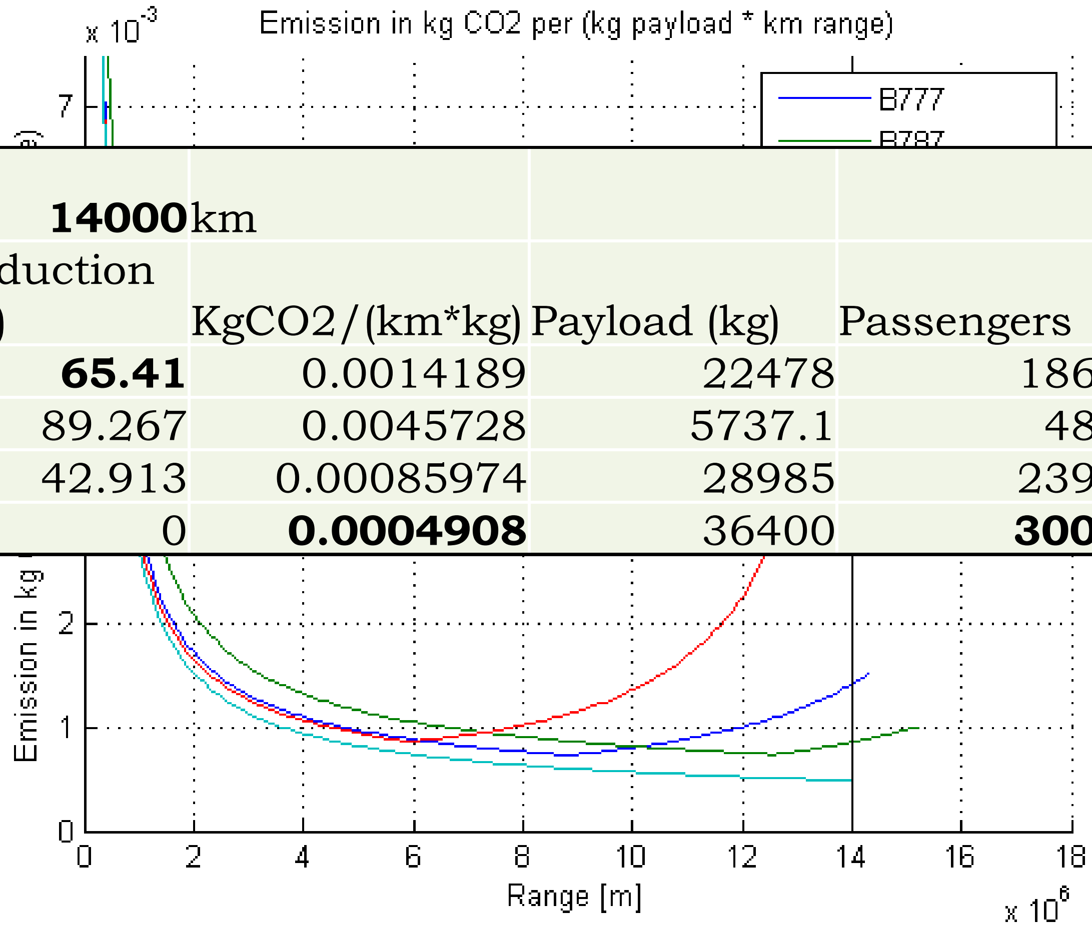

range	**14000**	km			
Aircraft	Reduction (%)	KgCO2/(km*kg)	Payload (kg)	Passengers	kgCO2/(Passenger*km)
B777	**65.41**	0.0014189	22478	186	0.172
A330	89.267	0.0045728	5737.1	48	0.554
B787	42.913	0.00085974	28985	239	0.104
BWB	0	**0.0004908**	36400	**300**	**0.059**

- Delft University of Technology
- WSK PZL-Rzeszow S.A
- Technical University of Berlin
- DLR, IAP
- Israel Institute of Technology-Technion
- Ad Cuenta b.v.

Questions?

www.ahead-euproject.eu

A.GangoliRao@tudelft.nl

MARS

Call identifier: “FP7-AAT.2010-RTD-CHINA” CSA Nº 266326

Manipulation of Reynolds Stress for Separation Control and Drag Reduction

Project Management

CIMNE

The University Of Sheffield.

中航工业空气动力研究院
AVIC AERODYNAMICS RESEARCH INSTITUTE

EASN Workshop
on Flight Physics and Propulsion
Prague, October 31st 2012

Project Overview

- History
- Consortium
- Coordination and Management
- Global objectives
- Technical objectives
- Work packages
- Work packages leaders
- Test cases
- Set up
- Conclusions

PROJECT BACKGROUND AND HISTORY

- Former networks: EUROVAL, EUROPT, ECARP, INGENET, FLOWNET, AEROSHAPE, QNET, PROMUVAL
- AeroChina: Identification of capabilities and partners
- AeroChina 2: Identification of topics of common interest
    - COLTS: Titanium casting
    - MARS: Flow Control
    - NEXTEP: Aeroacoustics
- GRAIN: Identification of topics on Greener Aeronautics

CONSORTIUM

Key Contact Persons: European Partners

Participant no.	Participant Name		Contact Names
EU1 (Coordinator)	CIMNE	ES	Prof. G. Bugeda, Prof. J. Periaux, Dr. J. Pons-Prats
EU2 (Coordinator)	Sheffield University	UK	Prof. N. QIN
EU3	Airbus	ES	Dr. A. Abbas
EU4	FOI	SW	Prof. S.H. Peng, Prof. P. Eliasson
EU5	Alenia	IT	Dr. N. Ceresola
EU6	DLR	GE	Dr. R. Geisler
EU7	Poitiers Univ. / LEA	FR	Prof. E. Moreau, Prof. J.P. Bonnet
EU8	Dassault Aviation	FR	Dr. J.C. Courty
EU9	Numeca	BE	Prof. C. Hirsch, Dr. L. Temmerman
EU10	Manchester University	UK	Prof. K. Kontis, Dr. E. Erdem
EU11	INRIA	FR	Dr. R. Duvigneau
EU12	EADS Innovation Works	UK	Dr. S. Rolston

Key Contact Persons: Chinese Partners

Participant no.	Participant Name		Contact Names
CH1 (Coordinator)	CAE	Ch	Ms. Sun Jian
CH2	NUAA	Ch	Prof. Ming Xiao, Porf. Tang Zhili
CH3	THU	Ch	Prof. Song Fu
CH4	NPU	Ch	Prof. GAO Zhenghong, Dr. LI Dong
CH5	PKU	Ch	Prof. Wu Jiezhi, Dr. Yang Yantao
CH6	BUAA	Ch	Prof. Liu Peiqing, Prof. Zhang Jinbai
CH7	ZJU	Ch	Dr. Yao Zheng

Chinese Subcontractors

S1 (Tech Leader)	AVIC-ARI	Ch	Prof. Dong Jun
S2	AVIC-FAI	Ch	Represented by CAE
S3	AVIC-ACTRI	Ch	Represented by CAE

Coordination and Management

China

SUN Jian, CAE: MARS Coordinators (General Management)
DONG Jun, ARI: MARS Coordinators (Technical Management)

Europe

G. Bugeda, J. Periaux, CIMNE:
MARS Coordinators (General Management)
N. QIN, SHEFFIELD Univ.:
MARS Coordinators (Technical Management)

Project Officer

D. Knoerzer, Senior Project Officer, EC, DG Research Aeronautics

Global OBJECTIVES

- To use the periodic flows embedded in the two identified flow cases as platforms in which direct control of discrete dynamic structures to manipulate the Reynolds stress can be observed, measured and simulated.
- To measure, simulate and understand the impact of certain actuators upon discrete structures in a turbulent shear layer and to identify candidate actuators for further development for skin friction reduction and flow separation control at flight scales.

Project Technical objectives

- To **control turbulent wall bounded shear flow** effectively from a more fundamental level by investigating directly the behaviour of Reynolds stresses and their response to the manipulation of the dynamic components of the flow
- To **conduct both experimental tests and computational simulations** to extract reliable flow physics, including Reynolds stresses, for a number of active flow control devices
- To **explore large scale unsteadiness** (unsteady jets, wakes and vortices) produced from the capability of these devices forto provide effective control of the dynamic components, and hence the Reynolds stresses, within the shear layers associated with large scale wakes and separations
- To **identify key strategies** that enable efficient control of dynamic fluid structures within shear layers and to design and optimise these devices for separation control (higher shear) and drag reduction (lower shear)
- To **demonstrate the most promising device/devices** at relevant scale, the ability to efficiently increase or decrease the Reynolds stresses
- To **investigate the application** of this capability within an aircraft context
- **To foster further collaboration between European and Chinese** researchers in the key technology area of flow control for the benefit of the civil aircraft industries on both sides.

Work Packages

WP #	WP Title	Type of activity	Lead participant Short name
1	Management, Data Tools and Communication	MGT	CIMNE/CAE SHEFFIELD/AVIC-ARI
2	Experimental Investigation Flow Control Mechanism	RTD	POITIERS/AVIC-ARI
3	Numerical Simulation for Flow Control	RTD	FOI/THU
4	Synthesis, Understanding and Design Optimisation of the control devices on Reynolds Stresses	RTD	SHEFFIELD/NPU
5	Industrial Demonstration and evaluation	RTD	AI/CAE, FAI

Work Package Leaders

Europe	China
G. Bugeda, J. Periaux, J. Pons, CIMNE General Coordinator and WP1 Leader	SUN Jian, CAE Deputy Coordinator
N. QIN, Sheffield Technical Coordinator & WP1 Leader	Dong Jun, ARI Technical Coordinator & WP1 Leader
N. Bernard, Poitiers, WP2 Leader	Dong Jun, ARI WP2 Leader
S.H. Peng, FOI WP3 Leader	Song Fu, THU WP3 Leader
G. Bugeda, CIMNE, N. QIN, Sheffield WP4 Leader	Gao Zhenghong, NPU WP4 Leader
A. Abbas, AIRBUS WP5 Leader	SUN Jian, CAE WP5 Leader

Test Cases

- Two test cases were defined:
  - Backward Facing Step
  - NACA 0015

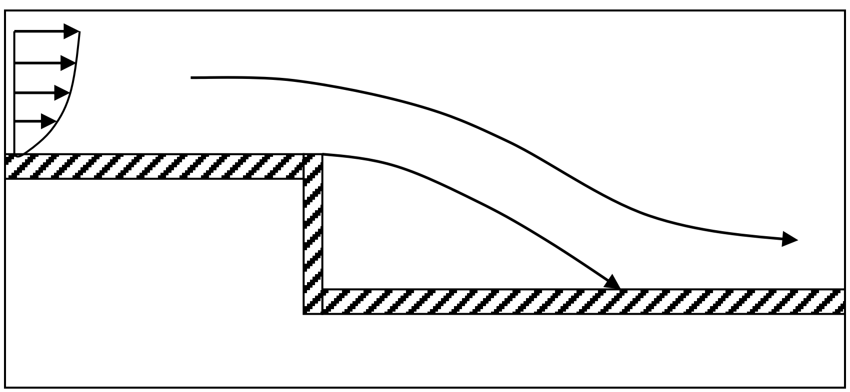

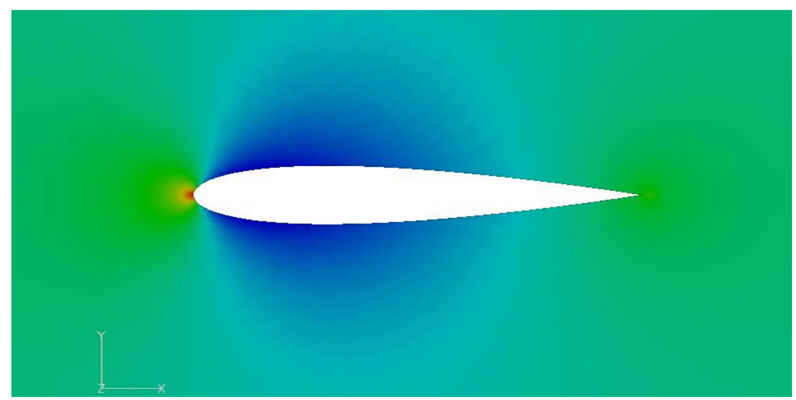

Experimental Facilities

- Wind tunnel (NUAA, NPU, ARI, UNIMAN, Poitiers, DLR)
- Measurement equipment (PIV, Hot Wire)

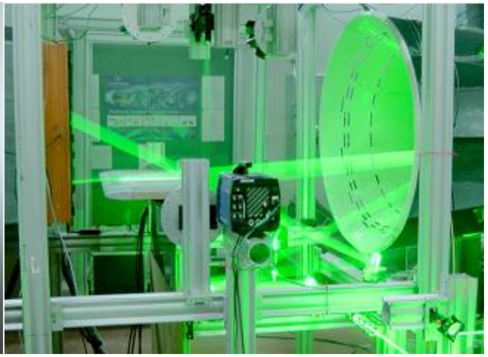

Experimental Set-up

- Piezo-electric actuators
- Plasma actuators

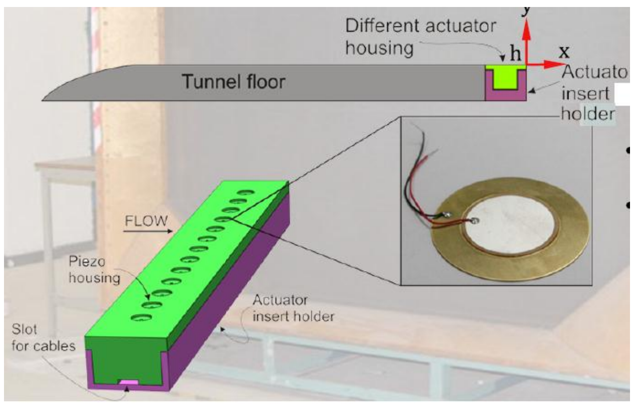

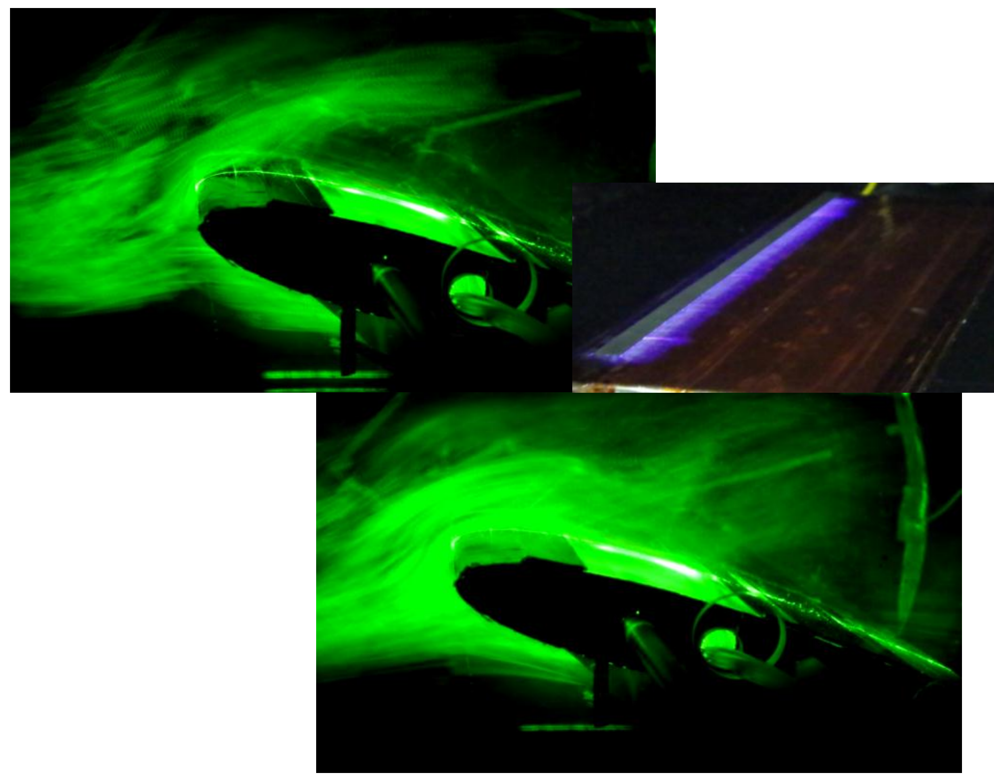

Numerical Set-up

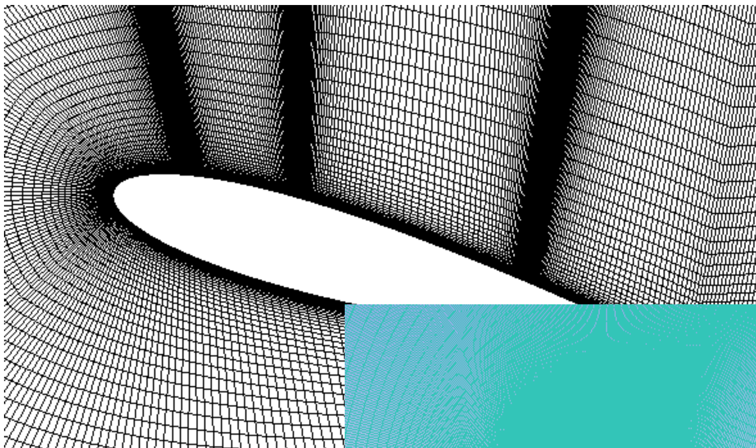

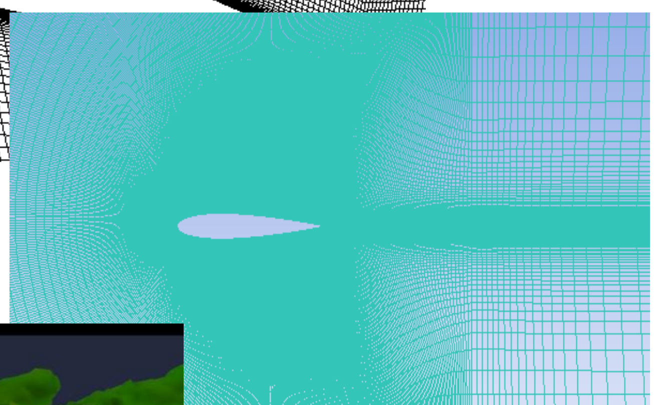

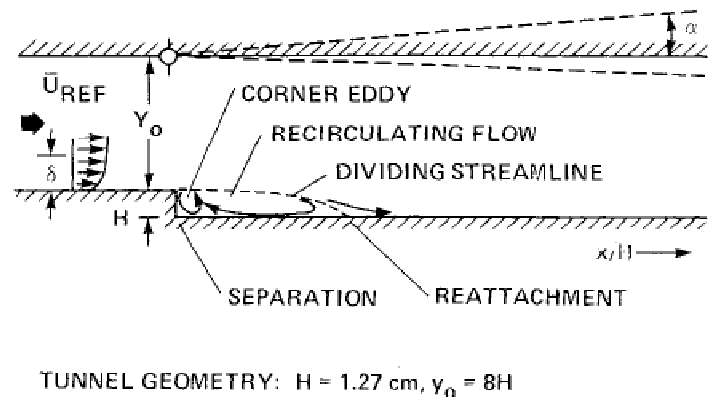

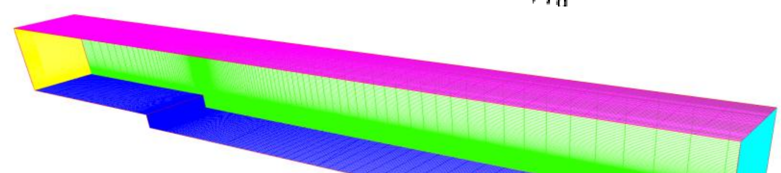

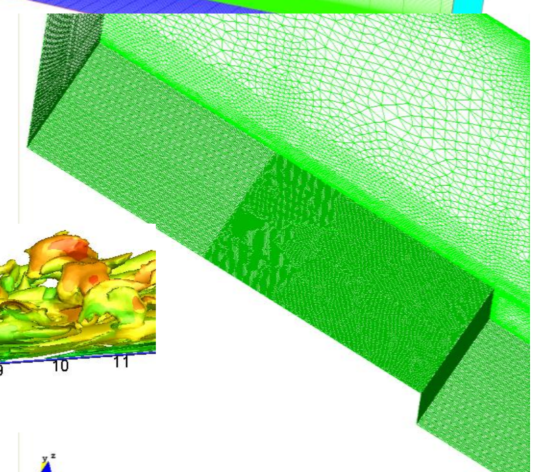

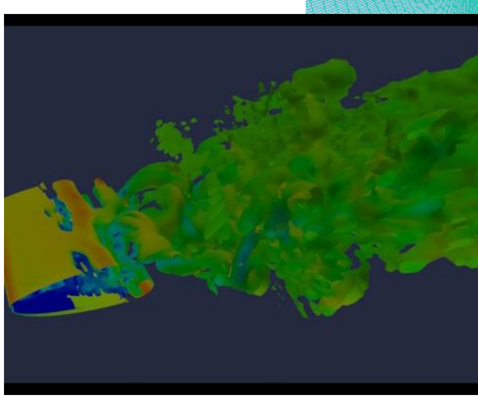

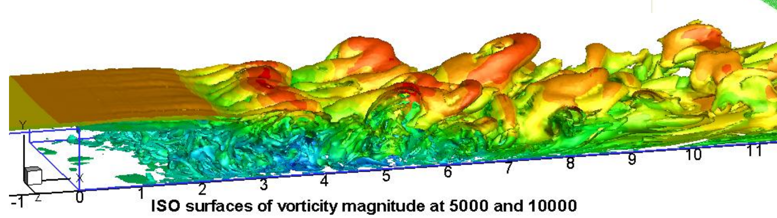

Conclusions

- First research project EU-CH
- Co-funded by EC and MIIT
- Cultural issues to be overcome
- Results and technical details in the following presentations

THANKS FOR YOUR ATTENTION

FP7-AAT.2010-RTD-CHINA
Project № 266326

MODIFICATIONS OF REYNOLDS STRESSES BY LOCALIZED UNSTEADY FORCING

N. Benard, P. Sujar-Garrido, V. Parezanovic, J.C. Laurentie, B. Noack, J.P. Bonnet and E. Moreau

Institut P' • UPR CNRS 3346
SP2MI • Téléport 2
Boulevard Marie et Pierre Curie • BP 30179
F86962 FUTUROSCOPE CHASSENEUIL Cedex

Primary objective of MARS EU project

The MARS project focus on the effects of a number of active flow control devices on periodic Reynolds stresses of turbulent shear flows.

Why looking at the Reynolds stresses?

Reynolds stresses

Major contribution to the momentum transfer in the wall bounded turbulent flow

Skin friction

Flow separation

More efficient air transportation

INSTITUT

Presentation of cases

Two fundamentals flow configurations

Backward Facing Step

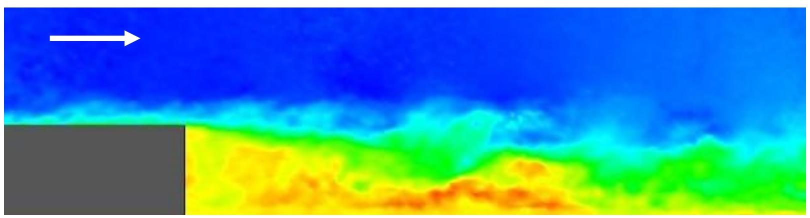

Airfoil NACA0015

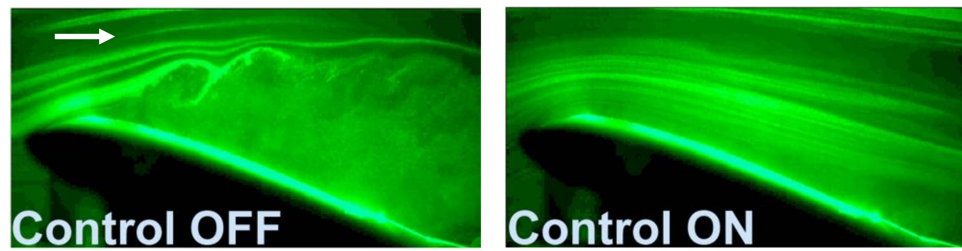

- Separated turbulent shear layer from a fixed sharp edge
- Periodic unsteady flows

- Massive or partial flow separation
- Periodicity of the dynamic components

Objectives and measurements techniques of the experimental investigations

Objectives

- Demonstrate the ability to measure the contribution of the periodic flow to the global Reynolds stresses
- Characterise the periodic component of the basic flow
- Understand the sensitivity of the base flow to small perturbations
- Demonstrate the capacity for the selected actuators to manipulate the Reynolds stresses

Measurement techniques

- Velocity field by PIV, TR-PIV, Tomo-PIV
- Hot-wire
- Wall pressure
- Skin friction

Partner list

Backward facing step

- University of Manchester, University of Poitiers, DLR Goettingen
- Northwestern Polytechnic University, Nanjing University of Aeronautics and Astronautics

Synthetic jet actuators, Plasma actuators, Oscillating surfaces

Airfoil NACA0015

- University of Manchester, University of Poitiers, DLR Goettingen
- BeiJing University of Aeronautics & Astronautics, AVIC Aerodynamics Research Institute

Fluidic vortex generators, Synthetic jet actuators, Plasma actuators, Oscillating surfaces

Investigations on BFS flow at University of Poitiers

A) Experimental setup

Wind-tunnel

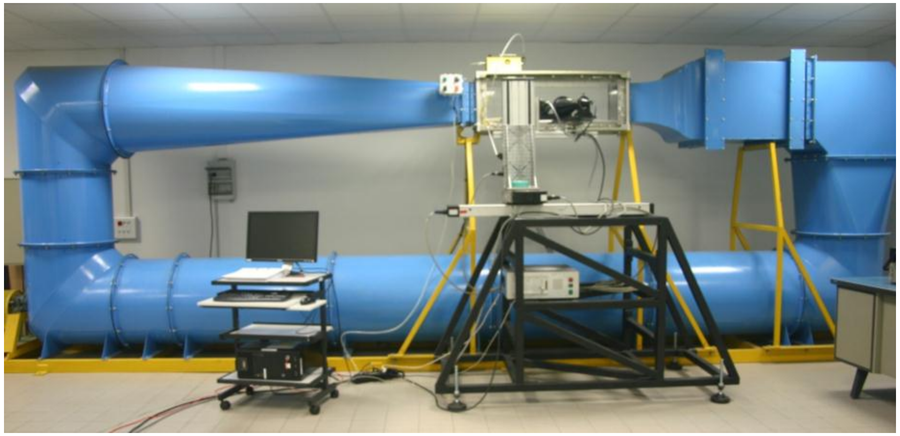

- Goettingen type wind-tunnel
- Velocity speed 5-50m/s
- Turbulent intensity < 1%
- Test section of 300x300x1000mm^3

Backward facing step model

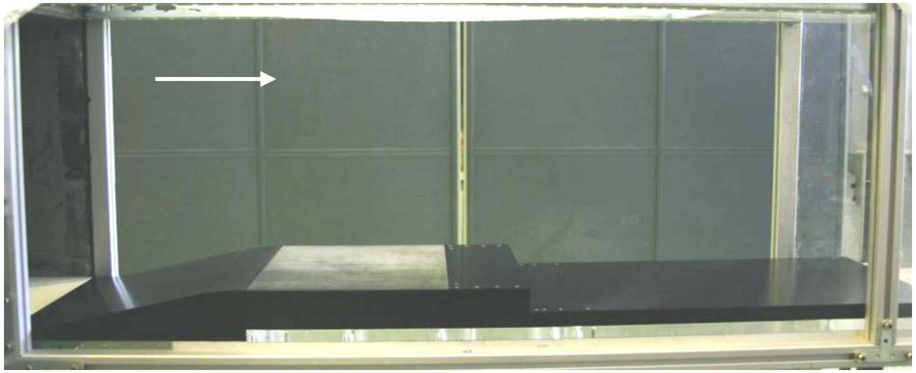

- Step height of 30 mm
- Aspect ratio of 10
- Expansion ratio of 1.11

Investigations on BFS flow at University of Poitiers

B) Control device based on plasma discharge

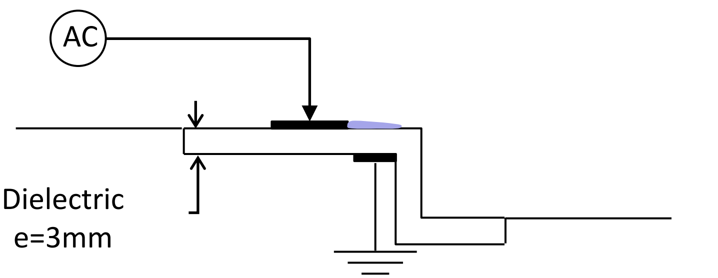

$E_{AC} \approx 20$ kV, $I < 40$ mA, $P \approx 200$ mW/cm^2

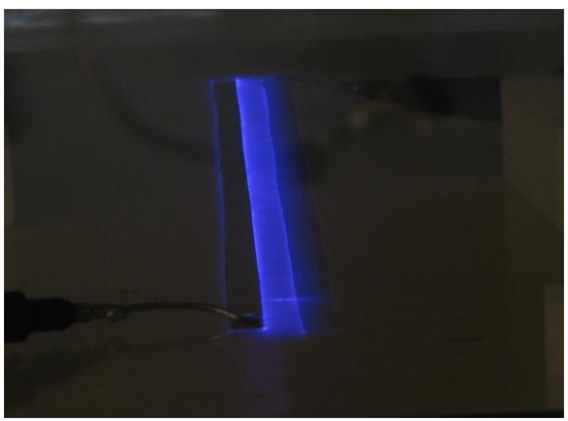

High electric field → **Production of charged species (ions and electrons)**

AC high-voltage → **Movement of the charged species**

↓

Collisions with neutral particles

↓

Electric wind production by momentum transfer

Plasma actuator = electromechanical converter

Investigations on BFS flow at University of Poitiers

C) Actuator locations and measurements

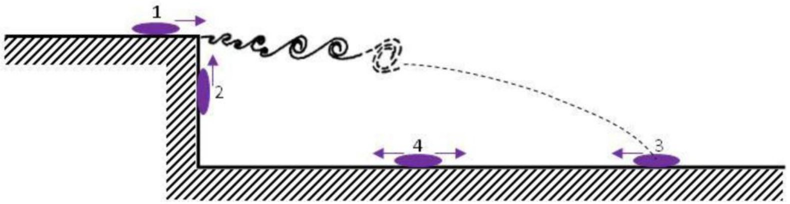

- Four different locations
- Investigation of directionnal effects
- Test matrix with a total of 75 independent cases

- Stereoscopic particle image velocimetry
- Velocity field with resolution of 1 vector per 1.5 mm
- Full resolution of the Reynolds stress tensor
- Acquisition of 1000 snapshots of the flow field

Investigations on BFS flow at University of Poitiers

D) Main results of the parametric study

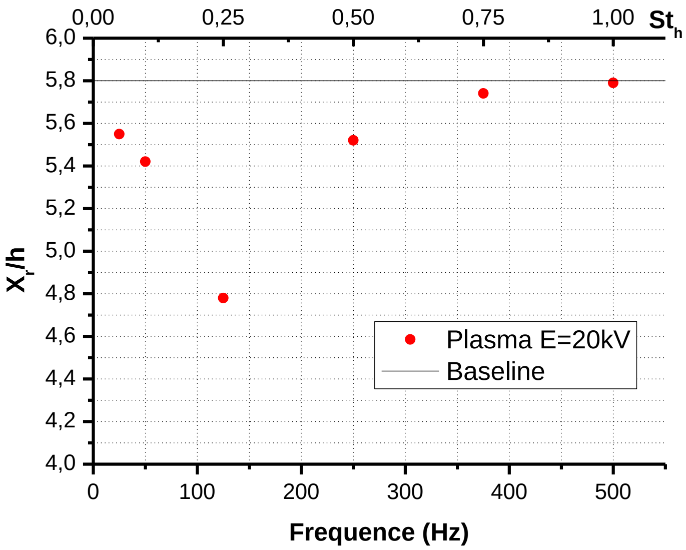

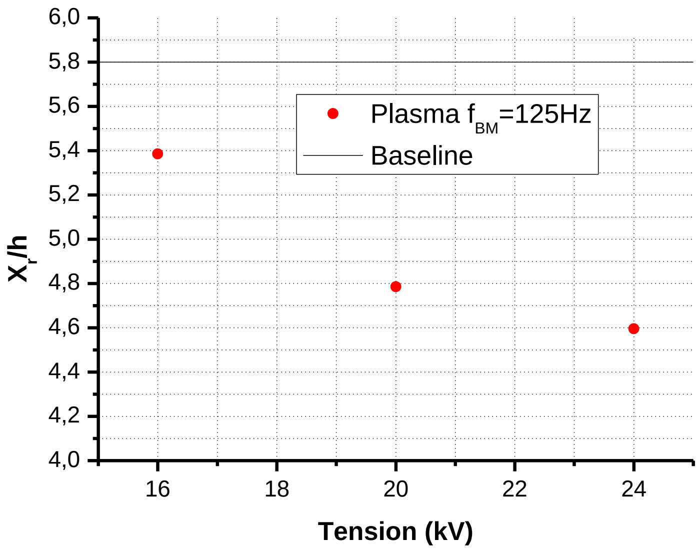

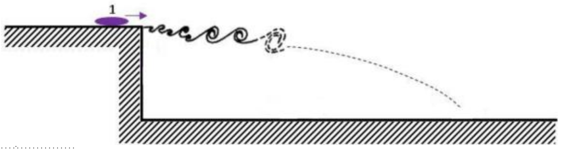

Large reduction of the recirculating region (17%) for unsteady forcing at the natural frequency of the free shear layer

Investigations on BFS flow at University of Poitiers

E) Mean flow characteristics and contribution to Reynolds stresses

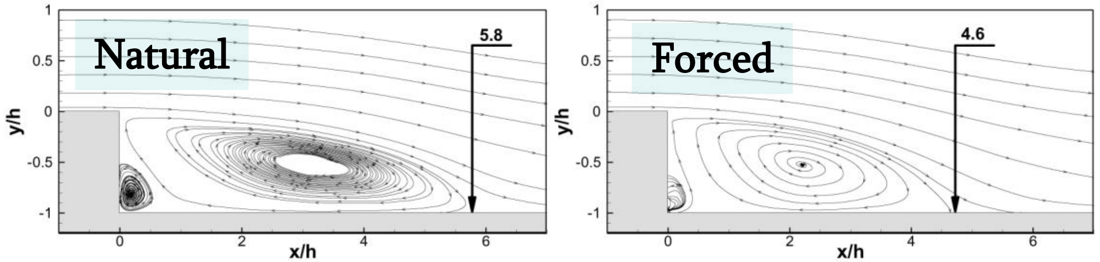

Figure 1: Streamlines of mean flow

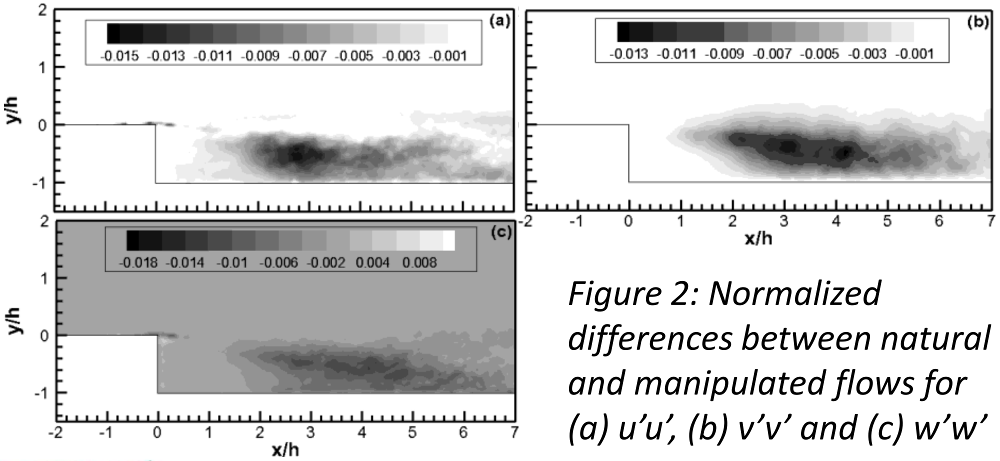

Figure 2: Normalized differences between natural and manipulated flows for (a) u'u', (b) v'v' and (c) w'w'

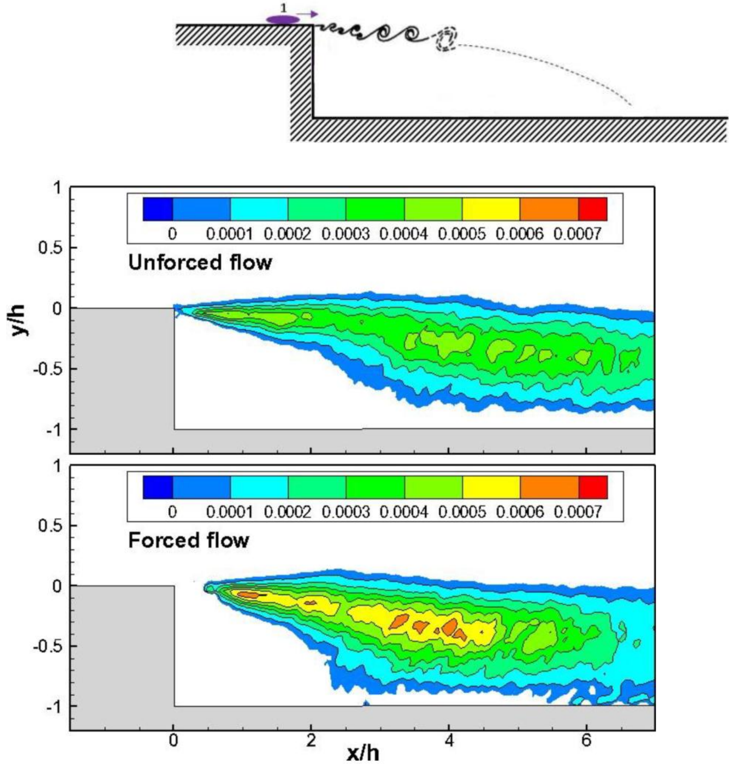

Figure 3: Production of Turbulent Kinetic Energy

Investigations on BFS flow at University of Poitiers

F) Extraction of vortical flow structures

Periodic components of the flow are extracted by using methods based on proper orthogonal decomposition (POD). This method is a coherent structure filtering that decomposes the whole turbulent flow according to turbulent energy levels

POD computed over the whole flow domain

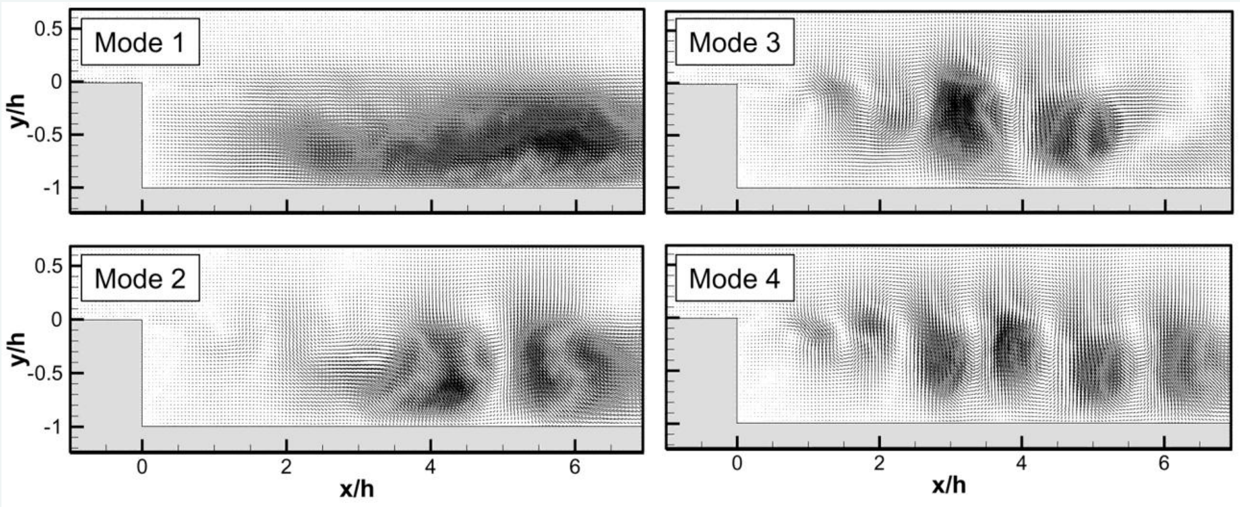

Dominant spatial modes issued from proper orthogonal decomposition computed on the whole flow domain

Investigations on BFS flow at University of Poitiers

F) Extraction of vortical flow structures

Periodic components of the flow are extracted by using methods based on proper orthogonal decomposition (POD). This method is a coherent structure filtering that decomposes the whole turbulent flow according to turbulent energy levels

POD computed over region of interest and projected on the whole flow domain (Extended POD)

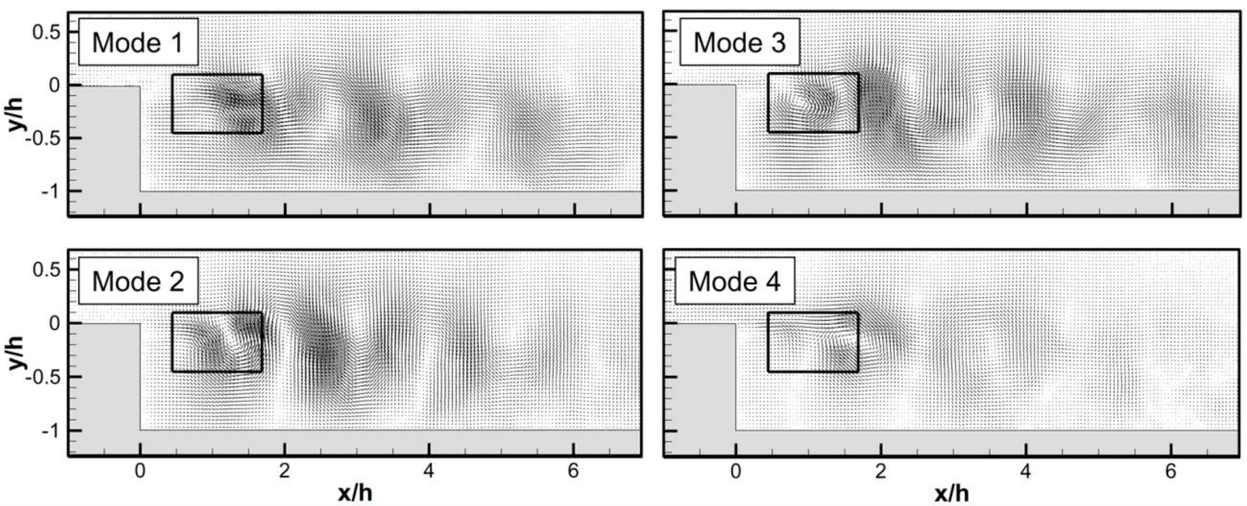

Dominant spatial modes issued from extended POD computed on the whole flow domain

Investigations on BFS flow at University of Poitiers

F) Extraction of vortical flow structures

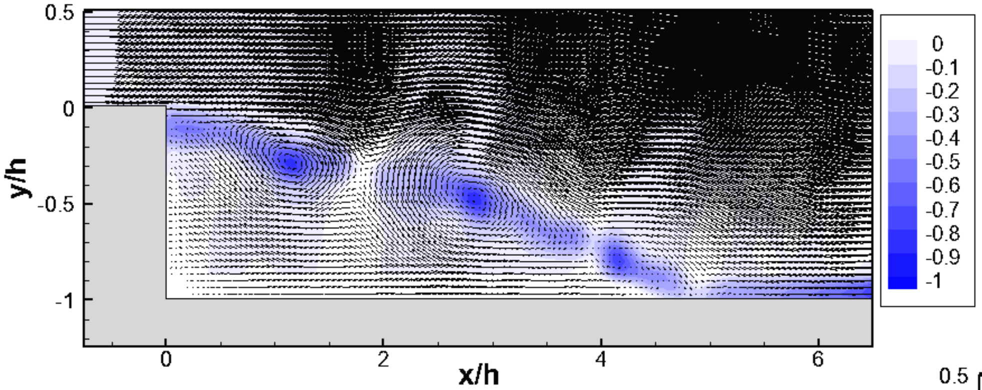

Figure 1: Reconstruction of turbulent coherent flow structures

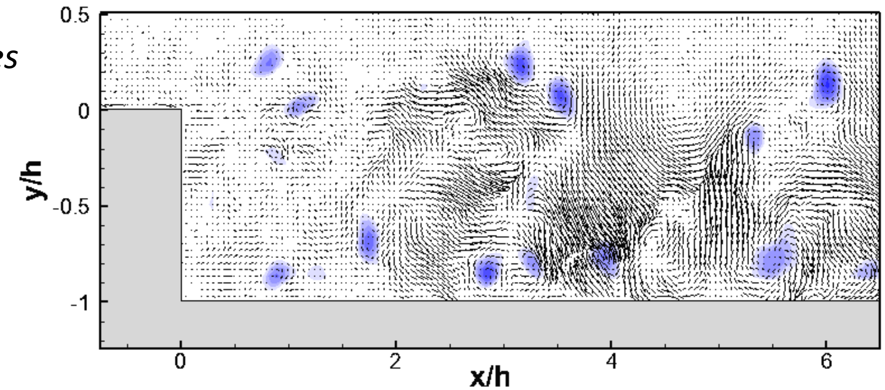

Figure 2: Reconstruction of turbulent stochastic contribution

Investigations on NACA0015 at University of Poitiers

A) Experimental setup

- Chord 350 mm
- Span 2.4 m (AR = 7)
- External velocity 40 m/s (**Re = 1 M**)
- Fixed incidence 11°

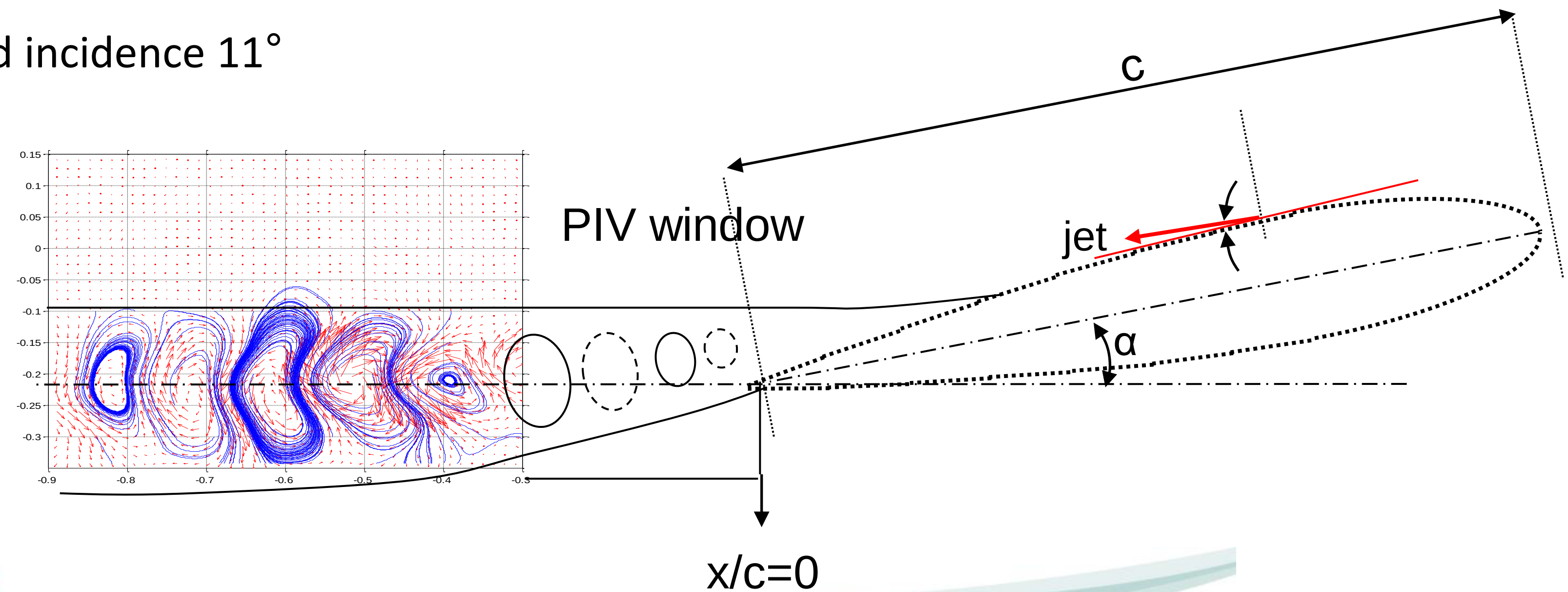

Investigations on NACA0015 at University of Poitiers

B) Fluidic vortex generators

- 44 FVG **Positioned at $x_A/c=0.3$**
- Pitch angle=30° and skew angle=60°
- 1 mm orifice diameter spaced 15 mm apart,

Inferred from open literatures

NO OPTIMIZATION

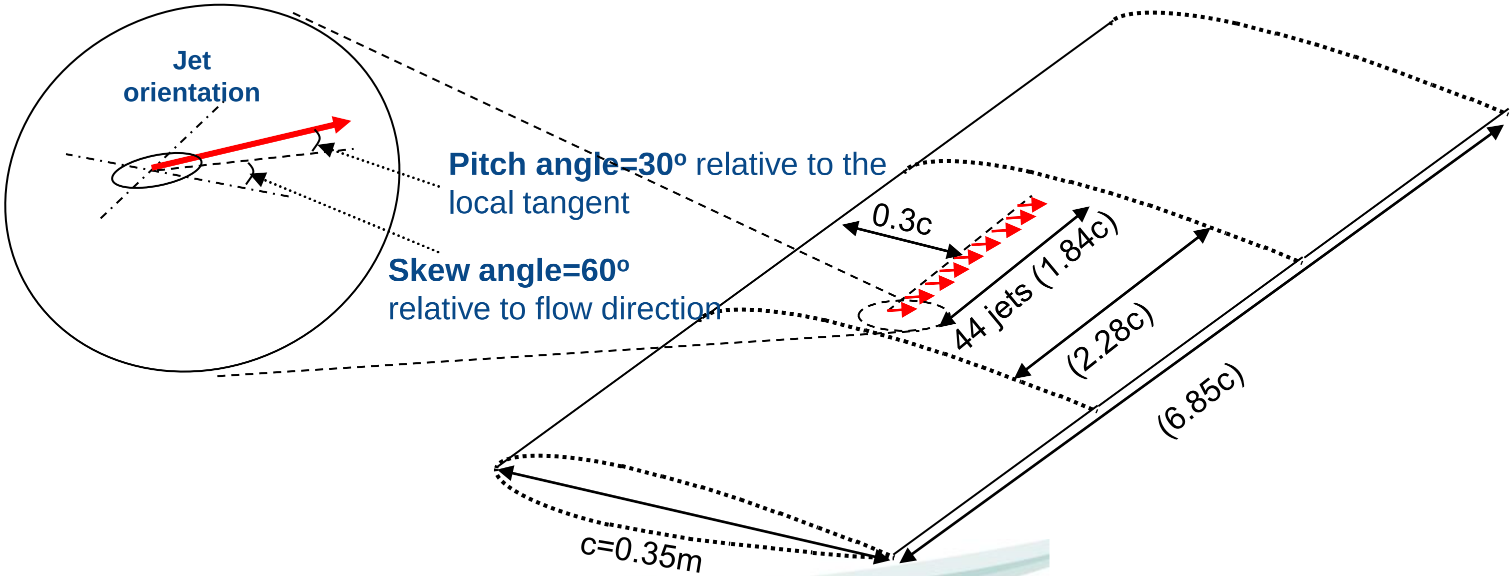

Investigations on NACA0015 at University of Poitiers

C) Study of transient regimes

The **dynamics** of flow **attachment/separation** over the airfoil surface of a NACA 0015 is analyzed in response to impulsive **deployment/removal** of fluidic vortex generators

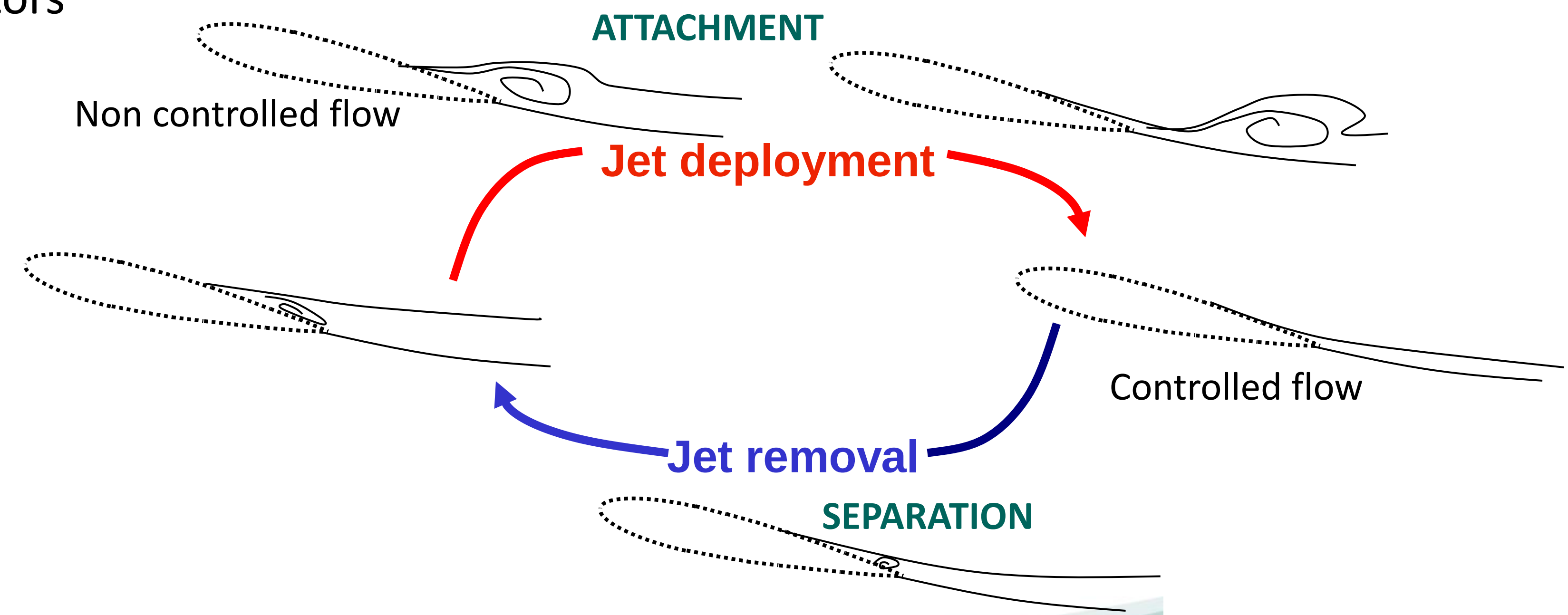

Investigations on NACA0015 at University of Poitiers

D) Time evolution of the mean V velocity component

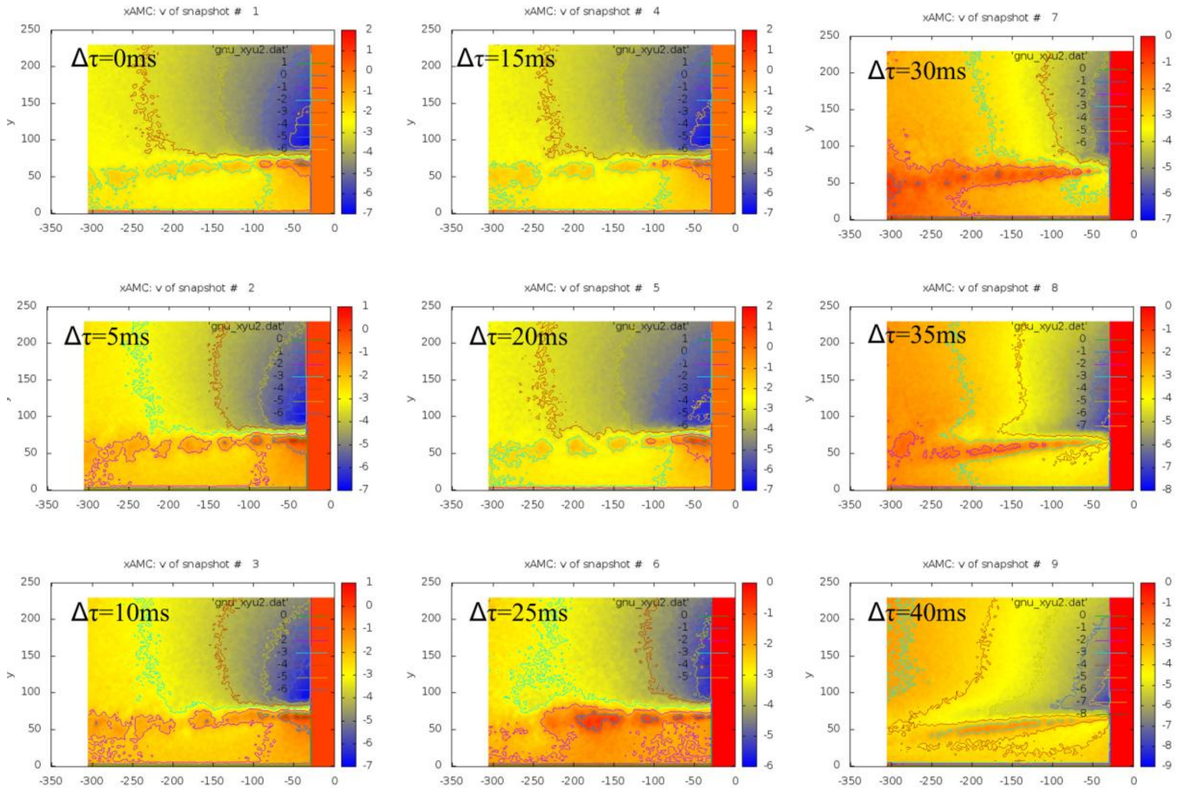

- Moderate flow response t<20 ms
- Wake width enlargement t=25-30 ms
- Mitigation of the flow separation at t=40 ms

Investigations on NACA0015 at University of Poitiers

E) Time evolution of the turbulent flow field

- $\Delta\tau$=10ms

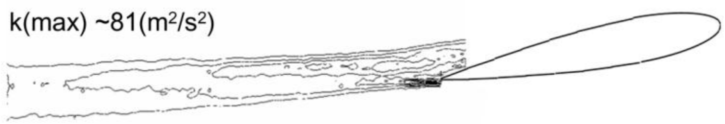

- $\Delta\tau$=30ms

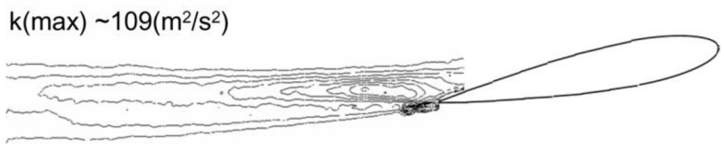

- $\Delta\tau$=50ms

Time evolution of the turbulent kinetic energy in the wake of the NACA0015

Investigations on NACA0015 at University of Poitiers

E) Time evolution of the turbulent flow field

- $\Delta\tau$=10ms
- $\Delta\tau$=30ms
- $\Delta\tau$=50ms

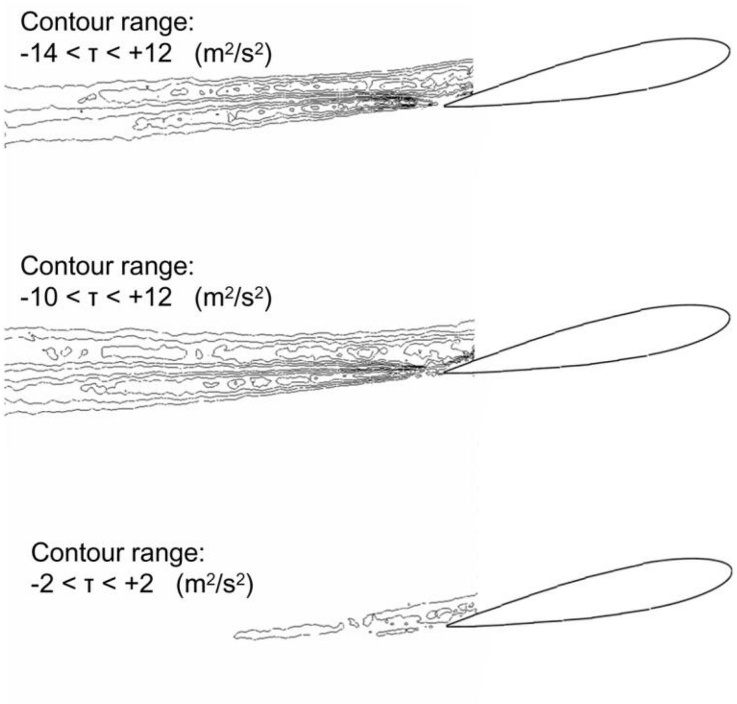

Time evolution of the Reynolds stress in the wake of the NACA0015

Ongoing researches

- A joint measurement campaign of 4 weeks was done this summer at DLR Gottingen:

Backward facing step

Time-resolved tomographic PIV
(University of Poitiers)

NACA 0015

Time-resolved stereoscopic PIV
(University of Manchester, Nanjing University of Aeronautics and Astronautics)

- Each partner conduced their own experiments according to defined test cases .

- Most of the experiments of MARS partners have been done, analysis, comparison and recommendation will be provided in M24-M36 report period.

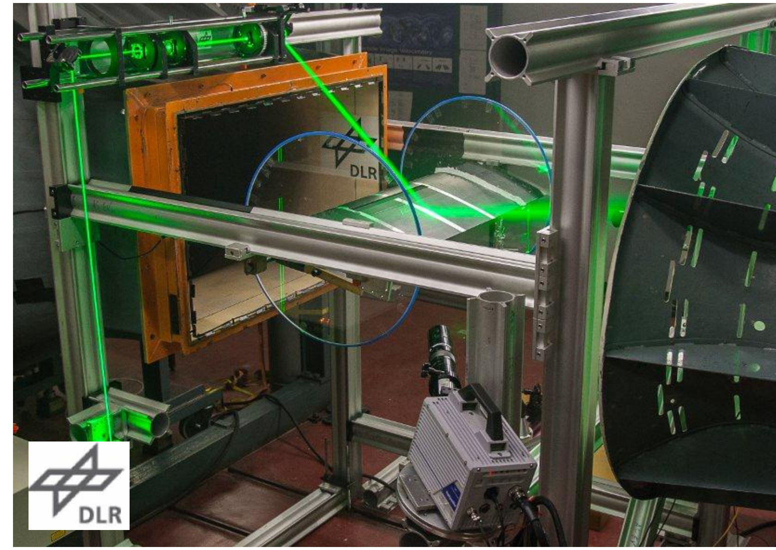

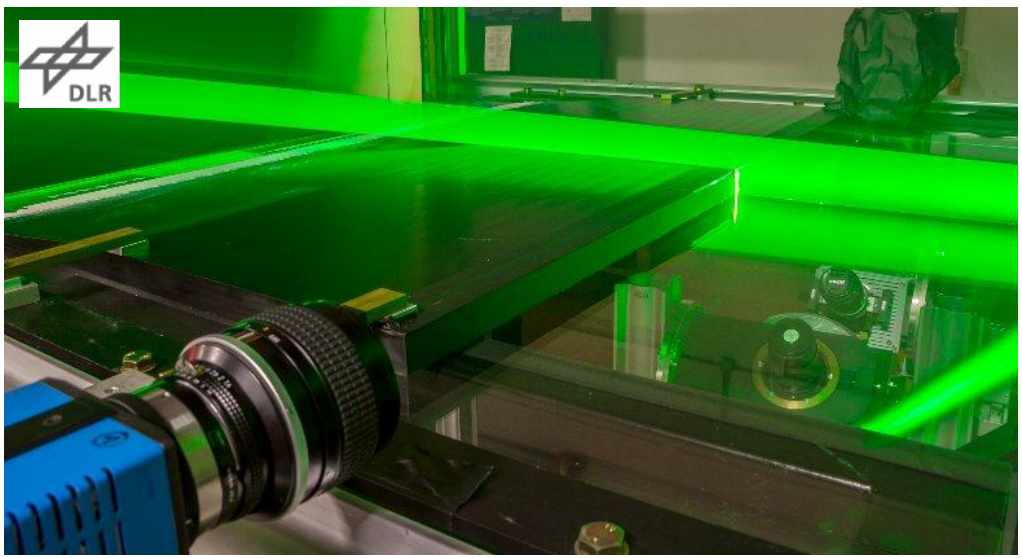

Questions ?

HYBRID RANS/LES FOR ACTIVE FLOW CONTROL USING OSCILLATING SURFACES AND FLUIDIC VORTEX GENERATOR

W. Wang, S. Siouris, and N. Qin
Department of Mechanical Engineering
University of Sheffield

The Second EASN Workshop on Flight Physics and Propulsion , Prague, Czech Republic
31st of October – 2nd of November 2012

Contents

- Introduction
- Methodology
  - Spatial and Temporal Discretisation
  - Turbulence Models
  - Dynamic Grid
- Modelling and Numerical Issues
  - Separation from a backward facing step
  - Separation from an aerofoil
- Simulations of flow control
  - Piezo oscillating surface on BFS
  - Pulse jets on NACA0015
- Conclusions

Introduction

- Part of FP7 MARS project, WP3, on numerical simulation of Reynolds stresses for flow control
- For aeronautical applications, flow control can have a significant impact on aircraft drag reduction and performance at off-design conditions
- Separation control
  - mild, moderate to massive separated flows, e.g. stall
  - fixed separation
  - separation from smooth surfaces
- Boundary layer control
  - laminar boundary layer control – to delay transition
  - turbulent boundary layer control – to reduce t.b.l. drag
- Numerical study of flow control requires
  - accurate prediction of flow separation
  - resolved Reynolds stresses to understand flow control effectiveness
  - moving mesh for active flow control actuators

Governing Equations

The N-S equations with ALE (Arbitrary Lagrange Eulerian) formulation

$$\frac{\partial}{\partial t}\int_{\Omega} U dV + \int_{S}\left(F^{c} - F^{\upsilon}\right)\cdot \vec{n} dS = 0$$

with

$$U = \begin{pmatrix} \bar{\rho} \\ \bar{\rho}\tilde{\vec{u}} \\ \tilde{E} \end{pmatrix}, F^{c} = \left(\tilde{\vec{u}} - \tilde{\vec{u}}_{g}\right)\begin{pmatrix} \bar{\rho} \\ \bar{\rho}\tilde{\vec{u}} \\ \tilde{E} \end{pmatrix} + \begin{pmatrix} 0 \\ \tilde{P}[\mathrm{I}] \\ \tilde{P}\tilde{\vec{u}} \end{pmatrix}, F^{\upsilon} = \begin{pmatrix} 0 \\ [\tau]^{eff} \\ \left([\tau]^{eff} \bullet \vec{u}\right) + \vec{q}^{\,eff} \end{pmatrix}$$

$$[\tau]^{eff} = [\tau] + [\tau]^{turb}$$

and the S-A equation

$$\frac{\partial}{\partial t}\int_{\Omega(t)} \tilde{\upsilon} d\Omega + \int_{\partial\Omega(t)}\left(\tilde{\upsilon}\vec{u} - \frac{1}{\sigma_{\tilde{\upsilon}}}(\upsilon + \tilde{\upsilon})\vec{\nabla}\tilde{\upsilon}\right)\cdot \vec{n} dS$$

$$= \int_{\Omega(t)}\left\{\left[C_{b1}(1 - f_{t2})\hat{S} + \vec{\nabla}\cdot\vec{u}\right]\tilde{\upsilon} + \frac{1}{\sigma_{\tilde{\upsilon}}}C_{b2}\left(\vec{\nabla}\tilde{\upsilon}\right)^{2} - \left(C_{w1}f_{w} - \frac{C_{b1}}{\varphi^{2}}f_{t2}\right)\left(\frac{\tilde{\upsilon}}{\tilde{d}}\right)^{2}\right\} dV$$

Turbulence or SSG Models

RANS: ✓Spalart Allmaras model (SA)	1) Simulate steady and small separation problems 2) Small computational cost
LES: ✓Smagorinksy model ✓Dynamic Smagorinksy model ✓Implicit LES (iLES)	1) Simulate separated turbulent flows 2) Large computation cost
Hybrid RANS/LES: ✓Detached Eddy Simulation (DES) ✓Delayed DES (DDES) ✓Improved DDES (IDDES) ✓iLES with SA wall modelled (SA-iLES)	1) Work as wall-modelled LES. 2) Simulate separated turbulent flows 3) Moderate computation cost

Hybrid RANS/LES Models

DES: hybrid method of RANS and LES by using the modified distance

$$\tilde{d} = \min\left(C_{DES}\Delta, d\right)$$

d<$C_{DES}\Delta$

$$\tilde{d} = d$$

RANS

$$\mu_{tur} = f_{v1}\rho\tilde{\upsilon}$$

otherwise

$$\tilde{d} = C_{DES}\Delta$$

LES: Smargorinsky-like SGS modeling

In equilibrium $\left[C_{b1}(1-f_{t2})\tilde{S}\right]\tilde{\upsilon} = \left(C_{w1}f_w - \frac{C_{b1}}{\varphi^2}f_{t2}\right)\left(\frac{\tilde{\upsilon}}{\tilde{d}}\right)^2$

$$\mu_{tur} = \rho_C l_C{}^2\left|\tilde{S}\right| = \rho_C l_C{}^2\sqrt{2\tilde{S}_{ij}\tilde{S}_{ij}}$$

For DES, the region of RANS and LES are determined by **the mesh only.**
DDES, IDDES and iLES have also been implemented.

Temporal Discretisation

The University Of Sheffield.

•**Dual Time Stepping Method**

$$\underbrace{\frac{\partial}{\partial t}\int_{\Omega}\mathbf{W}d\Omega}_{\text{Physical time}}+\underbrace{\frac{\partial \mathbf{W}}{\partial \mathbf{Q}}\cdot\frac{\partial}{\partial \tau}\int_{\Omega}\mathbf{Q}d\Omega}_{\text{pseudo time}}=\text{-}\Re$$

•**Second Order Euler's backward difference on physical time term:**

$$\underbrace{\Gamma^n\Omega^n\left(\frac{\partial \vec{Q}}{\partial \tau}\right)^n}_{\text{pseudo time}}=\text{-}\left[\Re^n+\frac{[W^{m-1}\Omega+\frac{\partial W}{\partial Q}(Q^m-Q^{m-1})\Omega]^n-(W\Omega)^{n-1}}{\Delta t}\right]$$

•**Explicit 4th order Runge Kutta methods on pseudo time:**

$$\mathbf{Q}^m=\mathbf{Q}^{m-1}-\Delta\tau\cdot\left[\frac{1}{\Omega}\left(\Gamma^{m-1}+\frac{\Delta\tau}{\Delta t}\frac{\partial \mathbf{W}}{\partial \mathbf{Q}}\right)^{-1}\right]^n\cdot\left[(\Re^{m-1})^n+\frac{(\mathbf{W}^{m-1}\Omega)^n-(\mathbf{W}\Omega)^{n-1}}{\Delta t}\right]$$

$\Delta t=\varepsilon$ →Unsteady Problems

$\Delta t \rightarrow \propto$ →Stead Problems

Convective Fluxes Discretisation

- **2^{nd} order Roe-type schemes**
  - Original Roe scheme
    - ✓Solve RANS problems stable and accurately
  - Preconditioning Roe scheme
    - ✓Simulate flow with low Mach number using compressible solver
  - Low/ALL speed Roe scheme
    - ✓Simulate flow involving both low and high speeds, e.g. cavitation in a rocket engine.

- **2^{nd} order Simple Low-dissipation AUSM (SLAU)**

- **Blending of upwind scheme and central difference scheme**
  - Simulate turbulent flows using LES, with low numerical dissipation
  - Obtain more resolved turbulence fluctuations

Dynamic Grid DES

Features of the DES code (DG-DES**)**:

- **Unstructured/hybrid** cell centered finite volume discretisation
- **Dual time** stepping: **implicit** physical time marching + 4-stage Runge-Kutta pseudo-time marching
- **ALE** (Arbitrary Lagrange Eulerian) formulation
- **Dynamic gridding** for moving boundaries, such as, synthetic jet membranes, flapping wings, fluid structure interaction, morphing and adaptive wings
- The DG-DES code is **fully parallelized** (using **METIS** for unstructured mesh) and have been ported to the local Linux clusters, the White Rose Clusters and the national HPC **HECToR**

Vortex Criteria for Post-processing

Vorticity vector : $\omega = \nabla \times V$

Q-criterion: $Q = ½ (\mathrm{trace}(\nabla u)^2 - \mathrm{trace}((\nabla u)^2)) = ½ (\|\Omega\|^2 - \|S\|^2)$

Balances between shear strain rate and vorticity magnitude

Lambda2-criterion: The middle eigenvalue of the matrix $S^2 + \Omega^2$

Removes unsteady irrotational strain and viscous effects

where: V, velocity vector

$S = ½ (\nabla V + (\nabla V)^T)$, symmetric part of the gradient of velocity

$\Omega = ½ (\nabla V - (\nabla V)^T)$, anti-symmetric part of the gradient

Pipe Flow Validation – Attached Flow

Mesh

Number of nodes	Number of elements	Type of cells		
		Brick	Tetrahedral	Pyramid
946,946	931,500	931,500	0	0

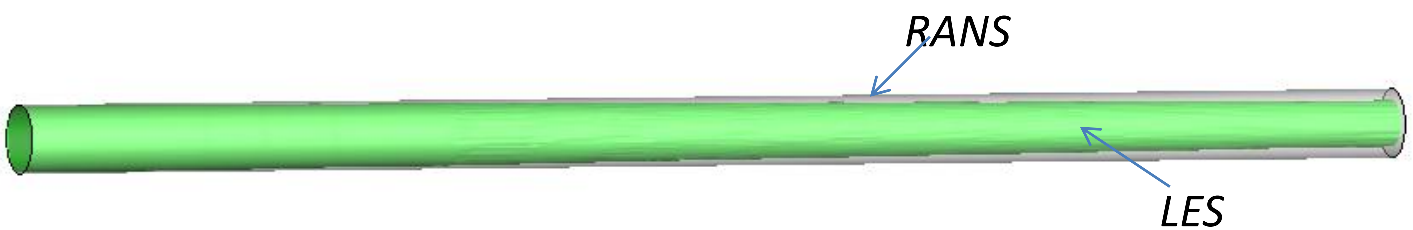

Result shows the velocity profile is better than pure RANS in the wake region

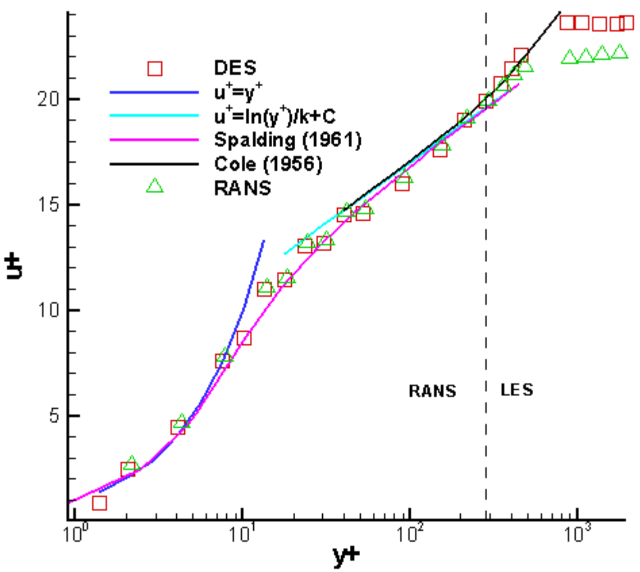

Spalding (1961) 's empirical formula in the sub-layer, buffer layer and log-layer

$$y^{+}=u^{+}+e^{-kB}\left[e^{ku^{+}}-1-ku^{+}-\frac{\left(ku^{+}\right)^{2}}{2}-\frac{\left(ku^{+}\right)^{3}}{6}\right]$$

Cole (1956) 's empirical formula in the wake region

$$u^{+}=1/\kappa\ln\left(y^{+}\right)+B+2\Pi/\kappa\cdot\sin^{2}\left(\frac{\pi y}{2\delta}\right)$$

BFS (Driver & Seegmiller) key comparisons – reattachment points and pressure rise

Comparison of numerical schemes on BFS

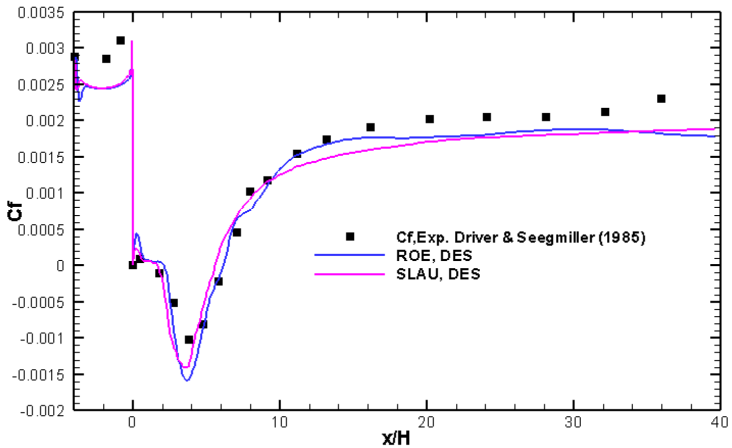

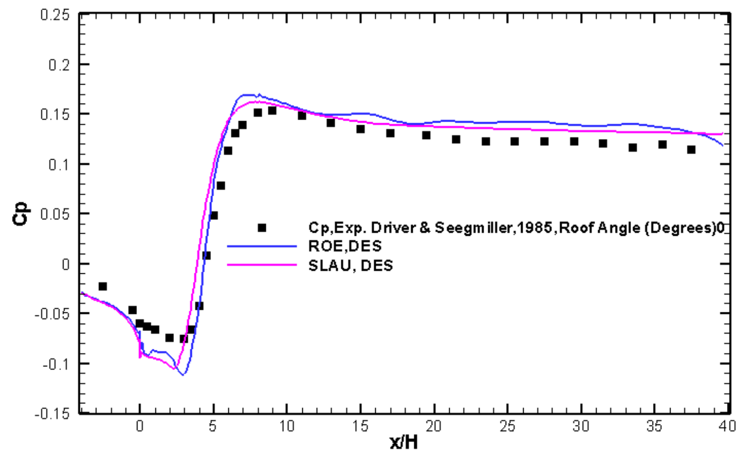

ROE and SLAU schemes give comparable results.

Comparison of turbulence/SGS models on BFS

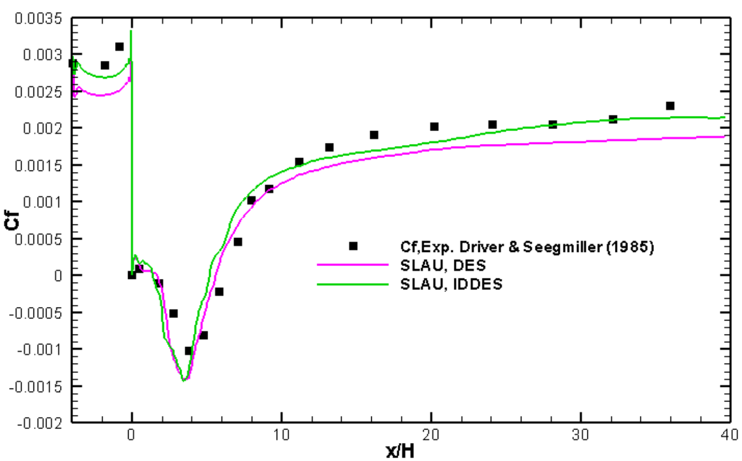

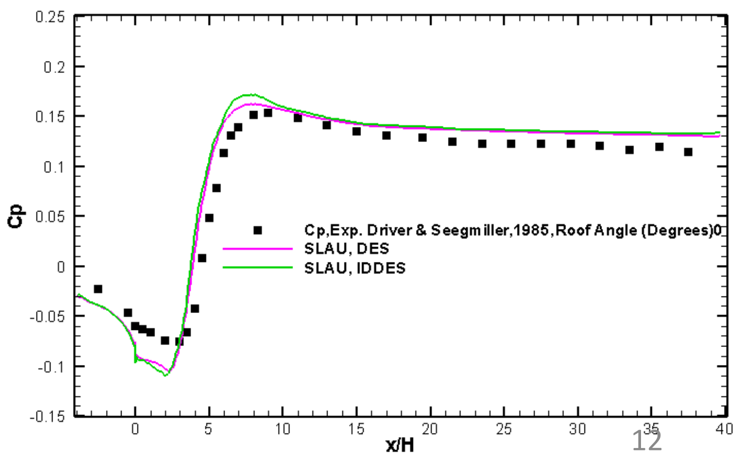

IDDES and DES performances similarly for the BSF case.

BFS (Driver & Seegmiller)

Comparison of velocity profiles and Reynolds shear stress ROE/DES

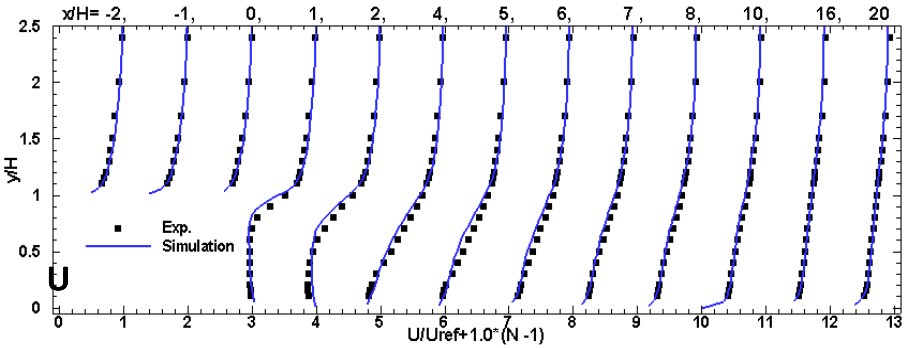

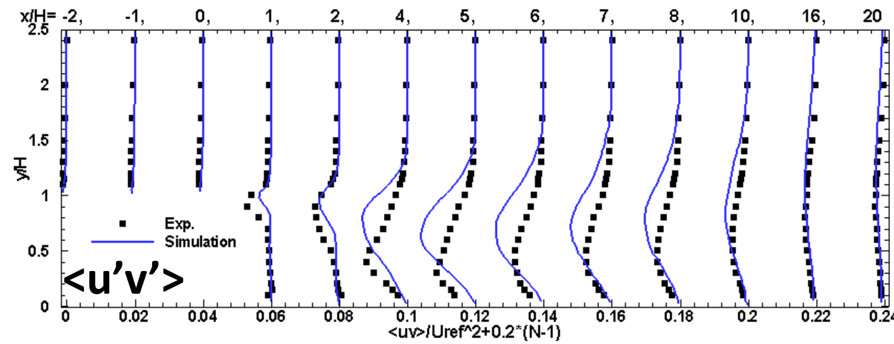

Time and spanwise averaged streamlines

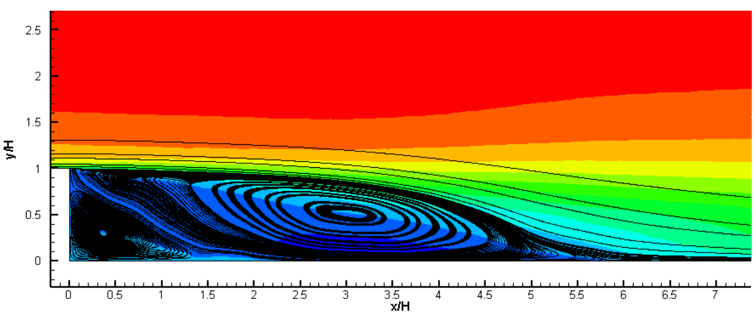

ISO surface of vorticity magnitude=5000 and 10000
Coloured with streamwise velocity

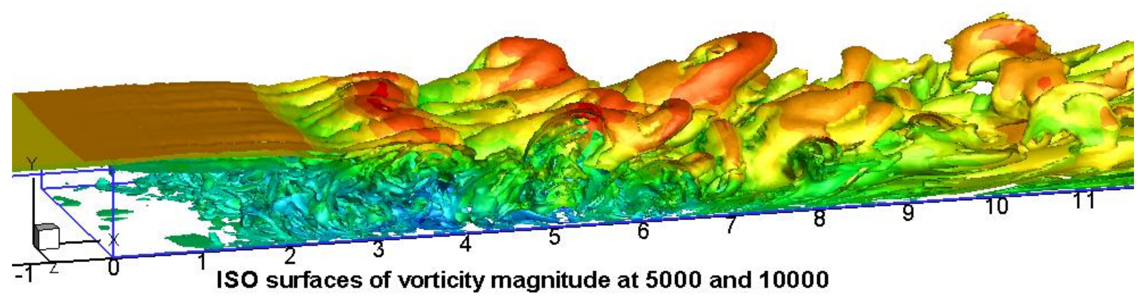

BFS UniMan Case: Baseline

Geometry, Mesh and Boundary Conditions

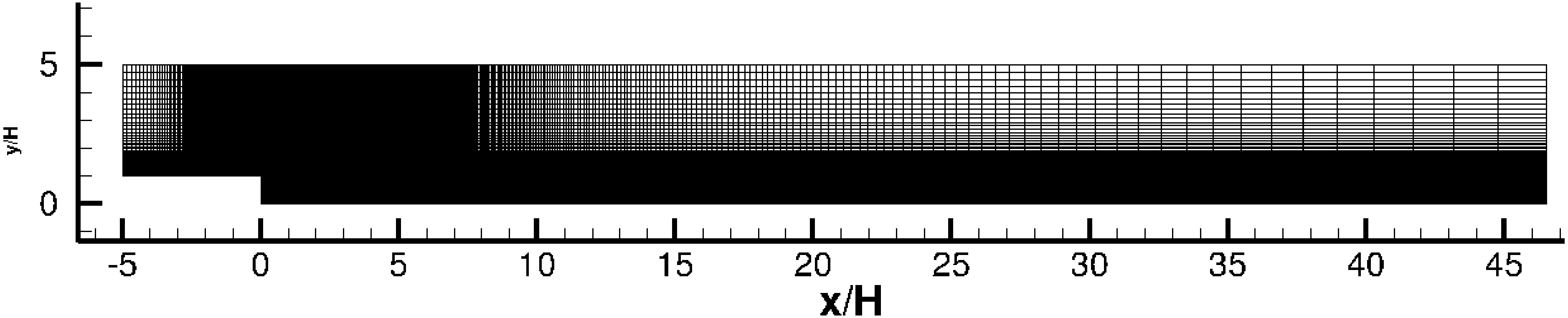

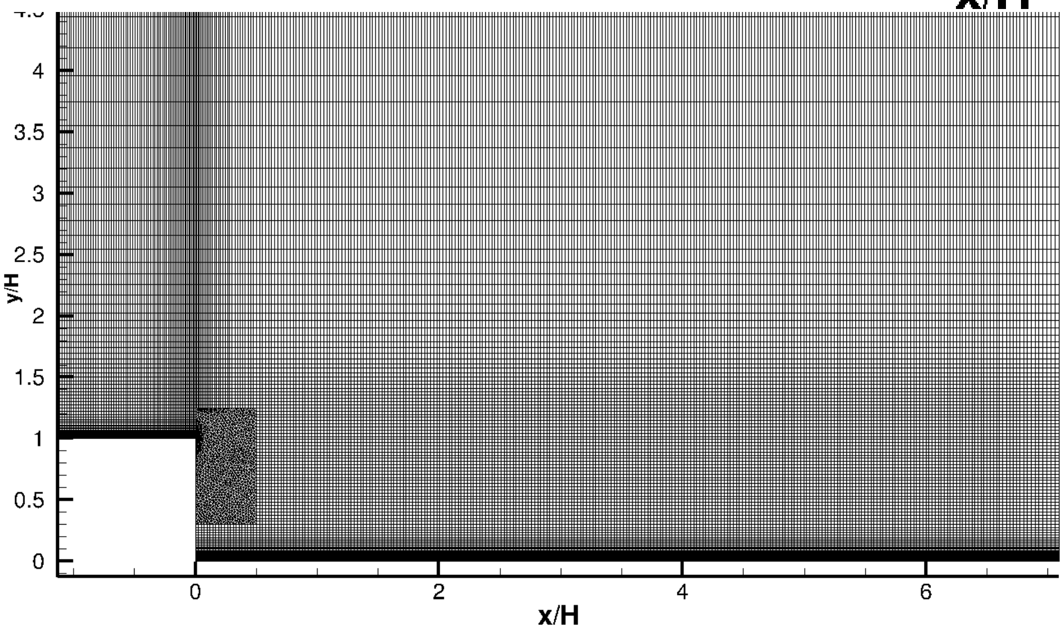

- Geometry:
  - Step Height = 0.065m
  - U_{ref} = 15m/s
  - Re_h = $6.4\text{x}10^{-4}$
  - ER = 1.08
  - Lz = 1.4H
- Mesh-Hybrid:
  - cells no. = 7,030,200
  - Nz = 100
- Boundary Conditions:
  - wind tunnel top : slip-WALL
  - wind tunnel bottom : no-slip WALL
  - inlet : VELOCITY INLET
  - outlet : PRESSURE OUTLET
  - spanwise : PERIODIC

BFS UniMan Case: Baseline

- **Time averaged streamlines:**

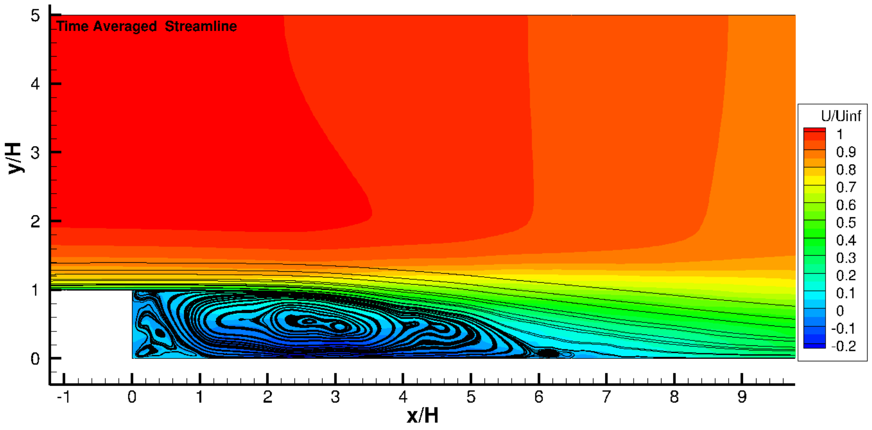

- **Instantaneous vorticity magnitude:**

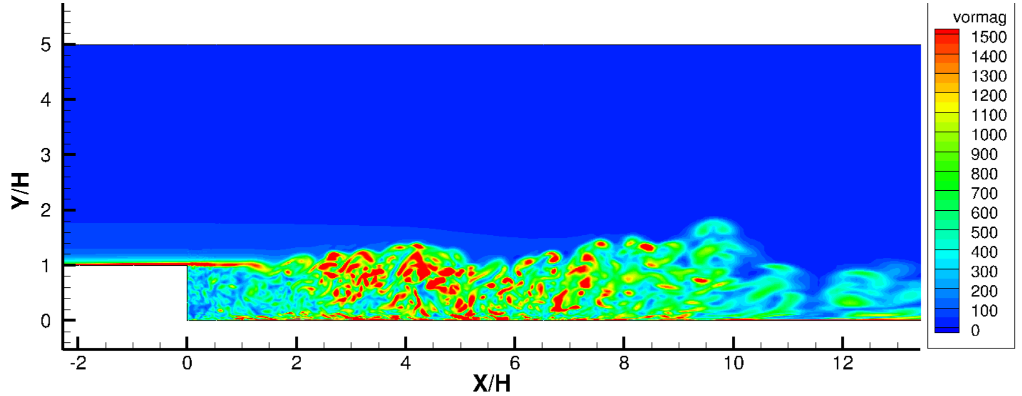

Comparison of separation: $Xr_{comp} = 6.6H$; $Xr_{exp} = 6.5H$

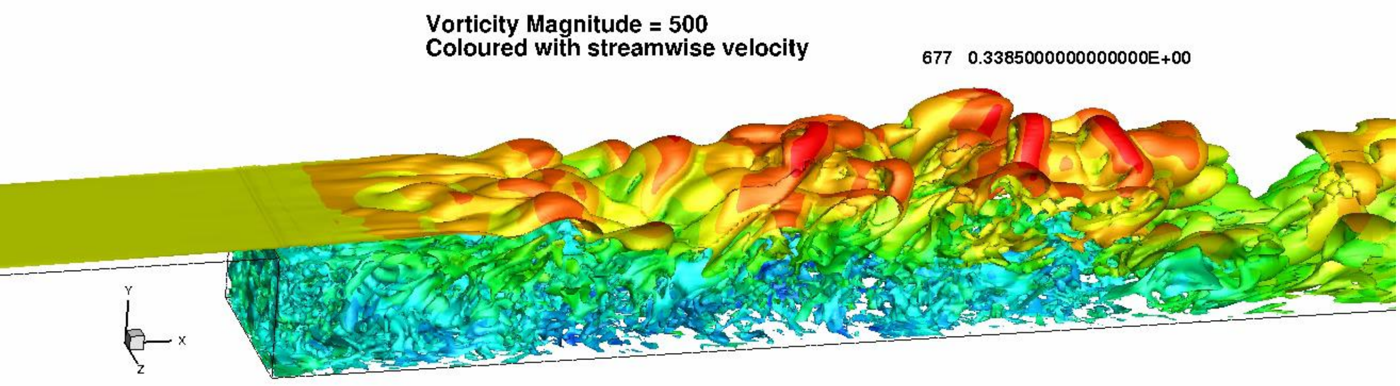

Some coherent hair pin edge structures can be observed travelling down stream

Geometry, Mesh and Boundary Conditions

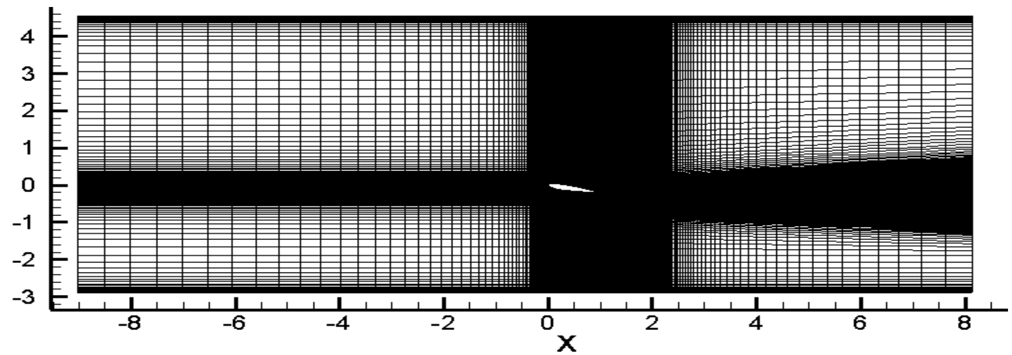

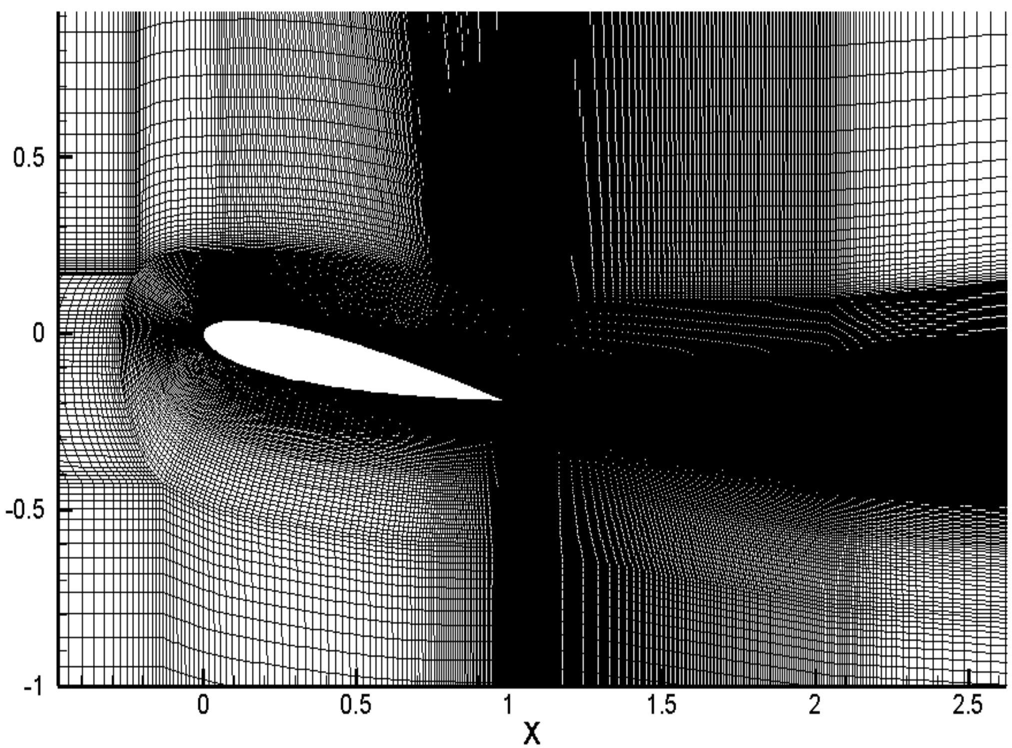

- **Geometry:**
  - chord = 0.35m
  - α = 18°
  - U_{ref} = 40m/s
  - Re = 0.933×10^6
  - Lz = 0.18c

- **Mesh-Multiblock Structured:**
  - cells no. = 8,511,000
  - Nz = 40

- **Boundary Conditions:**
  - wind tunnel: WALL
  - aerofoil: WALL
  - inlet: VELOCITY INLET
  - outlet: PRESSURE OUTLET
  - spanwise: PERIODIC

NACA0015 Poitier Case – Effects of models

The University Of Sheffield.

Comparison of RANS, DES, IDDES

2D RANS

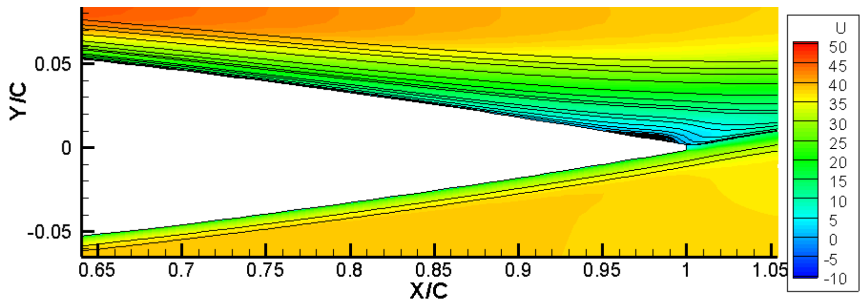

3D URANS (Lz/Nz = 0.2c/25)

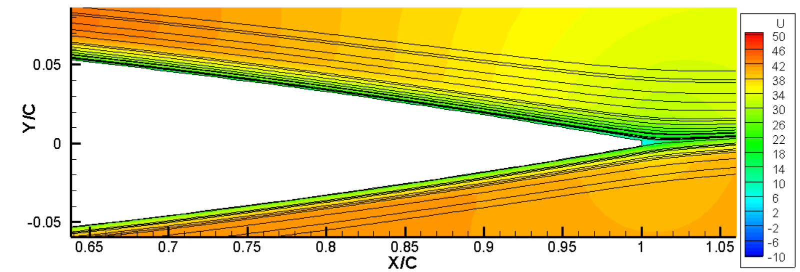

3D DES (3.7M)

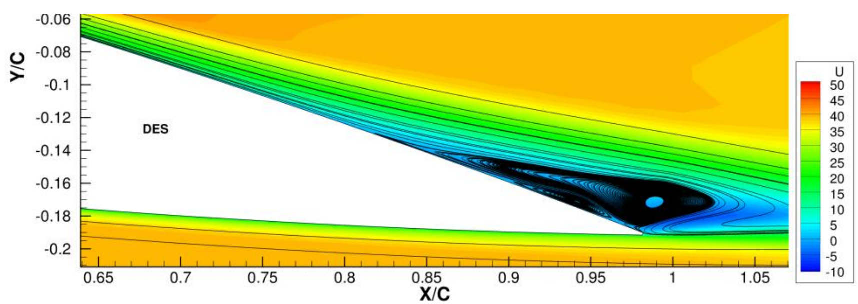

3D IDDES (3.7M instantaneous)

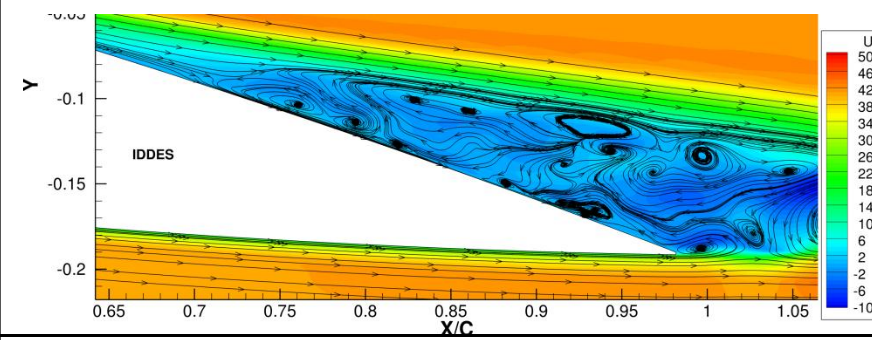

Lessons learned

- RANS and URANS(3D) failed to predict separation
- With the same mesh, IDDES performances better than DES in capturing separation region.
- IDDES with sufficient mesh gives good separation as compared with exp at 70%c

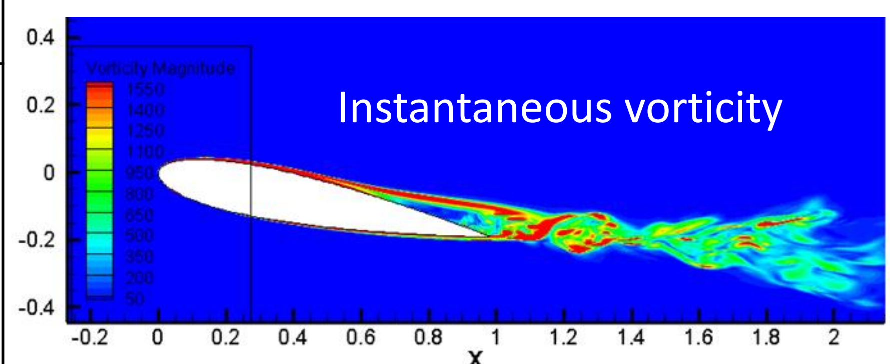

NACA0015 Poitier Case: Baseline

Results of IDDES in the wake

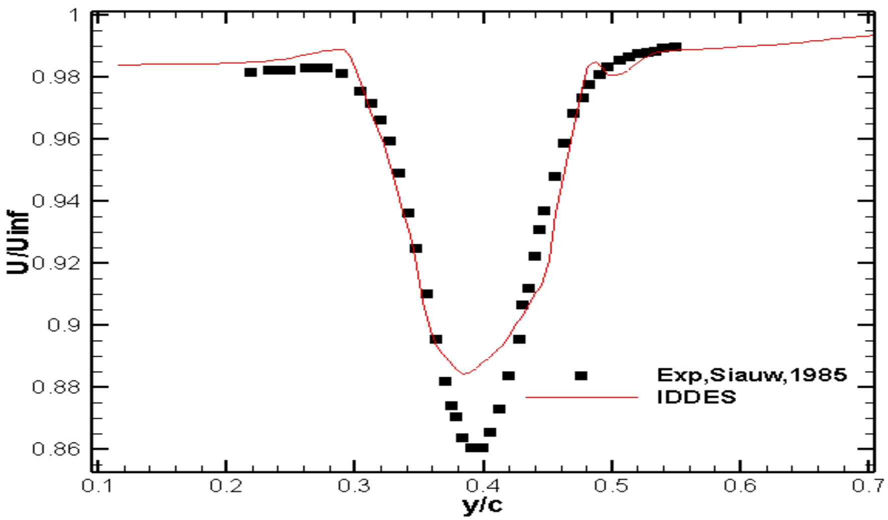

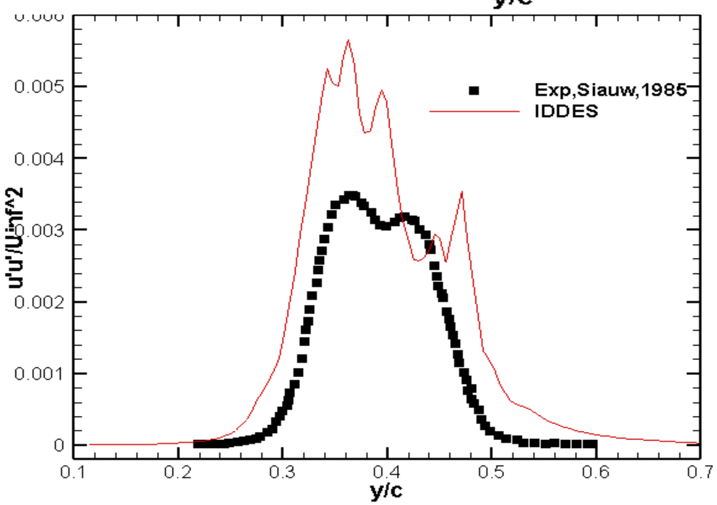

Power Spectral Density of v-velocity at x/c=1.98c

Frequency
Comp = 437.5 Hz
Exp = 474 Hz

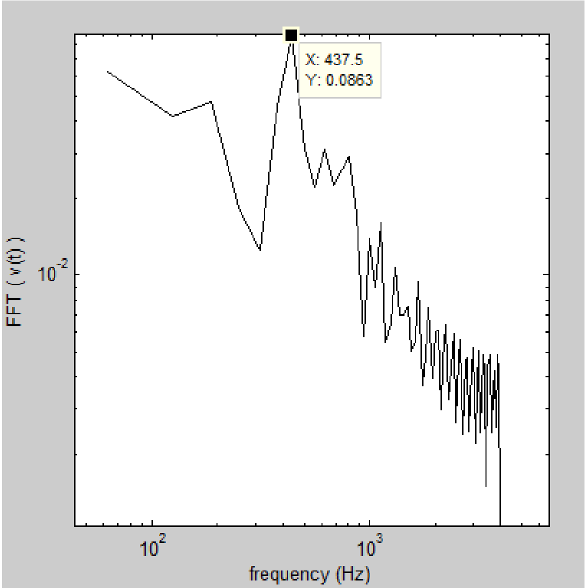

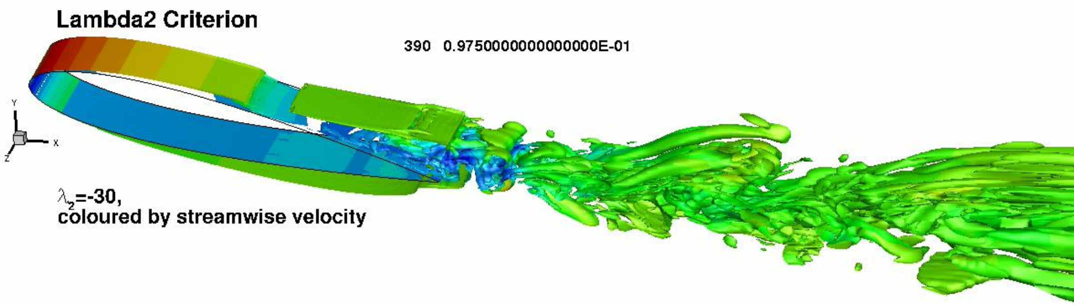

NACA0015 (α = 16.6º) – Massive Separation

Gilarranz, *et al*. J Fluid Eng, vol.127(2), 2005. Re=8.96x10^5, U_∞ =35m/s, c=0.375m

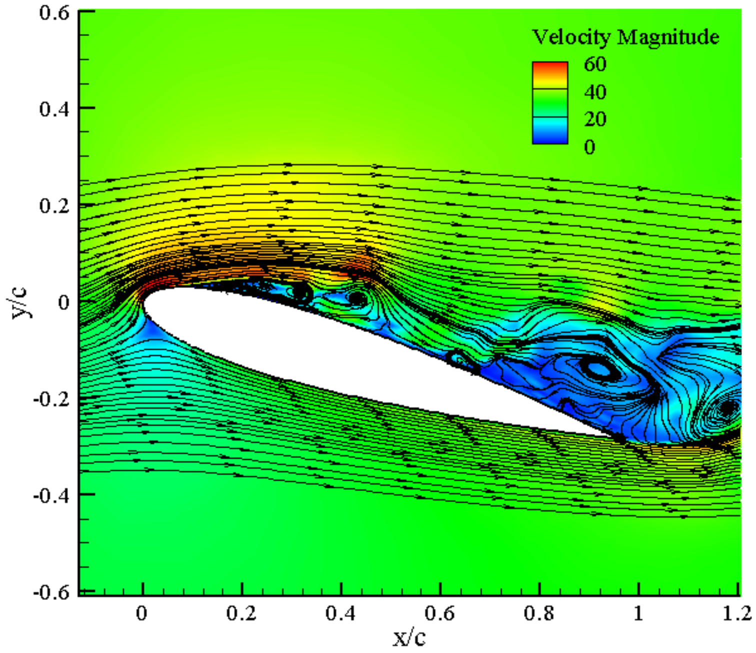

Contour plots of the instantaneous streamwise velocity.

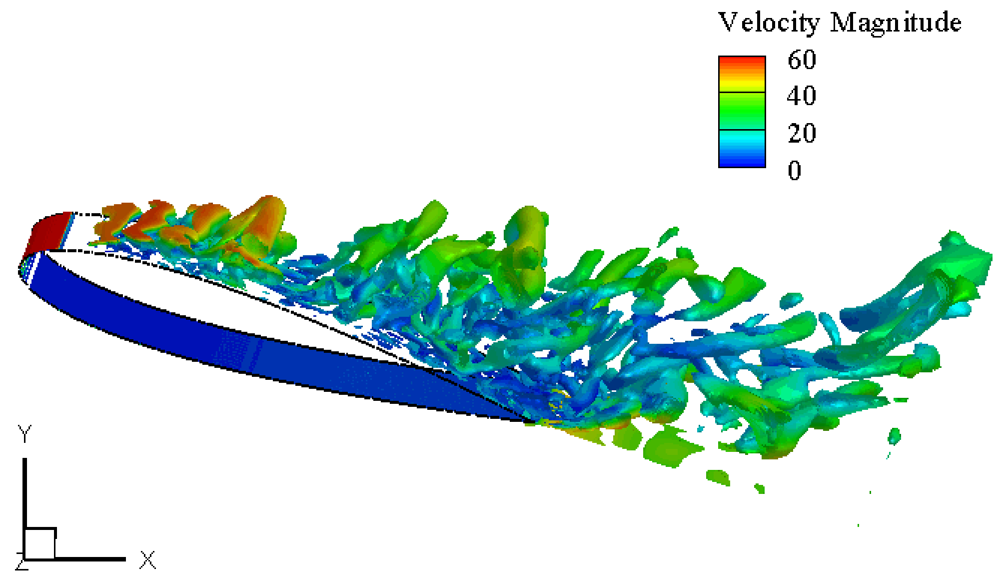

Iso-surface for the instantaneous Q-Criteria overlapped with velocity magnitude.

Case	Aerodynamic Characteristics	
	CL	CD
Exp.	0.84	0.25
LES (8 million mesh)	0.83	0.28
LES (15 million mesh)	0.81	0.28
Present DES (4 million)	0.844	0.212

Separation control using synthetic jet

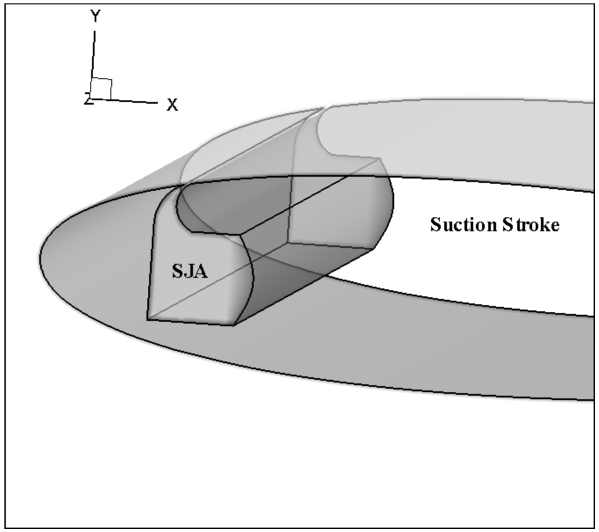

Actuator at max. suction

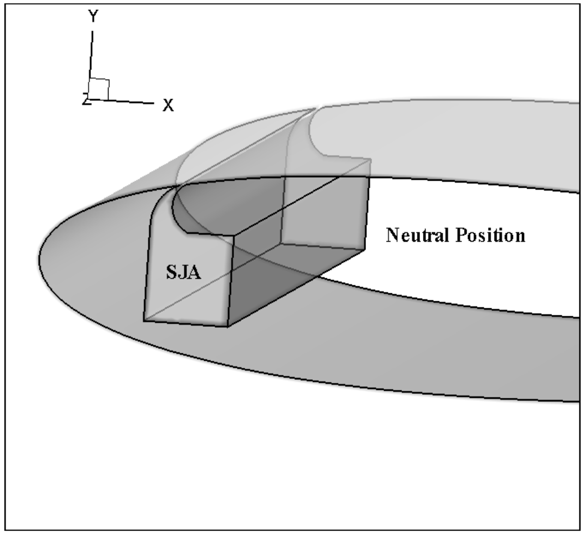

Actuator at neutral position

Control Parameters

- Slot jet location: 12%c from the leading edge
- Slot width: 2 mm
- Maximum jet momentum coefficient: Cμ = 0.0123.
- The actuator operating frequency = 120 *Hz*
- Dynamic hybrid mesh
- 4 millions cells

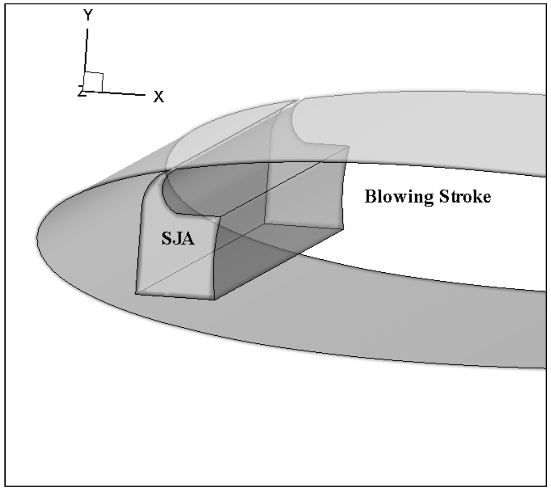

Actuator at max. blowing

Stall Control at 25°

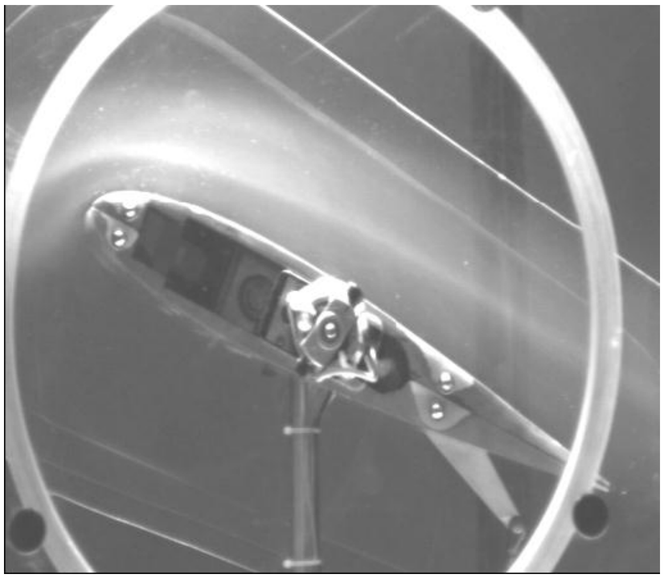

Controlled wing, Exp.

α=25 °

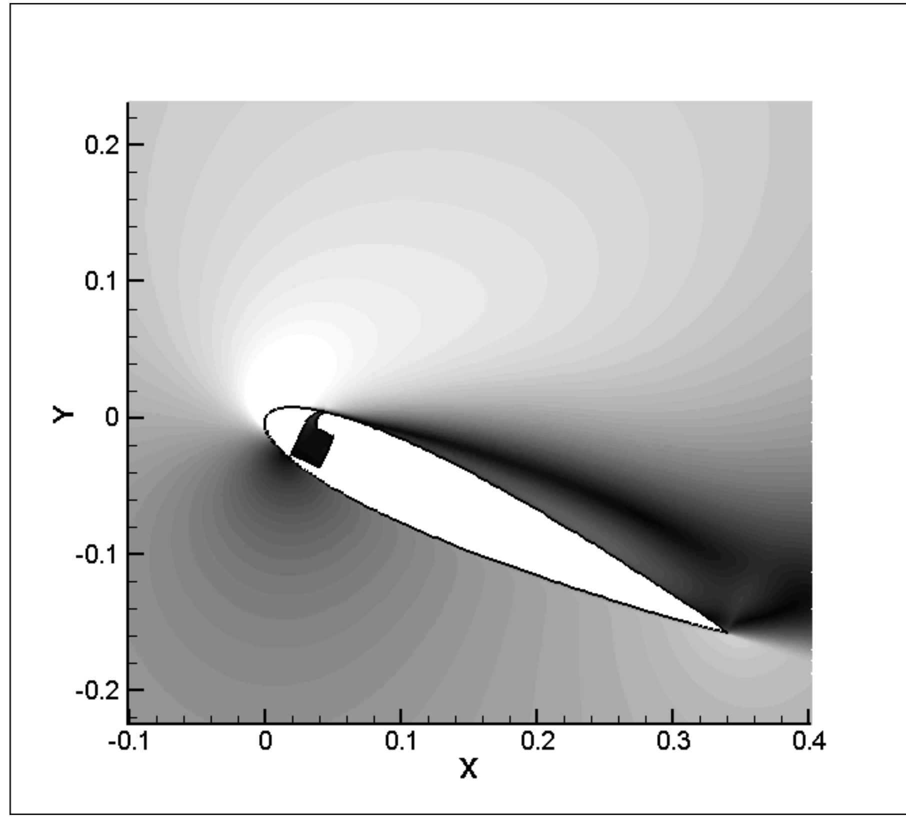

Controlled wing, DG-DES with Moving Grid. Mean velocity magnitude

BFS oscillating surface flow control

The University Of Sheffield.

Mesh and boundary condition

the same as the baseline case

Flow control geometrical parameter

Diameter of Oscillating surface : 0.041m = 0.631H

Position of the centre of controlled surface : -0.095m =-1.462H

Distance between two controlled surfaces : 45mm = 0.692H

Flow control parameter

Max. displacement of the surface = $9.55\text{x}10^{-6}$ m

Max. velocity of the surface = 0.006 m/s

Frequency = 100Hz

Probed vertical velocity and displacement in the centre of the controlled surface

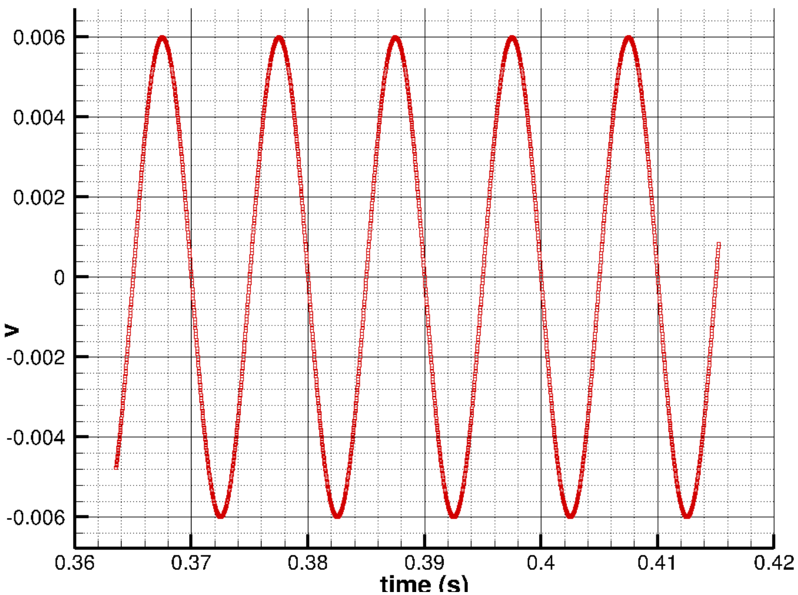

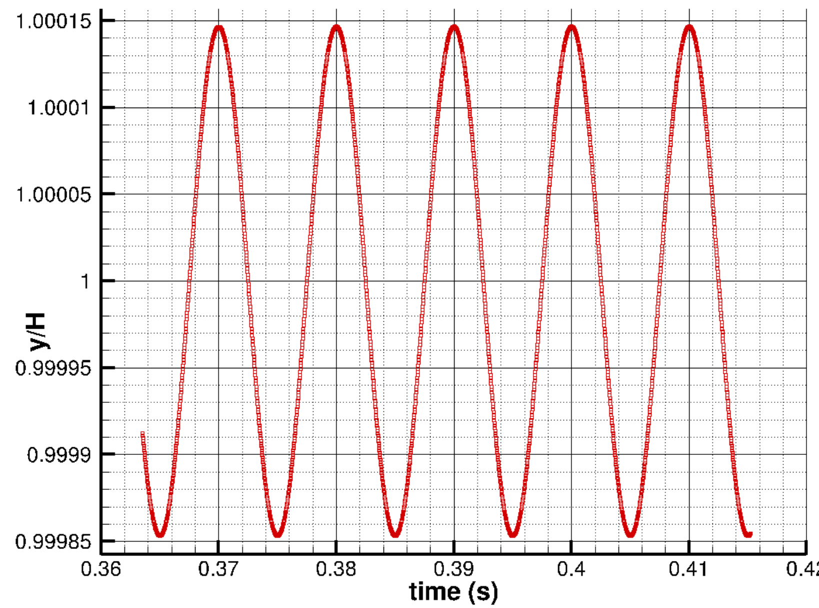

Results of DES

❑ Short-Time averaged Result:

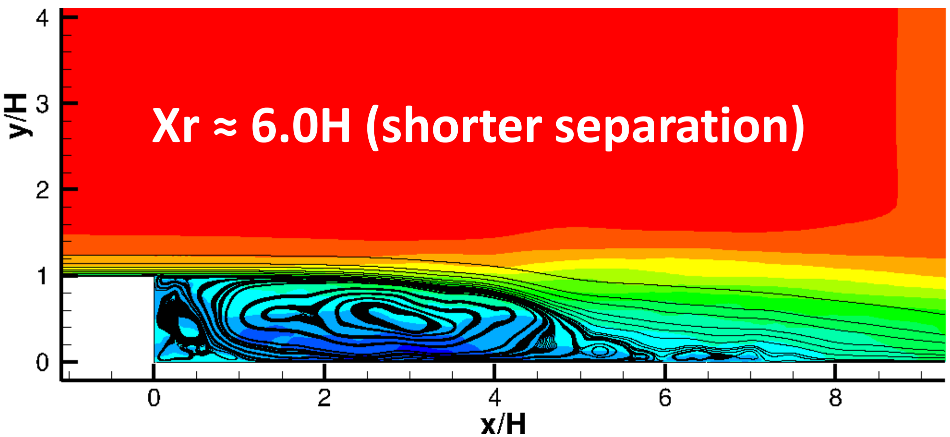

❑ Instantaneous Results:

Vertical velocity at the cell-centre of the first layer cell

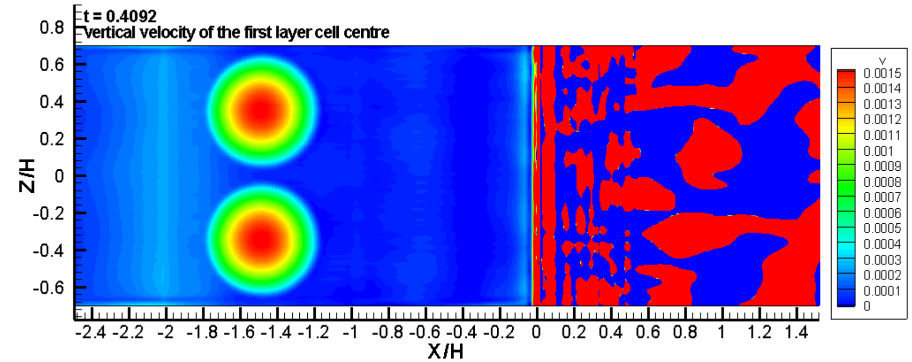

❑ Instantaneous Results:

Q-criterion at the cell-centre of the first layer cell

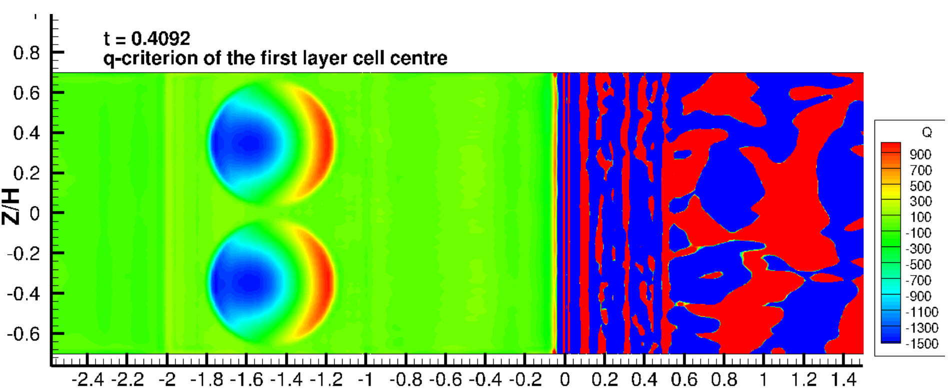

x-vorticity at the cell-centre of the first layer cell

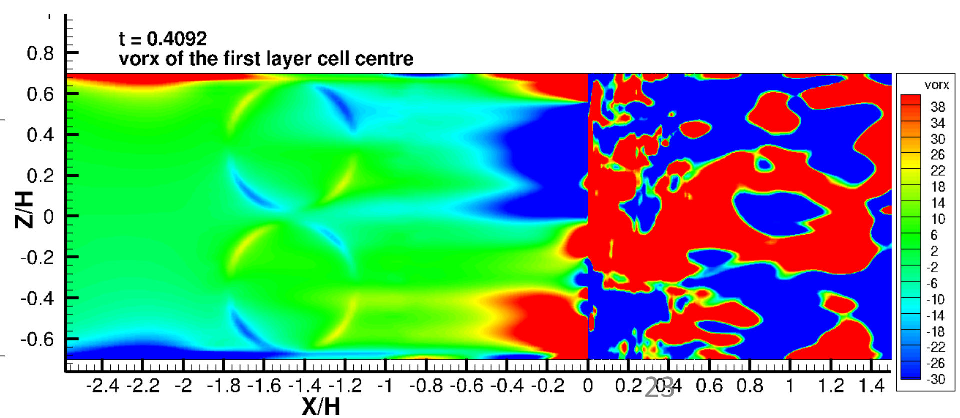

BFS oscillating surface flow control

- **Manchester Pezioactuator oscillating surface control device**

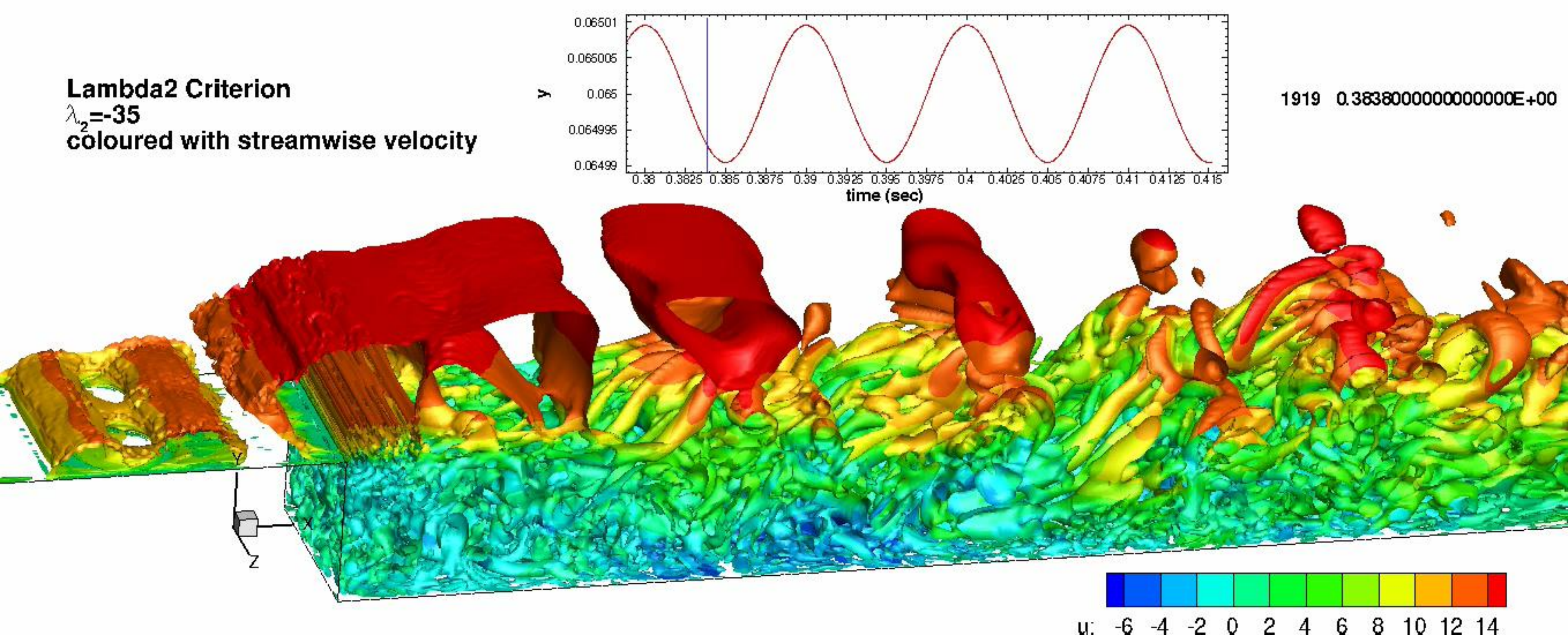

Oscillating surface flow control

Reynolds stress comparison of the baseline case and controlled case

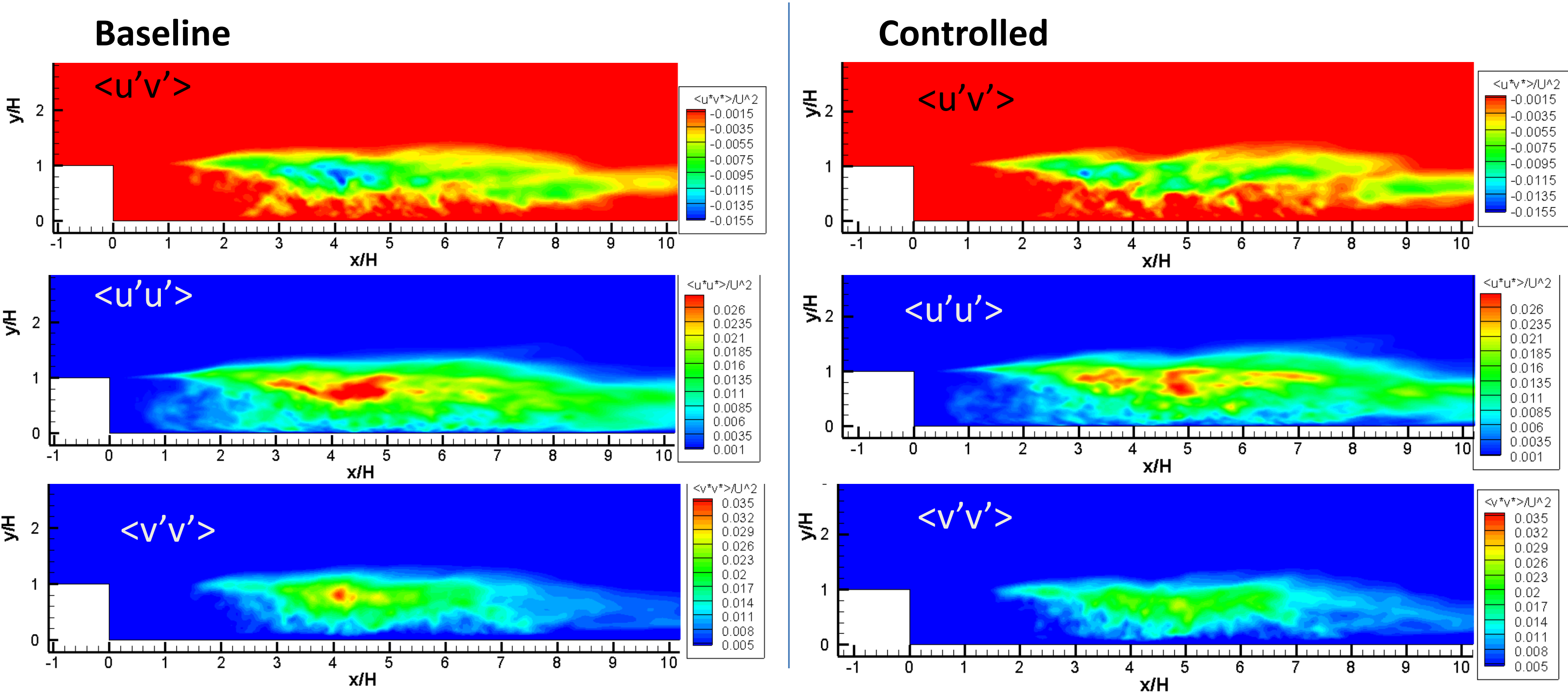

All three Reynolds stresses of the controlled case decrease and the peak values moves towards the step, which may explain the reattachment point moving towards the step.

NACA0015 Pulse Jets (Fluidic VG)

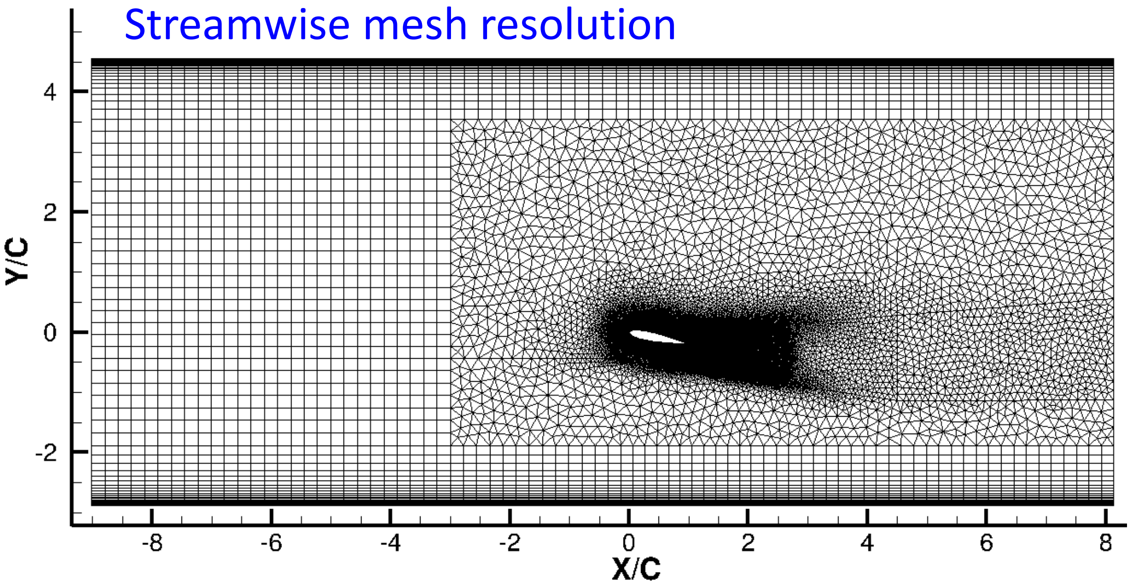

- **Mesh-Hybrid Mesh**

  1) Near the airfoil, structured mesh. Finer mesh near the jet position compared with the baseline mesh
  2) Unstructured mesh is used to decrease total cell number.
  3) In spanwise, mesh refinement near the jet positions is also applied.

- **Mesh-parameters**

  Four jets simulated in this case
  Cells no. = 15,048,560
  Lz = 15mmx4 = 0.1714c
  Nz = 80

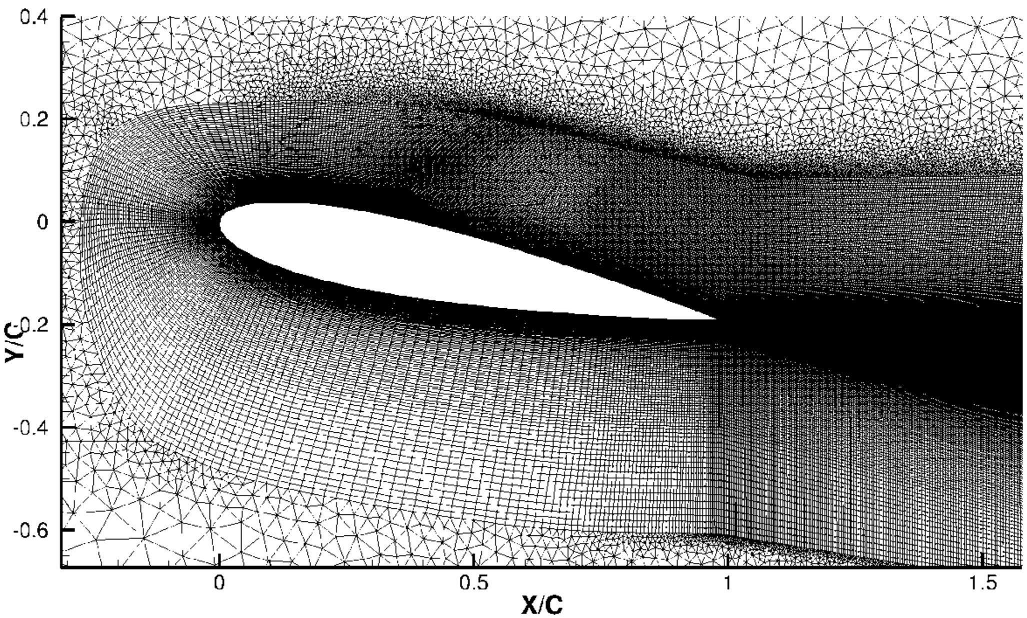

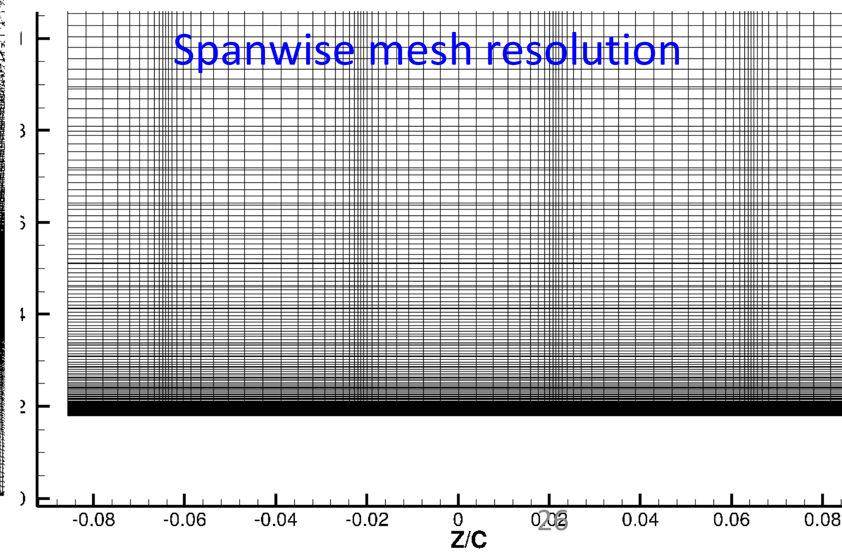

NACA0015 Pulse Jets

❑ Flow control parameter

Diameter of FVG jet = 1mm
Distance between two jets= 15mm
Pitch angle = 30°
Skew angle = 60°
Max. Velocity = 200 m/s
$C\mu$ = 0.67%

❑ Instantaneous Results

ISO-surface of z-vorticity = -500, coloured with streamwise velocity

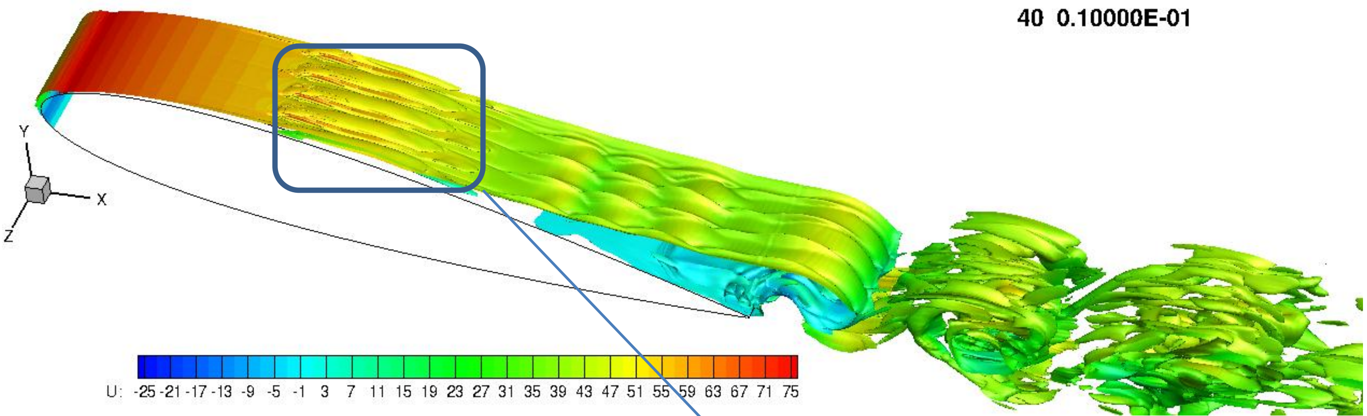

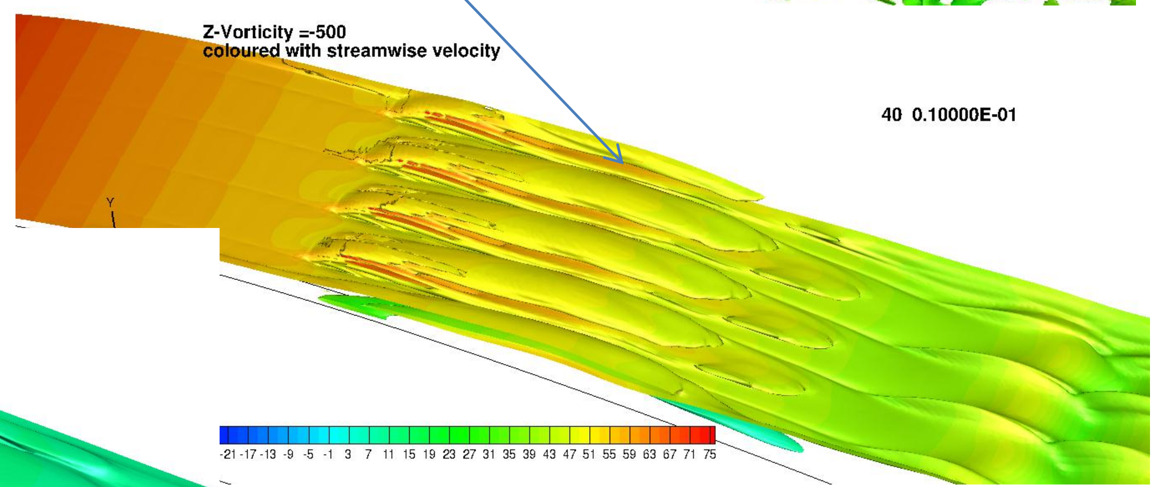

ISO-surface of v-velocity= -3,
coloured with streamwise velocity

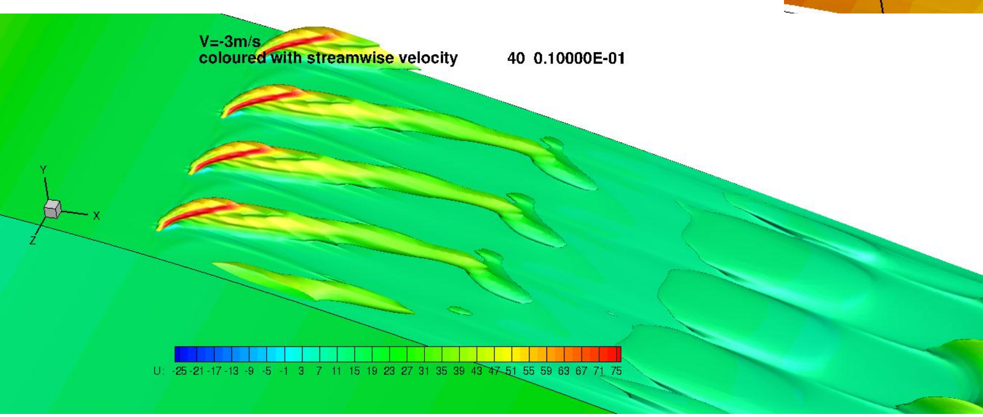

Conclusions

- Hybrid RANS/LES provides a feasible tool for flow control studies of aeronautical interests
- For fixed separation, different hybrid RANS/LES models do not give substantially different results
- For separation from smooth surfaces, the solutions are very sensitive to the models and IDDES gives satisfactory capability in capturing the separation position
- Dynamic mesh with ALE formulation allows detailed simulation of actuator movement and the flow around and in the device
- Meshing resolution plays an important role in resolving the Reynolds stresses
- Piezo actuator oscillation surface has very limited effects on the Reynolds stresses for the current case and the effects of amplitude and frequency are yet to be further studied for optimum control
- Dynamics of the pulse jets is yet to be understood

Acknowledgements

- Funding from the European Union Framework 7 Programme MARS Project: Manipulation of Reynolds Stress for Separation Control and Drag Reduction

- UK HPC HECToR Computing Time from both the Applied Aerodynamic Consortium and the Turbulence Consortium

Research problematic to increase fire safety and survival of the passengers in the new generation of aircraft

AircraftFire - FP7 project

Jean-Michel MOST
Jean-michel.most@isae-ensma.fr

Introduction

For 20 years the fire threat in aeronautics has been reduced, but more efforts are still necessary, particularly for new generation of Aircraft (A350 or B787 families), to :

- ✓reduce the incident / accident rate
- ✓increase the passenger and crew survivability

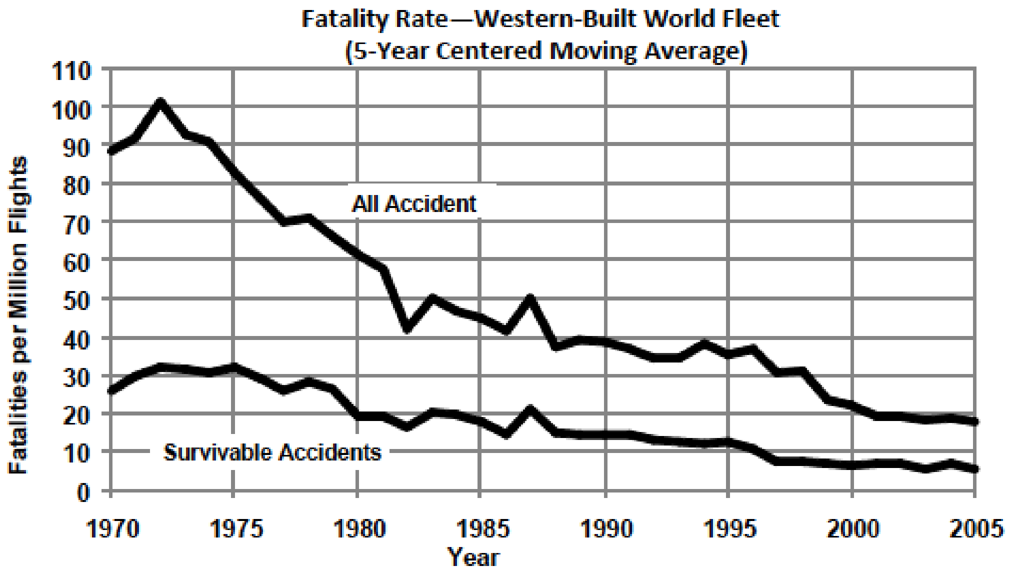

Figure 10. Fatality Rate—All Accidents and Survivable Accidents—World Fleet

The trend seems reducing

Introduction

For 20 years the fire threat in aeronautics has been reduced, but more efforts are still necessary, particularly for new generation of Aircraft (A350 or B787 families), to :

- ✓reduce the incident / accident rate
- ✓increase the passenger and crew survivability

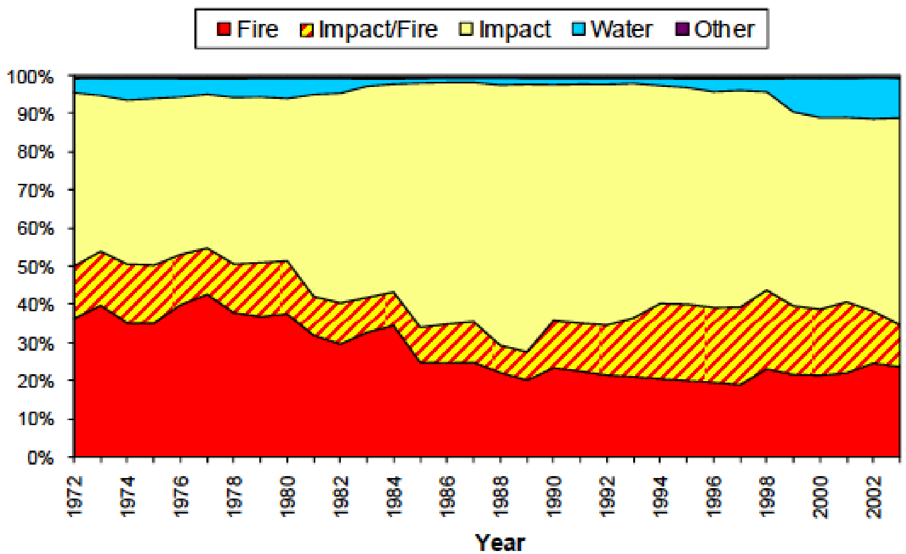

Figure 15. Proportion of Fatalities by Cause in a Survivable Accident—World Fleet

Impact stays the main cause of accident but the fire risk is also important

➔ Fire safety must stay a priority for aircraft manufacturers and companies

Does the Fire Threat increase?

The fire threat can increase in new generation of aircrafts

Aluminium is substituted by composites for hull, wing and structure to…

- Reduce the weight of the aircraft
- Increase the hull resistance to pressure (comfort, temperature and wetness control)
- Reduce the maintenance costs (best properties of the materials for fatigue, endurance, corrosion)

Flammable polymers and composites materials significantly increase…

- The fire threat in high temperature environment
- The total aircraft fuel load
- The toxicity of the smokes

CAA, Airbus, EADS, Fraunhofer

Higher energy supply for avionics and electronics

→ fire risks (ignition,…)

Composite materials in aircrafts

A composite material =
matrix + Fibres
(1D fibres or wooden fabric)

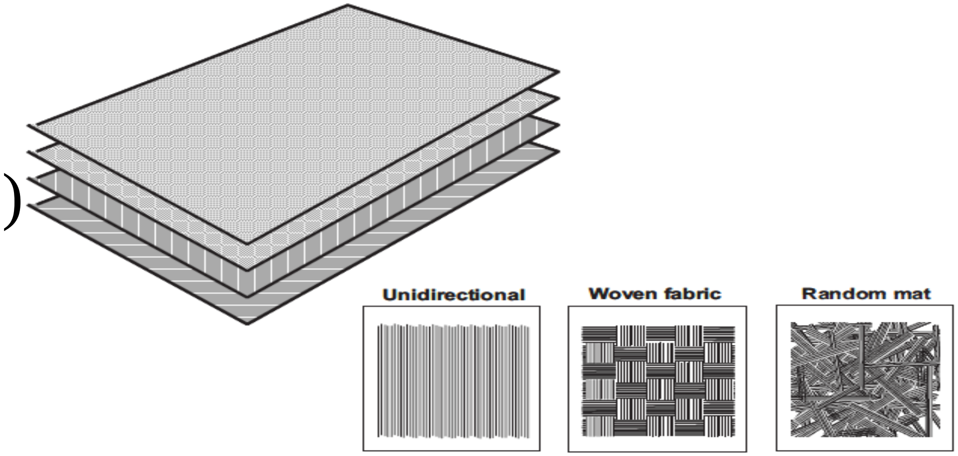

Figure 6.1. Ply structure of laminated composites and common examples of ply architecture.

Thermoset

- **Carbon fibres reinforced epoxy composites** (hull, wing, structure)
  flammable and decompose when exposed to fire
- **Glass fibres reinforced phenolic composites** (decorative panels)
  low flammability and good fire resistance

Thermoplast

- **Seats, next aircraft generation**

  best mechanical properties, recycling

Their burning properties must be equal or better than present ones

Fire resistance from outside fire

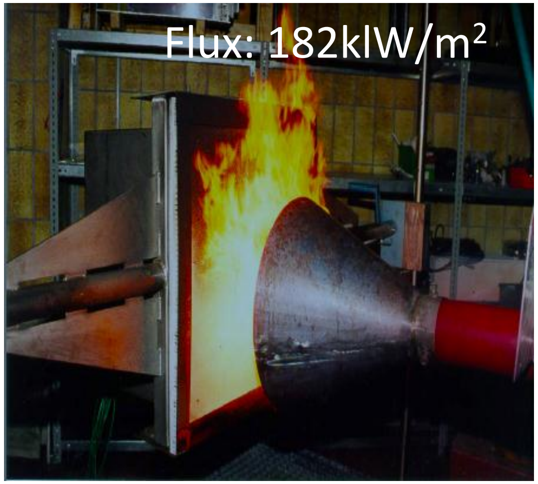

Passed – Failed standard tests

Tests for hull, wing and structure composites

The burnthrough test

- **The drilling time of the flame**
- **Regular fuel burners with**
  - ✓ Given gas temperature
  - ✓ Given total heat flux

at the material level

New behaviour

- **Resin burns very fast**
- **but fibres act as a barrier to the flame penetration**

Reduce the fire threat in the cabin

Tests for cabin materials

- **Heat release rate (peak and mean values)**
- **Self extinction** after a time limited external ignition

Heat release OSU

Radiant panels

Smoke chamber

Combustion propagation chamber

Flammability test

Calorimeter

Passed – Failed standard tests

Research objectives for Fire Safety

- To determine the physical/chemical/thermal flammability and burning properties of composites for aircraft design and fire safety modelling

- To develop and validate physical models correlated to the evolution of the fire scenario

- To model the cabin fire growing and evacuation procedures

- To act on recommendations for the development of efficient industrial technologies and aviation regulation

AircraftFire Project organisation

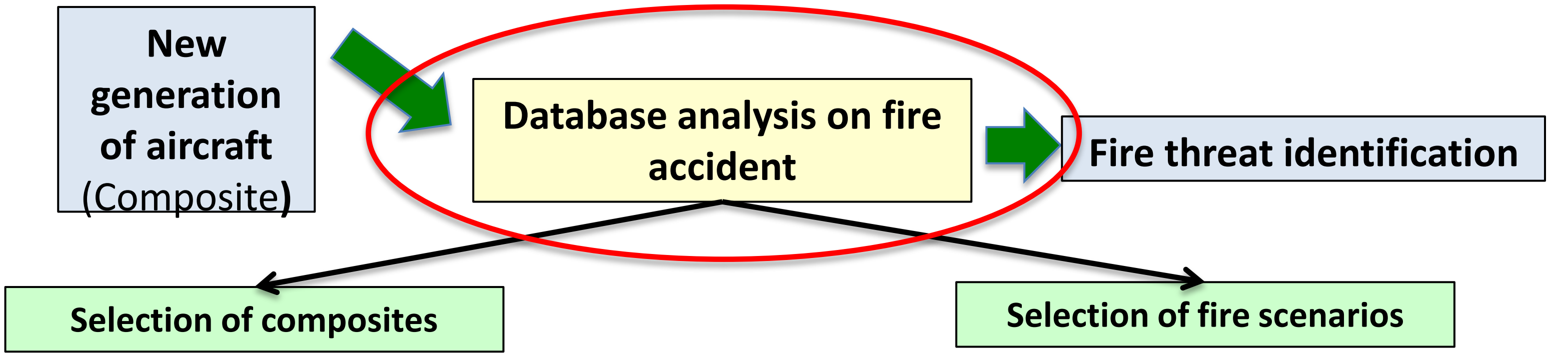

AircraftFire Project organisation

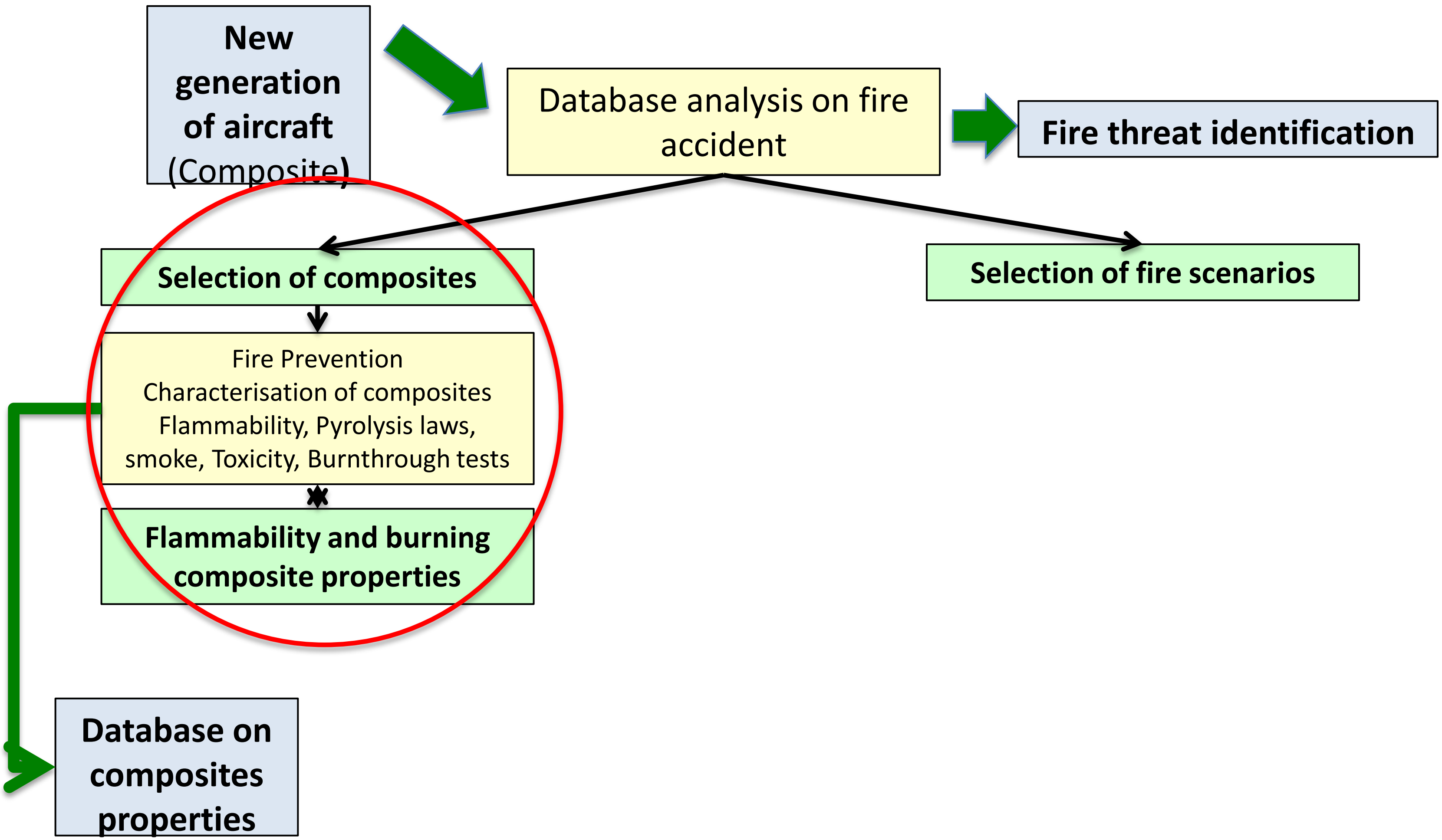

Challenges for material characterisation
Fire prevention

AircraftFire

advancing the frontiers

SEVENTH FRAMEWORK PROGRAMME

Smoke chamber

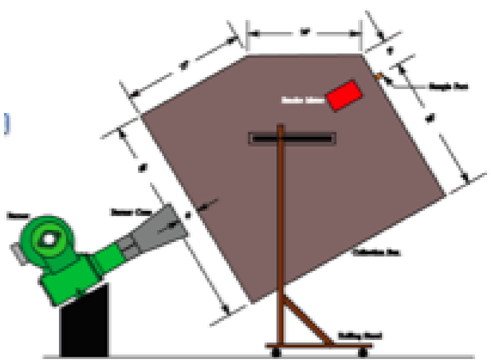

Diagnostics

- Cone calorimeter,
- Thermogravimetric analysis (TGA)
- Differential scanning calorimeter (DSC)
- Smoke chamber and SOD
- Tube furnace
- Heat transfer (thermal characterisation 3D medium)

Deliverables

Flammability and burning properties of composites

- Conduction, Specific heat
- Ignition temperature and flux
- Heat of combustion, efficiency of combustion
- Pyrolysis law
- Heat of pyrolysis
- CO, CO2 and smoke and toxic gas yields
- Smoke point height
- Kinetic parameters for reaction
- Fuel concentration in the pyrolysis gases
- Char properties

Firesert, Insa, Univ. Patras, Pprime, Trefle, Univ. Iceland

AircraftFire Project organisation

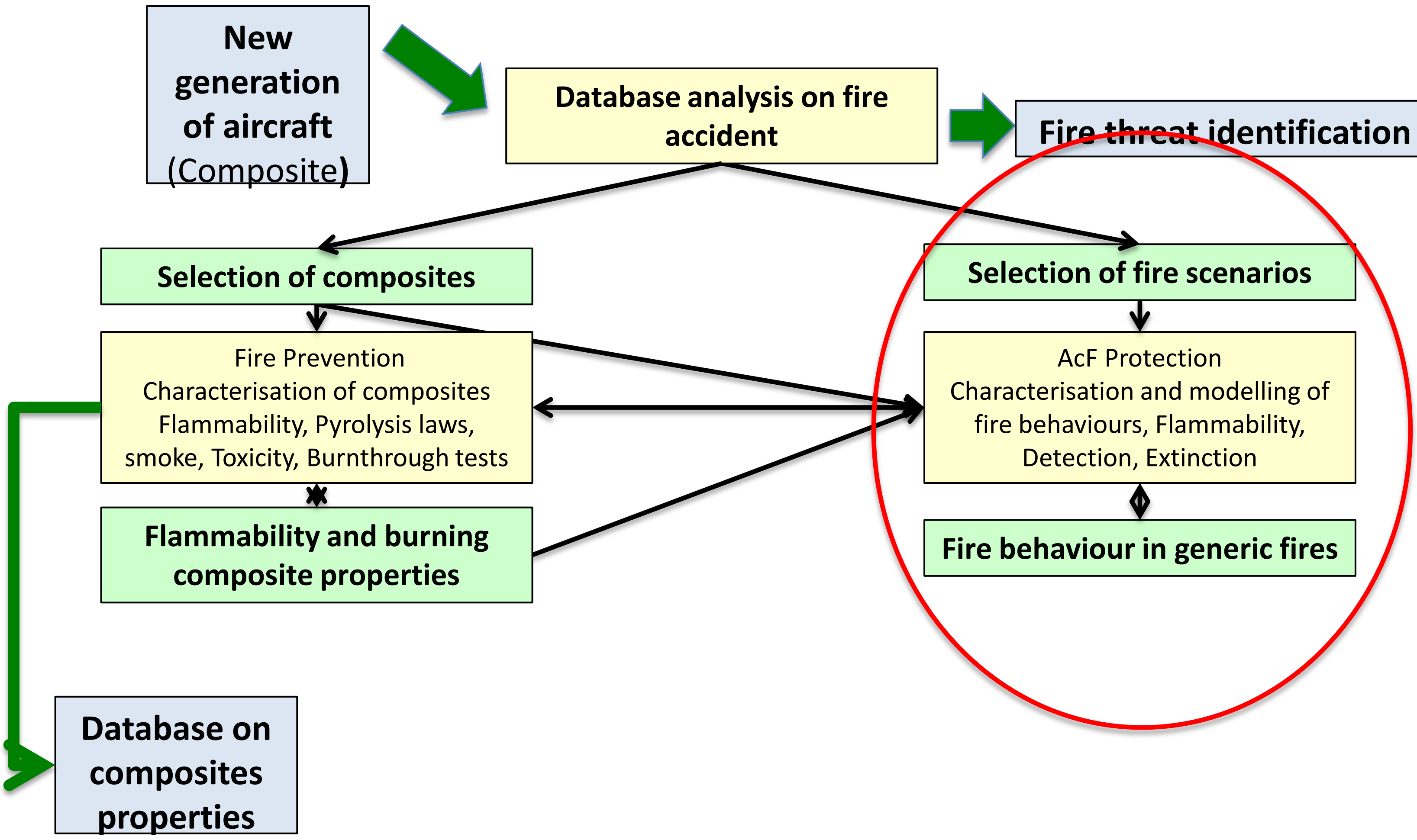

In flight fire behaviour
Hidden fire

- **Experimental characterisation** of **cabin materials** (partition walls, thermoacoustic insulation, ducting, seating, cabling, carpet, curtain, .) and **fire scenarios** (hidden fire)
- **Generic hidden fire configuration** (Univ. Patras)

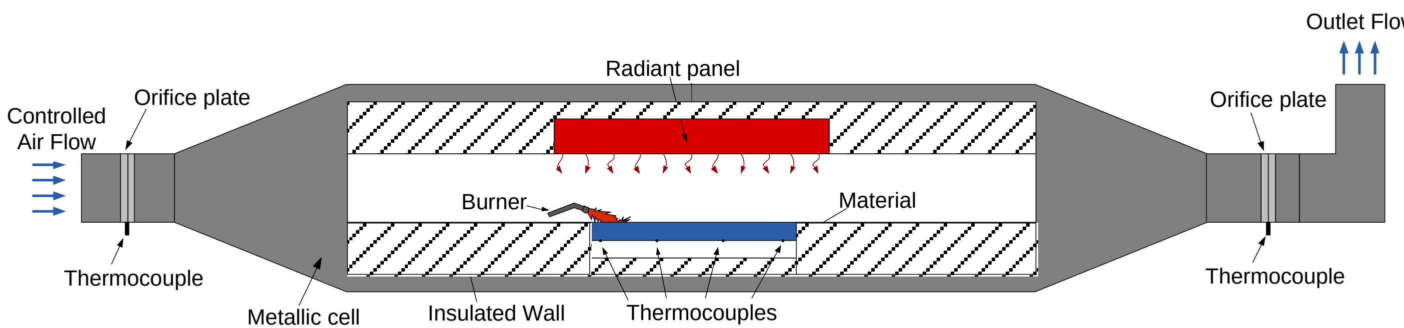

Experimental and numerical studies

- **Detection and extinction** (Univ. Edinburgh)
- **Scaling laws** (Univ. Iceland)

In flight fire behaviour
engine fire

- **Measurement of the burning properties of composites;**
  - ✓ Effect of flame impingement on the burning of composites in reduced pressure (altitude)
  - ✓ Flame sustainability at high altitude

- **Small size burnthrough test**

Pprime

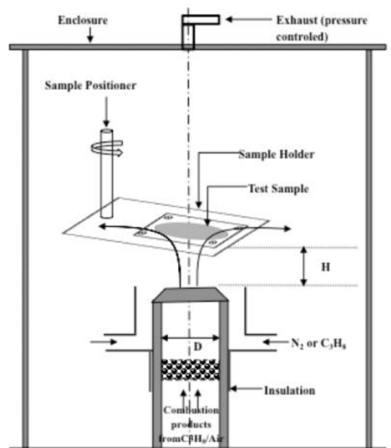

T_{gas}=1100°C
Flux=180kW/m²
Variation of Y_{ox}

Experimental Setup

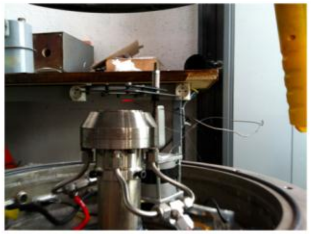

Burnthrough: Pyrolysis of the composite

Burnthrough: Pyrolysis and burning of the composite

Burnthrough: drilling of the sample

Flame sustainability experiment

In flight fire
Composite burning under loading conditions

- **Flammability and burning behaviour of materials under loading condition, effects on**
  - ✓ Mechanical properties
  - ✓ Flammability and burning properties

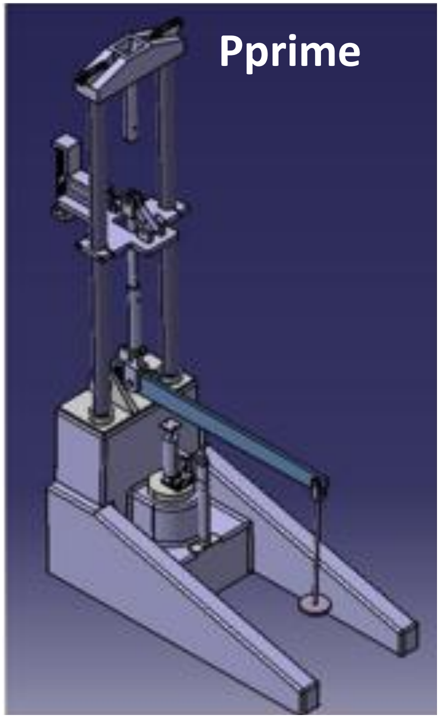

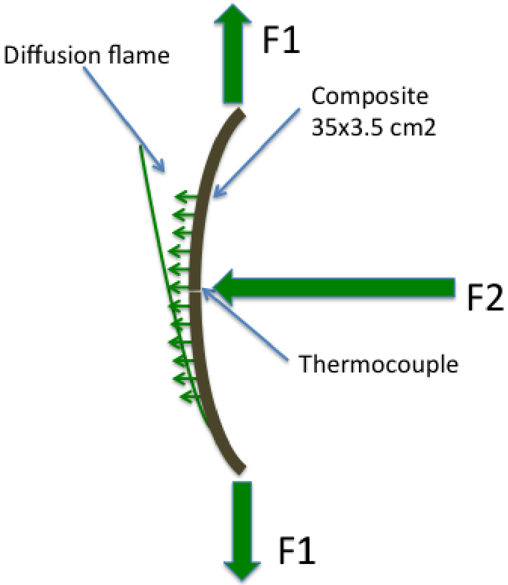

Post-crash fire

- **Integrity of structure during crash** (TUDelft)
- **Parallel wall fire characterisation *(burn-through test*) in real fire conditions** (deep characterisation of heat flux inside the material with burning of the surface)

Pprime

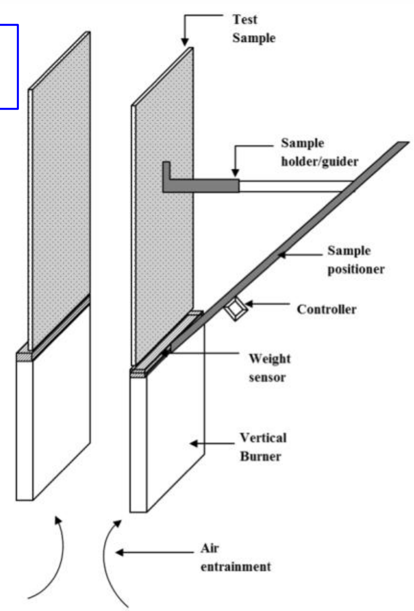

Parallel wall fire with material burning

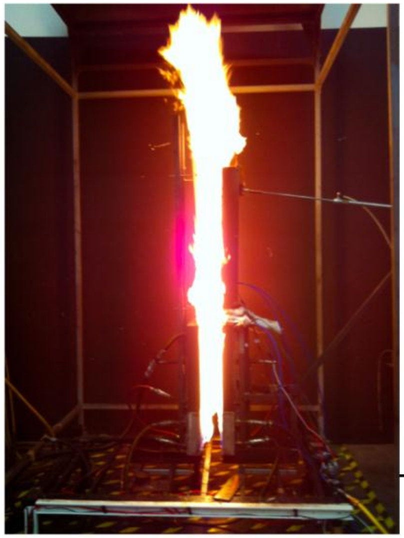

Photo of the parallel wall fire

Post-crash fire

➢ **Large scale pool fire modeling** (Pprime)

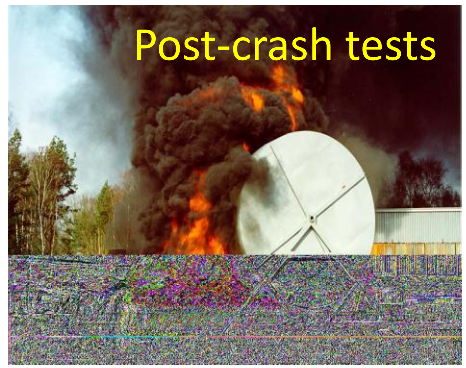

Time of fire penetration in the cabin

- Wind intensity and direction
- Pool fire thermal power

Pprime

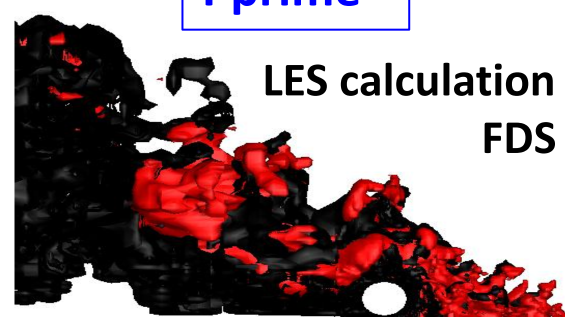

AircraftFire Project organisation

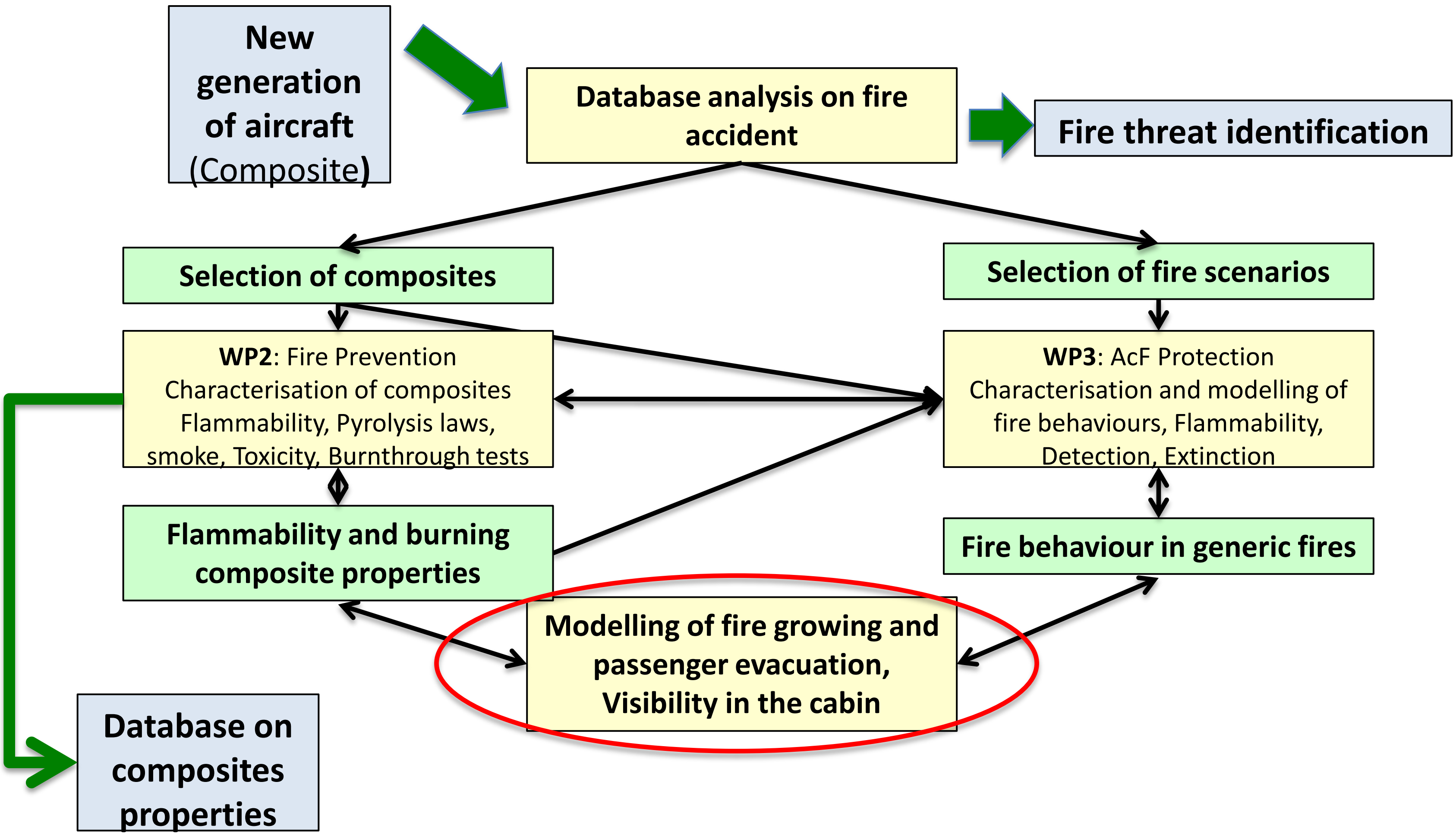

Fire growth and evacuation modelling

•Simulation of fire growth in the cabin: Code **SMARTFIRE**

•Simulation of evacuation: code **air EXODUS** (Univ. Greenwich)

•Simulation of **visibility in the cabin during fire** (EADS)

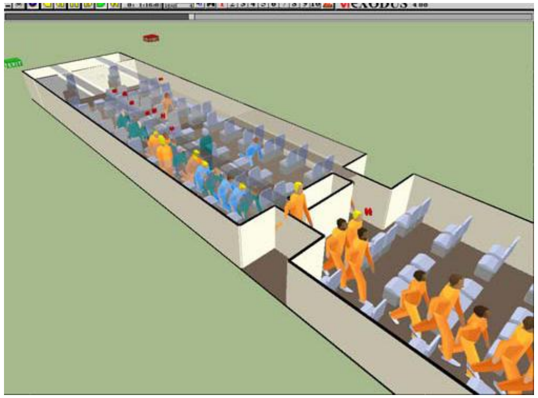

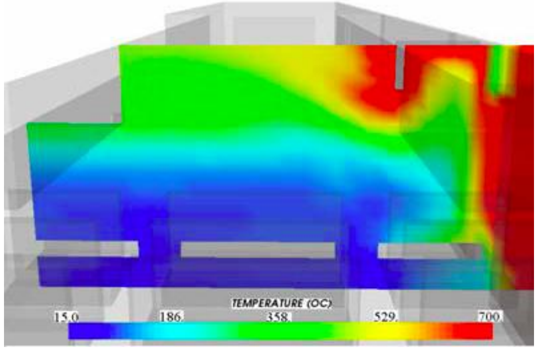

E. Galea (University of Greenwitch documents)

AircraftFire Project organisation

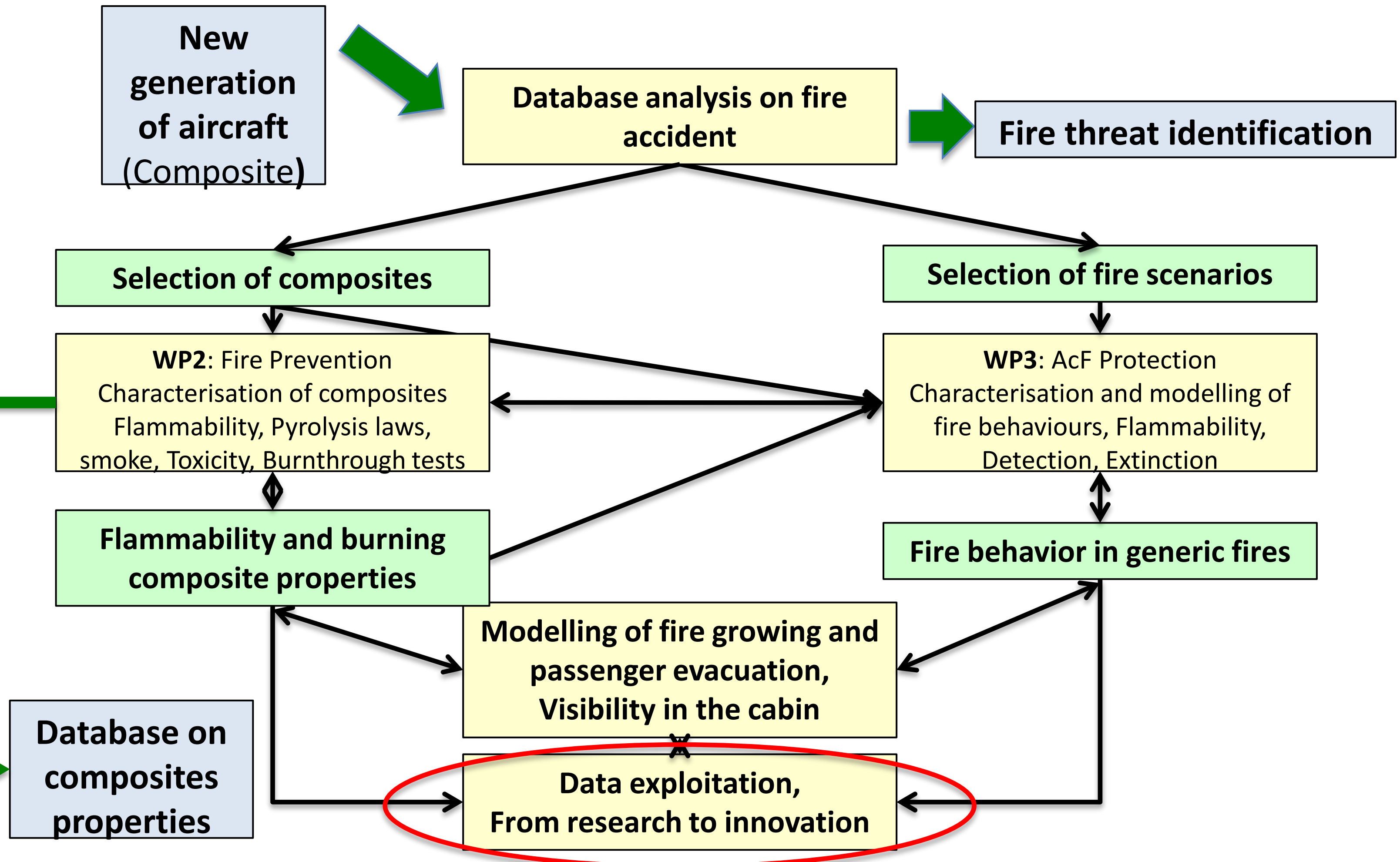

Airbus, CAA, EADS

AircraftFire Project organisation

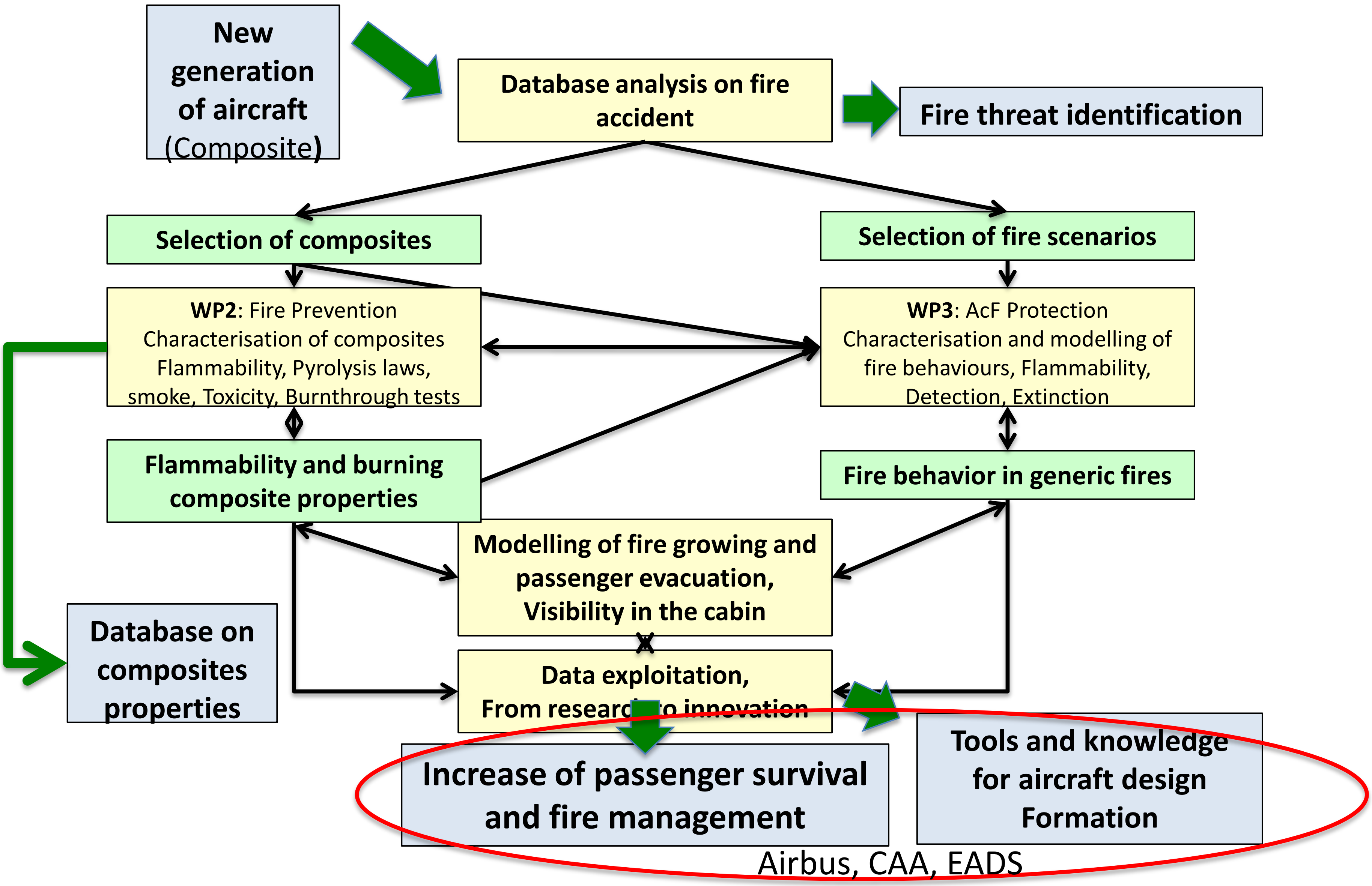

Conclusion

AcF contributes to the Increase of fire safety

- Identification of the **major fire incident/accident causes**
- **Elaboration of a complete data base on flammability and burning properties of composites and cabin materials** (data not presently available)
- **Material ranking** (flammability and burning properties)
- **Major fire scenarios are studied** (hidden fire, behaviour in altitude, under load, etc.)
- **Modelling** of large scale **kerosene pool fire**
- **Tools for cabin fire growth and passenger evacuation**
- **Recommendations** and proposal for:
  - ✓ regulation evolution
  - ✓ formation

Perspectives

- Is the fire safety reduced *or increased* in new generation of aircrafts?
- Are the present standard tests still adapted?
- Can the regulation evaluate?
- Needs of formation in fire safety (and security)?

Thank you for your attention

FP7 - AircraftFire

www.aircraftfire.eu

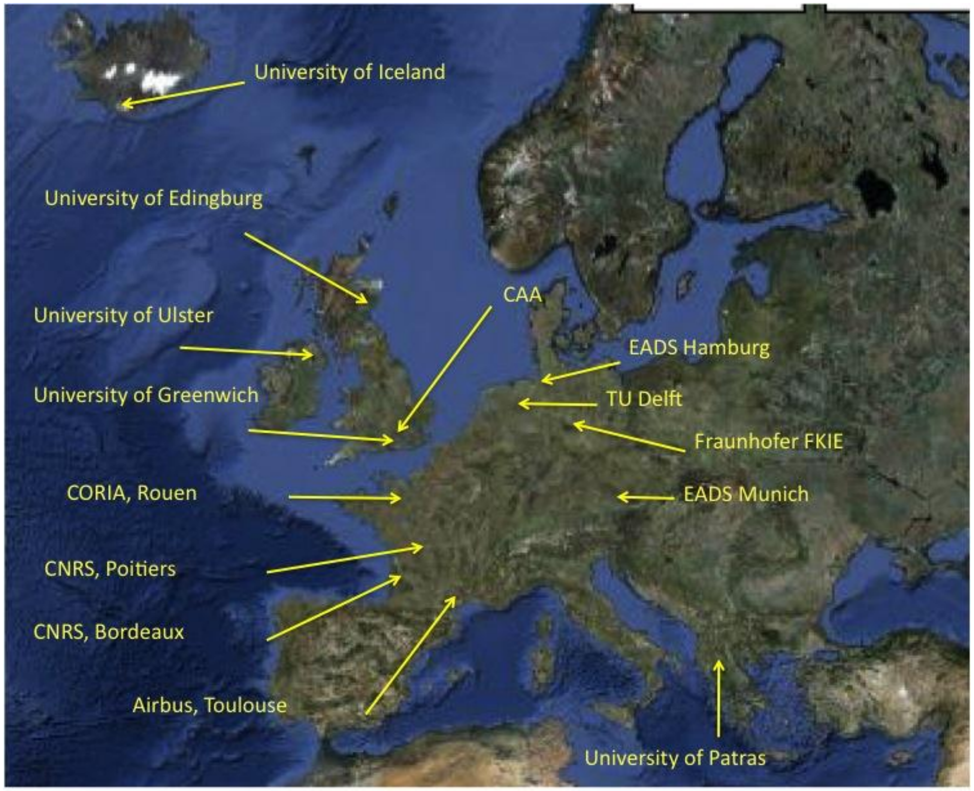

AcF Total Budget: 4 200 557€
EU contribution : 3 220 690€
Total effort : 379 p.m.

The partners

- 13 partners
- 9 Universities or Research Establisments
- 4 Industrials or Technical Centres

SEVENTH FRAMEWORK PROGRAMME

FACTOR

Insight on combustor-turbine interactions

Full Aerothermal Combustor-Turbine interactiOns Research

Address the lack of confidence in the prediction of combustor-turbine interactions so as to preserve High Pressure Turbine (HPT) life and performance when optimising the design of new HPT.

EASN, Prague, 31/10/2012

Friedrich Kost (DLR)

William Playford (University of Cambridge)

Camille Battisti (Snecma)

FACTOR Insight on Combustor-Turbine Interactions

SEVENTH FRAMEWORK PROGRAMME

Contents:

- ❑ **FACTOR project overview (F. Kost)**
- ❑ **Experimental Facilities**
- ❑ **Measurement techniques overview (next presentation by W. Playford)**

Objectives

- **Develop an experimental infrastructure using most advanced measurement techniques.**
  - Continuous test rig hosted at DLR, Göttingen
  - Complementary blow-down facility hosted by Univ. Oxford to supplement the analysis and to go deeper in the aero-thermal measurements.
  - Test rig at Univ. Firenze to reproduce a combustor sector with 3 swirlers.

- **Such infrastructure will allow collecting the data needed to:**
  - Investigate the behaviour of a realistic combustor outlet profile in the HP turbine to better understand the interaction with the coolant system, the transport (secondary flows) and mixing mechanisms.
  - Characterise the HP turbine aerodynamic performances under representative inlet flow conditions found in a real engine
  - Achieve wall heat flux measurements to be able to qualify each numerical model independently
  - Exploit the experimental data to validate next generation of CFD techniques and design tools

Objectives

SEVENTH FRAMEWORK PROGRAMME

- **Optimising the combustor-HPT interaction, FACTOR project will contribute to achieving the 50% CO2 and 80% NOx reductions of ACARE 2020 environmental objectives.**
    - reduce SFC by 2%, HPT weight by 1.5% and accordingly engine cost by 3% compared to the results from the TATEF2 and AITEB2 projects.

- **FACTOR will also strengthen the competitiveness of the European aero-engine industry by making available a new test infrastructure with experimental abilities beyond those of the US.**

Overall approach

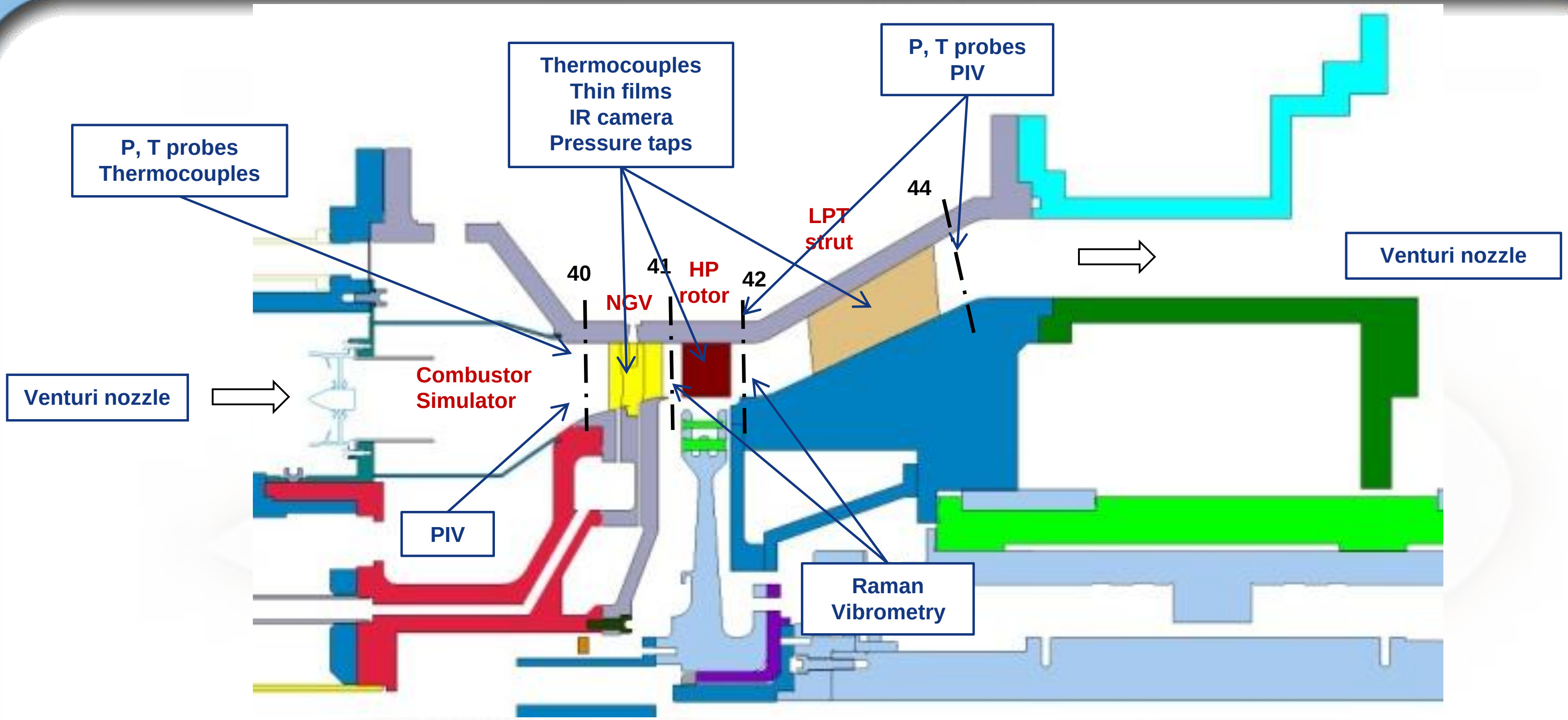

- **Develop and exploit an innovative test infrastructure coupling a combustor simulator with a HPT** *(Highly instrumented test rig)*
  - Collect experimental data to feed design techniques and simulation software
  - Validate advanced CFD → new knowledge

Consortium

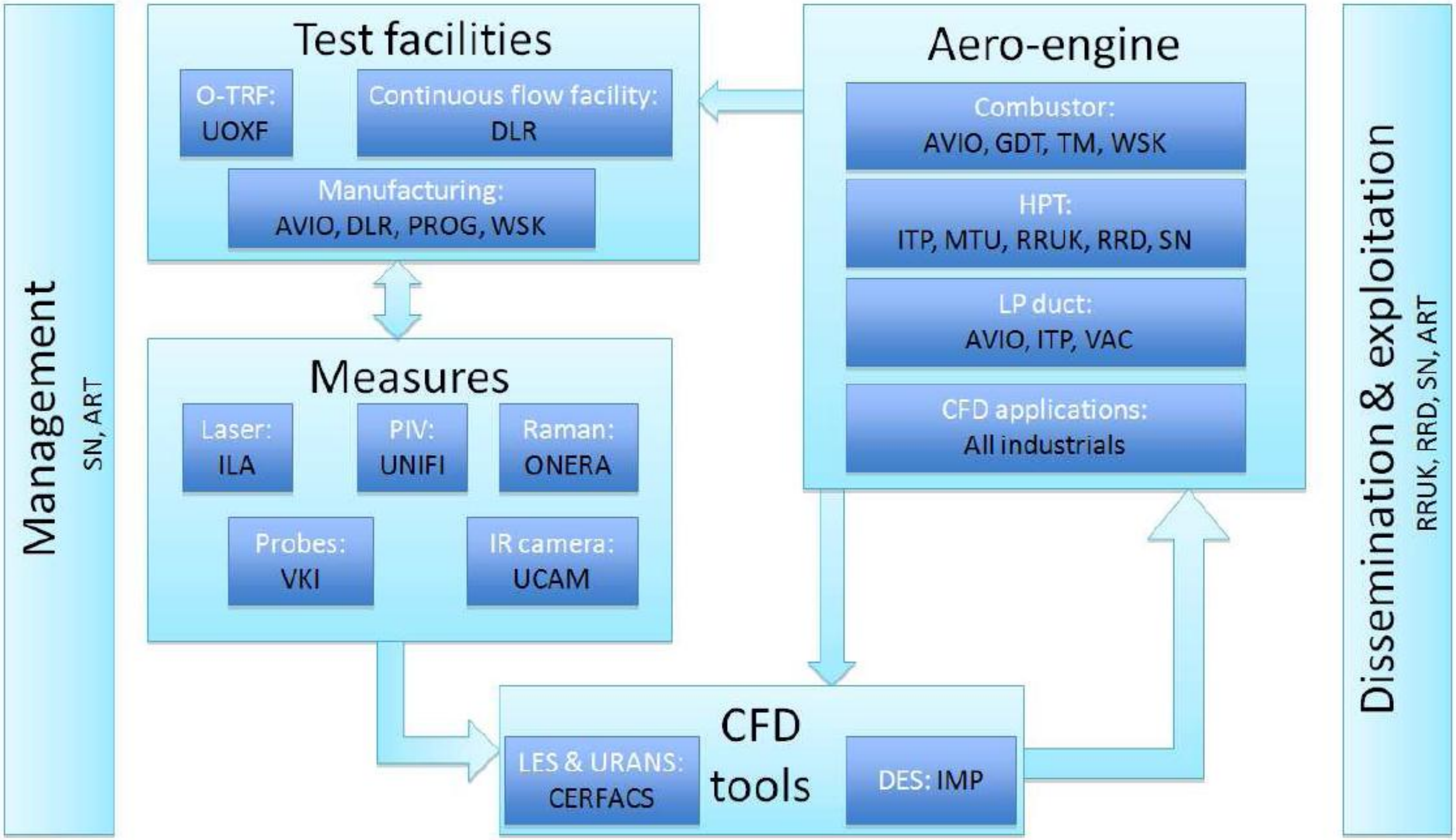

Figure 14: Consortium structure and expertise

WP1 - *Components design and manufacturing*

- Leader → **SNECMA**

- **Design components matching mechanical, thermal and aerodynamic performances specifications**
- **Manufacture the non-reacting combustor simulator, the HP turbine module and the LP duct that will be integrated together**

Turbine flow path
ITP

Combustor simulator
TURBOMECA

NGV
RR-UK

HP blade
SNECMA

HP disk
RRD

LP inter-duct
GKN Aerosp.

SAS
MTU

WP1 - *Components design and manufacturing*

SEVENTH FRAMEWORK PROGRAMME

- **Status**

  - ➢Combustor simulator has been designed
  - ➢HPT and LPT design are being finalized
  - ➢Critical Design Review planned for 2013

    → **Manufacturing will start in June 2013**

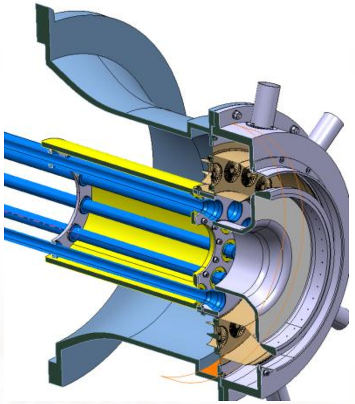

Combustor geometry and supporting structure - TM

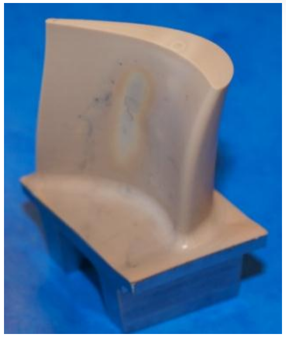

Sample of the HP rotor blade in Peek - PROGESA

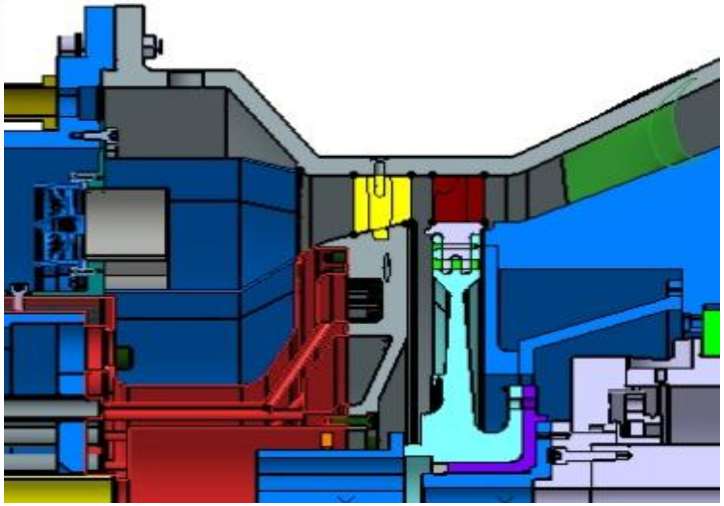

WP2 - *Instrumentation design & manufacturing and rig adaptation*

- Leader → **DLR**

- **To perform the necessary modifications to the turbine test rig**
- **To integrate the modules (CS, HPT, LP duct) in the facility**
- **To design and implement the instrumentation**

- **Measurement techniques overview (see next presentation by W. Playford)**

WP3 - *Integration*

- Leader → **TURBOMECA**
- **To integrate a combustor / turbine assembly compliant with the functional specification of the rig.**
- **To conduct CAD analysis.**
- **To carry out preliminary mechanical, thermal and aero thermal modeling of the assembly**

WP3 - *Integration*

- **Status**
  - Integration digital assessment is ongoing
  - CAD mock-up of the rig is available and in continuous improvement
  - Thermo-mechanical analysis of the whole is ongoing

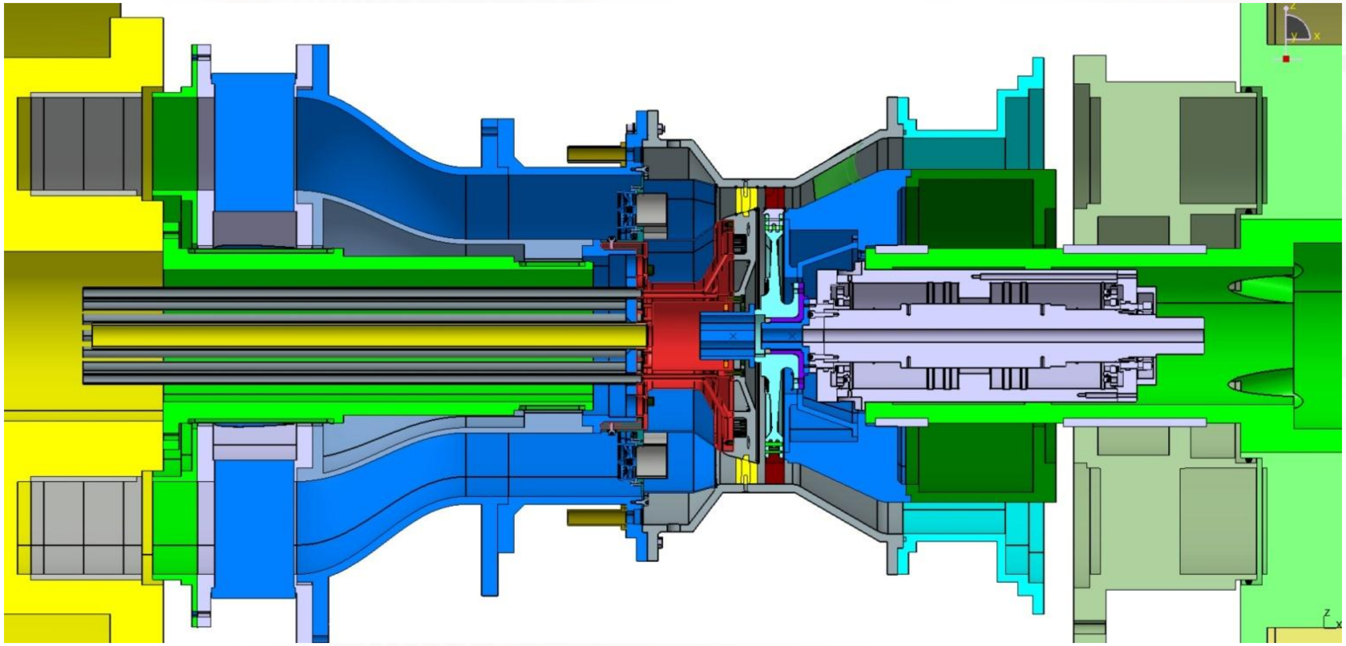

***CAD mock-up of the rig* – TURBOMECA, DLR**

WP4 - *Measurement campaign at DLR*

- Leader → **DLR**

- **To perform all measurements on the NGTurb rig in Göttingen needed to fill a detailed database**
- **Partners:**
  - **University of Florence (UNIFI)**
  - **University of Cambridge (UCAM)**
  - **Van Karman Institute (VKI)**
  - **ONERA**
  - **SIEMENS (SIT)**
  - **ILA**

WP5 - *Lean burn influences on low turning strut HT in Oxford O-TRF rig*

SEVENTH FRAMEWORK PROGRAMME

- Leader → **GKN Aerospace**
- **To analyse the impact of lean burn combustor type inlet flows on a HP Stage and a downstream duct.**
- **To understand the effect of clocking on the aerodynamics and HT of an HP stage and downstream duct.**
- **To assist the development of HT measurements on the DLR continuous flow facility, as LP duct/strut configuration is designed to be similar to DLR configuration**

WP5 - *Lean burn influences on low turning strut HT in Oxford O-TRF rig*

SEVENTH FRAMEWORK PROGRAMME

- **Status**
  - Design and manufacturing of low turning strut, duct and deswirl vanes completed
  - Instrumentation design is finished, hardware is instrumented (9 low turning vanes)
  - 1st rig runs in July 2012
  - End of testing is planned for October 2013

U-OXF stage working section

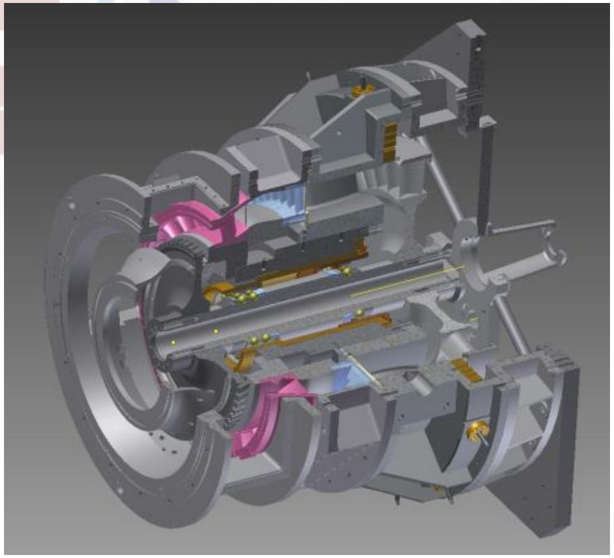

Low turning strut manufacture – GKN

WP6 - *Synthesis of experiments and computations*

SEVENTH FRAMEWORK PROGRAMME

- Leader → **RRD**

- **To define, set-up and maintain database for experimental and numerical data from the relevant work-packages.**
- **To conduct the CFD work and its validation using the experimental results.**
- **To derive best practice guidelines on modeling the combustor-turbine interaction.**

- **Status:**
  - CFD database is open and ready to use

Overall Time Schedule

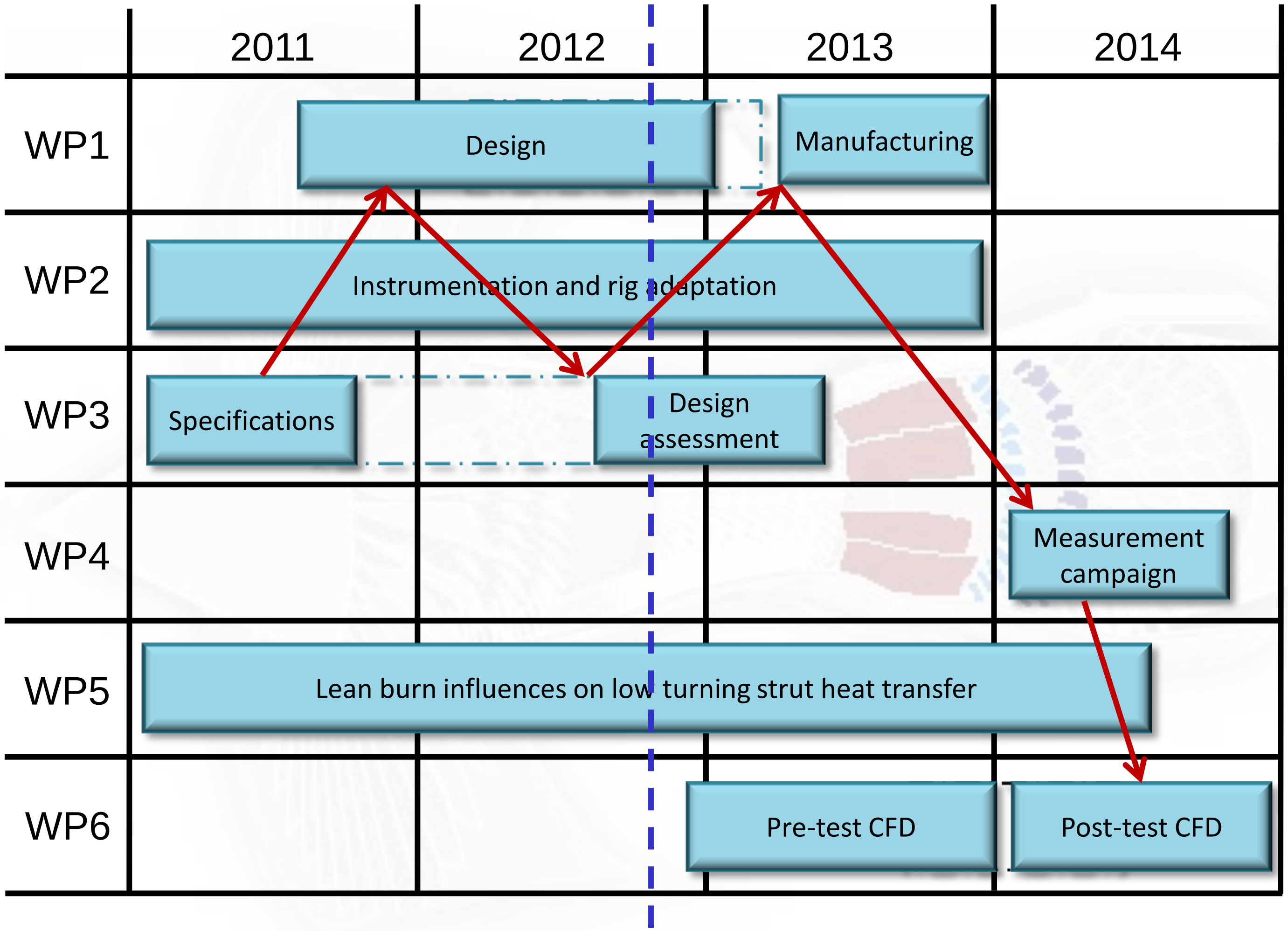

Experimental Facilities

Experimental facilities // *UOXF - TRF*

P_{01} = 4.6 bar	T_{01} = 440 K	RPM = 9500
Mass Flow = 17.4 kg/s		P = 1.726 MW

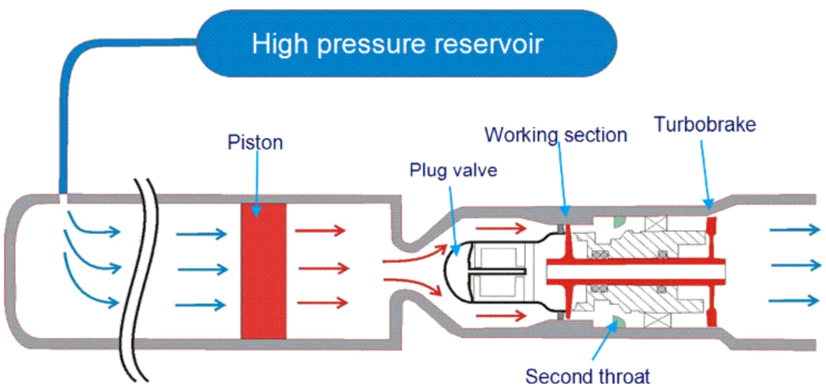

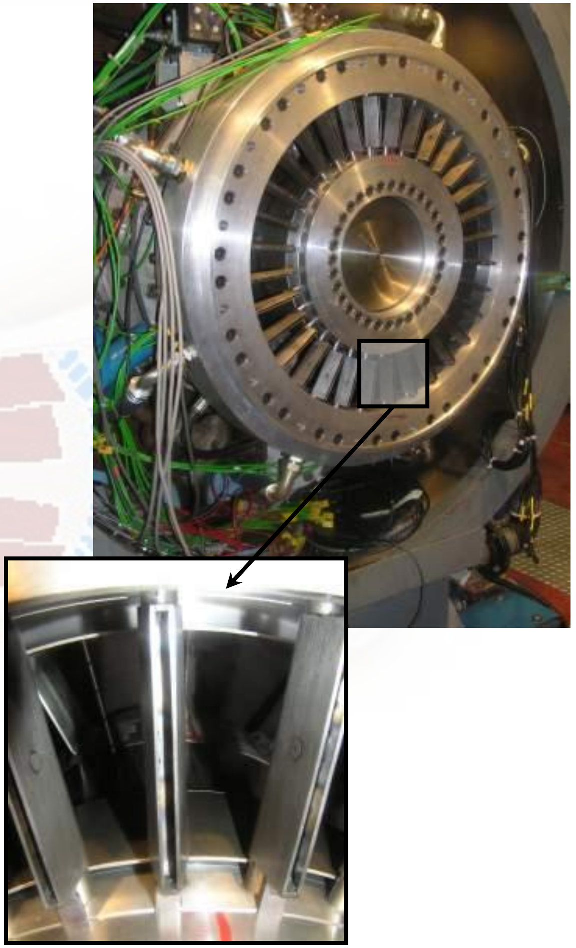

Experimental facilities
DLR – NGTurb flow circuit

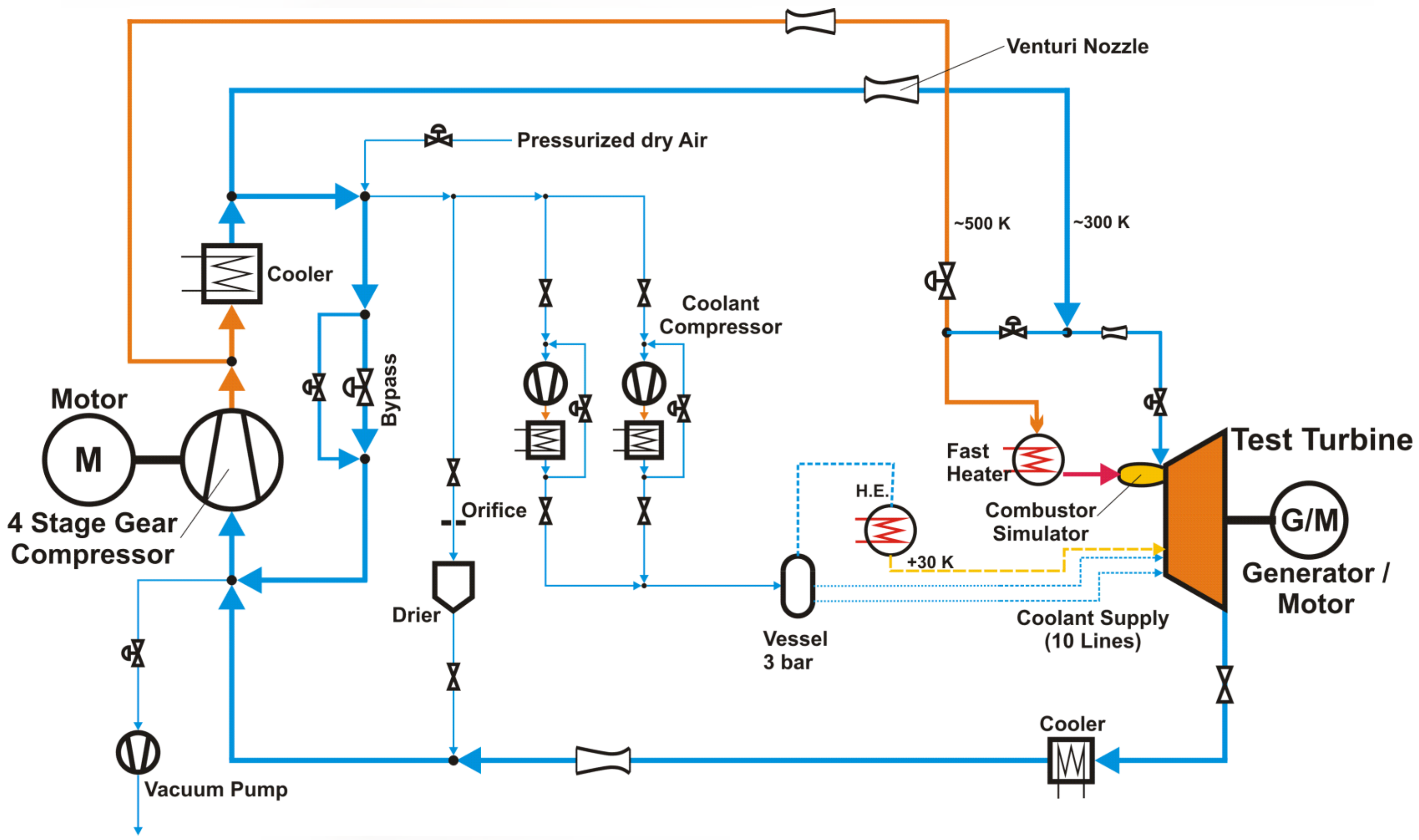

Experimental facilities
DLR – NGTurb characteristic values

SEVENTH FRAMEWORK PROGRAMME

Gear compressor (4 stages, radial)	MAN Diesel & Turbo SE
Maximum pressure ratio	12
Volume flow	< 230 000 m^3/h
Power	< 3.7 MW

Compressor performance data

Type (Test duration)	Continuous (6hrs)
Total inlet pressure p_t	10 – 200 kPa
Total inlet temperature T_t	300 – 600K
Pressure ratio (turbine)	≤ 10
Mass-flow	< 9 kg / s
Shaft Power (HPT)	≤ 1.5 MW
Rotational speed	≤ 13.000 rpm
Blade height / Turbine diameter	≤ 100 mm / ≤ 900 mm

Characteristic parameters of a test

Experimental facilities
DLR – NGTurb Test rig

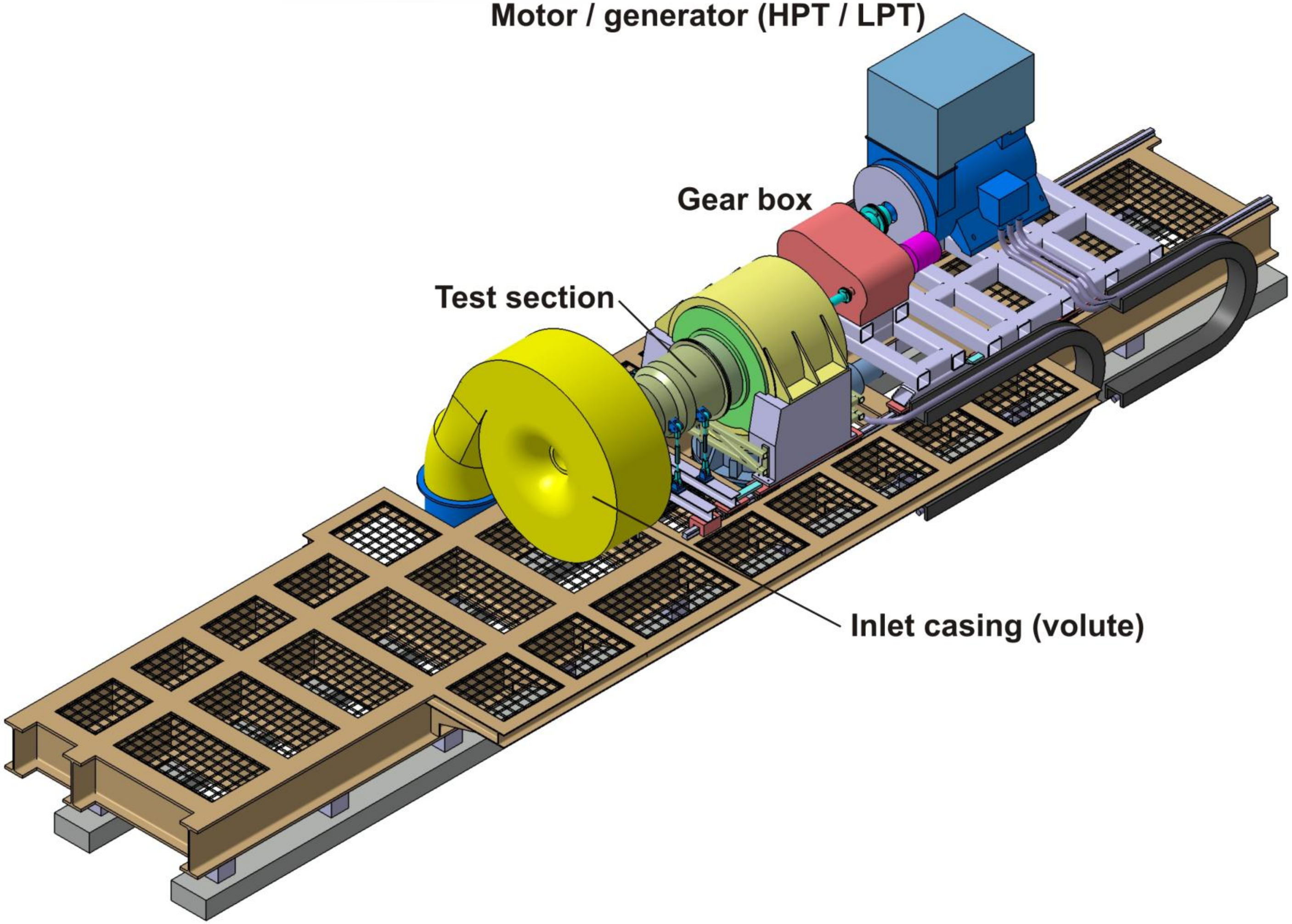

FACTOR Turbine in NGTurb test section

SEVENTH FRAMEWORK PROGRAMME

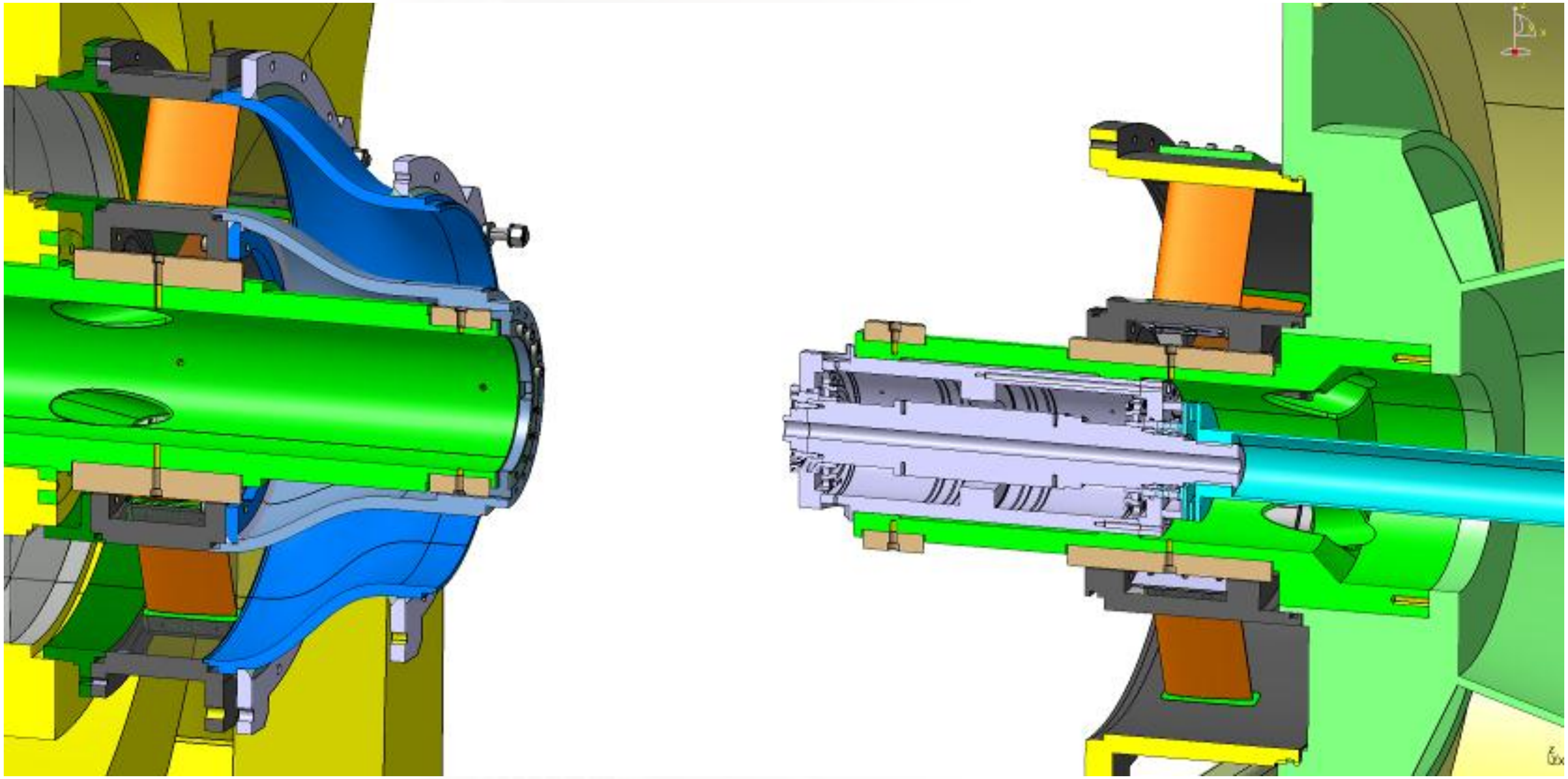

FACTOR Turbine in NGTurb test section

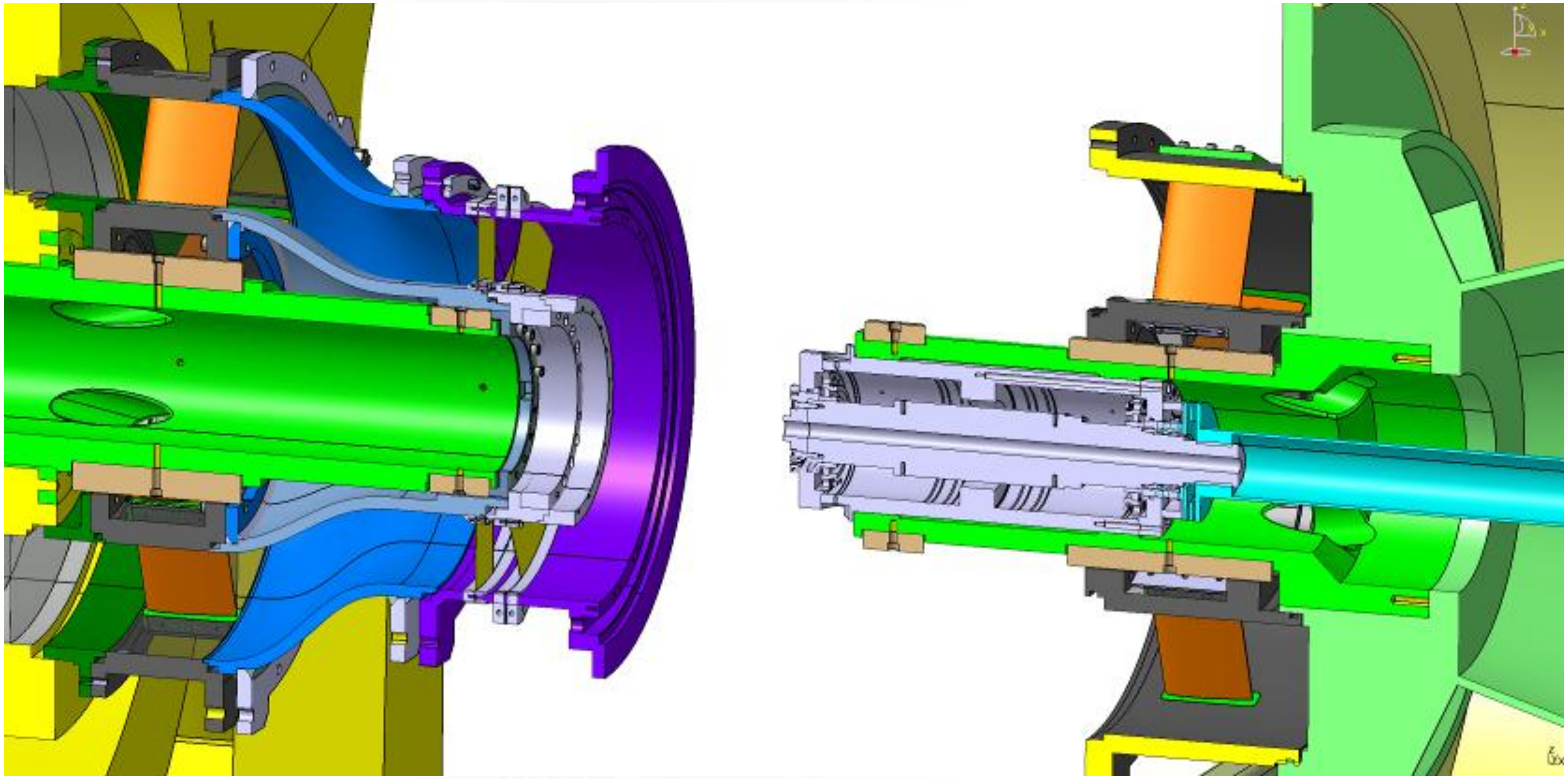

FACTOR Turbine in NGTurb test section

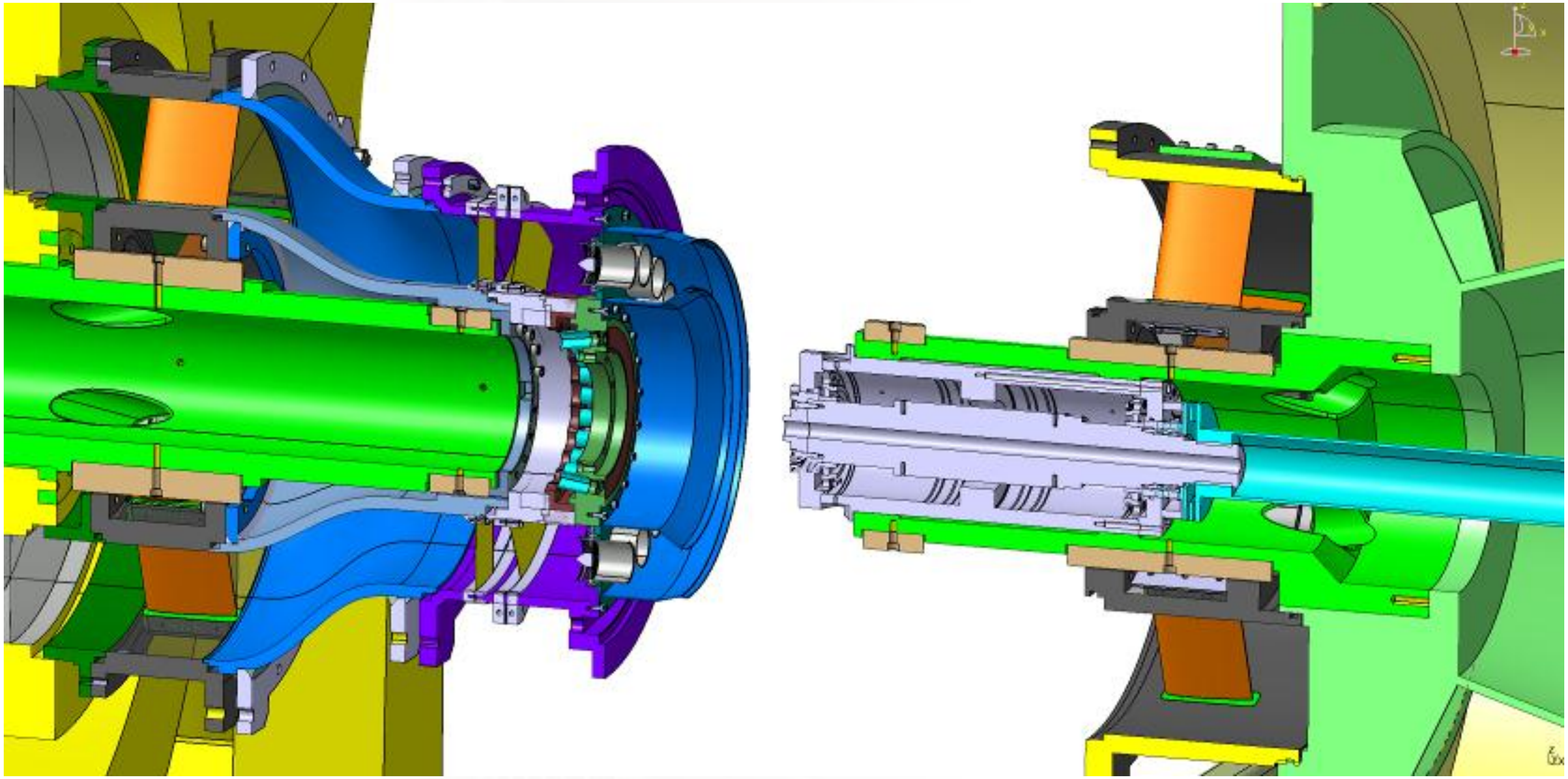

FACTOR Turbine in NGTurb test section

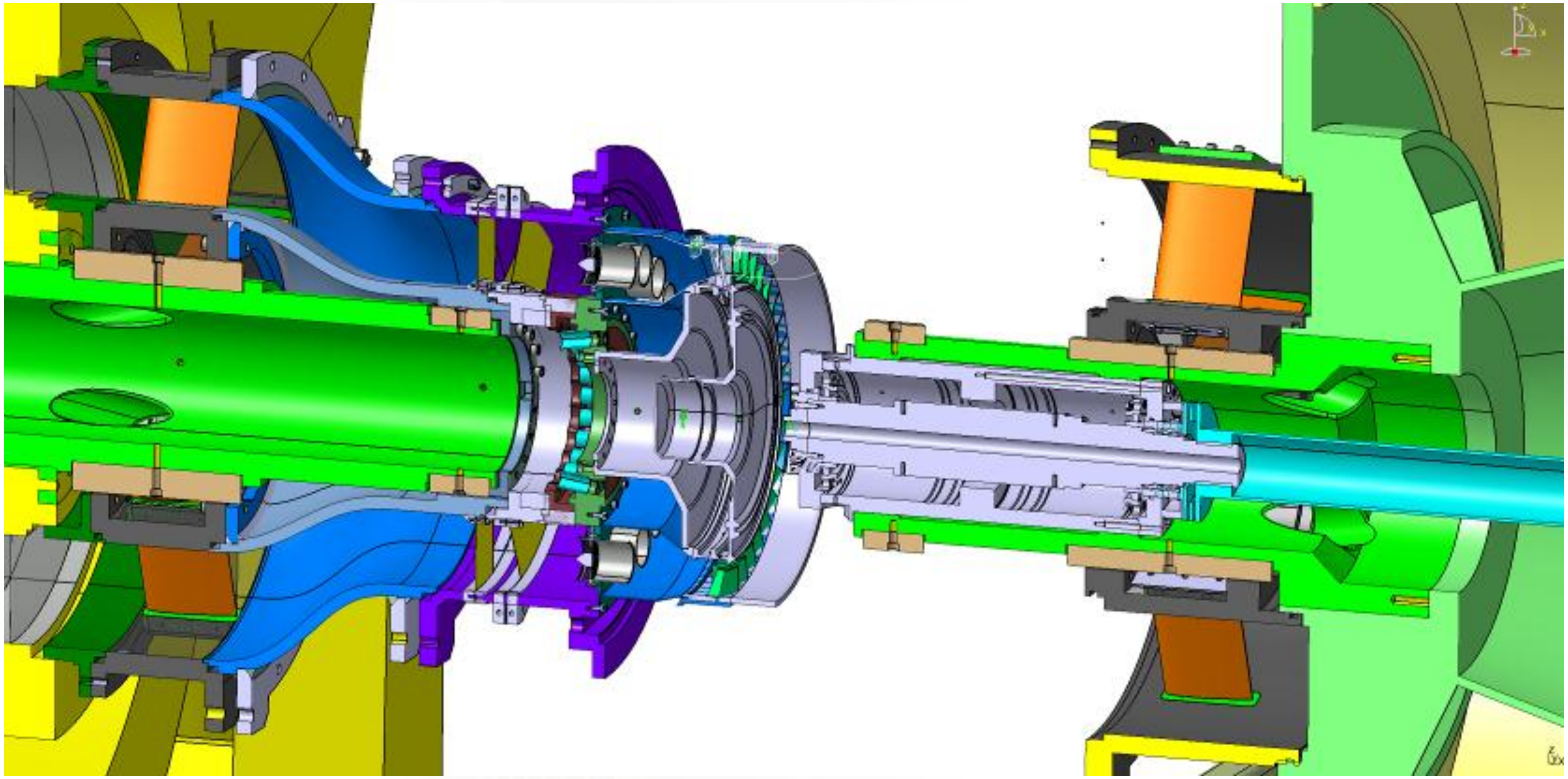

FACTOR Turbine in NGTurb test section

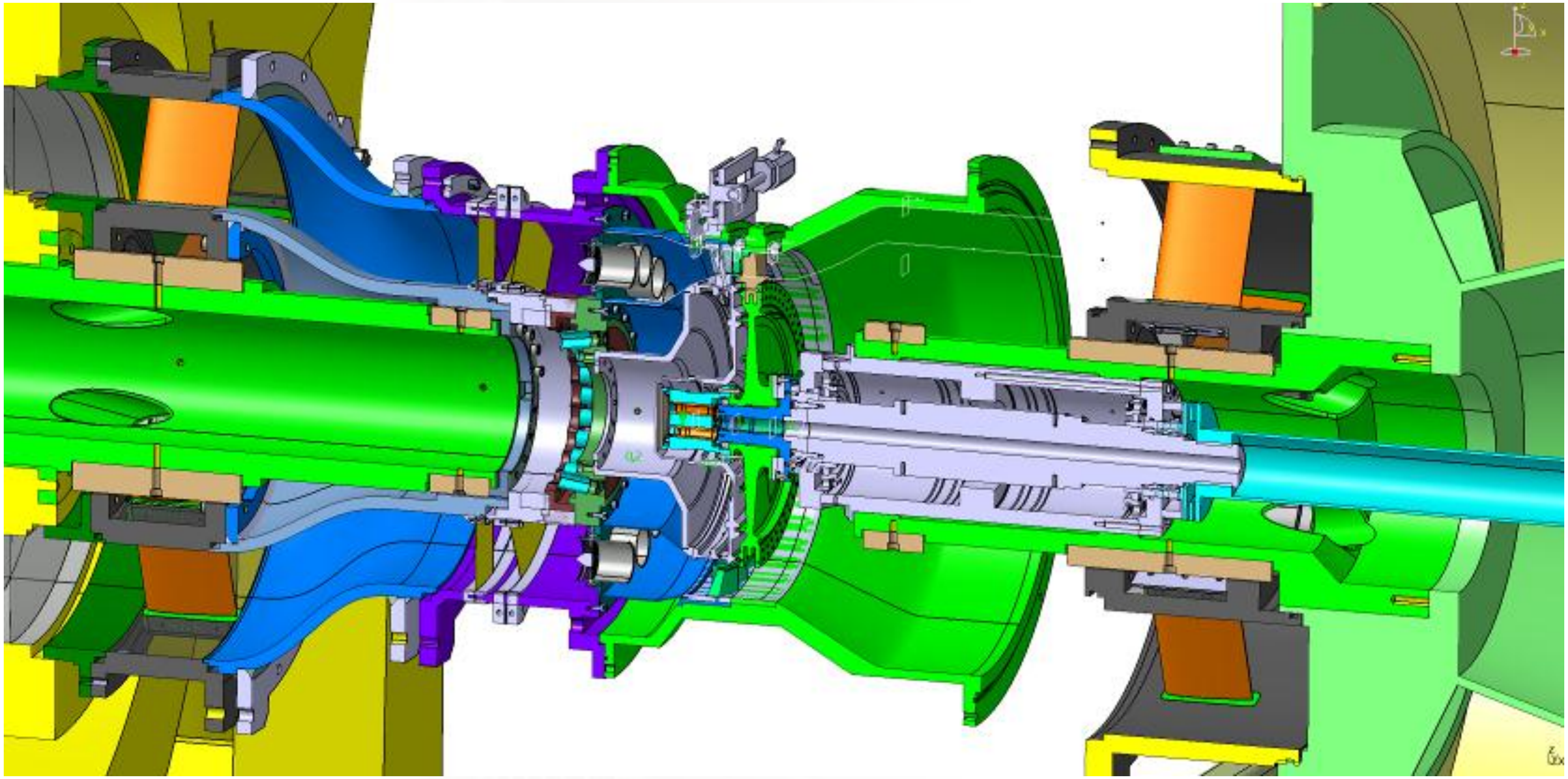

FACTOR Turbine in NGTurb test section

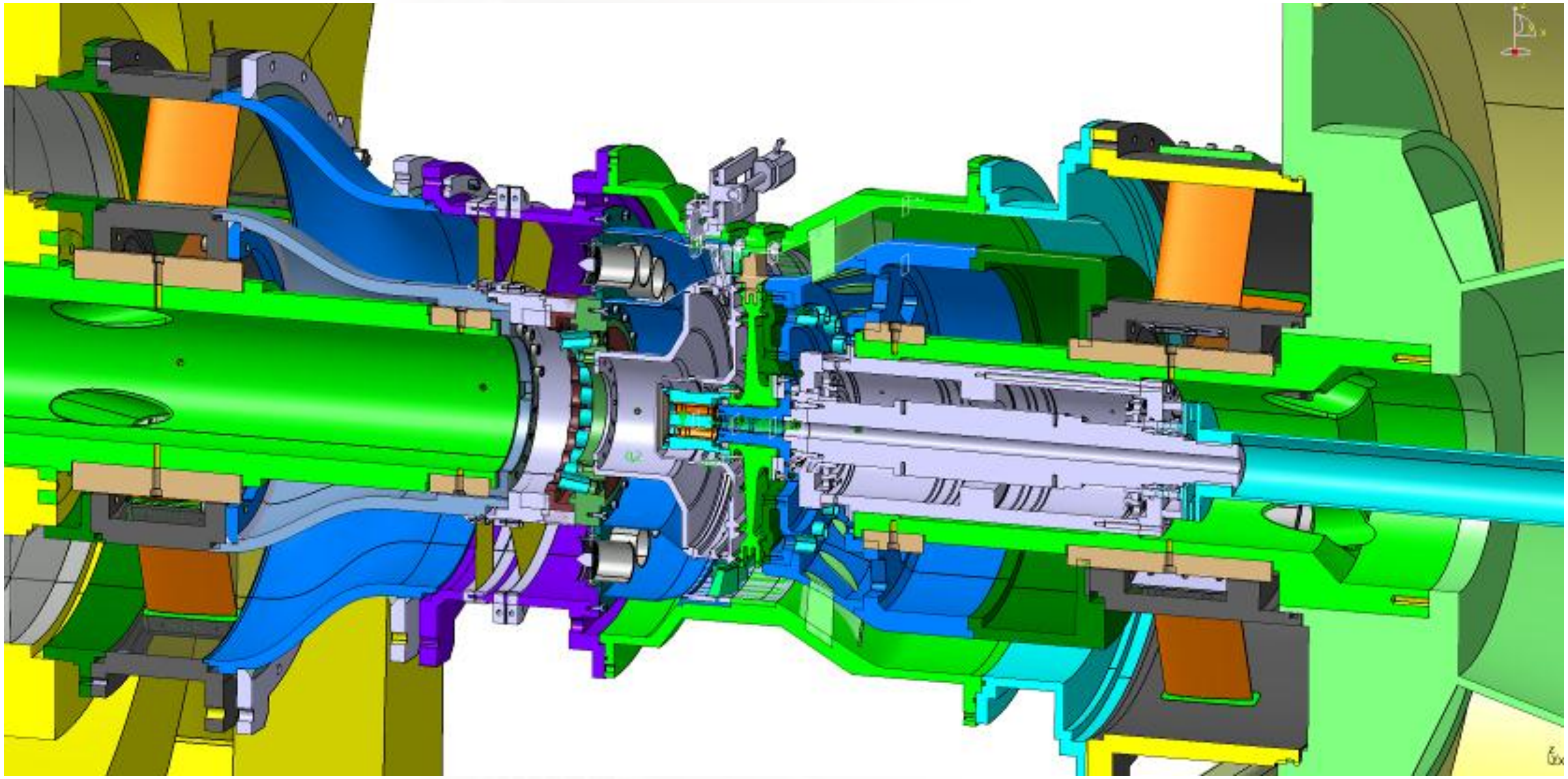

SEVENTH FRAMEWORK PROGRAMME

Measurement Techniques Overview

William Playford (The University of Cambridge)

Presentation Structure

- The FACTOR Measurement Campaign at NG-Turb
  - DLR – 5 Hole Probe Measurements
  - ILA - Laser Doppler vibrometry
  - VKI – FRAP Probe
  - UNIFI - PIV, HWA
  - ONERA - Raman Spectroscopy
- High Speed IR Heat Transfer Measurements: Cambridge University
  - Impulse Response Technique
  - Measurement Complexities

Presentation Structure

- **The FACTOR Measurement Campaign at NG-Turb**
- **High Speed IR Heat Transfer Measurements: Cambridge University**
  - Impulse Response Technique
  - Measurement Complexities

The FACTOR Measurement Campaign at NG-Turb

SEVENTH FRAMEWORK PROGRAMME

- 6 academic/research institutions performing the measurements

DLR

UNIVERSITAS STUDIORUM FLORENTINA

D•E Dipartimento di Energetica "Sergio Stecco"

VON KARMAN INSTITUTE

UNIVERSITY OF CAMBRIDGE

ILA Intelligent Laser Applications GmbH

ONERA THE FRENCH AEROSPACE LAB

SIEMENS

1: DLR – 5 Hole Probe Measurements

- **5 Hole probe measurements of steady flow field**
  - Plane 40, 41, 42 and 44

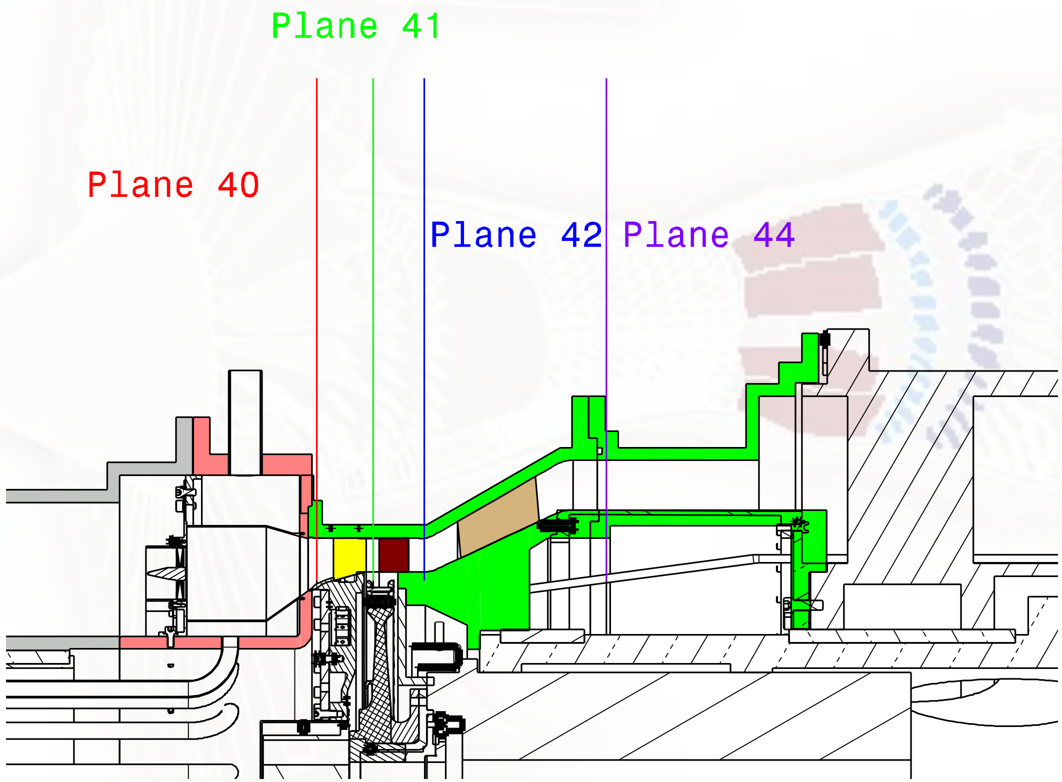

2: ILA – Intelligent Laser Applications

- **Flow field measurements using:**
  - Laser Doppler vibrometer with tomographic reconstruction
  - Background oriented Schlieren technique

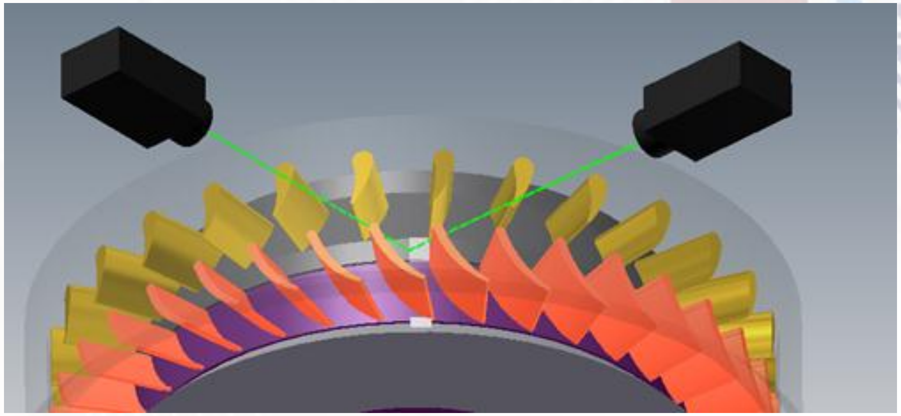

3: Von Karman Institute – FRAP Probe

- **Fast Response Pressure Measurements**
  - Developing a custom probe
  - Max temp. 500ºC
  - Frequency up to 240kHz

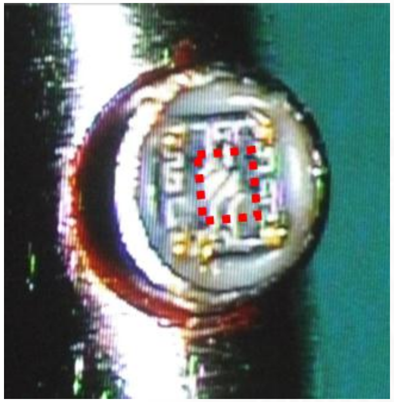

0.6mm x 0.6mm

4: University of Florence – PIV, HWA

SEVENTH FRAMEWORK PROGRAMME

- **PIV, Hot Wire Anemometry, steady temperature and pressure measurement**
  - Initial measurements being conducted on a sector rig at the University of Florence

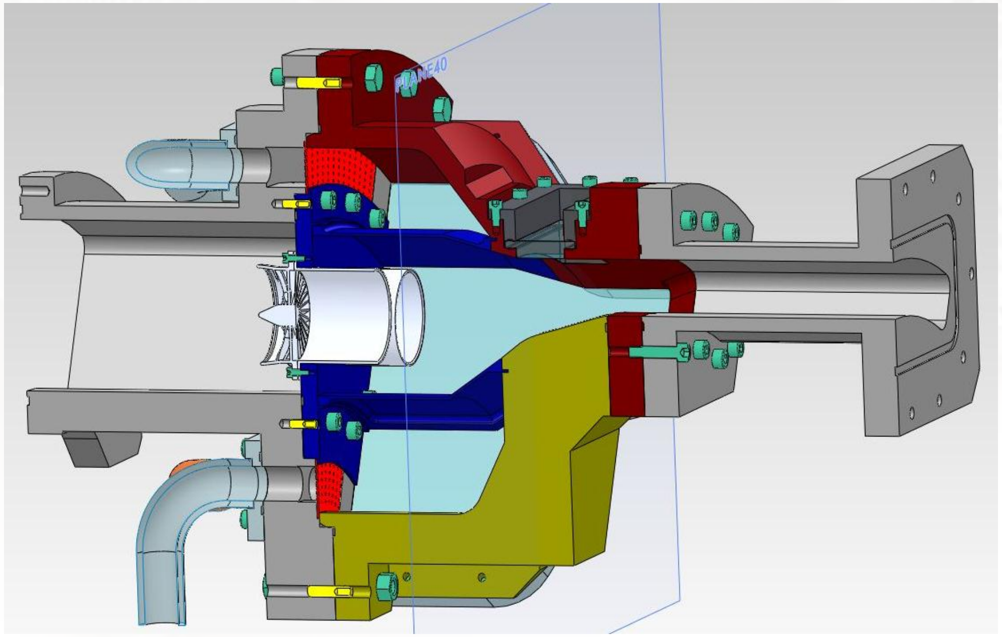

EASN Workshop (31/10/12)

4: University of Florence – PIV, HWA

SEVENTH FRAMEWORK PROGRAMME

- **Measurement plan planned with TM**

Coolant Mass flow

Mainstream Mass flow

Coolant Mass flow

- ▼ **Ts** fluid
- ▲ Twall
- ● **Ps** (tappings)
- ● HWA
- **Rack**
  P (Kiel)
  T (thermocouple)

Plane 40

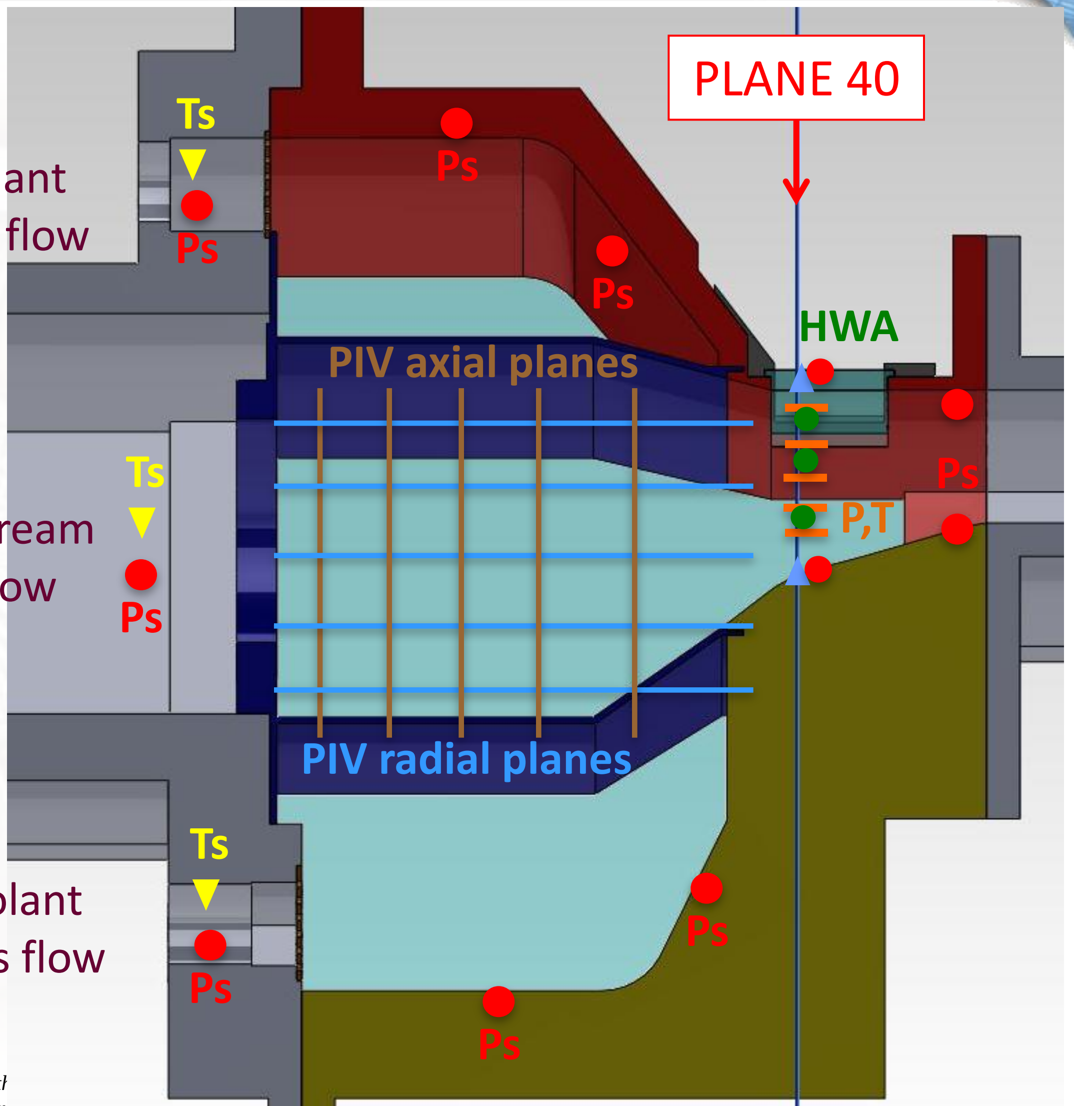

5: Onera– Raman Spectroscopy

SEVENTH FRAMEWORK PROGRAMME

❑ Raman Spectroscopy

- Static temperature measurements
- Full field measurements in the rotating frame
- Radial profiles of ~3° in the static frame
- Measurements down to 2mm from end walls

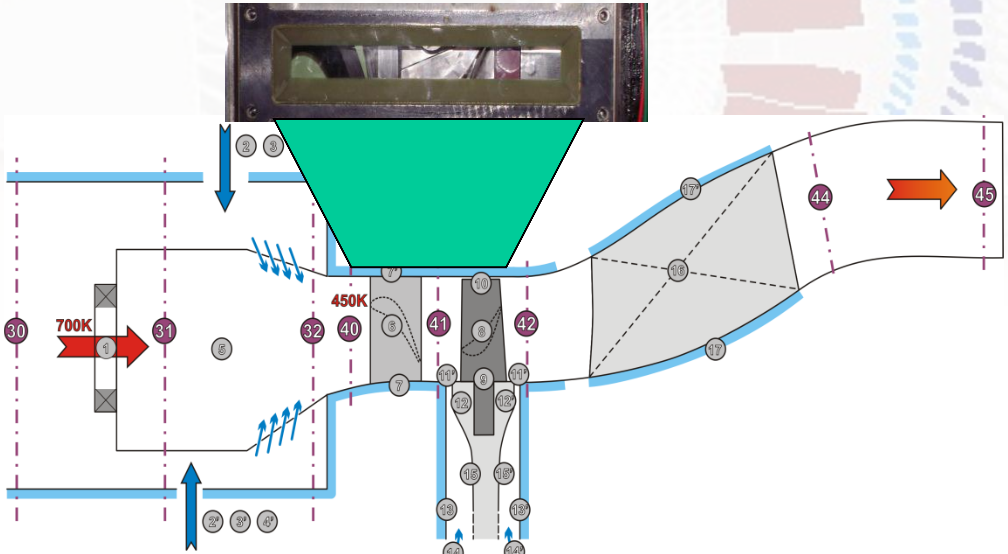

Presentation Structure

- The FACTOR Measurement Campaign
- **High Speed IR Heat Transfer Measurements: Cambridge University**
  - Impulse Response Technique
  - Signal/Noise

6: University of Cambridge – Heat Transfer

SEVENTH FRAMEWORK PROGRAMME

Our objective:

- NGV, HPT & IPV surface measurements of:
  - Local heat transfer coefficient (HTC) [W/m^{2}K]
  - Local adiabatic film cooling effectiveness (η)
- Using a transient infrared thermography technique
- Probably the first use of this *transient* HTC measurement technique with *IR thermography* on *high-speed* machinery

Presentation Structure

- The FACTOR Measurement Campaign
- High Speed IR Heat Transfer Measurements: Cambridge University
  - Impulse Response Technique
  - Signal/Noise

Impulse Response Technique

1. Impulse — Heat Transfer System — 2. Output

Step Change in Mainstream Temp →  → Surface Temperature Response in time

Impulse Response Technique

1. Impulse	Heat Transfer System	2. Output
Step Change in Mainstream Temp	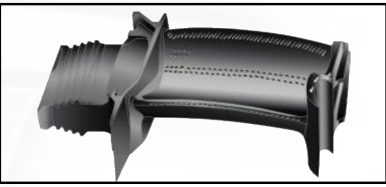	Surface Temperature Response in time
$T_\infty(\mathrm{t})$	h, ρck	$T_w(\mathrm{t})$

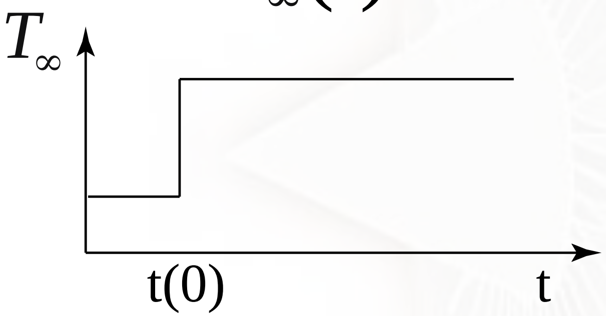

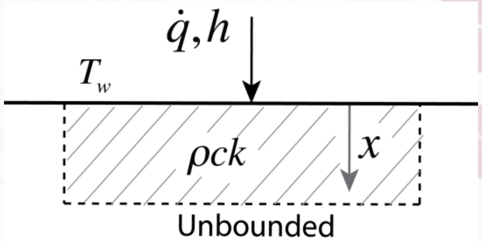

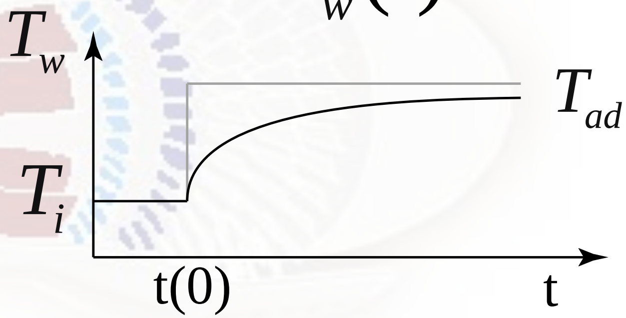

Impulse Response Technique

1. Impulse	Heat Transfer System	2. Output
Step Change in Mainstream Temp		Surface Temperature Response in time
$T_\infty(t)$	h, ρck	$T_w(t)$

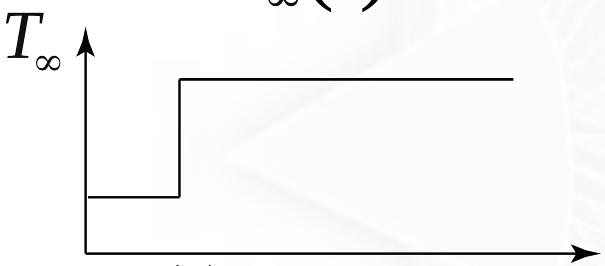

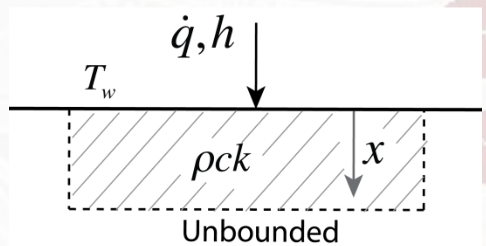

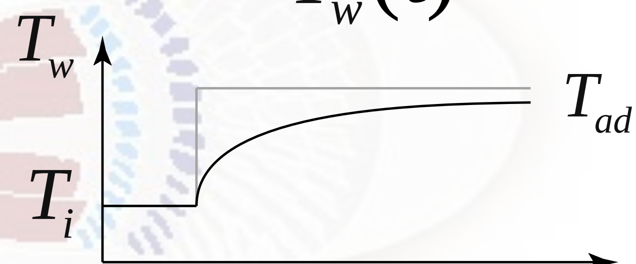

Analytical 1D surface temperature response to a step:

$$\frac{T_w - T_i}{T_{ad} - T_i} = 1 - \exp\left(\frac{h^2 t}{\rho ck}\right) erfc\left(\frac{h\sqrt{t}}{\sqrt{\rho ck}}\right)$$

Impulse Response Technique

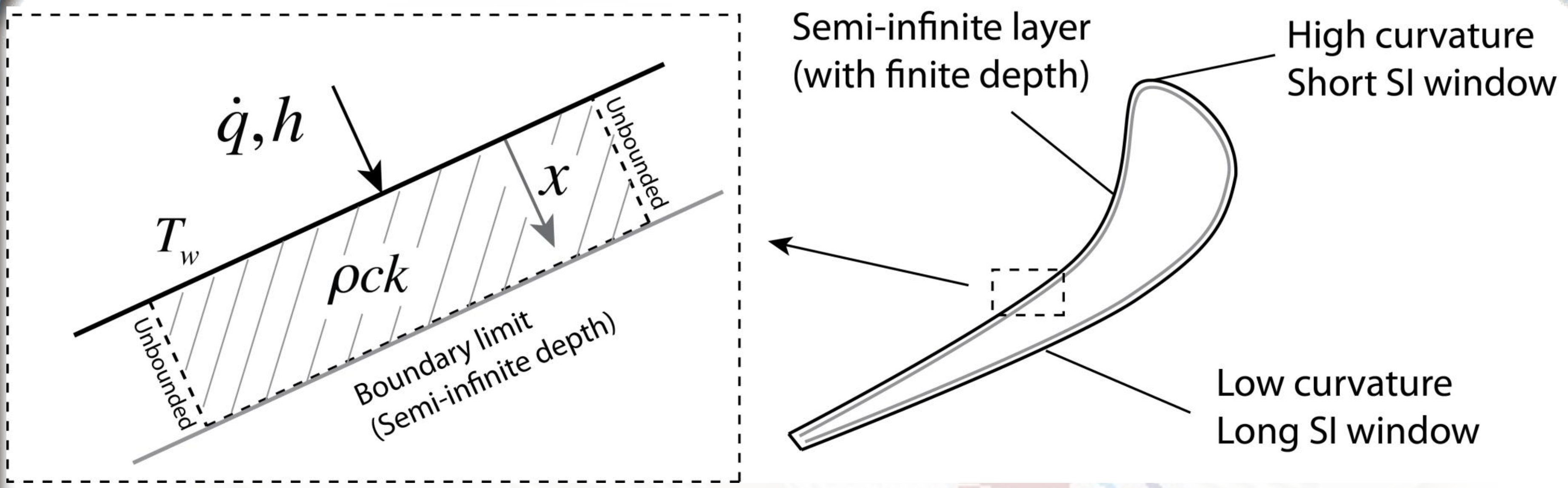

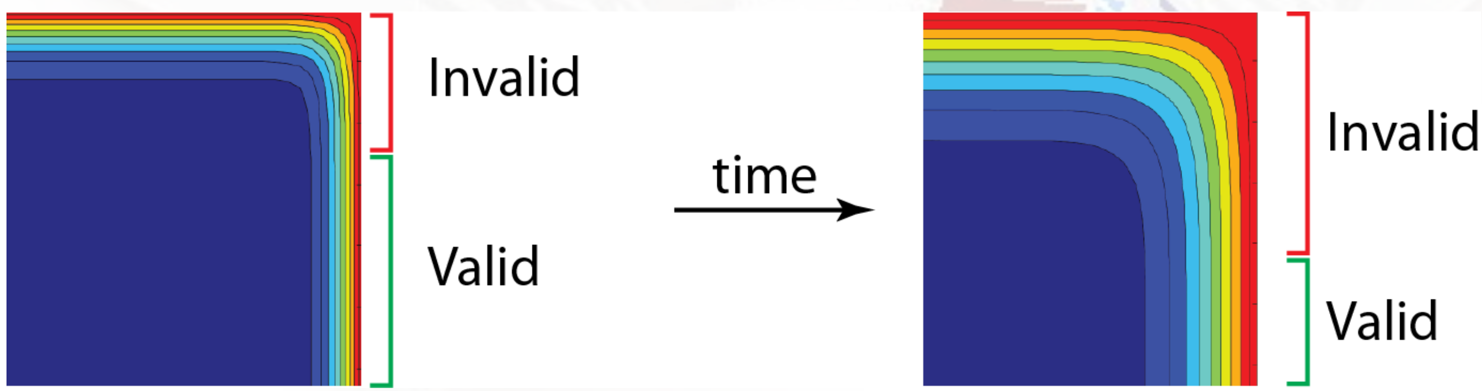

Presentation Structure

- The FACTOR Measurement Campaign
- High Speed IR Heat Transfer Measurements: Cambridge University
  - Impulse Response Technique
  - Measurement Complexities

Measurement Complexities

SEVENTH FRAMEWORK PROGRAMME

- **Complexities with the IR measurements:**
  - Moving target – rotor tip speed 210m/s
  - Slow transient relative to semi-infinite window

Measurement Complexities

SEVENTH FRAMEWORK PROGRAMME

- **Complexities with the IR measurements:**
  - Moving target – rotor tip speed 210m/s
  - Slow transient relative to semi-infinite window

- **Consequences**
  - Reduction in signal/noise ratio
  - Loss of depth of field
  - Need to model impulse function
  - Image acquisition timing

Measurement Complexities

- Complexities with the IR measurements:
  - Moving target – rotor tip speed 210m/s
  - Slow transient relative to semi-infinite window
- Consequences
  - Reduction in signal/noise ratio
  - Loss of depth of field
  - Need to model impulse function
  - Image acquisition timing

SEVENTH FRAMEWORK PROGRAMME

- **How do we address the signal/noise problem?**
  - Low thermal diffusivity surfaces
  - Impulse coolant flows as well as mainstream flow
  - Internally cooled IR cameras

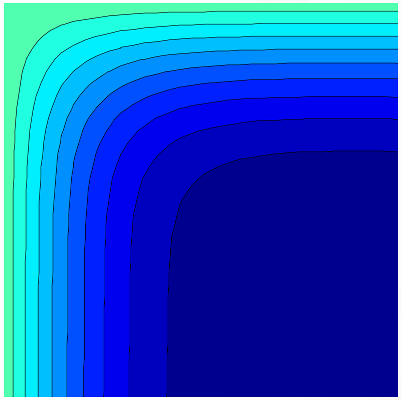

High Diffusivity

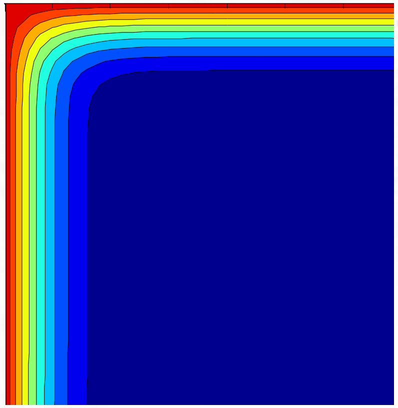

Low Diffusivity

Low Diffusivity Rotor Blade

Summary of Measurement Techniques

SEVENTH FRAMEWORK PROGRAMME

Summary of Measurement Techniques

1. DLR – 5 Hole Probe Traverse
2. ILA – Laser Doppler Vibrometry
3. VKI – Fast Response Pressure Measurement
4. University of Florence – PIV and Hot Wire Anemometry
5. Onera – Raman Spectroscopy
6. Cambridge University – Heat Transfer Measurement

Conclusion on FACTOR project

- **FACTOR is a four-year project** (2011 – 2014)
- **Objective:** To develop an experimental infrastructure using most advanced measurement techniques and to collect experimental data that will allow to draw up guidelines on CFD modelling of combustor-turbine interactions.
- **Facilities**
  - NG-Turb @ DLR, Göttingen (continuous test rig)
  - O-TRF @ Oxford University (blow-down rig)
  - Sector rig @ Firenze University (combustor with 3 swirlers)
- **Current status of the project:**
  - Finalization of components design
  - Manufacturing of DLR rig to start in June 2013
  - Start of experimental campaign @ DLR beginning 2014
- **The programme strategy, technology and skills to be deployed here are challenging and world class. FACTOR should be taking great strides to support the future of European propulsion.**

Thank you

for your attention

Back-up

Starting point

- **NASA and US Air Force Research Laboratory (Wright Patterson Air force base) developed a facility in early 2002 to operate a combustor simulator in interaction with a turbine operating at realistic Reynolds and Mach numbers.**
  - MD. Polanka, ASME Turbo expo *GT2004-53613, GT2006-90401, GT2008-50281*

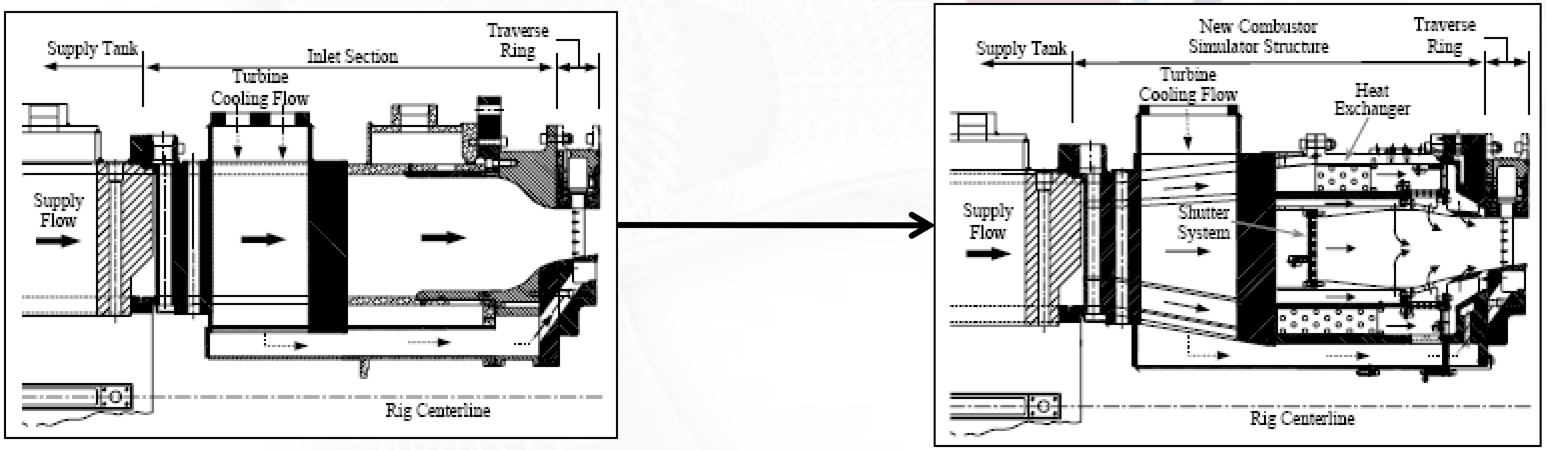

Fundamental idea

Turbine Aero-thermo-mechanical design requires complete knowledge of 3D flow

Need for

Experimental characterisation and CFD validation

In order to

Adapt the most suitable degree of complexity in current design process

Consortium

SEVENTH FRAMEWORK PROGRAMME

SAFRAN Snecma

Avio

CERFACS

DLR

GDTECH engineering

ILA Intelligent Laser Applications GmbH

IMP PAN GDANSK

ITP Industria de Turbo Propulsores, S.A.

MTU Aero Engines

ONERA THE FRENCH AEROSPACE LAB

Progesa

Rolls-Royce

SIEMENS

SAFRAN Turbomeca

UNIVERSITY OF CAMBRIDGE

STUDIORUM UNIVERSITAS FLORENTINA

D·E Dipartimento di Energetica "Sergio Stecco"

UNIVERSITY OF OXFORD

VOLVO AERO

VON KARMAN INSTITUTE

WK RZESZÓW

ARTTIC

Work Breakdown Structure

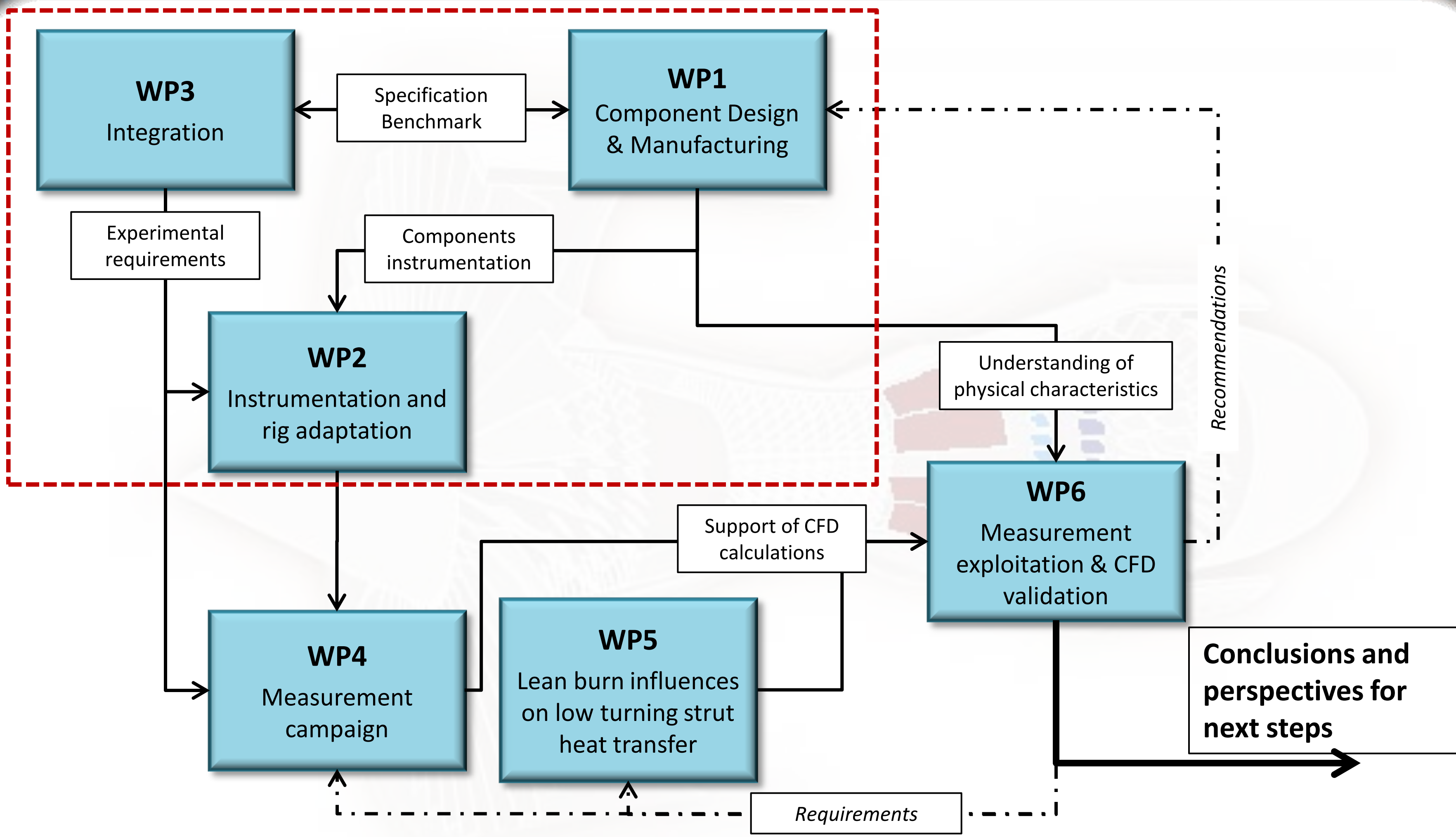

Work Breakdown Structure

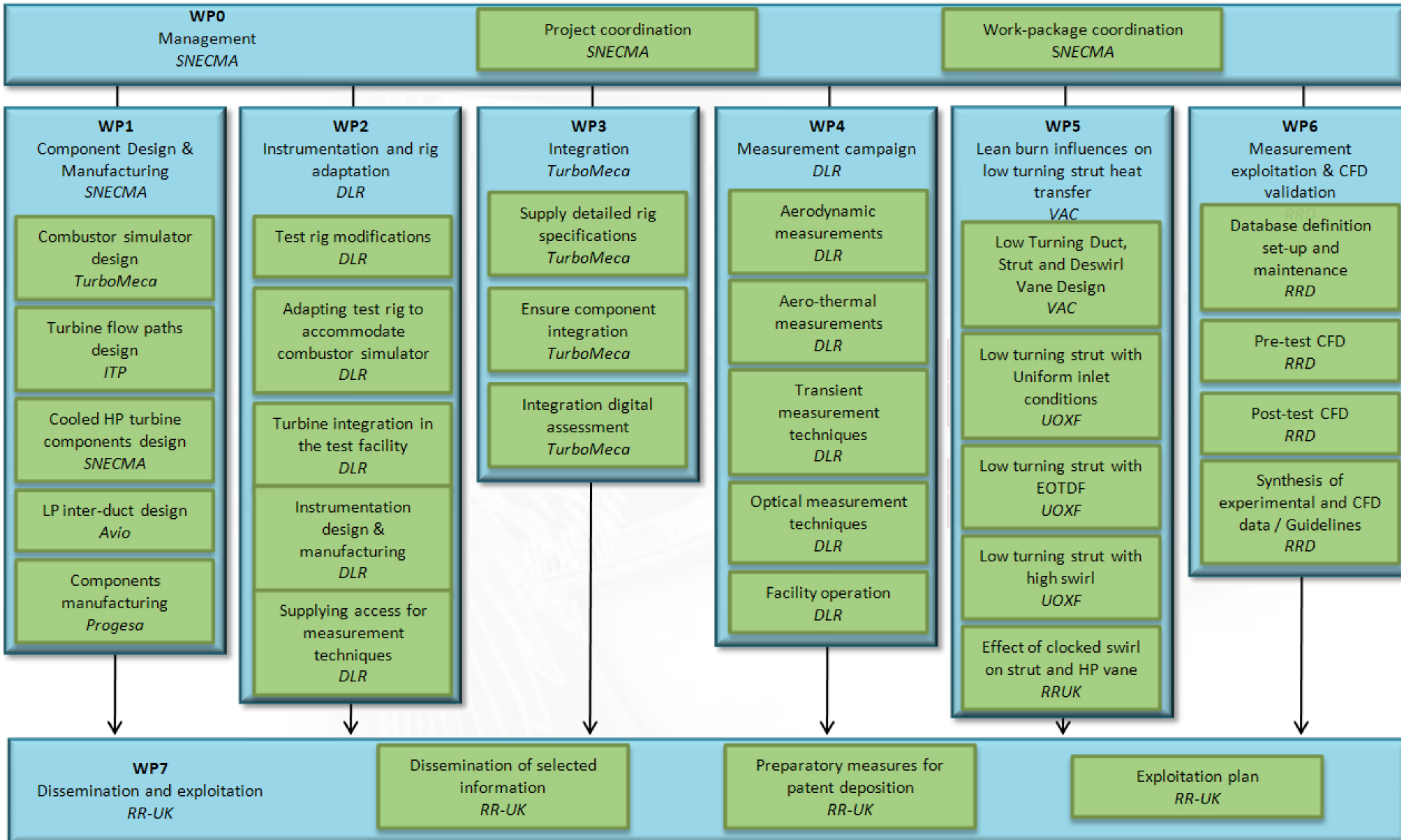

EASN Workshop (31/10/12)

GABRIEL project

Using the magnetic levitation technology to assist the aircraft take-off and landing

Dr. Jozsef Rohacs
Rea- Tech Ltd.

Introduction
1 . Actuality
2. The project
3.. Technology evaluation
4. Possible solutions
Summary

2012, Budapest, Hungary

Introduction

GABRIEL - Integrated Ground and on-Board system for Support of the Aircraft Safe Take-off and Landing

Type of funding scheme:
Collaborative Projects - Small or medium-scale focused research project

Work programme topics addressed:
FP7- AERONAUTICS and AIR TRANSPORT (AAT) - 2011- RTD-1
Activity 7.1.6 Pioneering the air transport of the future
Area 7.1.6.3 Promising Pioneering Ideas in Air Transport

AAT.2011.6.3-2 Take-off and Landing with Ground-based Power

Here are the first results of investigations

1. Actuality

- air transport at the starting the third „S” curve of development
- innovative or sustainable technology

  improving the existing system
- disruptive technology

  broadening and developing new markets

  and providing new functionality,

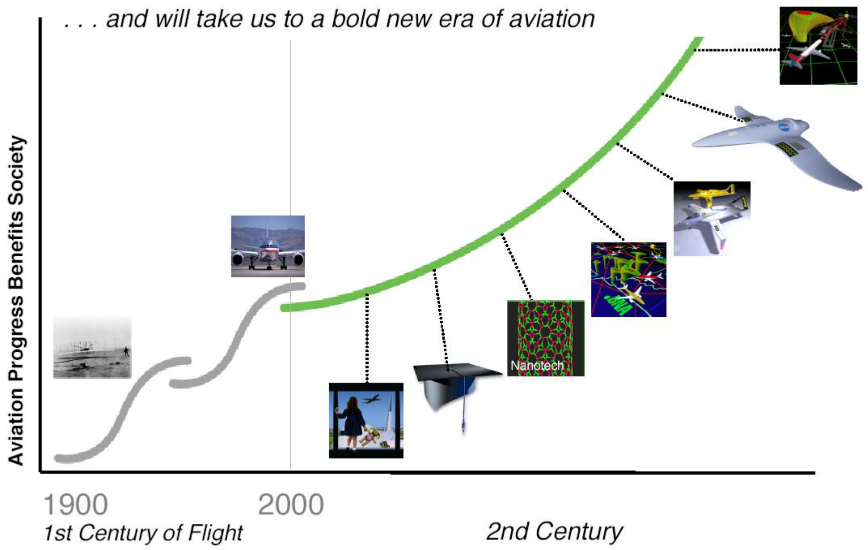

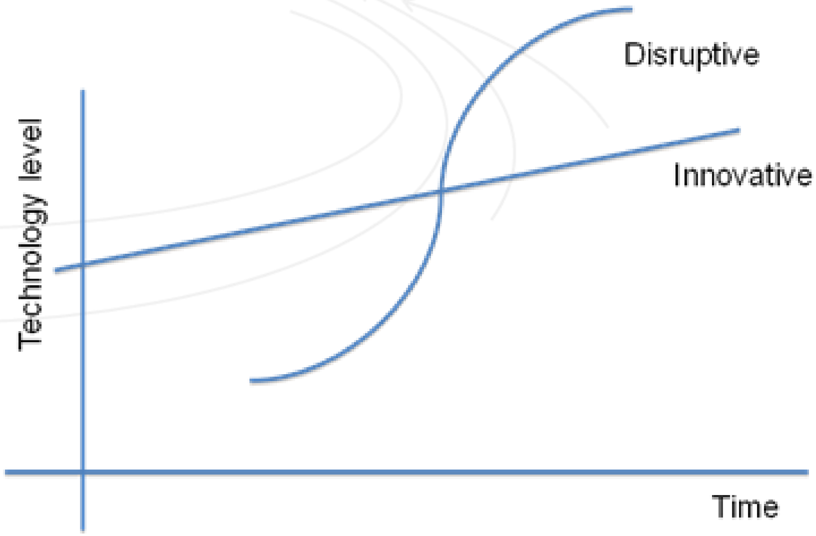

1. Actuality – cont'd.

- the are take-off weight and speed is growing
- environmental effect is contiously reducing
- further considerable changes are required

growth in efficiency, decreasing in environmental impact

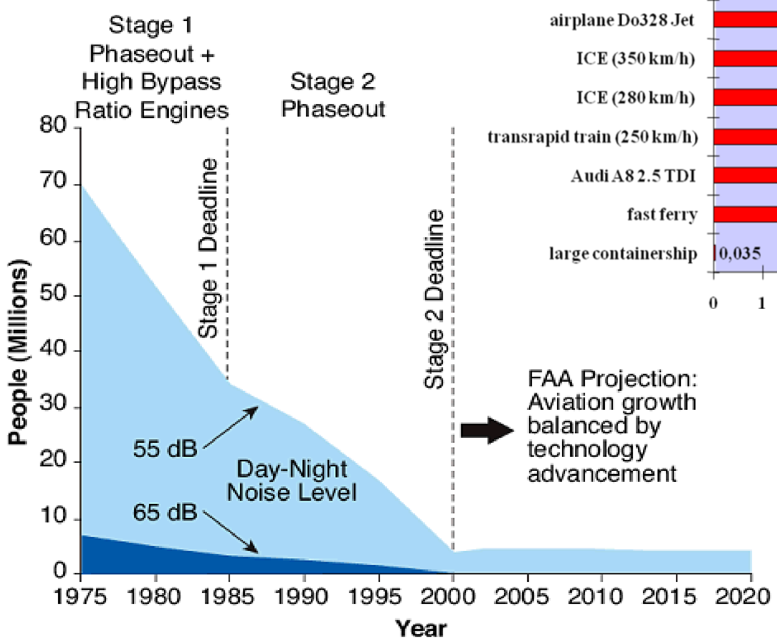

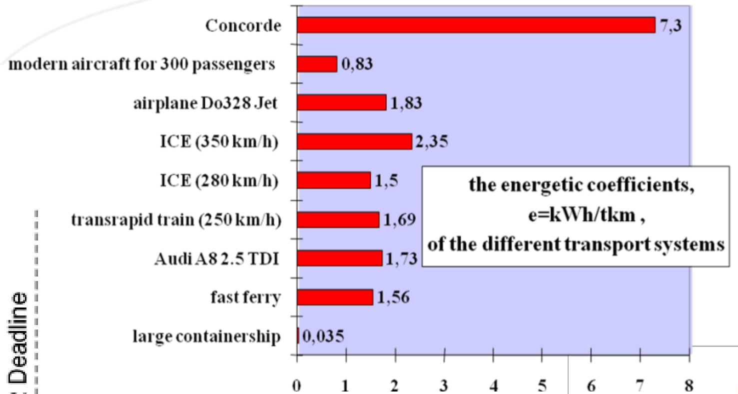

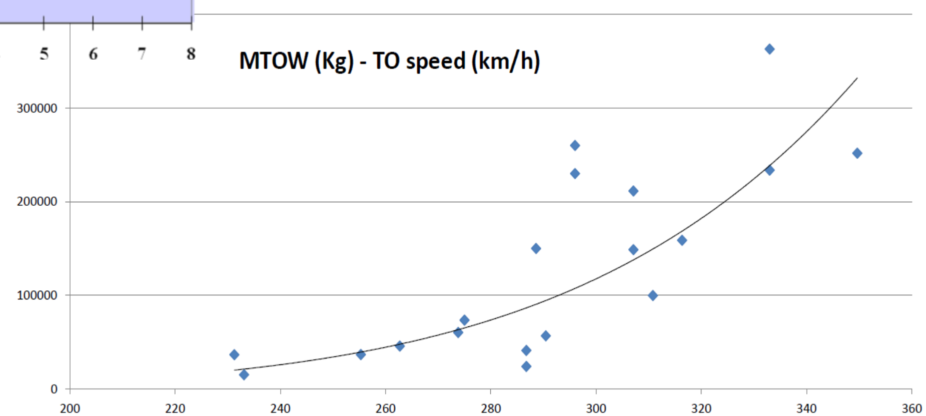

2. The project
2.1. The team

List of participants:

Participant no.	Participant organisation name	Country
1	REA-TECH Engineering and Architect Ltd. (REA)	Hungary
2	Slot Consulting (SLOT)	Hungary
3	Delft University of Technology (TUD)	Netherlands
4	The French Aerospace Lab (ONERA)	France
6	RWTH Aachen University (RWTH)	Germany
6	Dieter Rogg (DRogg)	Germany
7	Ad Cuenta (AdC)	Netherlands
8	National Aerospace Laboratory (NLR)	Netherlands
9	Rezeszov University of Technology (RzUT)	Poland
10	Wroclav University of Technology (WrUT)	Poland
11	Italian Airspace Research Center (CIRA)	Italy
12	University of Salerno (UoS)	Italy

- 1946: US Naval Air Test Center investigated an electric catapult.
- Since 1990: the magnetic levitation system has implemented by rapid train systems, widely.

- 2000: US Naval Air System Command and General Atomic started work on the Electromagnetic Aircraft Lunch System.

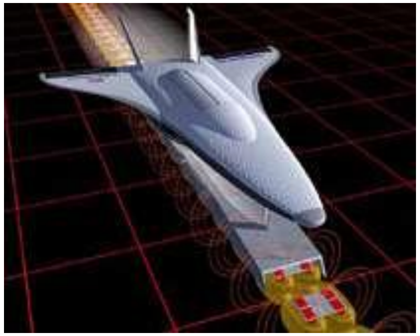

- 2008: Gabriel project has initiated
- Gabriel system – use of magnetic levitation system to ground based assisting the aircraft take-off and landing.

2. The project
2. 3. Vision

The air transport rapidly grorwth and causes further problems of

- capacity,
- efficiency
- safety and
- greeening.

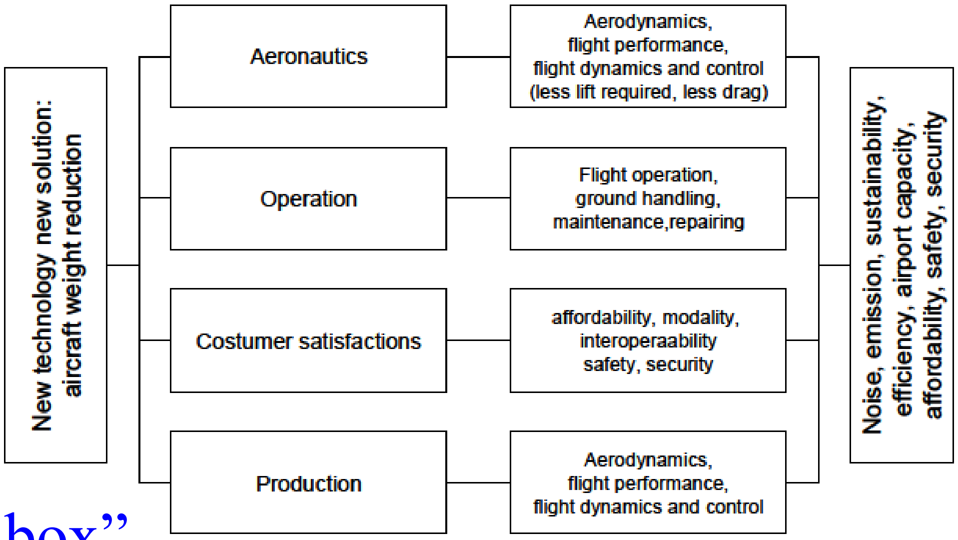

Solution: development of the revolutionary new technologies, by reforcing „thinking out of the box”.

Magnetic leviation is a reliable safe new technology

- that may generated real added values, but
- it needs fundamental studies in its
  - possible implementation
  - efficiency and
  - safety (!).

2.4. Goal and Objectives

Goal:

Gabriel will investigate if using the magnetic levitation system to assist the ***aircraft take-off and landing*** is

- feasible,
- cost effective and
- safe.

Objectives:

- concept exploration and analysis;
- concept development;
- concept validation;
- impact assessment.

2. The project

2.5. Project structure

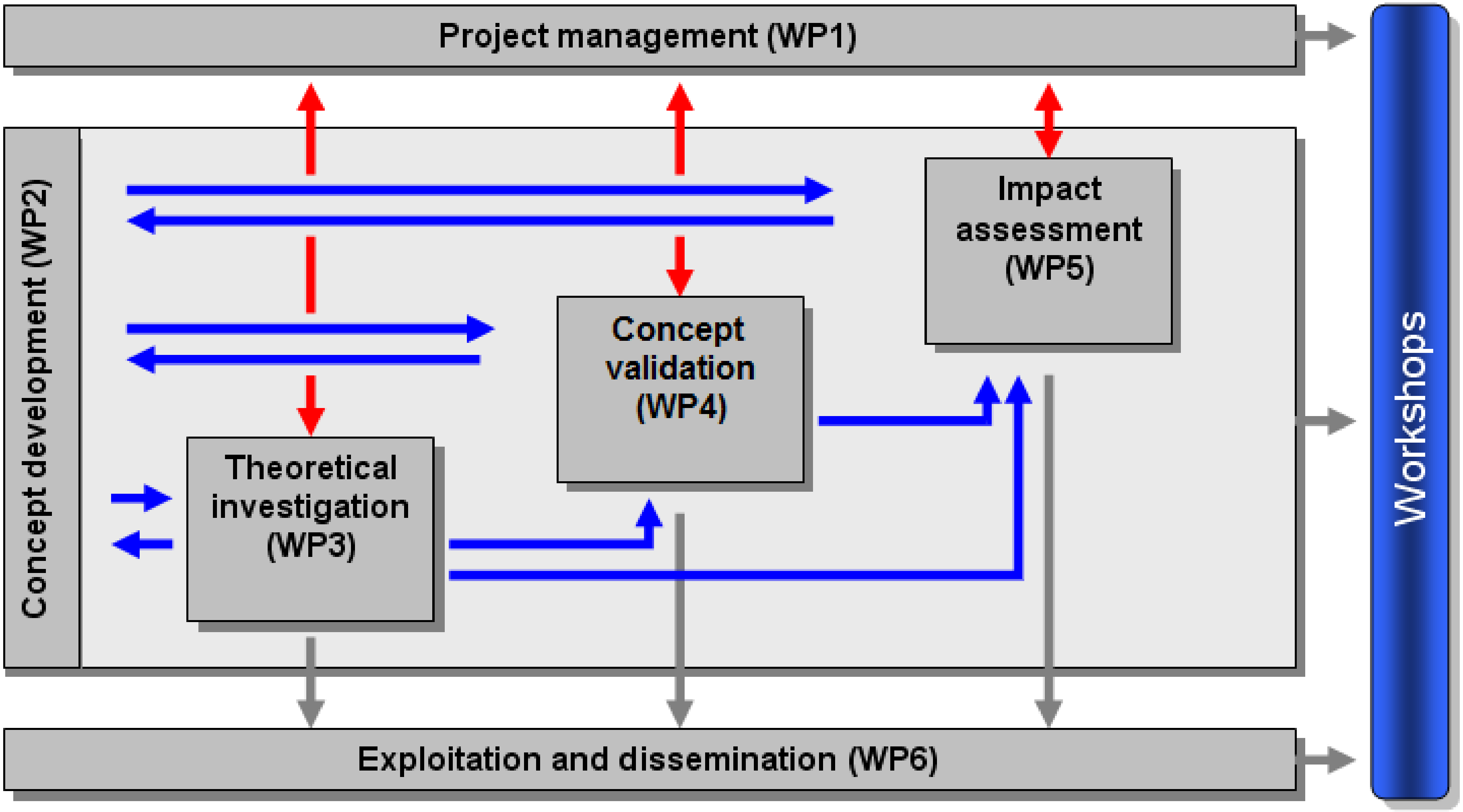

2.6. Planned results

The Gabriel deals with first step: (extended) theoretical investigation.

The theoretical investigations:

- energetic analysis,
- structural analysis,
- control sysnthesis,
- safety investigation
- Impact assestment analysis

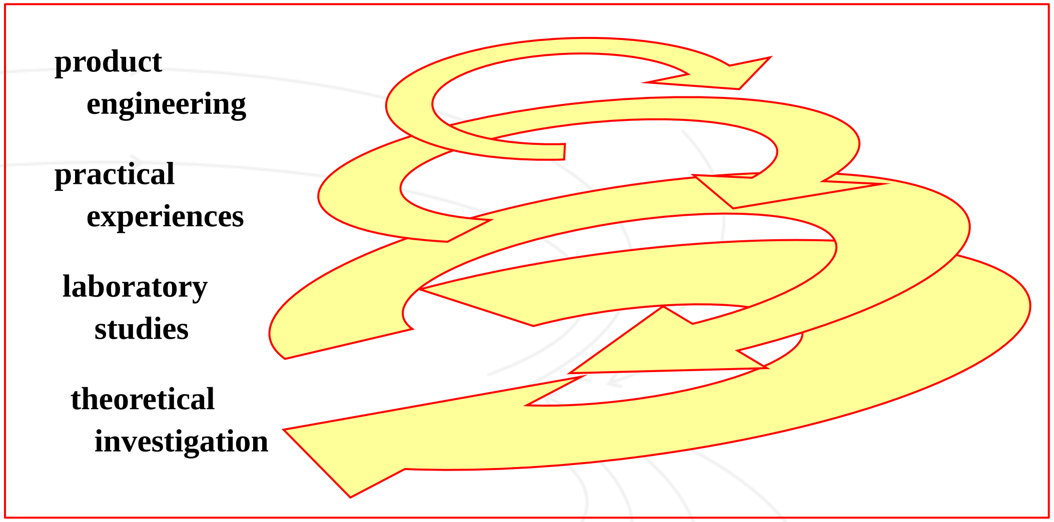

and practical studies

- with small aircraft model
- magnetic test bench

must results to decision about the

- applicability and efficiency of the Gabriel concept,
- possible solution of the safety problem (landing in emergency situation)
- impact assestments

and should result to validated operation concept.

3. Possible solutions
3.1. Innovative solutions

Effects of thrust increasing, weight decreasing for 10 % on flight performances

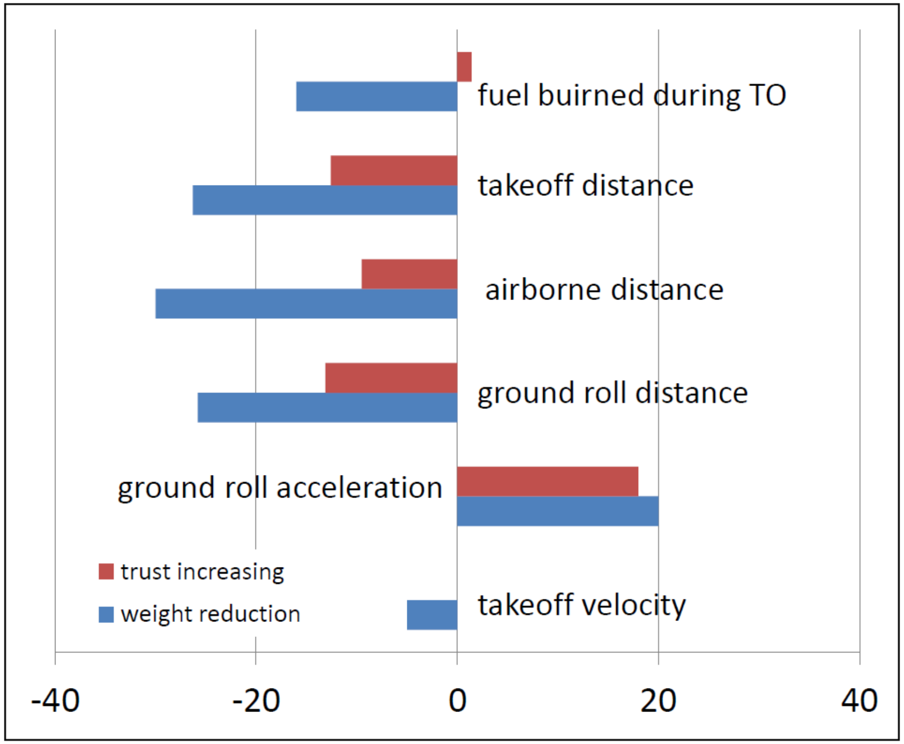

New (unconventional) flight procedures

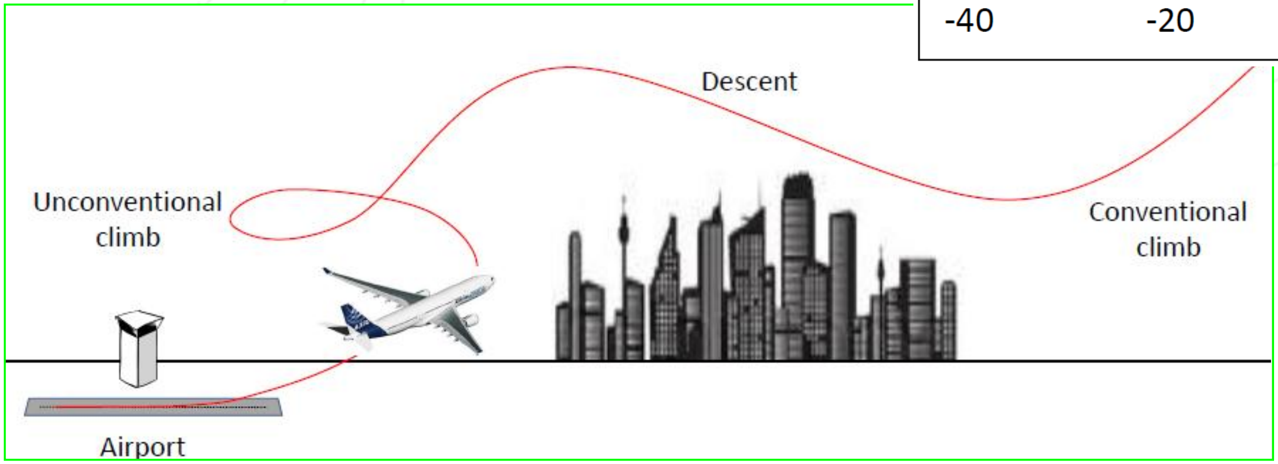

Disruptive solutions – thinking out of the box

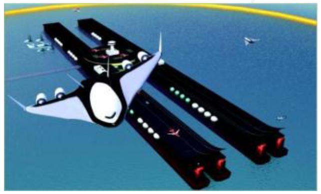

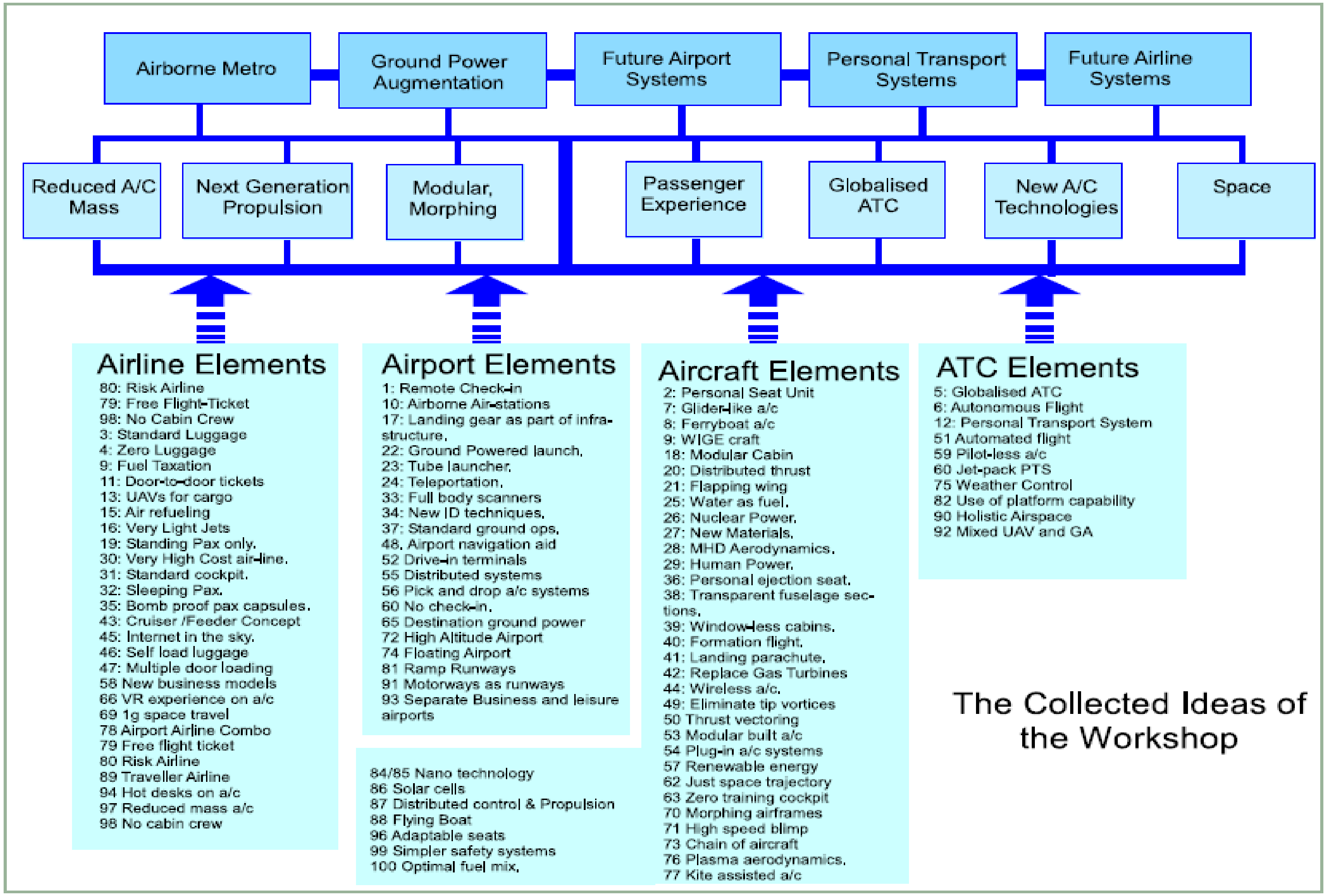

Possible solutions:

Takeoff with limited fuel and fuelling at the high altitude

Lifting up - down the aircraft by aerostatic ships

Airport in the sky – high altitude airport

Cruiser - feeder concept

Airport above the city

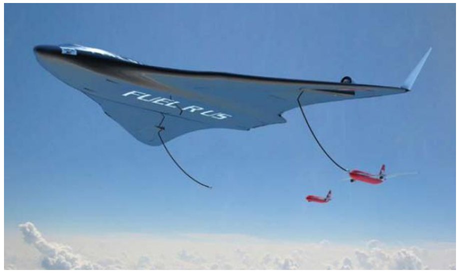

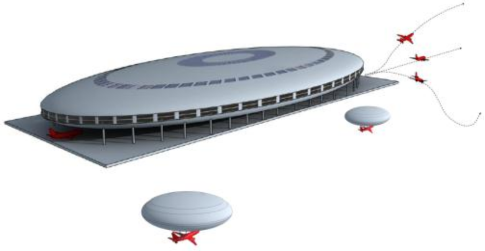

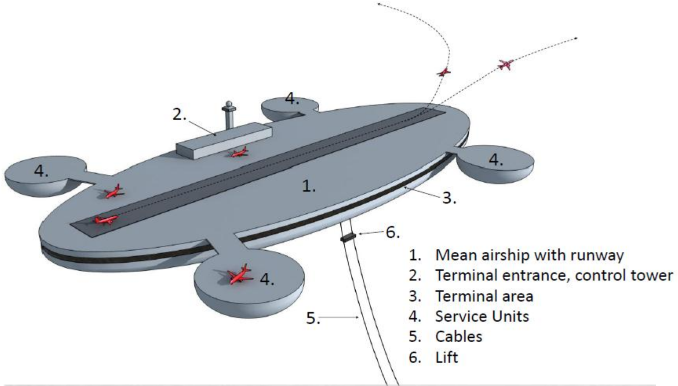

3. Possible solutions
3.3. Set of solutions – cont'd.

Underground airport
Ground assisted lift generation
Ground based energy supply –
microwave energy supply
Electric engine accelerators
Electromagnetic aircraft launch
system (EMALS)

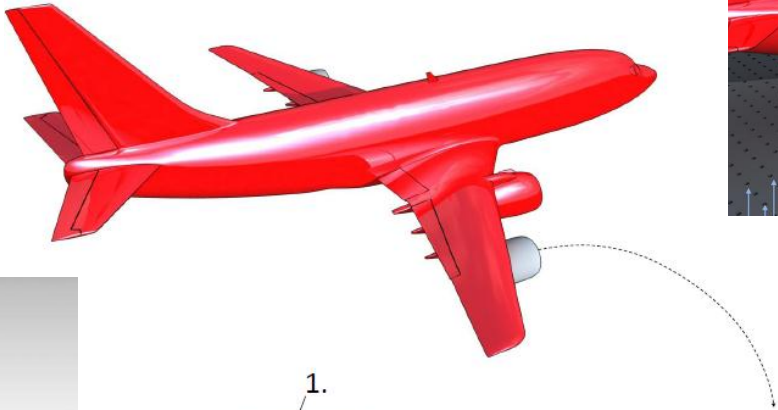

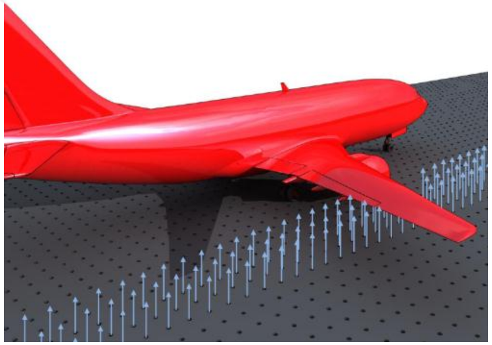

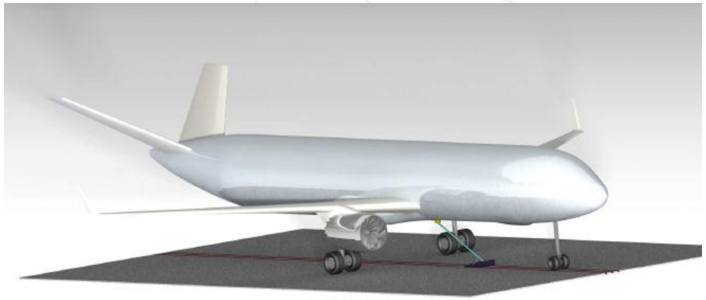

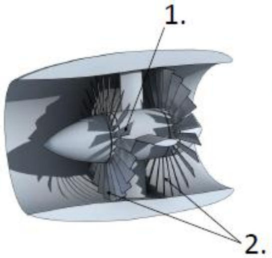

1. Electric motor
   + accumulator
   + control unit
2. Propellers

The solution – MagLev track and cart – sledge system

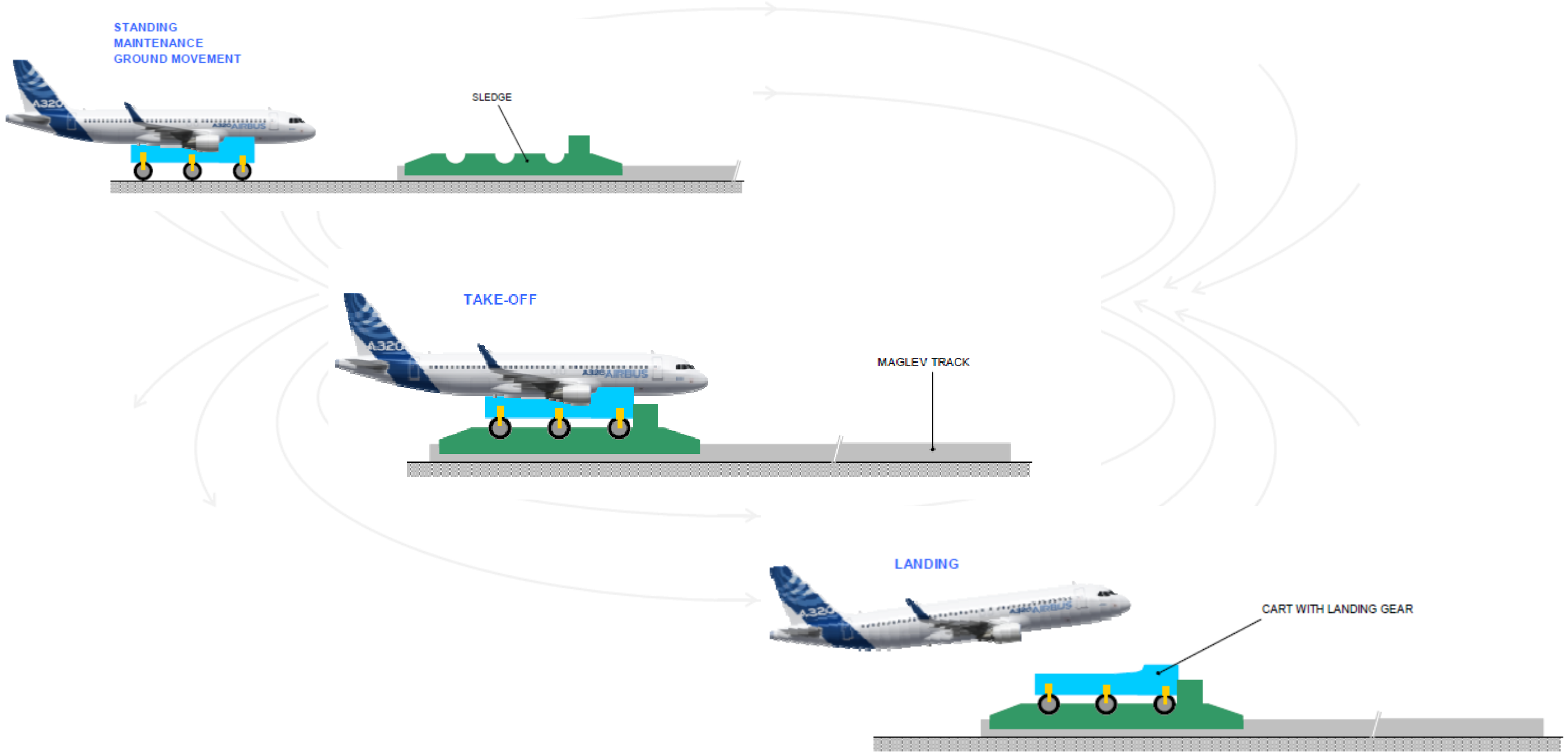

G. Further considerations – vision on operational concept

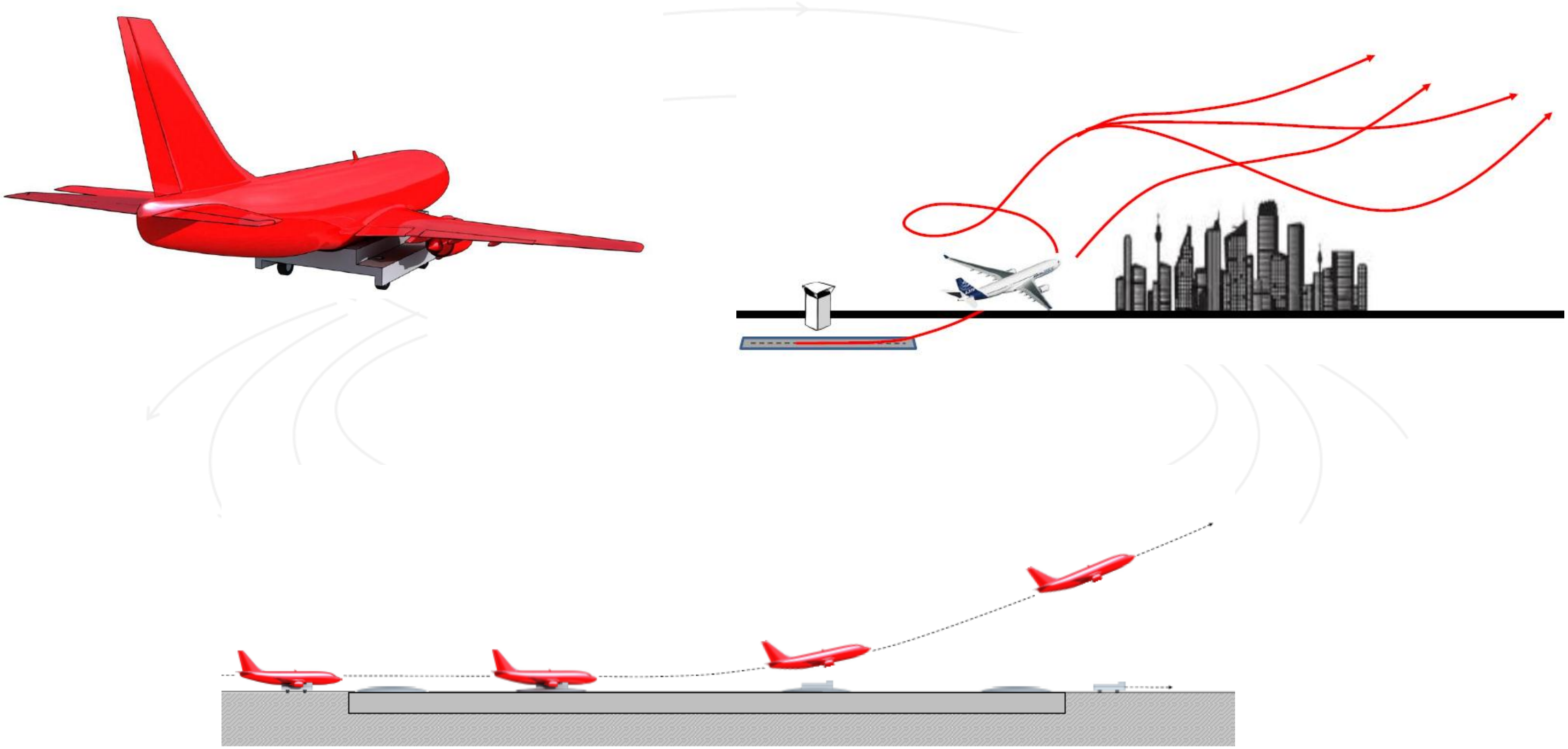

4. Technology evaluation
4.1. MAGLEV

- Review of existing maglev technologies (electrodynamic, eletromagnetic, indutrack)

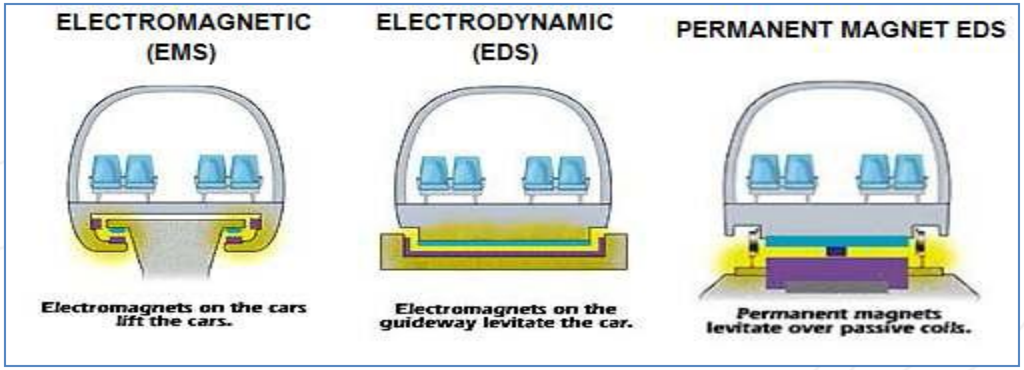

- Lessons learned:
  - It can improve **safety**: levitation, control and operation is fully automated, no room for human error
  - It can improve **efficiency**: no rolling friction
  - It can decrease the impact on the **environment**: no fossil fuel is burned, trains are virtually silent at 200km/h (no friction, engine)
  - Acceleration and supported weight is **relevant**
  - Permits a climb gradient up to 10 degrees
  - **Magnetic effects**: only at EDS and could be shielded

4. Technology evaluation
4.1. MAGLEV – cont’d. I.

- Review of existing maglev tracks in air transportation
  - Foster-Miller / NASA track (1997-2000):
    - NASA contract,40ft, with permanent magnets, desingned for spacecraft
    - Budget: 545 184 USD
  - RT Advanced Maglev System / NASA Marshall (1999)
    - NASA contract, 50ft, outdoor track, desing for spacecraft
  - Lawrence Livermore National Laboratory / NASA track
    - NASA contract, desing for launching rockets
    - Indutrack system: permanents magnets placed in **Hallbach array**

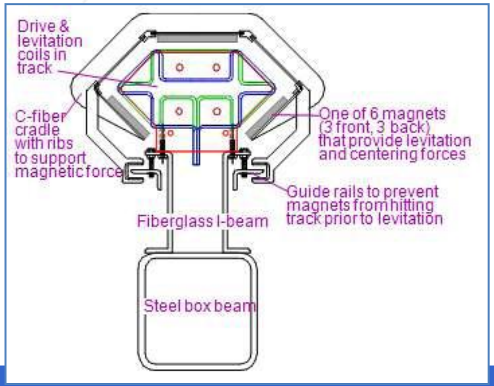

4. Technology evaluation
4.1. MAGLEV - cont'd. II.

- Review of existing maglev tracks in air transportation
  - Egeneral Atomic EMALS track (300 ft long)
    - Contracted in 2000 by the US NAVY, to launch military a/c
    - 2010/12/18: successfully tested on an F/A-18 fighter

- Lessons learned:
  - Maglev **could be adapted** to air transportation (***<u>already tested</u>***)
  - **Fulfills the requiremenets of GABRIEL** (acceleration, speed, weight)
  - Effects og magnetic fileds on the a/c is eigher not significant, or could be shielded

- Preliminary analysis of major meglev technologies

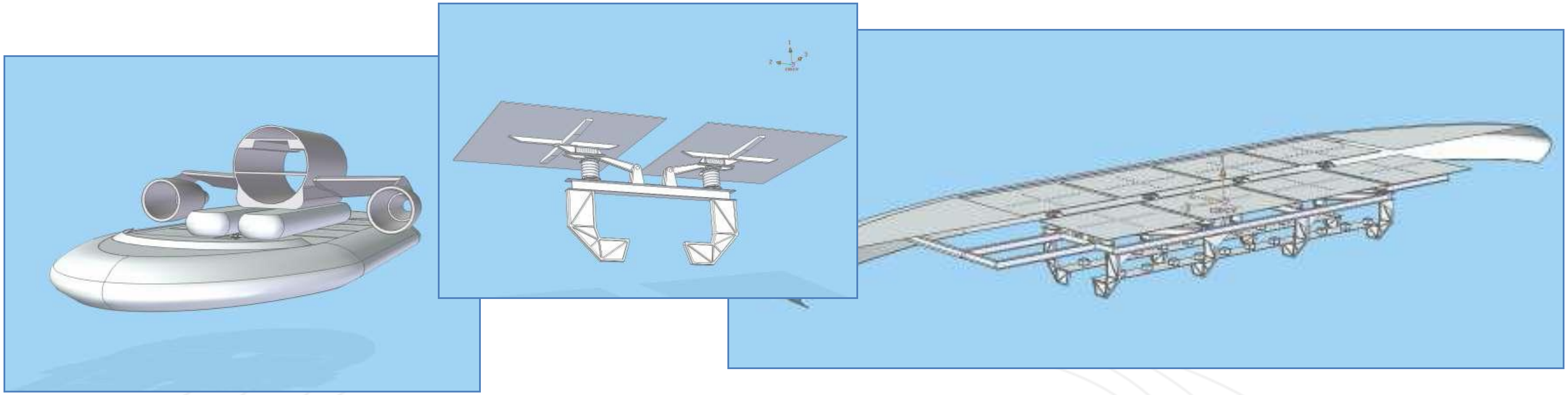

- Lessons learned:
  - use of **sledge**: no need to mount anything on the a/c (e.g. mangnets)
  - EMS could significantly **cut the required thrust**, and levitate even at zero speed
  - EDS requires **magnets with significant weight** (>950kg), generates **magnetic field and requires wheels**
  - **Indutrack** requires a small magnetic surface, can keep constant airgap

- Evaluation procedure

General Preconditions

Overview over Maglev Technologies

Detailed Description and Data Acquisition of Candidates

Definition of special Requirements of GABRIEL

Concepts, adjusted to the Requirements of GABRIEL

Evaluation Procedure

Definition of Criteria

Definition of Degree of Fulfillment

Definition of Priority Factors

Evaluation of the Candidates

Selection of the most suitable Candidate(s)

4. Technology evaluation
4.3. Methodology – cont’d.

Technology identification, evaluation and selection

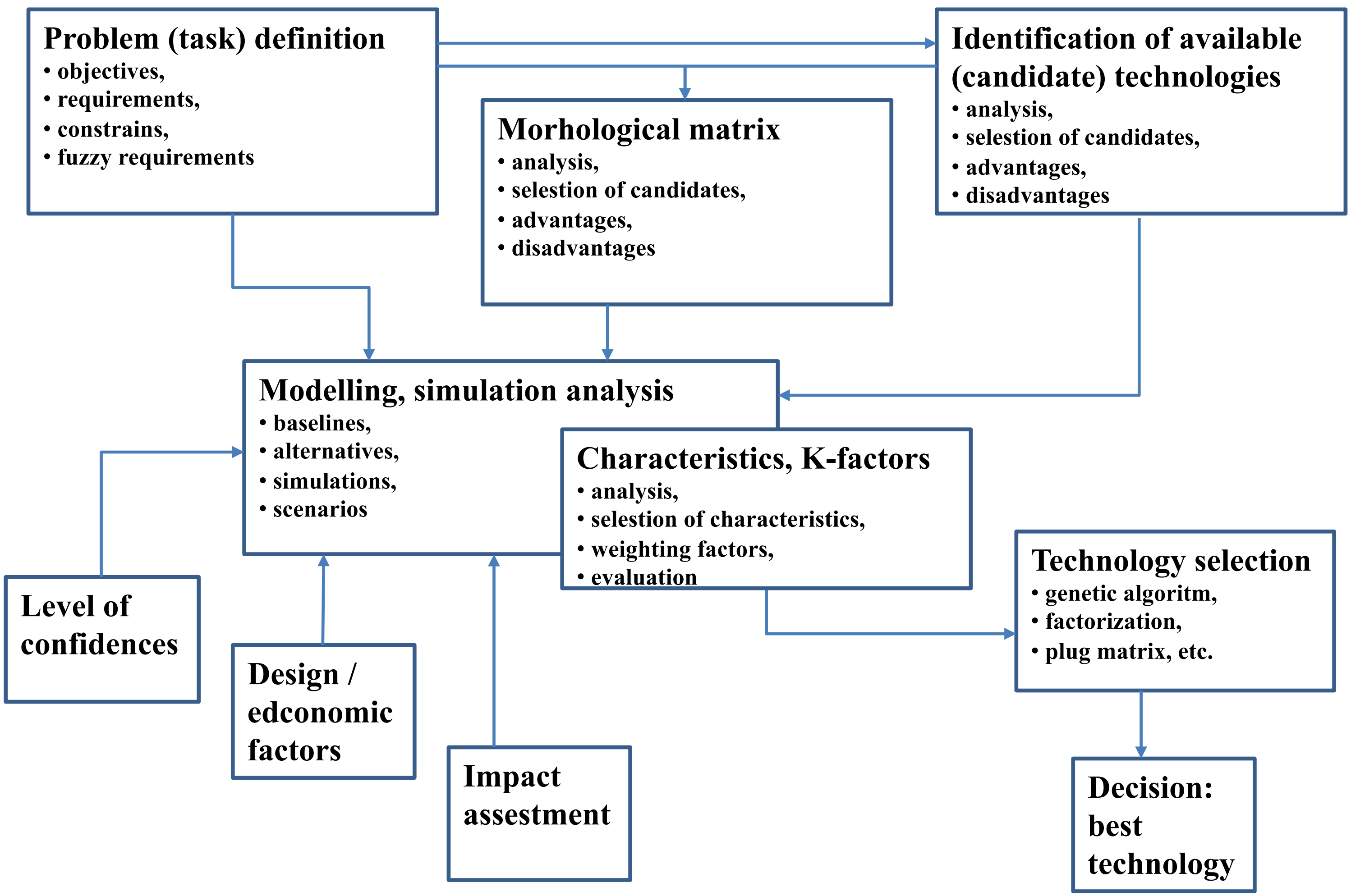

4.3. Methodology – cont'd. I.

General Preconditions

- The intention of "Gabriel" ***should not be to develop a fully new version*** of magnetic suspension and electrical linear propulsion, a matter of very high financial expenditure and long duration from the concept until getting the license for public transport.
- The intention should rather be, to ***evaluate existing and successfully tested technologies and to select and to adapt the most suitable*** combination.
- To get as high as possible an acceptance of "GABRIEL", especially from industry and airlines, ***major changes of the airframe should be avoided***. Therefore levitation and propulsion components should be mounted to a ***sled***, which carries the aircraft and not to the aircraft itself.

4. Technology evaluation
4.3. Methodology – cont'd. II.

Evaluation Criteria

- Levitation Capability
- Speed / Acceleration Capability
- Complexity of Guideway
- Complexity of Vehicle
- Electrical Power to be installed
- Energy Consumption per Launch
- Levitation at Standstill / Take Off- and Landing Velocity
- Magnetic Stray Fields 0,5 m Above Magnets
- Safety of Suspension System
- State of Development / Development Risks
- Potential of Further Development
- Operation / Maintenance easy – difficult

Anything wrong? Additional Criteria necessary?

Candidates:

- Electrodynamic suspension with superconducting, liquid Helium cooled magnets ("Chuo-Express", Japanese Railway Central)
- Electrodynamic suspension with permanent magnets in Halbach Arrays ("Inductrack", Lawrence Livermore National Labaratory, General Atomics, USA)
- Electromagnetic suspension with linear synchronous long stator motor (Transrapid International, Germany)
- Electromagnetic suspension with linear induction short stator motor (Linimo-System, Japan; Rotem Train, South Korea)

4. Technology evaluation
4.4. Techn. definition – cont'd. I.

Electrodynamic Suspension with Superconducting Magnets

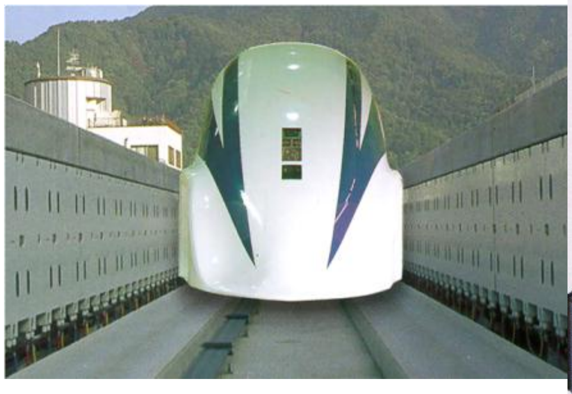

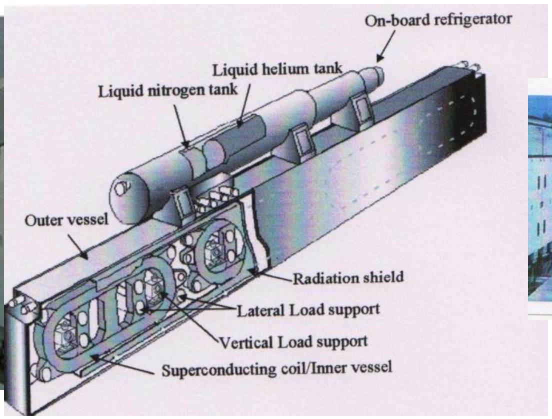

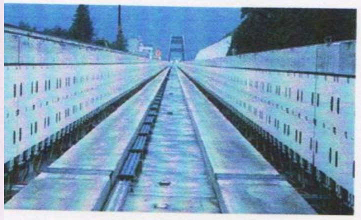

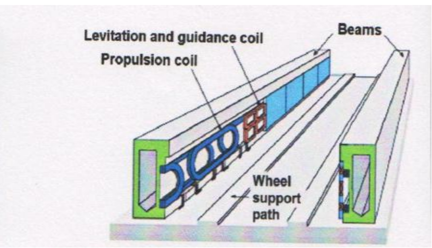

Large suspension gaps
High power propulsion system
Not disturbed by lifting force

Complex vehicle with cryogenic equipment
Complex suspension coils at the guideway
Levitation only above 100 km/h
High magnetic stray fields

Electrodynamic Suspension with Permanent Magnets

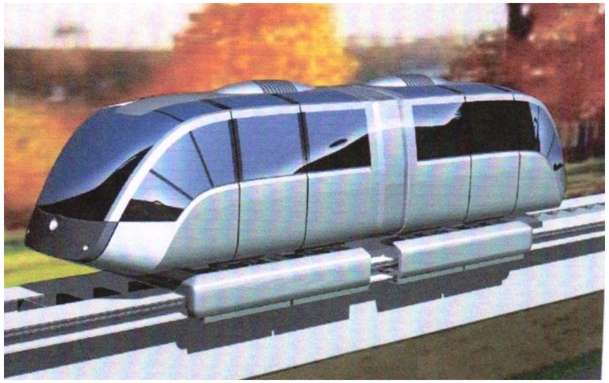

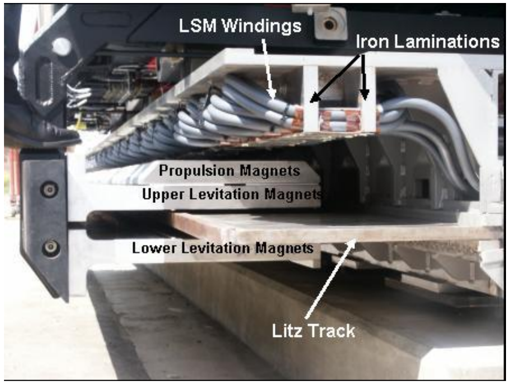

Passive, stable, uncomplicated suspension
Not disturbed by lifting force

Levitation only above 5 to 10 km/h
Only component tests up to now

Electromagnetic Suspension with Longstator Propulsion

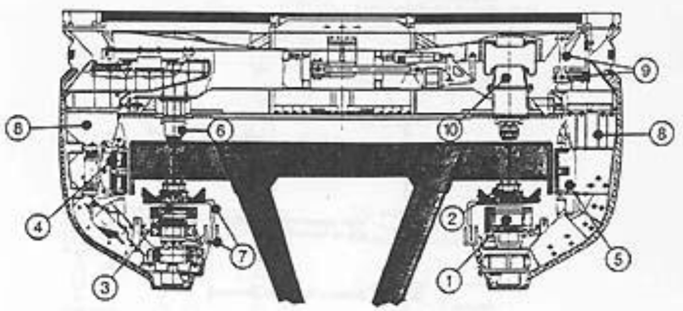

Cross section of the support, guidance and propulsion system: 1 — support electromagnet, 2 — LSM armature stack with windings, 3 — linear generator windings, 4 — guidance magnet, 5 — eddy-current brake electromagnet, 6 — support skids, 7 — *Inkrefa* sensor (vehicle location), 8 — levitation bogies, 9 — cabin suspension, 10 — pneumatic spring. Courtesy of *Thyssen Transrapid System, GmbH*, München, Germany.

- Levitation at standstill
- Low magnetic drag
- Low magnetic stray field

- Unstable levitation, complex electronic controlling
- Small levitation gap
- Problems with lifting force

4. Technology evaluation
4.4. Techn. definition – cont'd. IV.

Electromagnetic Suspension with Induction Motor

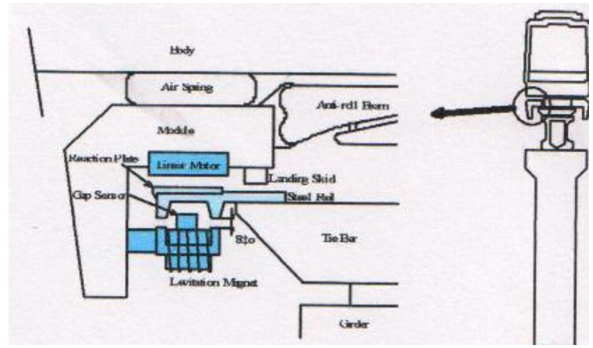

Levitation at standstill
Low magnetic drag
Low magnetic stray field

Unstable levitation, complex electronic controlling
Small levitation gap
Steeply increasing weight of propulsion equipment on board with higher speed

Preliminary Result of the Preliminary Evaluation

➢Electrodynamic superconducting suspension	152
➢Electrodynamic permanent magnets suspension	**188**
➢Electromagnetic suspension synchronous motor	163
➢Electromagnetic suspension with LIM)	130

Maximum Score: 240

Operational concept

description of operation of system from user (stakeholders) point of view.

The GABRIEL concept has no major influence on the passengers' or cargo handling processes, however will introduce a series of changes in aircraft structural solutions, take-off, climb and landing procedures, airport operation, ground handling and will have a significantly positive effect on the environmental load of airports' regions.

5. Solution – operational concept
5.2. Regulatory aspects

Regulatory aspects:

- required knowledge on MagLev,
- demonstration of stability and controlability
- certification
- randevous control
- abnormal flights
- emergency situation management
- operability, maintenability
- security problems
- non-technical and societical aspects

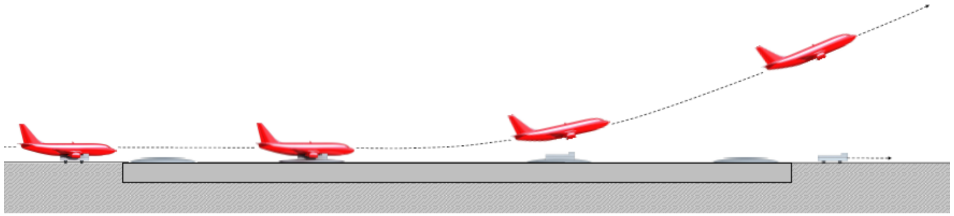

Aircraft design – flight operation.

- safety – at least as safe as conventional air transportation
- changes in thrust, fuselage lower part, missing the under carriage systems, etc.
- cart for aircraft classes,
- take-off and landing with use

of cart – sledge system

- cart is moving

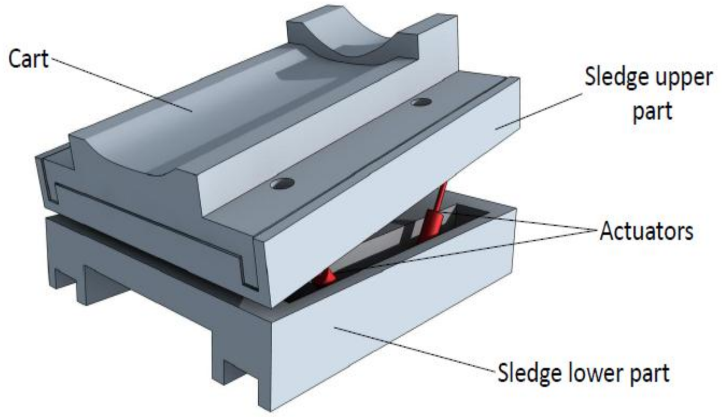

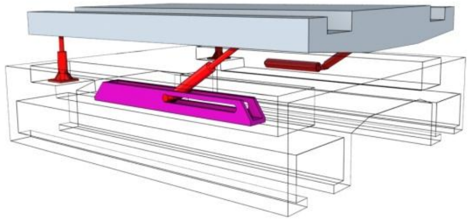

5. Solution – operational concept
5.3. Design – cont'd.

- cart is moving
- fixation elements, vacuum pads or air ballons
- Rendez-vous system sensor nets, side wind control, aircraft side motion control, rotating sledge, …
- skids or parachutes for emergency landing

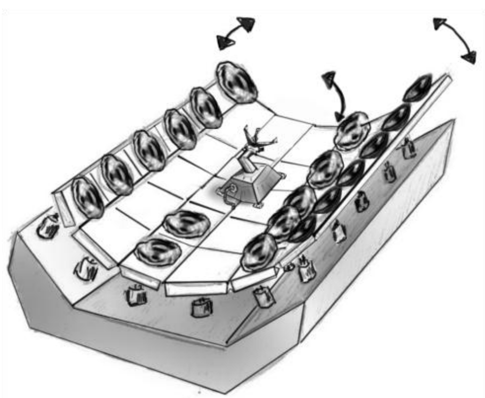

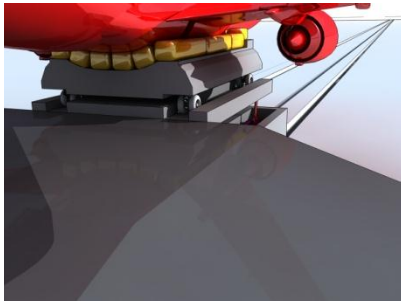

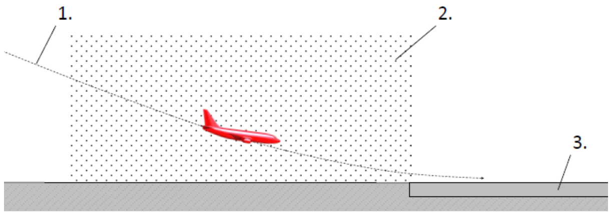

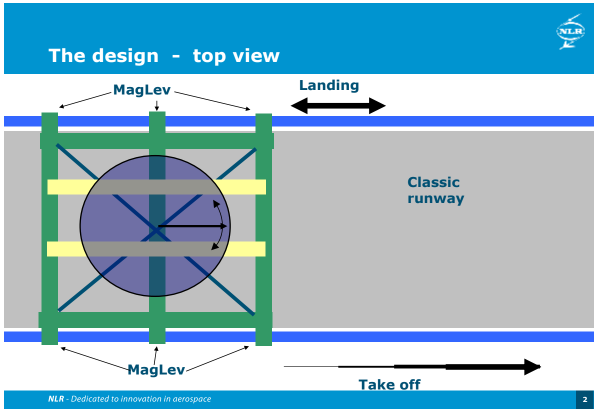

Impacts on all the elements of the air transport system

Airport site.

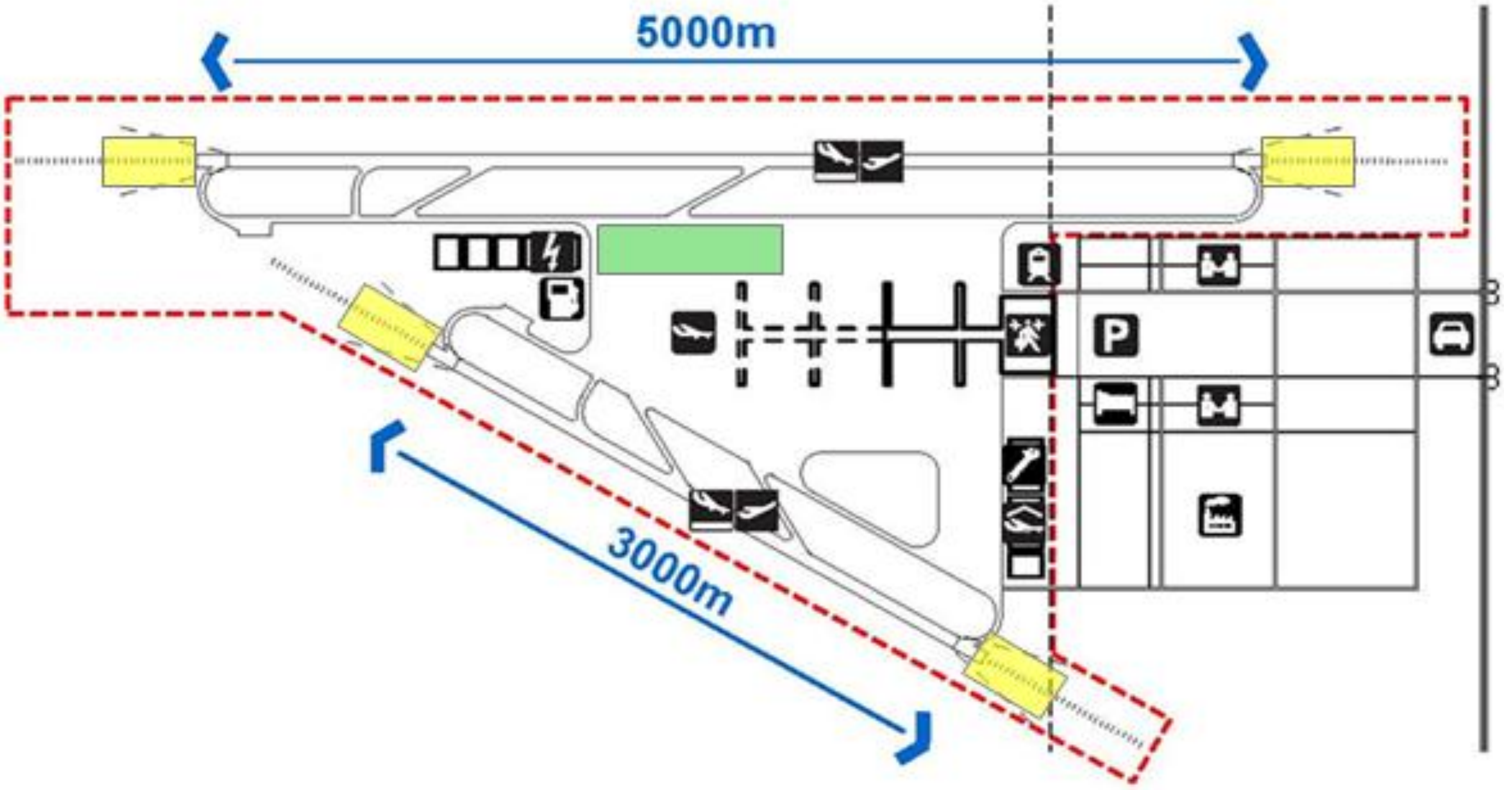

Summary

- **Gabriel** – L1 pioneering project in which
  - 12 partners from 7 countries
  - works on utilization of the magnetic levitation as
  - ground based system assisting the aircraft take-off and landing.
- Gabriel will investigate if such a system is feasible and cost effective.
- The project deals with
  - concept exploration and analysis;
  - concept development;
  - concept validation;
  - impact assessment.
- The first results show that, the maglev technology may use for assisting the aircraft takeoff and landing

Establishing a Comprehensive Transport Research Information Management and Exchange System
"HERMES"

2nd EASN Workshop on Flight Physics &Propulsion
Prague
31st October – 1st November, 2012

Contents

- Background
- Project Overview
- Results to date
- Concluding remarks

Background

- HERMES is a EU FP7 CSA project, commenced 1st November 2011 – ends 1st February 2014.

- It was created in response to the European Commission's call for
  - "*providing the means of enacting productive international transport research cooperation in the future*",
  - "*encouraging participation and dissemination of research results*."
- Transportation research is a priority area because an efficient and effective transport system is a fundamental prerequisite for economic growth.

- International collaboration in transport research is the best means of creating fertile conditions for research innovations, understanding and common solutions to common problems.

HERMES

OVERVIEW

Aims

- To fulfil its aims, the HERMES project has been divided into a number of work packages addressing various aspects of the work. The core of the project involves three main activities:
  - Creation of a “transport research database access portal” to facilitate access to information on transportation research carried out internationally,
  - Engage researchers in discussions to address the issues that inhibit a closer international collaboration in transportation research,
  - Perform comparative studies of transportation research topics from round the world to assess the potential for future research collaboration.

HERMES Portal

- This forms the major part of the HERMES project and undertakes all necessary activities for the creation of a common portal that will allow access to all identified transport research databases within the EU, US, Australia, Japan and other countries of interest.
  - Identify transportation research databases worldwide
  - Establish a dialogue between database managers
  - Investigate database accessibility, architecture and compatibility
  - Identify the major players and centres of excellence in transport research (Universities, Research Institutions, Government Agencies, NPOs and private industry)

Engagement of researchers

- HERMES aims to facilitate the creation of an environment for long term international collaboration in transport research.
- Organisation of a conference(to take place April or May 2013) to bring together researchers from around the world, with similar research interests to:
  - identify obstacles to closer long term collaboration and
  - express their opinions on the policies/measures that need to be taken to eliminate those obstacles.
- The output from this dialogue will be used to draw up a list of enabling policies that need to be in place for the establishment of long term collaboration.

Comparative studies

- The aim of the comparative studies is to investigate whether there are synergies in transportation research carried out worldwide by identifying similar projects conducted in the EU, US, Australia and Japan and compare and assess them in terms of their impact.
- Four case studies from each of the four transport modes will be selected. Assessment will include:
  - market uptake,
  - new product, process, policy, etc.
  - economic benefit,
  - new industry standards, etc
- provide recommendations/topics for future international collaborative research projects.

HERMES Consortium

Newcastle University	*UK*
Foundation WEGEMT	*Netherlands*
European Aeronautics Science Network	*Belgium*
International Union of Railways	*France*
Euromobilita s.r.o.	*Czech Republic*

Non EU collaborating organisations

Transportation Research Board	*USA*
ARRB Group Ltd	*Australia*
Institute of Transport Economics Japan	*Japan*

Advisory committee

B. Sandstedt	*VTI*
M. Violand	*OECD*
G. Woodroffe	*RSSB (SPARK)*

HERMES

RESULTS TO DATE

Identification of databases

- A list of worldwide databases of transportation research by transport mode has been compiled (work ongoing)
  - Aeronautics 62 databases
  - Marine 31 databases
  - Rail 41 databases
  - Road 34 databases
- 70% of identified databases are European.
- Databases have been ranked in three categories
  - Simple databases
  - Searchable databases
  - Full databases

Categories of databases

- **Simple database:** Lists of projects with very basic information (title, description of the main topic of the project, project manager) most of them are under html format and without any search engine.
- **Searchable database:** Detailed description of work (pdf often attached) with precise information about the consortium, contact persons, etc. Most of them accessible through a simple searching engine (neither keywords nor thesaurus) and no translation of the information in English.
- **Full database:** Database organised through a precise search engine with keywords and thesaurus, and with detailed information about the projects.

Differences in search filters

Australian Road Research Register	TRID (US)	TRIP (EU)
Assets Bridge design and management Environment Freight transport and logistics Heavy Vehicles Intelligent Transport System ITS Materials Pavement structures Public transport Registration and Licensing Road design Road Safety (Engineering) Road Safety (Human factors) Road Safety (Vehicles) Skills and Education Technology Traffic management and planning Transport economics Travel behaviour	Administration and Management Aviation Bridges and other structures Construction Data and Information Technology Design Economics Education and Training Energy Environment Finance Freight Transportation Geotechnology Highways History Hydraulics and Hydrology Law Maintenance and Preservation Marine Transportation Materials Motor Carriers Operations and Traffic Management Passenger Transportation Policy Public Transportation Railroads Research Safety and Human Factors Security and Emergencies Society Terminals and Facilities	**Modes** Air transport Rail transport Road transport Urban transport Water transport Multimodal transport **Sectors** Passenger transport Freight transport **Technology** Intelligent transport systems Innovative technologies Transport management **Policies** Financing, pricing and taxation Regulation, competition and public services Infrastructure and TEN-T Land-use and transport planning Climate policy and energy efficiency Security and Safety Assessment and decision support Environmental impacts Economic and regional impacts Accessibility, social and equity impacts

There is not a universally agreed system for categorising transportation research

Differences in search filters

- Filter by transport mode
- Filter by publication or project
- Filter by region
- Use of wildcards to catch additional characters without duplication of search results, e.g. use of [“ ”] and or [*], (Bridge* returns results for both Bridge and Bridges)

Language

- An important issue is **language**
- Not all databases available in English language.
- In TRID, a search using the keywords
  - “Heavy vehicle*” in all fields, brings up only 8 results.
  - “Truck” returns 85 results**.**
- In the Australian Road Register, the keyword
  - ‘Truck” returns 50 results and
  - “Heavy vehicle*” returns144 results
- Restricted access databases (Commercial organisations)

Engagement of researchers

Existing collaboration initiatives

- EU-US “Agreement for Scientific and Technological Cooperation” 2004 & 2009
- A Memorandum of Understanding (MoU) that was signed on January 2006 between the *European Conference of Transport Research Institutes (ECTRI)* and the *Transportation Research Board* of the United States Academy of Sciences (US/TRB).
- The MoU was translated into practice through a 10 point 2-year Action Plan. As part of this Action Plan, a joint working group on EU/US collaboration was established, known informally as Working Group 10 (WG 10)
- The output from this is a report, entitled **“*EU/US Transport Research Collaboration: Challenges and Opportunities*”** and is an important first step in establishing a structure for pooling finite resources to discover new solutions.
- This is an example of collaboration specific to transportation research
- Further talks are currently taking place between TRB/DG MOVE/DG Research. Initiatives mainly in the aeronautics sector.

Engagement of researchers

Existing collaboration initiatives

- Research collaboration between the European Union and Australia was formalised in 1994 with the *Science & Technology Agreement* – the first ever such agreement that the EU had concluded with a third country.
- The Agreement allows for European and Australian researchers to take part in each others programs primarily on a self funding basis.
- In 1997, the Agreement was further expanded to include all areas of research. BUT little to nothing has been done on transportation research

Engagement of researchers

Existing collaboration initiatives

- EU-Japan Cooperation Forum on ICT Research, 2008
- EU-Japan “J-BILAT” – 2010
- Japan has established centres for the promotion of Science around the world
  - Japan Science & Technology Agency (JST) Offices in Paris, Washington, Singapore, Beijing
  - Japan Society for the Promotion of Science (JSPS) – Offices in many EU and non EU countries

Comparative studies

- Case studies from all transport modes from EU, US, AUS and Japan have been selected for comparative studies.
- A search was made on ROAD related projects using the theme of “Aerodynamics” because it relates to safety, environmental impact , energy efficiency.
  - Considerable differences in the quantity of this research topic being carried out between the regions, according to the databases used.
  - The search term ‘Aerodynamic*’ in all fields brought up 0 results in Australia, 2 in the US and 45 in the EU.
  - However, it is known that there is research in Australia relating to this theme, and there is also research in Japan and more than two projects in the US.

HERMES

CONCLUDING REMARKS

Concluding remarks

- HERMES has identified a number of challenges facing the creation of the portal.
- Several issues resolved and work ongoing to develop suitable code. HERMES portal on target to go live - April 2013.
- Discussions with database managers worldwide making good progress.
- Preparations for the “International Conference on Transportation Research Collaboration” have commenced and Questionnaire for the scientific community to express their views on policies to facilitate international collaboration is prepared.
- The response for international collaboration in transportation research information sharing has been remarkably better than anticipated

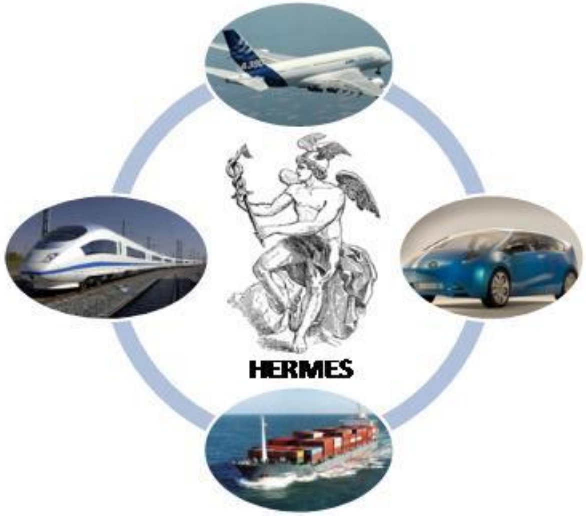

Thank you

Coordinator: **Dr George Kotsikos**
Tel: +44 (0)191 222 5889
Fax: +44 (0)191 222 8600
Email: george.kotsikos@ncl.ac.uk
Website: www.hermes-project.net

CORSAIR:
Cold Spray Radical Solutions for Aeronautic Improved Repairs

Funding scheme: CP-FP

Topic call: AREA 7.1.1.2 ECOLOGICAL PRODICTION AND MAINTENANCE

Work program topics addressed: ***AAT.2012.1.2-2. Maintenance and disposal***

Project Coordinator: **Simone Vezzù (Veneto Nanotech scpa, ITALY)**

Speaker: **Prof. Mario Guagliano (Politecnico di Milano, ITALY)**

The Cold Spray Technology

Cold Spray is a Solid State Deposition Process **and it is classified as a thermal spray processes.** It uses high-pressure (up to 5.0 MPa) and high-temperature (up to 1000°C) carrier gas in order to accelerate micrometric metallic particles at velocities higher than the speed of sound. The impact with a metallic substrate lead to plastic deformation of both particle and substrate responsible of coating adhesion.

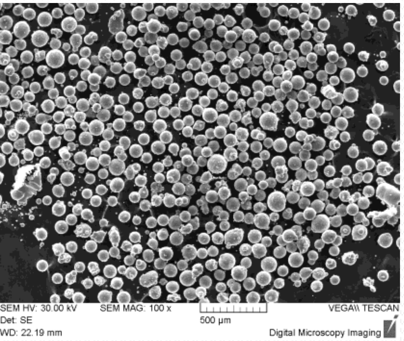

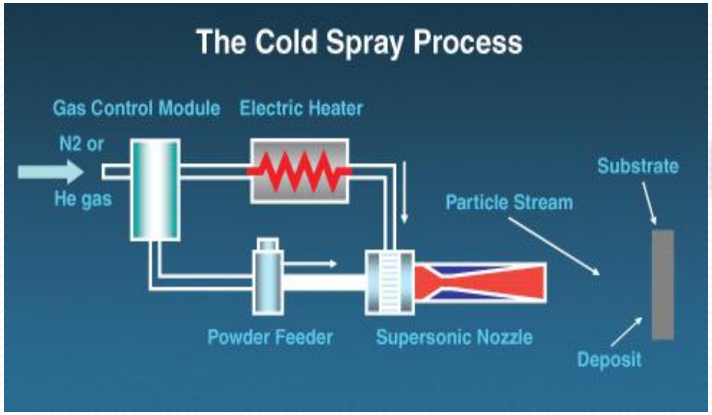

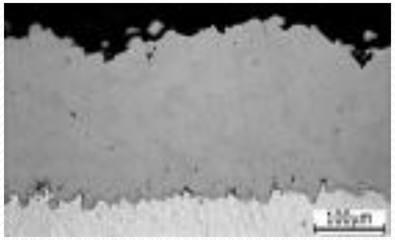

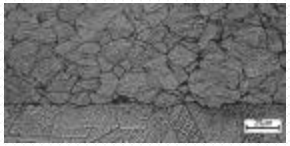

Feedstock materials:
Metal, Ceramic, Composite powders

Cold spray process

Coating:
Metal, Ceramic, Composite.
Thickness 0.01 – 50

Advantages of cold spray coating

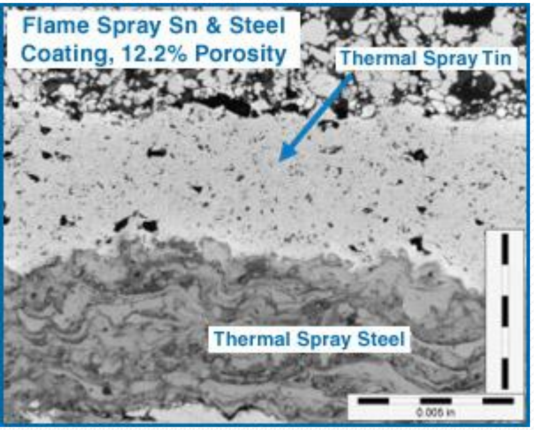

- Low temperature process
- Solid state bonding
- High density deposits

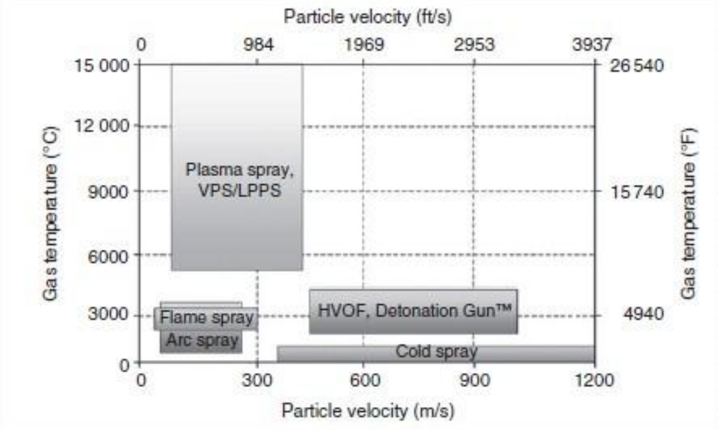

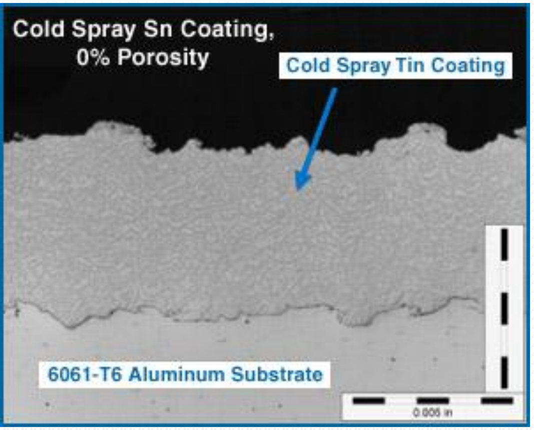

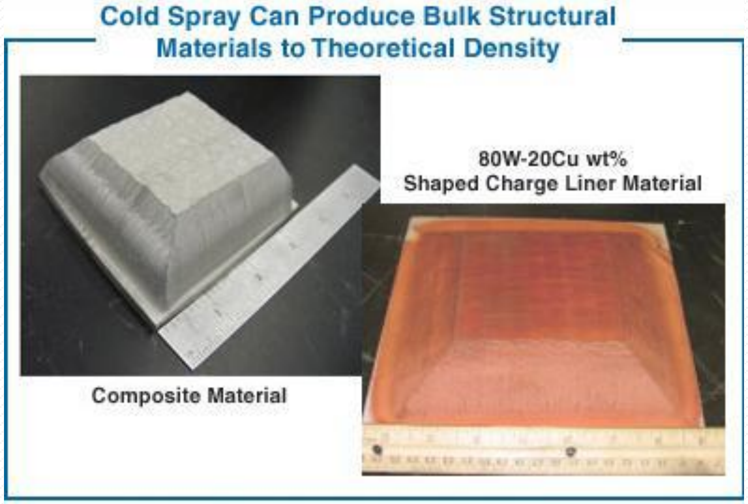

The Cold Spray opportunity for MRO of aeronautic components

The European aerospace sector seriously lags North America and Australia in terms of Cold Spray technology readiness, as evidenced, for example, by the fact that unlike the US, Europe has no relevant Cold Spray process, materials or manufacturing-related Cold Spray standard.

In the last 5 years, several organisations (e.g. the US Army Research Laboratory (US ARL) and the Australian Military) have funded major programmes to qualify the repair of helicopter engine gearboxes using Cold Spray deposition.

Currently, Cold Spray repairs are limited to a few non-structural parts in Al and Mg alloys, where the requirements for repair operations are relatively simple and the process validation easier.

The CORSAIR challange

To explore the real capabilities of Cold Spray in several practical examples of aeronautic application, thus extending its utilization to repair a wide range of defects (corrosion, fretting, scratch, wrong machining…) meeting the request of high performances processes for MRO of light alloy components (Al, Ti, Mg alloys), even for structural parts.

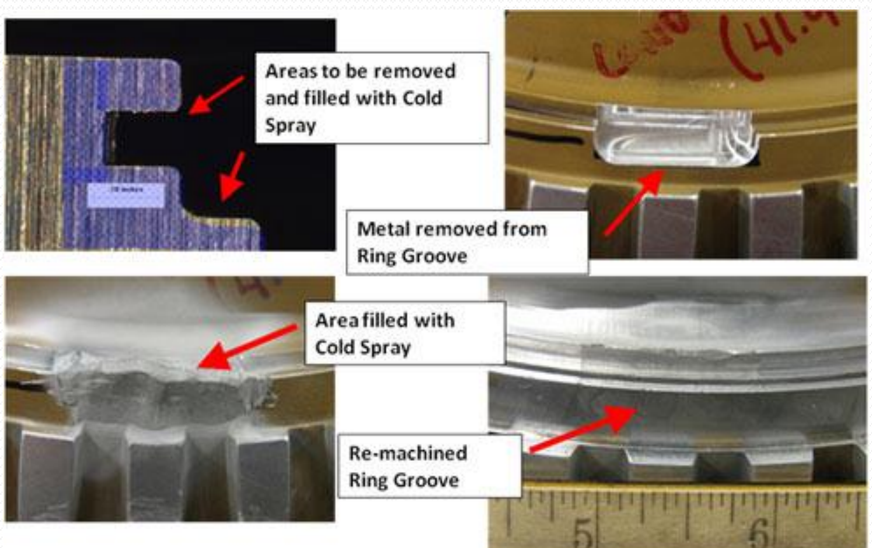

Ring Grove Repair at ARL. www.arl.army.mil

Worn Bearing Seats Repair at SST Windsor www.supersonicspray.com

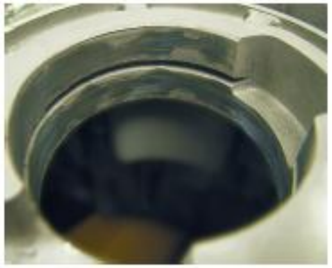

CORSAIR: concept and objectives

CORSAIR: S/T methodology and associated WorkPlan

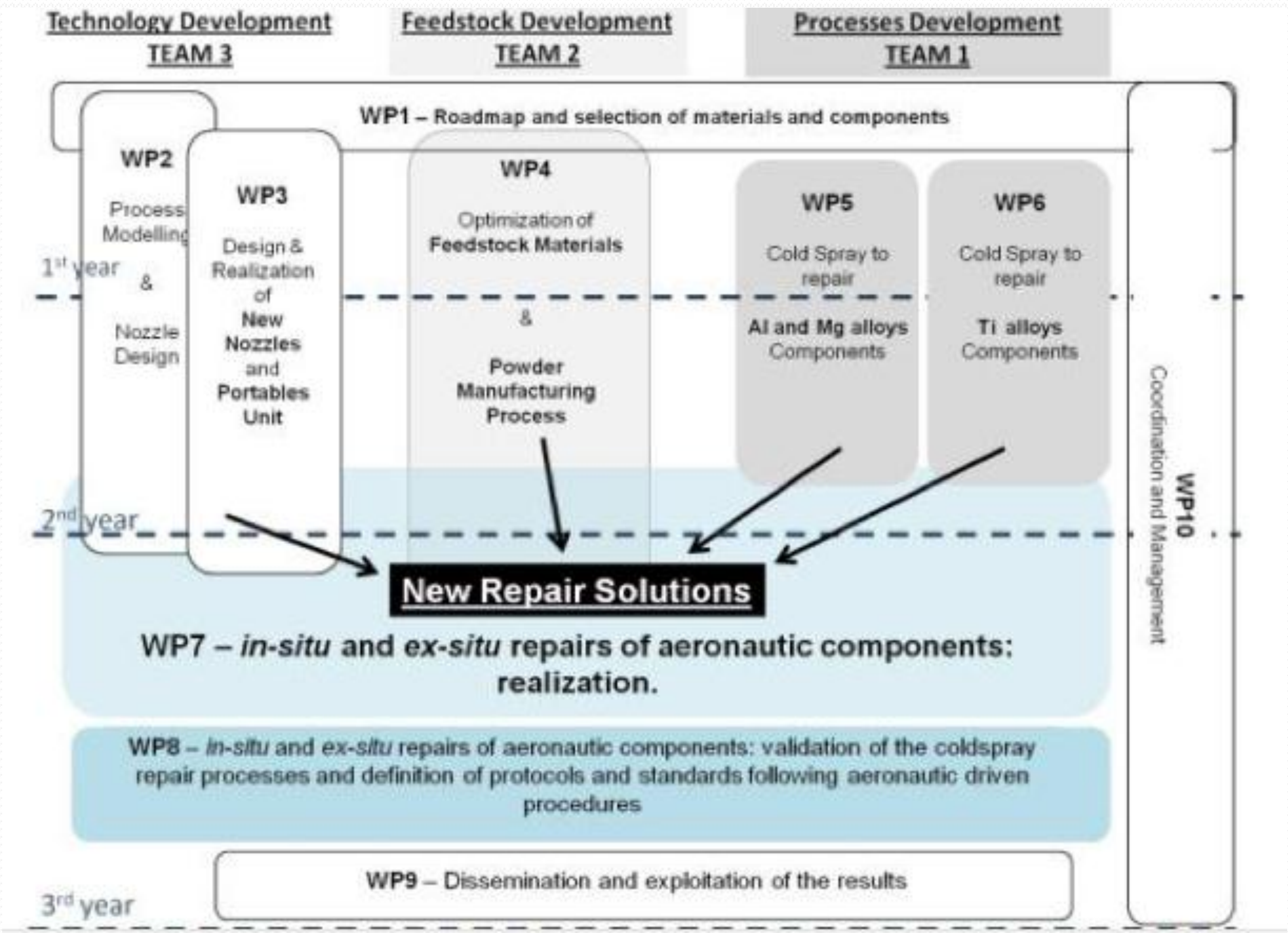

Main Expected impacts:

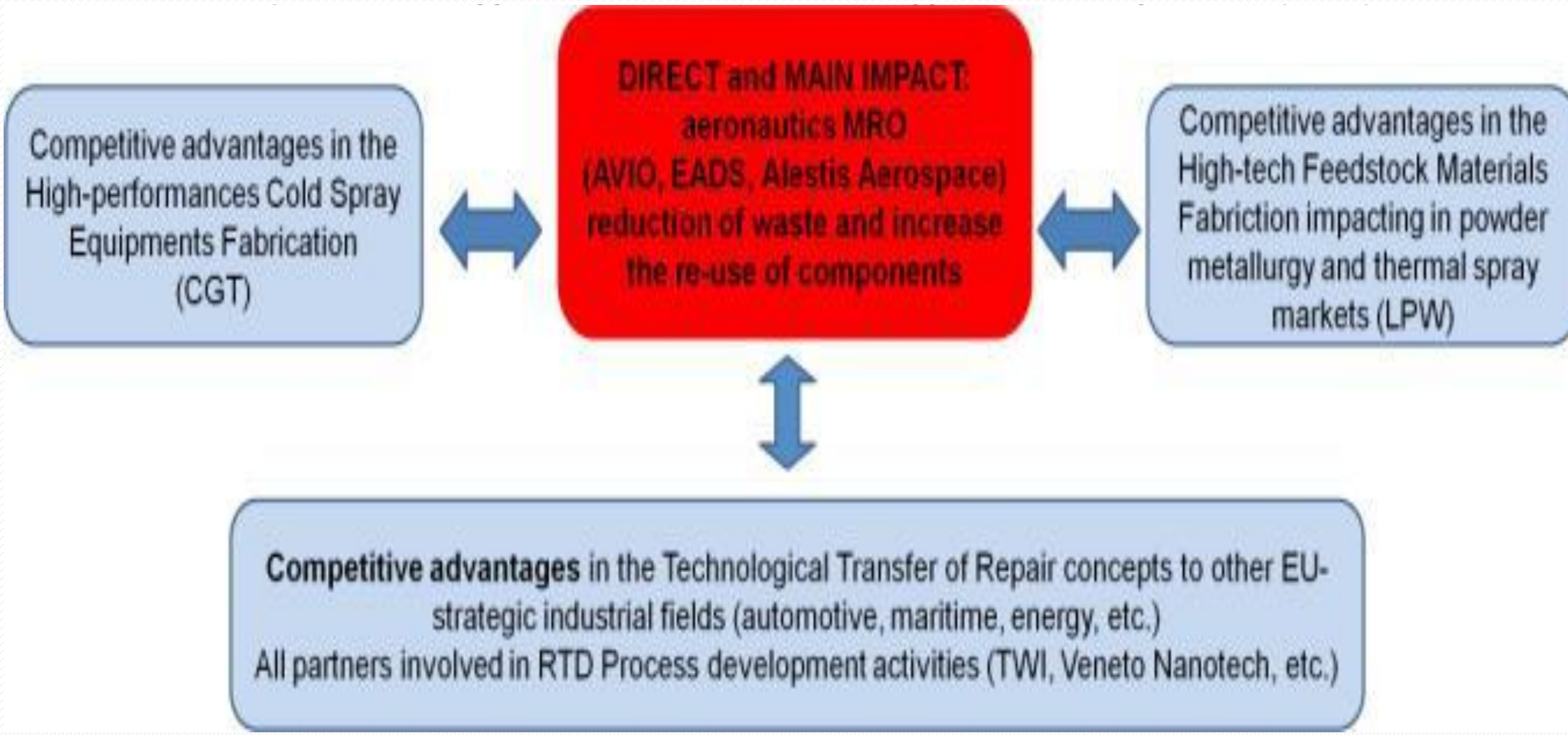

Main Expected impacts:

Improving the greening of air transport by increasing both the full recyclability and full lifetime of components and by substituting actually processes by using a eco-friendly repair technology (Cold Spray)

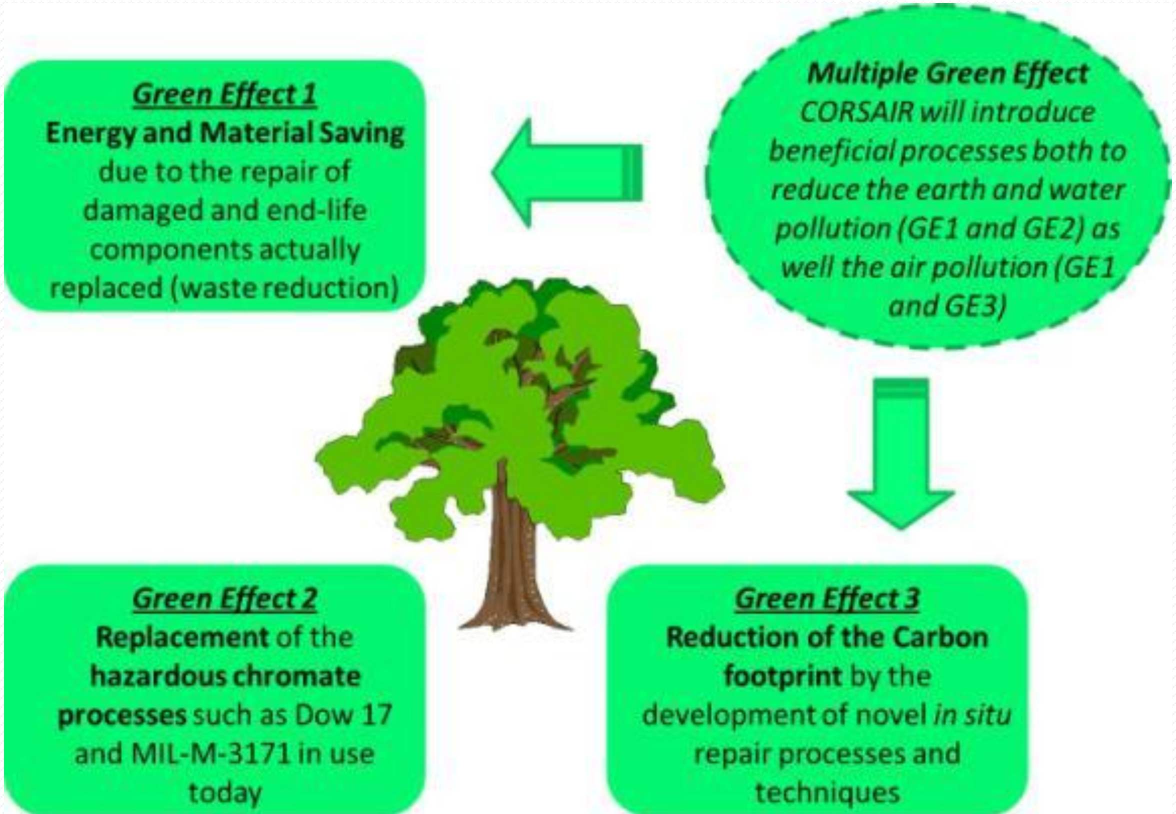

CORSAIR: the Consortium

Participant no./Type of participant	Participant organization name	Participant organization short name	Nation
1 / RTD (Coordinator)	VENETO NANOTECH	VN	I
2 / RTD	TWI	TWI	UK
3 / RTD	National Aerospace University “KHAI”	KHAI	UA
4 / RTD	POLITECNICO DI MILANO	POLIMI	I
5 / RTD	UNIVERSIDAD REY JUAN CARLOS	URJC	ES
6 / SME	METALOGIC	MLOG	BE
7 / IND	AVIO SpA	AVIO	I
8 / IND	EADS DEUTSCHLAND GMBH	EADS	D
9 / IND	ALESTIS AEROSPACE Engineering	AAE	ES
10 / SME	LPW Technology	LPW	UK
11 / SME	IMPACT-Innovations-GmbH	IMP	D
12 / SME	EASN-Technology Innovation Service	EASN	BE
13 / IND	IBERIA	IBERIA	ES

Thank you for your kind attention!

Proposed M^2 Vision

Meeting Date: ***27-September-2012***

MOVER2 TEAM

M^2 is

Multi level and Multi disciplinary optimization for design of aeronautical structures

Part. no.	Participant organisation name	Country	Participant org. short name
1	Alenia Aeronautica S.p.A.	Italy	ALA
2	Imperial College London	UK	IC
3	University of A Coruña	Spain	UDC
4	Modelling&Simulation s.r.l.	Italy	M&S
5	European Aeronautic Science Network	Belgium	EASN
6	Delft University of Technology	Netherlands	TU DELFT
7	German Aerospace Centre	Germany	DLR
8	University of Patras	Greece	UPAT
9	Swedish Defence Research Agency	Sweden	FOI
10	Politecnico di Milano	Italy	POLIMI

MOVER2 Goals

Development and Verification **by**
analytical, numerical means of
innovative design methodology and design approach
for composite structures**:**
Fully automated methodology for component sizing

in such a way *aiming to*
Reduce 30% the design lead time

MOVER2 30% lead time reduction

WHY? HOW?

1. Extensive utilization of HPC FERMI about 120.000 nodes 16 GB per node per Verification

2. Multilevel optimization using closed form integrated methodology for minimum weight (platform II) and minimum cost (platform I) mathematical link between the platform

3. After verification platform (platform3) eventually architecture modification will be reanalyzed using the linked platforms

   Having fast Multidisciplinary /Multilevel optimization

MOVER2 Application subject

The target substructure will be an outer wing of a 130 seats regional aircraft (see JTI)

The sizing procedure has the objective to define the sub-structure design that fulfills all the performance requirements / design rules with the minimum weight and cost.

The innovative design methodology and design approach proposed in MOVER2 will unify into an unique platform all the design phases, minimizing the design lead time

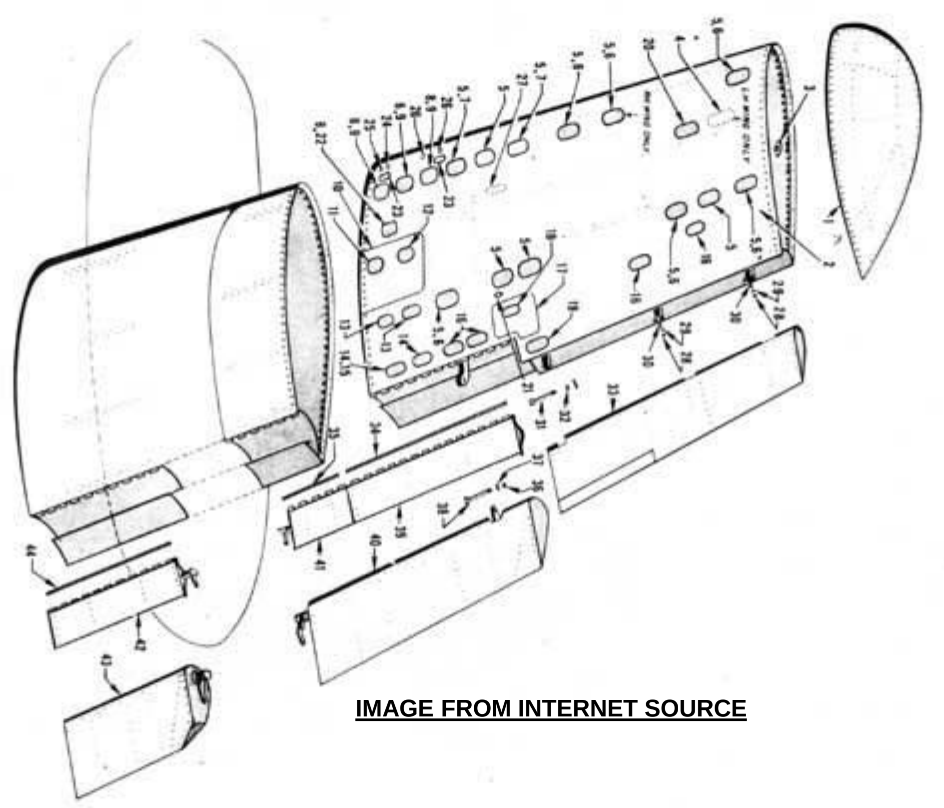

IMAGE FROM INTERNET SOURCE

The application will involve the minimum number of disciplines to demonstrate the validity of the M^2 concept/methodology

Current design Philosophy

STARTING POINT:

Certification Requirements

- *non detectable flaws are not critical to the structural integrity and do not grow to a critical size before the next inspection.*
- *the ultimate residual strength of the structure must be maintained for damage which may grow from an* undetectable (via NDI) size over a defined inspection interval.

Application of High deterministic KnockDown factors to the nominal material mechanical properties

- *environmental effects (moisture and temperature),*
- *low energy impacts (BVID)*
- *defects induced by the manufacturing process,*

Conservative design approach

- *First Ply Failure criteria*
- *No buckling up to Ultimate Loads*
- *Knockdown factors applied homogeneously on the whole component*
- *mechanical joints and mechanical repairs*
- *No-growth approach for BVID (the structures with this type of damage will carry design Ultimate Loads for the operational life of the aircraft)*
- *VID will not reach a critical size under Limit Load conditions over inspection intervals based on previous experiences and/or common considerations developed during the years, to take into account the effects of the degradation of the composite material performances.*

MOVER2 Design Strategy

The structure will be sized by evaluating the
real Barely Visible Impact Damage (BVID), VID and Crack Growth
of the part considering the structure in a “real” damaged condition
distributed over three analysis level

Example:

Fatigue problems could be highlighted using full scale progressive failure analysis and this would lead to a full damage tolerance design approach.

MOVER2 Design Strategy

Innovative Design methodology by Multilevel approach for Damage Tolerance

The application of damage tolerance through levels allows realization of *minimum weight and manufactoring cost CFRP structures* by establishing structural behaviour at full scale level in an unique platform.

Fuselage stiffened panel example: Large Damage Capability Design Criteria

Traditional design philosophy required by authorities CS 25 → The structure has to withstand a crack in the fuselage skin over two stringer bays up to assuming broken stringer

Level two linear / non linear analysis using shell elements
Level three progressive failure analysis shell elements (ply by ply)

Prevalently bonded joints and riveted joints will be considered for the composite structures

MOVER2 Design Strategy

Extensive use of bonded joints and bonding

AC 20-107 B (USA) / AMC 20-29 (EU)

(a) For bonded joints, CS 23.573(a)(5) states:

"For any bonded joint, the failure of which would result in catastrophic loss of the aeroplane, the limit load capacity must be substantiated by one of the following methods:

(i) The maximum disbonds of each bonded joint consistent with the capability to withstand the loads in paragraph (a)(3) of this section must be determined by analysis, tests, or both. Disbonds of each bonded joint greater than this must be prevented by design features; or

(ii) Proof testing must be conducted on each production article that will apply the critical limit design load to each critical bonded joint; or

(iii) Repeatable and reliable non-destructive inspection techniques must be established that ensure the strength of each joint."

MOVER2 Design Strategy (Damage classification)

Damage Category

Category	Examples (not inclusive of all damage types)
Category 1: Allowable damage that may go undetected by scheduled or directed field inspection (or allowable manufacturing defects)	BVID, minor environmental degradation, scratches, gouges and allowable mfg. defects that must retain ultimate load for the specified life
Category 2: Damage detected by scheduled or directed field inspection @ specified intervals (repair scenario)	VID (ranging small to large), deep gouges, mfg. defects/mistakes, major *local* heat or environmental degradation that must retain limit load until found
Category 3: Obvious damage detected within a few flights by operations focal (repair scenario)	Damage obvious to operations in a "walk-around" inspection or due to loss of form/fit/function that must retain limit load until found by operations
Category 4: Discrete source damage known by pilot to limit flight maneuvers (repair scenario)	Damage in flight from events that are obvious to pilot (rotor burst, bird-strike, lightning, exploding gear tires, severe in-flight hail)
Category 5: Severe damage created by anomalous ground or flight events (repair scenario)	Damage occurring due to rare service events or to an extent beyond that considered in design, which must be reported by operations for immediate action

AC 20-107 B (USA) / AMC 20-29 (EU)

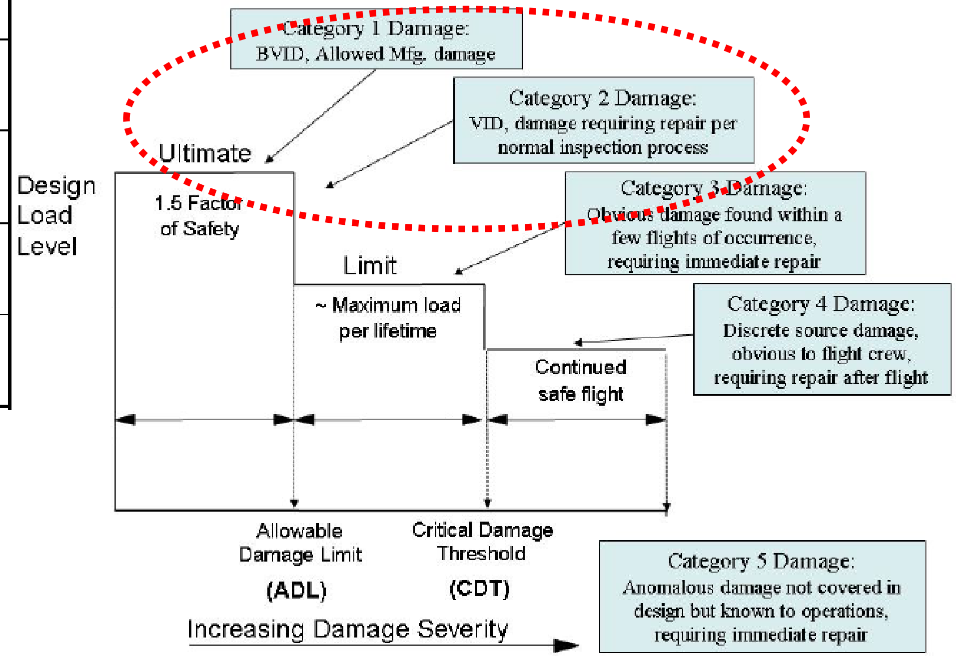

Schematic diagram showing design load levels versus categories of damage severity.

Category 1: *Allowable damage that may go undetected by scheduled or directed field inspection* (or allowable manufacturing defects)

Category 2: *Damage detected by scheduled or directed field inspection at specified intervals* (repair scenario)

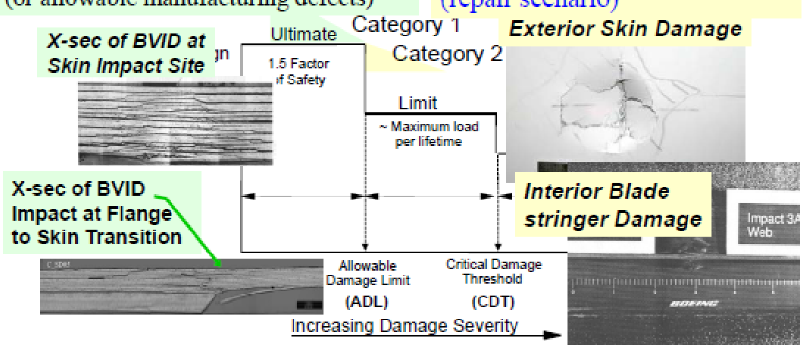

DECOHEMO will be focused only on

- **Category 1** ***(BVID, Allowed Mfg damage – NO repair scenario)***
- **Category 2** ***(VID, damage repair scenario/inspetion process VID***
  Example Disbonding ....)

MOVER 2 GLOBAL OVERVIEW

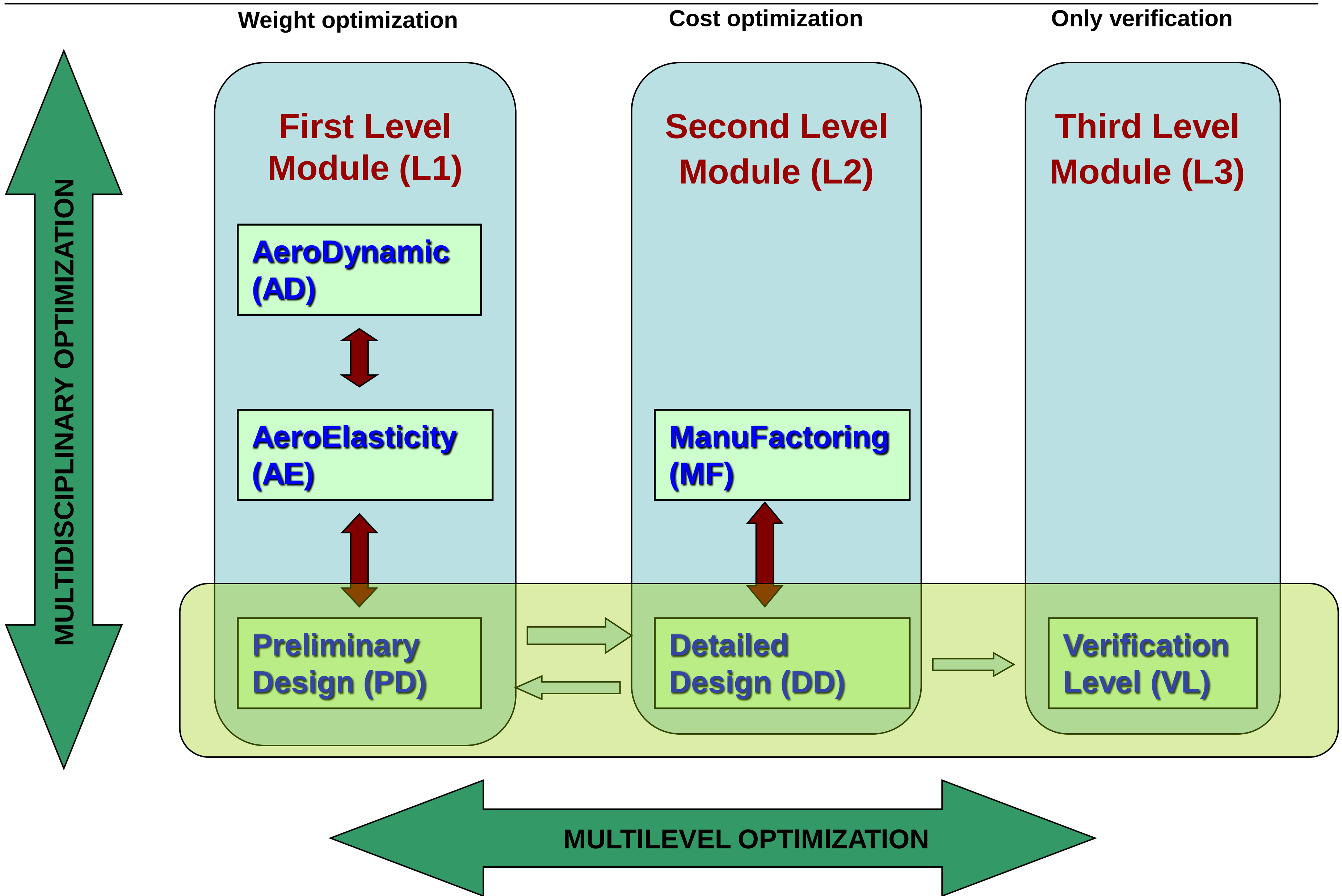

MOVER2 Requirements Summary

First Level Optimization Module (L1)

Objective(s)
Minimize weight

Design variables
Stringers / ribs number, position, section area

Constraints
Structural strength (stress and strain level)
Linear buckling
Maximize aerodynamic performance

Estimated degrees of freedom per run (shell/beams FE model): 10^5

Second Level Optimization Module (L2)

Objective(s)
Minimize manufactoring cost

Design variables
Stringers / ribs section area shape, layers lay-up joining technology (bonding, co-bonding, riveting…)

Constraints
Static failure
Buckling, Postbuckling, linear damage tolerance

Estimated degrees of freedom per run (shell FE model): 10^6

Third Level Module(L3)

Verification using progressive failure analysis on the damaged structure.

Detail of simulation:
3D material representation along thickness

Estimated degrees of freedom per run (solid elements FE model): 10^8

MOVER2 WPs list

WP1 Building **Multidisciplinary First level (Preliminary Design)** platform for structural sizing

WP2 Building **Multidisciplinary Second level (Detailed Design)** platform for structural sizing

WP3 Building **Verification level** platform for structural sizing

WP4 Building the **Integrated Multidisciplinary/Multilevel** platform for structural sizing

WP5 Coordination / Management

WP6 Exploitation /dissemination

MOVER2 WPs essential information flow

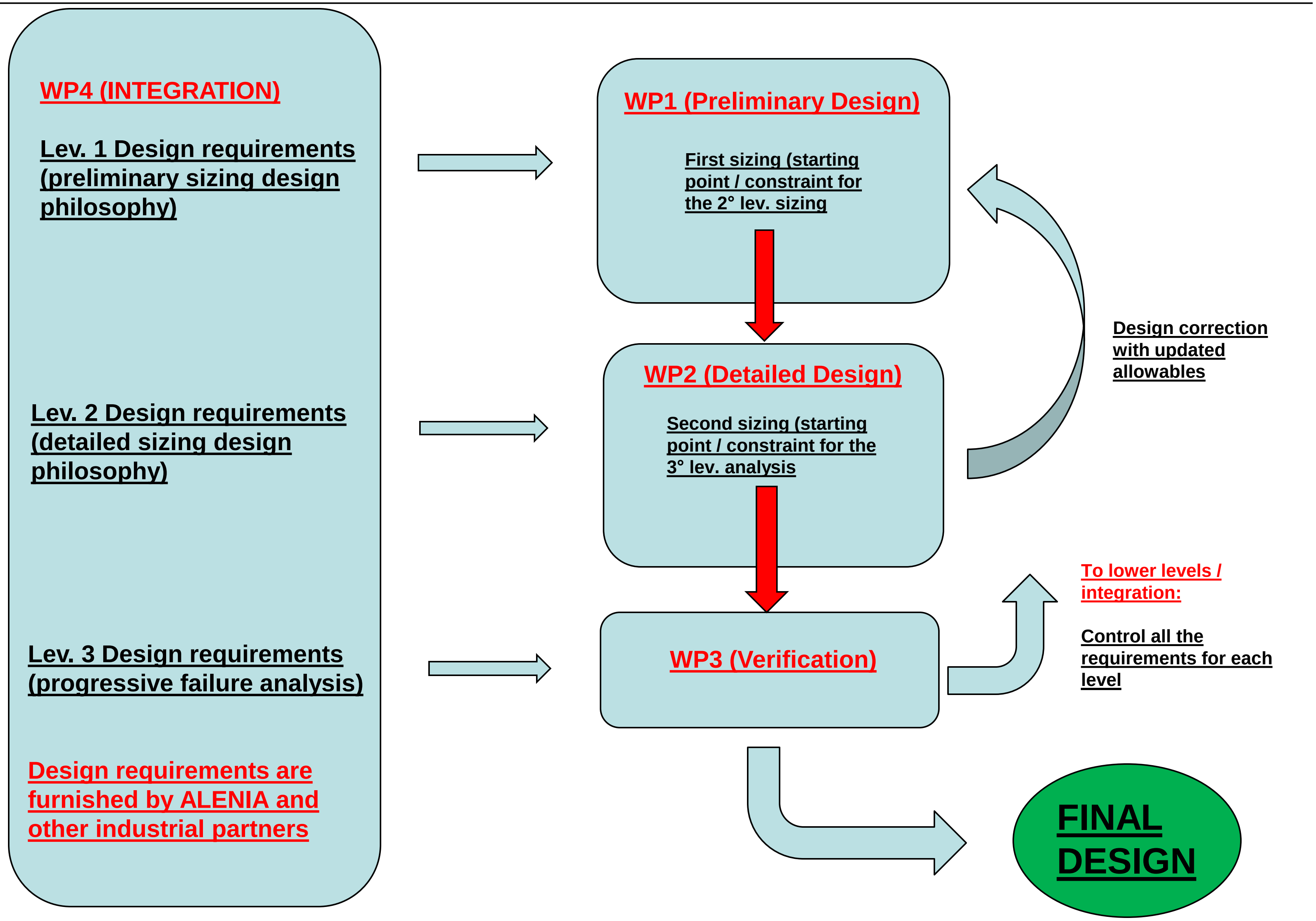

european aeronautics science network

European Aeronautics Science Network

VIVID: virtual assessment of low-velocity impact damage in composite airframes

Coordinated by: University of Parma (IT), Prof. Alessandro Pirondi

Partnership: Politecnico di Milano (IT), Prof. Alberto Corigliano
LMT Cachan (FR), Prof. Olivier Allix
Lublin University of Technology (PL), Prof. Tomasz Sadowski
University of Patras (EL), Prof. George Labeas
Bercella srl (IT), Mr. Massimo Bercella (SME)
EASN-TIS (BE), Prof. Spiros Pantelakis
SAMTECH (BE), Dr. Michael Bruyneel
ALENIA (IT), Dr. Alfonso Apicella

- **Challenge:** 1. ECO-INNOVATION; 3. COMPETITIVENESS THROUGH INNOVATION
- **Activity in Work Programme:** 7.1.1 THE GREENING OF AIR TRANSPORT; 7.1.4 IMPROVING COST EFFICIENCY
- **Topic in Work Programme:** *AAT.2013.1-2. Aerostructures; AAT.2013.4.-2. Design systems and tools*

European Aeronautics Science Network

- **Project content and goals:** the project is aimed at developing and validating experimentally advanced modeling tools for the **virtual assessment** of the airframe with respect to **low-velocity impact (LVI) damage tolerance.** Typical example: impact from tools falling during maintenance.

1. In order to provide a good usage of these advanced capabilities, correct values for model parameters should be used. This can be done thanks to a large numerical tests campaign, to be compared to a corresponding experimental test campaign for validation.
2. A distinctive point of VIVID is to implement new models into SAMCEF, an existent commercial finite element software developed by SAMTECH. This allows to make the developments durable in a European software and to solve problems with a complexity level that cannot be reached with the academic in-house finite element codes.
3. Fatigue delamination and damage growth capabilities will also be developed. Fatigue prediction in composites is clearly becoming a hot topic for the aerospace industry.
4. Efficient optimization methods will be incorporated to optimize composite structures with respect to LVI from the experimental data base of damage scenarios developed in VIVID.
5. A demonstrator of the model capabilities in predicting LVI will be developed by ALENIA

Outline of impact-related issues considered in VIVID

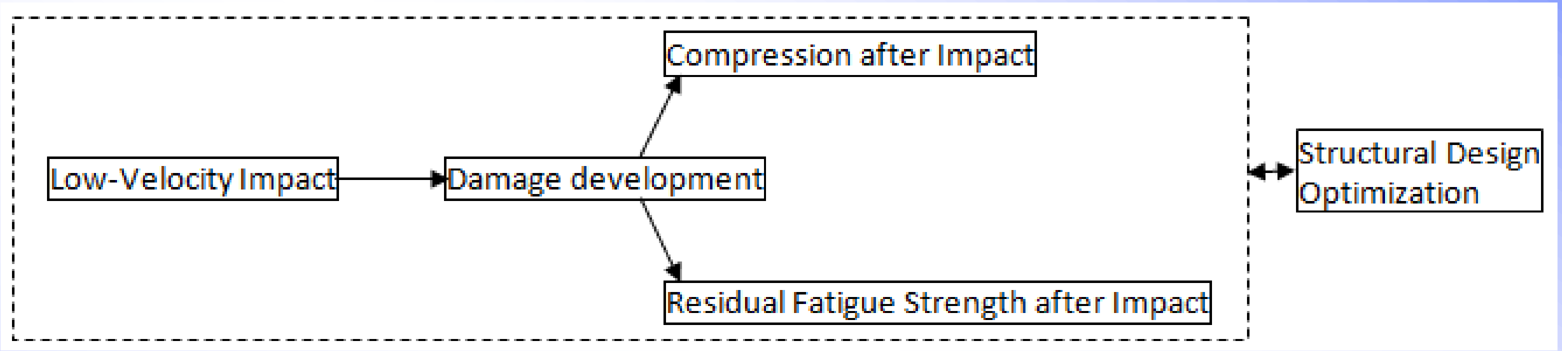

Model development assignments

Module	Specific task	Partner
LVI	Abrupt and progressive ply degradation	PoliMI
	Progressive ply degradation (PDM)	LTSM-UP
CaI	With each LVI-generated transverse crack and coupling with geometrical non-linearities in a parallel framework	ENS
RFSI	With single or multiple delamination cracks	UniPR
SDO	-	SMT

European Aeronautics Science Network

Expected impact:

Aircraft Safety, Development and Operation Cost, Environment

- to reduce uncertainties regarding the safety-critical decision of inspecting the airframe;
- to be able to precisely predict the scenario of damage tolerance of the design adopted and improve it exploring virtually several different materials and design solutions reducing the need of demanding experimental campaigns.
- to define more precisely inspection intervals, maintenance procedure, life extension or disposal at the design stage and during service improving both scheduled and unscheduled maintenance, avoiding unnecessary inspections and extending allowable damage limits, which means in turn a less grounded aircraft.
- to reduce direct operation costs (reduction of fuel consumption due to lower weight, which impacts the Greening of Air Transport).
- to reduce purchase costs due to **lower development cost** because of the physically-based nature of damage models that allows a less demanding experimental plan to transfer damage tolerance information from coupon to structure.

Cross-fertilization in other industrial sectors

- aircraft engines, automotive, train, shipbuilding, mechatronics.

CAPPADOCIA
Coordination Action Pro « Production, Avionics, Design » On Cost-efficiency In Aeronautics.

Project proposal for CSA-CA - Call: FP7-AAT-2013-RTD-1

Coordinated by: Efficient Innovation
Coordinator contact: Fabien Marty

01/11/2012 EASN Workshop' presenter : Jean-Louis BONAFE Euromart IMG, SMEs representative

CAPPADOCIA detailed positioning on the AAT.2013.7-1 objective with "Winning themes"

- Relevance to the work programme 2013
  - ***AAT.2013.7-1.*** Coordinating research and innovation in the field of Aeronautics and Air Transport
  - ***Topic***: Cost Efficiency (Design Systems and Tools, Production, and Avionics)

- The deal offered in the call
  - 5 CSA-CA in the Call for 6 €M
    - Environmental related research and innovation etc
    - **Cost Efficiency (Design, Production, and Avionics)**
    - Time Efficiency (Airports, ATM, aircraft separation, etc.)
    - Safety research (Coordination of Safety research, support to Safety Management System for Europe, and ATM)
    - Alternative fuels for aviation (AAT.2013.7-2)
  - Only one proposal should be selected per topic

CAPPADOCIA detailed positioning on the AAT.2013.7-1 objective with "Winning Partnership"

- Project partnership:

Participant organisation name	Country	Membership
Efficient Innovation	France	Aerospace Valley
Eurocopter	Germany	Euromart IMG
Airbus	France	Euromart IMG
EASN	Belgium	
CIRA	Italy	EREA
AERNNOVA	Spain	Euromart IMG
Aerospace Valley	France	EACP
Tusas Turkish Aerospace Industries	Turkey	Euromart IMG
NLR	Netherlands	EREA
INCAS	Romania	EREA
Apulian Aerospace District	Italy	EACP

Project duration 4 years   Project budget 1,2 M€

CAPPADOCIA detailed positioning on the AAT.2013.7-1 Commission objectives

- **EUROPEAN COMMISSION EXPECTATIONS**

- The objectives of the Commission within AAT.2013.7-1.
  - Annual review "of the state" of the state of the art of research and innovation (capacity, main performers)
  - Identify of gaps…. formulate strategic recommendations
  - Based on on-going and completed projects, assess
    - the impact of the EU-funded projects (FP7, CleanSky, JU SESAR, Eureka-Eurostars)
    - the impact of national funded projects
    - contribution to progress towards ACARE or other goals
  - Centralise information via a website and harmonise the dissemination of past and ongoing FP7 project

CAPPADOCIA detailed positioning on the AAT.2013.7-1 objective with "Winning themes"

- **Project objectives:**
  - Issue a yearly strategic recommendation paper policy
  - Creation of aeronautics cost efficiency database from impact assessment of relevant ongoing and past funded projects (FP7, CleanSky, JU SESAR, Eureka-Eurostars and national funding)
  - Dissemination throughout European Aeronautical networks and beyond (other funded CSAs in same call and EC funded past projects)
- **Expected achievements of the project**
  - Gather the scientific and industrial community to designing an annual review of the state of the art and recommend for future “tactical” actions
  - Confirm the coherence of the « Aeronautical » work programme calls with the SRA from ACARE and other relevant goals
  - Improve the “Aeronautical” R&D impact through dissemination in the field of aeronautics cost efficiency research
  - Coordination with other CSA funded by the addressed call

CAPPADOCIA overall methodology

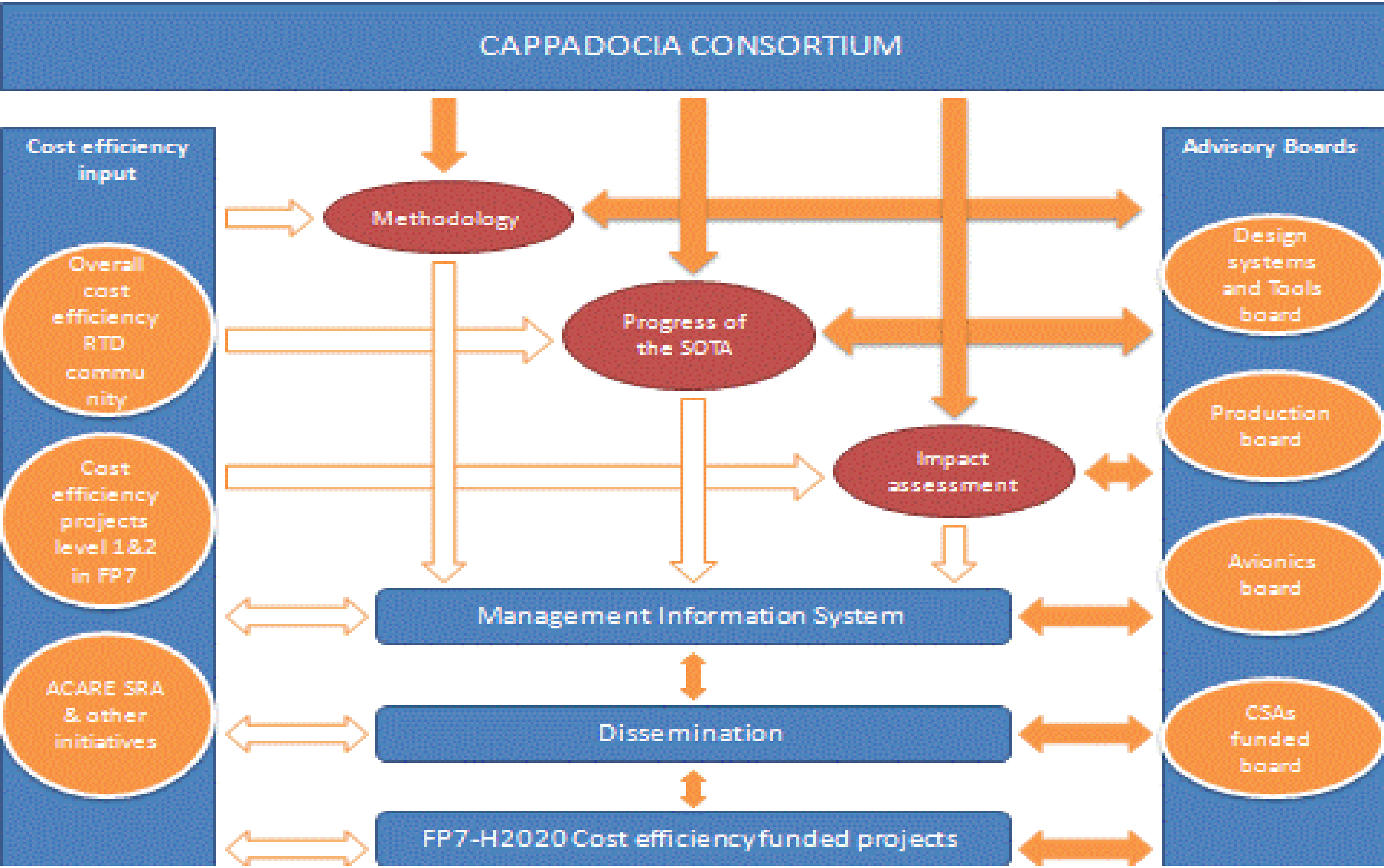

Work Packages' detailed content and organisation

Workplan

Title	Leader
CAPPADOCIA multidimensional methodological approach	Efficient Innovation
Analysis of the state of the art of research and innovation for the targeted CAPPADOCIA target research area (Production, Design system and tools, Avionics)	NLR
Impact assessment of relevant ongoing and past EU funded projects	Eurocopter
CAPPADOCIA Management Information System and Dissemination and Coordination of dissemination activities.	EASN
Management of the project	Efficient Innovation

WP1 – CAPPADOCIA multidimensional methodological approach (Efficient Innovation)

- **Objective: Define the operational character of the set up Advisory Boards as well as the proposed overall multidimensional methodological approach of the CAPPADOCIA project.**
- **T1.1: Identification, selection, integration and distribution of Advisory Board Members according to CAPPADOCIA cost-efficiency targeted research topics (Design Systems and Tools, Production, Avionics).**
- ***Start & end date: M01 – M02***
- **T1.2: Identification and mapping of EC FP7 funded projects and other relevant main projects (European and national funding programmes) according to CAPPADOCIA cost-efficiency targeted research topics (Production, Design system and tools, Avionics).**
- ***Start & end date: M01 – M03 / M28 / M39***
- **T1.3: Review and identification of ACARE & other relevant initiatives objectives and solutions taking into account external influencing factors (according to qualitative and quantitative metrics and indicators) towards progress in CAPPADOCIA cost-efficiency targeted research topics (Production, Design system and tools, Avionics).**
- ***Start & end date: M01 – M03 / M28 / M39***
- **T1.4: CAPPADOCIA overall multidimensional state-of-the-art and impact assessment methodology evaluation and grid definition per CAPPADOCIA targeted research topics (Production, Design system and tools, Avionics) and aircraft type.**
- ***Start & end date: M02 – M06 / M27 – M28 / M38 – M39***

Project Advisory Board committees

- **Three advisory board committees will be present all along the project corresponding to the 3 areas addressed by the call description:**

Design and tools committee	Production committee	Avionics committee

- **Selected accordingly to their expertise, the role of the Advisory Board Members will be mostly devoted to:**
  - **Assess the methodology set up during the first phase of the project**
  - **Control and check if the funded projects list is sufficiently broad and large to ensure a complete analysis of the SOTA and the progress of the SOTA**
  - **Dedicate time to be interviewed during the second phase of the project (analysis of the SOTA)**
  - **Contribution to recommendation and review white paper compilation in their respective research area**

- **The Advisory Board members will not be in charge of deliverables production but rather contribute as reviewer.**

Advisory Board Members
(confirmed and in discussion)

Legal entity	Country
EADS	France
EADS IW	France
ONERA	France
Rockwell Collins	France
Thales Avionics	France
Safran	France
AREA – Aragonian Aerospace Cluster	Spain
FADA-CATEC	Spain
Novabase	Portugal
Active Space Technologies	Portugal
Rolls Royce	United Kingdom
GE	United Kingdom
Liebherr	Germany
Alenia	Italy
SAAB	Sweden
DLR	Germany
Institute of Aerospace Engineering	Czech Republic

WP2: Analysis of the state of the art of research and innovation for the CAPPADOCIA targeted research area (Production, Design system and tools, Avionics) (Leader : NLR)

- **Objective: Review of the state of the art of research and innovation, identify gaps in the research landscape as well as bottlenecks to innovation in order to formulate strategic recommendations to improve and address gaps and bottlenecks to innovation related to Cost Efficiency.**

- **T2.1: EU-funded Cost Efficiency projects and relevant practices analysis**
- ***Start & end date: M06 – M10 / M17 – M20 / M28 – M31 / M39 – M42***

- **T2.2: Identification of gaps in the Cost Efficiency research landscape**
- ***Start & end date: M07 – M11 / M18 – M22 / M29 – M33 / M40 – M44***

- **T2.3: Identification of bottlenecks to innovation in the Cost Efficiency research landscape**
- ***Start & end date: M07 – M11 / M18 – M22 / M29 – M33 / M40 – M44***

- **T2.4: Formulation of strategic recommendations towards Cost Efficiency state of the art**
- ***Start & end date: M10 – M15 / M21 – M26 / M32 – M37 / M43 – M48***

WP3 – Impact assessment of relevant ongoing and past EU funded projects (Leader: Eurocopter)

- **Objective: Assess the impact of EC funded projects towards ACARE goals and solutions achievements by analyzing data collected from the impact assessment in order to formulate strategic recommendations to progress towards ACARE goals and solutions.**

- **T3.1: Impact assessment with respect to ACARE goals and solutions as well as other relevant initiatives**
- ***Start & end date: M04 – M12 / M16 / M18 / M20 / M22 / M27 / M29 / M31 / M33 / M37 / M39 / M41 / M43 / M 45***

- **T3.2: Formulation of recommendations to progress towards ACARE goals and solutions achievements**
- ***Start & end date: M11 – M17 / M24 – M28 / M34 – M38 / M45 – M48***

WP4 – CAPPADOCIA management information system and dissemination and coordination of dissemination activities (Leader: European Aeronautics Science Network)

- **Objective: Promote the broad dissemination of the CAPPADOCIA outcomes while at the same time developing a common coordination and dissemination policy with the other CSAs-funded dealing with the three other domains of the call topic.**

- **T4.1: CAPPADOCIA Management Information System and general communication pack**
- ***Start & end date: M01 – M48***

- **T4.2: Dissemination and Coordination with other CSAs-funded (from the same call)**
- ***Start & end date: M01 – M48***

- **T4.3: Dissemination coordination with FP7 and H2020 funded cost efficiency related projects**
- ***Start & end date: M01 – M48***

WP5 – Management of the CAPPADOCIA (leader Efficient Innovation)

- **Objective**: assure an effectiveness and quality management, ensuring that the project achieves successfully its objectives.

- T5.1: Administrative management
- *Start & end date: M01 – M48*

- T5.2: Financial management
- *Start & end date: M01 – M48*

Contact person

Coordinator contact: Fabien Marty
cappadocia@efficient-innovation.fr
0033 1 44 71 93 96 0033 6 85 21 12 14

–Coordination Actions Inter-coordination

- **Objectives**:
  - Benefit from synergy between CSA-CAs born from **AAT.2013.7-1**
  - Save funds and avoid duplication and burden.
- **Means**:
  - To exchange on best practices and align as deemed useful methodology for analysis.
  - To harmonise contact with stakeholder groups including ACARE, IMG4, ARG, EASN.
  - To harmonise R&D Projects approach in order to get sufficient and valuable input and avoid duplication of work.
  - To grant coherence by commonly establishing a list of projects that are of interest and pertinent to each CA' domain.
  - Joint and coordinated dissemination to allow for addressees to have easy access to outcomes and ensure a large visibility vis-à-vis the interested public/institutions.

MULMON

EASN Endorsed Project

Multilevel data integration for structural health monitoring

FP7-AAT-2013-RTD-1

Prague, November 1, 2012

outline

1. consortium
2. road map
3. workflow
4. impact in aeronautics
5. worksharing

1. consortium

no.	participant organisation name	status	country	short name
1	Università di Bologna - subcontractor CINECA (ITA)	Univ.	Italy	UNIBO
2	Alenia Aeronautica S.p.A.	Indus.	Italy	ALA
3	Silkan	SME	France	SILKAN
4	European Aeronautics Science Network	SME	Belgium	EASN
5	Imperial College London	Univ.	Great Britain	ICL
6	Modeling & Simulations	SME	Italy	M&S
7	University of Patras	Univ.	Greece	UPAT

1. consortium

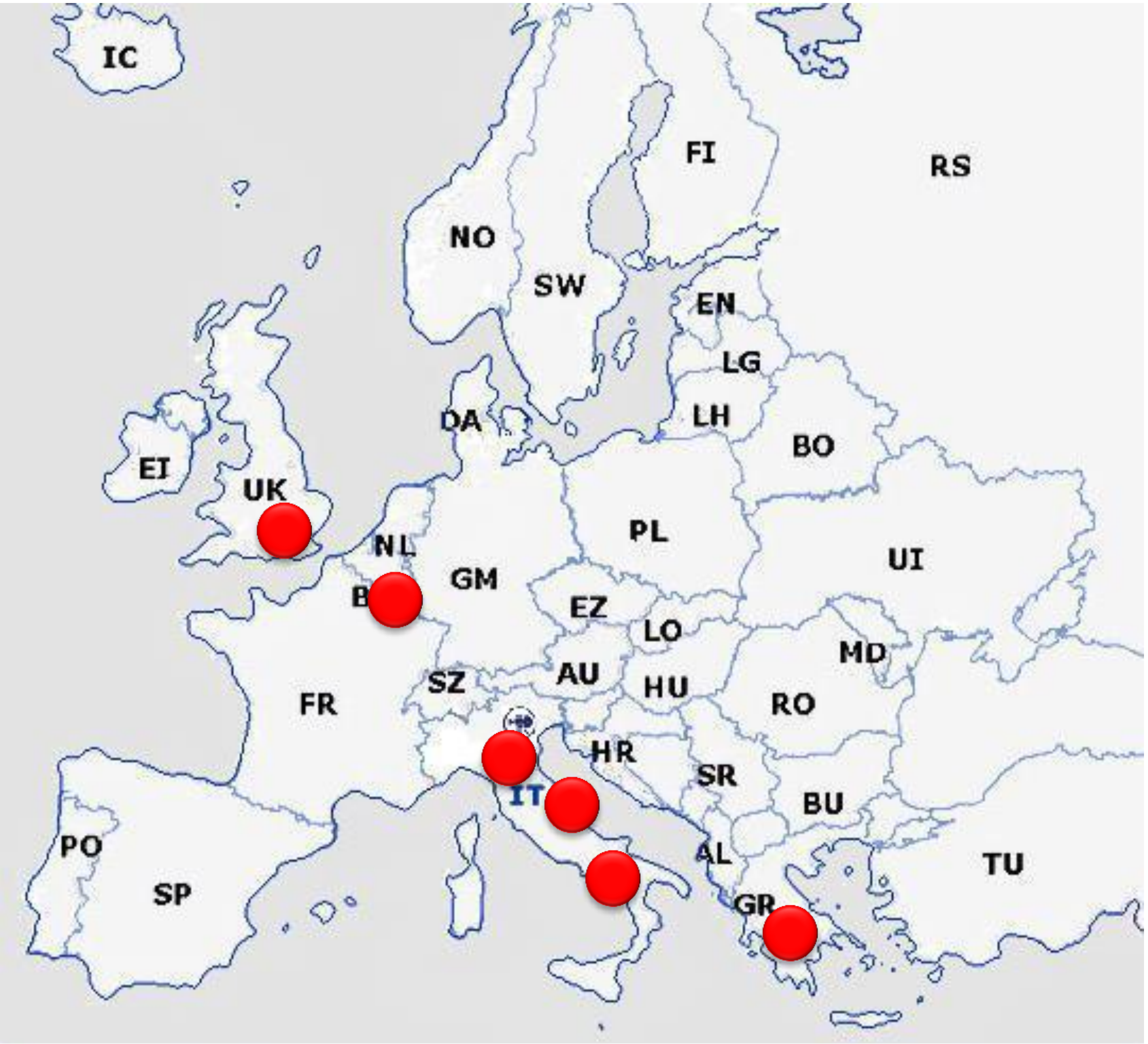

2. MULMON road map

extend the use of composites in aerospace

LIMITATIONS AND IMPLICATIONS

EFFECTS

RESEARCH NEEDS

Manufacturing

Design

Life performances

composites are prone to impact damage

barely visible defects (BVID) do reduce residual strenght to an unknown degree

no methodology is available for linking impact to damage

no methodology to link damage to residual strength

long and intricate certification processes

time-based maintenance (no damage growth during inspection intervals)

damage tolerance design (no damage growth during service life)

skepticism against the use of composites

negative expectation about investements and returns

oversizing in design

costly maintanence

BVID should be detected at an early stage without recurring to visual inspeciton

&

if the effect of BVIDs on the residual strength is known big savings in the maintenance cost

3. MULMON workflow

SOLUTION	TO DATE	CAUSES	INNOVATION	RESOURCES
embedded guided waves based SHM to map impact/damage in real time	not optimized	exclusive/new methodologies	optimize SHM methodology for comp. curved structures	Solid knowledge from previous/current EU projects (ALCAS, MAAXIMUS, JTI, SARISTU) *CONSORTIUM*
	numerically tested only on small samples	absence of a suitable simulation tool	Database: SHM impact – damage	
	limited realibility in mapping defects	impossibility to test advanced inverse approaches	design superior FEM for real large scale analysis (1 GDOFs)	Unique FE parallel software for SHM & RSE simulation (MAAXIMUS, JTI, SARISTU) *ALA, ICL & M&S*
&			perform full scale impact analysis to determine damage and sensors output	
residual strength evaluation due to low velocity impact at full scale level	no methodology is available for residual strenght prediction	No software No hardware	perform full scale residual strenght of fuselage section	New 160k cores computer resource available to MULMON *IBM BG/Q FERMI*
			Database: damage – residual strength	

4. MULMON impact in aeronautics

INNOVATION	OUTPUT	IMPACT

INNOVATION

- optimize SHM methodology for comp. curved structures
- Database: SHM impact – damage
- design superior FEM for real large scale analysis (1 GDOFs)
- perform full scale impact analysis to determine damage and sensors output
- perform full scale residual strenght of fuselage section
- Database: damage – residual strength

OUTPUT

a reliable methodology for diagnosis by having access to

1. SHM data
2. Damage characterization
3. Residual strength evaluation

IMPACT

- the first level of inspection In the maintenance process (visual inpection) can be simplified
  - reduce maintenance cost
  - speed up maintenance stage
- increased fleet availability
- quicker turnaround time
- reduced total ownership cost over the life cycle
- decrease the skepticism on the use of composites

5. worksharing

WP	NAME	LEADER	TASKS - Leader
WP1	Finite element meshes of GRA components and fuselage section	M&S	WP1.1 – Components and Full scale model description - ALA WP1.2 – Impact modeling and simulation requirements – ICL WP1.3 – Analysis of complete fuselage subject to impact - SILKAN WP1.4 – Implicit Finite elements model design – M&S WP1.5 – Simulations and Data storage – ICL WP1.6 – Data diagnosis – M&S
WP2	Damage identification on sensorized panels	ICL	WP2.1 – GW based passive methodologies – ICL WP2.2 – Multilevel passive methodologies - M&S WP2.3 – Active/passive methodologies – ICL WP2.4 – Sensors network optimization - ICL
WP3	Impact detection on a sensorized barrel	UNIBO	WP3.1 - verification of optimized sensorized at a barrel level – UNIBO WP3.2 - Data fusion methodology – M&S
WP4	Residual strenght analysis of damaged barrel	SILKAN	WP4.1 – Requirements – ALA WP4.2 – Residual strength analysis of full fuselage after impact - SILKAN WP4.3 – Finale assessment – ALA WP4.4 – Cause-effect e-database - UNIBO

5. worksharing

WP	NAME	LEADER	TASKS - Leader
WP5	Dissemination and exploitation	EASN	WP5.1 – Project communication pack - EASN WP5.2 – MULMON dissemination activities - EASN WP5.3 – MULMON exploitation activities – ALENIA
WP6	Management	UNIBO	WP6.1 – Communication management - UNIBO WP6.2 – Organisation of Kick-off and periodical meetings - UNIBO WP6.3 – Coordination and reporting - ALL WP6.4 –Monitoring of project Activities and work Packages - UNIBO WP6.5 - Legal and Contractual Management - UNIBO WP6.6 - Financial and Administrative Management - UNIBO WP6.7 - Coordination of Knowledge Management and Other Innovation-related Activities – ALL

ALMA MATER STUDIORUM
UNIVERSITÀ DI BOLOGNA

EFRA
Environmental FRiendly Aircraft

SEVENTH FRAMEWORK PROGRAMME

2nd EASN Conference, 31st Oct – 2nd Nov, Prague

Arvind G. Rao

Faculty of Aerospace Engineering, TU Delft

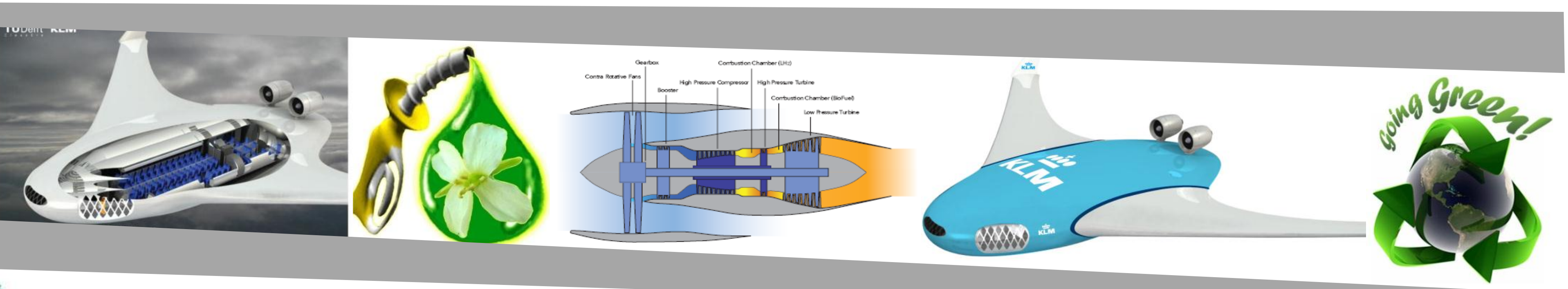

Main Challenges of Civil Aviation

ACARE Goals for EU

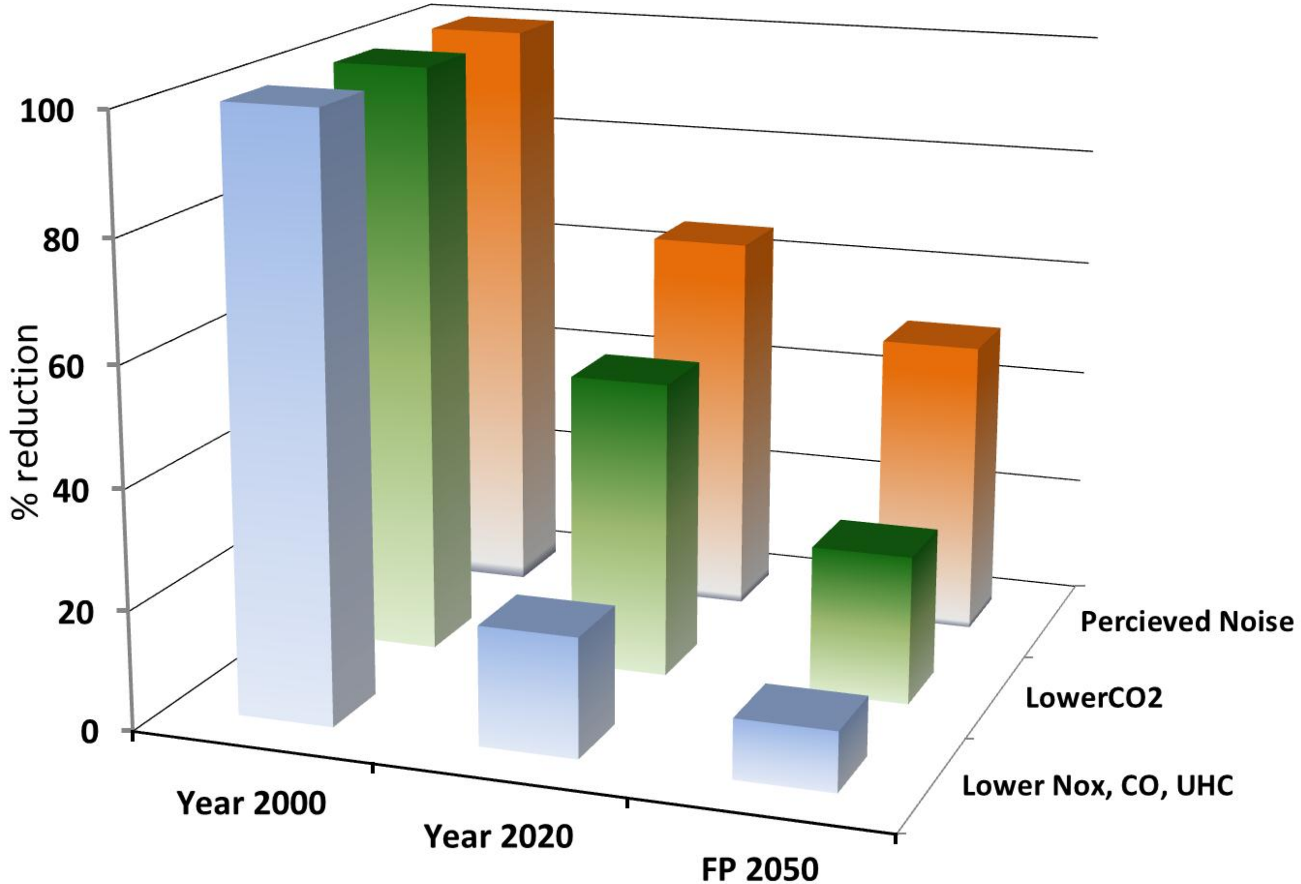

Air traffic over Europe (planefinder.net)

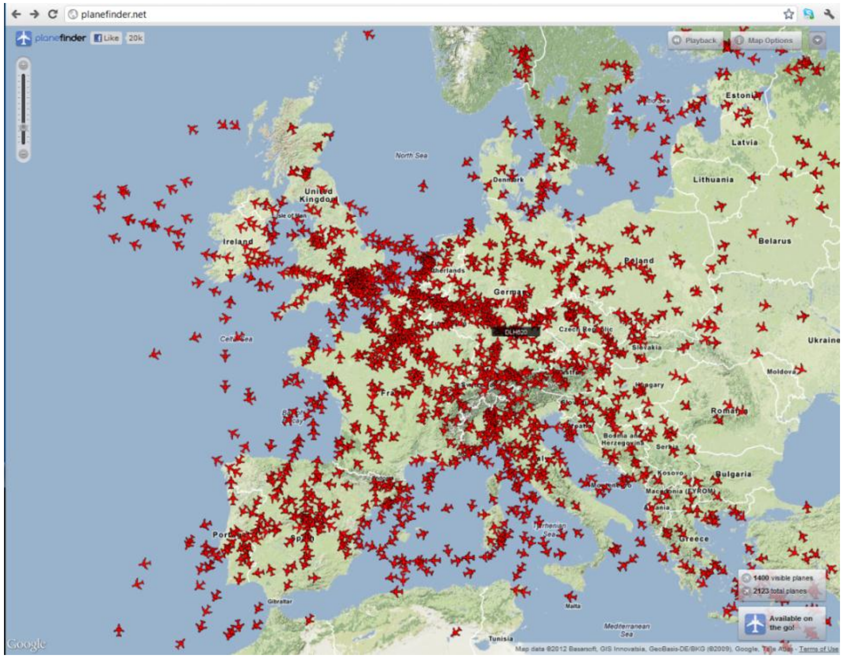

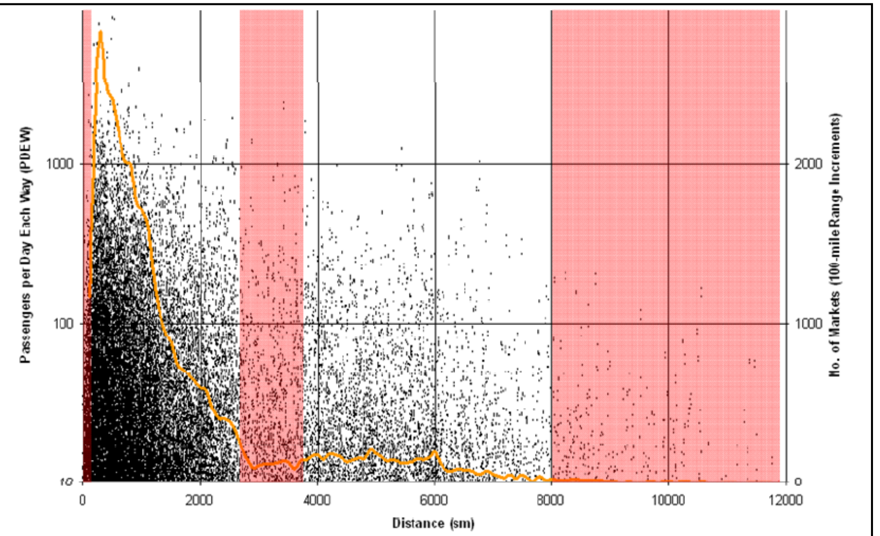

Figure 2.6 – World Ticketed Origin and Destinations

- Data from planefinder.net on 2nd April 2012 at 14:00.
- Total of approx 1400 airplane.
- Large number of these aircraft are regional and single aisle aircraft for travel within EU
- If ACARE goals are to be met, then regional air traffic and aircraft has to be improved dramatically!

Regional Air Transport

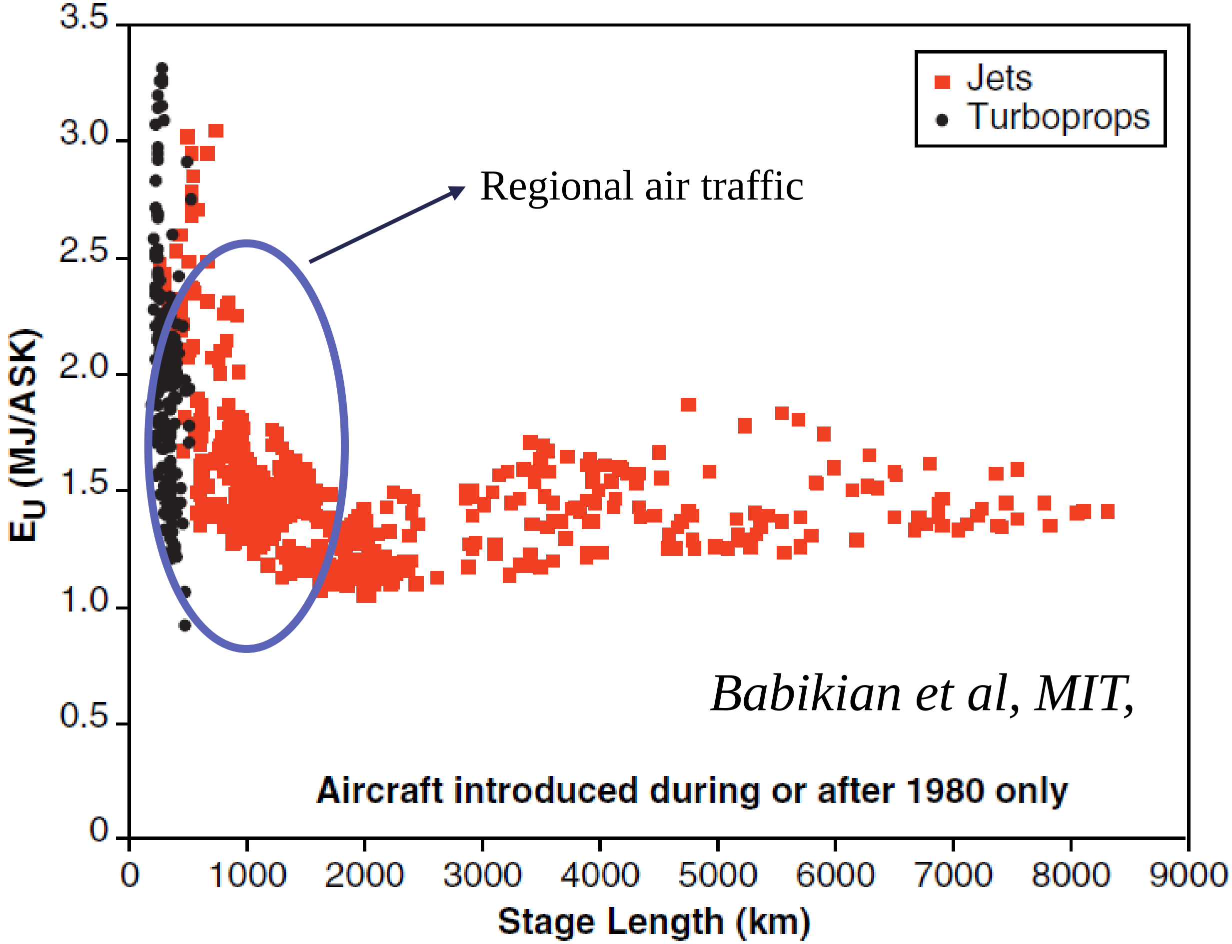

If ACARE goals are to be met, then regional air traffic and aircraft has to be improved dramatically!

Conventional Regional Aircraft Configurations

- Typical configuration characteristics of regional aircraft
  - Cylindrical fuselages (4- or 5 abreast) with high or low wing configuration.
  - Landing gear mounted in belly fairings
  - Engines wing or fuselage mounted
- Configuration advantages:
  - Structurally efficient and easy in manufacturing
  - Can be made into a family of aircraft
- Configuration disadvantages:
  - High fuselage drag
  - Power plant installation:
    - Fuselage mounted: small engines with low bypass ratio can be used, reducing propulsive efficiency
    - Wing mounted: interference and scrubbing drag, limited laminar flow
  - The space within the fuselage is cramped

Evolution in Regional Aircraft

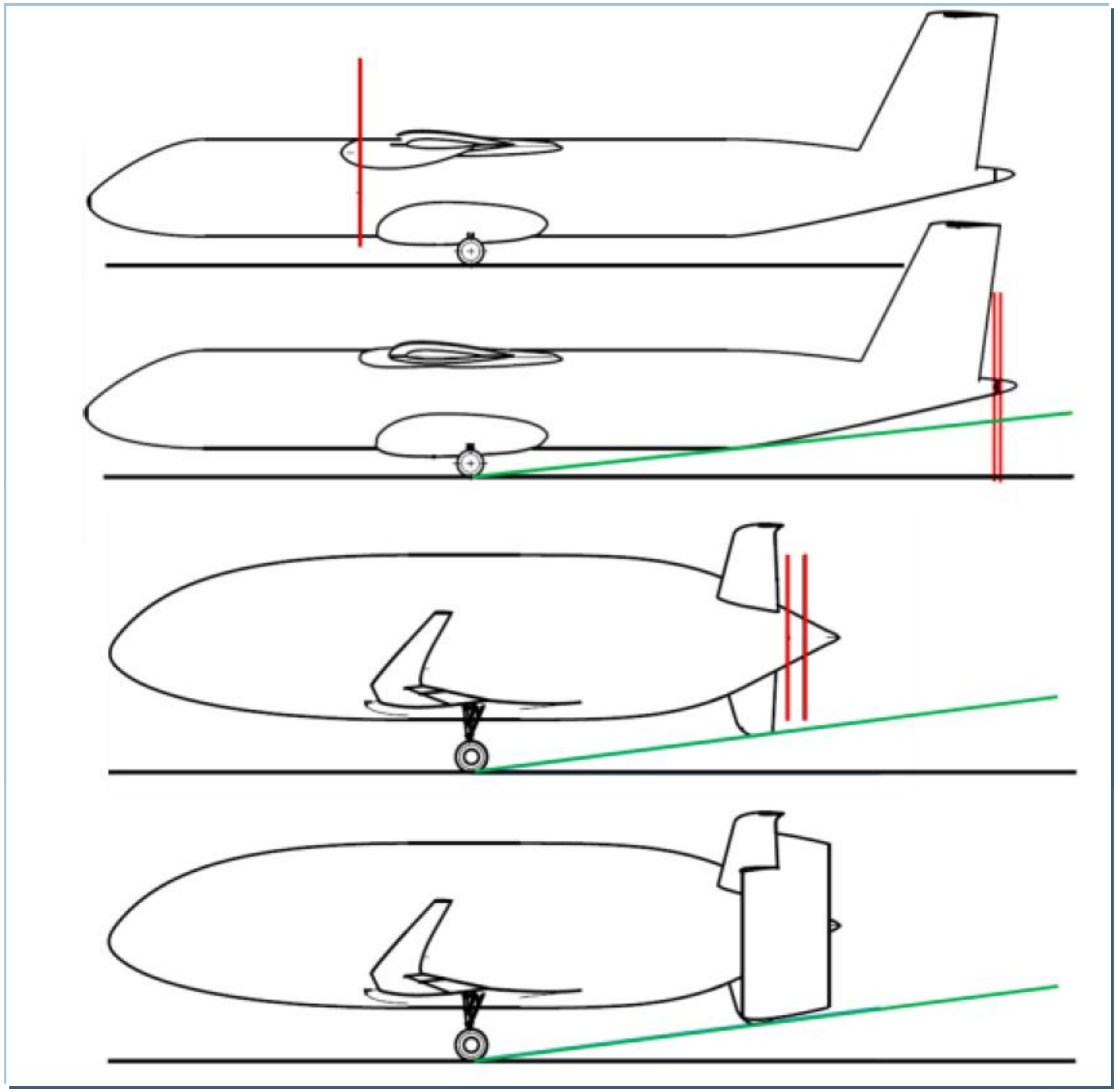

S. Stückl, J. van Toor, H. Lobentanzer, "voltair - the all electric propulsion concept platform" ICAS 2012,

Radical Approach in Aircraft Design: EFRA

- Boundary Layer Ingestion: Flow ingestion by the rear-mounted shrouded propellers reenergize this low energy boundary layer.
  → increase in propulsive efficiency.
- The bypass ratio of the propulsion system is very high, increasing the propulsive efficiency.
- Fuselage slenderness ratio: an optimal fuselage thickness to length ratio is achieved for low aerodynamic drag and maximum useful internal volume → comfortable 6-abreast fuselage with low drag landing gear installation .
- Aerodynamically clean wing design resulting in up to 60% laminar flow on wing surfaces, significantly improving aerodynamic efficiency.

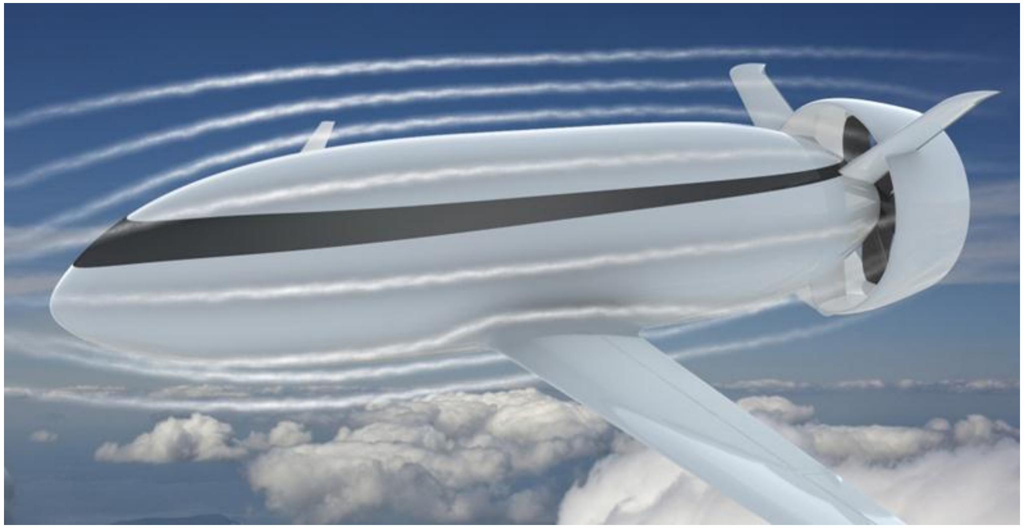

Highly-integrated aircraft-power plant installation: the logical step towards environmental friendly flight.

Power Plant Architecture: Two Counter-rotating Propeller

- Two co-axial, counter-rotating propellers with swept blades are individually driven by two engines via concentric shafts.
- A different number of blades at the two propellers results in better propulsive efficiency and less noise.
- The shroud enhances thrust at low speed (takeoff), protects the propellers in case of a tail strike, enables propeller noise shielding and contributes to the flight stability of the aircraft.

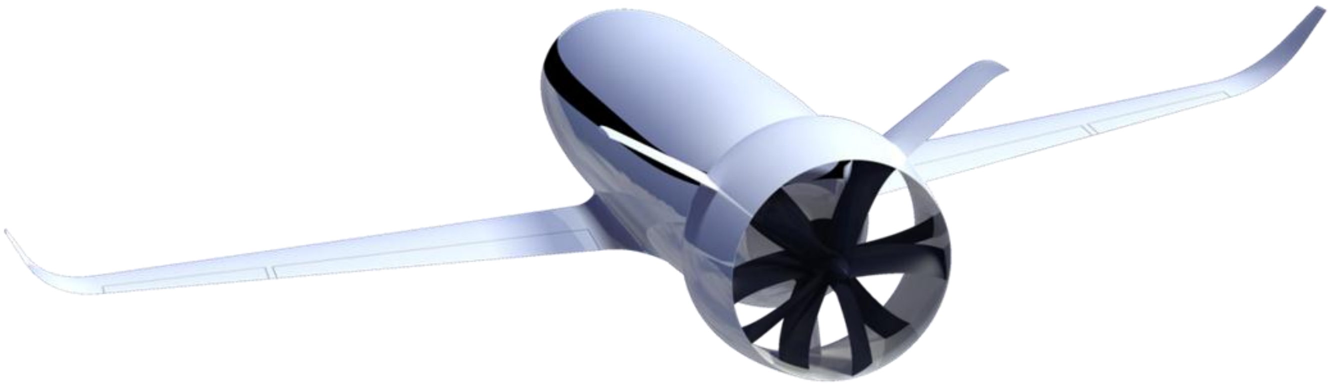

- The contra-rotating configuration reduces the residual swirl in the flow, increasing the propulsive efficiency further.
- Such an aircraft configuration is very well-suited for electric propulsion.

Low noise emission power plant will solve the night-flight dilemma.

Power Plant Architecture: Energy Storage

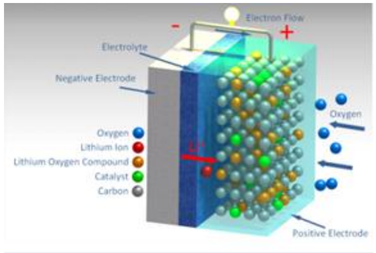

- Fully electric propulsion is at present not viable.
- Trends predict sufficient battery performance within the next two decades
- Hybrid concepts are viable intermediate solutions.

Type	Energy / Weight (Wh/kg)	Energy Density (MJ/kg)	Energy/ Size (Wh/L)	Power/ weight (W/kg)	Recharge Efficiency (%)
Ni Cd	60	0.2	150	150	80
Lead Acid	40	0.14	75	180	40
Ni Metal Hyd	80	0.28	300	1000	80
Lithium-ion	160	0.58	360	350	90
Lithium-Sulphur	600	2	350	NA	80
Kerosene	12000	43	9000	No Limit	–
Hydrogen	33000	120	2500	No Limit	–

If electric energy storage/kg is doubled and aircraft efficiency is doubled, then electric short range flight will become feasible.

Study: Environmental Friendly Regional Aircraft EFRA

>> *Main Research Approach*

- Investigate the aero-propulsion-structural integration of novel fuselage shapes with integrated propulsion concepts
- Suggest how the benefits of these concepts can be maximized at the global aircraft level for target year 2030
- Investigate in terms of realistic aircraft systems integration and application with regards to aircraft performance and operation
- **Develop roadmap for further** research and development, and, derive recommendations for potential concept implementation

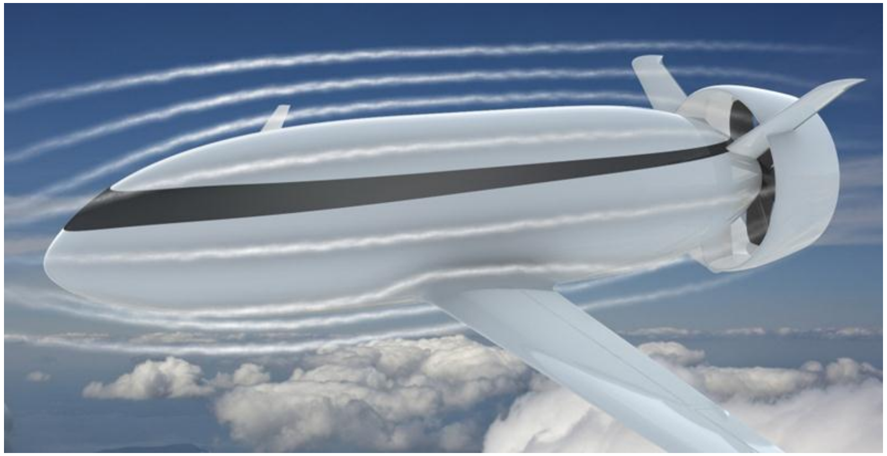

The EFRA CONSORTIUM

TU Delft

Bauhaus Luftfahrt
Neue Wege.

UNIVERSITY OF CAMBRIDGE

EADS INNOVATION WORKS

ONERA
THE FRENCH AEROSPACE LAB

PIAGGIO AERO

Universität Stuttgart

easn
european aeronautics science network

The future belongs to those who anticipate it first

Thank You

European Aeronautics Science Network

Validation of Quality Assurance Concepts for Adhesive Bonding of Aircraft Composite Structures by Extended NDT – ENCOMB+

Project proposal for AAT-2013-RTD-1

EASN Workshop, 31st October - 2nd November 2012, Prague

Motivation

Airbus has about 345 bonding features in all aircraft programmes...
...but is still procuring rivets to build 144 Eiffel-Towers / year.

➡ **Rivetless assembly:**

Concept of reduction or elimination of mechanically fastened joints in primary structures (➡ joining technique: adhesive bonding)

Rivetless assembly → Improved material usable → Increased structural efficiency → Decreased airframe weight → Decreased fuel consumption → Decreased CO_2 footprint

➡ **Improved eco-efficiency**

➡ **High rate & low cost manufacturing capability**

Motivation

How to ensure adhesive bond performance?

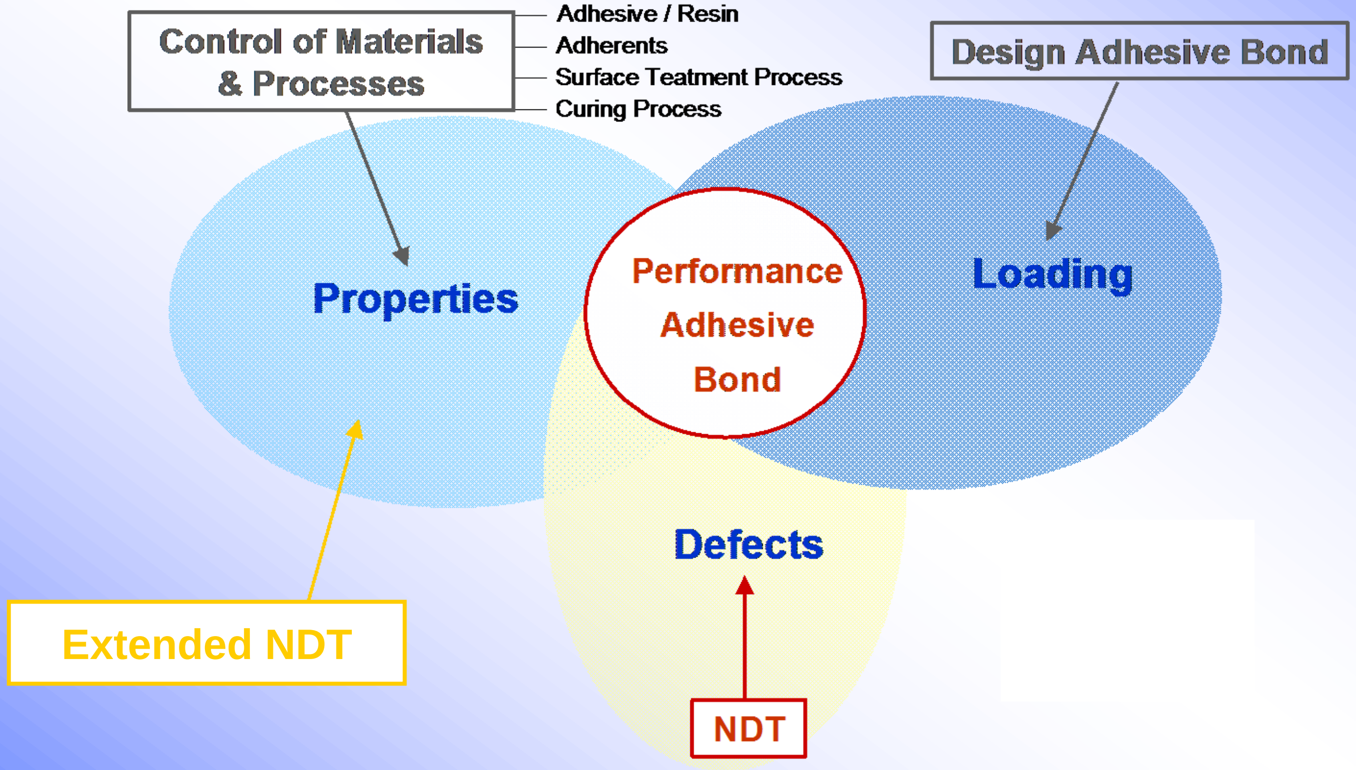

Bond quality assurance – an extended approach is needed! ➡ ENCOMB (3rd call)

Background – achievements of ENCOMB

Over 20 ENDT technologies for CFRP surface and bondline characterisation have been tested and further developed for the investigation of relevant **application scenarios**:

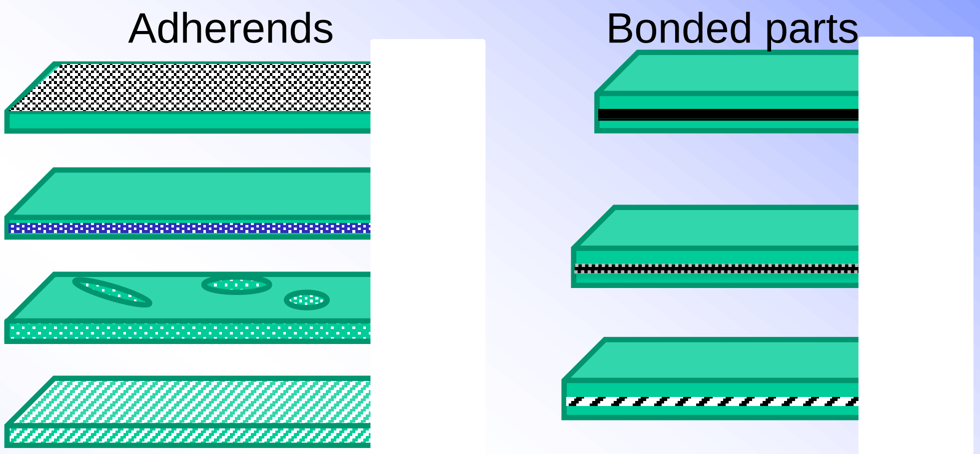

Surface contaminations:

- Silicone-based release agent
- Moisture
- Hydraulic fluid (Skydrol)
- Thermal degradation

Bondline characterisation:

- Silicone-based release agent
- Moisture
- Poorly cured adhesive

The majority of the tested ENDT techniques was able to detect differences between the contaminated/treated and the clean reference samples. Further developments are needed with regard to:

- realistic sample geometries/surfaces (curved, scarfed)
- more complex and undefined contaminations that reflect surfaces states from real processes
- reliability, robustness, in-line/mobile operation

Objectives

Development of ENDT technologies that can be integrated into future adhesive bonding process chains and that will allow

I. the assessment of surface quality before bonding
II. quality assessment of the finished adhesive joint
   - reliable and reproducible detection of undefined and potentially multiple contaminations on adherends' surfaces
   - reliable and reproducible detection of poor bond quality
   - robustness of methods, suitability for field measurements in aircraft manufacturing and repair environments
   - sufficient detection sensitivity
   - adequate measurement speed
   - potential for semi-automated operation

Complemented by SHM tools for in-service quality monitoring

Concept and WBS

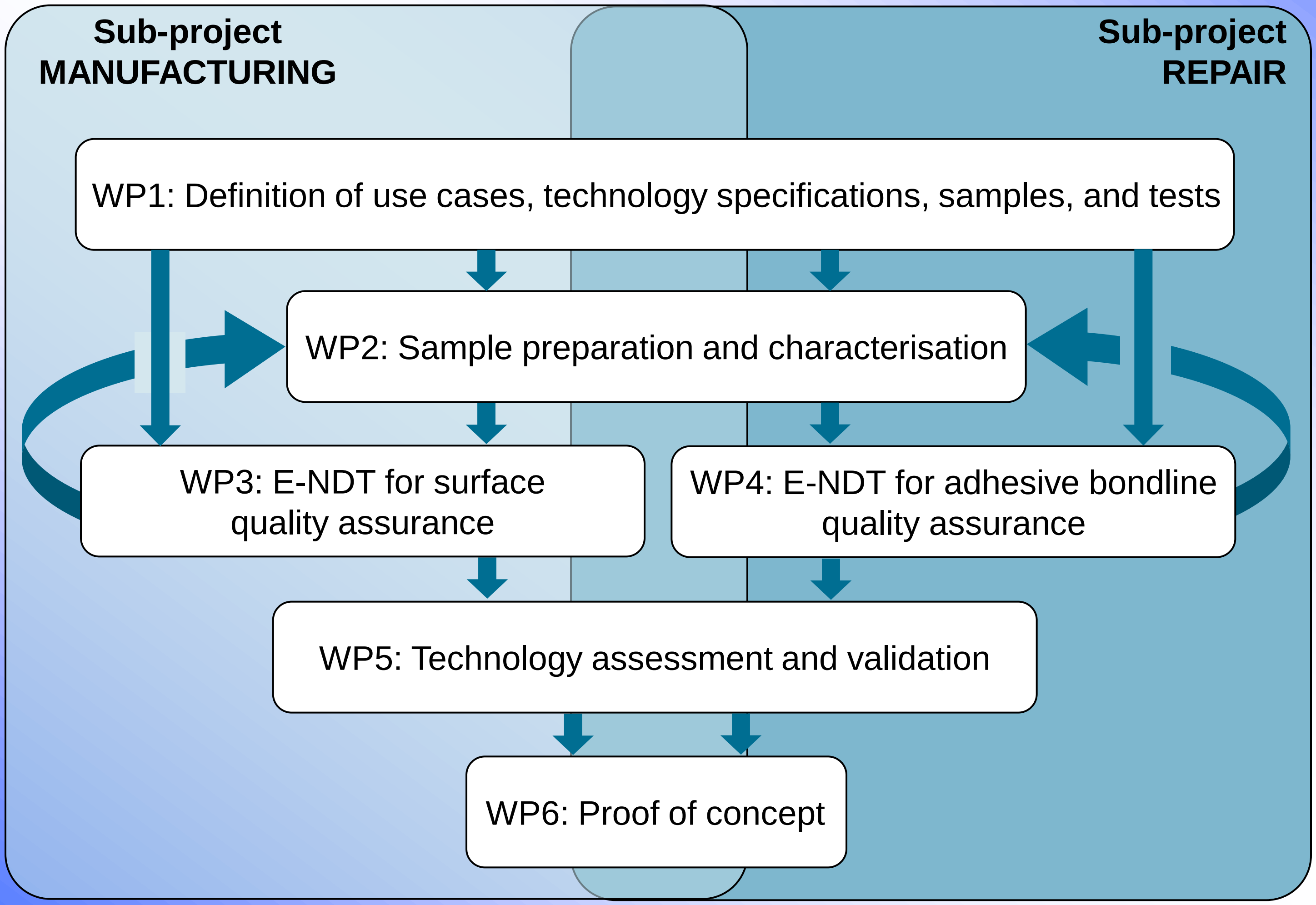

European Aeronautics Science Network

Consortium

Participant no.	Participant organisation name	Country
1 (Coordinator)	Fraunhofer-Gesellschaft zur Förderung der Angewandten Forschung e.V.	Germany
2	Airbus Deutschland GmbH	Germany
3	Agenzia Nazionale per le Nuove Tecnologie, l'Energia e lo Sviluppo Economico Sostenibile	Italy
4	Agilent Technologies Ltd	United Kingdom
5	Centre National de la Recherche Scientifique	France
6	EADS Deutschland GmbH	Germany
7	EADS France S.A.S.	France
8	École Polytechnique Fédérale de Lausanne	Switzerland
9	GMI AERO	France
10	Instytut Maszyn Przeplywowych-Polskiej Akademii Nauk	Poland
11	University of Patras	Greece
12	EASN Technology Innovation Services	Belgium

european aeronautics science network

European Aeronautics Science Network

PIONEERING AIRCRAFT-INTEGRATED STRUCTURAL SENSORS

Coordinated by: KU Leuven (University of Leuven) - Belgium
Core Partnership: Collaborative projects

PACIS

- **Challenge 3:** COMPETITIVENESS THROUGH INNOVATION
- **Activity in Work Programme**
  - 7.1.4. IMPROVING COST EFFICIENCY
- **Topic in Work Programme**
  - AAT.2013.4-4 MAINTENANCE, repair and disposal

- **Challenge 1:** ECO-INNOVATION
- **Activity in Work Programme**
  - 7.1.1 THE GREENING OF AIR TRANSPORT
- **Topic in Work Programme**
  - AAT.2013.1.1-2 AEROSTRUCTURES

European Aeronautics Science Network

european aeronautics science network

PIONEERING AIRCRAFT-INTEGRATED STRUCTURAL SENSORS

PACIS

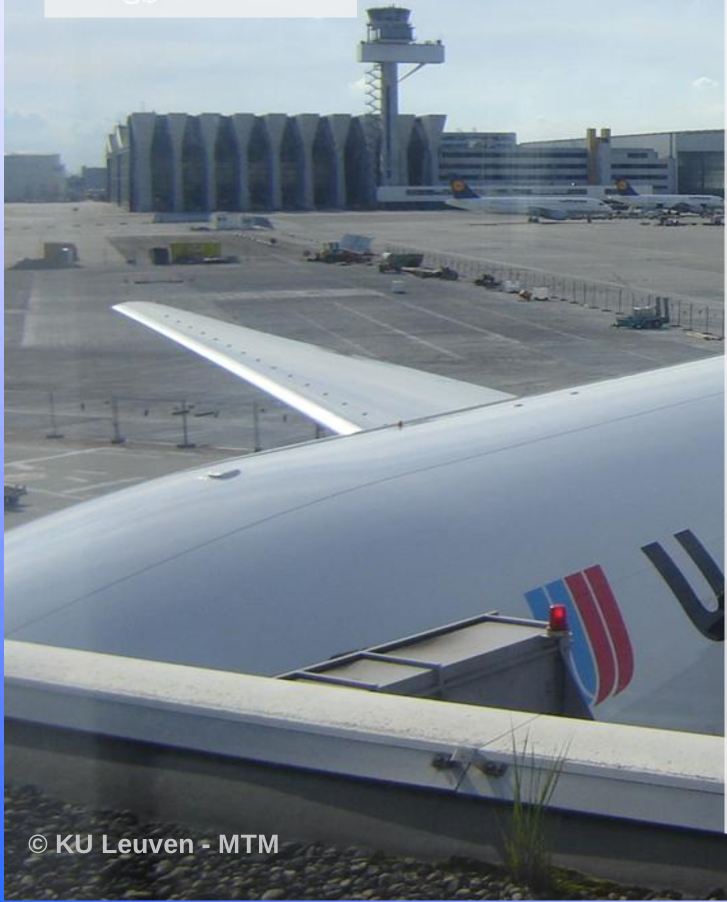

PROJECT

Finally, structural health monitoring (SHM) can replace traditional non-destructive testing. Meanwhile, **indicative low-end SHM** combined with advanced non-destructive testing (**aNDT**) is the optimum choice.

→ Implementation of SHM in relevant full-scale aircraft structures (metals and composites undergoing fatigue, impact, corrosion damage) provided by **maintenance companies/departments**.

→ Use of **percolation** sensors (leakage detection), **ultrasonic** guided waves (non-linear ultrasonics, time-of-flight, full-field imaging), **optical** methods (polarisation enhanced visual inspection) and corrosion monitoring with **electrochemical** methods.

→ Finally, the target are robust sensor networks while **avoiding complex on-board systems**.

European Aeronautics Science Network

european aeronautics science network

PIONEERING AIRCRAFT-INTEGRATED STRUCTURAL SENSORS

PACIS

KEY PARTNERS

… with practice in **aircraft operations** (such as airlines, maintenance, repair and overhaul companies (MRO) to provide **access** to relevant full-scale parts for the implementation of SHM systems within in the scope of the project

IMPACT

Use the experience from the **FP7 AISHA II** project (e.g. a floorbeam sensor was certified and successfully implemented in three **operational airliners**) and give it a new dimension by focusing on further implementation at TLR6. SHM sensors should be designed and performed as **minor modifications** whenever possible to reduce the time to market.

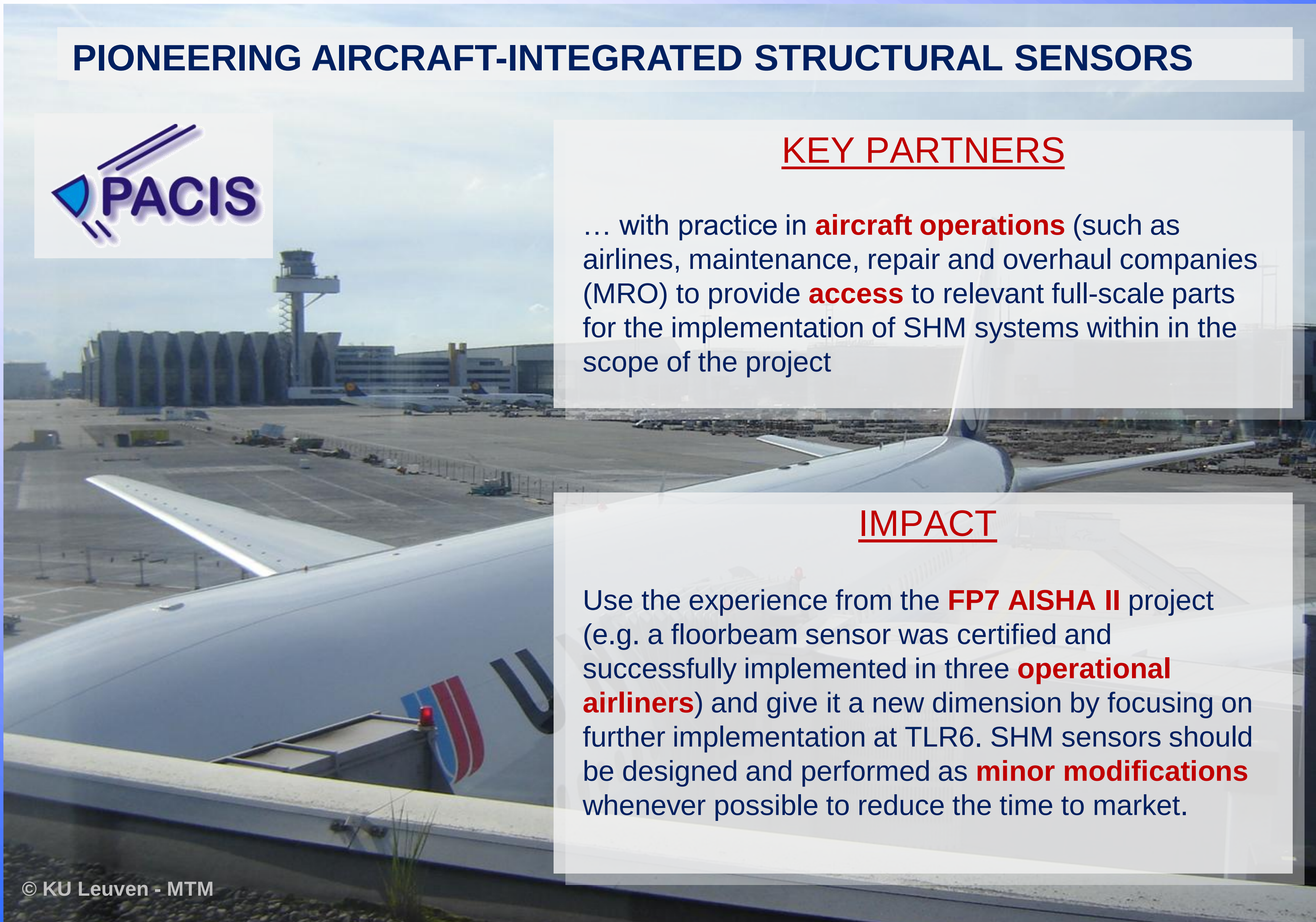

European Aeronautics Science Network

european aeronautics science network

PIONEERING AIRCRAFT-INTEGRATED STRUCTURAL SENSORS

PACIS

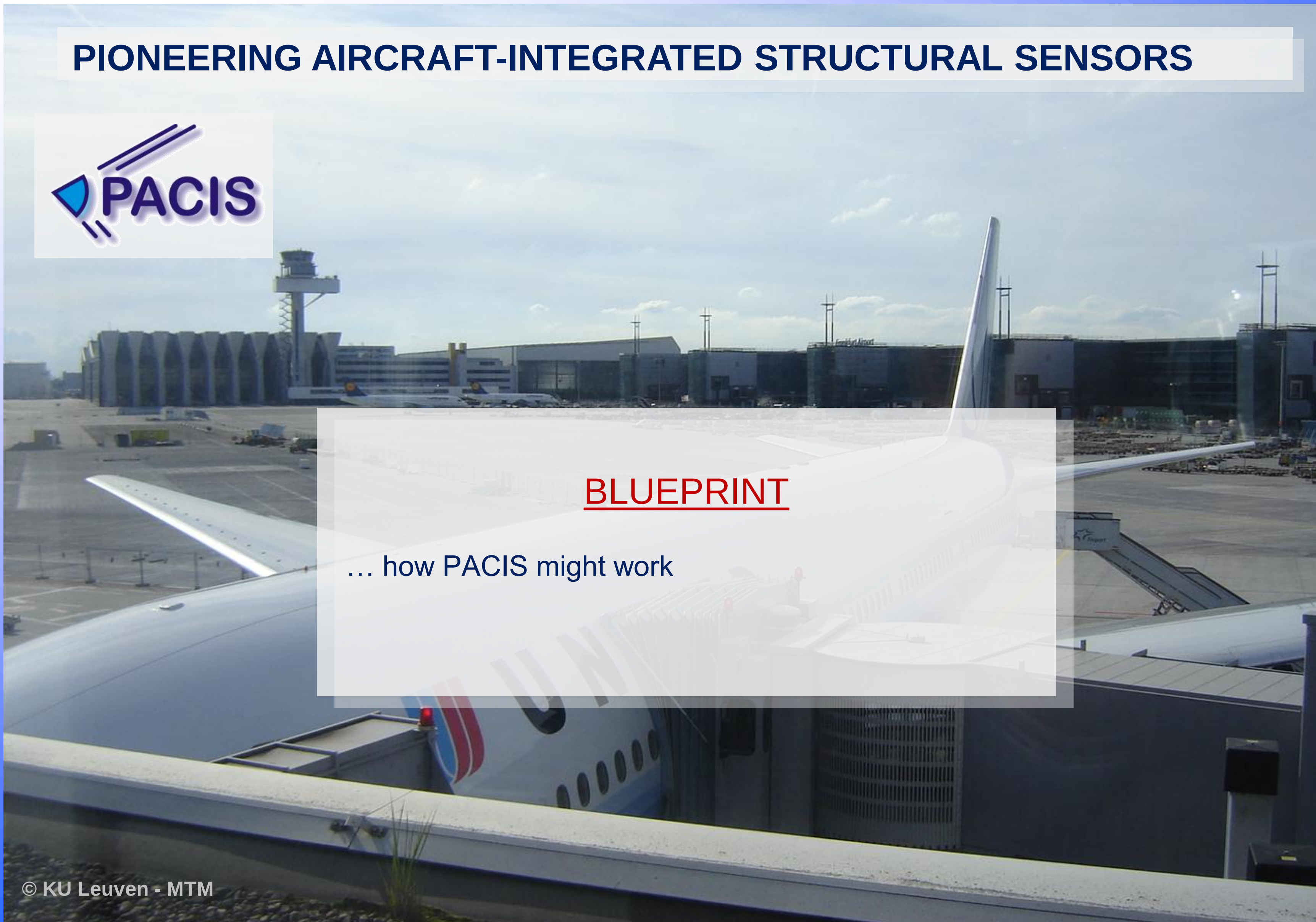

BLUEPRINT

… how PACIS might work

Floor beam – corrosion and corrosion prevention

Floor beam – corrosion and corrosion prevention

Floor beam – corrosion and corrosion prevention

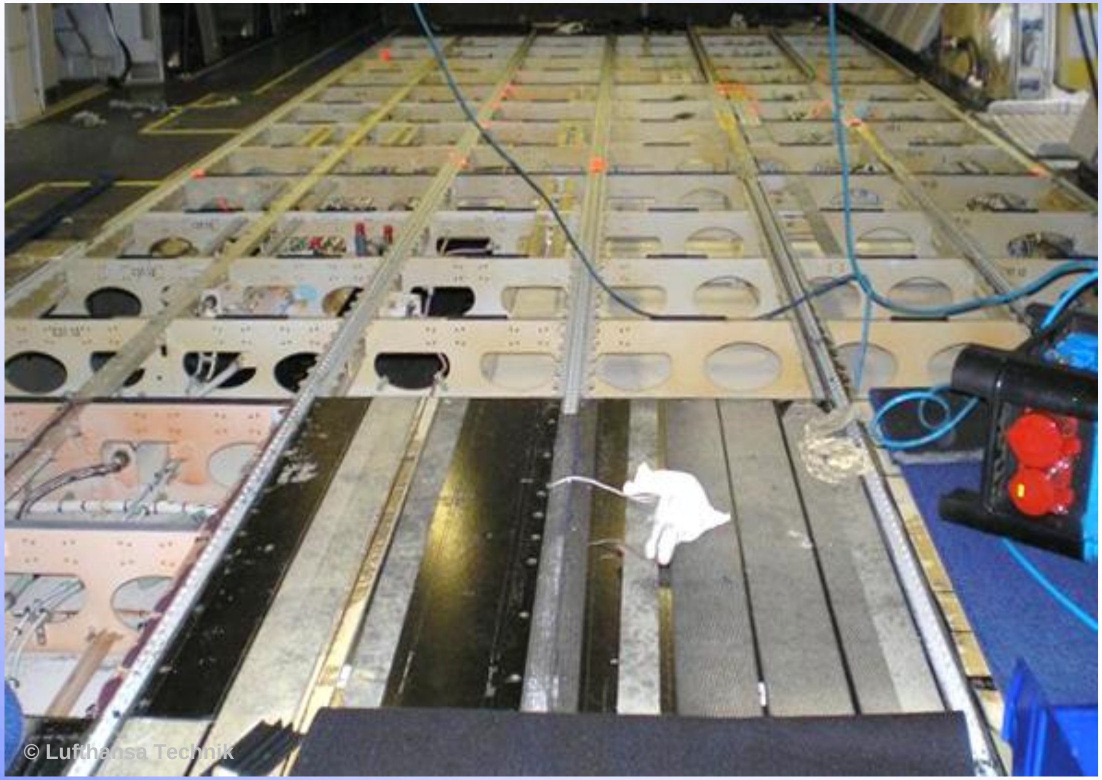

Floor beam – corrosion and corrosion prevention

European Aeronautics Science Network

european aeronautics science network

HOT SPOT
Monitoring

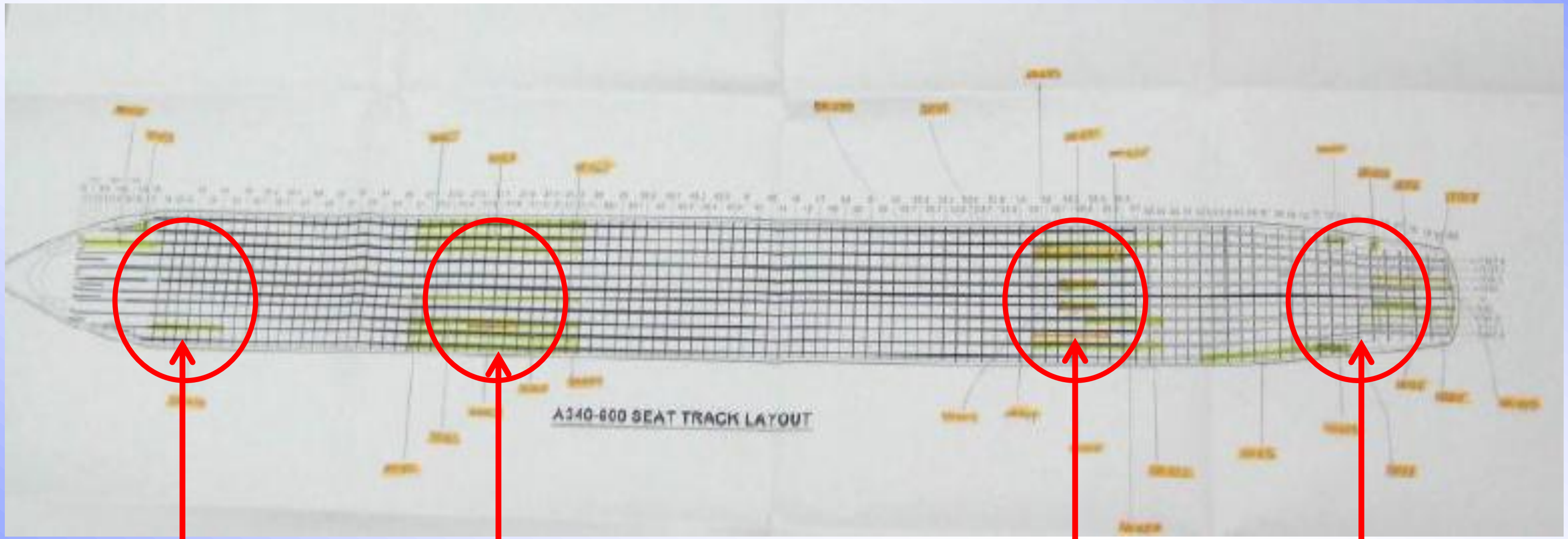

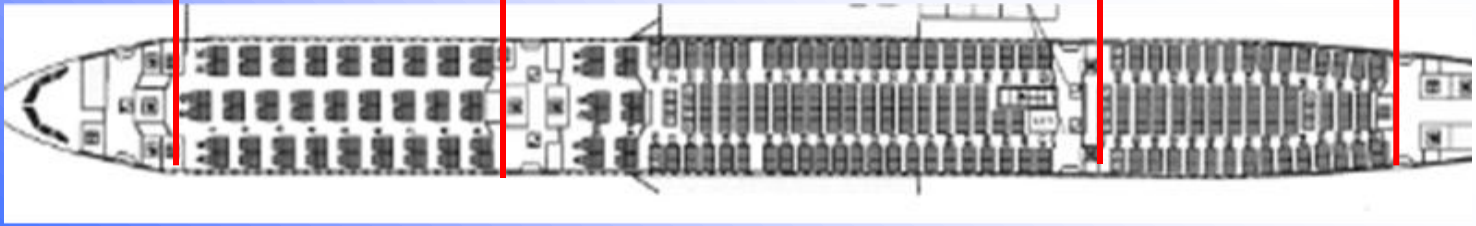

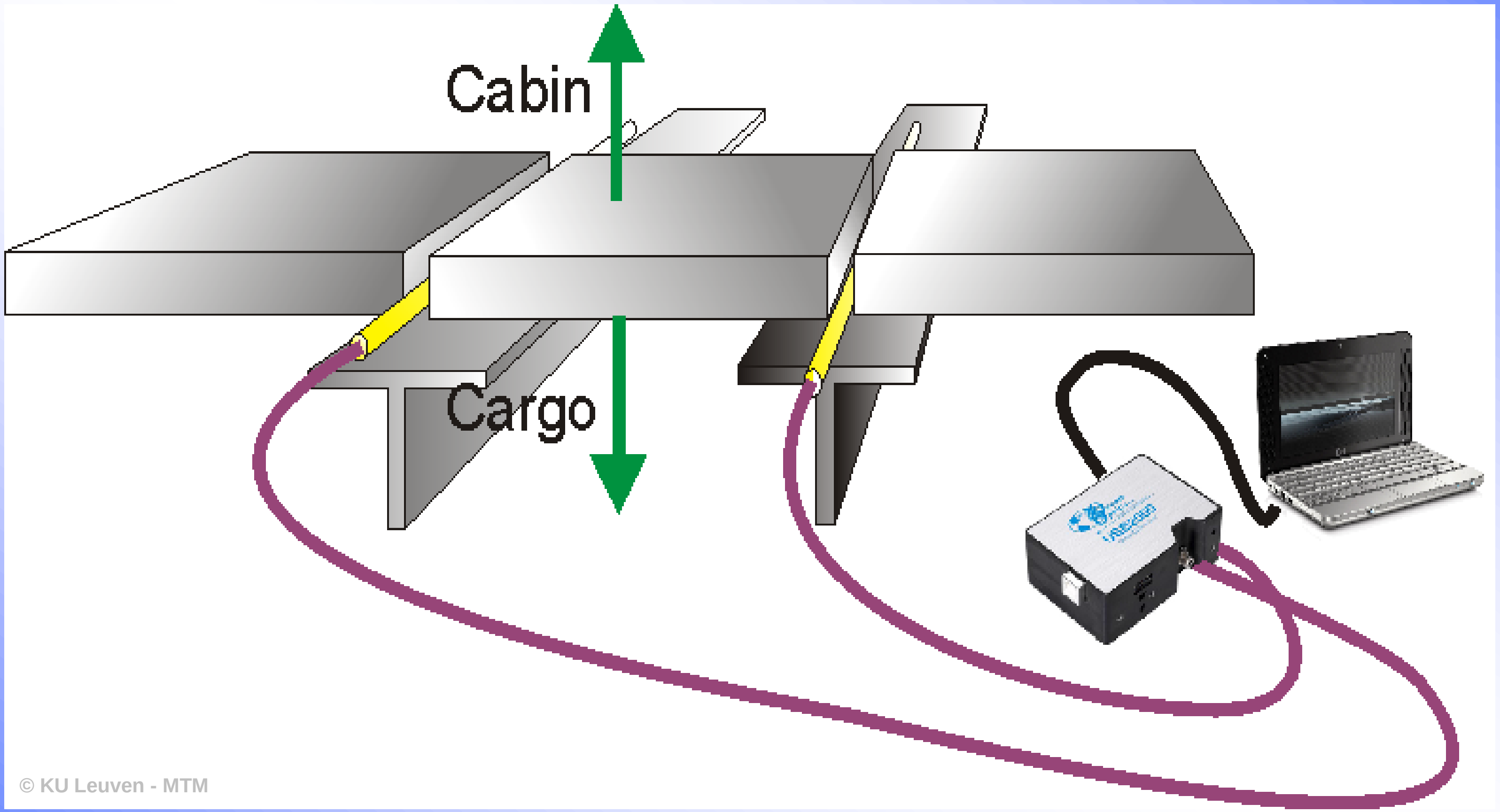
Cabin
Cargo
© KU Leuven - MTM

Lufthansa-Technik in Sofia/Bulgaria - April 2011

European Aeronautics Science Network

Lufthansa-Technik in Sofia/Bulgaria - April 2011

PCS – Percolation conductivity sensor

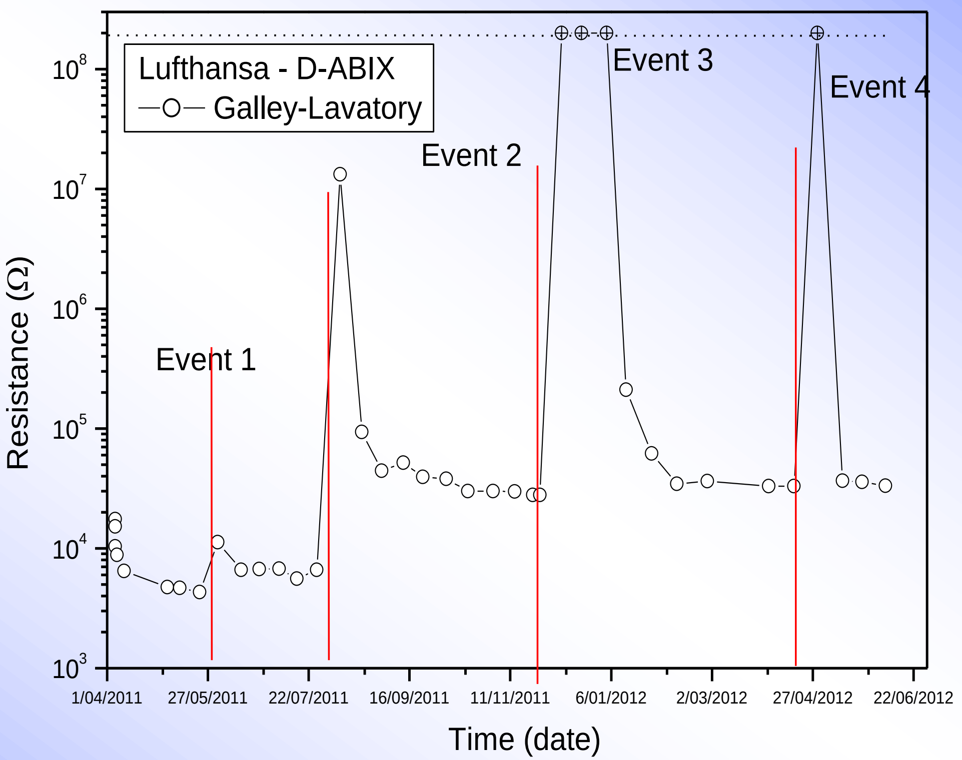

BRING THE COMPONENT (SENSOR/SENSOR MATERIAL) AS SOON AS POSSIBLE INTO THE AIRPLANE (TRL4) TO ACHIEVE TRL6 BY UNDER OPERATIONAL CONTRAINTS, NOT AS A COMPLETE SYSTEM/SUBSYSTEM BUT FOR THE COMPONENT

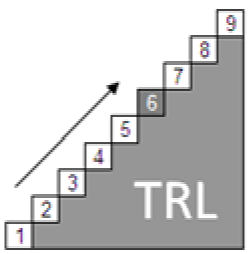

TRL1	Basic principles observed and reported
TRL2	Technology concept and/or application formulated
TRL3	Analytical & experimental critical function and/or characteristic proof-of-concept
TRL4	Component and/or breadboard validation in laboratory environment
TRL5	Component and/or breadboard validation in relevant environment
TRL6	COMPONENT l or prototype demonstration in a relevant environment (ground or in-flight)
TRL7	System prototype demonstration in-flight
TRL8	Actual system completed and "Flight qualified" through test and demonstration (ground or in-flight)
TRL9	Actual system "flight proven" through successful operations

european aeronautics science network

European Aeronautics Science Network

Towards an “indicative SHM (I-SHM)” as intermediate step

Traditional NDT
Provides damage size

High-end SHM
Provides damage size

Indicative SHM (I-SHM)
Provides semi-quantitative alert for traditional NDT and repair (preferentially without on-board electronics) →
- It is **just** the ”FUSE” not the “ELECTRICIAN”
- It is **just** the ”PAIN” not the “DIAGNOSTICIAN”

source: Holger Speckmann, Airbus
© Airbus

BENEFITS
Technically less challenging
Lower **certification** thresholds/less **risks/cheaper**
Enables **fading out** of **scheduled inspections**
Earlier **added values** for maintenance
Enables **smoother transition** to high-end **SHM**

European Aeronautics Science Network

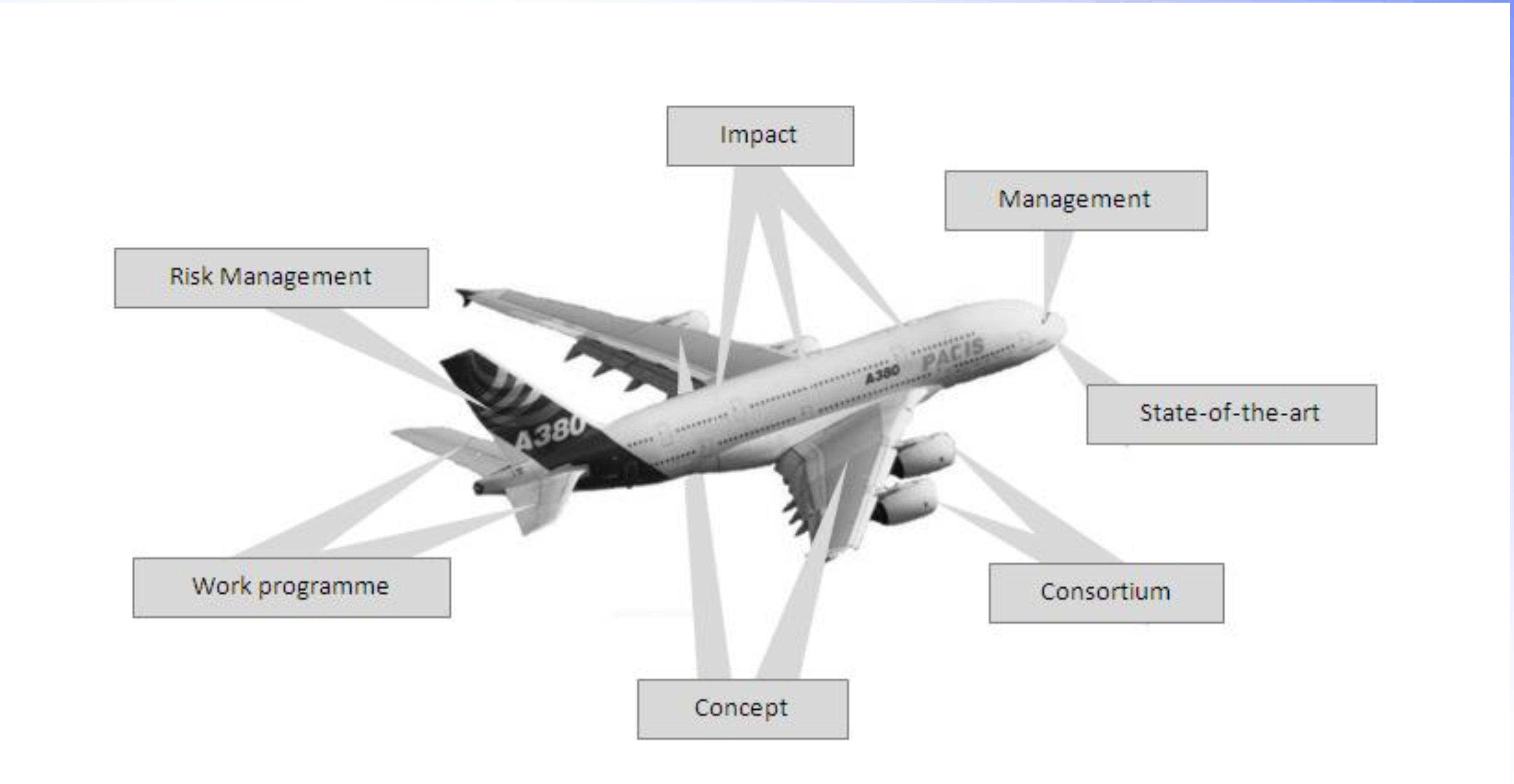

Technologies for Environmentally Friendly Aero Engines of the Future

Uwe Hessler
Head of Research & Technology
Rolls-Royce Deutschland

2nd EASN Workshop
31st October 2012

Agenda

- *Rolls-Royce*
- *Aviation and the environment*
- *Flightpath 2050*
- *Future technologies*
- *Conclusion*

Agenda

- *Rolls-Royce*
- *Aviation and the environment*
- *Flightpath 2050*
- *Future technologies*
- *Conclusion*

Four global markets – Sales £11.3bn*

Civil Aerospace

£5.6bn

Defence Aerospace

£2.2bn

Marine

£2.3bn

Energy

£1.2bn

****2011 results***

Civil aerospace

Powering over 30 types of commercial aircraft. We have a good presence in narrowbody and a strong position in widebody, regional and corporate aircraft. A Rolls-Royce powered aircraft takes off or lands every 2.5 seconds.

- over 13,000 engines currently in service
- more than 500 airline customers
- 4,000 corporate operators

2011 financial data

order book	**£51.9bn**
revenue*	**£5,572m**
profit*	**£499m**

*Underlying figures

Market opportunity over 20 years

original equipment	**US$800bn**	services	**US$600bn**

Research and development

We develop technologies and intellectual property that allow us to compete on a global basis in highly competitive markets.

- £908m invested in R&D in 2011
- £7.5bn invested in R&D over the past ten years
- 475 patent applications in 2011
- 28 University Technology Centres worldwide

Gross research and development expenditure (£m)

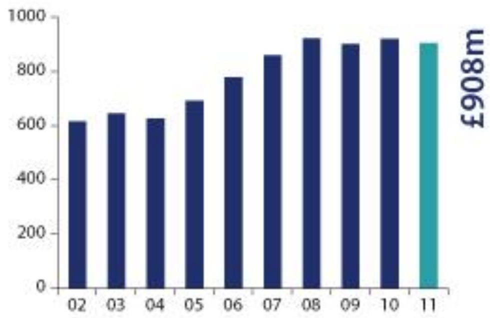

Global Research Network

North America

UTC at Purdue, partnership with Virginia Tech and Virginia, links to MIT, Georgia Tech, Illinois in the US

Exploring relationships in Canada

Asia

Pusan in Korea. Xian in China

Research centres in Singapore and Japan

Exploring options in India

Europe

18 UTCs in the UK

Cottbus, Dresden, Darmstadt, Karlsruhe, DLR in Germany

Chalmers in Sweden. Trondheim in Norway

Genoa in Italy

Agenda

- *Rolls-Royce*
- *Aviation and the environment*
- *Flightpath 2050*
- *Future technologies*
- *Conclusion*

The Environmental Challenge

- ICAO* set global minimum standards but regional concerns vary
- Global (Carbon Dioxide)
  - Climate change (and fuel use)
- Local
  - Local air quality (NOx and particulates)
  - Noise

Pasterze Glacier, Austria

Circa 1900

Recent

*** International Civil Aviation Organization**

Greenhouse gas emissions for 2005

All gasses

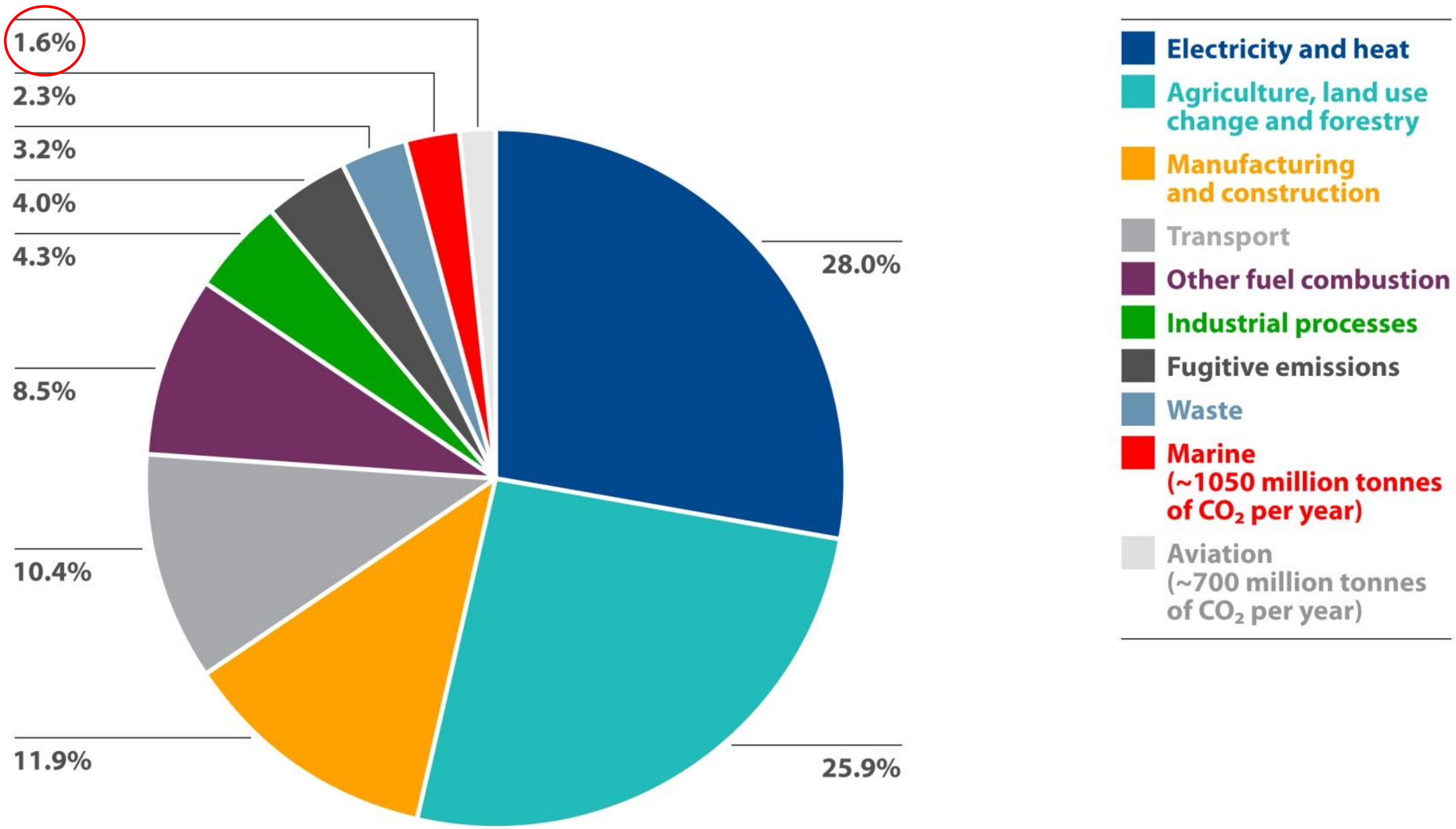

Source: World Resources Institute

Rolls-Royce Environmental Strategy

- Maintain our drive to reduce the environmental impact of all our business activities;
- Further reduce the environmental impact of our products; and
- Develop entirely new low-emission and renewable energy products

Factories and facilities

Efficient products

Future products

Rolls-Royce will apply its knowledge and technology to develop profitable solutions to the challenge of climate change

Agenda

- Rolls-Royce
- Aviation and the environment
- Flightpath 2050
- Future technologies
- Conclusion

Flightpath 2050

Goals to take ACARE* beyond 2020

*Advisory Council for Aviation Research in Europe

ACARE

By 2050 compared to year 2000 datum

- 75% reduction in CO_2 per passenger kilometre
- 90% reduction in NOx emissions
- 65% reduction in noise

Requires Improvement in all areas

Airframe

Engine

ATM & Operations

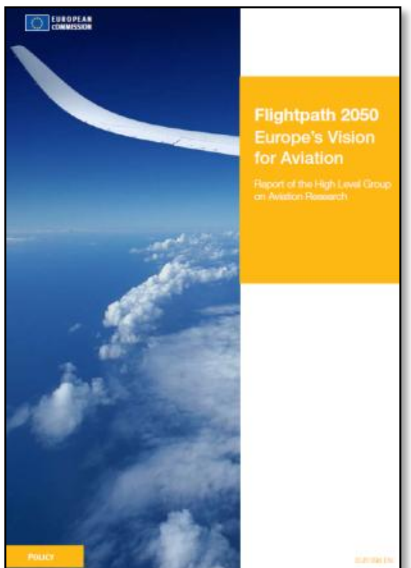

Strategic Research & Innovation Agenda – goals:
Meeting Societal and Market Needs
Maintaining and Extending Industrial Leadership
Protecting the Environment and the Energy Supply
Ensuring Safety and Security
Prioritising Research, Testing Capabilities & Education

Civil Aerospace - Reducing environmental impact

20% lower CO_2

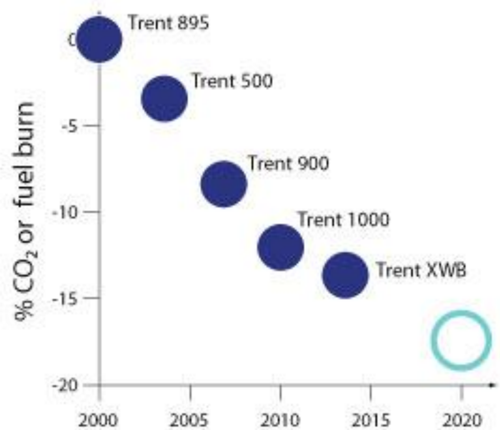

Target 50%
CO_2 overall reduction:

- 15-20% from engine
- 20-25% from airframe
- 5-10% from operations

60% lower NOx

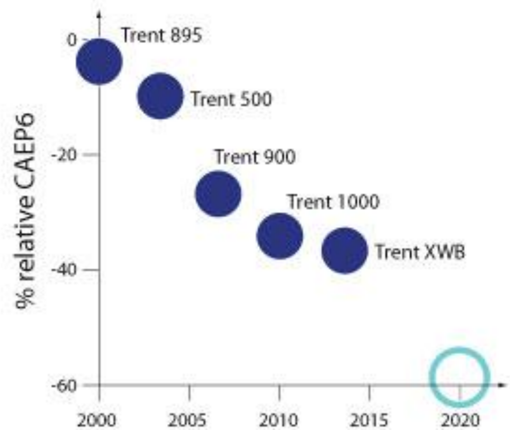

Target 80%
NOx overall reduction:

- 60% from engine technology
- 20% from operational efficiency improvements

Half perceived noise

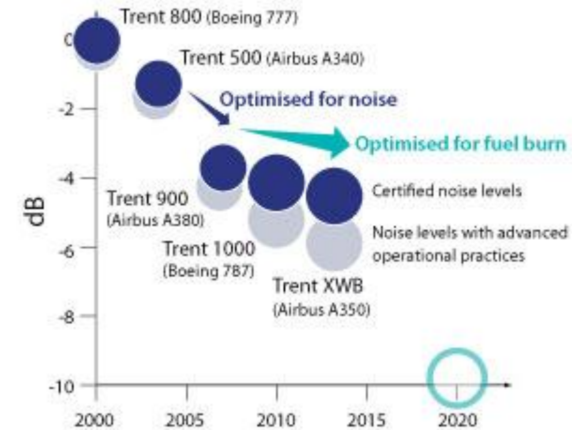

Target 50%
aircraft noise reduction:

- 30dB cumulative
- 10dB average at each condition

Trent family

ACARE target (Advisory Council for Aeronautics Research in Europe)

Agenda

- *Rolls-Royce*
- *Aviation and the environment*
- *Flightpath 2050*
- *Future technologies*
- *Conclusion*

Long-term consistent technology strategy

VISION

Vision 5

Near term products
Off the shelf technologies
In-service upgrades

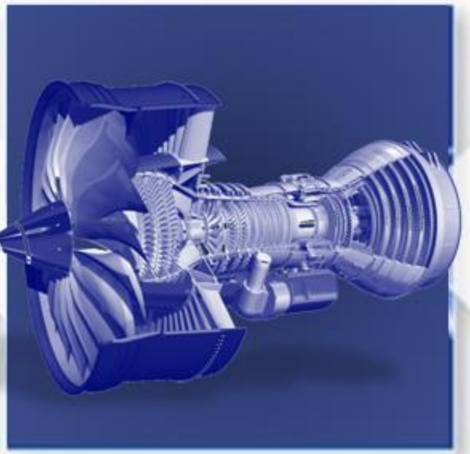

Vision 10

Next generation
Technology demonstration

Vision 20

Future generation
Emerging technologies

EIS ***2016*** ***2021*** ***2031***

Vision 10 technologies

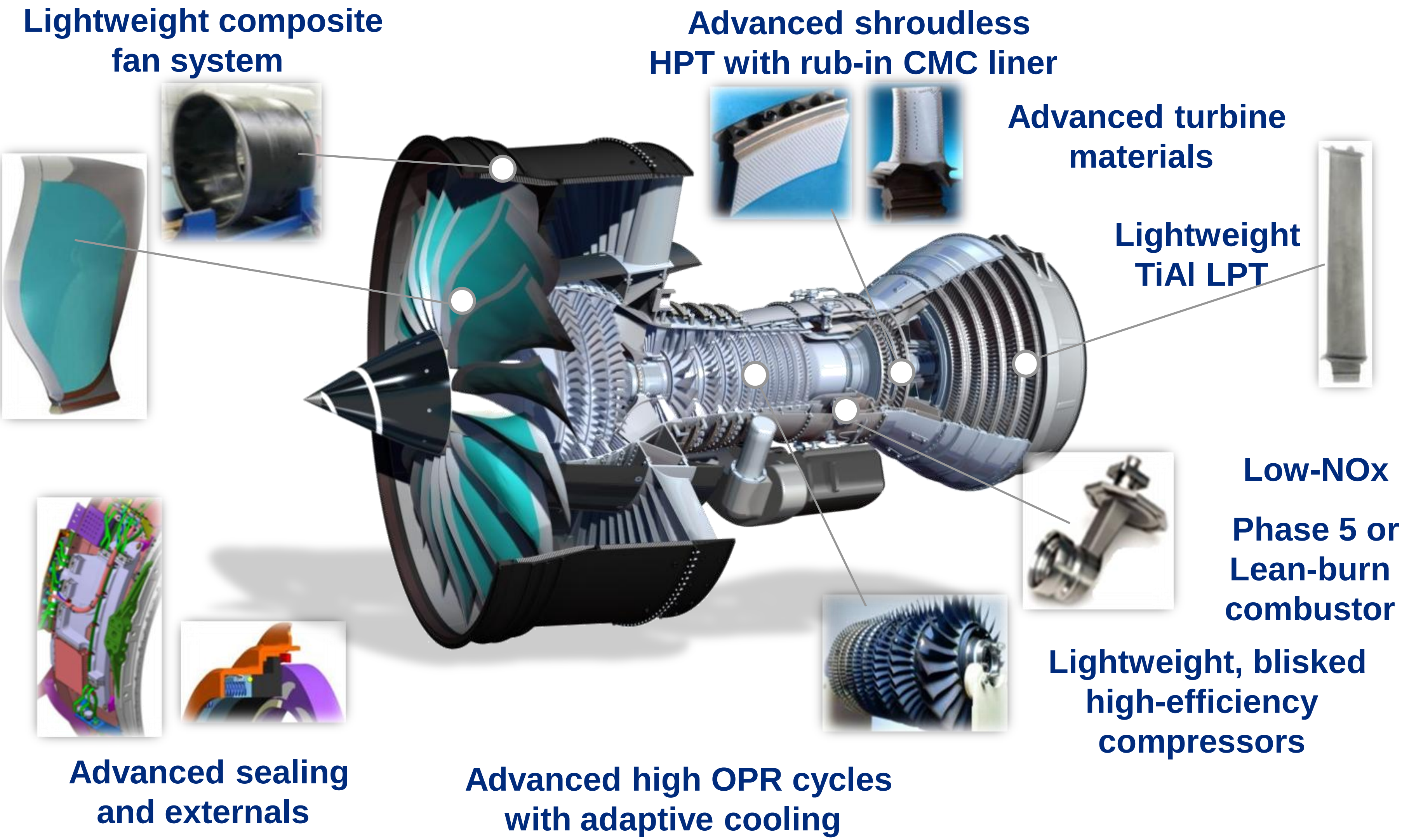

Turbofan Thermodynamic Cycle Efficiencies:

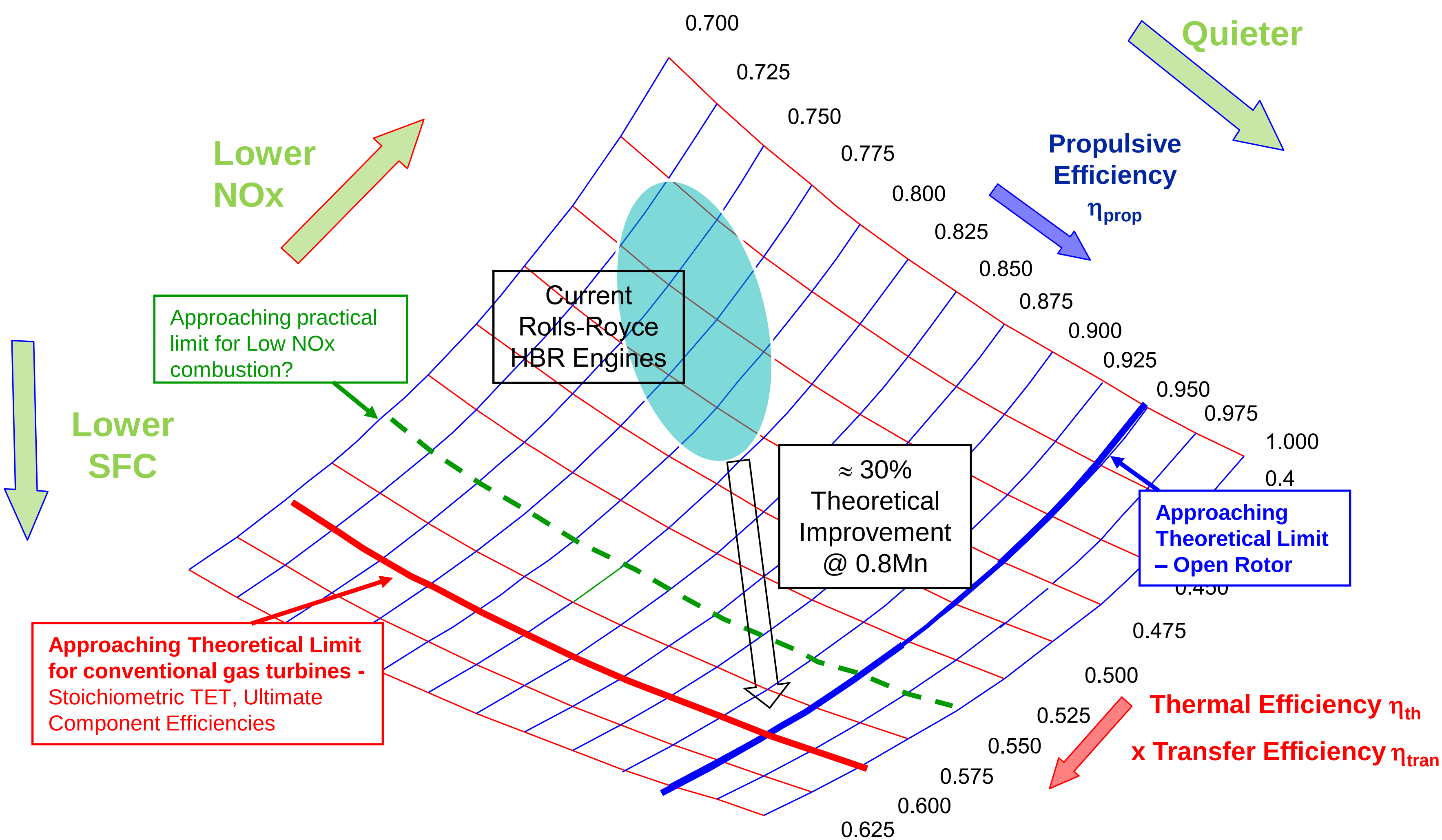

Driving thermal efficiency

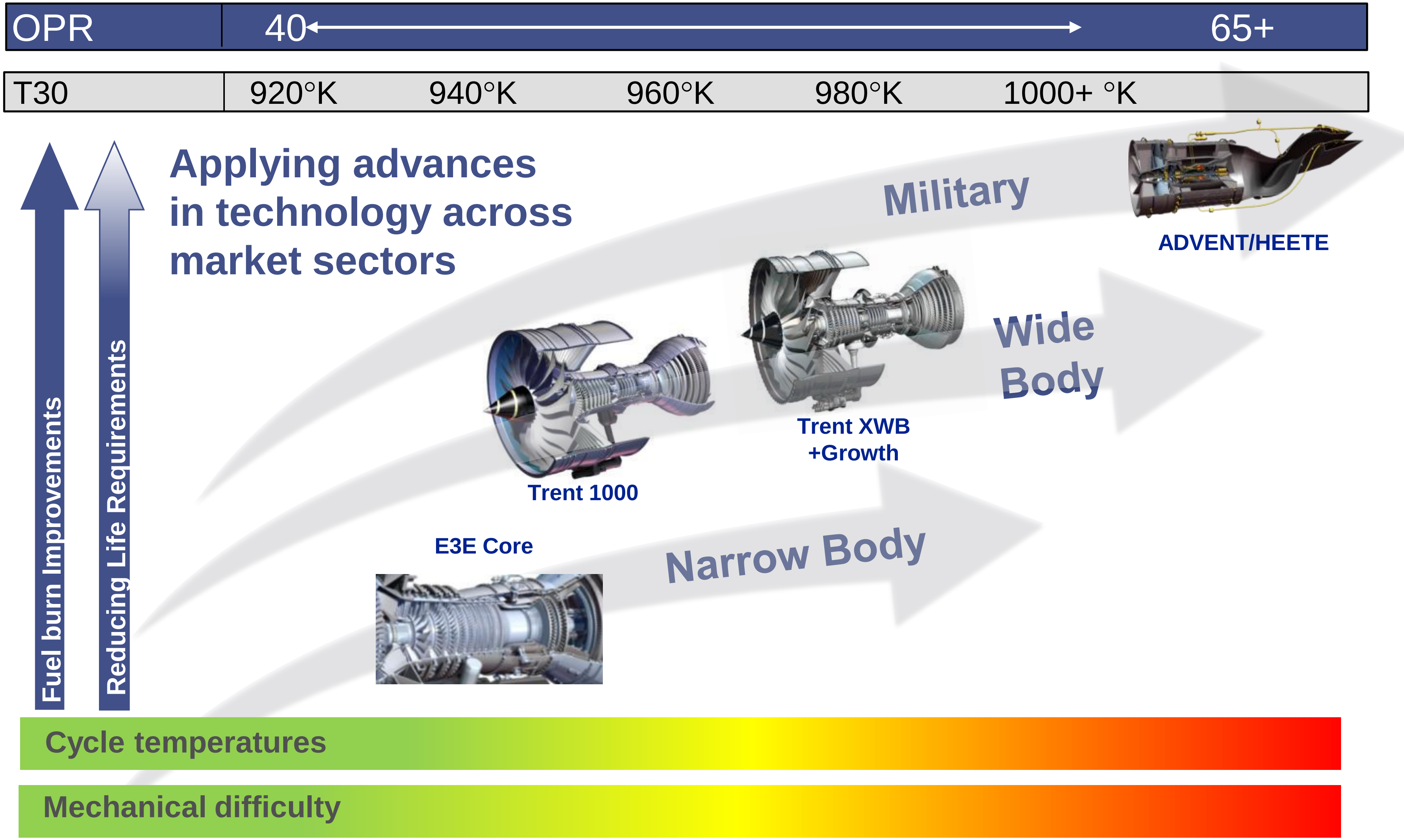

Driving propulsive efficiency

BPR	10+ ⟷ 50+
Technology	Direct Drive — UHBR Turbofan — Open Rotor

SFC

Fuel burn

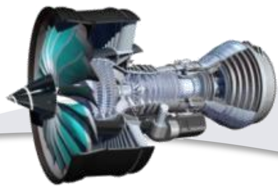

Advanced HBR turbofan
- Lightweight fan & LPT
- Integrated propulsion system
- High efficiency LP system

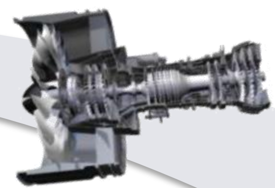

Geared-Drive turbofan
- Power gearbox
- High-speed LPT
- Variable Area Nozzle (VAN)

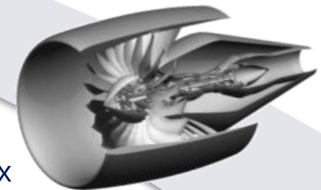

UHBR turbofan
- Power gearbox
- High-speed LPT
- Variable pitch fan / VAN
- Integrated slim-line nacelle / no TRU

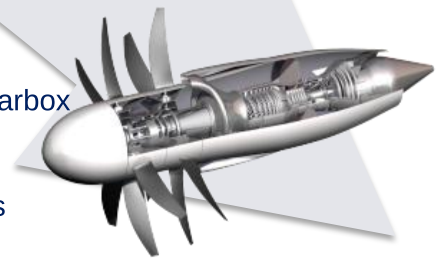

Open Rotor
- Counter rotating gearbox
- High-speed LPT
- Composite props
- Variable pitch props
- Integrated nacelle

Installation issues

Technical risk

Optimised Bypass Ratio

As Bypass ratio increases, then noise and efficiency improve

But as fan diameter increases then weight and drag of the LP system also increase

The optimum design point occurs where weight and drag balance the improving efficiency

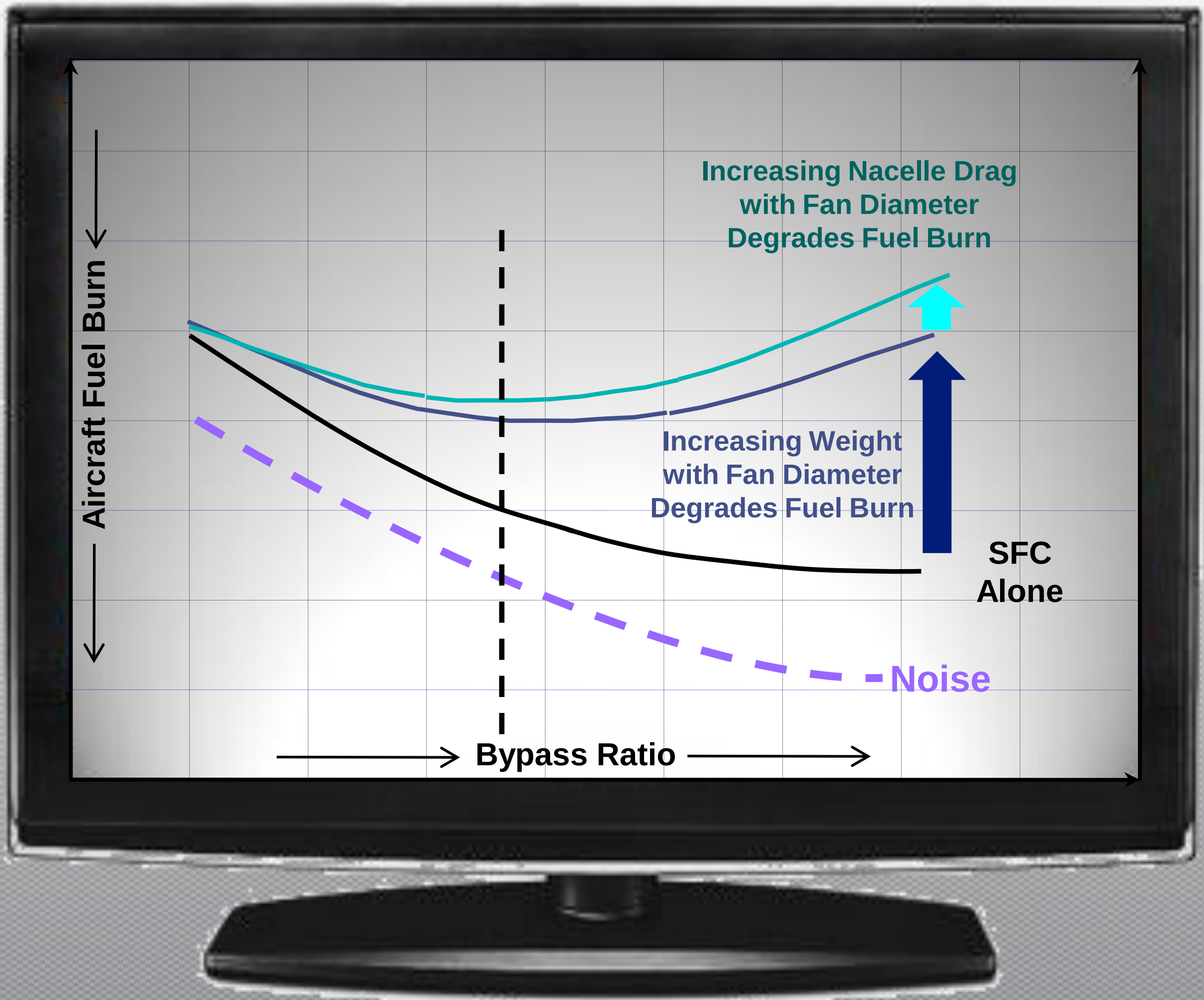

Gearing-up the turbine

As bypass ratio increases, the fan speed reduces and the number of stages of LP turbine increases – increasing the weight of the engine

A geared system increases the speed of the LP turbine and reduces the number of stages required

Consequently the pivot point occurs where the weight saved equals the weight added via the gear system

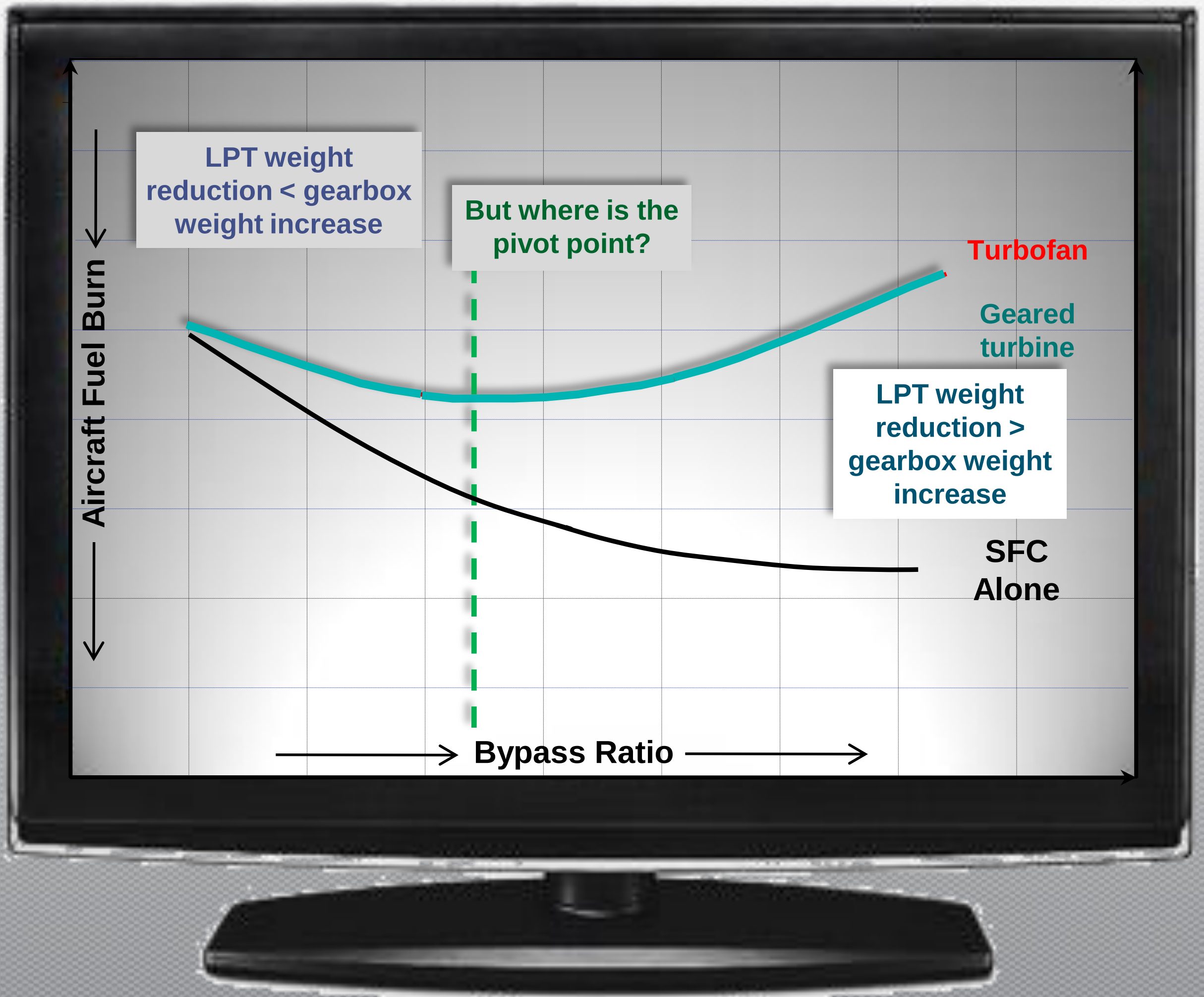

Gearing-up – the addition of advanced technology

Any improvement to the engine core is independent of engine architecture

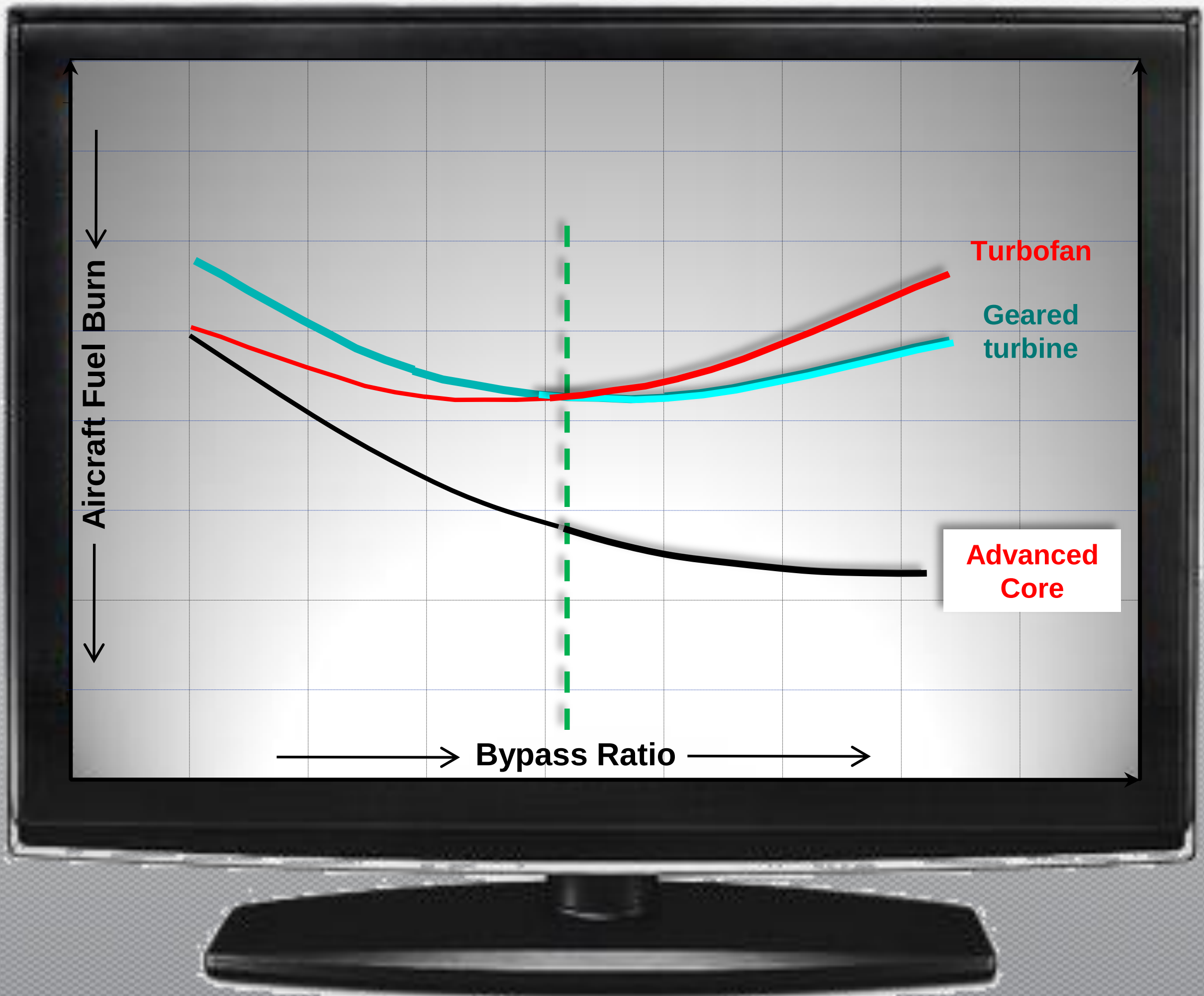

Gearing-up – the addition of advanced technology

Any improvement to the engine core is independent of engine architecture

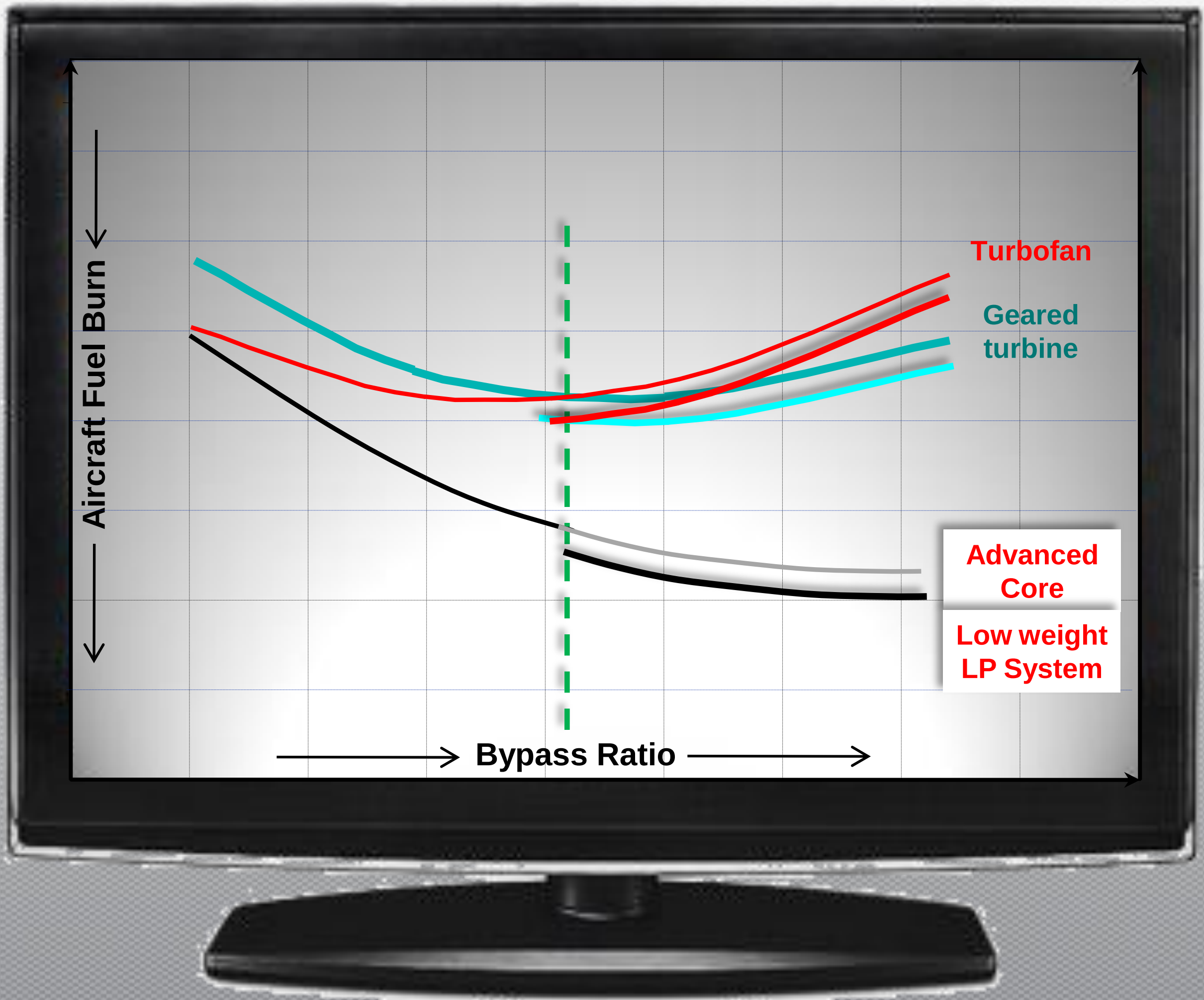

Propulsive efficiency comparison

150 seater

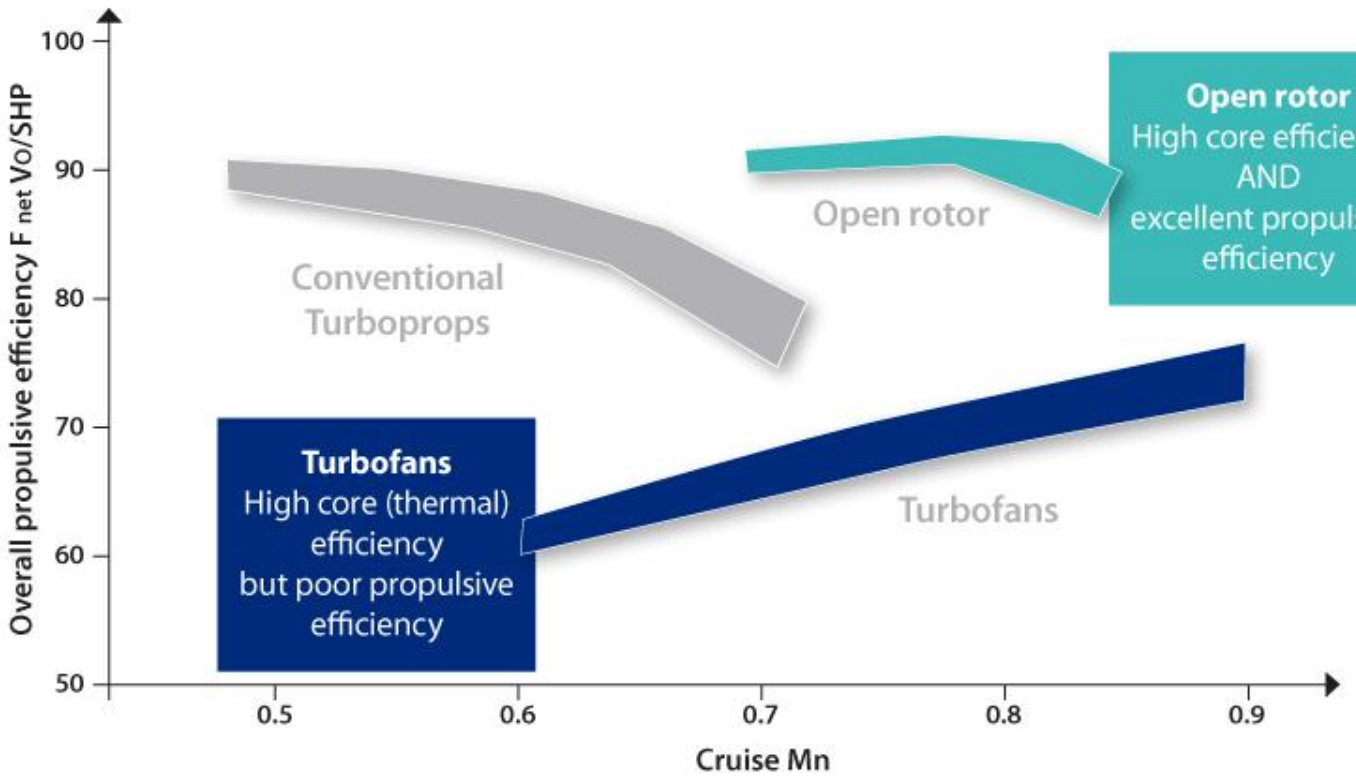

Open rotor

Vcom 14702

Vision 20 – open rotor

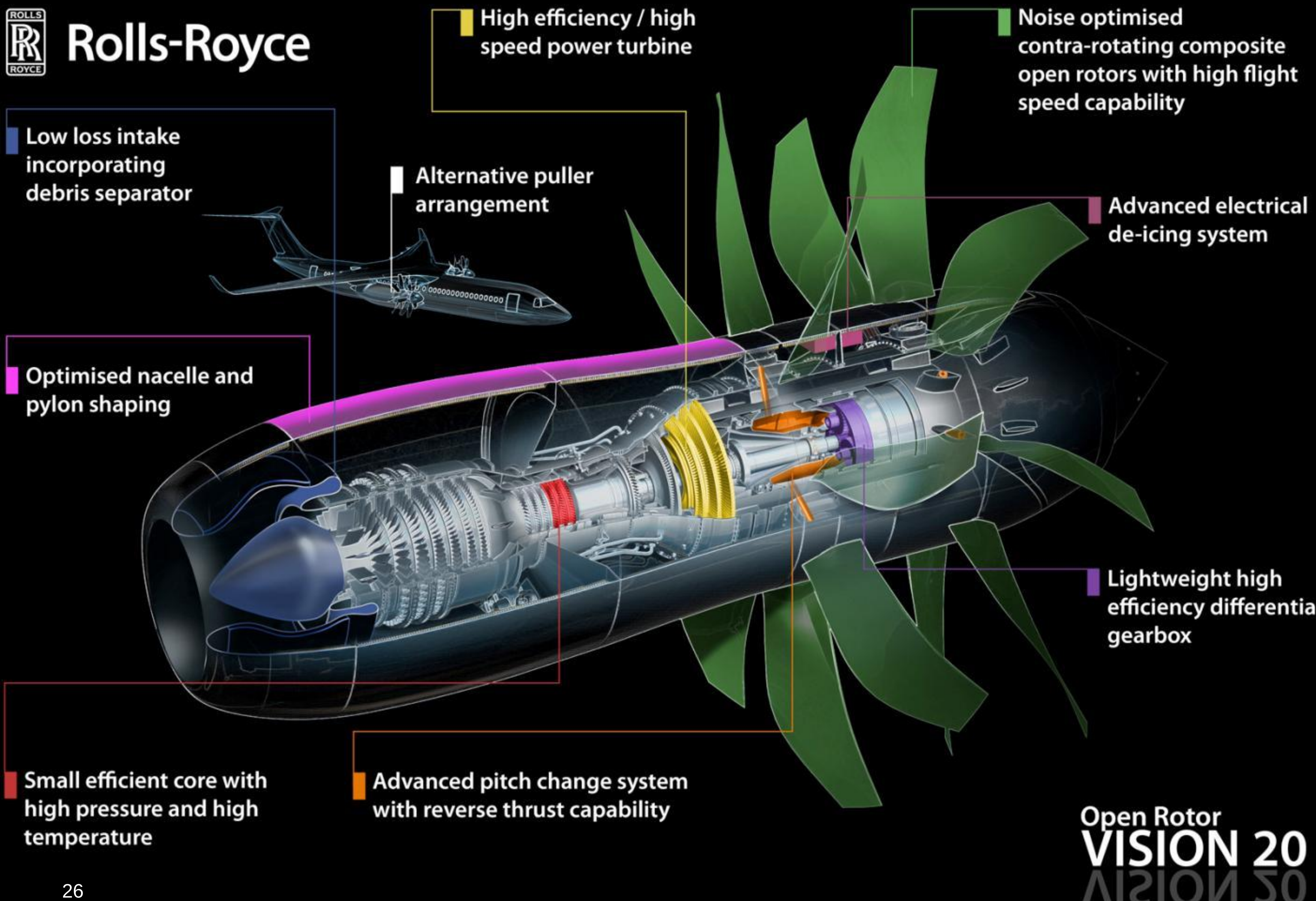

Engine / Aircraft configurations

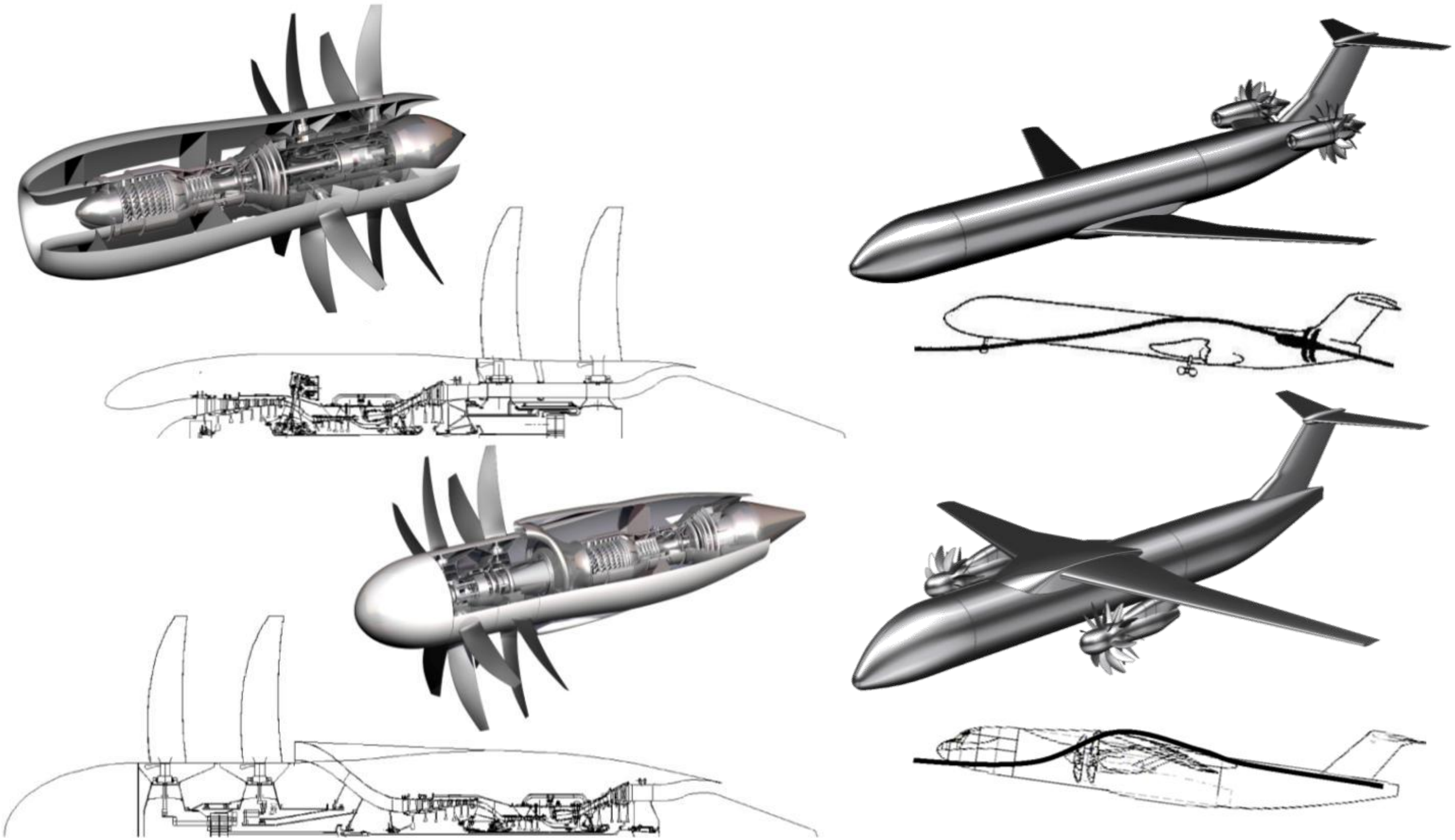

Fuel Consumption / CO2 improvements

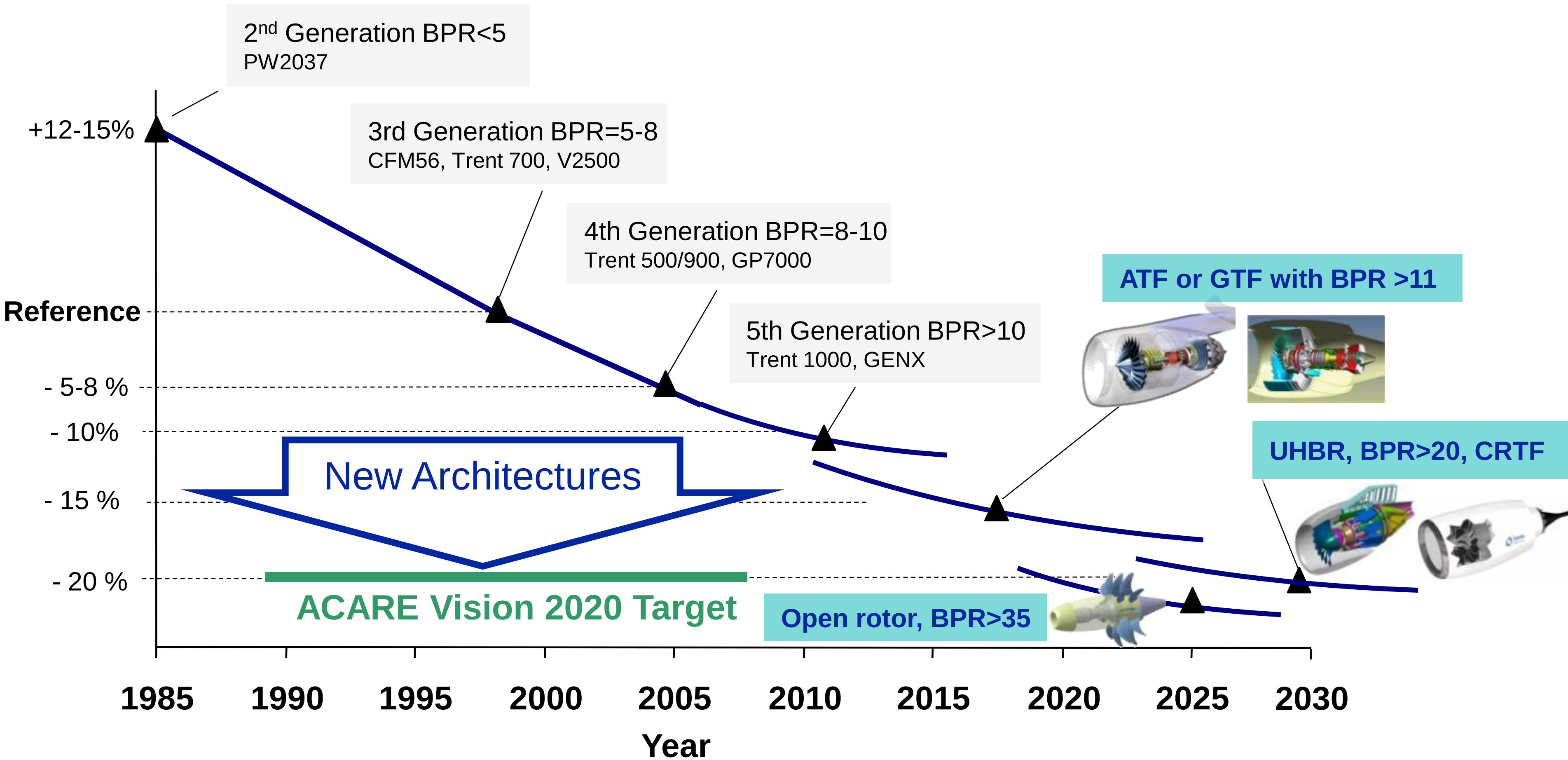

Future System Opportunities

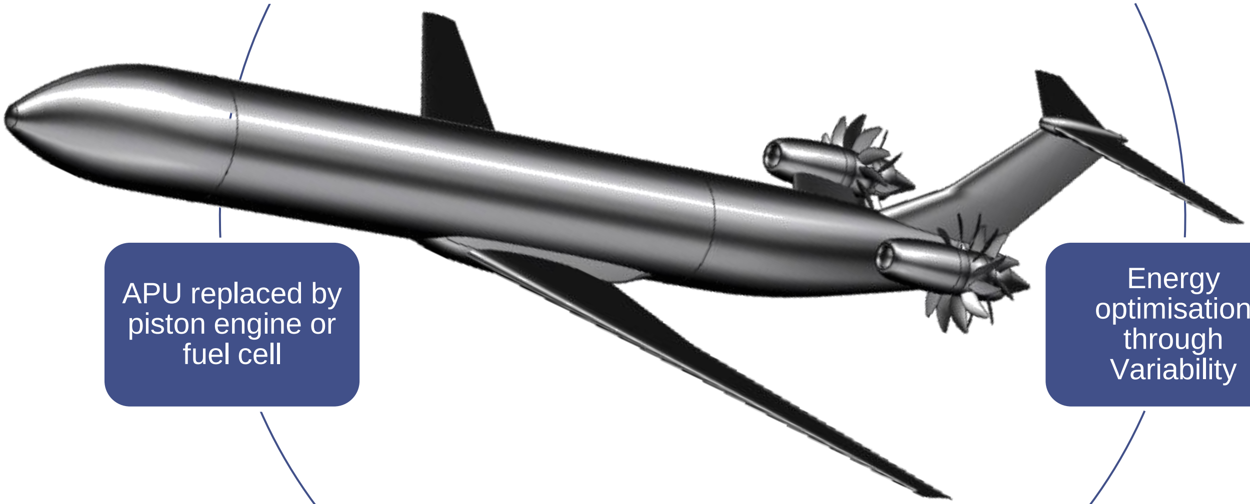

Energy recovery from exhaust and in descent

Energy optimisation through Power Management

Energy optimisation through Variability

Integrate APU and cabin air system

Electric taxi and engine start

APU replaced by piston engine or fuel cell

Lightweight electrical storage and solar cells on wing

Integrated more electric engine

Aircraft level interaction
- Integrated system simulation model
- Integrated power distribution system architecture
- Supports alternative manufacturing techniques (composite structure)

Power Electronic Units

Shared Oil-Cooling System
- Potential slim-line generator
- Heat management
- Reduce LRU count

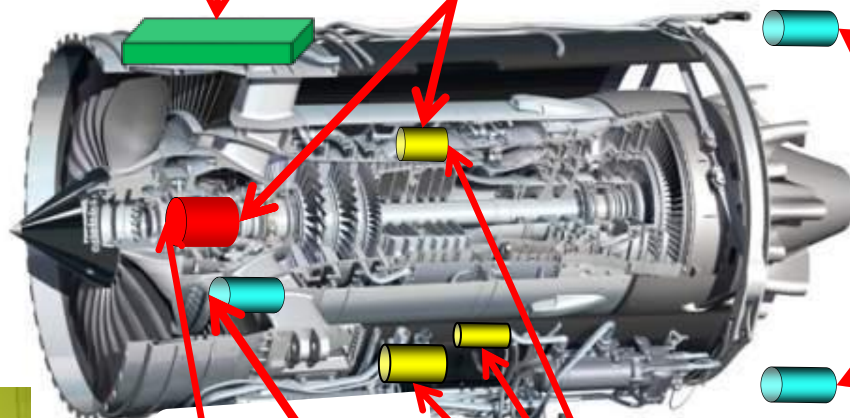

Electric Thrust Reverser Actuation

AGB Removed

Off Gearbox Generator

Electric Engine Actuators

Electric Oil Pump
- Flow rates
- Heat management

Fuel Pumps
- Reduction in heat to fuel
- Potential zero spill system

Servicing, maintainability and monitoring

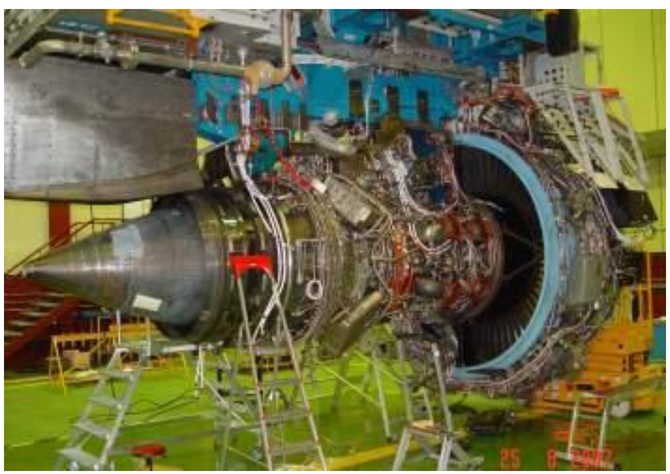

POA - Power optimised Aircraft

Potential Game Changers

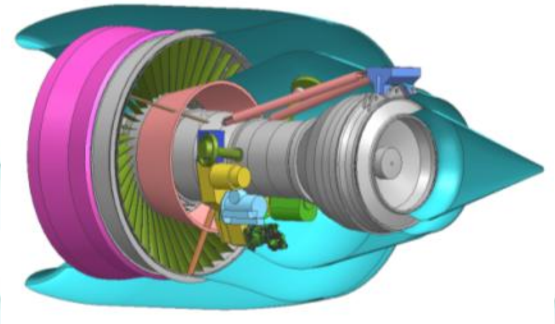

Hybrid Electric Propulsion

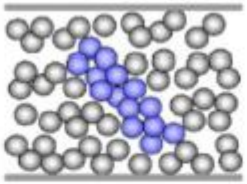

Materials

Engine – Airframe Optimization

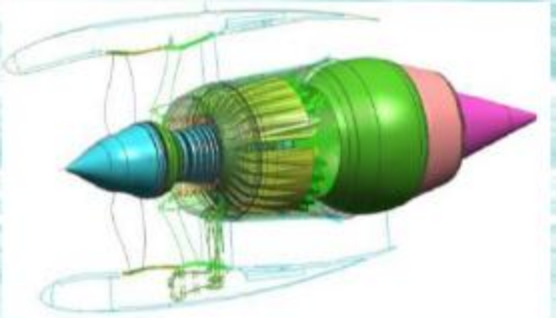

Advanced Cycles

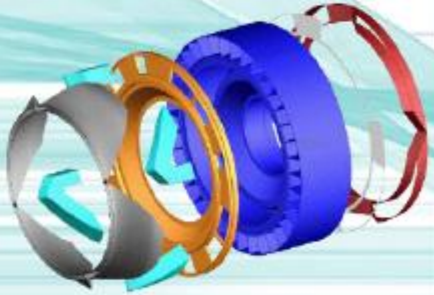

Pressure Gain Combustion

Adaptive cycles

…… and where can EASN help?

- **To develop & secure RR's & your Institutes future with new technologies, methods, processes through sharing of knowledge between all of us**
- **To generate views and options on technology which RR could not develop by in-house research**
- **To develop the next generation of RR Engineers by utilizing university education through R&T programmes**

Agenda

- *Rolls-Royce*
- *Aviation and the environment*
- *Flightpath 2050*
- *Future technologies*
- *Conclusion*

Conclusion

- Global warming is real and aviation makes a small but significant contribution
- Flightpath 2050 sets exacting targets which industry has agreed for 2050
- The *ACARE SRIA launched in September will chart the route to achieve this
- Novel propulsion systems will be key to achieving environmental targets
- Cooperation across Europe can provide the technology solutions
- It is an exciting time to be in propulsion technology

*Advisory Committee for Aviation Research in Europe - Research and Innovation Agenda

Delivering today,
investing for the future

Future technologies that could revolutionise propulsion?

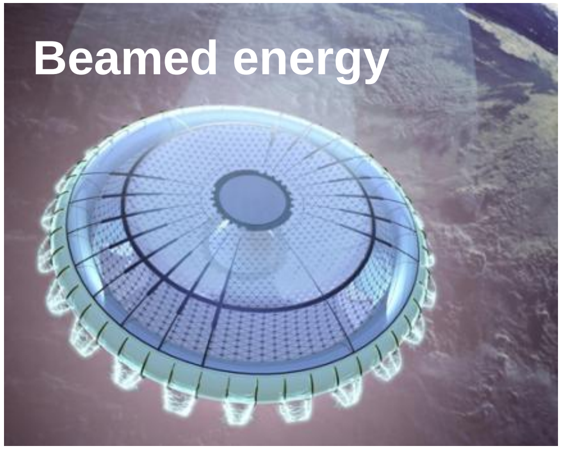

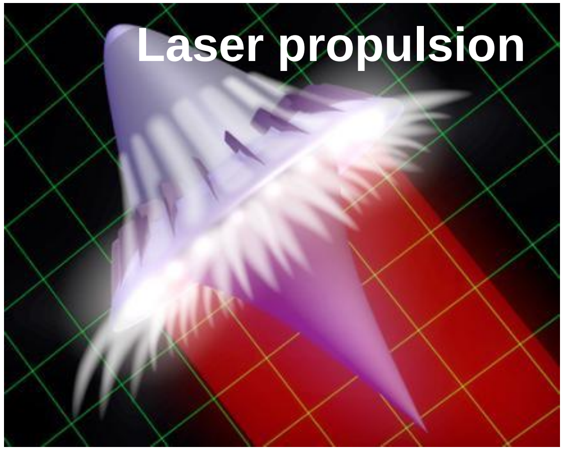

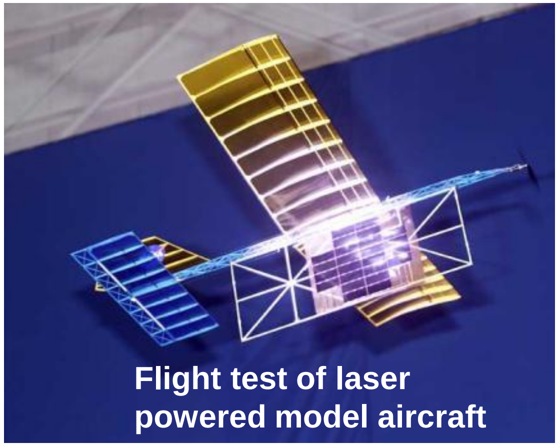

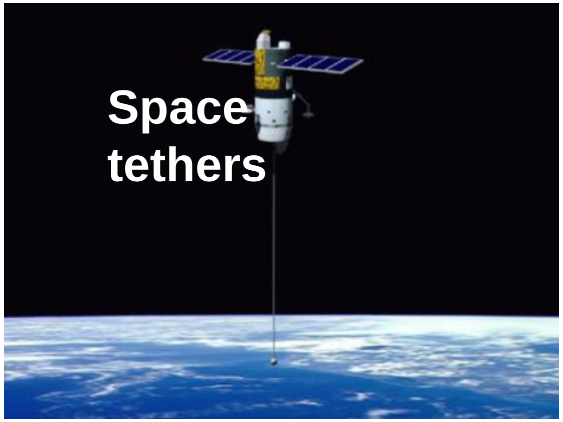

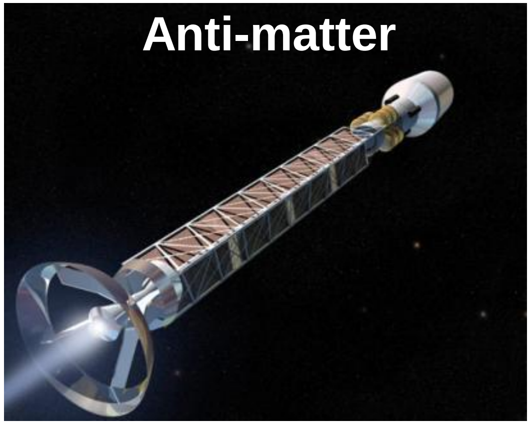

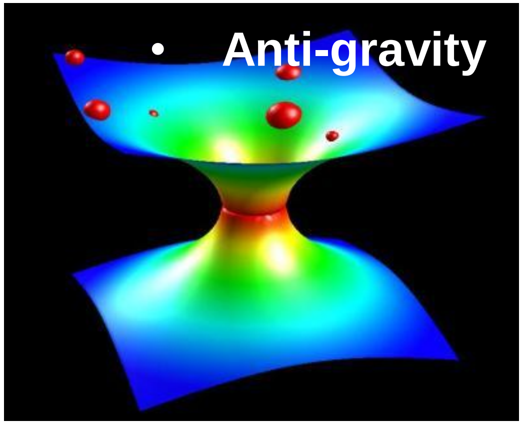

Driving Thermal Efficiency

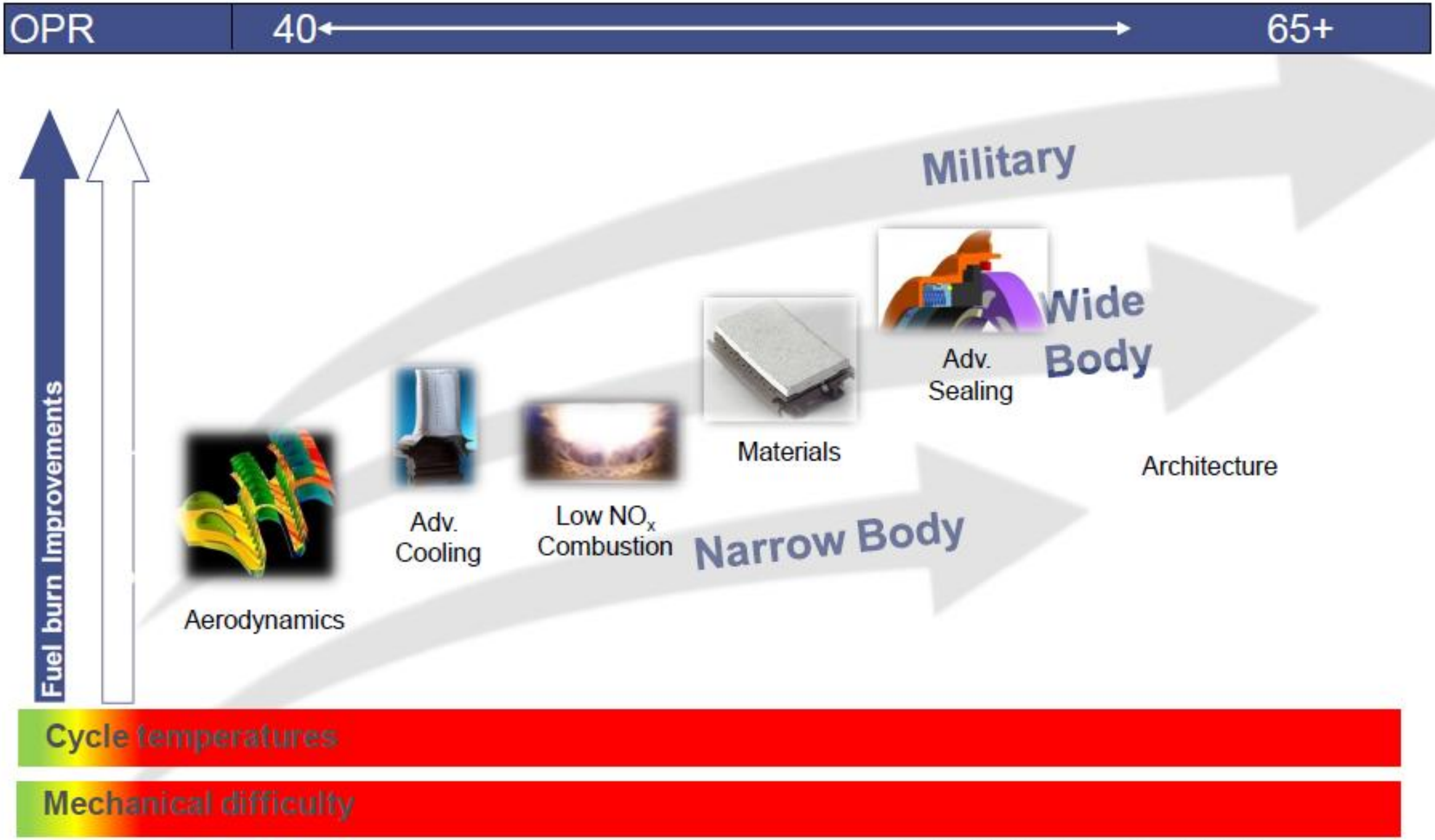

Electrical Power Systems (EPS) for Future Aircraft

Peter Malkin

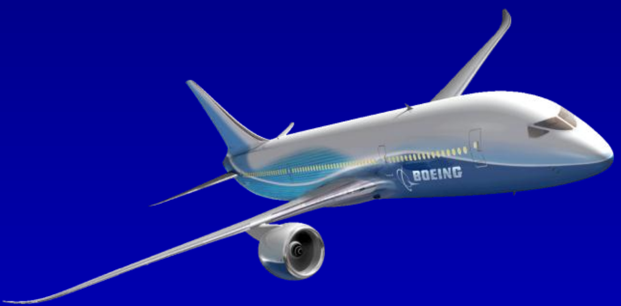

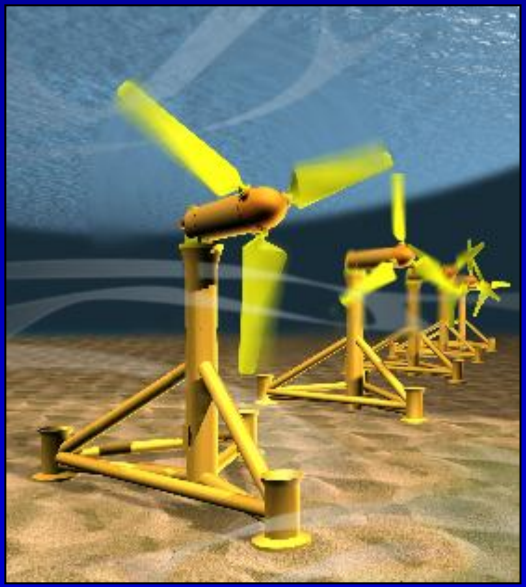

Contents

- The need for new aircraft designs
- BWB Hybrid Electric Distributed Propulsion Aircraft
- Electrical Power Systems requirements and current capabilities
- New technologies and their timescales
- High-Temperature Superconductors
- Summary and Conclusions

What are the drivers for radical change?

- Air travel is already under the spotlight from an environmental viewpoint.
  - Counter argument that CA represents only 2-4% of CO2 emissions
  - Other major areas (road transport and Powergen) will cut emissions radically
- Cost of Jet-fuel has risen dramatically
  - Now the largest cost to airlines
  - One airline has bought an oil refinery
  - Trends suggest this will increase in future
- However air travel growth is already >5% per year
  - This will increase the profile of this sector as a major CO2 target
  - Effect of altitude and contrails are complicating factors
  - Industry has set targets with ACARE and more aggressively with NASA N+3

Industry response

- Target set of >1% SFC reduction pa
- Has been achieved by improving GTs, move to composite aircraft, systems, MEA etc.
- However these are unlikely to continue indefinitely as these are mature technologies
- …and CO_2,NO_x and noise give conflicting drivers
- New entrants are coming into the civil aircraft market (China, Russia, Japan)…
- ..the industry may decide to look at step change technologies sooner rather than later!

NASA Subsonic Transport System Level Metrics

…. technology for dramatically improving noise, emissions, & performance

CORNERS OF THE TRADE SPACE	N+1 (2015)*** Technology Benefits Relative to a Single Aisle Reference Configuration	N+2 (2020)*** Technology Benefits Relative to a Large Twin Aisle Reference Configuration	N+3 (2025)*** Technology Benefits
Noise (cum below Stage 4)	- 32 dB	- 42 dB	- 71 dB
LTO NOx Emissions (below CAEP 6)	-60%	-75%	better than -75%
Performance: Aircraft Fuel Burn	-33%**	-40%**	better than -70%
Performance: Field Length	-33%	-50%	exploit metroplex* concepts

*** Technology Readiness Level for key technologies = 4-6

** An additional gains may be possible through operational improvements

* Concepts that enable optimal use of runways at multiple airports within the metropolitan areas

Step–Change Aircraft Design Options

- There is a strong view that major savings can be made by addressing the propulsive efficiency of commercial aircraft
- One of the key options is to move towards a blended-wing-body (BWB) with distributed propulsion (DP)
  - Conventional propulsion would create too much drag and limit the benefits of this approach
- However various ways of creating a distributed propulsion systems have been examined and found to be unsatisfactory.
- The best way of achieving this would be to use a hybrid-electrical system to drive a large number of small fans

Hybrid-electric Distributed Propulsion (HEDP) advantages

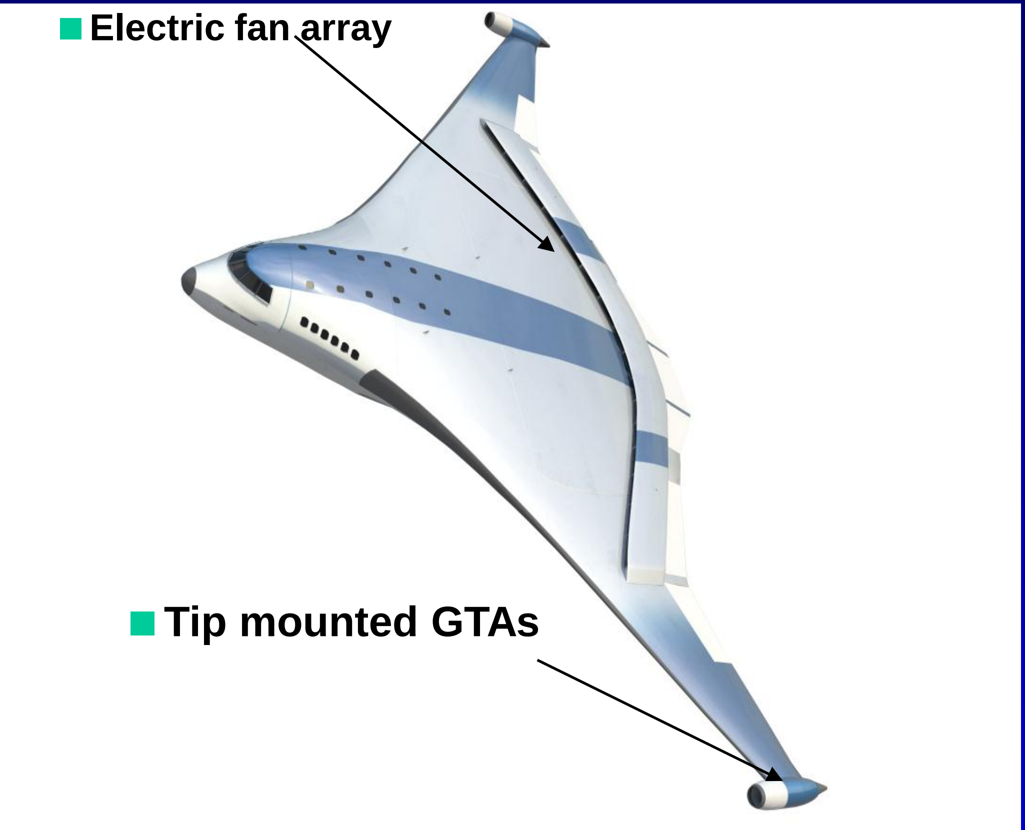

Fuel Burn and Emission:

- 2 large engine cores and multiple motor-driven fans give very high effective BPR.
- Higher propulsive efficiency via spanwise BLI and wake fill-in
- High engine core inlet pressure recovery
- Reduced Cdi (induced drag) due to wing-tip mounted engine core/electric generator

Noise:

- Low community noise due to low pressure fans, airframe shielding
- Low core jet exhaust noise
- Low cabin noise due to remote location of propulsion systems

Models show that this approach can meet'N+3' targets

Courtesy of NASA

What are the design benefits of HEDP?

- Uses GTs to provide electric power to multiple electric fans (c.f Electric Ships)
- Decouples propulsive device from the power-producing device gives a paradigm shift to design principles
    - For the fans, this gives very high effective BPR and design flexibility.
    - Speed of the power turbine shaft in the turbine engine is independent of the propulsor shaft speed. -> Electrical system as a gearbox
    - Minimal engine core jet noise due to maximum energy extraction
    - Symmetric fan thrust with an engine failure (rudder is no longer sized to OEI condition) & Asymmetric thrust for vehicle control
    - Easy to take other electric power source such as fuel cell, battery, etc.
    - Fans arranged to give Boundary Layer Ingestion with reduced drag

Electrical Power Systems

- This whole concept relies on Electrical Power Systems operating at multi-megawatt levels. Is this possible? Can aircraft be powered by electrical power systems?

EPS Systems

- EPS have evolved very little in the last 100 years with their major applications in the Power Generation and Transmission and Large Industrial fields.
- In both these fields the main drivers have been for simplicity and low costs. Weight and volume are not generally issues in these markets.
- It is only recently that new markets have developed in transport applications including rail, Marine, Automotive and Aerospace.
- These new markets are bringing through new technologies

Multi-megawatt electrical power systems

- The hybrid –electric principal on a multi-megawatt scale has already been demonstrated and is in service..
- ....for example on recent large naval ships
- However the electrical system here weighs well over 100 tons!

- However these are very low-speed applications

New Electric Power Technologies

- **New Semiconductors**
  - Silicon devices are not well suited to Power applications. At last better materials are now available (SIC and GaN) and even better materials under development (Diamond)
    - Both SiC and GaN have performance factors(Figures of Merit) between 400 -2000 times that of Silicon.
    - Diamond has FoMs between 10,000-50,000 that of Silicon
    - High quality 6" wafers of SiC are available now, Small wafers of GaN are available now. Diamond semiconductors are not yet on the market
- **Energy Storage**
  - Batteries and capacitors are improving with some breakthroughs expected soon.
- **High-temperature Superconductors**
  - This is the most crucial development for these new aircraft
  - I will now focus on this technology

Superconductivity – the basics

- Complete loss of resistance in some metals
  - discovered in 1911:
  - examples: Al, Hg, Pb, Sn, … but not Cu
  - Typically current densities can be increased by two or three orders of magnitude!
- Low temperature superconductors (LTS)
  - Liquid helium cooled ~ 4K
  - examples: Nb-Ti, Nb_3Sn
  - Widely used for medical scanners
- High Temperature Superconductors (HTS) examples: BSCCO, YBCO ~ 77K (liquid nitrogen)
- Newcomer: MgB_2 ~ 30K (He gas or liquid H_2 coolant)
  - However HTS suffers from a poor reputation –why?

The Superconductivity Revolution

Press Coverage of High temperature Superconductivity

What stirred all the excitement at that tumultuous meeting in March was a discovery that could change the world, a startling breakthrough in achieving an esoteric phenomenon long relegated to the backwaters of science: superconductivity. That discovery, most scientists believe, could lead to incredible savings in energy; trains that speed across the countryside at hundreds of miles per hour on a cushion of magnetism; practical electric cars and aircraft; powerful, yet smaller computers and particle accelerators; safer reactors operating on nuclear fusion rather than fission and a host of other rewards still undreamed of.

The date was May the 11th 1987

Current HTS Technology

- Ceramic Copper Oxides
  - These were the materials discovered in the 1980s that launched the interest in HTS materials. (BiSSCO and YBCO)
  - Both give high critical temperatures between 70 and 80K but have proved very difficult and expensive to manufacture in quantity.
  - Lot of work (US and Japan) can be made in bulk or tapes but wire still not possible. High costs and very fragile.
  - These material issues have been the major cause of delays in delivering this technology
- MgB2
  - This is a relatively new material discovered in 2001 but largely ignored as it has a Tc of only 40K
  - However it is a cheap and relatively easy material to manufacture and can be produced in a wire that can almost be handled as copper wire!
    - In fact the lower Tc turns out to be a minor issue….

Cooling the New Superconductors

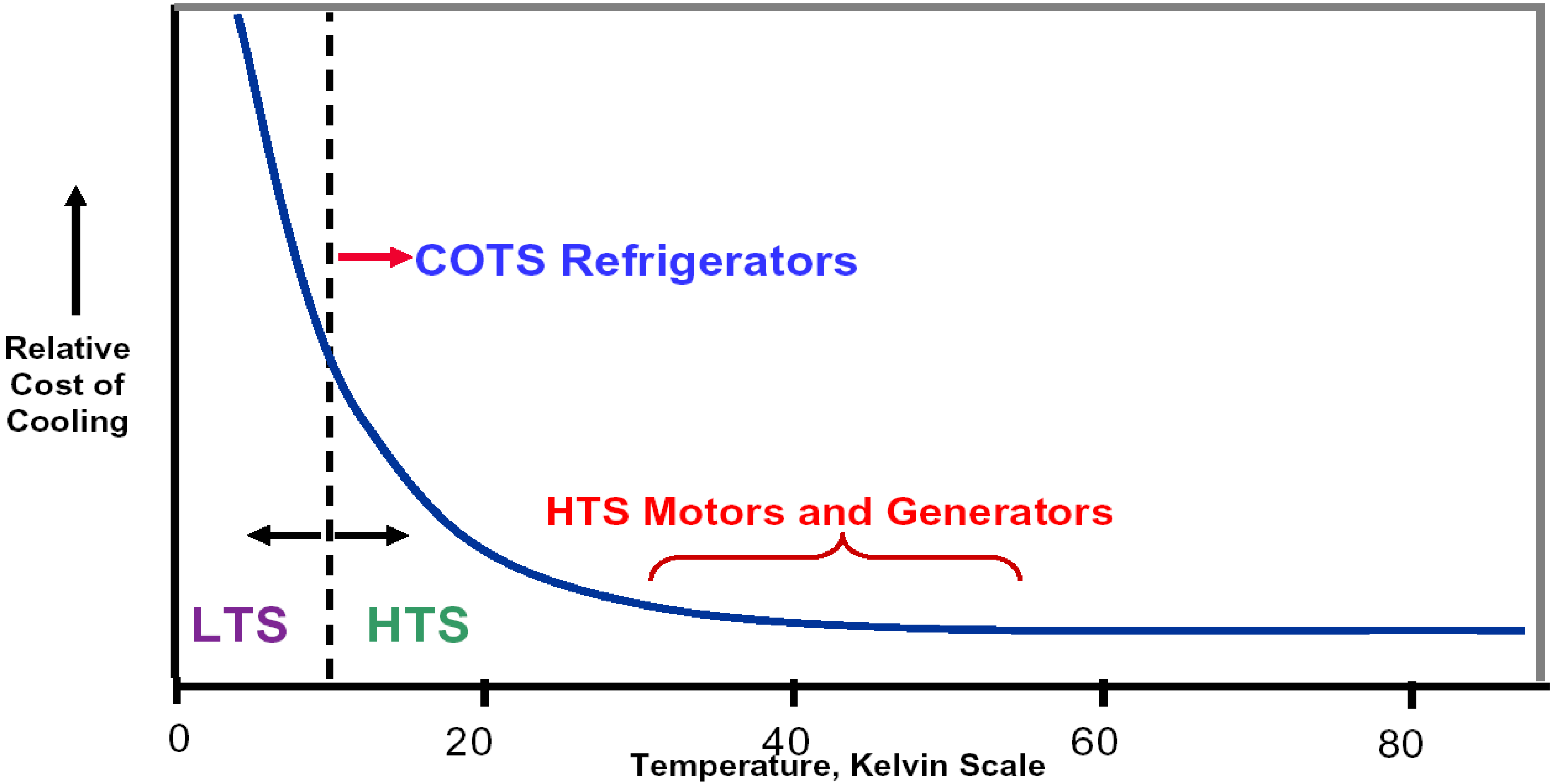

HTS Enables Reliable and Cost Effective Cooling

Superconductor Formats for Machine Applications

- Tape format - BSCCO, YBCO
  - Susceptible to variations in magnetic field perpendicular ($B_\perp$) to the tape
    - Risk of quench (i.e. return to resistive state)
    - Use Flux Diverters to reduce $B_\perp$
      - Diverters compromise rotor rigidity
        - » Laminated rotor
    - Tapes not used in conventional m/c design as DC only
- Round Wire format – only MgB_2
  - Conventional winding technology
  - Conventional rotor body – single piece forging
  - Use in AC systems as normal wire.

Superconducting (HTS) Electrical Machines

- **Present HTS Machines**

  A few large machines have been produced using a BiSSCo materials mainly aimed at Marine applications.

  These have been complex and expensive to manufacture for several reasons;

  The material is very costly (high silver content)

  Due to the nature of the material these have been superconducting rotor machines. This requires rotating cooling couplings which are difficult and add much complexity.

  Nevertheless these still give improvements over conventional machines

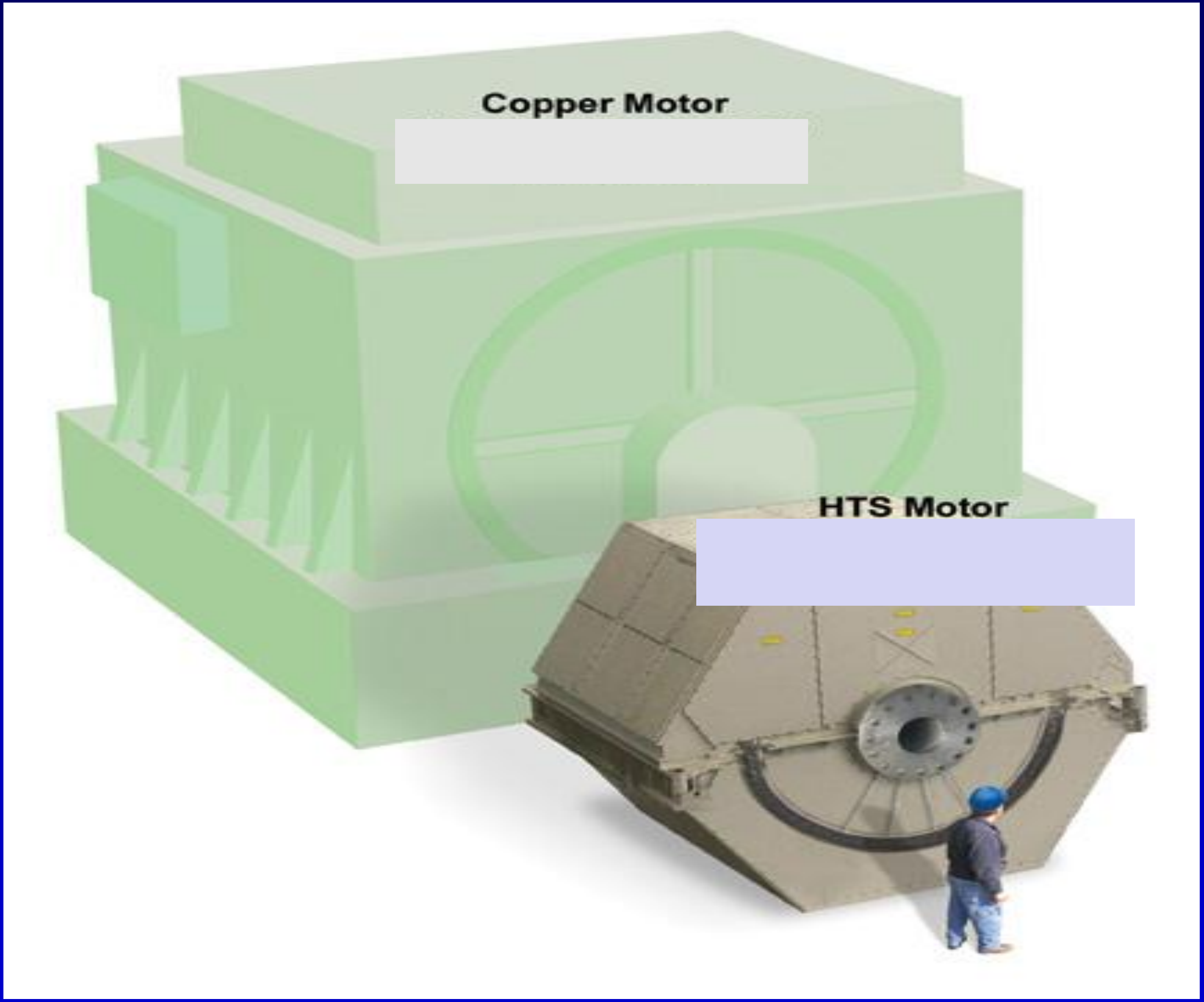

- An early US designed Marine motor showing the difference in size

Next generation HTS Machines

- Work is ongoing in the UK to develop HTS machines based on MgB_2 wire.
- An HTS stator machine based on MgB_2 wire is now being built in the UK.
  - This is a vital step to make these machines practical
- The most recent MgB_2 wire is capable of carrying up to 3×10^6 amps/cm^2
- The power density of these new machines is not yet known but seems likely to come close to the required weight targets

Low Temperature – Cryogenic Operation

- MgB2 operates as a superconductor below 39K
- Whilst this is a significant improvement over LTS systems (~5K) significant cooling would be required.
- However the cost and size of mechanical cryo-coolers has improved significantly recently as has their reliabilities
- However there has been no requirement for a lightweight cryo-cooler system and this would have to be developed
- Another interesting alternative would be to use a cryogenic liquid and Hydrogen gives a good temperature match for MgB2
  - This would undoubtedly give a lighter aircraft
  - And could be used partially or totally as fuel
  - Power system losses would pre-heat the fuel

Conclusions

- The HEDP concept is a radical but promising concept.
- The viability of this concept depends crucially on developing a high power density electrical power system.
- However new high temperature superconducting materials are available now that could deliver these systems.
- These seem to be a focus of attention in the US
- More work needs to be done to explore the potential impacts of HTS and other new electrical technologies in aerospace

Superconducting Surface – varies with material

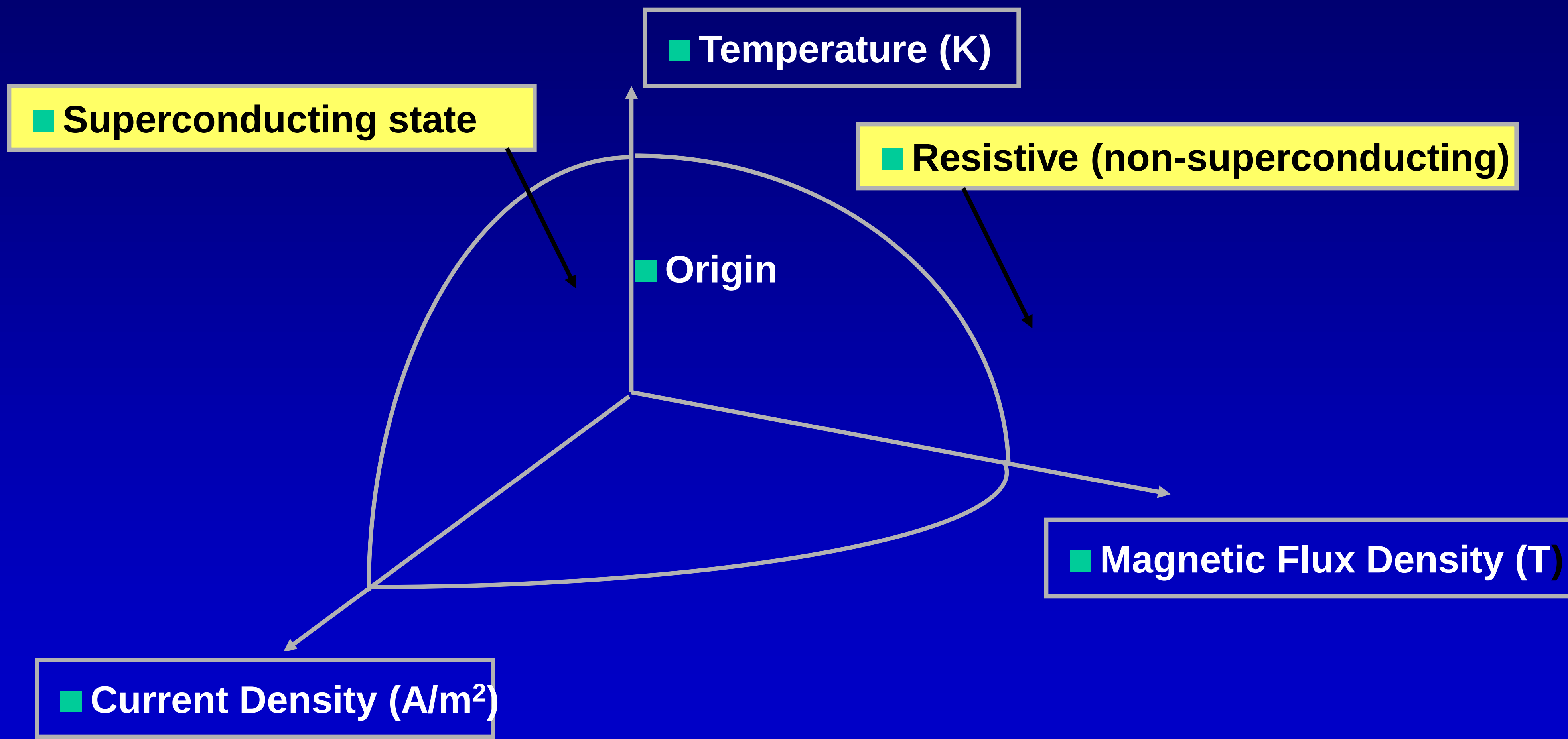

The EU Research Framework Programmes Contributing to Europe's Vision for a Sustainable Aviation

AWIATOR Project A340 Flight Test (Nov. 2006)

Dietrich Knoerzer
DG Research & Innovation
RTD-H.3 Aeronautics

Prague, 30th October 2012

European Commission

Content

- Policy Related Framework
- Environmental Issues
- Europe's Strategic Approach for Aviation
- Aeronautics in the Framework Programme
- ‘Horizon 2020’ and the Future

European Commission

European Commission President José Manuel Barroso

*'The next Commission needs to maintain the momentum towards a **low emission economy**, and in particular towards decarbonising our electricity supply and the **transport sector** – all transport, including maritime transport and **aviation**, as well as the development of clean and electric cars.'*

(From : Political guidelines to the next Commission, Brussels, 3 Sept. 2009)

The European Union

European Commission

President
J. M. Barroso

proposes

(e. g. 'Horizon 2020')

Annual Budget
112 billions €

Amendments

Amendments

Council of the European Union

decides

Presidency
changes every
6 months

Co-decision procedure

European Parliament

is consulted, co-decides

785 representatives
elected directly
by citizens

Court of Auditors

advises

Committee of the Regions

advises

European Economic and Social Committee - European Investment Bank -
European Central Bank - European Ombudsman - European Data Protection Supervisor - ...

Policy related Framework:

Global Energy Use in Transport (left) and Use of Biofuels in Different Transport Modes (right) in 2050

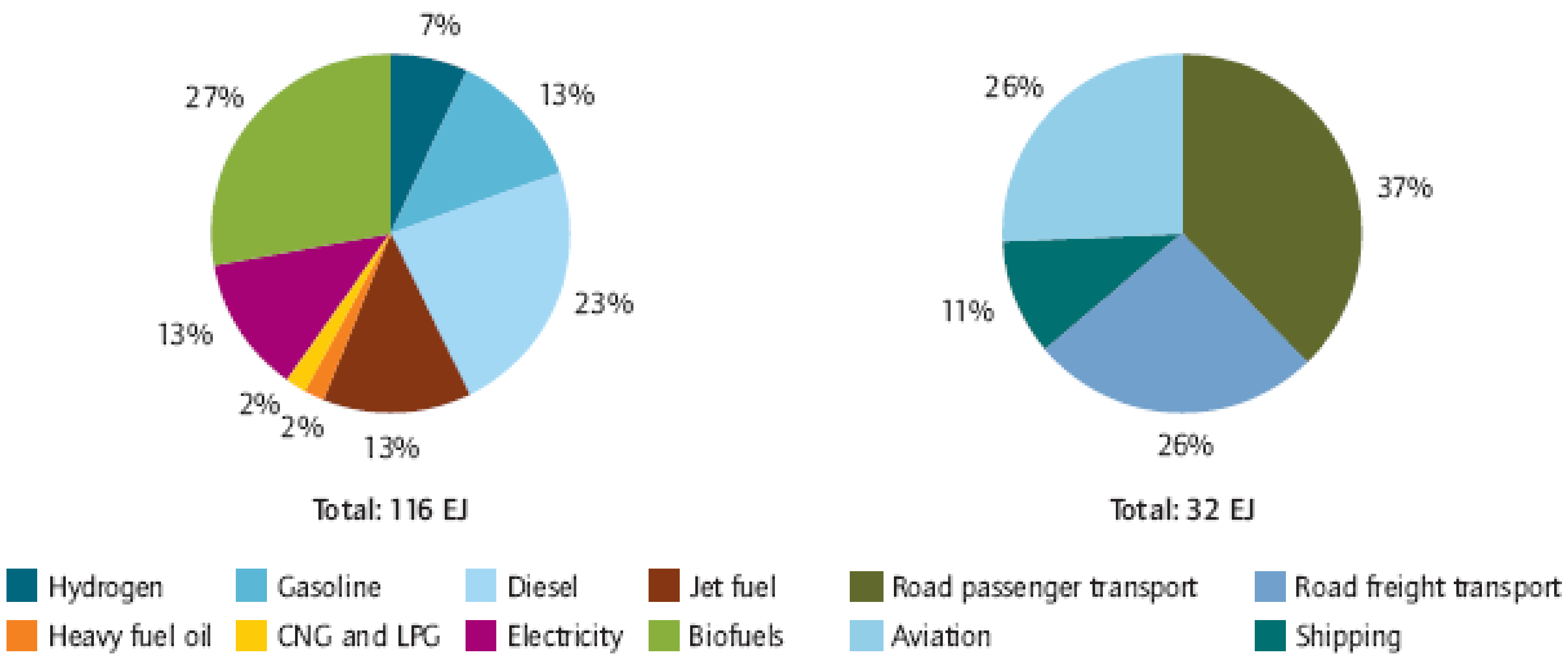

Note: CNG= compressed natural gas; LPG= liquefied petroleum gas.

Source: IEA, 2010c.

Industrial Framework

European Commission

CO_2 Emissions from Commercial Airlines Global Fuel Burn

(Economic Model)

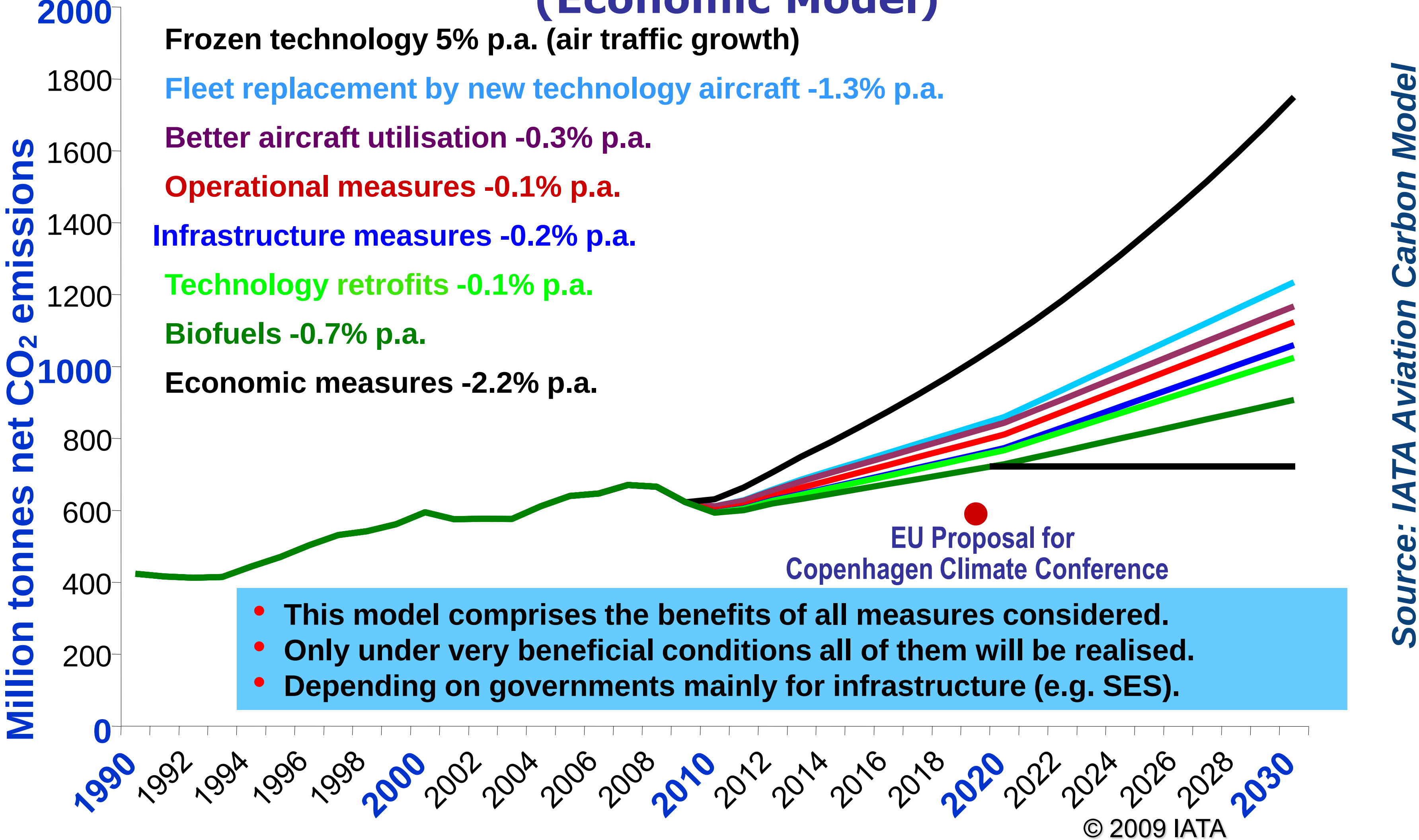

The EU Emission Trading Scheme (ETS) for Aviation from 2012

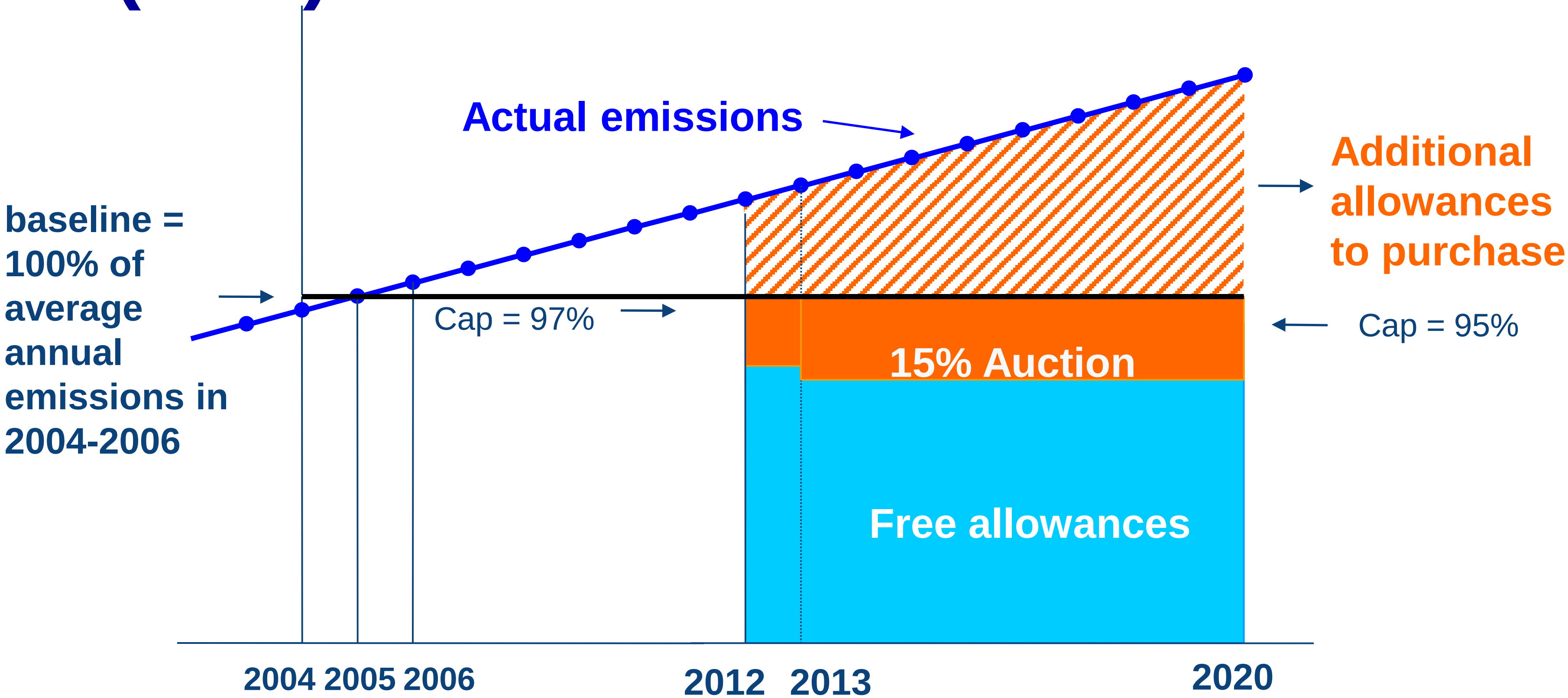

Source: IATA Training & Development Institute

Lufthansa Biofuel Tests on Scheduled Flights
(2011)

// Biofuel in practical tests

- Duration: 6 months
- Type: Airbus A321
- Biofuel ratio: 50% on one engine
- Each litre is produced sustainably

In the six-month practical trial involving biosynthetic fuel, 1187 biofuel flights were operated between Hamburg and Frankfurt. According to initial calculations, CO2 emissions were reduced by 1471 tons. Total consumption of the bio-kerosene mix amounted to 1,556 tons.

The highlight of the biofuel trial at Lufthansa was the first scheduled transatlantic flight to the United States on 12th Jan. 2012. A Boeing 747-400, carrying about 40 tons of a biosynthetic fuel mix, flew from Frankfurt to Washington.

Policy related Framework:

European Commission

Addressing Aviation's Climate Impacts

- **FP7 Research and Development of New Technologies**
  - Advanced technologies for next generation aircraft (Level 1 & Level 2)
  - Clean Sky Joint Technology Initiative (€1.6 billion over 7 years)
  - Sustainable alternative fuels
- **ATM Modernisation:** Single European Sky, SESAR Joint Undertaking
- **New Standards:** Through ICAO, e.g. new aircraft CO_2 standard
- **Market-Based Measures**
  - **EU Emissions Trading Scheme ETS for Aviation**
    - gives a long-term, predictable commercial incentive to use things like biofuels

Goals of 'Vision 2020' and ACARE

ACARE

2000

- 80% cut in NOx emissions
- Halving perceived aircraft noise
- Five-fold reduction in accidents
- Air traffic system capable of handling 16 million flights a year
- **50% cut in CO2 emissions per passenger/km**
- 99% of all flights within 15 min. of timetable

2020

Airframe 20-25%

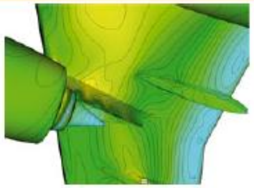

Engines 15-20%

Operations 5-10%

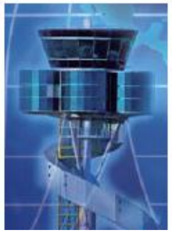

How is the 50% CO_2 Reduction Achieved ?

ACARE
Achievements so far

European Commission

A comprehensive response to Vision 2020

Strategic Research Agenda

- _Responding to society's needs_
- _Securing global leadership for Europe_

SRA-1

SRA-2

Addendum

A decade of Successful Innovation

New thinking to go beyond 2020

Flightpath 2050

SRIA- 2012

www.acare4europe.org

Flightpath 2050

Vision 2050

- Responding to society's needs
- Securing global leadership for Europe

Five Objectives of the Strategic Research & Innovation Agenda

- Meeting Societal and Market Needs
- Maintaining and Extending Industrial Leadership
- Protecting the Environment and the Energy Supply
- Ensuring Safety and Security
- Prioritising Research, Testing Capabilities & Education

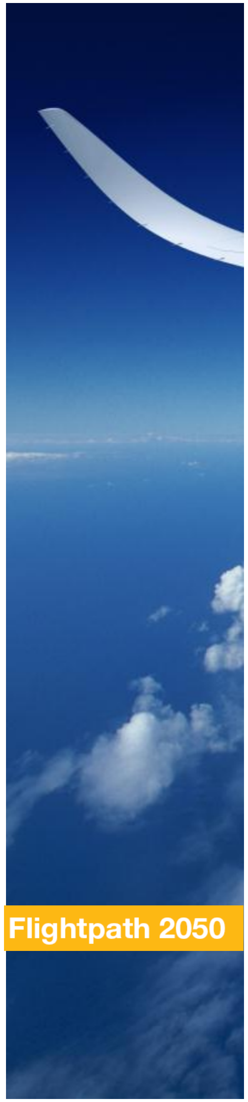

Europe's Vision for Aviation 'Flightpath 2050'

Protecting the Environment and the Energy Supply

- **75% reduction in CO_2 emissions** per passenger kilometre to support the ATAG target, a 90% reduction in NO_x emissions, 65% reduction of the perceived noise (Reference: 2000).
- Aircraft movements are emission-free when taxiing.
- Air vehicles are designed and manufactured to be recyclable.
- Europe is established as a centre of excellence on **sustainable alternative fuels**
- Europe is at the forefront of atmospheric research

Europe's Vision for Aviation 'Flightpath 2050'

Prioritising Research, Testing Capabilities and Education

- European research and innovation strategies are jointly defined by all stakeholders
- Networks of multi-disciplinary technology clusters are created
- Strategic European aerospace test, simulation and development facilities are identified, maintained and continuously developed
- Students are attracted to careers in aviation. Courses offered by European Universities closely match the needs of the Aviation Industry

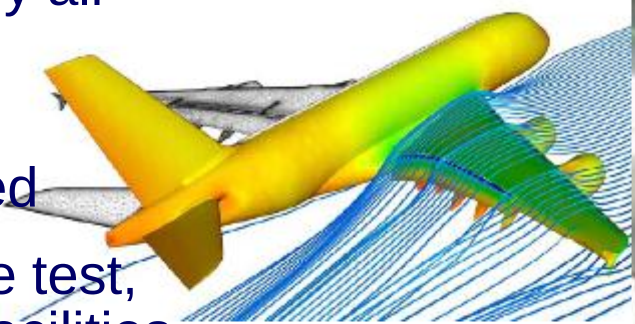

European
Commission

States Contributing to FP7

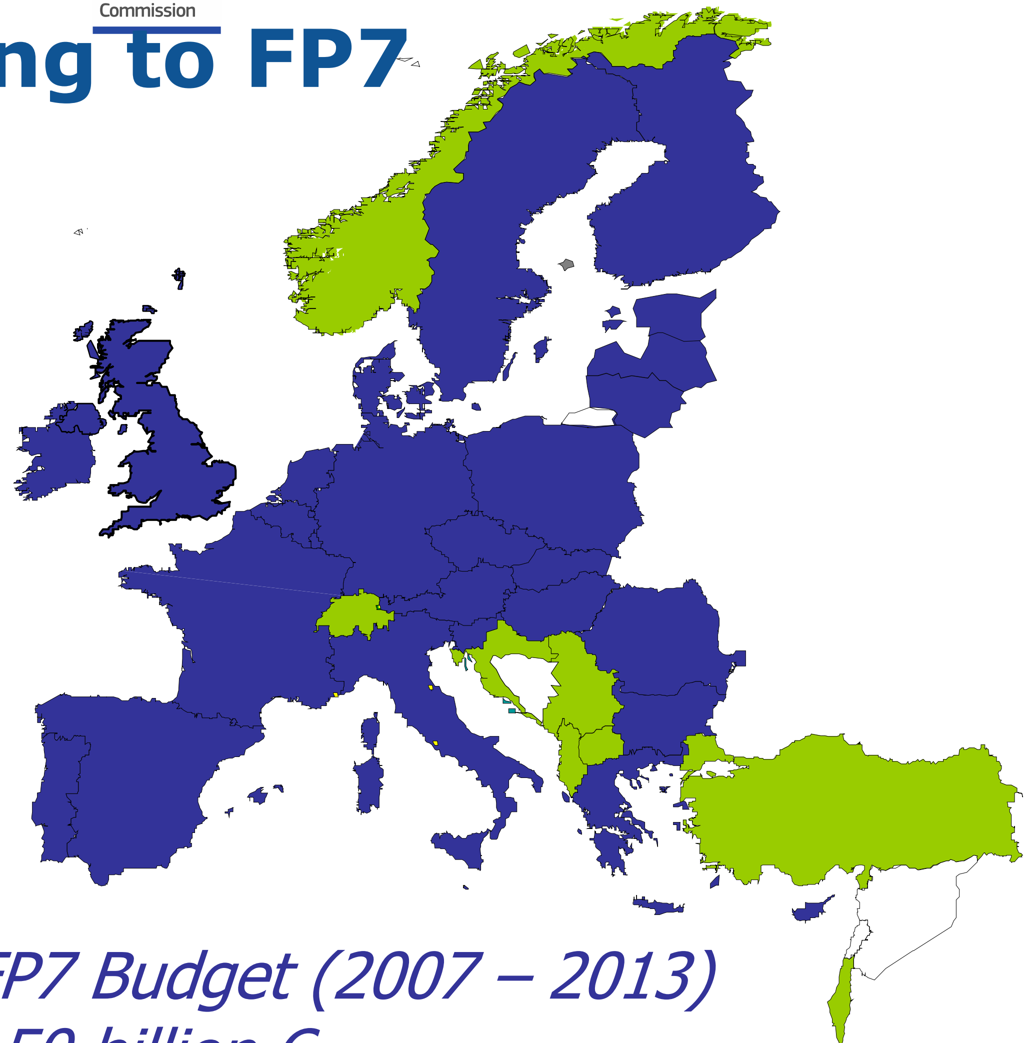

- 27 EU Member States
- FP7 Associated States
  - Israel
  - Norway
  - Switzerland
  - Turkey
  - Iceland
  - Croatia
  - Serbia
  - Albania
  - FYRoMacedonia

Total FP7 Budget (2007 – 2013)
above 50 billion €

Research versus Product Development

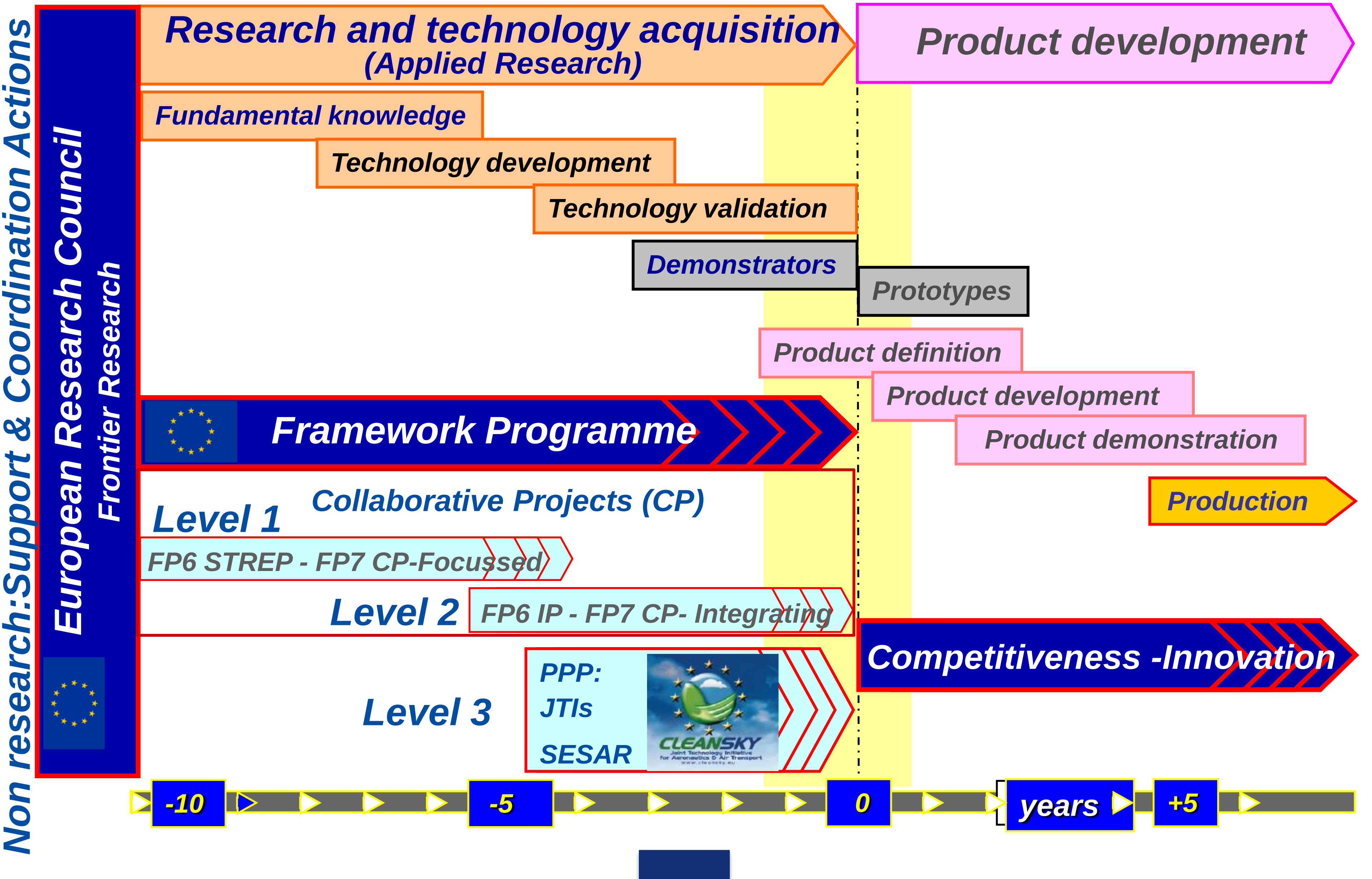

The Criteria of FP7

Evaluation Criteria Applicable to Collaborative Project Proposals		
Scientific & Technological Quality "Scientific and/or technological excellence (relevant to the topics addressed by the call)"	**Implementation** "Quality and efficiency of the implementation and the management"	**Impact** "Potential impact through the development, dissemination and use of project results"
• Soundness of concept, and quality of objectives • Progress beyond the state-of-the-art • Quality and effectiveness of the S/T methodology and associated work plan	• Appropriateness of the management structure and procedures • Quality and relevant experience of the individual participants • Quality of the consortium as a whole (including complementarity, balance) • Appropriateness of the allocation and justification of the resources to be com-mitted (staff, equipment…)	• Contribution, at the European and/or international level, to the expected impacts listed in the work programme under the relevant topic/activity • Appropriateness of measures for the dissemination and/or exploitation of project results, and management of intellectual property.

RTD Funding for Specific Aeronautics Research on EU Level

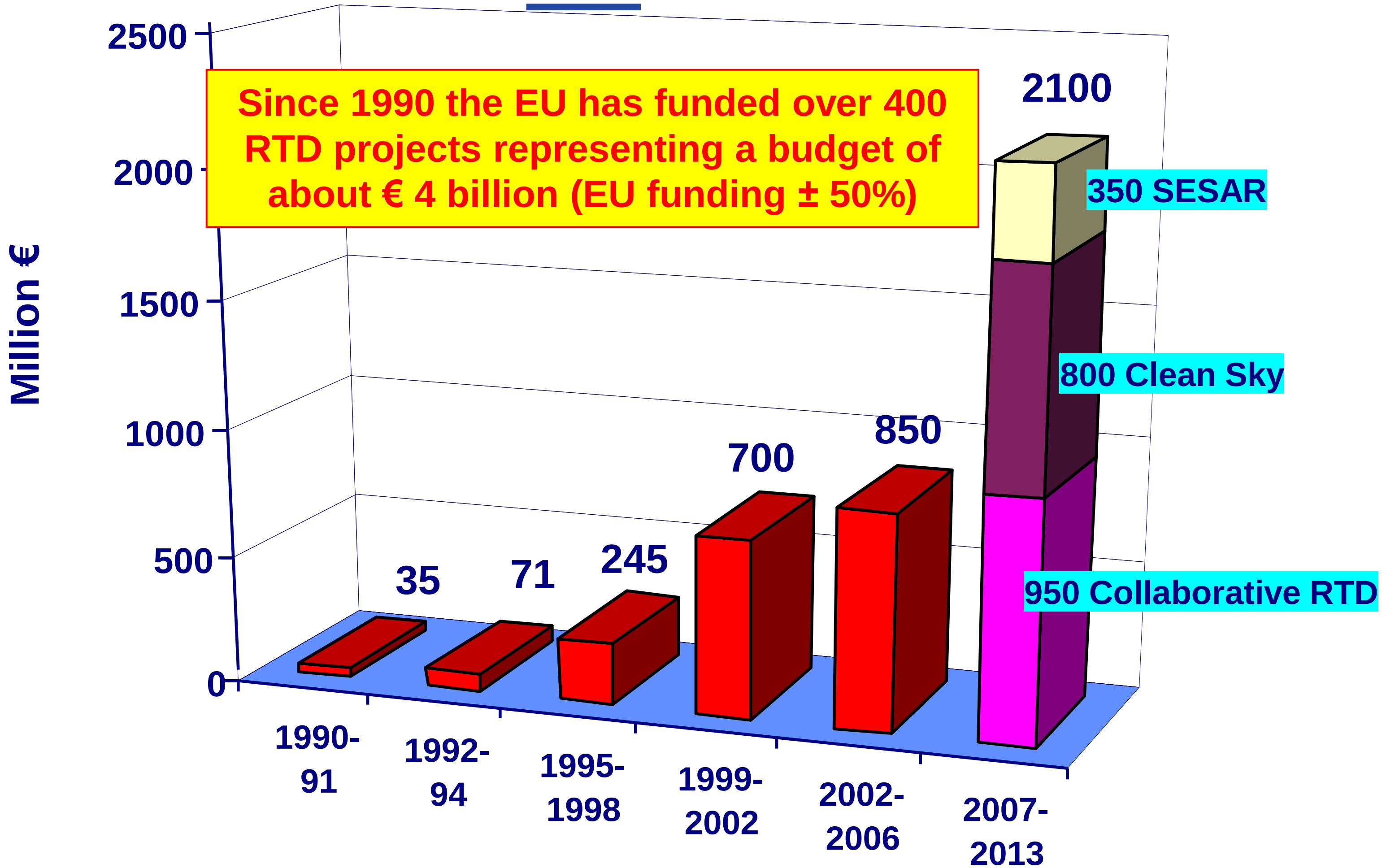

Clean Sky* – *Joint Technology Initiative to improve the impact of air transport on the environment

SESAR* – *Joint Undertaking on the Single European Sky Air Traffic Management Research

Airbus A380 Technology:
Framework Programme Origins

European Commission

On-board maintenance system

Upper fuselage skin in Glare®
TANGO

Integrated and modular avionics architecture (IMA)
NEVADA, PAMELA, VICTORIA, NATACHA

Horizontal tail plane designed for relaxed stability

Dual air conditioning Pack concept
ASICA, CABINAIR

High Reynolds Number; Low drag wing design
ECARP, EUROLIFT, AWIATOR
C-WAKE, HiReTT

Carbon Composite rear fuselage (Section 19)
ADPRIMAS, APRICOS, TANGO

Variable frequency Power generation

Skin to stringer welding (first on A318)
WAFS

New low weight front fuselage structure
ADPRIMAS, APRICOS, TANGO

Centre wing box in CFRP
TANGO

Electro-hydraulic Actuators
EPICA, ELISA, EHA

Electric thrust reverse control

2 hydraulic (5000psi) + 2 electrical channel architecture for flight controls and landing gear
POA

New four post main landing gear (4-6-6-4 wheels configuration)
ELGAR

Aeronautics and Air Transport in FP7

- **Total Budget: 2.1 billion Euro** (2007 – 2013)
  - **958 million € Collaborative RTD (Level 0, Level 1, Level 2)**
  - **800 million € Clean Sky (Level 3)**
  - **350 million € SESAR (Single European Sky ATM Research)**
- **6 Calls for Proposals (for Collaborative RTD)**
  - **2007 (220.6 million €)**
  - **2008 (211.7 million €)**
  - **2010 (108 million €)**
  - **2011 (121.3 million €)**
  - **2012 (150 million €)**
  - **2013 (135 million €) – Call to be published in July 2012**

Deadline of Call on 14th Nov. 2012

EUROPEAN COMMISSION

Community Research

Aeronautics Research

Research Projects in Flight Physics

- **Representativity of Wind Tunnel Testing**
- **Natural Laminar Flow for Drag Reduction**
- **New Aircraft Concepts** (noise, drag, payload)

FLIRET, Co-ord. Airbus-D

Flight Reynolds Number Testing

2005 - 2008

TELFONA, Co-ord. Airbus UK

Testing for Laminar Flow of New Aircraft

2005 - 2009

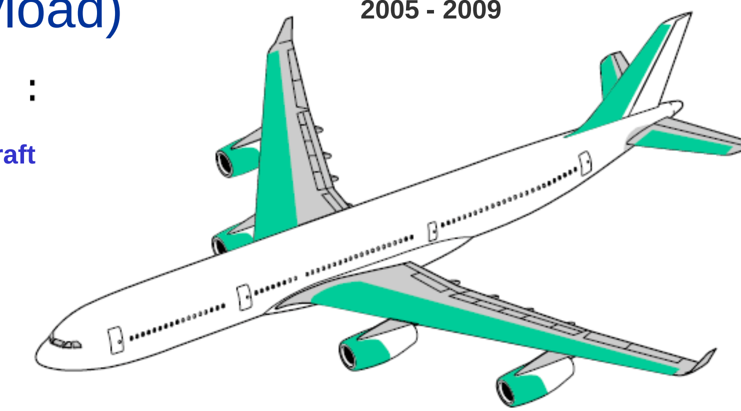

NACRE, Co-ord. Airbus

New Aircraft Concepts, 2005 - 2008

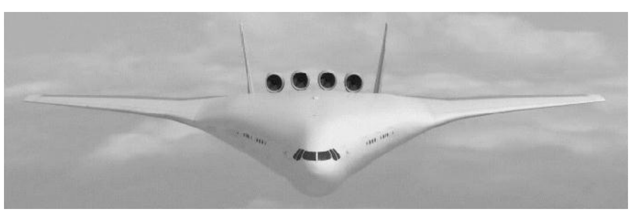

HISAC, Co-ord. Dassault

Environmentally Friendly High-Speed Aircraft

2005 - 2009

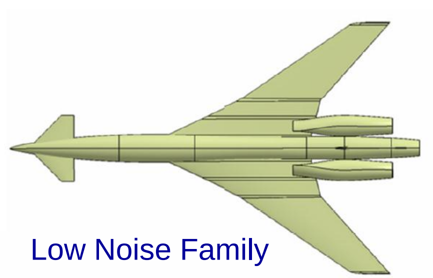

Low Noise Family

Low Sonic Boom Family

SUPERTRAC, Co-ord. ONERA

Supersonic Transition Control

2005 - 2008

PLASMAERO, Co-ord. ONERA

Flow Control by Plasma Actuators

2009 - 2012

SEVENTH FRAMEWORK PROGRAMME

EUROPEAN COMMISSION
Community Research

Aeronautics Research
FP7 Research Projects in CFD Methods

Adaptive Higher-Order Variational Methods for Aerodynamic Applications in Industry - ADIGMA (22 partners)
Co-ordinator: Prof. Dr. Norbert Kroll, DLR Braunschweig
Duration: 40 Months
Total Costs: 4.887.080,- Euro

Advanced Turbulence Simulation for Aerodynamic Application Challenges ATTAC (16 partners)
Co-ordinator: Dr. Dieter Schwamborn, DLR Göttingen
Duration: 36 Months
Total Costs: 6.760.375,- Euro

Industrialisation of High-Order Methods – A Top-Down Approach IDIHOM (21 partners)
Co-ordinator: Prof. Dr. Norbert Kroll, DLR Braunschweig
Duration: 36 Months
Total costs: 5 659 942 €

SEVENTH FRAMEWORK PROGRAMME

European Commission

DREAM (Validation of radical engine architecture systems)

The large–scale integrated project addresses the goals of reducing CO_2 and the increasing cost of Jet A1 fuel through:

- Increasing rotor efficiency
- Novel enabling architectures and structures
- Characterising alternative fuels and demonstrating the operation of a small turbofan engine with the selected alternative fuel

dream
Validation of radical engine architecture systems

Co-ordinator: Rolls-Royce Plc	
Total cost:	€ 39 994 957
EU contribution:	€ 24 999 999
1st Febr. 2008 to 31st Jan. 2012	
45 Partners	

COOPERATION

Horizon 2020

The Future

Common Strategic Framework of the European Union

Name:	**'Horizon 2020' - Framework Programme for Research & Innovation**
Time Frame:	**7 years (2014-2020) and beyond**
Budget:	**80 billion Euro proposed by the Commission**
Funding Schemes:	**fewer, more flexible and user-friendly**

Tentative Implementation Time Schedule:

Dec. 2011	Presentation of 'Horizon 2020' to the Council of Member States
During 2012	Consultation Process of European Parliament and Council
1st Half 2013	Decision of Parliament and Council on 'Horizon 2020'
Jan. 2014	**Start of 'Horizon 2020' Framework Programme for Research Innovation**

'Horizon 2020' Objectives & Structure

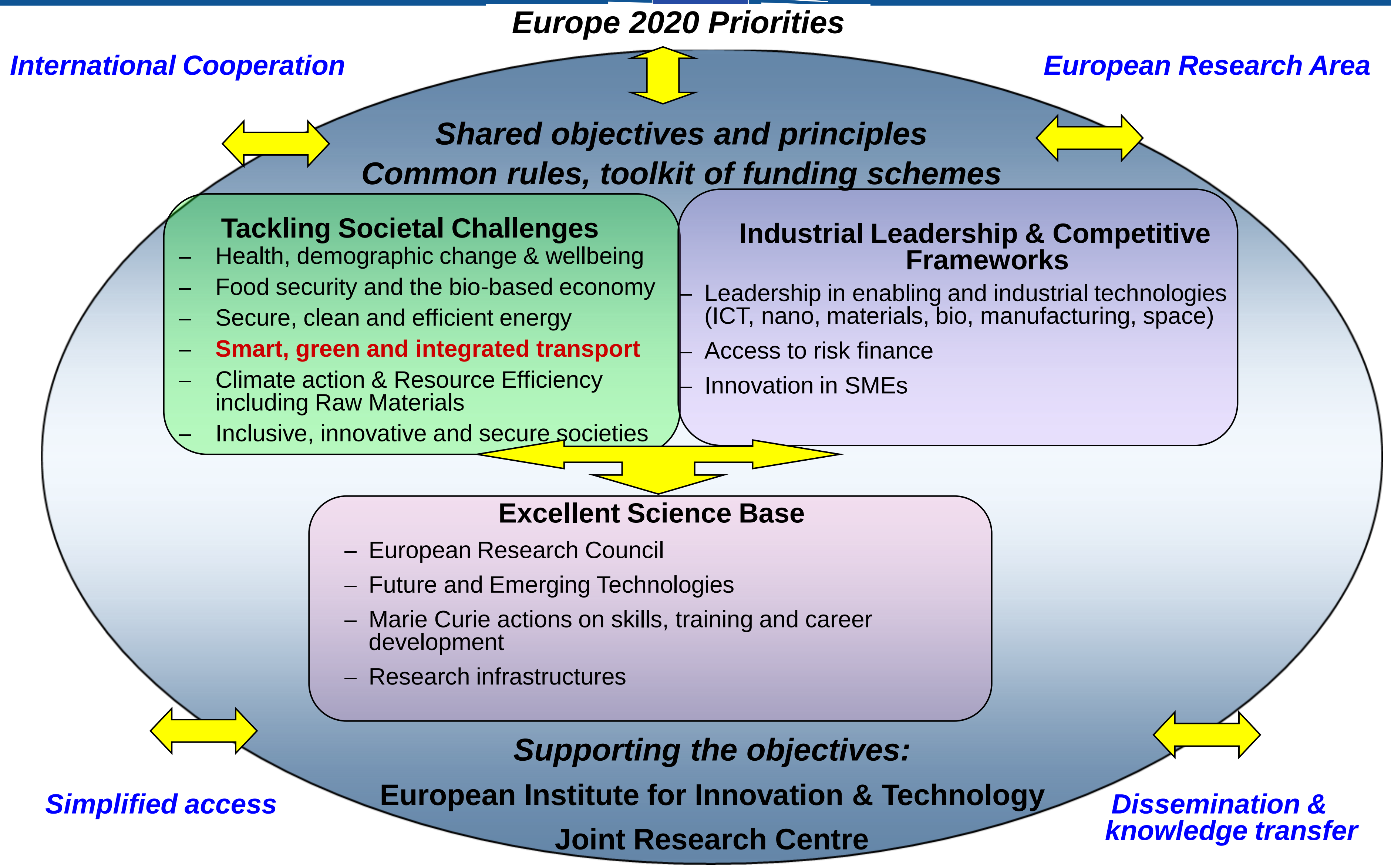

The Future

Where are we?

- Europe's Vision for Aviation and the SRIA of ACARE address the challenge of future needs
- Solutions have to involve national, European and international level (e.g. ICAO works on global ETS)
- For alternative fuels the aviation stakeholders look for
  - Sustainability
  - Availability
  - Price
  - Certification of new fuels

- Europe's new Framework Programme 'Horizon 2020' offers an opportunity and a multi-national platform for the need technologies

European Commission

Thank you for your attention!

dietrich.knoerzer@ec.europa.eu